

DAVID H EBERLY

GAME PHYSICS

SECOND EDITION

M K
MORGAN KAUFMANN

Morgan Kaufmann is an imprint of Elsevier
30 Corporate Drive, Suite 400, Burlington, MA 01803, USA
The Boulevard, Langford Lane, Kidlington, Oxford, OX5 1GB, UK

Copyright © 2010, Elsevier Inc. All rights reserved.

No part of this publication may be reproduced or transmitted in any form or by any means, electronic or mechanical, including photocopying, recording, or any information storage and retrieval system, without permission in writing from the publisher. Details on how to seek permission, further information about the Publisher's permissions policies and our arrangements with organizations such as the Copyright Clearance Center and the Copyright Licensing Agency, can be found at our website: www.elsevier.com/permissions.

This book and the individual contributions contained in it are protected under copyright by the Publisher (other than as may be noted herein).

Notices

Knowledge and best practice in this field are constantly changing. As new research and experience broaden our understanding, changes in research methods, professional practices, or medical treatment may become necessary.

Practitioners and researchers must always rely on their own experience and knowledge in evaluating and using any information, methods, compounds, or experiments described herein. In using such information or methods they should be mindful of their own safety and the safety of others, including parties for whom they have a professional responsibility.

To the fullest extent of the law, neither the Publisher nor the authors, contributors, or editors assume any liability for any injury and/or damage to persons or property as a matter of products liability, negligence or otherwise, or from any use or operation of any methods, products, instructions, or ideas contained in the material herein.

Library of Congress Cataloging-in-Publication Data

Eberly, David H.

Game physics / David H. Eberly. – 2nd ed.

p. cm.

Includes bibliographical references and index.

ISBN 978-0-12-374903-1 (hardcover : alk. paper)

1. Computer games—Programming. 2. Physics—Computer simulation. 3. Computer graphics.
4. Three-dimensional display systems. I. Title.

QA76.76.C672E24 2010

794.8'1526—dc22

2009049828

British Library Cataloguing-in-Publication Data

A catalogue record for this book is available from the British Library.

ISBN: 978-0-12-374903-1

For information on all Morgan Kaufmann publications
visit our Web site at www.elsevierdirect.com

Typeset by: diacriTech, India

Printed in the United States of America

10 11 12 13 10 9 8 7 6 5 4 3 2 1

Working together to grow
libraries in developing countries

www.elsevier.com | www.bookaid.org | www.sabre.org

ELSEVIER BOOKAID International Sabre Foundation

DEDICATION

After surgery for Stage 4 gallbladder cancer, aggressive chemotherapy, and radiation treatments, it was not clear I would ever have a chance to write the second edition of this book. My survival is a testament to the advances that modern medicine has made. The unselfish caregiving by my loving wife, Shelly, her support through difficult times, and her encouragement for me to recover and continue writing are things for which I am extremely grateful. I have finished this book and look forward to writing many more with her at my side.

TRADEMARKS

The following trademarks, mentioned in this book and the accompanying CD-ROM, are the property of the following organizations.

- DirectX, Direct3D, Visual C++, DOS, Windows, and Xbox 360 are trademarks of Microsoft Corporation.
- Playstation 3 is a trademark of Sony Corporation.
- OpenGL is a trademark of Silicon Graphics, Inc.
- Radeon is a trademark of ATI Technologies, Inc.
- NVIDIA, GeForce, PhysX, and the Cg Language are trademarks of NVIDIA Corporation.
- NetImmerse and R-Plus are trademarks of Numerical Design, Ltd.
- MathEngine is a trademark of Criterion Studios.
- The Havok physics engine is a trademark of Havok.com Inc.
- SoftImage is a trademark of Avid Technology, Inc.
- Prince of Persia 3D is a trademark of Brøderbund Software, Inc.
- XS-G and Canyon Runner are trademarks of Greystone Technology.
- Mathematica is a trademark of Wolfram Research, Inc.
- Turbo Pascal is a trademark of Borland Software Corporation.
- The 8086 and Pentium are trademarks of Intel Corporation.
- Macintosh and Xcode are trademarks of Apple Corporation.
- Gigi and VAX are trademarks of Digital Equipment Corporation.
- MASPAR is a trademark of MasPar Computer Corporation.

FIGURES

COLOR PLATES

- 3.3 The Foucault pendulum.
- 3.7 A ball rolling down a hill.
- 3.14 A mass pulley spring system shown at two different times.
- 3.25 Two snapshots of a freely spinning top.
- 4.2 A rope modeled as a linear chain of springs.
- 4.4 A cloth modeled as a rectangular array of springs.
- 4.6 A gelatinous cube that is oscillating because of random forces.
- 4.7 A gelatinous blob that is oscillating because of small, random forces.
- 4.15 A skirt modeled by a generalized cylinder surface.
- 4.17 A water drop modeled as a control point surface of revolution.
- 4.18 A closed tube surface whose central axis is a helix.
- 4.19 A wriggling snake modeled as a tube surface whose central curve is a control point curve.
- 4.20 Free-form deformation.
- 4.29 A bouncing ball with deformation based on implicit surfaces.
- 5.4 Image (a) [upper left]: The initial density is generated by a uniform random number generator. Image (b) [upper right]: The evolved density after a small period of time. The only force is due to a spike of wind moving from the left-center of the grid. The bright blob-like region is a density source. The dark blob-like region is a density sink. Image (c) [lower left]: Starting from the random initial density, eight vortices were added to the grid. They are shown in white in the equivalent gray-scale image of [Figure 5.4](#); the direction of rotation is indicated by the arrows. You can see the swirl-like effects of the vortices. Image (d) [lower right]: The grid of image (c) is allowed to evolve further. The density source and sink are more pronounced, and the density is starting to become more homogeneous in regions centered at the vortices.
- 5.5 Image (a) [upper left]: The initial density is a spherical blob of constant density. Image (b) [upper right]: The evolved density after a small period of time. The only force is due to a spike of wind moving from the right-center of the grid; the scene has been rotated slightly so you can see the portion of the sphere on which the wind interacted first. There are no density sources or sinks. You can see the material being pushed out of the sphere by the wind. Image (c) [lower left]: Eight vortices were added to the grid, which causes the density to swirl

- around a bit. The scene was rotated so you can see the tunnel carved out by the wind. Image (d) [lower right]: The lower-left grid is allowed to evolve further.
- 5.6 Image (a) [top] shows the initial $128 \times 128 \times 64$ gray scale image (a CT image). The boundary voxels are drawn in light gray. The $z = 0$ slice is the upper left tile. The $z = 63$ slice is the lower right tile. Image (b) [bottom] shows the 3D image after a number of blurring operations.

FIGURES IN CHAPTERS

2.1	A couple of coordinate systems at points on a curve.	16
2.2	A polar coordinate frame at a point on a curve.	18
2.3	A curve, a tangent vector at a point, and the circle of choices for the normal vector. The circle lies in the plane containing the point and perpendicular to the tangent.	20
2.4	Cylindrical coordinates $(x, y, z) = (r \cos \theta, r \sin \theta, z)$.	22
2.5	Spherical coordinates $(x, y, z) = (\rho \cos \theta \sin \phi, \rho \sin \theta \sin \phi, \rho \cos \phi)$.	24
2.6	Motion of a particle about a fixed axis, a constant distance from the axis.	25
2.7	(a) The body coordinate system as seen by the body observer. (b) The body coordinate system as seen by the world observer.	28
2.8	Gravitational forces on objects located at various places around the Earth.	32
2.9	Gravitational forces on objects located nearly on the Earth's surface, viewed as a flat surface.	33
2.10	(a) Unstretched spring. (b) Force due to stretching the spring. (c) Force due to compressing the string.	34
2.11	A block in contact with an inclined plane. (a) Static friction is dominant and the block remains at rest. (b) Gravity is dominant and the block slides, so kinetic friction applies.	35
2.12	Torque from a force exerted on a particle.	36
2.13	A force couple.	37
2.14	(a) All forces applied to a point mass are concurrent but are not balanced, so the point moves. (b) All forces are concurrent but do balance, so the point does not move. (c) A rigid rod with nonconcurrent forces applied to the endpoints. The forces are equal in magnitude but opposite in direction. The rod rotates about its center. (d) Nonconcurrent forces are applied to three locations, two forces of equal magnitudes and directions at the endpoints and one force of twice the magnitude of an endpoint force but opposite in direction applied to the rod center. The rod is balanced and does not rotate about its center.	38

2.15	Balancing discrete masses on a line. The center of mass for two masses viewed as the balance point for a seesaw on a fulcrum.	43
2.16	Balancing continuous masses on a line. The center of mass for the wire is viewed as the balance point for a seesaw on a fulcrum. A general point location x is shown, labeled with its corresponding mass density $\delta(x)$.	44
2.17	Balancing discrete masses in a plane.	45
2.18	Balancing discrete masses in a plane on a fulcrum.	46
2.19	Balancing continuous masses in a plane. The shades of gray indicate variable mass density.	47
2.20	A continuous mass bounded by a parabola and a line.	48
2.21	A continuous mass in the shape of a hemicircle.	49
2.22	A force applied to a particle traveling on a straight line from position \mathbf{x}_0 to \mathbf{x}_1 .	78
3.1	The infinitesimal area dA swept out by motion of the earth over an infinitesimal change in position $d\mathbf{r}$. The swept region is effectively a triangle whose sides are \mathbf{r} and $\mathbf{r} + d\mathbf{r}$.	88
3.2	The Foucault pendulum. The pendulum joint is at \mathcal{O} , the mass is m and is attached to the pendulum rod of length L . The gravitational force acts in the direction k , a unit-length vector from the joint to the center of the Earth.	92
3.3	The Foucault pendulum. The figures show the path of the pendulum tip in the horizontal plane. New points on the path are colored white, but the intensity of the older points along the path gradually decreases.	95
3.4	The simple pendulum. The motion is constrained to a plane. The mass is located at position $\mathcal{X}(t)$ at time t and is always a fixed length L from the joint \mathcal{P} . The angle formed by the pendulum rod with the vertical is $\theta(t)$. The curve of motion is a circle with tangent $\mathbf{T}(t)$ and outward pointing normal $\mathbf{N}(t)$. The only force acting on the mass is gravitational, $-mg\mathbf{j}$, where m is the mass of the particle, g is the gravitational constant, and $-\mathbf{j}$ is the direction of the force (vertically downward). The joint \mathcal{P} provides no frictional force.	99
3.5	A ball of mass m on a flat table. A rubber band connects the ball to a fixed point on the table. The force \mathbf{F} due to the rubber band is shown. The position \mathbf{x} of the ball is shown together with its velocity $\dot{\mathbf{x}}$.	104
3.6	A ball is at the top of a frictionless hill. With a small push, the ball will roll down the hill.	105
3.7	A ball rolling down a hill. Image (b) shows the path of the center of the ball as it rolls down the hill. The ball rotates at a speed commensurate with its downhill velocity. (See also Color Plate 3.7.)	108

3.8	(a) A metal chute of length L , one end attached to the origin, the other end raised by a height H . (b) Side view of the chute.	109
3.9	The initial configuration of a rigid rod containing a mass that is attached to a spring.	114
3.10	Three masses aligned vertically and subject to gravitational force.	116
3.11	A modification of the simple pendulum problem.	118
3.12	A triangle pendulum.	121
3.13	A system consisting of two masses, a pulley with mass, and a spring.	122
3.14	A mass pulley spring system shown at two different times. The spring expands and compresses and the pulley disk rotates during the simulation. The system stops when a mass reaches the center line of the pulley or the ground. (See also Color Plate 3.14 .)	125
3.15	A system of two pulleys, two springs, and a mass.	125
3.16	A physical system with a bent pipe rotating about the z -axis and a disk rotating about its axis.	126
3.17	A solid disk that rolls on a rough, inclined plane.	128
3.18	A simple diving board.	129
3.19	An inclined plane that forms an angle ϕ with the horizontal. The particle has mass m . It is located at $\mathbf{r}_0 = (x_0, y_0, z_0)$; hash marks are shown on the axes corresponding to x_0 , y_0 , z_0 , and w_0 , where $y_0 = w_0 \cos \phi$ and $z_0 = w_0 \sin \phi$.	137
3.20	Two particles, connected by a massless rod, that slide along a rough plane.	138
3.21	A flat board on a rough plane.	144
3.22	A side view of a solid box on a rough, inclined plane.	146
3.23	The world coordinates and body coordinates for a rigid body where both systems have the same origin.	148
3.24	A freely spinning top with tip fixed at the origin of the world coordinate system.	150
3.25	Two snapshots of a freely spinning top. The black line is the vertical axis. The white line is the axis of the top. (See also Color Plate 3.25 .)	154
4.1	Two curve mass objects represented as mass–spring systems.	159
4.2	A rope modeled as a linear chain of springs. Image (a) shows the rope at rest with only gravity acting on it. Image (b) shows the rope subject to a wind force whose direction changes by small random amounts. (See also Color Plate 4.2 .)	161
4.3	A surface mass represented as a mass–spring system with the masses organized as a two-dimensional array.	162

4.4	A cloth modeled as a rectangular array of springs. Wind forces make the cloth flap about. Notice that the cloth in image (b) is stretched in the vertical direction. The stretching occurs while the gravitational and spring forces balance out in the vertical direction during the initial portion of the simulation. (See also Color Plate 4.4 .)	163
4.5	A volume mass represented as a mass–spring system with the masses organized as a three-dimensional array. Only the masses and springs on the three visible faces are shown. The other connections are shown, but without their springs.	164
4.6	A gelatinous cube that is oscillating because of random forces. The cube is modeled by a three-dimensional array of mass connected by springs. (See also Color Plate 4.6 .)	166
4.7	A gelatinous blob that is oscillating because of small, random forces. This blob has the masses located at the vertices of an icosahedron with additional masses of infinite weight to help stabilize the oscillations. The springs connecting the blob to the infinite masses are shown in white. (See also Color Plate 4.7 .)	167
4.8	Six pairs of B-spline curves of various types. The right image of each pair shows the deformed curve by modifying one control point.	176
4.9	The initial control points and curve are shown at the top of the figure. The evolved control points and curve are shown at three later times, with time increasing from top to bottom in the figure.	179
4.10	The control points and curve at later times in the evolution.	180
4.11	Deformation of a line segment into a closed curve that splits away from the original curve.	181
4.12	The decomposition of (u, v) space into an $n \times m$ grid of rectangles, each rectangle consisting of two triangles. A typical rectangle is shown in (b), with lower corner index (i, j) corresponding to $u = i/n$ and $v = j/m$.	184
4.13	A cylinder surface (b) obtained by extruding the curve (a) in a direction oblique to the plane of the curve.	186
4.14	A generalized cylinder surface obtained by linearly interpolating pairs of points on two curves.	187
4.15	A skirt modeled by a generalized cylinder surface. Wind-like forces are acting on the skirt and are applied in the radial direction. Image (a) shows the skirt after wind is blowing it about. Image (b) shows a wireframe view of the skirt so that you can see it consists of two closed curve boundaries and is tessellated between. (See also Color Plate 4.15 .)	188
4.16	A surface of revolution.	189
4.17	A water drop modeled as a control point surface of revolution. The surface dynamically changes to show the water drop forming, separating from the main body of water, then falling to the floor. The	

evolution is from left to right and top to bottom. (See also Color Plate 4.17.)	190
4.18 A closed tube surface whose central axis is a helix. (See also Color Plate 4.18.)	191
4.19 A wriggling snake modeled as a tube surface whose central curve is a control point curve. (See also Color Plate 4.19.)	193
4.20 Free-form deformation. Image (a) shows the initial configuration where all control points are rectangularly aligned. Image (b) shows that some control points have been moved and the surface is deformed. The control point shown in red in (b) is the point at which the mouse was clicked on and moved. (See also Color Plate 4.20.)	197
4.21 A disk-shaped body and various deformations of it.	198
4.22 This is an illustration of a level surface $F(x, y, z) = 0$, a cube whose eight corners correspond to image samples. Four of the image values are shown, one positive and three negative. Assuming the image values vary continuously, each edge connecting a positive and negative value must have a point where the image is zero. The level surface $F(x, y, z) = 0$ necessarily passes through those zero points, as illustrated by the triangular-shaped surface shaded in dark gray.	200
4.23 The 16 possible sign configurations for a pixel.	202
4.24 The three possible resolutions for the ambiguous pixel case.	203
4.25 Two possible configurations for hyperbolic isocurves with pixels superimposed. The four edge intersections are P_0 , P_1 , P_2 , and P_3 as marked.	204
4.26 Topological inconsistencies introduced in two voxels sharing an ambiguous face.	207
4.27 A voxel and its extracted edge mesh.	208
4.28 Triangle removal in the edge mesh of Figure 4.27 . The sequence is from (a) to (h).	209
4.29 A bouncing ball with deformation based on implicit surfaces. Image (a) shows the bouncing ball with only the implicit surface deformation. Image (b) shows an additional deformation of nonuniform scaling by applying an affine transformation. (See also Color Plate 4.29.)	211
 5.1 The left image shows the vector field $\mathbf{v} = (x, y)$, which has a divergence $\nabla \cdot \mathbf{v} = 2$. The flow lines are expanding at the indicated point (black dot), illustrated by flow lines with directions \mathbf{v}^+ and \mathbf{v}^- . The right image shows the vector field $\mathbf{v} = (-x, -y)$, which has a divergence $\nabla \cdot \mathbf{v} = -2$. The flow lines are compressing at the indicated point (black dot).	241

5.2	A typical lattice of points, where $i_{\max} = j_{\max} = 5$. The lattice cell centers are shown as black dots. The interior cells have a white background. The boundary corner cells have a dark gray background. The boundary edge–interior cells have a light gray background.	248
5.3	Left: Forward transport of the density from three cell centers. The cell with light gray background contains two transported centers. Right: Backward transport of the density from three cell centers. One of the transported cell centers is shown contained in a square formed by four cell centers.	259
5.4	Image (a) [upper left]: The initial density is generated by a uniform random number generator. Image (b) [upper right]: The evolved density after a small period of time. The only force is due to a spike of wind moving from the left-center of the grid. The bright blob-like region is a density source. The dark blob-like region is a density sink. Image (c) [lower left]: Starting from the random initial density, eight vortices were added to the grid. They are shown in white in the figure; the direction of rotation is indicated by the arrows. You can see the swirl-like effects of the vortices. Image (d) [lower right]: The grid of image (c) is allowed to evolve further. The density source and sink are more pronounced, and the density is starting to become more homogeneous in regions centered at the vortices. (See also Color Plates 5.4(ab) and 5.4(cd) .)	275
5.5	Image (a) [upper left]: The initial density is a spherical blob of constant density. Image (b) [upper right]: The evolved density after a small period of time. The only force is due to a spike of wind moving from the right-center of the grid; the scene has been rotated slightly so you can see the portion of the sphere on which the wind interacted first. There are no density sources or sinks. You can see the material being pushed out of the sphere by the wind. Image (c) [lower left]: Eight vortices were added to the grid, which causes the density to swirl around a bit. The scene was rotated so you can see the tunnel carved out by the wind. Image (d) [lower right]: The lower-left grid is allowed to evolve further. (See also Color Plates 5.5(ab) and 5.5(cd) .)	288
5.6	Image (a) [top] shows the initial $128 \times 128 \times 64$ gray scale image (a CT image). The boundary voxels are drawn in light gray. The $z = 0$ slice is the upper left tile. The $z = 63$ slice is the lower right tile. Image (b) [bottom] shows the 3D image after a number of blurring operations. (See also Color Plate 5.6 .)	291
6.1	Culling of bounding spheres against a view frustum.	299
6.2	Decomposition of space to reduce the number of comparisons between pairs of objects.	301

6.3	The sweep phase of the algorithm.	305
6.4	The update phase of the algorithm when intervals have moved.	310
6.5	Axis-aligned rectangles overlap when both their x -intervals and y -intervals overlap.	313
6.6	The relationships among the CPU, SPU, send queue, receive port, CPU memory, and SPU memory. The gray-background items are the shared heaps.	336
6.7	E_1 is contained in E_0 . The maximum E_0 -level-curve value λ_1 for E_1 is negative.	354
6.8	E_1 transversely intersects E_0 . The minimum E_0 -level-curve value λ_0 for E_1 is negative, the maximum value λ_1 is positive.	355
6.9	E_1 is separated from E_0 . The minimum E_0 -level-curve value λ_0 for E_1 is positive.	355
6.10	Intersection of two ellipses.	357
6.11	The configuration of two ellipses at contact time. The contact point is \mathbf{P} .	359
6.12	The transformed configuration to a circle of radius 1 with center at the origin and an axis-aligned ellipse.	360
6.13	The transformed configuration to a circle of radius 1, with center at the origin and an axis-aligned ellipse. The circle and ellipse are separated. The point \mathbf{P} is the ellipse point that is closest to the origin. An outer-pointing normal at this point is $\nabla Q(\mathbf{P})$.	361
6.14	The left-most branch of the graph of $f(s)$. The vertical asymptote is at $s = 1/d_1$ when $k_1 \neq 0$, or at $s = 1/d_0$ when $k_1 = 0$.	363
6.15	The ellipse sweeps a region bounded by two parallel lines. Left: The ellipse will intersect the circle when the circle intersects the swept region. Right: The ellipse will not intersect the circle when the circle is disjoint from the swept region.	365
6.16	Possibilities for the graph of $h(t)$. Upper left: The ellipse is moving away from the circle, so there is no intersection at any time. Upper right: The ellipse initially moves towards the circle, but then veers away and passes it without intersection. Lower left: The ellipse moves towards the circle and just grazes it at the contact time. Lower right: The ellipse moves towards the circle, just touching the circle at contact time, and then interpenetrates for a period of time.	367
6.17	(a) Object at time t_0 . (b) Object at time $t_0 + \Delta t/2$. (c) Object at time $t_0 + \Delta t$.	392
6.18	(a) A convex set. No matter which two points you choose in the set, the line segment connecting them is in the set. (b) A nonconvex set. The line segment connecting two specific points is not (fully) contained in the set.	394

6.19	Nonintersecting convex objects and a separating line for them. The algebraic condition for separation is $\lambda_{\max}^{(0)}(\mathbf{D}) < \lambda_{\min}^{(1)}(\mathbf{D})$ as indicated in equation (6.58).	395
6.20	(a) Nonintersecting convex polygons. (b) Intersecting convex polygons.	397
6.21	(a) edge–edge contact. (b) vertex–edge contact. (c) vertex–vertex contact.	397
6.22	Two polygons separated by an edge-normal direction of the first polygon.	398
6.23	(a) A convex polygon. (b) A unit circle whose vertices correspond to normal directions of the polygon and whose arcs connecting the vertices correspond to vertices of the polygon (the <i>polar dual</i> of the polygon).	403
6.24	A BSP tree constructed by recursive splitting of the unit disk. Each node is labeled with the test used for the split. The subsectors consisting of points satisfying the test are shaded in dark gray. The leaf nodes are shaded in light gray and labeled with a vertex that is extremal.	404
6.25	Two views of two cubes that are not separated by any face normal but are separated by a cross product of two edges, one from each cube.	409
6.26	(a) A tetrahedron. (b) A unit sphere whose vertices correspond to normal directions of the tetrahedron, whose great circle arcs connecting the vertices correspond to edges of the tetrahedron, and whose spherical polygons correspond to vertices of the tetrahedron (the <i>spherical dual</i> of the tetrahedron).	414
6.27	The root of the BSP tree and the two hemispheres obtained by splitting. Both children are displayed with a viewing direction $(0, 0, -1)$. The right child is the top of the sphere viewed from the outside and the left child is the bottom of the sphere viewed from the inside.	415
6.28	The BSP trees for the children of the root.	416
6.29	Left: A convex polyhedron for which the point-in-spherical-polygon test, using only the original arcs, is $O(n)$ (the figure shows $n = 8$, but imagine a very large n). Right: The inscribed convex polyhedron whose edges generate the arcs of the spherical convex polygons.	417
6.30	A convex polygon with bisectors used for an $O(\log n)$ point-in-polygon query. The polygon is partitioned into four triangles labeled T_0 through T_3 .	418
6.31	(a) Edge–edge intersection predicted. (b) Vertex–vertex intersection predicted. (c) No intersection predicted.	426
6.32	Edge–edge contact for two moving triangles.	432

6.33	An OBB with center point \mathcal{C} , coordinate axis directions \mathbf{U}_0 , \mathbf{U}_1 , and \mathbf{U}_2 , and extents e_0 , e_1 , and e_2 along the coordinate axes. The object bounded by the box is shown in gray.	446
6.34	The projection intervals of two OBBs onto a line $\mathcal{P} + t\mathbf{D}$. (a) The intervals are disjoint, so the OBBs are separated. (b) The intervals overlap, so the line is not a separating axis.	447
6.35	Two projected intervals, one stationary and one moving.	457
6.36	Triangles A and B and sets $A + B$, $-B$, and $A - B$. The black dots on the grid are the origin $(0, 0)$. The gray point in the lower right grid is the closest point on $A - B$ to the origin.	460
6.37	The first iteration in the GJK algorithm.	462
6.38	The second iteration in the GJK algorithm.	462
6.39	The third iteration in the GJK algorithm.	463
6.40	The fourth iteration in the GJK algorithm.	463
6.41	Left: Construction of \mathbf{V}_{k+1} in the convex hull of $\mathbf{S}_k \cup \{\mathbf{W}_k\}$. Right: The new simplex $\bar{\mathbf{S}}_{k+1}$ generated from $M = \{\mathbf{W}_0, \mathbf{W}_2, \mathbf{W}_3\}$.	464
6.42	(a) Colliding contact. Body A attempts to penetrate into body B. (b) Resting contact. Body A rests on body B and attempts neither to penetrate into B nor to separate from B. Body A is allowed to slide along B. (c) Separation. Body A has a velocity that separates it from body B.	474
6.43	The reduced contact set for two convex polyhedra A and B.	475
6.44	The effects on $p(t)$ as ε approaches zero: (a) Small ε ; (b) Smaller ε ; and (c) Really small ε (like zero).	477
6.45	(a) Reflection of the preimpulse velocity \mathbf{v}^- through the contact normal to obtain the postimpulse velocity \mathbf{v}^+ . (b) An imperfect reflection that represents a loss of kinetic energy. (c) An imperfect reflection that represents a maximum loss of kinetic energy.	479
6.46	(a) The square traveling towards a sloped plane. (b) The preimpulse configuration at the instant of contact. (c) The postimpulse configuration at the instant of contact. (d) The square moving away from the plane.	482
6.47	An axis-aligned box colliding with a sloped plane along an entire edge of the box, $(1-s)\mathcal{P}_0 + s\mathcal{P}_1$ for $s \in [0, 1]$.	483
6.48	A rectangle travels downwards and intersects two objects simultaneously.	489
6.49	Four rigid bodies with six points of contact. The centers of mass of the four bodies are also shown.	494
6.50	A book resting on a table. Forces applied to the book include only gravitational (force vertically downward) and those used to push the book around the table (force has only a horizontal component).	511

6.51	Two rigid bodies in contact at point K . The centers of mass are \mathbf{x}_i and the offsets to the contact point are \mathbf{r}_i . The normal \mathbf{N}_1 is for rigid body 1.	529
7.1	(a) Two nonparallel lines. (b) Two parallel and disjoint lines. (c) Two coincident lines (shown in bold black).	553
7.2	(a) Two nonparallel planes. (b) Two parallel and disjoint planes. (c) Two coincident planes (shown in bold black).	554
7.3	The coincident planes are shown in bold (black for visible portions, gray for hidden portions).	555
7.4	A vector \mathbf{v} at two locations in the plane.	579
7.5	Addition of \mathbf{u} and \mathbf{v} .	579
7.6	Addition of \mathbf{u} , \mathbf{v} , and \mathbf{w} . Which pair of vectors is added first is irrelevant.	580
7.7	Addition of \mathbf{u} and \mathbf{v} . The order of the vectors is irrelevant.	580
7.8	A vector \mathbf{v} and its additive identity $-\mathbf{v}$.	581
7.9	The vectors \mathbf{u} and \mathbf{v} and the difference $\mathbf{u} - \mathbf{v}$.	581
7.10	The vectors \mathbf{u} and \mathbf{v} , the parallelogram formed by them, and the sum $\mathbf{u} + \mathbf{v}$ and difference $\mathbf{u} - \mathbf{v}$ shown as diagonals of the parallelogram.	582
7.11	The vector \mathbf{v} and two scalar multiples of it, one positive and one negative.	582
7.12	(a) Distributing across a scalar sum. (b) Distributing across a vector sum.	583
7.13	(a) Two orthogonal vectors drawn in the plane spanned by them. (b) Two nonorthogonal vectors and the angle between them.	596
7.14	The projection of vectors onto a unit length vector \mathbf{u} . (a) \mathbf{v} projects to $L\mathbf{u}$ with $L > 0$. The angle θ between \mathbf{u} and \mathbf{v} is shown. The vector \mathbf{w} is obtained as $\mathbf{w} = \mathbf{v} - L\mathbf{u}$ and is itself a projection. (b) \mathbf{v} is perpendicular to \mathbf{u} , so the projection onto \mathbf{u} is the zero vector $\mathbf{0}$. (c) The projection is $L\mathbf{u}$ with $L < 0$.	597
7.15	Gram–Schmidt orthonormalization applied to two vectors in the plane.	598
7.16	Gram–Schmidt orthonormalization applied to three vectors in space.	599
7.17	(a) The cross product of \mathbf{u} and \mathbf{v} according to the right-hand rule. (b) The parallelogram formed by \mathbf{u} and \mathbf{v} with angle θ and parallelogram base length and height marked.	600
7.18	A parallelepiped formed by vectors \mathbf{u} , \mathbf{v} , and \mathbf{w} where \mathbf{u} forms an acute angle with $\mathbf{v} \times \mathbf{w}$. The angle between \mathbf{v} and \mathbf{w} is θ and the angle between \mathbf{u} and $\mathbf{v} \times \mathbf{w}$ is ϕ .	603
7.19	The triple vector product $\mathbf{p} = \mathbf{u} \times (\mathbf{v} \times \mathbf{w})$. Note that \mathbf{p} must lie in the plane spanned by \mathbf{v} and \mathbf{w} .	605

7.20	A subspace U of \mathbb{R}^3 and its orthogonal complement U^\perp .	608
7.21	The four fundamental subspaces.	613
7.22	The projection $\mathbf{p} \in S$ of $\mathbf{b} \in \mathbb{R}^3$, where S is a two-dimensional subspace of \mathbb{R}^3 (a plane through the origin).	614
7.23	A linear transformation from V to V with respect to two different bases (horizontal arrows). The change of basis for V (vertical arrows).	624
7.24	(a) A unit-area square. (b) The parallelogram obtained by transforming the square when the transformed basis vectors have the same order as the basis vectors. (c) The parallelogram obtained by transforming the square when the transformed basis vectors have the opposite order as the basis vectors. (d) The basis vectors mapped to parallel vectors, in which case A is not invertible.	627
7.25	An illustration of the butterfly rule for the determinant of a 3×3 matrix.	629
7.26	(a) A unit-volume cube. (b) The parallelepiped obtained by transforming the cube when the transformed basis vectors have the same order as the basis vectors.	630
7.27	Three graphs showing critical points. (a) $f(x_0)$ is a local minimum. (b) $f(x_0)$ is a local maximum. (c) $(x_0, f(x_0))$ is a point of inflection for the graph of f .	655
7.28	Three graphs showing critical points. (a) $f(x_0)$ is a local minimum. (b) $f(x_0)$ is a local minimum. (c) $(x_0, f(x_0))$ is a saddle point on the graph of f . The tangent planes at the graph points are shown in all three figures.	657
8.1	(a) A vector \mathbf{v} connecting two points \mathcal{P} and \mathcal{Q} . (b) The sum of vectors, each vector determined by two points.	660
8.2	The parallelogram law for affine algebra.	661
8.3	Three coordinate systems in the plane. Observe that the vectors in the coordinate system are not required to be unit length or perpendicular in pairs.	663
8.4	An illustration of condition 1 of the definition for affine transformation.	666
8.5	Various barycentric combinations of two points \mathcal{P} and \mathcal{Q} .	668
8.6	The triangle partitions the plane into seven regions. The signs of c_1 , c_2 , and c_3 are listed as ordered triples.	669
8.7	(a) A triangle with base length b and height h marked. The area of the triangle is $bh/2$. (b) A triangle viewed as a union of an infinite number of line segments of varying lengths (only a few are shown). The area of the triangle is the sum of the lengths of those line segments.	672

8.8	A tetrahedron with base formed by \mathcal{P}_0 , \mathcal{P}_1 , and \mathcal{P}_2 . A triangle slice parallel to the base is shown. The direction perpendicular to the base is marked as the positive z -axis.	674
9.1	The graph of $f(x) = x^2 + x$ for x near 1.	683
9.2	The graph of a function that is discontinuous at $x = 0$.	686
9.3	The graph of $x(t) = t(1 - t)$ with two points marked at times t_1 and t_2 . The light gray lines connecting the origin $(0, 0)$ to $(t_1, x(t_1))$ and $(t_2, x(t_2))$ are secant lines to the graph. The dark gray line is the tangent line to the graph at $(0, x(0)) = (0, 0)$.	687
9.4	An attempt to compute the area bounded by a parabola and the x -axis by filling it with rectangles.	690
9.5	Bases of some rectangular solids as an attempt to fill the domain \mathcal{D} .	696
9.6	The graph of a function $f(x)$ on its domain $[a, b]$.	699
10.1	A right-handed orthonormal set of vectors. A rotation is desired about \mathbf{d} by the angle $\theta > 0$.	715
10.2	A 3D rotation about the z -axis that is represented as the product of two 4D rotations.	724
10.3	Illustration of the spherical linear interpolation, or slerp, of two vectors.	728
10.4	Four points forming a convex quadrilateral. Any interior point of the quadrilateral can be generated using bilinear interpolation with parameters s and t . The curve connecting \mathbf{v}_0 and \mathbf{v}_3 indicates that we want a particular function $s = f(t)$ with $f(0) = f(1) = 0$.	729
13.1	(a) Area under a curve. (b) Approximation of the area by a rectangle (leads to Euler's method). (c) Approximation of the area by a trapezoid (leads to the modified Euler method).	770
13.2	The explicit Euler's method applied to the simple pendulum problem. The image shows a plot of the pendulum angles over time.	801
13.3	The implicit Euler method applied to the simple pendulum problem. The image shows a plot of the pendulum angles over time.	803
13.4	The Runge–Kutta fourth-order method applied to the simple pendulum problem. The image shows a plot of the pendulum angles over time.	804
13.5	The leapfrog method applied to the simple pendulum problem. The image shows a plot of the pendulum angles over time.	805
13.6	The region of stability for the explicit Euler method is shown in gray.	806

13.7	The region of stability for the implicit Euler method is shown in gray.	807
13.8	The region of stability for the Runge–Kutta fourth-order method is shown in gray.	808
13.9	The region of stability for the leapfrog method is shown in black and consists of a line segment on the imaginary axis.	809
13.10	(a) An approximation to $x(t)$ using the Runge–Kutta fourth-order method. (b) The graph of the actual solution $x_0 e^{-ct}$.	810
14.1	(a) Various level curves $f(x_1, x_2) = c$ (straight lines) superimposed on the quadrilateral region implied by the constraints. (b) The graph of $x_3 = f(x_1, x_2)$ (a plane) over the quadrilateral region. The x_3 values at four points on the plane are shown.	815
14.2	(a) Constraints with no solution. The hash marks indicate on which side of the lines the half planes occur. (b) Constraints defining an unbounded convex set. (c) Constraints defining a bounded convex set.	815
14.3	(a) All five constraints are relevant to forming the convex domain. (b) Two of the six constraints are redundant, because only four of the constraints form the convex domain.	817
14.4	The convex domain implied by the two nonnegativity constraints and three linear inequality constraints of the example.	820
14.5	Graph of $f(u, v) = \pi / \sqrt{uv}$ in the first quadrant.	840
14.6	(a) The graph of a convex function. Any line segment connecting two graph points is always above the graph. (b) The graph of a nonconvex function. The line segment connecting two graph points is not always above the graph.	841
14.7	The graph of a convex function $f(x, y)$.	842

TABLES

2.1	Moments and Products of Inertia for Vertices	61
2.2	Moments and Products of Inertia for Edges	62
2.3	Moments and Products of Inertia for Faces	63
2.4	Generation of Polynomials by Vector Fields	66
4.1	Recursive Dependencies for B-Spline Basis Functions for $n = 4$ and $d = 2$	170
4.2	Nonzero Values (Boxed) from Table 4.1 for $N_{3,0}(u) = 1$	172
4.3	Knot Vectors and Parameter Intervals Affected by Modifying the Control Point	176
4.4	The Vertex–Edge Configurations for a Pixel	205
6.1	Timing for the Project-All and BSP-Tree Extremal Queries	420
6.2	Potential Separating Directions for OBBs and Values for r_0 , r_1 , and r	449
9.1	Average Speed Calculations on Intervals $[0, \Delta t]$ with Decreasing Δt	681
9.2	Function Values for x Near c	682
9.3	Derivatives of Some Common Functions	688
9.4	Parameters for Various Finite Difference Approximations	708
13.1	The Actual and Approximate Values for the Solution to the System of Equations	811
14.1	Solving All Possible Systems of Two Equations in Two Unknowns	816
14.2	Tableau of Coefficients and Constants (Example 14.1)	821
14.3	Updated Tableau: Exchanging w_2 with x_2	822
14.4	Updated Tableau: Exchanging x_1 with w_3	822
14.5	Updated Tableau: Exchanging w_1 with s_1	823
14.6	Maximizing f	824
14.7	Maximizing f : Exchanging s_1 with s_2	825

PREFACE TO THE SECOND EDITION

The first edition of *Game Physics* appeared in December 2003. At that time physics was quite a popular topic in games – it still is. I had mentioned in the introductory chapter of the first edition that we should expect physics hardware soon. In fact, Ageia Technologies produced their *physics processing unit* (PPU), but since then, NVIDIA Corporation acquired the company and provides PhysX® to access the physics hardware. However, some physics computations can even be performed on the graphics processing unit (GPU). And with all the power of multiple processors and cores on current generation desktop computers and game consoles, highly performing complex physical simulations are becoming a reality at minimal cost to the consumer.

A lot of research has been done over the years, so much so that it is difficult to keep up with and determine which are the important results and which are not. In this, the second edition, I have added some new material to address some of the criticisms about the first edition. The main criticism was that the impulse-based approach I discussed in the physics engine chapter is not what most commercial or Open Source engines use. The Wild Magic physics engine did (and does) contain a global LCP solver, and there was (and is) a sample application that illustrates its use. However, the number of interacting objects is small. The global solver is not suitable for a large number of objects. I had not discussed iterative dynamics in the first edition, but have remedied that in the second edition with a new section that describes the more common velocity-based dynamics. I had planned on adding a section on position-based dynamics, but the papers of interest to me are very dense in content. I prefer spending a lot of time dissecting the methods and researching the references of those papers before I am comfortable writing about them. Position-based dynamics will have to wait until a third edition.

The second edition also contains a lengthy chapter about fluid dynamics, both in 2D and 3D. The vector calculus background is extensive, and the goal is to derive the partial differential equations of motion from conservation of mass (density equation) and conservation of momentum (Navier–Stokes equation for velocity). Solving these equations on moderate-sized grids still takes a large number of CPU cycles, so much so that it would not be correct to say they are real-time algorithms. However, with multiple cores and processors these days, it is possible to obtain real-time rates. In fact, the source code on the CD-ROM contains a GPU-based implementation for a 2D Navier–Stokes solver that runs in real time. I have provided the framework in the Wild Magic libraries to solve the 3D problem on a GPU. A sample application that uses the library involves Gaussian blurring of a 3D image. I leave it as a project to implement the 3D fluid solver on top of this framework, although I am certain I will post my own implementation at some time after this book is released. The framework

is where most of the work is done anyway. The application work involves writing the shaders and setting up all the render targets necessary to run the application with a minimum amount of video memory and a minimum of transfer of data from system memory to video memory. This work is at a high level and relatively easy to do.

The broad-phase collision culling using axis-aligned boxes and space-time coherency was a topic in the first edition, and there was an implementation for the CPU on the CD-ROM. I greatly expanded this section to discuss how to move the broad-phase culling onto its own CPU core and use multithreading to support it. This is useful when programming on a Microsoft Xbox 360. I also added a discussion on how to move the broad-phase culling onto a specialized processor such as an SPU of the Sony Playstation 3. I have implemented this on the aforementioned consoles, and it was absolutely essential for good performance in a physics-heavy racing game with lots of interacting objects.

Of course, books have bugs just as source code does. The second edition contains as many corrections to typographical errors and content errors as I could possibly find.

The CD-ROM for the book contains a new version of Wild Magic, version 5.0. This is a significant rewrite of Wild Magic 4, except for the mathematics library (some ancient topics never change). I have greatly modified the graphics engine to have its own general FX system. Adding specialized shaders in Wild Magic 4 was a bit tedious and not general. The same thing in Wild Magic 5 is straightforward – the engine design for managing renderer resources does not get in your way. For example, the rewrite made it easy to implement the fluid solvers that are part of the sample applications. Perhaps superficial yet wanted by many users, I have eliminated the verbose Hungarian-style variable naming conventions (and there was great rejoicing ...). Finally, the Wild Magic 5 engine uses the Boost License, which is as liberal as you can get. I hope you enjoy playing with the new version.

As always, my thanks go to the Elsevier and Focal Press folks for their diligence and hard work to make this book possible: Laura Lewin (Senior Acquisitions Editor), Chris Simpson (Associate Acquisitions Editor), Anaïs Wheeler (Assistant Editor), Julie Ochs (Project Manager), and the entire production team at Elsevier.

PREFACE TO THE FIRST EDITION

The evolution of the games industry has been motivated clearly by the gamers' demands for more realistic environments. 3D graphics on a 2D graphics card requires necessarily a classical software renderer. Historically, rasterization of triangles was the bottleneck on 2D cards because of the low *fill rate*, the rate at which you can draw pixels during rasterization. To overcome fill rate limitations on consumer cards the *graphics hardware accelerator* was born in order to off-load the rasterization from the 2D card and the *central processing unit* (CPU) to the accelerator. Later generations of graphics cards, called 3D graphics cards, took on the role of handling the standard work of a 2D graphics card (drawing windows, bitmaps, icons, etc.) as well as supporting rasterization that the 3D graphics requires. In this sense the adjective accelerator for a combined 2D/3D card is perhaps a misnomer, but the term remains in use.

As fill rates increased, the complexity of models increased, further driving the evolution of graphics cards. Frame buffer and texture memory sizes increased in order to satisfy the gamers' endless desires for visual realism. With enough power to render a large number of triangles at real-time rates, the bottleneck of the cards was no longer the fill rate. Rather it was the front end of the graphics pipeline that provides the rasterizers with data. The process of transforming the 3D triangle meshes from world coordinates to camera coordinates, lighting vertices, clipping, and finally projecting and scaling to screen coordinates for the purposes of rasterization became a performance issue. The next generation of graphics cards arrived, called *hardware transform and lighting* (HW T&L) cards, the name referring to the fact that now the work of the graphics pipeline has been off-loaded from the CPU to the *graphics processing unit* (GPU). Although the intent of HW T&L cards was to support the standard graphics pipeline, most of these cards also supported some animation, namely *skin-and-bones* or *skinning* where the vertices of a triangle mesh (the skin) are associated with a matrix hierarchy (the bones), and a set of offsets and a set of weights relative to the bones. As the matrices vary during run time, the vertices are computed from the matrices, offsets, and weights, and the triangle mesh deforms in a natural way. Thus, we have some hardware support for *deformable bodies*.

The standard graphics pipeline is quite low-level when it comes to lighting of vertices. Dynamic lights in a scene and normal vectors at vertices of a triangle mesh are combined to produce vertex colors that are interpolated across the triangles by the rasterizer. Textured objects are rendered by assigning texture coordinates to the vertices of a mesh, the coordinates used as a lookup into a texture image. The rasterizer interpolates these coordinates during rasterization, then performs a lookup on a per-pixel basis for each triangle it rasterizes in the mesh. With a lot of creativity on the artists' end, the vertex coloring and texturing functions can be used to produce high

quality, realistic renderings. Fortunately, artists and programmers can create more interesting effects than a standard graphics pipeline can handle, producing yet more impetus for graphics cards to evolve. The latest generation of graphics cards now are programmable and support *vertex shading*, the ability to incorporate per-vertex information in your models and tell the rasterizer how to interpolate them. Clever use of vertex shading allows you to control more than color. For example, displacement mapping of vertices transfers some control of positional data to the rasterizer. And the cards support *pixel shading*, the ability to incorporate per-pixel information via images that no longer are required to represent texture data. Dot3 bumpmapping is the classic example of an effect obtained by a pixel shader function. You may view vertex shading as a generalization of the vertex coloring function and pixel shading as a generalization of the basic texturing function.

The power of current generation graphics cards to produce high quality visual effects is enormous. Much of the low-level programming you would do for software rendering is now absorbed in the graphics card drivers and the graphics APIs built on top of them, such as OpenGL and DirectX, allowing the programmers to concentrate at a higher level in a graphics engine. From a visual perspective, game designers and programmers have most of what they need to create realistic looking worlds for their gamer customers. But since you are reading this preface, you already know that visual realism is only half the battle. *Physical realism* is the other half. A well-crafted, good-looking character will attract your attention for the wrong reasons if it walks through a wall of a room. And if the characters cannot realistically interact with objects in their physical environment, the game will not be as interesting as it could be.

Some day we programmers will see significant hardware support for physics by off-loading work from the CPU to a *physics processing unit* (PPU). Until that day arrives we are, so to speak, at the level of software rendering. We need to implement everything ourselves, both low level and high level, and it must run on the CPU. Moreover we need real-time rates. Even if the renderer can display the environment at 60 frames per second, if the physics system cannot handle object interactions fast enough, the frame rate for the game will be abysmally low. We are required to understand how to model a physical environment and implement that model in a fast, accurate, and robust manner. Physics itself can be understood in an intuitive manner – after all it is an attempt to quantify the world around us. Implementing a physical simulation on a computer, though, requires more than intuition. It requires mathematical maturity as well as the ability and patience to synthesize a large system from a collection of sophisticated, smaller components. This book is designed to help you build such a large system, a *physics engine* as it were.

I believe this book is a good companion to my book *3D Game Engine Design*, a large tome that discusses the topic of constructing a real-time graphics engine for consumer hardware. *Game Physics* focuses on the topic of real-time physical simulation on consumer hardware. The two, of course, will be used simultaneously in a game application. *Game Physics* has a similar philosophy to *3D Game Engine Design* in two ways. First, both books were conceived while working on commercial engines and tools to be used for building games. The occurrence of the word “game” in the

titles reflects this. The material in both books applies to more than just game applications. For example, it is possible to build a virtual physics laboratory for students to explore physical concepts. Second, both books assume that the reader's background includes a sufficient level of mathematics. In fact, *Game Physics* requires a bit more background. To be comfortable with the material presented in this book, you will need some exposure to linear algebra, calculus, differential equations, and numerical methods for solving differential equations. All of these topics are covered in an undergraduate program in mathematics or computer science. Not to worry, though. As a refresher, the appendices contain a review of the essential concepts of linear algebra, affine algebra, calculus, and difference equations that you will need to read this book. Two detailed chapters are included that cover differential equations and numerical methods for solving them.

I did not call the book *3D Game Physics* because the material is just as appropriate for one- or two-dimensional settings. Many of the constrained physical models are of lower dimension. For example, a simple pendulum is constrained to move within a plane, even though a rendering of the physical system is in three dimensions. In fact, the material is applicable even to projects that are not game related, for example, supporting a virtual physics laboratory for students to explore physical concepts. I did call the book *Game Physics* and I expect that some readers might object to the title when in fact I do not cover all possible topics one might encounter in a game environment. Moreover, some topics I discuss are not in as much depth as some might like to see. Spending even a few years to write a book, I believe it is impossible to cover all the relevant topics in significant detail to support building a fully featured physics engine that rivals what you see commercially. Some projects just require a team of more than one. For example, I specifically avoided getting into fluid dynamics because that is an enormous topic all on its own. I chose to focus on the mechanics of rigid bodies and deformable bodies so that you can build a reasonable, working system for physical simulation. Despite this restricted coverage, I believe there is a significant amount of content in this book that will make it worth every minute of your reading time. This content includes both the written text *and* a vast amount of source code on the CD-ROM that accompanies the book, including both the Wild Magic graphics engine and components and applications for physics support. I have made every attempt at presenting all the content in a manner that will suit your needs.

As in the production of any book, the author is only part of the final result. The reviewers for an early draft of this book have been extremely helpful in providing guidance for the direction the book needed to take. The original scope of the book was quite large, but the reviewers' wisdom led me to reducing the scope to a manageable size by focusing on a few topics rather than providing a large amount of background material that would detract from the main purpose of the book – showing you the essentials of physical simulation on a computer. I wish to personally thank the reviewers for their contributions: Ian Ashdown (byHeart Consultants), Colin Barrett (Havok), Michael Doherty (University of the Pacific), Eric Dybsand (Glacier Edge Technology), David Eberle (Havok), Todd Gowney (Electronic Arts), Paul Hemler (Wake Forest University), Jeff Lander (Darwin 3D), Bruce Maxim (University of

Michigan–Dearborn), Doug McNabb (Rainbow Studios), Jon Purdy (University of Hull), and Craig Reinhart (California Lutheran University). Thanks also go to Tim Cox, my editor, Stacie Pierce, editorial coordinator, and Rick Camp, editorial assistant for the book. Tim has been patient with my seemingly endless delays in getting a final draft to him. Well, the bottom line is that the draft arrived. Now it is your turn to enjoy reading the book!

ABOUT THE CD-ROM

License Agreement

The accompanying CD-ROM contains source code that illustrates the ideas in the book. Each source file has a preamble stating that the source code is subject to the Boost License (http://www.boost.org/LICENSE_1_0.txt), which is quite simple:

Boost Software License – Version 1.0 – August 17th, 2003

Permission is hereby granted, free of charge, to any person or organization obtaining a copy of the software and accompanying documentation covered by this license (the “Software”) to use, reproduce, display, distribute, execute, and transmit the Software, and to prepare derivative works of the Software, and to permit third-parties to whom the Software is furnished to do so, all subject to the following:

The copyright notices in the Software and this entire statement, including the above license grant, this restriction and the following disclaimer, must be included in all copies of the Software, in whole or in part, and all derivative works of the Software, unless such copies or derivative works are solely in the form of machine-executable object code generated by a source language processor.

THE SOFTWARE IS PROVIDED “AS IS”, WITHOUT WARRANTY OF ANY KIND, EXPRESS OR IMPLIED, INCLUDING BUT NOT LIMITED TO THE WARRANTIES OF MERCHANTABILITY, FITNESS FOR A PARTICULAR PURPOSE, TITLE AND NON-INFRINGEMENT. IN NO EVENT SHALL THE COPYRIGHT HOLDERS OR ANYONE DISTRIBUTING THE SOFTWARE BE LIABLE FOR ANY DAMAGES OR OTHER LIABILITY, WHETHER IN CONTRACT, TORT OR OTHERWISE, ARISING FROM, OUT OF OR IN CONNECTION WITH THE SOFTWARE OR THE USE OR OTHER DEALINGS IN THE SOFTWARE.

Installing and Compiling the Source Code

The Wild Magic 5 engine is portable and runs on desktop computers running the Microsoft Windows XP/Vista/7 operating systems or Linux operating systems. Renderers are provided for both OpenGL (version 2.x) and Direct3D (version 9). The engine also runs on Apple computers, whether PowerPC- or Intel-powered, with the Macintosh OS X operating system (version 10.5.x or higher). Project files are provided for Microsoft Visual Studio (version 2009) on Microsoft Windows. Make files are provided for Linux. Xcode 3.x project files are provided for the Macintosh.

The CD-ROM includes a file, *Wm5p0InstallationRelease.pdf*, that contains the installation directions. You must read this first as it addresses various computing environment issues that you must be aware of, such as setting environment variables and project path settings.

Updates and Bug Fixes

Regularly visit the Geometric Tools, LLC web site, <http://www.geometrictools.com>, for updates and bug fixes. Histories of source code changes, book corrections, and known problems are maintained at the web site.

CHAPTER

INTRODUCTION

1.1 A BRIEF HISTORY OF THE WORLD

The first real experience I had with a “computing device” was in the early 1970s when I attended my first undergraduate college, Albright College in Reading, Pennsylvania, as a premedical student. The students with enough financial backing could afford handheld calculators. The rest of us had to use slide rules – and get enough significant digits using them in order to pass our examinations. I was quite impressed with the power of the slide rule. It definitely was faster than the previous generation of computing to which I was accustomed: pencil and paper. I did not survive the program at the college (my grades were low enough that I was asked to leave) and took a few years’ break to explore a more lucrative career.

“There is no reason anyone would want a computer in their home.”

Ken Olson, founder and president of Digital Equipment Corp

Deciding that managing a fast-food restaurant was not quite the career I thought it would be, I returned to the college track and attended Bloomsburg University (BU) in Bloomsburg, Pennsylvania as a mathematics major, a field that suited me more than chemistry and biology did. During my stay I was introduced to an even more powerful computing device, a mainframe computer. Writing Fortran programs by punching holes in Hollerith cards¹ was even better than having to use a slide rule,

1. Herman Hollerith used punched cards to represent the data gathered for the 1890 American census. The cards were then used to read and collate the data by machines. Hollerith’s company became International Business Machines (IBM) in 1924.

except for the occasional time or two when the high-speed card reader decided it was really hungry. By the end of my stay I had access to a monitor/terminal, yet another improvement in the computing environment. Linear programming problems were a lot easier to solve this way than with the slower modes of computing! I finished up at BU and decided graduate school was mandated.

"I think there is a world market for maybe five computers."

Thomas J. Watson, former chairman of IBM

Next stop, the University of Colorado at Boulder (CU) in 1979. I took a liking to differential equations and got another shot at punching cards, this time to numerically solve the differential equations of motion for a particular physical system. I understood the theory of differential equations and could properly analyze the phase space of the nonlinear equations to understand why I should expect the solution to have certain properties. However, I could not compute the solution that I expected – my first introduction to being careless about applying a numerical method without understanding its stability and how that relates to the physical system. The remainder of my stay at CU was focused on partial differential equations related to combustion with not much additional computer programming.

"Computers are useless. They can only give you answers."

Pablo Picasso, Spanish painter

After graduating in 1984, I started my academic career at the University of Texas at San Antonio (UTSA) in the Division of Mathematics, Computer Science, and Statistics. The university had recently started an engineering program and designed four courses for applied mathematics and computer science relevant to the new program. The two applied mathematics courses were your standard fare for an engineering program and included topics on differential equations, numerical methods, and physics concepts. The two computer science courses were somewhat unique in that both required students to work on the fast personal computers that were available at the time: 4.77 MHz Intel 8086 machines. The first course was introductory programming with Borland's Turbo Pascal 3. The second course was on computer graphics. Although Turbo Pascal supported graphics primitives, my requirements for the course included writing device drivers for the state-of-the-art graphics card: the Enhanced Graphics Adapter (EGA). With a blazingly fast CPU, Microsoft's Disk Operating System (DOS), 20M of hard disk space, 640K of accessible system memory, and an EGA card with four 64K memory chips (one chip per color plane), we were able to produce some fine quality output rivaling that of the 2D computer games of that era. The output was almost as good as what we could produce on the department's DEC Gigi that was attached to a VAX 730 and allowed you to draw to the monitor

by sending cryptic escape sequences of the type that you normally see in printer drivers.

"640K ought to be enough for anybody."

William ("Bill") H. Gates

During my tenure at UTSA, I became more involved in computer-related topics and less involved in theoretical considerations in my research field of differential equations. In particular I became involved with the University of Texas Health Science Center's Department of Radiology. The field of medical imaging was quite interesting to me with its inherent connection to computer graphics and visualization, but also of interest were aspects of geometry and numerical methods since we were interested in analyzing and extracting anatomical information from 3D medical images. My interest in the topic was strong enough that I decided to leave UTSA in 1991 and become a "retread" by studying computer science and medical imaging at the University of North Carolina (UNC) at Chapel Hill.

While at UNC I had access to more powerful equipment. We did not have a Cray supercomputer with a couple of powerful processors, but we did have a massively parallel machine appropriately named the MASPAC with 8,196 processors, individually not very powerful, but a natural architecture for 2D image processing.

"If you were plowing a field, which would you rather use?

Two strong oxen or 1024 chickens?"

Seymour Cray, father of supercomputing

Still, there was a strong attraction to compute numerically on a personal computer, to see the results graphically and immediately, if not sooner.

"The PC is the LSD of the 90's."

Timothy Leary, educator and psychologist

At the time I had upgraded my Intel 8086 machine to an Intel 80486 machine with a floating point coprocessor. I was able to implement many algorithms of interest in image analysis, including constructing something called *ridges* that are defined in terms of differential equations. The same programming issues that arose at CU bit me again: applying numerical methods for differential equation solvers without thought about the stability of the methods or about their applicability to the problem at hand. Another problem of interest was to compute *geodesic curves* on surfaces, curves that represent the shortest surface path between two points on the surface.

The formulation of the problem is akin to what you see in Lagrangian dynamics in physical modeling and results in yet more differential equations to solve numerically.²

After leaving UNC, I eventually found my way into the games industry in 1997 by signing on at Numerical Design Ltd. (www.ndl.com), a company cofounded by J. Turner Whitted, credited with the invention of ray tracing, and Robert Whitton, a mathematics professor at Davidson College. The company's business model had been focused on contract work in computer graphics, and they had developed a photorealistic ray tracing package called R-Plus. Times were changing, and they had decided that a product-oriented business model was better than a contract-based model. When I arrived the code base for NetImmerse was in its infancy. The goal of the product was a real-time graphics engine for 3D games. At the time, the Voodoo 1 graphics accelerator from the company 3Dfx (now defunct) had arrived on the scene. This was a true accelerator in the sense that it coexisted with a standard 2D graphics card. As you are already aware, this type of graphics technology started a whole new trend in the computer industry leading to significant evolution of central processing units (CPUs) and off-loading of a lot of work to graphics processing units (GPUs). The standard development machine at NDL in 1997 was a Pentium 133 MHz with 32M of system memory, not a lot of power compared to present-day machines but at the time quite a good system.

One of the first customers for NetImmerse was Broderbund, a software company that intended to use the package for their upcoming game *Prince of Persia 3D* (*POP3D*). The game engine needed a lot of help to evolve and keep up with the features that *POP3D* required. In particular, the collision detection system of NetImmerse was crude and needed improvement. The game engine was overhauled, including the addition of quaternions to support fast keyframe animations. The collision detection and response system was built from scratch, used hierarchical culling for collision purposes, and used an oriented bounding box tree-based hierarchy to support collision detection of the triangle mesh geometry [GLM96], but with an enhancement to predict the time of first contact of moving objects (see Section 6.4). The system also implemented 3D picking (intersection of line/ray/segment with objects), something heavily used in *POP3D* to allow the Prince to jump and catch ledges, and other related movements with constraints. The collision system was functional, but not what I would call sophisticated. CPUs were finally reaching speeds of 800 MHz by the time *POP3D* shipped in 1999, but they still did not have sufficient power for complex geometric environments. The collision system was also used successfully in an arcade game called *XS-G* (originally called *Canyon Runner*) that was shipped by Greystone Technology in 1998.

As CPUs and GPUs evolved because of consumer demands in the gaming arena, the graphics cards became powerful enough to give players a visually rich and

2. Specifically, a geodesic curve on a surface is the natural extension of a straight line in a plane – it has zero curvature. The physical analogy is that a particle traveling along a geodesic has zero acceleration while satisfying the constraint of remaining on the surface.

convincing environment for the games. But consumers are relentless and wanted more *physical realism*. Predicting a trend in this direction, the company MathEngine was started to build what was called a *physics engine*. The product was a good one, but some of the demonstrations showed *jittering* objects in resting contact with a flat surface. The problem is that applying numerical methods to the differential equations of motion is not enough. Stability of the methods is important, but also important is having a robust system that integrates collision detection and collision response involving multiple rigid bodies. Resting contact is now a classic problem that requires great care when implementing to avoid the jittering objects. While I was at NDL, Steven Collins, the CTO of a Dublin-based company called Telekinesys, Inc., contacted us to see what we thought about their physics engine and how it handled problems like resting contact. The demonstrations were very convincing and showed that, in fact, you can obtain physical realism with good frame rates even on current consumer CPUs. Eventually Telekinesys announced their new technology, and the company name changed to Havok.com. Their commercial physics engine is an extremely good product. Many of the robustness issues that show up in any product attempting to handle geometric queries on a computer with floating point arithmetic have been solved by the Havok folks. In fact, in January of 2003 I walked into my favorite store, Intrex Computers, to satisfy my latest silicon craving. On display was a computer with an ATI Radeon 9700 graphics card running a demonstration from Havok.com that showed a creature in exotic garb dancing about. The clothing was flowing in a very believable manner – no self-intersections of the cloth – and running at real-time rates. All I wanted was a hard drive, but I also walked out with a new graphics card *and* the desire to write my own physics engine. You know the feeling.

Other companies, of course, bought into the idea that you can do realistic physics in real time. AGEIA Technologies, Inc., produced PhysX, hardware support for real-time physics. They were acquired later by NVIDIA Corporation. Intel Corporation acquired Havok, Inc. Various open source packages are available for download – one of the most popular is the Bullet Physics Engine (www.bulletphysics.com). Other packages include the Open Dynamics Engine (ode.org), Newton Game Dynamics (www.newtondynamics.com), the Box2D Engine (www.gphysics.com), and the Tokamak Open Source Physics Engine (www.tokamakphysics.com) among others.

The games industry has gone through quite an evolutionary period over the past few decades. The computers of 10 years ago are nowhere near the powerful machines we have today. I started out with a 4.77 MHz Intel 8086 machine and a 2D EGA graphics card. Now I have machines with very fast CPUs and lots of system memory, and they all have 3D graphics hardware. These include a Macintosh system, a Linux system, and a few Microsoft Windows PCs (maintaining portable source code comes at a price). These systems are all capable of real-time graphics and real-time physics, whereas the systems of a decade ago just did not have that kind of power. In recent years, I have programmed on Microsoft's Xbox 360 and on Sony's Playstation 3. These are quite powerful machines, each with multiple processors, and both capable of handling complex physics. With current generation consoles and CPUs, you now get to enjoy the pleasure (and pain) of multiprocessor/multithreaded programming.

I have added some discussion about this regarding the broad-phase collision culling using axis-aligned bounding boxes and space-time coherency, including pseudocode for consoles as well as desktop computers.

“Grove giveth and Gates taketh away.”

Bob Metcalfe, Ethernet inventor and founder of 3Com Corporation, on the trend of hardware speedups not keeping up with software demands

Nevertheless, a major theme in this brief historical journey of mine is, *The mathematics and physics that you will deal with in this book is not new*. Much of the computer graphics research that appears in the literature of the past decade is motivated by the power that machines have now (or soon will have).

“A mathematician is a device for turning coffee into theorems.”

Paul Erdos, mathematician. My variant: “A computer graphics researcher is a device for turning coffee into SIGGRAPH papers.”

Much of what occurs in that research is a reapplication of classic mathematical and physical concepts and shows that the researchers appreciate the importance and power of mathematics and physics in achieving their goals.

“For the things of this world cannot be made known without a knowledge of mathematics.”

Roger Bacon, philosopher from the 12th century

Thus, you too should appreciate the power of all things mathematical and physical.

“It is the merest truism, evident at once to unsophisticated observation, that mathematics is a human invention.”

from. The Logic of Modern Physics, by P. W. Bridgman, physicist

As readers of my books certainly know, I have not shied away from mathematics, because it is my language for understanding the technical world around me.

“Omnia apud me mathematica fiunt”
(With me everything turns into mathematics).

Rene Descartes

“A mathematician, like a painter or a poet, is a maker of patterns. If his patterns are more permanent than theirs, it is because they are made with ideas.”

G. H. Hardy, mathematician

I wish it to be your language, too. After all, you will need it to appreciate fully the complexities and difficulties in implementing a robust physical simulation on a computer. What else can I say!

1.2 A SUMMARY OF THE TOPICS

Physics concepts and their application to games is quite a large topic. Rather than attempt to provide brief summaries of all possible topics, in other words a survey book, I decided to focus on the subset that most programmers seem to ask questions about in the various Usenet news groups: mechanics, rigid bodies, deformable bodies, and collision detection and response systems. These topics are discussed in depth and require a minimum mathematical background that includes linear algebra and calculus, both univariate and multivariate. Also helpful would be some exposure to ordinary differential equations and to numerical methods that solve these, but if you have not had this exposure, a couple of chapters provide enough material to support what you will need for implementing a physical simulation.

[Chapter 2](#) introduces curves in two dimensions and in three dimensions as representative paths of a particle. The chapter introduces the physical concepts of position, velocity, and acceleration. The choice of coordinate system is important in an application, so the standard systems are covered, including polar coordinates, cylindrical coordinates, and spherical coordinates. The motion of particles along paths in the absence of forces is called kinematics. In addition to kinematics of a single particle, we also look into the kinematics of a particle system. This material is the all important foundation for the physics engines discussed in [Chapter 6](#).

The remainder of [Chapter 2](#) is an introduction to the standard concepts that you see in a course on physics, starting with Newton’s laws of motion. The topics of force, torque, equilibrium, linear and angular momentum, center of mass, moments and products of inertia, and kinetic and potential energy are discussed in detail, with the goal of being able to calculate these quantities on a computer. Computing the center of mass and the inertia tensor for a solid convex polyhedron is necessary for the physics engines of [Chapter 6](#).

[Chapter 3](#) is about dynamics: the interaction of rigid bodies when forces and torques are present in the physical system. The classical approach in an introductory physics course uses Newtonian dynamics and the famous formula of Newton’s second law of motion, $F = ma$, where m is the constant mass of an object, a is its acceleration, and F is the applied force. I do not spend a lot of time delving into this

approach. The coverage is sufficient to support the general purpose physics engines that use Newton's second law for simulation.

The majority of [Chapter 3](#) is spent on Lagrangian dynamics, a framework for setting up the equations of motion for objects when constraints are present. In Lagrangian dynamics, the equations of motion naturally incorporate the constraints. A Newtonian formulation requires that forces of constraint be part of the term \mathbf{F} in the equation of motion, and the constraint forces are sometimes difficult to derive. For example, you will see in the Lagrangian approach that frictional forces are easier to deal with than in the Newtonian approach. For many games, a designer's specific knowledge of the physical system can be exploited to good effect by formulating the simulation using Lagrangian dynamics, the result being that the computational time of the simulation is reduced, compared to a general purpose system using Newtonian dynamics.

Euler's equations of motion are also discussed in [Chapter 3](#), because a few problems are more naturally formulated in terms of Euler angles than in terms of other dynamics systems. Although Hamiltonian dynamics is of importance, especially in dealing with the n -body problem, I made the decision not to include a discussion of it in this book, since the other approaches are sufficient to allow implementations on a computer.

[Chapter 4](#) is about deformable bodies. There are many ways to simulate deformation; we will address a subset in this book. In all cases you should consider these "hacked" physics in the sense that at no time do we use a real physical model for the actual material that makes up the bodies. The real models do not lend themselves to the fast computation that a game requires. All that is required of a hacked physics approach in a game is that the deformations look believable to the player. I do cover mass-spring systems for the purposes of deformation, but even these might not be as realistic a model for deformable objects as you might wish.

Another method that I have included for describing deformable objects includes the use of control point surfaces, where you vary the control points in some suitable manner to cause the surface to deform as you desire. A brief discussion is given for B-spline curves and surfaces and for nonrational uniform B-spline (NURBS) curves and surfaces. The presentation is limited to the computational aspects of curves and surfaces, including optimizations that allow fast evaluation. You are referred to other sources for a more detailed look at the properties of B-splines and NURBS.

Free-form deformation is a method for deforming an object and uses a volumetric approach. The object is embedded in a portion of space that is defined via a control-point lattice. The volume of space is deformed, causing the object itself to deform.

The final deformation method is based on the object's surface being defined implicitly. The popular term for such surfaces is metaballs. I prefer to call them what they are, implicit surfaces. The discussion of this topic shows how you define a 3D lattice of sample points, trilinearly interpolate to obtain a continuous representation of a function defined on the volume occupied by the lattice, then extract the implicit surface as the level surface of the constructed function. Implicit surfaces are deformed by varying the constructed function itself.

[Chapter 5](#) is a new chapter on fluid dynamics. The primary focus is on using conservation laws to derive partial differential equations for the density of the fluid (conservation of mass) and for the velocity of the fluid (conservation of momentum, the Navier–Stokes equation). Stability of the numerical methods for solving these equations is of importance. More important, though, is that the numerical methods are quite expensive. Current generation CPUs have the power to solve the 2D equations in real time for a moderate-sized grid, but the 3D equations require a lot of cycles even for small grids. Sample applications that solve the equations on the CPU are provided. Better yet, a sample application is provided for the 2D implementation on the GPU – this certainly runs at real-time rates for moderate-to-large-sized grids. The framework is provided for the 3D implementation, illustrated by a 3D Gaussian blurring application, but the framework easily allows you to solve the 3D fluid equations on the GPU (a suitable class project).

[Chapter 6](#) is about what most readers probably think of as the meat of game physics – the physics engine. The chapter describes a general system for handling a collection of rigid bodies, including collision detection and collision response. A general system is one that uses Newton’s second law of motion, $F = ma$, to control the motion of objects. The constraint forces are unknown to the system and must be calculated based on the information that is provided by the collision detection system.

[Section 6.1](#) discusses the game loop and the *physics tick* as one of the subsystems managed by the loop. In computer graphics, it is said that the fastest way to draw something is not to draw it at all. Practitioners use various culling algorithms to determine objects that are not in the view frustum – such objects are not sent to the renderer for drawing. This process is part of the graphics tick. The physics tick has a similar philosophy. If it is possible to quickly determine that two objects are not close enough to be in contact, then that pair of objects need not be processed by the collision response system. [Section 6.2](#) discusses *broad-phase collision culling* using axis-aligned bounding boxes and takes advantage of space–time coherency for speed. Detailed pseudocode is provided that allows you to implement this in a single-threaded application on a CPU, in a multicore/multithreaded application for the CPU (good for desktop PCs or Xbox 360), and in an application using specialized processors (good for Playstation 3). Test-intersection queries for *medium-phase collision culling* are discussed briefly in [Section 6.3](#) for bounding volumes that are spheres, ellipsoids, or cylinders. However, more popular and useful are those queries for oriented bounding boxes and convex polyhedra, the topic of [Section 6.4](#). This section covers the *method of separating axes*, for overlap tests of a pair of convex polyhedra, and the *GJK algorithm*, for computing the distance between convex polyhedra. Good books with a lot more details about collision detection are [[Eri03](#)], which has a lot of hands-on information, and [[vdB03](#)], which has a lot of details about the GJK algorithm and how it may be used robustly in a physics engine.

[Section 6.5](#) is about unconstrained motion. This gives you an idea of how to design a data structure to represent a rigid body and how to solve the differential equations of motion for a body that does not interact with other bodies in its environment. [Sections 6.6](#) and [6.7](#) complicate matters by allowing interaction between bodies,

referred to as constrained motion. As you will see, building a collision detection and response system for constrained motion is a formidable task! I have provided enough pseudocode to allow you to build a working engine if you choose to do so. Source code is provided for a working engine with which you can experiment. A lot of code was written by George Innis of Magic Software, Inc., after reading a draft of this book – hopefully evidence that other folks will be able to implement real systems from my descriptions.

I discuss the impulse-based approach that [Brian Mirtich \[Mir96b\]](#) and [David Baraff \[Bar01\]](#) made popular, but by all means this is not the only approach one can take. My goal is to go into significant detail about the impulse-based approach so that you (1) understand the layout of a general physics engine, (2) see what complications arise, and (3) learn to evaluate what are its strengths and weaknesses. Other approaches to building a robust physics engine are based on trying to fix the weaknesses of the previous generation engine. Once you understand the impulse-based engine, you should be able to start experimenting with modifications; references to other approaches are provided, so you have a nearly endless supply of ideas to investigate. For instance, a good tutorial site for rigid body dynamics is [\[Hec98\]](#). I refer to the impulse-based approach as *acceleration-based constrained motion*. A new section provides a discussion of *velocity-based constrained motion*. Researchers are still investigating the various approaches and trying to make improvements in speed and robustness. Some papers on *position-based constrained motion*, [\[MHR06\]](#) and [\[Mü108\]](#), are of importance. You can spend a lot of time tracking down what is the latest and greatest.

[Chapters 7 through 9](#) provide mathematical background. The chapters on linear algebra, affine algebra, and calculus are intended as brief reviews of the material you would see in undergraduate college courses.

[Chapter 10](#) is on quaternions, one of the most misunderstood and abused topics in the Usenet newsgroups (in my opinion). Yes, these are mathematical in flavor, but in fact a physical simulation benefits from using these because of the resulting reduced memory in representing rotations and in the reduced computation time in actually rotating or updating the equations of motion for a physical system. The molecular dynamics folks have been using these for a really long time, so you can find a lot of online material discussing quaternions in the context of that field, including higher-order methods for numerically solving the quaternion differential equation that shows up in the physical simulation. I provide the classical approach to how quaternions relate to rotations and I provide a linear algebraic approach to try to motivate the connection by considering rotation in four dimensions. The final sections involve interpolation of quaternions and derivatives of time-varying quaternions, the latter section being related to how you derive the equation of motion for updating orientations of rigid bodies when quaternions are used to represent the orientations.

[Chapter 11](#) is a brief overview of the theory of differential equations. This material is provided for those readers who want to understand the basic theory of differential

equations relevant to physical simulation. The overview is at the level of what you will find in an undergraduate textbook on the topic; it is intentionally limited in scope but should give you enough of the flavor of what analysis of differential equations is all about. Numerical methods for solving differential equations (ordinary or partial) involve finite-difference algorithms. Chapter 12 on ordinary difference equations shows some general concepts for solving such equations. This material is usually not presented together with a course on differential equations or on numerical methods.

Chapter 13 is on numerical methods for solving differential equations. This is a large chapter that shows you a vast collection of methods, including how the methods are derived using basic mathematical principles. The methods include Euler's method, higher-order Taylor methods, methods obtained by an integral formulation, and the all-popular and robust Runge–Kutta methods. These are all *single-step methods* that require information only at the previous time step to generate information at the current time step. I also discuss *multistep methods* that use multiple previous times to generate information at the current step. These methods include the concept of a predictor–corrector that attempts to provide good estimates of the solution from ones that are less precise. Extrapolation methods are also covered, leading to the Bulirsch–Stoer method that uses rational polynomial extrapolation to produce highly accurate results with a minimum of computation cost. A class of methods that is very popular now in the games arena, and has been used for a long time in molecular dynamics, is the *Verlet methods*. A section of the chapter is devoted to these methods, including the standard Verlet method, the Leap Frog method, and the Velocity Verlet method. I also included a reasonable alternative called the Gear fifth-order predictor–corrector method. Thus, you have a large collection of solvers, all of them implemented in the source code on the CD-ROM that accompanies the book.

Implementing a numerical method is only half the battle. Understanding the stability of a method, how to choose an appropriate step size, and how to evaluate the trade-offs between accuracy and computation time is the other half of the battle. Perhaps the most important part of Chapter 13 is the section on numerical stability and its relationship to physical stability of equilibrium solutions. You might think of this as an irrelevant mathematical exercise, but in fact I provide a stability analysis for a handful of methods when applied to the simple pendulum problem. This gives you the blueprint to follow when analyzing the stability of methods for your particular applications. The last section of the chapter discusses the problem of *stiffness*, another issue related to the stability of numerical solvers.

Finally, Chapter 14 is on the topics of linear programming (LP), the linear complementarity problem (LCP), and mathematical programming (MP) generally. One application of the material is to use LCP methods to compute the distance between points, convex polygons, and convex polyhedra. Another application is to use LCP methods to compute resting contact forces and to use MP methods, namely constrained quadratic minimization, to compute impulsive contact forces at the points of contact among a collection of interacting rigid bodies.

1.3 EXAMPLES AND EXERCISES

Quite a few examples and exercises are provided in this book. The examples are worked through in detail, of course, with some of them implemented in source code, which is on the CD-ROM. The exercises are for you to try. They vary in difficulty. In the first edition of the book, I marked the exercises as easy, medium, or hard. Apparently my marking algorithm is no different from a random number generator, so in the second edition I have removed the classifications. The answers to the exercises are on the CD-ROM. I recommend that you make a significant attempt to answer the questions before looking up the answers.



CHAPTER

2

BASIC CONCEPTS FROM PHYSICS

In this chapter we review some of the basic concepts of physics that are relevant to the analysis of motion and interaction of *rigid bodies*. A rigid body is classified according to the type of region that contains its mass, the topic of [Section 2.1](#). [Section 2.2](#) introduces curves in two or three dimensions as representative paths of a particle in the absence of forces. This topic is referred to as *kinematics*. The section introduces the physical concepts of position, velocity, and acceleration. Many applications are better handled with an appropriate choice of coordinate system. The Cartesian system is usually convenient, but we also take a look at polar coordinates, cylindrical coordinates, and spherical coordinates. In addition to kinematics of a single particle, we also look into the kinematics of particle systems and of solid bodies. This material is the foundation for the physics engines discussed in [Chapter 6](#).

The remainder of this chapter is an introduction to the standard concepts that you see in a course on physics, starting with Newton's Laws of Motion in [Section 2.3](#). The topic of forces is discussed in [Section 2.4](#) with specific reference to forces you will see throughout the book in the examples: gravitational forces, spring forces, and frictional forces. The closely related topics of torque and equilibrium are also covered in the section. Various measures of momenta are discussed in [Section 2.5](#), including linear and angular momenta, first-order moments and their relationship to the center of mass of an object, and moments and products of inertia. The last part of [Section 2.5](#) shows how to compute the center of mass and the inertia tensor for a solid polyhedron of constant mass, something you will need to implement in the physics engines discussed in [Chapter 6](#). Work and energy are the final topic of the chapter. The kinetic

energy is an important quantity in the development of Lagrangian dynamics. The potential energy is important when dealing with conservative forces such as gravity.

2.1 RIGID BODY CLASSIFICATION

A rigid body is characterized by the region that its mass lives in. The simplest body is a *single particle* of mass m that occupies a single location \mathbf{x} . A *particle system* is a collection of a finite number of particles, say p of them, the i th particle having mass m_i and located at \mathbf{x}_i , $1 \leq i \leq p$. Single particles and particle systems are examples of *discrete material* since the number of particles is finite. Various physical quantities involve summations over the particles in a system. The standard notation is

$$Q_{\text{total}} = \sum_{i=1}^p Q_i$$

where Q_i is some physical quantity associated with the i th particle, and Q_{total} is the summary quantity for all the particles. Although the equation here involves a scalar-valued physical quantity, vector-valued quantities will be encountered as well.

Another type of body is referred to as a *continuous material*, consisting of infinitely many particles that lie in a bounded region of space, denoted R . We refer to such a rigid body as a *continuum of mass*. Within the category of a continuum of mass we have a further set of classifications. The region R can be a bounded segment of a curve, whether in one, two, or three dimensions. Mathematically we may refer to such a rigid body as a *curve mass*. Physically we may call the body a *wire*. R can be a bounded region in the plane (two-dimensional mass living in two dimensions) or a bounded portion of a surface in space (two-dimensional mass living in three dimensions). Mathematically we may refer to such a rigid body as a *surface mass*. Physically we may call the body a *lamina* or, in two dimensions, a *planar lamina*. Finally, R can be a solid occupying a bounded region of space. Mathematically we may refer to such a body as a *volume mass*. Physically we may call the body a *solid*.

Various physical quantities involve summations over all particles of mass in the region. The summation notation for particle systems no longer applies and is replaced by integration over the region. The method of integration depends on the category of region. Generically we will use the notation

$$Q_{\text{total}} = \int_R Q \, dR$$

where R is the region, dR is an infinitesimal portion of the region, and Q is the physical quantity of interest and can be scalar- or vector-valued. An analysis for a particular type of rigid body, whether for mathematical purposes or for a computer implementation, must provide the specific type of integration in order to compute the integral. For a curve mass, the integration is computed as a line integral, where the curve is

parameterized by a single parameter and the limits of integration depend on that parameterization. For a surface mass in the plane, the integration is computed as a double integral, where the limits of integration depend on how the region is represented. For a surface mass in space, the integration is via a surface integral whose evaluation may very well involve Stokes' theorem. For a volume mass, the integration is computed as a triple integral, where the limits of integration depend on how the region is represented. Throughout the book I will use the generic notation $\int_R Q \, dR$ when presenting general physical topics. I will resort to the specific type of integration when demonstrating the concepts with examples.

2.2 RIGID BODY KINEMATICS

The study of motion of objects without considering the influence of external forces is referred to as *kinematics*. The basics of the topic are presented in this section. We look at the three basic types of rigid bodies: a single particle, a particle system, and a continuum of mass. For the purposes of rigid body kinematics, the analyses for particle systems and continuous materials are the same.

2.2.1 SINGLE PARTICLE

Let us focus first on the kinematics of a single particle. Although we might start directly with the analysis of a particle moving through space, many situations arise where the particle is constrained to moving within a plane. We start our analysis with particle motion in the xy -plane, ignoring the z -component of the position. If the constraining plane is another one at some arbitrary orientation in space, basic methods of linear algebra may be applied to represent the particle's position with respect to an orthonormal basis of two vectors in that plane. The ideas we present here for the xy -plane apply directly to the coordinates within the general plane.

Whether in two or three dimensions we may choose Cartesian coordinates to represent the particle's position. However, some problems are better formulated in different coordinate systems. Particle motion is first discussed in Cartesian coordinates, but we also look at polar coordinates for 2D motion and at cylindrical or spherical coordinates for 3D motion, because these coordinate systems are the most common ones you will see in applications.

Planar Motion in Cartesian Coordinates

First let us consider when the particle motion is constrained to be planar. In Cartesian coordinates, the *position* of the particle at time t is

$$\mathbf{r}(t) = x(t) \mathbf{i} + y(t) \mathbf{J} \quad (2.1)$$

where $\boldsymbol{\iota} = (1, 0)$ and $\boldsymbol{J} = (0, 1)$. The *velocity* of the particle at time t is

$$\mathbf{v}(t) = \dot{\mathbf{r}} = \dot{x}\boldsymbol{\iota} + \dot{y}\boldsymbol{J} \quad (2.2)$$

The dot symbol denotes differentiation with respect to t . The *speed* of the particle at time t is the length of the velocity vector, $|\mathbf{v}|$. If $s(t)$ denotes the arc length measured along the curve, the speed is $\dot{s} = |\mathbf{v}|$. The quantity $\dot{s} = ds/dt$ is intuitively read as “change in distance per change in time,” what you expect for speed. The *acceleration* of the particle at time t is

$$\mathbf{a}(t) = \dot{\mathbf{v}} = \ddot{\mathbf{r}} = \ddot{x}\boldsymbol{\iota} + \ddot{y}\boldsymbol{J} \quad (2.3)$$

At each point on the curve of motion we can define a unit-length tangent vector by normalizing the velocity vector,

$$\mathbf{T}(t) = \frac{\mathbf{v}}{|\mathbf{v}|} = (\cos(\phi(t)), \sin(\phi(t))) \quad (2.4)$$

The right-hand side of equation (2.4) defines $\phi(t)$ and is valid since the tangent vector is unit length. A unit-length normal vector is chosen as

$$\mathbf{N}(t) = (-\sin(\phi(t)), \cos(\phi(t))) \quad (2.5)$$

The normal vector is obtained by rotating the tangent vector $\pi/2$ radians counter-clockwise in the plane. A *coordinate system* at a point on the curve is defined by *origin* $\mathbf{r}(t)$ and *coordinate axis directions* $\mathbf{T}(t)$ and $\mathbf{N}(t)$. Figure 2.1 illustrates the coordinate systems at a couple of points on a curve. The coordinate system $\{\mathbf{r}(t); \mathbf{T}(t), \mathbf{N}(t)\}$ is called a *moving frame*.

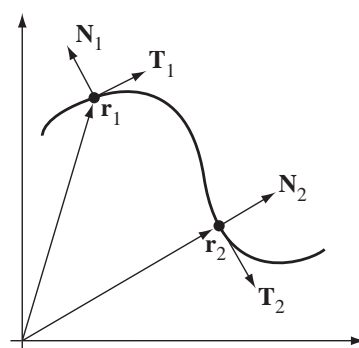


Figure 2.1 A couple of coordinate systems at points on a curve.

The velocity and acceleration vectors may be represented in terms of the curve tangent and normal. The velocity is a minor rearrangement of [equation \(2.4\)](#),

$$\mathbf{v} = |\mathbf{v}| \mathbf{T} = \dot{s} \mathbf{T} \quad (2.6)$$

The acceleration is obtained by differentiating the last equation,

$$\mathbf{a} = \dot{\mathbf{v}} = \frac{d}{dt} (\dot{s} \mathbf{T}) = \ddot{s} \mathbf{T} + \dot{s} \frac{d\mathbf{T}}{dt} = \ddot{s} \mathbf{T} + \dot{s}^2 \frac{d\mathbf{T}}{ds}$$

Differentiating the tangent vector in [equation \(2.4\)](#) with respect to arc length s produces

$$\frac{d\mathbf{T}}{ds} = \frac{d}{ds} (\cos \phi, \sin \phi) = \frac{d\phi}{ds} (-\sin \phi, \cos \phi) = \kappa \mathbf{N}(s)$$

where $\kappa = d\phi/ds$ is the *curvature* of the curve at arc length s . Observe that large angular changes in the normal vector over a small length of curve equate to large curvature values. The acceleration is therefore

$$\mathbf{a} = \ddot{s} \mathbf{T} + \kappa \dot{s}^2 \mathbf{N} \quad (2.7)$$

The component $\ddot{s}\mathbf{T}$ is called the *tangential acceleration*, the acceleration in the direction of motion. The component $\kappa \dot{s}^2 \mathbf{N}$ is called the *normal acceleration* or *centripetal acceleration*, the acceleration that is perpendicular to the direction of motion. [Equations \(2.6\)](#) and [\(2.7\)](#) may be used to show that the curvature is

$$\kappa = \frac{\mathbf{v} \cdot \mathbf{a}^\perp}{|\mathbf{v}|^3} = \frac{\dot{x}\ddot{y} - \dot{y}\ddot{x}}{(\dot{x}^2 + \dot{y}^2)^{3/2}} \quad (2.8)$$

where $\mathbf{a}^\perp = (\alpha, \beta)^\perp = (\beta, -\alpha)$.

The rate of change of the tangent vector with respect to arc length is related to the normal vector. You might be curious about the rate of change of the normal vector with respect to arc length. It is

$$\frac{d\mathbf{N}}{ds} = \frac{d}{ds} (-\sin \phi, \cos \phi) = \frac{d\phi}{ds} (-\cos \phi, -\sin \phi) = -\kappa \mathbf{T}$$

Summarizing the s -derivatives in a formal matrix notation:

$$\begin{bmatrix} \frac{d\mathbf{T}}{ds} \\ \frac{d\mathbf{N}}{ds} \end{bmatrix} = \begin{bmatrix} 0 & \kappa \\ -\kappa & 0 \end{bmatrix} \begin{bmatrix} \mathbf{T} \\ \mathbf{N} \end{bmatrix} \quad (2.9)$$

Observe that the coefficient matrix is skew-symmetric, a common theme when computing the derivatives of the vectors in a frame.

EXAMPLE

2.1

Construct the various vectors and quantities mentioned earlier for a parabolic curve $\mathbf{r}(t) = t\mathbf{i} + t^2\mathbf{j}$. For simplicity of notation, we use $\mathbf{r} = (t, t^2)$. The velocity is $\mathbf{v} = (1, 2t)$, and the speed is just the length of the velocity vector, $\dot{s} = \sqrt{1 + 4t^2}$.

(Example 2.1
continued)

The magnitude of tangential acceleration is $\ddot{s} = 4t/\sqrt{1+4t^2}$. The acceleration is $\mathbf{a} = (0, 2)$. The unit-length tangent and normal vectors are

$$\mathbf{T} = \frac{(1, 2t)}{\sqrt{1+4t^2}}, \quad \mathbf{N} = \frac{(-2t, 1)}{\sqrt{1+4t^2}}$$

Finally, the curvature is $\kappa = 2/(1+4t^2)^{3/2}$. ■

Planar Motion in Polar Coordinates

The particle motion may also be represented using polar coordinates. The choice of Cartesian form versus polar form depends on your application. The position vector is represented as a unit-length vector $\mathbf{R} = \mathbf{r}/|\mathbf{r}|$ and a distance $r = |\mathbf{r}|$ from the origin,

$$\mathbf{r} = |\mathbf{r}| \frac{\mathbf{r}}{|\mathbf{r}|} = r\mathbf{R} \quad (2.10)$$

Since $\mathbf{R} = \mathbf{r}/|\mathbf{r}|$ is unit length, we may write it as $\mathbf{R} = (\cos \theta, \sin \theta)$, where θ depends on t . A unit-length vector perpendicular to \mathbf{R} is $\mathbf{P} = (-\sin \theta, \cos \theta)$ and is obtained by a $\pi/2$ counterclockwise rotation of \mathbf{R} in the plane. The moving frame $\{\mathbf{r}(t); \mathbf{R}(t), \mathbf{P}(t)\}$ provides an alternate coordinate system to the tangent-normal one. Figure 2.2 shows the polar frames at points on a curve, the same curve shown in Figure 2.1.

The derivatives of the frame directions with respect to time are summarized in formal matrix notation:

$$\begin{bmatrix} \dot{\mathbf{R}} \\ \dot{\mathbf{P}} \end{bmatrix} = \begin{bmatrix} 0 & \dot{\theta} \\ -\dot{\theta} & 0 \end{bmatrix} \begin{bmatrix} \mathbf{R} \\ \mathbf{P} \end{bmatrix} \quad (2.11)$$

Notice the similarity to equation (2.9).

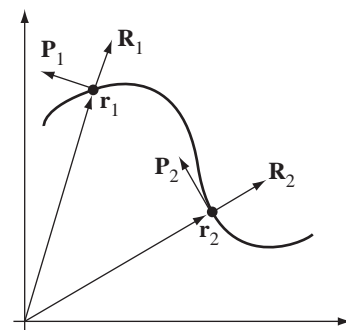


Figure 2.2 A polar coordinate frame at a point on a curve.

The velocity is represented in the polar frame by

$$\mathbf{v} = \dot{\mathbf{r}} = \frac{d}{dt}(r\mathbf{R}) = \dot{r}\mathbf{R} + r\dot{\mathbf{R}} = \dot{r}\mathbf{R} + r\dot{\theta}\mathbf{P} \quad (2.12)$$

The acceleration is represented in the polar frame by

$$\mathbf{a} = \ddot{\mathbf{v}} = \ddot{r}\mathbf{R} + \dot{r}\dot{\mathbf{R}} + \frac{d}{dt}(r\dot{\theta})\mathbf{P} + r\dot{\theta}\dot{\mathbf{P}} = (\ddot{r} - r\dot{\theta}^2)\mathbf{R} + (r\ddot{\theta} + 2\dot{r}\dot{\theta})\mathbf{P} \quad (2.13)$$

EXAMPLE
2.2

Construct the various quantities for a spiral $r = \theta$, where θ is a function of time t . The position is $\mathbf{r} = \theta\mathbf{R} = (\theta \cos \theta, \theta \sin \theta)$, the velocity is $\mathbf{v} = \dot{\theta}\mathbf{R} + \theta\dot{\theta}\mathbf{P} = \dot{\theta}(\cos \theta - \theta \sin \theta, \sin \theta + \theta \cos \theta)$, and the acceleration is $\mathbf{a} = (\ddot{\theta} - \theta\dot{\theta}^2)\mathbf{R} + (\theta\ddot{\theta} + 2\dot{\theta}\dot{\theta})\mathbf{P} = \ddot{\theta}(\cos \theta - \theta \sin \theta, \sin \theta + \theta \cos \theta) + \dot{\theta}^2(-\theta \cos \theta - 2 \sin \theta, -\theta \sin \theta + 2 \cos \theta)$. ■

Spatial Motion in Cartesian Coordinates

We now consider the spatial case. In Cartesian coordinates the position of a particle at time t is

$$\mathbf{r}(t) = x(t)\mathbf{i} + y(t)\mathbf{j} + z(t)\mathbf{k} \quad (2.14)$$

where $\mathbf{i} = (1, 0, 0)$, $\mathbf{j} = (0, 1, 0)$, and $\mathbf{k} = (0, 0, 1)$. The *velocity* of the particle at time t is

$$\mathbf{v}(t) = \dot{\mathbf{r}} = \dot{x}\mathbf{i} + \dot{y}\mathbf{j} + \dot{z}\mathbf{k} \quad (2.15)$$

The *speed* of the particle at time t is the length of the velocity vector, $|\mathbf{v}|$. If $s(t)$ denotes the arc length measured along the curve, the speed is $\dot{s} = |\mathbf{v}|$. The *acceleration* of the particle at time t is

$$\mathbf{a}(t) = \dot{\mathbf{v}} = \ddot{\mathbf{r}} = \ddot{x}\mathbf{i} + \ddot{y}\mathbf{j} + \ddot{z}\mathbf{k} \quad (2.16)$$

At each point on the curve of motion we can define a unit-length tangent vector by normalizing the velocity vector:

$$\mathbf{T}(t) = \frac{\mathbf{v}}{|\mathbf{v}|} \quad (2.17)$$

In 2D we had only two choices for unit-length vectors that are perpendicular to the curve. We chose the one that is always a counterclockwise rotation from the tangent vector. As long as the tangent vector is a continuous function of t (the angle $\phi(t)$ is a continuous function), the normal vector is also a continuous function. In 3D there are infinitely many choices for a unit-length vector perpendicular to the tangent vector, an entire circle of them in the plane that is perpendicular to \mathbf{T} and centered at the point on the curve. Figure 2.3 shows a curve, a tangent at a point, and the circle of choices for the normal.

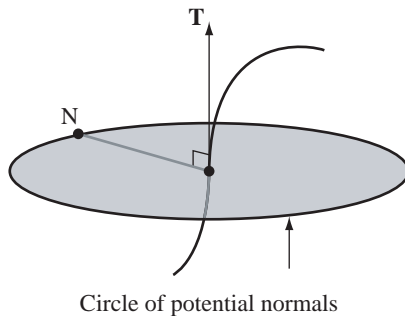


Figure 2.3 A curve, a tangent vector at a point, and the circle of choices for the normal vector. The circle lies in the plane containing the point and perpendicular to the tangent.

Which one do we choose for a normal vector \mathbf{N} ? Keeping consistent with the 2D setting, $\mathbf{T} \cdot \mathbf{T} = 1$ because \mathbf{T} is a unit length vector. Differentiating with respect to the arc length parameter s yields $\mathbf{T} \cdot d\mathbf{T}/ds = 0$, and as a result the vector $d\mathbf{T}/ds$ is perpendicular to the tangent. We use this vector to define both the normal vector and the curvature κ as a function of the arc length s ,

$$\frac{d\mathbf{T}}{ds} = \kappa(s)\mathbf{N}(s) \quad (2.18)$$

The velocity satisfies equation (2.6) and the acceleration satisfies equation (2.7), the vector quantities living in three dimensions in both cases.

The normal is a unit-length vector in the direction of $d\mathbf{T}/ds$, but notice that there are two choices for such a vector. Think of the second choice as the negative of the first, $-\mathbf{N}(s)$. The curvature function that must be associated with the second choice is the negative of the first, $-\kappa(s)$, so that the product of curvature and normal still produces $d\mathbf{T}/ds$. If the curve were planar, we could resort to the two-dimensional construction and select a normal that is a counterclockwise rotation from the tangent within that plane. This reasoning does not apply to a nonplanar curve. The choice of normal should be made in an attempt to maintain a continuous function $\mathbf{N}(s)$. Exercise 2.1 is designed to show that it is not always possible to do this. Once a choice is made for the normal vector, the curvature is $\kappa = \mathbf{N} \cdot d\mathbf{T}/ds$. The sign of the curvature depends on which of the two possible \mathbf{N} was chosen.

EXERCISE 2.1

Consider a curve defined in two pieces. The first piece is $\mathbf{r}(t) = (t, t^3, 0)$ for $t \leq 0$ and the second piece is $\mathbf{r}(t) = (t, 0, t^3)$ for $t \geq 0$. Prove that \mathbf{r} , \mathbf{v} , and \mathbf{a} are continuous at $t = 0$ by showing $\lim_{t \rightarrow 0^-} \mathbf{r}(t) = \mathbf{r}(0)$, $\lim_{t \rightarrow 0} \mathbf{v}(t) = \mathbf{v}(0)$, and $\lim_{t \rightarrow 0} \mathbf{a}(t) = \mathbf{a}(0)$. Construct the normal vectors for each piece as a function of t ; call this $\mathbf{N}(t)$. Prove that $\lim_{t \rightarrow 0^-} \mathbf{N}(t) = (0, 1, 0)$ and $\lim_{t \rightarrow 0^+} \mathbf{N}(t) = (0, 0, 1)$. Since the one-sided limits

have different values, $\mathbf{N}(t)$ is not continuous at $t = 0$. Changing the sign of the normal on one piece of the curve cannot change the conclusion. ■

The acceleration vector in 3D satisfies the relationship shown in equation (2.7). The curvature, however, is

$$\kappa = \sigma \frac{|\mathbf{v} \times \mathbf{a}|}{|\mathbf{v}|^3} \quad (2.19)$$

where σ is a sign parameter that is 1 or -1 and chosen, if possible, to make the normal vector continuous. A formula for the normal vector may be derived that contains the sign parameter,

$$\mathbf{N} = \frac{\sigma(\mathbf{v} \times \mathbf{a}) \times \mathbf{v}}{|\mathbf{v} \times \mathbf{a}| |\mathbf{v}|} \quad (2.20)$$

The tangent \mathbf{T} and normal \mathbf{N} only account for two of the three degrees of freedom in space. A third unit-length vector, called the *binormal vector*, is defined by

$$\mathbf{B} = \mathbf{T} \times \mathbf{N} \quad (2.21)$$

The coordinate system $\{\mathbf{r}(t); \mathbf{T}(t), \mathbf{N}(t), \mathbf{B}(t)\}$ is a moving frame for the curve. The binormal is perpendicular to the tangent and normal vectors, so $\mathbf{B} \cdot \mathbf{T} = 0$ and $\mathbf{B} \cdot \mathbf{N} = 0$ for all t . Differentiating with respect to arc length s , we obtain

$$0 = \frac{d\mathbf{B}}{ds} \cdot \mathbf{T} + \mathbf{B} \cdot \frac{d\mathbf{T}}{ds} = \frac{d\mathbf{B}}{ds} \cdot \mathbf{T} + \kappa \mathbf{B} \cdot \mathbf{N} = \frac{d\mathbf{B}}{ds} \cdot \mathbf{T}$$

The binormal is unit length, so $\mathbf{B} \cdot \mathbf{B} = 1$ for all t . Differentiating with respect to s and dividing by 2, we obtain

$$0 = \mathbf{B} \cdot \frac{d\mathbf{B}}{ds}$$

The last two displayed equations show that the derivative of the binormal is perpendicular to both \mathbf{T} and \mathbf{B} . It must therefore be parallel to \mathbf{N} and represented as

$$\frac{d\mathbf{B}}{ds} = -\tau \mathbf{N} \quad (2.22)$$

for some scalar function τ , called the *torsion* of the curve. The choice of minus sign is the standard convention. The curvature measures how the curve wants to bend within the plane spanned by the tangent and normal to the curve. The torsion measures how the curve wants to bend out of that plane.

To this point we know how the derivatives $d\mathbf{T}/ds$ and $d\mathbf{B}/ds$ relate to the tangent, normal, and binormal. We may complete the set of relationships by computing $d\mathbf{N}/ds$. The normal is $\mathbf{N} = \mathbf{B} \times \mathbf{T}$. Differentiating with respect to s yields

$$\frac{d\mathbf{N}}{ds} = \mathbf{B} \times \frac{d\mathbf{T}}{ds} + \frac{d\mathbf{B}}{ds} \times \mathbf{T} = \kappa \mathbf{B} \times \mathbf{N} - \tau \mathbf{N} \times \mathbf{T} = -\kappa \mathbf{T} + \tau \mathbf{B} \quad (2.23)$$

Equations (2.18), (2.22), and (2.23) are called the *Frenet–Serret equations* for the curve. In a formal matrix notation,

$$\begin{bmatrix} \frac{d\mathbf{T}}{ds} \\ \frac{d\mathbf{N}}{ds} \\ \frac{d\mathbf{B}}{ds} \end{bmatrix} = \begin{bmatrix} 0 & \kappa & 0 \\ -\kappa & 0 & \tau \\ 0 & -\tau & 0 \end{bmatrix} \begin{bmatrix} \mathbf{T}(s) \\ \mathbf{N}(s) \\ \mathbf{B}(s) \end{bmatrix} \quad (2.24)$$

An explicit formula for the torsion is obtained as follows. The derivative of acceleration, sometimes called a measure of *jerk* is

$$\ddot{\mathbf{a}} = \frac{d}{dt} (\ddot{s} \mathbf{T} + \kappa \dot{s}^2 \mathbf{N}) = (\ddot{s} - \kappa^2 \dot{s}^3) \mathbf{T} + \left[\frac{d}{dt} (\kappa \dot{s}^2) + \kappa \ddot{s} \right] \mathbf{N} + (\tau \kappa \dot{s}^3) \mathbf{B}$$

A simple calculation shows that $\mathbf{v} \times \mathbf{a} = \kappa \dot{s}^3 \mathbf{B}$. Consequently, $\mathbf{v} \times \mathbf{a} \cdot \dot{\mathbf{a}} = \tau \kappa^2 \dot{s}^6 = \tau |\mathbf{v} \times \mathbf{a}|^2$. The torsion is

$$\tau = \frac{\mathbf{v} \times \mathbf{a} \cdot \dot{\mathbf{a}}}{|\mathbf{v} \times \mathbf{a}|^2} \quad (2.25)$$

Spatial Motion in Cylindrical Coordinates

A point (x, y, z) is represented in cylindrical coordinates as $x = r \cos \theta$, $y = r \sin \theta$, and z as given, where r is the distance in the xy -plane from the origin $(0, 0, 0)$ to (x, y, z) , and z is the vertical height of the point above that plane. The angle satisfies $\theta \in [0, 2\pi)$. Figure 2.4 shows a typical point (x, y, z) and its related parameters r and θ .

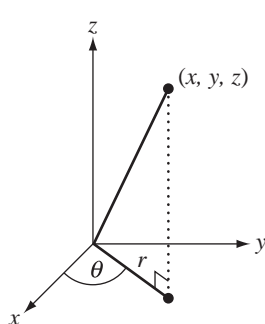


Figure 2.4 Cylindrical coordinates $(x, y, z) = (r \cos \theta, r \sin \theta, z)$.

Using notation similar to that of planar motion in polar coordinates, a unit-length vector in the xy -plane is $\mathbf{R} = (\cos \theta, \sin \theta, 0)$. A perpendicular vector in the plane is $\mathbf{P} = (-\sin \theta, \cos \theta, 0)$. The vertical direction is $\mathbf{k} = (0, 0, 1)$. The moving frame for the curve is $\{\mathbf{r}(t); \mathbf{R}(t), \mathbf{P}(t), \mathbf{k}\}$. The position of a point is

$$\mathbf{r} = r\mathbf{R} + zk \quad (2.26)$$

The velocity is

$$\mathbf{v} = \dot{\mathbf{r}} = \dot{r}\mathbf{R} + r\dot{\theta}\mathbf{P} + zk \quad (2.27)$$

The acceleration is

$$\mathbf{a} = \ddot{\mathbf{v}} = (\ddot{r} - r\dot{\theta}^2)\mathbf{R} + (r\ddot{\theta} + 2\dot{r}\dot{\theta})\mathbf{P} + zk \quad (2.28)$$

Observe that the position, velocity, and acceleration have the same \mathbf{R} and \mathbf{P} components as the polar representations in two dimensions, but have additional components in the z -direction. The time derivatives of the frame vectors are shown below in formal matrix notation:

$$\begin{bmatrix} \dot{\mathbf{R}} \\ \dot{\mathbf{P}} \\ \dot{\mathbf{k}} \end{bmatrix} = \begin{bmatrix} 0 & \dot{\theta} & 0 \\ -\dot{\theta} & 0 & 0 \\ 0 & 0 & 0 \end{bmatrix} \begin{bmatrix} \mathbf{R} \\ \mathbf{P} \\ \mathbf{k} \end{bmatrix} \quad (2.29)$$

As always, the coefficient matrix for rates of change of frame vectors is skew-symmetric.

EXERCISE 2.2

Construct the position, velocity, and acceleration vectors in cylindrical coordinates for the helix $(\cos(t), \sin(t), t)$. ■

Spatial Motion in Spherical Coordinates

A point (x, y, z) is represented in spherical coordinates as $x = \rho \cos \theta \sin \phi$, $y = \rho \sin \theta \sin \phi$, and $z = \rho \cos \phi$, where $\theta \in [0, 2\pi)$ and $\phi \in [0, \pi]$. Figure 2.5 shows a typical point (x, y, z) and its related parameters ρ , θ , and ϕ .

The position of a point is

$$\mathbf{r} = \rho \mathbf{R} \quad (2.30)$$

where $\mathbf{R} = (\cos \theta \sin \phi, \sin \theta \sin \phi, \cos \phi)$ is a unit-length vector. Two unit-length vectors that are perpendicular to \mathbf{R} are $\mathbf{P} = (-\sin \theta, \cos \theta, 0)$ and $\mathbf{Q} = \mathbf{R} \times \mathbf{P} = (-\cos \theta \cos \phi, -\sin \theta \cos \phi, \sin \phi)$. A moving frame for the curve is

$$\{\mathbf{r}(t); \mathbf{P}(t), \mathbf{Q}(t), \mathbf{R}(t)\}$$

The derivatives of the moving frame are shown in equation (2.31). The formal representation in terms of vectors and matrices is intended to emphasize that the coefficient

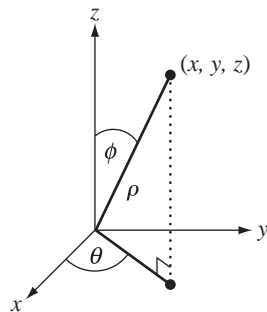


Figure 2.5 Spherical coordinates $(x, y, z) = (\rho \cos \theta \sin \phi, \rho \sin \theta \sin \phi, \rho \cos \phi)$.

matrix is skew-symmetric:

$$\begin{bmatrix} \dot{\mathbf{P}} \\ \dot{\mathbf{Q}} \\ \dot{\mathbf{R}} \end{bmatrix} = \begin{bmatrix} 0 & \dot{\theta} \cos \phi & -\dot{\theta} \sin \phi \\ -\dot{\theta} \cos \phi & 0 & \dot{\phi} \\ \dot{\theta} \sin \phi & -\dot{\phi} & 0 \end{bmatrix} \begin{bmatrix} \mathbf{P} \\ \mathbf{Q} \\ \mathbf{R} \end{bmatrix} \quad (2.31)$$

The proof of these equations is left as an exercise. The velocity of a point is

$$\mathbf{v} = \dot{\rho}\mathbf{R} + \rho\dot{\mathbf{R}} = (\rho\dot{\theta} \sin \phi)\mathbf{P} + (-\rho\dot{\phi})\mathbf{Q} + (\dot{\rho})\mathbf{R} \quad (2.32)$$

where equation (2.31) was used to replace the derivative of \mathbf{R} . Another application of a time derivative and equation (2.31) produces the acceleration of a point,

$$\begin{aligned} \mathbf{a} = & ((\rho\ddot{\theta} + 2\dot{\rho}\dot{\theta}) \sin \phi + 2\rho\dot{\theta}\dot{\phi} \cos \phi)\mathbf{P} + (\rho(\dot{\theta}^2 \sin \phi \cos \phi - \ddot{\phi}) - 2\dot{\rho}\dot{\phi})\mathbf{Q} \\ & + (\ddot{\rho} - \rho(\dot{\phi}^2 + \dot{\theta}^2 \sin^2 \phi))\mathbf{R} \end{aligned} \quad (2.33)$$

EXERCISE 2.3

Construct the position, velocity, and acceleration in spherical coordinates for the spherical helix $(\cos(t), \sin(t), t)/\sqrt{1+t^2}$. What happens to the helix as time increases without bound? ■

EXERCISE 2.4

Verify the formulas in equation (2.31). Hint: Compute the partial derivatives with respect to θ and ϕ of \mathbf{R} , \mathbf{P} , and \mathbf{Q} ; then use the chain rule from calculus to obtain the time derivatives. ■

Motion About a Fixed Axis

A classic question is how to compute the position, velocity, and acceleration of a particle that is rotating about a fixed axis and is a constant distance from that axis. For the

sake of argument, assume that the axis is a line that contains the origin and whose unit-length direction is \mathbf{D} . We may choose the coordinate system so that \mathbf{D} plays the role of \mathbf{k} in equation (2.26) and $\mathbf{R}(t) = (\cos \theta(t), \sin \theta(t), 0)$ is radial to that axis. The 3-tuple shown in Figure 2.6 is relative to a fixed coordinate system at the origin with an orthonormal set of axes ξ , η , and \mathbf{D} . That is, $\mathbf{R} = (\cos \theta)\xi + (\sin \theta)\eta$. In this system, the *angular speed* is $\sigma(t) = \dot{\theta}(t)$. The *angular velocity* is $\mathbf{w}(t) = \sigma(t)\mathbf{D}$. The *angular acceleration* is $\boldsymbol{\alpha}(t) = \dot{\sigma}(t)\mathbf{D}$. Figure 2.6 illustrates the motion.

The position for the particle in motion about the axis is

$$\mathbf{r}(t) = r_0\mathbf{R}(t) + h_0\mathbf{D} \quad (2.34)$$

where r_0 is the constant distance from the particle to the axis and where h_0 is the constant height above the plane $\mathbf{D} \cdot \mathbf{r} = 0$. From equation (2.27) the velocity is

$$\mathbf{v}(t) = r_0\sigma\mathbf{P} = r_0\sigma\mathbf{D} \times \mathbf{R} = \mathbf{w} \times \mathbf{r} \quad (2.35)$$

where we have used the facts that r_0 and h_0 are constants, so their derivatives are always zero, and $\dot{\theta} = \sigma$. This formula should be intuitive. The cross product of the axis direction and the position vector is tangent to the circle of motion. From equation (2.28) the acceleration is

$$\mathbf{a}(t) = -r_0\sigma^2\mathbf{R} + r_0\ddot{\theta}\mathbf{P} = -r_0\sigma^2\mathbf{R} + r_0\dot{\sigma}\mathbf{D} \times \mathbf{R} = -r_0\sigma^2\mathbf{R} + \boldsymbol{\alpha} \times \mathbf{r} \quad (2.36)$$

The vector $-r_0\sigma^2\mathbf{R}$ is the *centripetal acceleration* of the particle. The vector $\boldsymbol{\alpha} \times \mathbf{r}$ is the *tangential acceleration* of the particle and, of course, is a vector that is tangent to the circle of motion.

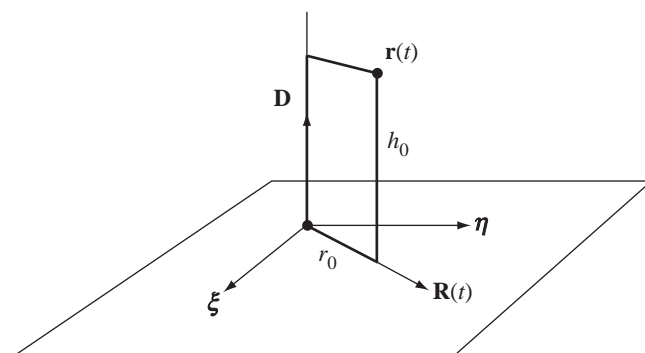


Figure 2.6 Motion of a particle about a fixed axis, a constant distance from the axis.

Motion About a Moving Axis

To motivate the concept of angular velocity for a time-varying axis with unit-length direction vector $\mathbf{D}(t)$, let us take a closer look at motion about a fixed axis. [Equation \(2.34\)](#) tells you the position of the particle that is rotating about the fixed axis, $\mathbf{r}(t) = r_0(\cos(\theta(t))\hat{\mathbf{x}} + \sin(\theta(t))\hat{\mathbf{y}}) + h_0\mathbf{D}$. The initial position is $\mathbf{r}_0 = \mathbf{r}(0) = r_0\hat{\mathbf{x}} + h_0\mathbf{D}$. Positions at later times are determined by a rotation of $\mathbf{r}(t)$ about the axis \mathbf{D} by an angle $\theta(t)$, namely $\mathbf{r}(t) = R(t)\mathbf{r}_0$ where $R(t)$ is the rotation matrix corresponding to the specified rotation about the axis. For any vector $\mathbf{u} = (u_1, u_2, u_3)$, define the skew-symmetric matrix:

$$\text{Skew}(\mathbf{u}) = \begin{bmatrix} 0 & -u_3 & u_2 \\ u_3 & 0 & -u_1 \\ -u_2 & u_1 & 0 \end{bmatrix}$$

This matrix has the property that $\text{Skew}(\mathbf{u})\mathbf{r} = \mathbf{u} \times \mathbf{r}$. The derivation in [Chapter 10](#) that leads to [equation \(10.14\)](#) shows that the rotation matrix is

$$R(t) = I + (\sin(\theta(t)))\text{Skew}(\mathbf{D}) + (1 - \cos(\theta(t)))\text{Skew}(\mathbf{D})^2$$

We can also write the linear velocity as

$$\dot{\mathbf{r}}(t) = \mathbf{w}(t) \times \mathbf{r}(t) = \text{Skew}(\mathbf{w}(t))\mathbf{r}(t)$$

where the angular velocity is $\mathbf{w}(t) = \dot{\theta}(t)\mathbf{D}$. Differentiating $\mathbf{r}(t) = R(t)\mathbf{r}_0$ directly, we obtain

$$\dot{\mathbf{r}}(t) = \dot{R}(t)\mathbf{r}_0 = \dot{R}(t)R^T R\mathbf{r}_0 = (\dot{R}(t)R^T)\mathbf{r}(t) \quad (2.37)$$

Equating this to the previously displayed equation, we have

$$\dot{R}(t)R^T = \text{Skew}(\mathbf{w}(t))$$

or

$$\dot{R}(t) = \text{Skew}(\mathbf{w}(t))R(t) \quad (2.38)$$

These equations tell us the rate of change of the rotation in terms of the current rotation and the current angular velocity.

Now consider what happens if we allow the unit-length direction vector to vary with time, $\mathbf{D}(t)$. The rotation matrix corresponding to this direction vector and rotation angle $\theta(t)$ is

$$R(t) = I + (\sin(\theta(t)))\text{Skew}(\mathbf{D}(t)) + (1 - \cos(\theta(t)))\text{Skew}(\mathbf{D}(t))^2 \quad (2.39)$$

The initial point \mathbf{r}_0 is still transformed by $\mathbf{r}(t) = R(t)\mathbf{r}_0$ and the linear velocity is still provided by [equation \(2.37\)](#). A rotation matrix satisfies the identity $I = RR^T$. Taking the time derivative, $0 = \dot{R}R^T + R\dot{R}^T = \dot{R}R^T + (\dot{R}R^T)^T$, or $(\dot{R}R^T)^T = -\dot{R}R^T$. Thus, $S(t) = \dot{R}(t)R^T(t)$ is a skew-symmetric matrix. We have already made this

observation for rotation matrices that arise in specific coordinate systems, namely equations (2.9) and (2.29). Since $S(t)$ is a skew-symmetric matrix, it can be written as $S(t) = \text{Skew}(\mathbf{w}(t))$.

We saw that for a fixed axis \mathbf{D} , the angular velocity is $\mathbf{w} = \dot{\theta}\mathbf{D}$. A natural question to ask is how the angular velocity relates to $\theta(t)$ and $\mathbf{D}(t)$ in the general case. We can directly calculate this by computing $\dot{R}(t)$ for the matrix in equation (2.39) followed by computing $\dot{R}R^T$. Some algebraic and trigonometric manipulations and the identity $\text{Skew}(\mathbf{D})^3 = -\text{Skew}(\mathbf{D})$ for a unit-length vector \mathbf{D} will lead you to

$$\mathbf{w} = \dot{\theta}\mathbf{D} + (\sin\theta)\dot{\mathbf{D}} + (\cos\theta - 1)\dot{\mathbf{D}} \times \mathbf{D} \quad (2.40)$$

Because \mathbf{D} is unit-length, $\mathbf{D} \cdot \dot{\mathbf{D}} = 0$, in which case $\dot{\mathbf{D}}$ is perpendicular to \mathbf{D} . Thus, \mathbf{D} , $\dot{\mathbf{D}}$, and $\dot{\mathbf{D}} \times \mathbf{D}$ are mutually orthogonal. The angular velocity is a linear combination of these three vectors.

EXERCISE

2.5

Prove equation (2.40) is true. ■

2.2.2 PARTICLE SYSTEMS AND CONTINUOUS MATERIALS

In the last section we discussed the basic concepts of kinematics for a single particle. Let us now look at the same concepts for a discrete set of particles, a particle system so to speak, or a continuous material. In this general discussion we are not assuming the body is rigid.

When a body moves through the world, each point in the body travels along a path that is measured in *world coordinates*. At time 0, if \mathcal{P} is a body point specified in world coordinates, the position after time t in world coordinates is denoted $\mathcal{X}(t; \mathcal{P})$. The inclusion of \mathcal{P} as an argument of the function indicates that we are thinking of many paths, each path generated by a starting point \mathcal{P} . By our definition, $\mathcal{X}(0; \mathcal{P}) = \mathcal{P}$. The world coordinates of the body points are what an observer measures when he is standing at the world origin using a known set of directions for the world coordinate axes. We will refer to this observer as the *world observer*.

We can also measure points in *body coordinates*. You can imagine such a coordinate system as the one that an observer situated in the body uses to measure the location of body points. We will refer to this observer as the *body observer*. The body observer stands at a special point that we call the *body origin*. He also has his own view of three coordinate axes called the *body axes*. The axis directions are assumed to form a right-handed orthonormal set. The body origin and axes never change from the body observer's point of view, but the world observer sees these change over time.

If the world observer measures the point at $\mathcal{X}(t; \mathcal{P})$, the body observer sees this point relative to his origin, measuring it as a vector $\mathbf{b}(t; \mathcal{P})$. Again the inclusion of \mathcal{P} as an argument indicates that there are many paths, one for each initial point \mathcal{P} . If the body is rigid, then necessarily \mathbf{b} is independent of time; its time derivative is identically zero. If \mathcal{C} is what the world observer sees as the body origin at time 0, at time t

he sees $\mathcal{X}(t; \mathcal{C})$. Of course the body observer always measures this as a relative difference $\mathbf{0}$ regardless of the time t . The world observer sees the body axis directions as orthonormal vectors measured in world coordinates; call these $\mathbf{U}_i(t)$ for $i = 0, 1, 2$. For convenience the world coordinate vectors can be stored as the columns of a rotation matrix $R(t) = [\mathbf{U}_0(t) \mathbf{U}_1(t) \mathbf{U}_2(t)]$. [Figure 2.7](#) illustrates the two coordinate systems, but in two dimensions to keep the diagrams simple.

The relative difference between the world point and world center is $\mathbf{r}(t; \mathcal{P}) = \mathcal{X}(t; \mathcal{P}) - \mathcal{X}(t; \mathcal{C}) = R(t)\mathbf{b}(t; \mathcal{P})$. The transformation that produces the world coordinates of body points at time t , given the location of points as measured by the body observer is

$$\mathcal{X}(t; \mathcal{P}) = \mathcal{X}(t; \mathcal{C}) + \mathbf{r}(t; \mathcal{P}) = \mathcal{X}(t; \mathcal{C}) + R(t)\mathbf{b}(t; \mathcal{P}) \quad (2.41)$$

The orientation changes are uncoupled from the translation changes.

Consider a time-varying vector written in the body coordinate system, $\xi(t) = R(t)\mathbf{s}(t)$. The body coordinates $\mathbf{s}(t)$ vary with time because $\xi(t)$ does. The time derivative is

$$\frac{d\xi}{dt} = R \frac{d\mathbf{s}}{dt} + \dot{R}\mathbf{s} = R \frac{d\mathbf{s}}{dt} + \dot{R}R^T \xi = \frac{D\xi}{Dt} + \mathbf{w} \times \xi \quad (2.42)$$

where $\dot{R}R^T = \text{Skew}(\mathbf{w})$ and \mathbf{w} is the angular velocity of the body measured in world coordinates as determined by [equation \(2.38\)](#). The last equality of [equation \(2.42\)](#) defines

$$\frac{D\xi}{Dt} = R(t) \frac{d\mathbf{s}}{dt}$$

a quantity that measures the rate of change of ξ relative to the body coordinate system. The rate of change $d\xi/dt$ is what the world observer sees. The quantity $D\xi/Dt$

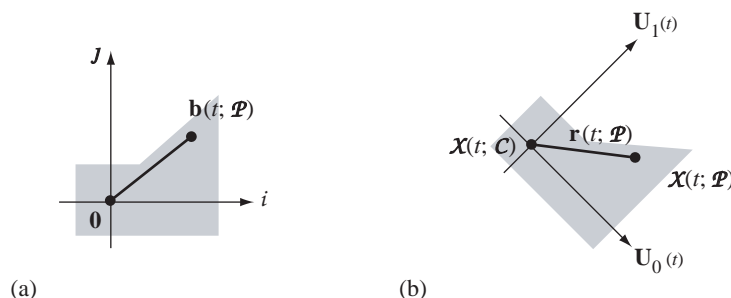


[Figure 2.7](#) (a) The body coordinate system as seen by the body observer. (b) The body coordinate system as seen by the world observer.

represents the time rate of change of ξ relative to the body coordinates because ds/dt is what the body observer measures. The body observer does not see the change $\mathbf{w} \times \xi$ because he is rotating with the body coordinate system.

The body origin has world velocity $\mathbf{v}_{\text{cen}} = d\mathcal{X}(t; \mathcal{C})/dt$ and world acceleration $\mathbf{a}_{\text{cen}} = d\mathbf{v}_{\text{cen}}/dt$. Differentiating equation (2.41) with respect to time, the world velocity $\mathbf{v}_{\text{wor}} = d\mathcal{X}(t; \mathcal{P})/dt$ is

$$\mathbf{v}_{\text{wor}} = \mathbf{v}_{\text{cen}} + R \frac{d\mathbf{b}}{dt} + \dot{R}\mathbf{b} = \mathbf{v}_{\text{cen}} + \frac{D\mathbf{r}}{Dt} + \mathbf{w} \times \mathbf{r} \quad (2.43)$$

where \mathbf{w} is the angular velocity of the body at time t in world coordinates. The terms of the equation are

- \mathbf{v}_{cen} , the velocity of the body origin relative to the world coordinates, sometimes referred to as the *drag velocity*,
- $D\mathbf{r}/Dt$, the velocity of \mathcal{P} measured relative to the body coordinates, and
- $\mathbf{w} \times \mathbf{r}$, the velocity due to rotation of the frame.

The world acceleration $\mathbf{a}_{\text{wor}} = d\mathbf{v}_{\text{wor}}/dt$ is obtained by differentiating equation (2.43) with respect to time,

$$\mathbf{a}_{\text{wor}} = \mathbf{a}_{\text{cen}} + \frac{d}{dt} \left(\frac{D\mathbf{r}}{Dt} \right) + \frac{d}{dt} (\mathbf{w} \times \mathbf{r})$$

The vector $D\mathbf{r}/Dt$ is measured in the body coordinate system, so equation (2.42) applies to it:

$$\frac{d}{dt} \left(\frac{D\mathbf{r}}{Dt} \right) = \frac{D}{Dt} \left(\frac{D\mathbf{r}}{Dt} \right) + \mathbf{w} \times \frac{D\mathbf{r}}{Dt} = \frac{D^2\mathbf{r}}{Dt^2} + \mathbf{w} \times \frac{D\mathbf{r}}{Dt}$$

Similarly, equation (2.42) is applied to $\mathbf{w} \times \mathbf{r}$ to obtain

$$\frac{d}{dt} (\mathbf{w} \times \mathbf{r}) = \frac{D(\mathbf{w} \times \mathbf{r})}{Dt} + \mathbf{w} \times (\mathbf{w} \times \mathbf{r}) = \mathbf{w} \times \frac{D\mathbf{r}}{Dt} + \frac{D\mathbf{w}}{Dt} \times \mathbf{r} + \mathbf{w} \times (\mathbf{w} \times \mathbf{r})$$

Observe that $D\mathbf{w}/Dt = d\mathbf{w}/dt$ since we may apply equation (2.42) to \mathbf{w} and use the identity $\mathbf{w} \times \mathbf{w} = \mathbf{0}$. The last three displayed equations combine to form an equation for the acceleration,

$$\mathbf{a}_{\text{wor}} = \mathbf{a}_{\text{cen}} + \mathbf{w} \times (\mathbf{w} \times \mathbf{r}) + \frac{D\mathbf{w}}{Dt} \times \mathbf{r} + 2\mathbf{w} \times \frac{D\mathbf{r}}{Dt} + \frac{D^2\mathbf{r}}{Dt^2} \quad (2.44)$$

The terms of the equation are

- \mathbf{a}_{cen} , the translational acceleration of the body origin relative to the world coordinates,
- $\mathbf{w} \times (\mathbf{w} \times \mathbf{r})$, the centripetal acceleration due to rotation of the frame,

- $(D\mathbf{w}/Dt) \times \mathbf{r}$, the tangential acceleration due to angular acceleration,
- $2\mathbf{w} \times (D\mathbf{r}/Dt)$, the Coriolis acceleration, and
- $D^2\mathbf{r}/Dt^2$, the acceleration of \mathcal{P} relative to the body.

The first three terms collectively are called the *drag acceleration*.

**EXERCISE
2.6**

Consider a rigid sphere of radius 1 and center at $\mathbf{0}$ that rotates about its center. The angular velocity is $\mathbf{w}(t) = (\cos(t), \sin(t), \sqrt{3})$. Does the path of the point starting at $(0, 0, 1)$ ever reach this same point at a later time? If it were not to reach $(0, 0, 1)$ again, is there some other constant angular speed for which it will reach that point again? ■

**EXERCISE
2.7**

Consider the same rigid sphere of the preceding example, but whose angular velocity is unknown. Suppose the path of the point starting at $(0, 0, 1)$ is $((1 - t^2) \cos(\pi t), (1 - t^2) \sin(\pi t), t^2)/\sqrt{(1 - t^2)^2 + t^4}$ for $t \in [-1, 1]$. What is the angular velocity $\mathbf{w}(t)$? If $\mathbf{r}(t)$ is the path traversed by $(1, 0, 0)$ over the time interval $[-1, 1]$, then by definition $\mathbf{r}(-1) = (1, 0, 0)$. What is $\mathbf{r}(1)$? If you have difficulties constructing all the components of this point, can you say something about any of the components? ■

**EXERCISE
2.8**

In the constructions of this section, the standard first-derivative operator d/dt was applied to vector quantities. This operator has certain rules associated with it. The operator D/Dt was introduced in this section, and I used the same rules for it. For example, I used the rule $D(\mathbf{A} \times \mathbf{B})/Dt = \mathbf{A} \times (D\mathbf{B}/Dt) + (D\mathbf{A}/Dt) \times \mathbf{B}$. What is the relationship between d/dt and D/Dt ? Use this relationship to prove that the differentiation rules for d/dt are equally valid for D/Dt . ■

2.3 NEWTON'S LAWS

We have seen the concepts of position, velocity, and acceleration of a point; all are relevant in describing the motion of an object. A key concept is *inertia*, the tendency of an object in motion to remain in motion. Although we tend to think of the *mass* of an object as a measure of the amount of matter making up the object, it is just as valid to think of mass as a measure of the inertia of the object. The standard unit of measurement for mass is a *kilogram*.

Another key concept is *force*, the general mechanism for changing the mechanical state of an object. Empirically we know that a force is a vector quantity, so it has a direction and a magnitude. For our purposes, forces are what lead to changes in velocity of an object and cause objects to interact with each other. An *external force* is one whose source is outside the system of interest. From experimental studies we know that the net external force on an object causes it to accelerate in the direction of the force. Moreover, the magnitude of the acceleration of the object is proportional to the magnitude of the force (the larger the force, the more the object accelerates) and inversely proportional to the mass of the object (the heavier the object, the less

it accelerates). The standard unit of measurement for the magnitude of a force is a *newton*. One newton is the required magnitude of a force to give a one kilogram mass an acceleration of one meter per second squared.

An introductory course to physics summarizes these concepts as a statement of *Newton's laws of physics*:

- **First Law.** In the absence of external forces, an object at rest will remain at rest. If the object is in motion and no external forces act on it, the object remains in motion with constant velocity. (*Only forces can change an object's motion.*)
- **Second Law.** For an object of constant mass over time, its acceleration \mathbf{a} is proportional to the force \mathbf{F} and inversely proportional to the mass m of the object: $\mathbf{a} = \mathbf{F}/m$. We normally see this written as $\mathbf{F} = m\mathbf{a}$. If the mass changes over time, the more general statement of the law is

$$\mathbf{F} = \frac{d}{dt}(m\mathbf{v}) = m\mathbf{a} + \frac{dm}{dt}\mathbf{v} \quad (2.45)$$

where \mathbf{v} is the velocity of the object. The quantity $m\mathbf{v}$ is the *linear momentum* of the object. Thus, the second law states that the application of an external force on an object causes a change in the object's momentum over time. (*An object's path of motion is determined from the applied forces.*)

- **Third Law.** If a force is exerted on one object, there is a force of equal magnitude but opposite direction on some other body that interacts with it. (*Action and reaction always occur between interacting objects.*)

The most important law for this book is the second one, although we will deal specifically with constant mass. The *equations of motion* $\mathbf{F} = m\mathbf{a}$ will be used to establish the path of motion for an object by numerically solving the second-order differential equations for position.

Each of the vector quantities of position, velocity, and acceleration is measured with respect to *some* coordinate system. This system is referred to as the *inertial frame*. If $\mathbf{x} = (x_1, x_2, x_3)$ is the representation of the position in the inertial frame, the components x_1, x_2 , and x_3 are referred to as the *inertial coordinates*. Although in many cases the inertial frame is considered to be fixed (relative to the stars as it were), the frame can have a constant linear velocity and no rotation and still be inertial. Any other frame of reference is referred to as a *noninertial frame*. In many situations it is important to know whether the coordinate system you use is inertial or noninertial. In particular, we will see later that kinetic energy must be measured in an inertial system.

2.4 FORCES

A few general categories of forces are described here. We restrict our attention to those forces that are used in the examples that occur throughout this book. For example, we are not going to discuss forces associated with electromagnetic fields.

2.4.1 GRAVITATIONAL FORCES

Given two point masses m and M that have gravitational interaction, they attract each other with forces of equal magnitude but opposite direction, as indicated by Newton's third law. The common magnitude of the forces is

$$F_{\text{gravity}} = \frac{GmM}{r^2} \quad (2.46)$$

where r is the distance between the points and $G \doteq 6.67 \times 10^{-11}$ newton-meters squared per kilogram squared. The units of G are selected, of course, so that F_{gravity} has units of newtons. The constant is empirically measured and is called the *universal gravitational constant*.

In the special case of the Earth represented as a single-point mass M located at the center of the Earth and an object represented as a single-point mass m located on or above the Earth's surface, the gravitational force exerted on the object by the Earth is

$$\mathbf{F} = -F_{\text{gravity}}\mathbf{R} \quad (2.47)$$

where \mathbf{R} is a unit-length vector whose direction is that of the vector from the center of the Earth to the center of the object. In the special case when the two objects are the Earth and the Sun, the equations of motion $\mathbf{F} = m\mathbf{a}$ that represent the path the Earth travels around the Sun may be solved in closed form to produce *Kepler's Laws*. We do so in detail in Section 2.3. Figure 2.8 shows the Earth and the forces exerted on various objects above its surface.

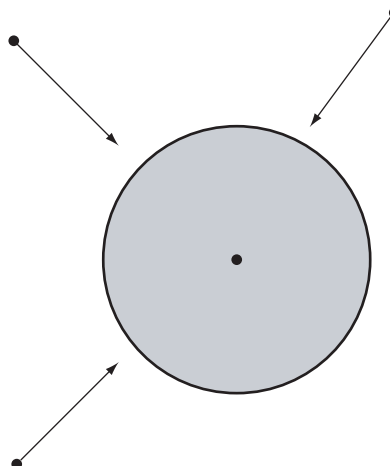


Figure 2.8 Gravitational forces on objects located at various places around the Earth.

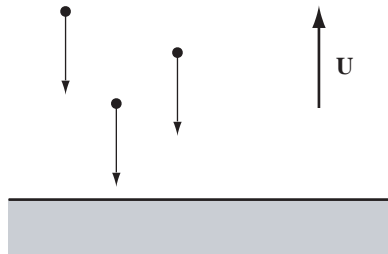


Figure 2.9 Gravitational forces on objects located nearly on the Earth's surface, viewed as a flat surface.

If the object does not vary much in altitude and its position does not move far from its initial position, we can make an approximation to the equation of gravitational force by assuming that the Earth's surface is flat (a plane), at least within the vicinity of the object, and that the direction of the gravitational force is normal to the plane. Moreover, the distance r is approximately a constant, the radius of the Earth, so $g = GM/r^2 \doteq 9.81$ meters per second squared is approximately a constant. If we choose \mathbf{U} as the unit-length upward direction (increasing altitude above the plane), the gravitational force exerted on the object by the Earth is

$$\mathbf{F} = -mg\mathbf{U} \quad (2.48)$$

Figure 2.9 shows the Earth viewed as a flat surface and the forces exerted on various objects above it.

The *weight* w of the object is different from its mass, namely, $w = mg$, the magnitude of the gravitational force exerted on the object. Astronauts of course are weightless when in orbit, but still have the same mass as on the Earth's surface.

2.4.2 SPRING FORCES

One end of a spring is attached to a fixed point. The other end is free to be pushed or pulled in any direction. The unstretched length of the spring is L . Experiments have shown that for small displacements Δ of the end of the spring, the force exerted by the spring on the end has a magnitude proportional to $|\Delta|$ and a direction opposite that of the displacement. That is, if the end of the spring is pulled away from the fixed point, the direction of the force is towards the fixed point, and vice versa. If \mathbf{U} is a unit-length vector pointing in the direction from the fixed end to the free end, the force is

$$\mathbf{F} = -c\Delta\mathbf{U} \quad (2.49)$$

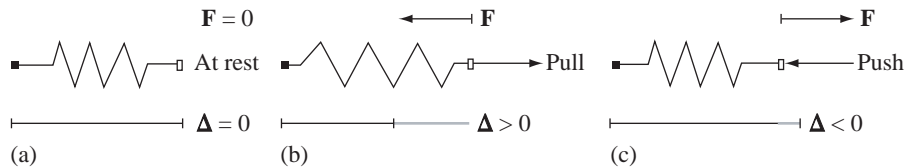


Figure 2.10 (a) Unstretched spring. (b) Force due to stretching the spring. (c) Force due to compressing the string.

where $c > 0$ is the constant of proportionality called the *spring constant*. For very stiff springs, c is large, and vice versa. This law for spring forces is known as *Hooke's Law*. The law breaks down if $|\Delta|$ is very large, so be careful if you have a physics application involving springs; you might want to modify the force equation when $|\Delta|$ is large. Figure 2.10 illustrates a spring that is stretched or compressed.

Hooke's Law will be applied in upcoming examples where we think of two points connected by an elastic line segment. This will be useful in modeling deformable objects as a system of masses connected by elastic threads.

2.4.3 FRICTION AND OTHER DISSIPATIVE FORCES

A *dissipative force* is one for which energy of the system decreases when motion takes place. Typically the energy is transferred out of the system by conversion to heat. A simple model for the magnitude of a dissipative force applied to a rigid object is

$$F_{\text{dissipative}} = c|\mathbf{v}|^n \quad (2.50)$$

where \mathbf{v} is the object's velocity, $c > 0$ is a scalar of proportionality, and $n \geq 0$ is an integer power. In most applications you probably will choose c to be a constant, but in general it may vary with position, for example when the underlying material on which the object moves is not homogeneous. The value c may also vary with time. A simple model for a dissipative force also usually includes the assumption that the direction of the force is opposite the motion of the object, that is, in the direction $-\mathbf{v}$. In our applications in this book we will consider two special types of dissipative forces, *friction* and *viscosity*.

Friction

A *frictional force* between two objects in contact opposes the sliding of one (moving) object over the surface of the adjacent (nonmoving) object. The frictional force is tangent to the surface of the adjacent object and opposite in direction to the

velocity of the moving object. The magnitude of the frictional force is assumed to be proportional to the magnitude of the *normal force* between surfaces. It is also assumed to be independent of the area of contact and independent of the speed of the object once that object starts to move. These assumptions argue that $n = 0$ in equation (2.50), so the frictional force is modeled as

$$\mathbf{F} = \begin{cases} -c_k \frac{\mathbf{v}}{|\mathbf{v}|}, & \mathbf{v} \neq \mathbf{0} \\ \mathbf{0}, & \mathbf{v} = \mathbf{0} \end{cases} \quad (2.51)$$

where c_k is referred to as the *coefficient of kinetic friction*. The coefficient is the ratio of the magnitudes of frictional force over normal force, $c_k = F_{\text{friction}}/F_{\text{normal}}$, but with the correct physical units so that the right-hand side of equation (2.51) has units of force.

Physically the transition between the nonzero and zero force cases involves another concept called *static friction*. For example, if an object is in contact with a flat surface and initially not moving, an external force is applied to the object to make it move. If the magnitude of the external force is sufficiently small, it is not enough to exceed the force due to static friction. As that magnitude increases, eventually the static friction is overcome and the object moves. At that instant the frictional force switches from static to kinetic; that is, the first case in equation (2.51) comes into play because the object is now moving. Another physical constant is the *coefficient of static friction*, denoted c_s . It is the ratio of the maximum frictional force over normal force, $c_s = \max(F_{\text{friction}})/F_{\text{normal}}$, and with the correct physical units assigned to it. The classical experiment to illustrate the transition from the static to kinetic case is a block of one material resting on an inclined plane of another material. Both materials are subject to gravitational force. Figure 2.11 illustrates.

Initially the angle of incline is small enough so that the static friction force dominates the gravitational force. The block remains at rest even though the plane is tilted. As the angle of incline increases, the gravitational force exerts a stronger influence on the block, enough so that it overcomes static friction. At that instant the block starts to slide down the plane. When it does, the frictional force switches from static to kinetic.

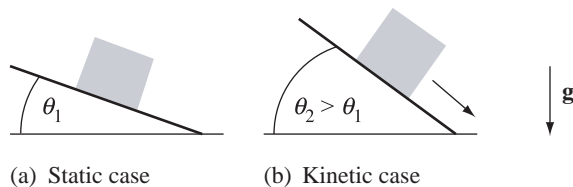


Figure 2.11 A block in contact with an inclined plane. (a) Static friction is dominant and the block remains at rest. (b) Gravity is dominant and the block slides, so kinetic friction applies.

Viscosity

A *viscous* force has magnitude, modeled by equation (2.50), when $n = 1$. The typical occurrence of this type of force is when an object is dragged through a thick fluid. The force is modeled to have direction opposite to that of the moving object:

$$\mathbf{F} = -F_{\text{dissipative}} \frac{\mathbf{v}}{|\mathbf{v}|} = -(c|\mathbf{v}|) \frac{\mathbf{v}}{|\mathbf{v}|} = -c\mathbf{v} \quad (2.52)$$

where $c > 0$ is a scalar of proportionality. Unlike friction that has a discontinuity when the speed is zero, a viscous force is continuous with respect to speed.

2.4.4 TORQUE

The concept of torque is one you are familiar with in everyday life. One example is replacing a tire on an automobile. You have to remove the lug nuts with a wrench. In order to turn a nut, you have to exert a force on the end of the wrench. The more force you apply, the easier the nut turns. You might also have noticed that the longer the wrench, the easier the nut turns. The ease of turning is proportional to both the magnitude of the applied force and the length of the wrench. This product is referred to as *torque* or *moment of force*. When you need a nut tightened, but not too much, you can use a tool called a torque wrench that is designed to stop turning the nut if the torque exceeds a specified amount.

The formal mathematical definition for torque applied to a single particle of mass m is given below. Let \mathbf{F} be the applied force. Let \mathbf{r} be the position of the particle relative to the origin. The torque is the quantity

$$\boldsymbol{\tau} = \mathbf{r} \times \mathbf{F} \quad (2.53)$$

In the analogy of a wrench and bolt, the bolt is located at the origin, the wrench lies along the vector \mathbf{r} , and the force \mathbf{F} is what you exert on the end of the wrench. Figure 2.12 illustrates torque due to a single force.

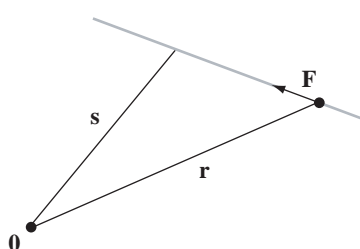


Figure 2.12 Torque from a force exerted on a particle.

Notice that \mathbf{F} is not necessarily perpendicular to \mathbf{r} . The applied force on the particle can be in any direction, independent of the position of the particle. The gray line indicates the line of force for \mathbf{F} . If the particle were on that line at a different position \mathbf{s} relative to the origin, the torque on it is $\mathbf{s} \times \mathbf{F}$. Since $\mathbf{r} - \mathbf{s}$ is a vector on the line of force, it must be that $(\mathbf{r} - \mathbf{s}) \times \mathbf{F} = \mathbf{0}$. That is, $\mathbf{r} \times \mathbf{F} = \mathbf{s} \times \mathbf{F}$ and the torque is the same no matter where the particle is located along the line of force.

Two forces of equal magnitude, opposite direction, but different lines of action are said to be a *couple*. Figure 2.13 shows two such forces. The torque due to the couple is $\tau = (\mathbf{r} - \mathbf{s}) \times \mathbf{F}$. The location of \mathbf{r} and \mathbf{s} on their respective lines is irrelevant. As you vary \mathbf{r} along its line, the torque does not change. Neither does the torque change when you vary \mathbf{s} along its line.

For a system of p particles located at positions \mathbf{r}_i with applied forces \mathbf{F}_i for $1 \leq i \leq p$, the torque is

$$\tau = \sum_{i=1}^p \mathbf{r}_i \times \mathbf{F}_i \quad (2.54)$$

If the object is a continuum of mass that occupies a region R , the torque is

$$\tau = \int_R \mathbf{r} \times \mathbf{F} dR \quad (2.55)$$

where \mathbf{F} is the applied force that varies with position \mathbf{r} .

Important: The torque due to internal forces in an object must sum to zero. This is an immediate consequence of Newton's third law. The essence of the argument is in considering two points in the object. The first point is at position \mathbf{r}_1 and exerts a force \mathbf{F} on the second point at position \mathbf{r}_2 . The second point exerts a force $-\mathbf{F}$ on the first point (Newton's third law). The lines of force are the same, having direction \mathbf{F} and containing both positions \mathbf{r}_1 and \mathbf{r}_2 . The total torque for the two points is $\mathbf{r}_1 \times \mathbf{F} + \mathbf{r}_2 \times (-\mathbf{F}) = (\mathbf{r}_1 - \mathbf{r}_2) \times \mathbf{F} = \mathbf{0}$. The last equality is true because $\mathbf{r}_1 - \mathbf{r}_2$ is on the line of force.

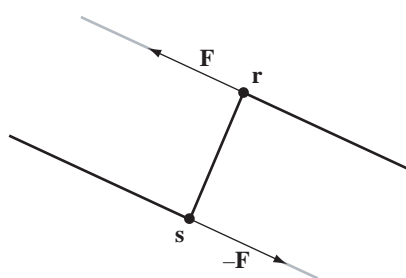


Figure 2.13 A force couple.

2.4.5 EQUILIBRIUM

Forces on an object are said to be *concurrent* if their lines of action all pass through a common point. If an object is a point mass, then all forces acting on the object are concurrent, the common point being the object itself. An example of nonconcurrent forces is a rigid rod with opposite direction forces applied at the endpoints. Figure 2.14 illustrates. The forces at the endpoints of the rod are parallel, but the lines through the endpoints and whose directions are those of the forces do not intersect in a common point, so those forces are not concurrent. In Figure 2.14 (c), the forces lead to a torque about the center of the rod.

An object is said to be in *equilibrium* if two conditions are met. The first condition is that the sum of all external forces acting on the object must be zero. That is, if \mathbf{F}_i for $1 \leq i \leq n$ are the external forces, then $\sum_{i=1}^n \mathbf{F}_i = \mathbf{0}$. The second condition is that the torques on the object must sum to zero, as we see intuitively in Figure 2.14 (d). The two endpoints have mass, but the rod connecting them is assumed to be massless. Let the

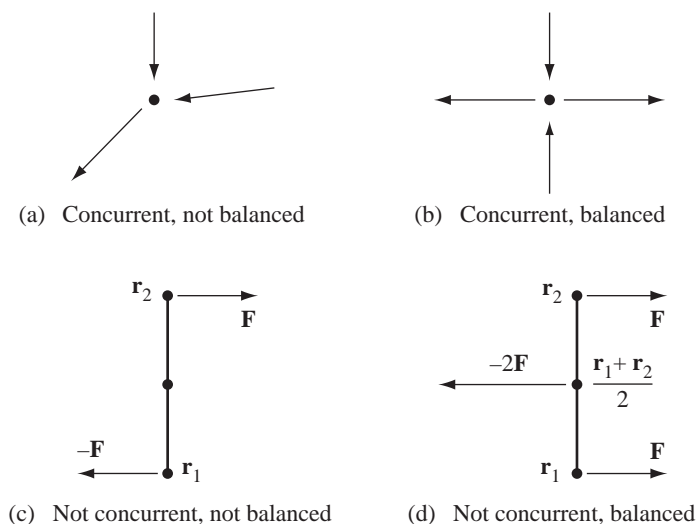


Figure 2.14 (a) All forces applied to a point mass are concurrent but are not balanced, so the point moves. (b) All forces are concurrent but do balance, so the point does not move. (c) A rigid rod with nonconcurrent forces applied to the endpoints. The forces are equal in magnitude but opposite in direction. The rod rotates about its center. (d) Nonconcurrent forces are applied to three locations, two forces of equal magnitudes and directions at the endpoints and one force of twice the magnitude of an endpoint force but opposite in direction applied to the rod center. The rod is balanced and does not rotate about its center.

lower endpoint be at position \mathbf{r}_1 and the upper endpoint be at position \mathbf{r}_2 . Let the force applied to the upper point be \mathbf{F} and the force applied to the lower point be $-\mathbf{F}$. We have a force couple with total torque $\tau = \mathbf{r}_2 \times \mathbf{F} + \mathbf{r}_1 \times (-\mathbf{F}) = (\mathbf{r}_2 - \mathbf{r}_1) \times \mathbf{F}$. The torque is a nonzero vector perpendicular to the plane of the diagram. The configuration in Figure 2.14 is not in equilibrium even though the sum of the forces is $\mathbf{F} + (-\mathbf{F}) = \mathbf{0}$. In Figure 2.14 (d), the center point is $(\mathbf{r}_1 + \mathbf{r}_2)/2$. The system shown has a total torque of zero, assuming the vectors at the endpoints are both \mathbf{F} and the vector at the center point $(\mathbf{r}_1 + \mathbf{r}_2)/2$ is $-2\mathbf{F}$. The total torque is $\tau = \mathbf{r}_1 \times \mathbf{F} + \mathbf{r}_2 \times \mathbf{F} + (\mathbf{r}_1 + \mathbf{r}_2)/2 \times (-2\mathbf{F}) = \mathbf{0}$. This system is in equilibrium since the forces sum to zero and the torques sum to zero.

An important observation is that an object in equilibrium is not necessarily stationary. It is possible that the inertial frame in which the object is measured is moving with constant velocity. However, another coordinate system may be chosen in which the object is not moving. A simple example, to a first approximation, is the fact that you are currently reading this book while in equilibrium sitting in your chair, even though the Earth is rotating with an angular speed of 1,000 miles per hour! The first approximation is that your current physical location moves along a straight line with constant velocity, at least over a short period of time, thus making it an inertial frame.

For a single particle, the second condition for equilibrium is a consequence of the first condition. Let the particle be located at \mathbf{r} and let the applied forces be \mathbf{F}_i for $1 \leq i \leq n$. Assume that the sum of forces is zero, $\sum_{i=1}^n \mathbf{F}_i = \mathbf{0}$. The total torque on the particle is

$$\tau = \sum_{i=1}^n \mathbf{r} \times \mathbf{F}_i = \mathbf{r} \times \sum_{i=1}^n \mathbf{F}_i = \mathbf{r} \times \mathbf{0} = \mathbf{0}$$

For a particle system whose external forces sum to zero, the total torque is not necessarily zero, in which case the second condition for equilibrium is independent of the first. However, it is true that the torque relative to one point is the same as the torque relative to another. Let the particles be at positions \mathbf{r}_i for $1 \leq i \leq p$. Let the forces on particle i be $\mathbf{F}_j^{(i)}$ for $1 \leq j \leq n_i$ (the number of forces per particle may vary). The torque relative to an origin \mathbf{A} for a single particle subject to a single force is

$$(\mathbf{r}_i - \mathbf{A}) \times \mathbf{F}_j^{(i)}$$

The total torque for the particle is

$$\sum_{j=1}^{n_i} (\mathbf{r}_i - \mathbf{A}) \times \mathbf{F}_j^{(i)}$$

The total torque for the particle system, relative to origin \mathbf{A} , is

$$\tau_A = \sum_{i=1}^p \sum_{j=1}^{n_i} (\mathbf{r}_i - \mathbf{A}) \times \mathbf{F}_j^{(i)} = \sum_{i=1}^p (\mathbf{r}_i - \mathbf{A}) \times \mathbf{G}^{(i)}$$

where

$$\mathbf{G}^{(i)} = \sum_{j=1}^{n_i} \mathbf{F}_j^{(i)}$$

is the total applied force on particle i . The total torque relative to another origin \mathbf{B} is

$$\boldsymbol{\tau}_{\mathbf{B}} = \sum_{i=1}^p (\mathbf{r}_i - \mathbf{B}) \times \mathbf{G}^{(i)}$$

The difference is

$$\boldsymbol{\tau}_{\mathbf{A}} - \boldsymbol{\tau}_{\mathbf{B}} = \sum_{i=1}^p (\mathbf{B} - \mathbf{A}) \times \mathbf{G}^{(i)} = (\mathbf{B} - \mathbf{A}) \times \sum_{i=1}^p \mathbf{G}^{(i)} = (\mathbf{B} - \mathbf{A}) \times \mathbf{0} = \mathbf{0}$$

where the $\mathbf{G}^{(i)}$ summing to zero is the mathematical statement that the net force on the particle system is zero. Thus, $\boldsymbol{\tau}_{\mathbf{A}} = \boldsymbol{\tau}_{\mathbf{B}}$ and the torque is the same about any point. A similar argument applies to a continuum of mass. When setting up equations of equilibrium, it is enough to require the sum of the external forces to be zero *and* the torque about a single point to be zero.

2.5 MOMENTA

In this section we are presented with the definitions for various physical quantities that are relevant to understanding the motion of an object undergoing external forces. We already saw one such quantity, torque. The first portion of this section introduces the concepts of linear and angular momentum. The second portion covers the concept you should be most familiar with, mass of an object. We derive formulas for computing the center of mass of an object, whether it consists of a finite number of point masses (discrete) or is a solid body (continuous). The construction of the center of mass involves a quantity called a *moment*, a summation for discrete masses and an integral for continuous masses. The third portion discusses moments and products of inertia, a topic that is particularly important when discussing motion of a rigid body.

2.5.1 LINEAR MOMENTUM

We have already seen the concept of *linear momentum* in the presentation of Newton's second law of motion for a single particle. The linear momentum is the product

$$\mathbf{p} = m\mathbf{v} \tag{2.56}$$

where m is the mass of the particle and \mathbf{v} is its velocity. The applied force and momentum are related by $\mathbf{F} = d\mathbf{p}/dt$; that is, an applied force on the particle causes a change in its linear momentum. For a system of p particles of masses m_i and velocities \mathbf{v}_i for $1 \leq i \leq p$, the linear momentum is

$$\mathbf{p} = \sum_{i=1}^p m_i \mathbf{v}_i \quad (2.57)$$

If the object is a continuum of mass that occupies a region R , the linear momentum is

$$\mathbf{p} = \int_R \mathbf{v} dm = \int_R \delta \mathbf{v} dR \quad (2.58)$$

where $dm = \delta dR$ is an infinitesimal measurement of mass. The function δ is the mass density. The density and velocity \mathbf{v} may depend on spatial location; they cannot be factored outside the integral. In a loose sense the integration over the region is a summation of the linear momenta of the infinitely many particles occupying that region. You will find the trichotomy represented by the equations (2.56), (2.57), and (2.58) throughout the rest of this book. We will consider physical systems that consist of a single particle, of multiple particles, or of a continuum of mass.

An important physical law is the *conservation of linear momentum*. The law states that if the net external force on a system of objects is zero, the linear momentum is a constant. This law is an immediate consequence of Newton's second law. In the single particle case, if \mathbf{F}_i for $1 \leq i \leq n$ are the external forces acting on the particle, then

$$\mathbf{0} = \sum_{i=1}^n \mathbf{F}_i = \frac{d(m\mathbf{v})}{dt} = \frac{d\mathbf{p}}{dt}$$

The derivative of \mathbf{p} is the zero vector, which implies that \mathbf{p} is a constant. Similar arguments apply in the cases of a discrete system and of a continuous system.

2.5.2 ANGULAR MOMENTUM

Linear momentum has some intuition about it. You think of it as a measure of inertia, the tendency to *remain in motion along a straight line* in the absence of any external forces. *Angular momentum* is less intuitive but is similar in nature. The quantity measures the tendency to *continue rotating about an axis*. For a single particle of mass m , the angular momentum of that particle about the origin is

$$\mathbf{L} = \mathbf{r} \times \mathbf{p} = \mathbf{r} \times m\mathbf{v} \quad (2.59)$$

where \mathbf{r} is the vector from the origin to the particle and \mathbf{v} is the velocity of the particle. The angular momentum vector \mathbf{L} is necessarily perpendicular to both \mathbf{r} and \mathbf{v} . The direction of \mathbf{L} is that of the axis of rotation at each instant of time. For a system

of p particles of masses m_i , positions \mathbf{r}_i relative to the origin, and velocities \mathbf{v}_i for $1 \leq i \leq p$, the angular momentum is

$$\mathbf{L} = \sum_{i=1}^p \mathbf{r}_i \times m_i \mathbf{v}_i \quad (2.60)$$

If the object is a continuum of mass that occupies a region R , the angular momentum is

$$\mathbf{L} = \int_R \mathbf{r} \times \mathbf{v} dm = \int_R \delta \mathbf{r} \times \mathbf{v} dR \quad (2.61)$$

where $dm = \delta dR$ is an infinitesimal measurement of mass. The function δ is the mass density. The density, position \mathbf{r} , and velocity \mathbf{v} may depend on spatial location.

Just as force is the time derivative of linear momentum, torque is the time derivative of angular momentum. To see this, differentiate equation (2.59) with respect to time:

$$\begin{aligned} \frac{d\mathbf{L}}{dt} &= \frac{d(\mathbf{r} \times \mathbf{p})}{dt} && \text{From equation (2.59)} \\ &= \mathbf{r} \times \frac{d\mathbf{p}}{dt} + \frac{d\mathbf{r}}{dt} \times \mathbf{p} && \text{Using the chain rule} \\ &= \mathbf{r} \times \mathbf{F} && \text{From Newton's Second Law and } \mathbf{v} \times \mathbf{v} = \mathbf{0} \\ &= \boldsymbol{\tau} && \text{From equation (2.53)} \end{aligned} \quad (2.62)$$

Similar constructions may be applied to the pair of equations (2.60) and (2.54) or to the pair (2.61) and (2.55).

Another important physical law is the *conservation of angular momentum*. The law states that if the net external torque on a system of objects is zero, the angular momentum is a constant. The proof is similar to that of the conservation of linear momentum. In the single-particle case, if \mathbf{F}_i for $1 \leq i \leq n$ are the external forces acting on the particle, then

$$\frac{d\mathbf{L}}{dt} = \sum_{i=1}^n \mathbf{r}_i \times \mathbf{F}_i = \mathbf{r} \times \sum_{i=1}^n \mathbf{F}_i = \mathbf{r} \times \mathbf{0} = \mathbf{0}$$

The derivative of \mathbf{L} is the zero vector, which implies that \mathbf{L} is a constant. Similar arguments apply in the cases of a discrete system and of a continuous system.

2.5.3 CENTER OF MASS

In many mechanical systems, each object can behave as if its mass is concentrated at a single point. The location of this point is called the *center of mass* of the object. This section shows how to define and compute the center of mass in one, two, and three dimensions, both for discrete sets of points and continuous materials.

Discrete Mass in One Dimension

Consider two masses m_1 and m_2 on the x -axis at positions x_1 and x_2 . The line segment connecting the two points is assumed to have negligible mass. Gravity is assumed to exert itself in the downward direction. You can imagine this system as a child's seesaw that consists of a wooden plank, a supporting base placed somewhere between the ends of the plank, and two children providing the masses at the ends. Figure 2.15 illustrates the system. The supporting base is drawn as a wedge whose uppermost vertex is positioned at \bar{x} .

If we select $\bar{x} = x_1$, clearly the system is not balanced because the torque induced by the mass m_2 will cause that mass to fall to the ground. Similarly, the system is not balanced for $\bar{x} = x_2$. Your intuition should tell you that there is a proper choice of \bar{x} between x_1 and x_2 at which the system is balanced. If $m_1 = m_2$, the symmetry of the situation suggests that $\bar{x} = (x_1 + x_2)/2$, the midpoint of the line segment. For different masses, the choice of \bar{x} is not immediately clear, but we can rely on equilibrium of forces to help us. The force on mass m_i due to gravity g is $m_i g$. The torque for mass m_i about the position \bar{x} is $m_i g(x_i - \bar{x})$. For the system to balance at \bar{x} , the total torque must be zero,

$$0 = m_1 g(x_1 - \bar{x}) + m_2 g(x_2 - \bar{x}) = g[(m_1 x_1 + m_2 x_2) - (m_1 + m_2) \bar{x}]$$

The solution to the equation is

$$\bar{x} = \frac{m_1 x_1 + m_2 x_2}{m_1 + m_2} = \frac{m_1}{m_1 + m_2} x_1 + \frac{m_2}{m_1 + m_2} x_2 = w_1 x_1 + w_2 x_2 \quad (2.63)$$

which is a weighted average of the positions of the masses called the *center of mass*. If m_1 is larger than m_2 , your intuition should tell you that the center of mass should be closer to x_1 than to x_2 . The coefficient of x_1 , $w_1 = m_1/(m_1 + m_2)$, is larger than the coefficient of x_2 , $w_2 = m_2/(m_1 + m_2)$, so in fact the center of mass is closer to x_1 , as expected.

A similar formula is derived for the center of mass \bar{x} of p masses m_1 through m_p located at positions x_1 through x_p . The total torque is zero, $\sum_{i=1}^p m_i g(x_i - \bar{x}) = 0$,



Figure 2.15 Balancing discrete masses on a line. The center of mass for two masses viewed as the balance point for a seesaw on a fulcrum.

the solution being

$$\bar{x} = \frac{\sum_{i=1}^p m_i x_i}{\sum_{i=1}^p m_i} = \sum_{i=1}^p \frac{m_i}{\sum_{j=1}^p m_j} x_i = \sum_{i=1}^p w_i x_i \quad (2.64)$$

The sum $\sum_{i=1}^p m_i$ is the *total mass of the system* and the sum $\sum_{i=1}^p m_i x_i$ is the *moment of the system about the origin*.

Continuous Mass in One Dimension

The center of mass for a discrete set of masses was simple enough to compute. All you need are the masses themselves and their locations on the x -axis. However, you might very well be interested in computing the center of mass for a wire of finite length. Let us assume that the endpoints of the wire are located at a and b , with $a < b$. The wire consists of a continuum of particles, infinitely many so to speak. Each particle has an infinitesimal amount of mass – call this dm – and is located at some position x . The infinitesimal mass is distributed over an infinitesimal interval of length dx . The mass values can vary over this interval, so we need to know the mass density $\delta(x)$ at each point x . The units of density are mass per unit length, from which it follows $dm = \delta(x)dx$. Figure 2.16 is the continuous analogy of Figure 2.15. The gray levels are intended to illustrate varying density, dark levels for large density and light levels for small density.

The infinitesimal force due to gravity is $g dm$ and the infinitesimal torque about a position \bar{x} is $(x - \bar{x})g dm$. For \bar{x} to be the center of mass, the total torque must be zero. You should recognize this as a problem suited for calculus. The summation that occurred for discrete point sets is replaced by integration for a continuum of points. The equilibrium condition for torque is

$$\int_a^b (x - \bar{x}) g dm = g \int_a^b (x - \bar{x}) \delta(x) dx = 0$$

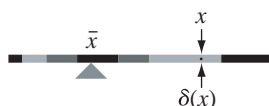


Figure 2.16 Balancing continuous masses on a line. The center of mass for the wire is viewed as the balance point for a seesaw on a fulcrum. A general point location x is shown, labeled with its corresponding mass density $\delta(x)$.

This equation can be solved to produce the center of mass:

$$\bar{x} = \frac{\int_a^b x\delta(x) dx}{\int_a^b \delta(x) dx} \quad (2.65)$$

The integral $\int_a^b \delta dx$ is the *total mass of the system* and the integral $\int_a^b x\delta dx$ is the *moment of the system about the origin*. If the density of the system is constant, say $\delta(x) = c$ for all x , equation (2.65) reduces to

$$\bar{x} = \frac{\int_a^b xc dx}{\int_a^b c dx} = \frac{\int_a^b x dx}{\int_a^b dx} = \frac{(b^2 - a^2)/2}{b - a} = \frac{b + a}{2}$$

As expected, the center of mass for a constant density wire is situated at the midpoint of the wire.

Discrete Mass in Two Dimensions

The extension of the computation of center of mass from one to two dimensions is straightforward. Let the p masses be m_i and located at (x_i, y_i) for $1 \leq i \leq p$. Imagine these lying on a thin, massless plate. Gravity is assumed to exert itself in the downward direction; the magnitude of the force is g . The center of mass is the point (\bar{x}, \bar{y}) , such that the plate balances when placed on a support at that location. Figure 2.17 illustrates this.

The gravitational force exerted on each mass is $m_i g$. The torque about (\bar{x}, \bar{y}) is $m_i g(x_i - \bar{x}, y_i - \bar{y})$. The total torque must be the zero vector,

$$\sum_{i=1}^p m_i g(x_i - \bar{x}, y_i - \bar{y}) = (0, 0)$$

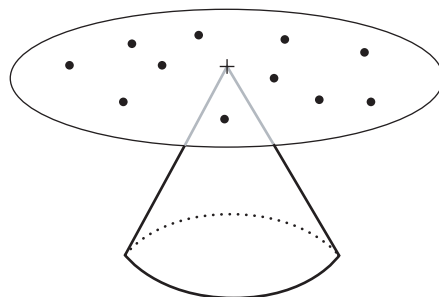


Figure 2.17 Balancing discrete masses in a plane.

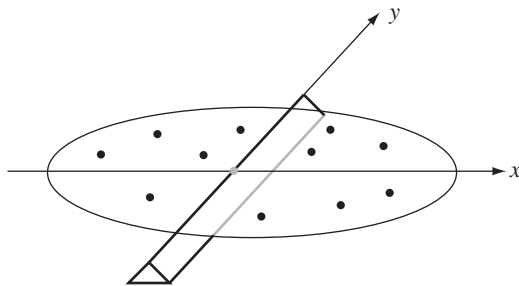


Figure 2.18 Balancing discrete masses in a plane on a fulcrum.

The equation is easily solved to produce the center of mass:

$$(\bar{x}, \bar{y}) = \frac{\sum_{i=1}^p m_i(x_i, y_i)}{\sum_{i=1}^p m_i} = \left(\frac{\sum_{i=1}^p m_i x_i}{\sum_{i=1}^p m_i}, \frac{\sum_{i=1}^p m_i y_i}{\sum_{i=1}^p m_i} \right) \quad (2.66)$$

The sum $m = \sum_{i=1}^p m_i$ is the *total mass of the system*. The sum $M_y = \sum_{i=1}^p m_i x_i$ is the *moment of the system about the y-axis* and the sum $M_x = \sum_{i=1}^p m_i y_i$ is the *moment of the system about the x-axis*.

The center of mass formula has some interesting interpretations. First, observe that if you look only at the x -components of the mass locations (i.e., project the masses onto the x -axis), \bar{x} is the center of mass of the projected points. Similarly, \bar{y} is the center of mass of the points projected onto the y -axis. Second, observe that the thin, massless plate containing the masses balances when placed on a fulcrum whose top edge contains the center of mass and is parallel to either of the coordinate axes. Figure 2.18 illustrates this.

EXERCISE
2.9

Show that the plate balances on a fulcrum containing the center of mass *regardless of the fulcrum's orientation*. ■

Continuous Mass in Two Dimensions

Now let us consider the case of a continuum of mass that lies in a bounded region R in the xy -plane. As in the one-dimensional case, each point in the region has an associated infinitesimal mass, dm . The mass is distributed over an infinitesimal rectangle of size dx by dy and having area $dA = dx dy$, the distribution represented by a density function $\delta(x, y)$ with units of mass per unit area. Thus, the infinitesimal mass is $dm = \delta dA = \delta dx dy$. Figure 2.19 illustrates.

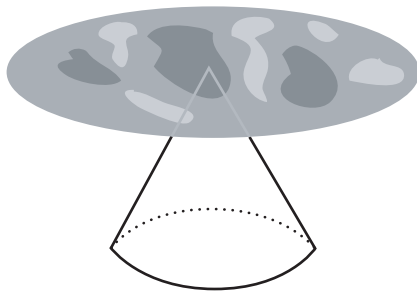


Figure 2.19 Balancing continuous masses in a plane. The shades of gray indicate variable mass density.

The infinitesimal torque relative to a location (\bar{x}, \bar{y}) is $(x - \bar{x}, y - \bar{y})g dm$. The equilibrium condition is

$$\iint_R (x - \bar{x}, y - \bar{y})g dm = 0$$

The center of mass is obtained by solving this equation:

$$(\bar{x}, \bar{y}) = \left(\frac{\iint_R x \delta(x, y) dx dy}{\iint_R \delta(x, y) dx dy}, \frac{\iint_R y \delta(x, y) dx dy}{\iint_R \delta(x, y) dx dy} \right) \quad (2.67)$$

The integral $m = \iint_R \delta dx dy$ is the *total mass of the system*. The integral $M_y = \iint_R x \delta dx dy$ is the *moment of the system about the y-axis* and the integral $M_x = \iint_R y \delta dx dy$ is the *moment of the system about the x-axis*.

EXAMPLE 2.3

Consider the region R bounded by the parabola $y = x^2$ and the line $y = 1$. Let the mass density be constant, $\delta(x, y) = 1$ for all (x, y) . Figure 2.20 shows the region.

Your intuition should tell you that the center of mass must lie on the y -axis, $\bar{x} = 0$, and the value \bar{y} should be closer to $y = 1$ than it is to $y = 0$. The total mass of the system is

$$m = \iint_R dy dx = \int_{-1}^1 \int_{x^2}^1 dy dx = \int_{-1}^1 1 - x^2 dx = \frac{4}{3}$$

The moment about the y -axis is

$$M_y = \iint_R x dy dx = \int_{-1}^1 \int_{x^2}^1 x dy dx = \int_{-1}^1 x(1 - x^2) dx = \frac{x^2}{2} - \frac{x^4}{4} \Big|_{-1}^1 = 0$$

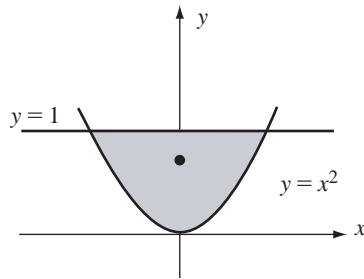
(Example 2.3
continued)

Figure 2.20

A continuous mass bounded by a parabola and a line.

The moment about the x -axis is

$$M_x = \iint_R y \, dy \, dx = \int_{-1}^1 \int_{x^2}^1 y \, dy \, dx = \int_{-1}^1 \frac{1-x^4}{2} \, dx = \frac{4}{5}$$

The center of mass is therefore $(\bar{x}, \bar{y}) = (M_y, M_x)/m = (0, 3/5)$. As predicted, the center of mass is on the y -axis and is closer to $y = 1$ than to $y = 0$. ■

In many situations the continuous mass is in a bounded region with positive area. But we must also consider the case where the mass is distributed along a curve. The typical physical example is one of computing the center of mass of a planar wire whose mass density varies with arc length along the wire. Let the curve be continuously differentiable and specified parametrically by $(x(t), y(t))$ for $t \in [a, b]$. In terms of arc length s , the mass density is $\bar{\delta}(s)$. In terms of the curve parameter, it is specified parametrically as $\delta(t)$. The infinitesimal mass at the position corresponding to t is distributed over an infinitesimal arc length ds of the wire. The infinitesimal mass is $dm = \delta(t) ds$, where $ds = \sqrt{\dot{x}^2 + \dot{y}^2} dt$ for parametric curves (again, the dot symbol denotes differentiation with respect to t). The total mass of the wire is therefore

$$m = \int_0^L \bar{\delta}(s) \, ds = \int_a^b \delta(t) \sqrt{\dot{x}^2 + \dot{y}^2} \, dt$$

where s is the arc length parameter and L is the total length of the curve. The rightmost integral is the formulation in terms of the curve parameter, making it the integral that is actually evaluated. The moment about the y -axis is

$$M_y = \int_0^L x \bar{\delta}(s) \, ds = \int_a^b x(t) \delta(t) \sqrt{\dot{x}^2 + \dot{y}^2} \, dt$$

and the moment about the x -axis is

$$M_x = \int_0^L y\delta(s) ds = \int_a^b y(t)\delta(t) \sqrt{\dot{x}^2 + \dot{y}^2} dt$$

The center of mass is

$$(\bar{x}, \bar{y}) = \frac{(M_y, M_x)}{m} = \frac{\left(\int_a^b x(t)\delta(t) \sqrt{\dot{x}^2 + \dot{y}^2} dt, \int_a^b y(t)\delta(t) \sqrt{\dot{x}^2 + \dot{y}^2} dt \right)}{\int_a^b \delta(t) \sqrt{\dot{x}^2 + \dot{y}^2} dt} \quad (2.68)$$

**EXAMPLE
2.4**

Compute the center of mass for a wire of constant density 1 and that lies on the hemicircle $x^2 + y^2 = 1$ for $y \geq 0$, as shown in Figure 2.21.

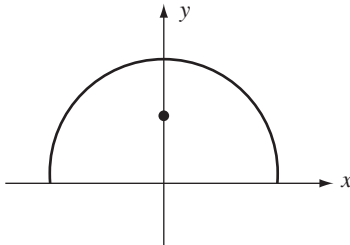


Figure 2.21

A continuous mass in the shape of a hemicircle.

By symmetry, the center of mass should lie on the y -axis, $\bar{x} = 0$, so let us calculate only the value for \bar{y} . The curve is parameterized by $(x(t), y(t)) = (\cos(t), \sin(t))$ for $t \in [0, \pi]$. The derivative of the curve is $(x'(t), y'(t)) = (-\sin(t), \cos(t))$. The total mass is

$$m = \int_0^\pi \sqrt{\dot{x}^2 + \dot{y}^2} dt = \int_0^\pi dt = \pi$$

The length of the hemicircle is π units of distance, but keep in mind that the units of mass are not distance. The moment about the x -axis is

$$M_x = \int_0^\pi y(t) \sqrt{\dot{x}^2 + \dot{y}^2} dt = \int_0^\pi \sin(t) dt = 2$$

The y -value for the center of mass is therefore $\bar{y} = M_x/m = 2/\pi \doteq 0.64$. The center of mass is clearly not on the wire itself. If the wire were to be placed on a thin, massless plate, the balancing point for the plate and wire would be at $(0, 2/\pi)$. ■

**EXERCISE
2.10**

Show that the center of mass for the half-disk $x^2 + y^2 \leq 1$, with $y \geq 0$, has $\bar{x} = 0$ and $\bar{y} = 4/(3\pi) \doteq 0.42$. The y -value is smaller than that of the wire, as is to be expected because the additional mass inside the hemicircle should bias the y -value toward the origin. ■

Discrete Mass in Three Dimensions

Let the p masses be m_i and located at (x_i, y_i, z_i) for $1 \leq i \leq p$. Imagine these lying within a massless gel. Gravity is assumed to exert itself in the downward direction; the magnitude of the force is g . The center of mass is the point $(\bar{x}, \bar{y}, \bar{z})$, such that the gel balances when a support is embedded at that location. The gravitational force exerted on each mass is $m_i g$. The torque about $(\bar{x}, \bar{y}, \bar{z})$ is $m_i g(x_i - \bar{x}, y_i - \bar{y}, z_i - \bar{z})$. The total torque must be the zero vector,

$$\sum_{i=1}^p m_i g(x_i - \bar{x}, y_i - \bar{y}, z_i - \bar{z}) = (0, 0, 0)$$

The equation is easily solved to produce the center of mass:

$$(\bar{x}, \bar{y}, \bar{z}) = \frac{\sum_{i=1}^p m_i (x_i, y_i, z_i)}{\sum_{i=1}^p m_i} = \left(\frac{\sum_{i=1}^p m_i x_i}{\sum_{i=1}^p m_i}, \frac{\sum_{i=1}^p m_i y_i}{\sum_{i=1}^p m_i}, \frac{\sum_{i=1}^p m_i z_i}{\sum_{i=1}^p m_i} \right) \quad (2.69)$$

The sum $m = \sum_{i=1}^p m_i$ is the *total mass of the system*. The sum $M_{yz} = \sum_{i=1}^p m_i x_i$ is the *moment of the system about the yz-plane*, the sum $M_{xz} = \sum_{i=1}^p m_i y_i$ is the *moment of the system about the xz-plane*, and the sum $M_{xy} = \sum_{i=1}^p m_i z_i$ is the *moment of the system about the xy-plane*.

Continuous Mass in Three Dimensions

We have three different possibilities to consider. The mass can be situated in a bounded volume, on a surface, or along a curve.

Volume Mass

In the case of a bounded volume V , the infinitesimal mass dm at (x, y, z) is distributed in an infinitesimal cube with dimensions dx , dy , and dz and volume $dV = dx dy dz$. The density of the distribution is $\delta(x, y, z)$, so the infinitesimal mass is $dm = \delta dV = \delta dx dy dz$. The total torque is the zero vector,

$$\iiint_V (x - \bar{x}, y - \bar{y}, z - \bar{z}) g dm = 0$$

The center of mass is obtained by solving this equation:

$$\begin{aligned} (\bar{x}, \bar{y}, \bar{z}) &= \frac{\iiint_V (x, y, z) \delta \, dx \, dy \, dz}{\iiint_V \delta \, dx \, dy \, dz} \\ &= \left(\frac{\iiint_V x \delta \, dx \, dy \, dz}{\iiint_V \delta \, dx \, dy \, dz}, \frac{\iiint_V y \delta \, dx \, dy \, dz}{\iiint_V \delta \, dx \, dy \, dz}, \frac{\iiint_V z \delta \, dx \, dy \, dz}{\iiint_V \delta \, dx \, dy \, dz} \right) \end{aligned} \quad (2.70)$$

The integral $m = \iiint_V \delta \, dx \, dy \, dz$ is the *total mass of the system*. The integral $M_{yz} = \iiint_V x \delta \, dx \, dy \, dz$ is the *moment of the system about the yz-plane*, the integral $M_{xz} = \iiint_V y \delta \, dx \, dy \, dz$ is the *moment of the system about the xz-plane*, and the integral $M_{xy} = \iiint_V z \delta \, dx \, dy \, dz$ is the *moment of the system about the xy-plane*.

EXAMPLE
2.5

Compute the center of mass of the solid hemisphere $x^2 + y^2 + z^2 \leq 1$, with $z \geq 0$, assuming the density is a constant $\delta \equiv 1$. From the symmetry, we know that $\bar{x} = \bar{y} = 0$. The numerical value of the total mass should be the same as the volume of the hemisphere, $m = 2\pi/3$. Let us verify that anyway. The mass integral is computed using a change to spherical coordinates:

$$\begin{aligned} m &= \iiint_V dx \, dy \, dz \\ &= \int_0^{\pi/2} \int_0^1 \int_0^{2\pi} \rho^2 \sin \phi \, d\theta \, d\rho \, d\phi \\ &= \left(\int_0^{\pi/2} \sin \phi \, d\phi \right) \left(\int_0^1 \rho^2 \, d\rho \right) \left(\int_0^{2\pi} d\theta \right) \\ &= (1)(1/3)(2\pi) \\ &= 2\pi/3 \end{aligned}$$

The moment about the xy -plane is

$$\begin{aligned} M_{xy} &= \iiint_V z \, dx \, dy \, dz \\ &= \int_0^{\pi/2} \int_0^1 \int_0^{2\pi} (\rho \cos \phi) \rho^2 \sin \phi \, d\theta \, d\rho \, d\phi \\ &= \left(\int_0^{\pi/2} \sin \phi \cos \phi \, d\phi \right) \left(\int_0^1 \rho^3 \, d\rho \right) \left(\int_0^{2\pi} d\theta \right) \\ &= (1/2)(1/4)(2\pi) \\ &= \pi/4 \end{aligned}$$

(Example 2.5
continued) | The z -value of the center of mass is $\bar{z} = M_{xy}/m = 3/8 = 0.375$. As you might have predicted, the point is closer to the xy -plane than to the pole of the hemisphere. ■

Surface Mass

In the case of a bounded surface S , the infinitesimal mass dm at (x, y, z) is distributed in an infinitesimal surface area dS . The representation of dS depends on how the surface is defined. If the surface is the graph of the function $z = f(x, y)$, then

$$dS = \sqrt{1 + \left(\frac{\partial f}{\partial x}\right)^2 + \left(\frac{\partial f}{\partial y}\right)^2} dx dy$$

If the surface is defined parametrically as $\mathbf{P}(u, v) = (x(u, v), y(u, v), z(u, v))$, then

$$dS = \left| \frac{\partial \mathbf{P}}{\partial u} \times \frac{\partial \mathbf{P}}{\partial v} \right| du dv$$

The density of the distribution is δ and is assumed to be a function defined at each point on the surface. Solving the equilibrium equation for torque, the center of mass for the surface is

$$(\bar{x}, \bar{y}, \bar{z}) = \frac{\iint_S (x, y, z) \delta \, dS}{\iint_S \delta \, dS} = \left(\frac{\iint_S x \delta \, dS}{\iint_S \delta \, dS}, \frac{\iint_S y \delta \, dS}{\iint_S \delta \, dS}, \frac{\iint_S z \delta \, dS}{\iint_S \delta \, dS} \right) \quad (2.71)$$

where the integration is performed over the two-dimensional surface (hence, the use of double integrals). The integral $m = \iint_S \delta \, dS$ is the *total mass of the system*. The integral $M_{yz} = \iint_S x \delta \, dS$ is the *moment of the system about the yz-plane*; the integral $M_{xz} = \iint_S y \delta \, dS$ is the *moment of the system about the xz-plane*; and the integral $M_{xy} = \iint_S z \delta \, dS$ is the *moment of the system about the xy-plane*.

EXAMPLE 2.6

Compute the center of mass of the hemisphere $x^2 + y^2 + z^2 = 1$, with $z \geq 0$, assuming the density is a constant $\delta \equiv 1$. From the symmetry, we know that $\bar{x} = \bar{y} = 0$. The numerical value of the total mass should be the same as the area of the hemisphere, $m = 2\pi$. The mass integral is computed using a change to spherical coordinates with $\delta = 1$:

$$\begin{aligned} m &= \iint_S dS \\ &= \int_0^{\pi/2} \int_0^{2\pi} \sin \phi \, d\theta \, d\phi \\ &= \left(\int_0^{\pi/2} \sin \phi \, d\phi \right) \left(\int_0^{2\pi} d\theta \right) \\ &= 2\pi \end{aligned}$$

(Example 2.6
continued)

The moment about the xy -plane is

$$\begin{aligned} M_{xy} &= \iint_S z \, dS \\ &= \int_0^{\pi/2} \int_0^{2\pi} (\cos \phi) \sin \phi \, d\theta \, d\phi \\ &= \left(\int_0^{\pi/2} \sin \phi \cos \phi \, d\phi \right) \left(\int_0^{2\pi} d\theta \right) \\ &= \pi \end{aligned}$$

The z -value of the center of mass is $\bar{z} = M_{xy}/m = 1/2 = 0.5$. This value is closer to the pole than its counterpart for the solid hemisphere, as expected. ■

Curve Mass

Last of all, suppose that the continuous material is a wire that consists of mass distributed along a curve in three dimensions. Let the curve be continuously differentiable and specified parametrically by $(x(t), y(t), z(t))$ for $t \in [a, b]$. In terms of arc length, s , the mass density is $\bar{\delta}(s)$. In terms of the curve parameter, it is specified parametrically as $\delta(t)$. The infinitesimal mass at the position corresponding to t is distributed over an infinitesimal arc length ds of the wire. The infinitesimal mass is $dm = \delta(t) ds$, where $ds = \sqrt{\dot{x}^2 + \dot{y}^2 + \dot{z}^2} dt$ for parametric curves in space; the dot symbol denotes differentiation with respect to t . The total mass of the wire is therefore

$$m = \int_0^L \bar{\delta}(s) \, ds = \int_a^b \delta(t) \sqrt{\dot{x}^2 + \dot{y}^2 + \dot{z}^2} \, dt$$

where s is the arc length parameter and L is the total length of the curve. The right-most integral is the formulation in terms of the curve parameter, making it the integral that is actually evaluated. The moment about the yz -plane is

$$M_{yz} = \int_0^L x \bar{\delta}(s) \, ds = \int_a^b x(t) \delta(t) \sqrt{\dot{x}^2 + \dot{y}^2 + \dot{z}^2} \, dt$$

the moment about the xz -plane is

$$M_{xz} = \int_0^L y \bar{\delta}(s) \, ds = \int_a^b y(t) \delta(t) \sqrt{\dot{x}^2 + \dot{y}^2 + \dot{z}^2} \, dt$$

and the moment about the xy -plane is

$$M_{xy} = \int_0^L z \bar{\delta}(s) \, ds = \int_a^b z(t) \delta(t) \sqrt{\dot{x}^2 + \dot{y}^2 + \dot{z}^2} \, dt$$

The center of mass is

$$(\bar{x}, \bar{y}, \bar{z}) = \frac{(M_{yz}, M_{xz}, M_{xy})}{m} = \frac{\int_a^b (x(t), y(t), z(t)) \delta(t) \sqrt{\dot{x}^2 + \dot{y}^2 + \dot{z}^2} dt}{\int_a^b \delta(t) \sqrt{\dot{x}^2 + \dot{y}^2 + \dot{z}^2} dt} \quad (2.72)$$

EXAMPLE
2.7

Compute the center of mass of a constant density wire in the shape of a helix, $(x(t), y(t), z(t)) = (\cos t, \sin t, t^2/2)$ for $t \in [0, 2\pi]$. For simplicity, set the density to 1. The mass of the wire is

$$\begin{aligned} m &= \int_0^{2\pi} \sqrt{\dot{x}^2 + \dot{y}^2 + \dot{z}^2} dt \\ &= \int_0^{2\pi} \sqrt{1+t^2} dt \\ &= \frac{1}{2} \left(t\sqrt{1+t^2} + \ln(t + \sqrt{1+t^2}) \right) \Big|_0^{2\pi} \\ &= \frac{2\pi\sqrt{1+4\pi^2} + \ln(2\pi + \sqrt{1+4\pi^2})}{2} \doteq 21.2563 \end{aligned}$$

The moment about the yz -plane is

$$M_{yz} = \int_0^{2\pi} x(t) \sqrt{\dot{x}^2 + \dot{y}^2 + \dot{z}^2} dt = \int_0^{2\pi} (\cos t) \sqrt{1+t^2} dt \doteq 0.386983$$

This integral cannot be evaluated in terms of elementary functions. A numerical integration leads to the approximation shown in the equation. Similarly,

$$M_{xz} = \int_0^{2\pi} y(t) \sqrt{\dot{x}^2 + \dot{y}^2 + \dot{z}^2} dt = \int_0^{2\pi} (\sin t) \sqrt{1+t^2} dt \doteq -5.82756$$

The last moment can be calculated in closed form and is

$$M_{xy} = \int_0^{2\pi} z(t) \sqrt{\dot{x}^2 + \dot{y}^2 + \dot{z}^2} dt = \int_0^{2\pi} \frac{t^2}{2} \sqrt{1+t^2} dt \doteq 199.610$$

The center of mass is

$$(\bar{x}, \bar{y}, \bar{z}) = (M_{yz}, M_{xz}, M_{xy}) / m \doteq (0.018206, -0.274157, 9.390627)$$

■

2.5.4 MOMENTS AND PRODUCTS OF INERTIA

Another moment quantity of physical significance is *moment of inertia*. This is a measure of the rotational inertia of a body about an axis. The more difficult it is to set the object into rotation, the larger the moment of inertia about that axis. Intuitively this happens if the object's mass is large or if its distance from the axis is large. Empirical studies for a single particle show that the moment of inertia is mr^2 , where m is the mass of the particle and r is its distance to the axis. For completeness, we also look at the one- and two-dimensional problems and define moment of inertia with respect to a point, because there is no concept of rotation about a line in those dimensions.

Moment of Inertia in One Dimension

Given a discrete set of p particles with masses m_i and located on the real line at positions x_i , the total mass is $m = \sum_{i=1}^p m_i$. The moment with respect to the origin $x = 0$ is $M_0 = \sum_{i=1}^p m_i x_i$. This quantity showed up when computing the center of mass $\bar{x} = \sum_{i=1}^p m_i x_i / \sum_{i=1}^p m_i = M_0/m$. The motivation for \bar{x} is that it is the location for which $\sum_{i=1}^p m_i(x_i - \bar{x}) = 0$. The quantities $\sum_{i=1}^p m_i$ and $\sum_{i=1}^p m_i x_i$ are special cases of $\sum_{i=1}^p m_i x_i^k$, where $k = 0$ for the mass and $k = 1$ for the moment. The special case $k = 2$ has great physical significance itself. The quantity

$$I_0 = \sum_{i=1}^p m_i x_i^2 \quad (2.73)$$

is referred to as the *moment of inertia with respect to the origin of the real line*. The *moment of inertia with respect to the center of mass* is

$$I = \sum_{i=1}^p m_i(x_i - \bar{x})^2 = I_0 - m\bar{x}^2 \quad (2.74)$$

For a continuous mass located on the interval $[a, b]$ of the real line and with mass density $\delta(x)$, the total mass is $m = \int_a^b \delta(x) dx$ and the moment about the origin is $M_0 = \int_a^b x\delta(x) dx$. The center of mass is $\bar{x} = M_0/m$. The *moment of inertia with respect to the origin* is

$$I_0 = \int_a^b x^2 \delta(x) dx \quad (2.75)$$

and the *moment of inertia with respect to the center of mass* is

$$I = \int_a^b (x - \bar{x})^2 \delta(x) dx = I_0 - m\bar{x}^2 \quad (2.76)$$

with the right-hand side occurring just as in the discrete case.

Moment of Inertia in Two Dimensions

Given a discrete set of p particles with masses m_i and located in the plane at positions (x_i, y_i) , the total mass is $m = \sum_{i=1}^p m_i$. The moment with respect to the y -axis was defined as $M_y = \sum_{i=1}^p m_i x_i$, and the moment with respect to the x -axis was defined as $M_x = \sum_{i=1}^p m_i y_i$. The center of mass is $(\bar{x}, \bar{y}) = (M_y/m, M_x/m)$. We define the *moment of inertia with respect to the origin* as

$$I_0 = \sum_{i=1}^p m_i (x_i^2 + y_i^2) \quad (2.77)$$

The *moment of inertia with respect to the center of mass* is

$$I = \sum_{i=1}^p m_i |(x_i, y_i) - (\bar{x}, \bar{y})|^2 = I_0 - m(\bar{x}^2 + \bar{y}^2) \quad (2.78)$$

For a continuous mass located in the region R of the plane and having mass density $\delta(x, y)$, the total mass is $m = \iint_R \delta(x, y) dx dy$ and the moments with respect to the y - and x -axes are $M_y = \iint_R x \delta(x, y) dx dy$ and $M_x = \iint_R y \delta(x, y) dx dy$. The center of mass is $(\bar{x}, \bar{y}) = (M_y/m, M_x/m)$. The *moment of inertia with respect to the origin* is

$$I_0 = \iint_R (x^2 + y^2) \delta(x, y) dx dy \quad (2.79)$$

and the *moment of inertia with respect to the center of mass* is

$$I = \iint_R ((x - \bar{x})^2 + (y - \bar{y})^2) \delta(x, y) dx dy = I_0 - m(\bar{x}^2 + \bar{y}^2) \quad (2.80)$$

with the right-hand side occurring just as in the discrete case.

Moment of Inertia in Three Dimensions

Of course the interesting case is in three dimensions. We could easily define a moment of inertia relative to a point, just as we did in one and two dimensions. However, keeping in mind that we are interested mainly in the motion of rigid bodies, if one point on the body rotates about a line (even if only instantaneously), then all other points rotate about that same line. In this sense it is more meaningful to define a moment of inertia relative to a line.

Given an origin \mathcal{O} and a discrete set of p particles with masses m_i located at $\mathbf{r}_i = (x_i, y_i, z_i)$ relative to \mathcal{O} , the total mass is $m = \sum_{i=1}^p m_i$. The moments with respect to

the xy -, xz -, and yz -planes were defined, respectively, as

$$M_{xy} = \sum_{i=1}^p m_i z_i, \quad M_{xz} = \sum_{i=1}^p m_i y_i, \quad \text{and} \quad M_{yz} = \sum_{i=1}^p m_i x_i$$

The center of mass is

$$(\bar{x}, \bar{y}, \bar{z}) = (M_{yz}/m, M_{xz}/m, M_{xy}/m)$$

The *moments of inertia about the x -, y -, and z -axes* are, respectively,

$$I_{xx} = \sum_{i=1}^p m_i (y_i^2 + z_i^2), \quad I_{yy} = \sum_{i=1}^p m_i (x_i^2 + z_i^2), \quad \text{and} \quad I_{zz} = \sum_{i=1}^p m_i (x_i^2 + y_i^2) \quad (2.81)$$

The *moment of inertia about a line L through O*, given parametrically as $O + t\mathbf{D}$ with unit-length direction vector $\mathbf{D} = (d_1, d_2, d_3)$, is the sum of $m_i r_i^2$, where r_i is the distance from \mathbf{r}_i to the line, or

$$\begin{aligned} I_L &= \sum_{i=1}^p m_i (|\mathbf{r}_i|^2 - (\mathbf{D} \cdot \mathbf{r}_i)^2) \\ &= d_1^2 \sum_{i=1}^p m_i (y_i^2 + z_i^2) + d_2^2 \sum_{i=1}^p m_i (x_i^2 + z_i^2) + d_3^2 \sum_{i=1}^p m_i (x_i^2 + y_i^2) \\ &\quad - 2d_1 d_2 \sum_{i=1}^p m_i x_i y_i - 2d_1 d_3 \sum_{i=1}^p m_i x_i z_i - 2d_2 d_3 \sum_{i=1}^p m_i y_i z_i \\ &= d_1^2 I_{xx} + d_2^2 I_{yy} + d_3^2 I_{zz} - 2d_1 d_2 I_{xy} - 2d_1 d_3 I_{xz} - 2d_2 d_3 I_{yz} \end{aligned} \quad (2.82)$$

where the first three terms contain the moments of inertia about the coordinate axes, and the last three terms have newly defined quantities called the *products of inertia*,

$$I_{xy} = \sum_{i=1}^p m_i x_i y_i, \quad I_{xz} = \sum_{i=1}^p m_i x_i z_i, \quad \text{and} \quad I_{yz} = \sum_{i=1}^p m_i y_i z_i \quad (2.83)$$

Equation (2.82) may be written in matrix form as

$$I_L = \mathbf{D}^T \begin{bmatrix} I_{xx} & -I_{xy} & -I_{xz} \\ -I_{xy} & I_{yy} & -I_{yz} \\ -I_{xz} & -I_{yz} & I_{zz} \end{bmatrix} \mathbf{D} =: \mathbf{D}^T J \mathbf{D} \quad (2.84)$$

where the last equality defines the symmetric matrix J , called the *inertia tensor* or *mass matrix*,

$$J = \begin{bmatrix} I_{xx} & -I_{xy} & -I_{xz} \\ -I_{xy} & I_{yy} & -I_{yz} \\ -I_{xz} & -I_{yz} & I_{zz} \end{bmatrix} \quad (2.85)$$

Moments and products of inertia are similar for a continuum of mass occupying a region R . The moments of inertia are

$$I_{xx} = \int_R y^2 + z^2 dm, \quad I_{yy} = \int_R x^2 + z^2 dm, \quad I_{zz} = \int_R x^2 + y^2 dm \quad (2.86)$$

and the products of inertia are

$$I_{xy} = \int_R xy dm, \quad I_{xz} = \int_R xz dm, \quad I_{yz} = \int_R yz dm \quad (2.87)$$

Equation (2.84) is the same whether the mass is discrete or continuous.

The reason for the use of the term *mass matrix* is clear by considering a single particle of mass m , located at \mathbf{r} relative to the origin, and that rotates about a fixed axis. As indicated by equations (2.34), (2.35), and (2.36), the position is $\mathbf{r} = (x, y, z)$; the velocity is $\mathbf{v} = \mathbf{w} \times \mathbf{r}$, where \mathbf{w} is the angular velocity; and the acceleration is $\mathbf{a} = -r_0\sigma^2\mathbf{R} + \boldsymbol{\alpha} \times \mathbf{r}$, where σ is the angular speed and $\boldsymbol{\alpha}$ is the angular acceleration. The angular momentum is

$$\mathbf{L} = \mathbf{r} \times m\mathbf{v} = m\mathbf{r} \times (\mathbf{w} \times \mathbf{r}) = m(|\mathbf{r}|^2 I - \mathbf{r}\mathbf{r}^T)\mathbf{w} = J\mathbf{w} \quad (2.88)$$

where the inertia tensor for a single particle is

$$J = m(|\mathbf{r}|^2 I - \mathbf{r}\mathbf{r}^T) = m \begin{bmatrix} y^2 + z^2 & -xy & -xz \\ -xy & x^2 + z^2 & -yz \\ -xz & -yz & x^2 + y^2 \end{bmatrix}$$

Notice the similarity of the angular momentum equation $\mathbf{L} = J\mathbf{w}$ to the linear momentum equation $\mathbf{p} = m\mathbf{v}$. The coefficient of linear velocity in the latter equation is the mass m . The coefficient of angular velocity in the former equation is the mass matrix J . Similarly, the torque is

$$\boldsymbol{\tau} = \mathbf{r} \times m\mathbf{a} = m\mathbf{r} \times (-\sigma^2\mathbf{r} + \boldsymbol{\alpha} \times \mathbf{r}) = m\mathbf{r} \times (\boldsymbol{\alpha} \times \mathbf{r}) = m(|\mathbf{r}|^2 I - \mathbf{r}\mathbf{r}^T)\boldsymbol{\alpha} = J\boldsymbol{\alpha} \quad (2.89)$$

Notice the similarity of the torque equation $\boldsymbol{\tau} = J\boldsymbol{\alpha}$ to Newton's second law, $\mathbf{F} = m\mathbf{a}$. The coefficient of linear acceleration in Newton's second law is the mass m , whereas the coefficient of angular acceleration in the torque equation is the mass matrix J . Equations (2.88) and (2.89) apply as well to particle systems and continuous mass, where the world and body origins coincide.

Equation (2.84) is a quadratic form that has a maximum and a minimum, both eigenvalues of the matrix J . From linear algebra (see [Str88] for example or see Chapter 7), a scalar λ is an eigenvalue of J with a corresponding eigenvector $\mathbf{V} \neq \mathbf{0}$, such that $J\mathbf{V} = \lambda\mathbf{V}$. The intuition, at least for real-valued eigenvalues, is that the vector \mathbf{V} has only its length changed by J but not its direction. The unit-length directions \mathbf{D} that generate the extreme values are eigenvectors corresponding to the eigenvalues. Using techniques from linear algebra and matrix theory, we can factor J using an eigendecomposition, $J = RMR^T$, where $M = \text{Diag}(\mu_1, \mu_2, \mu_3)$ is a diagonal matrix whose diagonal entries are the eigenvalues of J . The matrix $R = [\mathbf{U}_1 \ \mathbf{U}_2 \ \mathbf{U}_3]$ is a rotation matrix whose columns are eigenvectors of J , listed in the order of the eigenvalues in M . The eigenvalues μ_i are called the *principal moments of inertia*, and the columns \mathbf{U}_i are called the *principal directions of inertia*.

Equation (2.62) shows us that torque is just the time derivative of angular momentum. Equation (2.42) shows us how to compute the time derivative of a vector in a moving frame for the rigid body. In particular, we can apply this formula to the angular momentum:

$$\begin{aligned}\boldsymbol{\tau} &= \frac{d\mathbf{L}}{dt} \\ &= \frac{D\mathbf{L}}{Dt} + \mathbf{w} \times \mathbf{L} \\ &= \frac{D(J\mathbf{w})}{Dt} + \mathbf{w} \times (J\mathbf{w}) \\ &= J \frac{D\mathbf{w}}{Dt} + \mathbf{w} \times (J\mathbf{w}) \\ &= J \frac{d\mathbf{w}}{dt} + \mathbf{w} \times (J\mathbf{w})\end{aligned}\tag{2.90}$$

This vector-valued equation may be viewed as equations of motion for a rigid body. When $\boldsymbol{\tau}$ and \mathbf{w} are represented in a body coordinate system where the coordinate axis directions are the principal directions of inertia, equation (2.90) reduces to

$$\boldsymbol{\tau} = M \frac{d\mathbf{w}}{dt} + \mathbf{w} \times (M\mathbf{w})\tag{2.91}$$

where M is the diagonal matrix of principal moments. This equation is referred to as *Euler's equation of motion*. Mathematically, equation (2.91) is derived from equation (2.90) by replacing J with $RM R^T$ and by replacing the world coordinate representations $\boldsymbol{\tau}$ and \mathbf{w} with the body coordinate representations $R^T\boldsymbol{\tau}$ and $R^T\mathbf{w}$. In the process you need to use the identity $(R\mathbf{a}) \times (R\mathbf{b}) = R(\mathbf{a} \times \mathbf{b})$ when R is a rotation matrix.

EXERCISE 2.11

Let \mathbf{a} and \mathbf{b} be vectors and let R be a rotation matrix. Prove that

$$(R\mathbf{a}) \times (R\mathbf{b}) = R(\mathbf{a} \times \mathbf{b})\tag{2.92}$$

In words, the cross product of rotated vectors is the rotated cross product of the vectors. This makes sense from a purely geometric perspective. ■

**EXAMPLE
2.8**

Compute the inertia tensor for a solid triangle of constant mass density $\delta = 1$ with vertices at $(0, 0)$, $(a, 0)$, and $(0, b)$.

The region of integration R is determined by $z = 0$, $0 \leq x \leq a$, and $0 \leq y \leq b(1 - x/a)$. Since the mass density is always 1, the mass is just the area of the triangle, $m = ab/2$. The quantity I_{xx} is

$$\begin{aligned} I_{xx} &= \iint_R (y^2 + z^2) dR \\ &= \int_0^a \int_0^{b(1-x/a)} y^2 dy dx \\ &= \int_0^a \frac{y^3}{3} \Big|_0^{b(1-x/a)} dx \\ &= \int_0^a \frac{(b(1-x/a))^3}{3} dx \\ &= -\frac{ab^3(1-x/a)^4}{12} \Big|_0^a \\ &= \frac{ab^3}{12} \\ &= \frac{mb^2}{6} \end{aligned}$$

Similar integrations yield $I_{yy} = ma^2/6$, $I_{zz} = m(a^2 + b^2)/6$, $I_{xy} = mab/12$, $I_{xz} = 0$, and $I_{yz} = 0$. ■

**EXAMPLE
2.9**

Consider a box centered at the origin with dimensions $2a > 0$, $2b > 0$, and $2c > 0$. The vertices are $(\pm a, \pm b, \pm c)$, where you have eight choices for the signs in the components. Let the mass density be 1.

1. Compute the inertia tensor for the eight vertices of the box where all masses are 1 (discrete points).
2. Compute the inertia tensor for the box treated as a wireframe of masses where the 12 edges are the wires (curve mass).
3. Compute the inertia tensor for the box treated as a hollow body (surface mass).
4. Compute the inertia tensor for the box treated as a solid (volume mass).

SOLUTION 1

The moments and products of inertia are easily calculated by setting up a table (Table 2.1). The total mass is $m = 8$.

Table 2.1

Moments and Products of Inertia for Vertices

Point	I_{xx}	I_{yy}	I_{zz}	I_{xy}	I_{xz}	I_{yz}
(a, b, c)	$b^2 + c^2$	$a^2 + c^2$	$a^2 + b^2$	ab	ac	bc
$(a, b, -c)$	$b^2 + c^2$	$a^2 + c^2$	$a^2 + b^2$	ab	$-ac$	$-bc$
$(a, -b, c)$	$b^2 + c^2$	$a^2 + c^2$	$a^2 + b^2$	$-ab$	ac	$-bc$
$(a, -b, -c)$	$b^2 + c^2$	$a^2 + c^2$	$a^2 + b^2$	$-ab$	$-ac$	bc
$(-a, b, c)$	$b^2 + c^2$	$a^2 + c^2$	$a^2 + b^2$	$-ab$	$-ac$	bc
$(-a, b, -c)$	$b^2 + c^2$	$a^2 + c^2$	$a^2 + b^2$	$-ab$	ac	$-bc$
$(-a, -b, c)$	$b^2 + c^2$	$a^2 + c^2$	$a^2 + b^2$	ab	$-ac$	$-bc$
$(-a, -b, -c)$	$b^2 + c^2$	$a^2 + c^2$	$a^2 + b^2$	ab	ac	bc
Sum	$m(b^2 + c^2)$	$m(a^2 + c^2)$	$m(a^2 + b^2)$	0	0	0

SOLUTION 2

The moments and products of inertia can be calculated for each of the 12 edges, then summed. Consider the edge (x, b, c) for $|x| \leq a$. The moments and products of inertia for this edge are

$$I_{xx} = \int_{-a}^a y^2 + z^2 dx = (b^2 + c^2) \int_{-a}^a dx = 2a(b^2 + c^2)$$

$$I_{yy} = \int_{-a}^a x^2 + z^2 dx = \int_{-a}^a x^2 + c^2 dx = x^3/3 + c^2 x \Big|_{-a}^a = 2(a^3/3 + ac^2)$$

$$I_{zz} = \int_{-a}^a x^2 + y^2 dx = \int_{-a}^a x^2 + b^2 dx = x^3/3 + b^2 x \Big|_{-a}^a = 2(a^3/3 + ab^2)$$

$$I_{xy} = \int_{-a}^a xy dx = b \int_{-a}^a x dx = 0$$

$$I_{xz} = \int_{-a}^a xz dx = c \int_{-a}^a x dx = 0$$

$$I_{yz} = \int_{-a}^a yz dx = bc \int_{-a}^a dx = 2abc$$

Table 2.2 Moments and Products of Inertia for Edges

Edge	I_{xx}	I_{yy}	I_{zz}	I_{xy}	I_{xz}	I_{yz}
(x, b, c)	$2a(b^2 + c^2)$	$2(a^3/3 + ac^2)$	$2(a^3/3 + ab^2)$	0	0	$2abc$
$(x, b, -c)$	$2a(b^2 + c^2)$	$2(a^3/3 + ac^2)$	$2(a^3/3 + ab^2)$	0	0	$-2abc$
$(x, -b, c)$	$2a(b^2 + c^2)$	$2(a^3/3 + ac^2)$	$2(a^3/3 + ab^2)$	0	0	$-2abc$
$(x, -b, -c)$	$2a(b^2 + c^2)$	$2(a^3/3 + ac^2)$	$2(a^3/3 + ab^2)$	0	0	$2abc$
(a, y, c)	$2(b^3/3 + bc^2)$	$2b(a^2 + c^2)$	$2(b^3/3 + ba^2)$	0	$2abc$	0
$(a, y, -c)$	$2(b^3/3 + bc^2)$	$2b(a^2 + c^2)$	$2(b^3/3 + ba^2)$	0	$-2abc$	0
$(-a, y, c)$	$2(b^3/3 + bc^2)$	$2b(a^2 + c^2)$	$2(b^3/3 + ba^2)$	0	$-2abc$	0
$(-a, y, -c)$	$2(b^3/3 + bc^2)$	$2b(a^2 + c^2)$	$2(b^3/3 + ba^2)$	0	$2abc$	0
(a, b, z)	$2(c^3/3 + cb^2)$	$2(c^3/3 + ca^2)$	$2c(a^2 + b^2)$	$2abc$	0	0
$(a, -b, z)$	$2(c^3/3 + cb^2)$	$2(c^3/3 + ca^2)$	$2c(a^2 + b^2)$	$-2abc$	0	0
$(-a, b, z)$	$2(c^3/3 + cb^2)$	$2(c^3/3 + ca^2)$	$2c(a^2 + b^2)$	$-2abc$	0	0
$(-a, -b, z)$	$2(c^3/3 + cb^2)$	$2(c^3/3 + ca^2)$	$2c(a^2 + b^2)$	$2abc$	0	0
Sum	$\frac{m}{3} \frac{(b+c)^3 + 3a(b^2 + c^2)}{a+b+c}$	$\frac{m}{3} \frac{(a+c)^3 + 3b(a^2 + c^2)}{a+b+c}$	$\frac{m}{3} \frac{(a+b)^3 + 3c(a^2 + b^2)}{a+b+c}$	0	0	0

Similar integrals must be evaluated for the other edges. Table 2.2 shows the moments and products of inertia for the edges. The total mass is the sum of the lengths of the edges, $m = 8(a + b + c)$.

SOLUTION 3

The moments and products of inertia can be calculated for each of six faces, then summed. Consider the face $z = c$ with $|x| \leq a$ and $|y| \leq b$. The moments and products of inertia for this face are

$$I_{xx} = \int_{-b-a}^b \int_{-a}^a y^2 + z^2 dx dy = 4a(b^3/3 + bc^2)$$

$$I_{yy} = \int_{-b-a}^b \int_{-a}^a x^2 + z^2 dx dy = 4b(a^3/3 + ac^2)$$

$$I_{zz} = \int_{-b-a}^b \int_{-a}^a x^2 + y^2 dx dy = 4ab(a^2 + b^2)/3$$

$$I_{xy} = \int_{-b-a}^b \int_{-a}^a xy dx dy = 0$$

Table 2.3 Moments and Products of Inertia for Faces

Face	I_{xx}	I_{yy}	I_{zz}	I_{xy}	I_{xz}	I_{yz}
$z = c$	$4ab(b^2 + 3c^2)/3$	$4ab(a^2 + 3c^2)/3$	$4ab(a^2 + b^2)/3$	0	0	0
$z = -c$	$4ab(b^2 + 3c^2)/3$	$4ab(a^2 + 3c^2)/3$	$4ab(a^2 + b^2)/3$	0	0	0
$y = b$	$4ac(c^2 + 3b^2)/3$	$4ac(a^2 + c^2)/3$	$4ac(a^2 + 3b^2)/3$	0	0	0
$y = -b$	$4ac(c^2 + 3b^2)/3$	$4ac(a^2 + c^2)/3$	$4ac(a^2 + 3b^2)/3$	0	0	0
$x = a$	$4bc(b^2 + c^2)/3$	$4bc(c^2 + 3a^2)/3$	$4bc(b^2 + 3a^2)/3$	0	0	0
$x = -a$	$4bc(b^2 + c^2)/3$	$4bc(c^2 + 3a^2)/3$	$4bc(b^2 + 3a^2)/3$	0	0	0
Sum	$\frac{m}{3} \frac{a(b+c)^3 + bc(b^2 + c^2)}{ab + ac + bc}$	$\frac{m}{3} \frac{b(a+c)^3 + ac(a^2 + c^2)}{ab + ac + bc}$	$\frac{m}{3} \frac{c(a+b)^3 + ab(a^2 + b^2)}{ab + ac + bc}$	0	0	0

(Example 2.9
continued)

$$I_{xz} = \int_{-b-a}^b \int_{-b-a}^a xz \, dx \, dy = 0$$

$$I_{yz} = \int_{-b-a}^b \int_{-b-a}^a yz \, dx \, dy = 0$$

Similar integrals must be evaluated for the other faces. Table 2.3 shows moments and products of inertia for the faces. The total mass is the sum of the areas of the faces, $m = 8(ab + ac + bc)$.

SOLUTION 4

The total mass is the volume of the box, $m = 8abc$. The moments and products of inertia are

$$I_{xx} = \int_{-c}^c \int_{-b-a}^b \int_{-a}^a y^2 + z^2 \, dx \, dy \, dz = \frac{8abc(b^2 + c^2)}{3} = \frac{m(b^2 + c^2)}{3}$$

$$I_{yy} = \int_{-c}^c \int_{-b-a}^b \int_{-a}^a x^2 + z^2 \, dx \, dy \, dz = \frac{8abc(a^2 + c^2)}{3} = \frac{m(a^2 + c^2)}{3}$$

$$I_{zz} = \int_{-c}^c \int_{-b-a}^b \int_{-a}^a x^2 + y^2 \, dx \, dy \, dz = \frac{8abc(a^2 + b^2)}{3} = \frac{m(a^2 + b^2)}{3}$$

$$I_{xy} = \int_{-c}^c \int_{-b-a}^b \int_{-a}^a xy \, dx \, dy \, dz = 0$$

(Example 2.9
continued)

$$I_{xz} = \int_{-c}^c \int_{-b}^b \int_{-a}^a xz \, dx \, dy \, dz = 0$$

$$I_{yz} = \int_{-c}^c \int_{-b}^b \int_{-a}^a yz \, dx \, dy \, dz = 0$$

EXERCISE
2.12

Repeat the experiment of Example 2.9 using a tetrahedron instead of a box. The vertices are $(0, 0, 0)$, $(a, 0, 0)$, $(0, b, 0)$, and $(0, 0, c)$, where $a > 0$, $b > 0$, and $c > 0$. ■

EXERCISE
2.13

Compute the inertia tensor for the planar object in Example 2.3, but treated as a 3D object (a surface mass). ■

EXERCISE
2.14

Compute the inertia tensor for the hemicircle wire in Example 2.4, but treated as a 3D object (a curve mass). ■

EXERCISE
2.15

Transfer of Axes. The derivation of equation (2.82) used any specified origin \mathcal{O} and produced the quantities I_{xx} , I_{yy} , I_{zz} , I_{xy} , I_{xz} , and I_{yz} . Let the total mass of the system be m . Suppose that the origin is chosen to be the center of mass $(\bar{x}, \bar{y}, \bar{z})$ and that coordinate axes are chosen so that they are parallel to those used at origin \mathcal{O} . If the corresponding inertia quantities are \bar{I}_{xx} , \bar{I}_{yy} , \bar{I}_{zz} , \bar{I}_{xy} , \bar{I}_{xz} , and \bar{I}_{yz} , show that $I_{xx} = \bar{I}_{xx} + m(\bar{y}^2 + \bar{z}^2)$, $I_{yy} = \bar{I}_{yy} + m(\bar{x}^2 + \bar{z}^2)$, $I_{zz} = \bar{I}_{zz} + m(\bar{x}^2 + \bar{y}^2)$, $I_{xy} = \bar{I}_{xy} + m\bar{x}\bar{y}$, $I_{xz} = \bar{I}_{xz} + m\bar{x}\bar{z}$, and $I_{yz} = \bar{I}_{yz} + m\bar{y}\bar{z}$. Compare this result with equations (2.74), (2.76), (2.78), and (2.80).

Conclude that the moment of inertia about a line L containing the center of mass and having unit-length direction \mathbf{D} is

$$I_L = \mathbf{D}^T \begin{bmatrix} \bar{I}_{xx} + m(\bar{y}^2 + \bar{z}^2) & -(\bar{I}_{xy} + m\bar{x}\bar{y}) & -(\bar{I}_{xz} + m\bar{x}\bar{z}) \\ -(\bar{I}_{xy} + m\bar{x}\bar{y}) & \bar{I}_{yy} + m(\bar{x}^2 + \bar{z}^2) & -(\bar{I}_{yz} + m\bar{y}\bar{z}) \\ -(\bar{I}_{xz} + m\bar{x}\bar{z}) & -(\bar{I}_{yz} + m\bar{y}\bar{z}) & \bar{I}_{zz} + m(\bar{x}^2 + \bar{y}^2) \end{bmatrix} \mathbf{D}$$

The significance of this result is that an application needs only to compute the inertia tensor relative to the body's center of mass. The inertia tensor for other coordinate frames is then easily calculated from this tensor. ■

We will look at moments of inertia in more detail in Section 3.2 when dealing with rigid body motion.

2.5.5 MASS AND INERTIA TENSOR OF A SOLID POLYHEDRON

In a game environment the objects that physically interact typically are constructed as simple polyhedra. In order to set up the equations of motion for such objects, we

need to compute the mass and inertia tensor for a solid polyhedron. This can be quite a difficult task if the mass density of the object is variable, but turns out to be relatively simple for constant mass density. For the sake of simplicity we will assume that the mass density is $\rho = 1$. For any other value you will need to multiply the mass and inertia tensors by that value.

A mathematical algorithm for computing the mass and inertia tensor for solid polyhedra of constant mass density is described by Mirtich [Mir96a]. The construction uses the divergence theorem from calculus for reducing volume integrals to surface integrals, a reduction from three-dimensional integrals to two-dimensional integrals. The polyhedron surface is a union of planar faces, so the surface integrals are effectively integrals in various planes. Projection of these faces onto coordinate planes are used to set up yet another reduction in dimension. Green's theorem, the two-dimensional analog of the divergence theorem, is used to reduce the planar integrals to line integrals around the boundaries of the projected faces.

Two important points emphasized in the paper are (1) the projection of the polyhedron faces onto the appropriate coordinate planes to avoid numerical problems; and (2) the reduction using Green's theorem to obtain common subexpressions, which are integrals of polynomials of one variable, to avoid redundant calculations. Item (2) occurs to handle polyhedron faces with four or more vertices. Item (1) is necessary in order to robustly compute what is required by item (2). When the polyhedron faces are triangles, neither item (1) nor (2) is necessary. A simpler construction is provided here when the polyhedron faces are triangles. A consequence of the formulas as derived in this document is that they require significantly less computational time than Mirtich's formulas.

Reduction of Volume Integrals

The mass, center of mass, and inertia tensor require computing volume integrals of the type,

$$\int_V p(x, y, z) dV$$

where V is the volumetric region of integration and dV is an infinitesimal measure of volume. The function $p(x, y, z)$ is a polynomial selected from $1, x, y, z, x^2, y^2, z^2, xy, xz$, and yz . We are interested in computing these integrals where V is the region bounded by a simple polyhedron. A volume integral may be converted to a surface integral via the divergence theorem from calculus:

$$\int_V p(x, y, z) dV = \int_V \nabla \cdot \mathbf{F} dV = \int_S \mathbf{N} \cdot \mathbf{F} dS$$

where S is the boundary of the polyhedron, a union of triangular faces, and where dS is an infinitesimal measure of surface area. The function $\mathbf{F}(x, y, z)$ is chosen so that

Table 2.4 Generation of Polynomials by Vector Fields

p	\mathbf{F}	p	\mathbf{F}
1	($x, 0, 0$)	y^2	($0, y^3/3, 0$)
x	($x^2/2, 0, 0$)	z^2	($0, 0, z^3/3$)
y	($0, y^2/2, 0$)	xy	($x^2y/2, 0, 0$)
z	($0, 0, z^2/2$)	xz	($0, 0, z^2x/2$)
x^2	($x^3/3, 0, 0$)	yz	($0, y^2z/2, 0$)

$\nabla \cdot \mathbf{F} = p$. The vector \mathbf{N} denotes outward-pointing, unit-length surface normals. The choices for \mathbf{F} in the Mirtich paper are given in Table 2.4.

The computational effort is now devoted to calculating the integrals $\int_S \mathbf{N} \cdot \mathbf{F} dS$. The boundary S is just the union of polyhedral faces \mathcal{F} . An outward-pointing, unit-length normal to face \mathcal{F} is denoted by $\mathbf{N}_{\mathcal{F}} = (\hat{\eta}_x, \hat{\eta}_y, \hat{\eta}_z)$. The surface integral decomposes to

$$\int_S \mathbf{N} \cdot \mathbf{F} dS = \sum_{\mathcal{F} \in S} \int_{\mathcal{F}} \mathbf{N}_{\mathcal{F}} \cdot \mathbf{F} dS \quad (2.93)$$

The integrals to be computed are now reduced to

$$\begin{array}{ll} \int_V dV = \sum_{\mathcal{F} \in S} \hat{\eta}_x \int_{\mathcal{F}} x dS & \int_V y^2 dV = \frac{1}{3} \sum_{\mathcal{F} \in S} \hat{\eta}_y \int_{\mathcal{F}} y^3 dS \\ \int_V x dV = \frac{1}{2} \sum_{\mathcal{F} \in S} \hat{\eta}_x \int_{\mathcal{F}} x^2 dS & \int_V z^2 dV = \frac{1}{3} \sum_{\mathcal{F} \in S} \hat{\eta}_z \int_{\mathcal{F}} z^3 dS \\ \int_V y dV = \frac{1}{2} \sum_{\mathcal{F} \in S} \hat{\eta}_y \int_{\mathcal{F}} y^2 dS & \int_V xy dV = \frac{1}{2} \sum_{\mathcal{F} \in S} \hat{\eta}_x \int_{\mathcal{F}} x^2 y dS \\ \int_V z dV = \frac{1}{2} \sum_{\mathcal{F} \in S} \hat{\eta}_z \int_{\mathcal{F}} z^2 dS & \int_V yz dV = \frac{1}{2} \sum_{\mathcal{F} \in S} \hat{\eta}_y \int_{\mathcal{F}} y^2 z dS \\ \int_V x^2 dV = \frac{1}{3} \sum_{\mathcal{F} \in S} \hat{\eta}_x \int_{\mathcal{F}} x^3 dS & \int_V xz dV = \frac{1}{2} \sum_{\mathcal{F} \in S} \hat{\eta}_z \int_{\mathcal{F}} z^2 x dS \end{array}$$

We now need to compute integrals of the form,

$$\hat{\eta}_\ell \int_{\mathcal{F}} q(x, y, z) dS \quad (2.94)$$

where ℓ is one of x, y , or z and where q is one of $x, x^2, y^2, z^2, x^3, y^3, z^3, x^2y, y^2z$, or z^2x .

Computation by Reduction to Line Integrals

Although we do not need to compute a surface integral when $q(x, y, z) = 1$, we use it as motivation. Notice that $\int_{\mathcal{F}} dS$ is the area A of the polygonal face. The area may be computed as a three-dimensional quantity:

$$A = \int_{\mathcal{F}} dS = \frac{1}{2} \mathbf{N}_{\mathcal{F}} \cdot \sum_{i=0}^{n-1} \mathbf{P}_i \times \mathbf{P}_{i+1}$$

where the polygon vertices are $\mathbf{P}_i = (x_i, y_i, z_i)$, $0 \leq i \leq n - 1$, and the vertices are ordered counterclockwise relative to the face normal $\mathbf{N}_{\mathcal{F}}$. Modular indexing is used so that $\mathbf{P}_n = \mathbf{P}_0$. This formula occurs in [Arv91] and is derived using Stokes' theorem from calculus. The computation is not as efficient as it can be. A discussion of various methods for computing area (and volume) is found in [SE02].

An efficient method for computing the area is to project the polygon onto a coordinate plane, compute the area in two dimensions, and adjust the result to account for the projection. The plane of the polygonal face is $\hat{\eta}_x x + \hat{\eta}_y y + \hat{\eta}_z z + w = 0$, where $w = -\mathbf{N}_{\mathcal{F}} \cdot \mathbf{P}_0$. As long as $\hat{\eta}_z \neq 0$, we may project onto the xy -plane. The plane equation is written $z = f(x, y) = -(w + \hat{\eta}_x x + \hat{\eta}_y y)/\hat{\eta}_z$. The infinitesimal surface area in terms of the independent variables x and y is

$$\begin{aligned} dS &= \sqrt{1 + \left(\frac{\partial f}{\partial x}\right)^2 + \left(\frac{\partial f}{\partial y}\right)^2} dx dy \\ &= \sqrt{1 + \left(\frac{-\hat{\eta}_x}{\hat{\eta}_z}\right)^2 + \left(\frac{-\hat{\eta}_y}{\hat{\eta}_z}\right)^2} dx dy \\ &= \frac{1}{|\hat{\eta}_z|} dx dy \end{aligned}$$

where we have used the fact that $|\mathbf{N}_{\mathcal{F}}| = 1$. The surface integral becomes

$$\int_{\mathcal{F}} dS = \frac{1}{|\hat{\eta}_z|} \int_R dx dy$$

where R is the region bounded by the projected polygon. That polygon has vertices $\mathbf{Q}_i = (x_i, y_i)$. A planar integral may be converted to a line integral via Green's theorem, the two-dimensional analog of the divergence theorem,

$$\int_R p(x, y) dx dy = \int_R \nabla \cdot \mathbf{G} dx dy = \int_L \mathbf{M} \cdot \mathbf{G} ds$$

where L is the boundary of the region R and where ds is an infinitesimal measure of arc length. The function $\mathbf{G}(x, y)$ is chosen so that $\nabla \cdot \mathbf{G} = p$. The vector \mathbf{M} denotes outward-pointing, unit-length curve normals. In our special case $p(x, y) = 1$ and L is

a polygon. Many choices exist for \mathbf{G} , one being $\mathbf{G} = (x, 0)$. The boundary is the union of edges \mathcal{E} . An outward-pointing, unit-length normal to the edge is denoted $\mathbf{M}_{\mathcal{E}}$. The area integral decomposes to

$$\int_L \mathbf{M} \cdot \mathbf{G} ds = \sum_{\mathcal{E}} \int_{\mathcal{E}} \mathbf{M}_{\mathcal{E}} \cdot \mathbf{G} ds \quad (2.95)$$

Note the similarity to [equation \(2.93\)](#). If edge \mathcal{E} is the line segment connecting \mathbf{Q}_i to \mathbf{Q}_{i+1} and has length $L_i = |\mathbf{Q}_{i+1} - \mathbf{Q}_i|$, then the edge is parameterized by $(x(s), y(s)) = (1 - s/L_i)\mathbf{Q}_i + (s/L_i)\mathbf{Q}_{i+1}$ for $s \in [0, L_i]$. At first glance you might choose the edge normals to be $\mathbf{M}_i = (y_{i+1} - y_i, x_i - x_{i+1})/L_i$. This is a correct choice if the \mathbf{Q}_i are counterclockwise ordered. When $\hat{\eta}_z > 0$, a counterclockwise traversal of the \mathbf{P}_i results in a counterclockwise traversal of the \mathbf{Q}_i . But when $\hat{\eta}_z < 0$, the \mathbf{Q}_i are traversed clockwise; the previous formula for \mathbf{M}_i must be negated. In general $\mathbf{M}_i = \text{Sign}(\hat{\eta}_z)(y_{i+1} - y_i, x_i - x_{i+1})/L_i$. The integral of [equation \(2.95\)](#) is rewritten as

$$\begin{aligned} \int_L \mathbf{M} \cdot \mathbf{G} ds &= \sum_{i=0}^{n-1} \int_0^{L_i} \mathbf{M}_i \cdot (x(s), 0) ds \\ &= \text{Sign}(\hat{\eta}_z) \sum_{i=0}^{n-1} \frac{y_{i+1} - y_i}{L_i} \int_0^{L_i} \left(1 - \frac{s}{L_i}\right) x_i + \left(\frac{s}{L_i}\right) x_{i+1} ds \\ &= \text{Sign}(\hat{\eta}_z) \sum_{i=0}^{n-1} (y_{i+1} - y_i) \int_0^1 (1-t)x_i + tx_{i+1} dt \\ &= \frac{\text{Sign}(\hat{\eta}_z)}{2} \sum_{i=0}^{n-1} (x_{i+1} + x_i)(y_{i+1} - y_i) \\ &= \frac{\text{Sign}(\hat{\eta}_z)}{2} \sum_{i=0}^{n-1} x_i(y_{i+1} - y_{i-1}) \end{aligned} \quad (2.96)$$

where the third equality is based on the change of variables $s = L_i t$. The last equality uses modular indexing ($y_n = y_0$ and $y_{-1} = y_{n-1}$); it results in a reduction of one third the arithmetic operations from the previous equation. The proof of equality is left as an exercise.

One potential source of numerical error is when $\hat{\eta}_z$ is nearly zero. The division by $|\hat{\eta}_z|$ is ill conditioned. In this case we may project onto another coordinate plane. The same ill conditioning can occur for one of those, but not both since at least one of the components of $\mathbf{N}_{\mathcal{F}}$ must be larger or equal to $1/\sqrt{3}$ in magnitude. The area of

the polygonal face is computed accordingly:

$$A = \begin{cases} \frac{\int_{R_{xy}} dx dy}{|\hat{\eta}_z|} = \frac{1}{2\hat{\eta}_z} \sum_{i=0}^{n-1} x_i(y_{i+1} - y_{i-1}), & |\hat{\eta}_z| = \max\{|\hat{\eta}_x|, |\hat{\eta}_y|, |\hat{\eta}_z|\} \\ \frac{\int_{R_{yz}} dy dz}{|\hat{\eta}_x|} = \frac{1}{2\hat{\eta}_x} \sum_{i=0}^{n-1} y_i(z_{i+1} - z_{i-1}), & |\hat{\eta}_x| = \max\{|\hat{\eta}_x|, |\hat{\eta}_y|, |\hat{\eta}_z|\} \\ \frac{\int_{R_{zx}} dz dx}{|\hat{\eta}_y|} = \frac{1}{2\hat{\eta}_y} \sum_{i=0}^{n-1} z_i(x_{i+1} - x_{i-1}), & |\hat{\eta}_y| = \max\{|\hat{\eta}_x|, |\hat{\eta}_y|, |\hat{\eta}_z|\} \end{cases} \quad (2.97)$$

where R_{xy} , R_{yz} , and R_{zx} are the regions of projection of the polygonal face.

The construction of $\int_S q(x, y, z) dS$ is handled in a similar manner except that now the integrand has variables, the dependent one needing replacement using the appropriate formulation of the plane equation:

$$\begin{aligned} & \int_S q(x, y, z) dS \\ &= \begin{cases} \frac{1}{|\hat{\eta}_z|} \int_{R_{xy}} q(x, y, -(w + \hat{\eta}_x x + \hat{\eta}_y y)/\hat{\eta}_z) dx dy, & |\hat{\eta}_z| = \max\{|\hat{\eta}_x|, |\hat{\eta}_y|, |\hat{\eta}_z|\} \\ \frac{1}{|\hat{\eta}_x|} \int_{R_{yz}} q(-(w + \hat{\eta}_y y + \hat{\eta}_z z)/\hat{\eta}_x, y, z) dy dz, & |\hat{\eta}_x| = \max\{|\hat{\eta}_x|, |\hat{\eta}_y|, |\hat{\eta}_z|\} \\ \frac{1}{|\hat{\eta}_y|} \int_{R_{zx}} q(x, -(w + \hat{\eta}_x x + \hat{\eta}_z z)/\hat{\eta}_y, z) dz dx, & |\hat{\eta}_y| = \max\{|\hat{\eta}_x|, |\hat{\eta}_y|, |\hat{\eta}_z|\} \end{cases} \end{aligned} \quad (2.98)$$

Each integrand is a polynomial of two independent variables. A function \mathbf{G} must be chosen so that $\nabla \cdot \mathbf{G}$ is that polynomial. When $|\hat{\eta}_z|$ is the maximum absolute normal component, \mathbf{G} will have components that depend on x and y . Using the same notation that led to [equation \(2.96\)](#), the integral is

$$\begin{aligned} & \int_S q(x, y, z) dS \\ &= \frac{1}{|\hat{\eta}_z|} \sum_{i=0}^{n-1} \int_0^{L_i} \mathbf{M}_i \cdot \mathbf{G}(x(s), y(s)) ds \\ &= \frac{\text{Sign}(\hat{\eta}_z)}{|\hat{\eta}_z|} \sum_{i=0}^{n-1} \frac{(y_{i+1} - y_i, x_i - x_{i+1})}{L_i} \cdot \int_0^{L_i} G\left(\left(1 - \frac{s}{L_i}\right)\mathbf{Q}_i + \left(\frac{s}{L_i}\right)\mathbf{Q}_{i+1}\right) ds \\ &= \frac{1}{\hat{\eta}_z} \sum_{i=0}^{n-1} (y_{i+1} - y_i, x_i - x_{i+1}) \cdot \int_0^1 G((1-t)\mathbf{Q}_i + t\mathbf{Q}_{i+1}) dt \end{aligned}$$

At this point the remaining work involves selecting \mathbf{G} for each integrand of [equation \(2.98\)](#) and computing the integral $\int_0^1 G((1-t)\mathbf{Q}_i + t\mathbf{Q}_{i+1}) dt$. See [\[Mir96a\]](#) for all the tedious details. I summarize the formulas below. The notation used in that paper is that (α, β, γ) is a permutation of the usual coordinates, chosen from one of (x, y, z) , (y, z, x) , or (z, x, y) . The projection integrals are $\pi_f = \int_R f d\alpha d\beta$, where R is the projection of the polygonal face onto the $\alpha\beta$ -plane and f is some polynomial function:

$$\begin{aligned}
\int_{\mathcal{F}} \alpha dS &= |\hat{\eta}_\gamma|^{-1} \pi_\alpha \\
\int_{\mathcal{F}} \beta dS &= |\hat{\eta}_\gamma|^{-1} \pi_\beta \\
\int_{\mathcal{F}} \gamma dS &= -|\hat{\eta}_\gamma|^{-1} \hat{\eta}_\gamma^{-1} (\hat{\eta}_\alpha \pi_\alpha + \hat{\eta}_\beta \pi_\beta + w \pi_1) \\
\int_{\mathcal{F}} \alpha^2 dS &= |\hat{\eta}_\gamma|^{-1} \pi_{\alpha^2} \\
\int_{\mathcal{F}} \beta^2 dS &= |\hat{\eta}_\gamma|^{-1} \pi_{\beta^2} \\
\int_{\mathcal{F}} \gamma^2 dS &= |\hat{\eta}_\gamma|^{-1} \hat{\eta}_\gamma^{-2} (\hat{\eta}_\alpha^2 \pi_{\alpha^2} + 2\hat{\eta}_\alpha \hat{\eta}_\beta \pi_{\alpha\beta} + \hat{\eta}_\beta^2 \pi_{\beta^2} \\
&\quad + 2w(\hat{\eta}_\alpha \pi_\alpha + \hat{\eta}_\beta \pi_\beta) + w^2 \pi_1) \\
\int_{\mathcal{F}} \alpha^3 dS &= |\hat{\eta}_\gamma|^{-1} \pi_{\alpha^3} \\
\int_{\mathcal{F}} \beta^3 dS &= |\hat{\eta}_\gamma|^{-1} \pi_{\beta^3} \\
\int_{\mathcal{F}} \gamma^3 dS &= -|\hat{\eta}_\gamma|^{-1} \hat{\eta}_\gamma^{-3} (\hat{\eta}_\alpha^3 \pi_{\alpha^3} + 3\hat{\eta}_\alpha^2 \hat{\eta}_\beta \pi_{\alpha^2\beta} + 3\hat{\eta}_\alpha \hat{\eta}_\beta^2 \pi_{\alpha\beta^2} + \hat{\eta}_\beta^3 \pi_{\beta^3} \\
&\quad + 3w(\hat{\eta}_\alpha^2 \pi_{\alpha^2} + 2\hat{\eta}_\alpha \hat{\eta}_\beta \pi_{\alpha\beta} + \hat{\eta}_\beta^2 \pi_{\beta^2}) \\
&\quad + 3w^2(\hat{\eta}_\alpha \pi_\alpha + \hat{\eta}_\beta \pi_\beta) + w^3 \pi_1) \\
\int_{\mathcal{F}} \alpha^2 \beta dS &= |\hat{\eta}_\gamma|^{-1} \pi_{\alpha^2\beta} \\
\int_{\mathcal{F}} \beta^2 \gamma dS &= -|\hat{\eta}_\gamma|^{-1} \hat{\eta}_\gamma^{-1} (\hat{\eta}_\alpha \pi_{\alpha\beta^2} + \hat{\eta}_\beta \pi_{\beta^3} + w \pi_{\beta^2}) \\
\int_{\mathcal{F}} \gamma^2 \alpha dS &= |\hat{\eta}_\gamma|^{-1} \hat{\eta}_\gamma^{-2} (\hat{\eta}_\alpha^2 \pi_{\alpha^3} + 2\hat{\eta}_\alpha \hat{\eta}_\beta \pi_{\alpha^2\beta} + \hat{\eta}_\beta^2 \pi_{\alpha\beta^2} \\
&\quad + 2w(\hat{\eta}_\alpha \pi_{\alpha^2} + \hat{\eta}_\beta \pi_{\alpha\beta}) + w^2 \pi_\alpha)
\end{aligned}$$

The projection integrals are

$$\begin{aligned}
\pi_1 &= \frac{\text{Sign}(\hat{\eta}_\gamma)}{2} \sum_{i=0}^{n-1} (\beta_{i+1} - \beta_i)(\alpha_{i+1} + \alpha_i) \\
\pi_\alpha &= \frac{\text{Sign}(\hat{\eta}_\gamma)}{6} \sum_{i=0}^{n-1} (\beta_{i+1} - \beta_i)(\alpha_{i+1}^2 + \alpha_{i+1}\alpha_i + \alpha_i^2) \\
\pi_\beta &= -\frac{\text{Sign}(\hat{\eta}_\gamma)}{6} \sum_{i=0}^{n-1} (\alpha_{i+1} - \alpha_i)(\beta_{i+1}^2 + \beta_{i+1}\beta_i + \beta_i^2) \\
\pi_{\alpha^2} &= \frac{\text{Sign}(\hat{\eta}_\gamma)}{12} \sum_{i=0}^{n-1} (\beta_{i+1} - \beta_i)(\alpha_{i+1}^3 + \alpha_{i+1}^2\alpha_i + \alpha_{i+1}\alpha_i^2 + \alpha_i^3) \\
\pi_{\alpha\beta} &= \frac{\text{Sign}(\hat{\eta}_\gamma)}{24} \sum_{i=0}^{n-1} (\beta_{i+1} - \beta_i)(\beta_{i+1}(3\alpha_{i+1}^2 + 2\alpha_{i+1}\alpha_i + \alpha_i^2) \\
&\quad + \beta_i(\alpha_{i+1}^2 + 2\alpha_{i+1}\alpha_i + 3\alpha_i^2)) \\
\pi_{\beta^2} &= -\frac{\text{Sign}(\hat{\eta}_\gamma)}{12} \sum_{i=0}^{n-1} (\alpha_{i+1} - \alpha_i)(\beta_{i+1}^3 + \beta_{i+1}^2\beta_i + \beta_{i+1}\beta_i^2 + \beta_i^3) \\
\pi_{\alpha^3} &= \frac{\text{Sign}(\hat{\eta}_\gamma)}{20} \sum_{i=0}^{n-1} (\beta_{i+1} - \beta_i)(\alpha_{i+1}^4 + \alpha_{i+1}^3\alpha_i + \alpha_{i+1}^2\alpha_i^2 + \alpha_{i+1}\alpha_i^3 + \alpha_i^4) \\
\pi_{\alpha^2\beta} &= \frac{\text{Sign}(\hat{\eta}_\gamma)}{60} \sum_{i=0}^{n-1} (\beta_{i+1} - \beta_i)(\beta_{i+1}(4\alpha_{i+1}^3 + 3\alpha_{i+1}^2\alpha_i + 2\alpha_{i+1}\alpha_i^2 + \alpha_i^3) \\
&\quad + \beta_i(\alpha_{i+1}^3 + 2\alpha_{i+1}^2\alpha_i + 3\alpha_{i+1}\alpha_i^2 + 4\alpha_i^3)) \\
\pi_{\alpha\beta^2} &= -\frac{\text{Sign}(\hat{\eta}_\gamma)}{60} \sum_{i=0}^{n-1} (\alpha_{i+1} - \alpha_i)(\alpha_{i+1}(4\beta_{i+1}^3 + 3\beta_{i+1}^2\beta_i + 2\beta_{i+1}\beta_i^2 + \beta_i^3) \\
&\quad + \alpha_i(\beta_{i+1}^3 + 2\beta_{i+1}^2\beta_i + 3\beta_{i+1}\beta_i^2 + 4\beta_i^3)) \\
\pi_{\beta^3} &= -\frac{\text{Sign}(\hat{\eta}_\gamma)}{20} \sum_{i=0}^{n-1} (\alpha_{i+1} - \alpha_i)(\beta_{i+1}^4 + \beta_{i+1}^3\beta_i + \beta_{i+1}^2\beta_i^2 + \beta_{i+1}\beta_i^3 + \beta_i^4)
\end{aligned}$$

Notice that the formula for π_1 is exactly what we derived for the area of the polygonal face.

An example of how these are used is

$$\hat{\eta}_x \int_S x \, dS = \begin{cases} |\hat{\eta}_z^{-1}| \hat{\eta}_x \pi_x, & |\hat{\eta}_z| = \max\{|\hat{\eta}_x|, |\hat{\eta}_y|, |\hat{\eta}_z|\} \\ |\hat{\eta}_y^{-1}| \hat{\eta}_x \pi_x, & |\hat{\eta}_y| = \max\{|\hat{\eta}_x|, |\hat{\eta}_y|, |\hat{\eta}_z|\} \\ -|\hat{\eta}_x^{-1}| (\hat{\eta}_y \pi_y + \hat{\eta}_z \pi_z + w \pi_1), & |\hat{\eta}_x| = \max\{|\hat{\eta}_x|, |\hat{\eta}_y|, |\hat{\eta}_z|\} \end{cases}$$

$$\begin{aligned}
& \left| \frac{\hat{\eta}_x}{6\hat{\eta}_z} \sum_{i=0}^{n-1} (y_{i+1} - y_i)(x_{i+1}^2 + x_{i+1}x_i + x_i^2), \quad |\hat{\eta}_z| = \max\{|\hat{\eta}_x|, |\hat{\eta}_y|, |\hat{\eta}_z|\} \right. \\
& \left| -\frac{\hat{\eta}_x}{6\hat{\eta}_y} \sum_{i=0}^{n-1} (z_{i+1} - z_i)(x_{i+1}^2 + x_{i+1}x_i + x_i^2), \quad |\hat{\eta}_y| = \max\{|\hat{\eta}_x|, |\hat{\eta}_y|, |\hat{\eta}_z|\} \right. \\
= & \left| -\frac{\hat{\eta}_y}{6\hat{\eta}_x} \sum_{i=0}^{n-1} (z_{i+1} - z_i)(y_{i+1}^2 + y_{i+1}y_i + y_i^2) \right. \\
& \left| \frac{\hat{\eta}_z}{6\hat{\eta}_x} \sum_{i=0}^{n-1} (y_{i+1} - y_i)(z_{i+1}^2 + z_{i+1}z_i + z_i^2) \right. \\
& \left. \frac{\hat{\eta}_x x_0 + \hat{\eta}_y y_0 + \hat{\eta}_z z_0}{2\hat{\eta}_x} \sum_{i=0}^{n-1} (z_{i+1} - z_i)(y_{i+1} + y_i), \quad |\hat{\eta}_x| = \max\{|\hat{\eta}_x|, |\hat{\eta}_y|, |\hat{\eta}_z|\} \right. \\
\end{aligned} \tag{2.99}$$

As we will see in the next section, these formulas reduce greatly when the polyhedron has triangle faces.

Computation by Direct Parameterization of Triangles

Let the triangular face be counterclockwise ordered and have vertices $\mathbf{P}_i = (x_i, y_i, z_i)$, $0 \leq i \leq 2$. Two edges are

$$\mathbf{E}_i = \mathbf{P}_i - \mathbf{P}_0 = (x_i - x_0, y_i - y_0, z_i - z_0) = (\alpha_i, \beta_i, \gamma_i)$$

for $1 \leq i \leq 2$. A parameterization of the face is

$$\begin{aligned}
\mathbf{P}(u, v) &= \mathbf{P}_0 + u\mathbf{E}_1 + v\mathbf{E}_2 \\
&= (x_0 + \alpha_1 u + \alpha_2 v, y_0 + \beta_1 u + \beta_2 v, z_0 + \gamma_1 u + \gamma_2 v) \\
&= (x(u, v), y(u, v), z(u, v))
\end{aligned} \tag{2.100}$$

where $u \geq 0$, $v \geq 0$, and $u + v \leq 1$. The infinitesimal measure of surface area is

$$dS = \left| \frac{\partial \mathbf{P}}{\partial u} \times \frac{\partial \mathbf{P}}{\partial v} \right| du dv = |\mathbf{E}_1 \times \mathbf{E}_2| du dv$$

and the outer-pointing unit-length face normal is

$$\mathbf{N}_F = \frac{\mathbf{E}_1 \times \mathbf{E}_2}{|\mathbf{E}_1 \times \mathbf{E}_2|} = \frac{(\beta_1 \gamma_2 - \beta_2 \gamma_1, \alpha_2 \gamma_1 - \alpha_1 \gamma_2, \alpha_1 \beta_2 - \alpha_2 \beta_1)}{|\mathbf{E}_1 \times \mathbf{E}_2|} = \frac{(\delta_0, \delta_1, \delta_2)}{|\mathbf{E}_1 \times \mathbf{E}_2|}$$

The integrals in equation (2.94) reduce to

$$(\mathbf{N}_F \cdot \boldsymbol{\ell}) \int_{\mathcal{F}} q(x, y, z) dS = (\mathbf{E}_1 \times \mathbf{E}_2 \cdot \boldsymbol{\ell}) \int_0^1 \int_0^{1-v} q(x(u, v), y(u, v), z(u, v)) du dv \quad (2.101)$$

where $x(u, v)$, $y(u, v)$, and $z(u, v)$ are the components of the parameterization in equation (2.100).

The integrals on the right-hand side of equation (2.101) can be computed symbolically, either by hand or by a symbolic algebra package. The formulas following these integrals were computed using Mathematica. Common subexpressions may be obtained by some additional factoring. Define

$$s_n(w) = \sum_{i=0}^n w_0^{n-i} w_1^i, \quad f_0(w) = 1, \quad \text{and} \quad f_n(w) = s_n(w) + w_2 f_{n-1}(w) \quad \text{for } n \geq 1$$

Think of these as macros where the input argument is a textual replacement wherever w occurs in the right-hand sides. Also define the macro

$$g_i(w) = f_2(w) + w_i f_1(w) + w_i^2$$

The specific expressions required in the surface integrals are listed below in terms of w . Each macro is expanded three times, once for each of x , y , and z :

$$\begin{aligned} f_1(w) &= w_0 + w_1 + w_2 = [w_0 + w_1] + w_2 \\ f_2(w) &= w_0^2 + w_0 w_1 + w_1^2 + w_2 f_1(w) \\ &= [[w_0^2] + w_1 \{w_0 + w_1\}] + w_2 \{f_1(w)\} \\ f_3(w) &= w_0^3 + w_0^2 w_1 + w_0 w_1^2 + w_1^3 + w_2 f_2(w) \\ &= w_0 \{w_0^2\} + w_1 \{w_0^2 + w_0 w_1 + w_1^2\} + w_2 \{f_2(w)\} \\ g_i(w) &= \{f_2(w)\} + w_i (\{f_1(w)\} + w_i) \end{aligned} \quad (2.102)$$

The square brackets [] indicate that the subexpression is computed and saved in temporary variables for later use. The curly braces {} indicate that the subexpression was computed earlier and can be accessed from temporary variables. The number of subexpressions that must be stored at any one time is small, so cache coherence should not be an issue when enough floating point registers are available for storing the subexpressions (see the pseudocode section on page 75 of this text).

The integrals are

$$\begin{aligned}
 (\mathbf{N}_{\mathcal{F}} \cdot \boldsymbol{\iota}) \int_{\mathcal{F}} x dS &= \frac{\delta_0}{6} f_1(x) & (\mathbf{N}_{\mathcal{F}} \cdot \mathbf{J}) \int_{\mathcal{F}} y^3 dS &= \frac{\delta_1}{20} f_3(y) \\
 (\mathbf{N}_{\mathcal{F}} \cdot \boldsymbol{\iota}) \int_{\mathcal{F}} x^2 dS &= \frac{\delta_0}{12} f_2(x) & (\mathbf{N}_{\mathcal{F}} \cdot \mathbf{k}) \int_{\mathcal{F}} z^3 dS &= \frac{\delta_2}{20} f_3(z) \\
 (\mathbf{N}_{\mathcal{F}} \cdot \mathbf{J}) \int_{\mathcal{F}} y^2 dS &= \frac{\delta_1}{12} f_2(y) & (\mathbf{N}_{\mathcal{F}} \cdot \boldsymbol{\iota}) \int_{\mathcal{F}} x^2 y dS &= \frac{\delta_0}{60} (y_0 g_0(x) + y_1 g_1(x) \\
 &&&\quad + y_2 g_2(x)) \\
 (\mathbf{N}_{\mathcal{F}} \cdot \mathbf{k}) \int_{\mathcal{F}} z^2 dS &= \frac{\delta_2}{12} f_2(z) & (\mathbf{N}_{\mathcal{F}} \cdot \mathbf{J}) \int_{\mathcal{F}} y^2 z dS &= \frac{\delta_1}{60} (z_0 g_0(y) + z_1 g_1(y) \\
 &&&\quad + z_2 g_2(y)) \\
 (\mathbf{N}_{\mathcal{F}} \cdot \boldsymbol{\iota}) \int_{\mathcal{F}} x^3 dS &= \frac{\delta_0}{20} f_3(x) & (\mathbf{N}_{\mathcal{F}} \cdot \mathbf{k}) \int_{\mathcal{F}} z^2 x dS &= \frac{\delta_2}{60} (x_0 g_0(z) + x_1 g_1(z) \\
 &&&\quad + x_2 g_2(z))
 \end{aligned}$$

Comparison to Mirtich's Formulas

Let us compare the formulas for $Q_x = (\mathbf{N}_{\mathcal{F}} \cdot \boldsymbol{\iota}) \int_{\mathcal{F}} x dS$. Our derivation led to the formula,

$$Q_x = \frac{\delta_0}{6} f_1(x) = \frac{\delta_0}{6} (x_0 + x_1 + x_2) \quad (2.103)$$

In equation (2.99) there are three possibilities for computing Q_x . In the case $\gamma = z$,

$$Q_x = \frac{\delta_0}{6} \frac{(y_1 - y_0)(x_1^2 + x_0 x_1 + x_0^2) + (y_2 - y_1)(x_2^2 + x_1 x_2 + x_1^2) + (y_0 - y_2)(x_0^2 + x_0 x_2 + x_2^2)}{(x_1 - x_0)(y_2 - y_0) - (x_2 - x_0)(y_1 - y_0)}$$

The final formula requires much more computational time than the one derived in this document. In fact, the numerator is exactly divisible by the denominator and the fraction reduces to $x_0 + x_1 + x_2$, as it should be equivalent to the Q_x in equation (2.103). The reduction was verified using Mathematica. If $\gamma = x$, equation (2.99) produces

$$\begin{aligned}
 Q_x = -\frac{1}{\delta_0} \left(& \frac{\delta_1}{6} \sum_{i=0}^2 (z_{i+1} - z_i) (y_{i+1}^2 + y_{i+1} y_i + y_i^2) \right. \\
 & - \frac{\delta_2}{6} \sum_{i=0}^2 (y_{i+1} - y_i) (z_{i+1}^2 + z_{i+1} z_i + z_i^2) \\
 & \left. - \frac{\delta_0 x_0 + \delta_1 y_0 + \delta_2 z_0}{2} \sum_{i=0}^2 (z_{i+1} - z_i) (y_{i+1} + y_i) \right)
 \end{aligned}$$

The correctness of this formula was verified using Mathematica; in fact it reduces to [equation \(2.103\)](#). The computational requirements for this expression are enormous compared to that of [equation \(2.103\)](#).

Comparisons between the formulas for the other integrals is possible, but you will find that the differences in computational time become even greater than in the example shown here.

Pseudocode



The pseudocode for computing the integrals is quite simple. The polyhedron vertices are passed as the array `p[]`. The number of triangles is `tmax`. The array `index[]` has `tmax` triples of integers that are indices into the vertex array. The return values are the mass, the center of mass, and the inertia tensor.

```

constant Real oneDiv6 = 1/6;
constant Real oneDiv24 = 1/24;
constant Real oneDiv60 = 1/60;
constant Real oneDiv120 = 1/120;

MACRO Subexpressions(w0,w1,w2,f1,f2,f3,g0,g1,g2)
{
    // These are the expressions discussed in equation (2.101).
    temp0 = w0 + w1;
    f1 = temp0 + w2;
    temp1 = w0 * w0;
    temp2 = temp1 + w1 * temp0;
    f2 = temp2 + w2 * f1;
    f3 = w0 * temp1 + w1 * temp2 + w2 * f2;
    g0 = f2 + w0 * (f1 + w0);
    g1 = f2 + w1 * (f1 + w1);
    g2 = f2 + w2 * (f1 + w2);
}

void Compute (Point p[], int tmax, int index[],
    Real& mass, Point& cm, Matrix& inertia)
{
    // order: 1, x, y, z, x^2, y^2, z^2, xy, yz, zx
    Real integral[10] = {0,0,0,0,0,0,0,0,0,0};
    for (t = 0; t < tmax; t++)
    {
        // get vertices of triangle t
        i0 = index[3 * t];
        i1 = index[3 * t + 1];
        i2 = index[3 * t + 2];
        x0 = p[i0].x;
        y0 = p[i0].y;
        z0 = p[i0].z;
    }
}

```

```

x1 = p[i1].x;
y1 = p[i1].y;
z1 = p[i1].z;
x2 = p[i2].x;
y2 = p[i2].y;
z2 = p[i2].z;

// get edges and cross product of edges
a1 = x1 - x0;
b1 = y1 - y0;
c1 = z1 - z0;
a2 = x2 - x0;
b2 = y2 - y0;
c2 = z2 - z0;
d0 = b1 * c2 - b2 * c1;
d1 = a2 * c1 - a1 * c2;
d2 = a1 * b2 - a2 * b1;

// compute integral terms
Subexpressions(x0,x1,x2,f1x,f2x,f3x,g0x,g1x,g2x);
Subexpressions(y0,y1,y2,f1y,f2y,f3y,g0y,g1y,g2y);
Subexpressions(z0,z1,z2,f1z,f2z,f3z,g0z,g1z,g2z);

// update integrals
integral[0] += d0 * f1x;
integral[1] += d0 * f2x;
integral[2] += d1 * f2y;
integral[3] += d2 * f2z;
integral[4] += d0 * f3x;
integral[5] += d1 * f3y;
integral[6] += d2 * f3z;
integral[7] += d0 * (y0 * g0x + y1 * g1x + y2 * g2x);
integral[8] += d1 * (z0 * g0y + z1 * g1y + z2 * g2y);
integral[9] += d2 * (x0 * g0z + x1 * g1z + x2 * g2z);
}

integral[0] *= oneDiv6;
integral[1] *= oneDiv24;
integral[2] *= oneDiv24;
integral[3] *= oneDiv24;
integral[4] *= oneDiv60;
integral[5] *= oneDiv60;
integral[6] *= oneDiv60;
integral[7] *= oneDiv120;
integral[8] *= oneDiv120;
integral[9] *= oneDiv120;

mass = integral[0];

```

```

// center of mass
cm.x = integral[1] / mass;
cm.y = integral[2] / mass;
cm.z = integral[3] / mass;

// inertia relative to world origin
inertia.xx = integral[5] + integral[6];
inertia.yy = integral[4] + integral[6];
inertia.zz = integral[4] + integral[5];
inertia.xy = -integral[7];
inertia.yz = -integral[8];
inertia.xz = -integral[9];

// inertia relative to center of mass
inertia.xx -= mass * (cm.y * cm.y + cm.z * cm.z);
inertia.yy -= mass * (cm.z * cm.z + cm.x * cm.x);
inertia.zz -= mass * (cm.x * cm.x + cm.y * cm.y);
inertia.xy += mass * cm.x * cm.y;
inertia.yz += mass * cm.y * cm.z;
inertia.xz += mass * cm.z * cm.x;
}

```

The format of the input vertices and triangle connectivity array is useful if the input comes from triangle meshes that are also used for drawing. However, for even greater speed you may exchange some memory usage by passing in a single array of a more complicated triangle data structure that stores the three vertices and the cross product of two edges. This format will avoid the indirect lookup of vertices, the vector subtraction used to compute edges, and the cross product operation.

EXERCISE
2.16

1. Implement the pseudocode for computing the mass, center of mass, and inertia tensor for a polyhedron.
2. Implement the Mirtich algorithm for computing the mass, center of mass, and inertia tensor for a polyhedron.
3. Set up a profiling experiment to compare the average time per polyhedron required to compute the physical quantities. ■

2.6 ENERGY

This section is a brief one and describes the concepts of work, kinetic energy, and potential energy. The concept of kinetic energy is important in the development of Lagrangian dynamics. The concept of potential energy is important in the realm of conservative forces.

2.6.1 WORK AND KINETIC ENERGY

Consider a particle of mass m that is constrained to travel along a straight line whose direction is the unit-length vector \mathbf{D} . Suppose that a constant force \mathbf{F} is applied to the particle while it is moving. Figure 2.22 illustrates the situation.

If $L = |\mathbf{x}_1 - \mathbf{x}_0|$ is the distance traveled by the particle over a given time interval, the *work* done by the force on the particle over that time is defined to be the product of the magnitude of the force along the direction of the line and the distance traveled. In the simple illustration of Figure 2.22, the work is

$$W = (|\mathbf{F}| \cos \theta)L = (\mathbf{F} \cdot \mathbf{D})L \quad (2.104)$$

Observe that the component of the force in the direction of the line is $(\mathbf{F} \cdot \mathbf{D})\mathbf{D}$. The work is just the magnitude of that component times the distance traveled.

The path of the particle may very well be any smooth curve $\mathbf{x}(t)$. In this case we resort to the usual infinitesimal argument from calculus. Over an infinitesimal amount of time dt , the path looks like a line, and that line is the tangent line to the curve at the initial position of the particle. The infinitesimal amount of distance traveled by the particle during this instant of time is ds , the element of arc length. The direction at the initial instant of time is the unit-length tangential direction $\mathbf{D} = d\mathbf{x}/ds$. Using equation (2.104) as our motivation, the infinitesimal amount of work dW done by the force on the particle is

$$dW = (\mathbf{F} \cdot \mathbf{D})ds = \left(\mathbf{F} \cdot \frac{d\mathbf{x}}{ds} \right) ds$$

The total work done by the force on the particle as it travels over an arc length L is

$$W = \int_0^L \mathbf{F} \cdot \frac{d\mathbf{x}}{ds} ds \quad (2.105)$$

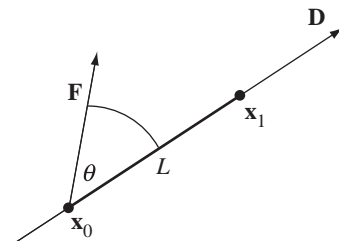


Figure 2.22 A force applied to a particle traveling on a straight line from position \mathbf{x}_0 to \mathbf{x}_1 .

However, we usually know the position as a function of time t rather than as a function of arc length s . The infinitesimal amount of work is

$$dW = \left(\mathbf{F} \cdot \frac{d\mathbf{x}}{ds} \right) ds = (\mathbf{F} \cdot d\mathbf{x}) = \left(\mathbf{F} \cdot \frac{d\mathbf{x}}{dt} \right) dt$$

The total work done by the force on the particle as it travels over a time interval $[t_0, t_1]$ is

$$W = \int_{t_0}^{t_1} \mathbf{F} \cdot \frac{d\mathbf{x}}{dt} dt = \int_{t_0}^{t_1} \mathbf{F} \cdot \mathbf{v} dt \quad (2.106)$$

where $\mathbf{v}(t)$ is the velocity of the particle.

In this development it is important to keep in mind that the position $\mathbf{x}(t)$ may not be entirely controlled by \mathbf{F} . Other forces can be acting on the particle at the same time. For example, the particle might be subject to gravitational force and \mathbf{F} represents a wind force. The quantity W in equation (2.106) represents the work done by the wind on the particle, but does not include work done by gravity.

EXAMPLE 2.10

A projectile of mass m follows a parabolic path $\mathbf{x}(t) = (t, 0, t(100 - t))$ for $t \in [0, 100]$. The projectile is subject to gravitational force $\mathbf{F} = (0, 0, -mg)$, where $g > 0$ is a constant. Compute the work done by the force over the specified interval.

The velocity of the projectile is $\mathbf{v} = (1, 0, 100 - 2t)$. The work done by the force is

$$\begin{aligned} W &= \int_0^{100} \mathbf{F} \cdot \mathbf{v} dt \\ &= \int_0^{100} (0, 0, -mg) \cdot (1, 0, 100 - 2t) dt \\ &= 2mg \int_0^{100} t - 50 dt \\ &= 0 \end{aligned}$$

EXERCISE 2.17

A particle travels along the circular path $\mathbf{x}(t) = (r \cos(\omega t), r \sin(\omega t), 1)$. A constant wind force is applied to the particle, $\mathbf{F} = (1, 1, 1)$. What is the work done by the wind on the particle during one period of rotation $0 \leq t \leq 2\pi/\omega$? What is a time interval over which the work is a maximum? Repeat the experiment, but for a time-varying wind $\mathbf{F} = (t, t, 1)$.

If \mathbf{F} is the net force on a particle and it does fully control the position, the integral in equation (2.106) can be integrated in closed form for a constant mass particle. In

this case Newton's Second Law allows us to use $\mathbf{F} = m\mathbf{a}$:

$$W = \int_{t_0}^{t_1} m\mathbf{a} \cdot \mathbf{v} dt = \int_{t_0}^{t_1} \frac{d}{dt} \left(\frac{m}{2} |\mathbf{v}|^2 \right) dt = \frac{m}{2} (|\mathbf{v}(t_1)|^2 - |\mathbf{v}(t_0)|^2)$$

The quantity W represents the work required to change the velocity of the particle from $\mathbf{v}(t_0)$ to $\mathbf{v}(t_1)$. If the particle starts out at rest, that is $\mathbf{v}(t_0) = \mathbf{0}$, then W is referred to as *kinetic energy*. In general, kinetic energy for a moving particle is

$$T = \frac{m}{2} |\mathbf{v}|^2 \quad (2.107)$$

By construction, kinetic energy is measured with respect to an inertial frame of reference. That frame is used to specify the position $\mathbf{x}(t)$ of the particle.

Kinetic energy is additive in the sense that for a system of particles, the kinetic energy of the system is the sum of the kinetic energies of the individual particles. For continuous material, the addition is in the sense of integration over a curve, surface, or volumetric region, just as we have seen in other parts of this chapter.

2.6.2 CONSERVATIVE FORCES AND POTENTIAL ENERGY

The work done by a force on a particle traveling along a path $\mathbf{x}(t)$ for $t \in [t_0, t_1]$ is defined by equation (2.106). The particle starts at $\mathbf{x}_0 = \mathbf{x}(t_0)$ and ends at $\mathbf{x}(t_1)$. By definition, the work done on the force depends on the path taken by the particle between the endpoints \mathbf{x}_0 and \mathbf{x}_1 . In many physical situations, though, the work is *independent of the path* given the right type of force. When this happens, the force is said to be *conservative*.

EXAMPLE 2.11

A particle is allowed to move between two points (x_0, y_0, z_0) and (x_1, y_1, z_1) along a smooth path $(x(t), y(t), z(t))$ connecting them, $t \in [t_0, t_1]$. The particle is subjected to a gravitational force $\mathbf{F} = -mg\mathbf{k}$. The work done by gravity is

$$\begin{aligned} W &= \int_{t_0}^{t_1} \mathbf{F} \cdot \mathbf{v} dt \\ &= \int_{t_0}^{t_1} -mg\mathbf{k} \cdot (\dot{\mathbf{x}}(t), \dot{\mathbf{y}}(t), \dot{\mathbf{z}}(t)) dt \\ &= -mg \int_{t_0}^{t_1} \dot{\mathbf{z}}(t) dt \\ &= -mg(z(t_1) - z(t_0)) \end{aligned} \quad (2.108)$$

Regardless of how you choose the path connecting the two points, the work is always a constant times the difference in heights of the endpoints. That is, W is independent of the path of the particle and gravitational force is a conservative force. ■

**EXAMPLE
2.12**

One end of a spring is attached to the origin $(0, 0, 0)$ and the other end is attached to a particle whose position $\mathbf{x}(t)$ varies with time, $t \in [t_0, t_1]$. The spring constant is $c > 0$ and the unstretched spring length is L . The force exerted on the particle by the spring is $\mathbf{F} = -c(\mathbf{x} - \ell)$ where $\ell = L\mathbf{x}/|\mathbf{x}|$, a vector of constant length L in the same direction as \mathbf{x} . The work done by the spring force is

$$\begin{aligned} W &= \int_{t_0}^{t_1} \mathbf{F} \cdot \mathbf{v} dt \\ &= \int_{t_0}^{t_1} -c(\mathbf{x} - \ell) \cdot \dot{\mathbf{x}} dt \\ &= \int_{t_0}^{t_1} -c(\mathbf{x} - \ell) \cdot (\dot{\mathbf{x}} - \dot{\ell}) dt \\ &= -c \int_{t_0}^{t_1} \frac{d}{dt} \frac{1}{2} |\mathbf{x} - \ell|^2 dt \\ &= -(c/2) (|\mathbf{x}(t_1) - \ell(t_1)|^2 - |\mathbf{x}(t_0) - \ell(t_0)|^2) \end{aligned} \tag{2.109}$$

The introduction of $(\mathbf{x} - \ell) \cdot \dot{\ell}$ in the integrand is valid because (1) $\mathbf{x} - \ell$ is parallel to ℓ , and (2) $\dot{\ell}$ is perpendicular to ℓ , because $\ell \cdot \ell = L^2$ implies $\ell \cdot \dot{\ell} = 0$. That is, $(\mathbf{x} - \ell) \cdot \dot{\ell} = 0$. The work depends only on the endpoints and not on the path connecting them, so the spring force is a conservative force. ■

**EXAMPLE
2.13**

A particle moves from $(0, 0, 0)$ to $(1, 1, 0)$ and is subject to the spatially varying force $\mathbf{F} = (y, -x, 0)$. This force is not conservative. The work done by the force when the particle travels along the line segment $(t, t, 0)$ for $t \in [0, 1]$ is

$$W_1 = \int_0^1 \mathbf{F} \cdot \mathbf{v} dt = \int_0^1 (t, -t, 0) \cdot (1, 1, 0) dt = 0$$

The work done by the force when the particle travels along the parabolic arc $(t, t^2, 0)$ for $t \in [0, 1]$ is

$$W_2 = \int_0^1 \mathbf{F} \cdot \mathbf{v} dt = \int_0^1 (t^2, -t, 0) \cdot (1, 2t, 0) dt = \int_0^1 -t^2 dt = -1/3 \neq W_1$$

The work done by the force depends on the path taken by the particle. ■

Other examples of nonconservative forces include friction, viscous drag when moving through a fluid, and many forces that have explicit dependence on time and velocity.

Consider a system of p particles with masses m_i and positions $(\hat{x}_i, \hat{y}_i, \hat{z}_i)$ for $1 \leq i \leq p$. These positions are referred to as the *reference system*. Conservative forces \mathbf{F}_i are applied to the particles in a *general system*, where the positions are (x_i, y_i, z_i) , and work is measured as the general system is transferred to the reference system. The work done by the forces in transferring the system is referred to as the *potential energy* that the general system has with respect to the reference system. This quantity is denoted V and is defined by

$$V = - \sum_{i=1}^p \int_0^1 \mathbf{F}_i \cdot \mathbf{v}_i \, dt \quad (2.110)$$

The paths implicit in the integration connect $(\hat{x}_i, \hat{y}_i, \hat{z}_i)$, at time 0, to (x_i, y_i, z_i) , at time 1. Because the forces are conservative, any smooth paths that are parameterized by $t \in [0, 1]$ will do. The potential energy is therefore dependent only on the general system; the reference positions are assumed to be constant. That is, as a function we have

$$V = V(x_1, y_1, z_1, \dots, x_p, y_p, z_p)$$

so that V is dependent on $3p$ variables. From calculus the total derivative of V is

$$\begin{aligned} dV &= \frac{\partial V}{\partial x_1} dx_1 + \frac{\partial V}{\partial y_1} dy_1 + \frac{\partial V}{\partial z_1} dz_1 + \dots + \frac{\partial V}{\partial x_p} dx_p + \frac{\partial V}{\partial y_p} dy_p + \frac{\partial V}{\partial z_p} dz_p \\ &= \sum_{i=1}^p \left(\frac{\partial V}{\partial x_i} dx_i + \frac{\partial V}{\partial y_i} dy_i + \frac{\partial V}{\partial z_i} dz_i \right) \end{aligned}$$

In terms of infinitesimal quantities, the potential energy is

$$dV = - \sum_{i=1}^p \mathbf{F}_i \cdot d\mathbf{x}_i = - \sum_{i=1}^p (F_{x_i} dx_i + F_{y_i} dy_i + F_{z_i} dz_i)$$

where each force is specified componentwise as $\mathbf{F}_i = (F_{x_i}, F_{y_i}, F_{z_i})$. In order to be independent of path, the right-hand sides of the last two differential equations must be equal. Thus,

$$F_{x_i} = -\frac{\partial V}{\partial x_i}, \quad F_{y_i} = -\frac{\partial V}{\partial y_i}, \quad F_{z_i} = -\frac{\partial V}{\partial z_i}$$

for all i . In compact vector notation, $\mathbf{F}_i = -\nabla_i V$, where ∇_i denotes the gradient operator with respect to the three variables x_i , y_i , and z_i .

By definition, if \mathbf{F} is a conservative force, there is a potential energy function V for which $\mathbf{F} = -\nabla V$. But how do you know if you have a conservative force? The answer lies in the same condition. If it were the case that $(F_1, F_2, F_3) = \mathbf{F} = -\nabla V$, then

$$F_1 = -\frac{\partial V}{\partial x}, \quad F_2 = -\frac{\partial V}{\partial y}, \quad F_3 = -\frac{\partial V}{\partial z}$$

Assuming V has continuous second-order partial derivatives, the mixed partials are equal. That is, $\partial^2 V / \partial x \partial y = \partial^2 V / \partial y \partial x$, $\partial^2 V / \partial x \partial z = \partial^2 V / \partial z \partial x$, and $\partial^2 V / \partial y \partial z = \partial^2 V / \partial z \partial y$. In terms of the function components, it is necessary that

$$\frac{\partial F_1}{\partial y} = \frac{\partial F_2}{\partial x}, \quad \frac{\partial F_1}{\partial z} = \frac{\partial F_3}{\partial x}, \quad \text{and} \quad \frac{\partial F_2}{\partial z} = \frac{\partial F_3}{\partial y} \quad (2.111)$$

The conditions in equation (2.111) are referred to as an *exactness test*. As it turns out, these conditions are sufficient as well as necessary for the existence of a potential energy function V for which $\mathbf{F} = -\nabla V$. If the conditions in the equation are satisfied, \mathbf{F} must be a conservative force. Note that equation (2.111) is written concisely as $\nabla \times \mathbf{F} = \mathbf{0}$; that is, the curl of \mathbf{F} is zero.

EXAMPLE 2.14

In Example 2.11 the gravitational force is $(F_1, F_2, F_3) = (0, 0, -mg)$, a constant force. The conditions in equation (2.111) are trivially satisfied because all the derivatives of the F_i are zero.

In Example 2.12 the spring force is $(F_1, F_2, F_3) = -c(x, y, z)$. The exactness conditions are satisfied,

$$\frac{\partial F_1}{\partial y} = 0 = \frac{\partial F_2}{\partial x}, \quad \frac{\partial F_1}{\partial z} = 0 = \frac{\partial F_3}{\partial x}, \quad \frac{\partial F_2}{\partial z} = 0 = \frac{\partial F_3}{\partial y}$$

so the force is conservative.

In Example 2.13 the force is $(F_1, F_2, F_3) = (y, -x, 0)$. This force is not conservative because

$$\frac{\partial F_1}{\partial y} = 1 \neq -1 = \frac{\partial F_2}{\partial x}$$

The other two exactness tests are true, but as long as one of the three fails, the force is not conservative. ■

One very important consequence of having a conservative force is that the total energy of the system is conserved. Let $\mathbf{F}(\mathbf{x})$ be the force and let $V(\mathbf{x})$ be the potential

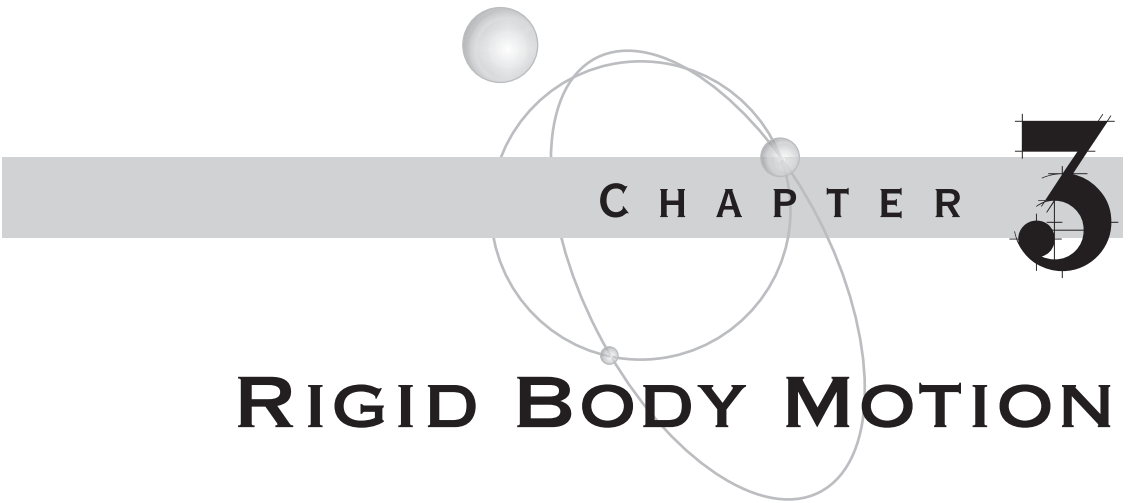
energy function for which $\mathbf{F} = -\nabla V$. The kinetic energy is $T = m|\dot{\mathbf{x}}|^2/2$ and the total energy is

$$E = T + V = \frac{1}{2} m|\dot{\mathbf{x}}|^2 + V(\mathbf{x}) \quad (2.112)$$

The time derivative of the energy is

$$\frac{dE}{dt} = \frac{d(T + V)}{dt} = m\dot{\mathbf{x}} \cdot \ddot{\mathbf{x}} + \dot{\mathbf{x}} \cdot \nabla V = \dot{\mathbf{x}} \cdot (m\ddot{\mathbf{x}} - \mathbf{F}) = 0$$

where the last equality follows from Newton's second law, $m\ddot{\mathbf{x}} = \mathbf{F}$.



CHAPTER

RIGID BODY MOTION

Chapter 2 introduced the topic of kinematics, the motion of a body along a path in the absence of external forces. Given the position, we can compute velocity and acceleration by differentiation. This chapter is about *dynamics*, the interaction of rigid bodies when forces and torques are present in the physical system. The classical approach in an introductory physics course uses Newtonian dynamics and the famous formula of Newton's second law of motion, $F = ma$, where m is the constant mass of an object, a is its acceleration, and F is the applied force. The applied force determines the acceleration of the object, so velocity and position are obtained by integration, exactly the opposite process we saw in kinematics. The coverage of Newtonian dynamics is brief yet sufficient to support the general purpose physics engines that use Newton's second law for simulation as described in [Chapter 6](#).

The majority of this chapter is on the topic of *Lagrangian dynamics*, a framework for setting up the equations of motion for objects when constraints are present. In Lagrangian dynamics, the equations of motion are derived from the kinetic energy function and naturally incorporate the constraints. A Newtonian formulation requires that forces of constraint be part of the term F in the equation of motion; the constraint forces are sometimes difficult to derive. Frictional forces are difficult to deal with in a general purpose physics engine that uses Newtonian dynamics. In the Lagrangian approach, frictional forces are easier to deal with. An entire section is devoted to various examples involving objects moving on a rough plane, that is, a plane whose material causes frictional forces.

A game designer's specific knowledge of what the game physics will entail can exploit that knowledge to good effect by formulating the simulations using Lagrangian dynamics. The result is that the computational time of the simulation

is reduced compared to a general purpose system using Newtonian dynamics. Even more important is that the robustness problems with enforcing nonpenetration in a general purpose engine are reduced. In the situation where you explicitly know the constraining surface on which an object must lie, you can periodically check if numerical round-off errors have caused the object to be slightly off the surface, then correct the position accordingly. On the other hand, a simulation modeled with Lagrangian dynamics is specific to each physics application, thus requiring more programming development time. My choice is to spend more time on the programming and gain the faster and more robust applications. In addition, Euler's equations of motion are discussed in this chapter because a few problems are more naturally formulated in terms of Euler angles than in terms of other dynamics systems.

The classic textbook covering mechanics, including the topics mentioned in this chapter, is [GPS02]. The text is on the heavy side with mathematics compared to what you see in a standard physics course. In my opinion, the ultimate textbook for Lagrangian dynamics is a title in the Schaum's Outline Series, [Wel67]. The presentation shirks away from many direct derivative computations and uses the infinitesimal approach that is popular among physicists to motivate some of the derivations (not my personal preference), but the book has a lot of good examples for you to try. If you are able to understand these and correctly work the exercises, you will be in a very good position to solve any similar problem that comes your way in an application.

3.1 NEWTONIAN DYNAMICS

The section on kinematics describes the position, velocity, and acceleration of a particle in motion along a curve and having no external forces acting on it. Dynamics, on the other hand, describes how the particle must move when external forces are acting on it. I assume that the mass m of the particle is constant over time, so Newton's law states that $\mathbf{F} = m\mathbf{a}$, where \mathbf{F} are the external forces acting on the particle and \mathbf{a} is the acceleration of the particle. If there are no external forces, $\mathbf{F} = \mathbf{0}$, the acceleration is $\mathbf{a}(t) = \mathbf{0}$. This equation integrates to $\mathbf{v}(t) = \mathbf{v}_0$, a constant. That is, the particle travels with constant velocity when the acceleration is zero. Integrating again yields $\mathbf{r}(t) = t\mathbf{v}_0 + \mathbf{r}_0$, where \mathbf{r}_0 is the initial location of the particle at time zero. The path of motion is a straight line, as expected when no forces act on the object.

In the case of kinematics, we postulated the path of a particle and computed the velocity and acceleration from it by differentiation. In the case of dynamics, we are specifying the acceleration and must integrate to obtain the velocity and acceleration. This is not always possible in a closed form, so many problems require numerical methods to approximate the solution.

EXAMPLE 3.1

Let us take a look at a classic problem of motion of the Earth about the Sun. The equations describing the motion are called *Kepler's Laws*, after Johann Kepler, who established the first two laws in 1609 and the third law in 1616. The basis for the equation is that the Sun exerts a gravitational force on the Earth according to an

inverse-squared-distance law. Let M be the mass of the Sun and m be the mass of the Earth. Let r be the distance between the Earth and Sun. Let the position of the Sun define the origin of the coordinate system. The force exerted is

$$\mathbf{F} = -\frac{GMm}{r^2}\mathbf{R}$$

where G is a positive constant whose value is determined by empirical means. The vector \mathbf{R} is unit length and in the direction of the vector from the Sun to the Earth. The minus sign states that the force on the Earth is attracting it towards the Sun. Newton's law states that the acceleration \mathbf{a} of the Earth is determined by

$$m\mathbf{a} = \mathbf{F} = -\frac{GMm}{r^2}\mathbf{R} = -\frac{GMm}{r^3}\mathbf{r}$$

where we have used $\mathbf{r} = r\mathbf{R}$. Dividing by the Earth's mass and using $\mathbf{a} = \dot{\mathbf{v}}$:

$$\dot{\mathbf{v}} = -\frac{GM}{r^3}\mathbf{r} \quad (3.1)$$

Now consider

$$\begin{aligned} \frac{d}{dt}(\mathbf{r} \times \mathbf{v}) &= \mathbf{r} \times \dot{\mathbf{v}} + \dot{\mathbf{r}} \times \mathbf{v} \\ &= \mathbf{r} \times \left(-\frac{GM}{r^3}\mathbf{r}\right) + \mathbf{v} \times \mathbf{v} \\ &= -\frac{GM}{r^3}\mathbf{r} \times \mathbf{r} + \mathbf{v} \times \mathbf{v} \\ &= \mathbf{0} \end{aligned}$$

This implies $\mathbf{r} \times \mathbf{v} = \mathbf{c}_0$, a constant vector for all time. Observe that the angular momentum of the Earth is $\mathbf{r} \times m\mathbf{v}$, so the implication is that the angular momentum is a constant vector for all time. Another immediate consequence of the constancy is that

$$\mathbf{0} = \mathbf{r} \cdot \mathbf{r} \times \mathbf{v} = \mathbf{r} \cdot \mathbf{c}_0$$

The motion is necessarily within a plane containing the Sun's location and having normal vector \mathbf{c}_0 .

KEPLER'S FIRST LAW *Equal areas in the plane of motion are swept out in equal time intervals.* To see that this is true, consider an infinitesimal area dA swept out by moving the Earth from current position \mathbf{r} by an infinitesimal change in position $d\mathbf{r}$. Figure 3.1 illustrates this.

The infinitesimal area is that of a triangle with two sides \mathbf{r} and $\mathbf{r} + d\mathbf{r}$. The area of the triangles is half the magnitude of the cross product of two edges, so

(Example 3.1
continued)

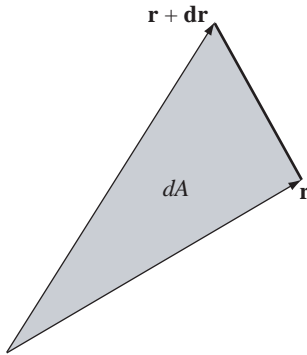


Figure 3.1

The infinitesimal area dA swept out by motion of the earth over an infinitesimal change in position $d\mathbf{r}$. The swept region is effectively a triangle whose sides are \mathbf{r} and $\mathbf{r} + d\mathbf{r}$.

$dA = |\mathbf{r} \times d\mathbf{r}|/2$. On the macroscopic level,

$$\dot{A} = \frac{1}{2} |\mathbf{r} \times \dot{\mathbf{r}}| = \frac{1}{2} |\mathbf{r} \times \mathbf{v}| = \frac{1}{2} |\mathbf{c}_0|$$

The rate of change in the swept area is constant, so equal areas are swept out in equal time intervals.

KEPLER'S SECOND LAW *The orbit of the Earth is an ellipse with the Sun as one of the focal points.* To see that this is true, consider:

$$\begin{aligned} \frac{d}{dt} (\mathbf{v} \times \mathbf{c}_0) &= \dot{\mathbf{v}} \times \mathbf{c}_0 \\ &= -\frac{GM}{r^3} \mathbf{r} \times \mathbf{c}_0 \\ &= -\frac{GM}{r^3} \mathbf{r} \times (\mathbf{r} \times \mathbf{v}) \\ &= -\frac{GM}{r^3} \mathbf{r} \times (\mathbf{r} \times (r\dot{\mathbf{R}} + \dot{r}\mathbf{R})) \\ &= -\frac{GM}{r^3} \mathbf{r} \times (r\mathbf{r} \times \dot{\mathbf{R}}) \\ &= -GMR \times (\mathbf{R} \times \dot{\mathbf{R}}) \\ &= -GM((\mathbf{R} \cdot \dot{\mathbf{R}})\mathbf{R} - (\mathbf{R} \cdot \mathbf{R})\dot{\mathbf{R}}) \\ &= GM\dot{\mathbf{R}} \end{aligned}$$

Integrating yields $\mathbf{v} \times \mathbf{c}_0 = GM\mathbf{R} + \mathbf{c}_1$ for some constant vector \mathbf{c}_1 . Define $\gamma_0 = |\mathbf{c}_0|$ and $\gamma_1 = |\mathbf{c}_1|$ and observe that

$$\begin{aligned}\gamma_0^2 &= |\mathbf{c}_0|^2 \\ &= \mathbf{r} \times \mathbf{v} \cdot \mathbf{c}_0 \\ &= \mathbf{r} \cdot \mathbf{v} \times \mathbf{c}_0 \\ &= \mathbf{r} \cdot (GM\mathbf{R} + \mathbf{c}_1) \\ &= GM\mathbf{r} + \mathbf{r} \cdot \mathbf{c}_1 \\ &= GM\mathbf{r} + r\gamma_1 \cos \theta\end{aligned}$$

where θ is the angle between \mathbf{r} and \mathbf{c}_1 . In polar coordinates (r, θ) , the equation is solved for r as a function of θ :

$$r(\phi) = \frac{\gamma_0^2}{GM + \gamma_1 \cos \theta} = \frac{e\rho}{1 + e \cos \theta} \quad (3.2)$$

which gives an ellipse with eccentricity $e = \gamma_1/(GM)$ and where $\rho = \gamma_0^2/\gamma_1$. The major axis length is $2a = r(0) + r(\pi) = 2\rho e/(1 - e^2)$. The minor axis length is $2b = 2a\sqrt{1 - e^2}$. The area of the ellipse is $A = \pi ab$.

KEPLER'S THIRD LAW *The square of the period of the motion is proportional to the cube of the major axis length.* The proof is as follows. The areal rate of change is $\dot{A} = \gamma_0/2$. Integrating over one period of time $t \in [0, T]$ yields the total area of the ellipse $A = \gamma_0 T/2$. Therefore, the period is

$$T = \frac{2A}{\gamma_0} = \frac{2\pi a^2 \sqrt{1 - e^2}}{\sqrt{GMa(1 - e^2)}} = \frac{2\pi}{\sqrt{GM}} a^{3/2}$$

or $T^2 = Ka^3$ for a constant of proportionality K . ■

EXERCISE
3.1

Convert [equation \(3.2\)](#) to Cartesian coordinates and verify that it does in fact represent an ellipse. ■

EXERCISE
3.2

Solve [equation \(3.1\)](#) using a differential equation solver. The left-hand side of that equation is replaced by $\ddot{\mathbf{r}}$, so the equation is second order in position. Use $GM = 1$ for the right-hand side of the equation. Choose an initial position $\mathbf{r}(0)$ and an initial velocity $\dot{\mathbf{r}}(0)$ that are perpendicular vectors. ■

EXERCISE
3.3

Consider the polar coordinate coordinate form for acceleration given in [equation \(2.13\)](#). We saw in [equation 3.2](#) that the motion of the Earth is along an elliptical path that defines r as a function of θ . However, we had not considered how θ varies in time. This exercise is designed to give you that information.

SOURCE CODE

KeplerPolarForm

1. Derive two second-order differential equations, $\ddot{r} - r\dot{\theta}^2 = -GM/r^2$ and $r\ddot{\theta} + 2r\dot{\theta}\dot{r} = 0$, that are the equations of motion in polar coordinates.
2. Show that the equation with $\ddot{\theta}$ implies $\alpha = Mr^2\dot{\theta}$ is a constant. The value α is angular momentum, so this physical system exhibits conservation of angular momentum as well as conservation of total energy. Since α is a constant, argue that $\dot{\theta}$ always has the same sign, in which case r may be thought of as a function of θ , $r = r(\theta)$.
3. Use the expression for α to eliminate $\dot{\theta}$ in the equation with \ddot{r} to obtain $\ddot{r} - \alpha^2/(M^2r^3) = -GM/r^2$. This may be solved numerically for $r(t)$, but you might find that the singularity at $r = 0$ causes quite a fuss!
4. The potential energy is $V(\phi) = -GM/r$. Equivalently, $r = -GM/V$. I emphasized earlier that I am thinking of r as a function of θ , so V is also a function of θ . Its first derivative with respect to θ is denoted V' and its second derivative with respect to θ is denoted V'' . Dots above variables will still be reserved to indicate time derivatives.
 - (a) Show that $\dot{r} = GMV'\dot{\theta}/V^2 = \alpha V'/(GM^2)$.
 - (b) Show that $\ddot{r} = \alpha V''\dot{\theta}/(GM^2) = \alpha^2 V''V^2/(G^3M^5)$.
 - (c) Use the last result in $\ddot{r} - \alpha^2/(M^2r^3) = -GM/r^2$ to obtain $V'' + V = -G^2M^4/\alpha^2$. Show that the general solution to this equation is $V(\theta) = c_0 \sin(\theta) + c_1 \cos(\theta) - G^2M^4/\alpha^2$.
 - (d) Determine c_0 and c_1 from the initial data r_0 , \dot{r}_0 , θ_0 , and $\dot{\theta}_0$.
5. From conservation of momentum, show that $\dot{\theta} = \alpha V^2/(G^2M^3)$.
6. Using the formula for $V(\theta)$ and the differential equation for θ , conclude that

$$\dot{\theta} = \frac{\alpha}{G^2M^3} \left(c_0 \sin(\theta) + c_1 \cos(\theta) - \frac{G^2M^4}{\alpha^2} \right)^2, \quad \theta(0) = \theta_0$$

The result of this exercise is a first-order nonlinear differential equation that can be solved by standard numerical methods. Can you solve for $\theta(t)$ in closed form? ■

EXAMPLE
3.2

Here is a second example and it is formulated for motion of a particle relative to the moving frame of a rigid body. Newton's second law is $\mathbf{F} = m\mathbf{a}$, where the acceleration \mathbf{a} is given in [equation \(2.44\)](#). The problem is to determine the path of motion of a particle that is freely falling towards the Earth, the rigid body, subject only to gravitational force. If the Earth were not rotating, the path of motion would clearly be a line containing the center of the Earth and the initial particle location. Fortunately, the Earth does rotate, so the problem is a bit more complex!

The world coordinate system is chosen so that its origin is at the center of the Earth. One of the coordinate axes is chosen to be in the direction from the Earth's

center to the north pole. The Earth rotates about this axis with angular velocity \mathbf{w} . Since we are dealing with a single particle, the center of mass is the particle's location and, subsequently, the origin of the moving frame. The moving frame directions are chosen to be those of spherical coordinates, $\xi_1 = \mathbf{P}$, $\xi_2 = \mathbf{Q}$, and $\xi_3 = \mathbf{R}$. The force on the particle due to gravity is $-mg\mathbf{R}$, where m is the mass of the particle and $g > 0$ is the gravitational constant. Since \mathbf{R} points away from the Earth's center, the minus sign in the force expression indicates the Earth is attracting the particle towards it. [Equation \(2.44\)](#) describes the path \mathbf{r} of the particle relative to the Earth's center.

We will take the usual liberties that you see in many physics applications. The equation of motion is quite complicated, so we will make a few simplifying assumptions that lead to a more tractable problem. First, let us assume that the time interval for which we want to know the path of motion is small. Over this time the difference between the particle and the world origin Δ is effectively a constant. If it were identically a constant, then $\dot{\Delta} = \mathbf{0}$. We also assume that the angular velocity does not change significantly during the time interval. The mathematical approximation is $\dot{\mathbf{w}} = \mathbf{0}$. Finally, the number of seconds per day is approximately 86,400. The angular speed is $|\mathbf{w}| \doteq 2\pi/86,400$. The radius of the Earth is approximately 6440 kilometers. Assuming the particle is relatively near the Earth's surface, its position \mathbf{r} is of the order of magnitude of the Earth's radius. The magnitude of $\mathbf{w} \times (\mathbf{w} \times \mathbf{r})$ is of the order of $|\mathbf{w}|^2 |\mathbf{r}| \doteq 3.4 \times 10^{-5}$, a very small number. The mathematical approximation to this term is $\mathbf{w} \times (\mathbf{w} \times \mathbf{r}) = \mathbf{0}$.

Using all the approximations in the equation of motion leads to

$$\frac{D^2\mathbf{r}}{Dt^2} = -2\mathbf{w} \times \frac{D\mathbf{r}}{Dt} - g\mathbf{R} \quad (3.3)$$

This is a linear second-order system of ordinary differential equations in the unknown $\mathbf{r}(t)$. If we supply an initial position $\mathbf{r}_0 = \mathbf{r}(0)$ and an initial velocity $\mathbf{v}_0 = D\mathbf{r}(0)/Dt$, the equation can be solved in closed form. We may integrate [equation \(3.3\)](#) to obtain

$$\frac{D\mathbf{r}}{Dt} = \mathbf{v}_0 - 2\mathbf{w} \times (\mathbf{r} - \mathbf{r}_0) - gt\mathbf{R} = -2\mathbf{w} \times \mathbf{r} + (\mathbf{v}_0 + 2\mathbf{w} \times \mathbf{r}_0) - gt\mathbf{R} \quad (3.4)$$

Define $\mathbf{w} = \omega\mathbf{u}$ where \mathbf{u} is the normalized vector for \mathbf{w} and $\omega = |\mathbf{w}|$. Using methods for solving linear systems of differential equations, [equation \(3.4\)](#) can be solved as

$$\mathbf{r} = \text{Rot}(-2\omega t, \mathbf{u})\mathbf{r}_0 + (\mathbf{v}_0 + 2\mathbf{w} \times \mathbf{r}_0)t - (gt^2/2)\mathbf{R} \quad (3.5)$$

where $\text{Rot}(\theta, \mathbf{u})$ denotes the rotation matrix about the axis with unit-length direction \mathbf{u} by the angle θ . Observe that if there were no rotation, that is, $\mathbf{w} = \mathbf{0}$, [equation \(3.5\)](#) is instead $\mathbf{r} = \mathbf{r}_0 + t\mathbf{v}_0 - (gt^2/2)\mathbf{R}$, exactly the equation you see in standard physics for a freely falling body where the Earth's rotation is considered negligible. ■

EXERCISE
3.4

Suppose that the particle represents a booster rocket that was fired from Cape Canaveral. Suppose the rocket traveled vertically upward to an altitude of 10 kilometers. At that point the rocket starts falling to Earth. Assuming the physical model of the last example applies for all time, how long does it take for the rocket to reach the ground? Where on Earth does it strike the ground? ■

EXAMPLE
3.3

This example is a model of the *Foucault pendulum*. The pendulum consists of a particle of mass m attached to one end of a wire of length L of negligible mass. The other end of the wire is attached to a joint at position O . The joint is assumed to be frictionless. The only forces acting on the particle are gravity and the tension in the wire. Figure 3.2 shows the pendulum relative to a fixed frame with origin O . We assume the Earth is rotating and that its angular velocity \mathbf{w} is in the direction from the center of the Earth C to the North Pole, just as in the previous example.

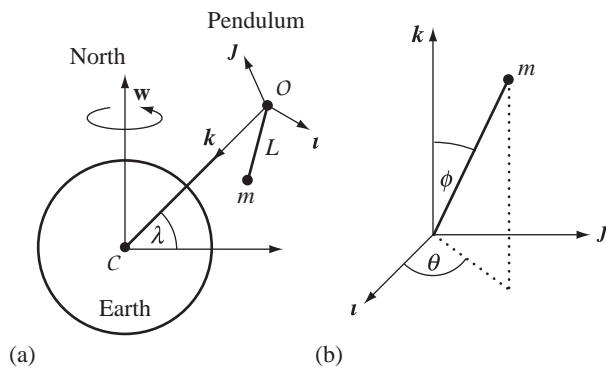


Figure 3.2

The Foucault pendulum. The pendulum joint is at O , the mass is m and is attached to the pendulum rod of length L . The gravitational force acts in the direction \mathbf{k} , a unit-length vector from the joint to the center of the Earth.

The fixed frame vectors are \mathbf{k} , a vector in the direction from O to the center of the earth; \mathbf{J} , a vector in the plane of \mathbf{w} and \mathbf{k} ; and \mathbf{i} , a vector pointing out of the page and perpendicular to the other two frame vectors. The mass at the end of the wire is represented in spherical coordinates relative to O . The position is

$$\mathbf{r} = LR(\theta, \phi)$$

where the angle ϕ is measured between the wire and the vertical \mathbf{k} , and the angle θ is measured from the \mathbf{i} axis in the (\mathbf{i}, \mathbf{J}) plane as shown in Figure 3.2(b). The angular

velocity is represented in the fixed frame as

$$\mathbf{w} = \omega [(\cos \lambda) \mathbf{J} - (\sin \lambda) \mathbf{k}]$$

where ω is the angular speed and λ is the latitude measured from the equator.

The simplifications that were made in the last example are also made here. The gravitational force is approximately $mg\mathbf{k}$ and the tension in the wire is $-m\tau\mathbf{R}$ for some scalar $\tau > 0$. The equation of motion for the pendulum is

$$\frac{D^2\mathbf{r}}{dt^2} = -2\mathbf{w} \times \frac{D\mathbf{r}}{dt} + g\mathbf{k} - \tau\mathbf{R} \quad (3.6)$$

Equations (2.32) and (2.33) apply, but with $\rho = L$, a constant for all time. The velocity is

$$\frac{D\mathbf{r}}{dt} = L [(\dot{\theta} \sin \phi) \mathbf{P} - (\dot{\phi}) \mathbf{Q}]$$

and the acceleration is

$$\frac{D^2\mathbf{r}}{dt^2} = L [(\ddot{\theta} \sin \phi + 2\dot{\theta}\dot{\phi} \cos \phi) \mathbf{P} + (\dot{\theta}^2 \sin \phi \cos \phi - \ddot{\phi}) \mathbf{Q} - (\dot{\phi}^2 + \dot{\theta}^2 \sin^2 \phi) \mathbf{R}]$$

These may be substituted into equation (3.6) to obtain three equations, one for each spherical frame direction.

The first equation of motion is

$$\begin{aligned} L(\ddot{\theta} \sin \phi + 2\dot{\theta}\dot{\phi} \cos \phi) &= \mathbf{P} \cdot \frac{D^2\mathbf{r}}{dt^2} \\ &= -2\mathbf{w} \times \frac{D\mathbf{r}}{dt} \cdot \mathbf{P} + g\mathbf{k} \cdot \mathbf{P} - \tau\mathbf{R} \cdot \mathbf{P} \\ &= -2\mathbf{w} \cdot \frac{D\mathbf{r}}{dt} \times \mathbf{P} \\ &= -2\mathbf{w} \cdot (L\dot{\phi}\mathbf{R}) \\ &= -2L\dot{\phi}(\mathbf{w} \cdot \mathbf{R}) \\ &= 2L\omega\dot{\phi}(-\cos \lambda \sin \theta \sin \phi + \sin \lambda \cos \phi) \end{aligned}$$

(Example 3.3
continued)

The L terms cancel, so the first equation of motion has been simplified to

$$\ddot{\theta} \sin \phi + 2\dot{\theta}\dot{\phi} \cos \phi = 2\omega\dot{\phi}(-\cos \lambda \sin \theta \sin \phi + \sin \lambda \cos \phi) \quad (3.7)$$

The second equation of motion is

$$\begin{aligned} L(\dot{\theta}^2 \sin \phi \cos \phi - \ddot{\phi}) &= \mathbf{Q} \cdot \frac{D^2 \mathbf{r}}{dt^2} \\ &= -2\mathbf{w} \times \frac{D\mathbf{r}}{dt} \cdot \mathbf{Q} + g\mathbf{k} \cdot \mathbf{Q} - \tau \mathbf{r} \cdot \mathbf{Q} \\ &= -2\mathbf{w} \cdot \frac{D\mathbf{r}}{dt} \times \mathbf{Q} + g \sin \phi \\ &= -2\mathbf{w} \cdot ((L\dot{\theta} \sin \phi)\mathbf{R}) + g \sin \phi \\ &= 2L\omega\dot{\theta} \sin \phi (-\cos \lambda \sin \theta \sin \phi + \sin \lambda \cos \phi) + g \sin \phi \end{aligned}$$

Dividing by the L term, the second equation of motion simplifies to

$$\dot{\theta}^2 \sin \phi \cos \phi - \ddot{\phi} = 2\omega\dot{\theta} \sin \phi (-\cos \lambda \sin \theta \sin \phi + \sin \lambda \cos \phi) + \frac{g}{L} \sin \phi \quad (3.8)$$

The third equation is

$$\begin{aligned} -L(\dot{\phi}^2 + \dot{\theta}^2 \sin^2 \phi) &= \mathbf{R} \cdot \frac{D^2 \mathbf{r}}{dt^2} \\ &= -2\mathbf{w} \times \frac{D\mathbf{r}}{dt} \cdot \mathbf{R} + g\mathbf{k} \cdot \mathbf{R} - \tau \mathbf{R} \cdot \mathbf{R} \\ &= 2L\mathbf{w} \cdot [(\dot{\phi})\mathbf{P} + (\dot{\theta} \sin \phi)\mathbf{Q}] + g(\mathbf{k} \cdot \mathbf{R}) - \tau \end{aligned}$$

which simplifies to

$$\tau = L[\dot{\phi}^2 + \dot{\theta}^2 \sin^2 \phi + 2\dot{\phi}(\mathbf{w} \cdot \mathbf{P}) + 2\dot{\theta} \sin \phi (\mathbf{w} \cdot \mathbf{Q})] + g(\mathbf{k} \cdot \mathbf{R}) \quad (3.9)$$

This is an equation of constraint and says that for static equilibrium, the tension in the wire, $-m\tau \mathbf{R}$, must have τ satisfy the equation. Therefore, only the two equations (3.7) and (3.8) control the motion through the time-varying angles $\theta(t)$ and $\phi(t)$. Figure 3.3 – also Color Plate 3.3 – shows some screen shots from the Foucault pendulum application found on the CD-ROM.

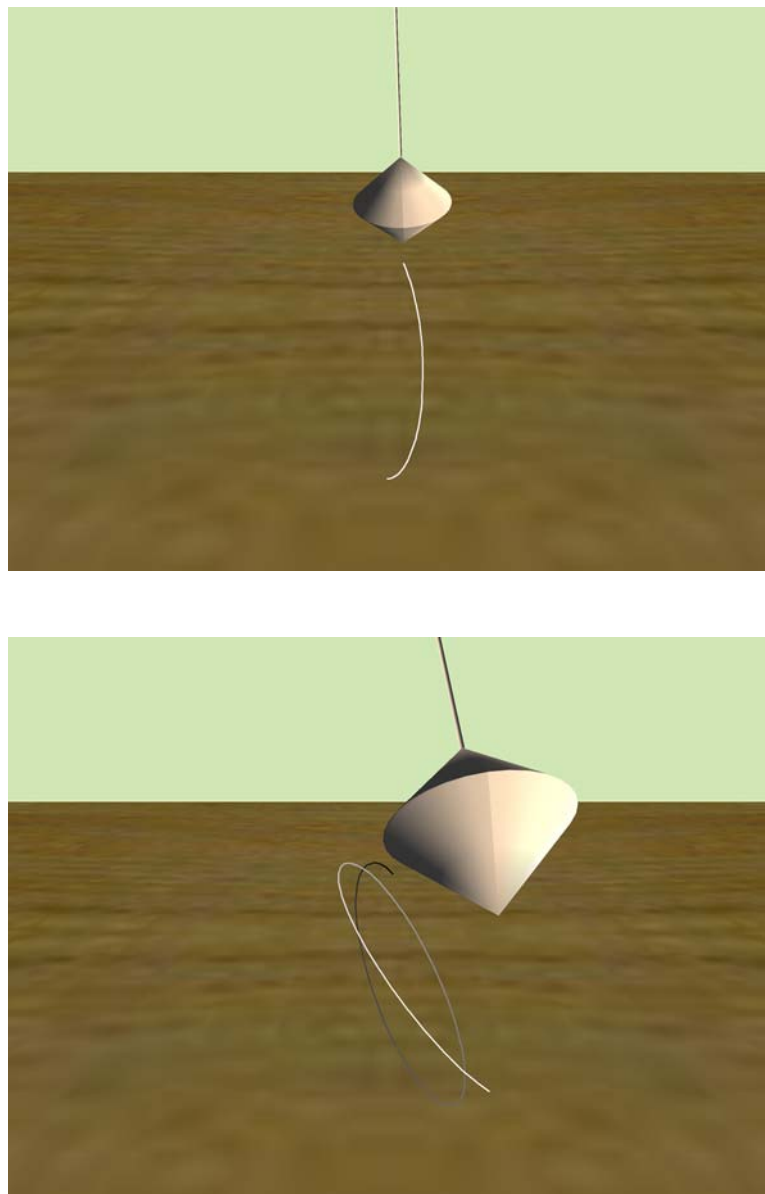


Figure 3.3

The Foucault pendulum. The figures show the path of the pendulum tip in the horizontal plane. New points on the path are colored white, but the intensity of the older points along the path gradually decreases. ■

EXAMPLE
3.4

The *simple pendulum* model is obtained by neglecting the angular velocity over a small period of time. The angle θ is constant, and the angular speed ω may as well be assumed to be zero. Under these assumptions, equation (3.7) is a tautology and offers no information. Equation (3.8) is a single nonlinear differential equation in ϕ :

$$\ddot{\phi} + \frac{g}{L} \sin \phi = 0 \quad (3.10)$$

Let the initial conditions be $\phi(0) = \phi_0 > 0$ and $\dot{\phi}(0) = 0$. That is, the mass at the end of the wire starts off at some nonzero angle from the vertical and is released with zero speed. Since the joint of the pendulum is frictionless, your intuition is that for some future time $T > 0$, the angle $\phi(T) = -\phi_0$, the motion is periodic, and T is the half period. So what is this time T ?

Multiply equation (3.10) by $2\dot{\phi}$ to obtain

$$0 = 2\dot{\phi}\ddot{\phi} + \frac{2g}{L}\dot{\phi}\sin\phi = \frac{d}{dt} \left(\dot{\phi}^2 - \frac{2g}{L} \cos\phi \right)$$

An integration leads to

$$\dot{\phi}^2 = \frac{2g}{L} (\cos\phi - \cos\phi_0)$$

We may take the square root and choose the appropriate sign to indicate that the angle is initially decreasing in time,

$$\dot{\phi} = -\sqrt{\frac{2g}{L} (\cos\phi - \cos\phi_0)}$$

In differential form, we have

$$\frac{d\phi}{\sqrt{\cos\phi - \cos\phi_0}} = -\sqrt{\frac{2g}{L}} dt$$

Integrating yields

$$\int_{\phi_0}^{\phi} \frac{d\psi}{\sqrt{\cos\psi - \cos\phi_0}} = -\sqrt{\frac{2g}{L}} t$$

Since we require $\phi(T) = -\phi_0$,

$$\int_{\phi_0}^{-\phi_0} \frac{d\psi}{\sqrt{\cos\psi - \cos\phi_0}} = -\sqrt{\frac{2g}{L}} T$$

Solving for the time,

$$T = \sqrt{\frac{L}{2g}} \int_{-\phi_0}^{\phi_0} \frac{d\psi}{\sqrt{\cos \psi - \cos \phi_0}} = \sqrt{\frac{2L}{g}} \int_0^{\phi_0} \frac{d\psi}{\sqrt{\cos \psi - \cos \phi_0}} \quad (3.11)$$

[Section 13.9](#) is about the stability of numerical solutions that solve differential equations. In particular, [Example 13.1](#) is provided for a stability analysis of the simple pendulum. It is not as easy as you might think to obtain a robust solution that exhibits periodic behavior.

Under the assumption that we want the pendulum to continue swinging with no other external forces acting on it, including friction, there is no reason to solve the problem for more than one period of oscillation. The differential equation can be solved over one period to produce a sequence of sampled angles. Angles for other times during that period can be interpolated from the samples, and we can use periodicity to calculate times larger than the first period. In order to proceed, we need to calculate the half period T , the time difference between the two angles where the pendulum has stopped. Once known, we can use a stable numerical method to solve the differential equation over that half period, store the computed samples for use by the application over its life time, and use periodicity and interpolate as needed.

The integral in [equation \(3.11\)](#) is not solvable in closed form. The integral is *improper* since the integrand becomes infinite at the upper limit of integration; that is, when ψ approaches ϕ_0 . Such integrals must be split into two integrals, the first integral numerically integrated by standard methods. The integrand of the second integral is approximated by some function to remove the singularity at the upper limit. [Equation \(3.11\)](#) is split into

$$\int_0^{\phi_0 - \varepsilon} \frac{d\psi}{\sqrt{\cos \psi - \cos \phi_0}} + \int_{\phi_0 - \varepsilon}^{\phi_0} \frac{d\psi}{\sqrt{\cos \psi - \cos \phi_0}}$$

for a sufficiently small $\varepsilon > 0$. The quadratic approximation from the Taylor series for $\cos \psi$ expanded about ϕ_0 is

$$\cos \theta \doteq \cos \phi_0 - (\sin \phi_0)(\psi - \phi_0) - \frac{1}{2}(\cos \phi_0)(\psi - \phi_0)^2$$

Substituting this in the second integrand and making the change of variables $z = \phi_0 - \psi$ leads to the approximation:

$$\int_{\phi_0 - \varepsilon}^{\phi_0} \frac{d\psi}{\sqrt{\cos \psi - \cos \phi_0}} \doteq \int_0^\varepsilon \frac{dz}{\sqrt{(\sin \phi_0)z - (\cos \phi_0)z^2/2}}$$

(Example 3.4
continued)

$$= \sqrt{\frac{2}{\cos \phi_0}} \left(\frac{\pi}{2} - \sin^{-1} \left(1 - \frac{\varepsilon \cos \phi_0}{\sin \phi_0} \right) \right)$$

As ε approaches zero, the approximation (and integral itself) goes to zero. You need to choose ε in your numerical methods so that the calculations in the first integral are well behaved; that is, the denominator of the integrand stays sufficiently away from zero to avoid introducing significant floating point errors. ■

EXERCISE
3.5

Selecting $2L/g = 1$ and $\phi_0 = \pi/6$, estimate T using numerical integration. ■

EXERCISE
3.6

Redo the derivation that led to the integral for T in [equation \(3.11\)](#) to take into account that the initial speed is $\dot{\phi}(0) = \dot{\phi}_0 > 0$. That is, the mass of the pendulum is initially positioned at a nonzero angle from the vertical and is then given a small push farther away from the vertical.

- What is the time $\tau > 0$ at which the mass reaches its maximum angle from the vertical? *Hint:* Notice that $\dot{\phi}(\tau) = 0$. If $\phi_1 = \phi(\tau)$ is the maximum angle, show that

$$\phi_1 = \cos^{-1} \left(\cos \phi_0 - \frac{L \dot{\phi}_0^2}{2g} \right)$$

Subsequently show that

$$\tau = \int_{\phi_0}^{\phi_1} \frac{d\psi}{\sqrt{\dot{\phi}_0^2 + 2g(\cos \psi - \cos \phi_0)/L}}$$

- What is the half period $T > 0$ of the pendulum? *Hint:* Use a numerical estimate obtained from [equation \(3.11\)](#) when the initial data of the pendulum is $\phi(0) = \phi_1$ and $\dot{\phi}_0 = 0$.

[Example 13.1](#) uses $\phi_0 = 0.1$, $\dot{\phi}_0 = 1$, and $g/L = 1$. In your constructions of the current example, show that $\tau \doteq 1.59$ and $T \doteq 3.37$ and compare to the numerical results obtained by the Runge-Kutta method in [Example 13.1](#) as some assurance that your results are good approximations. ■

3.2 LAGRANGIAN DYNAMICS

Let us revisit the basic formulation of Newton's second law. For a constant mass m undergoing a force \mathbf{F} , the motion of the mass over time is governed by

$$\mathbf{F} = m\mathbf{a} = m\dot{\mathbf{v}} = m\ddot{\mathbf{x}} \quad (3.12)$$

where $\mathbf{x}(t)$ is the position, $\mathbf{v}(t) = \dot{\mathbf{x}}(t)$ is the velocity, and $\mathbf{a}(t) = \ddot{\mathbf{x}}(t)$ is the acceleration of the mass at time t . Each of these vector quantities is measured with respect to *some* coordinate system. This system is referred to as the *inertial frame*. If $\mathbf{x} = (x_1, x_2, x_3)$ is the representation of the position in the inertial frame, the components x_1 , x_2 , and x_3 are referred to as the *inertial coordinates*. Although in many cases the inertial frame is considered to be fixed (relative to the stars as it were), the frame can have a constant linear velocity and no rotation and still be inertial. Any other frame of reference is referred to as a *noninertial frame*. Newton's second law, which we saw in [equation \(3.12\)](#), is simple to state and remember, but its simplicity can disguise the complexity of the problem at hand. Consider the simple pendulum problem from the last section, shown in [Figure 3.4](#).

The only postulated force is gravitational, $\mathbf{F} = -mg\mathbf{j}$, where g is a positive constant. You might be tempted to directly apply Newton's second law to obtain the equations of motion $m\ddot{\mathbf{x}} = -mg\mathbf{j}$. An integration of these will show that the mass drops straight to the ground, which is not the correct motion! The problem is that \mathbf{F} must represent all relevant forces. The pendulum has an additional force, the force that constrains the mass to be attached to the end of the rod, thus causing the mass to move along a circular path over time. This force is referred to as a *constraining force* or a *reactive force*. Newton's second law requires that the constraining forces occur in addition to the external forces applied to the mass. This example motivates what is called *Lagrangian dynamics*. We will discuss this topic, then return to the pendulum example to illustrate how to construct the *Lagrangian equations of motion*.

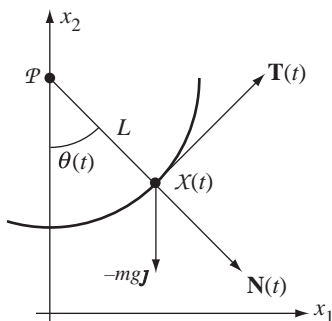


Figure 3.4 The simple pendulum. The motion is constrained to a plane. The mass is located at position $\mathcal{X}(t)$ at time t and is always a fixed length L from the joint \mathcal{P} . The angle formed by the pendulum rod with the vertical is $\theta(t)$. The curve of motion is a circle with tangent $\mathbf{T}(t)$ and outward pointing normal $\mathbf{N}(t)$. The only force acting on the mass is gravitational, $-mg\mathbf{j}$, where m is the mass of the particle, g is the gravitational constant, and $-\mathbf{j}$ is the direction of the force (vertically downward). The joint \mathcal{P} provides no frictional force.

3.2.1 EQUATIONS OF MOTION FOR A PARTICLE

From Newton's second law, [equation \(3.12\)](#), we may compute the small amount of work dW that is done by \mathbf{F} when we move the mass at position \mathbf{x} by a small displacement $d\mathbf{x}$. Recall from [Section 2.6.1](#) that the work done is

$$dW = \mathbf{F} \cdot d\mathbf{x}$$

The displacement of the mass and the force need not be in the same direction. Using [equation \(3.12\)](#) we have

$$m\ddot{\mathbf{x}} \cdot d\mathbf{x} = \mathbf{F} \cdot d\mathbf{x} \quad (3.13)$$

The right-hand side is the small amount of work done by the force for the given displacement. The left-hand side is the corresponding small change in the kinetic energy of the mass. [Equation \(3.13\)](#) is referred to as *D'Alembert's equation*.

Let $\mathbf{x} = (x_1, x_2, x_3)$ and $\mathbf{F} = (F_1, F_2, F_3)$. With no constraints on the position, the displacement can be in any direction. In particular, setting $d\mathbf{x} = \mathbf{i}$ and substituting into D'Alembert's equation produces $m\ddot{x}_1 = m\ddot{\mathbf{x}} \cdot \mathbf{i} = \mathbf{F} \cdot \mathbf{i} = F_1$. Similarly, the displacement can be \mathbf{j} or \mathbf{k} , producing $m\ddot{x}_2 = F_2$ or $m\ddot{x}_3 = F_3$. The three equations written in vector form are $m\ddot{\mathbf{x}} = \mathbf{F}$, which is Newton's second law. Of course this should come as no surprise. The power of D'Alembert's equation is in naturally supporting the idea of constraints on the position, as we now demonstrate.

Motion on a Curve

Consider the simplest situation when the mass is constrained to follow a curve in space. The curve may be parameterized by a variable q , say $\mathbf{x}(q)$. The derivative vector $d\mathbf{x}/dq$ is tangent to the path of motion. The small displacements $d\mathbf{x}$ can now occur only so that the mass remains on the curve. In this sense the displacement is *infinitesimal*. The infinitesimal displacements $d\mathbf{x}$ in D'Alembert's equation may be replaced by positional derivatives:

$$m\ddot{\mathbf{x}} \cdot \frac{d\mathbf{x}}{dq} = \mathbf{F} \cdot \frac{d\mathbf{x}}{dq} \quad (3.14)$$

This equation will be reformulated, the construction requiring a few derivative identities from calculus. An application of the chain rule yields

$$\dot{\mathbf{x}} = \frac{d\mathbf{x}}{dt} = \frac{d\mathbf{x}}{dq} \frac{dq}{dt} = \frac{d\mathbf{x}}{dq} \dot{q} \quad (3.15)$$

Treating $\dot{\mathbf{x}}$ as a formal function of both q and \dot{q} , we may compute the partial derivative of [equation \(3.15\)](#) with respect to \dot{q} to obtain

$$\frac{\partial \dot{\mathbf{x}}}{\partial \dot{q}} = \frac{\partial}{\partial \dot{q}} \left(\frac{d\mathbf{x}}{dq} \dot{q} \right) = \frac{d\mathbf{x}}{dq} \quad (3.16)$$

Another identity is

$$\frac{d}{dt} \left(\frac{d\mathbf{x}}{dq} \right) = \frac{d}{dq} \left(\frac{d\mathbf{x}}{dq} \right) \dot{q} = \frac{\partial}{\partial q} \left(\frac{d\mathbf{x}}{dq} \dot{q} \right) = \frac{\partial \dot{\mathbf{x}}}{\partial q} \quad (3.17)$$

where the first equality is an application of the chain rule, the second equality treats \dot{q} as a variable independent of q , and the third equality uses [equation \(3.15\)](#). Finally, the product rule

$$\frac{d}{dt} \left(\frac{d\mathbf{x}}{dt} \cdot \frac{d\mathbf{x}}{dq} \right) = \frac{d^2\mathbf{x}}{dt^2} \cdot \frac{d\mathbf{x}}{dq} + \frac{d\mathbf{x}}{dt} \cdot \frac{d}{dt} \left(\frac{d\mathbf{x}}{dq} \right)$$

produces the identity

$$\ddot{\mathbf{x}} \cdot \frac{d\mathbf{x}}{dq} = \frac{d}{dt} \left(\dot{\mathbf{x}} \cdot \frac{d\mathbf{x}}{dq} \right) - \dot{\mathbf{x}} \cdot \frac{d}{dt} \left(\frac{d\mathbf{x}}{dq} \right) \quad (3.18)$$

Substituting [equations \(3.16\)](#) and [\(3.17\)](#) into [\(3.18\)](#) and multiplying by the mass m yields

$$\begin{aligned} m\ddot{\mathbf{x}} \cdot \frac{d\mathbf{x}}{dq} &= \frac{d}{dt} \left(m\dot{\mathbf{x}} \cdot \frac{\partial \dot{\mathbf{x}}}{\partial \dot{q}} \right) - m\dot{\mathbf{x}} \cdot \frac{\partial \dot{\mathbf{x}}}{\partial q} \\ &= \frac{d}{dt} \left(\frac{\partial}{\partial \dot{q}} \left(\frac{1}{2} m |\dot{\mathbf{x}}|^2 \right) \right) - \frac{\partial}{\partial q} \left(\frac{1}{2} m |\dot{\mathbf{x}}|^2 \right) \\ &= \frac{d}{dt} \left(\frac{\partial T}{\partial \dot{q}} \right) - \frac{\partial T}{\partial q} \end{aligned} \quad (3.19)$$

where $T = m|\dot{\mathbf{x}}|^2/2$ is the kinetic energy of the system. Substituting [equation \(3.19\)](#) into [equation \(3.14\)](#) and defining $F_q = \mathbf{F} \cdot d\mathbf{x}/dq$, we have the *Lagrangian equation of motion* for a single particle constrained to a curve:

$$\frac{d}{dt} \left(\frac{\partial T}{\partial \dot{q}} \right) - \frac{\partial T}{\partial q} = F_q \quad (3.20)$$

The scalar value F_q is referred to as a *generalized force*. Although called a force, it is not a force since it is not vector valued and since the physical units are not those of a force. An important distinction between the Newtonian equations of motion, [equation \(3.12\)](#), and the Lagrangian equations of motion, [equation \(3.20\)](#), is that the force term in [equation \(3.12\)](#) includes external and constraining forces, but the force term in [equation \(3.20\)](#) eliminates the constraining forces.

EXAMPLE 3.5

Returning to our simple pendulum problem, let us set up the Lagrangian equations of motion. The mass is constrained to lie on a circle of radius L centered at \mathbf{P} . The position is parameterized by the angle θ , the constraint variable that we named q in the general discussion of the Lagrangian equations of motion. The position is

$$\mathbf{X}(\theta) = \mathbf{P} + L\mathbf{n}(\theta)$$

(Example 3.5
continued)

where $\mathbf{N}(\theta) = (\sin \theta, -\cos \theta)$ is normal to the circle and where $\mathbf{T}(\theta) = (\cos \theta, \sin \theta)$ is tangent to the circle. The derivative of position with respect to θ and the velocity are, respectively,

$$\frac{d\mathbf{x}}{d\theta} = L \frac{d\mathbf{N}}{d\theta} = L\mathbf{T} \quad \text{and} \quad \dot{\mathbf{x}} = \frac{d\mathbf{x}}{dt} = \frac{d\mathbf{x}}{d\theta} \frac{d\theta}{dt} = L\dot{\theta}\mathbf{T}$$

The kinetic energy is

$$T = \frac{1}{2}m|\dot{\mathbf{x}}|^2 = \frac{1}{2}mL^2\dot{\theta}^2$$

and its derivatives with respect to θ and $\dot{\theta}$ are

$$\frac{\partial T}{\partial \theta} = 0 \quad \text{and} \quad \frac{\partial T}{\partial \dot{\theta}} = mL^2\dot{\theta}$$

The left-hand side of equation (3.20) becomes

$$\frac{d}{dt} \left(\frac{\partial T}{\partial \dot{\theta}} \right) - \frac{\partial T}{\partial \theta} = \frac{d}{dt} (mL^2\dot{\theta}) = mL^2\ddot{\theta}$$

The right-hand side of equation (3.20) becomes

$$F_\theta = \mathbf{F} \cdot \frac{d\mathbf{x}}{d\theta} = (-mg\mathbf{j}) \cdot (L\mathbf{T}) = -mgL \sin \theta$$

Equating the left-hand and right-hand sides produces $mL^2\ddot{\theta} = -mgL \sin \theta$, or $\ddot{\theta} + (g/L)\sin \theta = 0$, just like we derived in equation (3.10). ■

EXERCISE 3.7

 SOURCE CODE
BeadSlide

A bead of mass m is attached to a frictionless wire whose shape is defined by the spiral curve $\mathbf{x}(q) = (q, q^2, q^3)$. The bead is subject to the gravitational force $\mathbf{F} = -mg\mathbf{k}$, where g is a positive constant. Initially, the bead is held fixed at $(1, 1, 1)$, then released to slide down the wire. How long does the bead take to reach the origin $(0, 0, 0)$? ■

Motion on a Surface

We now constrain the mass to lie on a parametric surface, $\mathbf{x}(q_1, q_2)$, where q_1 and q_2 are independent parameters. The infinitesimal displacements in equation (3.13) are now constrained to be tangential to the surface at the point in question. In particular, the derivatives $\partial\mathbf{x}/\partial q_1$ and $\partial\mathbf{x}/\partial q_2$ are tangent vectors, so D'Alembert's equation becomes

$$m\ddot{\mathbf{x}} \cdot \frac{\partial \mathbf{x}}{\partial q_i} = \mathbf{F} \cdot \frac{\partial \mathbf{x}}{\partial q_i}, \quad i = 1, 2 \quad (3.21)$$

The construction used in the case of motion on a curve applies to these equations as well to produce the Lagrangian equations of motion. An application of the chain rule

to the velocity yields

$$\dot{\mathbf{x}} = \frac{d\mathbf{x}}{dt} = \frac{\partial \mathbf{x}}{\partial q_1} \frac{dq_1}{dt} + \frac{\partial \mathbf{x}}{\partial q_2} \frac{dq_2}{dt} = \frac{\partial \mathbf{x}}{\partial q_1} \dot{q}_1 + \frac{\partial \mathbf{x}}{\partial q_2} \dot{q}_2 \quad (3.22)$$

Treating $\dot{\mathbf{x}}$ as a formal function of q_1 , q_2 , \dot{q}_1 , and \dot{q}_2 , we may compute the partial derivative of equation (3.22) with respect to \dot{q}_i to obtain

$$\frac{\partial \mathbf{x}}{\partial \dot{q}_i} = \frac{\partial}{\partial \dot{q}_i} \left(\frac{\partial \mathbf{x}}{\partial q_1} \dot{q}_1 + \frac{\partial \mathbf{x}}{\partial q_2} \dot{q}_2 \right) = \frac{\partial \dot{\mathbf{x}}}{\partial \dot{q}_i}, \quad i = 1, 2 \quad (3.23)$$

Another identity is

$$\begin{aligned} \frac{d}{dt} \left(\frac{\partial \mathbf{x}}{\partial q_1} \right) &= \frac{\partial}{\partial q_1} \left(\frac{\partial \mathbf{x}}{\partial q_1} \right) \dot{q}_1 + \frac{\partial}{\partial q_2} \left(\frac{\partial \mathbf{x}}{\partial q_1} \right) \dot{q}_2 \quad \text{By the chain rule} \\ &= \frac{\partial}{\partial q_1} \left(\frac{\partial \mathbf{x}}{\partial q_1} \right) \dot{q}_1 + \frac{\partial}{\partial q_1} \left(\frac{\partial \mathbf{x}}{\partial q_2} \right) \dot{q}_2 \quad \text{Order of differentiation unimportant} \\ &= \frac{\partial}{\partial q_1} \left(\frac{\partial \mathbf{x}}{\partial q_1} \dot{q}_1 + \frac{\partial \mathbf{x}}{\partial q_2} \dot{q}_2 \right) \quad \text{Differentiation is linear} \\ &= \frac{\partial \dot{\mathbf{x}}}{\partial q_1} \quad \text{Using equation (3.22)} \end{aligned}$$

A similar construction applies to differentiating with respect to q_2 . The two formulas are jointly represented as

$$\frac{d}{dt} \left(\frac{\partial \mathbf{x}}{\partial q_i} \right) = \frac{\partial \dot{\mathbf{x}}}{\partial q_i}, \quad i = 1, 2 \quad (3.24)$$

Just as in equation (3.18), the product rule may be applied to obtain

$$\ddot{\mathbf{x}} \cdot \frac{d\mathbf{x}}{dq} = \frac{d}{dt} \left(\dot{\mathbf{x}} \cdot \frac{d\mathbf{x}}{dq} \right) - \dot{\mathbf{x}} \cdot \frac{d}{dt} \left(\frac{d\mathbf{x}}{dq} \right) \quad (3.25)$$

Substituting equations (3.23) and (3.24) into (3.25) and multiplying by the mass m yields

$$\begin{aligned} m\ddot{\mathbf{x}} \cdot \frac{\partial \mathbf{x}}{\partial q_i} &= \frac{d}{dt} \left(m\dot{\mathbf{x}} \cdot \frac{\partial \dot{\mathbf{x}}}{\partial \dot{q}_i} \right) - m\dot{\mathbf{x}} \cdot \frac{\partial \dot{\mathbf{x}}}{\partial q_i} \\ &= \frac{d}{dt} \left(\frac{\partial}{\partial \dot{q}_i} \left(\frac{1}{2} m|\dot{\mathbf{x}}|^2 \right) \right) - \frac{\partial}{\partial q_i} \left(\frac{1}{2} m|\dot{\mathbf{x}}|^2 \right) \\ &= \frac{d}{dt} \left(\frac{\partial T}{\partial \dot{q}_i} \right) - \frac{\partial T}{\partial q_i} \end{aligned} \quad (3.26)$$

where $T = m|\dot{\mathbf{x}}|^2/2$ is the kinetic energy of the system. Substituting [equation \(3.26\)](#) into [equation \(3.21\)](#) and defining $F_{q_i} = \mathbf{F} \cdot \partial \mathbf{x} / \partial q_i$, we have the *Lagrangian equations of motion* for a single particle constrained to a surface:

$$\frac{d}{dt} \left(\frac{\partial T}{\partial \dot{q}_i} \right) - \frac{\partial T}{\partial q_i} = F_{q_i}, \quad i = 1, 2 \quad (3.27)$$

EXAMPLE
3.6


We have a ball constrained to lie on a flat, frictionless table. A rubber band is attached to the ball, the other end attached to a point on the table. The rubber band is unstretched when the ball is located at the same attachment point on the table. What are the Lagrangian equations of motion?

The ball has mass m . The forces on the ball due to the rubber band are assumed to follow Hooke's law: The magnitude of the force is negatively proportional to the length of the rubber band. If the ball is pulled to stretch the rubber band, the force is in the direction along the rubber band away from the ball and has magnitude cL , where $c > 0$ is a constant and L is the length of the stretched rubber band. [Figure 3.5](#) illustrates.

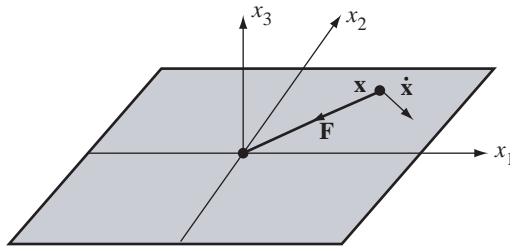


Figure 3.5

A ball of mass m on a flat table. A rubber band connects the ball to a fixed point on the table. The force \mathbf{F} due to the rubber band is shown. The position \mathbf{x} of the ball is shown together with its velocity $\dot{\mathbf{x}}$.

We may assume that the table surface is in the x_1x_2 -plane, $x_3 = 0$, in which case $\mathbf{x} = (x_1, x_2, 0)$. The kinetic energy is $T = m(\dot{x}_1^2 + \dot{x}_2^2)/2$ and the force is $\mathbf{F} = -c(x_1, x_2, 0)$ for some positive constant c . The constraint variables are $q_1 = x_1$ and $q_2 = x_2$, so we will use just the x -names rather than keep track of the q -names. The relevant partial derivatives in [equation \(3.27\)](#) are

$$\begin{aligned} \frac{\partial T}{\partial x_1} &= 0, & \frac{\partial T}{\partial x_2} &= 0, \\ \frac{\partial T}{\partial \dot{x}_1} &= m\dot{x}_1, & \frac{\partial T}{\partial \dot{x}_2} &= m\dot{x}_2, \\ \frac{d}{dt} \left(\frac{\partial T}{\partial \dot{x}_1} \right) &= m\ddot{x}_1, & \frac{d}{dt} \left(\frac{\partial T}{\partial \dot{x}_2} \right) &= m\ddot{x}_2 \end{aligned}$$

The generalized forces are

$$F_{x_1} = \mathbf{F} \cdot \frac{\partial \mathbf{x}}{\partial x_1} = -c(x_1, x_2, 0) \cdot (1, 0, 0) = -cx_1$$

$$F_{x_2} = \mathbf{F} \cdot \frac{\partial \mathbf{x}}{\partial x_2} = -c(x_1, x_2, 0) \cdot (0, 1, 0) = -cx_2$$

The Lagrangian equations of motion are therefore,

$$m\ddot{x}_1 = -cx_1, \quad m\ddot{x}_2 = -cx_2$$

Consequently each component of the position adheres to simple harmonic motion with frequency $\omega = \sqrt{c/m}$. For an initial position $\mathbf{x}(0) = (p_1, p_2, 0)$ and velocity $\dot{\mathbf{x}}(0) = (v_1, v_2, 0)$, the solutions to the differential equations are $x_1(t) = p_1 \cos(\omega t) + (v_1/\omega) \sin(\omega t)$ and $x_2(t) = p_2 \cos(\omega t) + (v_2/\omega) \sin(\omega t)$. ■

EXERCISE
3.8

In [Example 3.6](#), show that the path of motion is an ellipse. At what time will the ball reach the origin? ■

EXERCISE
3.9

In [Example 3.6](#), assume that the table is covered with a viscous fluid. Let the viscous force on the ball be in the opposite direction of motion of the ball, say $\mathbf{G} = -a\dot{\mathbf{x}}$ for some constant $a > 0$. What are the Lagrangian equations of motion? At what time will the ball reach the origin? ■

EXAMPLE
3.7
SOURCE CODE
BallHill

A ball is placed at the top of a hill whose shape is an elliptical paraboloid. The hill is assumed to be frictionless. The only force acting on the ball is gravitational force. The ball is slightly pushed so that it may roll down the hill. What are the Lagrangian equations of motion? [Figure 3.6](#) illustrates.

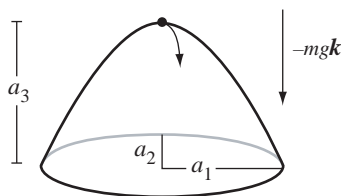


Figure 3.6

A ball is at the top of a frictionless hill. With a small push, the ball will roll down the hill.

The vertical axis is assumed to be the x_3 -axis. The gravitational force is $\mathbf{F} = -mgk$. The height of the hill is $a_3 > 0$, so the ground is considered to be the plane $x_3 = 0$. The cross section of the hill on the ground is an ellipse with semimajor axis length a_1 (in

(Example 3.7
continued)

the x_1 direction) and semiminor axis length a_2 (in the x_2 direction). The equation of the paraboloid is $x_3 = a_3 - (x_1/a_1)^2 - (x_2/a_2)^2$. The ball is constrained to

$$\mathbf{x} = \left(x_1, x_2, a_3 - \left(\frac{x_1}{a_1} \right)^2 - \left(\frac{x_2}{a_2} \right)^2 \right)$$

so once again $q_1 = x_1$ and $q_2 = x_2$ and we will just use the x -names.

The time derivative of x_3 is

$$\dot{x}_3 = -\frac{2x_1\dot{x}_1}{a_1^2} - \frac{2x_2\dot{x}_2}{a_2^2}$$

The kinetic energy is

$$T = \frac{m}{2} (\dot{x}_1^2 + \dot{x}_2^2 + \dot{x}_3^2) = \frac{m}{2} \left(\dot{x}_1^2 + \dot{x}_2^2 + \left(\frac{2x_1\dot{x}_1}{a_1^2} + \frac{2x_2\dot{x}_2}{a_2^2} \right)^2 \right)$$

The relevant terms in equation (3.27) are

$$\frac{\partial T}{\partial x_1} = \frac{4m\dot{x}_1}{a_1^2} \left(\frac{x_1\dot{x}_1}{a_1^2} + \frac{x_2\dot{x}_2}{a_2^2} \right)$$

$$\frac{\partial T}{\partial x_2} = \frac{4m\dot{x}_2}{a_2^2} \left(\frac{x_1\dot{x}_1}{a_1^2} + \frac{x_2\dot{x}_2}{a_2^2} \right)$$

$$\frac{\partial T}{\partial \dot{x}_1} = m \left(\ddot{x}_1 + \frac{4x_1}{a_1^2} \left(\frac{x_1\dot{x}_1}{a_1^2} + \frac{x_2\dot{x}_2}{a_2^2} \right) \right)$$

$$\frac{\partial T}{\partial \dot{x}_2} = m \left(\ddot{x}_2 + \frac{4x_2}{a_2^2} \left(\frac{x_1\dot{x}_1}{a_1^2} + \frac{x_2\dot{x}_2}{a_2^2} \right) \right)$$

$$\frac{d}{dt} \left(\frac{\partial T}{\partial \dot{x}_1} \right) = m \left(\ddot{x}_1 + \frac{4x_1}{a_1^2} \left(\frac{x_1\ddot{x}_1 + \dot{x}_1^2}{a_1^2} + \frac{x_2\ddot{x}_2 + \dot{x}_2^2}{a_2^2} \right) + \frac{4\dot{x}_1}{a_1^2} \left(\frac{x_1\dot{x}_1}{a_1^2} + \frac{x_2\dot{x}_2}{a_2^2} \right) \right)$$

$$\frac{d}{dt} \left(\frac{\partial T}{\partial \dot{x}_2} \right) = m \left(\ddot{x}_2 + \frac{4x_2}{a_2^2} \left(\frac{x_1\ddot{x}_1 + \dot{x}_1^2}{a_1^2} + \frac{x_2\ddot{x}_2 + \dot{x}_2^2}{a_2^2} \right) + \frac{4\dot{x}_2}{a_2^2} \left(\frac{x_1\dot{x}_1}{a_1^2} + \frac{x_2\dot{x}_2}{a_2^2} \right) \right)$$

$$\frac{\partial \mathbf{x}}{\partial x_1} = \left(1, 0, -\frac{2x_1}{a_1^2} \right)$$

$$\frac{\partial \mathbf{x}}{\partial x_2} = \left(0, 1, -\frac{2x_2}{a_2^2} \right)$$

$$F_{x_1} = (-mg\mathbf{k}) \cdot \frac{\partial \mathbf{x}}{\partial x_1} = \frac{2mgx_1}{a_1^2}$$

$$F_{x_2} = (-mg\mathbf{k}) \cdot \frac{\partial \mathbf{x}}{\partial x_2} = \frac{2mgx_2}{a_2^2}$$

The Lagrangian equations of motion are

$$\ddot{x}_1 + \frac{4x_1}{a_1^2} \left(\frac{x_1 \ddot{x}_1 + \dot{x}_1^2}{a_1^2} + \frac{x_2 \ddot{x}_2 + \dot{x}_2^2}{a_2^2} \right) = \frac{2gx_1}{a_1^2}$$

$$\ddot{x}_2 + \frac{4x_2}{a_2^2} \left(\frac{x_1 \ddot{x}_1 + \dot{x}_1^2}{a_1^2} + \frac{x_2 \ddot{x}_2 + \dot{x}_2^2}{a_2^2} \right) = \frac{2gx_2}{a_2^2}$$

Observe that this is a coupled system of second-order differential equations since \ddot{x}_1 and \ddot{x}_2 appear implicitly in both equations. The equations may be algebraically manipulated to obtain two explicit equations, one for each of the second derivatives. [Figure 3.7](#) – also [Color Plate 3.7](#) – shows some screen shots from the ball/hill application found on the CD-ROM.

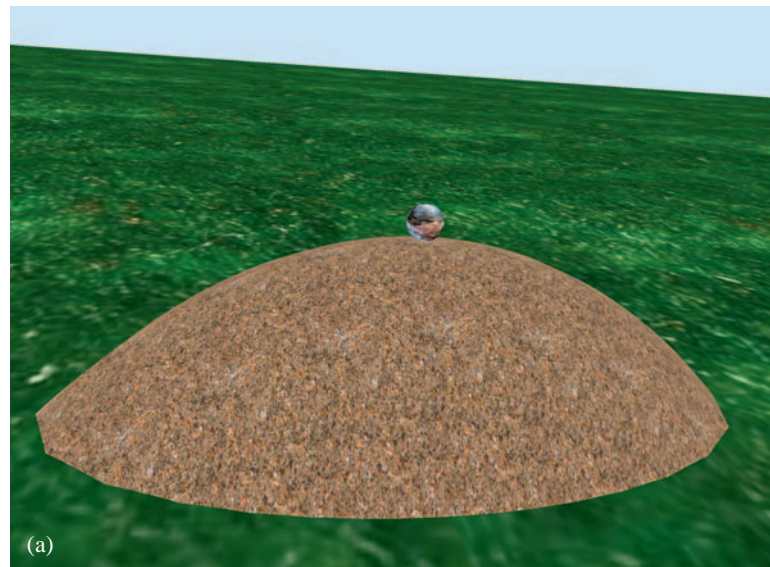


Figure 3.7 (Continued)

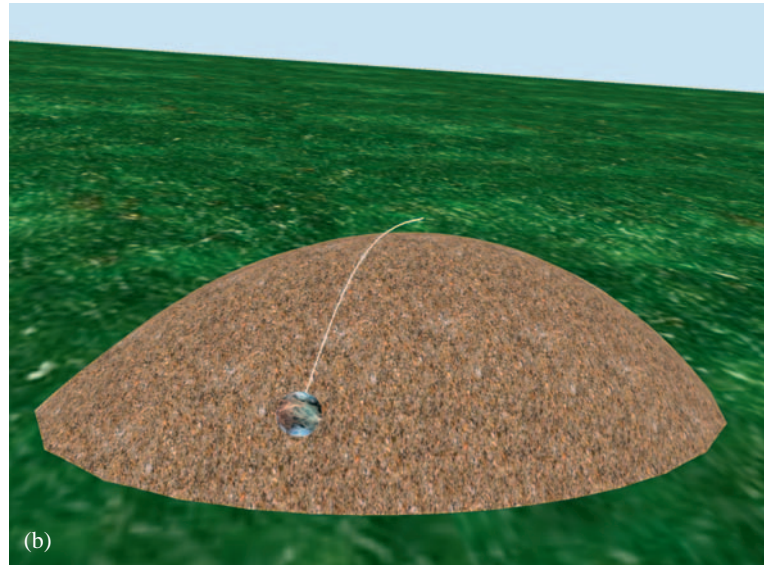
(Example 3.7
continued)

Figure 3.7

A ball rolling down a hill. Image (b) shows the path of the center of the ball as it rolls down the hill. The ball rotates at a speed commensurate with its downhill velocity. (See also [Color Plate 3.7](#).) ■

EXERCISE
3.10

The equations of the [Example 3.7](#) appear to be quite complex. However, if the paraboloid is circular, say $a_1 = a_2 = 1$, the radial symmetry of the surface should stoke your intuition and allow you to deduce that the ball will roll directly down the hill. That is, the path in the x_1x_2 plane is along a ray that starts at the origin. If r is the radial distance in the plane from the origin, prove that

$$\ddot{r} + \frac{2r(2\dot{r}^2 - g)}{1 + 4r^2} = 0$$

Choose $a_3 = 1$ so that the intersection of the hill and the ground plane occurs at $r = 1$. Numerically solve this differential equation for $g = 1$ with the initial conditions $r(0) = 0$ and $\dot{r}(0) = 1$. Estimate the time $T > 0$ when the ball reaches the ground, that is, the time T at which $r(T) = 1$. ■

EXERCISE
3.11

In [Example 3.7](#) with the elliptical paraboloid, verify that a solution to the system of differential equations is $(x_1(t), x_2(t)) = (v_1 t, v_2 t)$. Does this mean that the path of motion will always project to a straight line in the plane $x_3 = 0$? Justify your answer. ■

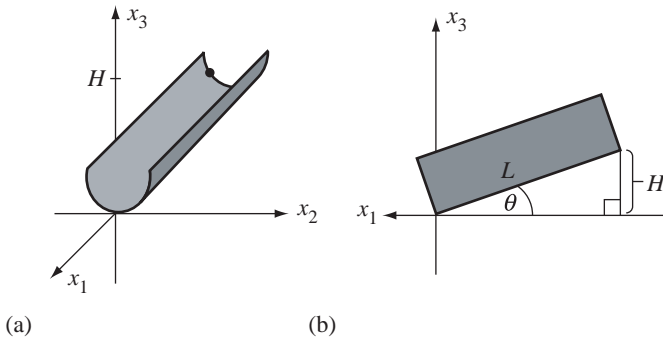


Figure 3.8 (a) A metal chute of length L , one end attached to the origin, the other end raised by a height H . (b) Side view of the chute.

EXERCISE
3.12

In [Example 3.7](#), include a second force in addition to the gravitational force. That force is due to wind blowing on the particle with constant velocity \mathbf{W} . Derive the Lagrangian equations of motion. Determine conditions on \mathbf{W} that prevent the ball from rolling to the ground plane. ■

EXERCISE
3.13

A frictionless metal chute is constructed in the shape of half a cylinder of radius R and length L . The chute is aligned to be parallel to the x_1 -axis. One end of the chute is attached to the ground plane $x_3 = 0$. The other end is raised by a height H . [Figure 3.8](#) illustrates the situation:

A ball is placed at the top of the chute and released (initial velocity is zero). The only force acting on the ball is gravitational force. Construct the Lagrangian equations of motion for the ball. What are these equations if you modify the problem by coating the chute with a viscous oil? Assume that the viscous force is negatively proportional to the ball's velocity. With or without viscosity, verify that if the ball starts in the middle of the chute, the path of motion is a straight line. ■

EXERCISE
3.14

For the mathematically inclined: If the mass always lies on a frictionless height field, the graph of the function $x_3 = h(x_1, x_2)$, and the only force acting on the mass is gravitational force, derive the Lagrangian equations of motion. ■

Determining Constraint Forces

In general you can think of having a Lagrangian equation for each degree of freedom in the system. When the particle is constrained to a curve, you have one degree of freedom and one equation governing the particle's motion. When constrained to a

surface, you have two degrees of freedom and two equations governing the motion. Later we will study particle systems with many degrees of freedom. Even though we are in three dimensions, the degrees of freedom may very well be greater than three. A Lagrangian equation occurs for each degree of freedom.

The construction that led to the Lagrangian equations applies equally well to additional parameters, even if those parameters are not freely varying. However, the generalized forces in these equations must include terms from the forces of constraint. These additional equations allow us to determine the actual constraint forces.

EXAMPLE
3.8

Consider the simple pendulum problem. In polar coordinates we can represent the position as $\mathbf{x}(r, \theta) = \mathbf{P} + r\mathbf{N}(\theta)$. The pendulum requires a constant radius, $r = L$ for all time. The radius is not free to vary. However, if we think of r as variable, we may construct two Lagrangian equations. In this setting we can think of the constraint force \mathbf{C} to be an applied force. The positional derivatives are

$$\frac{\partial \mathbf{x}}{\partial \theta} = r\mathbf{T}, \quad \frac{\partial \mathbf{x}}{\partial r} = \mathbf{N}, \quad \frac{d\mathbf{x}}{dt} = \frac{\partial \mathbf{x}}{\partial \theta}\dot{\theta} + \frac{\partial \mathbf{x}}{\partial r}\dot{r} = r\dot{\theta}\mathbf{T} + \dot{r}\mathbf{N}$$

The kinetic energy is

$$T = \frac{m}{2}(r^2\dot{\theta}^2 + \dot{r}^2)$$

and the relevant derivatives are

$$\frac{\partial T}{\partial \theta} = 0$$

$$\frac{\partial T}{\partial r} = mr\dot{\theta}^2$$

$$\frac{\partial T}{\partial \dot{\theta}} = mr^2\dot{\theta}$$

$$\frac{\partial T}{\partial \dot{r}} = m\dot{r}$$

$$\frac{d}{dt} \left(\frac{\partial T}{\partial \dot{\theta}} \right) = m(r^2\ddot{\theta} + 2r\dot{r}\dot{\theta})$$

$$\frac{d}{dt} \left(\frac{\partial T}{\partial \dot{r}} \right) = m\ddot{r}$$

The generalized force for the θ variable is

$$F_\theta = (-mg\mathbf{J} + \mathbf{C}) \cdot \frac{\partial \mathbf{x}}{\partial \theta} = (-mg \sin \theta + \mathbf{C} \cdot \mathbf{T})r$$

The generalized force for the r variable is

$$F_r = (-mg\mathbf{J} + \mathbf{C}) \cdot \frac{\partial \mathbf{x}}{\partial r} = mg \cos \theta + \mathbf{C} \cdot \mathbf{N}$$

The equations of motion are

$$0 = \frac{d}{dt} \left(\frac{\partial T}{\partial \dot{\theta}} \right) - \frac{\partial T}{\partial \theta} - F_\theta = mL\ddot{\theta} + 2m\dot{r}\dot{\theta} + mg \sin \theta - \mathbf{C} \cdot \mathbf{T}$$

and

$$0 = \frac{d}{dt} \left(\frac{\partial T}{\partial \dot{r}} \right) - \frac{\partial T}{\partial r} - F_r = m\ddot{r} - mr\dot{\theta}^2 - mg \cos \theta - \mathbf{C} \cdot \mathbf{N}$$

These may be solved to obtain $\mathbf{C} \cdot \mathbf{N} = m(\ddot{r} - r\dot{\theta}^2) - mg \cos \theta$ and $\mathbf{C} \cdot \mathbf{T} = m(r\ddot{\theta} + 2\dot{r}\dot{\theta}) + mg \sin \theta$. Using the normal and tangent vectors as a basis, we have

$$\mathbf{C} = (m(\ddot{r} - r\dot{\theta}^2) - mg \cos \theta)\mathbf{N} + (m(r\ddot{\theta} + 2\dot{r}\dot{\theta}) + mg \sin \theta)\mathbf{T}$$

When $r = L$ for all time, we found earlier that $L\ddot{\theta} + g \sin \theta = 0$ for all time. The constraint function reduces to

$$\mathbf{C} = -m(L\dot{\theta}^2 + g \cos \theta)\mathbf{N}(\theta)$$

Just to verify that this makes sense, consider when the mass is at the origin and not moving; that is, $\theta = 0$ and $\dot{\theta} = 0$. The constraint force is $\mathbf{C} = -mg\mathbf{N}(0) = -mg(\sin(0), -\cos(0)) = mg\mathbf{J}$. It exactly balances the gravitational force $-mg\mathbf{J}$, as expected.

Also observe that the normal component of the gravitational force is $-mg \cos \theta$. You might have tried selecting $-mg \cos \theta$ as the constraining force, but the actual force has the term $-mL\dot{\theta}^2$ in addition to the gravitational one. The constraining force, therefore, also must counter a force due to the motion of the particle itself. ■

3.2.2 TIME-VARYING FRAMES OR CONSTRAINTS

If the frame of reference varies over time or if the constraining curve or surface varies over time, the Lagrangian equations of motion in [equations \(3.20\)](#) or [\(3.27\)](#) still apply. The method of proof is general, so it covers both the curve and surface cases. The constraining parameters may be written as a vector \mathbf{q} . In the case of a curve, the vector has one component $\mathbf{q} = (q_1)$. In the case of a surface it is $\mathbf{q} = (q_1, q_2)$. In general let n denote the number of constraining variables. The position as a function of the constraining parameters and time is $\mathbf{x}(t, \mathbf{q})$. You need to be careful now about what the time derivatives mean. The velocity vector is the *total derivative* of position with respect to time. As such, you use ordinary differentiation with respect to t :

$$\dot{\mathbf{x}} = \frac{d\mathbf{x}}{dt}$$

But now the position has an explicit dependency on time that represents either the reference frame moving or the constraining curve/surface changing. The rate of change

of position with respect to time in that sense is represented by the partial derivative with respect to t . The chain rule from calculus relates the two:

$$\frac{d\mathbf{x}}{dt} = \frac{\partial \mathbf{x}}{\partial t} + \sum_{i=1}^m \frac{\partial \mathbf{x}}{\partial q_i} \dot{q}_i \quad (3.28)$$

Observe that this is the analogy of the identity from [equation \(3.22\)](#). The extension of [equation \(3.23\)](#) to our new situation is

$$\frac{\partial \mathbf{x}}{\partial \dot{q}_j} = \frac{\partial}{\partial \dot{q}_j} \left(\frac{\partial \mathbf{x}}{\partial t} + \sum_{i=1}^n \frac{\partial \mathbf{x}}{\partial q_i} \dot{q}_i \right) = \frac{\partial \dot{\mathbf{x}}}{\partial \dot{q}_j} \quad (3.29)$$

The extension of [equation \(3.24\)](#) is

$$\begin{aligned} \frac{d}{dt} \left(\frac{\partial \mathbf{x}}{\partial q_j} \right) &= \frac{\partial}{\partial t} \left(\frac{\partial \mathbf{x}}{\partial q_j} \right) + \sum_{i=1}^n \frac{\partial}{\partial q_i} \left(\frac{\partial \mathbf{x}}{\partial q_j} \right) \dot{q}_i && \text{By the chain rule} \\ &= \frac{\partial}{\partial q_j} \left(\frac{\partial \mathbf{x}}{\partial t} \right) + \sum_{i=1}^n \frac{\partial}{\partial q_j} \left(\frac{\partial \mathbf{x}}{\partial q_i} \right) \dot{q}_i && \text{Order of differentiation unimportant} \\ &= \frac{\partial}{\partial q_j} \left(\frac{\partial \mathbf{x}}{\partial t} + \sum_{i=1}^n \frac{\partial \mathbf{x}}{\partial q_i} \dot{q}_i \right) && \text{Differentiation is linear} \\ &= \frac{\partial \dot{\mathbf{x}}}{\partial q_j} && \text{Using equation (3.28)} \end{aligned} \quad (3.30)$$

Since all the identities are used in deriving the Lagrangian equations of motion, whether [equation \(3.20\)](#) or [\(3.27\)](#), these identities must equally apply when the position function has the explicit time component. The equations of motion for time-varying frames or constraints are still

$$\frac{d}{dt} \left(\frac{\partial T}{\partial \dot{q}_j} \right) - \frac{\partial T}{\partial q_j} = F_{q_j} \quad (3.31)$$

for all indices j .

EXAMPLE 3.9

Let us revisit the simple pendulum problem that is illustrated in [Figure 3.4](#) and whose equations of motion are derived in [Example 3.5](#). Rather than having the joint remain fixed over time, we allow it to vary in time, say $\mathbf{P}(t)$. The position function is

$$\mathbf{x}(t, \theta) = \mathbf{P}(t) + L\mathbf{N}(\theta)$$

The total time derivative is

$$\dot{\mathbf{x}} = \frac{d\mathbf{x}}{dt} = \frac{\partial \mathbf{x}}{\partial t} + \frac{\partial \mathbf{x}}{\partial \theta} \dot{\theta} = \dot{\mathbf{P}} + L\dot{\theta}\mathbf{T}$$

The kinetic energy is

$$T = \frac{m}{2} |\dot{\mathbf{P}} + L\dot{\theta}\mathbf{T}|^2 = \frac{m}{2} (\dot{\mathbf{P}} \cdot \dot{\mathbf{P}} + 2L\dot{\theta}\dot{\mathbf{P}} \cdot \mathbf{T} + L^2\dot{\theta}^2)$$

The relevant derivatives are

$$\frac{\partial T}{\partial \theta} = \frac{m}{2} \left(2L\dot{\theta}\dot{\mathbf{P}} \cdot \frac{d\mathbf{T}}{d\theta} \right) = -mL\dot{\theta}\dot{\mathbf{P}} \cdot \mathbf{N}$$

$$\frac{\partial T}{\partial \dot{\theta}} = \frac{m}{2} (2L\dot{\mathbf{P}} \cdot \mathbf{T} + 2L^2\ddot{\theta}) = mL(\dot{\mathbf{P}} \cdot \mathbf{T} + L\ddot{\theta})$$

and

$$\frac{d}{dt} \left(\frac{\partial T}{\partial \dot{\theta}} \right) = mL(\dot{\mathbf{P}} \cdot \dot{\mathbf{T}} + \ddot{\mathbf{P}} \cdot \mathbf{T} + L\ddot{\theta}) = mL(\ddot{\mathbf{P}} \cdot \mathbf{T} - \dot{\theta}\dot{\mathbf{P}} \cdot \mathbf{N} + L\ddot{\theta})$$

The generalized force is

$$F_\theta = (-mg\mathbf{J}) \cdot \frac{\partial \mathbf{x}}{\partial \theta} = (-mg\mathbf{J}) \cdot (L\mathbf{T}) = -mgL \sin \theta$$

Combining these into equation (3.20) produces

$$L\ddot{\theta} + \ddot{\mathbf{P}} \cdot \mathbf{T} + g \sin \theta = 0$$

In the case where $\mathbf{P}(t)$ is a constant (the joint is immovable as in the original problem), we obtain $L\ddot{\theta} + g \sin \theta = 0$ as before. However, you should also notice that if the joint has constant linear velocity, $\mathbf{P}(t) = \mathbf{A} + t\mathbf{B}$, then we still obtain $L\ddot{\theta} + g \sin \theta = 0$. This should come as no surprise because the frame of reference is moving with constant linear velocity and is still an inertial frame.

Also curious is that if you were to hold the pendulum joint in the fingers of one hand, hold the mass away from the vertical with the fingers of your other hand, then drop the entire system, the angle formed by the mass never changes! Assuming no air resistance, the joint acceleration is controlled by gravity, $\ddot{\mathbf{P}} = -g\mathbf{J}$. The differential equation reduces to $L\ddot{\theta} = 0$. The initial angle is $\theta(0) = \theta_0$ and the initial angular speed is $\dot{\theta}(0) = 0$. The solution to the equation is $\theta(t) = \theta_0$ for all $t \geq 0$. ■

EXERCISE 3.15

A rigid, frictionless rod of length L has one end attached to the origin of three-dimensional space. The initial direction of the rod is $(1, 0, 1)/\sqrt{2}$. Thus, the other end of the rod is at $L(1, 0, 1)/\sqrt{2} = (a, 0, a)$. A mass m is constrained to move on the rod and has initial location at $(b, 0, b)$, where $0 < b < a$. One end of a spring is attached to the mass. The other end is attached to a joint at location $(c, 0, 0)$ for some positive constant c . The spring is unstretched in this initial configuration. Figure 3.9 illustrates the setup.

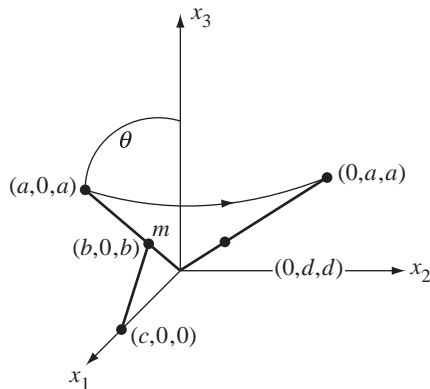


Figure 3.9 The initial configuration of a rigid rod containing a mass that is attached to a spring.

The rod is rotated about the x_3 -axis so that the angle θ between the rod and axis remains constant. The rotation occurs with angular speed θt for $t \geq 0$. Determine the equations of motion for the mass. What is the position $(0, d, d)$ of the mass when the rod reaches the $x_1 x_3$ -plane for the first time? ■

3.2.3 INTERPRETATION OF THE EQUATIONS OF MOTION

We now look at a simple, yet elegant way of interpreting the Lagrangian equations of motion. The position of the particle constrained to a curve or surface is $\mathbf{x}(t, \mathbf{q})$, where $\mathbf{q} = (q_1)$ for a curve or $\mathbf{q} = (q_1, q_2)$ for a surface. The partial derivatives of position with respect to the q_j are tangent vectors. Unit-length tangent vectors are therefore,

$$\mathbf{T}_j = \frac{1}{|\partial \mathbf{x}/\partial q_j|} \frac{\partial \mathbf{x}}{\partial q_j} = \frac{1}{L_j} \frac{\partial \mathbf{x}}{\partial q_j}$$

where the last equality defines L_j as the length of the partial derivative vector. The component of acceleration of the particle in each of the tangent directions, denoted by a_{q_j} , is computed by projection onto the tangent:

$$\begin{aligned} a_{q_j} &= \mathbf{a} \cdot \mathbf{T}_j = \frac{1}{L_j} \left(\ddot{\mathbf{x}} \cdot \frac{\partial \mathbf{x}}{\partial q_j} \right) \\ &= \frac{1}{m L_j} \left(\frac{d}{dt} \left(\frac{\partial T}{\partial \dot{q}_j} \right) - \frac{\partial T}{\partial q_j} \right) \\ &= \frac{1}{m L_j} F_{q_j} \end{aligned}$$

We have used the Lagrangian equations of motion, [equation \(3.31\)](#), in this construction. Now recall that the generalized force is

$$F_{q_j} = \mathbf{F} \cdot \frac{\partial \mathbf{x}}{\partial q_j} = L_j \mathbf{F} \cdot \mathbf{T}_j$$

Define the quantity $f_{q_j} = \mathbf{F} \cdot \mathbf{T}_j$, the projection of the force onto the tangent vector \mathbf{T}_j . That is, f_{q_j} is the component of force in the tangent direction. Thus, $a_{q_j} = F_{q_j}/(mL_j)$ or

$$ma_{q_j} = f_{q_j} \quad (3.32)$$

for each constraining variable q_j . You should recognize the similarity to Newton's second law. As a matter of fact, the Lagrangian formulation is the natural extension of Newton's second law when the motion is constrained to a manifold (curve or surface).

3.2.4 EQUATIONS OF MOTION FOR A SYSTEM OF PARTICLES

Consider a system of p particles, particle i having mass m_i and located at position \mathbf{x}_i , $1 \leq i \leq p$. D'Alembert's [equation \(3.13\)](#) applies to each particle when displaced by an infinitesimal amount $d\mathbf{x}_i$ and influenced by a force \mathbf{F}_i . The derivations for the equations of motion are applied for each such particle, to produce a Lagrangian equation of motion for each constraint of interest:

$$\frac{d}{dt} \left(\frac{\partial K_i}{\partial \dot{q}_j} \right) - \frac{\partial K_i}{\partial q_j} = \mathbf{F}_i \cdot \frac{\partial \mathbf{x}_i}{\partial q_j}$$

where $K_i = m_i |\dot{\mathbf{x}}_i|^2 / 2$ is the kinetic energy of the particle. The total kinetic energy is

$$T = \sum_{i=1}^p K_i = \frac{1}{2} \sum_{i=1}^p m_i |\dot{\mathbf{x}}_i|^2$$

and the total generalized force for the q_j coordinate is

$$F_{q_j} = \sum_{i=1}^p \mathbf{F}_i \cdot \frac{\partial \mathbf{x}_i}{\partial q_j}$$

The Lagrangian equations of motion are obtained by summing those for the individual particles, leading to

$$\frac{d}{dt} \left(\frac{\partial T}{\partial \dot{q}_j} \right) - \frac{\partial T}{\partial q_j} = F_{q_j}, \quad j \geq 1 \quad (3.33)$$

EXAMPLE
3.10

Three masses m_1 , m_2 , and m_3 are aligned vertically and are subject to gravitational force. The first two masses are attached by a spring with spring constant c_1 and unstretched length L_1 . The second two masses are attached by a spring with spring constant c_2 and unstretched length L_2 . The mass m_i is located at z_i vertical units with respect to the ground plane. The particle system has three degrees of freedom represented by the variables z_i , $1 \leq i \leq 3$. Figure 3.10 illustrates the situation.

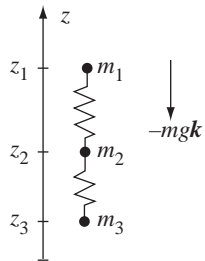


Figure 3.10

Three masses aligned vertically and subject to gravitational force.

The force due to gravity on mass m_i is $\mathbf{G}_i = -m_i g \mathbf{k}$ for $1 \leq i \leq 3$. The force due to the spring connecting masses m_1 and m_2 is

$$\mathbf{G}_4 = -c_1(z_1 - z_2 - L_1)\mathbf{k}$$

The leading sign is negative as shown by the following argument. When the spring is unstretched, the magnitude of the spring force is zero. The separation between the two masses is $z_1 - z_2 = L_1$. If the mass m_2 is pulled upwards to a new position $z_1 + \delta$, where $\delta > 0$, the force on m_2 must be in the downward direction. This force is $-c_1 \delta \mathbf{k}$. Since both c_1 and δ are positive, the leading negative sign guarantees that the force is downward. Similarly, the force due to the spring connecting masses m_2 and m_3 is

$$\mathbf{G}_5 = -c_2(z_2 - z_3 - L_2)\mathbf{k}$$

The force on m_1 is $\mathbf{F}_1 = \mathbf{G}_1 + \mathbf{G}_4$. The force on m_2 is $\mathbf{F}_2 = \mathbf{G}_2 - \mathbf{G}_4 + \mathbf{G}_5$. The negative sign on the \mathbf{G}_4 term occurs because an increase in z_2 causes the first spring to compress, in which case that spring must exert a force in the opposite direction. The force on m_3 is $\mathbf{F}_3 = \mathbf{G}_3 - \mathbf{G}_5$. The negative sign on the \mathbf{G}_5 term occurs because an increase in z_3 causes the second spring to compress, in which case that spring must exert a force in the opposite direction.

The kinetic energy for the system is

$$T = \frac{1}{2} \sum_{i=1}^3 m_i \dot{z}_i^2$$

The relevant derivatives are $\partial T / \partial z_i = 0$, $\partial T / \partial \dot{z}_i = m_i \dot{z}_i$, and $d(\partial T / \partial \dot{z}_i) / dt = m_i \ddot{z}_i$ for $1 \leq i \leq 3$.

The Lagrangian equations of motion are therefore $m_i \ddot{z}_i = \mathbf{F}_i \cdot \mathbf{k}$, or

$$\begin{aligned} m_1 \ddot{z}_1 &= -c_1(z_1 - z_2 - L_1) - m_1 g \\ m_2 \ddot{z}_2 &= -c_2(z_2 - z_3 - L_2) + c_1(z_1 - z_2 - L_1) - m_2 g \\ m_3 \ddot{z}_3 &= c_2(z_2 - z_3 - L_2) - m_3 g \end{aligned}$$

Setting $\mathbf{z} = [z_1 \ z_2 \ z_3]^T$, the system of equations in matrix form is

$$\ddot{\mathbf{z}} = \begin{bmatrix} -\frac{c_1}{m_1} & \frac{c_1}{m_1} & 0 \\ \frac{c_1}{m_2} & -\frac{c_1 + c_2}{m_2} & \frac{c_2}{m_2} \\ 0 & \frac{c_2}{m_3} & -\frac{c_2}{m_3} \end{bmatrix} \mathbf{z} + \begin{bmatrix} \frac{c_1 L_1}{m_1} - g \\ \frac{c_2 L_2 - c_1 L_1}{m_2} - g \\ -\frac{c_2 L_2}{m_3} - g \end{bmatrix}$$

This is a second-order linear system of differential equations. Using methods from linear systems of differential equations, it may be reduced to a first-order system by setting

$$\mathbf{x} = [x_1 \ x_2 \ x_3 \ x_4 \ x_5 \ x_6] = [z_1 \ z_2 \ z_3 \ \dot{z}_1 \ \dot{z}_2 \ \dot{z}_3]^T$$

leading to

$$\dot{\mathbf{x}} = \begin{bmatrix} 0 & 0 & 0 & 1 & 0 & 0 \\ 0 & 0 & 0 & 0 & 1 & 0 \\ 0 & 0 & 0 & 0 & 0 & 1 \\ -\frac{c_1}{m_1} & \frac{c_1}{m_1} & 0 & 0 & 0 & 0 \\ \frac{c_1}{m_2} & -\frac{c_1 + c_2}{m_2} & \frac{c_2}{m_2} & 0 & 0 & 0 \\ 0 & \frac{c_2}{m_3} & -\frac{c_2}{m_3} & 0 & 0 & 0 \end{bmatrix} \mathbf{x} + \begin{bmatrix} 0 \\ 0 \\ 0 \\ \frac{c_1 L_1}{m_1} - g \\ \frac{c_2 L_2 - c_1 L_1}{m_2} - g \\ -\frac{c_2 L_2}{m_3} - g \end{bmatrix}$$

This is of the form $\dot{\mathbf{x}} = A\mathbf{x} + \mathbf{b}$ and may be solved in closed form using the methods of linear systems of differential equations. The matrix A happens to be invertible, so the solution is

$$\mathbf{x} = e^{At} \mathbf{x}_0 - A^{-1} \mathbf{b}$$

where \mathbf{x}_0 is an initial condition (see Section 11.5). However, this solution will involve trigonometric functions. Because these are expensive to calculate, a numerical differential equation solver may be used instead to obtain a good approximation to the solution while requiring less computational time to calculate. ■

EXERCISE
 3.16

 **SOURCE CODE**
 DoublePendulum

Consider a modification of the simple pendulum problem, a *double pendulum problem* so to speak. In addition to the mass m_1 attached to a rigid rod of length r_1 , a second mass m_2 is attached via a rigid rod of length r_2 to the first mass. The second rod pivots at the location of m_1 and does so without friction. Figure 3.11 illustrates.

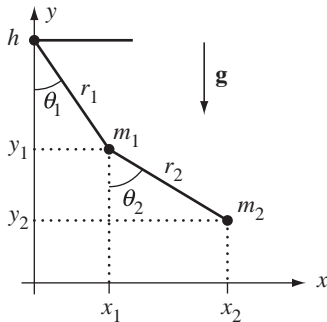


Figure 3.11 A modification of the simple pendulum problem.

Construct the equations of motion as two coupled differential equations in the unknown angles $\theta_1(t)$ and $\theta_2(t)$. ■

3.2.5 EQUATIONS OF MOTION FOR A CONTINUUM OF MASS

As expected, the Lagrangian equations of motion are also valid for a continuum of mass, whether a curve mass, a surface mass, or a volume mass. The summations that occur in the formulas for kinetic energy and generalized forces for particle systems are replaced by integrals. Rather than write separate formulas for curve masses (single integral), surface masses (double integral), and volume masses (triple integral), we use a suggestive notation with one integral whose domain of integration R generically refers to the correct type of object. The mass density is δ and varies over R . The infinitesimal measure of mass is $dm = \delta dR$, where dR is an infinitesimal measure of arc length, surface area, or volume, depending on what type of object R represents. The kinetic energy is

$$T = \frac{1}{2} \int_R |\mathbf{v}|^2 dm$$

where the world velocity is \mathbf{v} . That is, the kinetic energy must be measured in an inertial frame; in our case this frame is labeled as the world frame. For each constraint

variable q_j , the generalized force is

$$F_{q_j} = \int_R \mathbf{F} \cdot \frac{\partial \mathbf{x}}{\partial q_j} dR$$

where \mathbf{F} represents the applied forces on the object. The Lagrangian equations of motion are

$$\frac{d}{dt} \left(\frac{\partial T}{\partial \dot{q}_j} \right) - \frac{\partial T}{\partial q_j} = F_{q_j}$$

for all j .

Although the kinetic energy is computed from the velocity in the inertial frame, we may compute it using a transformation to local coordinates. For a rigid body we do this by [equation \(2.43\)](#):

$$\mathbf{v} = \mathbf{v}_{\text{cen}} + \mathbf{w} \times \mathbf{r}$$

where \mathbf{v}_{cen} is the velocity of the point \mathcal{C} identified as the origin of the body and where \mathbf{w} is the angular velocity of the body measured in the inertial frame. The relative position \mathbf{r} is from a rigid body point to the body origin. The kinetic energy in this case is

$$\begin{aligned} T &= \frac{1}{2} \int_R |\mathbf{v}|^2 dm \\ &= \frac{1}{2} \int_R |\mathbf{v}_{\text{cen}}|^2 + 2\mathbf{v}_{\text{cen}} \cdot \mathbf{w} \times \mathbf{r} + |\mathbf{w} \times \mathbf{r}|^2 dm \\ &= \frac{1}{2} |\mathbf{v}_{\text{cen}}|^2 \int_R dm + \mathbf{v}_{\text{cen}} \cdot \mathbf{w} \int_R \mathbf{r} dm + \frac{1}{2} \int_R (|\mathbf{w}|^2 |\mathbf{r}|^2 - (\mathbf{w} \cdot \mathbf{r})^2) dm \\ &= \frac{1}{2} m |\mathbf{v}_{\text{cen}}|^2 + m \mathbf{v}_{\text{cen}} \cdot \mathbf{w} \times \mathbf{r}_{\text{cm}} + \frac{1}{2} \mathbf{w}^T J \mathbf{w} \end{aligned}$$

where m is the total mass of the body, \mathbf{r}_{cm} is the position of the center of mass of the rigid body relative to \mathcal{C} , and J is the inertia tensor of the rigid body as specified in [equation \(2.84\)](#). If we choose \mathcal{C} to be the center of mass, the middle term vanishes since $\mathbf{r}_{\text{cm}} = \mathbf{0}$. We may also choose the local coordinate basis vectors to be the principal directions of motion (see [Section 2.5.4](#), the portion on inertia of 3D objects). If the principal directions are \mathbf{u}_i , $1 \leq i \leq 3$, they may be written as the columns of a rotation matrix $Q = [\mathbf{u}_1 \mid \mathbf{u}_2 \mid \mathbf{u}_3]$. By definition of principal directions, the inertia tensor satisfies the equation $J = Q D Q^T$, where D is a diagonal matrix whose diagonal entries μ_1 , μ_2 , and μ_3 are the principal moments. The world angular velocity \mathbf{w} is represented in terms of the principal direction basis as $\mathbf{w} = Q \boldsymbol{\xi}$. Consequently, $\mathbf{w}^T J \mathbf{w} = \boldsymbol{\xi}^T D \boldsymbol{\xi}$. If $\boldsymbol{\xi} = [\xi_1 \xi_2 \xi_3]^T$, then the kinetic energy in this special case is

$$T = \frac{1}{2} m |\mathbf{v}_{\text{cm}}|^2 + \frac{1}{2} (\mu_1 \xi_1^2 + \mu_2 \xi_2^2 + \mu_3 \xi_3^2) \quad (3.34)$$

where \mathbf{v}_{cm} is the world velocity of the center of mass. The formula is quite aesthetic. The first term is the energy due to the linear velocity of the center of mass. The last terms are the energies due to the angular velocity about principal direction lines through the center of mass. Although these formulas for kinetic energy were derived using integrals, they apply equally well to particle systems (the construction works for sums and integrals).

Equation (2.44) allows a similar simplification to the generalized force integral. Using Newton's law, an infinitesimal force $d\mathbf{F}$ applied to a particle in R of infinitesimal mass dm satisfies the relationship $d\mathbf{F} = \mathbf{a} dm$, where \mathbf{a} is the acceleration applied to that particle. Integrating over the entire region to obtain the total force \mathbf{F} and applying the aforementioned equation:

$$\begin{aligned}\mathbf{F} &= \int_R \mathbf{a} dm \\ &= \int_R \mathbf{a}_{\text{cen}} + \mathbf{w} \times (\mathbf{w} \times \mathbf{r}) + \frac{d\mathbf{w}}{dt} \times \mathbf{r} dm \\ &= \mathbf{a}_{\text{cen}} \int_R dm + \mathbf{w} \times \left(\mathbf{w} \times \int_R \mathbf{r} dm \right) + \frac{d\mathbf{w}}{dt} \times \int_R \mathbf{r} dm \\ &= m\mathbf{a}_{\text{cen}} + m\mathbf{w} \times (\mathbf{w} \times \mathbf{r}_{\text{cm}}) + m \frac{d\mathbf{w}}{dt} \times \mathbf{r}_{\text{cm}}\end{aligned}$$

where m is the total mass of the body, \mathbf{a}_{cen} is the world acceleration of the point C identified as the body origin, and \mathbf{r}_{cm} is the position of the center of mass relative to C . If we choose C to be the center of mass, then $\mathbf{r}_{\text{cm}} = \mathbf{0}$ and

$$\mathbf{F} = m\mathbf{a}_{\text{cm}} \quad (3.35)$$

That is, the external forces applied to the rigid body act as if they are applied to a single particle located at the center of mass of the body and having mass equal to the total mass of the body. The generalized force for the rigid body may be calculated based only on the center of mass and how it is constrained.

EXAMPLE 3.11

This example is a modification of the simple pendulum problem, but we treat this as a fully 3D problem. The z -axis is perpendicular to the plane of the diagram. The simple pendulum consists of a single point mass located at the end of a rigid, massless rod. The other end of the rod is attached to a frictionless joint at $(0, y_0, 0)$. The rod–point object is replaced by a triangular object as shown in Figure 3.12.

The triangle is isosceles with base length b and height h . Its mass density is constant, $\delta = 1$, so the total mass is the area of the triangle (in units of mass), $m = bh/2$. The center of mass is located at $(\bar{x}, \bar{y}, \bar{z})$. The distance from the pendulum joint to the center of mass is L and the angle formed with the vertical is θ , so the center of mass location is $(\bar{x}, \bar{y}, \bar{z}) = (L \sin \theta, y_0 - L \cos \theta, 0)$.

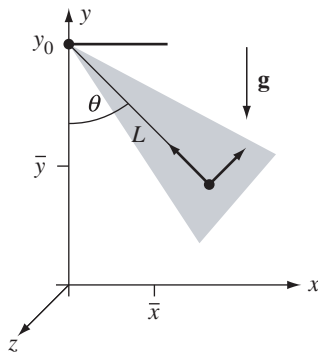


Figure 3.12

A triangle pendulum.

We assign a local coordinate frame using the principal directions of motion associated with the inertia tensor. From the symmetry of the object, the principal directions are $(\cos \theta, \sin \theta, 0)$, $(-\sin \theta, \cos \theta, 0)$, and $(0, 0, 1)$. The first two of these are drawn in the figure as small black arrows at the center of mass. Although we could compute the principal moments associated with the first two principal directions, it is not necessary since the world angular velocity, $\mathbf{w} = (0, 0, \dot{\theta})$, is already a multiple of the principal direction. The zero components of this vector multiply the principal moments in equation (3.34). The only relevant moment is μ_3 associated with the direction $(0, 0, 1)$. The kinetic energy is

$$T = \frac{1}{2} m L^2 \dot{\theta}^2 + \frac{1}{2} \mu_3 \dot{\theta}^2 = \frac{m L^2 + \mu_3}{2} \dot{\theta}^2$$

Since the body is rigid, according to equation (3.35) the gravitational force $\mathbf{F}_{\text{grav}} = -mg \mathbf{J}$ acts as if it is applied at the center of mass. The generalized force is

$$F_\theta = \mathbf{F}_{\text{grav}} \cdot \frac{\partial(\bar{x}, \bar{y}, \bar{z})}{\partial \theta} = (-mg \mathbf{J}) \cdot L(\cos \theta, \sin \theta, 0) = -mgL \sin \theta$$

The Lagrangian equation of motion is

$$(mL^2 + \mu_3)\ddot{\theta} = \frac{d}{dt} \left(\frac{\partial T}{\partial \dot{\theta}} \right) - \frac{\partial T}{\partial \theta} = F_\theta = -mgL \sin \theta$$

or $\ddot{\theta} + c \sin \theta = 0$, where $c = mgL/(mL^2 + \mu_3)$. Note the similarity to the equation of motion for the simple pendulum. As the base of the triangle shrinks to zero, all the while maintaining constant mass, the limiting case is the rod itself (of the simple pendulum problem). The principal moment μ_3 is zero in the limiting case and $c = g/L$, exactly what occurs in the simple pendulum problem. ■

A couple of observations about the last example are in order. Although we have set up the equations of motion, a numerical implementation must have available the values of the mass m and the principal moment μ_3 . Under the stated assumptions, the center of mass is the area of the triangle. In your implementation, you simply need to supply the dimensions of the triangle. However, if the triangle is more complicated – namely the mass density ρ is not constant – you must compute the center of mass for the triangle, most likely using a numerical integrator applied to $m = \int_R \delta \, dR$, where R is the region of the plane that the triangle occupies. Also, the principal moment μ_3 must be computed, also by numerical integration when δ is not a constant. In general for any rigid body, in order to construct the kinetic energy specified by [equation \(3.34\)](#), you will need to compute the mass and inertia tensor of the body. These calculations are typically done before the simulation starts and stored with the data structures representing the rigid body and its motion.

The second observation is that if the triangle in the last example is replaced by another planar object of the same mass m and having the same principal directions of motion and principal moments leading to the same value μ_3 , the equation of motion for the planar object is identical to that of the triangle. The triangle and planar object are said to be *dynamically equivalent*.

EXERCISE 3.17

In the Foucault pendulum [Example 3.3](#), replace the massless rod and single-point mass by a cone of height h and base radius r . Compute the equations of motion. ■

EXAMPLE 3.12

 SOURCE CODE
MassPulleySpring

Consider the physical system shown in [Figure 3.13](#). This example has a mixture of point-mass objects and a planar mass.

A gravitational force is applied, but note that the y -axis has been selected to point downward, so $\mathbf{g} = g \mathbf{j}$ where $g > 0$. The masses and locations are labeled in the figure, as is the radius of the pulley. The other relevant quantities are the spring constant $c > 0$, the unstretched spring length $L > 0$, and the principal moment of inertia of

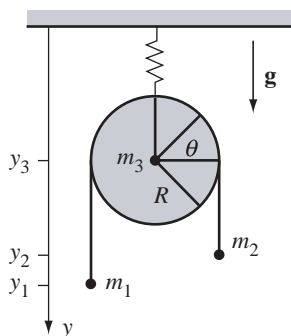


Figure 3.13

A system consisting of two masses, a pulley with mass, and a spring.

the pulley I , measured with respect to the z -axis that is perpendicular to the plane of the figure.

This system has two degrees of freedom, the vertical distance y_3 from the ceiling to the center of mass of the pulley and the vertical distance y_1 from the vertical location of the center of mass of the pulley to the mass m_1 . The vertical distance y_2 is automatically determined, because the length of the wire connecting m_1 and m_2 , namely $y_1 + y_2 + \pi R = \ell$, a constant.

The kinetic energy of the first mass is $m_1(\dot{y}_3 + \dot{y}_1)^2/2$ and the kinetic energy of the second mass is $m_2(\dot{y}_3 - \dot{y}_1)^2/2 = m_2(\dot{y}_3 - \dot{y}_1)^2/2$. The kinetic energy of the pulley is calculated using equation (3.34). The component associated with the velocity of the center of mass is $m_3\dot{y}_3^2/2$. The component associated with the angular velocity is $I\dot{\theta}^2/2$, where θ is an angle measured from the horizontal line through the center of the pulley, as shown in Figure 3.13. Notice that for an angle θ as shown, the length of the subtended arc on the pulley circumference is $R\theta$. The rate of change is $R\dot{\theta}$, where $\dot{\theta}$ is the angular speed of the pulley. Any change in arc length amounts to a change in the y_1 vertical distance; that is, $\dot{y}_1 = R\dot{\theta}$. The kinetic energy component is therefore, $I(\dot{y}_1/R)^2/2$. The total kinetic energy is

$$T = \frac{m_1}{2}(\dot{y}_3 + \dot{y}_1)^2 + \frac{m_2}{2}(\dot{y}_3 - \dot{y}_1)^2 + \frac{m_3}{2}\dot{y}_3^2 + \frac{I}{2R^2}\dot{y}_1^2$$

The principal moment, measured with respect to the center of the pulley, is $I = \int_D r^2 r dr d\theta$, where D is the disk $r \leq R$. The integral is easily calculated to produce $I = \pi R^4/2$.

The relevant derivatives of the kinetic energy are (1) $\partial T / \partial y_3 = 0$, $\partial T / \partial y_1 = 0$, $\partial T / \partial \dot{y}_3 = \alpha \dot{y}_3 + \beta \dot{y}_1$, where $\alpha = m_1 + m_2 + m_3$ and $\beta = m_1 - m_2$, and (2) $\partial T / \partial \dot{y}_1 = \beta \dot{y}_3 + \gamma \dot{y}_1$, where $\gamma = m_1 + m_2 + I/R^2$.

The position of mass m_1 is $(y_3 + y_1)\mathbf{J}$. The generalized forces for this mass are

$$\begin{aligned} F_{y_3} &= m_1 g \mathbf{J} \cdot \frac{\partial((y_3 + y_1)\mathbf{J})}{\partial y} = m_1 g \\ F_{y_1} &= m_1 g \mathbf{J} \cdot \frac{\partial((y_3 + y_1)\mathbf{J})}{\partial y_1} = m_1 g \end{aligned}$$

The position of mass m_2 is $(y_3 + y_2)\mathbf{J}$. The generalized forces for this mass are

$$\begin{aligned} F_{y_3} &= m_2 g \mathbf{J} \cdot \frac{\partial((y_3 + y_2)\mathbf{J})}{\partial y} = m_2 g \\ F_{y_1} &= m_2 g \mathbf{J} \cdot \frac{\partial((y_3 + y_2)\mathbf{J})}{\partial y_1} = -m_2 g \end{aligned}$$

The negative sign on the right-hand side occurs because $y_1 + y_2 = \ell - \pi R$ (a constant) implies $dy_2/dy_1 = -1$. The position of the center of the pulley is $y_3\mathbf{J}$. The

(Example 3.12
continued)

generalized forces for the pulley are

$$F_{y_3} = (m_3g + c(L - y_3))\mathbf{J} \cdot \frac{\partial(y_3\mathbf{J})}{\partial y} = m_3g + c(L - y_3)$$

$$F_{y_1} = (m_3g + c(L - y_3))\mathbf{J} \cdot \frac{\partial(y_3\mathbf{J})}{\partial y_1} = 0$$

The Lagrangian equations of motion are

$$\alpha\ddot{y}_3 + \beta\ddot{y}_1 = F_{y_3} = m_1g + m_2g + m_3g + c(L - y_3) = \alpha g + c(L - y_3)$$

and

$$\beta\ddot{y}_3 + \gamma\ddot{y}_1 = F_{y_1} = m_1g - m_2g = \beta g$$

The equations are uncoupled by solving the second for \ddot{y}_1 and replacing in the first,

$$\ddot{y}_3 = \frac{c\gamma}{\alpha\gamma - \beta^2}(L - y_3) + g$$

This is a second-order linear differential equation with a nonhomogeneous term. [Figure 3.14](#) – also [Color Plate 3.14](#) – shows some screen shots from the mass/pulley/spring application found on the CD-ROM.

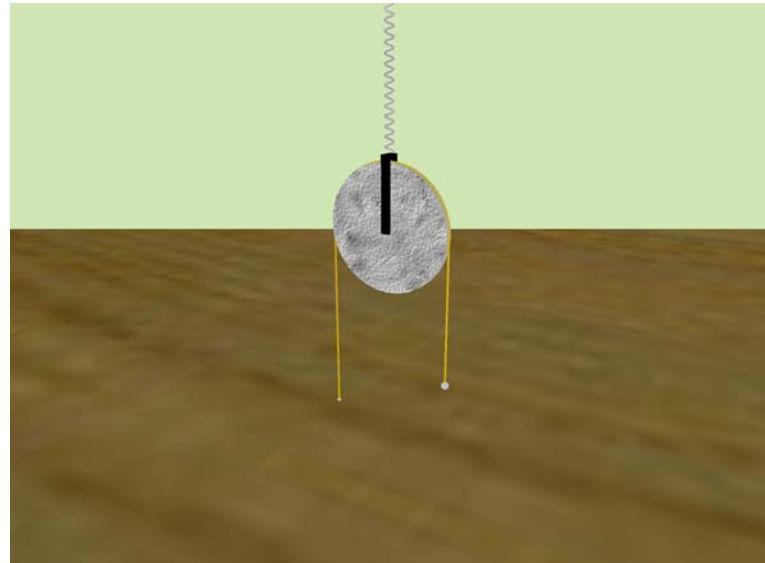


Figure 3.14 (Continued)

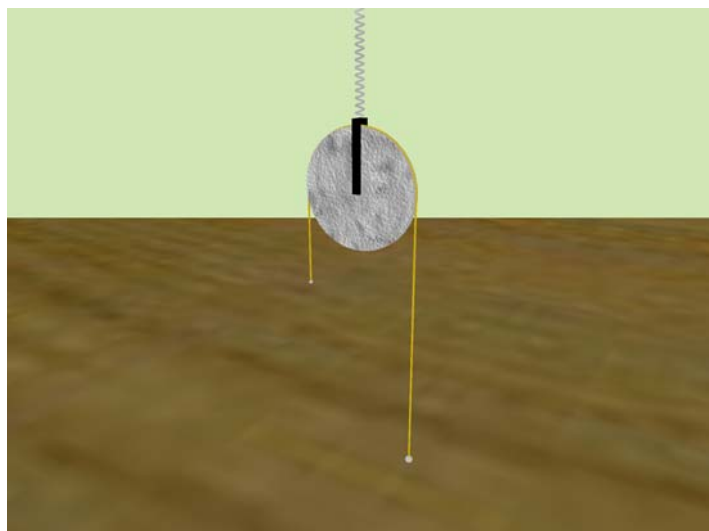


Figure 3.14

A mass pulley spring system shown at two different times. The spring expands and compresses and the pulley disk rotates during the simulation. The system stops when a mass reaches the center line of the pulley or the ground. (See also [Color Plate 3.14](#).)

EXERCISE
3.18

In [Example 3.12](#), solve the final differential equation explicitly for y , then solve for y_1 and y_2 explicitly.

EXERCISE
3.19

Compute the equations of motion for the physical system shown in Figure 3.15.

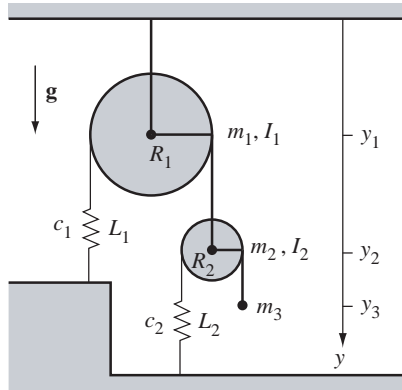


Figure 3.15 A system of two pulleys, two springs, and a mass.

The spring constants c_1 and c_2 and the unstretched lengths L_1 and L_2 are labeled in the figure. The masses, moments of inertia, and radii of the pulleys are shown, as well as the mass of the single particle. ■

EXAMPLE
3.13

Figure 3.16 shows a physical system consisting of a rigid, but massless, pipe that has a slight bend in it. The vertical portion of the pipe freely rotates about the z -axis with angular speed $\dot{\theta}$. At the end of the pipe is a solid, cylindrical disk of constant mass density. The radius of the disk is a and the thickness is b . The disk freely rotates about the cylinder axis with angular speed $\dot{\psi}$. The force acting on the system is given generically by \mathbf{F} . We wish to determine the equations of motion for the system.

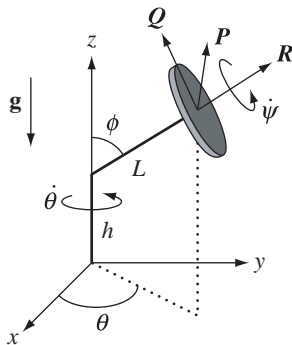


Figure 3.16

A physical system with a bent pipe rotating about the z -axis and a disk rotating about its axis.

The bend in the joint is h units above the end of the pipe. The bent portion of the pipe has length L . The local coordinate system at the center of mass uses spherical coordinates, where $\mathbf{P} = (-\sin \theta, \cos \theta, 0)$, $\mathbf{Q} = (-\cos \theta \cos \phi, -\sin \theta \cos \phi, \sin \phi)$, and $\mathbf{R} = (\cos \theta \sin \phi, \sin \theta \sin \phi, \cos \phi)$. If \mathcal{O} denotes the origin of the physical system, the center of mass \mathcal{C} of the disk is located relative to the origin by

$$\mathbf{r} = \mathcal{C} - \mathcal{O} = h\mathbf{k} + L\mathbf{R}$$

The velocity of the center of mass is

$$\mathbf{v}_{cm} = \frac{d\mathbf{r}}{dt} = L\dot{\mathbf{R}} = L(\dot{\theta} \sin \phi \mathbf{P} - \dot{\phi} \mathbf{Q})$$

The world coordinates of the angular velocity of the pipe about its shaft is $\mathbf{w}_{pipe} = \dot{\theta}\mathbf{k}$. The world coordinates of the angular velocity of the disk is $\mathbf{w}_{disk} = \dot{\psi}\mathbf{R}$, where $\dot{\psi}$ is the angular measurement made in the plane of \mathbf{P} and \mathbf{Q} . The world coordinates of the

angular velocity of the physical system as a whole is the sum of the angular velocities,

$$\mathbf{w} = \mathbf{w}_{\text{pipe}} + \mathbf{w}_{\text{disk}} = \dot{\theta}\mathbf{k} + \dot{\psi}\mathbf{R}$$

We may write the angular velocity in local coordinates using the fact that $\mathbf{k} = \cos\phi\mathbf{R} + \sin\phi\mathbf{Q}$:

$$\mathbf{w} = 0\mathbf{P} + \dot{\theta}\sin\phi\mathbf{Q} + (\dot{\psi} + \dot{\theta}\cos\phi)\mathbf{R}$$

in which case the local coordinates are

$$\xi = (0, \dot{\theta}\sin\phi, \dot{\psi} + \dot{\theta}\cos\phi)$$

From equation (3.34) the kinetic energy is

$$T = \frac{1}{2}mL^2(\dot{\theta}^2\sin^2\phi + \dot{\phi}^2) + \frac{1}{2}\mu_2\dot{\theta}^2\sin^2\phi + \frac{1}{2}\mu_3(\dot{\psi} + \dot{\theta}\cos\phi)^2$$

where m is the mass of the disk and where μ_2 and μ_3 are principal moments for the disk. Although we do not need the value here, by symmetry $\mu_1 = \mu_2$. The only degrees of freedom are θ and ψ , because ϕ is constant. The relevant derivatives are

$$\begin{aligned} \frac{\partial T}{\partial \theta} &= 0, \quad \frac{\partial T}{\partial \psi} = 0 \\ \frac{\partial T}{\partial \dot{\theta}} &= (mL^2 + \mu_2)\dot{\theta}\sin^2\phi + \mu_3(\dot{\psi} + \dot{\theta}\cos\phi)\cos\phi, \\ \frac{\partial T}{\partial \dot{\psi}} &= \mu_3(\dot{\psi} + \dot{\theta}\cos\phi) \\ \frac{d}{dt} \left(\frac{\partial T}{\partial \dot{\theta}} \right) &= (mL^2 + \mu_2)\ddot{\theta}\sin^2\phi + \mu_3(\ddot{\psi} + \ddot{\theta}\cos\phi)\cos\phi, \\ \frac{d}{dt} \left(\frac{\partial T}{\partial \dot{\psi}} \right) &= \mu_3(\ddot{\psi} + \ddot{\theta}\cos\phi) \end{aligned}$$

The generalized forces are

$$F_\theta = \mathbf{F} \cdot \frac{\partial \mathbf{r}}{\partial \theta} = \mathbf{F} \cdot \frac{\partial(h\mathbf{k} + L\mathbf{R})}{\partial \theta} = \mathbf{F} \cdot L(-\sin\theta\sin\phi, \cos\theta\sin\phi, 0)$$

and

$$F_\psi = \mathbf{F} \cdot \frac{\partial \mathbf{r}}{\partial \psi} = \mathbf{F} \cdot \frac{\partial(h\mathbf{k} + L\mathbf{R})}{\partial \psi} = \mathbf{F} \cdot (0, 0, 0) = 0$$

The fact that $F_\psi = 0$ is to be expected. The center of mass is invariant with respect to the rotation of the disk, so the applied force cannot affect it.

The equations of motion are therefore,

$$(mL^2 + \mu_2)\ddot{\theta}\sin^2\phi + \mu_3(\ddot{\psi} + \ddot{\theta}\cos\phi)\cos\phi = F_\theta$$

and

$$\mu_3(\ddot{\psi} + \ddot{\theta}\cos\phi) = 0$$

(Example 3.13
continued)

The equations may be solved explicitly for the second derivative terms:

$$\ddot{\theta} = \frac{F_\theta}{(mL^2 + \mu_2) \sin^2 \phi}, \quad \ddot{\psi} = \frac{-F_\theta \cos \phi}{(mL^2 + \mu_2) \sin^2 \phi}$$

The principal moment μ_3 does not enter into the solution. This does not mean the angular speeds of the pipe and disk are unaffected by physical characteristics of the disk. The solution still has μ_2 in it. If you increase μ_2 (i.e., make the disk heavier, increase its radius, or make it thicker), the right-hand sides of the differential equations become smaller because of the presence of μ_2 in the denominators. This in turn causes the angular accelerations to become smaller, leading to reduced angular speeds. ■

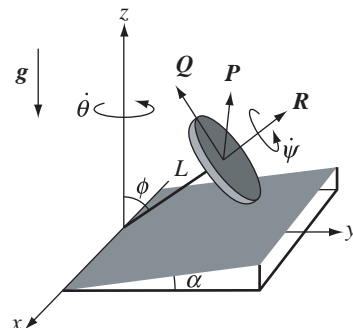
EXERCISE
3.20In Example 3.13, show that $\mu_2 = m(a^2/2 + b^2/12)$ and $\mu_3 = ma^2/2$. ■**EXERCISE**
3.21In Example 3.13, if the only applied force is gravitational, say $\mathbf{F} = -mg\mathbf{k}$, show that the angular speeds of the pipe and disk are constant over time. ■**EXERCISE**
3.22Consider a solid disk that is attached by a massless rod to the origin. The disk rolls on the plane $z = y \tan \alpha$ for a small positive angle α . Gravitational forces are present and the plane is assumed to be rough so that frictional forces come into play. Figure 3.17 illustrates.

Figure 3.17 A solid disk that rolls on a rough, inclined plane.

The disk has radius $a > 0$ and thickness $b > 0$. One end of the rod is attached to the origin, the other end to the center of the face closest to the origin. The distance from the rod to the center of mass is L units. The physical system has one degree of freedom, the angle θ . Construct the equation of motion for θ . (See Section 3.2.7 for a model of motion of a solid box over a plane with frictional forces.) ■

3.2.6 EXAMPLES WITH CONSERVATIVE FORCES

Recall that a Lagrangian equation of motion for the constraint variable q , is of the form

$$\frac{d}{dt} \left(\frac{\partial T}{\partial \dot{q}} \right) - \frac{\partial T}{\partial q} = F_q$$

where $F_q = \mathbf{F} \cdot d\mathbf{x}/dq$ is a generalized force. If \mathbf{F} is a conservative force, then $\mathbf{F} = -\nabla V$ for some potential energy function V , in which case,

$$F_q = \mathbf{F} \cdot \frac{d\mathbf{x}}{dq} = -\nabla V \cdot \frac{d\mathbf{x}}{dq} = -\frac{\partial V}{\partial q}$$

The Lagrangian equation of motion for a conservative force is

$$\frac{d}{dt} \left(\frac{\partial T}{\partial \dot{q}} \right) - \frac{\partial T}{\partial q} = -\frac{\partial V}{\partial q}$$

The potential function in mechanical problems is almost always independent of time derivatives \dot{q} , so if we define the scalar function $L = T - V$, called a *Lagrangian function*, the equation of motion for a conservative force is

$$\frac{d}{dt} \left(\frac{\partial L}{\partial \dot{q}} \right) - \frac{\partial L}{\partial q} = 0 \quad (3.36)$$

EXAMPLE
3.14

A simple model of a diving board is presented here. [Figure 3.18](#) illustrates.

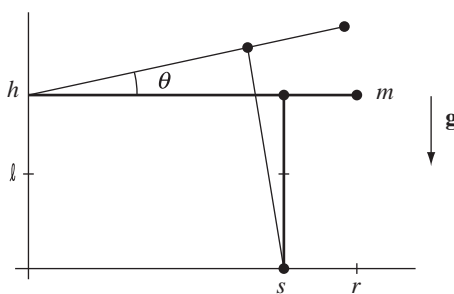


Figure 3.18

A simple diving board.

The board has length r and is massless, but has a mass m on the end that represents someone standing on the end of the board (and can be affected by gravity). The flexibility of the board is modeled by a spring attached between the board and the ground.

(Example 3.14
continued)

This spring affects the angular motion of the board about the joint at $(0, h)$. The spring is located at position s and has spring constant $c > 0$. The spring is unstretched with length ℓ , not necessarily the height h of the joint above the ground. The location of the mass is measured by the angle θ relative to the horizontal. The position of the mass is $\mathbf{x} = (0, h) + r(\cos \theta, \sin \theta)$. The velocity is $\dot{\mathbf{x}} = r(-\sin \theta, \cos \theta)\dot{\theta}$. The kinetic energy is $T = mr^2\dot{\theta}^2/2$.

The potential energy due to a change in height from the board's horizontal position is the magnitude of the force multiplied by the change in height, as seen in [equation \(2.108\)](#). For an angle θ , the change in height is $r \sin \theta$. The contribution to potential energy is $V_{\text{gravity}} = mgr \sin \theta$. The potential energy due to the spring stretching was derived in [equation \(2.109\)](#). It only depends on the endpoints (s, h) and $(s \cos \theta, h + s \sin \theta)$. The stretched length at the first endpoint is $h - \ell$. The stretched length at the second endpoint is the value

$$\sqrt{s^2(\cos \theta - 1)^2 + (h + s \sin \theta)^2} - \ell$$

The contribution is

$$V_{\text{spring}} = \frac{c}{2} \left(\left(\sqrt{s^2(\cos \theta - 1)^2 + (h + s \sin \theta)^2} - \ell \right)^2 - (h - \ell)^2 \right)$$

The total potential energy is $V = V_{\text{gravity}} + V_{\text{spring}}$. The constant $(h - \ell)^2$ may be ignored because the derivative of V is all that matters in the Lagrangian equations of motion. Moreover, if you want to make an approximation by allowing θ to be only a small angle, then $\cos \theta \doteq 1$ and $\sin \theta \doteq \theta$, so $V \doteq (c/2)(h + s\theta - \ell)^2 + mgr\theta$ is a reasonable approximation.

Using the approximation for potential energy, the Lagrangian is

$$L = T - V = \frac{1}{2}mr^2\dot{\theta}^2 - \frac{1}{2}c(h + s\theta - \ell)^2 - mgr\theta$$

The Lagrangian equation of motion is

$$\begin{aligned} 0 &= \frac{d}{dt} \left(\frac{\partial L}{\partial \dot{\theta}} \right) - \frac{\partial L}{\partial \theta} = \frac{d}{dt} (mr^2\dot{\theta}) - (-cs(h + s\theta - \ell) - mgr) \\ &= mr^2\ddot{\theta} + cs(h + s\theta - \ell) + mgr \end{aligned}$$

If the spring is such that the diving board is in static equilibrium at $\theta = 0$, that is $cs(h - \ell) + mgr = 0$, then the equation of motion is $\ddot{\theta} + ((cs^2)/(mr^2))\theta = 0$, and the board exhibits simple harmonic motion. ■

EXERCISE
3.23

Construct the equations of motion for the [Example 3.14](#), but without the approximation involving a small angle θ . ■

EXAMPLE
3.15

Consider a double pendulum that consists of two rigid and massless rods. The first rod is attached to a frictionless joint on the ceiling and has length r_1 . The other end of the rod has a mass m_1 attached. The second rod is attached to the other end of the first rod, this joint also frictionless, and has length r_2 . A mass m_2 is attached to the other end of the second rod. The only applied force is gravitational. See [Figure 3.11](#) for an illustration.

Mass m_i is located at (x_i, y_i) for $i = 1, 2$. The kinetic energy is $T = m_1(\dot{x}_1^2 + \dot{y}_1^2)/2 + m_2(\dot{x}_2^2 + \dot{y}_2^2)/2$. However, we have only two degrees of freedom, which may as well be chosen to be the angles θ_1 and θ_2 . Trigonometric identities lead to $x_1 = r_1 \sin \theta_1$, $h - y_1 = r_1 \cos \theta_1$, $x_2 - x_1 = r_2 \sin \theta_2$, and $y_1 - y_2 = r_2 \cos \theta_2$. Solving for the components:

$$x_1 = r_1 \sin \theta_1$$

$$y_1 = h - r_1 \cos \theta_1$$

$$x_2 = r_1 \sin \theta_1 + r_2 \sin \theta_2$$

$$y_2 = h - r_1 \cos \theta_1 - r_2 \cos \theta_2$$

and the derivatives are

$$\dot{x}_1 = r_1 \dot{\theta}_1 \cos \theta_1$$

$$\dot{y}_1 = r_1 \dot{\theta}_1 \sin \theta_1$$

$$\dot{x}_2 = r_1 \dot{\theta}_1 \cos \theta_1 + r_2 \dot{\theta}_2 \cos \theta_2$$

$$\dot{y}_2 = r_1 \dot{\theta}_1 \sin \theta_1 + r_2 \dot{\theta}_2 \sin \theta_2$$

The kinetic energy is therefore,

$$T = \frac{m_1}{2} r_1^2 \dot{\theta}_1^2 + \frac{m_2}{2} (r_1^2 \dot{\theta}_1^2 + r_2^2 \dot{\theta}_2^2 + 2r_1 r_2 \dot{\theta}_1 \dot{\theta}_2 \cos(\theta_1 - \theta_2))$$

The contribution to potential energy from mass m_1 is $-m_1 g(h - y_1)$ and the contribution from mass m_2 is $-m_2 g(h - y_2)$, so the total potential energy is

$$V = -m_1 g(h - y_1) - m_2 g(h - y_2) = -(m_1 + m_2)gr_1 \cos \theta_1 - m_2 gr_2 \cos \theta_2$$

The Lagrangian $L = T - V$ is

$$L = \frac{m_1}{2} r_1^2 \dot{\theta}_1^2 + \frac{m_2}{2} (r_1^2 \dot{\theta}_1^2 + r_2^2 \dot{\theta}_2^2 + 2r_1 r_2 \dot{\theta}_1 \dot{\theta}_2 \cos(\theta_1 - \theta_2)) \\ + (m_1 + m_2)gr_1 \cos \theta_1 + m_2 gr_2 \cos \theta_2$$

(Example 3.15
continued)

and its relevant derivatives are

$$\begin{aligned}\frac{\partial L}{\partial \theta_1} &= -m_2 r_1 r_2 \dot{\theta}_1 \dot{\theta}_2 \sin(\theta_1 - \theta_2) - (m_1 + m_2) g r_1 \sin \theta_1 \\ \frac{\partial L}{\partial \theta_2} &= m_2 r_1 r_2 \dot{\theta}_1 \dot{\theta}_2 \sin(\theta_1 - \theta_2) - m_2 g r_2 \sin \theta_2 \\ \frac{\partial L}{\partial \dot{\theta}_1} &= m_1 r_1^2 \dot{\theta}_1 + m_2 (r_1^2 \dot{\theta}_1 + r_1 r_2 \dot{\theta}_2 \cos(\theta_1 - \theta_2)) \\ \frac{\partial L}{\partial \dot{\theta}_2} &= m_2 (r_2^2 \dot{\theta}_2 + r_1 r_2 \dot{\theta}_1 \cos(\theta_1 - \theta_2)) \\ \frac{d}{dt} \left(\frac{\partial L}{\partial \dot{\theta}_1} \right) &= m_1 r_1^2 \ddot{\theta}_1 + m_2 (r_1^2 \ddot{\theta}_1 + r_1 r_2 (-\dot{\theta}_2 (\dot{\theta}_1 - \dot{\theta}_2) \sin(\theta_1 - \theta_2) + \ddot{\theta}_2 \cos(\theta_1 - \theta_2))) \\ \frac{d}{dt} \left(\frac{\partial L}{\partial \dot{\theta}_2} \right) &= m_2 (r_2^2 \ddot{\theta}_2 + r_1 r_2 (-\dot{\theta}_1 (\dot{\theta}_1 - \dot{\theta}_2) \sin(\theta_1 - \theta_2) + \ddot{\theta}_1 \cos(\theta_1 - \theta_2)))\end{aligned}$$

The two Lagrangian equations of motion are

$$\begin{aligned}0 &= \frac{d}{dt} \left(\frac{\partial L}{\partial \dot{\theta}_1} \right) - \frac{\partial L}{\partial \theta_1} \\ &= (m_1 + m_2) r_1 (r_1 \ddot{\theta}_1 + g \sin \theta_1) + m_2 r_1 r_2 (\ddot{\theta}_2 \cos(\theta_1 - \theta_2) + \dot{\theta}_2^2 \sin(\theta_1 - \theta_2)) \\ 0 &= \frac{d}{dt} \left(\frac{\partial L}{\partial \dot{\theta}_2} \right) - \frac{\partial L}{\partial \theta_2} \\ &= m_2 r_2 (r_2 \ddot{\theta}_2 + g \sin \theta_2) + m_2 r_1 r_2 (\ddot{\theta}_1 \cos(\theta_1 - \theta_2) - \dot{\theta}_1^2 \sin(\theta_1 - \theta_2))\end{aligned}$$

The two equations may be solved simultaneously to produce explicit formulas for the second derivatives $\ddot{\theta}_1$ and $\ddot{\theta}_2$. ■

EXERCISE 3.24

In the double pendulum problem, replace the rigid rods by massless springs whose spring constants are c_1 and c_2 and whose unstretched lengths are ℓ_1 and ℓ_2 . Calculate the kinetic energy, the potential energy, the Lagrangian, and the equations of motion. ■

EXERCISE 3.25

Compute the equations of motion for the triple pendulum problem where all the rods are rigid. This problem adds one more massless rod to the system: one end is attached to mass m_2 (the joint is frictionless) and the free end has a mass m_3 attached to it. The rod length is r_3 . ■

EXAMPLE 3.16

Two-body problem. This is the same problem discussed in Example 3.1 that was derived with Newtonian dynamics and that led to Kepler's Laws. We now derive the equations of motion using Lagrangian dynamics. Consider two particles with masses m_i and positions (x_i, y_i, z_i) for $i = 1, 2$. The center of mass is $(x, y, z) = (m_1(x_1, y_1, z_1) +$

$m_2(x_2, y_2, z_2))/(m_1 + m_2)$. The particles may be represented in the coordinate system whose origin is the center of mass and whose axes are parallel to the world coordinate axes. Specifically,

$$(x_i, y_i, z_i) = (x, y, z) + r_i \mathbf{R}(\theta, \phi)$$

where $\mathbf{R}(\theta, \phi) = (\cos \theta \sin \phi, \sin \theta \sin \phi, \cos \phi)$ is in the direction from particle 1 to particle 2. Using the fact that the total moment about the center of mass is zero, namely $\sum_{i=1}^2 m_i(x_i - x, y_i - y, z_i - z) = (0, 0, 0)$, the radial values must satisfy $m_1 r_1 + m_2 r_2 = 0$. Define r to be the distance between the particles, so $r = r_2 - r_1$. Consequently, $r_1 = -m_2 r / (m_1 + m_2)$ and $r_2 = m_1 r / (m_1 + m_2)$. In this notation the gravitational force exerted by particle 1 on particle 2 is

$$\mathbf{F} = -\frac{Gm_1 m_2}{r^2} \mathbf{R}(\theta, \phi)$$

where G is the gravitational constant. This force is conservative with potential energy $V = -Gm_1 m_2 / r$. The kinetic energy is

$$\begin{aligned} T &= \frac{1}{2} \sum_{i=1}^2 m_i (\dot{x}_i^2 + \dot{y}_i^2 + \dot{z}_i^2) \\ &= \frac{m_1 + m_2}{2} (\dot{x}^2 + \dot{y}^2 + \dot{z}^2) + \frac{m_1 m_2}{2(m_1 + m_2)} (\dot{r}^2 + r^2 (\dot{\phi}^2 + \dot{\theta}^2 \sin^2 \phi)) \end{aligned}$$

For simplicity we will assume that the center of mass travels through space with constant linear velocity. In this case the Lagrangian function is

$$L = T - V = \frac{c_1}{2} (\dot{r}^2 + r^2 (\dot{\phi}^2 + \dot{\theta}^2 \sin^2 \phi)) + \frac{c_2}{r}$$

where $c_1 = m_1 m_2 / (m_1 + m_2)$ and $c_2 = Gm_1 m_2$.

The relevant derivatives of L are

$$\begin{array}{ll} \frac{\partial L}{\partial r} = c_1 r (\dot{\phi}^2 + \dot{\theta}^2 \sin^2 \phi) - \frac{c_2}{r^2} & \frac{\partial L}{\partial \dot{r}} = c_1 \dot{r} \\ \frac{\partial L}{\partial \theta} = 0 & \frac{\partial L}{\partial \dot{\theta}} = c_1 r^2 \dot{\theta} \sin^2 \phi \\ \frac{\partial L}{\partial \phi} = c_1 r^2 \dot{\theta}^2 \sin \phi \cos \phi & \frac{\partial L}{\partial \dot{\phi}} = c_1 r^2 \dot{\phi} \end{array}$$

The Lagrangian equations of motion are

$$\begin{aligned} 0 &= \frac{d}{dt} \left(\frac{\partial L}{\partial \dot{r}} \right) - \frac{\partial L}{\partial r} = c_1 \ddot{r} - c_1 r (\dot{\phi}^2 + \dot{\theta}^2 \sin^2 \phi) + \frac{c_2}{r} \\ 0 &= \frac{d}{dt} \left(\frac{\partial L}{\partial \dot{\theta}} \right) - \frac{\partial L}{\partial \theta} = c_1 \frac{d}{dt} (r^2 \dot{\theta} \sin^2 \phi) \end{aligned}$$

(Example 3.16
continued)

$$0 = \frac{d}{dt} \left(\frac{\partial L}{\partial \dot{\phi}} \right) - \frac{\partial L}{\partial \phi} = c_1 \left(\frac{d}{dt} (r^2 \dot{\phi}) - r^2 \dot{\theta}^2 \sin \phi \cos \phi \right)$$

The second equation implies $r^2 \dot{\theta} \sin^2 \phi = \alpha$ is a constant. If we choose $\dot{\theta}(0) = 0$, then $\alpha = 0$, which in turn implies $\dot{\theta}(t) = 0$ for all time. Therefore, the motion of the two particles must be in the plane $\theta = \theta_0$. If the value $\dot{\theta}(0) \neq 0$, it is still the case that the motion is in a plane, but the analysis is a bit more complicated and left as an exercise. The third equation of motion reduces to $d(r^2 \dot{\phi})/dt = 0$, so $r^2 \dot{\phi} = \beta$, a constant for all time. Replacing this in the first equation of motion, dividing by c_1 , and defining $\gamma = c_2/c_1$, we have

$$\ddot{r} = \frac{\beta^2}{r^3} - \frac{\gamma}{r^2}$$

This equation may be solved numerically for $r(t)$ when initial conditions $r(0)$ and $\dot{r}(0)$ are selected. The angle is obtained by one more integration, $\phi(t) = \phi(0) + \int_0^t \beta/r^2(\tau) d\tau$, with $\phi(0)$ selected as an initial condition.

How does this relate back to Example 3.1 on Kepler's laws? At first glance you might have thought we found explicit solutions for $r(t)$ and $\phi(t)$. This is not so. What we found was a relationship between the two,

$$r(t) = \frac{e\rho}{1 + e \cos \phi(t)}$$

an equation of an ellipse. To obtain a numerical solution for r and ϕ as functions of time, you would need to solve $\ddot{\mathbf{r}} = -(Gm_1/r^2)\mathbf{r}$, where $\mathbf{r} = r\mathbf{R}$. In the derivation in that example we also showed that $\mathbf{r} \times \dot{\mathbf{r}} = \mathbf{c}_0$ for some constant vector \mathbf{c}_0 . This constant is determined from the initial position $\mathbf{r}(0)$ and initial velocity $\dot{\mathbf{r}}(0)$, namely $\mathbf{c}_0 = \mathbf{r}(0) \times \dot{\mathbf{r}}(0)$. This information can be used to reduce the differential equation to one involving motion in a plane whose normal is \mathbf{c}_0 .

As it turns out, the ellipse equation does satisfy the second-order equation for $r(t)$ that we just derived using Lagrangian dynamics. Taking a derivative leads to

$$\dot{r} = \frac{e^2 \rho \dot{\phi} \sin \phi}{(1 + e \cos \phi)^2} = \frac{r^2 \dot{\phi} \sin \phi}{\rho} = \frac{\beta \sin \phi}{\rho}$$

Taking another derivative:

$$\ddot{r} = \frac{\beta}{\rho} \cos \phi = \frac{\beta}{\rho} \frac{\beta}{r^2} \frac{1}{e} \left(\frac{e\rho}{r} - 1 \right) = \frac{\beta^2}{r^3} - \frac{\beta^2}{e\rho} \frac{1}{r^2}$$

For this to equate to our Lagrangian equation, we need $\beta^2 = e\rho\gamma$. ■

EXERCISE
3.26

In Example 3.16, if $\dot{\theta}(0) \neq 0$, show that the motion of the particles is still in a plane. What is the equation of that plane? Hint: The plane will depend on the choices for $\dot{\theta}(0)$ and $\dot{\phi}(0)$. ■

EXERCISE
3.27

Write a computer program to solve the Lagrangian equations of motion in exercise 3.16. ■

3.2.7 EXAMPLES WITH DISSIPATIVE FORCES

This section contains some examples for setting up the equations of motion when at least one of the applied forces is dissipative. The first example is a slight modification of the simple pendulum. Other examples are slightly more complicated.

EXAMPLE
3.17

SOURCE CODE
SimplePendulumFriction

Consider the simple pendulum problem that is illustrated in Figure 3.4. The joint at \mathcal{P} is now assumed to apply a frictional force \mathbf{F}_{fric} to impede the motion of the rod. The gravitational force is $\mathbf{F}_{\text{grav}} = -mg\mathbf{j}$. The position of the mass is $\mathbf{x} = (r \sin \theta, h - r \cos \theta)$, where the joint is a height h above the ground. The velocity is $\mathbf{v} = \dot{\mathbf{r}}(\cos \theta, \sin \theta)$. The kinetic energy is $T = m|\mathbf{v}|^2/2 = mr^2\dot{\theta}^2/2$. The generalized force is $F_\theta = (\mathbf{F}_{\text{grav}} + \mathbf{F}_{\text{fric}}) \cdot d\mathbf{x}/d\theta$. The Lagrangian equation of motion is

$$mr^2\ddot{\theta} = \frac{d}{dt}\left(\frac{\partial T}{\partial \dot{\theta}}\right) - \frac{\partial T}{\partial \theta} = F_\theta = -mgr \sin \theta + \mathbf{F}_{\text{fric}} \cdot \mathbf{r}(\cos \theta, \sin \theta)$$

The frictional force is assumed not to contain a static friction component.

If the frictional force is kinetic friction, the force is modeled by $\mathbf{F}_{\text{fric}} = -c\mathbf{v}/|\mathbf{v}|$ for some constant $c > 0$. The force is in the opposite direction of velocity. The equation of motion reduces to

$$0 = \ddot{\theta} + \frac{c}{mr} \frac{\dot{\theta}}{|\dot{\theta}|} + \frac{g}{r} \sin \theta = \ddot{\theta} + a\sigma(\dot{\theta}) + b \sin \theta$$

where $a = c/(mr)$, $b = g/r$, and $\sigma(\dot{\theta})$ acts as a switch. If $\dot{\theta} > 0$, then $\sigma(\dot{\theta}) = 1$. If $\dot{\theta} < 0$, then $\sigma(\dot{\theta}) = -1$. To avoid the singularity at $\dot{\theta} = 0$, we define $\sigma(0) = 0$.

If the dissipative force is viscous, for example when the joint has a layer of oil to prevent overheating, the force is modeled by $\mathbf{F}_{\text{fric}} = -c\mathbf{v}$ for some constant $c > 0$. The equation of motion reduces to

$$\ddot{\theta} + \frac{c}{m} \dot{\theta} + \frac{g}{r} \sin \theta = 0$$

If the pendulum has only small oscillations about the vertical so that θ is nearly zero and $\sin \theta \doteq \theta$, an approximation to the equation of motion is

$$\ddot{\theta} + \frac{c}{m} \dot{\theta} + \frac{g}{r} \theta = 0$$

This is a second-order linear differential equation whose solution may be written in closed form (see Section (11.3)). If we set $a = c/m$ and $b = g/r$, the characteristic equation is $\lambda^2 + a\lambda + b = 0$. If $a^2 > 4b$, this equation has two negative real-valued

(Example 3.17
continued)

roots, $\lambda_1 = (-a - \sqrt{a^2 - 4b})/2$ and $\lambda_2 = (-a + \sqrt{a^2 - 4b})/2$. The solution to the differential equation with initial conditions $\theta(0) = \theta_0 \neq 0$ and $\dot{\theta}(0) = \dot{\theta}_0$ is

$$\theta(t) = \frac{(\lambda_2 \theta_0 - \dot{\theta}_0) \exp(\lambda_1 t) - (\lambda_1 \theta_0 - \dot{\theta}_0) \exp(\lambda_2 t)}{\lambda_2 - \lambda_1}$$

No sinusoidal terms occur, so the pendulum cannot continually oscillate about its rest position. In the limit as $t \rightarrow \infty$ (physically after a large amount of time), the right-hand side of the equation becomes zero, that is, $\theta(\infty) = \lim_{t \rightarrow \infty} \theta(t) = 0$. The condition $a^2 > 4b$ is equivalent to $c > 2m\sqrt{g/r}$. The coefficient of friction of the joint is sufficiently large to prevent oscillation about the rest position, and after a large amount of time the damping causes the pendulum to stop. (**Question:** If $\theta_0 > 0$ and $\dot{\theta}_0 = 0$, does the pendulum ever pass the origin? That is, does there exist a time $T > 0$ for which $\theta(T) < 0$? How about when $\dot{\theta}_0 < 0$?)

If $a^2 = 4b$, the characteristic equation has a repeated real-valued root, $\lambda = -a/2$. The solution to the differential equation is

$$\theta(t) = ((\dot{\theta}_0 - \lambda \theta_0)t + \theta_0) \exp(\lambda t)$$

Just as in the previous case, $\theta(\infty) = \lim_{t \rightarrow \infty} \theta(t) = 0$ and the pendulum eventually stops. The condition $a^2 = 4b$ is equivalent to $c = 2m\sqrt{g/r}$ and the coefficient is still large enough to prevent oscillation about the rest position. (**Question:** If $\theta_0 > 0$ and $\dot{\theta}_0 = 0$, does the pendulum ever pass the origin? That is, does there exist a time $T > 0$ for which $\theta(T) < 0$? How about when $\dot{\theta}_0 < 0$?)

The last case is $a^2 < 4b$. The characteristic equation has two nonreal roots, $\lambda_1 = \rho - i\omega$ and $\lambda_2 = \rho + i\omega$, where $\rho = -a/2$ and $\omega = \sqrt{4b - a^2}/2$. The solution to the differential equation is

$$\theta(t) = \exp(\rho t) \left(\theta_0 \cos(\omega t) + \frac{\dot{\theta}_0 - \rho \theta_0}{\omega} \sin(\omega t) \right)$$

In this case the pendulum does oscillate about the rest position, but the amplitude of the oscillation decays exponentially over time. Once again $\theta(\infty) = \lim_{t \rightarrow \infty} \theta(t) = 0$, so the pendulum eventually stops. The condition $a^2 < 4b$ is equivalent to $c < 2m\sqrt{g/r}$. Physically this means the coefficient of friction is sufficiently small and cannot prevent the oscillations, but the slightest amount of friction is enough to stop the pendulum after a long time. ■

EXERCISE 3.28

Compute the equations of motion for the double pendulum of Example 3.15 assuming that both joints have kinetic friction. Repeat the exercise when both joints have a dissipative viscous force. ■

The next few examples deal with kinetic friction on flat surfaces. The examples increase in complexity. The first involves a single particle, the second involves multiple particles, the third involves a curve mass, and the fourth involves an areal mass. The last example is typical of what you can expect in a 3D simulation when one object slides over another.



SOURCE CODE
RoughPlaneParticle1

One Particle on a Rough Plane

A single particle is constrained to move on an inclined plane and is subject to gravitational force. The plane forms an acute angle ϕ with the horizontal, so the height relative to the horizontal is $z = y \tan \phi$. The plane is two dimensional. We choose coordinates x and w with w shown in Figure 3.19. Basic trigonometric definitions show us that $y = w \cos \phi$ and $z = w \sin \phi$. A single particle with mass m , initial position $\mathbf{r}_0 = (x_0, y_0, z_0)$, and initial velocity $\mathbf{v}_0 = (\dot{x}_0, \dot{y}_0, \dot{z}_0)$ is shown.

A portion of the path $\mathbf{r}(t)$ traveled by the particle is also shown. The velocity, of course, is $\mathbf{v}(t) = \dot{\mathbf{r}}(t)$.

In terms of x and w , the kinetic energy is

$$T(x, w) = \frac{m}{2} (\dot{x}^2 + \dot{y}^2 + \dot{z}^2) = \frac{m}{2} (\dot{x}^2 + \dot{w}^2)$$

The relevant derivatives are $\partial T / \partial x = 0$, $\partial T / \partial w = 0$, $\partial T / \partial \dot{x} = m\dot{x}$, $\partial T / \partial \dot{w} = m\dot{w}$, $d(\partial T / \partial \dot{x})/dt = m\ddot{x}$, and $d(\partial T / \partial \dot{w})/dt = m\ddot{w}$.

The gravitational force is $\mathbf{F}_{\text{grav}} = -mg\mathbf{k}$. The frictional force is $\mathbf{F}_{\text{fric}} = -c\mathbf{v}/|\mathbf{v}|$, where $c = \mu mg \cos \phi > 0$. The constant μ depends on the material properties of the mass and inclined plane. The generalized forces are

$$\begin{aligned} F_x &= (\mathbf{F}_{\text{grav}} + \mathbf{F}_{\text{fric}}) \cdot \frac{d\mathbf{r}}{dx} \\ &= \left(-mg\mathbf{k} - c \frac{\mathbf{v}}{|\mathbf{v}|} \right) \cdot (1, 0, 0) \\ &= -\frac{c\dot{x}}{\sqrt{\dot{x}^2 + \dot{w}^2}} \end{aligned}$$

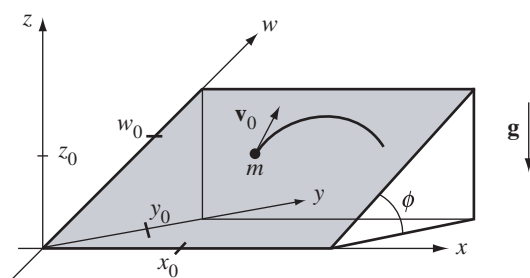


Figure 3.19 An inclined plane that forms an angle ϕ with the horizontal. The particle has mass m . It is located at $\mathbf{r}_0 = (x_0, y_0, z_0)$; hash marks are shown on the axes corresponding to x_0 , y_0 , z_0 , and w_0 , where $y_0 = w_0 \cos \phi$ and $z_0 = w_0 \sin \phi$.

and

$$\begin{aligned} F_w &= (\mathbf{F}_{\text{grav}} + \mathbf{F}_{\text{fric}}) \cdot \frac{d\mathbf{r}}{dw} \\ &= \left(-mg\mathbf{k} - c \frac{\mathbf{v}}{|\mathbf{v}|} \right) \cdot (0, \cos \phi, \sin \phi) \\ &= -mg \sin \phi - \frac{c \dot{w}}{\sqrt{\dot{x}^2 + \dot{w}^2}} \end{aligned}$$

The Lagrangian equations of motion are

$$m\ddot{x} + \frac{c\dot{x}}{\sqrt{\dot{x}^2 + \dot{w}^2}} = 0, \quad m\ddot{w} + \frac{c\dot{w}}{\sqrt{\dot{x}^2 + \dot{w}^2}} + mg \sin \phi = 0$$

Just as in the pendulum example, the frictional terms are undefined at zero velocity, when $\dot{x}^2 + \dot{w}^2 = 0$. When this happens, define the ratios to be zero (no friction at that instant). In the event that the inclined surface is exactly on the horizontal, the angle is $\phi = 0$ and $w = y$. The generalized force due to gravity has no effect on the particle's motion since $mg \sin \phi = 0$.

Two Particles on a Rough Plane

Consider two particles with positions $\mathbf{r}_i = (x_i, y_i)$ and masses m_i for $i = 1, 2$. The xy -plane is a rough surface and so provides a frictional force on the particles. The particles are interconnected with a massless rod that does not touch the plane. Thus, the particle system is a rigid body that has three degrees of freedom: the location (x, y) of the center of mass and an orientation angle θ formed by the rod with the x -axis. Figure 3.20 illustrates.

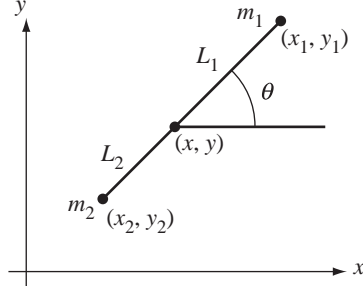


Figure 3.20 Two particles, connected by a massless rod, that slide along a rough plane.

The lengths L_i are measured from the center of mass to the particles. The particle positions are $\mathbf{r}_1 = (x + L_1 \cos \theta, y + L_1 \sin \theta)$ and $\mathbf{r}_2 = (x - L_2 \cos \theta, y - L_2 \sin \theta)$. The velocities are $\mathbf{v}_1 = (\dot{x} - L_1 \dot{\theta} \sin \theta, \dot{y} + L_1 \dot{\theta} \cos \theta)$ and $\mathbf{v}_2 = (\dot{x} + L_2 \dot{\theta} \sin \theta, \dot{y} - L_2 \dot{\theta} \cos \theta)$. The frictional forces are $\mathbf{F}_i = -c_i \mathbf{v}_i / |\mathbf{v}_i|$, where $c_i = \mu m_i g$ with μ depending on the material properties, and g is the gravitational constant.

The kinetic energy is

$$\begin{aligned} T(x, y, \theta) &= \sum_{i=1}^2 \frac{m_i}{2} (\dot{x}_i^2 + \dot{y}_i^2) \\ &= \frac{m_1}{2} ((\dot{x} - L_1 \dot{\theta} \sin \theta)^2 + (\dot{y} + L_1 \dot{\theta} \cos \theta)^2) \\ &\quad + \frac{m_2}{2} ((\dot{x} + L_2 \dot{\theta} \sin \theta)^2 + (\dot{y} - L_2 \dot{\theta} \cos \theta)^2) \\ &= \frac{m_1 + m_2}{2} (\dot{x}^2 + \dot{y}^2) + \frac{m_1 L_1^2 + m_2 L_2^2}{2} \dot{\theta}^2 \\ &= \frac{\mu_0}{2} (\dot{x}^2 + \dot{y}^2) + \frac{\mu_2}{2} \dot{\theta}^2 \end{aligned} \quad (3.37)$$

where the last equality defines the constants μ_0 and μ_2 . Formally, a term with $(m_1 L_1 - m_2 L_2)$ appears, but just as in [Example 3.16](#) on the two-body problem, $m_1 L_1 - m_2 L_2 = 0$. If $L = L_1 - L_2$, then $L_1 = m_2 L / (m_1 + m_2)$ and $L_2 = m_1 L / (m_1 + m_2)$. The relevant derivatives of kinetic energy are

$$\begin{aligned} \frac{\partial T}{\partial x} &= 0, & \frac{\partial T}{\partial y} &= 0, & \frac{\partial T}{\partial \theta} &= 0, \\ \frac{\partial T}{\partial \dot{x}} &= \mu_0 \dot{x}, & \frac{\partial T}{\partial \dot{y}} &= \mu_0 \dot{y}, & \frac{\partial T}{\partial \dot{\theta}} &= \mu_2 \dot{\theta}, \\ \frac{d}{dt} \left(\frac{\partial T}{\partial \dot{x}} \right) &= \mu_0 \ddot{x}, & \frac{d}{dt} \left(\frac{\partial T}{\partial \dot{y}} \right) &= \mu_0 \ddot{y}, & \frac{d}{dt} \left(\frac{\partial T}{\partial \dot{\theta}} \right) &= \mu_2 \ddot{\theta} \end{aligned}$$

The generalized force corresponding to x is

$$\begin{aligned} F_x &= \sum_{i=1}^2 \mathbf{F}_i \cdot \frac{\partial \mathbf{r}_i}{\partial x} \\ &= \sum_{i=1}^2 -c_i \frac{\mathbf{v}_i}{|\mathbf{v}_i|} \cdot (1, 0) \end{aligned}$$

$$= -\frac{c_1(\dot{x} - L_1\dot{\theta}\sin\theta)}{\sqrt{(\dot{x} - L_1\dot{\theta}\sin\theta)^2 + (\dot{y} + L_1\dot{\theta}\cos\theta)^2}} - \frac{c_2(\dot{x} + L_2\dot{\theta}\sin\theta)}{\sqrt{(\dot{x} + L_2\dot{\theta}\sin\theta)^2 + (\dot{y} - L_2\dot{\theta}\cos\theta)^2}}$$

The generalized force corresponding to y is

$$\begin{aligned} F_y &= \sum_{i=1}^2 \mathbf{F}_i \cdot \frac{\partial \mathbf{r}_i}{\partial y} \\ &= \sum_{i=1}^2 -c_i \frac{\mathbf{v}_i}{|\mathbf{v}_i|} \cdot (0, 1) \\ &= -\frac{c_1(\dot{y} + L_1\dot{\theta}\cos\theta)}{\sqrt{(\dot{x} - L_1\dot{\theta}\sin\theta)^2 + (\dot{y} + L_1\dot{\theta}\cos\theta)^2}} - \frac{c_2(\dot{y} - L_2\dot{\theta}\cos\theta)}{\sqrt{(\dot{x} + L_2\dot{\theta}\sin\theta)^2 + (\dot{y} - L_2\dot{\theta}\cos\theta)^2}} \end{aligned}$$

The generalized force corresponding to θ is

$$\begin{aligned} F_\theta &= \sum_{i=1}^2 \mathbf{F}_i \cdot \frac{\partial \mathbf{r}_i}{\partial \theta} \\ &= -\frac{c_1 \mathbf{v}_1}{|\mathbf{v}_1|} \cdot L_1(-\sin\theta, \cos\theta) - \frac{c_2 \mathbf{v}_2}{|\mathbf{v}_2|} \cdot L_2(\sin\theta, -\cos\theta) \\ &= -\frac{c_1 L_1(-\dot{x}\sin\theta + \dot{y}\cos\theta + L_1\dot{\theta})}{\sqrt{(\dot{x} - L_1\dot{\theta}\sin\theta)^2 + (\dot{y} + L_1\dot{\theta}\cos\theta)^2}} - \frac{c_2 L_2(\dot{x}\sin\theta - \dot{y}\cos\theta + L_2\dot{\theta})}{\sqrt{(\dot{x} + L_2\dot{\theta}\sin\theta)^2 + (\dot{y} - L_2\dot{\theta}\cos\theta)^2}} \end{aligned}$$

The Lagrangian equations of motion are

$$\mu_0 \ddot{x} = F_x, \quad \mu_0 \ddot{y} = F_y, \quad \mu_2 \ddot{\theta} = F_\theta \quad (3.38)$$

Multiple Particles on a Rough Plane

The example for two particles on a rough plane can be extended to more particles, leading to only a slightly more complicated set of equations. Consider $p > 1$ particles with positions $\mathbf{r}_i = (x_i, y_i)$ and masses m_i for $1 \leq i \leq p$. The particle system is a rigid body that has three degrees of freedom: the location (x, y) of the center of mass and an orientation angle θ . At least one point is not located at the center of mass. With a renumbering of the particles if necessary, let that point be (x_1, y_1) . We choose θ to be the angle between $(x_1 - x, y_1 - y)$ and the x -axis direction $(1, 0)$. Thus, $x_1 = x + L_1 \cos\theta$ and $y_1 = L_1 \sin\theta$, where L_1 is the length of $(x_1 - x, y_1 - y)$. The differences between the points and the center of mass form fixed angles with $(x_1 - x, y_1 - y)$:

$$x_i = x + L_i \cos(\theta + \phi_i), \quad y_i = y + L_i \sin(\theta + \phi_i), \quad 1 \leq i \leq p$$

where L_i is the length of $(x_i - x, y_i - y)$ and ϕ_i is the angle between $(x_i - x, y_i - y)$ and $(x_1 - x, y_1 - y)$. By definition of θ , it is the case that $\phi_1 = 0$. The frictional forces are $\mathbf{F}_i = -c_i \mathbf{v}_i / |\mathbf{v}_i|$, where $\mathbf{v}_i = \dot{\mathbf{r}}_i$, $c_i = \mu m_i g$ with μ depending on the material properties, and g is the gravitational constant.

The kinetic energy is

$$\begin{aligned} T &= \sum_{i=1}^p \frac{m_i}{2} (\dot{x}_i^2 + \dot{y}_i^2) \\ &= \sum_{i=1}^p \frac{m_i}{2} \left((\dot{x} - L_i \dot{\theta} \sin(\theta + \phi_i))^2 + (\dot{y} + L_i \dot{\theta} \cos(\theta + \phi_i))^2 \right) \\ &= \left(\sum_{i=1}^p m_i \right) \frac{1}{2} (\dot{x}^2 + \dot{y}^2) + \left(\sum_{i=1}^p m_i L_i^2 \right) \frac{1}{2} \dot{\theta}^2 \\ &= \frac{\mu_0}{2} (\dot{x}^2 + \dot{y}^2) + \frac{\mu_2}{2} \dot{\theta}^2 \end{aligned} \quad (3.39)$$

where the last equation defines the constants μ_0 and μ_2 . Just as in the case of two particles, the choice of center of mass as the origin causes a few formal terms to vanish when computing kinetic energy. Specifically, that choice implies

$$\sum_{i=1}^p m_i L_i \cos(\theta + \phi_i) = 0 \quad \text{and} \quad \sum_{i=1}^p m_i L_i \sin(\theta + \phi_i) = 0$$

This is exactly the same form as [equation \(3.37\)](#). The generalized forces are

$$\begin{aligned} F_x &= \sum_{i=1}^p \mathbf{F}_i \cdot \frac{\partial \mathbf{r}_i}{\partial x} = \sum_{i=1}^p -\frac{c_i \mathbf{v}_i}{|\mathbf{v}_i|} \cdot (1, 0) = -\sum_{i=1}^p \frac{c_i (\dot{x} - L_i \dot{\theta} \sin(\theta + \phi_i))}{|\mathbf{v}_i|} \\ F_y &= \sum_{i=1}^p \mathbf{F}_i \cdot \frac{\partial \mathbf{r}_i}{\partial y} = \sum_{i=1}^p -\frac{c_i \mathbf{v}_i}{|\mathbf{v}_i|} \cdot (0, 1) = -\sum_{i=1}^p \frac{c_i (\dot{y} + L_i \dot{\theta} \cos(\theta + \phi_i))}{|\mathbf{v}_i|} \\ F_\theta &= \sum_{i=1}^p \mathbf{F}_i \cdot \frac{\partial \mathbf{r}_i}{\partial \theta} = \sum_{i=1}^p -\frac{c_i \mathbf{v}_i}{|\mathbf{v}_i|} \cdot L_i (-\sin(\theta + \phi_i), \cos(\theta + \phi_i)) \\ &= -\sum_{i=1}^p \frac{c_i L_i (-\dot{x} \sin(\theta + \phi_i) + \dot{y} \cos(\theta + \phi_i) + L_i \dot{\theta})}{|\mathbf{v}_i|} \end{aligned}$$

The Lagrangian equations of motion are

$$\mu_0 \ddot{x} = F_x, \quad \mu_0 \ddot{y} = F_y, \quad \mu_2 \ddot{\theta} = F_\theta \quad (3.40)$$

which are the same as for two particles, [equation \(3.38\)](#).

A Thin Rod on a Rough Plane

This example is an extension of the one for two particles connected by a thin, massless rod. Now the rod itself has mass and is in contact with the rough plane at every point. The system still has three degrees of freedom: the center of mass (x, y) of the rod and the angle θ formed by the rod with the positive x -axis direction. The rod is parameterized by $\mathbf{r}(L) = (x + L \cos \theta, y + L \sin \theta)$ for $L \in [-L_2, L_1]$. The velocity is $\mathbf{v}(L) = (\dot{x} - L\dot{\theta} \sin \theta, \dot{y} + L\dot{\theta} \cos \theta)$. The total length of the rod is $L_1 + L_2$. The mass distribution is not necessarily uniform; mass density is the function $\delta(L)$. The total mass μ_0 and second moment μ_2 are

$$\mu_0 = \int_{-L_2}^{L_1} \delta(L) dL \quad \text{and} \quad \mu_2 = \int_{-L_2}^{L_1} \delta(L)L^2 dL$$

The kinetic energy is

$$\begin{aligned} T(x, y, \theta) &= \int_{-L_2}^{L_1} \frac{1}{2} \delta(L) |\mathbf{v}(L)|^2 dL \\ &= \int_{-L_2}^{L_1} \frac{1}{2} \delta(L) ((\dot{x} - L\dot{\theta} \sin \theta)^2 + (\dot{y} + L\dot{\theta} \cos \theta)^2) dL \\ &= \frac{\mu_0}{2} (\dot{x}^2 + \dot{y}^2) + \frac{\mu_2}{2} \dot{\theta}^2 \end{aligned} \tag{3.41}$$

Just as in the case of particle systems, some terms in the formal construction of kinetic energy vanish due to the choice of the center of mass as the origin. Specifically, $\int_{-L_2}^{L_1} \delta L \cos \theta dL = 0$ and $\int_{-L_2}^{L_1} \delta L \sin \theta dL = 0$. This is exactly of the form shown in [equation \(3.37\)](#).

The frictional force is $\mathbf{F}(L) = -c\mathbf{v}(L)/|\mathbf{v}(L)|$, where c is allowed to vary for each particle in the rod (c is allowed to be a function of L) but is assumed not to vary with position or velocity. The generalized force F_x is now formulated as an integral rather than as a sum:

$$\begin{aligned} F_x &= \int_{-L_2}^{L_1} \mathbf{F}(L) \cdot \frac{\partial \mathbf{r}(L)}{\partial x} dL \\ &= \int_{-L_2}^{L_1} -c \frac{\mathbf{v}}{|\mathbf{v}|} \cdot (1, 0) dL \end{aligned}$$

$$= \int_{-L_2}^{L_1} \frac{-c(\dot{x} - L\dot{\theta} \sin \theta)}{\sqrt{(\dot{x} - L\dot{\theta} \sin \theta)^2 + (\dot{y} + L\dot{\theta} \cos \theta)^2}} dL$$

Similarly, the generalized force F_y is

$$\begin{aligned} F_y &= \int_{-L_2}^{L_1} \mathbf{F}(L) \cdot \frac{\partial \mathbf{r}(L)}{\partial y} dL \\ &= \int_{-L_2}^{L_1} -c \frac{\mathbf{v}}{|\mathbf{v}|} \cdot (1, 0) dL \\ &= \int_{-L_2}^{L_1} \frac{-c(\dot{y} + L\dot{\theta} \cos \theta)}{\sqrt{(\dot{x} - L\dot{\theta} \sin \theta)^2 + (\dot{y} + L\dot{\theta} \cos \theta)^2}} dL \end{aligned}$$

and the generalized force F_θ is

$$\begin{aligned} F_\theta &= \int_{-L_2}^{L_1} \mathbf{F}(L) \cdot \frac{\partial \mathbf{r}(L)}{\partial \theta} dL \\ &= \int_{-L_2}^{L_1} -c \frac{\mathbf{v}}{|\mathbf{v}|} \cdot L(-\sin \theta, \cos \theta) dL \\ &= \int_{-L_2}^{L_1} \frac{-cL(-\dot{x} \sin \theta + \dot{y} \cos \theta + L\dot{\theta})}{\sqrt{(\dot{x} - L\dot{\theta} \sin \theta)^2 + (\dot{y} + L\dot{\theta} \cos \theta)^2}} dL \end{aligned}$$

The Lagrangian equations of motion are the same as those in [equation \(3.38\)](#).

EXERCISE
3.29

How do the formulas for kinetic energy, generalized forces, and the Lagrangian equations of motion change if the mass is distributed along a curve rather than a straight line segment? ■

A Flat Board on a Rough Plane

This example is an extension of the one for multiple particles on a rough surface. We now consider a continuum of mass in the region R , as shown in [Figure 3.21](#).

The system has three degrees of freedom: the center of mass (x, y) of the rod and an angle θ that represents the orientation of the region relative to the positive x -axis.

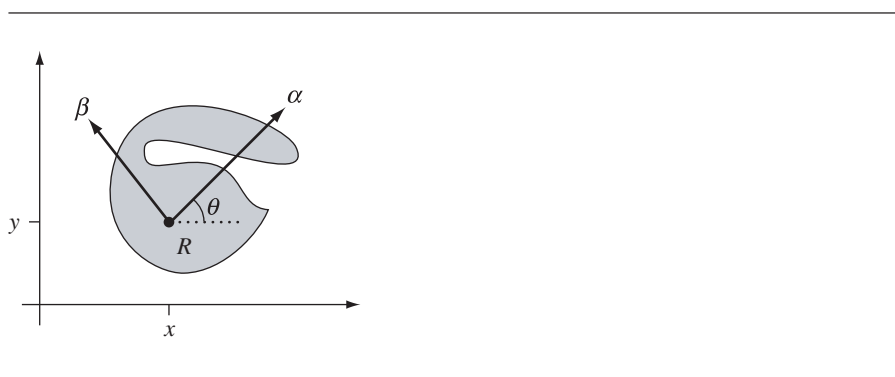


Figure 3.21 A flat board on a rough plane.

The rod is parameterized in a local coordinate system whose origin is the center of mass and whose orthonormal axes are chosen to be $(\cos \theta, \sin \theta)$ and $(-\sin \theta, \cos \theta)$:

$$\mathbf{r}(\alpha, \beta) = (x, y) + \alpha(\cos \theta, \sin \theta) + \beta(-\sin \theta, \cos \theta)$$

The velocity is

$$\mathbf{v}(\alpha, \beta) = (\dot{x}, \dot{y}) + \dot{\theta}(\alpha(-\sin \theta, \cos \theta) - \beta(\cos \theta, \sin \theta))$$

Since the region R represents a rigid body, the local coordinates (α, β) for a particle are independent of the orientation of the body. The distance between the particle at (α, β) and the center of mass is $L = \sqrt{\alpha^2 + \beta^2}$. The mass density is the function $\delta(\alpha, \beta)$ and is allowed to vary over the region. In the integral quantities used in the following, the infinitesimal for the region is $dR = d\alpha d\beta$.

The kinetic energy is

$$\begin{aligned}
 T &= \frac{1}{2} \int_R \delta |\mathbf{v}|^2 dR \\
 &= \frac{1}{2} \int_R \delta ((\dot{x} - \dot{\theta}(\alpha \cos \theta + \beta \sin \theta))^2 + (\dot{y} + \dot{\theta}(\alpha \cos \theta - \beta \sin \theta))^2) dR \\
 &= \left(\int_R \delta dR \right) \frac{1}{2} (\dot{x}^2 + \dot{y}^2) + \left(\int_R (\alpha^2 + \beta^2) \delta dR \right) \frac{1}{2} \dot{\theta}^2
 \end{aligned} \tag{3.42}$$

$$= \frac{\mu_0}{2} (\dot{x}^2 + \dot{y}^2) + \frac{\mu_2}{2} \dot{\theta}^2$$

where

$$\mu_0 = \int_R \delta \, dR \quad \text{and} \quad \mu_2 = \int_R (\alpha^2 + \beta^2) \delta \, dR$$

Once again some formal terms in the computation of kinetic energy vanish due to the choice of center of mass as the origin. Specifically, $\int_R \delta(\alpha \sin \theta + \beta \cos \theta) \, dR = 0$ and $\int_R \delta(\alpha \cos \theta - \beta \sin \theta) \, dR = 0$. The form of the kinetic energy is the same as in equation (3.39).

The frictional forces are $\mathbf{F} = -c\mathbf{v}/|\mathbf{v}|$, where c is allowed to vary with α and β . The generalized force F_x is

$$\begin{aligned} F_x &= \int_R \mathbf{F} \cdot \frac{\partial \mathbf{r}}{\partial x} \, dR \\ &= \int_R -c \frac{\mathbf{v}}{|\mathbf{v}|} \cdot (1, 0) \, dR \\ &= \int_R \frac{-c(\dot{x} - \dot{\theta}(\alpha \sin \theta + \beta \cos \theta))}{|\mathbf{v}|} \, dR \end{aligned}$$

The generalized force F_y is

$$\begin{aligned} F_y &= \int_R \mathbf{F} \cdot \frac{\partial \mathbf{r}}{\partial y} \, dR \\ &= \int_R -c \frac{\mathbf{v}}{|\mathbf{v}|} \cdot (0, 1) \, dR \\ &= \int_R \frac{-c(\dot{y} + \dot{\theta}(\alpha \cos \theta - \beta \sin \theta))}{|\mathbf{v}|} \, dR \end{aligned}$$

The generalized force F_θ is

$$\begin{aligned} F_\theta &= \int_R \mathbf{F} \cdot \frac{\partial \mathbf{r}}{\partial \theta} \, dR \\ &= \int_R -c \frac{\mathbf{v}}{|\mathbf{v}|} \cdot (-\alpha \sin \theta - \beta \cos \theta, \alpha \cos \theta - \beta \sin \theta) \, dR \\ &= \int_R \frac{-c(-(\alpha \sin \theta + \beta \cos \theta)\dot{x} + (\alpha \cos \theta - \beta \sin \theta)\dot{y} + (\alpha^2 + \beta^2)\dot{\theta})}{|\mathbf{v}|} \, dR \end{aligned}$$

The Lagrangian equations of motion are exactly the ones shown in equation (3.40).

 SOURCE CODE
RoughPlaneSolidBox

A Solid Box on a Rough Plane

The problem we now look at is a variation on the one involving a particle on an inclined plane as shown in Figure 3.19. Instead of a particle, we have a solid box of dimensions $2a$, $2b$, and $2h$. The box has constant mass density. A side view of the box and plane is shown in Figure 3.22.

In addition to sliding down the plane, the box is also rotating about its local vertical axis with angular speed $\dot{\theta}$. The center of mass is located at $\mathbf{r} = (x, w \cos \phi - h \sin \phi, w \sin \phi + h \cos \phi)$. The contribution to the kinetic energy due to the velocity of the center of mass is $m(\dot{x}^2 + \dot{w}^2)/2$, where m is the mass of the box. Because the box has angular velocity, we need to compute the contribution due to the rotation as indicated by equation (3.34). The angular velocity in world coordinates is $\mathbf{w} = \dot{\theta}(0, -\sin \phi, \cos \phi)$. Local coordinates for the box are as follows. The box's vertical direction is $\mathbf{u}_3 = [0 \ -\sin \phi \ \cos \phi]^T$. The other two coordinate axes vary with θ because of the rotation. A reference frame is $\mathbf{u}'_1 = [1 \ 0 \ 0]^T$ and $\mathbf{u}'_2 = [0 \ \cos \phi \ \sin \phi]^T$. The frame that rotates with the box as θ varies is

$$\mathbf{u}_1 = \cos \theta \mathbf{u}'_1 - \sin \theta \mathbf{u}'_2 = [\cos \theta \ -\sin \theta \cos \phi \ -\sin \theta \sin \phi]^T$$

and

$$\mathbf{u}_2 = \sin \theta \mathbf{u}'_1 + \cos \theta \mathbf{u}'_2 = [\sin \theta \ \cos \theta \cos \phi \ \cos \theta \sin \phi]^T$$

The local coordinates for the angular velocity are $\boldsymbol{\xi} = [\xi_1 \ \xi_2 \ \xi_3]^T$, where $\mathbf{w} = \sum_{i=1}^3 \xi_i \mathbf{u}_i$. In our case, $\mathbf{w} = \dot{\theta} \mathbf{u}_3$, so $\boldsymbol{\xi} = [0 \ 0 \ \dot{\theta}]^T$. From Example 2.9 we saw that the principal moment for the vertical axis is $\mu_3 = (a^2 + b^2)/3$, so the contribution of the angular velocity to the kinetic energy is $\dot{\theta}^2 m(a^2 + b^2)/3$. The total kinetic energy is

$$T = \frac{1}{2}m(\dot{x}^2 + \dot{w}^2) + \frac{1}{6}m(a^2 + b^2)\dot{\theta}^2 \quad (3.43)$$

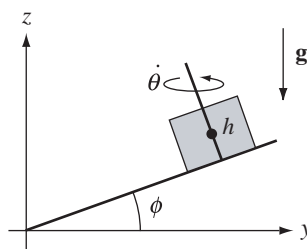


Figure 3.22 A side view of a solid box on a rough, inclined plane.

The system has three degrees of freedom given by x , w , and θ , so there will be three Lagrangian equations of motion: $m\ddot{x} = F_x$, $m\ddot{w} = F_w$, and $m(a^2 + b^2)\ddot{\theta}/3 = F_\theta$, where the right-hand sides of the equations are the generalized forces.

The center of mass is located at \mathbf{r} as mentioned earlier. You might be tempted to construct the generalized forces by dotting the applied forces $\mathbf{F}_{\text{grav}} + \mathbf{F}_{\text{fric}}$ with the partial derivatives of \mathbf{r} with respect to x , w , and θ . However, that would be an error in analysis. The contributions of the gravitational force to the generalized forces may be computed by assuming that gravity applies only to the center of mass. The frictional forces apply only to the face of the box that is sliding on the plane. In this sense we need to compute the contribution of friction to the generalized forces in the same manner as in the example of a flat board on a rough plane (see Figure 3.21). In that example, replace y with w and use the generalized forces exactly as shown in the example.

EXERCISE

3.30

In the discussion about a box sliding on a rough plane, the kinetic energy in equation (3.43) was computed using equation (3.34). First, the box half height h does not appear to affect the kinetic energy. Does this make sense to you? Second, the expression does not have terms of the form $\dot{x}\dot{\theta}$ or $\dot{w}\dot{\theta}$. In the example of a flat board sliding over a rough plane, the kinetic energy in equation (3.42) was computed directly as an integral over the velocity of points in the board. This latter formula has terms involving $\dot{x}\dot{\theta}$ and $\dot{y}\dot{\theta}$ (thinking of y and w as the same variable). From the perspective of friction, the sliding box and sliding flat board are identical in nature since the friction of the sliding box is only relevant for its bottom flat face. Why is it, then, that one expression has the $\dot{x}\dot{\theta}$ and $\dot{w}\dot{\theta}$ terms but not the other expression? ■

EXERCISE

3.31

Write a computer program that implements the example of a box sliding on a rough plane. The example, as modeled, uses only kinetic friction. Incorporate static friction into your program by specifying a minimum angle $\phi_{\min} > 0$ for which static friction prevents the box from moving when the plane is inclined at an angle ϕ smaller than ϕ_{\min} but allows movement when the angle of inclination is larger than ϕ_{\min} . ■

3.3 EULER'S EQUATIONS OF MOTION

Sometimes a physical application is more naturally modeled in terms of rotations about axes in a coordinate system. The prototypical example is that of a spinning top, where the top rotates about its axis of symmetry but simultaneously the entire top is rotating about a vertical axis. Euler's equations of motion are the likely choice for determining the motion of such an object. These equations are the focus of this section.

Consider a rigid body with origin \mathcal{O} that coincides with the origin of the world coordinate system. The basis vectors for the world are $\boldsymbol{\eta}_i$ for $1 \leq i \leq 3$. The rigid body is given its own basis vectors $\boldsymbol{\xi}_i$ for $1 \leq i \leq 3$, such that $\boldsymbol{\eta}_3$ and $\boldsymbol{\xi}_3$ are not parallel. The plane spanned by $\boldsymbol{\eta}_1$ and $\boldsymbol{\eta}_2$ intersects the plane spanned by $\boldsymbol{\xi}_1$ and $\boldsymbol{\xi}_2$ in a line. That line passes through the origin and has unit-length direction \mathbf{N} . Figure 3.23(a) illustrates the two coordinate systems.

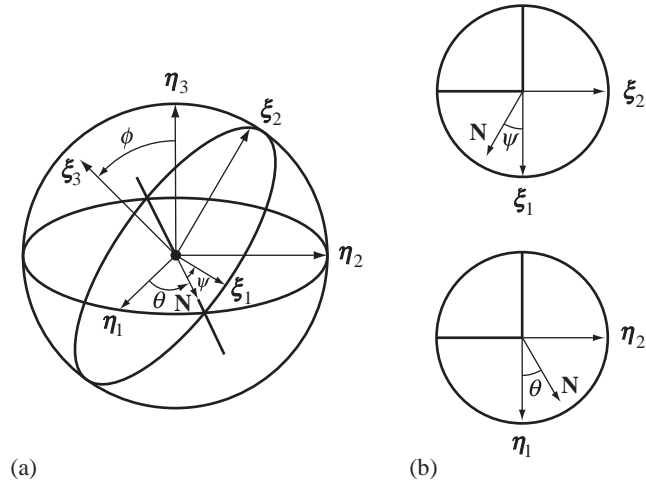


Figure 3.23 The world coordinates and body coordinates for a rigid body where both systems have the same origin.

The angle between η_3 and ξ_3 is ϕ , the angle between \mathbf{N} and η_1 is θ , and the angle between \mathbf{N} and ξ_1 is ψ . The positive direction for the angles is shown in Figure 3.23. By definition, \mathbf{N} lies in the plane spanned by η_1 and η_2 . Moreover, it must lie on the unit circle centered at the origin. The vector also lies on the unit circle centered at the origin of the plane spanned by ξ_1 and ξ_2 . As such we may write it as

$$\mathbf{N} = (\cos \theta)\eta_1 + (\sin \theta)\eta_2 = (\cos \psi)\xi_1 - (\sin \psi)\xi_2 \quad (3.44)$$

Figure 3.23(b) illustrates the location of \mathbf{N} relative to the various axes of the planes.

The three angles ϕ , θ , and ψ completely determine the orientation of the body relative to the world coordinates. Observe that $\dot{\phi}$ is the angular speed of rotation about \mathbf{N} , $\dot{\theta}$ is the angular speed of rotation about η_3 , and $\dot{\psi}$ is the angular speed of rotation about ξ_3 . The angular velocity of the rigid body is the sum of the axial angular velocities $\mathbf{w} = \dot{\phi}\mathbf{N} + \dot{\theta}\eta_3 + \dot{\psi}\xi_3$. The vector ξ_3 is obtained from η_3 by a rotation about the \mathbf{N} axis through an angle ϕ . Using a standard rotation formula and using equation (3.44) for cross products:

$$\begin{aligned} \xi_3 &= \eta_3 + (\sin \phi)\mathbf{N} \times \eta_3 + (1 - \cos \phi)\mathbf{N} \times (\mathbf{N} \times \eta_3) \\ &= \eta_3 + (\sin \phi)(-(\cos \theta)\eta_2 + (\sin \theta)\eta_1) + (1 - \cos \phi)(-\eta_3) \\ &= (\sin \theta \sin \phi)\eta_1 - (\cos \theta \sin \phi)\eta_2 + (\cos \phi)\eta_3 \end{aligned} \quad (3.45)$$

The angular velocity in world coordinates is

$$\begin{aligned}
 \mathbf{w} &= \dot{\phi}\mathbf{N} + \dot{\theta}\boldsymbol{\eta}_3 + \dot{\psi}\boldsymbol{\xi}_3 \\
 &= \dot{\phi}((\cos\theta)\boldsymbol{\eta}_1 + (\sin\theta)\boldsymbol{\eta}_2) + \dot{\theta}\boldsymbol{\eta}_3 + \dot{\psi}((\sin\theta\sin\phi)\boldsymbol{\eta}_1 \\
 &\quad - (\cos\theta\sin\phi)\boldsymbol{\eta}_2 + (\cos\phi)\boldsymbol{\eta}_3) \\
 &= (\dot{\phi}\cos\theta + \dot{\psi}\sin\theta\sin\phi)\boldsymbol{\eta}_1 + (\dot{\phi}\sin\theta - \dot{\psi}\cos\theta\sin\phi)\boldsymbol{\eta}_2 \\
 &\quad + (\dot{\theta} + \dot{\psi}\cos\phi)\boldsymbol{\eta}_3
 \end{aligned} \tag{3.46}$$

Similarly, the vector $\boldsymbol{\eta}_3$ is obtained from $\boldsymbol{\xi}_3$ by a rotation about the \mathbf{N} axis through an angle $-\phi$. Using a standard rotation formula and using equation (3.44) for cross products:

$$\begin{aligned}
 \boldsymbol{\eta}_3 &= \boldsymbol{\xi}_3 - (\sin\phi)\mathbf{N} \times \boldsymbol{\xi}_3 + (1 - \cos\phi)\mathbf{N} \times (\mathbf{N} \times \boldsymbol{\xi}_3) \\
 &= \boldsymbol{\xi}_3 - (\sin\phi)(-(\cos\psi)\boldsymbol{\xi}_2 - (\sin\psi)\boldsymbol{\xi}_1) + (1 - \cos\phi)(-\boldsymbol{\xi}_3) \\
 &= (\sin\psi\sin\phi)\boldsymbol{\xi}_1 + (\cos\psi\sin\phi)\boldsymbol{\xi}_2 + (\cos\phi)\boldsymbol{\xi}_3
 \end{aligned} \tag{3.47}$$

The angular velocity in body coordinates is

$$\begin{aligned}
 \mathbf{w} &= \dot{\phi}\mathbf{N} + \dot{\theta}\boldsymbol{\eta}_3 + \dot{\psi}\boldsymbol{\xi}_3 \\
 &= \dot{\phi}((\cos\psi)\boldsymbol{\xi}_1 - (\sin\psi)\boldsymbol{\xi}_2) + \dot{\theta}((\sin\psi\sin\phi)\boldsymbol{\xi}_1 + (\cos\psi\sin\phi)\boldsymbol{\xi}_2 \\
 &\quad + (\cos\phi)\boldsymbol{\xi}_3) + \dot{\psi}\boldsymbol{\xi}_3 \\
 &= (\dot{\phi}\cos\psi + \dot{\theta}\sin\psi\sin\phi)\boldsymbol{\xi}_1 + (-\dot{\phi}\sin\psi + \dot{\theta}\cos\psi\sin\phi)\boldsymbol{\xi}_2 \\
 &\quad + (\dot{\psi} + \dot{\theta}\cos\phi)\boldsymbol{\xi}_3
 \end{aligned} \tag{3.48}$$

The angular velocity in world coordinates is useful in setting up Euler's general equations of motion, equation (2.90). The angular velocity in body coordinates, when the $\boldsymbol{\xi}$ are chosen to be principal directions of the inertia tensor, is useful in setting up Euler's special equations of motion, equation (2.91). If the principal moments are μ_i , the body coordinates of the torque are τ_i , and the body coordinates of the angular velocity are w_i , then the special equations are

$$\begin{aligned}
 \mu_1\dot{w}_1 + (\mu_3 - \mu_2)w_2w_3 &= \tau_1 \\
 \mu_2\dot{w}_2 + (\mu_1 - \mu_3)w_1w_3 &= \tau_2 \\
 \mu_3\dot{w}_3 + (\mu_2 - \mu_1)w_1w_2 &= \tau_3
 \end{aligned} \tag{3.49}$$

EXAMPLE
3.18

Consider a freely spinning top whose tip is fixed in place. The top is assumed to be symmetric about the axis of the third principal direction vector, in which case $\mu_1 = \mu_2$. We assume no torques on the top, a situation that can be approximated by assuming the center of mass is effectively at the tip of the top. Figure 3.24 shows the configuration.

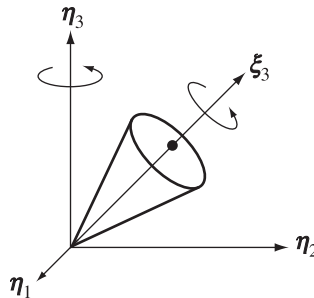


Figure 3.24

A freely spinning top with tip fixed at the origin of the world coordinate system.

The world coordinate axes η_i are shown. The body coordinate axes are ξ_i , which are the principal directions of the inertia tensor, but only the axis of symmetry is shown.

The Euler equations, equation (3.49), reduce to

$$\mu_1 \dot{w}_1 + (\mu_3 - \mu_1) w_2 w_3 = 0, \quad \mu_1 \dot{w}_2 - (\mu_1 - \mu_3) w_1 w_3 = 0, \quad \mu_3 \dot{w}_3 = 0$$

The last equation implies the component $w_3 = c$, a constant. Define $\lambda = c(\mu_3 - \mu_1)/\mu_1$. The first two equations are then $\dot{w}_1 + \lambda w_2 = 0$ and $\dot{w}_2 - \lambda w_1 = 0$. Taking derivatives and replacing one equation in the other leads to $\ddot{w}_1 + \lambda^2 w_1 = 0$. This is the differential equation for simple harmonic motion. A solution is $w_1 = \alpha \cos(\lambda t)$. The other component is determined from the second differential equation by substituting in w_1 , the result being $w_2 = \alpha \sin(\lambda t)$. The angular velocity of the top in body coordinates is

$$\mathbf{w} = (\alpha \cos(\lambda t)) \xi_1 + (\alpha \sin(\lambda t)) \xi_2 + c \xi_3$$

The angular speed is $|\mathbf{w}| = \sqrt{\alpha^2 + c^2}$, a constant. If the top rotates only about its axis of symmetry, then $\alpha = 0$ must occur so that \mathbf{w} is parallel to ξ_3 . However, the top can be rotating about the η_3 axis while simultaneously rotating about its axis of symmetry. In this case the angular velocity is not parallel to ξ_3 , and $\alpha \neq 0$ is required.

In world coordinates the torque τ and angular momentum \mathbf{L} are related by $\tau = d\mathbf{L}/dt$. Since the torque is assumed to be zero, the rate of change of angular momentum is zero. Thus, the angular momentum vector is constant. Moreover, we know

that $\mathbf{L} = J\mathbf{w}$ in world coordinates. For \mathbf{L} to be a constant and \mathbf{w} to be time-varying, J must also be time varying. In the specified body coordinates, the angular momentum vector is

$$\mathbf{L} = M\mathbf{w} = (\mu_1 \alpha \cos(\lambda t))\boldsymbol{\xi}_1 + (\mu_1 \alpha \sin(\lambda t))\boldsymbol{\xi}_2 + (\mu_3 c)\boldsymbol{\xi}_3$$

The first two coefficients are time varying, but so are the principal directions, and all must do so in order to guarantee the angular momentum vector is constant. This equation says that the angular momentum vector rotates about the body axis $\boldsymbol{\xi}_3$ with constant angular speed λ . However, we know \mathbf{L} is fixed in world space, and it must be parallel to $\boldsymbol{\eta}_3$, so the body axis $\boldsymbol{\xi}_3$ is rotating about $\boldsymbol{\eta}_3$ with angular speed $-\lambda$. ■

EXAMPLE
3.19

 SOURCE CODE
FreeTopFixedTip

This example is a modification of [Example 3.18](#). Now we assume that the center of mass is located ℓ units of distance from the origin along the axis of symmetry. The total mass of the top is m . Using the same notation as in our general discussion earlier in this section, the torque is

$$\begin{aligned}\boldsymbol{\tau} &= \mathbf{r} \times \mathbf{F}_{\text{grav}} \\ &= (\ell \boldsymbol{\xi}_3) \times (-mg \boldsymbol{\eta}_3) \\ &= (mg\ell \sin \phi) \mathbf{N} \\ &= (mg\ell \sin \phi \cos \psi) \boldsymbol{\xi}_1 + (-mg\ell \sin \phi \sin \psi) \boldsymbol{\xi}_2\end{aligned}$$

Euler's equations of motion are

$$\begin{aligned}\mu_1 \dot{w}_1 + (\mu_3 - \mu_1) w_2 w_3 &= mg\ell \sin \phi \cos \psi \\ \mu_1 \dot{w}_2 - (\mu_3 - \mu_1) w_1 w_3 &= -mg\ell \sin \phi \sin \psi \\ \mu_3 \dot{w}_3 &= 0\end{aligned}$$

As in the previous example, $w_3 = c$, a constant. Define $\lambda = c(\mu_3 - \mu_1)/\mu_1$ and $\alpha = mg\ell/\mu_1$. The first two equations of motion are

$$\dot{w}_1 + \lambda w_2 = \alpha \sin \phi \cos \psi, \quad \dot{w}_2 - \lambda w_1 = -\alpha \sin \phi \sin \psi$$

Multiplying the first by w_1 , the second by w_2 , and adding:

$$\frac{d}{dt}(w_1^2 + w_2^2) = 2\alpha \sin \phi (w_1 \cos \psi - w_2 \sin \psi)$$

[Equation \(3.48\)](#) may be used to show that $w_1^2 + w_2^2 = \dot{\phi}^2 + \dot{\theta}^2 \sin^2 \phi$ and $w_1 \cos \psi - w_2 \sin \psi = \dot{\phi}$. Consequently,

$$\frac{d}{dt}(\dot{\phi}^2 + \dot{\theta}^2 \sin^2 \phi) = 2\alpha \dot{\phi} \sin \phi = -\frac{d}{dt}(2\alpha \cos \phi)$$

(Example 3.19
continued)

Integrating leads to

$$\dot{\phi}^2 + \dot{\theta}^2 \sin^2 \phi = \beta - 2\alpha \cos \phi$$

where the right-hand side is a constant.

In body coordinates we know that the angular momentum is

$$\mathbf{L} = M\mathbf{w} = \mu_1 w_1 \boldsymbol{\xi}_1 + \mu_1 w_2 \boldsymbol{\xi}_2 + c\mu_3 \boldsymbol{\xi}_3$$

Dotting with $\boldsymbol{\eta}_3$ and defining $\gamma = \mathbf{L} \cdot \boldsymbol{\eta}_3$, we have

$$\begin{aligned}\gamma &= \mathbf{L} \cdot \boldsymbol{\eta}_3 \\ &= \mu_1 w_1 \boldsymbol{\xi}_1 \cdot \boldsymbol{\eta}_3 + \mu_1 w_2 \boldsymbol{\xi}_2 \cdot \boldsymbol{\eta}_3 + c\mu_3 \boldsymbol{\xi}_3 \cdot \boldsymbol{\eta}_3 \\ &= \mu_1 w_1 \sin \psi \sin \phi + \mu_1 w_2 \cos \psi \sin \phi + c\mu_3 \cos \phi\end{aligned}$$

where the last equality follows from dotting equation (3.47) with the $\boldsymbol{\xi}_i$. But $\boldsymbol{\tau} = d\mathbf{L}/dt$ and $\boldsymbol{\tau} \cdot \boldsymbol{\eta}_3 = 0$ imply that $d(\mathbf{L} \cdot \boldsymbol{\xi}_3)/dt = 0$, so $\gamma = \mathbf{L} \cdot \boldsymbol{\xi}_3$ is a constant. Once again we may substitute the body coordinates for \mathbf{w} from equation (3.48) to obtain

$$\mu_1 \dot{\theta} \sin^2 \phi + c\mu_3 \cos \phi = \gamma$$

Finally, equation (3.48) is used once more to produce

$$c = w_3 = \dot{\psi} + \dot{\theta} \cos \phi$$

This has been a long mathematical construction. Let us summarize what we have so far, three differential equations involving the three angles ϕ , θ , and ψ :

$$\dot{\phi}^2 + \dot{\theta}^2 \sin^2 \phi = \beta - 2\alpha \cos \phi, \quad \mu_1 \dot{\theta} \sin^2 \phi + c\mu_3 \cos \phi = \gamma, \quad \dot{\psi} + \dot{\theta} \cos \phi = c$$

The second equation can be solved for $\dot{\theta} = (\gamma - c\mu_3 \cos \phi)/(\mu_1 \sin^2 \phi)$. Defining the constants $\delta = \gamma/\mu_1$ and $\varepsilon = c\mu_3/\mu_1$ and replacing $\dot{\theta}$ in the first equation:

$$\dot{\phi}^2 + \left(\frac{\delta - \varepsilon \cos \phi}{\sin \phi} \right)^2 = \beta - 2\alpha \cos \phi$$

This differential equation involves only the angle ϕ . Solving for the first derivative:

$$\frac{d\phi}{dt} = \sqrt{(\beta - 2\alpha \cos \phi) - \left(\frac{\delta - \varepsilon \cos \phi}{\sin \phi} \right)^2}$$

You should convince yourself why the positive square root is chosen instead of the negative one. In a numerical implementation, to avoid the many trigonometric function calls that can be expensive to evaluate, the change of variables $p = \cos \phi$ may be used. The derivative is $\dot{p} = -\dot{\phi} \sin \phi$ and $\sin^2 \phi = 1 - p^2$. The differential equation becomes

$$\frac{dp}{dt} = -\sqrt{(1 - p^2)(\beta - 2\alpha p) - (\delta - \varepsilon p)^2} \tag{3.50}$$

This equation cannot be solved in closed form, even if we were to separate variables and solve for t as an integral of a function of p . It may be solved numerically to obtain p as a function of t , say $p(t)$. The other angles are computed by numerically integrating

$$\frac{d\theta}{dt} = \frac{\gamma - c\mu_3 \cos\phi}{\mu_1 \sin^2\phi} = \frac{\delta - \varepsilon p}{1 - p^2} \quad (3.51)$$

and

$$\frac{d\psi}{dt} = c - \dot{\theta} \cos\phi = c - p \frac{\delta - \varepsilon p}{1 - p^2} \quad (3.52)$$

Although you can solve equations (3.50), (3.51), and (3.52) as a system of differential equations, an alternative is to solve the first equation by generating a sequence of samples (t_i, p_i) , fitting those samples with a parametric curve in t , then using that curve in a numerical integration of the second and third equations with respect to t . Yet another alternative is to multiply the second and third equations by dt/dp to obtain $d\theta/dp = F(p)$ and $d\psi/dp = G(p)$, where the right-hand sides are functions of only p . Numerical integrators may be applied to solve for θ and ψ as functions of p . Figure 3.25 – also [Color Plate 3.25](#) – shows some screen shots from the free top application found on the CD-ROM.

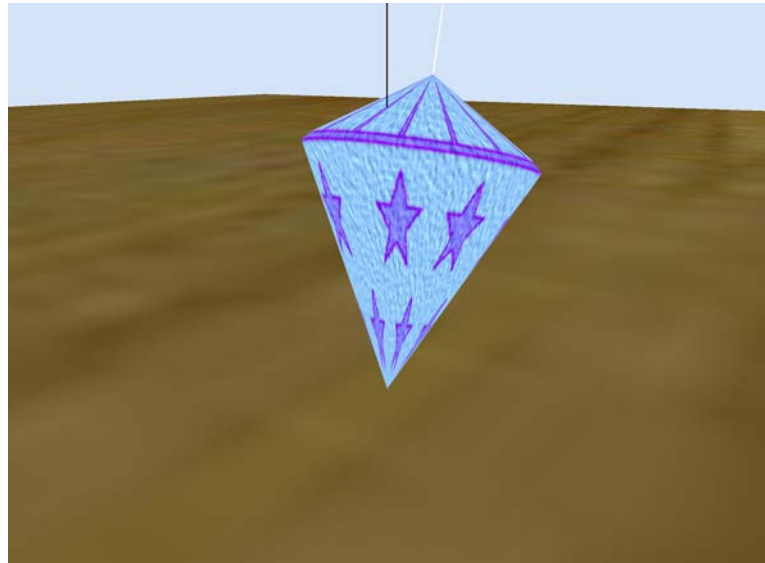


Figure 3.25 (Continued)

(Example 3.19
continued)

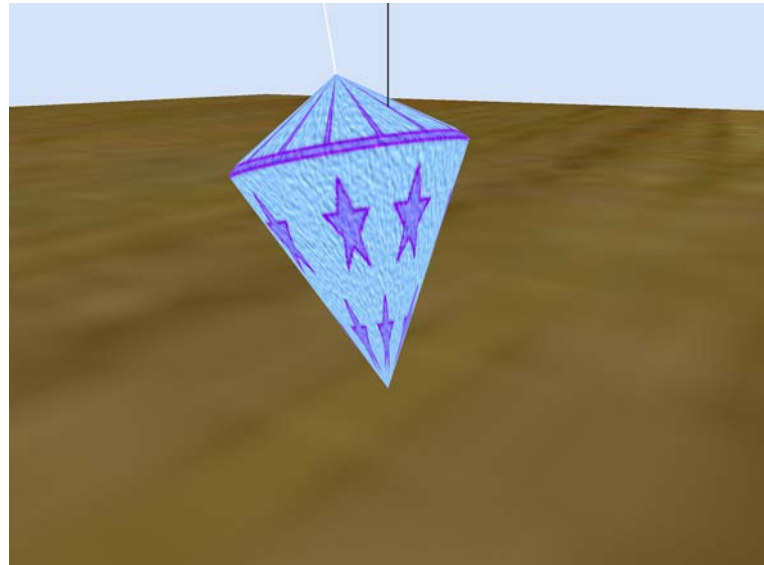


Figure 3.25

Two snapshots of a freely spinning top. The black line is the vertical axis. The white line is the axis of the top. (See also [Color Plate 3.25](#).)

EXERCISE
3.32

Write a computer program that uses a differential equation solver to solve [equations \(3.50\), \(3.51\), and \(3.52\)](#).

If you are feeling bold, add the following to your program. Assuming the top is a cone of height h and radius r , detect when $\phi(t)$ reaches an angle for which the cone becomes tangent to the horizontal plane. At that instant, the physical system should change to one that models the cone rolling around the plane, still with its tip connected to the origin (see [Exercise 3.22](#)). The plane is considered rough, so friction comes into play. In this mode the cone should eventually stop rolling.

EXERCISE
3.33

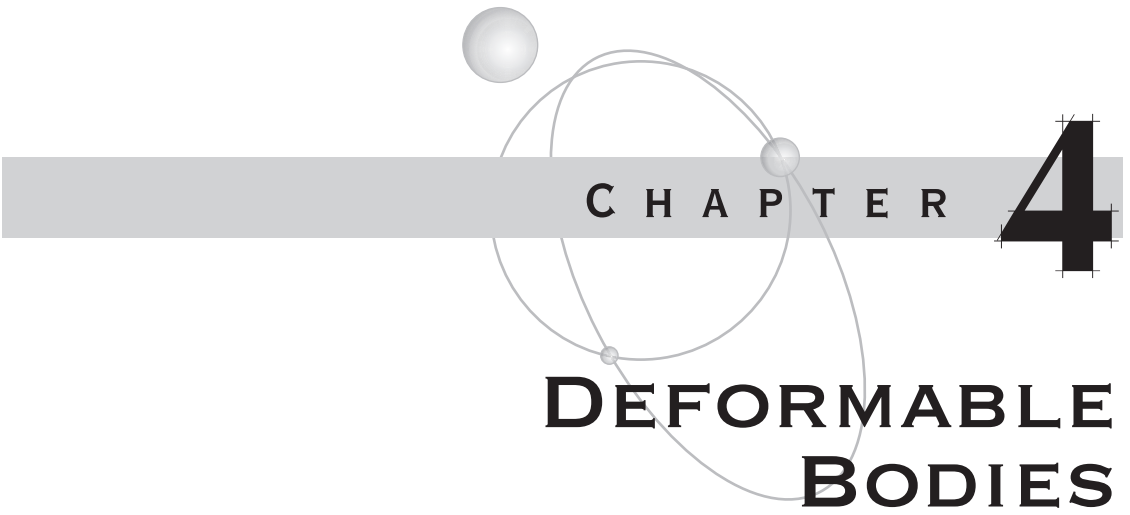
Compute the Lagrangian equations of motion for the freely spinning top subject to torque as in [Example 3.19](#).

EXERCISE
3.34

Compute equations of motion (Eulerian or Lagrangian) for the freely spinning top with no torque, where the tip is allowed to move on the xy -plane.

EXERCISE
3.35

Compute equations of motion (Eulerian or Lagrangian) for the freely spinning top with torque, where the tip moves in the x -direction of the xy -plane according to $x(t) = \alpha \sin \lambda t$, $y(t) = 0$.



CHAPTER

DEFORMABLE BODIES

In the last chapter we focused on rigid bodies and their behavior under various forces. In reality, no body is rigid, but for many bodies the assumption of rigidity is a close approximation to the actual physical conditions. For example, a ball bearing made of steel may be treated as a spherical rigid body. The equations of motion for reasonable forces applied to the ball bearing are good approximations to the physics. However, if the ball bearing is struck with a hard hammer with sufficient force, the bearing will deform, most likely into an elliptically shaped object.

In some physics applications, the objects we want to model are considered to be *deformable bodies*, ones for which the rigid body analyses do not apply. [Section 4.1](#) gives you a brief description of some concepts related to deformation. The other sections provide alternatives for modeling deformable bodies in a manner that is computationally reasonable on current computers.

A calculus-based approach to understanding deformation of a solid material is typically used in a course on continuum mechanics. Although current hardware may be of assistance in computing deformations through this approach, in particular GPU support for physics, it is still worthwhile to use a few alternatives to modeling deformable bodies. These are useful for maintaining a reasonable frame rate for a physics simulation involving the bodies. The first one is based on physical principles and requires solving systems of differential equations. The other alternatives are not physically based, but as long as the results look physically correct, they are good choices for deformation in that they avoid the numerical stability issues associated with differential equation solvers.

[Section 4.2](#) shows how to model a body as a system of point masses connected by springs. The quantity of masses, the configuration of springs, and the choice of spring constants depend on the particular needs of an application. The mathematical model of such a system will involve Hooke's Law and result in a system of differential equations that must be numerically solved.

[Section 4.3](#) shows how to model a body by explicitly defining its boundary to be a parametric surface with control points. In order to localize the deformation to small portions of the surface, we would like a surface with local control. This suggests using B-spline or NURBS surfaces. The control points may be varied over time to simulate time-varying forces applied to the surface of the body.

Free-form deformation of the region that contains the body is another practical alternative, one described in [Section 4.4](#). The surface of the body may be represented as a triangle mesh or as a parametric surface with control points. In the latter case a triangle mesh can be generated from the parametric surface for the purposes of display of the physical simulation. The idea is that the deformation region is parameterized by three variables and has a small number of control points that can be modified by the application. As the control points change, the region is deformed. The vertices for the triangle mesh or the control points for the parametric surface are located in the deformation region. As the region is deformed, the vertices or surface control points are moved about, causing the corresponding triangle meshes to deform.

The boundary of the region occupied by a body may be modeled as a surface implicitly by $F(x, y, z) = 0$ for a suitably chosen function F . This is the topic of [Section 4.5](#). We will choose the convention that the interior of the body is the set of points for which $F(x, y, z) < 0$. A force on the body is simulated by adding a deformation function $D(x, y, z)$ to $F(x, y, z)$ and setting the deformed surface to be that defined implicitly by $F(x, y, z) + D(x, y, z) = 0$. The interior of the deformed body is defined by $F(x, y, z) + D(x, y, z) < 0$.

4.1 ELASTICITY, STRESS, AND STRAIN

The primary concept for a deformable body is *elasticity*. This is the property by which the body returns to its original shape after the forces causing the deformation are removed. A plastic rod in the shape of a line segment can be easily bent and returned to its original form. A similarly shaped rod made of steel is more difficult to bend but will bend slightly and return to its original shape once the bending force is removed. The rod can be significantly bent so that it does not return to its initial shape once the force is removed. Such catastrophic behavior will not be dealt with in this book. Clearly, the amount of force necessary to deform a steel rod is greater than that required to deform a plastic rod.

The *stress* within a solid object is the magnitude of the applied force divided by the surface area over which the force acts. The stress is large when the force magnitude

is large or when the surface area is small, both intuitive behaviors. For example, if a heavy rigid body of mass m subject to gravitational force sits on the circular top of a cylinder of radius r , the stress on the cylinder is $mg/(\pi r^2)$, where g is the gravitational constant. A heavier mass causes more stress. A thinner cylinder has more stress generated by the same body. Since stress is the ratio of force magnitude to area of influence, it is effectively *pressure* and has the units of pressure, *pascals*. One pascal is defined to be one newton per meter squared.

The *strain* on an object is the fractional deformation caused by stress. The quantity is dimensionless since it measures a change in a dimension relative to the original dimension. Although the method of measuring a change depends on the particular type of object and how a force is applied, the simplest example to illustrate is a thin rod of elastic material that is fixed at one end, the other end pulled. If the rod has initial length L and changes length by ΔL due to the force pulling on the end, the strain on the rod is $\Delta L/L$.

By themselves, stress and strain do not appear to contain information about the specific material to which a force is applied. The amount of stress to produce a strain in a material does depend on that material. This suggests calculating the ratio of stress to strain for materials. Three variations of this ratio are presented here: *Young's modulus*, the *shear modulus*, and the *bulk modulus*. Loosely speaking, the three moduli represent the stress to strain ratio in a linear direction, along a planar region, and throughout a volume region.

If a wire of length L and cross-sectional area A has a force with magnitude F applied to one end, a change in length ΔL occurs. Young's modulus is the ratio of stress to strain:

$$Y = \frac{\text{linear stress}}{\text{linear strain}} = \frac{F/A}{\Delta L/L}$$

Consider a thin rectangular slab whose thickness is L units and whose other dimensions are x and y . L is assumed to be small relative to x and y . The large faces have area $A = xy$. One face is attached to a flat table. A tangential force of magnitude F and direction that of the x dimension is applied to the other face. This causes a shearing stress of F/A units. The rectangular slab slightly deforms into a parallelepiped whose volume is the same as the slab. The area of the large faces also remains the same. The slab has an edge length of L , but increases slightly by an amount ΔL due to the shearing. The shearing strain is $\Delta L/L$ and represents the strain of the one face attempting to move parallel to the other. The shearing modulus is

$$S = \frac{\text{planar stress}}{\text{planar strain}} = \frac{F/A}{\Delta L/L}$$

Finally, consider a material occupying a region of volume V . A force of magnitude F is uniformly distributed over the surface of the material, the direction of the force perpendicular at each point of the surface. You may consider the application of the

force as an attempt to compress the material. If the surface area is A , the pressure on the material is $P = F/A$. If the pressure is increased by an amount ΔP , the volume decreases by an amount ΔV . The volume stress is ΔP and the volume strain is $\Delta V/V$. The bulk modulus is

$$B = \frac{\text{volume stress}}{\text{volume strain}} = \frac{\Delta P}{\Delta V/V}$$

In all three cases the measurement is stress versus strain, but the difference lies in the dimensionality, so to speak, of how the material changes shape due to the stress.

4.2 MASS-SPRING SYSTEMS

A deformable body can be modeled as a system of point masses connected by springs. The bodies can be curve masses (e.g., hair or rope), surface masses (e.g., cloth or the surface of a body of water), or volume masses (e.g., a gelatinous blob or a moving, viscous material). The time complexity of the system is related to the number of masses and how they are interconnected. We will look at some simple configurations to illustrate the key ideas. Curve masses are modeled as a one-dimensional array of particles, surface masses as two-dimensional arrays, and volume masses as three-dimensional arrays. Sections 4.2.1 through 4.2.3 cover those cases. Section 4.2.4 discusses less regular configurations and the issues that arise when implementing them.

4.2.1 ONE-DIMENSIONAL ARRAY OF MASSES

A curve mass is thought of as a polyline, open with two endpoints or closed with no endpoints. Each vertex of the polyline represents a mass. Each edge represents a spring connecting the two masses at the endpoints of the edge. Figure 4.1 shows two such configurations.

A motivating example we looked at previously is Example 3.10, in which three masses aligned in the vertical direction were connected with two springs and allowed to fall due to gravitational forces. The masses are m_i and located at height z_i for $1 \leq i \leq 3$. Two springs connect the masses, one between m_1 and m_2 with spring constant $c_1 > 0$ and rest length L_1 and one between m_2 and m_3 with spring constant $c_2 > 0$. The gravitational force constant is $g > 0$. We determined the equations of motion to be

$$\begin{aligned} m_1 \ddot{z}_1 &= -c_1(z_1 - z_2 - L_1) - m_1 g \\ m_2 \ddot{z}_2 &= +c_1(z_1 - z_2 - L_1) - c_2(z_2 - z_3 - L_2) - m_2 g \\ m_3 \ddot{z}_3 &= +c_2(z_2 - z_3 - L_2) - m_3 g \end{aligned}$$

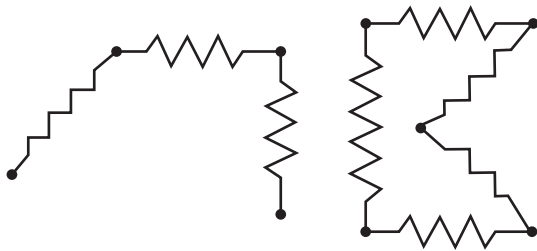


Figure 4.1 Two curve mass objects represented as mass–spring systems.

The organization of the terms on the right-hand side of the equation are suggestive of the pattern that occurs if more masses are added to a vertical chain of particles. The force on the boundary particle at z_1 has a contribution due to the spring below the mass, that contribution prefixed by a minus sign. The force on the boundary particle at z_3 has a contribution due to the spring above the mass, that contribution prefixed by a plus sign. The force on the interior particle at z_2 has two contributions, one from the spring above the mass (prefixed with a plus sign) and one from the spring below the mass (prefixed with a minus sign).

We can generalize the equations of motion to handle p particles in the chain. The masses are m_i and the positions are z_i for $1 \leq i \leq p$. The system has $p - 1$ springs with constants $c_i > 0$ and rest lengths L_i for $1 \leq i \leq p - 1$. Spring i connects masses m_i and m_{i+1} . The boundary points are at z_1 and z_p . All other points are interior points. The equation of motion for an interior point is modeled by

$$m_i \ddot{z}_i = c_{i-1}(z_{i-1} - z_i - L_{i-1}) - c_i(z_i - z_{i+1} - L_i) - m_i g \quad (4.1)$$

for $2 \leq i \leq p - 1$. If we define $c_0 = z_0 = L_0 = c_p = L_p = z_{p+1} = 0$, then this equation applies to all points in the system.

In our example every particle is falling because of gravitational forces. If we were to attach the boundary point z_1 to some stationary rigid object, perhaps the ceiling in a room, a constraint is introduced into the system. Since z_1 is now a constant over time, the first differential equation no longer applies in solving the remaining equations, and in fact becomes $m_1 \ddot{z}_1 = 0$. The force terms previously on the right-hand side of the equation are cancelled by the constraint forces (see [Section 3.2.1](#) for determining constraint forces). Similarly, other particles in the system can be tacked down and their differential equations removed from the system. If you tack down an interior point z_i , the linear chain is decomposed into two smaller linear chains, each with a fixed boundary point. The smaller systems may be solved separately.

Also in our example, the vertical chain of masses is only one-dimensional with regard to position, in this case vertical position z . In general, the masses can be located anywhere in space. When formulated in a full spatial setting, another variation is allowed: masses m_1 and m_p can be connected by yet another spring. If that spring has constant $c_p > 0$ and rest length L_p , [equation \(4.1\)](#) still applies, but wrapped indexing is required: $c_0 = c_p$, $\mathbf{x}_0 = \mathbf{x}_{p+1}$, and $L_0 = L_p$. Finally, forces other than gravitational ones can be applied to the particles.

The general formulation for an open linear chain is as follows. The masses m_i are located at positions \mathbf{x}_i for $1 \leq i \leq p$. The system has $p - 1$ springs connecting the masses, spring i connecting m_i and m_{i+1} . At an interior point i , two spring forces are applied, one from the spring shared with point $i - 1$ and one from the spring shared with point $i + 1$. The differential equation for this point is

$$\begin{aligned} m_i \ddot{\mathbf{x}}_i = & c_{i-1} (|\mathbf{x}_{i-1} - \mathbf{x}_i| - L_{i-1}) \frac{\mathbf{x}_{i-1} - \mathbf{x}_i}{|\mathbf{x}_{i-1} - \mathbf{x}_i|} \\ & + c_i (|\mathbf{x}_{i+1} - \mathbf{x}_i| - L_i) \frac{\mathbf{x}_{i+1} - \mathbf{x}_i}{|\mathbf{x}_{i+1} - \mathbf{x}_i|} + \mathbf{F}_i \end{aligned} \quad (4.2)$$

where \mathbf{F}_i represents other forces acting on particle i , such as gravitational or wind forces. Just as in the case of vertical masses, with the proper definitions of c_0 , c_p , L_0 , L_p , \mathbf{x}_0 , and \mathbf{x}_{p+1} , [equation \(4.2\)](#) also handles fixed boundary points and closed loops.

EXAMPLE 4.1

This application shows how to solve the equations of motion for a one-dimensional array of masses connected by springs. [Figure 4.2](#) – also [Color Plate 4.2](#) – shows some screen shots from this application found on the CD-ROM. ■



SOURCE CODE
Rope

4.2.2 TWO-DIMENSIONAL ARRAY OF MASSES

The equations of motion for a linear chain of masses are provided by [equation \(4.2\)](#). At an interior particle i , the two force terms due to Hooke's law occur because two springs are attached to the particle and its neighbors. A surface mass can be represented by a collection of particles arranged as a two-dimensional array. An interior particle has four neighbors as shown in [Figure 4.3](#).

The masses are m_{i_0, i_1} and are located at \mathbf{x}_{i_0, i_1} for $0 \leq i_0 < n_0$ and $0 \leq i_1 < n_1$. The spring to the right of a particle has spring constant $c_{i_0, i_1}^{(0)}$ and resting length $L_{i_0, i_1}^{(0)}$. The spring below a particle has spring constant $c_{i_0, i_1}^{(1)}$ and resting length $L_{i_0, i_1}^{(1)}$. The understanding is that the spring constants and resting lengths are zero if the particle has no such spring in the specified direction.

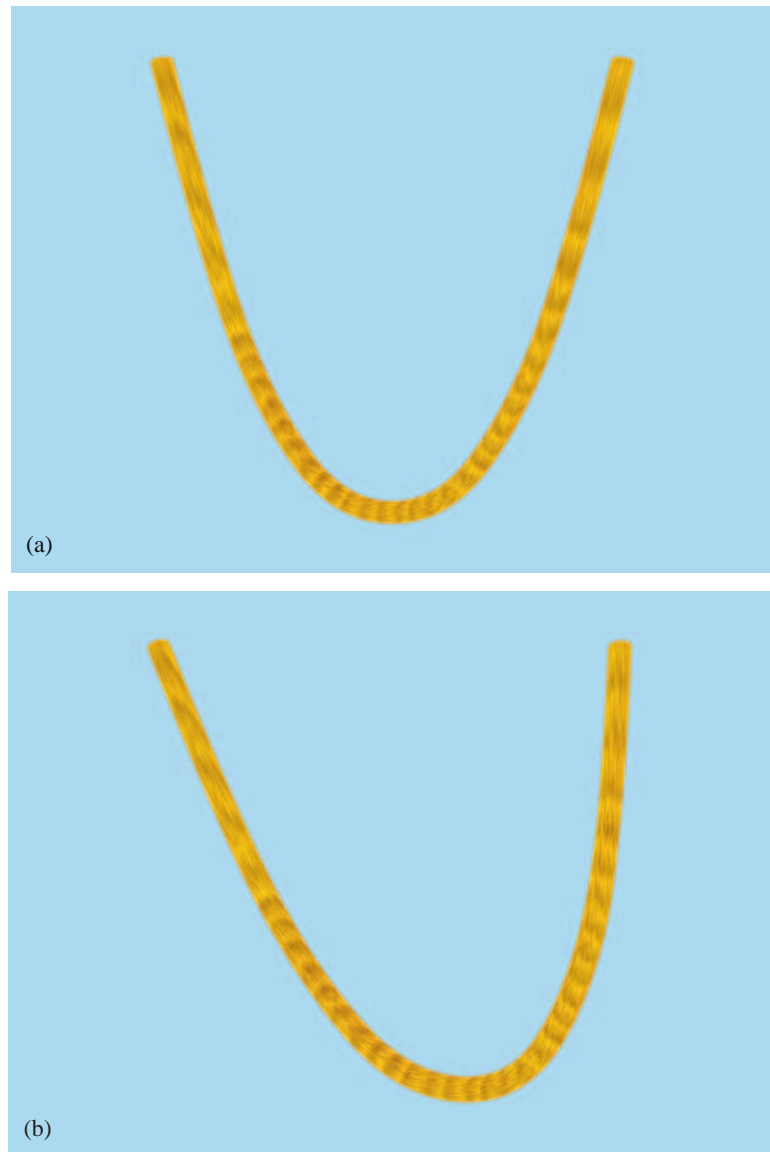


Figure 4.2 A rope modeled as a linear chain of springs. Image (a) shows the rope at rest with only gravity acting on it. Image (b) shows the rope subject to a wind force whose direction changes by small random amounts. (See also [Color Plate 4.2](#).)

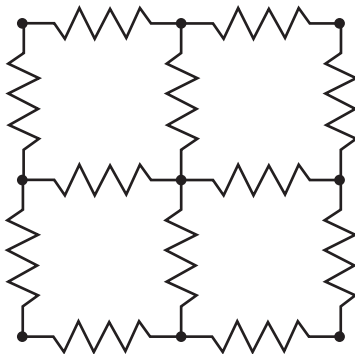


Figure 4.3 A surface mass represented as a mass–spring system with the masses organized as a two-dimensional array.

The equation of motion for particle (i_0, i_1) has four force terms due to Hooke's law, one for each neighboring particle. That equation is

$$\begin{aligned}
 m_{i_0, i_1} \ddot{\mathbf{x}}_{i_0, i_1} = & c_{i_0-1, i_1} \left(|\mathbf{x}_{i_0-1, i_1} - \mathbf{x}_{i_0, i_1}| - L_{i_0-1, i_1} \right) \frac{\mathbf{x}_{i_0-1, i_1} - \mathbf{x}_{i_0, i_1}}{|\mathbf{x}_{i_0-1, i_1} - \mathbf{x}_{i_0, i_1}|} \\
 & + c_{i_0+1, i_1} \left(|\mathbf{x}_{i_0+1, i_1} - \mathbf{x}_{i_0, i_1}| - L_{i_0+1, i_1} \right) \frac{\mathbf{x}_{i_0+1, i_1} - \mathbf{x}_{i_0, i_1}}{|\mathbf{x}_{i_0+1, i_1} - \mathbf{x}_{i_0, i_1}|} \\
 & + c_{i_0, i_1-1} \left(|\mathbf{x}_{i_0, i_1-1} - \mathbf{x}_{i_0, i_1}| - L_{i_0, i_1-1} \right) \frac{\mathbf{x}_{i_0, i_1-1} - \mathbf{x}_{i_0, i_1}}{|\mathbf{x}_{i_0, i_1-1} - \mathbf{x}_{i_0, i_1}|} \\
 & + c_{i_0, i_1+1} \left(|\mathbf{x}_{i_0, i_1+1} - \mathbf{x}_{i_0, i_1}| - L_{i_0, i_1+1} \right) \frac{\mathbf{x}_{i_0, i_1+1} - \mathbf{x}_{i_0, i_1}}{|\mathbf{x}_{i_0, i_1+1} - \mathbf{x}_{i_0, i_1}|} \\
 & + \mathbf{F}_{i_0, i_1}
 \end{aligned} \tag{4.3}$$

As in the case of linear chains, with the proper definition of the spring constants and resting lengths at the boundary points of the mesh, equation (4.3) applies to the boundary points as well as the interior points.

EXAMPLE 4.2

This application shows how to solve the equations of motion for a two-dimensional array of masses connected by springs. Figure 4.4 – also Color Plate 4.4 – shows some screen shots from this application found on the CD-ROM. ■



SOURCE CODE

Cloth

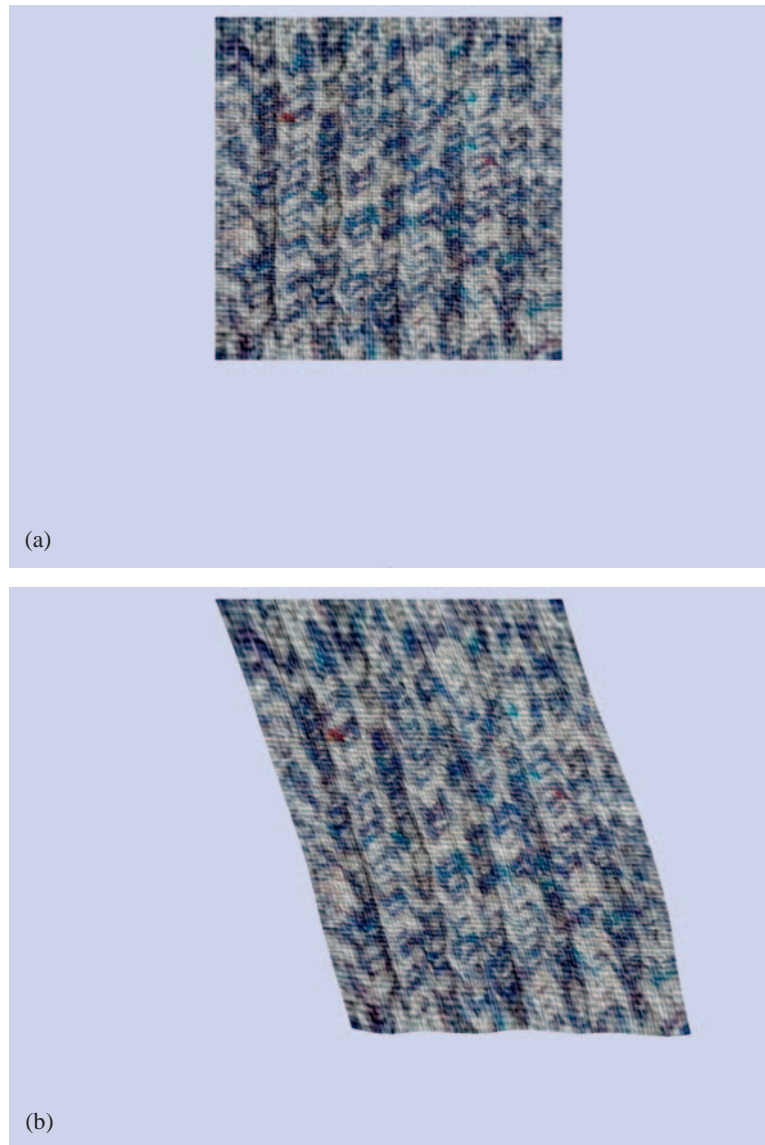


Figure 4.4 A cloth modeled as a rectangular array of springs. Wind forces make the cloth flap about. Notice that the cloth in image (b) is stretched in the vertical direction. The stretching occurs while the gravitational and spring forces balance out in the vertical direction during the initial portion of the simulation. (See also [Color Plate 4.4](#).)

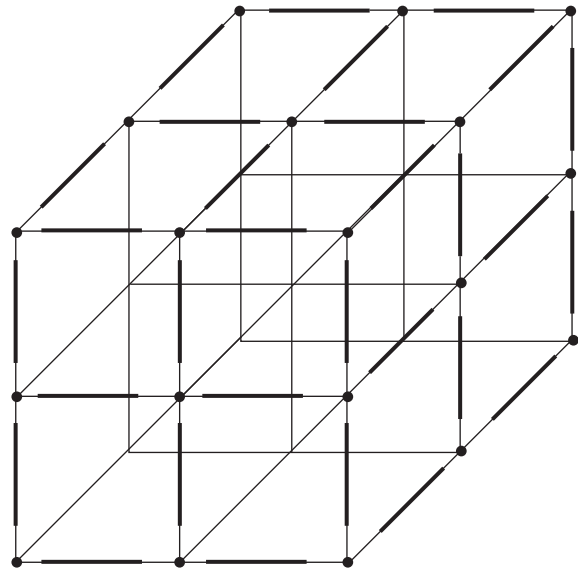


Figure 4.5 A volume mass represented as a mass–spring system with the masses organized as a three-dimensional array. Only the masses and springs on the three visible faces are shown. The other connections are shown, but without their springs.

4.2.3 THREE-DIMENSIONAL ARRAY OF MASSES

A volume mass can be represented by a collection of particles arranged as a three-dimensional array. An interior particle has eight neighbors as shown in Figure 4.5.

The masses are m_{i_0, i_1, i_2} and are located at $\mathbf{x}_{i_0, i_1, i_2}$ for $0 \leq i_j < n_j$, $j = 0, 1, 2$. In the direction of positive increase of index i_j , the spring has a spring constant $c_{i_0, i_1, i_2}^{(j)}$ and resting length $L_{i_0, i_1, i_2}^{(j)}$ for $j = 0, 1, 2$. The understanding is that the spring constants and resting lengths are zero if the particle has no such spring in the specified direction.

The equation of motion for particle (i_0, i_1, i_2) has six force terms due to Hooke's law, one for each neighboring particle. That equation is

$$\begin{aligned} m_{i_0, i_1, i_2} \ddot{\mathbf{x}}_{i_0, i_1, i_2} &= c_{i_0-1, i_1, i_2} \left(|\mathbf{x}_{i_0-1, i_1, i_2} - \mathbf{x}_{i_0, i_1, i_2}| - L_{i_0-1, i_1, i_2} \right) \frac{\mathbf{x}_{i_0-1, i_1, i_2} - \mathbf{x}_{i_0, i_1, i_2}}{|\mathbf{x}_{i_0-1, i_1, i_2} - \mathbf{x}_{i_0, i_1, i_2}|} \\ &\quad + c_{i_0+1, i_1, i_2} \left(|\mathbf{x}_{i_0+1, i_1, i_2} - \mathbf{x}_{i_0, i_1, i_2}| - L_{i_0+1, i_1, i_2} \right) \frac{\mathbf{x}_{i_0+1, i_1, i_2} - \mathbf{x}_{i_0, i_1, i_2}}{|\mathbf{x}_{i_0+1, i_1, i_2} - \mathbf{x}_{i_0, i_1, i_2}|} \end{aligned}$$

$$\begin{aligned}
& + c_{i_0, i_1-1, i_2} (|\mathbf{x}_{i_0, i_1-1, i_2} - \mathbf{x}_{i_0, i_1, i_2}| - L_{i_0, i_1-1, i_2}) \frac{\mathbf{x}_{i_0, i_1-1, i_2} - \mathbf{x}_{i_0, i_1, i_2}}{|\mathbf{x}_{i_0, i_1-1, i_2} - \mathbf{x}_{i_0, i_1, i_2}|} \\
& + c_{i_0, i_1+1, i_2} (|\mathbf{x}_{i_0, i_1+1, i_2} - \mathbf{x}_{i_0, i_1, i_2}| - L_{i_0, i_1+1, i_2}) \frac{\mathbf{x}_{i_0, i_1+1, i_2} - \mathbf{x}_{i_0, i_1, i_2}}{|\mathbf{x}_{i_0, i_1+1, i_2} - \mathbf{x}_{i_0, i_1, i_2}|} \\
& + c_{i_0, i_1, i_2-1} (|\mathbf{x}_{i_0, i_1, i_2-1} - \mathbf{x}_{i_0, i_1, i_2}| - L_{i_0, i_1, i_2-1}) \frac{\mathbf{x}_{i_0, i_1, i_2-1} - \mathbf{x}_{i_0, i_1, i_2}}{|\mathbf{x}_{i_0, i_1, i_2-1} - \mathbf{x}_{i_0, i_1, i_2}|} \\
& + c_{i_0, i_1, i_2+1} (|\mathbf{x}_{i_0, i_1, i_2+1} - \mathbf{x}_{i_0, i_1, i_2}| - L_{i_0, i_1, i_2+1}) \frac{\mathbf{x}_{i_0, i_1, i_2+1} - \mathbf{x}_{i_0, i_1, i_2}}{|\mathbf{x}_{i_0, i_1, i_2+1} - \mathbf{x}_{i_0, i_1, i_2}|} \\
& + \mathbf{F}_{i_0, i_1, i_2}
\end{aligned} \tag{4.4}$$

With the proper definition of the spring constants and resting lengths at the boundary points of the mesh, the equation (4.4) applies to the boundary points as well as interior points.

EXAMPLE
4.3

 **SOURCE CODE**
GelatinCube

This application shows how to solve the equations of motion for a three-dimensional array of masses connected by springs. Figure 4.6 – also Color Plate 4.6 – shows some screen shots from this application found on the CD-ROM. ■

4.2.4 ARBITRARY CONFIGURATIONS

In general you can set up an arbitrary configuration for a mass–spring system of p particles with masses m_i and location \mathbf{x}_i . Each spring added to the system connects two masses, say, m_i and m_j . The spring constant is $c_{ij} > 0$, and the resting length is L_{ij} .

Let \mathcal{A}_i denote the set of indices j such that m_j is connected to m_i by a spring, the set of *adjacent indices* so to speak. The equation of motion for particle i is

$$m_i \ddot{\mathbf{x}}_i = \sum_{j \in \mathcal{A}_i} c_{ij} (|\mathbf{x}_j - \mathbf{x}_i| - L_{ij}) \frac{\mathbf{x}_j - \mathbf{x}_i}{|\mathbf{x}_j - \mathbf{x}_i|} + \mathbf{F}_i \tag{4.5}$$

The technical difficulty in building a differential equation solver for an arbitrary graph is encapsulated solely by a vertex–edge table that stores the graph. Whenever the numerical solver must process particle i via equation (4.5), it must be able to iterate over the adjacent indices to evaluate the Hooke's law terms.

EXAMPLE
4.4

 **SOURCE CODE**
GelatinBlob

This application shows how to solve the equations of motion for a collection of masses connected by springs. The mass–spring configuration forms an arbitrary topology that is not representable as a two- or three-dimensional array of connections. Figure 4.7 – also Color Plate 4.7 – shows some screen shots from this application found on the CD-ROM. ■

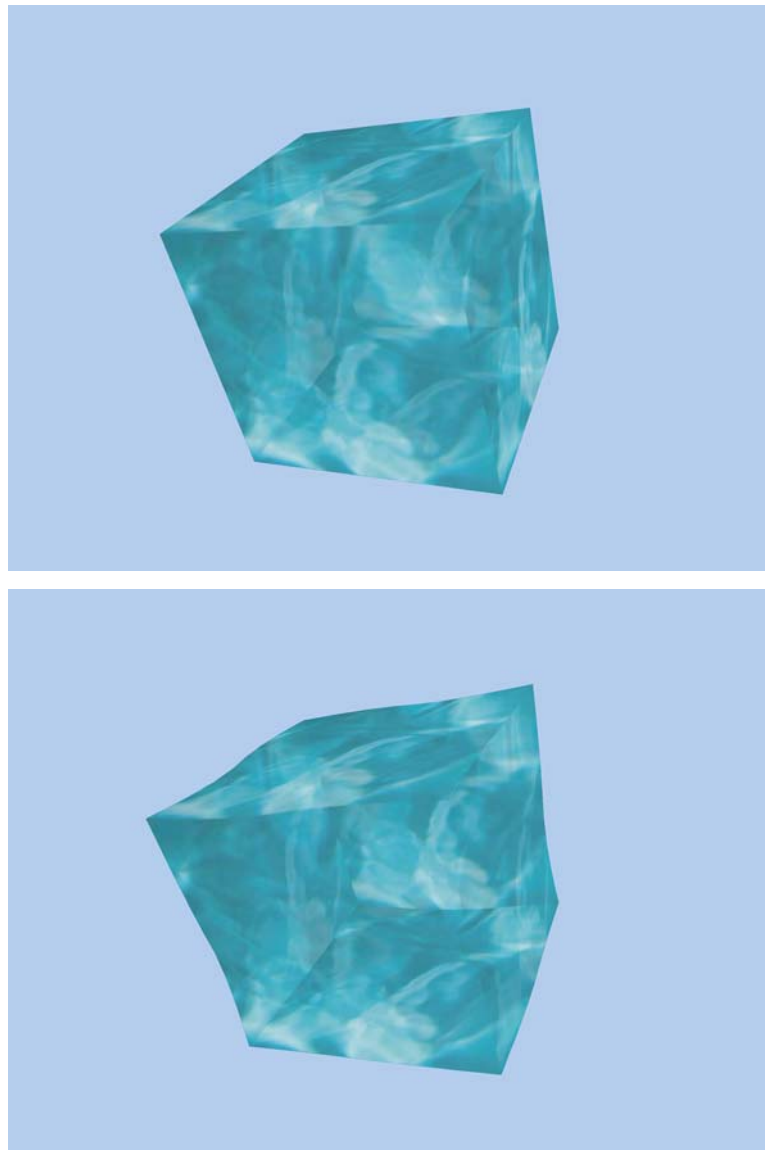


Figure 4.6 A gelatinous cube that is oscillating because of random forces. The cube is modeled by a three-dimensional array of mass connected by springs. (See also [Color Plate 4.6](#).)

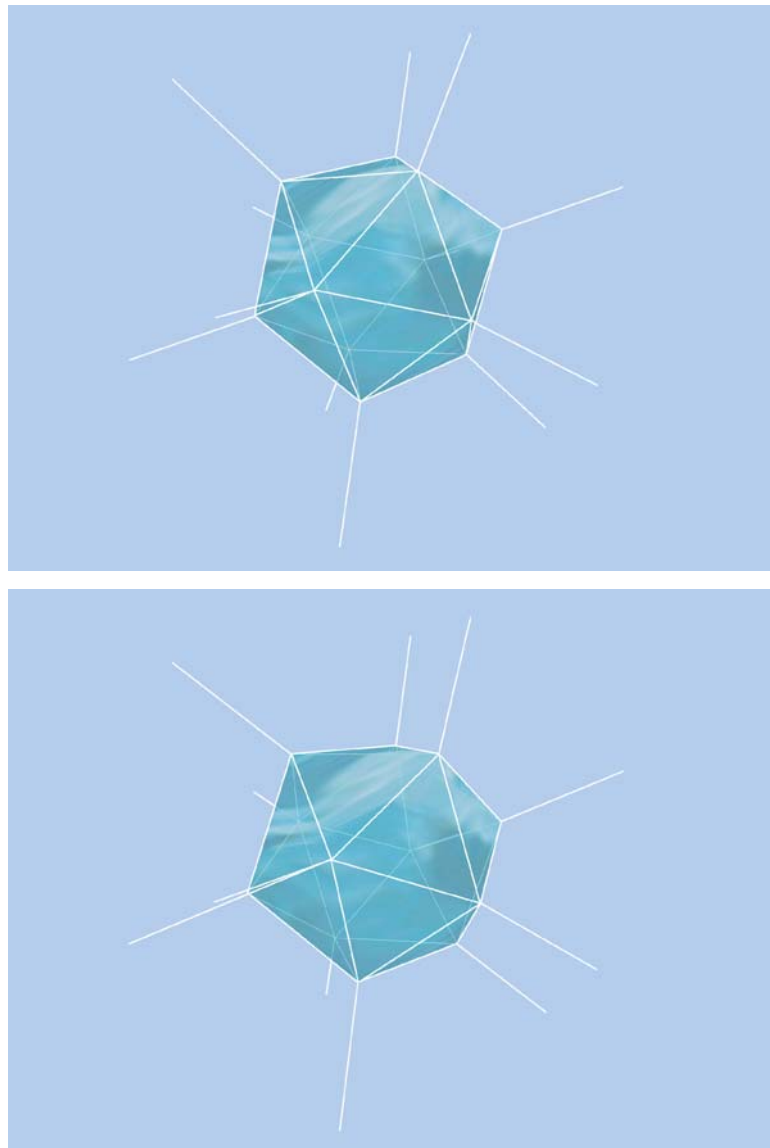


Figure 4.7 A gelatinous blob that is oscillating because of small, random forces. This blob has the masses located at the vertices of an icosahedron with additional masses of infinite weight to help stabilize the oscillations. The springs connecting the blob to the infinite masses are shown in white. (See also [Color Plate 4.7](#).)

4.3 CONTROL POINT DEFORMATION

A deformable body can be modeled as a parametric surface with control points that are varied according to the needs of an application. Although this approach is not physically based, a careful adjustment of control points can make the surface deform in a manner that is convincing to the viewer. To obtain localized deformations to small portions of a surface, a good choice for surface representation is B-splines or NURBS. A surface need not be a spline patch; it can be constructed from curves in a couple of ways. A tube surface can be constructed from a central curve and a radius function. If the control points of the central curve and the radius are time varying, the resulting tube surface deforms. A surface may also be generated from a spline curve as a surface of revolution or as a cylinder surface.

This chapter provides a brief summary of B-spline and NURBS curves, B-spline and NURBS surfaces, tube surfaces, and cylinder surfaces. The summary is confined to the processes of how such curves and surfaces are evaluated. The focus on evaluation is because you will want your deformable surfaces to be updated as rapidly as possible so as not to unnecessarily consume cycles during the game application runtime. A more thorough understanding of B-spline and NURBS curves and surfaces may be obtained by reading books such as [CRE01, Far90, Far99, Rog01]. The construction here is closest to that of [Rog01], a good book for an engineering-style approach to NURBS. Section 4.3.5 describes the applications on the CD-ROM that use ideas reviewed in Sections 4.3.1–4.3.4.

4.3.1 B-SPLINE CURVES

The control points for a B-spline curve are \mathbf{B}_i , $0 \leq i \leq n$. The construction is dimensionless, so the control points can be in whatever dimension interests you. The degree d of the curve must be selected so that $1 \leq d \leq n$. The curve itself is defined by

$$\mathbf{X}(u) = \sum_{i=0}^n N_{i,d}(u) \mathbf{B}_i \quad (4.6)$$

where the functions $N_{i,d}(u)$ are called the *B-spline basis functions*. These functions are defined recursively and require selection of a sequence of scalars u_i for $0 \leq i \leq n + d + 1$. The sequence must be nondecreasing, that is $u_i \leq u_{i+1}$. Each u_i is referred to as a *knot*, the total sequence a *knot vector*. The basis function that starts the recursive definition is

$$N_{i,0}(u) = \begin{cases} 1, & u_i \leq u < u_{i+1} \\ 0, & \text{otherwise} \end{cases} \quad (4.7)$$

for $0 \leq i \leq n + d$. The recursion itself is

$$N_{i,j}(u) = \frac{u - u_i}{u_{i+j} - u_i} N_{i,j-1}(u) + \frac{u_{i+j+1} - u}{u_{i+j+1} - u_{i+1}} N_{i+1,j-1}(u) \quad (4.8)$$

for $1 \leq j \leq d$ and $0 \leq i \leq n + d - j$. The *support* of a function is the smallest closed interval on which the function has at least one nonzero value. The support of $N_{i,0}(u)$ is clearly $[u_i, u_{i+1}]$. In general, the support of $N_{i,j}(u)$ is $[u_i, u_{i+j+1}]$. We will use this information later to show how $\mathbf{X}(u)$ for a specific value of u depends only on a small number of control points, the indices of those points related to the choice of u . This property is called *local control* and will be important when you want to deform a portion of a curve (or surface) by varying only those control points affecting that portion.

The knots can be within any domain, but I will choose them to be in $[0, 1]$ to provide a standardized interface for B-spline and NURBS curves and surfaces.

Types of Knot Vectors

The main classification of the knot vector is that it is either *open* or *periodic*. If open, the knots are either *uniform* or *nonuniform*. Periodic knot vectors have uniformly spaced knots. The use of the term *open* is perhaps a misnomer since you can construct a closed B-spline curve from an open knot vector. The standard way to construct a closed curve uses periodic knot vectors.

An open, uniform knot vector is defined by

$$u_i = \begin{cases} 0, & 0 \leq i \leq d \\ \frac{i-d}{n+1-d}, & d+1 \leq i \leq n \\ 1, & n+1 \leq i \leq n+d+1 \end{cases}$$

An open, nonuniform knot vector is in the same format except that the values u_i for $d+1 \leq i \leq n$ are user defined. These must be selected to maintain monotonicity $0 \leq u_{d+1} \leq \dots \leq u_{n+1} \leq 1$. A periodic knot vector is defined by

$$u_i = \frac{i-d}{n+1-d}, \quad 0 \leq i \leq n+d+1$$

Some of the knots are outside the domain $[0, 1]$, but this occurs to force the curve to have period 1. When evaluating $\mathbf{X}(u)$, any input value of u outside $[0, 1]$ is reduced to this interval by periodicity before evaluation of the curve point.

Evaluation

The straightforward method for evaluation of $\mathbf{X}(u)$ is to compute all of $N_{i,d}(u)$ for $0 \leq i \leq n$ using the recursive formulas from [equations \(4.7\)](#) and [\(4.8\)](#). The pseudocode to compute the basis function values is shown below. The value n , degree d , knots $u[]$, and control points $B[]$ are assumed to be globally accessible.

```
float N (int i, int j, float u)
{
}
```

```

if (j > 0)
{
    c0 = (u - u[i]) / (u[i + j] - u[i]);
    c1 = (u[i + j + 1] - u) / (u[i + j + 1] - u[i + 1]);
    return c0 * N(i,j - 1,u) + c1 * N(i + 1,j - 1,u);
}
else // j == 0
{
    if (u[i] <= u && u < u[i + 1])
    {
        return 1;
    }
    else
    {
        return 0;
    }
}
}

Point X (float u)
{
    Point result = ZERO;
    for (i = 0; i <= n; ++i)
    {
        result += N(i,d,u) * B[i];
    }
    return result;
}

```

This is an inefficient algorithm because many of the basis functions are evaluated twice. For example, the value $N_{0,d}(u)$ requires computing $N_{0,d-1}(u)$ and $N_{1,d-1}(u)$. The value $N_{1,d}(u)$ also requires computing $N_{1,d-1}(u)$, as well as $N_{2,d-1}(u)$. The recursive dependencies are illustrated in Table 4.1 for $n = 4$ and $d = 2$. The various types of knot vectors are shown below the table of basis function values. The

Table 4.1 Recursive Dependencies for B-spline Basis Functions for $n = 4$ and $d = 2$

	$N_{0,2}$	$N_{1,2}$	$N_{2,2}$	$N_{3,2}$	$N_{4,2}$		
	↓	↓	↓	↓	↓	↓	↓
	$N_{0,1}$	$N_{1,1}$	$N_{2,1}$	$N_{3,1}$	$N_{4,1}$	$N_{5,1}$	
	↓	↓	↓	↓	↓	↓	↓
	$N_{0,0}$	$N_{1,0}$	$N_{2,0}$	$N_{3,0}$	$N_{4,0}$	$N_{5,0}$	$N_{6,0}$
Open uniform	0	0	[0	$\frac{1}{3}$	$\frac{2}{3}$	1)	1
Open nonuniform	0	0	[0	u_3	u_4	1)	1
Periodic	$-\frac{2}{3}$	$-\frac{1}{3}$	[0	$\frac{1}{3}$	$\frac{2}{3}$	1)	$\frac{4}{3}$
							$\frac{5}{3}$

rows of knot vectors include brackets [and parentheses). These indicate that an evaluation for a specified $u \in [0, 1]$ requires searching for the bounding interval $[u_i, u_{i+1})$ containing u . Only those knots in the bracketed portion need to be searched. The search returns the index of the left endpoint i , where $d \leq i \leq n$. For an open knot vector, the knots corresponding to other indices are included for padding. For a periodic knot vector, the knots corresponding to other indices are included to force the periodicity.

To avoid the redundant calculations, you might think to evaluate the table from the bottom up rather than from the top down. In our example you would compute $N_{i,0}(u)$ for $0 \leq i \leq 6$ and save these for later access. You would then compute $N_{i,1}(u)$ for $0 \leq i \leq 5$ and look up the values $N_{j,0}(u)$ as needed. Finally, you would compute $N_{i,2}(u)$ for $0 \leq i \leq 4$. The pseudocode follows.

```

Point X (float u)
{
    float basis[d + 1][n + d + 1]; // basis[j][i] = N(i,j)

    for (i = 0; i <= n + d; ++i)
    {
        if (u[i] <= u && u < u[i + 1])
        {
            basis[0][i] = 1;
        }
        else
        {
            basis[0][i] = 0;
        }
    }

    for (j = 1; j <= d; ++j)
    {
        for (i = 0; i <= n + d - j; ++i)
        {
            c0 = (u - u[i]) / (u[i + j] - u[i]);
            c1 = (u[i + j + 1] - u) / (u[i + j + 1] - u[i + 1]);
            basis[i][j] = c0 * basis[j - 1][i]
                + c1 * basis[j - 1][i + 1];
        }
    }

    Point result = ZERO;
    for (i = 0; i <= n; ++i)
    {
        result += basis[d][i] * B[i];
    }
    return result;
}

```

Table 4.2 Nonzero Values (boxed) from Table 4.1 for $N_{3,0}(u) = 1$

$N_{0,2}$	$N_{1,2}$	$N_{2,2}$	$N_{3,2}$	$N_{4,2}$		
\downarrow	\searrow	\downarrow	\searrow	\downarrow	\searrow	\downarrow
$N_{0,1}$	$N_{1,1}$	$N_{2,1}$	$N_{3,1}$	$N_{4,1}$	$N_{5,1}$	
\downarrow	\searrow	\downarrow	\searrow	\downarrow	\searrow	\downarrow
$N_{0,0}$	$N_{1,0}$	$N_{2,0}$	$N_{3,0}$	$N_{4,0}$	$N_{5,0}$	$N_{6,0}$

This is a reasonable modification but still not as efficient as it could be. For a single value of u , only *one* of $N_{i,0}(u)$ is 1; the others are all zero. In our example, suppose that $u \in [u_3, u_4]$, so that $N_{3,0}(u)$ is 1 and all other $N_{i,0}(u)$ are 0. The only nonzero entries from Table 4.1 are shown as boxed quantities in Table 4.2.

The boxed entries cover a triangular portion of the table. The values on the left diagonal edge and on the right vertical edge are computed first since each value effectively depends only on one previous value, the other value already known to be zero. If $N_{i,0}(u) = 1$, the left diagonal edge is generated by

$$N_{i-j,j}(u) = \frac{u_{i+1} - u}{u_{i+1} - u_{i-j+1}} N_{i-j+1,j-1}(u)$$

and the right vertical edge is generated by

$$N_{i,j}(u) = \frac{u - u_i}{u_{i+j} - u_i} N_{i,j-1}(u)$$

both evaluated for $1 \leq j \leq d$. The interior values are computed using the recursive formula, equation (4.8). The pseudocode for computing the curve point follows.

```

Point X (float u)
{
    float basis[d + 1][n + d + 1]; // basis[j][i] = N(i,j)

    // get i for which u[i] <= u < u[i + 1]
    i = GetKey(u);

    // evaluate left-diagonal and right-vertical edges
    for (j = 1; j <= d; ++j)
    {
        c0 = (u - u[i]) / (u[i + j] - u[i]);
        c1 = (u[i + 1] - u) / (u[i + 1] - u[i - j + 1]);
        basis[j][i] = c0 * basis[j-1][i];
        basis[j][i - j] = c1 * basis[j - 1][i - j + 1];
    }

    // evaluate interior
    for (j = 2; j <= d; ++j)

```

```

{
    for (k = i - j + 1; k < i; ++k)
    {
        c0 = (u - u[k]) / (u[k + j] - u[k]);
        c1 = (u[k + j + 1] - u) / (u[k + j + 1] - u[k + 1]);
        basis[j][k] = c0 * basis[j - 1][k] * fInvD0 +
                      c1 * basis[j - 1][k + 1];
    }

    Point result = ZERO;
    for (j = i - d; j <= i; ++j)
    {
        result += basis[d][j] * B[j];
    }
    return result;
}

```

The only remaining issue is how to compute index i from the input parameter u . For optimal efficiency, the computation should take into account whether the knot vector is open or periodic and if open, whether the knots are uniformly or nonuniformly spaced. The pseudocode follows. Observe that the choice is made to clamp u to $[0,1]$ when the spline is open and to wrap u to $[0,1]$ when the spline is periodic.

```

int GetKey (float& u) const
{
    if (knot vector is open) // open splines clamp to [0,1]
    {
        if (u <= 0)
        {
            u = 0;
            return d;
        }
        if (u >= 1)
        {
            u = 1;
            return n;
        }
    }
    else // periodic splines wrap to [0,1]
    {
        if (u < 0 || u > 1)
        {
            u -= floor(u);
        }
    }
}

int i;

```

```

        if (knots are uniformly spaced)
        {
            i = d + floor((n + 1 - d) * u);
        }
        else // knots are nonuniformly spaced
        {
            for (i = d + 1; i <= n + 1; ++i)
            {
                if (u < u[i])
                {
                    break;
                }
            }
            --i;
        }
        return i;
    }
}

```

In all cases the search for the bounding interval $[u_i, u_{i+1}]$ of u produces an index i , for which $d \leq i \leq n$, according to the discussion immediately following Table 4.1.

The basis function data and operations can be encapsulated into a class `BasisFunction` so that a B-spline curve class has a basis function objects for the parameter u . For the purpose of curve evaluation, only two public interface functions must exist for a `BasisFunction` class. One function computes the basis function values at u and returns the index i of the nonzero basis value $N_{i,0}(u)$, call it `int Compute(float u)`. The function returns the index i . The `GetKey` function described earlier becomes a nonpublic helper function for `Compute`. Another function is an accessor to the values $N_{i,d}(u)$, call it `float Basis(int i)`. The `BasisFunction` class stores the degree d internally, so only i needs to be passed. The curve evaluator does not need access to basis function values $N_{i,j}(u)$ for $j < d$. The B-spline curve itself can be encapsulated in a class `BSplineCurve`. This class manages the control points `B[]`, knows the degree d of the curve, and has a `BasisFunction` member called `Nu`. The curve evaluator becomes a member function of `BSplineCurve` and is

```

Point BSplineCurve::X (float u)
{
    int i = Nu.Compute(u);
    Point result = ZERO;
    for (int j = i - d; j <= i; ++j)
    {
        result += Nu.Basis(j) * B[j];
    }
    return result;
}

```

Local Control

Our goal is to dynamically modify the control points of the B-spline curve in order to deform only a portion of that curve. If we were to change exactly one control point \mathbf{B}_j in [equation \(4.6\)](#), what part of the curve is affected? The modified \mathbf{B}_j is blended into the curve equation via the basis function $N_{j,d}(u)$. The curve associated with those parameters u for which this function is not zero is affected by the change. The set of such u is exactly what we called the support of the function, in this case the interval $[u_j, u_{j+d+1}]$. The property such that changing a control point affects only a small portion of the curve is referred to as *local control*.

The practical application of local control is that in drawing the curve, you create a polyline approximation by selecting samples $\bar{u}_k \in [0, 1]$ for $0 \leq k < m$, with $\bar{u}_k < \bar{u}_{k+1}$ for all k . The curve points are $\mathbf{P}_k = \mathbf{X}(\bar{u}_k)$. The polyline consists of the line segments $\langle \mathbf{P}_k, \mathbf{P}_{k+1} \rangle$ for $0 \leq k < m - 1$. If we were to change control point \mathbf{B}_j , only some of the line segments need to be recomputed. Specifically, define k_{\min} and k_{\max} to be the extreme indices for which $\bar{u}_k \in [u_j, u_{j+d+1}]$. The polyline points \mathbf{P}_k for $k_{\min} \leq k \leq k_{\max}$ are the only ones to be recomputed.

Closed Curves

In order to obtain closed curves, additional control points must be included by the curve designer or automatically generated by the B-spline curve implementation. If the latter, and the implementation allows the user to dynamically modify control points, the additional control points must be modified accordingly.

Closing a B-spline curve with an open knot vector is simple. If the curve has control points \mathbf{B}_i for $0 \leq i \leq n$, the first control point must be duplicated, $\mathbf{B}_{n+1} = \mathbf{B}_0$. An additional knot must also be added. The extra knot is automatically calculated for uniformly spaced knots, but the curve designer must specify the extra knot for nonuniformly spaced knots.

Closing a B-spline curve with a periodic knot vector requires the first d control points to be duplicated, $\mathbf{B}_{n+i} = \mathbf{B}_i$ for $0 \leq i < d$. Since a periodic knot vector has uniformly spaced knots, the d additional knots are automatically calculated.

EXAMPLE 4.5

 SOURCE CODE
BSplineCurve-
Examples

[Figure 4.8](#) shows six pairs of B-spline curves, pairs (a)–(f). The left image in each pair is generated from the eight ordered control points $(0, 0)$, $(1, 0)$, $(2, 0)$, $(2, 1)$, $(2, 2)$, $(1, 2)$, $(0, 2)$, and $(0, 1)$. The right image uses the same control points except that $(2, 2)$ is replaced by $(2.75, 2.75)$. Also, the light gray portions of the curves in the right images are those points that were affected by modifying the control point $(2, 2)$ to $(2.75, 2.75)$. In order to avoid confusion between the two uses of the term open, a curve is labeled as either closed or not closed.

[Table 4.3](#) shows the knot vectors and the parameter intervals affected by modifying the control point $(2, 2)$. The nonuniform knot vectors were just chosen arbitrarily. The other knot vectors were automatically generated. ■

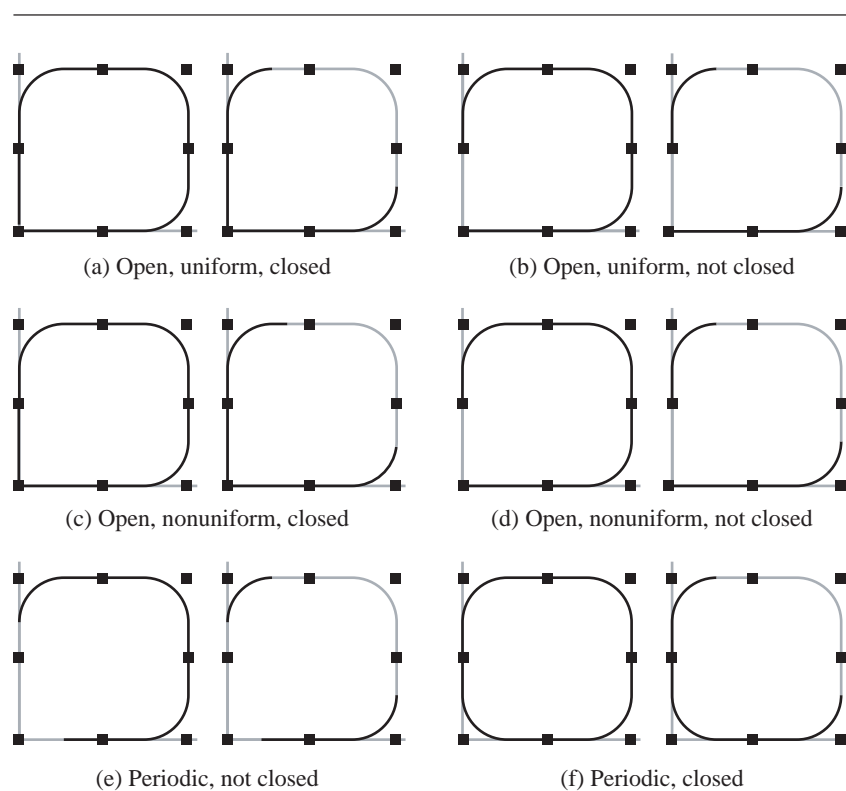


Figure 4.8 Six pairs of B-spline curves of various types. The right image of each pair shows the deformed curve by modifying one control point.

Table 4.3 Knot Vectors and Parameter Intervals Affected by Modifying the Control Point

Open, uniform, not closed	$\{0, 0, 0, \frac{1}{6}, \frac{2}{6}, \frac{3}{6}, \frac{4}{6}, \frac{5}{6}, 1, 1, 1\}$	$[\frac{2}{6}, \frac{5}{6}]$
Open, nonuniform, not closed	$\{0, 0, 0, 0.1, 0.2, 0.4, 0.7, 0.8, 1, 1, 1\}$	$[0.2, 0.8]$
Periodic, not closed	$\{-\frac{2}{6}, -\frac{1}{6}, 0, \frac{1}{6}, \frac{2}{6}, \frac{3}{6}, \frac{4}{6}, \frac{5}{6}, 1, \frac{7}{6}, \frac{8}{6}\}$	$[\frac{2}{6}, \frac{5}{6}]$
Open, uniform, closed	$\{0, 0, 0, \frac{1}{7}, \frac{2}{7}, \frac{3}{7}, \frac{4}{7}, \frac{5}{7}, \frac{6}{7}, 1, 1, 1\}$	$[\frac{2}{7}, \frac{5}{7}]$
Open, nonuniform, closed	$\{0, 0, 0, 0.1, 0.2, 0.4, 0.7, 0.8, 0.9, 1, 1, 1\}$	$[0.2, 0.8]$
Periodic, closed	$\{-\frac{2}{8}, -\frac{1}{8}, 0, \frac{1}{8}, \frac{2}{8}, \frac{3}{8}, \frac{4}{8}, \frac{5}{8}, \frac{6}{8}, \frac{7}{8}, 1, \frac{9}{8}, \frac{10}{8}\}$	$[\frac{2}{8}, \frac{5}{8}]$

4.3.2 NURBS CURVES

As we touched on earlier, NURBS is an acronym for **N**on**U**niform **R**ational **B**-**S**plice(s). B-spline curves are piecewise polynomial functions. The concept of NURBS provides a level of generality by allowing the curves to be piecewise, rational polynomial functions; that is, the curve components are ratios of polynomial functions. The mathematics of NURBS is quite deep and is described concisely in [Far99]. Not to de-emphasize the theoretical foundations, but for our purposes the use of NURBS is for the greater flexibility in constructing shapes than what B-splines provide.

The control points for a NURBS curve are \mathbf{B}_i for $0 \leq i \leq n$, just as in the case of B-spline curves. However, *control weights* are also provided, w_i for $0 \leq i \leq n$. The construction is dimensionless; the control points can be m -tuples. The idea for defining NURBS is quite simple. The $(m+1)$ -tuples $(w_i \mathbf{B}_i, w_i)$ are used to create a B-spline curve $(\mathbf{Y}(u), w(u))$. These tuples are treated as homogeneous coordinates. To project back to m -dimensional space, you divide by the last component: $\mathbf{X}(u) = \mathbf{Y}(u)/w(u)$. The degree d of the curve is selected so that $1 \leq d \leq n$. The NURBS curve is defined by

$$\mathbf{X}(u) = \frac{\sum_{i=0}^n N_{i,d}(u) w_i \mathbf{B}_i}{\sum_{i=0}^n N_{i,d}(u) w_i} \quad (4.9)$$

where $N_{i,d}(u)$ are the B-spline basis functions discussed earlier.

EXAMPLE 4.6

The classical example of the greater flexibility of NURBS compared to B-splines is illustrated in 2D. A quadrant of a circle cannot be represented using polynomial curves, but it can be represented as a NURBS curve of degree 2. The curve is $x^2 + y^2 = 1, x \geq 0, y \geq 0$. The general parameterization is

$$(x(u), y(u)) = \frac{w_0(1-u)^2(1,0) + w_1 2u(1-u)(1,1) + w_2 u^2(0,1)}{w_0(1-u)^2 + w_1 2u(1-u) + w_2 u^2}$$

for $u \in [0, 1]$. The requirement that $x^2 + y^2 = 1$ leads to the weights constraint $2w_1^2 = w_0 w_2$. The choice of weights $w_0 = 1$, $w_1 = 1$, and $w_2 = 2$ leads to a well-known parameterization:

$$(x(u), y(u)) = \frac{(1-u^2, 2u)}{1+u^2}$$

If you were to tessellate the curve with an odd number of uniform samples of u , say $u_i = i/(2n)$ for $0 \leq i \leq 2n$, then the resulting polyline is not symmetric about the midpoint $u = 1/2$. To obtain a symmetric tessellation, you need to choose $w_0 = w_2$. The weight constraint then implies $w_0 = w_1 \sqrt{2}$. The parameterization is then

$$(x(u), y(u)) = \frac{(\sqrt{2}(1-u)^2 + 2u(1-u), 2u(1-u) + \sqrt{2}u^2)}{\sqrt{2}(1-u)^2 + 2u(1-u) + \sqrt{2}u^2}$$

(Example 4.6
continued)

In either case we have a ratio of quadratic polynomials.

An algebraic construction of the same type, but quite a bit more tedious to solve, produces a ratio of quartic polynomials. The control points and control weights are required to be symmetric to obtain a tessellation that is symmetric about its midpoint. The middle weight is chosen as $w_2 = 4$ as shown:

$$(x(u), y(u)) = \frac{(1-u)^4 w_0(1,0) + 4(1-u)^3 u w_1(x_1, y_1) + 24(1-u)^2 u^2 (x_2, x_2) + 4(1-u) u^3 w_1(y_1, x_1) + u^4 w_0}{(1-u)^4 w_0 + 4(1-u)^3 u w_1 + 24(1-u)^2 u^2 + 4(1-u) u^3 w_1 + u^4 w_0}$$

The parameters are $x_1 = 1$, $y_1 = (\sqrt{3} - 1)/\sqrt{3}$, $x_2 = (\sqrt{3} + 1)/(2\sqrt{3})$, $w_0 = 4\sqrt{3}(\sqrt{3} - 1)$, and $w_1 = 3/\sqrt{2}$. ■

We already have all the machinery in place to deal with the basis functions. The NURBS curve can be encapsulated in a class `NURBSCurve` that manages the control points `B[]`, the control weights `W[]`, the degree `d`, and has a `BasisFunction` member `Nu`. The curve evaluator is

```
Point NURBSCurve::X (float u)
{
    int i = Nu.Compute(u);
    Point result = ZERO;
    float totalW = 0;
    for (int j = i-d; j <= i; ++j)
    {
        float tmp = Nu.Basis(j) * W[j];
        result += tmp * B[j];
        totalW += tmp;
    }
    result /= totalW;
    return result;
}
```

The next example shows a dynamic deformation of a planar NURBS curve and is used as the foundation for the three-dimensional deformation that we will see in Example 4.10

EXAMPLE 4.7

 SOURCE CODE
`NURBSCurveExample`

Consider a NURBS curve with 13 control points that are initially on the same straight line. The knot vector is open with uniformly spaced knots. The curve is necessarily a line segment. The control points must be moved to deform the central portion of the curve into a closed loop. The control weights are all 1 except for points 3, 5, 7, and 9, whose weights are 3/10. These weights were chosen to produce a final closed loop that is nearly circular. Figure 4.9 shows the initial line segment and its control points. It also shows how the control points evolve early in the process.

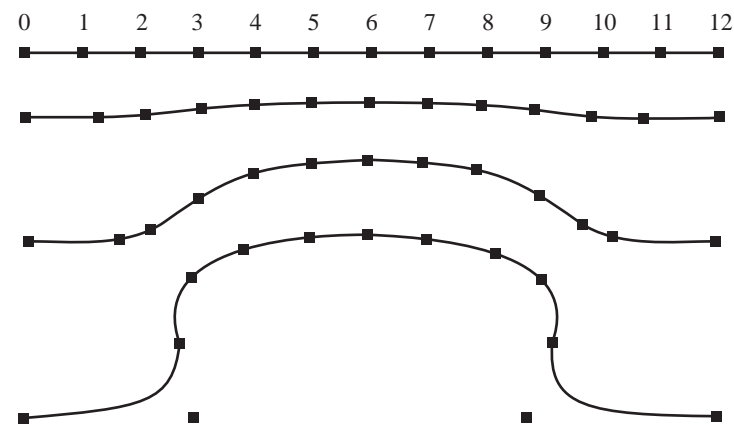


Figure 4.9

The initial control points and curve are shown at the top of the figure. The evolved control points and curve are shown at three later times, with time increasing from top to bottom in the figure.

The end control points 0 and 12 remain fixed. Control points 1 and 11 are constrained to lie on the initial line segment, but move towards the midpoint of the segment with constant speed; they will eventually coincide. Control points 5, 6, and 7 move vertically upward with constant speed. Control points 3 and 4 move towards the vertical line containing point 5. Control points 8 and 9 move towards the vertical line containing point 7. Control points 2 and 6 move towards the vertical line containing point 6 and will eventually coincide.

Figure 4.10 shows the control points and curves much further along in time. The time sequence is from (a) to (f). In image (e), control points 1 and 11 finally coincide, as do control points 2 and 6. At that instant the NURBS curve is split into two NURBS curves, as shown in image (f). The closed curve has a periodic knot vector. The closed curve continues to move vertically upward by uniform translations of the control points. The other curve has 5 control points with points 1 and 3 coinciding. The curve evolves back to a line segment by translating the middle control point 2 so that it too coincides with control points 1 and 3. Figure 4.11 shows an entire sequence of frames of the deformation. The sequence of images is top row to bottom row, left to right in each row. ■

4.3.3 B-SPLINE SURFACES

The simplest extension of the concept of B-spline curves to surfaces is to blend a rectangular array of control points \mathbf{B}_{i_0, i_1} for $0 \leq i_0 \leq n_0$ and $0 \leq i_1 \leq n_1$. The blending occurs separately in each dimension, leading to a *rectangle surface patch*. The degree

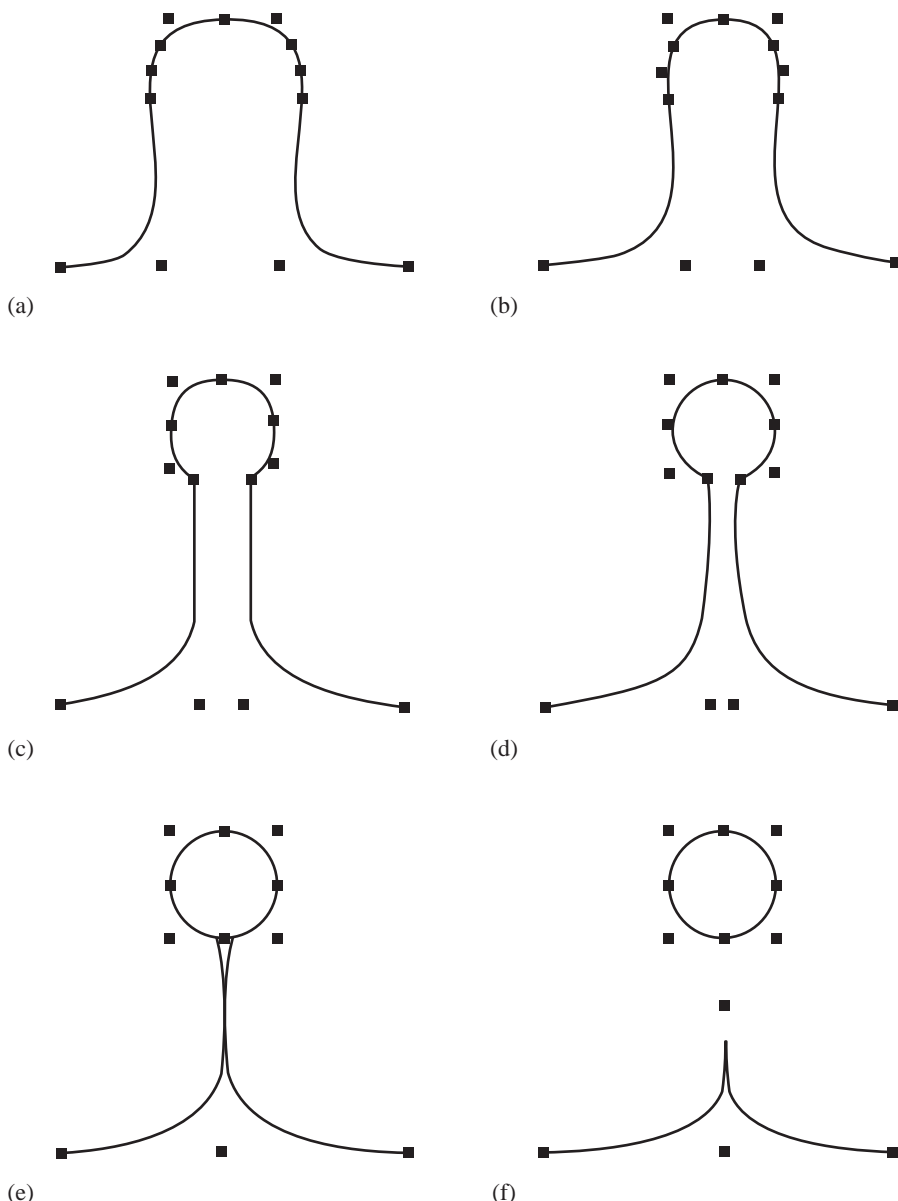


Figure 4.10 The control points and curve at later times in the evolution.

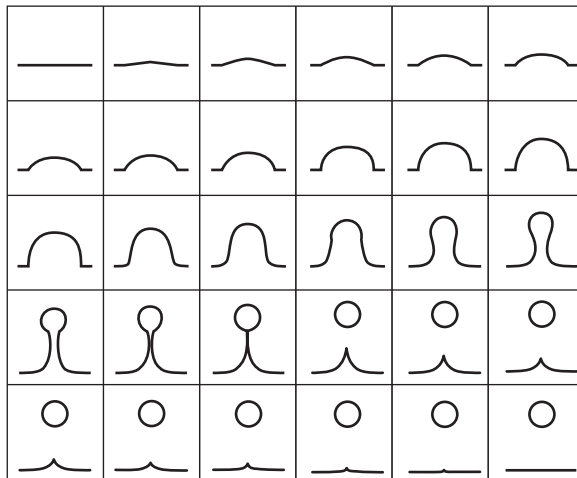


Figure 4.11 Deformation of a line segment into a closed curve that splits away from the original curve.

must be specified for each dimension, d_0 and d_1 with $1 \leq d_i \leq n_i$. The surface patch is defined by

$$\mathbf{X}(u, v) = \sum_{i_0=0}^{n_0} \sum_{i_1=0}^{n_1} N_{i_0, d_0}(u) N_{i_1, d_1}(v) \mathbf{B}_{i_0, i_1} \quad (4.10)$$

Once again we already have the mechanism in place for computing the basis functions. The B-spline surface is encapsulated in a class `BSplineSurface` and manages the control points `B[][]`, the degrees `d0` and `d1`, and has `BasisFunction` objects `Nu` and `Nv`. The surface evaluation is

```
Point BSplineSurface::X (float u, float v)
{
    int i0 = Nu.Compute(u), i1 = Nv.Compute(v);
    Point result = ZERO;
    for (int j0 = i0 - d0; j0 <= i0; ++j0)
    {
        for (int j1 = i1 - d1; j1 <= i1; ++j1)
        {
            result += Nu.Basis(j0) * Nv.Basis(j1) * B[j0][j1];
        }
    }
    return result;
}
```

4.3.4 NURBS SURFACES

B-spline surface patches are piecewise polynomial functions of two variables. NURBS surface patches are piecewise rational polynomial functions of two variables. Just as for curves, the construction involves fitting homogeneous points in one higher dimension with a B-spline surface ($\mathbf{Y}(u, v), w(u, v)$), then projecting back to your application space by dividing by the $w(u, v)$ term: $\mathbf{X}(u, v) = \mathbf{Y}(u, v)/w(u, v)$. NURBS surfaces have greater flexibility than B-spline surfaces.

A NURBS *rectangle surface patch* is built from control points \mathbf{B}_{i_0, i_1} and weights w_{i_0, i_1} for $0 \leq i_0 \leq n_0$ and $0 \leq i_1 \leq n_1$. The degrees d_i are user selected with $1 \leq d_i \leq n_i$. The surface patch is defined by

$$\mathbf{X}(u, v) = \frac{\sum_{i_0=0}^{n_0} \sum_{i_1=0}^{n_1} N_{i_0, d_0}(u) N_{i_1, d_1}(v) w_{i_0, i_1} \mathbf{B}_{i_0, i_1}}{\sum_{i_0=0}^{n_0} \sum_{i_1=0}^{n_1} N_{i_0, d_0}(u) N_{i_1, d_1}(v) w_{i_0, i_1}} \quad (4.11)$$

The B-spline construction in one higher dimension uses the homogeneous control points $(w_{i_0, i_1} \mathbf{B}_{i_0, i_1}, w_{i_0, i_1})$.

EXAMPLE
4.8

The classical example of the greater flexibility of NURBS compared to B-splines is illustrated in 3D. An octant of a sphere cannot be represented using a polynomial surface patch, but it can be represented as a triangular NURBS surface patch of degree 4. A simple parameterization of $x^2 + y^2 + z^2 = 1$ can be made by setting $r^2 = x^2 + y^2$. The sphere is then $r^2 + z^2 = 1$. Now apply the parameterization for a circle,

$$(r, z) = \frac{(1 - u^2, 2u)}{1 + u^2}$$

But $(x/r)^2 + (y/r)^2 = 1$, so another application of the parameterization for a circle is

$$\frac{(x, y)}{r} = \frac{(1 - v^2, 2v)}{1 + v^2}$$

Combining these produces

$$(x(u, v), y(u, v), z(u, v)) = \frac{((1 - u^2)(1 - v^2), (1 - u^2)2v, 2u(1 + v^2))}{(1 + u^2)(1 + v^2)}$$

The components are ratios of quartic polynomials. The domain is $u \geq 0, v \geq 0$, and $u + v \leq 1$. In barycentric coordinates, set $w = 1 - u - v$ so that $u + v + w = 1$ with u, v , and w nonnegative. In this setting, you can think of the octant of the sphere as a mapping from the uvw -triangle with vertices $(1, 0, 0)$, $(0, 1, 0)$, and $(0, 0, 1)$. Although a valid parameterization, a symmetric subdivision of the the uvw -triangle does not lead to a symmetric tessellation of the sphere.

Another parameterization is provided in [Far90]. This one chooses symmetric control points and symmetric weights:

$$(x(u, v), y(u, v), z(u, v)) = \frac{\sum_{i=0}^4 \sum_{j=0}^{4-i} w_{i,j,4-i-j} \mathbf{P}_{i,j,4-i-j} B_{i,j}(u, v)}{\sum_{i=0}^4 \sum_{j=0}^{4-i} w_{i,j,4-i-j} B_{i,j}(u, v)}$$

where

$$B_{i,j}(u, v) = \frac{4!}{i! j! (4-i-j)!} u^i v^j (1-u-v)^{4-i-j}, \quad u \geq 0, \quad v \geq 0, \quad u+v \leq 1$$

are the Bernstein polynomials. The control points $\mathbf{P}_{i,j,k}$ are defined in terms of three constants, $a_0 = (\sqrt{3}-1)/\sqrt{3}$, $a_1 = (\sqrt{3}+1)/(2\sqrt{3})$, and $a_2 = 1 - (5 - \sqrt{2})(7 - \sqrt{3})/46$:

$$\begin{array}{lll} \mathbf{P}_{040} & & (0, 1, 0) \\ \mathbf{P}_{031} \quad \mathbf{P}_{130} & & (0, 1, a_0) \quad (a_0, 1, 0) \\ \mathbf{P}_{022} \quad \mathbf{P}_{121} \quad \mathbf{P}_{220} & = & (0, a_1, a_1) \quad (a_2, 1, a_2) \quad (a_1, a_1, 0) \\ \mathbf{P}_{013} \quad \mathbf{P}_{112} \quad \mathbf{P}_{211} \quad \mathbf{P}_{310} & & (0, a_0, 1) \quad (a_2, a_2, 1) \quad (1, a_2, a_2) \quad (1, a_0, 0) \\ \mathbf{P}_{004} \quad \mathbf{P}_{103} \quad \mathbf{P}_{202} \quad \mathbf{P}_{301} \quad \mathbf{P}_{400} & & (0, 0, 1) \quad (a_0, 0, 1) \quad (a_1, 0, a_1) \quad (1, 0, a_0) \quad (1, 0, 0) \end{array}$$

The control weights $w_{i,j,k}$ are defined in terms of four constants, $b_0 = 4\sqrt{3}(\sqrt{3}-1)$, $b_1 = 3\sqrt{2}$, $b_2 = 4$, and $b_3 = \sqrt{2}(3 + 2\sqrt{2} - \sqrt{3})/\sqrt{3}$:

$$\begin{array}{lll} w_{040} & & b_0 \\ w_{031} \quad w_{130} & & b_1 \quad b_1 \\ w_{022} \quad w_{121} \quad w_{220} & = & b_2 \quad b_3 \quad b_2 \\ w_{013} \quad w_{112} \quad w_{211} \quad w_{310} & & b_1 \quad b_3 \quad b_3 \quad b_1 \\ w_{004} \quad w_{103} \quad w_{202} \quad w_{301} \quad w_{400} & & b_0 \quad b_1 \quad b_2 \quad b_1 \quad b_0 \end{array}$$

Both the numerator and denominator polynomial are quartic polynomials. Notice that each boundary curve of the triangle patch is a quartic polynomial of one variable that is exactly what was shown previously for a quadrant of a circle. ■

We can encapsulate NURBS rectangle patches into a class `NURBSSurface` and give it two `BasisFunction` members, just like we did for `BSplineSurface`. The class manages the control points `B[] []` and the control weights `W[] []`. The surface evaluation is

```
Point NURBSSurface::X (float u, float v)
{
    int i0 = Nu.Compute(u), i1 = Nv.Compute(v);
    Point result = ZERO;
    float totalW = 0;
    for (int j0 = i0 - d0; j0 <= i0; ++j0)
    {
        for (int j1 = i1 - d1; j1 <= i1; ++j1)
        {
```

```

        float tmp = Nu.Basis(j0) * Nv.Basis(j1) * W[j0][j1];
        result += tmp * B[j0][j1];
        totalW += tmp;
    }
}
result /= totalW;
return result;
}

```

4.3.5 SURFACES BUILT FROM CURVES

In order to avoid the complexity of dealing with a naturally defined surface patch such as B-spline or NURBS rectangle patches, sometimes it is convenient to build a surface from curves. The idea is that the curves are easier to work with and potentially lead to less expensive dynamic updates of the surface. A few types of surfaces built from curves are described here. In all cases the parameter space is $(u, v) \in [0, 1]$.

A triangle mesh is constructed by partitioning the parameter space into a rectangular grid, each rectangle representing two triangles. Figure 4.12 illustrates this.

The numbers n and m do not have to be the same. Generally you want a lot of samples in u to capture the shape of the curve (n large), but fewer samples in v since the surface is relatively flat in that direction (m small). The grid samples are $(u_i, v_j) =$

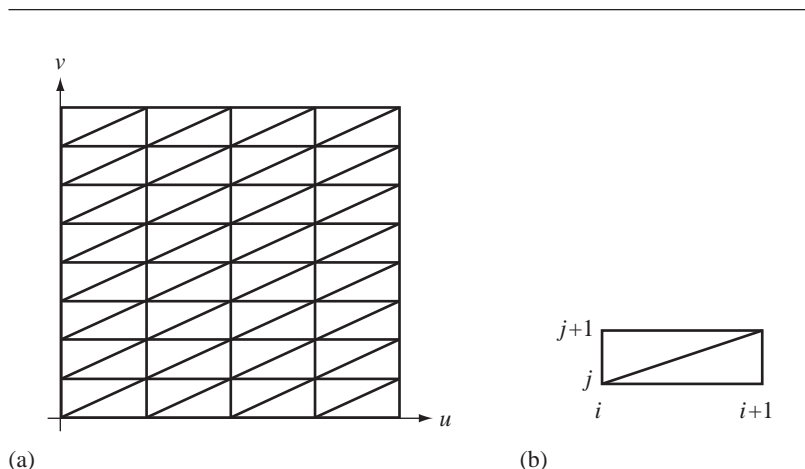


Figure 4.12 The decomposition of (u, v) space into an $n \times m$ grid of rectangles, each rectangle consisting of two triangles. A typical rectangle is shown in (b), with lower corner index (i, j) corresponding to $u = i/n$ and $v = j/m$.

$(i/n, j/m)$ for $0 \leq i < n$ and $0 \leq j < m$. The vertices are stored in a single array in lexicographic order: $k = i + nj$ where $0 \leq k < nm$. The triangles are stored in an array of triples of k -indices, a total of $2(n-1)(m-1)$ triples. Pseudocode to generate the vertices, normals, uniform texture coordinates, and triangles is as follows:

```

// generate vertices
//   X(u,v) = point on the surface at (u,v)
//   N(u,v) = normal on the surface at (u,v)
int vquantity = n*m;
Point3 vertex[vquantity], normal[vquantity];
Point2 texcoord[vquantity];

for (j = 0, k = 0; j < m; ++j)
{
    float v = j / (m - 1.0);
    for (i = 0; i < n; ++i)
    {
        float u = i / (n - 1.0);
        vertex[k] = X(u,v);
        normal[k] = N(u,v);
        texcoord[k] = Point2(u,v);
        k++;
    }
}

// generate triangles
int tquantity = 2 * (n - 1) * (m - 1);
int indices[3 * tquantity];
for (j = 0, k = 0; j < m - 1; ++j)
{
    for (i = 0; i < n - 1; i++)
    {
        int v0 = i + n * j;
        int v1 = v0 + 1;
        int v2 = v1 + n;
        int v3 = v0 + n;
        indices[k++] = v0;
        indices[k++] = v1;
        indices[k++] = v2;
        indices[k++] = v0;
        indices[k++] = v2;
        indices[k++] = v3;
    }
}

```

If the surface is closed in the u -direction, that is, $\mathbf{X}(1, v) = \mathbf{X}(0, v)$, the first and last columns of vertices of the mesh coincide. The texture coordinates of the first and last columns do not coincide, since the first column has $u = 0$ and the last column

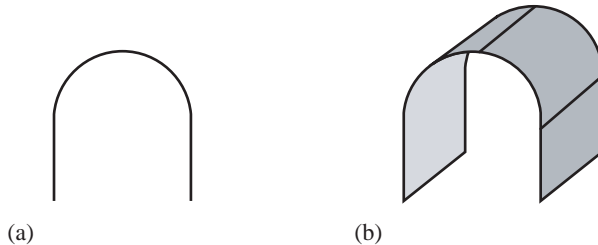


Figure 4.13 A cylinder surface (b) obtained by extruding the curve (a) in a direction oblique to the plane of the curve.

has $u = 1$. The texture image should be designed accordingly to make sure the seam is not visible. The same care must be taken if the surface is closed in the v -direction or in both directions.

Cylinder Surfaces

Surface patches might provide more curvature variation than is needed for a particular model. For example, a curved archway is curved in one dimension and flat in another. A single curve may be built to represent the curved dimension, then extruded linearly for the flat dimension. The surface obtained by this operation is said to be a *cylinder surface*. Figure 4.13 illustrates the process.

If $\mathbf{Y}(u)$ is a parameterization of the curve for $u \in [0, 1]$, and if \mathbf{D} is the desired amount of linear translation of the curve, the cylinder surface is parameterized by

$$\mathbf{X}(u, v) = \mathbf{Y}(u) + v\mathbf{D}$$

for $v \in [0, 1]$. First-order partial derivatives are $\partial \mathbf{X} / \partial u = \mathbf{Y}'(u)$ and $\partial \mathbf{X} / \partial v = \mathbf{D}$. Normal vectors to the surface are the cross product of the derivatives,

$$\mathbf{N}(u) = \frac{\mathbf{Y}'(u) \times \mathbf{D}}{|\mathbf{Y}'(u) \times \mathbf{D}|}$$

Notice that the normal does not depend on v .

Generalized Cylinder Surfaces

Some applications might require that a starting and ending curve be specified and an interpolation applied between them to generate a surface. This is called a *generalized cylinder surface*. Figure 4.14 illustrates.

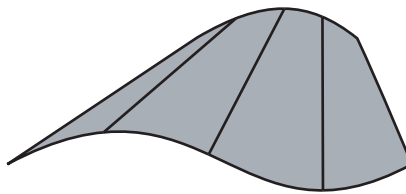


Figure 4.14 A generalized cylinder surface obtained by linearly interpolating pairs of points on two curves.

If $\mathbf{Y}_0(u)$ and $\mathbf{Y}_1(u)$ are the starting and ending curves, $u \in [0, 1]$, the generalized cylinder surface is parameterized by

$$\mathbf{X}(u, v) = (1 - v)\mathbf{Y}_0(u) + v\mathbf{Y}_1(u)$$

for $v \in [0, 1]$. The first-order derivatives are $\partial \mathbf{X} / \partial u = (1 - v)\mathbf{Y}'_0(u) + v\mathbf{Y}'_1(u)$ and $\partial \mathbf{X} / \partial v = \mathbf{Y}_1(u) - \mathbf{Y}_0(u)$. Normal vectors to the surface are

$$\mathbf{N}(u, v) = \frac{((1 - v)\mathbf{Y}'_0(u) + v\mathbf{Y}'_1(u)) \times (\mathbf{Y}_1(u) - \mathbf{Y}_0(u))}{|((1 - v)\mathbf{Y}'_0(u) + v\mathbf{Y}'_1(u)) \times (\mathbf{Y}_1(u) - \mathbf{Y}_0(u))|}$$

EXAMPLE 4.9



SOURCE CODE FlowingSkirt

This application shows a flowing skirt. The skirt is modeled as a generalized cylinder surface whose control points are varied over time to produce the deformation. [Figure 4.15](#) – also [Color Plate 4.15](#) – shows some screen shots from this application found on the CD-ROM. ■

Revolution Surfaces

A *revolution surface* is obtained by revolving a curve about a line that does not intersect the curve. To simplify the discussion, suppose that the line is the z -axis and the curve is $(x(u), z(u))$ in the xz -plane. The parameter $u \in [0, 1]$ and $x(u) > 0$. The intersection of the surface and a plane of constant z , given by $z(u)$ for a specified u , is a circle whose radius is $x(u)$ as shown by [Figure 4.16](#).

The surface is parameterized as

$$\mathbf{X}(u, v) = (x(u) \cos(2\pi v), x(u) \sin(2\pi v), z(u))$$

for $(u, v) \in [0, 1]^2$.

EXAMPLE 4.10



SOURCE CODE WaterSphere-Formation

The curve deformation in [Example 4.7](#) may be used to generate a control point deformation of a surface. The surface is constructed as a surface of revolution of the curve about the vertical axis. [Figure 4.17](#) – also [Color Plate 4.17](#) – shows some screen shots from this application found on the CD-ROM. ■

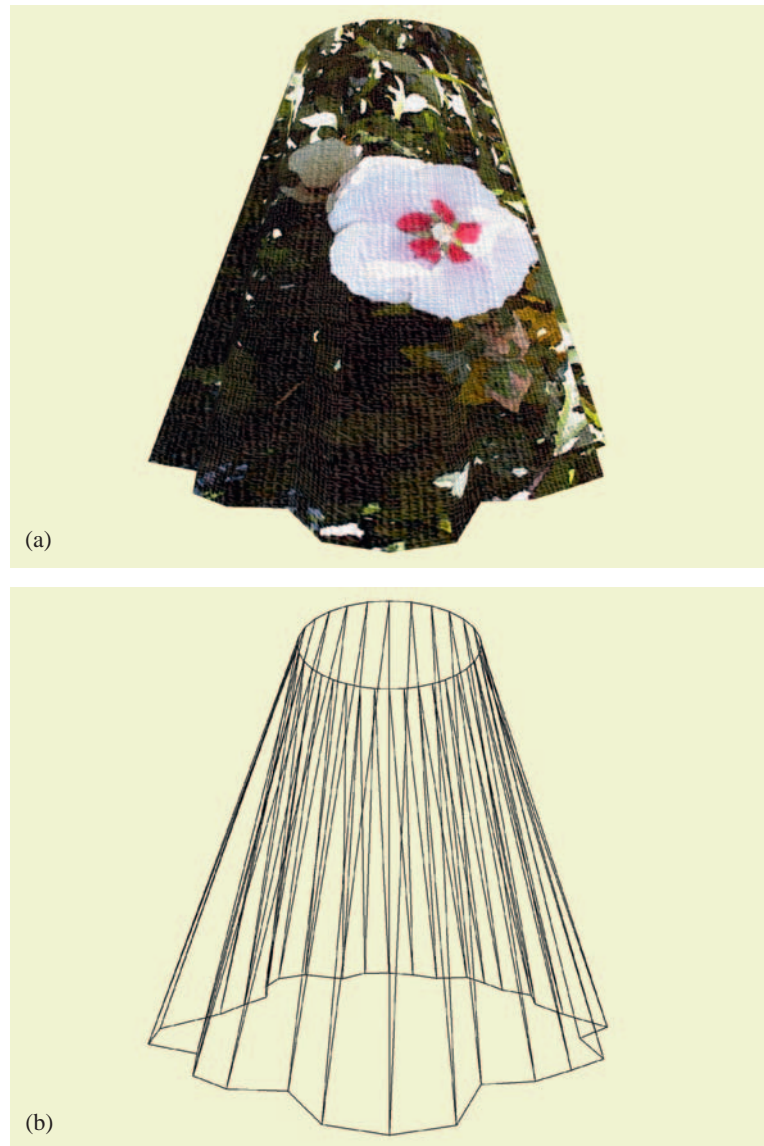


Figure 4.15 A skirt modeled by a generalized cylinder surface. Wind-like forces are acting on the skirt and are applied in the radial direction. Image (a) shows the skirt after wind is blowing it about. Image (b) shows a wireframe view of the skirt so that you can see it consists of two closed curve boundaries and is tessellated between. (See also [Color Plate 4.15](#).)

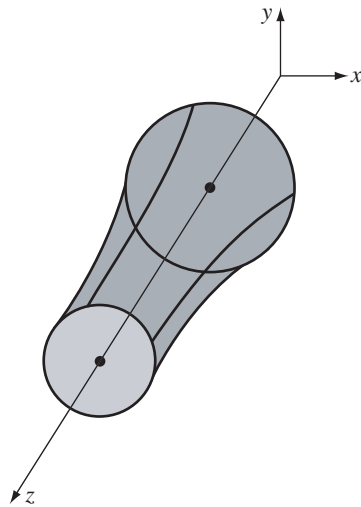


Figure 4.16 A surface of revolution.



Tube Surfaces

A surface in the shape of a tube can be generated by specifying the central curve of the tube, say $\mathbf{C}(v)$ for $v \in [0, 1]$, and by specifying a closed planar curve $\mathbf{Y}(u) = (y_1(u), y_2(u))$ to represent the boundary of a cross section of the surface. The cross section for a given v is within a plane whose coordinate system has origin $\mathbf{C}(v)$ and one unit-length coordinate direction $\mathbf{T}(v) = \mathbf{C}'(v)/|\mathbf{C}'(v)|$, a tangent to the central curve. The other two unit-length coordinate directions are chosen as desired, call them $\mathbf{N}(v)$ and $\mathbf{B}(v)$. The three vectors form a right-handed orthonormal set. The names are suggestive of using the Frenet frame for the curve, where \mathbf{N} is the curve normal and $\mathbf{B} = \mathbf{T} \times \mathbf{N}$ is the curve binormal. However, other choices are always possible. The tube surface is constructed as

$$\mathbf{X}(u, v) = \mathbf{C}(v) + y_1(u)\mathbf{N}(v) + y_2(u)\mathbf{B}(v)$$

for $(u, v) \in [0, 1]^2$. The classical tube surface is one whose cross sections are circular, $\mathbf{Y}(u) = r(\cos u, \sin u)$ for a positive radius r . More generally, the radius can be allowed to vary with v . For example, a surface of revolution is a tube surface whose central curve is a line segment and whose radius varies based on the curve that was revolved about the line segment. Figure 4.18 – also Color Plate 4.18 – shows a tube surface that was built so that the inside surface is visible to the camera.

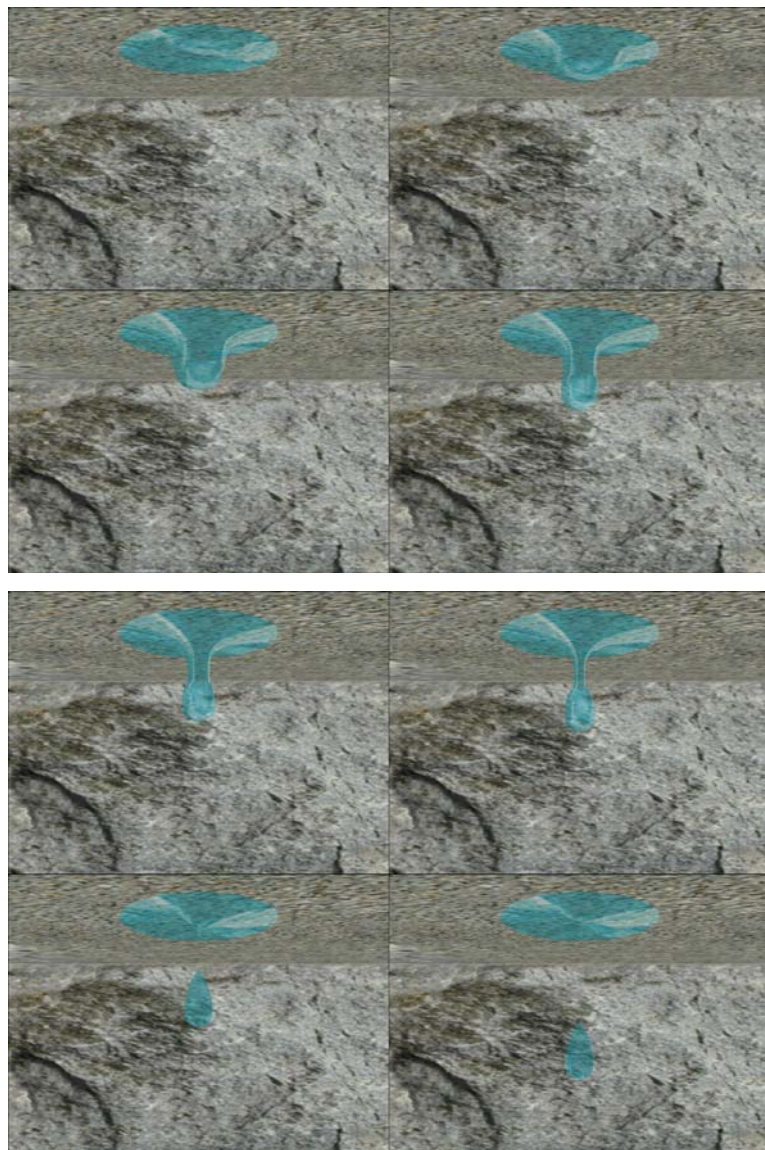


Figure 4.17 A water drop modeled as a control point surface of revolution. The surface dynamically changes to show the water drop forming, separating from the main body of water, then falling to the floor. The evolution is from left to right and top to bottom. (See also Color Plate 4.17.)

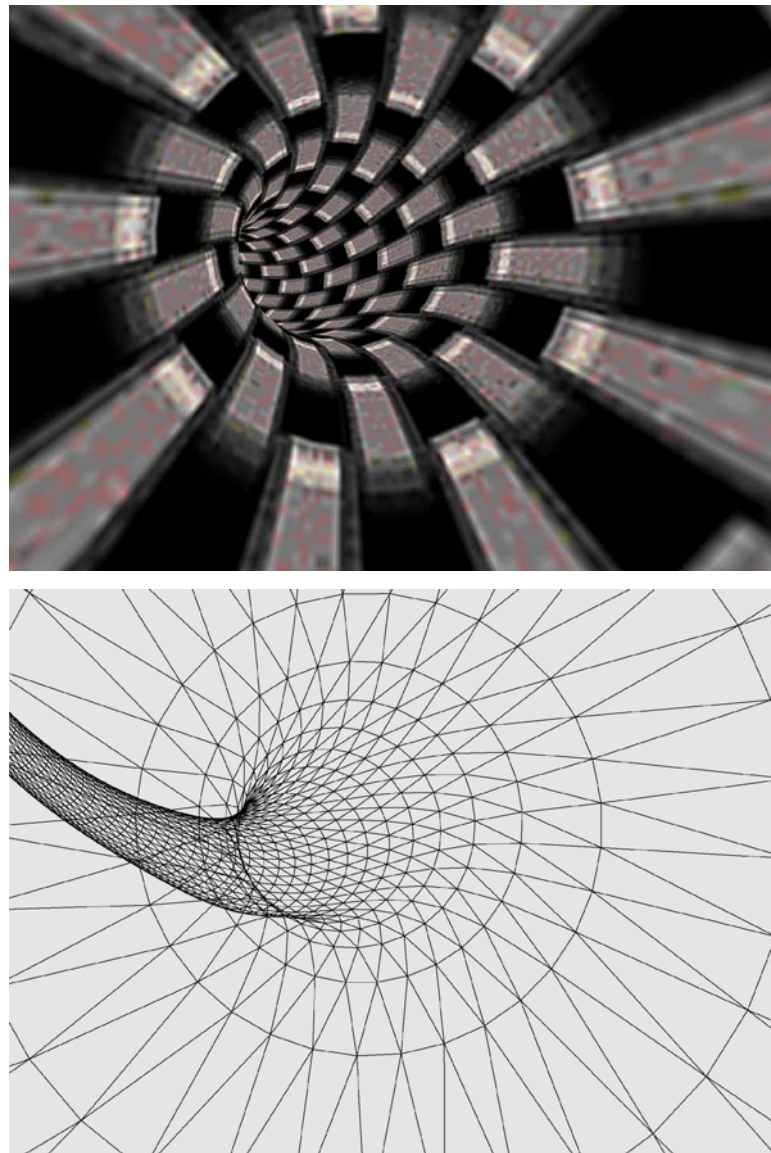


Figure 4.18 A closed tube surface whose central axis is a helix. (See also [Color Plate 4.18](#).)

We now look at an example of a deformation of a tube surface. The central curve of the tube is a control point curve. The control points are modified over time, thereby causing the tube surface itself to deform over time.

EXAMPLE
4.11


SOURCE CODE
WrigglingSnake

This application shows a wriggling snake. The snake is modeled as a tube surface whose central curve is a control point curve. The control points are varied over time to produce the deformation. [Figure 4.19](#) – also [Color Plate 4.19](#) – shows some screen shots from this application found on the CD-ROM. ■

4.4 FREE-FORM DEFORMATION

The deformation methods of the last section are useful for deforming a surface that is defined parametrically based on user-specified control points. In a game environment we need to display the deforming object in addition to handling it in a physical simulation. The typical representation of an object in the game is a triangle mesh. The parametric surface may be tessellated to produce that representation. Although the resulting mesh is required for display, that same mesh might also be used if the object participates in a collision detection system. The mesh dynamically changes as the control points are deformed, the vertices having to be recalculated after each modification of the control points. The triangle connectivity can be calculated once and maintained during the deformations.

In many cases, though, the triangle meshes are constructed by artists using a modeling package. No underlying control point surface is used to build those meshes. If the game application requires deforming these meshes, how do we do this? Certainly it is possible to construct a control point surface that, in some sense, approximates the triangle mesh. However, that is generally a difficult algorithm to implement and even more difficult to obtain approximations that an artist will agree looks like the original mesh.

A good alternative is to embed the triangle mesh in a volume of space that itself may be deformed via control points. The parameterization of the volume by three parameters is just the natural extension of the parameterization of surfaces by two parameters. The vertices of the triangle mesh initially are assigned parameters based on where they lie in the volume. The control points of the volume are then modified dynamically, causing a deformation of the volume, which in turn causes the vertices to move about. This process is called *free-form deformation* (FFD) and was formally introduced in [SP86], but earlier works exist regarding volume deformation with the goal of analyzing surface deformation, for example [Bar84]. The FFD algorithm uses a blending of control points using Bernstein polynomials, producing a Bézier volume patch that is a natural extension of a Bézier rectangle patch. A B-spline representation of the volume may be used instead [GP89].

Equation (4.10) extends to a lattice of control points $\mathbf{B}_{i_0, i_1, i_2}$ for $0 \leq i_0 \leq n_0$, $0 \leq i_1 \leq n_1$, and $0 \leq i_2 \leq n_2$. The degree must be specified for each dimension, d_0 , d_1 , and

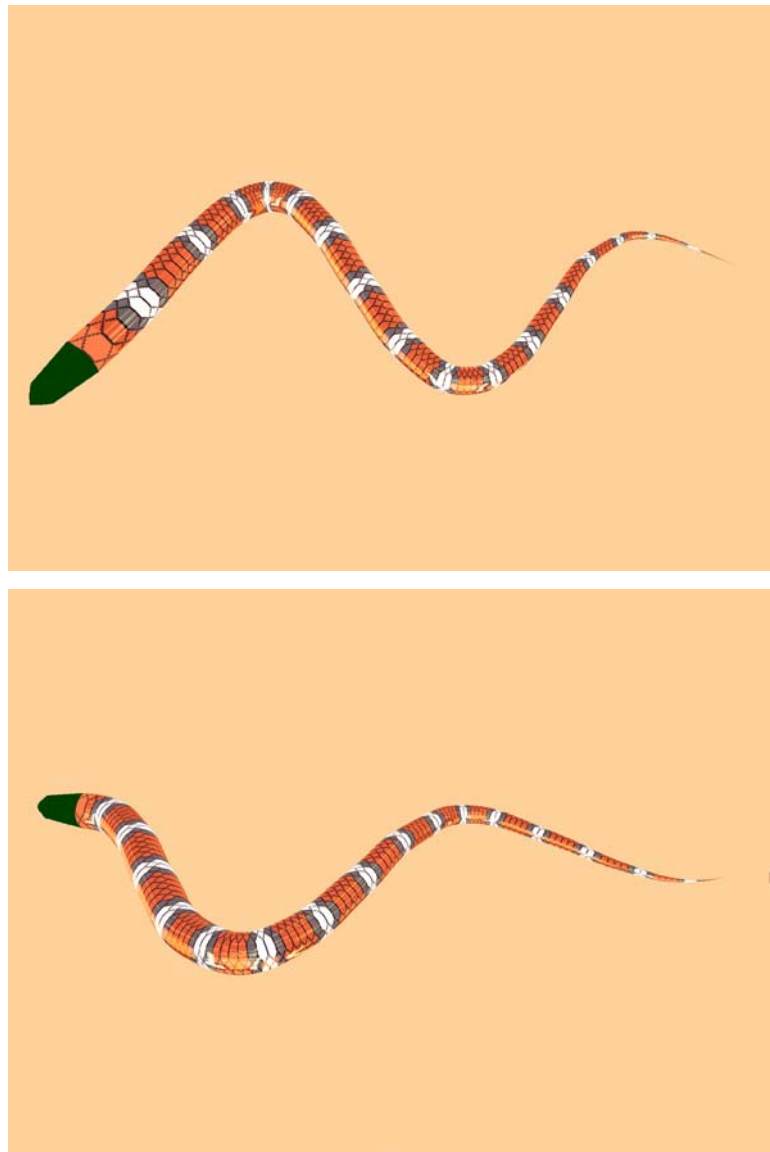


Figure 4.19 A wriggling snake modeled as a tube surface whose central curve is a control point curve. (See also [Color Plate 4.19](#).)

d_2 with $1 \leq d_i \leq n_i$. The volume patch is defined by

$$\mathbf{X}(u, v, w) = \sum_{i_0=0}^{n_0} \sum_{i_1=0}^{n_1} \sum_{i_2=0}^{n_2} N_{i_0, d_0}(u) N_{i_1, d_1}(v) N_{i_2, d_2}(w) \mathbf{B}_{i_0, i_1, i_2} \quad (4.12)$$

Just as for B-spline curves and surfaces, we have the mechanism in place for computing the basis functions. The B-spline volume is encapsulated in a class `BSplineVolume` and manages the control points `B[][][]` and the degrees `d0`, `d1`, and `d2` and has `BasisFunction` objects `Nu`, `Nv`, and `Nw`. The volume evaluation is

```
Point BSplineVolume::X (float u, float v, float w)
{
    int i0 = Nu.Compute(u);
    int i1 = Nv.Compute(v);
    int i2 = Nw.Compute(w);
    Point result = ZERO;
    for (int j0 = i0 - d0; j0 <= i0; ++j0)
    {
        for (int j1 = i1 - d1; j1 <= i1; ++j1)
        {
            for (int j2 = i2 - d2; j2 <= i2; ++j2)
            {
                result += Nu.Basis(j0) * Nv.Basis(j1) *
                           Nw.Basis(j2) * B[j0][j1][j2];
            }
        }
    }
    return result;
}
```

Assuming the control points are selected so that the volume patch encloses the application's triangle mesh, for each mesh vertex \mathbf{P}_i we need to compute the corresponding parameters (u_i, v_i, w_i) so that $\mathbf{X}(u_i, v_i, w_i) = \mathbf{P}_i$. In general, this is a difficult problem in that this equation represents three polynomial equations of three unknown variables that must be solved by some numerical method. Keeping in mind our application is to deform the mesh, we can make this a simple problem. Choose the control points so that the initial volume is an axis-aligned box containing the triangle mesh. If the box is $[x_{\min}, x_{\max}] \times [y_{\min}, y_{\max}] \times [z_{\min}, z_{\max}]$, then the control points are

$$\mathbf{B}_{i_0, i_1, i_2} = \mathbf{M} + (\Delta_x i_0, \Delta_y i_1, \Delta_z i_2)$$

where $\mathbf{M} = (x_{\min}, y_{\min}, z_{\min})$, $\Delta_x = (x_{\max} - x_{\min})/n_0$, $\Delta_y = (y_{\max} - y_{\min})/n_1$, and $\Delta_z = (z_{\max} - z_{\min})/n_2$. The volume function reduces as follows:

$$\begin{aligned} \mathbf{X}(u, v, w) &= \sum_{i_0=0}^{n_0} \sum_{i_1=0}^{n_1} \sum_{i_2=0}^{n_2} N_{i_0, d_0}(u) N_{i_1, d_1}(v) N_{i_2, d_2}(w) (\mathbf{M} + (\Delta_x i_0, \Delta_y i_1, \Delta_z i_2)) \\ &= c_0 \mathbf{M} + c_1 \Delta_x \mathbf{i} + c_2 \Delta_y \mathbf{j} + c_3 \Delta_z \mathbf{k} \end{aligned}$$

where

$$\begin{aligned}
c_0 &= \sum_{i_0=0}^{n_0} \sum_{i_1=0}^{n_1} \sum_{i_2=0}^{n_2} N_{i_0, d_0}(u) N_{i_1, d_1}(v) N_{i_2, d_2}(w) \\
&= \left(\sum_{i_0=0}^{n_0} N_{i_0, d_0}(u) \right) \left(\sum_{i_1=0}^{n_1} N_{i_1, d_1}(v) \right) \left(\sum_{i_2=0}^{n_2} N_{i_2, d_2}(w) \right) \\
&= 1 \cdot 1 \cdot 1 = 1
\end{aligned}$$

We used the well-known property for basis functions, $\sum_{i=0}^n N_{i,d}(t) = 1$ for all $t \in [0, 1]$. Similarly,

$$\begin{aligned}
c_1 &= \sum_{i_0=0}^{n_0} \sum_{i_1=0}^{n_1} \sum_{i_2=0}^{n_2} i_0 N_{i_0, d_0}(u) N_{i_1, d_1}(v) N_{i_2, d_2}(w) \\
&= \left(\sum_{i_0=0}^{n_0} i_0 N_{i_0, d_0}(u) \right) \left(\sum_{i_1=0}^{n_1} N_{i_1, d_1}(v) \right) \left(\sum_{i_2=0}^{n_2} N_{i_2, d_2}(w) \right) \\
&= u \cdot 1 \cdot 1 = u
\end{aligned}$$

where we use the property $\sum_{i=0}^n N_{i,d}(t) = t$ for $t \in [0, 1]$. The same argument shows that $c_2 = v$ and $c_3 = w$. Therefore,

$$\mathbf{X}(u, v, w) = \mathbf{M} + n_0 \Delta_x u \mathbf{i} + n_1 \Delta_y v \mathbf{j} + n_2 \Delta_z w \mathbf{k}$$

for the initially selected control points. The parameters to locate a mesh vertex $\mathbf{P}_i = \mathbf{X}(u_i, v_i, w_i)$ are simply $u_i = \mathbf{i} \cdot (\mathbf{P}_i - \mathbf{M})/\Delta_x$, $v_i = \mathbf{j} \cdot (\mathbf{P}_i - \mathbf{M})/\Delta_y$, and $w_i = \mathbf{k} \cdot (\mathbf{P}_i - \mathbf{M})/\Delta_z$.

The straightforward approach to deforming the surface is to modify the control points and recompute $\mathbf{X}(u_i, v_i, w_i)$ for all i . Although this certainly works, it is less efficient than it can be. The input parameters never change for a mesh vertex. Each time the B-spline volume function is calculated, the basis functions $N_{i_0, d_0}(u_i)$, $N_{i_1, d_1}(v_i)$, and $N_{i_2, d_2}(w_i)$ are calculated. These may be calculated once and stored for use in later volume evaluations. Another optimization is possible if only a few control points are modified at each step. To indicate the dependence of the volume function on the control points, let us write the function as $\mathbf{X}(u, v, w; \mathbf{B})$. The mesh vertex positions for the initial set of control points are

$$\mathbf{P}_i = \mathbf{X}(u_i, v_i, w_i; \mathbf{B})$$

for all i . The control points are modified to $\mathbf{B}_{i_0, i_1, i_2} + \mathbf{d}\mathbf{B}_{i_0, i_1, i_2}$ where the control point perturbations might be nonzero only for a few control points. In an interactive modeling package, the interface will most likely support dragging one control point at a time, in which case $\mathbf{d}\mathbf{B}_{i_0, i_1, i_2}$ is nonzero for exactly one triple of indices, but zero for all the others. The new mesh vertex positions are

$$\mathbf{Q}_i = \mathbf{X}(u_i, v_i, w_i; \mathbf{B} + \mathbf{d}\mathbf{B}) = \mathbf{X}(u_i, v_i, w_i; \mathbf{B}) + \mathbf{X}(u_i, v_i, w_i; \mathbf{d}\mathbf{B}) = \mathbf{P}_i + \mathbf{d}\mathbf{P}_i$$

where the perturbation of the old mesh vertices is denoted by $\mathbf{dP}_i = \mathbf{X}(u_i, v_i, w_i; \mathbf{dB})$. If you keep track of the original mesh vertices and measure only the control point perturbations, the new mesh vertices may be rapidly computed. The evaluation of the perturbation $\mathbf{X}(u_i, v_i, w_i; \mathbf{dB})$ is implemented to avoid multiplying the basis functions by a point $\mathbf{dB}_{i_0, i_1, i_2}$ when that point is the zero vector.

EXAMPLE
4.12


This programming example is a full implementation of the free-form deformation using a B-spline volume function. The application constructs the axis-aligned bounding box for a triangle mesh, computes the parameter triples for the mesh vertices, and displays the mesh. The volume is drawn as a wireframe box with line segments connecting the control points. The interface allows you to select a control point and drag it with the mouse. For each change the embedded triangle mesh is updated. The program also has an option for randomly perturbing the current set of control points so that the mesh wiggles. This option is toggled with the r/R keys. Figure 4.20 – also Color Plate 4.20 – shows some screen shots from this application on the CD-ROM. ■

The ideas of FFD have been extended by various researchers. An *extended free-form deformation* (EFFD) was developed in [Coq90], and it allows the surface to be embedded in a collection of multiple volumes to gain better control over the spatial deformations. These results were developed more from an engineering perspective than from a desire to obtain physically meaningful deformations. Along the latter lines the paper [HML99] describes an algorithm to preserve the total volume enclosed by the surface during the deformation. This is a reasonable goal, but it implicitly assumes that the object's mass density is constant throughout the deformation. For some objects this assumption makes sense, but for others it does not. Consider a foam ball that is deformed by squeezing it. Clearly, the volume is not preserved, but the total mass is preserved. The next step in developing deformation models of the free-form type should have the goal of modifying the mass density function so that the total mass is preserved. By accurately computing the mass density during deformation, the inertia tensor for the deformed object can then be calculated for use in physical simulations.

4.5 IMPLICIT SURFACE DEFORMATION

A body is modeled as the region $F(x, y, z) \leq 0$ for a suitably chosen function F . The surface of the body is implicitly defined by $F(x, y, z) = 0$. A force on the body is simulated by adding a deformation function $D(x, y, z)$ to $F(x, y, z)$. The deformed body is the region $F(x, y, z) + D(x, y, z) \leq 0$ and has a surface implicitly defined by $F(x, y, z) + D(x, y, z) = 0$. A simple example in two dimensions will illustrate the concept.

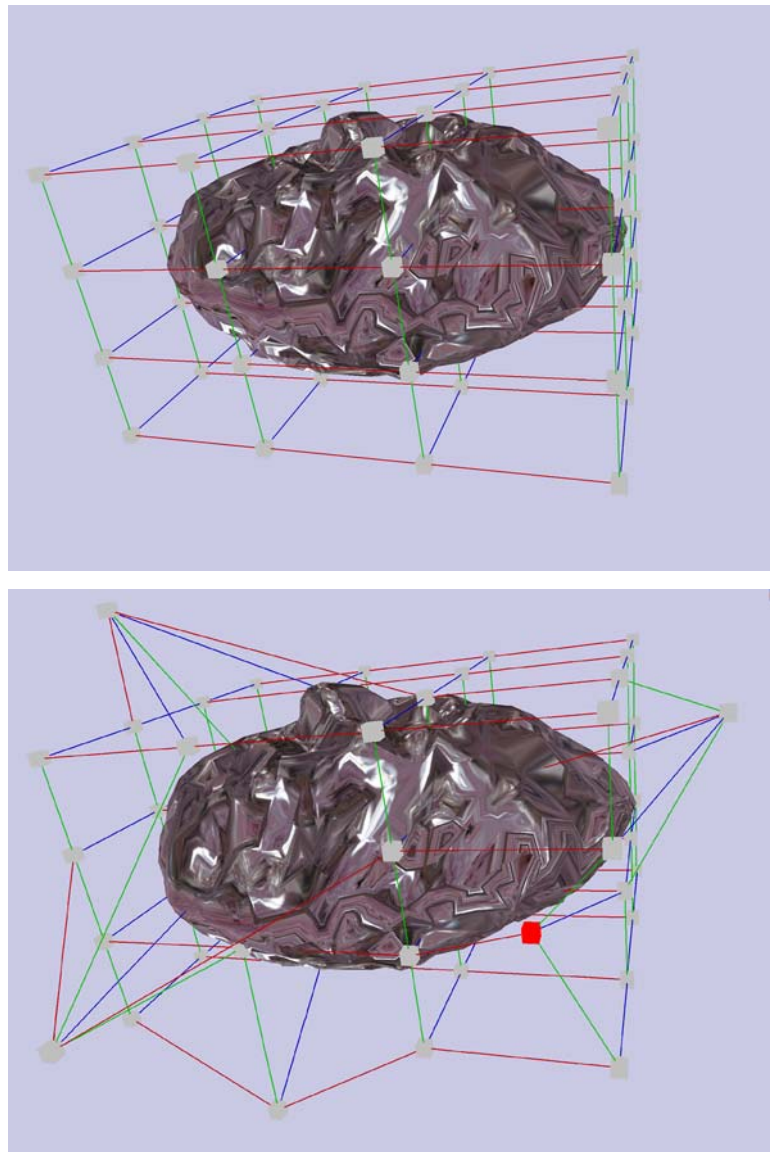


Figure 4.20 Free-form deformation. Image (a) shows the initial configuration where all control points are rectangularly aligned. Image (b) shows that some control points have been moved and the surface is deformed. The control point shown in red in (b) is the point at which the mouse was clicked on and moved. (See also Color Plate 4.20.)

EXAMPLE
4.13

Consider a planar body in the shape of a circular disk defined by $F(x, y) = x^2 + y^2 - 1 \leq 0$. The boundary of the object is the circle defined by $F(x, y) = 0$, namely $x^2 + y^2 = 1$. Figure 4.21(a) illustrates the object before deformation.

A force is to be applied to the body at the point $(1, 0)$ to produce a deformed body, with some possibilities shown in Figure 4.21(c)–(f). You have a lot of flexibility in choosing the deformation functions. A simple one to illustrate is

$$D(x, y) = \begin{cases} A(1 - 4((x - 1)^2 + y^2)), & (x - 1)^2 + y^2 < 1/4 \\ 0, & \text{otherwise} \end{cases}$$

This function is continuous. It is differentiable everywhere except on the circle $(x - 1)^2 + y^2 = 1/4$. This small circle intersects the original one at $x = 7/8$. Outside this circle the level curve is defined by $F(x, y) = 0$ and produces a large circular arc $x^2 + y^2 = 1$ for $x \leq 7/8$. Inside this circle the level curve is

$$0 = F(x, y) + D(x, y) = (1 - 4A)x^2 + (1 - 4A)y^2 + 8Ax - (1 + 3A)$$

If $A = 1/4$, the level curve is the line segment $x = 7/8$ with $|y| \leq \sqrt{15}/8$. For $A \neq 1/4$, divide by $1 - 4A$ and complete the square on x to obtain the factored equation:

$$\left(x + \frac{4A}{1 - 4A}\right)^2 + y^2 = \frac{1 - A + 4A^2}{(1 - 4A)^2}$$

This is the equation for a circle. Notice that the endpoints of the large circular arc, $(7/8, \pm\sqrt{15}/8)$, are always on the arc defined by this new circle.

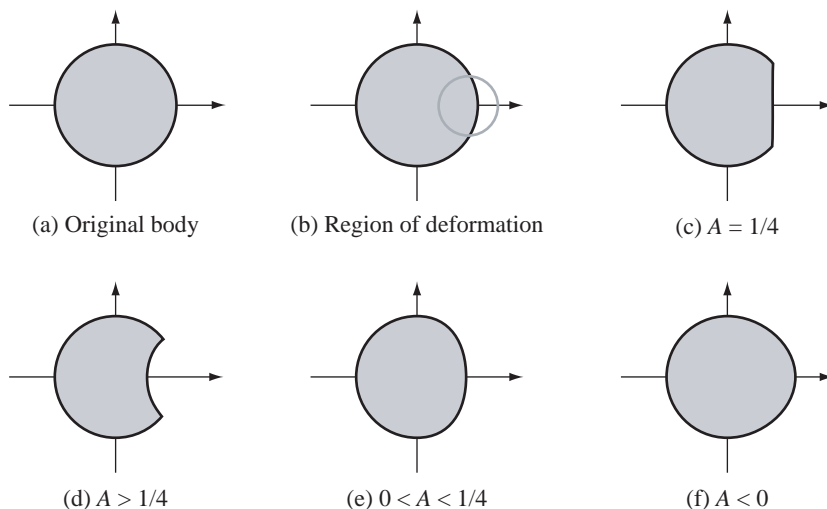


Figure 4.21

A disk-shaped body and various deformations of it.

A time-varying deformation may be induced by allowing the amplitude A of the deformation to vary with time. For example, $A(t) = ct$ for a positive constant c causes a gradual depression in the disk. Oscillatory behavior can be induced by something like $A(t) = c \sin(t)$ for a positive constant c . ■

In the example the deformation $D(x, y)$ is symmetric about the point $(1, 0)$, that center point considered to be the point of application of the simulated force. Generally, D is neither required to be symmetric nor to be viewed as having a center point that is on the boundary of the object. We could just have easily added $D(x, y) = A(1 - 4((x - x_0)^2 + (y - y_0)^2))$ for any point (x_0, y_0) in the plane. Of course if the region of influence does not intersect the level curve defining the object boundary, no deformation occurs.

The example is also a continuous one. In practice we will have discrete objects, polygonal objects in the plane (approximations to the level curve object boundaries), and triangle mesh objects in space (approximations to the level surface object boundaries). Given a continuous representation $F = 0$ of the object boundary, we need to construct the approximations. This requires extraction of curves or surfaces from data generated by sampling F on a regular lattice. The curves and surfaces are extracted from the data using methods from image analysis. Keeping in mind we want to have a reasonably fast simulation, the deformation D can be defined to be nonzero within a small region so that only a handful of pixels/voxels will be affected by the deformation. The level curves/surfaces need be updated only at those pixels/voxels.

4.5.1 LEVEL SET EXTRACTION

A standard isosurface extraction algorithm for a 3D image is the Marching Cubes algorithm [LC87]. The image is assumed to be defined on a regular lattice of size $N_0 \times N_1 \times N_2$ with integer points (x, y, z) , where $0 \leq x < N_0$, $0 \leq y < N_1$, and $0 \leq z < N_2$. The image values themselves are $F(x, y, z)$. An isosurface is of the form $F(x, y, z) = c$ for some specified level value c , where x , y , and z are treated as continuous variables. A voxel in the image is a rectangular solid whose corners are eight neighboring lattice points (x_0, y_0, z_0) , $(x_0 + 1, y_0, z_0)$, $(x_0, y_0 + 1, z_0)$, $(x_0 + 1, y_0 + 1, z_0)$, $(x_0, y_0, z_0 + 1)$, $(x_0 + 1, y_0, z_0 + 1)$, $(x_0, y_0 + 1, z_0 + 1)$, and $(x_0 + 1, y_0 + 1, z_0 + 1)$. Figure 4.22 illustrates the level surface contained by a single voxel.

The Marching Cubes algorithm analyzes each voxel in the image and determines if the isosurface intersects it. If so, the algorithm produces a triangle mesh for the voxel that is intended to approximate that portion of the isosurface inside the voxel. By selecting a level value that cannot be an image value, for example, by selecting a noninteger value when the image has only integer values, the voxel analysis requires determining the signs of $G(x, y, z) = F(x, y, z) - c$ at the eight corners, each sign positive or negative. If two adjacent corners have opposite signs, and if the image values are assumed to be linear along the edge connecting the corners, the isosurface $G(x, y, z) = 0$ must intersect the edge in a single point somewhere along the edge. The

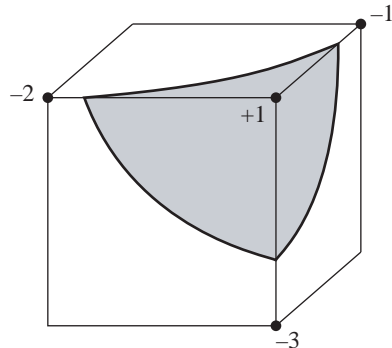


Figure 4.22 This is an illustration of a level surface $F(x, y, z) = 0$, a cube whose eight corners correspond to image samples. Four of the image values are shown, one positive and three negative. Assuming the image values vary continuously, each edge connecting a positive and negative value must have a point where the image is zero. The level surface $F(x, y, z) = 0$ necessarily passes through those zero points, as illustrated by the triangular-shaped surface shaded in dark gray.

complexity of the surface of intersection is related to the sign changes that occur on all the edges of the voxel.

The heart of the Marching Cubes algorithm is that only a small number of sign combinations is possible, 2 signs at each of 8 corners for a total of 256 combinations. Each combination is analyzed to determine the nature of the isosurface of intersection; a triangle mesh is selected to represent that intersection. These meshes are stored in a table of size 256. The sign analysis for a voxel leads to an index into the table to select a triangle mesh representing the surface of intersection for that voxel. The strength of this algorithm is the speed in which the triangle meshes are generated for the entire isosurface, the performance due to the simplicity of the table lookups.

The Marching Cubes algorithm has two undesirable consequences. The first consequence is that for a typical 3D medical image and typical isosurface, the number of triangles in the mesh is on the order of a million. The generation of the mesh certainly requires only a small amount of time, but most rendering systems are slow to render millions of triangles per frame, even with graphics hardware acceleration. Of course, the large number of triangles is a problem with any isosurface extraction algorithm that works at the voxel level. The second undesirable consequence is that the triangle mesh table can lead to topological inconsistencies in the mesh. Specifically, the two meshes generated at adjacent voxels might have triangles that should share edges, but do not, thereby producing holes in the final mesh. How these holes occur will be discussed later in this section.

One approach that addresses the issue of the large number of triangles is to apply mesh reduction algorithms to the extracted surface [DZ91, GH97, HDD⁺93, SZL92, Tur92]. The idea is to extract the triangles at the voxel level, build the triangle mesh using data structures that store the adjacency information for vertices, edges, and triangles, then attempt to reduce triangles according to some heuristic. The algorithm in [GH97] is based on the concept of an edge collapse, where an edge is removed, the triangles sharing the edge are removed, and the remaining triangles affected by the removed triangles are modified to preserve the local topology. Although the reduced meshes are quality representations of the isosurface and can be quickly rendered, the reduction scheme is computationally expensive, thus offsetting the speed of an extraction algorithm such as Marching Cubes. In our context of deformable surfaces, the computation time is kept to a minimum by selecting deformation functions that require updating only a small subset of voxels in the lattice.

In this section I provide an extraction algorithm that has no ambiguities and preserves the topology of the isosurface itself when the image data within each voxel has a continuous representation using trilinear interpolation of the image values at the eight corners. The table lookup of Marching Cubes is replaced by constructing an edge mesh on the voxel faces. That mesh approximates the intersection of the isosurface with the faces. The mesh is then triangulated using an extension of an ear-clipping algorithm for planar polygons [O'R98] to three dimensions. The triangulation does not introduce new points (called Steiner points in the computational geometry literature), something other researchers have tried in attempts to remove the topological ambiguities of Marching Cubes. The triangulation is fast and efficient, but it is also possible to avoid the runtime cost by having a table lookup. The table has 256 entries, just as in Marching Cubes, but each entry that has potential ambiguities stores multiple triangle meshes. Selection of the correct mesh in the table entry is based on a secondary index. The concepts are first discussed for 2D images to give the reader intuition on how the algorithms apply to 3D images.

4.5.2 ISOCURVE EXTRACTION IN 2D IMAGES

A 2D image is assumed to be defined on a regular lattice of size $N_0 \times N_1$ with integer points (x, y) , where $0 \leq x < N_0$ and $0 \leq y < N_1$. The image values themselves are $F(x, y)$. An isocurve is of the form $F(x, y) = c$ for some specified level value c , where x and y are treated as continuous variables. A pixel in the image is a rectangle whose corners are four neighboring lattice points (x_0, y_0) , $(x_0 + 1, y_0)$, $(x_0, y_0 + 1)$, and $(x_0 + 1, y_0 + 1)$. I choose $F(x, y)$ to be a bilinear interpolation of the four image values F_{00} , F_{10} , F_{01} , and F_{11} at the corners, respectively. The continuous representation of the image over the entire pixel is given below, where $\delta_x = x - x_0$ and $\delta_y = y - y_0$:

$$F(x, y) = (1 - \delta_y)((1 - \delta_x)F_{00} + \delta_x F_{10}) + \delta_y((1 - \delta_x)F_{01} + \delta_x F_{11}) \quad (4.13)$$

The equation $F(x, y) = c$ is a quadratic equation in x and y when the xy term appears, a linear equation when xy does not. The isocurves for F when viewed as a function

on all of the plane are either hyperbolas or lines. As in 3D, I make the simplifying assumption that the level value c is chosen not to be an image value. The isocurves can intersect interior edge points of a pixel, but cannot intersect the corner points. I also work with $G(x, y) = F(x, y) - c$ and its isocurves generated by $G(x, y) = 0$.

The specialization of Marching Cubes to 2D images is usually referred to as Marching Squares. The isocurve extraction for $G(x, y) = 0$ on a pixel is performed by analyzing the signs of G at the four corners. Since the signs can be only $+1$ or -1 , there are 16 possible sign configurations. Figure 4.23 shows these.

In the case of sign changes on two edges, clearly we can connect the two edge points with a line segment. The actual isocurve is either a portion of a hyperbola or a line segment. In the first case, the segment connecting the two edge points is a reasonable approximation to the isocurve. In the second case, the segment is exactly the isocurve. Figure 4.23 shows the approximating segments in the unambiguous cases. However, two cases are ambiguous and are labeled with question marks. The possible resolutions are shown in Figure 4.24.

The question is how to select one of the three possibilities in Figure 4.24 to obtain a mesh that is topologically consistent with the isocurves. The answer is based on an analysis of the quadratic equation $G(x, y) = 0$ to actually determine what the isocurves look like. For simplicity, we may consider the problem when $0 \leq x \leq 1$ and $0 \leq y \leq 1$ and where the pixel-image values are $(0, 0, G_{00})$, $(1, 0, G_{10})$, $(0, 1, G_{01})$, and

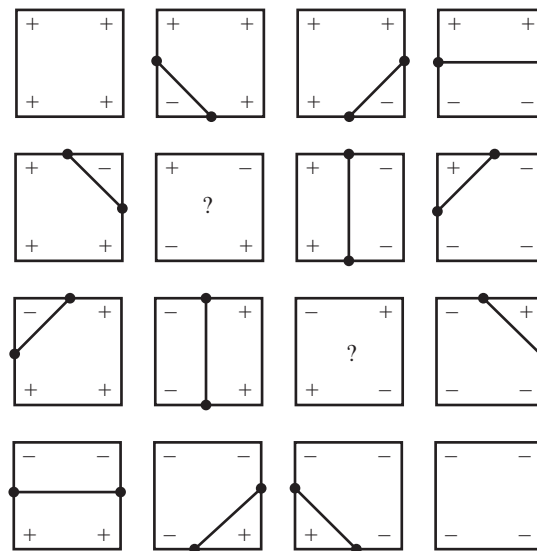


Figure 4.23 The 16 possible sign configurations for a pixel.

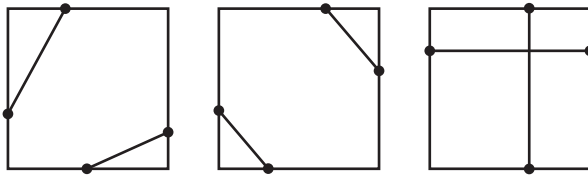


Figure 4.24 The three possible resolutions for the ambiguous pixel case.

$(1, 1, G_{11})$. The equation is of the form,

$$G(x, y) = a_{00} + a_{10}x + a_{01}y + a_{11}xy$$

where $a_{00} = G_{00}$, $a_{10} = G_{10} - G_{00}$, $a_{01} = G_{01} - G_{00}$, and $a_{11} = G_{00} - G_{10} - G_{01} + G_{11}$. Of course the interesting case is when all four edges have sign changes. We may consider the case $G_{00} < 0$, $G_{10} > 0$, $G_{01} > 0$, and $G_{11} < 0$. The opposite signs case has a similar analysis. Notice that $a_{00} < 0$, $a_{10} > 0$, $a_{01} > 0$, and $a_{11} < 0$. The four edge points where $G(x, y) = 0$ are $(0, \bar{y}_0)$, $(1, \bar{y}_1)$, $(\bar{x}_0, 0)$, and $(\bar{x}_1, 0)$. The linear interpolation will show that

$$\bar{x}_0 = \frac{-G_{00}}{G_{10} - G_{00}}, \quad \bar{x}_1 = \frac{-G_{01}}{G_{11} - G_{01}}, \quad \bar{y}_0 = \frac{-G_{00}}{G_{01} - G_{00}}, \quad \bar{y}_1 = \frac{-G_{10}}{G_{11} - G_{10}}$$

Because $a_{11} \neq 0$, the product $a_{11}G(x, y)$ is not formally zero and can be factored as

$$a_{11}G(x, y) = (a_{00}a_{11} - a_{01}a_{10}) + (a_{01} + a_{11}x)(a_{10} + a_{11}y)$$

Moreover, some algebra will show that $a_{00}a_{11} - a_{01}a_{10} = G_{00}G_{11} - G_{01}G_{10}$. Define $\Delta = G_{00}G_{11} - G_{01}G_{10}$. I consider the two cases when Δ is zero or nonzero.

If $\Delta = 0$, then $a_{11}G(x, y) = (a_{01} + a_{11}x)(a_{10} + a_{11}y)$. The isocurves $G = 0$ occur when $x = -a_{01}/a_{11}$ and $y = -a_{10}/a_{11}$. The isocurves in the entire plane consist of the vertical and horizontal lines defined by the two equations. Thus, the right-most pixel in Figure 4.24 shows the isocurve structure within the pixel. In this case the line segments forming the plus sign are exactly the isocurves. The center of the plus sign was not found by edge intersections but is added to the vertex-edge data structure for storing the edge mesh representing the total isocurve for the image. That is, when a plus sign configuration is encountered, we add the four edge intersections and plus-sign center as vertices to the mesh and we add the four segments to the mesh edges that connect the edge intersections with the center point.

If $\Delta \neq 0$, then the isocurves of $G = 0$ are hyperbolas with asymptotes $x = -a_{01}/a_{11}$ and $y = -a_{10}/a_{11}$. The two possible graphs are shown in Figure 4.25.

To distinguish which configuration is correct for the given pixel, observe that a pair of edge points is on the same hyperbolic component whenever the signs

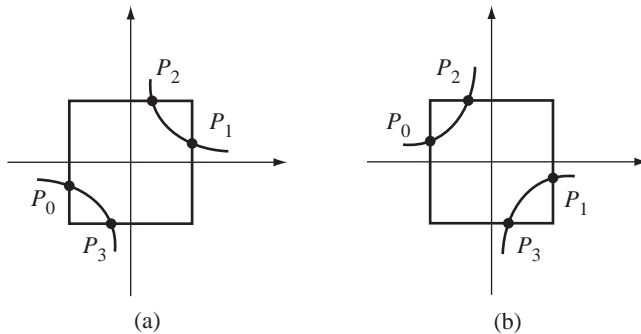


Figure 4.25 Two possible configurations for hyperbolic isocurves with pixels superimposed. The four edge intersections are P_0 , P_1 , P_2 , and P_3 as marked.

of the expression $a_{01} + a_{11}x$ are the same at those points. This test follows from the observation that points (x, y) on the vertical asymptote satisfy $a_{01} + a_{11}x = 0$. Points to the right of the vertical asymptote satisfy $a_{01} + a_{11}x > 0$ for Figure 4.25(a) and $a_{01} + a_{11}x < 0$ for Figure 4.25(b). Points to the left of the vertical asymptote have opposite sign, $a_{01} + a_{11}x < 0$ for Figure 4.25(a) and $a_{01} + a_{11}x > 0$ for Figure 4.25(b). Let $\sigma(P)$ denote the sign of $a_{01} + a_{11}x$ for point $P = (x, y)$. Some simple computations produce

$$\sigma(P_0) = \text{Sign}(a_{01}) = \text{Sign}(G_{01} - G_{00}) = -\text{Sign}(G_{00})$$

and

$$\sigma(P_1) = \text{Sign}(a_{01} + a_{11}) = \text{Sign}(G_{11} - G_{10}) = \text{Sign}(G_{00})$$

Now $\sigma(P_2) = \text{Sign}(a_{01} + a_{11}\bar{x}_0)$. Some algebra will show that the argument of the right-hand side is

$$a_{01} + a_{11}\bar{x}_0 = \frac{G_{01}G_{10} - G_{00}G_{11}}{G_{10} - G_{00}}$$

Therefore,

$$\sigma(P_2) = \text{Sign}(G_{01}G_{10} - G_{00}G_{11})\text{Sign}(G_{10} - G_{00}) = -\text{Sign}(\Delta)\text{Sign}(G_{00})$$

Similarly, $\sigma(P_3) = \text{Sign}(a_{01} + a_{11}\bar{x}_1)$ where

$$a_{01} + a_{11}\bar{x}_1 = \frac{G_{01}G_{10} - G_{00}G_{11}}{G_{11} - G_{01}}$$

Therefore,

$$\sigma(P_3) = \text{Sign}(G_{01}G_{10} - G_{00}G_{11})\text{Sign}(G_{10} - G_{00}) = \text{Sign}(\Delta)\text{Sign}(G_{00})$$

Each of the four signs is computed and the points are grouped into two pairs, each pair having the same sign. Equivalently, we may analyze the signs of $\text{Sign}(G_{00})\sigma(P_i)$ and pair the points accordingly. In this formulation, the modified signs are

$$\begin{aligned}\text{Sign}(G_{00})\sigma(P_0) &= -1 \\ \text{Sign}(G_{00})\sigma(P_1) &= +1 \\ \text{Sign}(G_{00})\sigma(P_2) &= -\text{Sign}(\Delta) \\ \text{Sign}(G_{00})\sigma(P_3) &= +\text{Sign}(\Delta)\end{aligned}$$

Clearly, P_0 and P_1 can never be paired just as P_2 and P_3 can never be paired. This should be clear geometrically from Figure 4.25. We pair (P_0, P_2) and (P_1, P_3) when $\Delta > 0$ or (P_0, P_3) and (P_1, P_2) when $\Delta < 0$.

Table 4.4 summarizes all the possible vertex–edge configurations based on analysis of the bilinear function for the pixel. The signs at the four pixels are written from left to right and correspond to the signs of G_{00} , G_{10} , G_{01} , and G_{11} , in that order. The

Table 4.4 The Vertex–edge Configurations for a Pixel

Signs				Sign of Δ	Edges
+	+	+	+		
+	+	+	-		$\langle P_0, P_3 \rangle$
+	+	-	+		$\langle P_1, P_3 \rangle$
+	+	-	-		$\langle P_0, P_1 \rangle$
+	-	+	+		$\langle P_1, P_2 \rangle$
				+	$\langle P_0, P_2 \rangle, \langle P_1, P_3 \rangle$
+	-	+	-	-	$\langle P_0, P_3 \rangle, \langle P_1, P_2 \rangle$
				0	$\langle P_0, C \rangle, \langle P_1, C \rangle, \langle P_2, C \rangle, \langle P_3, C \rangle$
+	-	-	+		$\langle P_2, P_3 \rangle$
+	-	-	-		$\langle P_0, P_2 \rangle$
-	+	+	+		$\langle P_0, P_2 \rangle$
-	+	+	-		$\langle P_2, P_3 \rangle$
				0	$\langle P_0, C \rangle, \langle P_1, C \rangle, \langle P_2, C \rangle, \langle P_3, C \rangle$
-	+	-	+	-	$\langle P_0, P_3 \rangle, \langle P_1, P_2 \rangle$
				+	$\langle P_0, P_2 \rangle, \langle P_1, P_3 \rangle$
-	+	-	-		$\langle P_1, P_2 \rangle$
-	-	+	+		$\langle P_0, P_1 \rangle$
-	-	+	-		$\langle P_1, P_3 \rangle$
-	-	-	+		$\langle P_0, P_3 \rangle$
-	-	-	-		

sign of Δ is only relevant in the ambiguous cases, so nothing is listed in this column in the unambiguous cases. The names P_0 , P_1 , P_2 , and P_3 always refer to edge points on the edges $x = 0$, $x = 1$, $y = 0$, and $y = 1$, respectively. The center point, if any, is labeled C .

4.5.3 ISOSURFACE EXTRACTION IN 3D IMAGES

A 3D image is assumed to be defined on a regular lattice of size $N_0 \times N_1 \times N_2$ with integer points (x, y, z) , where $0 \leq x < N_0$, $0 \leq y < N_1$, and $0 \leq z < N_2$. The image values themselves are $F(x, y, z)$. An isosurface is of the form $F(x, y, z) = c$ for some specified level value c , where x , y , and z are treated as continuous variables. A voxel in the image is a rectangular solid whose corners are eight neighboring lattice points (x_0, y_0, z_0) , $(x_0 + 1, y_0, z_0)$, $(x_0, y_0 + 1, z_0)$, $(x_0 + 1, y_0 + 1, z_0)$, $(x_0, y_0, z_0 + 1)$, $(x_0 + 1, y_0, z_0 + 1)$, $(x_0, y_0 + 1, z_0 + 1)$, and $(x_0 + 1, y_0 + 1, z_0 + 1)$. I choose $F(x, y, z)$ to be a trilinear interpolation of the eight image values, which are F_{000} , F_{100} , F_{010} , F_{110} , F_{001} , F_{101} , F_{011} , and F_{111} at the corners, respectively. The continuous representation of the image over the entire voxel follows, where $\delta_x = x - x_0$, $\delta_y = y - y_0$, and $\delta_z = z - z_0$:

$$\begin{aligned} F(x, y, z) = & (1 - \delta_z)((1 - \delta_y)((1 - \delta_x)F_{000} + \delta_x F_{100}) \\ & + \delta_y((1 - \delta_x)F_{010} + \delta_x F_{110})) \\ & + \delta_z((1 - \delta_y)((1 - \delta_x)F_{001} + \delta_x F_{101}) \\ & + \delta_y((1 - \delta_x)F_{011} + \delta_x F_{111})) \end{aligned} \quad (4.14)$$

The equation $F(x, y, z) = c$ is a cubic equation in x , y , and z when the xyz term appears, a quadratic equation when xyz does not, and a linear equation when none of xyz , xy , xz , or yz occurs. I make the simplifying assumption that the level value c is chosen not to be an image value. The isosurfaces can intersect interior edge points of any of the 12 edges of a voxel, but cannot intersect the corner points. I also work with $G(x, y, z) = F(x, y, z) - c$ and its isosurfaces generated by $G(x, y, z) = 0$.

Table-Based Mesh Selection

As I mentioned in the introduction, the Marching Cubes algorithm is based on the fact that each corner has an image value that is either positive or negative, leading to 256 possible sign configurations. The corner sign values are used to construct an index into a precomputed table of 256 triangle meshes. I discussed the analogy of this in 2D and showed the ambiguities that arise in two sign configurations. In 2D, rather than having a precomputed table of 16 edge meshes, we needed a secondary index to select one of three edge meshes that can occur in each of the two ambiguous cases. Thus, we have a total of 20 edge meshes from which to select. The same ambiguities arise in 3D. In fact, the ambiguities have a more serious consequence: the triangle mesh

generated by adjacent voxels can have topological inconsistencies. In particular, when two voxels share a face that is ambiguous in the 2D sense, the table lookup can produce triangle meshes that do not properly share edges on the common face. [Figure 4.26](#) illustrates this.

The voxel on the right had its edge points on the ambiguous face paired differently than the voxel on the left. This leads to a triangle mesh where a pair of triangles occurs, one triangle from each voxel, but the triangles touch at a single edge point rather than sharing an entire edge. To remedy this, all we need to do is make sure that the pairing of edge points on ambiguous faces occur according to the scheme I constructed for 2D. Interpolating each face bilinearly is consistent with the trilinear interpolation assumed for the entire voxel.

In the 2D setting, I mentioned that the precomputed table of edge meshes has a primary and a secondary index. The primary index takes on 16 values, each value representing a sign configuration for the corners of the pixel. The secondary index is 0 for the nonambiguous cases; that is, if the primary index corresponds to a nonambiguous case, the entry in the table stores a single edge mesh. Assuming the edge meshes in the table entry are stored as an array with zero-based indexing, the secondary index of 0 will always locate the correct (and only) mesh. For the ambiguous case, the secondary index takes on three values that represent whether the quantity Δ I defined previously is zero, positive, or negative. The table entries for the ambiguous cases have arrays of three edge meshes.

A similar construction can be applied in 3D. However, the table construction can be a bit tedious. An ambiguity for a voxel occurs whenever one or more of its faces is an ambiguous case in 2D. Suppose that exactly one face is ambiguous (e.g., [Figure 4.26](#)). Marching Cubes has a single triangle mesh to approximate the isosurface of the voxel. However, the ambiguous face has one of three possible interpretations, so the table entry for this case really needs an array of three triangle meshes. As in 2D,

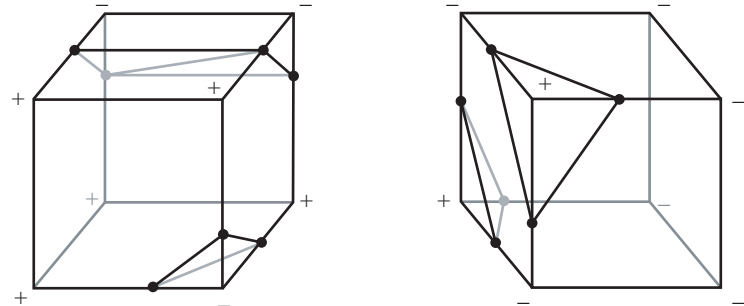


Figure 4.26 Topological inconsistencies introduced in two voxels sharing an ambiguous face.

a secondary index can be used to select the correct mesh. Now suppose that exactly two faces are ambiguous. Each face can be resolved in one of three ways, thus leading to nine possible triangle meshes for the table entry of the given primary index. Worst case, of course, is that all six faces are ambiguous, requiring a secondary index that takes on $3^6 = 729$ values. Consequently, the tables will be quite large but still constructible.

Ear-Clipping-Based Mesh Construction

An alternative to the table lookup is to generate the triangle mesh for each voxel at runtime. The concept is quite simple. The edge meshes of a voxel are generated for each face of the voxel. A vertex–edge data structure is used to store the isosurface points on the edges of the voxel and to keep track of which points are paired by an edge. The assumptions that the image is trilinearly interpolated on the voxel and that the level values are not image values guarantees that isosurface points on the voxel edges share exactly two mesh edges.

If a plus-sign configuration occurs on the face of a voxel, then the center point of that configuration is added as a vertex of the mesh. That point shares four edges. Thus, a vertex shares either two or four edges. The triangle generation amounts to finding a vertex sharing two edges, locating its two adjacent vertices, adding the triangle formed by those three vertices to a list, then removing the original vertex and the two edges it shares. If necessary, an edge is added to connect the remaining adjacent vertices. This process is repeated until no more vertices exist that share exactly two edges. I illustrate with an example. Figure 4.27 shows a voxel and the edge mesh generated by analyzing the six faces using the 2D algorithm.

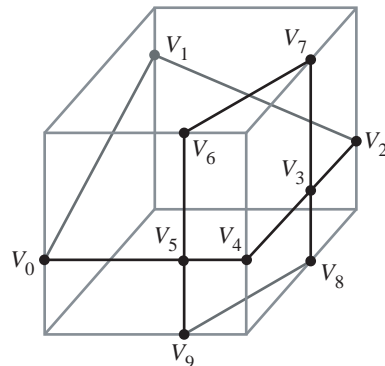


Figure 4.27 A voxel and its extracted edge mesh.

Vertices V_3 and V_5 are centers of plus-sign configurations and share four edges each. The other vertices share two edges each. Vertex V_0 shares two edges. The adjacent vertices are V_1 and V_5 . The triangle $\langle V_5, V_0, V_1 \rangle$ is added to a list. V_0 and its edges to the adjacent vertices are removed from the edge mesh. A new edge is added to connect V_5 and V_1 . Figure 4.28(a) shows the resulting edge mesh.

V_1 shares two edges. The adjacent vertices are V_5 and V_2 . The triangle $\langle V_5, V_1, V_2 \rangle$ is added to the list. V_1 and its edges to the adjacent vertices are removed from the edge mesh. A new edge is added to connect V_5 and V_2 . Figure 4.28(b) shows the resulting edge mesh.

V_2 shares two edges. The adjacent vertices are V_5 and V_3 . The triangle $\langle V_5, V_2, V_3 \rangle$ is added to the list. V_2 and its edges to the adjacent vertices are removed from the edge mesh. A new edge is added to connect V_5 and V_3 . Figure 4.28(c) shows the resulting edge mesh.

V_4 shares two edges. The adjacent vertices are V_5 and V_3 . The triangle $\langle V_5, V_4, V_3 \rangle$ is added to the list. V_4 and its edges to the adjacent vertices are removed from the edge mesh. An edge already exists between V_5 and V_3 , so a new one does not have to be added. Figure 4.28(d) shows the resulting edge mesh.

V_6 shares two edges. The adjacent vertices are V_5 and V_7 . The triangle $\langle V_5, V_6, V_7 \rangle$ is added to the list. V_6 and its edges to the adjacent vertices are removed from the edge

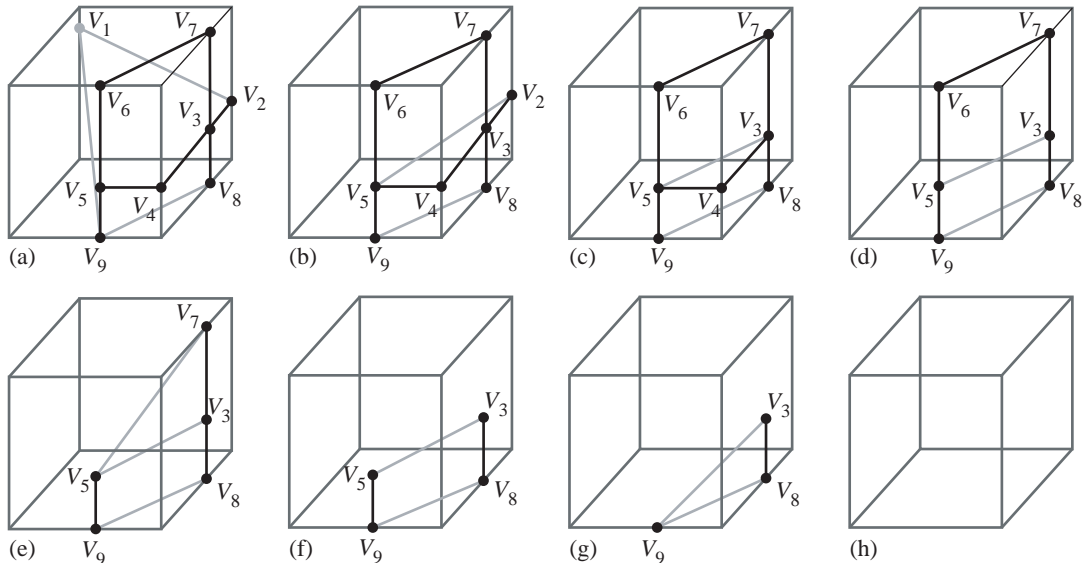


Figure 4.28 Triangle removal in the edge mesh of Figure 4.27. The sequence is from (a) to (h).

mesh. A new edge is added to connect V_5 and V_7 . Figure 4.28(e) shows the resulting edge mesh.

V_7 shares two edges. The adjacent vertices are V_5 and V_3 . The triangle $\langle V_5, V_7, V_3 \rangle$ is added to the list. V_7 and its edges to the adjacent vertices are removed from the edge mesh. An edge already exists between V_5 and V_3 , so a new one does not have to be added. Figure 4.28(f) shows the resulting edge mesh.

V_5 shares two edges. The adjacent vertices are V_3 and V_9 . The triangle $\langle V_3, V_5, V_9 \rangle$ is added to the list. V_5 and its edges to the adjacent vertices are removed from the edge mesh. A new edge is added to connect V_3 and V_9 . Figure 4.28(g) shows the resulting edge mesh.

Finally, V_3 shares two edges. The adjacent vertices are V_8 and V_9 . The triangle $\langle V_8, V_3, V_9 \rangle$ is added to the list. V_3 and its edges to the adjacent vertices are removed from the edge mesh. No more vertices exist, so the triangulation is finished. Figure 4.28(h) shows the voxel with all vertices and edges removed.

EXAMPLE 4.14



An example of implicit surface deformation is provided in the source code on the CD-ROM. A deformable body initially in the shape of a sphere is bounced on a floor. When the body hits the floor, it starts to deform. At the instant of maximum deformation, the body bounces off the floor and gradually returns to its spherical shape.

The floor is represented by the xy -plane ($z = 0$). The spherical body is defined implicitly at time 0 by $F(x, y, z) = x^2 + y^2 + (z - 1)^2 - 1 = 0$. The center point of the body is denoted $C(t) = (c_1(t), 0, c_3(t))$ and is a hard-coded path for the purposes of simplifying the demonstration. The body bounces back and forth striking the plane in only the points $(2, 0, 0)$ and $(-2, 0, 0)$. At time zero the center is at $(0, 0, 2)$ and the body is not in contact with the floor. The x -coordinate of the center is $c_1(t) = 2 \sin(\pi t/2)$ for $t \in [0, 1]$. During that same time interval the z -coordinate is defined as $c_3(t) = 2 - t^2$. The body is not in contact with the floor until the time reaches one. At that instant a time-varying deformation is applied to the body. The path of the center during the deformation is allowed to be downward only.

A slight complication arises because of the body motion. The body surface can be defined implicitly using world coordinates, but then F should additionally depend on t . To avoid this we will use a local coordinate system for the body and define the deformations within that system. We may therefore consider $F(x, y, z) = x^2 + y^2 + (z - 1)^2 - 1 = 0$ as defining the body surface in local coordinates but translate the surface itself to world coordinates when displaying the object.

The time interval of deformation and the actual z -value of the path of the center depend on how the deformation is defined. Consider using

$$D(x, y, z; t) = \begin{cases} A(t)(1 - x^2 - y^2 - z^2); & x^2 + y^2 + z^2 \leq 1, t \in [1, 1+d] \\ 0; & \text{otherwise} \end{cases}$$

where $A(t) = 4(t - 1)(1 + d - t)/d^2$. The time interval over which the deformation is applied is $[1, 1 + d]$ for some selected duration $d > 0$. The amplitude $A(t)$ varies

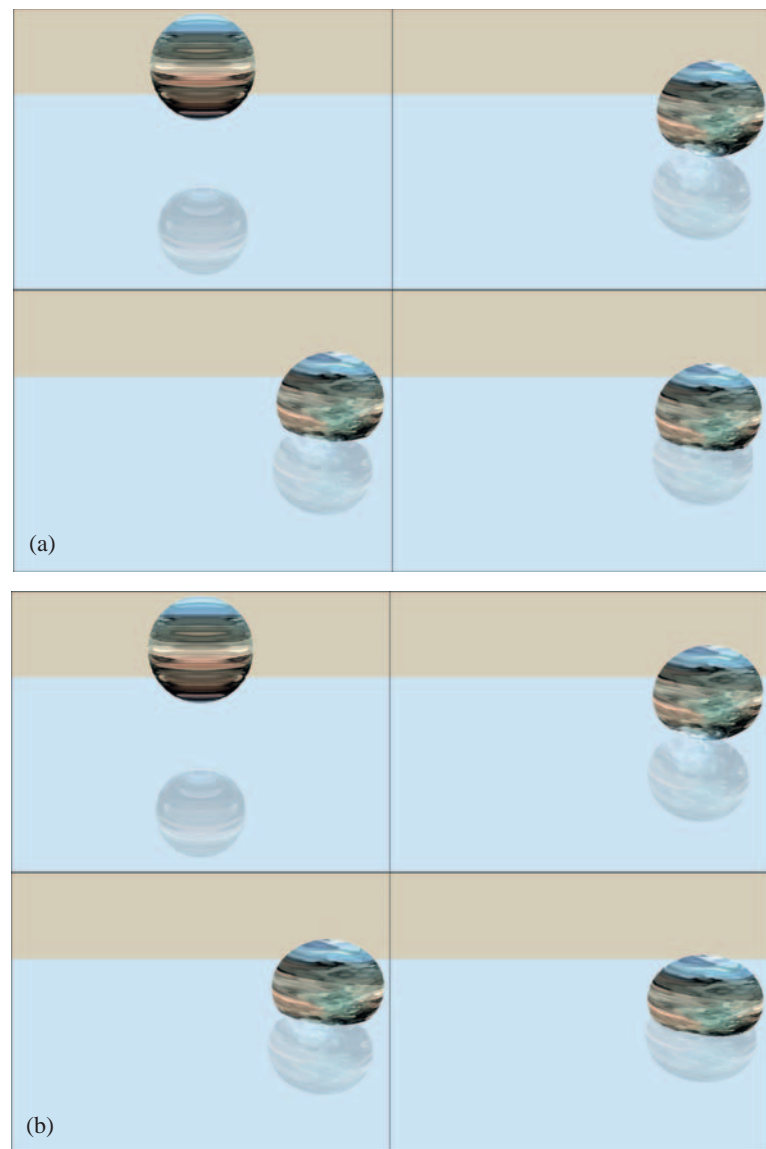


Figure 4.29

A bouncing ball with deformation based on implicit surfaces. Image (a) shows the bouncing ball with only the implicit surface deformation. Image (b) shows an additional deformation of nonuniform scaling by applying an affine transformation. (See also [Color Plate 4.29](#).)

(Example 4.14
continued)

from 0 at time $t = 1$, to 1 at time $t = 1 + d/2$, back to 0 at time $t = 1 + d$. The deformation is implicitly defined by $F(x, y, z) + D(x, y, z) = 0$, leading to

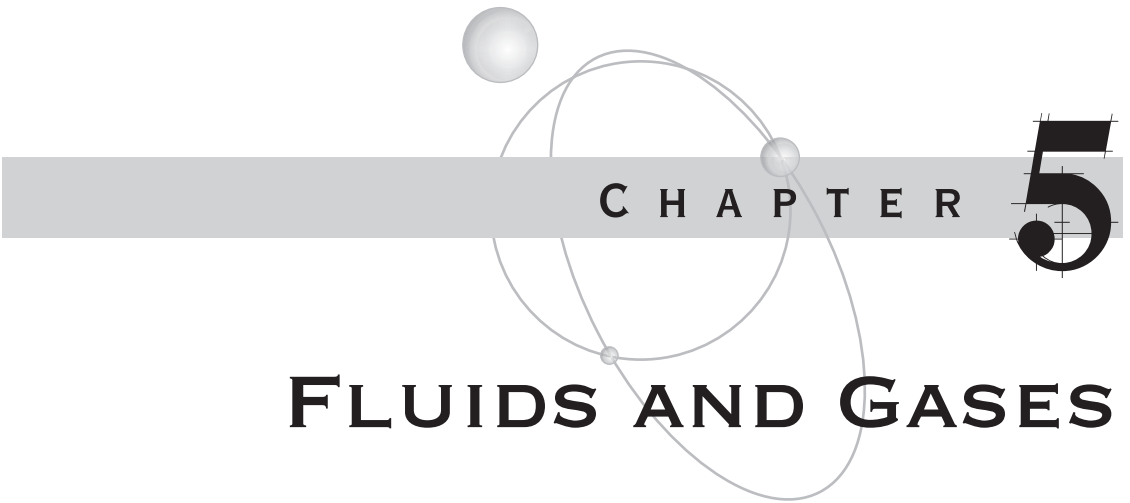
$$x^2 + y^2 + \left(z - \frac{1}{1-A}\right)^2 = \frac{1-A+A^2}{(1-A)^2}$$

which is the equation for a sphere. The portion of the original sphere contained in the region of influence $x^2 + y^2 + z^2 \leq 1$ is replaced by a spherical section from the previously displayed equation. By symmetry, the minimum point of that section occurs at $x = y = 0$, so $z_{\min} = (1 - \sqrt{1 - A + A^2})/(1 - A) \in [0, 1/2]$ for $A \in [0, 1]$. In the limit as A approaches 1, z_{\min} approaches 1/2. When that limit is reached, the deformed section of the body is a flat disk. So that the visual display of the body will make it appear as if it is in contact with the floor, the locally defined level surface for the deformed body should be translated downward by subtracting z_{\min} from the z -coordinates of the vertices.

[Figure 4.29](#) – also [Color Plate 4.29](#) – shows some screen shots from this application found on the CD-ROM.

The level surface extractor is configured to update only those voxels that are affected by the deformation. We know by design that only the portion of the body below $z = 1/2$ is affected. Moreover, we can limit our search for new voxels that define the next deformable surface by examining those vertically neighboring voxels intersected by the current deformable surface, thus taking advantage of continuity in time.

The deformed ball as constructed here most likely does not look physically realistic. You would expect a ball hitting the ground to flatten vertically and expand horizontally about its middle. The deformation function we used does not cause that to happen. Although we could choose a different deformation function and/or increase the region of influence of the function, a cheaper alternative involving more hacked physics is to apply a nonuniform scaling to the vertices of the triangle mesh after the effects of the deformation are calculated. The x and y components may be scaled by a factor $\sigma_1 > 1$. The z component may be scaled by a factor $\sigma_2 < 1$. [Figure 4.29\(b\)](#) shows some screen shots for the modified physical simulation that uses the affine deformation to get nonuniform scaling.



CHAPTER

5

FLUIDS AND GASES

This chapter introduces some basic concepts for fluid dynamics, allowing us to model fluid flow and to implement algorithms that run in real time.

Section 5.1 is a summary of topics in vector calculus that are applicable to fluid dynamics. This is a lengthy section about the gradient, directional derivatives, vector fields, divergence, curl, and integration (line, surface, volume integrals). A few important results are mentioned: divergence theorem, Stokes' theorem, and Green's theorem. Applications are shown for solving some partial differential equations, namely, Laplace's equation and Poisson's equation. The final result of the section is the Helmholtz decomposition that shows a vector field may be decomposed into a gradient vector field and a curl vector field. This result plays an important role in the numerical methods for solving the equations of fluid motion.

Section 5.2 contains a discussion about strain and stress of fluids. Under special assumptions about the fluid, the stress tensor is simplified to a form that at least gives us hope of numerically solving the equations of fluid motion.

Conservation of mass and conservation of momentum are the topics of Section 5.3. Conservation of mass leads to a partial differential equation that models the density of a fluid moving within a bounded region. Conservation of momentum leads to a partial differential equation that models the velocity of the fluid; this equation is called the Navier–Stokes equation. The density and velocity occur in both equations, so the equations are coupled, which makes the numerical solution a bit of a challenge.

With more assumptions, the density equation and Navier–Stokes equation are simplified to a form that allows us to solve them with some standard numerical methods. The solutions may be generated in real time. Section 5.4 presents the ideas leading to the equations used in the real-time fluids for games paper [Sta03].

Section 5.5 covers the implementation of the simplified model in two dimensions where the region of fluid is a rectangle. Pseudocode is provided for all the details. Section 5.6 summarizes the implementation in three dimensions where the region of fluid is a cube. Pseudocode is also provided. The CD-ROM has implementations for both two and three dimensions.

A few variations on the simplified model are mentioned in Section 5.7. The most important one is called vorticity confinement [FSJ01] and helps to keep the vortices that one associates with motion of smoke.

5.1 VECTOR CALCULUS

Rather than make this a section in Chapter 9 on calculus, I decided it would be more useful to include it here. The derivations for the partial differential equations related to fluid flow are heavily dependent on topics in vector calculus, so it is convenient to have this material here for quick reference.

5.1.1 GRADIENT, DIRECTIONAL DERIVATIVE, AND TOTAL DERIVATIVE

Consider three-dimensional space with position $\mathbf{x} = (x_0, x_1, x_2)$. The *gradient operator* in three dimensions is

$$\nabla = \left(\frac{\partial}{\partial x_0}, \frac{\partial}{\partial x_1}, \frac{\partial}{\partial x_2} \right) \quad (5.1)$$

and is applied to a function $f(\mathbf{x})$ to obtain the *gradient* of f ,

$$\nabla f = \left(\frac{\partial f}{\partial x_0}, \frac{\partial f}{\partial x_1}, \frac{\partial f}{\partial x_2} \right) \quad (5.2)$$

which is the 3-tuple of first-order partial derivatives of f .

Sometimes we wish to compute the rate of change of f at a point \mathbf{x} in a specified direction \mathbf{u} . According to convention, the direction is a unit-length vector. The rate of change of f at \mathbf{x} in the direction \mathbf{u} is the *directional derivative*

$$\mathbf{u} \cdot \nabla f(\mathbf{x}) = \mathbf{u} \cdot \left(\frac{\partial f}{\partial x_0}, \frac{\partial f}{\partial x_1}, \frac{\partial f}{\partial x_2} \right) = u_0 \frac{\partial f}{\partial x_0} + u_1 \frac{\partial f}{\partial x_1} + u_2 \frac{\partial f}{\partial x_2} \quad (5.3)$$

In fact, $\mathbf{u} \cdot \nabla f = (\mathbf{u} \cdot \nabla) f$, which defines the *directional derivative operator*

$$\mathbf{u} \cdot \nabla = \left(u_0 \frac{\partial}{\partial x_0}, u_1 \frac{\partial}{\partial x_1}, u_2 \frac{\partial}{\partial x_2} \right) \quad (5.4)$$

where $\mathbf{u} = (u_0, u_1, u_2)$.

The *total derivative* of a function $f(\mathbf{x})$ is defined as the differential form,

$$df = dx_0 \frac{\partial f}{\partial x_0} + dx_1 \frac{\partial f}{\partial x_1} + dx_2 \frac{\partial f}{\partial x_2} = d\mathbf{x} \cdot \nabla f = (d\mathbf{x} \cdot \nabla) f \quad (5.5)$$

where the coordinate differentials are summarized in vector form as $d\mathbf{x} = (dx_0, dx_1, dx_2)$. The equation $f(\mathbf{x}) = c$ for constants c defines a family of surfaces (possibly degenerate to a curve or point) called *level surfaces*. If \mathbf{x} varies only within one level surface, then f is constant for those \mathbf{x} and the total derivative is zero, $df = 0$. Consequently, $d\mathbf{x} \cdot \nabla f = 0$, which says that if you start on the surface and then move an infinitesimal amount $d\mathbf{x}$ while staying on the surface, the gradient of f remains perpendicular to $d\mathbf{x}$. Because such an infinitesimal amount keeps you on the surface, $d\mathbf{x}$ is tangent to the surface and ∇f must be perpendicular to the surface. Thus, $\nabla f(\mathbf{x})$ is a normal vector to the level surface at the point \mathbf{x} on that surface.

5.1.2 VECTOR FIELDS, DIVERGENCE, AND LAPLACIAN

A *vector field* is a vector-valued function of a vector-valued variable. Specifically, if \mathbf{x} is position, a vector field is $\mathbf{f}(\mathbf{x})$. You may think of the vector field in terms of its components,

$$\mathbf{f}(\mathbf{x}) = (f_0(\mathbf{x}), f_1(\mathbf{x}), f_2(\mathbf{x}))$$

Although the motivation for directional derivative involved application of the operator $\mathbf{u} \cdot \nabla$ to scalar-valued functions, we may also apply the operator to vector fields \mathbf{f} ,

$$(\mathbf{u} \cdot \nabla) \mathbf{f} = u_0 \frac{\partial \mathbf{f}}{\partial x_0} + u_1 \frac{\partial \mathbf{f}}{\partial x_1} + u_2 \frac{\partial \mathbf{f}}{\partial x_2} \quad (5.6)$$

EXERCISE

5.1

For any vector field \mathbf{f} , prove that

$$(\mathbf{f} \cdot \nabla) \mathbf{x} = \mathbf{f} \quad (5.7)$$

An expression involving the gradient operator and vector fields that shows up frequently in physics topics is the *divergence*, defined by

$$\nabla \cdot \mathbf{f} = \frac{\partial f_0}{\partial x_0} + \frac{\partial f_1}{\partial x_1} + \frac{\partial f_2}{\partial x_2} = \left(\frac{\partial}{\partial x_0}, \frac{\partial}{\partial x_1}, \frac{\partial}{\partial x_2} \right) \cdot (f_0, f_1, f_2) \quad (5.8)$$

The right-most equality shows that, formally, you may think of the divergence as a dot product of the gradient operator and the vector field.

EXERCISE
5.2 Prove that $\nabla \cdot \mathbf{x} = 3$.

EXERCISE
5.3 In [Example 3.1](#), Newton's law led to the equation involving gravitational force,

$$m\mathbf{a} = -\frac{GMm}{r^2}\mathbf{R}$$

where G , M , and m are constants and where $\mathbf{R} = \mathbf{r}/r$ is a unit-length direction vector. The right-hand side is referred to as an *inverse-square force*. Let $\mathbf{x} = \mathbf{r}$ and $|\mathbf{x}| = r$. The equation becomes

$$m\mathbf{a} = -GMm\frac{\mathbf{x}}{|\mathbf{x}|^3}$$

Prove that

$$\nabla \cdot \left(\frac{\mathbf{x}}{|\mathbf{x}|^3} \right) = 0$$

which says that the divergence of an inverse-square force is always zero.

EXERCISE
5.4 Let $\phi(\mathbf{x})$ be a scalar-valued function. Let $\mathbf{f}(\mathbf{x})$ be a vector field. Prove that

$$\nabla \cdot (\phi\mathbf{f}) = \phi\nabla \cdot \mathbf{f} + \nabla\phi \cdot \mathbf{f} \quad (5.9)$$

This equation has the flavor of a product rule for differentiation.

EXERCISE
5.5 Let \mathbf{f} be a vector field. Let M be a constant 3×3 matrix. Prove that

$$\nabla \cdot (M\mathbf{f}) = (M^T\nabla) \cdot \mathbf{f} \quad (5.10)$$

Observe that $\mathbf{g} \cdot M\mathbf{f} = \mathbf{g}^T M\mathbf{f} = (M^T\mathbf{g})^T \mathbf{f} = (M^T\mathbf{g}) \cdot \mathbf{f}$. [Equation \(5.10\)](#) says that you may formally apply this construction with $\mathbf{g} = \nabla$.

An important concept that shows up in fluid flow is *diffusion*. This involves the *Laplacian operator*

$$\nabla^2 = \frac{\partial^2}{\partial x_0^2} + \frac{\partial^2}{\partial x_1^2} + \frac{\partial^2}{\partial x_2^2} \quad (5.11)$$

and is applied to a scalar-valued function $\phi(\mathbf{x})$ as

$$\nabla^2\phi = \nabla \cdot (\nabla\phi) = \frac{\partial^2\phi}{\partial x_0^2} + \frac{\partial^2\phi}{\partial x_1^2} + \frac{\partial^2\phi}{\partial x_2^2} \quad (5.12)$$

The Laplacian of f is the divergence of the gradient of ϕ . We may also formally apply the Laplacian operator to a vector field \mathbf{f} ,

$$\nabla^2 \mathbf{f} = \frac{\partial^2 \mathbf{f}}{\partial x_0^2} + \frac{\partial^2 \mathbf{f}}{\partial x_1^2} + \frac{\partial^2 \mathbf{f}}{\partial x_2^2} \quad (5.13)$$

The result, of course, is vector-valued.

5.1.3 CURL

Another useful operation involving the gradient operator is the *curl* of a vector field $\mathbf{f}(\mathbf{x})$. This is defined by

$$\nabla \times \mathbf{f} = \left(\frac{\partial f_2}{\partial x_1} - \frac{\partial f_1}{\partial x_2}, \frac{\partial f_0}{\partial x_2} - \frac{\partial f_2}{\partial x_0}, \frac{\partial f_1}{\partial x_0} - \frac{\partial f_0}{\partial x_1} \right) = \det \begin{bmatrix} \mathbf{i} & \mathbf{j} & \mathbf{k} \\ \frac{\partial}{\partial x_0} & \frac{\partial}{\partial x_1} & \frac{\partial}{\partial x_2} \\ f_0 & f_1 & f_2 \end{bmatrix} \quad (5.14)$$

The right-most equality shows that, formally, the curl may be computed using the butterfly rule for determinants applied to the gradient operator and the vector field. Here are a few exercises involving the curl operator.

EXERCISE

5.6

Prove that $\nabla \times \mathbf{x} = \mathbf{0}$.

EXERCISE

5.7

Let $\phi(\mathbf{x})$ be a scalar-valued function. Let $\mathbf{f}(\mathbf{x})$ be a vector field. Prove that

$$\nabla \times (\phi \mathbf{f}) = \phi \nabla \times \mathbf{f} + \nabla \phi \times \mathbf{f} \quad (5.15)$$

This equation has the flavor of a product rule for differentiation.

EXERCISE

5.8

Let $\mathbf{f}(\mathbf{x})$ be a vector field and let R be a rotation matrix that is constant (independent of \mathbf{x}). Prove that

$$(R \nabla) \times (R \mathbf{f}) = R (\nabla \times \mathbf{f}) \quad (5.16)$$

Compare this with [equation \(2.92\)](#).

EXERCISE

5.9

Let $\phi(\mathbf{x})$ be a scalar-valued function. Prove that

$$\nabla \times (\nabla \phi) = \mathbf{0} \quad (5.17)$$

The curl of a gradient is always the zero vector. You may also think of this in operator form, $(\nabla \times \nabla)\phi = \mathbf{0}$, which says that the operator $\nabla \times \nabla$ applied to scalar functions is always the zero vector.

Here are some additional exercises involving the divergence and the curl operators.

EXERCISE Let \mathbf{f} be a vector field. Prove that
5.10

$$\nabla \cdot (\nabla \times \mathbf{f}) = \mathbf{0} \quad (5.18)$$

The divergence of a curl is always the zero vector. ■

EXERCISE Let \mathbf{f} and \mathbf{g} be vector fields. The cross product $\mathbf{f} \times \mathbf{g}$ is also a vector field, so we may compute its divergence. Prove that
5.11

$$\nabla \cdot (\mathbf{f} \times \mathbf{g}) = (\nabla \times \mathbf{f}) \cdot \mathbf{g} - (\nabla \times \mathbf{g}) \cdot \mathbf{f} \quad (5.19)$$

This is not quite a product rule because the antisymmetry of the cross product ($\mathbf{g} \times \mathbf{f} = -\mathbf{f} \times \mathbf{g}$) causes the minus sign to occur rather than a plus sign. ■

EXERCISE Let \mathbf{f} and \mathbf{g} be vector fields. The cross product $\mathbf{f} \times \mathbf{g}$ is also a vector field, so we may compute its curl. Prove that
5.12

$$\nabla \times (\mathbf{f} \times \mathbf{g}) = \mathbf{f}(\nabla \cdot \mathbf{g}) - \mathbf{g}(\nabla \cdot \mathbf{f}) + (\mathbf{g} \cdot \nabla) \mathbf{f} - (\mathbf{f} \cdot \nabla) \mathbf{g} \quad (5.20)$$

The equation makes use of the application of the directional derivative operator to vector fields; see [equation \(5.6\)](#). ■

EXERCISE Let \mathbf{f} and \mathbf{g} be vector fields. The dot product $\mathbf{f} \cdot \mathbf{g}$ is a scalar-valued function, so we may compute its gradient. Prove that
5.13

$$\nabla(\mathbf{f} \cdot \mathbf{g}) = \mathbf{f} \times (\nabla \times \mathbf{g}) + \mathbf{g} \times (\nabla \times \mathbf{f}) + (\mathbf{f} \cdot \nabla) \mathbf{g} + (\mathbf{g} \cdot \nabla) \mathbf{f} \quad (5.21)$$

The equation makes use of the application of the directional derivative operator to vector fields; see [equation \(5.6\)](#). ■

EXERCISE Let \mathbf{f} be a vector field. The curl of \mathbf{f} is itself a vector field, so we may apply the curl to it. Prove that
5.14

$$\nabla \times (\nabla \times \mathbf{f}) = \nabla(\nabla \cdot \mathbf{f}) - \nabla^2 \mathbf{f} \quad (5.22)$$

The equation makes use of the Laplacian operator applied to a vector field; see [equation \(5.13\)](#). ■

EXERCISE [Exercise 5.14](#) provides a formula for the application of the curl twice to a vector field \mathbf{f} . Let us refer to the *curl operator* as $\nabla \times$. The curl of \mathbf{f} is therefore $(\nabla \times) \mathbf{f} = \nabla \times \mathbf{f}$. The curl of the curl of \mathbf{f} is

$$(\nabla \times)^2 \mathbf{f} = (\nabla \times)(\nabla \times \mathbf{f}) = \nabla \times (\nabla \times \mathbf{f})$$

Derive a formula for $(\nabla \times)^3 \mathbf{f}$. Be daring and try to derive a formula for $(\nabla \times)^n \mathbf{f}$ for any positive integer n . ■

5.1.4 LINE INTEGRALS

Let $\mathbf{f}(\mathbf{x})$ be a vector field. Let $\mathbf{x}(s)$ be a curve that is parameterized by arc length s . The derivative is $\mathbf{x}'(s) = d\mathbf{x}/ds$ and is a unit-length tangent to the curve. The projection of \mathbf{f} onto the tangents is

$$[\mathbf{f}(\mathbf{x}(s)) \cdot \mathbf{x}'(s)] \mathbf{x}'(s)$$

We may add up the dot products along a segment of the curve in the sense of integration,

$$\int_{s_0}^{s_1} \left(\mathbf{f}(\mathbf{x}(s)) \cdot \frac{d\mathbf{x}}{ds} \right) ds$$

where the curve segment corresponds to the interval $[s_0, s_1]$. An arc-length parameterization is not usually readily available, so we may write the previous integral in a parameterless format,

$$\int_C \mathbf{f} \cdot d\mathbf{x} \tag{5.23}$$

where C denotes the curve and where $d\mathbf{x} = (dx_0, dx_1, dx_2)$ is the infinitesimal position that we have seen previously in this chapter. The integral of equation (5.23) is referred to as a *line integral*. Perhaps a better name would have been *curve integral*, but that's history.

If instead we have a curve parameterization $\mathbf{x}(t)$, then equation (5.23) may be written as

$$\int_{t_0}^{t_1} \left(\mathbf{f}(\mathbf{x}(t)) \cdot \frac{d\mathbf{x}(t)}{dt} \right) dt$$

where the curve segment of interest is that corresponding to the parameter interval $[t_0, t_1]$. We have already seen such integrals when computing the total work done by a force; see Section 2.6.

5.1.5 SURFACE INTEGRALS AND STOKES' THEOREM

The concept of a line integral extends naturally to integrals over a surface. We have already seen this in Section 2.5.3 for continuous mass in three dimensions, under the heading *Surface Mass*. In that example, we computed the mass of a surface for a parametric function of two variables.

Generally, let $\mathbf{f}(\mathbf{x})$ be a vector field. Consider a surface S for which the normal vector at position \mathbf{x} is the unit-length normal vector $\mathbf{n}(\mathbf{x})$. The projection of \mathbf{f} onto

the normals is

$$[\mathbf{f}(\mathbf{x}) \cdot \mathbf{n}(\mathbf{x})] \mathbf{n}(\mathbf{x})$$

We may add up the normal projections in the sense of integration,

$$\int_S \mathbf{f} \cdot \mathbf{n} dS = \int_S \mathbf{f} \cdot d\mathbf{S} \quad (5.24)$$

where dS is an infinitesimal amount of surface area and where $d\mathbf{S} = \mathbf{n} dS$ is an infinitesimal amount of surface. The integrals of equation (5.24) are referred to as *surface integrals*.

An important result that is important in physics applications is *Stokes' theorem*, which is stated here without proof. Let \mathbf{f} be a vector field. Let S be a surface patch whose boundary is the closed curve C . The surface integral of the curl of \mathbf{f} may be reduced to a line integral of \mathbf{f} on the boundary C .

$$\int_S (\nabla \times \mathbf{f}) \cdot d\mathbf{S} = \int_C \mathbf{f} \cdot d\mathbf{x} \quad (5.25)$$

where $d\mathbf{S}$ is an infinitesimal amount of surface and $d\mathbf{x}$ is an infinitesimal amount of curve.

5.1.6 VOLUME INTEGRALS AND THE DIVERGENCE THEOREM

Integrals of functions defined on a region of space V are naturally covered in a multivariate calculus course. For a scalar function $\phi(\mathbf{x})$, the *volume integral* of ϕ is

$$\int_V \phi dV \quad (5.26)$$

where $dV = dx_0 dx_1 dx_2$ is an infinitesimal amount of volume of the region. We have already seen such an integral when computing the total mass of an object occupying the region V ; see Section 2.5.3 for continuous mass in three dimensions, under the heading *Volume Mass*. In that example, the function to be integrated is the density function $\delta(\mathbf{x})$.

We may compute volume integrals for vector fields as well, by integrating each of the components of the vector field. For a vector field $\mathbf{f}(\mathbf{x})$, the *volume integral* of \mathbf{f} is

$$\int_V \mathbf{f} dV = \left(\int_V f_0 dV, \int_V f_1 dV, \int_V f_2 dV \right) \quad (5.27)$$

An important result in physics applications is the *divergence theorem*, which is stated here without proof. Let \mathbf{f} be a vector field. Let V be a region of space whose

boundary is the closed surface S . The volume integral of the divergence of \mathbf{f} may be reduced to a surface integral of \mathbf{f} on the boundary S .

$$\int_V \nabla \cdot \mathbf{f} dV = \int_S \mathbf{f} \cdot d\mathbf{S} \quad (5.28)$$

where dV is an infinitesimal amount of volume and $d\mathbf{S}$ is an infinitesimal amount of surface.

5.1.7 GREEN'S THEOREM, LAPLACE'S EQUATION, AND POISSON'S EQUATION

Another important result is *Green's theorem*, which states that for twice continuously differentiable functions u and v defined on a region V with boundary S ,

$$\int_V (u \nabla^2 v - v \nabla^2 u) dV = \int_S (u \nabla v - v \nabla u) \cdot d\mathbf{S} \quad (5.29)$$

The proof is simple. The divergence theorem applied to $u \nabla v$ is

$$\int_V (u \nabla^2 v + \nabla u \cdot \nabla v) dV = \int_V \nabla \cdot (u \nabla v) dV = \int_S u \nabla v \cdot d\mathbf{S}$$

The divergence theorem applied to $v \nabla u$ is

$$\int_V (v \nabla^2 u + \nabla v \cdot \nabla u) dV = \int_V \nabla \cdot (v \nabla u) dV = \int_S v \nabla u \cdot d\mathbf{S}$$

Subtracting the second displayed equation from the first displayed equation produces [equation \(5.29\)](#).

A function ϕ for which $\nabla^2 \phi = 0$ is said to be a *harmonic function*. The differential equation is referred to as *Laplace's equation*. Consider $\nabla^2 \phi = 0$ for ϕ defined on a region V with boundary S . We may specify *boundary conditions* for ϕ on S . The *Dirichlet boundary conditions* involve specifying the function values on the boundary,

$$\begin{aligned} \nabla^2 \phi(\mathbf{x}) &= 0, & \mathbf{x} \in V \\ \phi(\mathbf{x}) &= B(\mathbf{x}), & \mathbf{x} \in S \end{aligned} \quad (5.30)$$

for some specified function B whose domain is the surface S . The *Neumann boundary conditions* involve specifying directional derivatives of the function values on the boundary,

$$\begin{aligned} \nabla^2 \phi(\mathbf{x}) &= 0, & \mathbf{x} \in V \\ \mathbf{n}(\mathbf{x}) \cdot \nabla \phi(\mathbf{x}) &= B(\mathbf{x}), & \mathbf{x} \in S \end{aligned} \quad (5.31)$$

for some specified function B whose domain is the surface S . The vector $\mathbf{n}(\mathbf{x})$ is the outer-pointing unit-length normal to the surface at the position \mathbf{x} . Equations (5.30) and (5.31) are referred to as *boundary value problems*. If $V = \mathbb{R}^3$ (all of space), then there are no boundary conditions.

For a known function $f(\mathbf{x})$, Poisson's equation is the differential equation $\nabla^2\phi = -f$. This is a generalization of Laplace's equation and reduces to it when $f = 0$. When defined on a region V with boundary S , we may set up boundary value problems. The problem with Dirichlet boundary conditions is

$$\begin{aligned}\nabla^2\phi(\mathbf{x}) &= -f(\mathbf{x}), \quad \mathbf{x} \in V \\ \phi(\mathbf{x}) &= B(\mathbf{x}), \quad \mathbf{x} \in S\end{aligned}\tag{5.32}$$

for some specified function B whose domain is the surface S . The problem with Neumann boundary conditions is,

$$\begin{aligned}\nabla^2\phi(\mathbf{x}) &= -f(\mathbf{x}), \quad \mathbf{x} \in V \\ \mathbf{n}(\mathbf{x}) \cdot \nabla\phi(\mathbf{x}) &= B(\mathbf{x}), \quad \mathbf{x} \in S\end{aligned}\tag{5.33}$$

for some specified function B whose domain is the surface S . If $V = \mathbb{R}^3$, then there are no boundary conditions. However, the integrals are defined on an unbounded region. To hope for a solution to the equation, it is necessary to impose *decay conditions* on f . The standard one is to require $|f(\mathbf{x})| = O(1/r^2)$ for $r = |\mathbf{x}|$. This is order notation that means there is a constant $K > 0$ and a value $r_0 > 0$ such that $|f(\mathbf{x})| \leq K/r^2$ for $r \geq r_0$. We also require that the solution and its derivative decay like $\phi = O(1/r)$ and $|\nabla\phi| = O(1/r^2)$.

The solutions to Laplace's equation and Poisson's equation involve constructing something called a *Green's function*. The mathematics is advanced, so only a brief but intuitive summary is presented here.

Given a linear differential operator $L(\mathbf{x})$, a Green's function is a solution $G(\mathbf{x}, \mathbf{y})$ to

$$L(\mathbf{x})G(\mathbf{x}, \mathbf{y}) = -\delta(\mathbf{x} - \mathbf{y})\tag{5.34}$$

where $\delta(\mathbf{z})$ is the *Dirac delta function* defined by

$$\delta(\mathbf{z}) = \begin{cases} 0, & \mathbf{z} \neq \mathbf{0} \\ \infty, & \mathbf{z} = \mathbf{0} \end{cases}$$

Technically, δ is not a function; rather, it is a *distribution* with the *substitution property*

$$\int_V \phi(\mathbf{y})\delta(\mathbf{x} - \mathbf{y}) dV = \begin{cases} \phi(\mathbf{x}), & \mathbf{x} \in V \\ 0, & \mathbf{x} \notin V \end{cases}\tag{5.35}$$

where dV is the infinitesimal with respect to the \mathbf{y} -variables; that is, if $\mathbf{y} = (y_0, y_1, y_2)$, then $dV = dy_0 dy_1 dy_2$. This is where the mathematics gets deep. Distributions are

part of the topic of *measure theory* and are not typically covered in detail until you have a graduate-level course on the topic.

A note on sign conventions: Physicists tend to use [equation \(5.34\)](#) to define a Green's function. Mathematicians tend to have $+\delta$ on the right-hand side of this equation. When reading about Green's functions, you need to be careful about which convention is used. For example, at the time of this writing, the Wikipedia page on Green's function mentions the varying sign conventions, chooses the mathematician's version for constructing a Green's function for the Laplace operator, and then uses the incorrect sign for the solution to Poisson's equation.

A Green's function for the Laplace operator ∇^2 is a solution $G(\mathbf{x}, \mathbf{y})$ to $\nabla^2 G(\mathbf{x}, \mathbf{y}) = -\delta(\mathbf{x} - \mathbf{y})$. In Green's theorem of [equation \(5.29\)](#), set $u = \phi$ and $v = G$; then

$$\int_V (\phi(\mathbf{y})\delta(\mathbf{x} - \mathbf{y}) - G(\mathbf{x}, \mathbf{y})\nabla^2\phi(\mathbf{y})) dV = \int_S (\phi(\mathbf{y})\nabla G(\mathbf{x}, \mathbf{y}) - G(\mathbf{x}, \mathbf{y})\nabla\phi(\mathbf{y})) \cdot d\mathbf{S}$$

where it is understood that \mathbf{x} is a free variable so that in the integrands, ∇ and ∇^2 are applied as \mathbf{y} -derivatives. For Poisson's equation and using [equation \(5.35\)](#) on the left-hand side, the previously displayed equation is rewritten as

$$\phi(\mathbf{x}) = \int_V G(\mathbf{x}, \mathbf{y})f(\mathbf{y}) dV + \int_S (G(\mathbf{x}, \mathbf{y})\nabla\phi(\mathbf{y}) - \phi(\mathbf{y})\nabla G(\mathbf{x}, \mathbf{y})) \cdot d\mathbf{S}$$

The solution to Poisson's equation has a volume integral dependent on f and a surface integral depending on ϕ and $\nabla\phi$. We have some latitude in selecting the Green's function. For the Dirichlet boundary value problem, G is chosen so that $G(\mathbf{x}, \mathbf{y}) = 0$ when either \mathbf{x} or \mathbf{y} is a surface point. The solution is

$$\phi(\mathbf{x}) = \int_V G(\mathbf{x}, \mathbf{y})f(\mathbf{y}) dV - \int_S B(\mathbf{y})\nabla G(\mathbf{x}, \mathbf{y}) \cdot \mathbf{n}(\mathbf{y}) dS \quad (5.36)$$

where B is the boundary function of [equation \(5.32\)](#). For the Neumann boundary value problem, G is chosen so that $\nabla G(\mathbf{x}, \mathbf{y}) \cdot \mathbf{n}(\mathbf{y}) = 0$ when either \mathbf{x} or \mathbf{y} is a surface point. The solution is

$$\phi(\mathbf{x}) = \int_V G(\mathbf{x}, \mathbf{y})f(\mathbf{y}) dV + \int_S G(\mathbf{x}, \mathbf{y})B(\mathbf{y}) dS \quad (5.37)$$

where B is the boundary function of [equation \(5.33\)](#). Constructing Green's functions for an arbitrary V is difficult, and cannot usually be done in closed form. Numerical methods are used instead to solve the boundary value problems.

When $V = \mathbb{R}^3$, the Green's function is $G(\mathbf{x}, \mathbf{y}) = 1/|\mathbf{x} - \mathbf{y}|$. The decay conditions on ϕ and $\nabla\phi$ guarantee that the surface integrals in [Equations \(5.36\)](#) and [\(5.37\)](#) tend to zero as S becomes unbounded (think of S as a sphere of radius r). The solution to

Poisson's equation is then

$$\phi(\mathbf{x}) = \int_{\mathbb{R}^3} \frac{f(\mathbf{y})}{|\mathbf{x} - \mathbf{y}|} dV \quad (5.38)$$

The decay condition on $|f|$ guarantees that the integral exists.

Equation (5.38) also produces the solution to Laplace's equation on \mathbb{R}^3 , because $f = 0$. Specifically, the solution is $\phi = 0$. You might have observed that $\nabla^2 c = 0$ for any constant c , so how can $\phi = 0$ be the unique solution? If $c \neq 0$, the decay conditions are no longer satisfied – the solution must decay to zero for large $|\mathbf{x}|$, which a nonzero constant does not do.

5.1.8 VECTOR FIELD DECOMPOSITION

This section contains some results to decomposing vector fields into other vector fields that have some physical significance. The end result will be to present the *fundamental theorem of vector calculus*, which gives us a decomposition of a vector field into a sum of three vector fields – a gradient of a scalar function, a curl of a vector function, and a harmonic vector function.

Scalar Potential

Consider a vector field defined by $\mathbf{f} = \nabla\phi$ for some scalar function ϕ . The vector field is said to be generated by the *scalar potential* ϕ . By Exercise 5.17, \mathbf{f} has the property that $\nabla \times \mathbf{f} = \nabla \times (\nabla\phi) = \mathbf{0}$. In words, a scalar potential-generated vector field has no curl; the vector field is said to be *curl free*.

Suppose that we are given a vector field \mathbf{f} for which $\nabla \times \mathbf{f} = \mathbf{0}$. Can we construct a scalar potential ϕ that generates \mathbf{f} ? The answer is “yes,” although not uniquely. Let $\mathbf{f} = (f_0, f_1, f_2)$ so that $\nabla \times \mathbf{f} = \mathbf{0}$ implies

$$\frac{\partial f_2}{\partial y} = \frac{\partial f_1}{\partial z}, \quad \frac{\partial f_0}{\partial z} = \frac{\partial f_2}{\partial x}, \quad \frac{\partial f_1}{\partial x} = \frac{\partial f_0}{\partial y} \quad (5.39)$$

Let us construct a function ϕ for which

$$\frac{\partial \phi}{\partial x} = f_0, \quad \frac{\partial \phi}{\partial y} = f_1, \quad \frac{\partial \phi}{\partial z} = f_2$$

Integrating the x -derivative equation,

$$\phi(x, y, z) = \int_{x_0}^x f_0(\bar{x}, y, z) d\bar{x} + A(y, z)$$

for an arbitrary constant x_0 and a function $A(y, z)$ that needs to be determined. Differentiate with respect to y to obtain

$$\begin{aligned}
 \frac{\partial \phi(x, y, z)}{\partial y} &= \frac{\partial}{\partial y} \int_{x_0}^x f_0(\bar{x}, y, z) d\bar{x} + \frac{\partial A(y, z)}{\partial y} \\
 &= \int_{x_0}^x \frac{\partial f_0(\bar{x}, y, z)}{\partial y} d\bar{x} + \frac{\partial A(y, z)}{\partial y} \\
 &= \int_{x_0}^x \frac{\partial f_1(\bar{x}, y, z)}{\partial x} d\bar{x} + \frac{\partial A(y, z)}{\partial y} && \text{by equation (5.39)} \\
 &= f_1(x, y, z) - f_1(x_0, y, z) + \frac{\partial A(y, z)}{\partial y} \\
 &= f_1(x, y, z) && \text{by requirement}
 \end{aligned}$$

To satisfy the requirement that $\partial \phi / \partial y = f_1$, we need $\partial A / \partial y = f_1(x_0, y, z)$. Integrating with respect to y leads to

$$A(y, z) = \int_{y_0}^y f_1(x_0, \bar{y}, z) d\bar{y} + B(z)$$

for an arbitrary constant y_0 and a function $B(z)$ that needs to be determined. Now we have

$$\phi(x, y, z) = \int_{x_0}^x f_0(\bar{x}, y, z) d\bar{x} + \int_{y_0}^y f_1(x_0, \bar{y}, z) d\bar{y} + B(z)$$

Differentiate with respect to z to obtain

$$\begin{aligned}
 \frac{\partial \phi(x, y, z)}{\partial z} &= \frac{\partial}{\partial z} \int_{x_0}^x f_0(\bar{x}, y, z) d\bar{x} + \frac{\partial}{\partial z} \int_{y_0}^y f_1(x_0, \bar{y}, z) d\bar{y} + B'(z) \\
 &= \int_{x_0}^x \frac{\partial f_0(\bar{x}, y, z)}{\partial z} d\bar{x} + \int_{y_0}^y \frac{\partial f_1(x_0, \bar{y}, z)}{\partial z} d\bar{y} + B'(z) \\
 &= \int_{x_0}^x \frac{\partial f_2(\bar{x}, y, z)}{\partial x} d\bar{x} + \int_{y_0}^y \frac{\partial f_2(x_0, \bar{y}, z)}{\partial y} d\bar{y} + B'(z) && \text{by equation (5.39)} \\
 &= f_2(x, y, z) - f_2(x_0, y_0, z) + B'(z) \\
 &= f_2(x, y, z) && \text{by requirement}
 \end{aligned}$$

To satisfy the requirement that $\partial\phi/\partial z = f_2$, we need $B'(z) = f_2(x_0, y_0, z)$. Integrating with respect to z leads to

$$B(z) = \int_{z_0}^z f_2(x_0, y_0, \bar{z}) d\bar{z} + C$$

for an arbitrary constant y_0 and an arbitrary constant C . Finally, we have

$$\phi(x, y, z) = \int_{x_0}^x f_0(\bar{x}, y, z) d\bar{x} + \int_{y_0}^y f_1(x_0, \bar{y}, z) d\bar{y} + \int_{z_0}^z f_2(x_0, y_0, \bar{z}) d\bar{z} + C \quad (5.40)$$

and by construction, $\mathbf{f} = \nabla\phi$.

Vector Field Uniquely Determined by Divergence and Curl

Suppose you have a vector field \mathbf{f} defined in a region V with boundary S . The divergence is $\nabla \cdot \mathbf{f}$, the curl is $\nabla \times \mathbf{f}$, and the boundary components are $\mathbf{f} \cdot \mathbf{n}$ where \mathbf{n} is the vector field of outer-pointing normals to S . Can there be another vector field \mathbf{g} with the same divergence, curl, and boundary components? The answer is “no”. If there were such a \mathbf{g} for which $\nabla \cdot \mathbf{g} = \nabla \cdot \mathbf{f}$, $\nabla \times \mathbf{g} = \nabla \times \mathbf{f}$, and $\mathbf{g} \cdot \mathbf{n} = \mathbf{f} \cdot \mathbf{n}$ on the boundary, then define the difference $\mathbf{h} = \mathbf{f} - \mathbf{g}$. Consequently, $\nabla \cdot \mathbf{h} = 0$, $\nabla \times \mathbf{h} = \mathbf{0}$, and $\mathbf{h} \cdot \mathbf{n} = 0$ on the boundary of S .

We had just argued that a vector field \mathbf{h} for which $\nabla \times \mathbf{h} = \mathbf{0}$ has a scalar potential ϕ . Thus,

$$\begin{aligned} \int_V |\mathbf{h}|^2 dV &= \int_V \phi \nabla \cdot \mathbf{h} + \mathbf{h} \cdot \nabla \phi dV && \text{because } \nabla \cdot \mathbf{h} = 0 \text{ and } \nabla \phi = \mathbf{h} \\ &= \int_V \nabla \cdot (\phi \mathbf{h}) dV \\ &= \int_S \phi \mathbf{h} \cdot d\mathbf{S} && \text{by the divergence theorem} \\ &= \int_S \phi \mathbf{h} \cdot \mathbf{n} dS \\ &= 0 && \text{because } \mathbf{h} \cdot \mathbf{n} = 0 \end{aligned}$$

The only way the integral of a nonnegative function can be zero is if the integrand is zero, $|\mathbf{h}|^2 = 0$, which implies that $\mathbf{h} = \mathbf{0}$. Consequently, $\mathbf{g} = \mathbf{f}$, so the divergence, curl, and boundary components of a vector field on V uniquely determine the vector field.

If $V = \mathbb{R}^3$ (all of space), then there is no boundary S . In this case, \mathbf{f} is uniquely determined by its divergence and curl as long as the infinite integrals involving \mathbf{f} are

valid. It is sufficient to require that $|\mathbf{f}| = O(1/r^2)$, which is order notation that translates to: There is a constant $K > 0$ and an $r_0 > 0$ such that $|\mathbf{f}| \leq K/r^2$ for $r \geq r_0$. In the vernacular, $|\mathbf{f}|$ tends to zero like $1/r^2$ as $r \rightarrow \infty$.

In the construction of the previous paragraph, let $V(r)$ be a solid sphere of radius r centered at the origin. Its boundary is the sphere $S(r)$. We have

$$\int_{V(r)} |\mathbf{h}|^2 dV = \int_{S(r)} \phi \mathbf{h} \cdot \mathbf{n} dS$$

Unlike the previous proof, the right-hand side is not zero because we have made no assumptions about the boundary components on $S(r)$. Using spherical coordinates for the boundary, $\mathbf{x} = r(\cos\theta \sin\phi, \sin\theta \sin\phi, \cos\phi)$, the element of surface area is $dS = r^2 \sin\phi d\theta d\phi$. For r sufficiently large,

$$\begin{aligned} \int_{V(r)} |\mathbf{h}|^2 dV &= \int_{S(r)} \phi \mathbf{h} \cdot \mathbf{n} r^2 \sin\phi d\theta d\phi \\ &= \left| \int_{S(r)} \phi \mathbf{h} \cdot \mathbf{n} r^2 \sin\phi d\theta d\phi \right| \\ &\leq \int_{S(r)} |\phi \mathbf{h} \cdot \mathbf{n}| r^2 \sin\phi d\theta d\phi \\ &\leq \int_{S(r)} |\phi| |\mathbf{h}| r^2 \sin\phi d\theta d\phi \\ &\leq \int_{S(r)} (K_1/r)(K_2/r^2) r^2 \sin\phi d\theta d\phi \\ &= K_3/r^2 \end{aligned}$$

I have used the fact that $|\mathbf{h}| = |\nabla\phi|$ is $O(1/r^2)$ which implies the antiderivative $\phi = O(1/r)$. Taking the limit as r becomes unbounded,

$$0 \leq \int_{\mathbb{R}^3} |\mathbf{h}|^2 dV = \lim_{r \rightarrow \infty} \int_{V(r)} |\mathbf{h}|^2 dV \leq \lim_{r \rightarrow \infty} (K_3/r^2) = 0$$

which forces the infinite integral to be zero and, consequently, $\mathbf{h} = \mathbf{0}$.

Vector Potential

Consider a vector field defined by $\mathbf{f} = \nabla \times \mathbf{g}$ for some vector field \mathbf{g} . The vector field \mathbf{f} is said to be generated by the *vector potential* \mathbf{g} . By [Exercise 5.18](#), \mathbf{f} has the property

$\nabla \cdot \mathbf{f} = \nabla \cdot \nabla \times \mathbf{g} = 0$. In words, a vector potential-generated vector field has no divergence; the vector field is said to be *divergence free*.

Suppose that we are given a vector field \mathbf{f} for which $\nabla \cdot \mathbf{f} = 0$. Can we construct a vector potential \mathbf{g} that generates \mathbf{f} ? The answer is “yes,” although not uniquely.

Let $\mathbf{f} = (f_0, f_1, f_2)$ be a vector field for which $\nabla \cdot \mathbf{f} = 0$. Let $\mathbf{g} = (g_0, g_1, g_2)$ be an as-yet-unknown vector field for which we want $\mathbf{f} = \nabla \times \mathbf{g}$; then

$$(f_0, f_1, f_2) = \left(\frac{\partial g_2}{\partial y} - \frac{\partial g_1}{\partial z}, \frac{\partial g_0}{\partial z} - \frac{\partial g_2}{\partial x}, \frac{\partial g_1}{\partial x} - \frac{\partial g_0}{\partial y} \right)$$

To simplify matters, let us try to construct a vector field for which $g_0 = 0$. The previous equation becomes

$$(f_0, f_1, f_2) = \left(\frac{\partial g_2}{\partial y} - \frac{\partial g_1}{\partial z}, -\frac{\partial g_2}{\partial x}, \frac{\partial g_1}{\partial x} \right)$$

We may integrate the last two components to obtain

$$\begin{aligned} g_1(x, y, z) &= \int_{x_0}^x f_2(x, y, z) dx + A(y, z) \\ g_2(x, y, z) &= - \int_{x_0}^x f_1(x, y, z) dx + B(y, z) \end{aligned} \tag{5.41}$$

for any choice of constant x_0 and for some as-yet-unknown functions $A(y, z)$ and $B(y, z)$.

In equation (5.41), differentiate g_1 with respect to z and g_2 with respect to y and combine to obtain

$$\begin{aligned} \frac{\partial g_2}{\partial y} - \frac{\partial g_1}{\partial z} &= - \int_{x_0}^x \left(\frac{\partial f_1}{\partial y} + \frac{\partial f_2}{\partial z} \right) dx + \frac{\partial B}{\partial y} - \frac{\partial A}{\partial z} \\ &= \int_{x_0}^x \frac{\partial f_0}{\partial x} dx + \frac{\partial B}{\partial y} - \frac{\partial A}{\partial z} \\ &= f_0(x, y, z) - f_0(x_0, y, z) + \frac{\partial B}{\partial y} - \frac{\partial A}{\partial z} \end{aligned} \tag{5.42}$$

where the second equality uses $\nabla \cdot \mathbf{f} = 0$, namely, by solving for $\partial f_0 / \partial x = -\partial f_1 / \partial y - \partial f_2 / \partial z$. Equation (5.41) also states that we want $f_0(x, y, z) = \partial g_2 / \partial y - \partial g_1 / \partial z$, so in equation (5.42) we need

$$-f_0(x_0, y, z) + \frac{\partial B}{\partial y} - \frac{\partial A}{\partial z} = 0$$

It is sufficient to choose $A = 0$ and $B = \int_{y_0}^y f_0(x_0, y, z) dy$ for any choice of constant y_0 . Thus,

$$\mathbf{g} = \left(0, \int_{x_0}^x f_2(x, y, z) dx, - \int_{x_0}^x f_1(x, y, z) dx + \int_{y_0}^y f_0(x_0, y, z) dy \right)$$

is a vector function for which $\mathbf{f} = \nabla \times \mathbf{g}$. The choice for \mathbf{g} is not unique. Given any continuously differentiable function $\psi(\mathbf{x})$, the function $\mathbf{g} + \nabla\psi$ also is a solution; see [Exercise 5.17](#). Solutions are

$$\mathbf{g} = \left(0, \int_{x_0}^x f_2(x, y, z) dx, - \int_{x_0}^x f_1(x, y, z) dx + \int_{y_0}^y f_0(x_0, y, z) dy \right) + \nabla\psi \quad (5.43)$$

for an arbitrary differentiable function ψ .

Fundamental Theorem of Vector Calculus

The *fundamental theorem of vector calculus*, also known as the *Helmholtz decomposition*, says that any twice continuously differentiable vector field \mathbf{f} defined on all of \mathbb{R}^3 , and for which $|\mathbf{f}| = O(1/r^2)$, can be decomposed into a gradient and a curl,

$$\mathbf{f} = -\nabla\phi + \nabla \times \mathbf{g} \quad (5.44)$$

where ϕ is a scalar potential and \mathbf{g} is a vector potential. The scalar potential is not unique, because $\nabla(\phi + c) = \nabla\phi$ for any constant c . The vector potential is not unique, because $\nabla \times (\mathbf{g} + \nabla\psi) = \nabla \times \mathbf{g}$ for any differentiable function ψ . However, the decomposition of \mathbf{f} is unique by our previous results that show \mathbf{f} is uniquely determined by its divergence and curl.

The construction is as follows. Let \mathbf{p} be a solution to Poisson's equation defined on \mathbb{R}^3 ; that is, \mathbf{p} is a solution to $\nabla^2 \mathbf{p} = -\mathbf{f}$. [Equation \(5.38\)](#) is the solution per component, so

$$\mathbf{p} = \int_{\mathbb{R}^3} \frac{\mathbf{f}(\mathbf{y})}{|\mathbf{x} - \mathbf{y}|} dV$$

[Exercise 5.14](#) states that

$$\nabla \times (\nabla \times \mathbf{p}) = \nabla(\nabla \cdot \mathbf{p}) - \nabla^2 \mathbf{p}$$

in which case

$$\mathbf{f} = -\nabla^2 \mathbf{p} = -\nabla(\nabla \cdot \mathbf{p}) + \nabla \times (\nabla \times \mathbf{p}) = -\nabla\phi + \nabla \times \mathbf{g}$$

where $\phi = \nabla \cdot \mathbf{p}$ and $\mathbf{g} = \nabla \times \mathbf{p}$. Observe that this decomposition implies

$$\nabla^2 \phi = \nabla^2(\nabla \cdot \mathbf{p}) = -\nabla \cdot \mathbf{f}, \quad \nabla^2 \mathbf{g} = \nabla^2(\nabla \times \mathbf{p}) = -\nabla \times \mathbf{f}$$

where

$$\nabla \cdot \mathbf{p} = \int_{\mathbb{R}^3} \mathbf{f}(\mathbf{y}) \nabla \cdot \frac{1}{|\mathbf{x} - \mathbf{y}|} dV, \quad \nabla \times \mathbf{p} = \int_{\mathbb{R}^3} \mathbf{f}(\mathbf{y}) \nabla \times \frac{1}{|\mathbf{x} - \mathbf{y}|} dV$$

In the integrands, ∇ is applied as \mathbf{x} -derivatives, whereas \mathbf{y} are the variables of integration.

5.2 STRAIN AND STRESS

This section provides the derivations for the *strain tensor*, the *deformation tensor*, and the *stress tensor* for a fluid. The development depends on analyzing the structure of the velocity field of a fluid locally at each point.

5.2.1 STRAIN TENSOR

Let \mathbf{p} be a point in the volume of fluid with velocity $\mathbf{v}(\mathbf{p})$. We will analyze points nearby, say $\mathbf{p} + \mathbf{x}$, where \mathbf{x} is a small displacement. The velocity at such a point is $\mathbf{v}(\mathbf{p} + \mathbf{x})$. We may use a Taylor polynomial to approximate the velocity at the neighboring points.

For a small displacement \mathbf{x} , define

$$\mathbf{g}(h) = \mathbf{v}(\mathbf{p} + h\mathbf{u})$$

where \mathbf{u} is a unit-length vector in the direction of the displacement \mathbf{x} . The derivative of \mathbf{g} is computed using the chain rule,

$$\mathbf{g}'(h) = (\mathbf{u} \cdot \nabla) \mathbf{v}(\mathbf{p} + h\mathbf{u})$$

From calculus, we may write

$$\mathbf{g}(h) = \mathbf{g}(0) + h\mathbf{g}'(0) + \varepsilon$$

where ε is an error that is on the order of h^2 for small h . The function $\mathbf{g}(h)$ is approximated by the Taylor polynomial of degree 1, $\mathbf{g}(h) \doteq \mathbf{g}(0) + h\mathbf{g}'(0)$.

In terms of the velocity,

$$\mathbf{v}(\mathbf{p} + h\mathbf{u}) = \mathbf{v}(\mathbf{p}) + h((\mathbf{u} \cdot \nabla) \mathbf{v})(\mathbf{p}) + \varepsilon$$

The parentheses around the expression $(\mathbf{u} \cdot \nabla)\mathbf{v}$ indicates that the derivative is computed *first* before evaluating the result *second* by substituting in \mathbf{p} . Setting $\mathbf{x} = h\mathbf{u}$, we have

$$\mathbf{v}(\mathbf{p} + \mathbf{x}) = \mathbf{v}(\mathbf{p}) + ((\mathbf{x} \cdot \nabla)\mathbf{v})(\mathbf{p}) + \varepsilon$$

Define

$$\mathbf{w} = ((\mathbf{x} \cdot \nabla)\mathbf{v})(\mathbf{p}) = x_0 \mathbf{v}_{x_0}(\mathbf{p}) + x_1 \mathbf{v}_{x_1}(\mathbf{p}) + x_2 \mathbf{v}_{x_2}(\mathbf{p}) \quad (5.45)$$

The term $\mathbf{v}_{x_i}(\mathbf{p})$ is the first-order partial derivative of \mathbf{v} with respect to x_i which is computed first and then evaluated at \mathbf{p} , which means the end results are all constants with respect to the x_i . It is easily shown that

$$(\mathbf{x} \cdot \nabla) \mathbf{w} = \mathbf{w} \quad (5.46)$$

and

$$\nabla \times \mathbf{w} = (\nabla \times \mathbf{v})(\mathbf{p}) \quad (5.47)$$

with the same convention that the curl of \mathbf{v} is computed first before the evaluation at \mathbf{p} . Also,

$$\begin{aligned} \nabla(\mathbf{x} \cdot \mathbf{w}) &= \mathbf{x} \times (\nabla \times \mathbf{w}) + \mathbf{w} \times (\nabla \times \mathbf{x}) + (\mathbf{x} \cdot \nabla) \mathbf{w} + (\mathbf{w} \cdot \nabla) \mathbf{x} \\ &\quad \text{using equation (5.21)} \\ &= \mathbf{x} \times (\nabla \times \mathbf{w}) + \mathbf{0} + (\mathbf{x} \cdot \nabla) \mathbf{w} + \mathbf{w} \\ &\quad \text{using Equations (5.6) and (5.7)} \\ &= \mathbf{x} \times ((\nabla \times \mathbf{v})(\mathbf{p})) + 2\mathbf{w} \\ &\quad \text{using Equations (5.46) and (5.47)} \end{aligned} \quad (5.48)$$

We may solve this for \mathbf{w} and obtain the velocity representation

$$\mathbf{v}(\mathbf{p} + \mathbf{x}) = \mathbf{v}(\mathbf{p}) + \frac{1}{2} ((\nabla \times \mathbf{v})(\mathbf{p})) \times \mathbf{x} + \frac{1}{2} \nabla(\mathbf{x} \cdot \mathbf{w}) + \varepsilon \quad (5.49)$$

Compute the dot product of \mathbf{x} and \mathbf{w} using equation (5.45) to obtain

$$\mathbf{x} \cdot \mathbf{w} = \mathbf{x}^T (\nabla \otimes \mathbf{v}) \mathbf{x} \quad (5.50)$$

where $M = \nabla \otimes \mathbf{v}$ is the matrix of first-order partial derivatives of \mathbf{v} . The symbol \otimes denotes a tensor product. If you are familiar with tensor index notation, this matrix has entry $v_{r,c}$ in row r and column c . It is the partial derivative of component r of \mathbf{v} with respect to the variable x_c . Equation (5.50) may look like a quadratic form, but technically it is not because quadratic forms $\mathbf{x}^T M \mathbf{x}$ require M to be a symmetric matrix. The matrix $\nabla \otimes \mathbf{v}$ is not symmetric. However, we can easily fix the problem by noticing that a matrix A may always be written as the sum of a symmetric matrix and a skew-symmetric matrix,

$$A = \frac{A + A^T}{2} + \frac{A - A^T}{2}$$

where $A + A^T$ is symmetric and $A - A^T$ is skew-symmetric. In such a factorization, notice that

$$\mathbf{x}^T A \mathbf{x} = \mathbf{x}^T \left(\frac{A + A^T}{2} \right) \mathbf{x}$$

because $\mathbf{x}^T (A - A^T) \mathbf{x} = \mathbf{0}$.

EXERCISE
5.16

Prove that $\mathbf{x}^T (A - A^T) \mathbf{x} = \mathbf{0}$ for a 3×3 matrix A and for any 3×1 vector \mathbf{x} . ■

Therefore, equation (5.50) may be written as the quadratic form

$$\mathbf{x} \cdot \mathbf{w} = \mathbf{x}^T M \mathbf{x} = \mathbf{x}^T \left(\frac{\nabla \otimes \mathbf{v} + (\nabla \otimes \mathbf{v})^T}{2} \right) \mathbf{x} = \mathbf{x}^T E \mathbf{x} \quad (5.51)$$

where the last equality defines the symmetric matrix E . The gradient is

$$\nabla(\mathbf{x} \cdot \mathbf{w}) = 2E\mathbf{x} \quad (5.52)$$

Also, define

$$\boldsymbol{\alpha} = \frac{1}{2} ((\nabla \times \mathbf{v})(\mathbf{p})) \quad (5.53)$$

Substitute equations (5.52) and (5.53) into equation (5.49) to obtain

$$\mathbf{v}(\mathbf{p} + \mathbf{x}) = \mathbf{v}(\mathbf{p}) + \boldsymbol{\alpha} \times \mathbf{x} + E\mathbf{x} + \boldsymbol{\varepsilon} \quad (5.54)$$

The matrix E is symmetric, so it may be decomposed using an eigensystem solver into $E = RE'R^T$, where R is a rotation matrix and $E' = \text{Diag}(e_0, e_1, e_2)$ is a diagonal matrix. Define $\mathbf{y} = R^T\mathbf{x}$, in which case $\mathbf{x} = Ry$. This is effectively a rotation of the \mathbf{x} -coordinate system into the \mathbf{y} -coordinate system. Equation (5.54) now reduces to

$$\mathbf{v}(\mathbf{p} + Ry) = \mathbf{v}(\mathbf{p}) + R(\boldsymbol{\beta} \times \mathbf{y}) + E'\mathbf{y} + \boldsymbol{\varepsilon} \quad (5.55)$$

where $\boldsymbol{\alpha} = R\boldsymbol{\beta}$ and where I have used the vector identity mentioned in Exercise 2.11.

In equation (5.55), treating the error term $\boldsymbol{\varepsilon}$ as negligible (displacements \mathbf{y} have very small length), the velocity at position $\mathbf{p} + Ry$ consists of three terms:

1. $\mathbf{v}(\mathbf{p})$ is a velocity that represents a linear translation at \mathbf{p} .
2. $\boldsymbol{\alpha} \times \mathbf{x} = R(\boldsymbol{\beta} \times \mathbf{y})$ is a velocity that corresponds to rotation about a line with direction $\boldsymbol{\alpha}$ and containing \mathbf{p} ; see equation (2.35).
3. $E'\mathbf{y} = e_0 y_0 + e_1 y_1 + e_2 y_2$ is a velocity that represents stretching of the volume at \mathbf{p} . This velocity is referred to as a *pure strain*.

Consider a point \mathbf{p} in the fluid. Over a small time period Δt , the point moves to $\mathbf{p} + \Delta t \mathbf{v}(\mathbf{p})$. A neighboring point is $\mathbf{p} + \mathbf{x}$ for a small displacement \mathbf{x} . This point also

moves over the time period to $\mathbf{p} + \mathbf{x} + \Delta t \mathbf{v}(\mathbf{p} + \mathbf{x})$. The displacement between the two moved points is

$$\mathbf{y} = \mathbf{x} + \Delta t [\mathbf{v}(\mathbf{p} + \mathbf{x} - \mathbf{v}(\mathbf{p}))] = \mathbf{x} + \Delta t [\boldsymbol{\alpha} \times \mathbf{x} + E\mathbf{x} + \boldsymbol{\varepsilon}]$$

The term \mathbf{x} is a displacement and the term $\Delta t (\boldsymbol{\alpha} \times \mathbf{x})$ corresponds to a rotation, both rigid motions. The term $\Delta t (E\mathbf{x})$ corresponds to a strain. We constructed the matrix

$$E = \frac{\nabla \otimes \mathbf{v} + (\nabla \otimes \mathbf{v})^T}{2} \quad (5.56)$$

see equation (5.51). E is referred to as the (*infinitesimal*) *strain tensor*. Sometimes it is called the *deformation tensor* since its eigenvalues and eigenvectors give you an idea of how the fluid deforms at a specified position.

5.2.2 STRESS TENSOR

Any strain within the fluid must be caused by forces called *stresses*. Consider a small amount of fluid that lies in a region V with boundary S . We may first consider such forces along coordinate-axis directions, called *stress vectors*,

$$\mathbf{T}^{(0)} = (\sigma_{00}, \sigma_{01}, \sigma_{02}), \quad \mathbf{T}^{(1)} = (\sigma_{10}, \sigma_{11}, \sigma_{12}), \quad \mathbf{T}^{(2)} = (\sigma_{20}, \sigma_{21}, \sigma_{22}) \quad (5.57)$$

The values $\sigma_{00}, \sigma_{11}, \sigma_{22}$ are called *normal stresses* and the other values are called *shear stresses*. Imagine $\mathbf{T}^{(0)}$ acting on a fluid surface that is planar with normal $(1, 0, 0)$. The component σ_{00} is the stress in the normal direction, which is why it is called a normal stress. The components σ_{01} and σ_{02} act within the plane perpendicular to the normal, so they have a shearing nature about them. The nine values of equation (5.57) may be written as a tensor, as indicated by the matrix

$$\boldsymbol{\sigma} = \begin{bmatrix} \sigma_{00} & \sigma_{01} & \sigma_{02} \\ \sigma_{10} & \sigma_{11} & \sigma_{12} \\ \sigma_{20} & \sigma_{21} & \sigma_{22} \end{bmatrix} \quad (5.58)$$

The stress vector in an arbitrary unit-length direction $\mathbf{n} = (n_0, n_1, n_2)$ is a combination of the coordinate-axis stress vectors. The argument is based on considering a tetrahedron of small volume that contains fluid. One vertex of the tetrahedron is at the origin. The slant face has outer-pointing normal \mathbf{n} and is a distance $h > 0$ from the origin. The equation of the plane is $\mathbf{n} \cdot \mathbf{x} = h$. The other vertices of the tetrahedron must be $(h/n_0, 0, 0)/3, (0, h/n_1, 0)/3$, and $(0, 0, h/n_2)/3$.

The area of the slant face is $A = h^2/(18n_0n_1n_2)$, the area of the face in the x_1x_2 -plane is $A_0 = h^2/(18n_1n_2)$, the area of the face in the x_0x_2 -plane is $A_1 = h^2/(18n_0n_2)$, and the area of the face in the x_0x_1 -plane is $A_2 = h^2/(18n_0n_1)$. Observe that $A_i = n_i A$ for all i . The height of the tetrahedron is h , measured from the origin to the slant face. The volume of the tetrahedron is one-third the area of the base (slant face)

times the height, $V = h^3 / (18n_0 n_1 n_2)$. The mass of the fluid is $m = \rho V$, where ρ is the (constant) density of the fluid.

The fluid adjacent to the slant face exerts a force $m\mathbf{a}$, where m is the mass of the fluid in the tetrahedron and \mathbf{a} is the acceleration of the fluid toward the slant face. The coordinate-axis stress vectors also induce forces on their corresponding faces, $\mathbf{T}^{(i)} A_i$ for all i . The stress vector for the slant face is denoted $\mathbf{T}^{(n)}$ and induces a force $\mathbf{T}^{(n)} A$ on the slant face. In equilibrium, the forces on the tetrahedron must balance,

$$\mathbf{T}^{(n)} A = \frac{\rho h^3}{18n_0 n_1 n_2} \mathbf{a} + \sum_{i=0}^2 \mathbf{T}^{(i)} A_i$$

Dividing by A and using $A_i = n_i A$ leads to

$$\mathbf{T}^{(n)} = \rho h \mathbf{a} + \sum_{i=0}^2 \mathbf{T}^{(i)} n_i$$

This is true no matter how small the tetrahedron, so it is true in the limit as h approaches zero. This leaves us with

$$\mathbf{T}^{(n)} = \sum_{i=0}^2 n_i \mathbf{T}^{(i)} = \mathbf{n}^T \boldsymbol{\sigma} \quad (5.59)$$

where $\boldsymbol{\sigma}$ is the stress tensor of equation (5.58).

Consider a small region V with boundary S . The surface forces are $\mathbf{T}^{(n)}$ and the body forces per unit volume are \mathbf{F} . In equilibrium, the resultant force must be zero, which can be summarized componentwise. In this construction, I use the tensor index notation that a repeated index in a term implies a summation over that term. For example, $a_{ij} b_j$ indicates to sum over the j index, leaving i as a free index. I also use the convention that for a 1-index tensor a_i that depends on position, the 2-index tensor $a_{i,j}$ represents the derivatives of the a_i with respect to the variable x_j . You can have any number of indices before the comma (tensor component indices) and any number of indices after the comma (positional indices).

$$\begin{aligned} 0 &= \int_S \mathbf{T}_i^{(n)} dS + \int_V F_i dV \\ &= \int_S \sigma_{ji} n_j dS + \int_V F_i dV \\ &= \int_V \sigma_{ji,j} dV + \int_V F_i dV \\ &= \int_V (\sigma_{ji,j} + F_i) dV \end{aligned}$$

The second equality uses the definition of the slant stress vector in [equation \(5.59\)](#). The term $\sigma_{ji} n_j$ is summed over j with free index i . The third equality is an application of the divergence theorem. The term $\sigma_{ji,j}$ indicates that you differentiate each entry of the stress tensor σ_{ji} with respect to x_j and then sum over j . The index i is free. The last equality lists an integral whose value is zero no matter how you choose the region V . The only way for this to happen is when the integrand is identically zero,

$$\sigma_{ji,j} + F_i = 0 \quad (5.60)$$

Similarly, equilibrium requires that the resultant moment about an arbitrary point is zero. In this construction I use a tensor notation for the cross product of vectors. The *permutation tensor* is the triply indexed quantity e_{ijk} and has 27 elements. They are $e_{123} = e_{312} = e_{231} = 1$, $e_{132} = e_{321} = e_{213} = -1$, and all other elements are zero. If $\mathbf{a} = [a_i]$ and $\mathbf{b} = [b_i]$, the cross product is written as $\mathbf{a} \times \mathbf{b} = [e_{ijk} a_j b_k]$, where the repeated indices mean sum over the j index and sum over the k index. The index i is free. In equilibrium,

$$\begin{aligned} \mathbf{0} &= \int_S \mathbf{x} \times \mathbf{T} dS + \int_V \mathbf{x} \times \mathbf{F} dV \\ &= \int_S e_{ijk} x_j \mathbf{T}_k^{(n)} dS + \int_V e_{ijk} x_j F_k dV \\ &= \int_S e_{ijk} x_j \sigma_{\ell k} n_\ell dS + \int_V e_{ijk} x_j F_k dV \\ &= \int_V (e_{ijk} x_j \sigma_{\ell k})_{,\ell} dV + \int_V e_{ijk} x_j F_k dV \\ &= \int_V e_{ijk} (x_{j,\ell} \sigma_{\ell k} + x_j \sigma_{\ell k,j}) dV + \int_V e_{ijk} x_j F_k dV \\ &= \int_V e_{ijk} [\delta_{j\ell} \sigma_{\ell k} + x_j (\sigma_{\ell k,\ell} + F_k)] dV \\ &= \int_V e_{ijk} (\delta_{j\ell} \sigma_{\ell k}) dV \\ &= \int_V e_{ijk} \sigma_{jk} dV \end{aligned}$$

The second equality defines what \mathbf{T} actually means, and the indexed quantities are used in the subsequent steps. The third equality uses the definition of the slant stress vector in [equation \(5.59\)](#). The fourth equality is an application of the divergence theorem. The parenthesized expression has a subscript with a comma followed by index ℓ . This means that the parenthesized expression, which is a tensor, must have its components differentiated with respect to x_ℓ . The fifth equality is an application

of the product rule for differentiation. The sixth equality has $x_{j,\ell} = \delta_{j\ell}$; the right-hand side is the identity matrix: $\delta_{00} = \delta_{11} = \delta_{22} = 1$ and all other entries zero. The right-hand side of the sixth equality also groups together the terms involving x_j . The seventh equality uses the equilibrium of forces condition in [equation \(5.60\)](#). The eighth equality uses the substitution property of δ_{ij} ; that is, in the expression $\delta_{j\ell}\sigma_{\ell k}$, anywhere there is an ℓ -index, substitute it with j and then throw away the δ -term.

In summary, we have $\int_V e_{ijk}\sigma_{jk} dV = 0$ no matter how we choose V . The only way this can happen is when the integrand is identically zero, $e_{ijk}\sigma_{jk}$, in which case

$$(0, 0, 0) = (e_{0jk}\sigma_{jk}, e_{1jk}\sigma_{jk}, e_{2jk}\sigma_{jk}) = (\sigma_{12} - \sigma_{21}, \sigma_{20} - \sigma_{02}, \sigma_{01} - \sigma_{10}) \quad (5.61)$$

which implies $\sigma_{01} = \sigma_{10}$, $\sigma_{02} = \sigma_{20}$, and $\sigma_{12} = \sigma_{21}$. Thus, the stress tensor σ is a symmetric matrix.

5.2.3 THE RELATIONSHIP BETWEEN STRAIN AND STRESS

In the previous sections we constructed the strain tensor E and the stress tensor σ . We had decomposed the strain tensor as $E = RE'R^T$, where R is a rotation matrix and $E' = \text{Diag}(e_0, e_1, e_2)$ is a diagonal matrix. I make the assumption that the fluid is *isotropic*; that is, an infinitesimal cube whose axes are the principal directions of strain (the column vectors of R) will deform only along those principal directions.

One of the consequences for isotropic fluids is that the stress tensor σ is *simultaneously diagonalizable* with E . That is, σ may be decomposed using an eigensolver as $\sigma = R\sigma'R^T$, where R is the *same* rotation matrix used to diagonalize E and where $\sigma' = \text{Diag}(s_0, s_1, s_2)$ is a diagonal matrix. Thus, the principal directions are the same for the strain and stress tensors. Empirical evidence shows that locally,

$$\begin{aligned} e_0 &= as_0 - b(s_1 + s_2) = (a + b)s_0 - b(s_0 + s_1 + s_2) \\ e_1 &= as_1 - b(s_0 + s_2) = (a + b)s_1 - b(s_0 + s_1 + s_2) \\ e_2 &= as_2 - b(s_0 + s_1) = (a + b)s_2 - b(s_0 + s_1 + s_2) \end{aligned} \quad (5.62)$$

for some (physical) constants a and b that depend on the fluid. Imagine an elastic linear strand of fluid. When you pull on both ends of the strand, the tension produces an extension along the axis of the strand that is proportional to the strand. This leads to the terms as_i in [equation \(5.62\)](#). That same tension causes contractions in the directions perpendicular to the axis of the strand. This leads to the terms of the form $b(s_i + s_j)$.

[Equation \(5.62\)](#) may be written succinctly as

$$E' = (a + b)\sigma' - b\text{Trace}(\sigma')I \quad (5.63)$$

where I is the identity matrix and where $\text{Trace}(A)$ is the sum of the diagonal entries of a matrix A . Applying R to the left and R^T to the right of these expressions, and using

$$E = RE'R^T \text{ and } \sigma = R\sigma'R^T,$$

$$E = (a + b)\sigma - b\text{Trace}(\sigma)I \quad (5.64)$$

where I used the identity $\text{Trace}(RAR^T) = \text{Trace}(A)$ for any rotation matrix R and any matrix A . Both $E = [E_{ij}]$ and $\sigma = [\sigma_{ij}]$ are symmetric, so we need only work with the upper triangular terms. Equation (5.64) leads to

$$\begin{aligned} E_{00} &= a\sigma_{00} - b\sigma_{11} - b\sigma_{22} \\ E_{01} &= (a + b)\sigma_{01} \\ E_{02} &= (a + b)\sigma_{02} \\ E_{11} &= -b\sigma_{00} + a\sigma_{11} - b\sigma_{22} \\ E_{12} &= (a + b)\sigma_{12} \\ E_{22} &= -b\sigma_{00} - b\sigma_{11} + a\sigma_{22} \end{aligned}$$

Using

$$\begin{bmatrix} a & -b & -b \\ -b & a & -b \\ -b & -b & a \end{bmatrix}^{-1} = \frac{1}{(a - 2b)(a + b)} \begin{bmatrix} a - b & b & b \\ b & a - b & b \\ b & b & a - b \end{bmatrix}$$

we may solve for the σ_{ij} in terms of the E_{ij} ,

$$\begin{aligned} \sigma_{00} &= [(a - b)E_{00} + b(E_{11} + E_{22})]/[(a - 2b)(a + b)] \\ \sigma_{01} &= E_{01}/(a + b) \\ \sigma_{02} &= E_{02}/(a + b) \\ \sigma_{11} &= [(a - b)E_{11} + b(E_{00} + E_{22})]/[(a - 2b)(a + b)] \\ \sigma_{12} &= E_{12}/(a + b) \\ \sigma_{22} &= [(a - b)E_{22} + b(E_{00} + E_{11})]/[(a - 2b)(a + b)] \end{aligned}$$

In matrix form this is

$$\sigma = \frac{1}{a + b} E + \frac{b}{(a - 2b)(a + b)} \text{Trace}(E)I \quad (5.65)$$

5.3 CONSERVATION LAWS

In physics, conservation laws are of utmost importance. They are typically formulated in terms of partial differential equations. We have already been exposed to these laws. For example, Section 2.5.1 appeals to the conservation of linear momentum to show that the linear momentum is constant for a system of objects with zero net external forces. Similarly, Section 2.5.2 appeals to the conservation of angular momentum.

Previous chapters made reference to conservation of energy. A summary of some basic conservation laws is provided here. The outcome is a set of differential equations we may use to model fluid flow.

5.3.1 CONSERVATION OF MASS

Consider a region V in three dimensions that contains a fluid. For the sake of argument, let the region have the topology of a solid sphere. Let the surface bounding V be named S . The fluid has a density $\rho(\mathbf{x}, t)$ that varies with position \mathbf{x} and with time t . The total mass of the fluid is

$$M(t) = \int_V dm = \int_V \rho(\mathbf{x}, t) dV \quad (5.66)$$

where the infinitesimal element of mass is $dm = \rho dV$ with dV an infinitesimal element of volume. The total mass varies with time because the density varies with time. The rate of change of mass is the time derivative

$$\frac{dM}{dt} = \frac{d}{dt} \int_V \rho dV = \int_V \frac{\partial \rho}{\partial t} dV \quad (5.67)$$

One way the mass of the fluid can change in the region V is that fluid may enter or leave through the boundary S . The amount of change is

$$-\int_S \rho \mathbf{v} \cdot \mathbf{n} dS \quad (5.68)$$

where \mathbf{v} is the velocity of the mass particles as they enter or leave the boundary, \mathbf{n} is a unit-length normal to the boundary, and dS is an infinitesimal element of surface area. At a boundary point, if \mathbf{v} points outside the region, then $\mathbf{v} \cdot \mathbf{n} > 0$, in which case equation (5.68) is a negative contribution; that is, the mass is decreasing inside V . The larger the magnitude of the velocity, the more the mass decreases. The larger the mass density at that boundary point, the larger the magnitude of the negative contribution, so the more the mass decreases. Similar intuition may be used for when \mathbf{v} points inside the region.

Another way the mass of the fluid can change is when matter is created or destroyed within V . The creation of matter is due to a *source* and the destruction of matter is due to a *sink*. Although we tend to think of sources and sink occurring at single points, the creation and destruction may be allowed to occur in a continuous manner, varying with space and time. Let the source-sink function be $s(\mathbf{x}, t)$, which measures the amount of matter created or destroyed per unit volume at the

specified location and time. Matter is created when $s > 0$ and destroyed when $s < 0$. The amount of change in mass due to the source–sink function is

$$\int_V s(\mathbf{x}, t) dV \quad (5.69)$$

Consider a small subregion $R \subset V$ with boundary B . The surface has a density flux, $\kappa \nabla \rho$, at each position. The coefficient κ is a constant that depends on the fluid and has units ℓ^2/t for length units ℓ and time units t . Adding the density flux over the surface gives us

$$\int_B \kappa \nabla \rho \cdot d\mathbf{S} = \int_B \kappa \nabla \rho \cdot \mathbf{n} dS$$

The units of ρ are m/ℓ^3 for mass units m , the units of $\nabla \rho$ are m/ℓ^4 , and the units of dS are ℓ^2 , so the integral has units m/t , which is the rate of change of mass through the surface B due to the gradient of density. An application of the divergence theorem converts the surface integral to a volume integral

$$\int_R \kappa \nabla^2 \rho dV$$

which has the same units m/t . The mass flux per unit volume is

$$\phi(R) = \frac{\int_R \kappa \nabla^2 \rho dV}{\int_R dV}$$

and is valid for any region R no matter how small. Thinking of this informally as taking the limit of $\phi(R)$ as the volume of R goes to zero – R shrinks to a point \mathbf{x} – we obtain $\phi(\mathbf{x}) = \kappa \nabla^2 \rho(\mathbf{x})$. In the large, we have

$$\int_V \kappa \nabla^2 \rho dV \quad (5.70)$$

as the contribution to the mass rate of change.

To motivate the idea of “shrinking to a point” with a formal argument, consider the one-dimensional problem. Let f and g be continuous functions. For a specified x , let $g(y)$ be the average of a function $f(y)$ over an interval $[x, y]$; that is,

$$g(y) = \frac{\int_x^y f(\xi) d\xi}{y - x}$$

Compute the following,

$$\begin{aligned}
 g(x) &= \lim_{y \rightarrow x} g(y) && \text{by continuity of } g \\
 &= \lim_{y \rightarrow x} \frac{\int_x^y f(\xi) d\xi}{y - x} && \text{by definition of } g \\
 &= \lim_{y \rightarrow x} \frac{\frac{d}{dy} \int_x^y f(\xi) d\xi}{\frac{d}{dy}(y - x)} && \text{by L'Hôpital's rule} \\
 &= \lim_{y \rightarrow x} \frac{f(y)}{1} && \text{numerator by fundamental theorem of calculus} \\
 &= f(x) && \text{by continuity of } f
 \end{aligned}$$

Therefore, by “shrinking to a point,” g is just the integrand f .

The net change in the mass in V is represented by equation (5.67). It is also represented by the sum of the quantities in equations (5.68), (5.70), and (5.69). Thus, the conservation of mass is stated mathematically as

$$\int_V \frac{\partial \rho}{\partial t} dV = \int_V (\kappa \nabla^2 \rho + s) dV - \int_S \rho \mathbf{v} \cdot \mathbf{n} dS \quad (5.71)$$

The divergence theorem may be applied to the boundary integral in equation (5.71), after which we may collect all terms to the left-hand side of the equation to obtain

$$\int_V \left(\frac{\partial \rho}{\partial t} + \nabla \cdot (\rho \mathbf{v}) - \kappa \nabla^2 \rho - s \right) dV = 0 \quad (5.72)$$

This equation states that the integral on the left-hand side is zero for all time t . The only way this can happen is when the integrand is zero for all time t . This leads us to a partial differential equation that represents conservation of mass,

$$\frac{\partial \rho}{\partial t} + \nabla \cdot (\rho \mathbf{v}) - \kappa \nabla^2 \rho - s = 0 \quad (5.73)$$

Applying the product rule for the term involving divergence, we have

$$\frac{\partial \rho}{\partial t} + \mathbf{v} \cdot \nabla \rho + \rho \nabla \cdot \mathbf{v} - \kappa \nabla^2 \rho - s = 0 \quad (5.74)$$

A fluid is said to be *incompressible* when the density is constant for all positions and time, in which case $\partial \rho / \partial t = 0$, $\nabla \rho = \mathbf{0}$, and $\nabla^2 \rho = 0$. Additionally, if there are no sources or sinks, then $s = 0$. Equation (5.74) becomes

$$\nabla \cdot \mathbf{v} = 0$$

that is, the divergence of the velocity vector field is zero. A *flow line* of the velocity vector field is a curve for which the tangents are velocity vectors. If $\mathbf{x}(t)$ is the position of a particle at time t , then the tangents are required to be

$$\frac{d\mathbf{x}}{dt} = \mathbf{v}, \quad t \geq 0; \quad \mathbf{x}(0) = \mathbf{x}_0 \quad (5.75)$$

The initial position is specified as \mathbf{x}_0 . The divergence of the velocity vector field measures the rate of expansion ($\nabla \cdot \mathbf{v} > 0$) or the rate of compression ($\nabla \cdot \mathbf{v} < 0$) of the flow lines. Figure 5.1 illustrates this.

For a fluid in region V without sources or sinks and without diffusion ($\kappa = 0$), constant density is a sufficient condition for zero divergence. With variable density and a velocity of zero divergence, equation (5.74) becomes

$$\frac{D\rho}{Dt} = \frac{\partial \rho}{\partial t} + \mathbf{v} \cdot \nabla p = 0$$

where $D/Dt = \partial/\partial t + \mathbf{v} \cdot \nabla$ is the *material derivative operator* with respect to the velocity. This equation states that when the velocity has zero divergence, the material derivative of density is zero. What does a zero material derivative say about the density itself? Define the function

$$f(t) = \rho(\mathbf{x}(t), t)$$

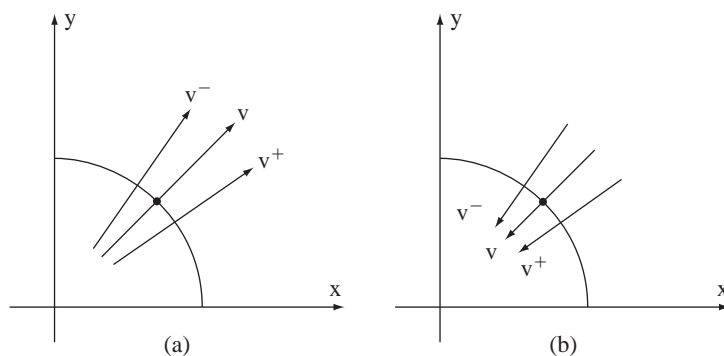


Figure 5.1 The left image shows the vector field $\mathbf{v} = (x, y)$, which has a divergence $\nabla \cdot \mathbf{v} = 2$. The flow lines are expanding at the indicated point (black dot), illustrated by flow lines with directions \mathbf{v}^+ and \mathbf{v}^- . The right image shows the vector field $\mathbf{v} = (-x, -y)$, which has a divergence $\nabla \cdot \mathbf{v} = -2$. The flow lines are compressing at the indicated point (black dot).

for a specific flow line $\mathbf{x}(t)$, so f measures the density along the flow line. The derivative is

$$\begin{aligned} f'(t) &= \frac{\partial \rho}{\partial t} + \mathbf{x}'(t) \cdot \nabla \rho, \quad \text{using the chain rule from calculus} \\ &= \frac{\partial \rho}{\partial t} + \mathbf{v} \cdot \nabla \rho, \quad \text{since } \mathbf{x}(t) \text{ is a flow line} \\ &= \frac{D\rho}{Dt}, \quad \text{by definition of the material derivatives} \\ &= 0, \quad \text{the material derivative of density is zero} \end{aligned}$$

The derivative $f'(t)$ is zero for all time, so $f(t)$ must be a constant. The implication is that *the density is constant along a flow line*.

Certainly if the density is a constant, it is constant along all flow lines. On the other hand, a zero material derivative says that density is constant along a flow line, but the actual density value can vary among flow lines. For example, the flow line containing a point \mathbf{x}_0 has constant density $\rho_0 = \rho(\mathbf{x}_0, 0) = \rho(\mathbf{x}(t), t)$ for all time, where $\mathbf{x}(t)$ is the flow line containing \mathbf{x}_0 . The flow line containing a point \mathbf{x}_1 has constant density $\rho_1 = \rho(\mathbf{x}_1, 0) = \rho(\mathbf{y}(t), t)$ for all time where $\mathbf{y}(t)$ is the flow line containing \mathbf{x}_1 . However, the values ρ_0 and ρ_1 can be unequal.

The intuition for constant density along a flow line matches the intuition for a velocity field of zero divergence. If the divergence of the velocity is negative, the flow lines are being compressed into each other. Particles from the various flow lines are being forced into the nearby flow lines due to the compression, which must cause the density to increase. Similarly, if the divergence of the velocity is positive, the flow lines are expanding away from each other. Particles from the various flow lines are free to flow away from their current flow lines due to the expansion, which must cause the density to decrease. A zero divergence means no expansion or compression, so the density of the particles is unvarying along the flow lines.

5.3.2 CONSERVATION OF MOMENTUM

Consider fluid in a region V with boundary S . The total linear momentum of the fluid is

$$\mathbf{M} = \int_V \rho \mathbf{v} dV$$

and the time derivative is

$$\frac{d\mathbf{M}}{dt} = \frac{d}{dt} \int_V \rho \mathbf{v} dV = \int_V \frac{\partial(\rho \mathbf{v})}{\partial t} dV \quad (5.76)$$

In the discussion about conservation of mass, mass enters or leaves the boundary S . The mass flux is shown in [equation \(5.68\)](#). The corresponding momentum

flux has a similar form, although it is vector-valued,

$$-\int_S (\rho \mathbf{v}) \mathbf{v} \cdot \mathbf{n} dS = -\int_S (\rho \mathbf{v} \mathbf{v}^T) \mathbf{n} dS = -\int_S \rho v_i v_j n_j dS \quad (5.77)$$

where the right-hand side uses tensor index notation. The summation is over the index j and i is a free index. An application of the divergence theorem leads to

$$-\int_V \nabla \cdot (\rho \mathbf{v} \mathbf{v}^T) dV = -\int_V (\rho v_i v_j)_{,j} dV \quad (5.78)$$

The left-hand side notation indicates that you apply the divergence to a 3-tuple by applying it to each component of the 3-tuple. The right-hand side uses tensor index notation. The parenthesized expression is a two-index tensor and is differentiated with respect to x_j , followed by summation over the j index. The index i is free. Observe that

$$(\rho v_i v_j)_{,j} = [(\rho v_j) v_i]_{,j} = (\rho v_j) v_{i,j} + (\rho v_j)_{,j} v_i = \rho (\mathbf{v} \cdot \nabla) \mathbf{v} + \nabla \cdot (\rho \mathbf{v}) \mathbf{v}$$

The integral of equation (5.78) becomes

$$-\int_V \rho (\mathbf{v} \cdot \nabla) \mathbf{v} + \nabla \cdot (\rho \mathbf{v}) \mathbf{v} dV \quad (5.79)$$

Various forces act on the fluid. External forces such as gravity may act on the fluid; call these \mathbf{f} , a force per unit mass. Pressure on the boundary S is specified by the function p . Stresses occur within the fluid, call them \mathbf{g} , a force per unit volume.

The contribution due to external forces is

$$\int_V \rho \mathbf{f} dV \quad (5.80)$$

where ρ is the density of the fluid.

The contribution from the pressure on the boundary is

$$-\int_S p dS = -\int_S p \mathbf{n} dS = -\int_V \nabla p dV \quad (5.81)$$

where the last equality is an application of the divergence theorem componentwise. Specifically, let \mathbf{e}_i be the unit-length vector with a 1 in entry i and 0 in the other two entries; then $\int_V \partial p / \partial x_i dV = \int_V \nabla \cdot p \mathbf{e}_i dV = \int_S p \mathbf{e}_i \cdot \mathbf{n} dS = \int_S p n_i dS$. The minus sign in the equation indicates that a positive pressure is applied into the surface.

The contribution from the stresses is slightly more complicated to derive. Consider a small region of fluid, call it R , with boundary B . The stress forces on the

boundary lead to a resultant force acting on the region of

$$\mathbf{g} = \frac{(\int_B \mathbf{T}^{(0)} \cdot d\mathbf{S}, \int_B \mathbf{T}^{(1)} \cdot d\mathbf{S}, \int_B \mathbf{T}^{(2)} \cdot d\mathbf{S})}{\int_R dR}$$

where $\mathbf{T}^{(i)}$ are the coordinate-axis stress vectors mentioned previously. The denominator is the volume of R , because \mathbf{g} is measured as force per unit volume. Applying the divergence theorem, we have

$$\begin{aligned}\mathbf{g} &= \frac{(\int_R \sigma_{00,0} + \sigma_{01,1} + \sigma_{02,2} dR, \int_R \sigma_{10,0} + \sigma_{11,1} + \sigma_{12,2} dR, \int_R \sigma_{20,0} + \sigma_{21,1} + \sigma_{22,2} dR)}{\int_R dR} \\ &= \frac{\int_R \nabla \cdot \boldsymbol{\sigma} dR}{\int_R dR}\end{aligned}$$

where $\nabla \cdot \boldsymbol{\sigma} = \sigma_{ij,j}$ using the tensor index and summation conventions. This result is true no matter how we choose R . Shrinking R to a point, we have $\mathbf{g} = \nabla \cdot \boldsymbol{\sigma}$. The total contribution from \mathbf{g} over all of V is

$$\int_V \nabla \cdot \boldsymbol{\sigma} dV \quad (5.82)$$

The sum of the external forces, including the momentum flux, satisfies the equation $\mathbf{F} = d\mathbf{M}/dt$. Combining equations (5.80), (5.81), (5.82), (5.79), and (5.76), we have

$$\mathbf{0} = \int_V \left(\frac{\partial(\rho\mathbf{v})}{\partial t} + \rho(\mathbf{v} \cdot \nabla)\mathbf{v} + \nabla \cdot (\rho\mathbf{v})\mathbf{v} - \rho\mathbf{f} + \nabla p - \nabla \cdot \boldsymbol{\sigma} \right) dV$$

This equation is true no matter the choice of V . The only way this can happen is when the integrand is zero, which leads us to the *Navier–Stokes equation*,

$$\frac{\partial(\rho\mathbf{v})}{\partial t} + \rho(\mathbf{v} \cdot \nabla)\mathbf{v} + \nabla \cdot (\rho\mathbf{v})\mathbf{v} = \rho\mathbf{f} - \nabla p + \nabla \cdot \boldsymbol{\sigma} \quad (5.83)$$

Applying the product rule to $\partial(\rho\mathbf{v})/\partial t$ and grouping terms, we have

$$\rho \left(\frac{\partial \mathbf{v}}{\partial t} + (\mathbf{v} \cdot \nabla)\mathbf{v} \right) + \left(\frac{\partial \rho}{\partial t} + \nabla \cdot (\rho\mathbf{v}) \right) \mathbf{v} = \rho\mathbf{f} - \nabla p + \nabla \cdot \boldsymbol{\sigma}$$

The standard assumption in derivations of the Navier–Stokes equations is that the system has no density sources or sinks and no density diffusion, in which case equation (5.73) is used with $s = 0$ and $\kappa = 0$,

$$\rho \left(\frac{\partial \mathbf{v}}{\partial t} + (\mathbf{v} \cdot \nabla)\mathbf{v} \right) = \rho\mathbf{f} - \nabla p + \nabla \cdot \boldsymbol{\sigma}$$

If you plan on including density sources or sinks and density diffusion, you must use instead the equation

$$\rho \left(\frac{\partial \mathbf{v}}{\partial t} + (\mathbf{v} \cdot \nabla) \mathbf{v} \right) + (\kappa \nabla^2 \rho + s) \mathbf{v} = \rho \mathbf{f} - \nabla p + \nabla \cdot \boldsymbol{\sigma} \quad (5.84)$$

We have some additional knowledge of the stress tensor $\boldsymbol{\sigma}$. Equation (5.65) has a relationship between the strain and stress tensors, but in the presence of a viscous fluid, the frictional forces lead to a similar relationship but with *dynamic viscosity* constant μ and a yet-to-be-determined constant μ' ,

$$\boldsymbol{\sigma} = 2\mu E + \mu' \text{Trace}(E) I$$

The trace of the stress tensor is an invariant for such fluids and must be zero in the static case, so

$$0 = \text{Trace}(\boldsymbol{\sigma}) = (2\mu + 3\mu') \text{Trace}(E)$$

It is sufficient to choose $\mu' = -2\mu/3$ for the trace to be zero. Also, from the definition of E note that $\text{Trace}(E) = \nabla \cdot \mathbf{v}$. Therefore,

$$\boldsymbol{\sigma} = 2\mu \left(E - \frac{\nabla \cdot \mathbf{v}}{3} I \right)$$

Recall that $2E = \nabla \otimes \mathbf{v} + (\nabla \otimes \mathbf{v})^T$, $\nabla \otimes \mathbf{v} = v_{i,j}$ in tensor index notation, where $\mathbf{v} = (v_0, v_1, v_2)$, and $\nabla \cdot \mathbf{v} = v_{k,k}$. Consequently,

$$\sigma_{ij} = \mu \left(v_{i,j} + v_{j,i} - \frac{2v_{k,k}}{3} \delta_{ij} \right)$$

The divergence of stress, $\nabla \cdot \boldsymbol{\sigma}$, in tensor index notation is

$$\begin{aligned} \sigma_{ij,j} &= \mu \left(v_{i,jj} + v_{j,ij} - \frac{2v_{k,kj}}{3} \delta_{ij} \right) \\ &= \mu \left(v_{i,jj} + v_{j,ij} - \frac{2v_{k,ki}}{3} \right) \\ &= \mu \left(v_{i,jj} + v_{j,ji} - \frac{2v_{j,ji}}{3} \right) \\ &= \mu \left(v_{i,jj} + \frac{v_{j,ji}}{3} \right) \end{aligned}$$

The second equality uses the substitution property of the δ tensor. The third equality just renames the summation index k to j and switches the order of differentiation (valid for functions that are twice continuously differentiable). Switching back to vector form, we have

$$\nabla \cdot \boldsymbol{\sigma} = \mu \left(\nabla^2 \mathbf{v} + \frac{1}{3} \nabla (\nabla \cdot \mathbf{v}) \right) \quad (5.85)$$

Equation (5.84) is now

$$\rho \left(\frac{\partial \mathbf{v}}{\partial t} + (\mathbf{v} \cdot \nabla) \mathbf{v} \right) + (\kappa \nabla^2 \rho + s) \mathbf{v} = \rho \mathbf{f} - \nabla p + \mu \left(\nabla^2 \mathbf{v} + \frac{1}{3} \nabla (\nabla \cdot \mathbf{v}) \right) \quad (5.86)$$

5.4 A SIMPLIFIED MODEL FOR FLUID FLOW

In summary, the equations for conservation of mass and momentum from the previous section are listed next, where the left-hand sides are the material derivatives of density ρ and velocity \mathbf{v} ,

$$\frac{\partial \rho}{\partial t} + (\mathbf{v} \cdot \nabla) \rho = \kappa \nabla^2 \rho + s - \rho \nabla \cdot \mathbf{v}$$

and

$$\frac{\partial \mathbf{v}}{\partial t} + (\mathbf{v} \cdot \nabla) \mathbf{v} = \mathbf{f} - \frac{1}{\rho} \nabla p + \frac{\mu}{\rho} \left(\nabla^2 \mathbf{v} + \frac{1}{3} \nabla (\nabla \cdot \mathbf{v}) \right) - \frac{1}{\rho} (\kappa \nabla^2 \rho + s) \mathbf{v}$$

A few more assumptions about the fluid allows us to simplify the equations. Let us assume that the fluid is incompressible, so $\nabla \cdot \mathbf{v} = 0$. The equations are then

$$\begin{aligned} \frac{\partial \rho}{\partial t} + (\mathbf{v} \cdot \nabla) \rho &= \kappa \nabla^2 \rho + s \\ \frac{\partial \mathbf{v}}{\partial t} + (\mathbf{v} \cdot \nabla) \mathbf{v} &= \mathbf{f} - \frac{1}{\rho} \nabla p + \frac{\mu}{\rho} \nabla^2 \mathbf{v} - \frac{1}{\rho} (\kappa \nabla^2 \rho + s) \mathbf{v} \end{aligned}$$

These equations *almost* look like those used in the paper [Sta03], which are

$$\begin{aligned} \frac{\partial \rho}{\partial t} + (\mathbf{v} \cdot \nabla) \rho &= \kappa \nabla^2 \rho + s \\ \frac{\partial \mathbf{v}}{\partial t} + (\mathbf{v} \cdot \nabla) \mathbf{v} &= v \nabla^2 \mathbf{v} + \mathbf{f} \end{aligned} \quad (5.87)$$

The expression $\mathbf{f} - (s/\rho)\mathbf{v} - (1/\rho)\nabla p$ is replaced by a single term, which is still called \mathbf{f} . You may think of this as having no pressure on the boundary of the fluid, $p = 0$, but unfortunately it is not possible to think that $\kappa = 0$ and $s = 0$ in the velocity equation. Any such assumptions for the velocity equation must then also be made for the density equation. Effectively, the term $(\kappa \nabla^2 \rho + s)\mathbf{v}/\rho$ is discarded, yet this term involves the state of the system (density and velocity).

The paper also has $v = \mu/\rho$. The numerator is the *dynamic viscosity*, which is a ratio of pressure exerted on the surface of the fluid in the lateral direction and the change in velocity of the fluid as you move through it. The value v is the *kinematic viscosity*, which is the ratio of viscous force (dynamic viscosity) to inertial force (from the fluid density). In the derivation of the stress tensor, μ was assumed to be a constant, so v is not a constant (varies with density). However, [Sta03] treats v as a constant. This

might be a reasonable assumption should the density be approximately a constant, but the simulations show otherwise.

The goal of [Sta03] is to obtain visually convincing simulations, not ones that are of high accuracy and match the actual physics models. For the purpose of fluid dynamics in games, equation (5.87) is as good a model as any. The remaining sections in this chapter are devoted to describing the algorithms in the paper.

5.5 IMPLEMENTING THE SIMPLIFIED 2D MODEL

A numerical method is formulated for solving the density equation in equation (5.87). This equation is a *parabolic partial differential equation*. To solve the equation for density $\rho(\mathbf{x}, t)$, we need to specify an *initial condition* $\rho(\mathbf{x}, t) = \rho_0(\mathbf{x})$, where the function ρ_0 is chosen however you like – a nonnegative function for this application, because ρ represents density. Our original region V of fluid is bounded with boundary S , so we also need to specify *boundary conditions*, which are the values of ρ on S for all time $t \geq 0$. The two classical choices are *Dirichlet conditions*, where $\rho(\mathbf{x}, t)$ is specified for all $\mathbf{x} \in S$, or *Neumann conditions*, where $\mathbf{n}(\mathbf{x}) \cdot \nabla \rho(\mathbf{x}, t)$ for all $\mathbf{x} \in S$ and where $\mathbf{n}(\mathbf{x})$ is the outer-pointing surface normal at \mathbf{x} .

Solving the differential equation on a general region V requires *finite element methods*, a way of decomposing the region to allow derivative approximations at various points in the region. Typical is to approximate a 2D region by a triangle mesh and a 3D region by a tetrahedron mesh. The approximations are computed at the vertices of the mesh.

5.5.1 THE DENSITY EQUATION

To simplify our problem for games, V will be a solid rectangle in 2D, say, $V = \{(x, y) : x \in [x_0, x_1], y \in [y_0, y_1]\}$. The velocity vector has components $u(x, y, t)$ and $v(x, y, t)$. The differential equation and initial conditions are

$$\begin{aligned}\rho_t &= \kappa (\rho_{xx} + \rho_{yy}) - u\rho_x - v\rho_y + s, \quad (x, y) \in [x_0, x_1] \times [y_0, y_1], \quad t \geq 0 \\ \rho(x, y, 0) &= \rho_0(x, y), \quad (x, y) \in [x_0, x_1] \times [y_0, y_1]\end{aligned}\tag{5.88}$$

where the subscripts on ρ indicate partial derivatives with respect to the variables t , x , and y . The initial-value function ρ_0 is specified by you.

The Dirichlet boundary conditions are

$$\begin{aligned}\rho(x_0, y, t) &= \phi_0(y, t), \quad y \in [y_0, y_1], \quad t \geq 0 \\ \rho(x_1, y, t) &= \phi_1(y, t), \quad y \in [y_0, y_1], \quad t \geq 0 \\ \rho(x, y_0, t) &= \psi_0(x, t), \quad x \in [x_0, x_1], \quad t \geq 0 \\ \rho(x, y_1, t) &= \psi_1(x, t), \quad x \in [x_0, x_1], \quad t \geq 0\end{aligned}\tag{5.89}$$

where the functions ϕ_0 , ϕ_1 , ψ_0 , and ψ_1 are specified by you. For continuity on the boundary at the corners, you must guarantee that $\phi_0(y_0, t) = \psi_0(x_0, t)$, $\phi_1(y_0, t) = \psi_0(x_1, t)$, $\phi_0(y_1, t) = \psi_1(x_0, t)$, and $\phi_1(y_1, t) = \psi_1(x_1, t)$. For continuity with the initial conditions, you must guarantee that $\rho_0(x_0, y) = \phi_0(y, 0)$, $\rho_0(x_1, y) = \phi_1(y, 0)$, $\rho_0(x, y_0) = \psi_0(x, 0)$, and $\rho_0(x, y_1) = \psi_1(x, 0)$.

The Neumann boundary conditions are

$$\begin{aligned}\rho_x(x_0, y, t) &= \phi'_0(y, t), & y \in [y_0, y_1], t \geq 0 \\ \rho_x(x_1, y, t) &= \phi'_1(y, t), & y \in [y_0, y_1], t \geq 0 \\ \rho_y(x, y_0, t) &= \psi'_0(x, t), & x \in [x_0, x_1], t \geq 0 \\ \rho_y(x, y_1, t) &= \psi'_1(x, t), & x \in [x_0, x_1], t \geq 0\end{aligned}\tag{5.90}$$

where the functions ϕ'_0 , ϕ'_1 , ψ'_0 , and ψ'_1 are specified by you. The prime symbols are part of the function names and are used solely to remind you that these functions produce derivative values. For continuity on the boundary at the corners, you must guarantee that $\phi'_0(y_0, t) = \psi'_0(x_0, t)$, $\phi'_1(y_0, t) = \psi'_0(x_1, t)$, $\phi'_0(y_1, t) = \psi'_1(x_0, t)$, and $\phi'_1(y_1, t) = \psi'_1(x_1, t)$. For continuity with the initial conditions, assume that the initial-value function is differentiable with partial derivatives $\rho_{0,x} = \partial\rho/\partial x$ and $\rho_{0,y} = \partial\rho/\partial y$. You must guarantee that $\rho_{0,x}(x_0, y) = \phi'_0(y, 0)$, $\rho_{0,x}(x_1, y) = \phi'_1(y, 0)$, $\rho_{0,y}(x, y_0) = \psi'_0(x, 0)$, and $\rho_{0,y}(x, y_1) = \psi'_1(x, 0)$.

The rectangular region is decomposed into a rectangular lattice of points, say, $(x[i], y[j])$ for $0 \leq i \leq i_{\max}$ and $0 \leq j \leq j_{\max}$. Each lattice cell is centered at $(x[i], y[j])$ and has dimensions $\Delta_x = (x_1 - x_0)/i_{\max}$ and $\Delta_y = (y_1 - y_0)/j_{\max}$. Thus, $x[i] = x_0 + i\Delta_x$ and $y[j] = y_0 + j\Delta_y$. [Figure 5.2](#) shows a typical lattice.

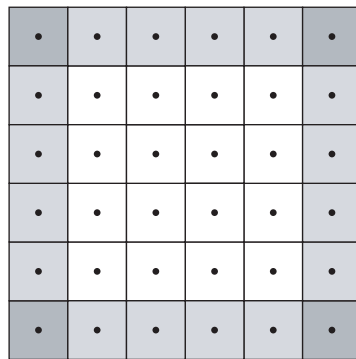


Figure 5.2 A typical lattice of points, where $i_{\max} = j_{\max} = 5$. The lattice cell centers are shown as black dots. The interior cells have a white background. The boundary corner cells have a dark gray background. The boundary edge-interior cells have a light gray background.

The time variable is also discretized by $t[k] = k\Delta_t$ for $k \geq 0$, where the time step $\Delta_t > 0$ is specified by the user. The choice for the time step can affect the numerical stability of the algorithm, so depending on how the differential equation is numerically solved, you might have restrictions on the size of the time step.

The initial-value function is needed at the lattice points. We could precompute the values and store them in a double array, but for simplicity the algorithm assumes that $\rho_0(x, y)$ is available as a function that can be evaluated at $(x[i], y[j])$. Similarly, the source–sink function $s(x, y, t)$ is assumed to be available for evaluation at the lattice points. If you were to store the source–sink values in a double array, you would have to update that array for each time step because of the time dependence of that function.

If you were considering the density equation as the only one to solve, the velocity components $u(x, y)$ and $v(x, y)$ could also be evaluated by the algorithm using function calls at the lattice points. However, the differential equations for density and velocity are generally coupled, so we will store estimated values of these quantities at the lattice points. Specifically, we store $\rho_k[j][i] \doteq \rho(x[i], y[j], t[k])$, $u_k[j][i] \doteq u(x[i], y[j], t[k])$, and $v_k[j][i] \doteq v(x[i], y[j], t[k])$, obtained by using finite-difference approximations in the differential equation. The choice of approximations is discussed later in this chapter. By using subscripts k , I mean that there is no persistent storage in the time variable; that is, we will not have a triple array $f[k][j][i]$ for any of the state variables ρ , u , or v . The estimates will be stored in a two-buffer system where the buffers represent state information for two consecutive time steps. The numerical method will swap the buffers for each iteration of time.

5.5.2 THE DIFFUSION TERM

Consider the density equation that contains only the time derivative and the diffusion term,

$$\rho_t = \kappa(\rho_{xx} + \rho_{yy})$$

In fact, this is the model for diffusion of heat. When the (x, y) domain is the entire xy -plane, the solution represents Gaussian blurring of the initial-value data when thought of as an image.

The classical numerical method to estimating ρ uses a forward difference to estimate the time derivative.

$$\rho_t(x, y, t) \doteq \frac{\rho(x, y, t + \Delta_t) - \rho(x, y, t)}{\Delta_t}$$

and centered differences to estimate the spatial derivatives,

$$\rho_{xx} \doteq \frac{\rho(x + \Delta_x, y, t) - 2\rho(x, y, t) + \rho(x - \Delta_x, y, t)}{\Delta_x^2}$$

and

$$\rho_{yy} \doteq \frac{\rho(x, y + \Delta_y, t) - 2\rho(x, y, t) + \rho(x, y - \Delta_y, t)}{\Delta_y^2}$$

Let $\rho_{i,j}^{(k)} = \rho(x[i], y[j], t[k])$. Substituting the finite differences into the differential equation, we have the approximation

$$\frac{\rho_{i,j}^{(k+1)} - \rho_{i,j}^{(k)}}{\Delta_t} = \kappa \left(\frac{\rho_{i+1,j}^{(k)} - 2\rho_{i,j}^{(k)} + \rho_{i-1,j}^{(k)}}{\Delta_x^2} + \frac{\rho_{i,j+1}^{(k)} - 2\rho_{i,j}^{(k)} + \rho_{i,j-1}^{(k)}}{\Delta_y^2} \right)$$

or

$$\rho_{i,j}^{(k+1)} = \rho_{i,j}^{(k)} + \lambda_x \left(\rho_{i+1,j}^{(k)} - 2\rho_{i,j}^{(k)} + \rho_{i-1,j}^{(k)} \right) + \lambda_y \left(\rho_{i,j+1}^{(k)} - 2\rho_{i,j}^{(k)} + \rho_{i,j-1}^{(k)} \right) \quad (5.91)$$

where $\lambda_x = \kappa \Delta_t / \Delta_x^2$ and $\lambda_y = \kappa \Delta_t / \Delta_y^2$. The density at time step $k+1$ for lattice cell (i, j) depends on the density at time step k at lattice cell (i, j) and at the four neighboring cells $(i+1, j)$, $(i-1, j)$, $(i, j+1)$, and $(i, j-1)$.

The algorithm starts with the initial values $\rho_{i,j}^{(0)} = \rho_0(x[i], y[j])$ for $0 \leq i \leq i_{\max}$ and $0 \leq j \leq j_{\max}$. At time zero, the boundary values at $i = 0$, $i = i_{\max}$, $j = 0$, and j_{\max} must match the initial values. The first iteration of the algorithm computes the update of [equation \(5.91\)](#) for the interior lattice cells, after which it fills in the boundary lattice cells by evaluating the boundary-value functions and either assigning them to those cells (Dirichlet boundary conditions) or determining them from derivatives (Neumann boundary conditions) also using finite difference estimates. Subsequent iterations duplicate the process. The pseudocode is presented next.

Much of the differential equation solver code can be shared when updating density or when updating the velocity components. The following pseudocode supports the sharing.

```
enum BoundaryType = { Dirichlet, Neumann };

typedef float (*Function2)(float, float);
typedef float (*Function3)(float, float, float);

struct BoundaryFunctions
{
    BoundaryType type;
    Function2 BoundaryX0, BoundaryX1, BoundaryY0, BoundaryY1;
};

void SwapBuffers (float*** addrBuffer0, float*** addrBuffer1)
{
    float** save = *addrBuffer0;
```

```

    *addrBuffer0 = *addrBuffer1;
    *addrBuffer1 = save;
}

```

Global variables, functions, local state arrays, and the simulation are shown in the next code.

```

// global values
float x0, y0, x1, y1; // rectangle bounds
int imax, jmax; // lattice bounds
float deltaT; // time step (positive)
float deltaX = (x1 - x0)/imax; // cell x-dimension
float deltaY = (y1 - y0)/jmax; // cell y-dimension

// global function for initial values
float RhoT0 (float x, float y);

// global functions for Dirichlet boundary conditions
float RhoX0 (float y, float t); // phi0
float RhoX1 (float y, float t); // phi1
float RhoY0 (float x, float t); // psi0
float RhoY1 (float x, float t); // psi1

// global functions for Neumann boundary conditions
float RhoDerX0 (float y, float t); // phi0'
float RhoDerX1 (float y, float t); // phi1'
float RhoDerY0 (float x, float t); // psi0'
float RhoDerY1 (float x, float t); // psi1'

// local values
float kappa; // density viscosity constant (positive)
float lambdaX = kappa*deltaT/(deltaX*deltaX);
float lambdaY = kappa*deltaT/(deltaY*deltaY);
BoundaryType type; // choose one of Dirichlet or Neumann
float x[imax], y[jmax]; // lattice cell centers
float rhoOld[jmax][imax]; // density, old time
float rhoNew[jmax][imax]; // density, new time
float t = 0.0; // initial time

BoundaryFunctions bf;
if (type == Dirichlet)
{
    bf.type = Dirichlet;
    bf.BoundaryX0 = RhoX0;
    bf.BoundaryX1 = RhoX1;
    bf.BoundaryY0 = RhoY0;
    bf.BoundaryY1 = RhoY1;
}

```

```

else // type == Neumann
{
    bf.type = Neumann;
    bf.BoundaryX0 = RhoDerX0;
    bf.BoundaryX1 = RhoDerX1;
    bf.BoundaryY0 = RhoDerY0;
    bf.BoundaryY1 = RhoDerY1;
}

// simulation code in the application
InitializeExplicit(x, y, RhoT0, rhoOld);
while (simulating)
{
    UpdateDiffusionExplicit(t, x, y, lambdaX, lambdaY, bf,
        rhoOld, rhoNew);
    SwapBuffers(&rhoOld, &rhoNew);
    t = t + deltaT;
}

```

The initialization function is

```

void InitializeExplicit (float* x, float* y, Function2 InitialT0,
    float** sOld)
{
    int i, j;
    for (i = 0; i <= imax; ++i)
    {
        x[i] = x0 + deltaX*i;
    }
    for (j = 0; j <= jmax; ++j)
    {
        y[j] = y0 + deltaY*j;
    }
    for (j = 0; j <= jmax; ++j)
    {
        for (i = 0; i <= imax; ++i)
        {
            sOld[j][i] = InitialT0(x[i], y[j]);
        }
    }
}

```

The update function is

```

void UpdateDiffusionExplicit (float t, float* x, float* y,
    float lambdaX, float lambdaY, BoundaryFunctions bf,
    float** sOld, float** sNew)
{
    // Update the interior cells.
    for (int j = 1; j < jmax; ++j)

```

```

    {
        for (int i = 1; i < imax; ++i)
        {
            sNew[j][i] = sOld[j][i]
                + lambdaX*(sOld[j][i+1] - 2*sOld[j][i]
                + sOld[j][i-1])
                + lambdaY*(sOld[j+1][i] - 2*sOld[j][i]
                + sOld[j-1][i]);
        }
    }

    UpdateBoundary(t, x, y, bf, sNew);
}

```

The boundary update function is

```

void UpdateBoundary (float t, float* x, float* y,
    BoundaryFunctions bf, float** sNew)
{
    int i, j;

    if (bf.type == Dirichlet)
    {
        // edge interiors
        for (j = 1; j < jmax; ++j)
        {
            sNew[j][0] = bf.BoundaryX0(y[j], t);
            sNew[j][imax] = bf.BoundaryX1(y[j], t);
        }
        for (i = 1; i < imax; ++i)
        {
            sNew[0][i] = bf.BoundaryY0(x[i], t);
            sNew[jmax][i] = bf.BoundaryY1(x[i], t);
        }

        // corners
        sNew[0][0] = bf.BoundaryX0(y[0], t);
        sNew[0][imax] = bf.BoundaryX1(y[0], t);
        sNew[jmax][0] = bf.BoundaryX0(y[jmax], t);
        sNew[jmax][imax] = bf.BoundaryX1(y[jmax], t);
    }
    else // Neumann
    {
        // Diagonally adjacent neighbor is farther away than
        // horizontal or vertical neighbor.
        float delta = sqrt(deltaX*deltaX + deltaY*deltaY);

        // edge interiors
        for (j = 1; j < jmax; ++j)

```

```

{
    sNew[j][0] = sNew[j][1] +
        delta*bf.BoundaryX0(y[j], t);
    sNew[j][imax] = sNew[j][imax-1] +
        delta*bf.BoundaryX1(y[j], t);
}
for (i = 1; i < imax; ++i)
{
    sNew[0][i] = sNew[1][i] +
        delta*bf.BoundaryY0(x[i], t);
    sNew[jmax][i] = sNew[jmax-1][i] +
        delta*bf.BoundaryY1(x[i], t);
}

// corners
sNew[0][0] = sNew[1][1] +
    delta*bf.BoundaryX0(y[0], t);
sNew[0][imax] = sNew[1][imax-1] +
    delta*bf.BoundaryX1(y[0], t);
sNew[jmax][0] = sNew[jmax-1][1] +
    delta*bf.BoundaryX0(y[jmax], t);
sNew[jmax][imax] = sNew[jmax-1][imax-1] +
    delta*bf.BoundaryX1(y[jmax], t);
}
}

```

All is well with this approach until you choose Δ_t to be sufficiently large, at which time you will notice that the density values start oscillating between positive and negative values. This is a problem, because we require that density be nonnegative. The issue is one of *numerical stability*. The finite-difference algorithm described here is only *conditionally stable*, requiring the time step to be relatively small. Specifically, rewrite equation (5.91) to

$$\rho_{i,j}^{(k+1)} = \left[1 - 2\kappa \Delta_t \left(\frac{1}{\Delta_x^2} + \frac{1}{\Delta_y^2} \right) \right] \rho_{i,j}^{(k)} + \lambda_x (\rho_{i+1,j}^{(k)} + \rho_{i-1,j}^{(k)}) + \lambda_y (\rho_{i,j+1}^{(k)} + \rho_{i,j-1}^{(k)}) \quad (5.92)$$

If the coefficient of $\rho_{i,j}^{(k)}$ is negative, imagine a time step for which $\rho_{i,j}^{(k)}$ is very large compared to its four neighboring values. It may be so large that the right-hand side sums to a negative number, in which case $\rho_{i,j}^{(k+1)}$ is negative. Once this happens, the oscillatory behavior begins.

To maintain numerical stability, we need the coefficient of $\rho_{i,j}^{(k)}$ to be positive, which implies

$$\Delta_t < \frac{1}{2\kappa \left(\frac{1}{\Delta_x^2} + \frac{1}{\Delta_y^2} \right)}$$

The coefficients of the density terms in the right-hand side of [equation \(5.92\)](#) are all positive, so as long as the density at the current time step is positive, the right-hand side is positive, which guarantees that the density at the next time step is positive.

The finite-difference scheme mentioned here uses a forward difference in time. This is called an *explicit method* because you can solve directly for the state at the next time from state at the current time. Explicit methods are typically only conditionally stable. We may instead use a backward difference in time, which is an *implicit method* that tends to be stable for any size time step. The explicit method of [equation \(5.91\)](#) is replaced by the implicit method

$$\rho_{i,j}^{(k+1)} = \rho_{i,j}^{(k)} + \lambda_x \left(\rho_{i+1,j}^{(k+1)} - 2\rho_{i,j}^{(k+1)} + \rho_{i-1,j}^{(k+1)} \right) + \lambda_y \left(\rho_{i,j+1}^{(k+1)} - 2\rho_{i,j}^{(k+1)} + \rho_{i,j-1}^{(k+1)} \right) \quad (5.93)$$

The equation is implicit in the following sense. The right-hand side contains a term for the density at the current time iteration k for the lattice cell (i, j) . The other right-hand side terms involve the as-yet-unknown density at neighboring lattice cells for the time iteration $k + 1$. We cannot simply update cell-by-cell as we did in the explicit method. Instead, [equation \(5.93\)](#) represents a linear system of equations in the unknown density values at time iteration $k + 1$. This finite-difference scheme is referred to as the *Crank–Nicholson scheme*.

If we were working in one spatial dimension, the linear system of the Crank–Nicholson scheme is tridiagonal. A linear system solver for a tridiagonal matrix is easy to implement and uses computational time that is linear in the number of spatial samples. The two-dimensional problem is more complicated to set up, but the matrix of coefficients is sparse. To avoid the complexities of solving the linear system directly, [\[PFTV88\]](#) suggests something called the *alternating-direction implicit method*, which is an *operator splitting method* that divides each time step into two time steps (half the time per step). Each substep involves solving a tridiagonal matrix system.

As is typical these days for sparse matrix systems in game applications, [\[Sta03\]](#) uses an iterative method called *Gauss–Seidel*, which is also an operator splitting method; see [Section 7.2.6](#) for details. [Equation \(5.93\)](#) may be solved for $\rho_{i,j}^{(k+1)}$ to obtain

$$\rho_{i,j}^{(k+1)} = \gamma_0 \rho_{i,j}^{(k)} + \gamma_1 \left(\rho_{i+1,j}^{(k+1)} + \rho_{i-1,j}^{(k+1)} \right) + \gamma_2 \left(\rho_{i,j+1}^{(k+1)} + \rho_{i,j-1}^{(k+1)} \right) \quad (5.94)$$

where

$$\gamma_0 = \frac{1}{1 + 2(\lambda_x + \lambda_y)}, \quad \gamma_1 = \frac{\lambda_x}{1 + 2(\lambda_x + \lambda_y)}, \quad \gamma_2 = \frac{\lambda_y}{1 + 2(\lambda_x + \lambda_y)}$$

[Equation \(5.94\)](#) is iterated some specified number of times. On the first iteration, the densities for the time iterate $k + 1$ are just the densities known for time iterate k . The equation modifies the $\rho_{i,j}^{(k+1)}$, so on the second and later iterations, the right-hand side densities for the time iterate $k + 1$ are different from those at time iterate k . The

function `UpdateDiffusionExplicit` is replaced by

```
// Global value chosen before starting the simulation.
int numGaussSeidelIterations; // your choice;

// Local values computed before starting the simulation.
float gamma0 = 1/(1 + 2*(lambdaX + lambdaY));
float gamma1 = lambdaX*gamma0;
float gamma2 = lambdaY*gamma0;

void UpdateDiffusionImplicit (float t, float* x, float* y,
    float gamma0, float gamma1, float gamma2,
    BoundaryFunctions bf, float** sOld, float** sNew)
{
    CopyArray(sOld, sNew); // copy elements of sOld to sNew
    for (int iter = 0; iter < numGaussSeidelIterations; ++iter)
    {
        // Update interior cells.
        for (int j = 1; j < jmax; ++j)
        {
            for (int i = 1; i < imax; ++i)
            {
                sNew[j][i] = gamma0*sOld[j][i]
                    + gamma1*(sNew[j][i+1] + sNew[j][i-1])
                    + gamma2*(sNew[j+1][i] + sNew[j-1][i]);
            }
        }
        UpdateBoundary(t, x, y, bf, sNew);
    }
}
```

The `CopyArray` function appears to be necessary to initialize the `sNew` values on the right-hand side of the assignment statement. Assuming that the number of Gauss–Seidel iterations are sufficient to guarantee convergence (within floating-point tolerances), we can avoid the copy per time iterate by initializing `rho[0]` and `rho[1]` to the same values,

```
initialize:
    rho[0] = density(0); // density at time iterate 0 (t = 0)
    rho[1] = density(0);
update:
    rho[0] = density(0);
    rho[1] = density(1); // density at time iterate 1
swap:
    rho[0] = density(1);
    rho[1] = density(0); // rho[1] starts at density(0)
```

```

update:
rho[0] = density(1);
rho[1] = density(2); // with CopyArray, rho[1] would have
                     // started at density(1), not density(0)

```

The initialization function to support this is

```

void InitializeImplicit (float* x, float* y, Function2 InitialT0,
                        float** sOld, float** sNew)
{
    for (int j = 0; j <= jmax; ++j)
    {
        y[j] = y0 + deltaY*j;
        for (int i = 0; i <= imax; ++i)
        {
            x[i] = x0 + deltaX*i;
            float value = InitialT0(x[i], y[j]);
            sOld[j][i] = value;
            sNew[j][i] = value;
        }
    }
}

```

5.5.3 THE ADVECTION TERM

Consider the partial differential equation for density but with only the time derivative and the velocity directional derivative term,

$$\rho_t = -u\rho_x - v\rho_y, \quad (x, y) \in [x_0, x_1] \times [y_0, y_1], \quad t \geq 0$$

For the sake of argument, assume that the initial values and boundary values are specified as for the diffusion equation. This is a *hyperbolic differential equation*. To solve this numerically, we can choose a forward difference in time and centered differences in space,

$$\frac{\rho_{i,j}^{(k+1)} - \rho_{i,j}^{(k)}}{\Delta t} = -u_{i,j}^{(k)} \left(\frac{\rho_{i+1,j}^{(k)} - \rho_{i-1,j}^{(k)}}{2\Delta x} \right) - v_{i,j}^{(k)} \left(\frac{\rho_{i,j+1}^{(k)} - \rho_{i,j-1}^{(k)}}{2\Delta y} \right)$$

where $u_{i,j}^{(k)} = u(x[i], y[j], t[k])$ and $v_{i,j}^{(k)} = v(x[i], y[j], t[k])$. The time update of density is

$$\rho_{i,j}^{(k+1)} = \rho_{i,j}^{(k)} + \frac{\Delta t}{2\Delta x} u_{i,j}^{(k)} \left(\rho_{i+1,j}^{(k)} - \rho_{i-1,j}^{(k)} \right) + \frac{\Delta t}{2\Delta y} v_{i,j}^{(k)} \left(\rho_{i,j+1}^{(k)} - \rho_{i,j-1}^{(k)} \right)$$

This explicit scheme has the same stability problems as that for the diffusion equation (conditional stability requires small time steps).

We could attempt to remedy the problem by using an implicit scheme, just as we did for diffusion,

$$\rho_{i,j}^{(k+1)} = \rho_{i,j}^{(k)} + \frac{\Delta_t}{2\Delta_x} u_{i,j}^{(k+1)} (\rho_{i+1,j}^{(k+1)} - \rho_{i-1,j}^{(k+1)}) + \frac{\Delta_t}{2\Delta_y} v_{i,j}^{(k+1)} (\rho_{i,j+1}^{(k+1)} - \rho_{i,j-1}^{(k+1)})$$

Solving this is much more complicated. The problem is that the velocity components at time iterate $k+1$ occur on the right-hand side. We can use Gauss–Seidel iterates for the density terms at time iterate $k+1$, but then we are required to compute the velocity terms at time iterate $k+1$. These values must be obtained from a similar numerical method applied to the Navier–Stokes equation. Thus, we have a coupling of density and velocity by the two partial differential equations. The resulting numerical method that has to deal with the coupling is complicated.

The approach in [Sta03] is a *transport algorithm*¹ that uses the velocity field to determine how density at time iterate $k+1$ was accumulated from nearby densities at time iterate k . Intuitively, this is the concept mentioned in the discussion of conservation of mass whereby the material derivative $\rho_t + u\rho_x + v\rho_y$ is the rate of change of density along flow lines; that is, the update function simply tracks density along the flow lines and adjusts over time as necessary. This mechanism is also referred to as *advection*.

Figure 5.3 shows two possible ways of implementing the transport algorithm. In Figure 5.3(a), the light gray cell contains two transported centers. How should we compute the densities at the transported center and how show these densities be used to update the density at the center of the light gray cell? In Figure 5.3(b), a transported cell center is shown contained in a square formed by four cell centers. The density at the transported center is computed using bilinear interpolation of the densities at the four cell centers (all correspond to time iterate k). This density is assigned to the source cell center’s density (the value for time iterate $k+1$).

In the forward transport method, we could also use bilinear interpolation for each transported cell center. However, if two transported cell centers are in the same cell, then one of the lattice cells will not contain a transported cell. Such a lattice cell will have no density update. This has the flavor of rotating a bitmap to generate another bitmap. If you iterate over the source bitmap pixels and rotate them, the destination bitmap will be missing some pixels. Instead, you iterate over the destination bitmap pixels, inverse-rotate each one, and then use bilinear interpolation in the source bitmap to obtain the value for the destination pixel.

1. This term is not used in [Sta03], but it is mentioned that this is a *semi-Lagrangian* method. However, it is used in a variety of fields. For example, in the field of air pollution, sensors at various locations measure particulate matter (pollutants). Naturally, it is important to know the source of the pollutants (so proper blame can be placed for polluting). Wind forces move the particulate matter from the sources to the sensors (forward transport). Given the sensor measurements and time-varying wind velocity field in a lattice of cells, the contributions at a sensor can be traced backward through time via the velocity field (backward transport), hopefully identifying the pollutant sources.

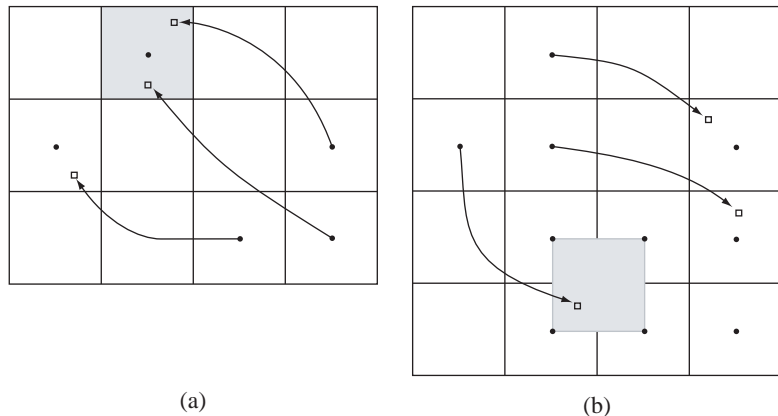


Figure 5.3 Left: Forward transport of the density from three cell centers. The cell with light gray background contains two transported centers. Right: Backward transport of the density from three cell centers. One of the transported cell centers is shown contained in a square formed by four cell centers.

The update function for the lattice cells is

```
// Global values computed before starting the simulation.
float dtDivDx = deltaT/deltaX;
float dtDivDy = deltaT/deltaY;

void UpdateAdvection (float t, float* x, float* y, float** uOld,
                      float** vOld, BoundaryFunctions bf, float** sOld,
                      float** sNew)
{
    // Update interior cells.
    for (int j = 1; j < jmax; ++j)
    {
        for (int i = 1; i < imax; ++i)
        {
            float iPrevious = i - dtDivDx*uOld[j][i];
            Clamp(iPrevious, 0.5, imax - 0.5);
            int i0 = Floor(iPrevious);
            int i1 = i0 + 1;
            float a1 = iPrevious - i0;
            float a0 = 1 - a1;

            float jPrevious = j - dtDivDy*vOld[j][i];
            Clamp(jPrevious, 0.5, jmax - 0.5);
            int j0 = Floor(jPrevious);
```

```

        int j1 = j0 + 1;
        float b1 = jPrevious - j0;
        float b0 = 1 - b1;

        sNew[j][i] =
            b0*(a0*sOld[j0][i0] + a1*sOld[j0][i1]) +
            b1*(a0*sOld[j1][i0] + a1*sOld[j1][i1]);
    }
}

UpdateBoundary(t, x, y, bf, sNew);
}

```

where `Clamp(z,a,b)` maps $z < a$ to a and $z > b$ to b , with all other z remaining the same, and where `Floor(z)` is the largest integer smaller or equal to z .

To explain the floating-point index `iPrevious`, observe that $u = dx/dt$ is the x -component of velocity. The units of u are length per unit time, where length has units of the original $x \in [x_0, x_1]$. The change in position is estimated by $\Delta_t u = \Delta_t(dx/dt)$, where Δ_t has units of time. This change still has units of length in the original x variable. To convert to units of the i -index of the lattice, notice that $x(i+h) - x(i) = (x_0 + (i+h)\Delta_x) - (x_0 + i\Delta_x) = h\Delta_x$. The left-hand side of the expression is change of x in units of length for the original variable. The value h is the change in the index i , so we need to divide by Δ_x to obtain the i -index units; that is, $(\Delta_t/\Delta_x)u = (\Delta_t/\Delta_x)(dx/dt)$ has units of the i -index. A similar argument for `jPrevious` shows that $(\Delta_t/\Delta_y)v$ has units of the j -index.

5.5.4 THE SOURCE–SINK TERM

Consider the density equation that contains only the time derivative and the source–sink term,

$$\rho_t = s$$

The update of density for a single time step is trivial. The pseudocode is

```

// global function
float RhoSource (float x, float y, float t);

void UpdateSource (float t, float* x, float* y, Function3 Source,
                   bool clampToZero, float** sOld, float** sNew)
{
    int i, j;

    if (clampToZero)
    {
        for (j = 0; j <= jmax; ++j)

```

```

    {
        for (i = 0; i <= imax; ++i)
        {
            sNew[j][i] = sOld[j][i] +
                deltaT*Source(x[i], y[j], t);
            if (sNew[j][i] < 0)
            {
                sNew[j][i] = 0;
            }
        }
    }
else
{
    for (j = 0; j <= jmax; ++j)
    {
        for (i = 0; i <= imax; ++i)
        {
            sNew[j][i] = sOld[j][i] +
                deltaT*Source(x[i], y[j], t);
        }
    }
}
}

```

Because we have no guarantee the source–sink function will keep the densities nonnegative, we must clamp the updated value to be nonnegative.

5.5.5 THE TOTAL DENSITY UPDATE

The following pseudocode combines the source–sink update, the diffusion update, and the advection update.

```

// global values
float x0, y0, x1, y1; // rectangle bounds
int imax, jmax; // lattice bounds
float deltaT; // time step (positive)
float deltaX = (x1 - x0)/imax; // cell x-dimension
float deltaY = (y1 - y0)/jmax; // cell y-dimension
float dtDivDx = deltaT/deltaX;
float dtDivDy = deltaT/deltaY;
float dtDivDxDx = dtDivDx/deltaX;
float dtDivDyDy = dtDivDy/deltaY;
int numGaussSeidelIterations; // your choice;
enum BoundaryType = { Dirichlet, Neumann };
BoundaryType type; // choose one of Dirichlet or Neumann

```

```

// global functions
float RhoT0 (float x, float y);
float RhoX0 (float y, float t);
float RhoX1 (float y, float t);
float RhoY0 (float x, float t);
float RhoY1 (float x, float t);
float RhoDerX0 (float y, float t);
float RhoDerX1 (float y, float t);
float RhoDerY0 (float x, float t);
float RhoDerY1 (float x, float t);
float RhoSource (float x, float y, float t);

// local values
float kappa; // density viscosity constant (positive)
float lambdaX = kappa*dtDivDxDx;
float lambdaY = kappa*dtDivDyDy;
float gamma0 = 1/(1 + 2*(lambdaX + lambdaY));
float gamma1 = lambdaX*gamma0;
float gamma2 = lambdaY*gamma0;
float x[jmax], y[jmax]; // lattice cell centers
float rhoOld[jmax][imax]; // density, old time
float rhoNew[jmax][imax]; // density, new time
float uOld[jmax][imax]; // current x-component of velocity
float vOld[jmax][imax]; // current y-component of velocity
float t = 0.0; // initial time

BoundaryFunctions bf;
if (type == Dirichlet)
{
    bf.type = Dirichlet;
    bf.BoundaryX0 = RhoX0;
    bf.BoundaryX1 = RhoX1;
    bf.BoundaryY0 = RhoY0;
    bf.BoundaryY1 = RhoY1;
}
else // type == Neumann
{
    bf.type = Neumann;
    bf.BoundaryX0 = RhoDerX0;
    bf.BoundaryX1 = RhoDerX1;
    bf.BoundaryY0 = RhoDerY0;
    bf.BoundaryY1 = RhoDerY1;
}

// simulation code in the application
InitializeImplicit(x, y, RhoT0, rhoOld, rhoNew);
while (simulating)
{

```

```

UpdateSource(t, x, y, bf, RhoSource, true, rhoOld, rhoNew);
SwapBuffers(&rhoOld, &rhoNew);

UpdateDiffusionImplicit(t, x, y, gamma0, gamma1, gamma2, bf,
    rhoOld, rhoNew);
SwapBuffers(&rhoOld, &rhoNew);

UpdateAdvection(t, x, y, uOld, vOld, bf, rhoOld, rhoNew);
SwapBuffers(&rhoOld, &rhoNew);

t = t + deltaT;
}

```



Here is a side note on the explicit method for solving the diffusion equation and for solving parabolic equations generally of the form

$$\rho_t = \kappa(\rho_{xx} + \rho_{yy}) + F(t, x, y, \rho, \rho_x, \rho_y)$$

where F is a function of the indicated variables, where an initial-value function is specified, and using Neumann boundary conditions with boundary derivatives set to zero. The numerical method may be solved by shader programming on a GPU. An implementation of Gaussian blurring ($F = 0$) is provided on the CD-ROM.

5.5.6 THE VELOCITY EQUATIONS

The simplified Navier–Stokes equation for 2D can be written componentwise as

$$\begin{aligned} u_t &= \nu(u_{xx} + u_{yy}) - uu_x - vu_y + f \\ v_t &= \nu(v_{xx} + v_{yy}) - uv_x - vv_y + g \end{aligned}$$

where the velocity is (u, v) and the external forces are summarized by (f, g) . The positive constant ν is the viscosity coefficient. The velocity components must have initial values specified at time zero as well as boundary conditions over time.

The velocity equations are structured exactly like the density differential equation, so we could use the previously developed pseudocode to solve these simultaneously with the density equation.

```

// global values
float x0, y0, x1, y1; // rectangle bounds
int imax, jmax; // lattice bounds
float deltaT; // time step (positive)
float deltaX = (x1 - x0)/imax; // cell x-dimension
float deltaY = (y1 - y0)/jmax; // cell y-dimension
float dtDivDx = deltaT/deltaX;
float dtDivDy = deltaT/deltaY;
float dtDivDxDx = dtDivDx/deltaX;

```

```

float dtDivDyDy = dtDivDy/deltaY;
int numGaussSeidelIterations; // your choice;
enum BoundaryType = { Dirichlet, Neumann };
BoundaryType rhoType, uType, vType; // Dirichlet or Neumann

// global functions
float RhoT0 (float x, float y);
float RhoX0 (float y, float t);
float RhoX1 (float y, float t);
float RhoY0 (float x, float t);
float RhoY1 (float x, float t);
float RhoDerX0 (float y, float t);
float RhoDerX1 (float y, float t);
float RhoDerY0 (float x, float t);
float RhoDerY1 (float x, float t);
float RhoSource (float x, float y, float t); // s(x,y,t)
float UTO (float x, float y);
float UX0 (float y, float t);
float UX1 (float y, float t);
float UYO (float x, float t);
float UY1 (float x, float t);
float UDerX0 (float y, float t);
float UDerX1 (float y, float t);
float UDerY0 (float x, float t);
float UDerY1 (float x, float t);
float USource (float x, float y, float t); // f(x,y,t)
float VT0 (float x, float y);
float VX0 (float y, float t);
float VX1 (float y, float t);
float VYO (float x, float t);
float VY1 (float x, float t);
float VDerX0 (float y, float t);
float VDerX1 (float y, float t);
float VDerY0 (float x, float t);
float VDerY1 (float x, float t);
float VSource (float x, float y, float t); // g(x,y,t)

// local values
float viscosity[2]; // viscosity[0] = kappa, viscosity[1] = nu
float lambdaX[2] =
{
    viscosity[0]*dtDivDxDx,
    viscosity[1] n*dtDivDxDx
};
float lambdaY[2] =
{
    viscosity[0]*dtDivDyDy,

```

```

    viscosity[1]*dtDivDyDy
};

float gamma0[2] =
{
    1/(1+2*(lambdaX[0]+lambdaY[0])),
    1/(1+2*(lambdaX[1]+lambdaY[1]))
};

float gamma1[2] = { lambdaX[0]*gamma0[0], lambdaX[1]*gamma0[1] };
float gamma2[2] = { lambdaY[0]*gamma0[0], lambdaY[1]*gamma0[1] };

float x[iMAX], y[jMAX]; // lattice cell centers
float rhoOld[jMAX][iMAX]; // density, old time
float rhoNew[jMAX][iMAX]; // density, new time
float uOld[jMAX][iMAX]; // x-component of velocity, old time
float uNew[jMAX][iMAX]; // x-component of velocity, new time
float vOld[jMAX][iMAX]; // y-component of velocity, old time
float vNew[jMAX][iMAX]; // y-component of velocity, new time
float t = 0.0; // initial time

BoundaryFunctions rhoBF;
if (rhoType == Dirichlet)
{
    rhoBF.type = Dirichlet;
    rhoBF.BoundaryX0 = RhoX0;
    rhoBF.BoundaryX1 = RhoX1;
    rhoBF.BoundaryY0 = RhoY0;
    rhoBF.BoundaryY1 = RhoY1;
}
else // type == Neumann
{
    rhoBF.type = Neumann;
    rhoBF.BoundaryX0 = RhoDerX0;
    rhoBF.BoundaryX1 = RhoDerX1;
    rhoBF.BoundaryY0 = RhoDerY0;
    rhoBF.BoundaryY1 = RhoDerY1;
}

BoundaryFunctions uBF;
if (uType == Dirichlet)
{
    uBF.type = Dirichlet;
    uBF.BoundaryX0 = UX0;
    uBF.BoundaryX1 = UX1;
    uBF.BoundaryY0 = UY0;
    uBF.BoundaryY1 = UY1;
}
else // type == Neumann
{
}

```



```

        gamma2[1], uBF, uOld, uNew);
UpdateDiffusionImplicit(t, x, y, gamma0[1], gamma1[1],
    gamma2[1], vBF, vOld, vNew);
SwapBuffers(&uOld, &uNew);
SwapBuffers(&vOld, &vNew);

UpdateAdvection(t, x, y, uOld, vOld, uBF, uOld, uNew);
UpdateAdvection(t, x, y, uOld, vOld, vBF, vOld, vNew);
SwapBuffers(&uOld, &uNew);
SwapBuffers(&vOld, &vNew);

t = t + deltaT;
}

```

A new numerical issue manifests itself. The continuous formulation of the partial differential equations included conservation of mass and the condition that $\nabla \cdot \mathbf{v} = 0$. The numerical algorithm using finite differences introduces error that causes the divergence not to be zero. Effectively, the mass conservation does not happen. To remedy this, the velocity field must be adjusted.

From the Helmholtz decomposition, equation (5.44), the velocity is

$$\mathbf{v} = -\nabla\phi + \nabla \times \mathbf{g}$$

where ϕ is a solution to $\nabla^2\phi = -\nabla \cdot \mathbf{v}$ and \mathbf{g} is a solution to $\nabla^2\mathbf{g} = -\nabla \times \mathbf{v}$ with $\nabla \cdot \mathbf{g} = 0$. If we were to treat the left-hand side of this equation as the velocity field produced by the numerical solver, we can add to it the gradient field

$$\mathbf{v}' = \mathbf{v} + \nabla\phi = \nabla \times \mathbf{g}$$

The new vector field on the left-hand side has the property $\nabla \cdot \mathbf{v}' = \nabla \cdot \nabla \times \mathbf{g} = 0$. The result is a velocity field \mathbf{v}' that is mass preserving.

This adjustment requires solving the Poisson equation for ϕ on our rectangular domain. Using centered differences in space, the numerical method is

$$\frac{\phi_{i+1,j} - 2\phi_{i,j} + \phi_{i-1,j}}{\Delta_x^2} + \frac{\phi_{i,j+1} - 2\phi_{i,j} + \phi_{i,j-1}}{\Delta_y^2} = -\left(\frac{u_{i+1,j} - u_{i-1,j}}{2\Delta_x} + \frac{v_{i,j+1} - v_{i,j-1}}{2\Delta_y}\right)$$

where $\phi_{i,j} = \phi(x[i], y[j])$, $u_{i,j} = u(x[i], y[j])$, and $v_{i,j} = v(x[i], y[j])$. Defining the right-hand side as $-d_{i,j}$, we may rewrite the equation as

$$\phi_{i,j} = \varepsilon_0 d_{i,j} + \varepsilon_1 (\phi_{i+1,j} + \phi_{i-1,j}) + \varepsilon_2 (\phi_{i,j+1} + \phi_{i,j-1})$$

where

$$\varepsilon_0 = \frac{\Delta_x^2 \Delta_y^2}{2(\Delta_x^2 + \Delta_y^2)}, \quad \varepsilon_1 = \frac{\Delta_y^2}{2(\Delta_x^2 + \Delta_y^2)}, \quad \varepsilon_2 = \frac{\Delta_x^2}{2(\Delta_x^2 + \Delta_y^2)}$$

We also need boundary conditions. In the absence of numerical errors, $\nabla \cdot \mathbf{v} = 0$ and $\phi = 0$. This indicates we should choose Dirichlet boundary conditions, $\phi(\mathbf{x}) = 0$ for

boundary points \mathbf{x} . In terms of finite differences, $\phi_{i,0} = 0$ for all i and $\phi_{0,j} = 0$ for all j . The finite-difference equation is implicit and may be solved using Gauss–Seidel iteration.

The pseudocode for computing the adjustment $\mathbf{v}' = \mathbf{v} + \nabla\phi$ is listed next.

```

// Global values computed before starting the simulation.
float halfDivDX = 0.5/deltaX;
float halfDivDY = 0.5/deltaY;
float deltaXSqr = deltaX*deltaX;
float deltaYSqr = deltaY*deltaY;
float invDenom = 0.5/(deltaXSqr + deltaYSqr);
float epsilon0 = deltaXSqr*deltaYSqr*invDenom;
float epsilon1 = deltaYSqr*invDenom;
float epsilon2 = deltaXSqr*invDenom;

void AdjustVelocity (float t, float* x, float* y,
BoundaryFunctions uBF, BoundaryFunctions vBF, float** u,
float** v)
{
    int i, j;

    // Approximate the divergence of velocity.
    float div[jmax][imax];
    for (j = 1; j < jmax; ++j)
    {
        for (i = 1; i < imax; ++i)
        {
            div[j][i] =
                halfDivDX*(u[j][i+1] - u[j][i-1]) +
                halfDivDY*(v[j+1][i] - v[j-1][i]);
        }
    }

    // Use zero-valued derivative on boundary to assign divergence.
    for (int i = 0; i <= imax; ++i)
    {
        div[0][i] = div[1][i];
        div[jmax][i] = div[jmax-1][i];
    }
    for (int j = 0; j <= jmax; ++j)
    {
        div[j][0] = div[j][1];
        div[j][imax] = div[j][imax-1];
    }

    // Initialize phi.
    float phi[jmax][imax];
    for (j = 0; j <= jmax; ++j)

```

```

{
    for (i = 0; i <= imax; ++i)
    {
        phi[j][i] = 0.0;
    }
}

// Numerically solve Poisson's equation for phi. The boundary
// values remain zero, so there is no need to call a boundary
// update function.
for (int iter = 0; iter < numGaussSeidelIterations; ++iter)
{
    for (j = 1; j < jmax; ++j)
    {
        for (i = 1; i < imax; ++i)
        {
            phi[j][i] = epsilon0*div[j][i] +
                epsilon1*(phi[j][i+1] + phi[j][i-1]) +
                epsilon2*(phi[j+1][i] + phi[j-1][i]);
        }
    }
}

// Adjust the velocity v' = v + gradient(phi).
for (j = 1; j < jmax; ++j)
{
    for (i = 1; i < imax; ++i)
    {
        u[j][i] = u[j][i] + halfDivDX*(phi[j][i+1]
            - phi[j][i-1]);
        v[j][i] = v[j][i] + halfDivDY*(phi[j+1][i]
            - phi[j-1][i]);
    }
}
UpdateBoundary(t, x, y, uBF, u);
UpdateBoundary(t, x, y, vBF, v);
}

```

The simulation portion of the pseudocode is now modified to

```

while (simulating)
{
    // density update
    UpdateSource(t, x, y, rhoBF, RhoSource, true, rhoOld, rhoNew);
    SwapBuffers(&rhoOld, &rhoNew);
    UpdateDiffusionImplicit(t, x, y, gamma0[0], gamma1[0],
        gamma2[0], rhoBF, rhoOld, rhoNew);
    SwapBuffers(&rhoOld, &rhoNew);
}

```

```

UpdateAdvection(t, x, y, uOld, vOld, rhoBF, rhoOld, rhoNew);
SwapBuffers(&rhoOld, &rhoNew);

// velocity update
UpdateSource(t, x, y, uBF, USource, false, uOld, uNew);
UpdateSource(t, x, y, vBF, VSource, false, vOld, vNew);
SwapBuffers(&uOld, &uNew);
SwapBuffers(&vOld, &vNew);

UpdateDiffusionImplicit(t, x, y, gamma0[1], gamma1[1],
    gamma2[1], uBF, uOld, uNew);
UpdateDiffusionImplicit(t, x, y, gamma0[1], gamma1[1],
    gamma2[1], vBF, vOld, vNew);
SwapBuffers(&uOld, &uNew);
SwapBuffers(&vOld, &vNew);

AdjustVelocity(t, x, y, uBF, vBF, uOld, vOld);
UpdateAdvection(t, x, y, uOld, vOld, uBF, uOld, uNew);
UpdateAdvection(t, x, y, uOld, vOld, vBF, vOld, vNew);
AdjustVelocity(t, x, y, uBF, vBF, uNew, vNew);
SwapBuffers(&uOld, &uNew);
SwapBuffers(&vOld, &vNew);

t = t + deltaT;
}

```

`AdjustVelocity` is called before `UpdateAdvection` so that the velocity is mass preserving before advection. It is also called after `UpdateAdvection` so that the velocity is mass preserving before the simulation loop repeats.

5.5.7 SPECIALIZED BOUNDARY HANDLING

In my development, the boundary value handling is general in that you call various functions to set the boundary values. In [Sta03], the boundary values are set by a single function shown next.

```

void set_bnd (int N, int b, float* x)
{
    int i;

    for (i = 1; i <= N; ++i)
    {
        x[IX(0, i)] = b == 1 ? -x[IX(1,i)] : x[IX(1,i)];
        x[IX(N+1,i)] = b == 1 ? -x[IX(N,i)] : x[IX(N,i)];
        x[IX(i, 0)] = b == 2 ? -x[IX(i,1)] : x[IX(i,1)];
        x[IX(i,N+1)] = b == 2 ? -x[IX(i,N)] : x[IX(i,N)];
    }
}

```

```

x[IX(0, 0)] = 0.5*(x[IX(1,0)] + x[IX(0,1)]);
x[IX(0, N+1)] = 0.5*(x[IX(1,N+1)] + x[IX(0,N)]);
x[IX(N+1,0)] = 0.5*(x[IX(N,0)] + x[IX(N+1,1)]);
x[IX(N+1,N+1)] = 0.5*(x[IX(N,N+1)] + x[IX(N+1,N)]);
}

```

The lattice is square with dimensions $(N + 2) \times (N + 2)$. The macro $IX(i, j)$ expands to $(i) + (N + 2) * (j)$. The input b is 0 for density ρ , 1 for the velocity component u , and 2 for the velocity component v .

The paper mentions that for the density, the boundary values are chosen by “continuity.” The boundary handling for density, written in the notation of this chapter, is equivalent to

```

void SetRhoBoundary (float** rho)
{
    for (int i = 1; i < imax; ++i)
    {
        rho[0][i] = rho[1][i];
        rho[jmax][i] = rho[jmax-1][i];
    }
    for (int j = 1; j < jmax; ++j)
    {
        rho[j][0] = rho[j][1];
        rho[j][imax] = rho[j][imax-1];
    }
    rho[0][0] = rho[1][1];
    rho[0][imax] = rho[1][imax-1];
    rho[jmax][0] = rho[jmax-1][1];
    rho[jmax][imax] = rho[jmax-1][imax-1];
}

```

The code is actually the standard implementation for Neumann boundary conditions where the boundary directional derivatives are all zero. Such conditions, when used in heat diffusion, indicated the boundary is *insulated*; that is, no heat is allowed to diffuse out of the domain. In the fluids application, the boundary conditions specify that no mass change occurs at the boundary.

The paper also mentions that the fluid is contained in the rectangle “with solid walls” and that no flow should exit the walls. The horizontal component of the velocity (u) should be zero on the vertical walls and the vertical component of the velocity (v) should be zero on the horizontal walls. The claim is that `set_bnd` implements this, but that does not appear to be the case. For example, the function when applied to u is equivalent to

```

void SetUBoundary (float** u)
{
    for (int i = 1; i < imax; ++i)
    {
        u[0][i] = u[1][i];
    }
}

```

```

        u[jmax][i] = u[jmax-1][i];
    }
    for (int j = 1; j < jmax; ++j)
    {
        u[j][0] = -u[j][1];
        u[j][imax] = -u[j][imax-1];
    }
    u[0][0] = 0;
    u[0][imax] = 0;
    u[jmax][0] = 0;
    u[jmax][imax] = 0;
}

```

The i -loop involves Neumann boundary conditions on the horizontal walls where the boundary directional derivatives are zero. The j -loop sets the vertical wall values, but the u -values are *negated* instead of being set to zero. It is not clear why the negation is used, but one consequence is that if $u[1][1] > 0$, then $u[1][0] < 0$ in which case the velocity vector at the boundary point is directed outside the lattice, which is probably not the desired behavior.

The negation of the components is not one of the standard Dirichlet or Neumann boundary conditions, because it involves setting the boundary based on u itself. Recall that the boundary conditions were functions that depend only on the surface positions, not on the state of the solution near the surface. Regardless, as long as the numerical solution has desired behavior for the simulation, it is reasonable to have boundary dependence on the solution. In the case at hand, to satisfy the requirement that u is zero on the vertical walls, we may use *mixed boundary conditions*. Dirichlet boundary conditions are used on the vertical walls where the boundary values are zero. Neumann boundary conditions are used on the horizontal walls where the boundary derivative values are zero.

```

void SetUBoundary (float** u)
{
    for (int i = 1; i < imax; ++i)
    {
        u[0][i] = u[1][i];
        u[jmax][i] = u[jmax-1][i];
    }
    for (int j = 1; j < jmax; ++j)
    {
        u[j][0] = 0;
        u[j][imax] = 0;
    }
    u[0][0] = 0;
    u[0][imax] = 0;
    u[jmax][0] = 0;
    u[jmax][imax] = 0;
}

```

Mixed boundary conditions can also be used for the velocity component v .

```
void SetVBoundary (float** v)
{
    for (int i = 1; i < imax; ++i)
    {
        v[0][i] = 0;
        v[jmax][i] = 0;
    }
    for (int j = 1; j < jmax; ++j)
    {
        v[j][0] = v[j][1];
        v[j][imax] = v[j][imax-1];
    }
    v[0][0] = 0;
    v[0][imax] = 0;
    v[jmax][0] = 0;
    v[jmax][imax] = 0;
}
```

Another possibility is to clamp the u values to zero on the vertical walls and to clamp the v values to zero on the horizontal walls. This has the consequence that the velocities on the boundary never point outside the lattice. This is also a nonstandard boundary condition, but if the simulation looks good, then so be it.

```
void SetUBoundary (float** u)
{
    for (int i = 1; i < imax; ++i)
    {
        u[0][i] = u[1][i];
        u[jmax][i] = u[jmax-1][i];
    }
    for (int j = 1; j < jmax; ++j)
    {
        u[j][0] = u[j][1];
        if (u[j][0] < 0) { u[j][0] = 0; }
        u[j][imax] = u[j][imax-1];
        if (u[j][imax] > 0) { u[j][imax] = 0; }
    }
    u[0][0] = 0;
    u[0][imax] = 0;
    u[jmax][0] = 0;
    u[jmax][imax] = 0;
}

void SetVBoundary (float** v)
{
    for (int i = 1; i < imax; ++i)
    {
```

```

v[0][i] = v[1][i];
if (v[0][i] < 0) { v[0][i] = 0; }
v[jmax][i] = v[jmax-1][i];
if (v[jmax][i] > 0) { v[jmax][i] = 0; }
}
for (int j = 1; j < jmax; ++j)
{
    v[j][0] = v[j][1];
    v[j][imax] = v[j][imax-1];
}
v[0][0] = 0;
v[0][imax] = 0;
v[jmax][0] = 0;
v[jmax][imax] = 0;
}

```



An implementation of this algorithm is provided on the CD-ROM. Dirichlet boundary conditions with zero values are used for density. Mixed boundary conditions with zero values or zero derivatives are used for velocity. In the pseudocode presented here, the update functions are applied separately to u and v . In the actual code, the updates are applied jointly to avoid the repeated double loops and to avoid the repeated bilinear interpolation setup in the advection update.

The physics library has a class `Fluid2Da` that implements the three-stage update algorithm of [Sta03] on the CPU. The class `Fluid2Db` has a single-stage update that combines the source–sink evaluation, the diffusion term, and the advection. The modified algorithm is only conditionally stable, but a reasonable time step can be chosen. For a 256×256 grid and running on a single 3 GHz core and an NVIDIA GeForce 9600 GT graphics card, the `Fluid2Da` algorithm ran at 7 frames per second. The `Fluid2Db` algorithm ran at 28 frames per second.

Figure 5.4 – also Color Plates 5.4(ab) and 5.4(cd) – shows some screen captures from the application running with the `Fluid2Db` class.



An implementation of this algorithm on the GPU is provided on the CD-ROM. The sample duplicates the behavior of the `Fluids2Db` sample. Running on a single 3 GHz core and an NVIDIA GeForce 9600 GT graphics card, the frame rate for the 256×256 grid was 135 frames per second.

5.6 IMPLEMENTING THE SIMPLIFIED 3D MODEL

The region V is chosen to be a solid cube in 3D, say, $V = \{(x, y, z) : x \in [x_0, x_1], y \in [y_0, y_1], z \in [z_0, z_1]\}$. The velocity vector has components $u(x, y, z, t)$, $v(x, y, z, t)$, and $w(x, y, z, t)$. The differential equations are

$$\begin{aligned}
\rho_t &= \kappa (\rho_{xx} + \rho_{yy} + \rho_{zz}) - u\rho_x - v\rho_y - w\rho_z + s \\
u_t &= v(u_{xx} + u_{yy} + u_{zz}) - uu_x - vu_y - wu_z + f \\
v_t &= v(v_{xx} + v_{yy} + v_{zz}) - uv_x - vv_y - wv_z + g \\
w_t &= v(w_{xx} + w_{yy} + w_{zz}) - uw_x - vw_y - ww_z + h
\end{aligned} \tag{5.95}$$

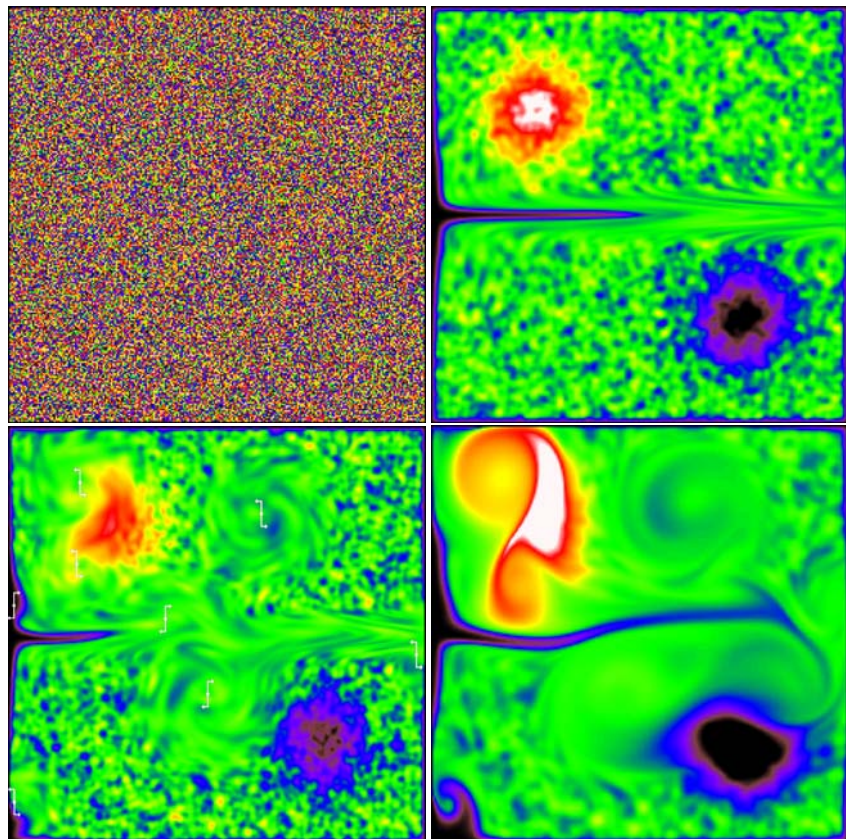


Figure 5.4 Image (a) [upper left]: The initial density is generated by a uniform random number generator. Image (b) [upper right]: The evolved density after a small period of time. The only force is due to a spike of wind moving from the left-center of the grid. The bright blob-like region is a density source. The dark blob-like region is a density sink. Image (c) [lower left]: Starting from the random initial density, eight vortices were added to the grid. They are shown in white in the figure; the direction of rotation is indicated by the arrows. You can see the swirl-like effects of the vortices. Image (d) [lower right]: The grid of image (c) is allowed to evolve further. The density source and sink are more pronounced, and the density is starting to become more homogeneous in regions centered at the vortices. (See also Color Plates 5.4(ab) and 5.4(cd).)

for $(x, y, z) \in [x_0, x_1] \times [y_0, y_1] \times [z_0, z_1]$ and $t \geq 0$. The subscripts on the functions indicate partial derivatives with respect to the variables t , x , y , and z . The density source–sink function is s and the velocity impulse function is (f, g, h) . Initial values and boundary values must be specified.

The cube is decomposed into a lattice of points, say, $(x[i], y[j], z[k])$ for $0 \leq i \leq i_{\max}$, $0 \leq j \leq j_{\max}$, and $0 \leq k \leq k_{\max}$. Each lattice cell is centered at $(x[i], y[j], z[k])$ and has dimensions $\Delta_x = (x_1 - x_0)/i_{\max}$, $\Delta_y = (y_1 - y_0)/j_{\max}$, and $\Delta_z = (z_1 - z_0)/k_{\max}$. Thus, $x[i] = x_0 + i\Delta_x$, $y[j] = y_0 + j\Delta_y$, and $z[k] = z_0 + k\Delta_z$.

The time variable is also discretized by $t[\ell] = \ell\Delta_t$ for $\ell \geq 0$, where the time step $\Delta_t > 0$ is specified by the user. The choice for the time step can affect the numerical stability of the algorithm, so depending on how the differential equation is numerically solved, you might have restrictions on the size of the time step.

The derivation of the numerical method for 3D is similar to that for 2D. The initial-value functions must be specified for each of ρ , u , v , and w . The boundary value functions must also be specified. There are two such functions for the x -faces of the cube, two for the y -faces, and two for the z -faces. The functions must be continuous as a whole over the six faces. In the pseudocode, the boundary values are set for voxels of type *face-interior*, *edge-interior*, and *corners*. Rather than having generic functions as in the 2D case, the pseudocode has functions specific to density (Neumann boundary conditions) and velocity (mixed boundary conditions).

The global and local data and functions are

```
// global values
float x0, y0, x1, y1, z0, z1; // cube bounds
int imax, jmax, kmax; // lattice bounds
float deltaT; // time step (positive)
float deltaX = (x1 - x0)/imax; // cell x-dimension
float deltaY = (y1 - y0)/jmax; // cell y-dimension
float deltaZ = (z1 - z0)/kmax; // cell z-dimension
float halfDivDX = 0.5/deltaX;
float halfDivDY = 0.5/deltaY;
float halfDivDZ = 0.5/deltaZ;
float deltaXSqr = deltaX*deltaX;
float deltaYSqr = deltaY*deltaY;
float deltaZSqr = deltaZ*deltaZ;
float epsilon0 = 0.5*deltaXSqr*deltaYSqr*deltaZSqr
    / (deltaXSqr + deltaYSqr + deltaZSqr);
float epsilonX = epsilon0/deltaXSqr;
float epsilonY = epsilon0/deltaYSqr;
float epsilonZ = epsilon0/deltaZSqr;
float dtDivDx = deltaT/deltaX;
float dtDivDy = deltaT/deltaY;
float dtDivDz = deltaT/deltaZ;
float dtDivDxDx = dtDivDx/deltaX;
float dtDivDyDy = dtDivDy/deltaY;
float dtDivDzDz = dtDivDz/deltaZ;

float denViscosity; // density viscosity, kappa
float denLambdaX = denViscosity*dtDivDxDx;
float denLambdaY = denViscosity*dtDivDyDy;
```

```

float denLambdaZ = denViscosity*dtDivDzDz;
float denGamma0 = 1/(1 + 2*(denLambdaX + denLambdaY + denLambdaZ));
float denGammaX = denLambdaX*denGamma0;
float denGammaY = denLambdaY*denGamma0;
float denGammaZ = denLambdaZ*denGamma0;

float velViscosity; // velocity viscosity, nu
float velLambdaX = velViscosity*dtDivDxDx;
float velLambdaY = velViscosity*dtDivDyDy;
float velLambdaZ = velViscosity*dtDivDzDz;
float velGamma0 = 1/(1 + 2*(velLambdaX + velLambdaY + velLambdaZ));
float velGammaX = velLambdaX*velGamma0;
float velGammaY = velLambdaY*velGamma0;
float velGammaZ = velLambdaZ*velGamma0;

int numGaussSeidelIterations; // your choice;

// global functions
float InitialDensity (float x, float y, float z);
float SourceDensity (float x, float y, float z, float t);
Vector3 InitialVelocity (float x, float y, float z);
Vector3 SourceVelocity (float x, float y, float z, float t);

void SwapBuffers (float**** oldBuffer, float**** newBuffer);
void SwapBuffers (Vector3**** oldBuffer, Vector3**** newBuffer);

// local values
float x[imax], y[jmax], z[kmax];
float densityOld[kmax][jmax][imax];
float densityNew[kmax][jmax][imax];
Vector3 velocityOld[kmax][jmax][imax];
Vector3 velocityNew[kmax][jmax][imax];
float t = 0.0; // initial time

```

The simulation portion of the pseudocode is

```

Initialize(x, y, z, densityOld, densityNew, velocityOld,
           velocityNew);
while (simulating)
{
    // density update
    UpdateDensitySource(t, x, y, z, densityOld, densityNew);
    SwapBuffers(&densityOld, &densityNew);
    UpdateDensityDiffusion(densityOld, densityNew);
    SwapBuffers(&densityOld, &densityNew);
    UpdateDensityAdvection(velocityOld, densityOld, densityNew);
    SwapBuffers(&densityOld, &densityNew);
}

```

```

// velocity update
UpdateVelocitySource(t, x, y, z, velocityOld, velocityNew);
SwapBuffers(&velocityOld, &velocityNew);
UpdateVelocityDiffusion(velocityOld, velocityNew);
SwapBuffers(&velocityOld, &velocityNew);
UpdateVelocityAdvection(velocityOld, velocityNew);
SwapBuffers(&velocityOld, &velocityNew);

t = t + deltaT;
}

```

where the `AdjustVelocity` calls are now made inside any function that updates the velocity field. This includes the functions `Initialize`, `UpdateVelocitySource`, `UpdateVelocityDiffusion`, and `UpdateAdvection`. The idea is that any “consumer” of the velocity field wants it to be divergence free.

The adjustment of velocity is

```

void AdjustVelocity (float*** velocity)
{
    int i, j, k;

    // Approximate the divergence of velocity.
    float div[kmax][jmax][imax];
    for (k = 1; k < kmax; ++k)
    {
        for (j = 1; j < jmax; ++j)
        {
            for (i = 1; i < imax; ++i)
            {
                div[k][j][i] =
                    halfDivDX*(velocity[k][j][i+1].x
                               - velocity[k][j][i-1].x) +
                    halfDivDY*(velocity[k][j+1][i].y
                               - velocity[k][j-1][i].y) +
                    halfDivDZ*(velocity[k+1][j][i].z
                               - velocity[k-1][j][i].z);
            }
        }
    }

    // Use zero-valued derivative on boundary to assign divergence.
    for (k = 0; k <= kmax; ++k)
    {
        for (j = 0; j <= jmax; ++j)
        {
            div[k][j][0] = div[k][j][1];
            div[k][j][imax] = div[k][j][imax-1];
        }
    }
}

```

```

}
for (k = 0; k <= kmax; ++k)
{
    for (i = 0; i <= imax; ++i)
    {
        div[k][0][i] = div[k][1][i];
        div[k][jmax][i] = div[k][jmax-1][i];
    }
}
for (j = 0; j <= jmax; ++j)
{
    for (i = 0; i <= imax; ++i)
    {
        div[0][j][i] = div[1][j][i];
        div[kmax][j][i] = div[kmax-1][j][i];
    }
}

// Initialize phi.
float phi[kmax][jmax][imax];
for (k = 0; k <= kmax; ++k)
{
    for (j = 0; j <= jmax; ++j)
    {
        for (i = 0; i <= imax; ++i)
        {
            phi[k][j][i] = 0;
        }
    }
}

// Numerically solve Poisson's equation for phi.  The
// boundary values remain zero, so there is no need to
// call a boundary update function.
for (int iter = 0; iter < numGaussSeidelIterations; ++iter)
{
    for (k = 1; k < kmax; ++k)
    {
        for (j = 1; j < jmax; ++j)
        {
            for (i = 1; i < imax; ++i)
            {
                phi[k][j][i] = epsilon0*div[k][j][i] +
                    epsilonX*(phi[k][j][i+1]
                        + phi[k][j][i-1]) +
                    epsilonY*(phi[k][j+1][i]
                        + phi[k][j-1][i]) +

```

```

        epsilonZ*(phi[k+1][j][i]
                  + phi[k-1][j][i]));
    }
}
}

// Adjust the velocity v' = v + gradient(phi).
for (k = 1; k < kmax; ++k)
{
    for (j = 1; j < jmax; ++j)
    {
        for (i = 1; i < imax; ++i)
        {
            velocity[k][j][i].x += halfDivDX*(phi[k][j][i+1]
                                              - phi[k][j][i-1]);
            velocity[k][j][i].y += halfDivDY*(phi[k][j+1][i]
                                              - phi[k][j-1][i]);
            velocity[k][j][i].z += halfDivDZ*(phi[k+1][j][i]
                                              - phi[k-1][j][i]);
        }
    }
    UpdateVelocityBoundary(velocity);
}

```

The initialization of density and velocity is

```

void Initialize (float* x, float* y, float* z,
                 float*** densityOld, float*** densityNew,
                 Vector3*** velocityOld, Vector3*** velocityNew)
{
    for (int k = 0; k <= kmax; ++k)
    {
        z[k] = z0 + deltaZ*k;
        for (int j = 0; j <= jmax; ++j)
        {
            y[j] = y0 + deltaY*j;
            for (int i = 0; i <= imax; ++i)
            {
                x[i] = x0 + deltaX*i;
                float density = InitialDensity(x[i], y[j], z[k]);
                densityOld[k][j][i] = density;
                densityNew[k][j][i] = density;
                velocityOld[k][j][i] =
                    InitialVelocity(x[i], y[j], z[k]);
            }
        }
    }
}

```

```

    AdjustVelocity(velocityOld);
    CopyArray(velocityOld, velocityNew);
}

```

The update of density on the boundary is

```

void UpdateDensityBoundary (float*** density)
{
    int i, j, k;

    // x-faces (i = 0, i = imax)
    for (k = 0; k <= kmax; ++k)
    {
        for (j = 0; j <= jmax; ++j)
        {
            density[k][j][0] = density[k][j][1];
            density[k][j][imax] = density[k][j][imax-1];
        }
    }

    // y-faces (j = 0, j = jmax)
    for (k = 0; k <= kmax; ++k)
    {
        for (i = 0; i <= imax; ++i)
        {
            density[k][0][i] = density[k][1][i];
            density[k][jmax][i] = density[k][jmax-1][i];
        }
    }

    // z-faces (k = 0, k = kmax)
    for (j = 0; j <= jmax; ++j)
    {
        for (i = 0; i <= imax; ++i)
        {
            density[0][j][i] = density[1][j][i];
            density[kmax][j][i] = density[kmax-1][j][i];
        }
    }
}

```

The update of velocity on the boundary is

```

void UpdateVelocityBoundary (Vector3*** velocity)
{
    int i, j, k;

    // (v,w) zero derivatives on x-faces (i = 0, i = imax)
    for (k = 0; k <= kmax; ++k)

```

```

{
    for (j = 0; j <= jmax; ++j)
    {
        velocity[k][j][0].y = velocity[k][j][1].y;
        velocity[k][j][0].z = velocity[k][j][1].z;
        velocity[k][j][imax].y = velocity[k][j][imax-1].y;
        velocity[k][j][imax].z = velocity[k][j][imax-1].z;
    }
}

// (u,w) zero derivatives on y-faces (j = 0, j = jmax)
for (k = 0; k <= kmax; ++k)
{
    for (i = 0; i <= imax; ++i)
    {
        velocity[k][0][i].x = velocity[k][1][i].x;
        velocity[k][0][i].z = velocity[k][1][i].z;
        velocity[k][jmax][i].x = velocity[k][jmax-1][i].x;
        velocity[k][jmax][i].z = velocity[k][jmax-1][i].z;
    }
}

// (u,v) zero derivatives on z-faces (k = 0, k = kmax)
for (j = 0; j <= jmax; ++j)
{
    for (i = 0; i <= imax; ++i)
    {
        velocity[0][j][i].x = velocity[1][j][i].x;
        velocity[0][j][i].y = velocity[1][j][i].y;
        velocity[kmax][j][i].x = velocity[kmax-1][j][i].x;
        velocity[kmax][j][i].y = velocity[kmax-1][j][i].y;
    }
}

// u = 0 on x-faces
for (k = 0; k <= kmax; ++k)
{
    for (j = 0; j <= jmax; ++j)
    {
        velocity[k][j][0].x = 0;
        velocity[k][j][imax].x = 0;
    }
}

// v = 0 on y-faces
for (k = 0; k <= kmax; ++k)
{
}

```

```

        for (i = 0; i <= imax; ++i)
        {
            velocity[k][0][i].y = 0;
            velocity[k][jmax][i].y = 0;
        }
    }

    // w = 0 on z-faces
    for (j = 0; j <= jmax; ++j)
    {
        for (i = 0; i <= imax; ++i)
        {
            velocity[0][j][i].z = 0;
            velocity[kmax][j][i].z = 0;
        }
    }
}

```

The updates of density and velocity sources are

```

void UpdateDensitySource (float t, float* x, float* y, float* z,
    float*** densityOld, float*** densityNew)
{
    for (int k = 0; k <= kmax; ++k)
    {
        for (int j = 0; j <= jmax; ++j)
        {
            for (int i = 0; i <= imax; ++i)
            {
                densityNew[k][j][i] = densityOld[k][j][i] +
                    deltaT*SourceDensity(x[i], y[j], z[k], t);
                if (densityNew[k][j][i] < 0)
                {
                    densityNew[k][j][i] = 0;
                }
            }
        }
    }
}

void UpdateVelocitySource (float t, float* x, float* y, float* z,
    Vector3*** velocityOld, Vector3*** velocityNew)
{
    for (int k = 0; k <= kmax; ++k)
    {
        for (int j = 0; j <= jmax; ++j)
        {
            for (int i = 0; i <= imax; ++i)

```

```

        {
            velocityNew[k][j][i] = velocityOld[k][j][i] +
                deltaT*SourceVelocity(x[i], y[j], z[k], t);
        }
    }
    AdjustVelocity(velocityNew);
}

```

The updates of density and velocity by diffusion are

```

void UpdateDensityDiffusion (Vector3*** densityOld,
    Vector3*** densityNew)
{
    for (int iter = 0; iter < numGaussSeidelIterations; ++iter)
    {
        for (int k = 1; k < kmax; ++k)
        {
            for (int j = 1; j < jmax; ++j)
            {
                for (int i = 1; i < imax; ++i)
                {
                    densityNew[k][j][i] =
                        denGamma0*densityOld[k][j][i] +
                        denGammaX*(densityNew[k][j][i+1]
                            + densityNew[k][j][i-1]) +
                        denGammaY*(densityNew[k][j+1][i]
                            + densityNew[k][j-1][i]) +
                        denGammaZ*(densityNew[k+1][j][i]
                            + densityNew[k-1][j][i]);
                }
            }
        }
    }
    UpdateDensityBoundary(densityNew);
}

void UpdateVelocityDiffusion (Vector3*** velocityOld,
    Vector3*** velocityNew)
{
    for (int iter = 0; iter < numGaussSeidelIterations; ++iter)
    {
        for (int k = 1; k < kmax; ++k)
        {
            for (int j = 1; j < jmax; ++j)
            {
                for (int i = 1; i < imax; ++i)

```

```

    {
        velocityNew[k][j][i] =
            velGamma0*velocityOld[k][j][i] +
            velGammaX*(velocityNew[k][j][i+1]
                + velocityNew[k][j][i-1]) +
            velGammaY*(velocityNew[k][j+1][i]
                + velocityNew[k][j-1][i]) +
            velGammaZ*(velocityNew[k+1][j][i]
                + velocityNew[k-1][j][i]);
    }
}
UpdateVelocityBoundary(velocityNew);
}
AdjustVelocity(velocityNew);
}

```

The updates of density and velocity by advection are

```

void UpdateDensityAdvection (Vector3*** velocityOld,
    float*** densityOld, float*** densityNew)
{
    for (int k = 1; k < kmax; ++k)
    {
        for (int j = 1; j < jmax; ++j)
        {
            for (int i = 1; i < imax; ++i)
            {
                float iPrevious =
                    i - dtDivDx*velocityOld[k][j][i].x;
                Clamp(iPrevious, 0.5, imax - 0.5);
                int i0 = Floor(iPrevious);
                int i1 = i0 + 1;
                float a1 = iPrevious - i0;
                float a0 = 1 - a1;

                float jPrevious =
                    j - dtDivDy*velocityOld[k][j][i].y;
                Clamp(jPrevious, 0.5, jmax - 0.5);
                int j0 = Floor(jPrevious);
                int j1 = j0 + 1;
                float b1 = jPrevious - j0;
                float b0 = 1 - b1;

                float kPrevious =
                    k - dtDivDz*velocityOld[k][j][i].z;
                Clamp(kPrevious, 0.5, kmax - 0.5);
                int k0 = Floor(kPrevious);

```

```

        int k1 = k0 + 1;
        float c1 = kPrevious - k0;
        float c0 = 1 - c1;

        densityNew[k][j][i] =
            c0*(
                b0*(a0*densityOld[k0][j0][i0] +
                    a1*densityOld[k0][j0][i1]) +
                b1*(a0*densityOld[k0][j1][i0] +
                    a1*densityOld[k0][j1][i1])
            )
            +
            c1*(
                b0*(a0*densityOld[k1][j0][i0] +
                    a1*densityOld[k1][j0][i1]) +
                b1*(a0*densityOld[k1][j1][i0] +
                    a1*densityOld[k1][j1][i1])
            );
    }
}

UpdateDensityBoundary(densityNew);
}

void UpdateVelocityAdvection (Vector3*** velocityOld,
    Vector3*** velocityNew)
{
    AdjustVelocity(velocityOld);

    for (int k = 1; k < kmax; ++k)
    {
        for (int j = 1; j < jmax; ++j)
        {
            for (int i = 1; i < imax; ++i)
            {
                float iPrevious =
                    i - dtDivDx*velocityOld[k][j][i].x;
                Clamp(iPrevious, 0.5, imax - 0.5);
                int i0 = Floor(iPrevious);
                int i1 = i0 + 1;
                float a1 = iPrevious - i0;
                float a0 = 1 - a1;

                float jPrevious =
                    j - dtDivDy*velocityOld[k][j][i].y;
                Clamp(jPrevious, 0.5, jmax - 0.5);
                int j0 = Floor(jPrevious);
            }
        }
    }
}

```

```

int j1 = j0 + 1;
float b1 = jPrevious - j0;
float b0 = 1 - b1;

float kPrevious =
    k - dtDivDz*velocityOld[k][j][i].z;
Clamp(kPrevious, 0.5, kmax - 0.5);
int k0 = Floor(kPrevious);
int k1 = k0 + 1;
float c1 = kPrevious - k0;
float c0 = 1 - c1;

velocityNew[k][j][i] =
c0*(
    b0*(a0*velocityOld[k0][j0][i0] +
    a1*velocityOld[k0][j0][i1]) +
    b1*(a0*velocityOld[k0][j1][i0] +
    a1*velocityOld[k0][j1][i1])
)
+
c1*(
    b0*(a0*velocityOld[k1][j0][i0] +
    a1*velocityOld[k1][j0][i1]) +
    b1*(a0*velocityOld[k1][j1][i0] +
    a1*velocityOld[k1][j1][i1])
);
}
}
}
UpdateVelocityBoundary(velocityNew);
AdjustVelocity(velocityNew);
}

```



An implementation of this algorithm is provided on the CD-ROM. The physics library has a class `Fluids3Da` that implements the three-stage update of [Sta03]. It also has a class `Fluids3Db` that has a single-stage update combining sources, diffusion, and advection, but it is only conditionally stable. A $24 \times 24 \times 24$ grid is used. On a single 3 GHz core, the three-stage algorithm runs at 20 frames per second. The density is displayed using billboarded particles. The single-state algorithm runs at 33 frames per second.

Figure 5.5 – also Color Plates 5.5(ab) and 5.5(cd) – shows some screen captures from the application running with the `Fluids3Db` class. The lattice is a 24^3 grid. The rendering uses cheesy looking particle billboards, each having a texture with a solid disk in the RGB channels and an alpha channel whose value is proportional to the density. The particles are sorted each time the camera moves or scene rotated, which really slows down the rendering. GPU support or use of multiple CPU cores is called for.

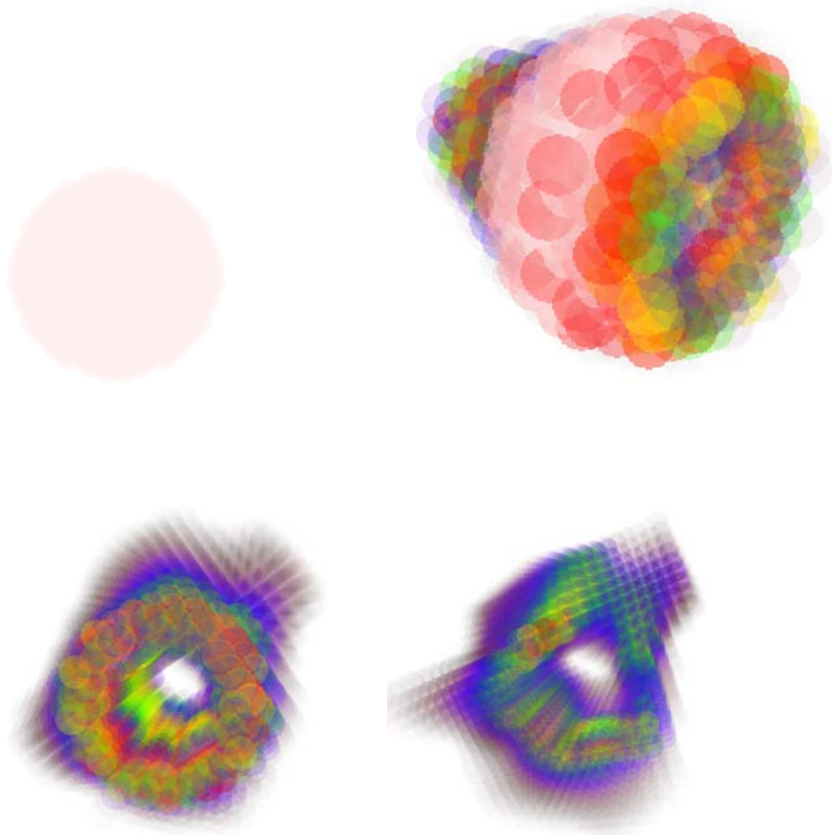


Figure 5.5 Image (a) [upper left]: The initial density is a spherical blob of constant density. Image (b) [upper right]: The evolved density after a small period of time. The only force is due to a spike of wind moving from the right-center of the grid; the scene has been rotated slightly so you can see the portion of the sphere on which the wind interacted first. There are no density sources or sinks. You can see the material being pushed out of the sphere by the wind. Image (c) [lower left]: Eight vortices were added to the grid, which causes the density to swirl around a bit. The scene was rotated so you can see the tunnel carved out by the wind. Image (d) [lower right]: The lower-left grid is allowed to evolve further. (See also [Color Plates 5.4\(ab\)](#) and [5.4\(cd\)](#).)

The images in the figure are gray scale. The application actually allows you to display the particles in pseudocolor using a rainbow palette. It is easier to see how the density evolves when using the pseudocolor.

Class Project. Here is a class project that will take some time. Implement the single-stage update algorithm for a 3D fluid on the GPU. The 2D fluid required writing to 2D render targets in a natural way; that is, samplers evaluated the state textures at a point and its neighboring points in order to estimate derivatives. The graphics APIs do not have the concept of a 3D render target, so the derivative estimation does not naturally map into a simple shader program using a 2D render target. The trick is to store the 3D state texture in a 2D render target as an array of 2D textures. For example, if you have a $2^{2n} \times 2^{2n} \times 2^{2n}$ state grid, map it to a $2^n \times 2^n$ array of tiles, each tile a z-slice of size $2^{2n} \times 2^{2n}$. Observe that this is *not* the standard lexicographical ordering that maps a grid point (x, y, z) to linear memory as $i = x + b_0(y + b_1z)$, when the 3D texture has dimensions $b_0 \times b_1 \times b_2$. The finite-difference estimates for x- and y-derivatives are computed using neighboring texel values. However, the finite-difference estimates for z-derivatives require texel values that are not immediate neighbors. A *z-offset texture* must be provided. The pixel shader looks up the z-offsets first and then uses these to form texture coordinates to look up the corresponding state values.

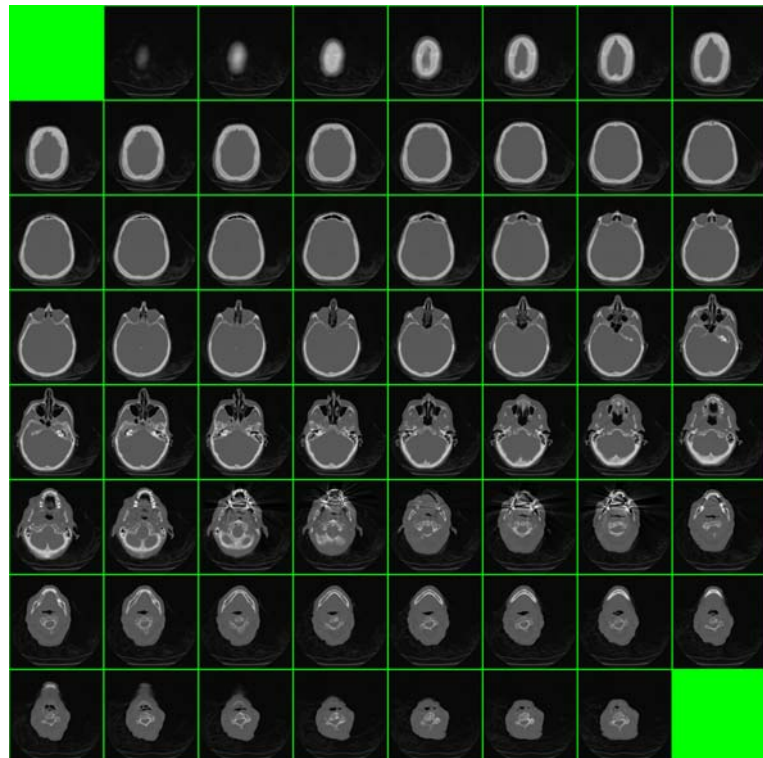


Figure 5.6 (Continued)

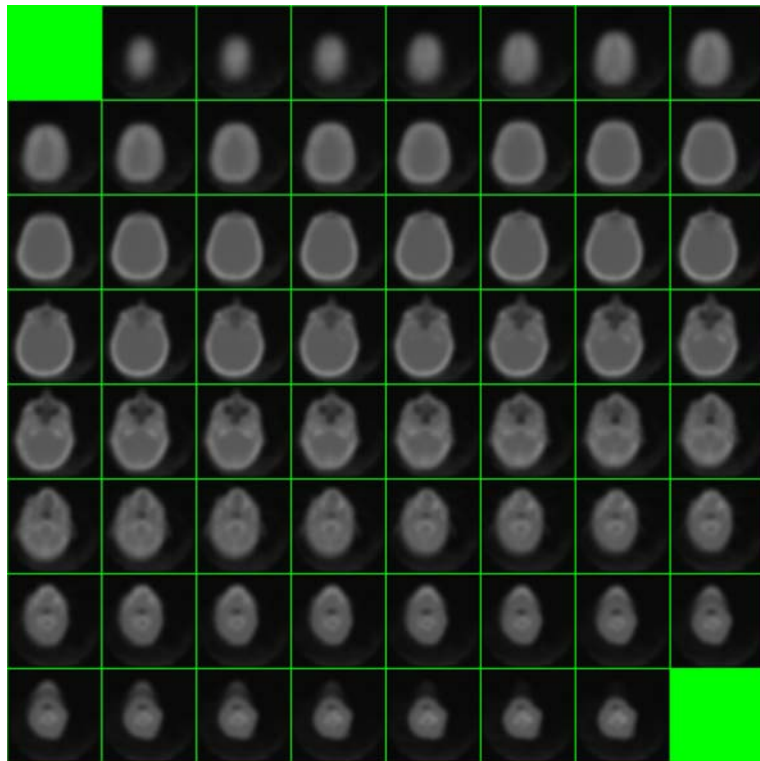


Figure 5.6 Image (a) [top] shows the initial $128 \times 128 \times 64$ gray scale image (a CT image). The boundary voxels are drawn in light gray. The $z = 0$ slice is the upper left tile. The $z = 63$ slice is the lower right tile. Image (b) [bottom] shows the 3D image after a number of blurring operations. (See also [Color Plate 5.6](#).)



SOURCE CODE
GpuGaussianBlur3

As a hint for the class project, this sample application implements Gaussian blurring for 3D images on the GPU. The framework for generating a 2D tiled render target from a 3D image is part of Wild Magic. On a 3 Ghz core and an NVIDIA GeForce 9600 GT graphics card, the application runs at 210 frames per second. [Figure 5.6](#) – also [Color Plate 5.6](#) – shows a couple of screen captures.

5.7 VARIATIONS OF THE SIMPLIFIED MODEL

The simplified model of [equation \(5.87\)](#) may be enhanced to obtain other visually realistic behavior in the simulation. This section describes a few variations.

5.7.1 VORTICITY CONFINEMENT AND VORTEX PARTICLES

The finite-difference approximations led to a velocity field that is not necessarily divergence free. The Helmholtz decomposition was used to adjust the velocity field by subtracting out the gradient field, leaving only a curl field (that is divergence free) and is mass preserving. Another consequence of the finite-difference approximations is that the system can lose energy. This manifests itself in that any vortex behavior of the fluid is damped over time. Instead, [FSJ01] introduced a modification that detects where the curl of velocity is large (curl is what causes the vorticity/circulation) and adds energy back into the system by including a force that encourages the velocity field to have vorticity. This process is referred to as *vorticity confinement*.

Another approach to modeling the vorticity behavior involves having separate sets of particles, those for the fluid (smoke) and those to model the vortex behavior. The latter set is referred to as *vortex particles*. The idea is to construct and evolve curves that “carry” the vorticity. See [SRF05] for details.

5.7.2 SEPARATE PRESSURE TERM

A simple change is to keep the pressure term separate from the force term

$$\mathbf{v}_t + (\mathbf{v} \cdot \nabla) \mathbf{v} = \nu \nabla^2 \mathbf{v} - \frac{1}{\rho} \nabla p + \mathbf{f}$$

The simulation can allow for user input to control the pressure within the fluid, handling this separately from forces such as gravity (that are still encapsulated by the \mathbf{f} term).

5.7.3 OMIT DIFFUSION TERMS

Some arguments have been made to ignore the density diffusion and velocity diffusion terms of equation (5.87). In theory, viscosity causes dampening of the fluid flow. However, the use of implicit numerical solvers for the differential equations also cause a dampening effect. The dampening of the solver helps with stability, as does the viscosity and diffusion terms, so in practice there might not be a need to have dampening from both processes.

5.7.4 DENSITY AND VELOCITY DISSIPATION

It is possible to make the density dissipate over time by including another term in the density differential equation,

$$\frac{\partial \rho}{\partial t} + (\mathbf{v} \cdot \nabla) \rho = -\lambda \rho + \kappa \nabla^2 \rho + s$$

for a positive constant λ . In absence of the other terms, we have $\rho_t = -\lambda\rho$, whose solution is

$$\rho(\mathbf{x}, t) = \rho_0(\mathbf{x})e^{-\lambda t}$$

As t increases, the density decreases. Such an effect might be useful for making smoke or clouds dissipate over time.

It is also possible to have a dissipation-like term in the velocity differential equation. This is accomplished by keeping the term involving the source–sink density function times velocity rather than absorbing it into the \mathbf{f} term,

$$\mathbf{v}_t + (\mathbf{v} \cdot \nabla)\mathbf{v} = v\nabla^2\mathbf{v} - \frac{s}{\rho}\mathbf{v} + \mathbf{f}$$

If the density has only source contributions (and no density sink), then $s/\rho \geq 0$ and the extra term acts as a velocity dissipation, much like that described for density dissipation.

5.7.5 INCLUDE TEMPERATURE

It is possible to include *conservation of energy* in the physical modeling. The derivation is complicated and not provided here. A simplified equation that involves the temperature T of the system is

$$\frac{\partial T}{\partial t} + (\mathbf{v} \cdot \nabla)T = c\nabla^2 T + H$$

where c is a nonnegative constant and H is a heat source–sink function. Just as for density and velocity, the left-hand side is the material derivative of the temperature. The right-hand side has a diffusion term and a term that models external heat added or subtracted in the system.

For a smoke simulation, it is intuitively clear that when you heat the air, the hot air rises and induces upward force on the smoke particles. Similarly, when you cool the air, a downward force is applied to the particles. The force from heating or cooling the air causes the smoke velocity to change, so the pressure term in the velocity differential equation should be included and contain a force whose magnitude is proportional to the difference between the temperature of the fluid and the ambient temperature.

5.7.6 COMPRESSIBLE FLOW

We made the assumption that the velocity field is incompressible; that is, $\nabla \cdot \mathbf{v} = 0$. This assumption may be discarded to produce a *compressible fluid*. For example, see [YOH00].

5.7.7 OBSTACLES IN THE FLUID REGION

The implementations of [Sections 5.5](#) and [5.6](#) involved a lattice of cells. The fluid is free to move about the region into and out of any cell it likes. In a more realistic situation, the fluid flow might be obstructed by an obstacle in the region. For example, imagine modeling the flow of a river (2D) within a rectangular strip. You might want to place rocks in the river to impede the flow. The fluid naturally will encounter the rocks and flow around them.

It is not too difficult to modify the implementations to allow the placement of obstacles. Additional storage is used for a Boolean variable that is true when a cell is an obstacle or false when it is not. The cells that are marked true and have at least one immediate neighbor that is marked false is a “boundary cell.” Such cells must also be assigned boundary values. The finite differences are used to approximate state at cells marked false and whose immediate neighbors (4 in 2D and 6 in 3D) are marked false. Inside the loops over the cells, the Boolean conditions are tested to decide whether you apply the finite difference. The boundary update functions must also test the Boolean conditions to decide whether you assign/compute a boundary value.

5.7.8 MOVING BOUNDARIES AND MULTIPLE FLUIDS

The simulations discussed here involve a region that is invariant over time. The boundaries are always in the same place. Consider, though, modeling water is poured onto a flat surface and that flows over the surface. The surface below the water acts as part of the boundary, but part of the boundary is also around the leading edge of the water puddle. This edge varies with time, which makes the simulation more difficult to implement.

Even more complicated is to have a simulation involving multiple fluids. The different species of fluid are separated from each other by boundaries that vary with time, and if the fluids are poured onto a surface, we have the additional complications to deal with regarding boundaries.

In both cases, allowing for *moving boundaries* makes the simulation difficult. I consider this beyond the scope of the book, but encourage you to study research papers that attempt to solve the inherent problems and provide simulations. The paper [[Sta03](#)] mentions a few early approaches. [[FF01](#)] and [[EMF02](#)] model water and air (both fluids) using a mixture of particles and level sets (level-set methods are a powerful technique; see the books [[Set99](#)] and [[OF03](#)]). [[NFJ02](#)] models fire and air.

5.7.9 FINDING PAPERS ON FLUID SIMULATION

The field of fluid simulation has grown substantially, so much that it is not difficult to perform an Internet search on some of the terms introduced in this chapter and find lots of papers to read. It is difficult, however, to read all those papers and still have a life...

One of the topics not discussed here is *smoothed particle hydrodynamics* (SPH), which was introduced in the field of astrophysics by [Mon92]. A detailed master's thesis on the topic applied to fluids is [Ves04]. The paper [MCG03] discusses the application of SPH to fluid simulation and addresses many of the inherent issues, including rendering aspects of the simulation. More recently, here is an SPH approach that avoids solving a pressure Poisson's equation (much like the divergence Poisson's equation used to correct the velocity field) yet allows large time steps while retaining stability [SP09].

[SB08] introduces an approach that uses typical fluid solvers to generate low-resolution behavior, but then adds on top of this some high-resolution turbulent behavior. A mixture of particles, double-density relaxation, and mass–springs is presented in [CBP05]. A lot of attention has been given lately to simulations that run with the aid of GPUs. For example, see [HKK07], [ZSP08], and [Har08].

These are just a handful of papers you can find by searching. Happy hunting.

CHAPTER 6

PHYSICS ENGINES

We arrive at the topic I believe most readers will think of as the heart of game physics – the physics engine. This chapter describes a general system for handling a collection of rigid bodies, including collision detection and collision response. The system uses Newton’s second law of motion, $F = ma$, to control the motion of objects. The constraint forces are unknown to the system and must be calculated based on the information that is provided by the collision detection system. A natural requirement for a general system is that the rigid bodies never interpenetrate. A model for satisfying the requirement is the impulse-based (or acceleration-based) approach that Brian Mirtich [Mir96b] and David Baraff [Bar01] made popular, but by all means this is not the only approach one can take. Velocity-based approaches are found in [Ani97], [AP97], and [Cat05]. Position-based approaches are found in [MHHR06] and [Mül08].

My goal is to go into significant detail about the impulse-based approach so that you

- Understand the layout of a general physics engine,
- See what complications arise, and
- Learn to evaluate its strengths and weaknesses.

I will also describe in lesser detail the velocity-based and position-based approaches. Other approaches to building a robust physics engine are based on trying to fix the weaknesses of the previous generation engine. Once you understand the impulse-based engine, you should be able to start experimenting with modifications;

references to other approaches are provided, so you have a nearly endless supply of ideas to investigate.

A physics engine naturally partitions the physical simulation into two phases, *collision detection* and *collision response*. Collision detection refers to the process of determining if two bodies are currently intersecting or will intersect at a future time. Even though we are concerned with nonpenetration, an implementation has to deal with penetration due to numerical round-off errors. A collision detection system must be prepared to deal with all cases and report time-zero intersections and/or penetrations when they occur. The time of intersection is important, especially in the case of moving objects that are currently not intersecting but will do so at a later time. The first such time is called the *contact time*. In many situations, just knowing that two objects will intersect is sufficient information. I refer to this as a *test-intersection query*, the end result a Boolean value: true if an intersection will occur, false if not. In other situations we will want to know *where* the objects intersect at the time of contact. The set of intersection points is referred to as the *contact set* or *contact manifold*, the latter term appropriate when the intersection set is not a finite set but a continuum of points. For example, the intersection set of a box sitting on a table is the set of points on a face of the box. When the contact set is desired, I refer to this as a *find-intersection query*. As you would expect, in most cases a find intersection query is more expensive than a test intersection query for a given pair of objects.

Collision detection is about determining the contact time and the contact set for two moving objects. At the time they intersect we need to decide how the objects will continue moving, the collision response so to speak. For example, if a rigid ball strikes a flat surface at an angle, you most likely want the ball to bounce away from the surface. In particular, you will want to reflect the velocity vector through the normal of the surface so that the angle of incidence is equal to the angle of reflection. The method of response falls into two categories based on how the objects collide: colliding contact and resting contact.

General analysis of two rigid bodies is quite intractable for real-time game physics. The geometric nature of the bodies can be quite complicated, preventing any reasonable attempt at modeling their dynamics. To simplify matters, we will restrict our attention to rigid bodies that are convex polyhedra.

This chapter describes the various stages of a physics engine. At its highest level, the application layer needs to control when the physics engine is executed. The game loop and various *ticks*, including the physics tick, are described in [Section 6.1](#).

An all-pairs comparison of interactable objects in a game application is expensive. Moreover, it is usually not necessary because not all objects interact with all other objects during the same physics frame. To rule out pairs of objects that cannot interact during a frame, [Section 6.2](#) describes a collision culling algorithm that uses axis-aligned bounding boxes and space–time coherency.

The collision culling algorithm of [Section 6.2](#) is referred to as a *broad-phase algorithm*. It uses coarse-fitting bounding volumes for the objects. If the bounding volumes of two objects are not intersecting, then the objects are not intersecting. When the bounding volumes intersect, the objects still might not intersect, which

is likely the case for coarse-fitting bounding volumes. As a *medium-phase algorithm*, tighter-fitting bounding volumes for the objects can be used. If two such bounding volumes do not intersect, then the objects do not intersect. [Section 6.3](#) describes various bounding volumes and the corresponding *test-intersection queries* that are used to determine if (and not where) the bounding volumes intersect. In applications that have a limited number of interacting objects, the broad-phase algorithm might be skipped completely in favor of only a medium-phase algorithm.

As mentioned previously, we consider rigid bodies that are convex polygons or convex polyhedra. A *narrow-phase algorithm* is used to determine when (contact time) and where (contact set) the polyhedra intersect. [Section 6.4](#) describes some of the ideas used for determining intersection of convex polyhedra.

Once the contact time and contact sets are known, the collision response must occur. This is inarguably the most complicated part of the physics engine. [Section 6.5](#) describes how the rigid bodies move about when unconstrained. This gives you a sense of the mathematics necessary to formulate the equations of motion. Constrained motion involves the constraints implied by the contact set and the equations of motion. [Section 6.6](#) describes in detail the impulse-based dynamics. [Section 6.7](#) is a summary of velocity-based dynamics.

6.1 THE PHYSICS TICK

A typical game application has a top-level *game loop* that executes until the user terminates the game. For example, the game loop might be structured as follows:

```
repeat
    gameLogic.Tick(currentTime);
    inputDevices.Tick(currentTime);
    physics.Tick(currentTime);
    network.Tick(currentTime);
    audio.Tick(currentTime);
    graphics.Tick(currentTime);
    userInterface.Tick(currentTime);
until game_over;
```

Each *tick* function represents the execution of one of the subengines of the game engine. The order of the ticks shown here is arbitrary, but in an actual game you probably will have constraints that cause some implied ordering.

The game logic tick encapsulates the game play itself. Of course, the complexity of this tick depends on the game itself. The input devices tick will involve processing events such as keyboard and gamepad input. The network tick (if any) encapsulates the network activities required for the game. For example, an online racing game will require your current vehicle information to be transmitted to all opponents in the game. Game statistics and leaderboards are also transmitted and received by the network layer. The audio tick (if any) encapsulates 2D sound and/or 3D sound. Some of

these sounds might be triggered based on the state of other ticks. For example, if your racing vehicle strikes another vehicle, this will trigger collision sounds that must be played by the audio system. The graphics tick involves rendering of the 3D environment and objects. The user interface tick displays menus, buttons, controls, and various information (game statistics and leaderboards) as overlays on the rendered scene.

The physics tick is what we are interested in. An abstract formulation is as follows. The axis-aligned bounding boxes (AABBS) are part of the broad-phase algorithm. The bounding volumes (BVs) are part of the medium-phase algorithm.

```

physics.Initialize:
    assign an AABB to each object that can interact;

physics.Tick:
    // collision culling
    update AABBs and compute overlapping pairs;

    // optional collision culling
    remove overlapping pairs using BV tests;

    // compute contact points, resolve interpenetrations
    do collision detection;

    // resolve constraints
    update physics state;

    // solve equations of motion
    move objects;

```

The narrow-phase algorithms are part of the “do collision detection” operation.

The order of the steps in the physics tick is reasonable for an application that is single threaded. However, the collision culling using AABBS can be quite expensive and moved to a separate unit of execution (a dedicated core or processor) to speed up the execution. In this case, the order will change slightly. Section 6.2 includes discussions about parallel execution of the AABB-based collision culling, including an implementation on a separate core of a CPU (the cores share memory) and on a specialized processor (the processor has its own local memory).

6.2 COLLISION CULLING

In a graphics system a standard approach to improving the performance of rendering is to avoid drawing objects that are outside the view frustum. This process is called *culling*. The classic algorithm is to associate a bounding volume with each drawable object and use plane-at-a-time culling. For each frustum plane, the bounding volume is tested to see whether it is on the side outside the frustum. If so, then the object contained by it is outside the frustum and need not be drawn. If the bounding volume is not outside any of the planes, the object is drawn. This is not an exact culling

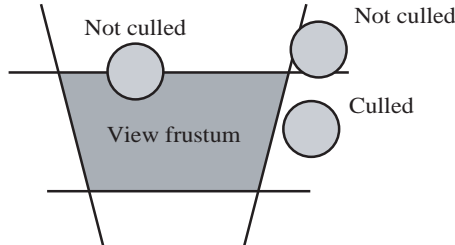


Figure 6.1 Culling of bounding spheres against a view frustum.

algorithm because the bounding volume can be outside the frustum even though not outside any of the six planes. Figure 6.1 illustrates this for bounding spheres.

However, any culling that occurs is better than attempting to draw all objects in the system. Of course, it is essential that the time it takes to cull an object is less than the time spent by the rendering system transforming its triangles into view space and clipping, only to find out that all triangle vertices are outside the frustum. The essence of view frustum culling is that a bounding volume is a simple geometric entity for which intersection testing with the frustum is much cheaper than intersection testing between the original object and the frustum. The performance of collision detection systems can be enhanced using culling in a similar manner.

One algorithm for determining whether two convex polyhedra are intersecting uses the *method of separating axes*. If the polyhedra are not intersecting, we will find that out once we project onto one of the $N_0 + N_1 + N_0 N_1$ potential separating directions, where polyhedra i has N_i faces. An object in the system tends to interact with only a small subset of the total objects, so you expect most pairs of objects at any given time not to be intersecting. The system can spend a lot of time telling you something you already know. Using view frustum culling as motivation, we should have a bounding volume per convex polyhedra that is simpler in structure and allows us to quickly determine whether two bounding volumes are (or are not) intersecting.

A drawback of the method of separating axes is that the number of potential separating can be quite large—quadratic in the number of polyhedra vertices. A better alternative for such polyhedra is to compute distance between them using the GJK algorithm [GJK88].

Section 6.4 presents discussions of both the method of separating axes and of the GJK algorithm. This section is about collision culling that uses space-time coherence to speed up the execution.

6.2.1 CULLING WITH BOUNDING SPHERES

An obvious choice for a bounding volume of a convex polyhedron is a sphere. Given spheres with centers C_i and radii r_i for $i = 0, 1$, the spheres do not intersect whenever

the distance between their centers is larger than the sum of their radii. The algebraic condition for nonintersection is $|\mathcal{C}_1 - \mathcal{C}_0| > r_0 + r_1$. This should look familiar to you because it is the same form as the inequality for specifying the separation of two projection intervals on a separating axis. The set of potential separating axes for a sphere is the set of *all* directions. When comparing two spheres, we need only project onto a line containing both centers. The separation test in practice is implemented using squared quantities, $|\mathcal{C}_1 - \mathcal{C}_0|^2 > (r_0 + r_1)^2$, to avoid the expensive square root calculation of distance between centers.

Suppose our environment has n convex polyhedra. Let c_p denote the average cost of the intersection testing for two convex polyhedra. Testing all pairs, the total cost for a test-intersection query is

$$c_1 = \frac{n(n-1)}{2} c_p \quad (6.1)$$

Let c_s denote the cost of the intersection testing for two spheres. We still compute an all-pairs, test-intersection query, this time for spheres. If two spheres intersect, the contained polyhedra might or might not intersect. We still have to perform the polyhedra intersection test in this case. If m pairs of spheres intersect where $0 \leq m \leq n(n-1)/2$, the total cost for a test-intersection query is

$$c_2 = \frac{n(n-1)}{2} c_s + mc_p \quad (6.2)$$

The culling system needs to be more efficient, so we require that $c_2 < c_1$. This happens when

$$\frac{c_s}{c_p} < 1 - \frac{2m}{n(n-1)}$$

If the expected number of separating axis tests for a pair of polyhedra is k where $1 \leq k \leq N_0 + N_1 + N_0 N_1$, then we expect the ratio to be $c_s/c_p = 1/k$ to a first approximation. Consequently, $c_2 < c_1$ implies

$$m < \left(1 - \frac{1}{k}\right) \frac{n(n-1)}{2}$$

That is, the sphere-based culling system is more efficient as long as the number of intersecting spheres does not exceed the fraction $(1 - 1/k)$ of total objects in the system.

Despite the benefits from sphere-based culling, the system requires a comparison of all pairs of n objects. The objects are moving about, so the comparisons occur at each time step. When n is large, this culling system still might not be enough to remedy the sluggishness of the application. Another improvement is called for, one that uses *coherence* of the objects in the system. We have two possibilities for coherence, *spatial coherence* where we take advantage of knowledge about the spatial locations of the objects in the system (locality in space), and *temporal coherence* where we take

advantage of the fact that with a small change in time, the new state of the system does not deviate much from its old state (locality in time).

We may modify the sphere-based culling to illustrate how to use spatial coherence to improve the performance of the collision system. A simple idea is to decompose the space known to be occupied by all the objects during the life of the simulation. If the total space is an axis-aligned box, we decompose it into a regular lattice of disjoint, smaller axis-aligned boxes. Each box maintains a list of spheres that are fully or partially inside the box. Figure 6.2 illustrates for a collection of 8 spheres and a partition into 4 boxes.

If B_{ij} denotes the bin in row i and column j , the bins are $B_{00} = \{A, C, D, E\}$, $B_{01} = \{B, D, E\}$, $B_{10} = \{E, F\}$, and $B_{11} = \{E, F, G\}$. As you can see, if a sphere overlaps any box in the decomposition, it is placed into the list of spheres for that bin. For the sake of argument, suppose that we have b bins labeled B_i and the spheres are uniformly distributed in the bins. The number of spheres in each bin is n/b , where n is the total number of spheres. Let m_i denote the number of intersecting spheres in bin B_i . The cost for the sphere-based culling in bin i is

$$\frac{(n/b)(n/b - 1)}{2} c_s + m_i c_p$$

The total cost is

$$c_3 = \sum_{i=1}^b \frac{(n/b)(n/b - 1)}{2} c_s + m_i c_p = \frac{n(n/b - 1)}{2} c_s + m c_p \quad (6.3)$$

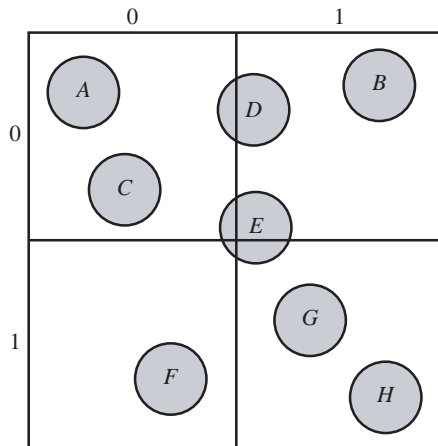


Figure 6.2 Decomposition of space to reduce the number of comparisons between pairs of objects.

where $m = \sum_{i=1}^b m_i$. The cost of the sphere comparisons in c_3 is approximately $1/b$ that of the cost in c_2 as shown in equation (6.2). If b is a small constant compared to n , the cost of sphere comparisons in equations (6.2) and (6.3) are both $O(n^2)$. However, if we choose b to be on the order of n , say $b = rn$ for some fraction $r \in (0, 1)$, then the cost of sphere comparisons is $((1/r - 1)/2)nc_s$, which is $O(n)$ in time, something quite desirable in a collision system.

Unfortunately, the analysis for the binning is not complete. We have forgotten to include the cost of determining which bins contain the spheres. The algorithm itself requires testing for overlap between a sphere with center C and radius r and an axis-aligned box $[x_{\min}, x_{\max}] \times [y_{\min}, y_{\max}] \times [z_{\min}, z_{\max}]$. To test for overlap it is sufficient to compute the distance from the center of the sphere to the solid box and show that it is less than the radius. The algorithm is listed next. The Sphere class is assumed to have members C for the center and r for the radius. The AxisAlignedBox class has six members for the minimum and maximum values on the coordinate axes.

```
bool TestIntersection (Sphere S, AxisAlignedBox B)
{
    double sqrDist = 0.0, d;

    if (S.C.x < B.xmin)
    {
        d = S.C.x - B.xmin;
        sqrDist += d * d;
    }
    else if (S.C.x > B.xmax)
    {
        d = S.C.x - B.xmax;
        sqrDist += d * d;
    }

    if (S.C.y < B.ymin)
    {
        d = S.C.y - B.ymin;
        sqrDist += d * d;
    }
    else if (S.C.y > B.ymax)
    {
        d = S.C.y - B.ymax;
        sqrDist += d * d;
    }

    if (S.C.z < B.zmin)
    {
        d = S.C.z - B.zmin;
        sqrDist += d * d;
    }
    else if (S.C.z > B.zmax)
```

```

{
    d = S.C.z - B.zmax;
    sqrDist += d * d;
}

return sqrDist < S.r * S.r;
}

```

The return value is true whenever the sphere intersects the box and the intersection has positive volume. The cost of this test is denoted c_t , a relatively small cost. The naive algorithm for determining the bins containing the spheres just iterates over all spheres and tests each sphere against all boxes, a double loop, leading to a cost of bnc_t . The cost of the sphere-based culling with binning is now

$$c_4 = \frac{n(n/b - 1)}{2} c_s + mc_p + bnc_t \quad (6.4)$$

We argued earlier that to make the cost of sphere comparisons $O(n)$, we needed $b = rn$ for some fraction r . Unfortunately, this makes the cost of binning $O(n^2)$. This is to be expected: The more bins you select, the cheaper the cost of sphere comparisons, but the more expensive the cost of deciding which bins contain the spheres.

EXERCISE

6.1

Develop a more efficient algorithm than the naive one for determining which bins are intersected by a sphere. How does the cost equation (6.4) change with your new algorithm? ■

In a dynamic simulation, the polyhedra (and spheres) will move each time step of the simulation. The binning algorithm can be applied at each step if you so desire, but we can do better by modifying the algorithm to take advantage of temporal coherence. When the simulation is initialized we can determine which boxes the spheres intersect. On the next step of the simulation the spheres are moved. Under reasonable assumptions on the speeds of the objects, the maximum distance traveled by the spheres should be small compared to the dimensions of a box in the partition, or at least no worse than a couple of box extents. The set of candidate boxes that a sphere now intersects should be quite small, restricted to the current boxes that the sphere intersects and a small ring of neighboring boxes. The set size is constant, compared to the total number of spheres in the system, so we can update for each bin the set of spheres overlapping it in $O(n)$ time.

EXERCISE

6.2

Develop an efficient algorithm that updates each bin's set of spheres overlapping it. (*Hint:* Use a breadth-first search starting with the current box containing the sphere.) ■

EXERCISE

6.3

Write a computer program to implement sphere-based culling as described in this section. The program should use binning to take advantage of spatial coherence and should efficiently update the overlap information of the bins to take advantage of temporal coherence. ■

One final issue is to be mentioned: The convex polyhedra are both translated and rotated at each time step of the simulation. The bounding spheres after the motion still must be bounds. Depending on how you chose your spheres, you might have to update the bounding spheres for each time step, adding yet one more term to the cost equation. However, we can avoid this extra cost by choosing the bounding sphere center to be the center of mass of the polyhedron. No matter how the polyhedron rotates about its center of mass, the bounding sphere will contain it. Consequently, the update of the bounding sphere requires translating its center, the exact same translation that is applied to the polyhedron.

6.2.2 CULLING WITH AXIS-ALIGNED BOUNDING BOXES

Here we investigate another culling system that uses both spatial and temporal coherence. This one performs particularly well in practice. To each convex polyhedron, we associate an AABB. If two AABBs do not intersect, then the convex polyhedra contained by them do not intersect. If the AABBs do intersect, we then test whether the enclosed polyhedra intersect. Of course, this is the same approach we used for bounding spheres.

We have the same issues to deal with as we did for sphere-based culling. Each time step the convex polyhedra move, their AABBs move. First, we need to update the AABB to make sure it contains the polyhedron. When we used a sphere whose center is the center of mass, only a translation was applied to the center since the sphere is guaranteed to contain the polyhedron regardless of its orientation. This is not the case for AABBs. If the polyhedron rotates, the current AABB is not necessarily a bound and we need to compute a new one. Certainly, an iteration over the vertices of the newly moved polyhedron may be used to compute the extremes along each coordinate axis, but if we have added the fast extremal query support to the convex polyhedra discussed earlier, we can use six queries to compute the AABB.

Second, once the AABBs are updated for all the polyhedra we expect that the intersection status of pairs of polyhedra/AABBs has changed – old intersections might no longer exist, new intersections might now occur. Spatial and temporal coherence will be used to make sure the update of status is efficient.

Intersecting Intervals

The idea of determining intersection between AABBs is based on sorting and update of intervals on the real line, a one-dimensional problem that we will analyze first. The method we describe here is mentioned in [Bar01]. A more general discussion of intersections of rectangles in any dimension is provided in [PS85]. Consider a collection of n intervals $I_i = [b_i, e_i]$ for $1 \leq i \leq n$. The problem is to efficiently determine all pairs of intersecting intervals. The condition for a single pair I_i and I_j to intersect is $b_j \leq e_i$ and $b_i \leq e_j$. The naive algorithm for the full set of intervals just compares all possible pairs, an $\tilde{O}(n^2)$ algorithm.

A more efficient approach uses a *sweep algorithm*, a concept that has been used successfully in many computational geometry algorithms. First, the interval endpoints are sorted into ascending order. An iteration is made over the sorted list (the sweep) and a set of *active intervals* is maintained, initially empty. When a beginning value b_i is encountered, all active intervals are reported as intersecting with interval I_i and I_i is added to the set of active intervals. When an ending value e_i is encountered, interval I_i is removed from the set of active intervals. The sorting phase is $O(n \log n)$. The sweep phase is $O(n)$ to iterate over the sorted list, clearly asymptotically faster than $O(n \log n)$. The intersecting reporting phase is $O(m)$ to report the m intersecting intervals. The total order is written as $O(n \log n + m)$. The worst case behavior is when all intervals overlap, in which case $m = O(n^2)$, but for our applications we expect m to be relatively small. Figure 6.3 illustrates the sweep phase of the algorithm.

The sorted interval endpoints are shown on the horizontal axis of the figure. The set of active intervals is initially empty, $A = \emptyset$. The first five sweep steps are enumerated as follows:

1. b_3 encountered. No intersections reported because A is empty. Update $A = \{I_3\}$.
2. b_1 encountered. Intersection $I_3 \cap I_1$ is reported. Update $A = \{I_3, I_1\}$.
3. b_2 encountered. Intersections $I_3 \cap I_2$ and $I_1 \cap I_2$ reported. Update $A = \{I_3, I_1, I_2\}$.
4. e_3 encountered. Update $A = \{I_1, I_2\}$.
5. e_1 encountered. Update $A = \{I_2\}$.

The remaining steps are easily stated and are left as an exercise.

A warning is in order here: The sorting of the interval endpoints must be handled carefully when equality occurs. For example, suppose that two intervals $[b_i, e_i]$

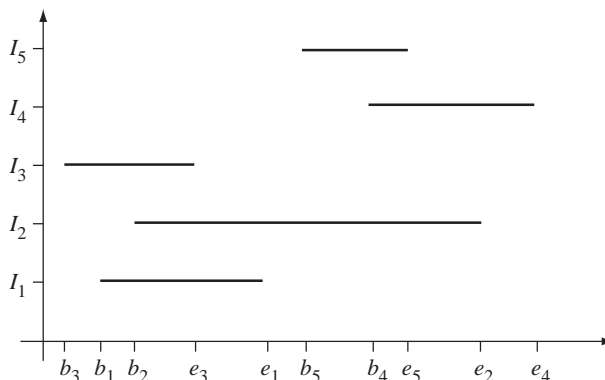


Figure 6.3 The sweep phase of the algorithm.

and $[b_j, e_j]$ intersect in a single point, $e_i = b_j$. If the sorting algorithm lists e_i before b_j , when e_i is encountered in the sweep we remove I_i from the set of active intervals. Next, b_j is encountered and intersections of I_j with the active intervals are reported. The interval I_i was removed from the active set on the previous step, so $I_j \cap I_i$ is *not reported*. In the sort suppose instead that b_j is listed before e_i by the sorting algorithm. Since b_j was encountered earlier in the sweep, the set of active intervals contains I_i . When b_j is encountered $I_j \cap I_i$ is *reported* as an intersection. Clearly, the order of equal values in the sort is important. Our application will require that we report just-touching intersections, so the interval endpoints cannot be sorted just as a set of floating point numbers. Tags need to be associated with each endpoint indicating whether it is a beginning point or an ending point. The sorting must take the tag into account to make sure that equal endpoint values are sorted so that values with a “begin” tag occur before values with an “end” tag. The tags are not a burden because, in fact, we need them anyway to decide during the sweep what type of endpoint we have encountered.

The basic data structures for the algorithm are `Endpoint`, to represent an interval endpoint and to contain necessary information for sorting, and `Interval`, to represent the interval itself,

```

struct Endpoint
{
    enum Type { BEGIN = 0, END = 1 };
    Type mType;
    float mValue;
    int mIndex; // index of interval containing this endpoint

    // Endpoint end0, end1;
    // end0 < end1 when
    //   end0.value < end1.value, or
    //   end0.value == end1.value AND end0.type < end1.type
}

// An interval [min,max].
struct Interval { float end[2]; }

// A pair of indices for overlapping intervals. A Pair instance
// is stored so that mI0 < mI1.
class Pair
{
public:
    Pair (int i0, int i1)
    {
        if (i0 < i1)
        {
            mI0 = i0;
            mI1 = i1;
        }
    }
}

```

```

        else
        {
            mI0 = i1;
            mI1 = io;
        }
    }

    int mI0, mI1;
};
```

The class managing the intervals and overlap status is

```

class IntervalManager
{
public:
    IntervalManager (array<Interval> intervals);
    void Set (int i, Interval interval);
    Interval Get (int i) { return mIntervals[i]; }
    void Update ();
    set<Pair> GetOverlaps () { return mOverlaps; }

private:
    array<Interval> mIntervals;
    array<Endpoint> mEndpoints;
    set<Pair> mOverlaps;
    array<int> mLookup;
}
```

The application will move the intervals about using the Set function. It is easy to set the `mIntervals` values for the specified index. However, `mEndpoints` is a sorting of the endpoints. If an interval of the array `mIntervals` is set, then the corresponding endpoints in `mEndpoints` must be set. This requires a lookup table to be maintained during the moving/sorting; the array `mLookup` is that table. The set function is

```

void IntervalManager::Set (int i, Interval interval)
{
    mIntervals[i] = interval;
    mEndpoints[mLookup[2*i]].mValue = interval.end[0];
    mEndpoints[mLookup[2*i+1]].mValue = interval.end[1];
}
```

The initialization of the system involves user specification of intervals whose endpoints are first sorted (the sort phase), and the intervals are then tested for overlap (the sweep phase) to build a set of pairs of indices. Each pair represents two overlapping intervals.

```

IntervalManager::IntervalManager (array<Interval> intervals)
{
    // Copy the intervals and create the endpoint array.
    mIntervals = intervals;
    mEndpoints.resize(2*mIntervals.size());
```

```

        for (i = 0; i < mIntervals.size(); ++i)
        {
            mEndpoints[2*i].mType = Endpoint::BEGIN;
            mEndpoints[2*i].mValue = mIntervals[i].end[0];
            mEndpoints[2*i].mIndex = i;
            mEndpoints[2*i+1].mType = Endpoint::END;
            mEndpoints[2*i+1].mValue = mIntervals[i].end[1];
            mEndpoints[2*i+1].mIndex = i;
        }

        // Use an O(n log n) in-place sort of the endpoints. The
        // ordering of the endpoints is specified in class Endpoint.
        Sort(mEndpoints);

        // Create the lookup table to allow setting of endpoint values
        // whenever interval values are modified.
        mLookup.resize(mEndpoints.size());
        for (j = 0; j < mEndpoints.size(); ++j)
        {
            mLookup[2*mEndpoints[j].mIndex + mEndpoints[j].mType] = j;
        }

        // The active set of intervals (stored by index in array).
        set<int> active = empty;

        // Sweep through the endpoints to determine overlapping
        // intervals. The presence of (i,j) in mOverlaps means
        // mIntervals[i] and mIntervals[j] overlap.
        mOverlaps = empty;
        for (i = 0; i < mEndpoints.size(); i++)
        {
            Endpoint end = mEndpoints[i];
            int index = end.mIndex;
            if (end.mType == Endpoint::BEGIN)
            {
                for (each activeIndex in active)
                {
                    mOverlaps.insert(Pair(activeIndex, index));
                }
                active.insert(index);
            }
            else // end.mType == Endpoint::END
            {
                active.remove(index);
            }
        }
    }
}

```

Once the sort and sweep has occurred, the intervals are allowed to move about, thus invalidating the order of the endpoints in the sorted list. We can re-sort the values and apply another sweep, an $O(n \log n + m)$ process. However, we can do better than that. The sort itself may be viewed as a way to know the spatial coherence of the intervals. If the intervals move only a small distance, we expect that not many of the endpoints will swap order with their neighbors. The modified list is *nearly sorted*, so we should re-sort using an algorithm that is fast for nearly sorted inputs. Taking advantage of the small number of swaps is our way of using temporal coherence to reduce our workload. The insertion sort is a fast algorithm for sorting nearly sorted lists. For general input it is $O(n^2)$, but for nearly sorted data it is $O(n + e)$, where e is the number of exchanges used by the algorithm. Pseudocode for the insertion sort is

```
// input: A[0] through A[n-1]
// output: array sorted in-place
void InsertionSort (int n, type A[])
{
    for (j = 1; j < n; ++j)
    {
        key = A[j];
        i = j-1;
        while (i >= 0 and A[i] > key)
        {
            Swap(A[i], A[i+1]);
            --i;
        }
        A[i+1] = key;
    }
}
```

The situation so far is that we applied the sort and sweep algorithm to our collection of intervals, a once-only step that requires $O(n \log n + m)$ time. The output is a set S of pairs (i, j) that correspond to overlapping intervals, $I_i \cap I_j$. Some intervals are now moved and the list of endpoints is re-sorted in $O(n + e)$ time. The set S might have changed. Two overlapping intervals might not overlap now. Two nonoverlapping intervals might now overlap. To update S we can simply apply the sweep algorithm from scratch, an $O(n + m)$ algorithm, and build S anew. Better, though, is to mix the update with the insertion sort. An exchange of two “begin” points with two “end” points does not change the intersection status of the intervals. If a pair of “begin” and “end” points is swapped, then we have either gained a pair of overlapping intervals or lost a pair. By temporal coherence, we expect the number of changes in status to be small. If c is the number of changes of overlapping status, we know that $c \leq e$, where e is the number of exchanges in the insertion sort. The value e is expected to be much smaller than m , the number of currently overlapping intervals. Thus, we would like to avoid the full sweep that takes $O(n + m)$ time and update during the insertion sort that takes smaller time $O(n + e)$.

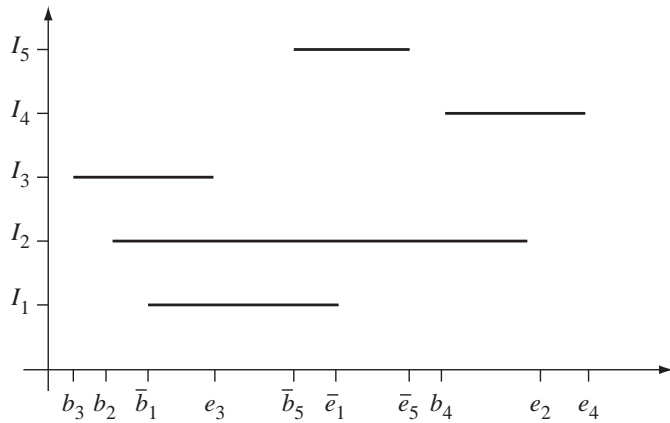


Figure 6.4 The update phase of the algorithm when intervals have moved.

Figure 6.4 illustrates the update phase of the algorithm applied to the intervals shown in Figure 6.3.

At the initial time the sorted endpoints are $\{b_3, b_1, b_2, e_3, e_1, b_5, b_4, e_5, e_2, e_4\}$. The pairs of indices for the overlapping intervals are $S = \{(1,2), (1,3), (2,3), (2,4), (2,5), (4,5)\}$. Now I_1 moves to the right and I_5 moves to the left. The new endpoints are denoted $\bar{b}_1, \bar{e}_1, \bar{b}_5$, and \bar{e}_5 . The list of endpoints that was sorted but now has had values changed is $\{b_3, \bar{b}_1, b_2, e_3, \bar{e}_1, \bar{b}_5, b_4, e_5, e_2, e_4\}$. The insertion sort is applied to this set of values. The steps follow.

1. Initialize the sorted list to be $L = \{b_3\}$.
2. Insert \bar{b}_1 , $L = \{b_3, \bar{b}_1\}$.
3. Insert b_2 , $L = \{b_3, \bar{b}_1, b_2\}$.
 - (a) Exchange \bar{b}_1 and b_2 , $L = \{b_3, b_2, \bar{b}_1\}$. No change to S .
4. Insert e_3 , $L = \{b_3, b_2, \bar{b}_1, e_3\}$.
5. Insert \bar{e}_1 , $L = \{b_3, b_2, \bar{b}_1, e_3, \bar{e}_1\}$.
6. Insert \bar{b}_5 , $L = \{b_3, b_2, \bar{b}_1, e_3, \bar{e}_1, \bar{b}_5\}$.
 - (a) Exchange \bar{e}_1 and \bar{b}_5 , $L = \{b_3, b_2, \bar{b}_1, e_3, \bar{b}_5, \bar{e}_1\}$. This exchange causes I_1 and I_5 to overlap, so insert $(1,5)$ into the set $S = \{(1,2), (1,3), (1,5), (2,3), (2,4), (2,5), (4,5)\}$.
7. Insert b_4 , $L = \{b_3, b_2, \bar{b}_1, e_3, \bar{b}_5, \bar{e}_1, b_4\}$.
8. Insert \bar{e}_5 , $L = \{b_3, b_2, \bar{b}_1, e_3, \bar{b}_5, \bar{e}_1, b_4, \bar{e}_5\}$.

- (a) Exchange b_4 and \bar{e}_5 , $L = \{b_3, b_2, \bar{b}_1, e_3, \bar{b}_5, \bar{e}_1, \bar{e}_5, b_4\}$. This exchange causes I_4 and I_5 to no longer overlap, so remove (4,5) from the set $S = \{(1,2), (1,3), (1,5), (2,3), (2,4), (2,5)\}$.
9. Insert e_2 , $L = \{b_3, b_2, \bar{b}_1, e_3, \bar{b}_5, \bar{e}_1, \bar{e}_5, b_4, e_2\}$.
 10. Insert e_4 , $L = \{b_3, b_2, \bar{b}_1, e_3, \bar{b}_5, \bar{e}_1, \bar{e}_5, b_4, e_2, e_4\}$.
 11. The new list is sorted and the set of overlaps is current.

The update function that implements this algorithm is

```
void IntervalManager::Update ()
{
    // Apply an insertion sort. Under the assumption that the
    // intervals have not changed much since the last call, the
    // endpoints are nearly sorted. The insertion sort should be
    // very fast in this case.
    for (int j = 1; j < mEndpoints.size(); ++j)
    {
        Endpoint key = mEndpoints[j];
        int i = j - 1;
        while (i >= 0 && key < mEndpoints[i])
        {
            Endpoint end0 = mEndpoints[i];
            Endpoint end1 = mEndpoints[i+1];

            // Update the overlap status.
            if (end0.mType == Endpoint::BEGIN)
            {
                if (end1.mType == Endpoint::END)
                {
                    // The 'b' of interval end0.mIndex was smaller
                    // than the 'e' of interval end1.mIndex and
                    // the intervals *might have been* overlapping.
                    // Now 'b' and 'e' are swapped and the intervals
                    // cannot overlap. Remove the pair from the
                    // overlap set. The removal operation needs to
                    // find the pair and erase it if it exists.
                    // Finding the pair is the expensive part of the
                    // operation.
                    mOverlaps.remove(Pair(end0.mIndex, end1.mIndex));
                }
            }
            else
            {
                if (end1.mType == Endpoint::BEGIN)
                {
                    // The 'b' of interval end1.mIndex was larger
                }
            }
        }
    }
}
```

```

        // than the 'e' of interval end0.mIndex and the
        // intervals were not overlapping. Now 'b' and
        // 'e' are swapped and the intervals *might be*
        // overlapping. Determine whether they are
        // overlapping and then insert.
        Interval interval0 = mIntervals[end0.mIndex];
        Interval interval1 = mIntervals[end1.mIndex];
        if (interval0.end[0] <= interval1.end[1])
        {
            mOverlaps.insert(
                Pair(end0.mIndex, end1.mIndex));
        }
    }

    // Reorder the items to maintain the sorted list.
    mEndpoints[i] = end1;
    mEndpoints[i+1] = end0;
    mLookup[2*end1.mIndex + end1.mType] = i;
    mLookup[2*end0.mIndex + end0.mType] = i+1;
    --i;
}
mEndpoints[i+1] = key;
mLookup[2*key.mIndex + key.mType] = i+1;
}

```

Intersecting Rectangles



SOURCE CODE

IntersectingRectangles

The algorithm for computing all pairs of intersecting axis-aligned rectangles is a simple extension of the algorithm for intervals. An axis-aligned rectangle is of the form $[x_{\min}, x_{\max}] \times [y_{\min}, y_{\max}]$. Two such rectangles intersect whenever there is overlap between both their x -intervals and their y -intervals, as shown in Figure 6.5.

The rectangles are $[x_0, x_1] \times [y_0, y_1]$ and $[x_2, x_3] \times [y_2, y_3]$. The rectangles overlap because $[x_0, x_1] \cap [x_2, x_3] \neq \emptyset$ and $[y_0, y_1] \cap [y_2, y_3] \neq \emptyset$.

In the two-dimensional setting we maintain two sorted lists, one for the endpoints of the x -intervals and one for the endpoints of the y -intervals. The initial step of the algorithm sorts the two lists. The sweep portion is only slightly more complicated than for one dimension. The condition for overlap is that the x -intervals *and* y -intervals overlap. If we were to sweep the sorted x -list first and determine that two x -intervals overlap, that is not sufficient to say that the rectangles of those x -intervals overlap. We could devise some fancy scheme to sweep both x - and y -lists at the same time, but it is simpler just to do a little extra work. If two x -intervals overlap, we will test for overlap of the corresponding rectangles in both dimensions and update the set of overlapping rectangles as needed.

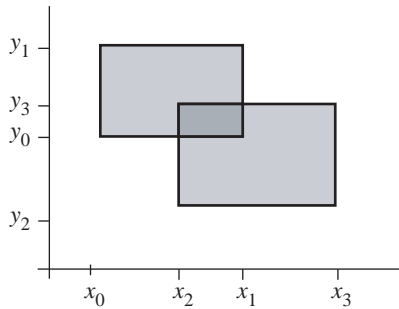


Figure 6.5 Axis-aligned rectangles overlap when both their x -intervals and y -intervals overlap.

Once we have the sorted lists and a set of overlapping rectangles, we will move the rectangles and must update the lists and set. The process will use an insertion sort to take advantage of spatial and temporal coherence. The x -list is processed first. If an exchange occurs so that two previously overlapping intervals no longer overlap, the corresponding rectangles no longer overlap so we can remove that pair from the set of overlaps. If an exchange occurs so that two previously nonoverlapping intervals now overlap, the corresponding rectangles may or may not overlap. Just as we did for the initialization phase, we will simply test the corresponding rectangles for overlap in both dimensions and adjust the set of overlaps accordingly.

The basic data structures for endpoints and index pairs are the same as for intervals. We need a data structure for the rectangle,

```
struct Rectangle { float xEnd[2]; float yEnd[2]; }
```

which represents an axis-aligned bounding box in two dimensions. The class managing the rectangles and overlap status is

```
class RectangleManager
{
public:
    RectangleManager (array<Rectangle> rectangles);
    void Set (int i, Rectangle rectangle);
    Rectangle Get (int i) { return mRectangles[i]; }
    void Update ();
    set<Pair> GetOverlaps () { return mOverlaps; }

private:
    void Update (array<Endpoint> endpoints, array<int> lookup);

    array<Rectangle> mRectangles;
    array<Endpoint> mXEndpoints, mYEndpoints;
```

```

    set<Pair> mOverlaps;
    array<int> mXLookup, mYLookup;
}

```

The sorting of endpoints requires lookup tables to be maintained during the moving/sorting; the arrays `mXLookup` and `mYLookup` are those tables. The set function is

```

void RectangleManager::Set (int i, Rectangle rectangle)
{
    mRectangles[i] = rectangle;
    mXEndpoints[mXLookup[2*i]].mValue = rectangle.xEnd[0];
    mXEndpoints[mXLookup[2*i+1]].mValue = rectangle.xEnd[1];
    mYEndpoints[mYLookup[2*i]].mValue = rectangle.yEnd[0];
    mYEndpoints[mYLookup[2*i+1]].mValue = rectangle.yEnd[1];
}

```

The initialization of the system involves user specification of rectangles whose endpoints are first sorted (the sort phase), and the rectangles are then tested for overlap (the sweep phase) to build a set of pairs of indices. Each pair represents two overlapping rectangles.

```

RectangleManager::RectangleManager (array<Rectangle> rectangles)
{
    // Copy the rectangles and create the endpoint arrays.
    mRectangles = rectangles;
    mXEndpoints.resize(2*mRectangles.size());
    mYEndpoints.resize(2*mRectangles.size());
    for (i = 0; i < mRectangles.size(); ++i)
    {
        mXEndpoints[2*i].mType = Endpoint::BEGIN;
        mXEndpoints[2*i].mValue = mRectangles[i].xEnd[0];
        mXEndpoints[2*i].mIndex = i;
        mYEndpoints[2*i].mType = Endpoint::BEGIN;
        mYEndpoints[2*i].mValue = mRectangles[i].yEnd[1];
        mYEndpoints[2*i].mIndex = i;
        mXEndpoints[2*i+1].mType = Endpoint::END;
        mXEndpoints[2*i+1].mValue = mRectangles[i].xEnd[1];
        mXEndpoints[2*i+1].mIndex = i;
        mYEndpoints[2*i+1].mType = Endpoint::END;
        mYEndpoints[2*i+1].mValue = mRectangles[i].yEnd[1];
        mYEndpoints[2*i+1].mIndex = i;
    }

    // Use an O(n log n) in-place sort of the endpoints. The
    // ordering of the endpoints is specified in class Endpoint.
    Sort(mXEndpoints);
    Sort(mYEndpoints);
}

```

```

// Create the lookup tables to allow setting of endpoint values
// whenever rectangle values are modified.
mXLookup.resize(mEndpoints.size());
mYLookup.resize(mEndpoints.size());
for (j = 0; j < mEndpoints.size(); ++j)
{
    mXLookup[2*mEndpoints[j].mIndex + mEndpoints[j].mType] = j;
    mYLookup[2*mEndpoints[j].mIndex + mEndpoints[j].mType] = j;
}

// The active set of rectangles (stored by index in array).
set<int> active = empty;

// Sweep through the endpoints to determine overlapping
// rectangles. The presence of (i,j) in mOverlaps means
// mRectangles[i] and mRectangles[j] overlap.
mOverlaps = empty;
for (i = 0; i < mEndpoints.size(); i++)
{
    Endpoint end = mEndPoints[i];
    int index = end.mIndex;
    if (end.mType == Endpoint::BEGIN)
    {
        // In the 1D problem, the current x-interval overlaps
        // with all the active x-intervals. In 2D, we also
        // need to check for y-overlap.
        for (each activeIndex in active)
        {
            Rectangle rectangle0 = mRectangles[activeIndex];
            Rectangle rectangle1 = mRectangles[index];
            if (rectangle0.HasYOverlapWith(rectangle1))
            {
                mOverlaps.insert(Pair(activeIndex, index));
            }
        }
        active.insert(index);
    }
    else // end.mType == Endpoint::END
    {
        active.remove(index);
    }
}
}

```

The update function must handle both the x - and y -dimensions of the problem.

```

void RectangleManager::Update()
{

```

```

        Update(mXEndpoints, mXLookup);
        Update(mYEndpoints, mYLookup);
    }
}

```

The update function with array inputs is identical to that for intervals except for the block of code where both endpoints are “begin” points. In the interval case, the block of code is

```

Interval interval0 = mIntervals[end0.mIndex];
Interval interval1 = mIntervals[end1.mIndex];
if (interval0.end[0] <= interval1.end[1])
{
    mOverlaps.insert(Pair(end0.mIndex, end1.mIndex));
}

```

In the rectangle case, the block of code is

```

Rectangle rectangle0 = mRectangles[end0.mIndex];
Rectangle rectangle1 = mRectangles[end1.mIndex];
if (Overlapping(rectangle0, rectangle1))
{
    mOverlaps.insert(Pair(end0.mIndex, end1.mIndex));
}

```

The overlap test for two axis-aligned rectangles is

```

bool Overlapping (Rectangle r0, Rectangle r1)
{
    if ((r0.xEnd[1] < r1.xEnd[0]) or (r0.xEnd[0] > r1.xEnd[1]))
    {
        return false;
    }
    if ((r0.yEnd[1] < r1.yEnd[0]) or (r0.yEnd[0] > r1.yEnd[1]))
    {
        return false;
    }
    return true;
}

```

Intersecting Boxes

You should see clearly that the algorithm for axis-aligned rectangles in two dimensions extends easily to axis-aligned boxes in three dimensions. The basic data structures for endpoints and index pairs are the same as for intervals. We need a data structure for the box,

```
struct Box { float xEnd[2]; float yEnd[2]; float zEnd[2]; }
```

which represents an axis-aligned bounding box in three dimensions. The class managing the boxes and overlap status is

```

class BoxManager
{
public:
    BoxManager (array<Box> boxes);
    void Set (int i, Box box);
    Box Get (int i) { return mBoxes[i]; }
    void Update ();
    set<Pair> GetOverlaps () { return mOverlaps; }

private:
    array<Box> mBoxes;
    array<Endpoint> mXEndpoints, mYEndpoints, mZEndpoints;
    set<Pair> mOverlaps;
    array<int> mXLookup, mYLookup, mZLookup;
}

```

The sorting of endpoints requires lookup tables to be maintained during the moving/sorting; the arrays `mXLookup`, `mYLookup`, and `mZLookup` are those tables. The `Set` function is

```

void BoxManager::Set (int i, Box box)
{
    mBoxes[i] = box;
    mXEndpoints[mXLookup[2*i]].mValue = box.xEnd[0];
    mXEndpoints[mXLookup[2*i+1]].mValue = box.xEnd[1];
    mYEndpoints[mYLookup[2*i]].mValue = box.yEnd[0];
    mYEndpoints[mYLookup[2*i+1]].mValue = box.yEnd[1];
    mZEndpoints[mZLookup[2*i]].mValue = box.zEnd[0];
    mZEndpoints[mZLookup[2*i+1]].mValue = box.zEnd[1];
}

```

The initialization of the system involves user specification of boxes whose endpoints are first sorted (the sort phase) and the boxes are then tested for overlap (the sweep phase) to build a set of pairs of indices. Each pair represents two overlapping boxes.

```

BoxManager::BoxManager (array<Box> boxes)
{
    // Copy the boxes and create the endpoint arrays.
    mBoxes = boxes;
    mXEndpoints.resize(2*mBoxes.size());
    mYEndpoints.resize(2*mBoxes.size());
    mZEndpoints.resize(2*mBoxes.size());
    for (i = 0; i < mBoxes.size(); ++i)
    {
        mXEndpoints[2*i].mType = Endpoint::BEGIN;
        mXEndpoints[2*i].mValue = mBoxes[i].xEnd[0];
        mXEndpoints[2*i].mIndex = i;
        mYEndpoints[2*i].mType = Endpoint::BEGIN;

```

```

mYEndpoints[2*i].mValue = mBoxes[i].yEnd[1];
mYEndpoints[2*i].mIndex = i;
mZEndpoints[2*i].mType = Endpoint::BEGIN;
mZEndpoints[2*i].mValue = mBoxes[i].zEnd[1];
mZEndpoints[2*i].mIndex = i;
mXEndpoints[2*i+1].mType = Endpoint::END;
mXEndpoints[2*i+1].mValue = mBoxes[i].xEnd[1];
mXEndpoints[2*i+1].mIndex = i;
mYEndpoints[2*i+1].mType = Endpoint::END;
mYEndpoints[2*i+1].mValue = mBoxes[i].yEnd[1];
mYEndpoints[2*i+1].mIndex = i;
mZEndpoints[2*i+1].mType = Endpoint::END;
mZEndpoints[2*i+1].mValue = mBoxes[i].zEnd[1];
mZEndpoints[2*i+1].mIndex = i;
}
}

// Use an O(n log n) in-place sort of the endpoints. The
// ordering of the endpoints is specified in class Endpoint.
Sort(mXEndpoints);
Sort(mYEndpoints);
Sort(mZEndpoints);

// Create the lookup tables to allow setting of endpoint values
// whenever box values are modified.
mXLookup.resize(mXEndpoints.size());
mYLookup.resize(mYEndpoints.size());
mZLookup.resize(mZEndpoints.size());
for (j = 0; j < mEndpoints.size(); ++j)
{
    mXLookup[2*mXEndpoints[j].mIndex + mXEndpoints[j].mType] = j;
    mYLookup[2*mYEndpoints[j].mIndex + mYEndpoints[j].mType] = j;
    mZLookup[2*mZEndpoints[j].mIndex + mZEndpoints[j].mType] = j;
}

// The active set of boxes (stored by index in array).
set<int> active = empty;

// Sweep through the endpoints to determine overlapping boxes.
// The presence of (i,j) in mOverlaps means mBoxes[i] and
// mBoxes[j] overlap.
mOverlaps = empty;
for (i = 0; i < mEndpoints.size(); i++)
{
    Endpoint end = mEndpoints[i];
    int index = end.mIndex;
    if (end.mType == Endpoint::BEGIN)
    {

```

```

// In the 1D problem, the current x-interval overlaps
// with all the active x-intervals. In 3D, we also
// need to check for y-overlap and for z-overlap.
for (each activeIndex in active)
{
    Box box0 = mBoxes[activeIndex];
    Box box1 = mBoxes[index];
    if (box0.HasYOverlapWith(box1) or
        box0.HasZOverlapWith(box1))
    {
        mOverlaps.insert(Pair(activeIndex, index));
    }
    active.insert(index);
}
else // end.mType == Endpoint::END
{
    active.remove(index);
}
}
}
}

```

The update function must handle the x -, y -, and z -dimensions of the problem.

```

void BoxManager::Update()
{
    Update(mXEndpoints, mXLookup);
    Update(mYEndpoints, mYLookup);
    Update(mZEndpoints, mZLookup);
}

```

The update function with array inputs is similar to that for intervals except for the block of code where both endpoints are “begin” points.

```

Box box0 = mBoxes[end0.mIndex];
Box box1 = mBoxes[end1.mIndex];
if (Overlapping(box0, box1))
{
    mOverlaps.insert(Pair(end0.mIndex, end1.mIndex));
}

```

The overlap test for two axis-aligned boxes is

```

bool Overlapping (Box b0, Box b1)
{
    if ((b0.xEnd[1] < b1.xEnd[0]) or (b0.xEnd[0] > b1.xEnd[1]))
    {
        return false;
    }
    if ((b0.yEnd[1] < b1.yEnd[0]) or (b0.yEnd[0] > b1.yEnd[1]))

```

```

    {
        return false;
    }
    if ((b0.zEnd[1] < b1.zEnd[0]) or (b0.zEnd[0] > b1.zEnd[1]))
    {
        return false;
    }
    return true;
}

```

6.2.3 AABB CULLING IN A SINGLE-THREADED ENVIRONMENT

This section describes an implementation for the three-dimensional AABB culling in a single-threaded computing environment. Moreover, it is designed to be extendable to a multithreading/multiprocessing computing environment with relatively few changes; the design choices reflect this need. You should read this section first, because the later sections refer back to the ideas in this one. One assumption is that the processors have a native word size of 32 bits. Another assumption is that memory is limited, so some concern must be given to how much memory the system uses.

The workhorse in the system is the `Update()` function. Although the insertion sort for nearly sorted data takes only a small amount of time compared to a full sort, it is still the bottleneck when you have thousands of objects (and corresponding AABBs) in the system. The `Update()` function calls three separate insertion sorts (the update function with array inputs), one for each dimension.

During an insertion sort, it is possible that (1) a pair of nonoverlapping boxes is inserted into the overlap set, or (2) a pair of overlapping boxes is removed from the overlap set. Each of these operations is referred to as an *event*. The system may itself manage the sorted endpoints and lookup tables, but it must communicate events (changes in the overlap set) to the application. The memory storage size for the endpoints and lookup tables is $O(n)$ in the number of boxes. However, it is $O(n^2)$ for the overlap set – in worst case the overlap set stores all pairs of boxes. This is not an issue for a single-threaded or single-core environment with shared memory, but it is an issue for a specialized processor with limited local memory. Even if there was enough local memory, it is not clear you want the specialized processor to deal with a complex data structure such as a set.

The compromise is to have an array of events. The array is of sufficient size to store a reasonable number of events during a physics tick. In the improbable case that you have more events than the array can store, the culling system will stall and make additional calls into the sorting and event-reporting subsystems. Situations like this can be avoided during game design; for example, the designer should ensure that not all pairs of objects are colliding at the same time.

Regarding memory usage, I introduced a data type called `Endpoint` that had three members. The member `mType` has one of two values indicating whether the endpoint is the initial endpoint or final endpoint of a projection interval of the AABB.

The member `mValue` stored the endpoint value. The member `mIndex` is the index of the AABB that generated the endpoint. These three members, presumably each requiring 32 bits of storage, may be combined into two members. The `mType` value requires only 1 bit of storage, which can be borrowed from the `mIndex` storage. For example, you could use the sign bit of the index as an indicator of type of endpoint. A negative index i refers to a minimum endpoint for box $|i|$ and a nonnegative index i refers to a maximum endpoint for box i . In fact, we will require the number of boxes to be relatively small, so the index storage is handled differently. Even with current generation powerful consoles, the number of boxes must be limited to obtain real-time frame rates (when lots of other systems are executing such as graphics and audio).

The basic design for the system uses the *producer-consumer model*. The application *produces* box moves and the box culling system *consumes* those moves. The box culling system then *produces* a sequence of events. The application *consumes* the events and decides which pairs of objects to process in the narrow-phase collision detection system.

Enumerations, Masks, and Endpoint

The following enumerations are used by the classes in the system.

```
enum
{
    // number of boxes in system
    NUM_BOXES = <desired number of boxes>,

    // number of bits per index
    LG2_NUM_BOXES = <ceil(log2(NUM_BOXES))>,

    // number of endpoints in system
    NUM_ENDPOINTS = 2*NUM_BOXES,

    // bit mask for maximum endpoint
    TYPE_MAXIMUM = 0x80000000,

    MAX_EVENTS = <maximum number of events for one physics frame>,

    // bit mask for insert event during update
    INSERT_EVENT = 0x80000000,

    // 1-value bits for low-order LG2_NUM_BOXES
    // 0-value bits otherwise;
    MASK_INDEX0 = <mask value>,

    // 0-value bits for low-order LG2_NUM_BOXES bits
    // 1-value bits for next LG2_NUM_BOXES bits
}
```

```
// 0-value otherwise
MASK_INDEX1 = <mask value>
};
```

The information stored by an event is the pair of indices for the boxes involved in the event and whether the event is an insertion into the overlap set or a removal from the overlap set. The insertion/removal requires 1 bit of storage. This leaves 31 bits for the pair of indices, so each index is allotted at most 15 bits. The type information in the Endpoint class requires 1 bit of storage, so it is combined with the box index member. In either case of event or type, the high-order bit is reserved for the 1-bit information. The masks for this bit are TYPE_MAXIMUM and INSERT_EVENT. The masks to extract box indices from an event are MASK_INDEX0 and MASK_INDEX1. For example, if LG2_NUM_BOXES is 10, then MASK_INDEX0 is 0x000003FF and MASK_INDEX1 is 0x000FFC00.

The endpoint class is chosen to be the following:

```
class Endpoint
{
public:
    Endpoint ();

    void Set (int i, float value, bool isMinimum)
    {
        mValue = value;
        mIndex = (isMinimum ? i : (i | TYPE_MAXIMUM));
    }

    int GetType () const
    {
        return (mIndex & TYPE_MAXIMUM) >> LG2_NUM_BOXES;
    }

    int GetIndex () const
    {
        return mIndex & ~TYPE_MAXIMUM;
    }

    int GetLookup () const
    {
        return 2*(mIndex & ~TYPE_MAXIMUM) +
            ((mIndex & TYPE_MAXIMUM) >> LG2_NUM_BOXES);
    }

    // The high-order bit stores the type information. The 15
    // low-order bits store the actual box index.
    int mIndex;
```

```

// The numerical value of the endpoint.
float mValue;

// Endpoints are ordered during a sort according to the
// total ordering:
bool operator< (const Endpoint& end) const
{
    if (mValue < end.mValue)
    {
        return true;
    }
    if (mValue > end.mValue)
    {
        return false;
    }
    return GetType() < end.GetType();
}
};

```

Class BoxManager

The class design for the box culling system is listed next. It is effectively identical to the one mentioned in the previous section, except that the event array replaces the overlap set and the class does not store the boxes themselves, only the endpoints and lookup tables. The class also has a queue of box indices. Whenever a box has been modified, its index must be inserted into the queue.

```

struct Box
{
    float mMin[3], mMax[3];
};

class BoxManager
{
public:
    BoxManager ();

    void InsertMoveQueue (int i);
    bool MoveBoxes (const Box* boxes);
    void Update ();
    bool ProcessEvents (std::set<Pair>& overlaps);

private:
    void Move (int i, const Box& box);
    bool Overlapping (int i0, int i1);

```

```

        bool Overlapping (int i0, int i1, Endpoint* endpoints,
                          int* lookup);
        void Update (Endpoint* endpoints, int* lookup);

        Endpoint mXEndpoints[NUM_ENDPOINTS];
        Endpoint mYEndpoints[NUM_ENDPOINTS];
        Endpoint mZEndpoints[NUM_ENDPOINTS];
        int mXLookup[NUM_ENDPOINTS];
        int mYLookup[NUM_ENDPOINTS];
        int mZLookup[NUM_ENDPOINTS];

        int mNumMoveQueue;
        int mMoveQueue[NUM_BOXES];
        int mNumEvents;
        int mEvents[MAX_EVENTS];
    };
}

```

The constructor handles the initialization of the system. Unlike the pseudocode of the previous section, the constructor is not passed the array of boxes. Instead, the application inserts into a queue the indices of those boxes that have been modified. When finished modifying, it calls `MoveBoxes(boxes)` followed by a call to `Update()`. On completion of the update, the application calls `ProcessEvents(overlaps)` so that its set of pairs of indices for overlapping boxes is made current. The constructor initializes the boxes to invalid values. The endpoints are already sorted in this construction, so there is no need to explicitly sort them.

```

BoxManager::BoxManager ()
{
    // Larger than any world coordinate of game.
    float invalid = SOME_LARGE_FLOAT;
    for (int i = 0, j = 0; i < NUM_BOXES; ++i)
    {
        mXEndpoints[j].Set(i, invalid, true);
        mYEndpoints[j].Set(i, invalid, true);
        mZEndpoints[j].Set(i, invalid, true);
        ++j;
        invalid += 1.0f;

        mXEndpoints[j].Set(i, invalid, false);
        mYEndpoints[j].Set(i, invalid, false);
        mZEndpoints[j].Set(i, invalid, false);
        ++j;
        invalid += 1.0f;
    }

    for (int j = 0; j < NUM_ENDPOINTS; ++j)
    {

```

```

        mXLookup[mXEndpoints[j].GetLookup()] = j;
        mYLookup[mYEndpoints[j].GetLookup()] = j;
        mZLookup[mZEndpoints[j].GetLookup()] = j;
    }

    // no pending moves
    mNumMoveQueue = 0;

    // no pending events
    mNumEvents = 0;
    memset(mEvents, 0, MAX_EVENTS*sizeof(int));
}

```

The function to insert an index into the queue is trivial.

```

void BoxManager::InsertMoveQueue (int i)
{
    mMoveQueue[mNumMoveQueue++] = i;
}

```

Once queue insertions are finished for the current physics frame, the endpoint arrays need to be updated.

```

bool BoxManager::MoveBoxes (const Box* boxes)
{
    for (int i = 0; i < mNumMoveQueue; ++i)
    {
        Move(mMoveQueue[i], boxes[mMoveQueue[i]]);
    }

    bool hasMoved = (mNumMoveQueue > 0);
    mNumMoveQueue = 0;
    return hasMoved;
}

```

The Boolean return value is true if and only if any of the boxes has moved. This is a hint to the application whether to continue the physics processing – if nothing has moved, there are no physics to apply.

The Move function uses the lookup tables, as before.

```

void BoxManager::Move (int i, const Box& box)
{
    mXEndpoints[mXLookup[2*i]].mValue = box.mMin[0];
    mXEndpoints[mXLookup[2*i+1]].mValue = box.mMax[0];
    mYEndpoints[mYLookup[2*i]].mValue = box.mMin[1];
    mYEndpoints[mYLookup[2*i+1]].mValue = box.mMax[1];
    mZEndpoints[mZLookup[2*i]].mValue = box.mMin[2];
    mZEndpoints[mZLookup[2*i+1]].mValue = box.mMax[2];
}

```

The `Update()` function of the previous section made three calls to the update function that takes array parameters. It is slightly more complicated when the number of events is limited.

```
void BoxManager::Update ()
{
    mNumEvents = 0;
    Update(mXEndpoints, mXLookup);

    if (mNumEvents < MAX_EVENTS)
    {
        Update(mYEndpoints, mYLookup);
    }

    if (mNumEvents < MAX_EVENTS)
    {
        Update(mZEndpoints, mZLookup);
    }
}
```

The issue is that if any of the individual updates fills the event array, the main update must terminate. The client of `BoxManager` is required to test `mNumEvents`. If it is equal to `MAX_EVENTS`, then the client must make an additional call to the update; this is the stall mentioned previously.

The per-dimension update is

```
void BoxManager::Update (Endpoint* endpoints, int* lookup)
{
    int i, j;
    for (j = 1; j < NUM_ENDPOINTS; ++j)
    {
        Endpoint key = endpoints[j];
        i = j - 1;
        while (i >= 0 && key < endpoints[i])
        {
            Endpoint end0 = endpoints[i];
            Endpoint end1 = endpoints[i + 1];
            if (end0.GetType() == 0)
            {
                if (end1.GetType() == 1)
                {
                    int i0 = end0.GetIndex();
                    int i1 = end1.GetIndex();
                    if (i0 != i1)
                    {
                        // Report boxes i0 and i1 no longer
                        // overlap.
                        mEvents[mNumEvents++] =
```

```

                i0 | (i1 << LG2_NUM_BOXES);
            }
        }
    }
else
{
    if (end1.GetType() == 0)
    {
        int i0 = end0.GetIndex();
        int i1 = end1.GetIndex();
        if (i0 != i1 && Overlapping(i0, i1))
        {
            // Report box0 and box1 are now
            // overlapping.
            mEvents[mNumEvents++] =
                i0 | (i1 << LG2_NUM_BOXES)
                | INSERT_EVENT;
        }
    }
}

// Reorder the items to maintain the sorted list.
endpoints[i] = end1;
endpoints[i + 1] = end0;
lookup[end1.GetLookup()] = i;
lookup[end0.GetLookup()] = i + 1;
--i;

if (mNumEvents == MAX_EVENTS)
{
    // The event array is full. Another update pass
    // is needed.
    break;
}
}

endpoints[i + 1] = key;
lookup[key.GetLookup()] = i + 1;

if (mNumEvents == MAX_EVENTS)
{
    // The event array is full. Another update pass is
    // needed.
    break;
}
}
}

```

The overlap tests are listed next. The per-dimension overlap test is slightly more complicated than that of the previous section, because BoxManager has access only to endpoints, not to the original boxes.

```
bool BoxManager::Overlapping (int i0, int i1)
{
    return Overlapping(i0, i1, mXEndpoints, mXLookup)
        && Overlapping(i0, i1, mYEndpoints, mYLookup)
        && Overlapping(i0, i1, mZEndpoints, mZLookup);
}

bool BoxManager::Overlapping (int i0, int i1, Endpoint* endpoints,
    int* lookup)
{
    float max0 = endpoints[lookup[2*i0+1]].mValue;
    float min1 = endpoints[lookup[2*i1]].mValue;
    if (max0 < min1)
    {
        return false;
    }
    float min0 = endpoints[lookup[2*i0]].mValue;
    float max1 = endpoints[lookup[2*i1+1]].mValue;
    return min0 <= max1;
}
```

The application needs to update its overlap set by

```
bool BoxManager::ProcessEvents (set<Pair>& overlaps)
{
    for (int i = 0; i < mNumEvents; ++i)
    {
        int i0 = mEvents[i] & MASK_INDEX0;
        int i1 = (mEvents[i] & MASK_INDEX1) >> LG2_NUM_BOXES;
        if (mEvents[i] & INSERT_EVENT)
        {
            overlaps.insert(Pair(i0, i1));
        }
        else
        {
            overlaps.erase(Pair(i0, i1));
        }
    }

    return mNumEvents == MAX_EVENTS;
}
```

The Boolean return value is true when the event queue was full. This is a message to the application that `Update()` must be called one or more additional times to ensure that all events are reported.

The application code is summarized abstractly as the following:

```

initialization:
    Box boxes[NUM_BOXES];
    BoxManager manager;
    set<Pair> overlaps = empty;
    for (int i = 0; i < NUM_BOXES; ++i)
    {
        <set the initial boxes[i] parameters>;
        manager.InsertMoveQueue(i);
    }

physics_tick:
    bool updateInProgress = manager.MoveBoxes(boxes);
    while (updateInProgress)
    {
        manager.Update();
        updateInProgress = manager.ProcessEvents(overlaps);
    }

    // The remaining steps in the physics tick; they use the
    // 'overlaps' set.
    <remove overlapping pairs using BV tests>;
    <do collision detection>;
    <update physics state (resolve constraints)>;
    <move objects>;
        // solve equations of motion;
        // set boxes[i] parameters for all moved boxes;
        for (each boxes[i] that has moved)
        {
            manager.InsertMoveQueue(i);
        }
    }
}

```

As mentioned previously, the expected number of times in the physics tick “while” loop (that tests `updateInProgress`) is 1. If a large number of boxes were involved in events, the number of loop passes will be larger than 1, but you can try to design the game environment so this will not happen. However, if it does, the code supports it (with a stall).

Notice that the manager is informed about the moved boxes, and then the manager is asked to perform an update to re-sort the endpoints. The update must be completed before the physics engine can continue with its work. This approach is acceptable when using sequential execution in a single thread. In fact, the function that processes the events can begin only after the `Update()` function returns.

When the update is moved to a separate execution unit, either in a second thread on a separate core or on a specialized processor, the ordering of the code is not reasonable. Specifically, when `manager.Update()` is called, the application must wait for the update to finish before it can consume its events. You certainly do not want to

wait, because that defeats the reason for having multiple execution units in the first place. A better choice is to have the `manager.Update()` call made *after* the final “move objects.” The update is initiated on the separate execution unit. The current execution unit is finished with the physics tick and then processes the other game loop ticks. By the time those ticks are finished, the chances are that the separate execution unit has completed its tasks (done in parallel with the other ticks). When you next enter the physics tick, the events are ready to be consumed and the overlaps set is updated. The next sections describe this process.

6.2.4 AABB CULLING USING A SEPARATE CORE OF A CPU

With only minor changes, the `BoxManager` class can perform the endpoint sorting in a separate thread that we will assume can be specified to run on a separate core. Depending on the computer, the operating system might not allow you to specify the core, but it should schedule the threads to balance the load between cores. The class interface has some additional members, as shown next.

```
class BoxManager
{
public:
    BoxManager ();
    ~BoxManager ();

    void InsertMoveQueue (int i);
    bool MoveBoxes (const Box* boxes);
    void Update ();
    void WaitForUpdateEnd();
    static void UpdateAsynchronous (void* userdata);
    bool ProcessEvents (std::set<Pair>& overlaps);

private:
    void Move (int i, const Box& box);
    bool Overlapping (int i0, int i1);
    bool Overlapping (int i0, int i1, Endpoint* endpoints,
                      int* lookup);
    void Update (Endpoint* endpoints, int* lookup);

    Endpoint mXEndpoints[NUM_ENDPOINTS];
    Endpoint mYEndpoints[NUM_ENDPOINTS];
    Endpoint mZEndpoints[NUM_ENDPOINTS];
    int mXLookup[NUM_ENDPOINTS];
    int mYLookup[NUM_ENDPOINTS];
    int mZLookup[NUM_ENDPOINTS];

    int mNumMoveQueue;
    int mMoveQueue[NUM_BOXES];
```

```

int mNumEvents;
int mEvents[MAX_EVENTS];

bool mUpdateBegin;
Event mUpdateEndEvent;
bool mTerminate;
Event mUpdateAsynchronousEndEvent;
int mThreadID;
};

}

```

The function `UpdateAsynchronous` will be managed by a thread that is separate from the main thread of the game (where the physics tick is executing). When an update is launched, in rare cases we might have to wait for it to finish when we return to the physics tick. The function `WaitForUpdateEnd` handles the waiting.

The Boolean variable `mUpdateBegin` is set to `true` when an update starts and is set to `false` when the update is finished. The event `mUpdateEndEvent` is used by the thread to let the main thread know that the update (sorting of endpoints) has finished. The state of this event is queried by `WaitForUpdateEnd`. The Boolean `mTerminate` and the event `mUpdateAsynchronousEndEvent` are used for proper cleanup once the `BoxManager` object is destroyed (at game exit). The member `mThreadID` is associated with the thread that manages `UpdateAsynchronous` on creation and is used for thread destruction.

The constructor has additional work to do other than that listed previously. The destructor now has work to do.

```

BoxManager::BoxManager ()
{
    float invalid = SOME_LARGE_FLOAT;
    for (int i = 0, j = 0; i < NUM_BOXES; ++i)
    {
        mXEndpoints[j].Set(i, invalid, true);
        mYEndpoints[j].Set(i, invalid, true);
        mZEndpoints[j].Set(i, invalid, true);
        ++j;
        invalid += 1.0f;

        mXEndpoints[j].Set(i, invalid, false);
        mYEndpoints[j].Set(i, invalid, false);
        mZEndpoints[j].Set(i, invalid, false);
        ++j;
        invalid += 1.0f;
    }

    for (int j = 0; j < NUM_ENDPOINTS; ++j)
    {
        mXLookup[mXEndpoints[j].GetLookup()] = j;
        mYLookup[mYEndpoints[j].GetLookup()] = j;
        mZLookup[mZEndpoints[j].GetLookup()] = j;
    }
}

```

```

    }

    mNumMoveQueue = 0;
    mNumEvents = 0;
    memset(mEvents, 0, MAX_EVENTS*sizeof(int));

    // Additional work.
    mUpdateBegin = false;
    mTerminate = false;
    mUpdateAsynchronousEndEvent = CreateEvent(false);
    mUpdateEndEvent = CreateEvent(true);
    mThreadID = CreateThread(UpdateAsynchronous, this, coreID);
}

BoxManager::~BoxManager ()
{
    mTerminate = true;
    WaitForObjectToSignal(mUpdateAsynchronousEndEvent, INFINITE);
    DestroyEvent(mUpdateAsynchronousEndEvent);
    DestroyEvent(mUpdateEndEvent);
}

```

In the constructor, the Boolean variable `mUpdateBegin` is set to `false`, indicating that no update is in progress. The Boolean variable `mTerminate` is set to `false`, indicating that the `BoxManager` object exists.

The `CreateEvent` creates events for interthread communication. The Boolean parameter of the creation function is `true` when the event must be initially in the signaled state and `false` when the event must be initially in the nonsignaled state. The event `mUpdateAsynchronousEndEvent` is initially nonsignaled, meaning that the thread is *not* ready to terminate. The event `mUpdateEndEvent` is in the signaled state, meaning that no update is in progress (the previous update, of which there is none, is at an end).

The `CreateThread` function creates a thread to manage the specified function (the first parameter). The second parameter is the user data that is passed to `UpdateAsynchronous`; in our case, this is a pointer to the `BoxManager` object. The third parameter is the core on which to execute the thread; of course, this input is allowed only if the operating system supports it. It is assumed that the thread will begin execution immediately on creation. Most operating systems allow you to specify that the thread is created in a suspended mode, and you have to activate it with something like a `ResumeThread` function call.

In the destructor, `mTerminate` is set to `false`. The `UpdateAsynchronous` function will notice this and terminate the thread. The destructor has to wait for the thread termination; it does so via the `WaitForObjectToSignal` function call. The second parameter of the call is the amount of time it should wait before giving up – in this case, it waits for as long as it takes. The `DestroyEvent` function calls destroy the two events of the class.

The class function `WaitForUpdateEnd` is a simple wrapper.

```
void BoxManager::WaitForUpdateEnd ()
{
    WaitForObjectToSignal(mUpdateEndEvent, INFINITE);
}
```

A call to this function causes the main thread to wait until the update is completed. It is with high probability that the update will be completed before the return to the physics tick. If it is not completed frequently, you have too many interacting objects to process in the given time slice. As mentioned previously, you can design your game environment to reduce the number of potentially interacting objects/boxes to avoid the stall caused by the wait. The `WaitForObjectToSignal` function resets `mUpdateEndEvent` to the nonsignaled state.

The asynchronous sorting function is shown next.

```
void BoxManager::UpdateAsynchronous (void* userdata)
{
    BoxManager* manager = (BoxManager*)userdata;
    while (!manager->mTerminate)
    {
        if (manager->mUpdateBegin)
        {
            // A request to update has been received.
            manager->mUpdateBegin = false;
            manager->Update();

            // Signal that the update is completed.
            SetEvent(manager->mUpdateEndEvent);
        }
        else
        {
            sleep(1);
        }
    }

    DestroyThread(manager->mThreadID);

    // Signal that the thread is destroyed, so termination of
    // the manager can continue in the main thread.
    SetEvent(manager->mSortAsyncEndEvent);
}
```

The parsing of events and updating of the overlaps set is the following:

```
void BoxManager::ProcessEvents (set<Pair>& overlaps)
{
    while (true)
    {
```

```

        int i;
        for (i = 0; i < mNumEvents; ++i)
        {
            int i0 = mEvents[i] & MASK_INDEX0;
            int i1 = (mEvents[i] & MASK_INDEX1) >> LG2_NUM_BOXES;
            if (mEvents[i] & INSERT_EVENT)
            {
                overlaps.insert(Pair(i0, i1));
            }
            else
            {
                overlaps.remove(Pair(i0, i1));
            }
        }

        if (mNumEvents < MAX_EVENTS)
        {
            // The high-frequency case.
            return;
        }

        // The low-frequency case. Too many events to process
        // in one frame. Stall by updating until no more events
        // occur.
        Update();
        WaitForUpdateEnd();
    }
}

```

The client code of the culling system now becomes the following:

```

initialization:
Box boxes[NUM_BOXES];
BoxManager manager;
set<Pair> overlaps = empty;
for (int i = 0; i < NUM_BOXES; ++i)
{
    <set the initial boxes[i] parameters>;
    manager.InsertMoveQueue(i);
}
manager.MoveBoxes(boxes);
manager.Update();
manager.WaitForUpdateEnd();
manager.ProcessEvents(overlaps);

physics_tick:
manager.WaitForUpdateEnd();
manager.ProcessEvents(overlaps);

```

```

// The remaining steps in the physics tick; they use the
// 'overlaps' set.
<remove overlapping pairs using BV tests>;
<do collision detection>;
<update physics state (resolve constraints)>;
<move objects>;
    // solve equations of motion;
    // set boxes[i] parameters for all moved boxes;
    for (each boxes[i] that has moved)
    {
        manager.InsertMoveQueue(i);
    }
manager.MoveBoxes(boxes);
manager.Update();

```

The algorithm and pseudocode presented here are ideal for implementing on a desktop computer with a multicore CPU or on the Xbox 360. On the latter, it is possible to specify which of the six cores that the update thread should run on.

6.2.5 AABB CULLING USING A SPECIALIZED PROCESSOR

Let us assume that we have a specialized processing unit (SPU) that can execute a single C++ program and that has a small amount of local memory. The CPU communicates with the SPU by sending messages to a send queue. The SPU receives messages from this queue by polling. The SPU communicates with the CPU by sending messages to a receive port. A CPU receive thread is responsible for processing these messages. Whenever the SPU sends a message to the receive port, a signal is sent to the CPU that the receive thread should be activated and the receive port message is passed to that thread. The CPU and SPU can access shared heaps that reside in CPU memory. The CPU accesses such memory in the standard way by dereferencing pointers to the heap storage. However, the SPU must access the shared heaps using direct memory access (DMA). [Figure 6.6](#) has a schematic of the relationships among the various components.

To make the situation slightly more complicated, let us assume that the amount of local memory for the SPU is limited, say, less than a megabyte. Although we could store some number of floating-point-valued endpoints and integer-valued indices for a specified number of boxes, we can store even more such values if we transform the floating-point values (32-bit quantities) and integer-valued indices (32-bit quantities) to short values and indices (16-bit quantities). These reduce the memory requirements by half for the `Endpoint` class.

Both the CPU and the SPU have implementations of `BoxManager`. Additionally, the SPU has an implementation of `Endpoint`. Let us look at the SPU implementation first.

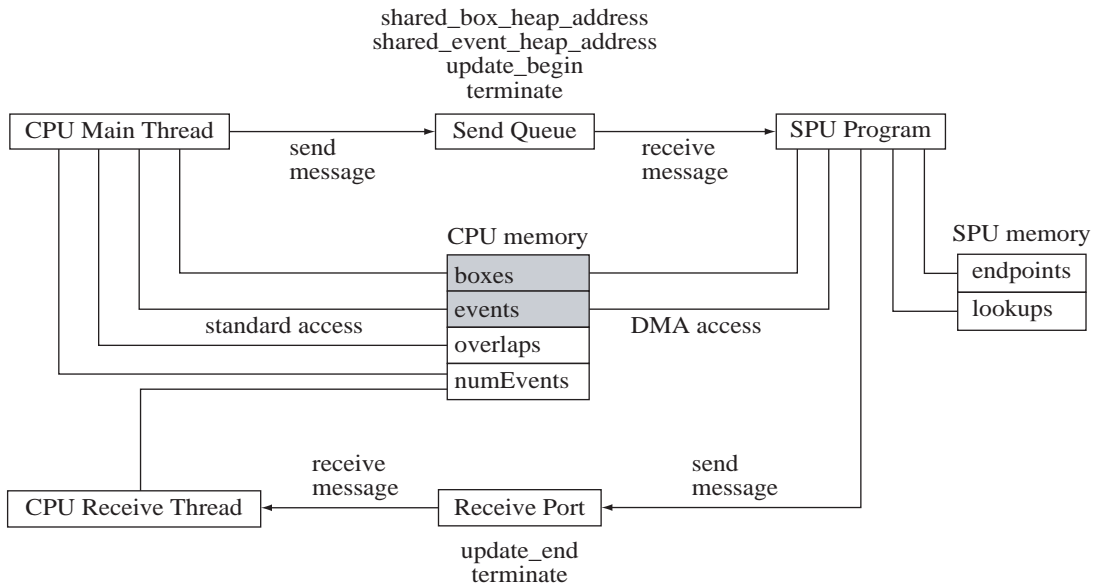


Figure 6.6 The relationships among the CPU, SPU, send queue, receive port, CPU memory, and SPU memory. The gray-background items are the shared heaps.

The SPU Implementation

Various enumerations supporting the system are listed next,

```

enum
{
    // number of boxes in system
    NUM_BOXES = <desired number of boxes>,

    // number of bits per index
    LG2_NUM_BOXES = <ceil(log2(NUM_BOXES))>,

    // number of endpoints in system
    NUM_ENDPOINTS = 2*NUM_BOXES,

    // bit mask for maximum endpoint
    TYPE_MAXIMUM = 0x8000,

    // maximum number of events for one physics frame
}
```

```

MAX_EVENTS = <value>,
// bit mask for insert event during update
INSERT_EVENT = 0x80000000,
// 1-value bits for low-order LG2_NUM_BOXES bits
// 0-value otherwise
MASK_INDEX0 = <mask value>,
// 0-value bits for low-order LG2_NUM_BOXES bits
// 1-value bits for next LG2_NUM_BOXES bits
// 0-value otherwise
MASK_INDEX1 = <mask value>,
// = moderately large 'short'
POS_INFINITY = SHRT_MAX - 2*NUM_BOXES + 1,
NEG_INFINITY = -POS_INFINITY,
// memory tag shared by CPU and SPU for box heap
BOX_DMA_TAG = <tag value>,
// memory tag shared by CPU and SPU for event heap
EVENT_DMA_TAG = <tag value>,
// messages between CPU and SPU
MSG_SHARED_BOX_HEAP_ADDRESS = 1,
MSG_SHARED_EVENT_HEAP_ADDRESS = 2,
MSG_UPDATE_BEGIN = 3,
MSG_UPDATE_END = 4,
MSG_TERMINATE = 5
};

```

The first eight enumerations are what we used for the CPU-only implementation, except that TYPE_MAXIMUM is now a 16-bit mask that will be used by the SPU's Endpoint class.

The floating-point box values will be transformed to short-valued data and stored on the SPU. The range of short values is specified by POS_INFINITY and NEG_INFINITY. The subtraction of twice the number of boxes from the maximum short value is designed to allow us to initialize the boxes to invalid state using values larger than or equal to POS_INFINITY, yet not exceeding the maximum value for short.

The CPU is responsible for creating two shared heaps. One heap stores an array of box information. Each box requires six short values for the two extremes in each of the three dimensions and one integer value for the box index. The other heap stores the array of events, each event represented by an integer value. The DMA tags BOX_DMA_TAG and EVENT_DMA_TAG are required by the SPU to access the shared heaps (by tag number).

The CPU sends messages of four types. Message `MSG_SHARED_BOX_HEAP_ADDRESS` is bundled with the address of the box heap and sent to the SPU. Likewise, message `MSG_SHARED_EVENT_HEAP_ADDRESS` is bundled with the address of the event heap and sent to the SPU. These messages are sent only once, when the CPU's box manager is created. The message `MSG_UPDATE_BEGIN` is bundled with the number of box-heap items (the number of moved boxes) and sent to the SPU during the physics simulation. When the CPU's box manager is to be destroyed (on game exit), the message `MSG_TERMINATE` is sent.

The SPU sends messages of two types. After receiving an update request from the CPU, the SPU re-sorts endpoints and stores events in the event array. Message `MSG_UPDATE_END` is bundled with the number of events in the event array and sent to the CPU. At game exit, the CPU sends the `MSG_TERMINATE` to the SPU. The SPU responds with the same message and self-terminates the thread running its main program.

At the highest level, the CPU creates the send queue, receive port, and tells the SPU to begin its main program. The queue and port are referenced by an integer-valued handle. This program is structured as shown next. For now observe that there is a singleton for the class `BoxManagerSPU`. We will look at the class details later. Also, note that the enumerations must be known to both the CPU and the SPU.

```
BoxManagerSPU manager;

int main (int sendQueue, int receivePort)
{
    // The box manager needs this to send messages to the CPU.
    manager.mReceivePort = receivePort;

    while (true)
    {
        // Poll the send-queue for any pending messages.
        int message, data;
        SpuReceiveMessage(sendQueue, &message, &data);

        // Process the message.
        switch (message)
        {
            case MSG_SHARED_BOX_HEAP_ADDRESS:
                manager.mBoxes = (BoxManagerSPU::BoxState*)data;
                break;

            case MSG_SHARED_EVENT_HEAP_ADDRESS:
                manager.mEvents = (int*)data;
                break;

            case MSG_UPDATE_BEGIN:
                // 'data' is the number of boxes to process in
                // manager.mBoxes
                manager.Update(data);
        }
    }
}
```

```
        break;

    case MSG_TERMINATE:
        // The CPU's box manager is in the process of being
        // destroyed. The SPU acknowledges this, breaks from
        // the loop, and terminates its main thread.
        SpuSendMessage(receivePort, MSG_TERMINATE, 0);

        // This function has an exit code that is returned
        // from 'main'.
        return SpuDestroyThread();
    }

}
```

The SPU's Endpoint class is listed next. Observe that the index and value members are now shorts, which cuts the memory usage by half compared to a floating-point value and an integer-valued index.

```

class Endpoint
{
public:
    Endpoint();

    void Set (int i, short value, bool isMinimum)
    {
        mValue = value;
        mIndex = (isMinimum ? i : (i | TYPE_MAXIMUM));
    }

    int GetType () const
    {
        return (mIndex & TYPE_MAXIMUM) >> LG2_NUM_BOXES;
    }

    int GetIndex () const
    {
        return mIndex & ~TYPE_MAXIMUM;
    }

    int GetLookup () const
    {
        return 2*(mIndex & ~TYPE_MAXIMUM) +
               ((mIndex & TYPE_MAXIMUM) >> LG2_NUM_BOXES);
    }

    // The high-order bit stores the type information.
    // low-order bits store the actual box index.
}

```

```

short mIndex;

// The value is in (NEG_INFINITY,POS_INFINITY).
short mValue;

// Endpoints are ordered during a sort according to the
// total ordering:
bool operator< (const Endpoint& end) const
{
    if (mValue < end.mValue)
    {
        return true;
    }
    if (mValue > end.mValue)
    {
        return false;
    }
    return GetType() < end.GetType();
}
};

The box manager class for the SPU is

```

```

class BoxManagerSPU
{
public:
    BoxManagerSPU ();

    void Update (int numBoxes);

    struct BoxState
    {
        int mXExtremes; // two shorts packed into one int
        int mYExtremes; // two shorts packed into one int
        int mZExtremes; // two shorts packed into one int
        int mIndex;     // index into the CPU box array
    };

    int mReceivePort;
    BoxState* mBoxes;
    int* mEvents;

private:
    bool Overlapping (int i0, int i1);
    bool Overlapping (int i0, int i1, Endpoint* endpoints,
                      short* lookup);
    void Update (Endpoint* endpoints, short* lookup);

    Endpoint mEndpoints[NUM_ENDPOINTS];

```

```

EndPoint mYEndpoints[NUM_ENDPOINTS];
EndPoint mZEndpoints[NUM_ENDPOINTS];
short mXLookup[NUM_ENDPOINTS];
short mYLookup[NUM_ENDPOINTS];
short mZLookup[NUM_ENDPOINTS];
int mNumEvents;
};

```

The constructor initializes the endpoints and lookup tables, just as we had seen for the CPU-only implementations.

```

BoxManagerSPU::BoxManagerSPU ()
{
    mReceivePort = 0;
    mBoxes = 0;
    mEvents = 0;
    mNumEvents = 0;

    short invalidValue = POS_INFINITY;
    for (int i = 0, j = 0; i < NUM_BOXES; ++i)
    {
        mXEndpoints[j].Set(i, invalidValue, true);
        mYEndpoints[j].Set(i, invalidValue, true);
        mZEndpoints[j].Set(i, invalidValue, true);
        ++j;
        ++invalidValue;

        mXEndpoints[end].Set(i, invalidValue, false);
        mYEndpoints[end].Set(i, invalidValue, false);
        mZEndpoints[end].Set(i, invalidValue, false);
        ++j;
        ++invalidValue;
    }

    for (int j = 0; j < NUM_ENDPOINTS; ++j)
    {
        mXLookup[mXEndpoints[j].GetLookup()] = j;
        mYLookup[mYEndpoints[j].GetLookup()] = j;
        mZLookup[mZEndpoints[j].GetLookup()] = j;
    }
}

```

The main update function is listed next. The extremes for a given dimension of the box are both short values but packed into an unsigned integer.

```

void BoxManagerSPU::Update (int numBoxes)
{
    // Update the endpoints for the boxes that were moved by
    // the CPU.

```

```

BoxState box;
BoxState* current = mBoxes;
for (int i = 0; i < numMoves; i++, current += sizeof(BoxState))
{
    DmaGet(BOX_DMA_TAG, &box, current, sizeof(BoxState));
    DmaWait(BOX_DMA_TAG);
    int j0 = 2*box.mIndex;
    int j1 = j0 + 1;
    mXEndpoints[mLookupX[j0]].mValue =
        (short)(box.mXExtremes & 0x0000FFFF);
    mXEndpoints[mLookupX[j1]].mValue =
        (short)((box.mXExtremes & 0xFFFF0000) >> 16);
    mYEndpoints[mLookupY[j0]].mValue =
        (short)(box.mYExtremes & 0x0000FFFF);
    mYEndpoints[mLookupY[j1]].mValue =
        (short)((box.mYExtremes & 0xFFFF0000) >> 16);
    mZEndpoints[mLookupZ[j0]].mValue =
        (short)(box.mZExtremes & 0x0000FFFF);
    mZEndpoints[mLookupZ[j1]].mValue =
        (short)((box.mZExtremes & 0xFFFF0000) >> 16);
}

// Re-sort the endpoints.
mNumEvents = 0;
Update(mXEndpoints, mXLookup);

if (mNumEvents < MAX_EVENTS)
{
    Update(mYEndpoints, mYLookup);
}

if (mNumEvents < MAX_EVENTS)
{
    Update(mZEndpoints, mZLookup);
}

SpuSendMessage(mReceivePort, MSG_UPDATE_END, mNumEvents);
}

```

The update per dimension is the following:

```

void BoxManagerSPU::Update (Endpoint* endpoints, short* lookup)
{
    int i, j, event;
    for (j = 1; j < NUM_ENDPOINTS; ++j)
    {
        Endpoint key = endpoints[j];

```

```

i = j - 1;
while (i >= 0 && key < endpoints[i])
{
    Endpoint end0 = endpoints[i];
    Endpoint end1 = endpoints[i + 1];

    if (end0.GetType() == 0)
    {
        if (end1.GetType() == 1)
        {
            int i0 = end0.GetIndex();
            int i1 = end1.GetIndex();
            if (i0 != i1)
            {
                // Report boxes i0 and i1 no longer
                // overlap.
                event = i0 | (i1 << LG2_NUM_BOXES);
                DmaWrite(EVENT_DMA_TAG,
                         &mEvents[mNumEvents++], event,
                         sizeof(int));
                DmaWait(EVENT_DMA_TAG);
            }
        }
    }
else
{
    if (end1.GetType() == 0)
    {
        int i0 = end0.GetIndex();
        int i1 = end1.GetIndex();
        if (i0 != i1 && Overlapping(i0, i1))
        {
            // Report boxes i0 and i1 are now
            // overlapping.
            event =
                i0 | (i1 << LG2_NUM_BOXES)
                | INSERT_EVENT;
            DmaWrite(EVENT_DMA_TAG,
                     &mEvents[mNumEvents++], event,
                     sizeof(int));
            DmaWait(EVENT_DMA_TAG);
        }
    }
}

// Reorder the items to maintain the sorted list.
endpoints[i] = end1;

```

```

        endpoints[i + 1] = end0;
        lookup[end1.GetLookup()] = i;
        lookup[end0.GetLookup()] = i + 1;
        --i;

        if (mNumEvents == MAX_EVENTS)
        {
            // The event array is full. Another update pass
            // is needed.
            break;
        }
    }

    endpoints[i + 1] = key;
    lookup[key.GetLookup()] = i + 1;

    if (mNumEvents == MAX_EVENTS)
    {
        // The event array is full. Another update pass is
        // needed.
        return;
    }
}
}

```

The overlap processing is implemented with the following functions:

```

bool BoxManagerSPU::Overlapping (int i0, int i1)
{
    return Overlapping(i0, i1, mXEndpoints, mXLookup)
        && Overlapping(i0, i1, mYEndpoints, mYLookup)
        && Overlapping(i0, i1, mZEndpoints, mZLookup);
}

bool BoxManagerSPU::Overlapping (int i0, int i1,
    Endpoint* endpoints, short* lookup)
{
    short max0 = endpoints[lookup[2*i0+1]].mValue;
    short min1 = endpoints[lookup[2*i1]].mValue;
    if(max0 < min1)
    {
        return false;
    }
    short min0 = endpoints[lookup[2*i0]].mValue;
    short max1 = endpoints[lookup[2*i1+1]].mValue;
    return min0 <= max1;
}

```

The CPU Implementation

The box manager class for the CPU is similar to what we had for the CPU-only implementation.

```
class BoxManagerCPU
{
public:
    BoxManagerCPU (float minWorld[3], float maxWorld[3]);
    ~BoxManagerCPU ();

    void InsertMoveQueue (int i);
    bool MoveBoxes (const Box* boxes);
    void Update ();
    void WaitForUpdateEnd();
    bool ProcessEvents (std::set<Pair>& overlaps);

private:
    static void ReceiveMessageFromSPU (int receiveQueue);

    float mMinWorld[3];
    float mMaxWorld[3];
    float mPosInfinity;
    float mNegInfinity;
    float mC0[3], mC1[3];

    struct BoxState
    {
        int mXExtremes, mYExtremes, mZExtremes, mIndex;
    };
    BoxState* mBoxes;
    int mNumMoveQueue;
    int mMoveQueue[NUM_BOXES];
    int mNumEvents;
    int* mEvents;
    Event mUpdateEvent;
    int mSendQueue;

    // The class represents a 'singleton'. The
    // ReceiveMessageFromSPU function needs access to the class
    // data. The message passing between CPU and SPUs can be
    // easily modified to support more instances, if necessary.
    static BoxManagerCPU* mThis;
};
```

Unlike the previous box manager classes, this constructor has inputs. These are used to map the floating point box values to short-valued quantities.

```

BoxManagerCPU::BoxManagerCPU (float minWorld[3], float maxWorld[3])
{
    // For access by ReceiveMessageFromSPU.
    mpThis = this;

    // This event signals when ReceiveMessageFromSPU receives the
    // update-end message.
    mUpdateEvent = CreateEvent(true);

    // Parameters for transforming the world coordinates to 'short'.
    mPosInfinity = (float)POS_INFINITY;
    mNegInfinity = (float)NEG_INFINITY;
    for (int i = 0; i < 3; ++i)
    {
        float twoInvRange = 2.0f/(maxWorld[i] - minWorld[i]);
        mC0[i] = mNegInfinity*(1.0f + twoInvRange*minWorld[i]);
        mC1[i] = mPosInfinity*twoInvRange;
    }

    mNumMoveQueue = 0;
    mNumEvents = 0;

    // Set up the SPU, including specifying the program it should
    // run and creating the send-queue, receive-port, and thread
    // associated with ReceiveMessageFromSPU. In practice, this
    // takes a lot of code. On the Sony Playstation 3, I factored
    // this support into a base class for any derived class wanting
    // to run an SPU program.
    SpuConnect(input, output);

    mBoxes = SpuAllocateSharedHeap(BOX_DMA_TAG,
        NUM_BOXES*sizeof(BoxState));
    mEvents = SpuAllocateSharedHeap(EVENT_DMA_TAG,
        MAX_EVENTS*sizeof(int));

    SpuSendMessage(mSendQueue, MSG_SHARED_BOX_HEAP_ADDRESS,
        mBoxes);
    SpuSendMessage(mSendQueue, MSG_SHARED_EVENT_HEAP_ADDRESS,
        mEvents);
}

```

The destructor cleans up resources and disconnects from the SPU.

```

BoxManagerCPU::~BoxManagerCPU ()
{
    SpuSendMessage(mSendQueue, MSG_TERMINATE, 0);

    // The 'input' parameter is whatever is needed by the SPU

```

```

// system to wait for the thread to terminate and to
// disconnect and destroy the send-queue, receive-queue,
// and thread that manages ReceiveMessageFromSPU.
SpuWaitForThreadTermination(input);
SpuDisconnect(input);

SpuDeallocateSharedHeap(BOX_DMA_TAG, mBoxes);
SpuDeallocateSharedHeap(EVENT_DMA_TAG, mEvents);
DestroyEvent(mUpdateEvent);
}

```

The functions InsertMoveQueue, MoveBoxes, WaitForUpdateEnd, and ProcessEvents have the same implementation as before, with the exception that MoveBoxes no longer sets mNumMoveQueue to zero. The Update function will do this. The Move function is different in that it must now transform the floating point box data to shorts.

```

void BoxManagerCPU::Move (int i, const Box& box)
{
    int smin[3], smax[3];
    for (int j = 0; j < 3; ++j)
    {
        float fmin = floorf(mC0[j] + mC1[j]*box.mMin[j]);
        if (fmin < mNegInfinity)
        {
            fmin = mNegInfinity + 1.0f;
        }
        else if (fmin > mPosInfinity)
        {
            fmin = mPosInfinity - 1.0f;
        }
        smin[j] = (int)fmin;

        float fmax = ceilf(mC0[j] + mC1[j]*box.mMax[j]);
        if (fmax < mNegInfinity)
        {
            fmax = mNegInfinity + 1.0f;
        }
        else if (fmax > mPosInfinity)
        {
            fmax = mPosInfinity - 1.0f;
        }
        smax[j] = (int)fmax;
    }

    BoxState& box = mBoxes[mNumMoves++];
    box.mXExtremes =
        (smin[0] & 0x0000FFFF) | ((smax[0] & 0x0000FFFF) << 16);
}

```

```

    box.mYExtremes =
        (smin[1] & 0x0000FFFF) | ((smax[1] & 0x0000FFFF) << 16);
    box.mZExtremes =
        (smin[2] & 0x0000FFFF) | ((smax[2] & 0x0000FFFF) << 16);
    box.mIndex = i;
}

```

The transformation is applied to the box extremes. The values are clamped to the desired short-valued range. The minimum values are rounded down to the nearest short and the maximum values are rounded up to the nearest short. This is a conservative approach that will lead to slightly larger boxes, and guarantees at least the same number of overlaps. We are guaranteed not to lose overlaps because of the conversion to shorts.

The update function is a simple wrapper for sending a message to the SPU. Setting mNumMoveQueue to zero here instead of MoveBoxes is necessary because its value must persist until we send it to the SPU.

```

void BoxManagerCPU::Update ()
{
    SpuSendMessage(mSendQueue, MSG_UPDATE_BEGIN, mNumMoveQueue);
    mNumMoveQueue = 0;
}

```

Finally, the function that is managed by a thread created during SPU set up is specified next.

```

void BoxManagerCPU::ReceiveMessageFromSPU (int receiveQueue)
{
    while (true)
    {
        int message, data;
        if (SpuReceiveMessage(receiveQueue, &message, &data))
        {
            switch (message)
            {
                case MSG_UPDATE_END:
                    mThis->mNumEvents = data;

                    // Signal that the update is finished.
                    SetEvent(mThis->mUpdateEvent);
                    break;

                case MSG_TERMINATE:
                    SpuDestroyThread();
                    return;
            }
        }
    }
}

```

```
    {  
        sleep(1);  
    }  
}
```

The application code that was presented for the CPU-only asynchronous updating remains the same for the SPU version. As you might have deduced, this implementation is ideal for the Playstation 3 with its *synergistic processing units* (SPUs).

6.3 TEST-INTERSECTION QUERIES

Axis-aligned bounding boxes were useful for the broad-phase collision culling algorithm that used space-time coherency. For medium-phase culling or for test-intersection queries generally, a few other bounding volumes might be of use.

Oriented bounding boxes (OBBs) are quite common for coarse-level intersection testing for objects. More generally, convex polyhedra may be used. The two approaches to testing for intersection are the *method of separating axes* and distance-based methods using the *GJK algorithm*. These concepts require a lot of discussion, so let us postpone that until Section 6.4.

6.3.1 SPHERES

Practitioners have used spheres as bounding volumes. The intersection testing algorithms are easy to implement. However, spheres are generally not a tight fit for an object; for example, consider a tall telephone pole on the side of a race track. Collision detection between race cars and telephone poles could use bounding spheres for medium-phase culling. You can see the problem – the bounding sphere of the telephone pole will have a radius that is half its length, so the sphere sticks out into the middle of the race track. Every race car will lead to a “potential intersection” because their bounding spheres will always intersect that of the telephone pole.

Ignoring the goodness-of-fit issue, a sphere has a center C and a radius r . Two spheres, $\{C_0, r_0\}$ and $\{C_1, r_1\}$, intersect when the distance between C_0 and C_1 is smaller than or equal to the sum of the radii $r_0 + r_1$. Pseudocode is

```
bool Overlapping (Sphere S0, Sphere S1)
{
    float rsum = S0.radius + S1.radius;
    Vector3 diff = S0.center - S1.center;
    float distance = Length(diff);
    return distance <= rsum;
}
```

6.3.2 CAPSULES

Alternatives to using spheres for obtaining a better fitting bounding volumes are *capsules*. A capsule has a line segment S and a radius r associated with it. The (solid) capsule consists of those points that are within a distance r of the segment S . Consequently, a capsule is the union of a cylinder and two hemispheres. The cylinder axis is the segment, has radius r , and has height equal to the length of the segment. The hemispheres have radii r and are centered at the endpoints of the segment.

The test-intersection query for two capsules, $\{S_0, r_0\}$ and $\{S_1, r_1\}$, is simply formulated. The capsules intersect when the distance between segments S_0 and S_1 is smaller than or equal to the sum of the radii $r_0 + r_1$. The query requires you to have an implementation of the algorithm for computing the distance between two line segments. Pseudocode is

```
bool Overlapping (Capsule C0, Capsule C1)
{
    float rsum = C0.radius + C1.radius;
    float distance = Distance(C0.segment, C1.segment);
    return distance <= rsum;
}
```

The Wild Magic files `Wm5DistSegment3Segment3.{h, cpp}` contain an implementation for computing the distance between line segments.

Consider two spheres, each moving with constant linear velocity over a specified time interval. Let sphere i be $\{C_i, r_i\}$ and have velocity V_i for $i = 0, 1$. The test-intersection query for the moving spheres becomes a test-intersection query for two capsules. If $[0, T]$ is the time interval, the capsules have line segments with endpoints $C_i + TV_i$ and radii r_i . Pseudocode is

```
bool WillOverlap (float tmin, float tmax, Sphere S0, Vector3 V0,
Sphere S1, Vector3 V1)
{
    Capsule C0(S0.center + tmin*V0, S0.center + tmax*V0,
S0.radius);
    Capsule C1(S1.center + tmin*V1, S1.center + tmax*V1,
S1.radius);
    return Overlapping(C0, C1);
}
```

The test-intersection query for two capsules, each moving with constant linear velocity, is more complicated. The set spanned by a segment moving with constant linear velocity is either a line segment (velocity is parallel to the capsule axis) or a parallelogram (velocity is not parallel to the capsule axis). The query for the moving capsules becomes a query for two stationary sets. The capsules will intersect during the specified time interval when the distance between the two sets is smaller than or equal to the sum of the radii. You will need a segment–segment

distance function, a segment–parallelogram distance function, and a parallelogram–parallelogram distance function. Pseudocode is

```

// A 'lozenge' is the set of points within a specified radius of
// a parallelogram.

bool Overlapping (Capsule C, Lozenge L)
{
    return Distance(C.segment, L.parallelogram) <=
        C.radius + L.radius;
}

bool Overlapping (Lozenge L0, Lozenge L1)
{
    return Distance(L0.parallelogram, L1.parallelogram) <=
        L0.radius + L1.radius;
}

bool WillOverlap (float tmin, float tmax, Capsule C0, Vector3 V0,
                  Capsule C1, Vector3 V1)
{
    if (Cross(V0, C0.segment.direction) != Vector3::ZERO)
    {
        Lozenge L0(
            C0.segment.end0 + tmin*V0,
            C0.segment.end1 + tmin*V0,
            C0.segment.end0 + tmax*V0,
            C0.segment.end1 + tmax*V0,
            C0.radius);

        if (Cross(V1, C1.segment.direction) != Vector3::ZERO)
        {
            Lozenge L1(
                C1.segment.end0 + tmin*V1,
                C1.segment.end1 + tmin*V1,
                C1.segment.end0 + tmax*V1,
                C1.segment.end1 + tmax*V1,
                C1.radius);

            return Overlapping(L0, L1);
        }
    }
    else
    {
        Capsule MC1;
        if (Dot(C1.segment.direction, V1) > 0)
        {
            MC1 = Capsule(
                C1.segment.end0 + tmin*V1,

```

```

        C1.segment.end1 + tmax*V1,
        C1.radius);
    }
    else
    {
        MC1 = Capsule(
            C1.segment.end1 + tmin*V1,
            C1.segment.end0 + tmax*V1,
            C1.radius);
    }

    return Overlapping(MC1, L0);
}
}
else
{
    Capsule MC0;
    if (Dot(C0.segment.direction, V0) > 0)
    {
        MC0 = Capsule(
            C0.segment.end0 + tmin*V0,
            C0.segment.end1 + tmax*V0,
            C0.radius);
    }
    else
    {
        MC0 = Capsule(
            C0.segment.end1 + tmin*V0,
            C0.segment.end0 + tmax*V0,
            C0.radius);
    }

    if (Cross(V1, C1.segment.direction) != Vector3::ZERO)
    {
        Lozenge L1(
            C1.segment.end0 + tmin*V1,
            C1.segment.end1 + tmin*V1,
            C1.segment.end0 + tmax*V1,
            C1.segment.end1 + tmax*V1,
            C1.radius);

        return Overlapping(MC0, L1);
    }
    else
    {
        Capsule MC1;
        if (Dot(C1.segment.direction, V1) > 0)

```

```

    {
        MC1 = Capsule(
            C1.segment.end0 + tmin*V1,
            C1.segment.end1 + tmax*V1,
            C1.radius);
    }
    else
    {
        MC1 = Capsule(
            C1.segment.end1 + tmin*V1,
            C1.segment.end0 + tmax*V1,
            C1.radius);
    }
    return Overlapping(MC0, MC1);
}
}

```

6.3.3 ELLIPSOIDS

Occasionally you will see on developer forums a post where the person wants to use ellipsoids as bounding volumes that fit better than spheres, but it is not clear how to perform the intersection testing. When confronted with the answer, the posters will frequently abandon the task and instead work with bounding volumes whose test-intersection queries are easier to implement. Intersection testing for ellipsoids is nontrivial. The algorithm is heavy on mathematics and is iterative, leading to a potentially expensive test. I will present the details here anyway to give you an idea of the complexity of the problem. The ideas are motivated first using ellipses in 2D and then extended to ellipsoids in 3D.

Test-Intersection Query for Stationary Ellipses

An ellipse is implicitly defined by a quadratic equation $Q(x, y) = 0$. Given two ellipses defined by $Q_0(x, y) = 0$ and $Q_1(x, y) = 0$, you may eliminate the y -variable and obtain a quartic equation $P(x) = 0$. The x -roots may be computed using closed-form equations or numerically. For each x -root you can compute corresponding y -values from the quadratic $Q_0(x, y) = 0$. It is possible that extraneous solutions occur (because of the elimination process). The end result is a set of points (\bar{x}, \bar{y}) that are intersection points of the ellipse (or extraneous pairs that occurred because of the elimination and can be discarded).

In collision culling, more information is needed other than just knowing points of intersection. Specifically, if the ellipses are used as bounding regions, it might be

important to know if one ellipse is fully contained in another. This information is not provided by the algebraic method applied to the two quadratic equations defining the ellipses. The more precise queries for ellipses E_0 and E_1 are:

- Do E_0 and E_1 intersect?
- Are E_0 and E_1 separated? That is, does there exist a line for which the ellipses are on opposite sides?
- Is E_0 properly contained in E_1 , or is E_1 properly contained in E_0 ?

Let the ellipse E_i be defined by the quadratic equation $Q_i(\mathbf{X}) = \mathbf{X}^T A_i \mathbf{X} + \mathbf{B}_i^T \mathbf{X} + C_i$ for $i = 0, 1$. It is assumed that the A_i are positive definite. In this case, $Q_i(\mathbf{X}) < 0$ defines the inside of the ellipse and $Q_i(\mathbf{X}) > 0$ defines the outside.

The discussion focuses on level curves of the quadratic functions. All level curves defined by $Q_0(x, y) = \lambda$ are ellipses, except for the minimum (negative) value λ for which the equation defines a single point, the center of every level curve ellipse. The ellipse defined by $Q_1(x, y) = 0$ is a curve that generally intersects many level curves of Q_0 . The problem is to find the minimum level value λ_0 and maximum level value λ_1 attained by any (x, y) on the ellipse E_1 . If $\lambda_1 < 0$, then E_1 is properly contained in E_0 . If $\lambda_0 > 0$, then E_0 and E_1 are separated. Otherwise, $0 \in [\lambda_0, \lambda_1]$ and the two ellipses intersect. Figures 6.7, 6.8, and 6.9 illustrate the three possibilities. The figures show the relationship of one ellipse E_1 to the level curves of another ellipse E_0 .

This can be formulated as a constrained optimization that can be solved by the method of Lagrange multipliers: Optimize $Q_0(\mathbf{X})$ subject to the constraint $Q_1(\mathbf{X}) = 0$. Define $F(\mathbf{X}, t) = Q_0(\mathbf{X}) + tQ_1(\mathbf{X})$. Differentiating with respect to the components of \mathbf{X} yields $\nabla F = \nabla Q_0 + t\nabla Q_1$. Differentiating with respect to t yields $\partial F / \partial t = Q_1$.

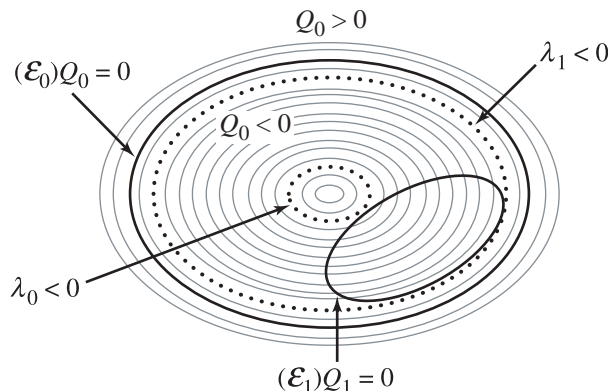


Figure 6.7 E_1 is contained in E_0 . The maximum E_0 -level-curve value λ_1 for E_1 is negative.

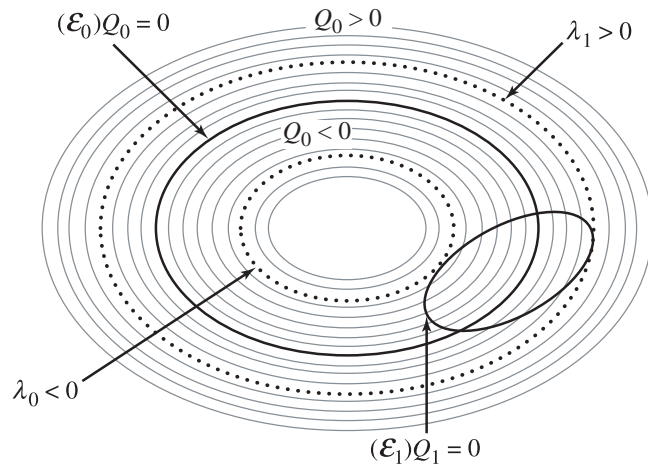


Figure 6.8 E_1 transversely intersects E_0 . The minimum E_0 -level-curve value λ_0 for E_1 is negative, the maximum value λ_1 is positive.

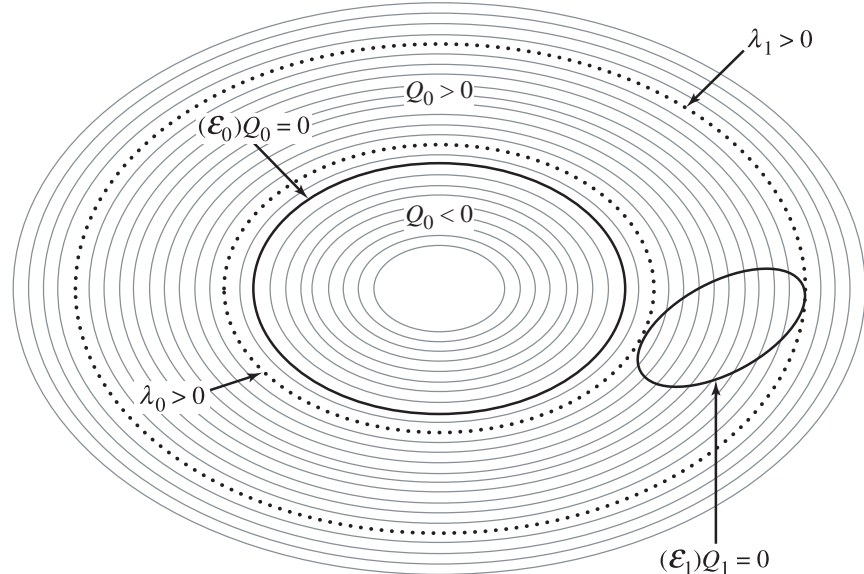


Figure 6.9 E_1 is separated from E_0 . The minimum E_0 -level-curve value λ_0 for E_1 is positive.

Setting the t -derivative equal to zero reproduces the constraint $Q_1 = 0$. Setting the \mathbf{X} -derivative equal to zero yields $\nabla Q_0 + t \nabla Q_1 = \mathbf{0}$ for some t . Geometrically this means that the gradients are parallel.

Note that $\nabla Q_i = 2A_i\mathbf{X} + \mathbf{B}_i$, so

$$\mathbf{0} = \nabla Q_0 + t \nabla Q_1 = 2(A_0 + tA_1)\mathbf{X} + (\mathbf{B}_0 + t\mathbf{B}_1).$$

Formally solving for \mathbf{X} yields

$$\mathbf{X} = -\frac{1}{2}(A_0 + tA_1)^{-1}(\mathbf{B}_0 + t\mathbf{B}_1) = \frac{1}{\delta(t)}\mathbf{Y}(t)$$

where $A_0 + tA_1$ is a matrix of linear polynomials in t and $\delta(t)$ is its determinant, a quadratic polynomial. The components of $\mathbf{Y}(t)$ are quadratic polynomials in t . Replacing this in $Q_1(\mathbf{X}) = 0$ leads to a polynomial equation,

$$p(t) = \mathbf{Y}(t)^T A_1 \mathbf{Y}(t) + \delta(t) \mathbf{B}_1^T \mathbf{Y}(t) + \delta(t)^2 C_1 = 0 \quad (6.5)$$

a quartic polynomial in t . The roots can be computed, the corresponding values of \mathbf{X} computed, and $Q_0(\mathbf{X})$ evaluated. The minimum and maximum values are stored as λ_0 and λ_1 , and the earlier comparisons with zero are applied.

This method leads to a quartic polynomial, just as the original algebraic method for finding intersection points did. But the current style of query does answer questions about the relative positions of the ellipses (separated or proper containment), whereas the original method does not.

EXAMPLE 6.1

Consider $Q_0(x, y) = x^2 + 6y^2 - 1$ and $Q_1(x, y) = 52x^2 - 72xy + 73y^2 - 32x - 74y + 28$. Figure 6.10 shows the plots of the two ellipses.

The various parameters are

$$A_0 = \begin{bmatrix} 1 & 0 \\ 0 & 6 \end{bmatrix}, \mathbf{B}_0 = \begin{bmatrix} 0 \\ 0 \end{bmatrix}, C_0 = -1,$$

$$A_1 = \begin{bmatrix} 52 & -36 \\ -36 & 73 \end{bmatrix}, \mathbf{B}_1 = \begin{bmatrix} -32 \\ -74 \end{bmatrix}, C_1 = 28$$

From these are derived

$$\mathbf{Y}(t) = \begin{bmatrix} 4t(625t + 24) \\ t(2500t + 37) \end{bmatrix}, \delta(t) = 2500t^2 + 385t + 6$$

The polynomial of equation (6.5) is $p(t) = -156250000t^4 - 48125000t^3 + 1486875t^2 + 94500t + 1008$. The two real-valued roots are $t_0 \doteq -0.331386$ and $t_1 \doteq 0.0589504$. The corresponding $\mathbf{X}(t)$ values are $\mathbf{X}(t_0) = (x_0, y_0) \doteq (1.5869, 1.71472)$ and $\mathbf{X}(t_1) = (x_1, y_1) \doteq (0.383779, 0.290742)$. The axis-aligned ellipse level values at these points are $Q_0(x_0, y_0) = -0.345528$ and $Q_0(x_1, y_1) = 19.1598$. Since $Q_0(x_0, y_0) < 0 < Q_0(x_1, y_1)$, the ellipses intersect. Figure 6.10 shows the two points on $Q_1 = 0$ that have extreme Q_0 values.

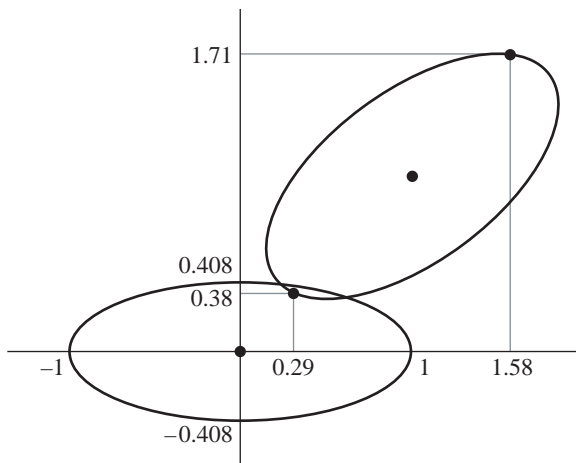


Figure 6.10

Intersection of two ellipses.

Test-Intersection Query for Stationary Ellipsoids

The algorithm for determining the relationship between two stationary ellipsoids is similar to that for ellipses. The precise queries we answer for testing for intersection of two ellipsoids E_0 and E_1 are

- Do E_0 and E_1 intersect?
- Are E_0 and E_1 separated? That is, does there exist a plane for which the ellipsoids are on opposite sides?
- Is E_0 properly contained in E_1 or is E_1 properly contained in E_0 ?

Finding the set of intersection points is more complicated. A couple of methods are discussed. An ellipsoid E_i is defined by the quadratic equation $Q_i(\mathbf{X}) = \mathbf{X}^T \mathbf{A} \mathbf{X} + \mathbf{B}_i^T \mathbf{X} + C_i = 0$ where \mathbf{A}_i is a 3×4 positive definite matrix, \mathbf{B}_i is a 3×1 vector, C_i is a scalar, and \mathbf{X}_i is a 3×1 vector that represents an ellipsoid point. Because \mathbf{A} is positive definite, $Q_i(\mathbf{X}) < 0$ defines the inside of the ellipsoid and $Q_i(\mathbf{X}) > 0$ defines the outside.

The test-intersection query is based on level surfaces of the quadratic functions. All level surfaces defined by $Q_0(x, y, z) = \lambda$ are ellipsoids, except for the minimum (negative) value λ for which the equation defines a single point, the center of every level surface ellipsoid. The ellipsoid defined by $Q_1(x, y, z) = 0$ is a surface that generally intersects many level surfaces of Q_0 . The problem is to find the minimum Q_0 -level

value λ_0 and the maximum Q_0 -level value λ_1 attained by any point (x, y, z) on the ellipsoid E_1 . If $\lambda_1 < 0$, E_1 is properly contained in E_0 . If $\lambda_0 > 0$, then E_0 and E_1 are separated. Otherwise, $0 \in [\lambda_0, \lambda_1]$ and the two ellipsoids intersect. Illustrations in two dimensions are shown in Figures 6.7, 6.8, and 6.9, but apply equally well to the three dimensional case.

The problem can be formulated as a constrained optimization that is solved by the method of Lagrange multipliers. Optimize $Q_0(\mathbf{X})$ subject to the constraint $Q_1(\mathbf{X}) = 0$. Define $F(\mathbf{X}, t) = Q_0(\mathbf{X}) + tQ_1(\mathbf{X})$. Differentiating with respect to the \mathbf{X} components yields $\nabla F = \nabla Q_0 + t\nabla Q_1$. Differentiating with respect to t yields $\partial F / \partial t = Q_1$. Setting the t -derivative equal to zero reproduces the constraint $Q_1 = 0$. Setting the \mathbf{X} -derivative equal to zero yields $\nabla Q_0 + t\nabla Q_1 = \mathbf{0}$ for some t . Geometrically this means the gradients are parallel.

Note that $\nabla Q_i = 2A_i\mathbf{X} + \mathbf{B}_i$, so

$$\mathbf{0} = \nabla Q_0 + t\nabla Q_1 = 2(A_0 + tA_1)\mathbf{X} + (\mathbf{B}_0 + t\mathbf{B}_1)$$

Formally solving for \mathbf{X} yields

$$\mathbf{X} = -\frac{1}{2}(A_0 + tA_1)^{-1}(\mathbf{B}_0 + t\mathbf{B}_1) = \frac{1}{\delta(t)}\mathbf{Y}(t)$$

where $A_0 + tA_1$ is a matrix of linear polynomials in t and $\delta(t)$ is its determinant, a cubic polynomial in t . The components of $\mathbf{Y}(t)$ are cubic polynomials in t . Replacing this in $Q_1(\mathbf{X}) = 0$ yields

$$\mathbf{Y}(t)^T A_1 \mathbf{Y}(t) + \delta(t) \mathbf{B}_1^T \mathbf{Y}(t) + \delta(t)^2 C_1 = 0$$

a degree six polynomial in t . The roots can be computed, the corresponding values of \mathbf{X} computed, and $Q_0(\mathbf{X})$ evaluated. The minimum and maximum values are stored as λ_0 and λ_1 , and the earlier comparisons with zero are applied.

Intersection of Moving Ellipses

Consider two ellipses that are initially separated and are moving with constant linear velocities. The first problem is to determine whether or not the ellipses intersect at a later time. If they do intersect, the second problem is to determine the contact time and contact point of the ellipses. The contact time is the smallest positive time $t_{\text{contact}} > 0$ such that the two ellipses are separated for times $0 \leq t < t_{\text{contact}}$ and just touching at time $t = t_{\text{contact}}$. This document describes an algorithm for solving these problems.

At time zero, the ellipses are defined by quadratic equations in standard form. The first ellipse is defined by

$$(\mathbf{X} - \mathbf{K}_0)^T M_0 (\mathbf{X} - \mathbf{K}_0) = 1 \quad (6.6)$$

The center of the ellipse is \mathbf{K}_0 . The matrix M_0 is positive definite and can be factored as $M_0 = R_0 D_0 R_0^T$, where R_0 is a rotation matrix and D_0 is a diagonal matrix whose

diagonal entries are positive. The diagonal values of D_0 are eigenvalues of M_0 , and the columns of R_0 are eigenvectors of M_0 . The second ellipse is defined by

$$(\mathbf{X} - \mathbf{K}_1)^T M_1 (\mathbf{X} - \mathbf{K}_1) = 1 \quad (6.7)$$

where \mathbf{K}_1 is the center and where $M_1 = R_1 D_1 R_1^T$ is positive definite.

The ellipses are moving with constant linear velocities \mathbf{V}_0 and \mathbf{V}_1 , where the indices make it clear which velocity goes with which ellipse. The ellipse centers at time $t \geq 0$ are $\mathbf{K}_0 + t\mathbf{V}_0$ and $\mathbf{K}_1 + t\mathbf{V}_1$. To simplify the problem, we may use relative velocity; the first ellipse is assumed to be stationary and the second ellipse is moving with constant linear velocity $\mathbf{V} = \mathbf{V}_1 - \mathbf{V}_0$.

The Configuration at Contact Time

At the contact time, the contact set must contain a single point because of the convexity of the ellipses. Moreover, the ellipses must be tangent at the contact point. [Figure 6.11](#) illustrates this.

Let us analyze this configuration to determine the location of the contact point. We make several changes of variables to reduce the problem to one involving a circle of radius 1 and centered at the origin and an ellipse that is axis-aligned. The transformations are affine and invertible, so the contact set still contains a single point. [Figure 6.12](#) shows such a configuration.

Reduction to Circle and Axis-Aligned Ellipse

For the sake of argument, we will use [equations \(6.6\)](#) and [\(6.7\)](#) as if the contact time were $T = 0$.

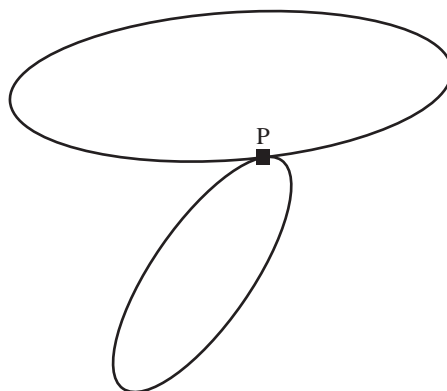


Figure 6.11 The configuration of two ellipses at contact time. The contact point is \mathbf{P} .

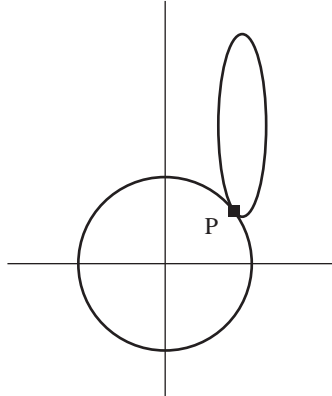


Figure 6.12 The transformed configuration to a circle of radius 1 with center at the origin and an axis-aligned ellipse.

The first change of variables is

$$\mathbf{Y} = D_0^{1/2} R_0^T (\mathbf{X} - \mathbf{K}_0) \quad (6.8)$$

where $D_0^{1/2}$ is the diagonal matrix whose diagonal entries are the square roots of the diagonal entries of D_0 . Equation (6.6) transforms to

$$\mathbf{Y}^T \mathbf{Y} = 1 \quad (6.9)$$

which represents a circle of radius 1 centered at the origin. Define

$$\mathbf{K}_2 = R_0^T D_0^{1/2} (\mathbf{K}_1 - \mathbf{K}_0) \quad (6.10)$$

and

$$M_2 = R_0^T D_0^{-1/2} R_1 D_1 R_1^T D_0^{-1/2} R_0 \quad (6.11)$$

Equations (6.8), (6.10), and (6.11) transform equation (6.7) to

$$(\mathbf{Y} - \mathbf{K}_2)^T M_2 (\mathbf{Y} - \mathbf{K}_2) = 1 \quad (6.12)$$

The matrix M_2 may be factored using an eigendecomposition to $M_2 = RDR^T$, where D is a diagonal matrix and R is a rotation matrix. The second change of variables is

$$\mathbf{Z} = R^T \mathbf{Y} \quad (6.13)$$

Equation (6.9) is transformed to

$$\mathbf{Z}^T \mathbf{Z} = 1 \quad (6.14)$$

which is the same circle, but rotated about the origin. Defining

$$\mathbf{K} = R^T \mathbf{K}_2 \quad (6.15)$$

Equation (6.12) is transformed to

$$(\mathbf{Z} - \mathbf{K})^T D (\mathbf{Z} - \mathbf{K}) = 1 \quad (6.16)$$

Because D is diagonal, this equation represents an axis-aligned ellipse with center point \mathbf{K} , as illustrated in Figure 6.13. Define

$$Q(\mathbf{Z}) = (\mathbf{Z} - \mathbf{K})^T D (\mathbf{Z} - \mathbf{K}) - 1 \quad (6.17)$$

The ellipse is implicitly defined by $Q(\mathbf{Z}) = 0$, and the gradient vector $\nabla Q(\mathbf{Z})$ is an outer-pointing normal to the point \mathbf{Z} on the ellipse.

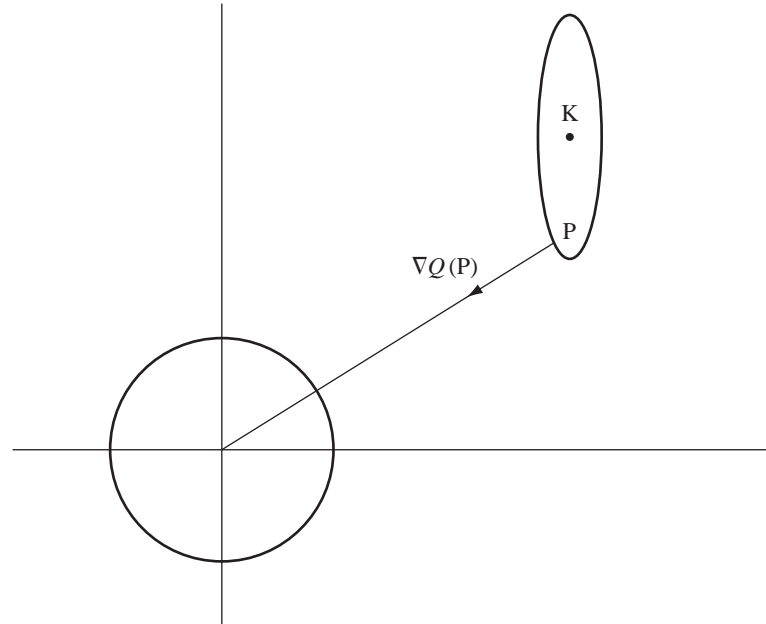


Figure 6.13 The transformed configuration to a circle of radius 1, with center at the origin and an axis-aligned ellipse. The circle and ellipse are separated. The point \mathbf{P} is the ellipse point that is closest to the origin. An outer-pointing normal at this point is $\nabla Q(\mathbf{P})$.

Computing the Closest Point \mathbf{P}

The point \mathbf{P} shown in Figure 6.13 is the ellipse point closest to the origin (and to the circle). We know that \mathbf{P} is on the ellipse, so $Q(\mathbf{P}) = 0$. An outer-pointing normal to the ellipse at \mathbf{P} is the gradient vector $\nabla Q(\mathbf{P}) = 2D(\mathbf{P} - \mathbf{K})$. In fact, this vector is parallel to \mathbf{P} but in the opposite direction; thus, there is some scalar $s < 0$ for which

$$sD(\mathbf{P} - \mathbf{K}) = \mathbf{P} \quad (6.18)$$

If $\mathbf{P} = (p_0, p_1)$, $\mathbf{K} = (k_0, k_1)$, and $D = \text{Diag}(d_0, d_1)$ with $d_1 \geq d_0$, then equation (6.18) may be solved for

$$p_0 = \frac{d_0 k_0 s}{d_0 s - 1}, \quad p_1 = \frac{d_1 k_1 s}{d_1 s - 1} \quad (6.19)$$

Knowing that \mathbf{P} is on the ellipse, we have

$$0 = Q(\mathbf{P}) = \frac{d_0 k_0^2}{(d_0 s - 1)^2} + \frac{d_1 k_1^2}{(d_1 s - 1)^2} - 1 \quad (6.20)$$

We will show that equation (6.20) has a unique negative root \bar{s} .

The summary of the algorithm is the following. It assumes that the eigen-decompositions for M_0 and M_1 are computed once and stored with the ellipse data structure.

1. Given two separated ellipses, $\mathcal{E}_0 = \{\mathbf{K}_0, R_0, D_0\}$ and $\mathcal{E}_1 = \{\mathbf{K}_1, R_1, D_1\}$.
2. Compute $\mathbf{K}_2 = R_0^T D_0^{1/2} (\mathbf{K}_1 - \mathbf{K}_0)$.
3. Compute $M_2 = R_0^T D_0^{-1/2} R_1 D_1 R_1^T D_0^{-1/2} R_0$.
4. Use an eigendecomposition to factor $M_2 = RDR^T$ with $D = \text{Diag}(d_0, d_1)$.
5. Compute $\mathbf{K} = R^T \mathbf{K}_2 = (k_0, k_1)$.
6. Compute the unique negative root \bar{s} to equation (6.20).
7. Compute $\mathbf{P} = (d_0 k_0 \bar{s} / (d_0 \bar{s} - 1), d_1 k_1 \bar{s} / (d_1 \bar{s} - 1))$.

What remains is to determine an algorithm for computing \bar{s} .

Computing the Negative Root

Equation (6.20) may be rewritten as a quartic polynomial equation:

$$p(s) = (d_0 s - 1)^2 (d_1 s - 1)^2 - d_0 k_0^2 (d_1 s - 1)^2 - d_1 k_1^2 (d_0 s - 1)^2 = 0 \quad (6.21)$$

The closed-form equations for the roots of a quartic may be used to compute the real-valued roots, one of which will be negative. These equations are known to be numerically ill-conditioned, and we do not need all the roots.

An algorithm that is better suited for numerical computations is described next. Define the function

$$f(s) = \frac{d_0 k_0^2}{(d_0 s - 1)^2} + \frac{d_1 k_1^2}{(d_1 s - 1)^2} - 1 \quad (6.22)$$

The sets of roots of $p(s)$ and $f(s)$ are the same. The first derivative is

$$f'(s) = \frac{-2d_0^2 k_0^2}{(d_0 s - 1)^3} + \frac{-2d_1^2 k_1^2}{(d_1 s - 1)^3} \quad (6.23)$$

and the second derivative is

$$f''(s) = \frac{6d_0^3 k_0^2}{(d_0 s - 1)^4} + \frac{6d_1^3 k_1^2}{(d_1 s - 1)^4} > 0 \quad (6.24)$$

I have indicated that the second derivative is always positive, which makes $f(s)$ a *convex function*. Such functions are ideal for locating roots using Newton's method.

Part of the graph of $f(s)$ is illustrated by Figure 6.14. Because we want only the negative roots, the left-most branch of the graph is of interest. A simple calculation shows that

$$f(0) = d_0 k_0^2 + d_1 k_1^2 - 1 = Q(\mathbf{0}) > 0 \quad (6.25)$$

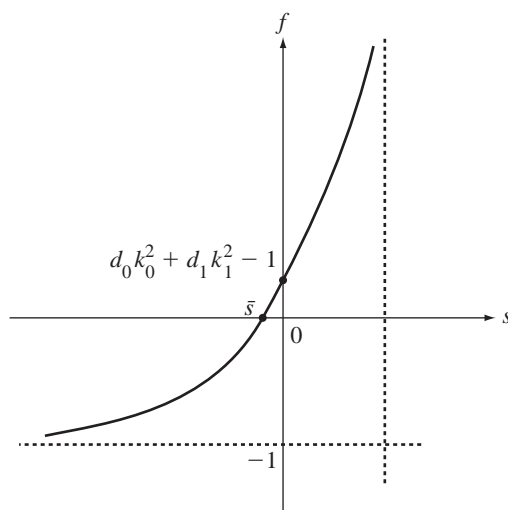


Figure 6.14 The left-most branch of the graph of $f(s)$. The vertical asymptote is at $s = 1/d_1$ when $k_1 \neq 0$, or at $s = 1/d_0$ when $k_1 = 0$.

The positivity is guaranteed because the origin $\mathbf{0}$ is outside the ellipse. Also,

$$\lim_{s \rightarrow -\infty} f(s) = -1 \quad (6.26)$$

The convexity of f and equations (6.25) and (6.26) guarantee that $f(s)$ has a unique negative root \bar{s} . We may use Newton's method to numerically estimate this root:

$$s_0 = 0; \quad s_{i+1} = s_i - \frac{f(s_i)}{f'(s_i)}, \quad i \geq 0 \quad (6.27)$$

The convexity of f guarantees convergence of the sequence, and in practice the number of iterates for an accurate estimate is small.

Computing the Contact Time

In the previous construction, the ellipses were stationary and assumed to be in tangential contact. When the ellipses are moving, we replace in the construction \mathbf{K}_0 by $\mathbf{K}_0 + t\mathbf{V}_0$ and \mathbf{K}_1 by $\mathbf{K}_1 + t\mathbf{V}_1$. The center of the axis-aligned ellipse is time varying,

$$\mathbf{C}(t) = R^T R_0^T D_0^{1/2} (\mathbf{K}_1 - \mathbf{K}_0 + t\mathbf{V}) = \mathbf{K} + t\mathbf{W} \quad (6.28)$$

where $\mathbf{V} = \mathbf{V}_1 - \mathbf{V}_0$ is the relative velocity. The last equality defines the velocity \mathbf{W} , which is the relative velocity of the axis-aligned ellipse compared to the stationary circle. For notation's sake, let $\mathbf{K} = (k_0, k_1)$, $\mathbf{W} = (w_0, w_1)$, and $\mathbf{C} = (c_0, c_1) = (k_0 + tw_0, k_1 + tw_1)$.

The circle and ellipse are initially separated, as Figure 6.13 illustrates. A quick-out test is convenient here. The initially closest point \mathbf{P} to the circle moves with velocity \mathbf{W} . If the velocity vector forms an acute angle with \mathbf{P} , then initially \mathbf{P} moves away from the circle and must do so for all later times. Thus, when $\mathbf{W} \cdot \mathbf{P} \geq 0$, the ellipse will never intersect the circle.

When $\mathbf{W} \cdot \mathbf{P} < 0$, we would like to know whether or not the ellipse will intersect the circle. The ellipse sweeps a region \mathcal{R} that is bounded by two parallel lines. An intersection between the ellipse and circle will occur if and only if the circle intersects the region \mathcal{R} . This is a tractable problem. The bounding parallel lines have direction \mathbf{W} and pass through the two extreme points in the perpendicular direction $\mathbf{W}^\perp = (w_1, -w_0)$. Determining whether or not the circle intersects these lines, or is between them, is a matter of algebra. Figure 6.15 illustrates the geometric relationship between the circle and \mathcal{R} .

The extreme points \mathbf{E}_0 and \mathbf{E}_1 are in the directions of $\pm\mathbf{N}$ where $\mathbf{N} = \mathbf{W}^\perp$. The point \mathbf{B}_0 is extreme in the direction of $-\mathbf{W}$. The extreme point $\mathbf{B}_1 = \mathbf{B}_0 + t_{\max}\mathbf{W}$ is chosen such that the moving ellipse has completely passed the circle. Thus, the contact time is in the interval $[0, t_{\max}]$.

The algorithm presented here for computing the contact point has the circle-region intersection test in it implicitly. There is a trade-off: The implicit test requires more computational cycles than the direct test. But the ideas here apply to higher-dimensional ellipsoids, where the direct test becomes more computationally intensive. For example, the direct test in 3D requires testing whether a sphere intersects the

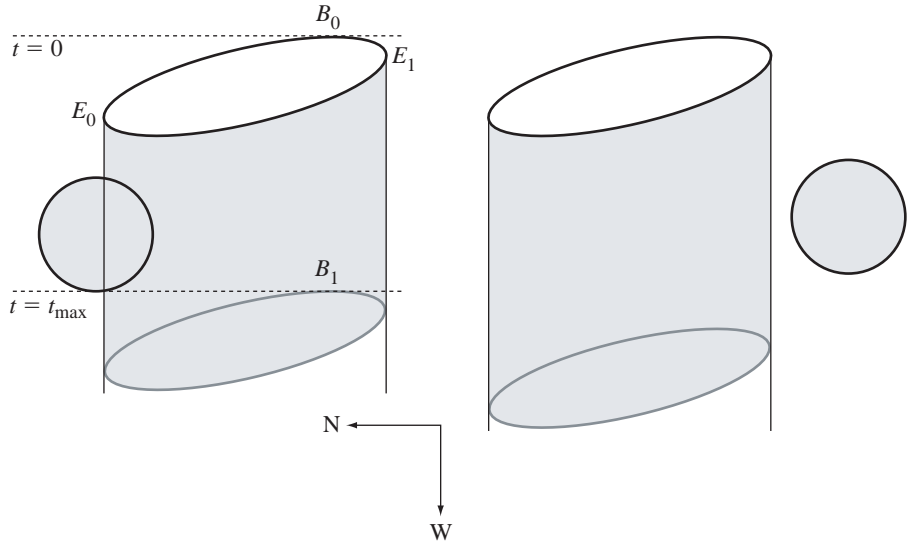


Figure 6.15 The ellipse sweeps a region bounded by two parallel lines. Left: The ellipse will intersect the circle when the circle intersects the swept region. Right: The ellipse will not intersect the circle when the circle is disjoint from the swept region.

ellipsoid-sweep region which happens to be a right-elliptical cylinder. Computing the equation of the elliptical cylinder is tedious, but tractable. The intersection test can then be reduced to a 2D problem of testing whether or not a circle and ellipse overlap. The algorithm here has no component for reduction of dimension, which makes it easy to adapt to higher dimensions.

With the introduction of the time parameter, the function of equation (6.22) is now dependent on two parameters,

$$f(s, t) = \frac{d_0 c_0^2}{(d_0 s - 1)^2} + \frac{d_1 c_1^2}{(d_1 s - 1)^2} - 1 \quad (6.29)$$

where c_0 and c_1 are linear functions of t . For each time t , we may compute the negative root of $f(s, t) = 0$, call it $s(t)$ to indicate that it now depends on the choice of t (it is a function of t). For notational simplicity, I have dropped the overbar on s . It is therefore the case that $f(s(t), t) \equiv 0$; as a function of t , f is zero for all t . This allows us to compute the rate of change of s with respect to t . Using the chain rule from calculus,

$$f_s(s(t), t)s'(t) + f_t(s(t), t) \equiv 0 \quad (6.30)$$

where $f_s = \partial f / \partial s$ and $f_t = \partial f / \partial t$ are the first-order partial derivatives of f ,

$$f_s = \frac{-2d_0^2 c_0^2}{(d_0 s - 1)^3} + \frac{-2d_1^2 c_1^2}{(d_1 s - 1)^3}, \quad f_t = \frac{d_0(c_0^2)'}{(d_0 s - 1)^2} + \frac{d_1(c_1^2)'}{(d_1 s - 1)^2} \quad (6.31)$$

The derivative of $s(t)$ is therefore

$$s'(t) = -\frac{f_t(s(t), t)}{f_s(s(t), t)} \quad (6.32)$$

Let $\mathbf{P}(t)$ be the ellipse point closest to the origin at time t . We are trying to compute the contact time t_{contact} for which the ellipse is just touching the circle. When this happens, the ellipse point $\mathbf{P}(t_{\text{contact}})$ closest to the origin must be on the circle; that is, $|\mathbf{P}(t_{\text{contact}})|^2 - 1 = 0$. Define the function $h(t) = |\mathbf{P}(t)|^2 - 1$. As a function of s and t , the right-hand side of the equation is

$$g(s, t) = \frac{d_0^2 c_0^2 s^2}{(d_0 s - 1)^2} + \frac{d_1^2 c_1^2 s^2}{(d_1 s - 1)^2} - 1 \quad (6.33)$$

in which case $h(t) = g(s(t), t)$, where s is the negative root at time t of $f(s, t) = 0$. Using the chain rule, the first derivative of $h(t)$ is

$$h'(t) = g_s(s(t), t)s'(t) + g_t(s(t), t) = \frac{2d_0(c_0^2)'s}{d_0 s - 1} + \frac{2d_1(c_1^2)'s}{d_1 s - 1} \quad (6.34)$$

where

$$g_s = \frac{-2d_0^2 c_0^2 s}{(d_0 s - 1)^3} + \frac{-2d_1^2 c_1^2 s}{(d_1 s - 1)^3}, \quad g_t = \frac{d_0^2(c_0^2)'s^2}{(d_0 s - 1)^2} + \frac{d_1^2(c_1^2)'s^2}{(d_1 s - 1)^2} \quad (6.35)$$

The right-most equality of equation (6.34) was obtained by substituting into $g_s(s, t)s' + g_t(t, s)$ the expressions of equations (6.35), (6.32), and (6.31). I used Mathematica to simplify the resulting expression to that shown in the right-most equality.

Half the second derivative of $h''(t)$ may be computed from the right-most equality of equation (6.34),

$$\frac{h''(t)}{2} = \left[\frac{d_0 s(c_0^2)''}{d_0 s - 1} + \frac{d_1 s(c_1^2)''}{d_1 s - 1} \right] - \left[\frac{\left(\frac{d_0(c_0^2)'}{(d_0 s - 1)^2} + \frac{d_1(c_1^2)'}{(d_1 s - 1)^2} \right)^2}{\left(\frac{d_0^2 c_0^2}{(d_0 s - 1)^3} + \frac{d_1^2 c_1^2}{(d_1 s - 1)^3} \right)} \right] > 0 \quad (6.36)$$

where the positivity is guaranteed as long as s is negative, which it is by construction (it is a negative root of a function). To verify the positivity, the first square-bracketed expression is positive because $(c_0^2)'' = 2w_0^2$, $(c_1^2)'' = 2w_1^2$ and because $d_0 s / (d_0 s - 1) > 0$ and $d_1 s / (d_1 s - 1) > 0$ as long as $s < 0$. The numerator of the second square-bracketed term is positive because it is the square of an expression. The denominator is negative because $(d_0 s - 1)^3 < 0$ and $(d_1 s - 1)^3 < 0$ as long as $s < 0$. The negative

sign in front of the second square-bracketed term makes the denominator positive. Thus, the combination of the expressions on the right-hand side of equation (6.36) are positive as long as s is negative.

I have shown that $h(0) > 0$, because the initial closest point is outside the circle, and that $h''(t) > 0$, in which case $h(t)$ is a convex function. Figure 6.16 illustrates four different possibilities for the graph of h .

Because $h(t)$ is convex, we may use Newton's method to locate the smallest positive root,

$$t_0 = 0; \quad t_{i+1} = t_i - \frac{h(t_i)}{h'(t_i)}, \quad i \geq 0 \quad (6.37)$$

but with one constraint. In the lower-left and lower-right images of Figure 6.16, the iterates are guaranteed to be on the left of the root of h . Moreover, the derivatives at the iterates are always negative. During Newton's method, if we ever discover that $h'(t_i) \geq 0$, then we know we have one of the graphs of the upper-left and upper-right images of the figure. In this case, we terminate the iteration and conclude that the ellipse and circle do not intersect.

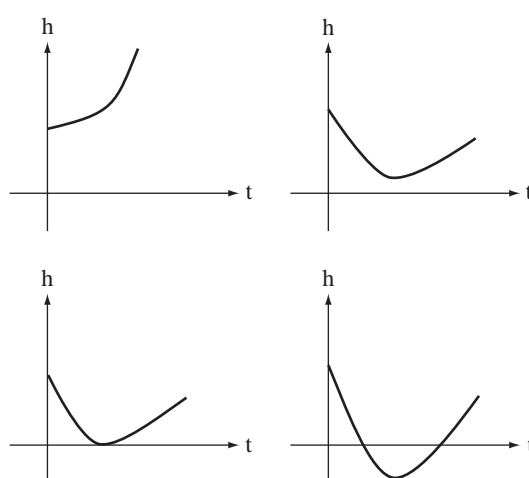


Figure 6.16 Possibilities for the graph of $h(t)$. Upper left: The ellipse is moving away from the circle, so there is no intersection at any time. Upper right: The ellipse initially moves towards the circle, but then veers away and passes it without intersection. Lower left: The ellipse moves towards the circle and just grazes it at the contact time. Lower right: The ellipse moves towards the circle, just touching the circle at contact time, and then interpenetrates for a period of time.

When we do have a contact point, it is in the transformed coordinates. Let the computed contact point be

$$\mathbf{Z}_{\text{contact}} = \mathbf{P}(t_{\text{contact}}) \quad (6.38)$$

We then compute

$$\mathbf{Y}_{\text{contact}} = R\mathbf{Z}_{\text{contact}} \quad (6.39)$$

In the original coordinate system, the contact point is

$$\mathbf{X}_{\text{contact}} = \mathbf{K}_0 + R_0 D_0^{-1/2} \mathbf{Y}_{\text{contact}} \quad (6.40)$$

Source Code

Here is Wild Magic code for computing the contact time and contact point, if they exist, for two moving ellipses.

```
double ComputeClosestPoint (const Matrix2d& D, const Vector2d& K,
                           Vector2d& closestPoint)
{
    double d0 = D[0][0], d1 = D[1][1];
    double k0 = K[0], k1 = K[1];
    double d0k0 = d0*k0;
    double d1k1 = d1*k1;
    double d0k0k0 = d0k0*k0;
    double d1k1k1 = d1k1*k1;

    if (d0k0k0 + d1k1k1 - 1.0 < 0.0)
    {
        // The ellipse contains the origin, so the ellipse and
        // circle are/ overlapping.
        return FLT_MAX;
    }

    const int maxIterations = 128;
    const double epsilon = 1e-08;

    double s = 0.0;
    int i;
    for (i = 0; i < maxIterations; ++i)
    {
        // Compute f(s).
        double tmp0 = d0*s - 1.0;
        double tmp1 = d1*s - 1.0;
        double tmp0sqr = tmp0*tmp0;
        double tmp1sqr = tmp1*tmp1;
        double f = d0k0k0/tmp0sqr + d1k1k1/tmp1sqr - 1.0;

        if (fabs(f) < epsilon)
```

```

    {
        // We have found a root.
        break;
    }

    // Compute f'(s).
    double tmp0cub = tmp0*tmp0sqr;
    double tmp1cub = tmp1*tmp1sqr;
    double fder = -2.0*(d0*d0k0k0/tmp0cub + d1*d1k1k1/tmp1cub);

    // Compute the next iterate sNext = s - f(s)/f'(s).
    s -= f/fder;
}

// assert: i < maxIterations

closestPoint[0] = d0k0*s/(d0*s - 1.0);
closestPoint[1] = d1k1*s/(d1*s - 1.0);
return s;
}

bool ComputeContact (const Matrix2d& D, const Vector2d& K,
                     const Vector2d& W, double& contactTime, Vector2d& Zcontact)
{
    double d0 = D[0][0], d1 = D[1][1];
    double k0 = K[0], k1 = K[1];
    double w0 = W[0], w1 = W[1];

    int maxIterations = 128;
    double epsilon = 1e-08;

    contactTime = 0.0;
    for (int i = 0; i < maxIterations; ++i)
    {
        // Compute h(t).
        Vector2d Kmove = K + contactTime*W;
        double s = ComputeClosestPoint(D, Kmove, Zcontact);
        double tmp0 = d0*Kmove[0]*s/(d0*s - 1.0);
        double tmp1 = d1*Kmove[1]*s/(d1*s - 1.0);
        double h = tmp0*tmp0 + tmp1*tmp1 - 1.0;

        if (fabs(h) < epsilon)
        {
            // We have found a root.
            return true;
        }
    }

    // Compute h'(t).
}

```

```

        double hder = 4.0*tmp0*w0 + 4.0*tmp1*w1;
        if (hder > 0.0)
        {
            // The ellipse cannot intersect the circle.
            return false;
        }

        // Compute the next iterate tNext = t - h(t)/h'(t).
        contactTime -= h/hder;
    }

    ComputeClosestPoint(D, K + contactTime*W, Zcontact);
    return true;
}

bool FindContact (const Ellipse2d &ellipse0,
                  const Vector2d& velocity0, const Ellipse2d &ellipse1,
                  const Vector2d& velocity1, double& contactTime,
                  Vector2d& contactPoint)
{
    // Get the parameters of ellipse0.
    Vector2d K0 = ellipse0.Center;
    Matrix2d R0(ellipse0.Axis, true);
    Matrix2d D0(
        1.0/(ellipse0.Extent[0]*ellipse0.Extent[0]),
        1.0/(ellipse0.Extent[1]*ellipse0.Extent[1]));

    // Get the parameters of ellipse1.
    Vector2d K1 = ellipse1.Center;
    Matrix2d R1(ellipse1.Axis, true);
    Matrix2d D1(
        1.0/(ellipse1.Extent[0]*ellipse1.Extent[0]),
        1.0/(ellipse1.Extent[1]*ellipse1.Extent[1]));

    // Compute K2.
    Matrix2d D0NegHalf(ellipse0.Extent[0], ellipse0.Extent[1]);
    Matrix2d D0Half(1.0/ellipse0.Extent[0], 1.0/ellipse0.Extent[1]);
    Vector2d K2 = (D0Half*(K1 - K0))*R0;

    // Compute M2.
    Matrix2d R1TD0NegHalfR0 = R1.TransposeTimes(D0NegHalf*R0);
    Matrix2d M2 = R1TD0NegHalfR0.TransposeTimes(D1)*R1TD0NegHalfR0;

    // Factor M2 = R*D*R^T.
    Matrix2d R, D;
    M2.EigenDecomposition(R, D);

    // Compute K.
}

```

```

Vector2d K = K2*R;

// Compute W.
Vector2d W = ((D0Half*(velocity1 - velocity0))*R0)*R;

// Transformed ellipse0 is Z^T*Z = 1 and transformed ellipself is
// (Z-K)^T*D*(Z-K) = 0.

// Compute the initial closest point.
Vector2d P0;
if (ComputeClosestPoint(D, K, P0) >= 0.0)
{
    // The ellipse contains the origin, so the ellipses were not
    // separated.
    return false;
}
double dist0 = P0.Dot(P0) - 1.0;
if (dist0 < 0.0)
{
    // The ellipses are not separated.
    return false;
}

Vector2d Zcontact;
if (!ComputeContact(D, K, W, contactTime, Zcontact))
{
    return false;
}

// Transform contactPoint back to original space.
contactPoint = K0 + R0*D0NegHalf*R*Zcontact;
return true;
}

```

Intersection of Moving Ellipsoids

The reduction of swept ellipses to the circle and axis-aligned ellipse is shown in [equations \(6.8\)](#) through [\(6.17\)](#). The construction is independent of dimension, so it also applies to swept ellipsoids.

Using the same notation as before, let $\mathbf{P} = (p_0, p_1, p_2)$, $\mathbf{K} = (k_0, k_1, k_2)$, and $D = \text{Diag}(d_0, d_1, d_2)$. [Equation \(6.20\)](#) becomes

$$0 = Q(\mathbf{P}) = \frac{d_0 k_0^2}{(d_0 s - 1)^2} + \frac{d_1 k_1^2}{(d_1 s - 1)^2} + \frac{d_2 k_2^2}{(d_2 s - 1)^2} - 1 \quad (6.41)$$

The function whose negative root determines the closest ellipse point is now as shown together with its derivatives

$$f(s) = \frac{d_0 k_0^2}{(d_0 s - 1)^2} + \frac{d_1 k_1^2}{(d_1 s - 1)^2} + \frac{d_2 k_2^2}{(d_2 s - 1)^2} - 1 \quad (6.42)$$

and

$$f'(s) = \frac{-2d_0^2 k_0^2}{(d_0 s - 1)^3} + \frac{-2d_1^2 k_1^2}{(d_1 s - 1)^3} + \frac{-2d_2^2 k_2^2}{(d_2 s - 1)^3} \quad (6.43)$$

and

$$f''(s) = \frac{6d_0^3 k_0^2}{(d_0 s - 1)^4} + \frac{6d_1^3 k_1^2}{(d_1 s - 1)^4} + \frac{6d_2^3 k_2^2}{(d_2 s - 1)^4} > 0 \quad (6.44)$$

so $f(s)$ is a convex function that has a unique negative root \bar{s} . Newton's method may be used to compute robustly \bar{s} .

The moving center of the axis-aligned ellipsoid is $\mathbf{C}(t) = (c_0, c_1, c_2) = \mathbf{K} + t\mathbf{W}$, just as in equation (6.28). The function $h(t)$ and its derivative $h'(t)$ are

$$h(t) = \frac{d_0^2 c_0^2 s^2}{(d_0 s - 1)^2} + \frac{d_1^2 c_1^2 s^2}{(d_1 s - 1)^2} + \frac{d_2^2 c_2^2 s^2}{(d_2 s - 1)^2} - 1 \quad (6.45)$$

and

$$h'(t) = \frac{2d_0(c_0^2)'s}{d_0 s - 1} + \frac{2d_1(c_1^2)'s}{d_1 s - 1} + \frac{2d_2(c_2^2)'s}{d_2 s - 1} \quad (6.46)$$

It may be shown that $h''(t) > 0$, so $h(t)$ is a convex function. Newton's method may be used to compute robustly t_{contact} .

Once we have the contact point, equations (6.38) through (6.40) may be used to transform back to the original coordinates.

Source Code

Here is Wild Magic code for computing the contact time and contact point, if they exist, for two moving ellipsoids.

```
double ComputeClosestPoint (const Matrix3d& D, const Vector3d& K,
                           Vector3d& closestPoint)
{
    double d0 = D[0][0], d1 = D[1][1], d2 = D[2][2];
    double k0 = K[0], k1 = K[1], k2 = K[2];
    double d0k0 = d0*k0;
    double d1k1 = d1*k1;
    double d2k2 = d2*k2;
    double d0k0k0 = d0k0*k0;
    double d1k1k1 = d1k1*k1;
    double d2k2k2 = d2k2*k2;
```

```

if (d0k0k0 + d1k1k1 + d2k2k2 - 1.0 < 0.0)
{
    // The ellipsoid contains the origin, so the ellipsoid and
    // sphere are overlapping.
    return FLT_MAX;
}

const int maxIterations = 128;
const double epsilon = 1e-08;

double s = 0.0;
int i;
for (i = 0; i < maxIterations; ++i)
{
    // Compute f(s).
    double tmp0 = d0*s - 1.0;
    double tmp1 = d1*s - 1.0;
    double tmp2 = d2*s - 1.0;
    double tmp0sqr = tmp0*tmp0;
    double tmp1sqr = tmp1*tmp1;
    double tmp2sqr = tmp2*tmp2;
    double f = d0k0k0/tmp0sqr + d1k1k1/tmp1sqr +
        d2k2k2/tmp2sqr - 1.0;

    if (fabs(f) < epsilon)
    {
        // We have found a root.
        break;
    }

    // Compute f'(s).
    double tmp0cub = tmp0*tmp0sqr;
    double tmp1cub = tmp1*tmp1sqr;
    double tmp2cub = tmp2*tmp2sqr;
    double fder = -2.0*(d0*d0k0k0/tmp0cub + d1*d1k1k1/tmp1cub
        + d2*d2k2k2/tmp2cub);

    // Compute the next iterate sNext = s - f(s)/f'(s).
    s -= f/fder;
}

// assert: i < maxIterations

closestPoint[0] = d0k0*s/(d0*s - 1.0);
closestPoint[1] = d1k1*s/(d1*s - 1.0);
closestPoint[2] = d2k2*s/(d2*s - 1.0);
return s;
}

```

```

bool ComputeContact (const Matrix3d& D, const Vector3d& K,
                     const Vector3d& W, double& contactTime, Vector3d& Zcontact)
{
    double d0 = D[0][0], d1 = D[1][1], d2 = D[2][2];
    double k0 = K[0], k1 = K[1], k2 = K[2];
    double w0 = W[0], w1 = W[1], w2 = W[2];

    int maxIterations = 128;
    double epsilon = 1e-08;

    contactTime = 0.0;
    for (int i = 0; i < maxIterations; ++i)
    {
        // Compute h(t).
        Vector3d Kmove = K + contactTime*W;
        double s = ComputeClosestPoint(D, Kmove, Zcontact);
        double tmp0 = d0*Kmove[0]*s/(d0*s - 1.0);
        double tmp1 = d1*Kmove[1]*s/(d1*s - 1.0);
        double tmp2 = d2*Kmove[2]*s/(d2*s - 1.0);
        double h = tmp0*tmp0 + tmp1*tmp1 + tmp2*tmp2 - 1.0;

        if (fabs(h) < epsilon)
        {
            // We have found a root.
            return true;
        }

        // Compute h'(t).
        double hder = 4.0*tmp0*w0 + 4.0*tmp1*w1 + 4.0*tmp2*w2;
        if (hder > 0.0)
        {
            // The ellipsoid cannot intersect the sphere.
            return false;
        }

        // Compute the next iterate tNext = t - h(t)/h'(t).
        contactTime -= h/hder;
    }

    ComputeClosestPoint(D, K + contactTime*W, Zcontact);
    return true;
}

bool FindContact (const Ellipsoid3d &ellipsoid0,
                  const Vector3d& velocity0, const Ellipsoid3d &ellipsoid1,
                  const Vector3d& velocity1, double& contactTime,
                  Vector3d& contactPoint)
{

```

```

// Get the parameters of ellipsoid0.
Vector3d K0 = ellipsoid0.Center;
Matrix3d R0(ellipsoid0.Axis, true);
Matrix3d D0(
    1.0/(ellipsoid0.Extent[0]*ellipsoid0.Extent[0]),
    1.0/(ellipsoid0.Extent[1]*ellipsoid0.Extent[1]),
    1.0/(ellipsoid0.Extent[2]*ellipsoid0.Extent[2]));

// Get the parameters of ellipsoid1.
Vector3d K1 = ellipsoid1.Center;
Matrix3d R1(ellipsoid1.Axis, true);
Matrix3d D1(
    1.0/(ellipsoid1.Extent[0]*ellipsoid1.Extent[0]),
    1.0/(ellipsoid1.Extent[1]*ellipsoid1.Extent[1]),
    1.0/(ellipsoid1.Extent[2]*ellipsoid1.Extent[2]));

// Compute K2.
Matrix3d D0NegHalf(ellipsoid0.Extent[0], ellipsoid0.Extent[1],
    ellipsoid0.Extent[2]);
Matrix3d D0Half(
    1.0/ellipsoid0.Extent[0],
    1.0/ellipsoid0.Extent[1],
    1.0/ellipsoid0.Extent[2]);
Vector3d K2 = (D0Half*(K1 - K0))*R0;

// Compute M2.
Matrix3d R1TD0NegHalfR0 = R1.TransposeTimes(D0NegHalf*R0);
Matrix3d M2 = R1TD0NegHalfR0.TransposeTimes(D1)*R1TD0NegHalfR0;

// Factor M2 = R*D*R^T.
Matrix3d R, D;
M2.EigenDecomposition(R, D);

// Compute K.
Vector3d K = K2*R;

// Compute W.
Vector3d W = ((D0Half*(velocity1 - velocity0))*R0)*R;

// Transformed ellipsoid0 is Z^T*Z = 1 and transformed
// ellipsoid1 is (Z-K)^T*D*(Z-K) = 0.

// Compute the initial closest point.
Vector3d P0;
if (ComputeClosestPoint(D, K, P0) >= 0.0)
{
    // The ellipsoid contains the origin, so the ellipsoids
    // were not separated.
}

```

```

        return false;
    }
    double dist0 = P0.Dot(P0) - 1.0;
    if (dist0 < 0.0)
    {
        // The ellipsoids are not separated.
        return false;
    }

    Vector3d Zcontact;
    if (!ComputeContact(D, K, W, contactTime, Zcontact))
    {
        return false;
    }

    // Transform contactPoint back to original space.
    contactPoint = K0 + R0*D0NegHalf*R*Zcontact;
    return true;
}

```

6.3.4 CYLINDERS

Practitioners also sometimes consider using cylinders as bounding volumes. The test-intersection query for two cylinders is even more difficult to derive than that for ellipsoids. My advice is to avoid cylinders and try to use capsules instead. That said, this section shows how to formulate an algorithm that uses the method of separating axes, although the construction is more complicated than one encounters when separating convex polyhedra (see [Section 6.4](#)). The resulting algorithm is a fairly expensive one.

Representation of a Cylinder

A cylinder has a center point \mathbf{C} , unit-length axis direction \mathbf{W} , radius r and height h . The end disks of the cylinder are centered at $\mathbf{C} \pm (h/2)\mathbf{W}$. Let \mathbf{U} and \mathbf{V} be any unit-length vectors for which $\{\mathbf{U}, \mathbf{V}, \mathbf{W}\}$ is a right-handed set of orthonormal vectors. That is, the vectors are unit length, mutually orthogonal, and $\mathbf{W} = \mathbf{U} \times \mathbf{V}$. Points in the cylinder are parameterized by

$$\mathbf{X}(\theta, t) = \mathbf{C} + (s \cos \theta) \mathbf{U} + (s \sin \theta) \mathbf{V} + t \mathbf{W}, \quad \theta \in [0, 2\pi), \quad 0 \leq s \leq r, \quad |t| \leq h/2 \quad (6.47)$$

The projections of a cylinder onto a line are determined solely by the cylinder wall, not the end disks.

The choice of \mathbf{U} and \mathbf{V} is arbitrary. Intersection queries between cylinders should be independent of this choice, but some of the algorithms are better handled if a

choice is made. A quadratic equation that represents the cylinder wall is $(\mathbf{X} - \mathbf{C})^T(I - \mathbf{W}\mathbf{W}^T)(\mathbf{X} - \mathbf{C}) = r^2$. The boundedness of the cylinder is specified by $|\mathbf{W} \cdot (\mathbf{X} - \mathbf{C})| \leq h/2$. This representation is dependent only on \mathbf{C} , \mathbf{W} , r , and h .

Nonintersection of Convex Objects by Projection Methods

Consider the problem of determining whether two convex objects in 3D are intersecting. This *test-intersection* geometric query is concerned only about whether the objects intersect, not about where they intersect. The latter problem is said to be a *find-intersection* geometric query. This document is about the test-intersection query for two bounded cylinders.

Separation by Projection onto a Line

A test for nonintersection of two convex objects is simply stated: If there exists a line for which the intervals of projection of the two objects onto that line do not intersect, then the objects do not intersect. Such a line is called a *separating line* or, more commonly, a *separating axis*. The translation of a separating line is also a separating line, so it is sufficient to consider lines that contain the origin. Given a line containing the origin and with unit-length direction \mathbf{D} , the projection of a compact convex set C onto the line is the interval

$$I = [\lambda_{\min}(\mathbf{D}), \lambda_{\max}(\mathbf{D})] = [\min\{\mathbf{D} \cdot \mathbf{X} : \mathbf{X} \in C\}, \max\{\mathbf{D} \cdot \mathbf{X} : \mathbf{X} \in C\}]$$

Two compact convex sets C_0 and C_1 are separated if there exists a direction \mathbf{D} such that the projection intervals I_0 and I_1 do not intersect, $I_0 \cap I_1 = \emptyset$. Specifically they do not intersect when

$$\lambda_{\min}^{(0)}(\mathbf{D}) > \lambda_{\max}^{(1)}(\mathbf{D}) \text{ or } \lambda_{\max}^{(0)}(\mathbf{D}) < \lambda_{\min}^{(1)}(\mathbf{D}). \quad (6.48)$$

The superscripts correspond to the indices of the convex set. Although the comparisons are made where \mathbf{D} has unit length, the comparison results are invariant to changes in length of the vector. This follows from $\lambda_{\min}(t\mathbf{D}) = t\lambda_{\min}(\mathbf{D})$ and $\lambda_{\max}(t\mathbf{D}) = t\lambda_{\max}(\mathbf{D})$ for $t > 0$. The Boolean value of the pair of comparisons is also invariant when \mathbf{D} is replaced by the opposite direction $-\mathbf{D}$. This follows from $\lambda_{\min}(-\mathbf{D}) = -\lambda_{\max}(\mathbf{D})$ and $\lambda_{\max}(-\mathbf{D}) = -\lambda_{\min}(\mathbf{D})$. When \mathbf{D} is not unit length, the intervals obtained for the separating axis tests are not the projections of the object onto the line; rather, they are scaled versions of the projection intervals. I make no distinction in this document between the scaled projection and regular projection. I will also use the terminology that the direction vector for a separating axis is called a *separating direction* and is not necessarily unit length.

For a pair of convex polyhedra, only a finite set of direction vectors needs to be considered for separation tests. That set includes the normal vectors to the faces of the

polyhedra and vectors generated by a cross product of two edges, one from each polyhedron. I am aware of no general theory for constructing the smallest set of potential separating directions for other convex objects.

In equation (6.48), allowing equality means that the two convex objects might be separated, but they also might be just touching. The intersection set does not have volume to it, so one might say that the objects are not overlapping. In this document, I will allow the equality because it allows for some simplification of the algorithm for separation testing. If you need strict separation, the algorithm may be modified appropriately to support this.

Projection of a Cylinder onto a Line

Let the line be $\lambda \mathbf{D}$ where \mathbf{D} is a nonzero vector. The projection of a cylinder wall point onto the line is

$$\lambda(\theta, t) = \mathbf{D} \cdot \mathbf{X}(\theta, t) = \mathbf{D} \cdot \mathbf{C} + (r \cos \theta) \mathbf{D} \cdot \mathbf{U} + (r \sin \theta) \mathbf{D} \cdot \mathbf{V} + t \mathbf{D} \cdot \mathbf{W} \quad (6.49)$$

The interval of projection has endpoints determined by the extreme values of this expression. The maximum value occurs when all three terms involving the parameters are made as large as possible. The t -term has a maximum of $(h/2)|\mathbf{D} \cdot \mathbf{W}|$. The θ -terms, not including the radius, can be viewed as a dot product $(\cos \theta, \sin \theta) \cdot (\mathbf{D} \cdot \mathbf{U}, \mathbf{D} \cdot \mathbf{V})$. This is maximized when $(\cos \theta, \sin \theta)$ is in the same direction as $(\mathbf{D} \cdot \mathbf{U}, \mathbf{D} \cdot \mathbf{V})$. Therefore,

$$(\cos \theta, \sin \theta) = \frac{(\mathbf{D} \cdot \mathbf{U}, \mathbf{D} \cdot \mathbf{V})}{\sqrt{(\mathbf{D} \cdot \mathbf{U})^2 + (\mathbf{D} \cdot \mathbf{V})^2}}$$

and the maximum projection value is

$$\lambda_{\max} = \mathbf{D} \cdot \mathbf{C} + r \sqrt{|\mathbf{D}|^2 - (\mathbf{D} \cdot \mathbf{W})^2} + (h/2)|\mathbf{D} \cdot \mathbf{W}| \quad (6.50)$$

The construction uses the identities

$$\begin{aligned} \mathbf{D} &= (\mathbf{D} \cdot \mathbf{U})\mathbf{U} + (\mathbf{D} \cdot \mathbf{V})\mathbf{V} + (\mathbf{D} \cdot \mathbf{W})\mathbf{W} \\ (\mathbf{D} \cdot \mathbf{U})^2 + (\mathbf{D} \cdot \mathbf{V})^2 + (\mathbf{D} \cdot \mathbf{W})^2 &= |\mathbf{D}|^2 \\ \mathbf{U}\mathbf{U}^T + \mathbf{V}\mathbf{V}^T + \mathbf{W}\mathbf{W}^T &= I \end{aligned} \quad (6.51)$$

where I is the 3×3 identity matrix. The minimum projection value is similarly derived,

$$\lambda_{\min} = \mathbf{D} \cdot \mathbf{C} - r \sqrt{|\mathbf{D}|^2 - (\mathbf{D} \cdot \mathbf{W})^2} - (h/2)|\mathbf{D} \cdot \mathbf{W}|$$

Separating Axis Tests for Two Cylinders

Given two cylinders with centers \mathbf{C}_i , axis directions \mathbf{W}_i , radii r_i , and heights h_i , for $i = 0, 1$, the cylinders are separated if there exists a nonzero direction \mathbf{D} such that

either

$$\begin{aligned}\mathbf{D} \cdot \mathbf{C}_0 - r_0 \sqrt{|\mathbf{D}|^2 - (\mathbf{D} \cdot \mathbf{W}_0)^2} - (h_0/2)|\mathbf{D} \cdot \mathbf{W}_0| &\geq \\ \mathbf{D} \cdot \mathbf{C}_1 + r_1 \sqrt{|\mathbf{D}|^2 - (\mathbf{D} \cdot \mathbf{W}_1)^2} + (h_1/2)|\mathbf{D} \cdot \mathbf{W}_1| &\end{aligned}$$

or

$$\begin{aligned}\mathbf{D} \cdot \mathbf{C}_0 + r_0 \sqrt{|\mathbf{D}|^2 - (\mathbf{D} \cdot \mathbf{W}_0)^2} + (h_0/2)|\mathbf{D} \cdot \mathbf{W}_0| &\leq \\ \mathbf{D} \cdot \mathbf{C}_1 - r_1 \sqrt{|\mathbf{D}|^2 - (\mathbf{D} \cdot \mathbf{W}_1)^2} - (h_1/2)|\mathbf{D} \cdot \mathbf{W}_1| &\end{aligned}$$

These are just a restatement of [equation \(6.48\)](#) for bounded cylinders.

Defining $\Delta = \mathbf{C}_1 - \mathbf{C}_0$, these tests can be combined into a single expression

$$f(\mathbf{D}) = r_0|P_0\mathbf{D}| + r_1|P_1\mathbf{D}| + (h_0/2)|\mathbf{D} \cdot \mathbf{W}_0| + (h_1/2)|\mathbf{D} \cdot \mathbf{W}_1| - |\mathbf{D} \cdot \Delta| \leq 0 \quad (6.52)$$

where $P_i = I - \mathbf{W}_i \mathbf{W}_i^T$ for $i = 0, 1$ are projection matrices.

If $\Delta = 0$, then $f > 0$. This is geometrically obvious because two cylinders with the same center always intersect. The remainder of the discussion assumes $\Delta \neq 0$. If \mathbf{D} is perpendicular to Δ , then $f(\mathbf{D}) > 0$. This shows that any line perpendicular to the line containing the two cylinder centers can never be a separating axis. This is also clear geometrically. The line of sight $\mathbf{C}_0 + s\Delta$ intersects both cylinders at their centers. If you project the two cylinders onto the plane $\Delta \cdot (\mathbf{X} - \mathbf{C}_0) = 0$, both regions of projection overlap. No matter which line you choose containing \mathbf{C}_0 in this plane, the line intersects both projection regions.

If \mathbf{D} is a separating direction, then $f(\mathbf{D}) \leq 0$. Observe that $f(t\mathbf{D}) = tf(\mathbf{D})$ for $t > 0$, so $f(t\mathbf{D}) \leq 0$. This is consistent with the geometry of the problem. Any nonzero multiple of a separating direction must itself be a separating direction. This allows us to restrict our attention to the unit sphere, $|\mathbf{D}| = 1$. Function f is continuous on the unit sphere, a compact set, so f must attain its minimum at some point on the sphere. This is a minimization problem in two dimensions, but the spherical geometry complicates the analysis somewhat. As we will see later, different restrictions on the set of potential separating directions can be made that yield minimization problems in a plane rather than on a sphere.

The analysis of f involves computing its derivatives to determine its critical points. These are points for which the derivative is zero or undefined. The latter category is easy to specify. The derivatives are undefined when any of the terms inside the five absolute value signs is zero. Thus, the derivatives are undefined at $\mathbf{W}_0, \mathbf{W}_1$, at vectors that are perpendicular to \mathbf{W}_0 , at vectors that are perpendicular to \mathbf{W}_1 , and at vectors that are perpendicular to Δ . I already argued that $f > 0$ for vectors perpendicular to Δ , so we may ignore this case.

The next two sections describe how to handle those directions for which the derivatives of f are undefined. The section after those describes how to handle those directions for which the derivatives of f are defined.

Separation Tests Involving the Cylinder Axis Directions

The cylinder axis directions themselves can be tested first for separation. The tests for separation are

$$f(\mathbf{W}_0) = r_1|\mathbf{W}_0 \times \mathbf{W}_1| + (h_0/2) + (h_1/2)|\mathbf{W}_0 \cdot \mathbf{W}_1| - |\mathbf{W}_0 \cdot \Delta| \leq 0$$

and

$$f(\mathbf{W}_1) = r_0|\mathbf{W}_0 \times \mathbf{W}_1| + (h_0/2)|\mathbf{W}_0 \cdot \mathbf{W}_1| + (h_1/2) - |\mathbf{W}_1 \cdot \Delta| \leq 0$$

If either condition is satisfied, the cylinders are separated.

The test for direction $\mathbf{W}_0 \times \mathbf{W}_1$ does not require many more operations and might lead to a quick no-intersection test,

$$f(\mathbf{W}_0 \times \mathbf{W}_1) = (r_0 + r_1)|\mathbf{W}_0 \times \mathbf{W}_1| - |\mathbf{W}_0 \times \mathbf{W}_1 \cdot \Delta| \leq 0$$

assuming that $\mathbf{W}_0 \times \mathbf{W}_1 \neq \mathbf{0}$. This vector is one for which the derivatives of f are undefined.

If \mathbf{W}_0 and \mathbf{W}_1 are parallel, then $\mathbf{W}_0 \times \mathbf{W}_1 = \mathbf{0}$, $|\mathbf{W}_0 \cdot \mathbf{W}_1| = 1$, and $|\mathbf{W}_0 \times \mathbf{W}_1|^2 = 1 - (\mathbf{W}_0 \cdot \mathbf{W}_1)^2$. The test for separation by \mathbf{W}_0 is

$$f(\mathbf{W}_0) = (h_0 + h_1)/2 - |\mathbf{W}_0 \cdot \Delta| \leq 0$$

If $f(\mathbf{W}_0) \geq 0$, the two cylinders are potentially separated by a direction that is perpendicular to \mathbf{W}_0 . Geometrically it is enough to determine whether or not the circles of projection of the cylinders onto the plane $\mathbf{W}_0 \cdot \mathbf{X} = \mathbf{0}$ intersect. These circles are disjoint if and only if the length of the projection of Δ onto that plane is larger than the sum of the radii of the circles. The projection of Δ is $\Delta - (\mathbf{W}_0 \cdot \Delta)\mathbf{W}_0$ and the separation test is

$$|\Delta - (\mathbf{W}_0 \cdot \Delta)\mathbf{W}_0| \geq r_0 + r_1$$

In fact, this test is equivalent to the separating axis test for the direction $\mathbf{D} = \Delta - (\mathbf{W}_0 \cdot \Delta)\mathbf{W}_0$. The test has a common factor $|\mathbf{D}|$ that may be divided out of the expression.

For the remainder of this document I assume that \mathbf{W}_0 and \mathbf{W}_1 are not parallel.

Separation Tests Involving the Cylinder Axis Perpendiculars

We now consider the directions \mathbf{D} perpendicular to \mathbf{W}_0 . The function of equation (6.52) becomes

$$f(\mathbf{D}) = r_0|\mathbf{D}| + r_1|P_0\mathbf{D}| + (h_1/2)|\mathbf{D} \cdot \mathbf{W}_1| - |\mathbf{D} \cdot \Delta| \quad (6.53)$$

We may choose $\mathbf{D}(\theta) = (\cos \theta)\mathbf{U}_0 + (\sin \theta)\mathbf{V}_0$, where $\{\mathbf{U}_0, \mathbf{V}_0, \mathbf{W}_0\}$ is a right-handed orthonormal set, giving us a circle of directions to analyze. We may then define $g(\theta) = f(\mathbf{D}(\theta))$. The analysis of the derivative of g in order to determine critical

points is complicated by the presence of the four absolute value signs. We discussed previously the cases when the derivative is undefined (in terms of f itself). To compute symbolically the values θ where $g'(\theta) = 0$ is an intractable task.

An alternative parameterization is the following and is equivalent to testing directions on a hemicircle. It is sufficient to consider only a hemicircle because $-\mathbf{D}$ is a separating direction if and only if \mathbf{D} is a separating direction. By assumption, \mathbf{W}_0 and \mathbf{W}_1 are not parallel. A normalized projection of \mathbf{W}_1 onto the plane perpendicular to \mathbf{W}_0 is

$$\mathbf{V}_0 = \frac{\mathbf{W}_1 - (\mathbf{W}_0 \cdot \mathbf{W}_1)\mathbf{W}_0}{|\mathbf{W}_1 - (\mathbf{W}_0 \cdot \mathbf{W}_1)\mathbf{W}_0|}$$

Define $\mathbf{U}_0 = \mathbf{V}_0 \times \mathbf{W}_0$. The set $\{\mathbf{U}_0, \mathbf{V}_0, \mathbf{W}_0\}$ is a right-handed orthonormal basis. Notice also that

$$\mathbf{U}_0 = \frac{\mathbf{W}_1 \times \mathbf{W}_0}{|\mathbf{W}_1 \times \mathbf{W}_0|}$$

Define $\mathbf{D}(t) = (1-t)\mathbf{U}_0 + t\mathbf{V}_0$ for $t \in [0, 1]$, which are nonzero vectors whose normalized values cover one quarter of a circle. Define

$$\begin{aligned} F(t) &= f(\mathbf{D}(t)) \\ &= r_0 \sqrt{(1-t)^2 + t^2} + r_1 \sqrt{(1-t)^2 + c_1^2 t^2} + h_1 b_1 t / 2 \\ &\quad - |(1-t)a_2 + tb_2| \end{aligned} \quad (6.54)$$

where $a_1 = \mathbf{W}_1 \cdot \mathbf{U}_0 = 0$, $b_1 = \mathbf{W}_1 \cdot \mathbf{V}_0 > 0$, $c_1 = \mathbf{W}_1 \cdot \mathbf{W}_0$, $a_2 = \Delta \cdot \mathbf{U}_0$, and $b_2 = \Delta \cdot \mathbf{V}_0$. Observe that the absolute value signs were discarded for the term corresponding to $|\Delta \cdot \mathbf{W}_1|$. This is a result of knowing that the directions \mathbf{D} for the hemicircle form an acute angle with \mathbf{W}_1 , so $\mathbf{D} \cdot \mathbf{W}_1 \geq 0$. I have also used the fact that $1 = a_1^2 + b_1^2 + c_1^2 = b_1^2 + c_1^2$, in which case $1 - b_1^2 = c_1^2$.

The first derivative of $F(t)$ is

$$\begin{aligned} F'(t) &= \frac{r_0(2t-1)}{\sqrt{(1-t)^2 + t^2}} + \frac{r_1((1+c_1^2)t-1)}{\sqrt{(1-t)^2 + c_1^2 t^2}} + h_1 b_1 / 2 \\ &\quad - (b_2 - a_2) \text{Sign}((1-t)a_2 + tb_2) \end{aligned} \quad (6.55)$$

where $\text{Sign}(x) = +1$ when $x > 0$, -1 when $x < 0$, and 0 when $x = 0$. The second derivative is

$$F''(t) = \frac{3r_0}{((1-t)^2 + t^2)^{3/2}} + \frac{r_1 c_1^2}{((1-t)^2 + c_1^2 t^2)^{3/2}} \quad (6.56)$$

The warning is that $F'(t)$ and $F''(t)$ are discontinuous when $\text{Sign}((1-t)a_2 + b_2) = 0$. Notice that $F''(t) > 0$, so $F(t)$ is a *strictly convex function*. One implication is that $F'(t)$ is a strictly increasing function. Another is that $F(t)$ must have a global minimum that

occurs for exactly one t on the interval $[0, 1]$. The minimum is either $F(0)$, $F(1)$, or $F(\bar{t})$ where $F'(\bar{t})$ is zero or undefined. If the global minimum is nonpositive, we have a separating direction.

The algorithm is as follows. If $F(0) \leq 0$, then \mathbf{U}_0 is a separating direction. If $F(1) \leq 0$, then \mathbf{V}_0 is a separating direction. Otherwise, $F(0) > 0$ and $F(1) > 0$. If $F'(0) \geq 0$, then the convexity of F guarantees that $F(0)$ is the global minimum. Since $F(0) > 0$, there is no separation. If $F'(1) \leq 0$, then the convexity of F guarantees that $F(1)$ is the global minimum. Since $F(1) > 0$, there is no separation. We are now at the point where $F(0) > 0$, $F(1) > 0$, $F'(0) < 0$, and $F'(1) > 0$. A global minimum must occur at an interior point $\bar{t} \in [0, 1]$ for which $F'(\bar{t})$ is zero or undefined. Use bisection based on the signs of $F'(t)$ to locate \bar{t} . At each iterate t_i it is worthwhile to test whether $F(t_i) \leq 0$. For if it is, we have found a separating direction. If the bisection terminates and $F(\bar{t}) > 0$, there is no separation.

The other line segment of directions to process has $\mathbf{D}(t) = (1-t)(-\mathbf{U}_0) + t\mathbf{V}$. The only thing that changes in equations (6.54), (6.55), and (6.56) is that a_2 is replaced by $-a_2$. The bisection algorithm is applied once again to compute the global minimum of F and test whether or not F is nonpositive at the iterates.

The same algorithm is applied when the two cylinders reverse roles.

Separation Tests Involving Other Directions

The idea is similar to what was discussed previously – to compute global minima of functions and determine whether any of the bisection iterates produces a separating direction.

The symmetry $f(-\mathbf{D}) = f(\mathbf{D})$ implies that we only need to analyze f on a hemisphere; the other hemisphere values are determined automatically. Since $f > 0$ on the great circle of vectors that are perpendicular to Δ , we can restrict our attention to the hemisphere whose pole is $\mathbf{W} = \Delta/|\Delta|$. Choose \mathbf{U} and \mathbf{V} such that the set $\{\mathbf{U}, \mathbf{V}, \mathbf{W}\}$ is right-handed and orthonormal.

The hemisphere is processed by decomposing it into octants and analyzing a function that is defined on a triangular surface in each octant. For example, in the first octant define $\mathbf{D}(s, t) = s\mathbf{U} + t\mathbf{V} + (1-s-t)\mathbf{W}$ and $G(s, t) = f(\mathbf{D}(s, t))$ for $s \geq 0$, $t \geq 0$, and $s+t \leq 1$,

$$\begin{aligned} G(s, t) = & r_0 \sqrt{s^2 + t^2 + (1-s-t)^2 - (a_0 s + b_0 t + c_0(1-s-t))^2} \\ & + r_1 \sqrt{s^2 + t^2 + (1-s-t)^2 - (a_1 s + b_1 t + c_1(1-s-t))^2} \\ & + (h_0/2)|a_0 s + b_0 t + c_0(1-s-t)| \\ & + (h_1/2)|a_1 s + b_1 t + c_1(1-s-t)| \\ & - (1-s-t)|\Delta| \end{aligned} \tag{6.57}$$

It turns out that $G(s, t)$ is a convex function. To simplify the presentation, define

$$L_i(s, t) = a_i s + b_i t + c_i(1-s-t)$$

and

$$Q_i(s, t) = s^2 + t^2 + (1 - s - t)^2 - (a_i s + b_i t + c_i(1 - s - t))^2$$

for $i = 0, 1$. The first-order derivatives are

$$\begin{aligned} Q_{i,s} &= 2s - 2(1 - s - t) - 2(a_i - c_i)(a_i s + b_i t + c_i(1 - s - t)) \\ Q_{i,t} &= 2t - 2(1 - s - t) - 2(b_i - c_i)(a_i s + b_i t + c_i(1 - s - t)) \end{aligned}$$

and the second-order derivatives are

$$\begin{aligned} Q_{i,ss} &= 4 - 2(a_i - c_i)^2 \\ Q_{i,st} &= 2 - 2(a_i - c_i)(b_i - c_i) \\ Q_{i,tt} &= 4 - 2(b_i - c_i)^2 \end{aligned}$$

The function G becomes

$$G(s, t) = r_0 \sqrt{Q_0} + r_1 \sqrt{Q_1} + (h_0/2)|L_0| + (h_1/2)|L_1| - (1 - s - t)|\Delta|$$

The first-order derivatives are

$$\begin{aligned} G_s &= r_0 \frac{Q_{0,s}}{2\sqrt{Q_0}} + r_1 \frac{Q_{1,s}}{2\sqrt{Q_1}} + (h_0/2)(a_0 - c_0)\text{Sign}(L_0) + (h_1/2)(a_1 - c_1)\text{Sign}(L_1) + |\Delta| \\ G_t &= r_0 \frac{Q_{0,t}}{2\sqrt{Q_0}} + r_1 \frac{Q_{1,t}}{2\sqrt{Q_1}} + (h_0/2)(b_0 - c_0)\text{Sign}(L_0) + (h_1/2)(b_1 - c_1)\text{Sign}(L_1) + |\Delta| \end{aligned}$$

The second-order derivatives are

$$\begin{aligned} G_{ss} &= r_0 \frac{2Q_0 Q_{0,ss} - Q_{0,s} Q_{0,s}}{4Q_0^{3/2}} + r_1 \frac{2Q_1 Q_{1,ss} - Q_{1,s} Q_{1,s}}{4Q_1^{3/2}} \\ G_{st} &= r_0 \frac{2Q_0 Q_{0,st} - Q_{0,s} Q_{0,t}}{4Q_0^{3/2}} + r_1 \frac{2Q_1 Q_{1,st} - Q_{1,s} Q_{1,t}}{4Q_1^{3/2}} \\ G_{tt} &= r_0 \frac{2Q_0 Q_{0,tt} - Q_{0,t} Q_{0,t}}{4Q_0^{3/2}} + r_1 \frac{2Q_1 Q_{1,tt} - Q_{1,t} Q_{1,t}}{4Q_1^{3/2}} \end{aligned}$$

where it is understood that the first- and second-order derivatives are discontinuous when $\text{Sign}(L_i) = 0$. If we define

$$\eta_i(s, t) = \sqrt{Q_i(s, t)}$$

then

$$G_{ss} = r_0 \eta_{0,ss} + r_1 \eta_{1,ss}, \quad G_{st} = r_0 \eta_{0,st} + r_1 \eta_{1,st}, \quad G_{tt} = r_0 \eta_{0,tt} + r_1 \eta_{1,tt}$$

The factorizations in the following were computed with the help of Mathematica, although that program needed quite a bit of manual guidance to complete the tasks. It was demonstrated that

$$Q_i^{3/2} \eta_{i,ss} = (2Q_i Q_{i,ss} - Q_{i,s} Q_{i,s})/4 = ((a_i + b_i + c_i)t - b_i)^2 \geq 0$$

and

$$Q_i^{3/2} \eta_{i,tt} = (2Q_i Q_{i,tt} - Q_{i,t} Q_{i,t})/4 = ((a_i + b_i + c_i)s - a_i)^2 \geq 0$$

These establish the facts that $G_{ss} \geq 0$ and $G_{tt} \geq 0$. The more challenging work was to factor $G_{ss} G_{tt} - G_{st}^2$. It was demonstrated that

$$\begin{aligned} Q_i^3 (\eta_{i,ss} \eta_{i,tt} - \eta_{i,st}^2) &= (2Q_i Q_{i,ss} - Q_{i,s} Q_{i,s})(2Q_i Q_{i,tt} - Q_{i,t} Q_{i,t}) \\ &\quad - (2Q_i Q_{i,st} - Q_{i,s} Q_{i,t})^2 \\ &= (a_i^2 + b_i^2 + c_i^2 - 1)p_i(s, t) \\ &= 0 \end{aligned}$$

where $p_i(s, t)$ are quadratic polynomials. However, we know that (a_i, b_i, c_i) are the coefficients of unit-length vectors \mathbf{W}_i with respect to the orthonormal basis $\{\mathbf{U}, \mathbf{V}, \mathbf{W}\}$, so $a_i^2 + b_i^2 + c_i^2 = 1$. The determinant of the second-derivative matrix for G is

$$\begin{aligned} G_{ss} G_{tt} - G_{st}^2 &= (r_0 \eta_{0,ss} + r_1 \eta_{1,ss})(r_0 \eta_{0,tt} + r_1 \eta_{1,tt}) - (r_0 \eta_{0,st} + r_1 \eta_{1,st})^2 \\ &= r_0^2(\eta_{0,ss} \eta_{0,tt} - \eta_{0,st}^2) + r_1^2(\eta_{1,ss} \eta_{1,tt} - \eta_{1,st}^2) \\ &\quad + r_0 r_1(\eta_{0,ss} \eta_{1,tt} + \eta_{1,ss} \eta_{0,tt} - 2\eta_{0,st} \eta_{1,st}) \\ &= r_0 r_1(\eta_{0,ss} \eta_{1,tt} + \eta_{1,ss} \eta_{0,tt} - 2\eta_{0,st} \eta_{1,st}) \end{aligned}$$

Finally, we were able to demonstrate that

$$Q_0^{3/2} Q_1^{3/2} (\eta_{0,ss} \eta_{1,tt} + \eta_{1,ss} \eta_{0,tt} - 2\eta_{0,st} \eta_{1,st}) = (\alpha s + \beta t + \gamma(1-s-t))^2$$

where $\alpha = b_0 c_1 - b_1 c_0$, $\beta = a_1 c_0 - a_0 c_1$, and $\gamma = a_0 b_1 - a_1 b_0$. Observe that $\mathbf{W}_0 \times \mathbf{W}_1 = \alpha \mathbf{U} + \beta \mathbf{V} + \gamma \mathbf{W}$ and $\mathbf{D} \cdot \mathbf{W}_0 \times \mathbf{W}_1 = \alpha s + \beta t + \gamma(1-s-t)$. This establishes the fact that $G_{ss} G_{tt} - G_{st}^2 \geq 0$, with equality occurring only when \mathbf{D} is perpendicular to $\mathbf{W}_0 \times \mathbf{W}_1$.

The conditions $G_{ss} \geq 0$, $G_{tt} \geq 0$, and $G_{ss} G_{tt} - G_{st}^2 \geq 0$ are sufficient to conclude that $G(s, t)$ is a convex function. Numerical minimizers tend to perform quite well for convex functions.

Pseudocode for the Algorithm

This section describes the high-level details for the test-intersection query between two bounded cylinders.

At the topmost level, the separation function is the following. It returns `true` whenever the cylinders are separated.

```

bool SeparatedCylinders (Point C0, Vector W0, Real r0, Real h0,
    Point C1, Vector W1, Real r1, Real h1)
{
    Vector Delta = C1 - C0;
    Vector W0xW1 = Cross(W0,W1);
    Real lenW0xW1 = |W0xW1|;
    Real h0Div2 = h0/2;
    Real h1Div2 = h1/2;
    Real rSum = r0 + r1;

    if (lenW0xW1 > 0)
    {
        // Test for separation by W0.
        if (r1*lenW0xW1 + h0Div2 + h1Div2*|Dot(W0,W1)|
            - |Dot(W0,Delta)| < 0) return true;

        // Test for separation by W1.
        if (r0*lenW0xW1 + h0Div2*|Dot(W0,W1)| + h1Div2
            - |Dot(W1,Delta)| < 0) return true;

        // Test for separation by W0xW1.
        if (rSum*lenW0xW1 - |Dot(W0xW1,Delta)| < 0) return true;

        // Test for separation by directions perpendicular to W0.
        if (SeparatedByCylinderPerpendiculars(C0,W0,r0,h0,
            C1,W1,r1,h1)) return true;

        // Test for separation by directions perpendicular to W1.
        if (SeparatedByCylinderPerpendiculars(C1,W1,r1,h1,
            C0,W0,r0,h0)) return true;

        // Test for separation by other directions.
        if (SeparatedByOtherDirections(W0,r0,h0,
            W1,r1,h1,Delta)) return true;
    }
    else
    {
        // Test for separation by height.
        if (h0Div2 + h1Div2 - |Dot(W0,Delta)| < 0) return true;

        // Test for separation radially.
        if (rSum - |Delta - Dot(W0,Delta)*W0| < 0) return true;

        // If parallel cylinders are not separated by height or
        // radial distance, then the cylinders must overlap.
    }
    return false;
}

```

Processing of directions perpendicular to the cylinder axes is handled by the following code.

```

Real F (Real t, Real r0, Real r1, Real h1b1Div2, Real c1sqr,
        Real a2, Real b2)
{
    Real omt = 1 - t;
    Real tsqr = t*t;
    Real omtsqr = omt*omt;
    Real term0 = r0*sqrt(omtsqr + tsqr);
    Real term1 = r1*sqrt(omtsqr + c1sqr*tsqr);
    Real term2 = h1b1Div2*t;
    Real term3 = |omt*a2 + t*b2|;
    return term0 + term1 + term2 - term3;
}

Real FDer (Real t, Real r0, Real r1, Real h1b1Div2, Real c1sqr,
            Real a2, Real b2)
{
    Real omt = 1 - t;
    Real tsqr = t*t;
    Real omtsqr = omt*omt;
    Real term0 = r0*(2*t-1)/sqrt(omtsqr + tsqr);
    Real term1 = r1*((1+c1sqr)*t - 1)/sqrt(omtsqr + c1sqr*tsqr);
    Real term2 = h1b1Div2;
    Real term3 = (b2 - a2)*sign(omt*a2 + t*b2);
    return term0 + term1 + term2 - term3;
}

bool SeparatedByCylinderPerpendiculars (Point C0, Vector W0,
                                         Real r0, Real h0, Point C1, Vector W1, Real r1, Real h1)
{
    Vector Delta = C1 - C0;
    Real c1 = Dot(W0,W1);
    Real b1 = sqrt(1 - c1*c1);
    Vector V0 = (W1 - c1*W0)/b1;
    Vector U0 = Cross(V0,W0);
    Real a2 = Dot(Delta,U0);
    Real b2 = Dot(Delta,V0);

    // Test directions (1-t)*U0 + t*V0.
    if (F(0) <= 0) return true; // U0 is a separating direction
    if (F(1) <= 0) return true; // V0 is a separating direction
    if (FDer(0) >= 0) return false; // no separation perp dirs
    if (FDer(1) <= 0) return false; // no separation perp dirs

    // Use bisection to locate t-bar for which F(t-bar) is a
    // minimum. The upper bound maxIterations may be chosen to

```

```

// guarantee a specified number of digits of precision in the
// t-variable.
Real t0, t1, fd0, fd1, tmid, fdmid;
int i;
t0 = 0;
t1 = 1;
for (i = 0; i < maxIterations; ++i)
{
    tmid = 0.5*(t0 + t1);
    if (F(tmid) <= 0)
    {
        // (1-t)*U0 + t*V0 is a separating direction
        return true;
    }
    fdmid = FDer(tmid);
    if (fdmid > 0)
    {
        t1 = tmid;
    }
    else if (fdmid < 0)
    {
        t0 = tmid;
    }
    else
    {
        break;
    }
}

// Test directions (1-t)*(-U0) + t*V0.
a2 = -a2;
if (F(0) <= 0) return true; // U0 is a separating direction
if (F(1) <= 0) return true; // V0 is a separating direction
if (FDer(0) >= 0) return false; // no separation perp dirs
if (FDer(1) <= 0) return false; // no separation perp dirs

// Use bisection to locate t-bar for which F(t-bar) is a
// minimum. The upper bound maxIterations may be chosen to
// guarantee a specified number of digits of precision in the
// t-variable.
t0 = 0;
t1 = 1;
for (i = 0; i < maxIterations; ++i)
{
    tmid = 0.5*(t0 + t1);
    if (F(tmid) <= 0)
    {

```

```

        // (1-t)*U0 + t*V0 is a separating direction
        return true;
    }
    fdmid = FDer(tmid);
    if (fdmid > 0)
    {
        t1 = tmid;
    }
    else if (fdmid < 0)
    {
        t0 = tmid;
    }
    else
    {
        break;
    }
}
}

```

Processing of other directions is handled by the following code.

```

Real G (Real s, Real t, Real r0, Real h0Div2, Real r1,
        Real h1Div2, Real a0, Real b0, Real c0, Real a1,
        Real b1, Real c1, Real lenDelta)
{
    Real omsmt = 1 - s - t;
    Real ssqr = s*s;
    Real tsqr = t*t;
    Real omsmtsqr = omsmt*omsmt;
    Real temp = ssqr + tsqr + omsmtsqr;
    Real L0 = a0*s + b0*t + c0*omsmt;
    Real L1 = a1*s + b1*t + c1*omsmt;
    Real Q0 = temp - L0*L0;
    Real Q1 = temp - L1*L1;
    return r0*sqrt(Q0) + r1*sqrt(Q1) + h0Div2*|L0|
           + h1Div2*|L1| - omsmt*lenDelta;
}

Vector GDer (Real s, Real t, Real r0, Real h0Div2,
             Real r1, Real h1Div2, Real a0, Real b0, Real c0,
             Real a1, Real b1, Real c1, Real lenDelta)
{
    Real omsmt = 1 - s - t;
    Real ssqr = s*s;
    Real tsqr = t*t;
    Real omsmtsqr = omsmt*omsmt;
    Real temp = ssqr + tsqr + omsmtsqr;
    Real L0 = a0*s + b0*t + c0*omsmt;
    Real L1 = a1*s + b1*t + c1*omsmt;

```

```

Real Q0 = temp - L0*L0;
Real Q1 = temp - L1*L1;
Real diffS = s - omsmt;
Real diffT = t - omsmt;
Real diffa0c0 = a0 - c0;
Real diffa1c1 = a1 - c1;
Real diffb0c0 = b0 - c0;
Real diffb1c1 = b1 - c1;
Real halfQ0s = diffS - diffa0c0*L0;
Real halfQ1s = diffS - diffa1c1*L1;
Real halfQ0t = diffT - diffb0c0*L0;
Real halfQ1t = diffT - diffb1c1*L1;
Real factor0 = r0/sqrt(Q0);
Real factor1 = r1/sqrt(Q1);
Real signL0 = sign(L0);
Real signL1 = sign(L1);

Vector gradient = (0,0);
gradient[0] += halfQ0s*factor0;
gradient[0] += halfQ1s*factor1;
gradient[0] += h0Div2*diffa0c0*signL0;
gradient[0] += h1Div2*diffa1c1*signL1;
gradient[0] += lenDelta;
gradient[1] += halfQ0t*factor0;
gradient[1] += halfQ1t*factor1;
gradient[1] += h0Div2*diffb0c0*signL0;
gradient[1] += h1Div2*diffb1c1*signL1;
gradient[1] += lenDelta;

return gradient;
}

bool SeparatedByOtherDirections (Vector W0, Real r0, Real h0,
                                 Vector W1, Real r1, Real h1, Vector Delta)
{
    // Minimize G(s,t) subject to s >= 0, t >= 0, and s+t <= 1.
    // If at any iterate you find a value for which G <= 0,
    // return 'true'. If no separating directions have been
    // found at the end of the minimization, return 'false'.
}

```

The function `SeparatedByOtherDirections` encapsulates a numerical method such as the conjugate gradient method or Powell's direction set method to minimize the function $G(s, t)$. In either case, the idea is to start at a parameter point (s_0, t_0) and choose the direction (d_0, d_1) for a line along which to minimize,

$$(s(r), t(r)) = (s_0, t_0) + r(d_0, d_1)$$

The interval for the line parameter r is determined by the intersection of the line with the triangular domain for s and t . Let this interval be denoted $[r_0, r_1]$. The function to minimize is

$$\gamma(r) = G(s(r), t(r))$$

and its derivative is

$$\gamma'(r) = G_s(s(r), t(r))d_0 + G_t(s(r), t(r))d_1 = (d_0, d_1) \cdot \nabla G(s(r), t(r))$$

Because $G(s, t)$ is a convex function, so is $\gamma(r)$. The algorithm for minimizing γ on $[r_0, r_1]$ is the same one mentioned previously for $F(t)$ on $[0, 1]$. If $\gamma(r_0) \leq 0$, then $\mathbf{D} = s(r_0)\mathbf{U} + t(r_0)\mathbf{V} + (1 - s(r_0) - t(r_0))\mathbf{W}$ is a separating direction. If $\gamma(r_1) \leq 0$, then $\mathbf{D} = s(r_1)\mathbf{U} + t(r_1)\mathbf{V} + (1 - s(r_1) - t(r_1))\mathbf{W}$ is a separating direction. Otherwise, $\gamma(r_0) > 0$ and $\gamma(r_1) > 0$. If $\gamma'(r_0) \geq 0$, then the convexity of γ guarantees that $\gamma(r_0)$ is the global minimum. Since $\gamma(r_0) > 0$, there is no separation *using directions along the current r-interval*. If $\gamma'(r_1) \leq 0$, then the convexity of γ guarantees that $\gamma(r_1)$ is the global minimum. Since $\gamma(r_1) > 0$, there is no separation *using directions along the current r-interval*. Otherwise, $\gamma(r_0) > 0$, $\gamma(r_1) > 0$, $\gamma'(r_0) < 0$, and $\gamma'(r_1) > 0$. A global minimum must occur at an interior point $\bar{r} \in [r_0, r_1]$ for which $\gamma'(\bar{r})$ is zero or undefined. Use bisection based on the signs of $\gamma'(r)$ to locate \bar{r} . At each iterate r_i it is worthwhile to test whether $\gamma(r_i) \leq 0$. For if it is, we have found a separating direction. If the bisection terminates and $\gamma(\bar{r}) > 0$, there is no separation *using directions along the current r-interval*.

Once a minimum has been located along the current r -interval, say, $\gamma(\bar{r})$, then the new starting point is $(s_0, t_0) = (s(\bar{r}), t(\bar{r}))$, and a new direction is chosen for (d_0, d_1) . If the minimum of the previous line occurs on a boundary of the triangular domain, then you need only search that boundaries of the triangular domain for the global minimum. Otherwise, the line search is repeated for the new line. If the global minimum is interior to the triangular domain, then you will never reach the boundary on a line search.

The choice of directions depends on the numerical minimizer you choose. The number of lines to search is usually based on convergence criteria – are you close enough to a global minimum?

6.4 COLLISION DETECTION WITH CONVEX POLYHEDRA

In this chapter our rigid bodies have been selected to be convex polyhedra of constant mass density. The short name for convex polyhedron is *polytope*, a term we will use throughout the remainder of this section. The invariant of the collision detection and response system is *nonpenetration of the polyhedra*. The collision detection system

must compute points of contact between each pair of polytopes. The response of the system is designed so that at all points of contact, the polytopes move with nonnegative velocity relative to the normal directions at the contact points, thus maintaining the nonpenetration invariant.

Now we take a close look at how to compute the contact points. Since we must find actual intersection points, a test-intersection geometric query will not suffice. A find-intersection geometric query must be formulated. For two stationary polytopes a find-intersection query must compute the polytope of intersection. If we were just to use a generic intersection algorithm, we would be ignoring the fact that our invariant prevents interpenetration. Because of our invariant, the intersection must consist of points, line segments, or convex polygons; intersection regions with volume are disallowed. Assuming a collision detection and response system designed to handle a finite set of contact points, the find-intersection query might very well detect a line segment of intersection but need only report the endpoints as the contact points. Similarly, only the vertices of a convex polygon of intersection need to be reported. Thus, a find-intersection query should be tailored to our needs.

We have an additional problem with which to deal. Time is a continuous variable in the physical setting, but we are using a differential equation solver to estimate motion over small time intervals. Let $\mathcal{P}(t)$ be the path of a point on a moving polytope. The equations of motion determine this path, but we do not know the path in closed form. Knowing the location of a point $\mathcal{P}_0 = \mathcal{P}(t_0)$ at the current time t_0 , our goal is to determine the location $\mathcal{P}_1 = \mathcal{P}(t_1)$ at the next sampled simulation time $t_1 = t_0 + \Delta t$. The differential equation solver produces a point \mathcal{Q}_1 that is an *approximation* to \mathcal{P}_1 . The collision system might very well report that \mathcal{Q}_1 is outside (or inside) another polytope when in fact \mathcal{P}_1 is inside (or outside), the collision result being in error. For most game applications, if a collision is reported when in fact there is none, the system is effectively conservative in its handling in that some action will be taken to “prevent” the collision; the only harm done is that some extra cycles are spent on the event. More serious, though, is for the collision system *not to report a collision* when in fact there is one. For those of you with some experience programming with collision detection systems, I am certain you have seen the situation where an object whose motion is controlled by an input device such as a mouse or joystick slightly interpenetrates a wall because the collision system failed to report the intersection. When you attempt to steer the object away from the wall, it becomes stuck because now the collision system *does detect an intersection*, this one between the object and the opposite side of the wall. In some collision detection systems you might even see the object stutter, a high-frequency oscillation of a system in conflict, one portion trying to pull the object out of the wall and another portion pulling it into the wall. We would like to avoid such behavior in our collision detection system.

Even if we were able to compute the exact value \mathcal{P}_1 , the system can still be in error. The problem now is that we have incremented t_0 to t_1 by a positive increment in time. It is possible that \mathcal{P}_0 and \mathcal{P}_1 are both outside another polytope, but at some time $t_2 \in [t_0, t_1]$ the point $\mathcal{P}(t_2)$ is inside that polytope. The time step Δt of the differential equation solver was too large to “notice” the collision event. Although your

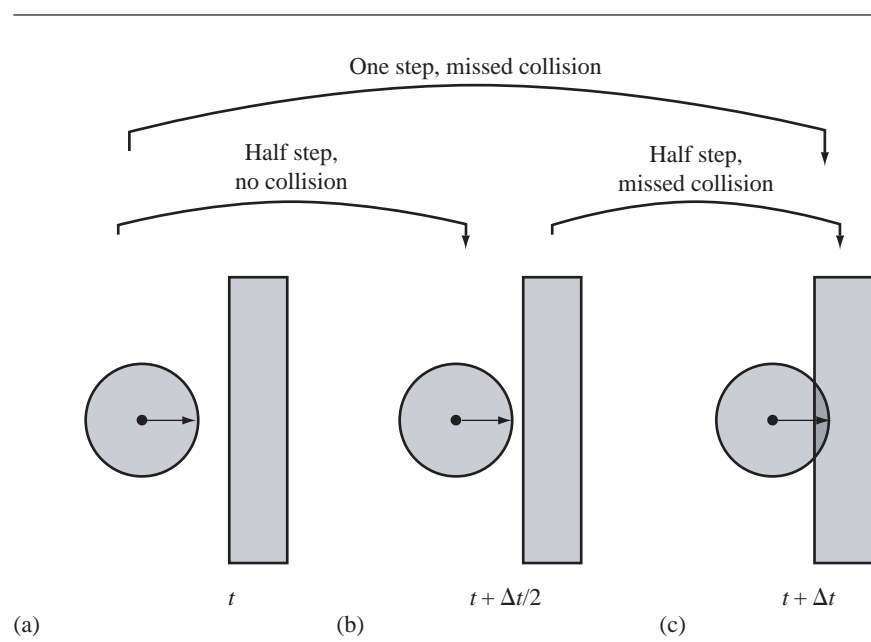


Figure 6.17 (a) Object at time t_0 . (b) Object at time $t_0 + \Delta t/2$. (c) Object at time $t_0 + \Delta t$.

instinct might be to choose a smaller value for Δt , you can do so, move the object in two time steps and miss the intersection again. Figure 6.17 illustrates.

In fact, the reduction in time step has problems *exactly* in those circumstances that we are interested in – contact without interpenetration.

A classical solution to the problem, and one mentioned in [Bar01], is to use a bisection method. Let $B_0(t)$ and $B_1(t)$ denote the solid polytopes at time t (as sets of points). The assumption is that two polytopes are not intersecting at time t_0 , $B_0(t_0) \cap B_1(t_0) = \emptyset$ (the intersection is the empty set). The polytopes are to be moved during the time interval $[t_0, t_1]$, the difference $\Delta t = t_1 - t_0$ supplied by the application. If $B_0(t_1)$ and $B_1(t_1)$ intersect and the intersection set has volume, say $I = B_0(t_1) \cap B_1(t_1) \neq \emptyset$ with $\text{Volume}(I) > 0$, the time step was too large. Now try the motion with half the time step, the final time being $t_m = (t_0 + t_1)/2$. The intersect set is $I = B_0(t_m) \cap B_1(t_m)$. If $I \neq \emptyset$ and $\text{Volume}(I) > 0$, the half step was also too large and we repeat the bisection of the time interval. If $I = \emptyset$, the half step was too large and we search for potential intersection on the other half interval $[t_m, t_1]$. Our goal is to obtain an intersection $I \neq \emptyset$ with $\text{Volume}(I) = 0$. The pseudocode is

```
void GetContactSet (double t0, double t1, polytope B0(t),
                    polytope B1(t), double& tContact, set& I)
{
    // precondition: B0(t0) and B1(t0) do not intersect
```

```

I = GetIntersection(B0(t1),B1(t1));
if (I is the empty_set)
{
    tContact = <irrelevant>;
    return;
}
if (Volume(I) == 0)
{
    tContact = t1;
    return;
}

for (i = 1; i <= maxIterations; ++i)
{
    tm = (t0 + t1) / 2;
    I = GetIntersection(B0(tm),B1(tm));
    if (I is the empty_set)
    {
        t0 = tm;
    }
    else if (Volume(I) > 0)
    {
        t1 = tm;
    }
    else
    {
        tContact = tm;
        return;
    }
}
}

```

Well, this is still not a correct algorithm for two reasons. First, it can terminate immediately when $B_0(t_1)$ and $B_1(t_1)$ do not intersect and the system reports that no intersection has occurred. Second, it is possible that the system reports contact points at the *last time of contact*. However, if the time steps are small compared to the sizes and velocities of the polytopes, the algorithm should have reasonable behavior. Observe that the pseudocode contains a function call `GetIntersection` that requires computing the polytope of intersection for two purposes, testing if the intersection is empty and measuring the volume if not. As mentioned earlier, we want to avoid a generic intersection calculator for polytopes because they can be somewhat expensive to execute. Moreover, it would be useful to have an intersection system that can *predict* the time of collision on the interval $[t_0, t_1]$ rather than search for one by sampling the interval.

This section addresses how we go about testing for intersection of polytopes and predicting when they intersect. A powerful algorithm is used, called the *method of*

separating axes. A detailed description of the method for moving as well as stationary objects and for 2D (convex polygons) and 3D (convex polyhedra) is provided in the books [Ebe07] and [SE02]. A summary of the method is provided here, but with some additional material that is relevant to objects participating in a constrained dynamics system. In particular, we want to take advantage of *time coherence* to help minimize calculations at the next time step by caching information from the previous time step.

6.4.1 THE METHOD OF SEPARATING AXES

We have been using the term *convex* when referring to the polyhedra that represent our rigid bodies. A reminder of what that term means is in order: A set C is convex if given any two points \mathcal{P} and \mathcal{Q} in C , the line segment $(1-t)\mathcal{P} + t\mathcal{Q}$ for $t \in [0, 1]$ is also in C . Figure 6.18 shows a convex set and a nonconvex set in the plane.

A test for nonintersection of two convex objects is simply stated: If there exists a line for which the intervals of projection of the two objects onto that line do not intersect, then the objects do not intersect. Such a line is called a *separating line* or, more commonly, a *separating axis*. Figure 6.19 illustrates.

The translation of a separating line is also a separating line, so it is sufficient to consider lines that contain the origin. Given a line containing the origin \mathcal{O} and with unit-length direction \mathbf{D} , the projection of a convex set C onto the line is the interval

$$I = [\lambda_{\min}(\mathbf{D}), \lambda_{\max}(\mathbf{D})] = [\min\{\mathbf{D} \cdot (\mathcal{X} - \mathcal{O}) : \mathcal{X} \in C\}, \max\{\mathbf{D} \cdot (\mathcal{X} - \mathcal{O}) : \mathcal{X} \in C\}]$$

where possibly $\lambda_{\min}(\mathbf{D}) = -\infty$ or $\lambda_{\max}(\mathbf{D}) = +\infty$, these cases arising when the convex set is unbounded. Two convex sets C_0 and C_1 are *separated* if there exists

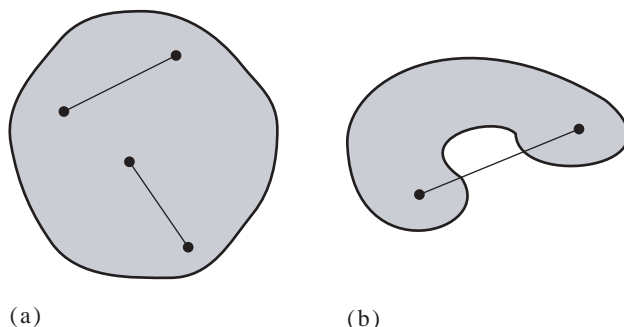


Figure 6.18 (a) A convex set. No matter which two points you choose in the set, the line segment connecting them is in the set. (b) A nonconvex set. The line segment connecting two specific points is not (fully) contained in the set.

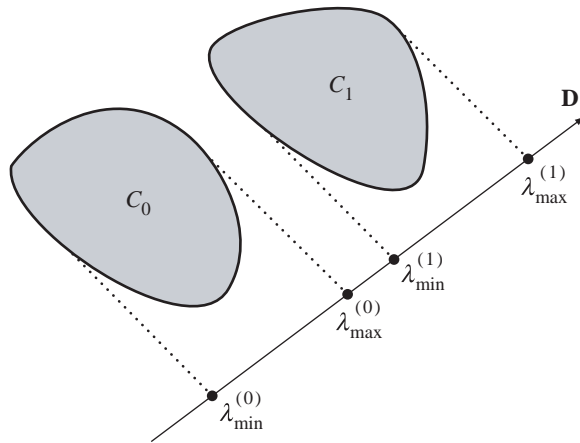


Figure 6.19 Nonintersecting convex objects and a separating line for them. The algebraic condition for separation is $\lambda_{\max}^{(0)}(\mathbf{D}) < \lambda_{\min}^{(1)}(\mathbf{D})$ as indicated in equation (6.58).

a direction \mathbf{D} such that the projection intervals I_0 and I_1 do not intersect. Specifically, they do not intersect when

$$\lambda_{\min}^{(0)}(\mathbf{D}) > \lambda_{\max}^{(1)}(\mathbf{D}) \quad \text{or} \quad \lambda_{\max}^{(0)}(\mathbf{D}) < \lambda_{\min}^{(1)}(\mathbf{D}) \quad (6.58)$$

The superscript corresponds to the index of the convex set. Although the comparisons are made where \mathbf{D} is unit length, the comparison results are invariant to changes in length of the vector. This follows from $\lambda_{\min}(t\mathbf{D}) = t\lambda_{\min}(\mathbf{D})$ and $\lambda_{\max}(t\mathbf{D}) = t\lambda_{\max}(\mathbf{D})$ for $t > 0$. The Boolean value of the pair of comparisons is also invariant when \mathbf{D} is replaced by the opposite direction $-\mathbf{D}$. This follows from $\lambda_{\min}(-\mathbf{D}) = -\lambda_{\max}(\mathbf{D})$ and $\lambda_{\max}(-\mathbf{D}) = -\lambda_{\min}(\mathbf{D})$. When \mathbf{D} is not unit length, the intervals obtained for the separating line tests are not the projections of the object onto the line, rather they are scaled versions of the projection intervals. We make no distinction between the scaled projection and regular projection. We will also use the terminology that the direction vector for a separating line is called a *separating direction*, a direction that is not necessarily unit length.

Please note that in two dimensions, the terminology for separating line or axis is potentially confusing. The separating line separates the *projections* of the objects on that line. The separating line does *not* partition the plane into two regions, each containing an object. In three dimensions, the terminology should not be confusing since a plane would need to be specified to partition space into two regions, each containing an object. No real sense can be made for partitioning space by a line.

6.4.2 STATIONARY OBJECTS

The method of separating axes for stationary objects determines whether or not two objects intersect, a test-intersection query. We will analyze the method for convex polygons in 2D to motivate the ideas, then extend the method to convex polyhedra in 3D.

Convex Polygons

The following notation is used throughout this section. Let C_j for $j = 0, 1$ be the convex polygons with vertices $\mathcal{P}_i^{(j)}$ for $0 \leq i < N_j$ that are counterclockwise ordered. The edges of the polygons have direction vectors $\mathbf{E}_i^{(j)} = \mathcal{P}_{i+1}^{(j)} - \mathcal{P}_i^{(j)}$ for $0 \leq i < N_j$ and where modular indexing is used to handle wraparound (index N is the same as index 0; index -1 is the same as index $N-1$). Outward normal vectors to the edges are $\mathbf{N}_i^{(j)}$. No assumption is made about the length of the normal vectors; an implementation may choose the length as needed. Regardless of length, the condition of outward pointing means $(\mathbf{N}_i^{(j)})^\perp \cdot \mathbf{E}_i^{(j)} > 0$, where $(x, y)^\perp = (-y, x)$. All the pseudocode relating to convex polygons will use the class shown:

```
class ConvexPolygon
{
public:
    // N, number of vertices
    int GetN();

    // V[i], counterclockwise ordered
    Point GetVertex (int i);

    // E[i] = V[i + 1]-V[i]
    Vector GetEdge (int i);

    // N[i], N[i].x * E[i].y - N[i].y * E[i].x > 0
    Vector GetNormal (int i);
};
```

All functions are assumed to handle the wraparound. For example, if the input value is N , the number of vertices, then `GetVertex` returns \mathcal{P}_0 and `GetEdge` returns $\mathcal{P}_1 - \mathcal{P}_0$. If the input value is -1 , then `GetVertex` returns \mathcal{P}_{N-1} and `GetEdge` returns $\mathcal{P}_0 - \mathcal{P}_{N-1}$. Only the relevant interface is supplied for clarity of the presentation. The implementation details will vary with the needs of an application.

For a pair of convex polygons, only a finite set S of direction vectors needs to be considered for separation tests. That set contains only the normal vectors to the edges of the polygons. Figure 6.20(a) shows two nonintersecting polygons that are separated along a direction determined by the normal to an edge of one polygon. Figure 6.20 shows two polygons that intersect; there are no separating directions.

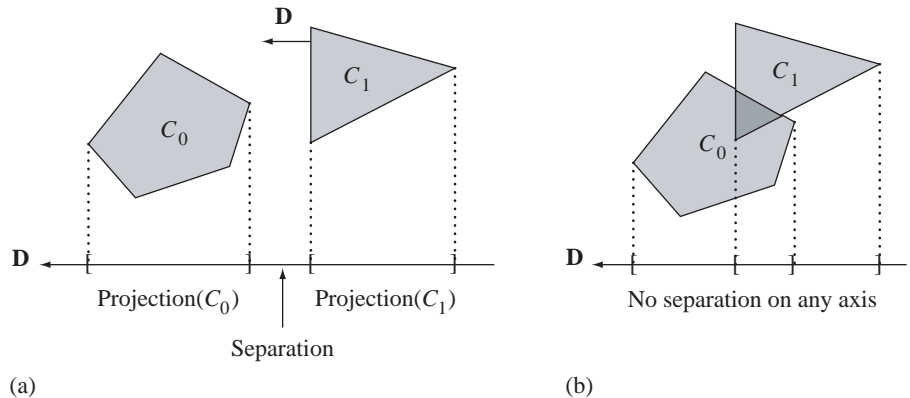


Figure 6.20 (a) Nonintersecting convex polygons. (b) Intersecting convex polygons.

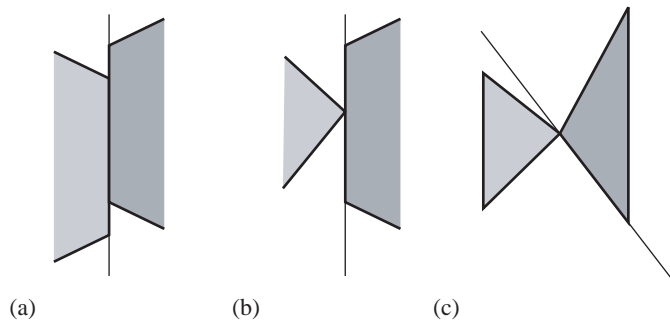


Figure 6.21 (a) edge–edge contact. (b) vertex–edge contact. (c) vertex–vertex contact.

The intuition for why only edge normals must be tested is based on having two convex polygons just touching with no interpenetration. Figure 6.21 shows the three possible configurations: edge–edge contact, vertex–edge contact, and vertex–vertex contact.

The lines between the polygons are perpendicular to the separation lines that would occur for one object translated away from the other by an infinitesimal distance. The vertex–vertex edge case has a low probability of occurrence. The collision system should report this as a vertex–face collision to be consistent with our classification of contact points (vertex–face or edge–edge with appropriately assigned normal vectors).

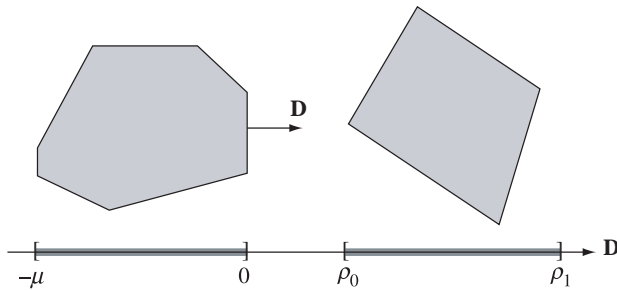


Figure 6.22 Two polygons separated by an edge-normal direction of the first polygon.

A naive implementation of the method of separating axes selects a potential separating direction \mathbf{D} , computes the intervals of projection by projecting the vertices of both polygons onto that line, then tests if the intervals are separated. This requires computing N_i projections for polygon C_i and keeping track of the minimum and maximum projection values for each polygon. In the worst case that the polygons intersect, N_0 directions are tested from C_0 , each requiring $N_0 + N_1$ projections, and N_1 directions are tested from C_1 , each requiring $N_0 + N_1$ projections. The total number of projections is $(N_0 + N_1)^2$.

A smarter algorithm avoids projecting all the vertices for the polygons by only testing for separation using the maximum of the interval for the first polygon and the minimum of the interval for the second polygon. If \mathbf{D} is an outward pointing normal for the edge $P_{i+1}^{(0)} - P_i^{(0)}$ of C_0 , then the projection of the C_0 onto the separating line $P_i^{(0)} + t\mathbf{D}$ is $[-\mu, 0]$, where $\mu > 0$. If the projection of C_1 onto this line is $[\rho_0, \rho_1]$, then the reduced separation test is $\rho_0 > 0$. Figure 6.22 illustrates two separated polygons using this scheme.

The value μ is irrelevant since we only need to compare ρ_0 to 0. Consequently, there is no need to project the vertices of C_0 to calculate μ . Moreover, the vertices of C_1 are projected one at a time until either the projected value is negative, in which case \mathbf{D} is no longer considered for separation, or until all projected values are positive, in which case \mathbf{D} is a separating direction.

```

bool TestIntersection (ConvexPolygon C0, ConvexPolygon C1)
{
    // Test edges of C0 for separation. Because of the
    // counterclockwise ordering, the projection interval for
    // C0 is [m,0] where m <= 0. Only try to determine if C1
    // is on the 'positive' side of the line.
    for (i0 = C0.GetN()-1, i1 = 0; i1 < C0.GetN(); i0 = i1++)
    {
        P = C0.GetVertex(i1);

```

```

D = C0.GetNormal(i0);
if (WhichSide(C1,P,D) > 0)
{
    // C1 is entirely on 'positive' side of line P + t * D
    return false;
}
}

// Test edges of C1 for separation. Because of the
// counterclockwise ordering, the projection interval for
// C1 is [m,0] where m <= 0. Only try to determine if C0
// is on the 'positive' side of the line.
for (i0 = C1.GetN()-1, i1 = 0; i1 < C1.GetN(); i0 = i1++)
{
    P = C1.GetVertex(i1);
    D = C1.GetNormal(i0);
    if (WhichSide(C0,P,D) > 0)
    {
        // C0 is entirely on 'positive' side of line P + t * D
        return false;
    }
}

return true;
}

int WhichSide (ConvexPolygon C, Point P, Vector D)
{
    // C vertices are projected onto line P+t*D. Return value
    // is +1 if all t > 0, -1 if all t < 0, or 0 if the line
    // splits the polygon.

    posCount = 0;
    negCount = 0;
    zeroCount = 0;
    for (i = 0; i < C.GetN(); ++i)
    {
        t = Dot(D,C.GetVertex(i) - P);
        if (t > 0)
        {
            posCount++;
        }
        else if (t < 0)
        {
            negCount++;
        }
        else
    }
}

```

```

    {
        zeroCount++;
    }

    if ((posCount > 0 and negCount > 0) or zeroCount > 0)
    {
        return 0;
    }
}
return posCount ? 1 : -1;
}

```

In the worst case, the polygons do intersect. We have processed N_0 edge normals of C_0 , each requiring N_1 projections for C_1 , and N_1 edge normals of C_1 , each requiring N_0 projections for C_0 . The total number of projections is $2N_0N_1$, still a quadratic quantity but considerably smaller than $(N_0 + N_1)^2$.

We can do even better in an asymptotic sense as the number of vertices becomes large. A form of bisection may be used to find an extreme point of the projection of the polygon [O'R98]. The bisection effectively narrows in on sign changes of the dot product of edges with the specified direction vector. For a polygon of N_0 vertices, the bisection is of order $O(\log N_0)$, so the total algorithm is $O(\max\{N_0 \log N_1, N_1 \log N_0\})$.

Given two vertex indices i_0 and i_1 of a polygon with N vertices, the *middle index* of the indices is described by the following pseudocode.

```

int GetMiddleIndex (int i0, int i1, int N)
{
    if (i0 < i1)
    {
        return (i0 + i1) / 2;
    }
    else
    {
        return ((i0 + i1 + N) / 2) (mod N);
    }
}

```

The division of two integers returns the largest integer smaller than the real-valued ratio and the `mod` operation indicates calculating the remainder after dividing the argument by N . Observe that if $i_0 = i_1 = 0$, the function returns a valid index. The condition when $i_0 < i_1$ has an obvious result – the returned index is the average of the input indices, certainly supporting the name of the function. For example, if the polygon has $N = 5$ vertices, inputs $i_0 = 0$ and $i_1 = 2$ lead to a returned index of 1. The other condition handles wraparound of the indices. If $i_0 = 2$ and $i_1 = 0$, the implied set of ordered indices is $\{2, 3, 4, 0\}$. The middle index is selected as 3 since $3 = (2 + 0 + 5)/2(\text{mod } 5)$.

The bisection algorithm to find the extreme value of the projection is

```
int GetExtremeIndex (ConvexPolygon C, Vector D)
```

```

{
    i0 = 0;
    i1 = 0;
    while (true)
    {
        mid = GetMiddleIndex(i0,i1,C.GetN());
        if (Dot(D,C.GetEdge(mid)) > 0)
        {
            if (mid != i0)
            {
                i0 = mid;
            }
            else
            {
                return i1;
            }
        }
        else
        {
            if (Dot(D,C.GetEdge(mid - 1)) < 0)
            {
                i1 = mid;
            }
            else
            {
                return mid;
            }
        }
    }
}

```

```

Using the bisection method, the intersection testing pseudocode is

bool TestIntersection (ConvexPolygon C0, ConvexPolygon C1)
{
    // Test edges of C0 for separation. Because of the
    // counterclockwise ordering, the projection interval for
    // C0 is [m,0] where m <= 0. Only try to determine if C1
    // is on the 'positive' side of the line.
    for (i0 = C0.GetN()-1, i1 = 0; i1 < C0.GetN(); i0 = i1++)
    {
        P = C0.GetVertex(i1);
        D = C0.GetNormal(i0);
        if (Dot(D,C1.GetVertex(GetExtremeIndex(C1,-D)) - P) > 0)
        {
            // C1 is entirely on 'positive' side of line P + t * D
            return false;
        }
    }
}

```

```

// Test edges of C1 for separation. Because of the
// counterclockwise ordering, the projection interval for
// C1 is [m,0] where m <= 0. Only try to determine if C0
// is on the 'positive' side of the line.
for (i0 = C1.N-1, i1 = 0; i1 < C1.N; i0 = i1++)
{
    P = C1.GetVertex(i1);
    D = C1.GetNormal(i0);
    if (Dot(D,C0.GetVertex(GetExtremeIndex(C0,-D)) - P) > 0)
    {
        // C0 is entirely on 'positive' side of line P + t * D
        return false;
    }
}
return true;
}

```

Let us consider an alternate formulation of the bisection problem. Just as we would do in the 3D problem, the vertices, edges, and normals of the convex polygon are stored in body coordinates. The polygon additionally stores the center of mass (the body origin) and an orientation matrix that transforms the body coordinate axes to the world coordinates. We will transform a potential separating direction \mathbf{D} from world coordinates to body coordinates and continue the separation process in those coordinates. Figure 6.23 illustrates the initial part of the process of determining which polygon vertex or edge is extremal.

If $\mathbf{D} = \mathbf{N}_i$, then all points on the edge E_i are extremal. If \mathbf{D} is strictly between \mathbf{N}_0 and \mathbf{N}_1 , then P_1 is the unique extremal point in that direction. Similar arguments apply for \mathbf{D} strictly between any pair of consecutive normals. The normal points on the circle decompose the circle into arcs, each arc corresponding to an extremal vertex of the polygon. An endpoint of an arc corresponds to an entire edge being extremal. The testing of \mathbf{D} to determine the full set of extremal points is summarized as follows.

- Vertex P_i is optimal when $\mathbf{N}_i^\perp \cdot \mathbf{D} > 0$ and $\mathbf{N}_{i-1}^\perp \cdot \mathbf{D} < 0$
- Edge E_i is optimal when $\mathbf{N}_{i-1}^\perp \cdot \mathbf{D} = 0$ and $\mathbf{N}_i^\perp \cdot \mathbf{D} < 0$

where $(x, y)^\perp = (-y, x)$. The indexing is computed in the modular sense, $\mathbf{N}_{-1} = \mathbf{N}_5$. Since we will be projecting the extremal point onto a potential separating axis, we can collapse the two tests into a single test and just use one vertex of an extremal edge as the to-be-projected point:

- Vertex P_i is optimal when $\mathbf{N}_{i-1}^\perp \cdot \mathbf{D} \geq 0$ and $\mathbf{N}_i^\perp \cdot \mathbf{D} < 0$

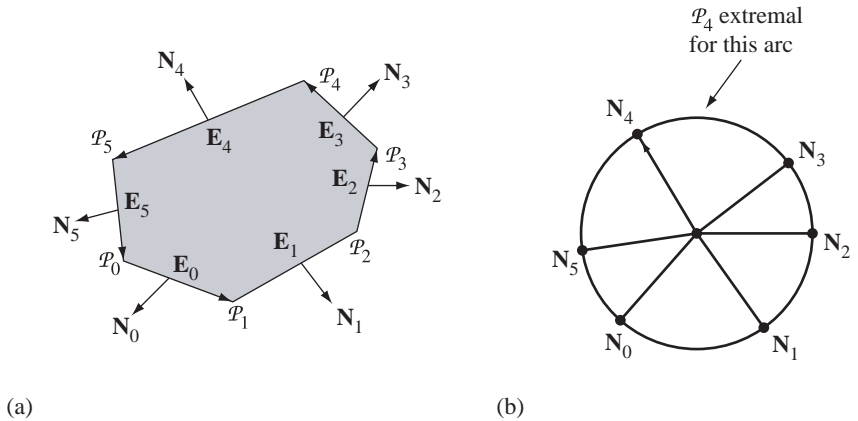


Figure 6.23 (a) A convex polygon. (b) A unit circle whose vertices correspond to normal directions of the polygon and whose arcs connecting the vertices correspond to vertices of the polygon (the *polar dual* of the polygon).

Generally, there are N arcs for an N -sided polygon. We could search the arcs one at a time and test if \mathbf{D} is on that arc, but then we are back to an $O(N)$ search. Instead, we can create a *binary space partitioning tree* (BSP tree) for the circle that supports an $O(\log N)$ search. Effectively, this is a binary search of an ordered array of numbers, so thinking of it as a BSP tree might not be useful to you. However, in 3D we will construct something similar that is a BSP tree in the sense you are used to. A simple illustration using the polygon of Figure 6.23 suffices. Figure 6.24 illustrates the construction of the BSP tree. The unit disk is recursively split into sectors, each split representing a test $\mathbf{N}_j^\perp \cdot \mathbf{D} \geq 0$.

The vertices on the circle are \mathbf{N}_i for $0 \leq i \leq 5$. The circular arcs are denoted $A_{ij} = \langle \mathbf{N}_i, \mathbf{N}_j \rangle$ where $j = (i + 1) \bmod 6$. The set of all vertices and the set of all arcs are used to initialize the process. These are shown at the top of Figure 6.24. The root node of the tree claims the first normal in the list, namely \mathbf{N}_0 , and uses it for computing dot products with other vectors, $\mathbf{N}_0^\perp \cdot \mathbf{D} \geq 0$. When creating the tree, the remaining normals in the input set are tested. If $\mathbf{N}_0^\perp \cdot \mathbf{N}_i \geq 0$, vector \mathbf{N}_i is placed in a set of vectors that will be used to create the right child of the root (marked as T in Figure 6.24); otherwise \mathbf{N}_i is placed in another set of vectors that will be used to create the left child of the root (marked as F in Figure 6.24).

The set of arcs is also processed at each node. The endpoints of the arc A_{ij} are normals for which we have already computed $d_i = \mathbf{N}_0^\perp \cdot \mathbf{N}_i$ and $d_j = \mathbf{N}_0^\perp \cdot \mathbf{N}_j$. If $d_i \geq 0$ and $d_j \geq 0$, then the arc is placed in a set of arcs that will be used to create the right child of the root. If $d_i \leq 0$ and $d_j \leq 0$, then the arc is placed in a set of arcs that will be

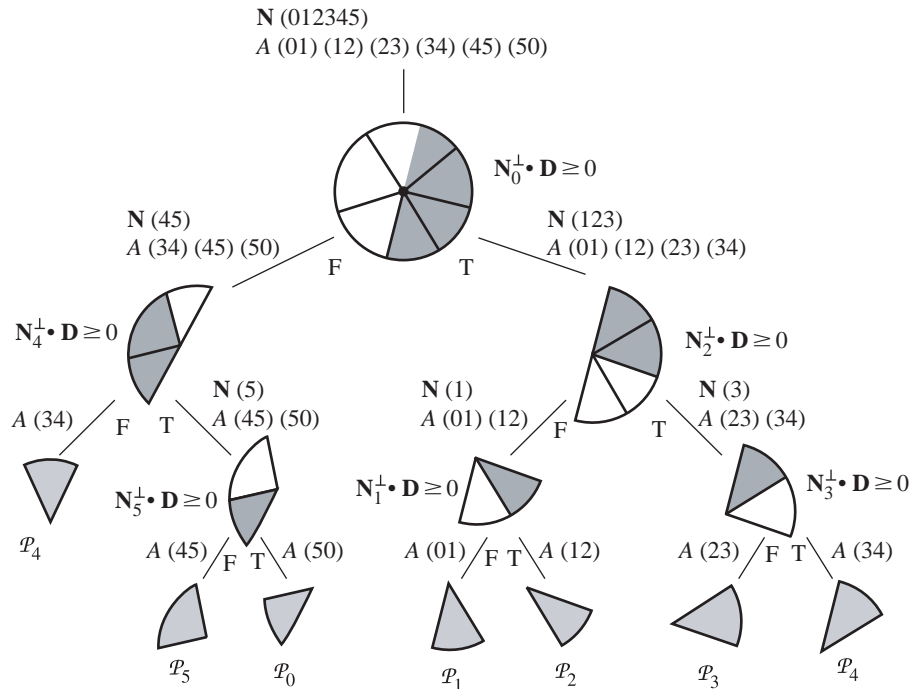


Figure 6.24 A BSP tree constructed by recursive splitting of the unit disk. Each node is labeled with the test used for the split. The subsectors consisting of points satisfying the test are shaded in dark gray. The leaf nodes are shaded in light gray and labeled with a vertex that is extremal.

used to create the left child. If $d_i d_j < 0$, then the arc is split in a sense, but we do not need to literally subdivide it into two subarcs. Instead, we just add that arc to both sets to be used in constructing the child subtrees. In our example the only arc that is split is A_{34} . In fact this will be the *only split* and represents the wraparound, so to speak, of the circle.

The process just described above is applied recursively. At the end, each interior node of the tree has been assigned a normal vector for testing purposes. Each leaf node was given an arc A_{ij} , but not a normal. The last index j is that of the extreme vertex represented by the leaf node.

Some pseudocode is provided. Let us assume a class for a BSP node as shown next. The class `ConvexPolygon` described earlier is given a new data member of type `BSPNode`.

```
class BSPNode
{
public:
```

```

// normal index (interior node), vertex index (leaf node)
int I;

// if Dot(E,D) >= 0, D gets propagated to this child
BSPNode R;

// if Dot(E,D) < 0, D gets propagated to this child
BSPNode L;
};

class ConvexPolygon
{
public:
    // N, number of vertices
    int GetN();

    // P[i], counterclockwise ordered
    Point GetVertex (int i);

    // E[i] = P[i + 1]-P[i]
    Vector GetEdge (int i);

    // N[i], N[i].x * E[i].y - N[i].y * E[i].x > 0
    Vector GetNormal (int i);

    BSPNode tree;
};

```

The BSP tree must be able to access the vertices and edges of the polygon, so the creation of the tree involves passing the polygon as a parameter. Because $N_i^\perp = E_i$, the direction of the edge, and since we are assuming the edges are stored in the polygon, we do not need a `Perp` function. The pseudocode is written for clarity and thus not optimized.

```

void CreateTree (ConvexPolygon C)
{
    // Create the root node first, knowing that the only split can
    // occur here.

    array<int> NIR, NIL; // normal index sets

    // Arc index sets, array element written {j0,j1},
    // AIR[i][0] = j0, AIR[i][1] = j1.
    array<int,int> AIR, AIL;
    array<int> d(C.GetN());
    d[0] = 0;
    for (i = 1; i < C.GetN(); ++i)
    {

```

```

d[i] = Dot(C.GetEdge(0), C.GetNormal(i));

if (d[i] >= 0)
{
    NIR.append(i);
}
else
{
    NIL.append(i);
}

if (d[i-1] >= 0 and d[i] >= 0)
{
    AIR.append({i-1,i});
}
else if (d[i-1] <= 0 and d[i] <= 0)
{
    AIL.append({i-1,i});
}
else // d[i-1]*d[i] < 0
{
    AIR.append({i-1,i});
    AIL.append({i-1,i});
}
}
AIL.append({C.GetN()-1,0}); // always left!

C.tree = CreateNode(0, CreateNode(C,NIR,AIR),
                    CreateNode(C,NIL,AIL));
}

BSPNode CreateNode (int I, BSPTree R, BSPTree L)
{
    BSPNode node;
    node.I = I;
    node.R = R;
    node.L = L;
    return node;
}

BSPNode CreateNode (ConvexPolygon C, array<int> NI,
                    array<int,int> AI)
{
    array<int> NIR, NIL;
    array<int> d(NI.size());
    d[0] = NI[0];
    for (i = 1; i < NI.size(); ++i)

```

```

    {
        d[i] = Dot(C.GetEdge(NI[0]), C.GetNormal(NI[i]));
        if (d[i] >= 0)
        {
            NIR.append(NI[i]);
        }
        else
        {
            NIL.append(NI[i]);
        }
    }

    array<int,int> AIR, AIL;
    for (i = 0; i < AI.size(); ++i)
    {
        if (d[AI[i][0]] >= 0 and d[AI[i][1]] >= 0)
        {
            AIR.append(AI[i]);
        }
        else
        {
            AIL.append(AI[i]);
        }
    }

    BSPNode RChild;
    if (NIR.size() > 0)
    {
        RChild = CreateNode(C,NIR,AIR);
    }
    else
    {
        RChild = CreateNode(AIR[0][1],null,null);
    }

    BSPNode LChild;
    if (NIL.size() > 0)
    {
        LChild = CreateNode(C,NIL,AIL);
    }
    else
    {
        LChild = CreateNode(AIL[0][1],null,null);
    }

    return CreateNode(NI[0],RChild,LChild);
}

```

Once the BSP tree has been constructed, locating an extreme vertex for a potential separating direction \mathbf{D} can be done using the following pseudocode. This function replaces the one that was used for the bisection of indices shown earlier. The `TestIntersection` function corresponding to that bisection remains the same.

```
int GetExtremeIndex (ConvexPolygon C, Vector D)
{
    BSPTree node = C.tree;
    while (node.R)
    {
        if (Dot(C.GetEdge(node.I), D) >= 0)
        {
            node = node.R;
        }
        else
        {
            node = node.L;
        }
    }
    return node.I;
}
```

The leaf nodes have no children and internal nodes have two children, so the test on one child pointer is sufficient to identify leaf nodes.

Convex Polyhedra

The following notation is used throughout this section. Let C_j for $j = 0, 1$ be the convex polyhedra with vertices $P_i^{(j)}$ for $0 \leq i < N_j$, edges with directions $E_i^{(j)}$ for $0 \leq i < M_j$, and faces that are planar convex polygons whose vertices are ordered counterclockwise as you view the face from outside the polyhedron. The outward normal vectors for the faces are $N_i^{(j)}$ for $0 \leq i < L_j$. All the pseudocode relating to convex polyhedra will use the class shown next.

```
class ConvexPolyhedron
{
public:
    int GetVCount (); // number of vertices
    int GetECount (); // number of edges
    int GetFCount (); // number of faces
    Point GetVertex (int i);
    Vector GetEdge (int i);
    Vector GetNormal (int i);
};
```

Only the relevant interface is supplied for clarity of the presentation. The implementation details will vary with the needs of an application.

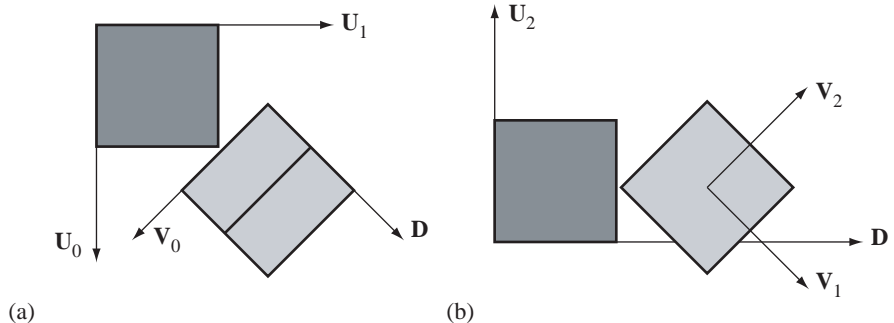


Figure 6.25 Two views of two cubes that are not separated by any face normal but are separated by a cross product of two edges, one from each cube.

The ideas of separation of convex polygons extend to convex polyhedra. For a pair of convex polyhedra, only a finite set of direction vectors needs to be considered for separating tests. The intuition is similar to that of convex polygons. If the two polyhedra are just touching with no interpenetration, the contact is one of face–face, face–edge, face–vertex, edge–edge, edge–vertex, or vertex–vertex. The set of potential separating directions that capture these types of contacts include the normal vectors to the faces of the polyhedra and vectors generated by a cross product of two edges, one from each polyhedron. The necessity of testing more than just the face normals is shown by Figure 6.25.

The first cube (dark gray) has unit-length face normals $\mathbf{U}_0 = (1, 0, 0)$, $\mathbf{U}_1 = (0, 1, 0)$, and $\mathbf{U}_2 = (0, 0, 1)$. The second cube (light gray) has unit-length face normals $\mathbf{V}_0 = (1, -1, 0)/\sqrt{2}$, $\mathbf{V}_1 = (1, 1, -\sqrt{2})/2$, and $\mathbf{V}_2 = (1, 1, \sqrt{2})/2$. The other vector shown in the figure is $\mathbf{D} = (1, 1, 0)/\sqrt{2}$. Figure 6.25(a) shows a view of the two cubes when looking in the direction $-\mathbf{U}_2$. Figure 6.25(b) shows a view when looking along the direction $\mathbf{U}_2 \times \mathbf{D}$. In view (a), neither \mathbf{U}_0 , \mathbf{U}_1 , nor \mathbf{V}_0 are separating directions. In view (b), neither \mathbf{U}_2 , \mathbf{V}_1 , nor \mathbf{V}_2 are separating directions. No face axis separates the two cubes, yet they are not intersecting. A separating direction is $\mathbf{D} = \mathbf{U}_2 \times \mathbf{V}_0$, a cross product of edges from the cubes.

The pseudocode for using the method of separating axes to test for intersection of two polyhedra, similar to the naive implementation in 2D, is

```

bool TestIntersection (ConvexPolyhedron C0, ConvexPolyhedron C1)
{
    // test faces of C0 for separation
    for (i = 0; i < C0.GetFCount(); ++i)
    {
        D = C0.GetNormal(i);
        ComputeInterval(C0,D,min0,max0);
    }
    // test faces of C1 for separation
    for (i = 0; i < C1.GetFCount(); ++i)
    {
        D = C1.GetNormal(i);
        ComputeInterval(C1,D,min1,max1);
    }
    if (min0 > max1 || min1 > max0)
        return false;
    else
        return true;
}

```

```

        ComputeInterval(C1,D,min1,max1);
        if (max1 < min0 || max0 < min1)
        {
            return false;
        }
    }

    // test faces of C1 for separation
    for (j = 0; j < C1.GetFCount(); ++j)
    {
        D = C1.GetNormal(j);
        ComputeInterval(C0,D,min0,max0);
        ComputeInterval(C1,D,min1,max1);
        if (max1 < min0 || max0 < min1)
        {
            return false;
        }
    }

    // test cross products of pairs of edges
    for (i = 0; i < C0.GetECount(); ++i)
    {
        for (j = 0; j < C1.GetECount(); ++j)
        {
            D = Cross(C0.Edge(i),C1.Edge(j));
            ComputeInterval(C0,D,min0,max0);
            ComputeInterval(C1,D,min1,max1);
            if (max1 < min0 || max0 < min1)
            {
                return false;
            }
        }
    }

    return true;
}

void ComputeInterval (ConvexPolyhedron C, Vector D, double& min,
                     double& max)
{
    min = Dot(D,C.GetVertex(0));
    max = min;
    for (i = 1; i < C.GetVCount(); ++i)
    {
        value = Dot(D,C.GetVertex(i));
        if (value < min)
        {

```

```
        min = value;  
    }  
    else  
    {  
        max = value;  
    }  
}
```

The function `ComputeInterval` is $O(N)$ for a polyhedron of N vertices. A quick glance at the code shows that you need $L_0(N_0 + N_1) + L_1(N_0 + N_1) + M_0 M_1(N_0 + N_1) = (L_0 + L_1 + M_0 M_1)(N_0 + N_1)$ units of time to execute the test (cubic order). Since all pairs of edges are tested in the worst case, the time is at least quadratic. Our only hope in reducing the time complexity is to have a faster algorithm for finding extreme vertices for convex polyhedra, just as we did for convex polygons.

The asymptotically better algorithm for finding the extreme points of a convex polygon in 2D does have a counterpart for polytopes in 3D. Given N vertices, it is possible to find extreme points in $O(\log N)$ time [Kir83, DK90]. The algorithm requires preprocessing the polytope to build a data structure, called the *Dobkin–Kirkpatrick hierarchy*, that supports the queries. The preprocessing requires $O(N)$ time. A well-written presentation of the algorithm is provided in [O'R98] and has enough information and pseudocode to assist you in implementing the algorithm. The idea is to construct a sequence of nested polytopes C_0, \dots, C_k , where the innermost polytope C_k is either a triangle or a tetrahedron and the outermost polytope C_0 is the original one. The extremal query relies on quickly finding the extreme point on C_i given the extreme point on C_{i+1} ; in fact, this can be done in constant time, $O(1)$. The construction of the nested polytopes shows that $k = O(\log N)$, so the total query executes in $O(\log N)$ time.

Here is a brief summary of the ideas presented in [O'R98] to give you an idea of the complexity of implementing the algorithm. The vertices and edges of a polytope form a planar graph. The construction of C_{i+1} from C_i is based on locating a *maximum independent set* of vertices for the graph of C_i . A set of vertices is *independent* if no two vertices are adjacent. An independent set S is *maximum* if no other independent set has more vertices than does S . The vertices in the maximum independent set are removed from C_i , one at a time. On removal of a vertex \mathcal{P} , a hole is introduced into the current polytope. The neighboring vertices of \mathcal{P} – call this set $N(\mathcal{P})$ – must be triangulated to generate the faces that fill in the hole. The triangulation is accomplished via a convex hull algorithm. After removal of a maximum independent set of vertices from C_i , we have C_{i+1} . However, the construction must support the extremal query; linking steps must occur between faces of C_{i+1} and C_i . The pseudocode mentioned in [O'R98] is

```
void ComputeHierarchy (ConvexPolyhedron C)
{
    int i = 0;
```

```

C.hier.poly[0] = C; // the assignment copies C into poly[0]
while ( C.hier.poly[0].N > 4 )
{
    set<point> S = GetMaximumIndependentSet(C.hier.poly[i]);
    C.hier.poly[i+1] = C.hier.poly[i];
    for (each P in S) do
    {
        delete P from C.hier.poly[i+1];
        triangulate the hole by constructing ConvexHull(N(V));
        insert the triangles into C.hier.poly[i+1];
        link each new triangle of C.hier.poly[i+1] to P;
    }
    link unchanged faces of C.hier.poly[i+1] to C.hier.poly[i];
}
}
}

```

As it turns out, constructing a maximum independent set of a graph is NP-complete [CLR90, ch. 36]. To obtain a polynomial time construction of the hierarchy, an approximation is required. This is provided by [Ede87, Theorem 9.8] and is proved that the hierarchy construction remains $O(N)$ and the extremal query remains $O(\log N)$. The approximation produces a sufficiently large independent set, although not necessarily a maximum independent set. The pseudocode is

```

set<point> GetLargeIndependentSet (ConvexPolyhedron C)
{
    set<point> S = empty;
    mark all vertices P in C of degree(P) >= 9;
    while (some nodes remain unmarked) do
    {
        choose an unmarked node P;
        mark P and all neighbors in N(P);
        S.insert(P);
    }
}

```

The function call `GetMaximumIndependentSet` in the hierarchy construction is replaced by a call to the function `GetLargeIndependentSet`.

The extremal query is based on the following result, formulated for the direction $\mathbf{D} = (0, 0, 1)$, but easily adaptable to other directions [EM85]. If \mathcal{M}_i is the extreme point for C_i and \mathcal{M}_{i+1} is the extreme point for C_{i+1} , then either $\mathcal{M}_i = \mathcal{M}_{i+1}$ or \mathcal{M}_{i+1} has the largest z -value among the vertices adjacent to \mathcal{M}_i . Although the obvious approach now is just to search the neighbors directly, the problem is that the number of neighbors can be quite large and lead to an $O(N)$ query rather than an $O(\log N)$ query. The search must be narrowed to some subset of neighbors.

The key is to project C_{i+1} onto a coordinate plane parallel to the z -axis. That projection is a convex polygon whose extreme vertex \mathcal{M}'_{i+1} in the z -direction is the projection of \mathcal{M}_{i+1} . Two edges of the convex polygon share \mathcal{M}'_{i+1} , call them \mathbf{L}'_{i+1}

and \mathbf{R}'_{i+1} . These edges are projections of some edges \mathbf{L}_{i+1} and \mathbf{R}_{i+1} that share \mathcal{M}_{i+1} . The *umbrella parents* of an edge \mathbf{E} of C_{i+1} are defined as follows. If \mathbf{E} is not an edge of C_i , then it was generated for C_{i+1} by the removal of a vertex \mathbf{V} from C_i . In this case \mathbf{V} is the sole umbrella parent of \mathbf{E} (“umbrella” refers to the umbrella of faces sharing \mathbf{V}). If \mathbf{E} is an edge of C_i , then its umbrella parents are the two vertices of C_i at the tips of the triangle faces that share \mathbf{E} . This allows us to narrow the search for the extreme point: If \mathcal{M}_i is the extreme point for C_i and \mathcal{M}_{i+1} is the extreme point for C_{i+1} , then either $\mathcal{M}_i = \mathcal{M}_{i+1}$ or \mathcal{M}_{i+1} has the largest z -value among the umbrella parents of the edges \mathbf{L}_{i+1} and \mathbf{R}_{i+1} . The pseudocode for the query as presented in [O'R98] is listed below. It is assumed that the sequence of nested polytopes was already constructed.

```

point GetExtremePoint (ConvexPolyhedron C, Vector D)
{
    // polys 0 through k = size - 1
    int k = C.hier.size() - 1;
    array<point> M[k + 1];

    // extreme of triangle or tetrahedron
    M[k] = GetExtremeVertex(C.hier.poly[k]);

    compute extreme edges L[k] and R[k];
    for (i = k - 1; i >= 0; --i)
    {
        M[i] = SelectExtremeFrom(M[i + 1], Parents(L[i + 1]),
                                  Parents(R[i + 1]));

        if (M[i] not equal to M[i + 1]) then
        {
            for (all edges incident to M[i]) do
            {
                save extreme edges L[i] and R[i];
            }
        }
        else
        {
            compute L[i] from L[i + 1];
            compute R[i] from R[i + 1];
        }
    }
    return M[0];
}

```

The summary here should give you the idea that the implementation of the Dobkin–Kirkpatrick hierarchy and the extremal queries is tractable, but tedious. An alternative that is easier to implement is presented here and is the extension of the BSP tree construction used for finding extreme points for convex polygons. The construction of the BSP tree is $O(N \log N)$ and the query is $O(\log N)$ as long as you have

a balanced tree. The asymptotic order of construction of the BSP data structure is worse than the $O(N)$ construction of the data structure for the Dobkin–Kirkpatrick hierarchy, but since a collision system does the constructions on start-up of the simulation, and since the BSP tree is easy code to write, the comparison of asymptotic times is irrelevant.

Extremal Query for a Convex Polyhedron

A convex polyhedron has vertices \mathbf{V}_i for $0 \leq i < n$ and a set of edges and a set of faces with outer pointing normals \mathbf{N}_j . The set of extremal points for a specified direction is either a polyhedron vertex, edge, or face. To illustrate, Figure 6.26 shows a tetrahedron and a unit sphere with vertices that correspond to the face normals of the tetrahedron, whose great circle arcs connecting the vertices correspond to the edges of the tetrahedron, and whose spherical polygons correspond to the vertices of the tetrahedron. This view of the sphere is called the *spherical dual* of the polyhedron.

The tetrahedron has vertices $\mathbf{V}_0 = (0, 0, 0)$, $\mathbf{V}_1 = (1, 0, 0)$, $\mathbf{V}_2 = (0, 1, 0)$, and $\mathbf{V}_3 = (0, 0, 1)$. The face normals are $\mathbf{N}_0 = (1, 1, 1)/\sqrt{3}$, $\mathbf{N}_1 = (-1, 0, 0)$, $\mathbf{N}_2 = (0, -1, 0)$, and $\mathbf{N}_3 = (0, 0, -1)$. The sphere is partitioned into four spherical triangles. The interior of the spherical triangle with $\langle \mathbf{N}_0, \mathbf{N}_1, \mathbf{N}_2 \rangle$ corresponds to those directions for which

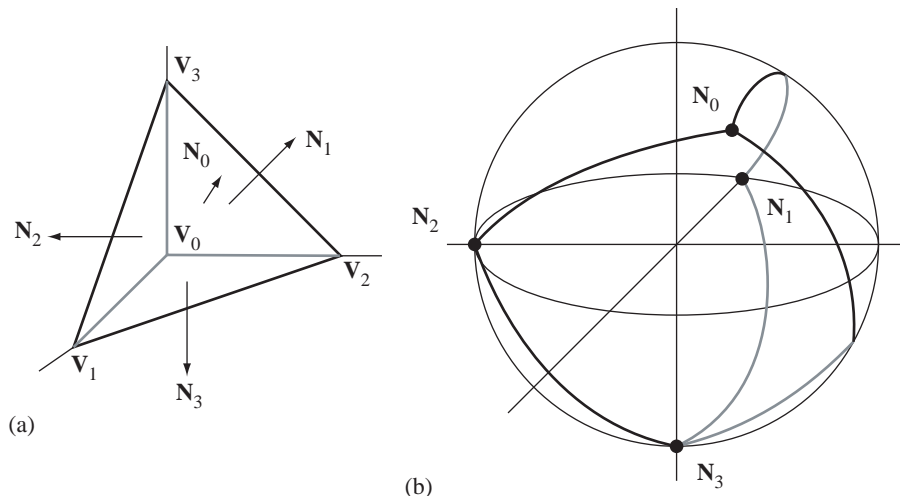


Figure 6.26 (a) A tetrahedron. (b) A unit sphere whose vertices correspond to normal directions of the tetrahedron, whose great circle arcs connecting the vertices correspond to edges of the tetrahedron, and whose spherical polygons correspond to vertices of the tetrahedron (the *spherical dual* of the tetrahedron).

V_3 is the unique extreme point. Observe that the three normals forming the spherical triangle are the normals for the faces that share vertex V_3 .

Generally, the normal and edge directions of a polytope lead to a partitioning of the sphere into spherical convex polygons. The interior of a single spherical convex polygon corresponds to the set of directions for which a vertex of the polytope is the unique extreme point. The number of edges of the spherical convex polygon is the number of polytope faces sharing that vertex. Just as for convex polygons in 2D, we can construct a BSP tree of the spherical polygons and use it for fast determination of extreme vertices. The method used for 2D extends to 3D with each node of the BSP tree representing a hemisphere determined by $\mathbf{N}_i \times \mathbf{N}_j \cdot \mathbf{D} \geq 0$, where \mathbf{N}_i and \mathbf{N}_j are unit-length normal vectors for two adjacent triangles.

The vector $\mathbf{H}_{ij} = \mathbf{N}_i \times \mathbf{N}_j$ is perpendicular to the plane containing the two normals. The hemispheres corresponding to this vector are $\mathbf{H}_{ij} \cdot \mathbf{D} \geq 0$ and $\mathbf{H}_{ij} \cdot \mathbf{D} < 0$. The tetrahedron of Figure 6.26 has six such vectors, listed as $\{\mathbf{H}_{12}, \mathbf{H}_{13}, \mathbf{H}_{23}, \mathbf{H}_{01}, \mathbf{H}_{02}, \mathbf{H}_{03}\}$. Please note that the subscripts correspond to normal vector indices, not to vertex indices. Each arc of the sphere connecting two normal vectors corresponds to an edge of the tetrahedron, label the arcs A_{ij} . The root node of the tree claims arc A_{12} for splitting. The condition $\mathbf{N}_1 \times \mathbf{N}_2 \cdot \mathbf{D} \geq 0$ splits the sphere into two hemispheres. Figure 6.27 shows those hemispheres with viewing direction $(0, 0, -1)$.

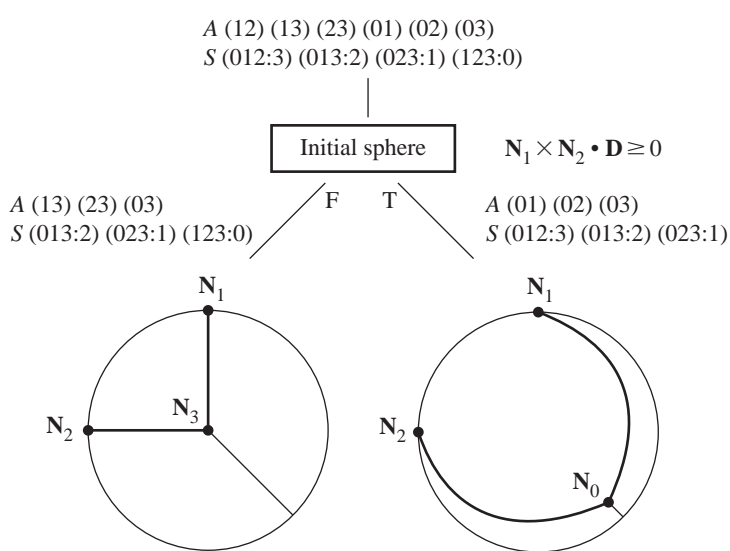


Figure 6.27 The root of the BSP tree and the two hemispheres obtained by splitting. Both children are displayed with a viewing direction $(0, 0, -1)$. The right child is the top of the sphere viewed from the outside and the left child is the bottom of the sphere viewed from the inside.

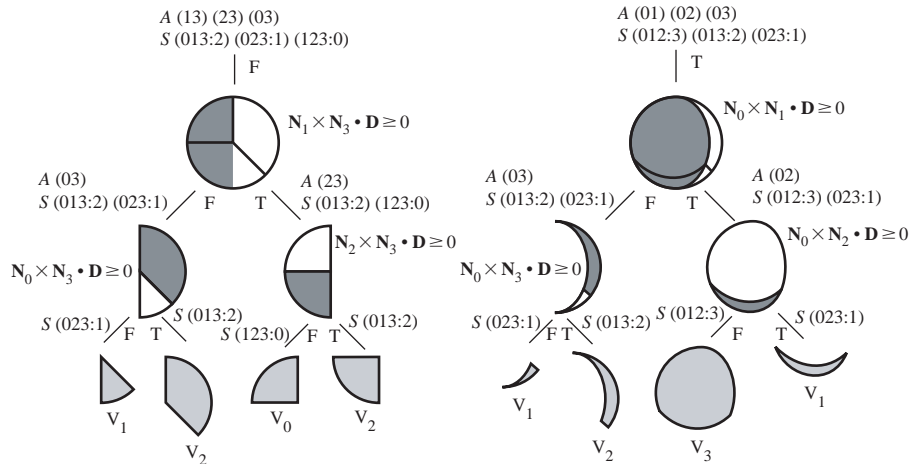


Figure 6.28 The BSP trees for the children of the root.

The set of arcs and the set of spherical polygons bounded by the arcs are the inputs to the BSP tree construction. These sets are shown at the top of the figure. An arc is specified by A_{ij} and connects \mathbf{N}_i and \mathbf{N}_j . A spherical polygon is $S_{i_1, \dots, i_n; \ell}$ and has vertices \mathbf{N}_{i_1} through \mathbf{N}_{i_n} . The vertex \mathbf{V}_ℓ of the original polyhedron is the extreme vertex corresponding to the spherical polygon. In our example the spherical polygons all have three vertices. Figure 6.28 shows the BSP trees for the children of the root.

During BSP tree construction, the root node claims the first arc A_{12} and uses the vector $\mathbf{E} = \mathbf{N}_1 \times \mathbf{N}_2$ for testing other vectors corresponding to arcs A_{ij} . Let $d_i = \mathbf{E} \cdot \mathbf{N}_i$ and $d_j = \mathbf{E} \cdot \mathbf{N}_j$. If $d_i \geq 0$ and $d_j \geq 0$, then the arc is completely on one side of the hemisphere implied by \mathbf{E} . A_{ij} is placed in a set that will be used to generate the BSP tree for the right child of the root. If $d_i \leq 0$ and $d_j \leq 0$, then the arc is completely on the other side of the hemisphere and is placed in a set that will be used to generate the BSP tree for the left child of the root. If $d_i d_j < 0$, then the arc is partially in each hemisphere and is added to both sets. This is exactly the algorithm we used in 2D.

In 3D we have some additional work in that the spherical faces must be processed by the tree to propagate to the leaf nodes the indices of the extreme vertices represented by those nodes. In fact, the processing is similar to that for arcs. Let $S_{i,j,k;\ell}$ be a face to be processed at the root node. Let $d_i = \mathbf{E} \cdot \mathbf{N}_i$, $d_j = \mathbf{E} \cdot \mathbf{N}_j$, and $d_k = \mathbf{E} \cdot \mathbf{N}_k$. If $d_i \geq 0$ and $d_j \geq 0$ and $d_k \geq 0$, then the spherical face is completely on one side of the hemisphere implied by \mathbf{E} . $S_{i,j,k;\ell}$ is placed in a set that will be used to generate the BSP tree for the right child of the root. If $d_i \leq 0$, $d_j \leq 0$, and $d_k \leq 0$, then the face is completely on the other side of the hemisphere and is placed in a set that will be used to generate the BSP tree for the right child of the root. Otherwise the arc is

partially in each hemisphere and is added to both sets. In general for a spherical face with n vertices, the face is used for construction of the right child if all dot products are nonnegative, for construction of the left child if all dot products are nonpositive, or for construction of both children if some dot products are positive and some are negative.

A query for a specified direction \mathbf{D} is structured the same as for convex polygons. The signs of the dot products of \mathbf{D} with the \mathbf{H} vectors in the BSP tree are computed, and the appropriate path is taken through the tree. A balanced tree will have depth $O(\log n)$ for a polyhedron of n vertices, so the query takes logarithmic time. However, there is a technical problem. The spherical arcs as described so far might not lead to a balanced tree. Consider a polyhedron formed by an $(n - 2)$ -sided convex polygon in the xy -plane with vertices $\mathbf{V}_i = (x_i, y_i, 0)$ for $1 \leq i \leq n - 2$ and by two vertices $\mathbf{V}_0 = (0, 0, z_0)$, with $z_0 < 0$, and $\mathbf{V}_{n-1} = (0, 0, z_{n-1})$, with $z_{n-1} > 0$. Figure 6.29 shows such a polyhedron.

The spherical dual has two spherical convex polygons, each with $n - 2$ arcs and $n - 2$ spherical convex polygons, each with 4 arcs. If \mathbf{D} is contained by one of

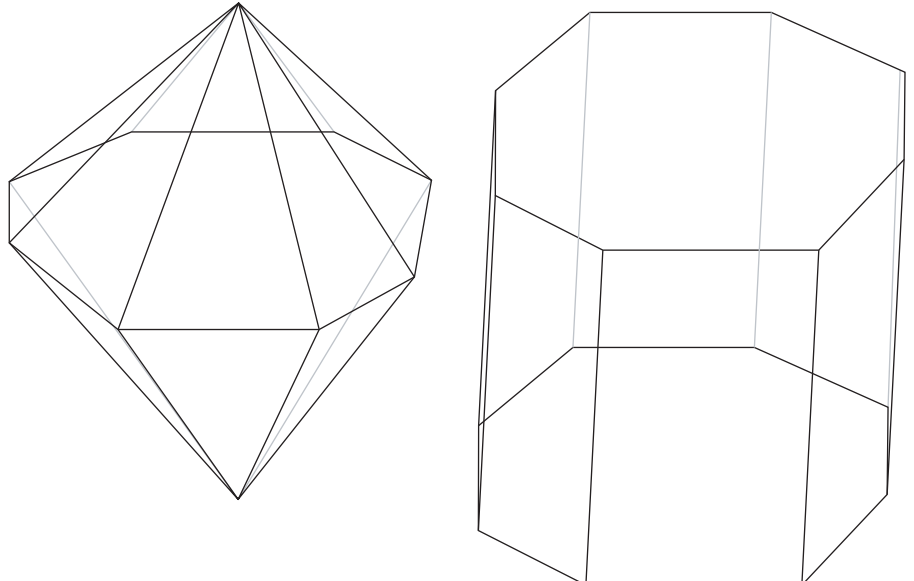


Figure 6.29 Left: A convex polyhedron for which the point-in-spherical-polygon test, using only the original arcs, is $O(n)$ (the figure shows $n = 8$, but imagine a very large n). Right: The inscribed convex polyhedron whose edges generate the arcs of the spherical convex polygons.

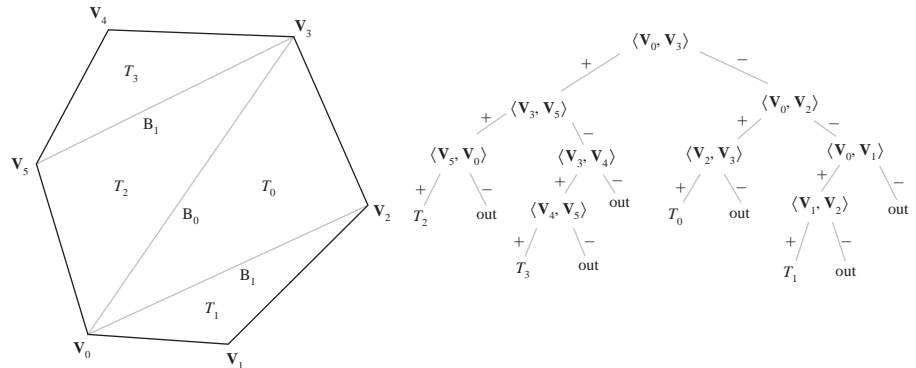


Figure 6.30 A convex polygon with bisectors used for an $O(\log n)$ point-in-polygon query. The polygon is partitioned into four triangles labeled T_0 through T_3 .

$(n - 2)$ -sided spherical polygons, the determination of this using only the given arcs requires $n - 2$ point-on-which-side-of-arc queries. This is an $O(n)$ algorithm.

The pathological problem mentioned previously is avoided by appealing to an $O(\log n)$ query for point-in-convex-polygon determination. In fact, this problem uses what you may think of as the Dobkin–Kirkpatrick hierarchy restricted to two dimensions. However, it is phrased in terms of a binary search using binary separating lines. Consider the convex polygon of Figure 6.30.

If we use only the polygon edges for containment testing, we would need six tests, each showing that the query point is to the left of the edges. Instead, we use *bisectors*. The first bisector is segment $\langle V_0, V_3 \rangle$ and is marked with B_0 in the figure. The query point P is either to the left of the bisector, where $(V_3 - V_0) \cdot (P - V_0)^\perp \geq 0$, or to the right of the bisector, where $(V_3 - V_0) \cdot (P - V_0)^\perp < 0$. The original polygon has six edges. The polygon to the left of the bisector has four edges, and the containment test is applied to that left polygon. The bisector edge has already been tested, so only the three remaining edges need to be tested for the containment.

The next bisector to be used is one of the segments marked with B_1 , either $\langle V_3, V_5 \rangle$ or $\langle V_0, V_2 \rangle$. Naturally, the choice depends on which side of the bisector $\langle V_0, V_3 \rangle$ the query point P occurs. If P is to the left of $\langle V_0, V_3 \rangle$ and to the left of $\langle V_3, V_5 \rangle$, then the only subpolygon that might contain P is a triangle. The remaining edge to test is $\langle V_5, V_0 \rangle$. If instead P is to the right of $\langle V_3, V_5 \rangle$, then P is potentially in triangle T_3 . There are two remaining edges to test, so we can consider this yet another bisection step.

The binary tree in the right image of Figure 6.30 shows the query tree implied by the bisectors and polygon edges. A tree link marked with a “+” indicates “to the left of,” and a link marked with a “-” indicates “to the right of.” The query point is

tested against each edge, leading to a path from the root of the tree to a leaf node. The leaves are labeled with the region defined by the path. Four of the leaf nodes represent the triangles that make up the convex polygon. Six of the leaf nodes represent the exterior of the polygon; that is, a query point can be “outside” one of the six edges of the polygon.

The choice of the bisectors is based on selecting the medians of the ranges of indices for the subpolygon of interest. This leads to a balanced tree, so a polygon of n edges. The point-in-polygon query requires computing vector differences and dot products for a linear path of nodes through the tree. Such a path has $O(\log n)$ nodes.

The same idea may be applied to determining whether a unit-length vector \mathbf{D} is contained in a spherical convex polygon on the unit sphere. In the 2D problem, the dot product whose sign determines which side of the bisector the point is on was of the form

$$d = (\mathbf{V}_i - \mathbf{V}_j) \cdot (\mathbf{P} - \mathbf{V}_j)^\perp$$

We cared about $d \geq 0$ or $d < 0$. In the 3D problem, we use the normal vectors as the vertices and the direction vector as the query point. The dot product of interest is

$$d = \mathbf{N}_i \times \mathbf{N}_j \cdot \mathbf{D}$$

Imagine walking along the spherical arc from \mathbf{N}_j to \mathbf{N}_i . The vector $\mathbf{N}_i \times \mathbf{N}_j$ points to your left as you walk along the arc. The spherical point \mathbf{D} is to your left whenever $d \geq 0$ and is to your right whenever $d < 0$.

What this means is that the BSP tree we build for the spherical dual must use the bisectors of the spherical polygons as well as the arcs which are their boundary edges. Moreover, we do not just have one spherical polygon to test – we have n such polygons, one for each of the n vertices of the original convex polyhedron. Given the collection of all bisector arcs and boundary edge arcs, we can build the BSP tree one arc at a time. Each arc is tested at a node of the BSP tree to see on which side of the node arc it lies. If fully on the left side, we send the arc to the left subtree of the node for further classification. If fully on the right side, we send the arc to the right subtree. When the arc arrives at a leaf node, it is similarly tested for sidedness and stored as the appropriate child of the leaf node (which now becomes an interior node). If an arc straddles the great circle containing the node arc – one arc endpoint is to the left of the node arc and one arc endpoint is to the right of the node arc – we send the arc to both subtrees of the node. That is, no actual splitting of the arc is performed. This avoids expensive arc–arc intersection finding.

The order of the arcs is important in determining the structure of the BSP tree. We do want a balanced tree. A heuristic to obtain a balanced tree is to sort the arcs. The bisector arcs occur first, the boundary edge arcs last. The first bisector arc of an n -sided spherical polygon splits the polygon into two subpolygons, each with half the number of boundary edge arcs. If we were to do a point-in-spherical-polygon query using such a bisector edge first, we will eliminate half of that spherical polygon’s bisectors and half of its boundary arcs from further processing. This suggests that we order the

bisector arcs based on how many other arcs they reject during a sidedness test. In the implementation, I maintain an ordered set of arcs, using a *separation* measure. The first bisector arc for an n -sided spherical polygon has a separation of $n/2$, measuring how many boundary arcs of that polygon separate the endpoints. A boundary arc itself has a separation measure of 1. The BSP tree is built using the arcs in decreasing order of separation. My numerical experiments showed that indeed the BSP trees are balanced.



SOURCE CODE

ExtremalQuery

An Implementation and Timing

The Foundation library files `Wm5ExtremalQuery3.h` and `Wm5ExtremalQuery3.cpp` are the base class for extremal queries for convex polyhedra. The straightforward $O(n)$ method for computing the extreme points just involves projecting the vertices onto the specified direction vector and computing the extreme projection values. This algorithm is implemented in `Wm5ExtremalQuery3PRJ.h` and `Wm5ExtremalQuery3PRJ.cpp`.

The files `Wm5ExtremalQuery3BSP.h` and `Wm5ExtremalQuery3BSP.cpp` implement the BSP tree algorithm described in this document. The identification of adjacent polyhedron normal vectors \mathbf{N}_i and \mathbf{N}_j requires building a vertex–edge–face data structure. The class implemented in `Wm5BasicMesh.h` and `Wm5BasicMesh.cpp` suffices, but the edges adjacent to a vertex are not required for the extremal queries. You could modify `BasicMesh` to eliminate this adjacency information.

Table 6.1 shows the results of the experiment to compare the BSP tree approach to a simple project-all-vertices approach. The column with header n is the number of vertices of the convex polyhedron. Each polyhedron was used in 10^7 extremal queries. The execution times are listed in the second and third columns, and are in seconds. The target machine was an AMD Athlon XP 2800+ (2.08GHz). The next to last column is the BSP time divided by $\log n$. This ratio is expected to be a constant for large n ;

Table 6.1 Timing for the Project-All and BSP-Tree Extremal Queries

n	BSP time t_b	project-all time t_p	$t_b / \log n$	t_p / n
4	2.141	0.812	1.0705	0.2030
8	3.922	1.547	1.3073	0.1933
16	5.422	2.563	1.3555	0.1601
32	5.937	4.328	1.1874	0.1352
64	6.922	7.765	1.1536	0.1213
128	7.922	14.391	1.1317	0.1124
256	9.281	27.359	1.1601	0.1068
512	10.250	53.859	1.1388	0.1051
1024	11.532	104.125	1.1532	0.1016
2048	12.797	210.765	1.1633	0.1029

that is, we expect the query to be $O(\log n)$. The last column is the project-all-vertices time divided by n , because we expect this algorithm to be $O(n)$.

Of interest is the break-even n . It is somewhere between 32 and 64. If the convex polyhedra in your applications have a small number of vertices, the project-all-vertices approach is clearly the choice. For a larger number of vertices, the BSP approach wins.

The sample application illustrates the queries. A convex polyhedron is displayed using an orthogonal camera. You may rotate it with the mouse. The extreme vertices in the x -direction are drawn as small spheres. The orthogonal camera is used to make it clear that the points are extreme.

6.4.3 OBJECTS MOVING WITH CONSTANT LINEAR VELOCITY

The method of separating axes is used to test for intersection of two stationary convex polyhedra. The set of potential separating axes consists of the face normals for the polyhedra and cross products of edges, each product using an edge from each of the participating polyhedra. As described earlier, a collision detection system can be implemented using a bisection technique. At the first time step, no polyhedra are intersecting. For the next time step, the physical simulation decides how each polyhedron should move based on constraints (using a differential equation solver for the equations of motion). All the polyhedra are moved to their desired locations. Each pair of convex polyhedra are tested for intersection using the method of separating axes. If any pair reports interpenetration, then the system is restarted at the first time step, but with a time increment that is half of what was tried the first time.

The strategy is not bad when only a small number of polyhedra are in the system and when the frequency of contact (or close contact) is small. However, for large numbers of polyhedra in close proximity, a lot of time can be spent in restarting the system. A quick hack to reduce the time is to restart the system only for those pairs that reported an interpenetration. When the bisection is completed, all the objects have been moved to a new state with no inter penetrations, but the time step is (potentially) different for the objects, an implied change in the speeds of some of the objects. For a system that runs on the order of 30 frames per second or larger, this is not usually a noticeable problem.

An alternative to the bisection approach is to attempt to predict the time of collision between two polyhedra. For a small change in time an assumption we can make is that the polyhedra are moving with constant linear velocity and zero angular velocity. Whether or not the assumption is reasonable will depend on your application. The method of separating axes can be extended to handle polyhedra moving with constant linear velocity and to report the first time of contact between a pair. The algorithm is attributed to Ron Levine in a post to the SourceForge game developer algorithms mailing list [Lev00]. As we did for stationary objects, let us first look at the problem for convex polygons to illustrate the ideas for convex polyhedra.

Separation of Convex Polygons

If C_0 and C_1 are convex polygons with linear velocities \mathbf{V}_0 and \mathbf{V}_1 , it can be determined via projections if the polygons will intersect for some time $T \geq 0$. If they do intersect, the first time of contact can be computed. It is enough to work with a stationary polygon C_0 and a moving polygon C_1 with velocity \mathbf{V} since one can always use $\mathbf{V} = \mathbf{V}_1 - \mathbf{V}_0$ to perform the calculations as if C_0 were not moving.

If C_0 and C_1 are initially intersecting, then the first time of contact is $T = 0$. Otherwise, the convex polygons are initially disjoint. The projection of C_1 onto a line with direction \mathbf{D} not perpendicular to \mathbf{V} is itself moving. The speed of the projection along the line is $\sigma = (\mathbf{V} \cdot \mathbf{D})/|\mathbf{D}|^2$. If the projection interval of C_1 moves away from the projection interval of C_0 , then the two polygons will never intersect. The cases when intersection might happen are those when the projection intervals for C_1 move towards those of C_0 .

The intuition for how to predict an intersection is much like that for selecting the potential separating directions in the first place. If the two convex polygons intersect at a first time $T_{\text{first}} > 0$, then their projections are not separated along any line at that time. An instant before first contact, the polygons are separated. Consequently there must be at least one separating direction for the polygons at time $T_{\text{first}} - \varepsilon$ for small $\varepsilon > 0$. Similarly, if the two convex polygons intersect at a last time $T_{\text{last}} > 0$, then their projections are also not separated at that time along any line, but an instant after last contact, the polygons are separated. Consequently there must be at least one separating direction for the polygons at time $T_{\text{last}} + \varepsilon$ for small $\varepsilon > 0$. Both T_{first} and T_{last} can be tracked as each potential separating axis is processed. After all directions are processed, if $T_{\text{first}} \leq T_{\text{last}}$, then the two polygons do intersect with first contact time T_{first} . It is also possible that $T_{\text{first}} > T_{\text{last}}$, in which case the two polygons cannot intersect.

Pseudocode for testing for intersection of two moving convex polygons is given next. The time interval over which the event is of interest is $[0, T_{\text{max}}]$. If knowing an intersection at *any* future time is desired, then set $T_{\text{max}} = \infty$. Otherwise, T_{max} is finite. The function is implemented to indicate there is no intersection on $[0, T_{\text{max}}]$, even though there might be an intersection at some time $T > T_{\text{max}}$.

```

bool TestIntersection (ConvexPolygon C0, Vector V0,
                      ConvexPolygon C1, Vector V1, double tmax, double& tfirst,
                      double& tlast)
{
    V = V1 - V0; // process as if C0 is stationary, C1 is moving
    tfirst = 0;
    tlast = INFINITY;

    // test edges of C0 for separation
    for (i0 = C0.GetN() - 1, i1 = 0; i1 < C0.GetN(); i0 = i1++)
    {
        D = C0.GetNormal(i0);
        ComputeInterval(C0,D,min0,max0);
    }
}

```

```

        ComputeInterval(C1,D,min1,max1);
        speed = Dot(D,V);
        if (NoIntersect(tmax,speed,min0,max0,min1,max1,tfirst,
                         tlast))
        {
            return false;
        }
    }

    // test edges of C1 for separation
    for (i0 = C1.N - 1, i1 = 0; i1 < C1.N; i0 = i1++)
    {
        D = C1.GetNormal(i0);
        ComputeInterval(C0,D,min0,max0);
        ComputeInterval(C1,D,min1,max1);
        speed = Dot(D,V);
        if (NoIntersect(tmax,speed,min0,max0,min1,max1,tfirst,
                         tlast))
        {
            return false;
        }
    }
    return true;
}

bool NoIntersect (double tmax, double speed, double min0,
                  double max0, double min1, double max1, double& tfirst,
                  double& tlast)
{
    if (max1 < min0)
    {
        // interval(C1) initially on 'left' of interval(C0)

        if (speed <= 0) // intervals moving apart
        {
            return true;
        }

        t = (min0 - max1)/speed;
        if (t > tfirst)
        {
            tfirst = t;
        }
        if (tfirst > tmax)
        {
            return true;
        }
    }
}

```

```
t = (max0 - min1)/speed;
if (t < tlast)
{
    tlast = t;
}
if (tfirst > tlast)
{
    return true;
}
}
else if ( max0 < min1 )
{
    // interval(C1) initially on 'right' of interval(C0)

    if (speed >= 0) // intervals moving apart
    {
        return true;
    }

    t = (max0 - min1)/speed;
    if (t > tfirst)
    {
        tfirst = t;
    }
    if (tfirst > tmax)
    {
        return true;
    }

    t = (min0 - max1)/speed;
    if (t < tlast)
    {
        tlast = t;
    }
    if (tfirst > tlast)
    {
        return true;
    }
}
else
{
    // interval(C0) and interval(C1) overlap

    if (speed > 0)
    {
        t = (max0 - min1)/speed;
```

```

        if (t < tlast)
        {
            tlast = t;
        }
        if (tfirst > tlast)
        {
            return true;
        }
    }
    else if (speed < 0)
    {
        t = (min0 - max1)/speed;
        if (t < tlast)
        {
            tlast = t;
        }
        if (tfirst > tlast)
        {
            return true;
        }
    }
    return false;
}

```

The function `ComputeInterval(C,D,min,max)` computes the projection interval $[min, max]$ of a convex polygon C onto the line of direction D using the fast extremal queries described earlier that use an approach based on BSP trees. The pseudocode as written projects the convex polygons onto the line tD . In an implementation, you most likely will want to avoid floating point problems in the projection values when the vertices have large components. An additional parameter to `ComputeInterval` should be a point approximately near one (or both) polygons, something as simple as choosing a vertex P of a polygon. The projection is onto $P + tD$ instead.

The following example illustrates the ideas. The first box is the unit cube $0 \leq x \leq 1$ and $0 \leq y \leq 1$ and is stationary. The second box is initially $0 \leq x \leq 1$ and $1 + \delta \leq y \leq 2 + \delta$ for some $\delta > 0$. Let its velocity be $(1, -1)$. Whether or not the second box intersects the first box depends on the value of δ . The only potential separating axes are $(1, 0)$ and $(0, 1)$. Figure 6.31 shows the initial configuration for three values of δ , one where there will be an edge–edge intersection, one where there will be a vertex–vertex intersection, and one where there is no intersection.

The black box is stationary. The dark gray box is moving. The black vector indicates the direction of motion. The dotted boxes indicate where the moving box first touches the stationary box. In Figure 6.31(c), the dotted line indicates that the moving box will miss the stationary box. For $D = (1, 0)$, the pseudocode produces $min0 = 0$, $max0 = 1$, $min1 = 0$, $max1 = 1$, and $speed = 1$. The projected intervals are initially overlapping. Since the speed is positive, $T = (max0-min1)/speed = 1 < TLast = INFINITY$

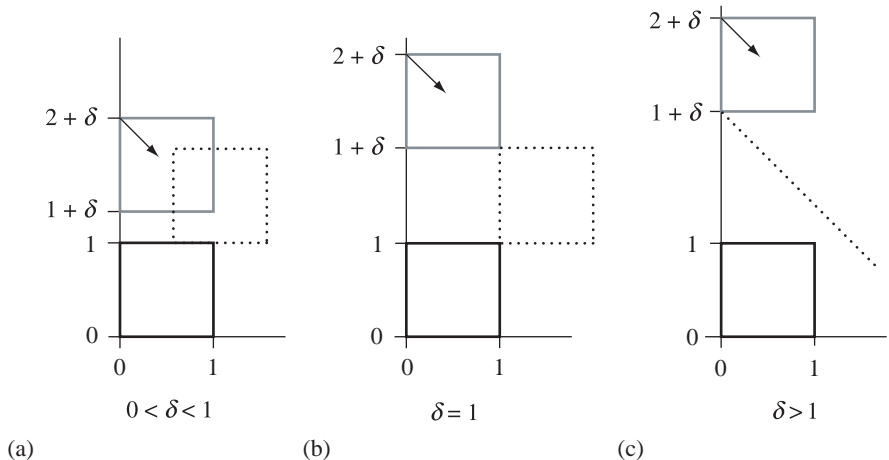


Figure 6.31 (a) Edge–edge intersection predicted. (b) Vertex–vertex intersection predicted. (c) No intersection predicted.

and T_{Last} is updated to 1. For $\vec{D} = (0, 1)$, the pseudocode produces $\min_0 = 0$, $\max_0 = 1$, $\min_1 = 1 + \delta$, $\max_1 = 2 + \delta$, and $\text{speed} = -1$. The moving projected interval is initially on the right of the stationary projected interval. Since the speed is negative, $T = (\max_0 - \min_1) / \text{speed} = \delta > T_{\text{First}} = 0$ and T_{First} is updated to δ . The next block of code sets $T = (\min_0 - \max_1) / \text{speed} = 2 + \delta$. The value T_{Last} is not updated since $2 + \delta < 1$ cannot happen for $\delta > 0$. On exit from the loop over potential separating directions, $T_{\text{First}} = \delta$ and $T_{\text{last}} = 1$. The objects intersect if and only if $T_{\text{first}} \leq T_{\text{last}}$, or $\delta \leq 1$. This condition is consistent with the images in Figure 6.31. Figure 6.31(a) has $\delta < 1$ and Figure 6.31(b) has $\delta = 1$, intersections occurring in both cases. Figure 6.31(c) has, $\delta > 1$ and no intersection occurs.

Contact Set for Convex Polygons

Although we are interested in nonpenetration intersections for moving objects, I mention the stationary case just for completeness. The find-intersection query for two stationary convex polygons is a special example of Boolean operations on polygons. If the polygons have N_0 and N_1 vertices, there is an intersection algorithm of order $O(N_0 + N_1)$ for computing the intersection [O'R98]. A less efficient algorithm is to clip the edges of each polygon against the other polygon. The order of this algorithm is $O(NM)$. Of course, the asymptotic analysis applies to large N and M , so the latter algorithm is potentially a good choice for triangles and rectangles.

Given two moving convex objects C_0 and C_1 , initially not intersecting and with velocities \mathbf{V}_0 and \mathbf{V}_1 , we showed earlier how to compute the first time of contact T , if it exists. Assuming it does, the sets $C_0 + T\mathbf{V}_0 = \{\mathcal{X} + T\mathbf{V}_0 : \mathcal{X} \in C_0\}$ and $C_1 + T\mathbf{V}_1 = \{\mathcal{X} + T\mathbf{V}_1 : \mathcal{X} \in C_1\}$ are just touching with no interpenetration. See Figure 6.21 for the various configurations.

The `TestIntersection` function can be modified to keep track of which vertices or edges are projected to the endpoints of the projection interval. At the first time of contact, this information is used to determine how the two objects are oriented with respect to each other. If the contact is vertex–edge or vertex–vertex, then the contact set is a single point, a vertex. If the contact is edge–edge, the contact set is a line segment that contains at least one vertex. Each endpoint of the projection interval is either generated by a vertex (unique extreme) or an edge (nonunique extreme). A class to store all the relevant projection information is

```
class ProjInfo
{
public:
    double min, max; // projection interval [min,max]
    int index[2];
    bool isUnique[2];
};
```

The zero-indexed entries of the array correspond to the minimum of the interval. If the minimum is obtained from the unique extreme vertex \mathbf{V}_i , then `index[0]` stores i and `isUnique[0]` is true. If the minimum is obtained from an edge E_j , then `index[0]` stores j and `isUnique[0]` stores false. The same conventions apply for the one-indexed entries corresponding to the maximum of the interval.

To support calculation of the contact set and the new configuration structure, we need to modify the extremal query `GetExtremeIndex`. The version we developed just returned the index of an extreme vertex with no information about whether it is unique or an endpoint of an extreme edge. We now need this information. The revised query is

```
int GetExtremeIndex (ConvexPolyhedron C, Vector D, bool& isUnique)
{
    BSPTree node = C.tree;
    isUnique = true;
    while (node.R)
    {
        d = Dot(C.GetEdge(node.I), D);
        if (d > 0)
        {
            node = node.R;
        }
        else if (d < 0)
        {
            node = node.L;
```

```

        }
    else // d == 0
    {
        // direction is an edge normal, edge is extreme
        isUnique = false;
        break;
    }
}
return node.I;
}

```

Of course, in an implementation using floating point numbers, the test on the dot product d would use some application-specified value $\varepsilon > 0$ and replace $d > 0$ by $d > \varepsilon$ and $d < 0$ by $d < -\varepsilon$. Function ComputeInterval must be modified to provide more information than just the projection interval.

```

void ComputeInterval (ConvexPolyhedron C, Vector D, ProjInfo& info)
{
    info.index[0] = GetExtremeIndex(C,-D,info.isUnique[0]);
    info.min = Dot(D,C.GetVertex(info.index[0]));
    info.index[1] = GetExtremeIndex(C,+D,info.isUnique[1]);
    info.max = Dot(D,C.GetVertex(info.index[1]));
}

```

The projection intervals for the two polygons were inputs to the NoIntersect function. Now those intervals are stored in the ProjInfo objects, so NoIntersect must be modified to reflect this. In the event that there will be an intersection between the moving polygons, it is necessary that the projection information be saved for later use in determining the contact set. As a result, NoIntersect must keep track of the ProjInfo objects corresponding to the current first time of contact. Finally, the contact set calculation will require knowledge of the order of the projection intervals. NoIntersect will set a flag `side` with value $+1$ if the intervals intersect at the maximum of the C_0 interval and the minimum of the C_1 interval, or with value -1 if the intervals intersect at the minimum of the C_0 interval and the maximum of the C_1 interval. The modified pseudocode is

```

bool NoIntersect (double tmax, double speed, ProjInfo info0,
                  ProjInfo info1, ProjInfo& curr0, ProjInfo& curr1, int& side,
                  double& tfirst, double& tlast)
{
    if (info1.max < info0.min)
    {
        if (speed <= 0)
        {
            return true;
        }

        t = (info0.min - info1.max)/speed;
        if (tfirst > t)
        {
            tfirst = t;
            curr0 = info0;
            curr1 = info1;
            side = -1;
        }
        else if (tlast < t)
        {
            tlast = t;
            curr0 = info1;
            curr1 = info0;
            side = +1;
        }
    }
}

```

```
if (t > tfirst)
{
    tfirst = t;
    side = -1;
    curr0 = info0;
    curr1 = info1;
}
if (tfirst > tmax)
{
    return true;
}

t = (info0.max - info1.min)/speed;
if (t < tlast)
{
    tlast = t;
}
if (tfirst > tlast)
{
    return true;
}
else if (info0.max < info1.min)
{
    if (speed >= 0)
    {
        return true;
    }
    t = (info0.max - info1.min)/speed;
    if (t > tfirst)
    {
        tfirst = t;
        side = +1;
        curr0 = info0;
        curr1 = info1;
    }
    if (tfirst > tmax)
    {
        return true;
    }

    t = (info0.min - info1.max)/speed;
    if (t < tlast)
    {
        tlast = t;
    }
    if (tfirst > tlast)
```

```

    {
        return true;
    }
}
else
{
    if (speed > 0)
    {
        t = (info0.max - info1.min)/speed;
        if (t < tlast)
        {
            tlast = t;
        }
        if (tfirst > tlast)
        {
            return true;
        }
    }
    else if (speed < 0)
    {
        t = (info0.min - info1.max)/speed;
        if (t < tlast)
        {
            tlast = t;
        }
        if (tfirst > tlast)
        {
            return true;
        }
    }
}
return false;
}

```

With the indicated modifications, `TestIntersection` has the equivalent formulation

```

bool TestIntersection (ConvexPolygon C0, Vector V0,
                      ConvexPolygon C1, Vector V1, double tmax, double& tfirst,
                      double& tlast)
{
    ProjInfo info0, info1, curr0, curr1;
    V = V1 - V0; // process as if C0 stationary and C1 moving
    tfirst = 0;
    tlast = INFINITY;

    // process edges of C0
    for (i0 = C0.GetN() - 1, i1 = 0; i1 < C0.GetN(); i0 = i1++)
    {

```

```

D = C0.GetNormal(i0);
ComputeInterval(C0,D,info0);
ComputeInterval(C1,D,info1);
speed = Dot(D,v);
if (NoIntersect(tmax,speed,info0,info1,curr0,curr1,side,
    tfirst,tlast))
{
    return false;
}
}

// process edges of C1
for (i0 = C1.GetN() - 1, i1 = 0; i1 < C1.GetN(); i0 = i1++)
{
    D = C1.GetNormal(i0);
    ComputeInterval(C0,D,info0);
    ComputeInterval(C1,D,info1);
    speed = Dot(D,v);
    if (NoIntersect(tmax,speed,info0,info1,curr0,curr1,side,
        tfirst,tlast))
    {
        return false;
    }
}

return true;
}

```

The `FindIntersection` pseudocode has exactly the same implementation as `TestIntersection`, but with one additional block of code after the two loops that is reached if there will be an intersection. When the polygons will intersect at time T , they are effectively moved with their respective velocities and the contact set is calculated. Let $\mathcal{Q}_i^{(j)} = \mathcal{P}_i^{(j)} + T\mathbf{V}^{(j)}$ represent the polygon vertices after motion. In the case of edge–edge contact, for the sake of argument, suppose that the contact edges are $\mathbf{E}_0^{(0)}$ and $\mathbf{E}_0^{(1)}$. Figure 6.32 illustrates the configurations for two triangles.

Because of the counterclockwise ordering of the polygons, observe that the two edge directions are parallel, but in opposite directions. The edge of the first polygon is parameterized as $\mathcal{Q}_0^{(0)} + s\mathbf{E}_0^{(0)}$ for $s \in [0, 1]$. The edge of the second polygon has the same parametric form, but with $s \in [s_0, s_1]$ where

$$s_0 = \frac{\mathbf{E}_0^{(0)} \cdot (\mathcal{Q}_1^{(1)} - \mathcal{Q}_0^{(0)})}{|\mathbf{E}_0^{(0)}|^2} \quad \text{and} \quad s_1 = \frac{\mathbf{E}_0^{(0)} \cdot (\mathcal{Q}_0^{(1)} - \mathcal{Q}_0^{(0)})}{|\mathbf{E}_0^{(0)}|^2}.$$

The overlap of the two edges occurs for $\bar{s} \in I = [0, 1] \cap [s_0, s_1] \neq \emptyset$. The corresponding points in the contact set are $\mathcal{P}_0^{(0)} + T\vec{W}^{(0)} + \bar{s}\vec{E}_0^{(0)}$ for $\bar{s} \in I$.

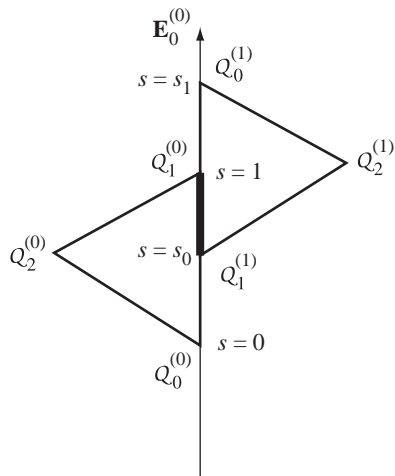


Figure 6.32 Edge–edge contact for two moving triangles.

In the event the two polygons are initially overlapping, the contact set is more expensive to construct. This set can be constructed by standard methods involving Boolean operations on polygons.

The pseudocode is shown next. The intersection is a convex polygon and is returned in the last two arguments of the function. If the intersection set is nonempty, the return value of the function is true. The set must itself be convex. The number of vertices in the set is stored in quantity and the vertices, in counterclockwise order, are stored in the array I []. If the return value is false, the last two arguments of the function are invalid and should not be used.

```

bool FindIntersection (ConvexPolygon C0, Vector V0,
                      ConvexPolygon C1, Vector W1, double tmax, double& tfirst,
                      double& tlast, int& quantity, Point I[])
{
    ProjInfo info0, info1, curr0, curr1;
    V = V1 - V0; // process as if C0 stationary and C1 moving
    tfirst = 0;
    tlast = INFINITY;

    // process edges of C0
    for (i0 = C0.GetN() - 1, i1 = 0; i1 < C0.GetN(); i0 = i1++)
    {
        D = C0.GetNormal(i0);
        ComputeInterval(C0,D,info0);
        ComputeInterval(C1,D,info1);
        speed = Dot(D,v);
    }
}

```

```

        if (NoIntersect(tmax,speed,info0,info1,curr0,curr1,side,
                         tfirst,tlast))
        {
            return false;
        }
    }

// process edges of C1
for (i0 = C1.GetN() - 1, i1 = 0; i1 < C1.GetN(); i0 = i1++)
{
    D = C1.GetNormal(i0);
    ComputeInterval(C0,D,info0);
    ComputeInterval(C1,D,info1);
    speed = Dot(D,v);
    if (NoIntersect(tmax,speed,info0,info1,curr0,curr1,side,
                     tfirst,tlast))
    {
        return false;
    }
}

// compute the contact set
GetIntersection(C0,V0,C1,V1,curr0,curr1,side,tfirst,
                 quantity,I);
return true;
}

```

The intersection calculator pseudocode is shown next. Observe how the projection types are used to determine if the contact is vertex–vertex, edge–vertex, or edge–edge.

```

void GetIntersection (ConvexPolygon C0, Vector V0,
                      ConvexPolygon C1, Vector V1, ProjInfo info0,
                      ProjInfo info1, int side, double tfirst, int& quantity,
                      Point I[])
{
    if (side == 1) // C0-max meets C1-min
    {
        if (info0.isUnique[1])
        {
            // vertex–vertex or vertex–edge intersection
            quantity = 1;
            I[0] = C0.GetVertex(info0.index[1]) + tfirst * V0;
        }
        else if (info1.isUnique[0])
        {
            // vertex–vertex or edge–vertex intersection
            quantity = 1;
            I[0] = C1.GetVertex(info1.index[0]) + tfirst * V1;
        }
    }
}

```

```

        }
    else
    {
        // edge-edge intersection
        P = C0.GetVertex(info0.index[1]) + tfirst * V0;
        E = C0.GetEdge(info0.index[1]);
        Q0 = C1.GetVertex(info1.index[0]);
        Q1 = C1.GetVertex(info1.index[0] + 1);
        s0 = Dot(E,Q1-P) / Dot(E,E);
        s1 = Dot(E,Q0-P) / Dot(E,E);
        FindIntervalIntersection(0,1,s0,s1,quantity,interval);
        for (i = 0; i < quantity; ++i)
        {
            I[i] = P + interval[i] * E;
        }
    }
}
else if (side == -1) // C1-max meets C0-min
{
    if (info1.isUnique[1])
    {
        // vertex-vertex or vertex-edge intersection
        quantity = 1;
        I[0] = C1.GetVertex(info1.index[1]) + tfirst * V1;
    }
    else if (info0.isUnique[0])
    {
        // vertex-vertex or edge-vertex intersection
        quantity = 1;
        I[0] = C0.GetVertex(info0.index[0]) + tfirst * V0;
    }
    else
    {
        // edge-edge intersection
        P = C1.GetVertex(info1.index[1]) + tfirst * V1;
        E = C1.GetEdge(info1.index[1]);
        Q0 = C0.GetVertex(info0.index[0]);
        Q1 = C0.GetVertex(info0.index[0] + 1);
        s0 = Dot(E,Q1-P) / Dot(E,E);
        s1 = Dot(E,Q0-P) / Dot(E,E);
        FindIntervalIntersection(0,1,s0,s1,quantity,interval);
        for (i = 0; i < quantity; ++i)
        {
            I[i] = P + interval[i] * E;
        }
    }
}
}

```

```

    else // polygons were initially intersecting
    {
        ConvexPolygon COMoved = C0 + tfirst * V0;
        ConvexPolygon C1Moved = C1 + tfirst * V1;
        FindPolygonIntersection(COMoved,C1Moved,quantity,I);
    }
}
}

```

The final case is the point at which the two polygons were initially overlapping so that the first time of contact is $T = 0$. `FindPolygonIntersection` is a general routine for computing the intersection of two polygons. In our collision detection system with the nonpenetration constraint, we should not need to worry about the last case, although you might want to trap the condition for debugging purposes.

Separation of Convex Polyhedra

The structure of the algorithm for convex polyhedra moving with constant linear velocity is similar to the one for convex polygons, except for the set of potential separating axes that must be tested. The pseudocode is listed

```

bool TestIntersection (ConvexPolyhedron C0, Vector V0,
                      ConvexPolyhedron C1, Vector V1, double tmax,
                      double& tfirst, double& tlast)
{
    V = V1 - V0; // process as if C0 stationary, C1 moving
    tfirst = 0;
    tlast = INFINITY;

    // test faces of C0 for separation
    for (i = 0; i < C0.GetFCount(); ++i)
    {
        D = C0.GetNormal(i);
        ComputeInterval(C0,D,min0,max0);
        ComputeInterval(C1,D,min1,max1);
        speed = Dot(D,V);
        if (NoIntersect(tmax,speed,min0,max0,min1,max1,tfirst,
                        tlast))
        {
            return false;
        }
    }

    // test faces of C1 for separation
    for (j = 0; j < C1.GetFCount(); ++j)
    {
        D = C1.GetNormal(j);
    }
}

```

```

        ComputeInterval(C0,D,min0,max0);
        ComputeInterval(C1,D,min1,max1);
        speed = Dot(D,V);
        if (NoIntersect(tmax,speed,min0,max0,min1,max1,tfirst,
                        tlast) )
        {
            return false;
        }
    }

    // test cross products of pairs of edges
    for (i = 0; i < C0.GetECount(); ++i)
    {
        for (j = 0; j < C1.GetECount(); ++j)
        {
            D = Cross(C0.GetEdge(i),C1.GetEdge(j));
            ComputeInterval(C0,D,min0,max0);
            ComputeInterval(C1,D,min1,max1);
            speed = Dot(D,V);
            if (NoIntersect(tmax,speed,min0,max0,min1,max1,tfirst,
                            tlast))
            {
                return false;
            }
        }
    }

    return true;
}

```

The function `NoIntersect` is exactly the one used in the two-dimensional problem.

Contact Set for Convex Polyhedra

The find-intersection query for two stationary convex polyhedra is a special example of Boolean operations on polyhedra. Since we are assuming nonpenetration in our collision system, we do not need to implement this.

Given two moving convex objects C_0 and C_1 , initially not intersecting, with velocities \mathbf{V}_0 and \mathbf{V}_1 , if $T > 0$ is the first time of contact, the sets $C_0 + TVW_0 = \{\mathcal{X} + TV_0 : \mathcal{X} \in C_0\}$ and $C_1 + TV_1 = \{\mathcal{X} + TV_1 : \mathcal{X} \in C_1\}$ are just touching with no interpenetration. As indicated earlier for convex polyhedra, the contact is one of face–face, face–edge, face–vertex, edge–edge, edge–vertex, or vertex–vertex. The analysis is slightly more complicated than that of the 2D setting, but the ideas are the same – the relative orientation of the convex polyhedra to each other must be known to properly compute the contact set.

The `TestIntersection` function can be modified to keep track of which vertices, edges, or faces are projected to the endpoints of the projection interval. At the first time of contact, this information is used to determine how the two objects are oriented with respect to each other. If the contact is vertex–vertex, vertex–edge, or vertex–face, then the contact point is a single point, a vertex. If the contact is edge–edge, the contact is typically a single point, but can be an entire line segment. If the contact is edge–face, the contact set is a line segment. Finally, if the contact is face–face, the intersection set is a convex polygon. This is the most complicated scenario and requires a two-dimensional convex polygon intersector. Each endpoint of the projection interval is either generated by a vertex, an edge, or a face. Similar to the implementation for the two-dimensional problem, a projection information class can be defined.

```
class ProjInfo
{
public:
    double min, max; // projection interval [min, max]
    int index[2];
    enum Type { V, E, F };
    Type type[2];
};
```

The zero-indexed values correspond to the minimum of the interval, the one-indexed values to the maximum. If the extreme point is exactly a vertex, the type is set to `V`. If the extreme points are exactly an edge, the type is set to `E`. If the extreme points are exactly a face, the type is set to `F`.

Just as for convex polygons, the extremal query must be modified to support calculation of the contact set via `ProjInfo`. In particular, we need to know the enumerated type to assign based on the extremal set.

```
int GetExtremeIndex (ConvexPolyhedron C, Vector D,
    ProjInfo::Type& type)
{
    BSPTree node = C.tree;
    array<int> edges;
    while (node.R)
    {
        d = Dot(C.GetEdge(node.i),D);
        if (d > 0)
        {
            node = node.R;
        }
        else if (d < 0)
        {
            node = node.L;
        }
        else
```

```

    {
        node = node.R;
        edges.append(node.I);
        ++type;
    }
}

if (edges.size() == 0)
{
    type = ProjInfo::V;
    return node.I; // vertex index at leaf node
}
else if (edges.size() == 1)
{
    type = ProjInfo::E;
    return edges[0]; // edge index at interior node
}
else
{
    type = ProjInfo::F;
    return C.GetFaceFromEdges(edges);
}
}
}

```

Note that you need another interface function for ConvexPolyhedron,

```

class ConvexPolyhedron
{
public:
    // other members...

    int GetFaceFromEdges (array<int> edges);
};

```

that can determine the face bounded by the input edges. Alternatively, you could build more information into the BSP tree nodes so that this information is immediately available. Function ComputeInterval must be modified to provide more information than just the projection interval.

```

void ComputeInterval (ConvexPolyhedron C, Vector D, ProjInfo& info)
{
    info.index[0] = GetExtremeIndex(C,-D,info.type[0]);
    info.min = Dot(D,C.GetVertex(info.index[0]));
    info.index[1] = GetExtremeIndex(C,+D,info.type[1]);
    info.max = Dot(D,C.GetVertex(info.index[1]));
}

```

The NoIntersect function that was modified in two dimensions to accept ProjInfo objects instead of projection intervals is used exactly as is for the

three-dimensional problem, so I do not restate that code here. With all modifications to this point, `TestIntersection` is rewritten as

```

bool TestIntersection (ConvexPolyhedron C0, Vector V0,
                      ConvexPolyhedron C1, Vector V1, double tmax, double& tfirst,
                      double& tlast)
{
    ProjInfo info0, info1, curr0, curr1;
    V = V1 - V0; // process as if C0 stationary, C1 moving
    tfirst = 0;
    tlast = INFINITY;

    // test faces of C0 for separation
    for (i = 0; i < C0.GetFCount(); ++i)
    {
        D = C0.GetNormal(i);
        ComputeInterval(C0,D,info0);
        ComputeInterval(C1,D,info1);
        speed = Dot(D,V);
        if (NoIntersect(tmax,speed,info0,info1,curr0,curr1,side,
                        tfirst,tlast))
        {
            return false;
        }
    }

    // test faces of C1 for separation
    for (j = 0; j < C1.GetFCount(); ++j)
    {
        D = C1.GetNormal(j);
        ComputeInterval(C0,D,info0);
        ComputeInterval(C1,D,info1);
        speed = Dot(D,V);
        if (NoIntersect(tmax,speed,info0,info1,curr0,curr1,side,
                        tfirst,tlast))
        {
            return false;
        }
    }

    // test cross products of pairs of edges
    for (i = 0; i < C0.GetECount(); ++i)
    {
        for (j = 0; j < C1.GetECount(); ++j)
        {
            D = Cross(C0.GetEdge(i),C1.GetEdge(j));
            ComputeInterval(C0,D,info0);
            ComputeInterval(C1,D,info1);
        }
    }
}

```

```

        speed = Dot(D,V);
        if (NoIntersect(tmax,speed,info0,info1,curr0,curr1,side,
                         tfirst,tlast))
        {
            return false;
        }
    }
}

return true;
}

```

The `FindIntersection` pseudocode has exactly the same implementation as that of `TestIntersection`, but with one additional block of code after all the loops that is reached if there will be an intersection. When the polyhedra intersect at time T , they are effectively moved with their respective velocities and the contact set is calculated. The pseudocode follows. The intersection is a convex polyhedron and is returned in the last argument of the function, but keep in mind that for nonpenetration we should have only a convex polygon in 3D. If the intersection set is nonempty, the return value is true. Otherwise, the original moving convex polyhedra do not intersect and the function returns false.

```

bool FindIntersection (ConvexPolyhedron C0, Vector V0,
                      ConvexPolyhedron C1, Point V1, double tmax, double& tfirst,
                      double& tlast, ConvexPolyhedron& I)
{
    ProjInfo info0, info1, curr0, curr1;
    V = V1 - V0; // process as if C0 stationary, C1 moving
    tfirst = 0;
    tlast = INFINITY;

    // test faces of C0 for separation
    for (i = 0; i < C0.GetFCount(); ++i)
    {
        D = C0.GetNormal(i);
        ComputeInterval(C0,D,info0);
        ComputeInterval(C1,D,info1);
        speed = Dot(D,V);
        if (NoIntersect(tmax,speed,info0,info1,curr0,curr1,side,
                        tfirst,tlast))
        {
            return false;
        }
    }

    // test faces of C1 for separation
    for (j = 0; j < C1.GetFCount(); ++j)

```

```

    {
        D = C1.GetNormal(j);
        ComputeInterval(C0,D,info0);
        ComputeInterval(C1,D,info1);
        speed = Dot(D,V);
        if (NoIntersect(tmax,speed,info0,info1,curr0,curr1,side,
                        tfirst,tlast))
        {
            return false;
        }
    }

// test cross products of pairs of edges
for (i = 0; i < C0.GetECount(); ++i)
{
    for (j = 0; j < C1.GetECount(); ++j)
    {
        D = Cross(C0.GetEdge(i),C1.GetEdge(j));
        ComputeInterval(C0,D,info0);
        ComputeInterval(C1,D,info1);
        speed = Dot(D,V);
        if (NoIntersect(tmax,speed,info0,info1,curr0,curr1,
                        side,tfirst,tlast))
        {
            return false;
        }
    }
}

// compute the contact set
GetIntersection(C0,V0,C1,V1,curr0,curr1,side,tfirst,I);
return true;
}

```

```

The intersection calculator pseudocode follows.

void GetIntersection (ConvexPolyhedron C0, Vector V0,
    ConvexPolyhedron C1, Vector V1, ProjInfo info0,
    ProjInfo info1, int side, double tfirst,
    ConvexPolyhedron& I)
{
    if (side == 1) // C0-max meets C1-min
    {
        if (info0.type[1] == ProjInfo::V)
        {
            // vertex-{vertex/edge/face} intersection
            I.InsertFeature(C0.GetVertex(info0.index[1])
                + tfirst * V0);
        }
    }
}

```

```

    }
    else if (info1.type[0] == ProjInfo::V)
    {
        // {vertex/edge/face}-vertex intersection
        I.InsertFeature(C1.GetVertex(info1.index[0])
            + tfirst * V1);
    }
    else if (info0.type[1] == ProjInfo::E)
    {
        Segment E0 = C0.GetESegment(info0.index[1])
            + tfirst * V0;
        if (info1.type[0] == ProjInfo::E)
        {
            Segment E1 = C1.GetESegment(info1.index[0])
                + tfirst * V1;
            I.InsertFeature(IntersectSegmentSegment(E0,E1));
        }
        else
        {
            Polygon F1 = C1.GetFPolygon(info1.index[0])
                + tfirst * V1;
            I.InsertFeature(IntersectSegmentPolygon(E0,F1));
        }
    }
    else if (info1.type[0] == ProjInfo::E)
    {
        Segment E1 = C1.GetESegment(info1.index[0])
            + tfirst * V1;
        if (info0.type[1] == ProjInfo::E)
        {
            Segment E0 = C0.GetESegment(info0.index[1])
                + tfirst * V0;
            I.InsertFeature(IntersectSegmentSegment(E1,E0));
        }
        else
        {
            Polygon F0 = C0.GetFPolygon(info0.index[1])
                + tfirst * V0;
            I.InsertFeature(IntersectSegmentPolygon(E1,F0));
        }
    }
    else // info0.type[1] and info1.type[0] both ProjInfo::F
    {
        // face-face intersection
        Polygon F0 = C0.GetFPolygon(info0.index[1])
            + tfirst * V0;
        Polygon F1 = C1.GetFPolygon(info1.index[0])
    }
}

```

```

        + tfirst * V1;
    I.InsertFeature(IntersectPolygonPolygon(F0,F1));
}
}
else if (side == -1) // C1-max meets C0-min
{
    if (info1.type[1] == ProjInfo::V)
    {
        // vertex-{vertex/edge/face} intersection
        I.InsertFeature(C1.GetVertex(info1.index[1])
            + tfirst * V1);
    }
    else if (info0.type[0] == ProjInfo::V)
    {
        // {vertex/edge/face}-vertex intersection
        I.InsertFeature(C0.GetVertex(info0.index[0])
            + tfirst * V0);
    }
    else if (info1.type[1] == ProjInfo::E)
    {
        Segment E1 = C1.GetESegment(info1.index[1])
            + tfirst * V1;
        if (info0.type[0] == ProjInfo::E)
        {
            Segment E0 = C0.GetESegment(info0.index[0])
                + tfirst * V0;
            I.InsertFeature(IntersectSegmentSegment(E1,E0));
        }
        else
        {
            Polygon F0 = C0.GetFPolygon(info0.index[0])
                + tfirst * V0;
            I.InsertFeature(IntersectSegmentPolygon(E1,F0));
        }
    }
    else if (info0.type[0] == ProjInfo::E)
    {
        Segment E0 = C0.GetESegment(info0.index[0])
            + tfirst * V0;
        if (info1.type[1] == ProjInfo::E)
        {
            Segment E1 = C1.GetESegment(info1.index[1])
                + tfirst * V1;
            I.InsertFeature(IntersectSegmentSegment(E0,E1));
        }
        else
        {

```

```

        Polygon F1 = C1.GetFPolygon(info1.index[1])
                    + tfirst * V1;
        I.InsertFeature(IntersectSegmentPolygon(E0,F1));
    }
}

else // info1.type[1] and info0.type[0] both ProjInfo::F
{
    // face-face intersection
    Polygon F0 = C0.GetFPolygon(info0.index[0])
                  + tfirst * V0;
    Polygon F1 = C1.GetFPolygon(info1.index[1])
                  + tfirst * V1;
    I.InsertFeature(Intersection(F0,F1));
}

else // polyhedra were initially intersecting
{
    ConvexPolyhedron M0 = C0 + tfirst * V0;
    ConvexPolyhedron M1 = C1 + tfirst * V1;
    I = IntersectionPolyhedronPolyhedron(M0,M1);
}
}

```

The type Segment refers to a line segment and the type Polygon refers to a convex polygon in 3D. The various functions `Intersect<Type1><Type2>` are almost generic intersection calculators. I say “almost,” meaning that you know the two objects *must* intersect because the separating axis results say so. Given that they intersect, you can optimize generic intersection calculators to obtain your results. The possible outputs from the intersection calculators are points, line segments, or convex polygons, referred to collectively as “features.” The class ConvexPolyhedron must support construction by allowing the user to insert any of these features. I simply used the name `InsertFeature` to cover all the cases (overloading of the function name, so to speak). The function `GetESegment` returns some representation of a line segment, for example, a pair of points. The calculation $S+t*V$ where S is a Segment, V is a vector, and t is a floating point number requires the vector class to support scalar-times-vector. Moreover, the expression requires addition to be defined for a Segment object and a Vector object. Similarly `GetFPolygon` returns some representation of the convex polygon face, for example an ordered array of points. The calculation $F+t*V$ requires addition to be defined for a Polygon object and a Vector object.

As you can see, this is the workhorse of the collision system, the geometric details of calculating intersections of line segments and convex polygons. You should expect that this is a likely candidate for the bottleneck in your collision system. For this reason you will see simplified systems such as [Bar01] where the contact set is reduced to a container of points. The preceding intersection calculator can be greatly optimized for such a system.

6.4.4 ORIENTED BOUNDING BOXES

So far we have discussed collision detection for convex polyhedra in general terms. A very common polyhedron used in applications is an *oriented bounding box*, the acronym *OBB* used for short. The term *box* is enough to describe the shape, but the modifier *bounding* applies when the box contains a more complex object and is used as a coarse measure of that portion of space the object occupies. The modifier *oriented* refers to the fact that the box axes are not necessarily aligned with the standard coordinate axes. Details are presented in [Section 6.2](#) on the use of bounding boxes (and volumes) in the context of minimizing the work the collision detection system must do by *not* processing pairs of objects, if you can cheaply determine that they will not intersect. A descriptive name for this process is *collision culling*, suggestive of the culling that a graphics engine does in order not to draw objects if you can cheaply determine that they are not visible.

An OBB is defined by a center point \mathcal{C} that acts as the origin for a coordinate system whose orthonormal axis directions are \mathbf{U}_i for $i = 0, 1, 2$. The directions are normal vectors to the faces of the OBB. The half-widths or *extents* of the box along the coordinate axes are $e_i > 0$ for $i = 0, 1, 2$. [Figure 6.33](#) shows an OBB and the intersection of the coordinate axes with three faces of the box.

The eight vertices of the OBB are of the form

$$\mathcal{P} = \mathcal{C} + \sigma_0 e_0 \mathbf{U}_0 + \sigma_1 e_1 \mathbf{U}_1 + \sigma_2 e_2 \mathbf{U}_2$$

where $|\sigma_i| = 1$ for $i = 0, 1, 2$; that is, we have eight choices for the signs σ_i .

Our interest is restricted to testing when two OBBs intersect, whether stationary or moving. As a convex polyhedron, an OBB has 6 faces and 12 edges. If we just blindly applied the test-intersection query for a pair of convex polyhedra, the number of potential separating axis tests is 156: 6 face normals for the first OBB, 6 face normals for the second OBB, and $144 = 12 * 12$ edge–edge pairs. In the worst case we would try all 156 axes only to find the OBBs are intersecting. That is quite a large number of tests for such simple looking objects! The nature of an OBB, though, is that the symmetry allows us to reduce the number of tests. You probably already observed that we have three pairs of parallel faces, so we only need to consider three face normals for an OBB for the purposes of separation. Similarly, only three edge directions are unique and happen to be those of the face normals. Thus, for a pair of OBBs we have only 15 potential separating axis tests: 3 face normals for the first OBB, 3 face normals for the second OBB, and $9 = 3 * 3$ edge–edge pairs.

We still have to project an OBB onto a potential separating axis $\mathcal{Q} + t\mathbf{D}$. Although the fast extremal query for general convex polyhedra may be applied, the symmetry of the OBB allows us to quickly determine the interval of projection. Because a vertex must be an extreme point, it suffices to try to find a vertex \mathcal{P} which maximizes the dot product

$$\mathbf{D} \cdot (\mathcal{P} - \mathcal{Q}) = \mathbf{D} \cdot (\mathcal{C} - \mathcal{Q}) + e_0 \sigma_0 \mathbf{D} \cdot \mathbf{U}_0 + e_1 \sigma_1 \mathbf{D} \cdot \mathbf{U}_1 + e_2 \sigma_2 \mathbf{D} \cdot \mathbf{U}_2$$

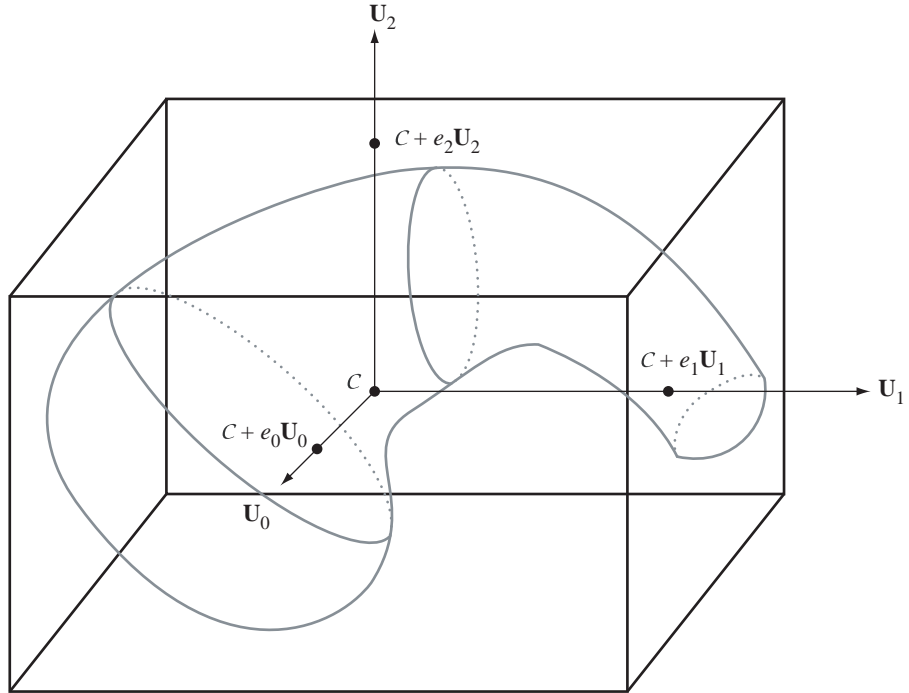


Figure 6.33 An OBB with center point C , coordinate axis directions \mathbf{U}_0 , \mathbf{U}_1 , and \mathbf{U}_2 , and extents e_0 , e_1 , and e_2 along the coordinate axes. The object bounded by the box is shown in gray.

The sign σ_0 is either 1 or -1 . To make the term $\sigma_0 \mathbf{D} \cdot \mathbf{U}_0$ as large as possible, we want $\sigma_0 = 1$ when $\mathbf{D} \cdot \mathbf{U}_0 > 0$ and $\sigma_0 = -1$ when $\mathbf{D} \cdot \mathbf{U}_0 < 0$. If $\mathbf{D} \cdot \mathbf{U}_0 = 0$, it does not matter what the choice is for σ_0 . The resulting quantity can be written as the single term $|\mathbf{D} \cdot \mathbf{U}_0|$. The same argument applies to the other terms, so

$$\max \mathbf{D} \cdot (\mathcal{P} - \mathcal{Q}) = \mathbf{D} \cdot (\mathcal{C} - \mathcal{Q}) + e_0 |\mathbf{D} \cdot \mathbf{U}_0| + e_1 |\mathbf{D} \cdot \mathbf{U}_1| + e_2 |\mathbf{D} \cdot \mathbf{U}_2|$$

Similarly, the minimum is

$$\min \mathbf{D} \cdot (\mathcal{P} - \mathcal{Q}) = \mathbf{D} \cdot (\mathcal{C} - \mathcal{Q}) - e_0 |\mathbf{D} \cdot \mathbf{U}_0| - e_1 |\mathbf{D} \cdot \mathbf{U}_1| - e_2 |\mathbf{D} \cdot \mathbf{U}_2|$$

Therefore, the projection interval is $[\gamma - r, \gamma + r]$, where $\gamma = \mathbf{D} \cdot (\mathcal{C} - \mathcal{Q})$ and $r = \sum_{i=0}^2 e_i |\mathbf{D} \cdot \mathbf{U}_i|$.

Given two oriented bounding boxes, one with center \mathbf{C}_0 , axes \mathbf{A}_i , and extents a_i , and one with center \mathbf{C}_1 , axes \mathbf{B}_i , and extents b_i , let the projection intervals onto a line

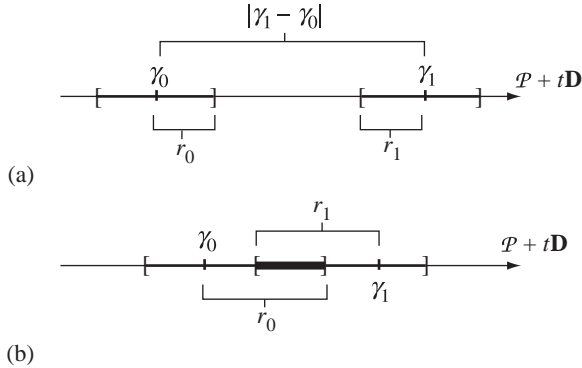


Figure 6.34 The projection intervals of two OBBs onto a line $\mathcal{P} + t\mathbf{D}$. (a) The intervals are disjoint, so the OBBs are separated. (b) The intervals overlap, so the line is not a separating axis.

$\mathcal{Q} + t\mathbf{D}$ be $[\gamma_0 - r_0, \gamma_0 + r_0]$ and $[\gamma_1 - r_1, \gamma_1 + r_1]$. Figure 6.34 shows two cases, one with separated intervals and one with overlapping intervals.

The algebraic condition that describes the separated intervals in Figure 6.34(a) is $|\gamma_1 - \gamma_0| > r_0 + r_1$. In words, this says that the distance between the centers of the projected intervals is larger than the sum of the radii of the intervals. The intervals in the bottom image of the figure overlap, so $|\gamma_1 - \gamma_0| < r_0 + r_1$. If the intervals are just touching, $|\gamma_1 - \gamma_0| = r_0 + r_1$. This last case is important when dealing with moving OBBs.

Define $r = |\gamma_1 - \gamma_0|$. A closer look at the algebraic condition for separation of the projected intervals shows that

$$r = |\gamma_1 - \gamma_0| = |\mathbf{D} \cdot (\mathcal{C}_1 - \mathcal{Q}) - \mathbf{D} \cdot (\mathcal{C}_0 - \mathcal{Q})| = |\mathbf{D} \cdot (\mathcal{C}_1 - \mathcal{C}_0)|$$

This means we need to specify only the direction \mathbf{D} and not worry about providing a point \mathcal{Q} on the line. Also,

$$r_0 = \sum_{i=0}^2 a_i |\mathbf{D} \cdot \mathbf{A}_i|, \quad r_1 = \sum_{i=0}^2 b_i |\mathbf{D} \cdot \mathbf{B}_i|$$

The condition for separation of the projection intervals is $r > r_0 + r_1$ and is formally expanded as

$$|\mathbf{D} \cdot \Delta| = r > r_0 + r_1 = \sum_{i=0}^2 a_i |\mathbf{D} \cdot \mathbf{A}_i| + \sum_{i=0}^2 b_i |\mathbf{D} \cdot \mathbf{B}_i| \quad (6.59)$$

where $\Delta = C_1 - C_0$. We have been thinking of \mathbf{D} as a unit-length direction vector. The face normals are already unit-length potential separating directions. A potential separating direction $\mathbf{D} = \mathbf{A}_i \times \mathbf{B}_j$ obtained as a cross product of edges, one edge from each of the OBBs, is not necessarily unit length. We should then use $\mathbf{D}/|\mathbf{D}|$ in equation (6.59) instead of \mathbf{D} . Notice, though, that the truth of the inequality is unchanged whether we use the vector or the normalized vector, since we can multiply through by $|\mathbf{D}|$. Consequently, we do not need to worry about normalizing the cross product.

A further optimization can be made. The formal sum for r_0 is a single term only when \mathbf{D} is a face normal of the first OBB. For example, if $\mathbf{D} = \mathbf{A}_0$, then $r_0 = a_0$. The formal sum for r_1 is also a single term only when \mathbf{D} is a face normal of the second OBB. The summation term of r_0 involves dot products $\mathbf{A}_i \cdot \mathbf{B}_j$ when using face normals of the second OBB for potential separating directions. The summation term of r_1 involves the same dot products when face normals of the first OBB are used for potential separating directions. When $\mathbf{D} = \mathbf{A}_j \times \mathbf{B}_k$, the summation term of r_0 is

$$\mathbf{D} \cdot \mathbf{A}_i = \mathbf{A}_j \times \mathbf{B}_k \cdot \mathbf{A}_i = \mathbf{A}_i \cdot \mathbf{A}_j \times \mathbf{B}_k = \mathbf{A}_i \times \mathbf{A}_j \cdot \mathbf{B}_k = \mathbf{A}_\ell \cdot \mathbf{B}_k$$

where $\{i, j, \ell\} = \{0, 1, 2\}$. For example, if $i = 2$ and $j = 0$, then $\ell = 1$. Similarly, the summation term of r_1 is

$$\mathbf{D} \cdot \mathbf{B}_i = \mathbf{A}_j \times \mathbf{B}_k \cdot \mathbf{B}_i = \mathbf{A}_j \cdot \mathbf{B}_k \times \mathbf{B}_i = \mathbf{A}_j \cdot \mathbf{B}_\ell$$

where again $\{i, j, \ell\} = \{0, 1, 2\}$. Therefore, all the separating axis tests require computing the quantities $c_{ij} = \mathbf{A}_i \cdot \mathbf{B}_j$ and do not need cross product operations. A convenient summary of the axes and quantities required by $r > r_0 + r_1$ are listed in Table 6.2. The table uses $\alpha_i = \Delta \cdot \mathbf{A}_i$ and $\beta_i = \Delta \cdot \mathbf{B}_i$.

A term of the form $c_{10}\alpha_2 - c_{20}\alpha_1$ occurs as a result of $\Delta = \alpha_0\mathbf{A}_0 + \alpha_1\mathbf{A}_1 + \alpha_2\mathbf{A}_2$, and

$$\begin{aligned} \mathbf{A}_0 \times \mathbf{B}_0 \cdot \Delta &= \alpha_0(\mathbf{A}_0 \times \mathbf{B}_0 \cdot \mathbf{A}_0) + \alpha_1(\mathbf{A}_0 \times \mathbf{B}_0 \cdot \mathbf{A}_1) + \alpha_2(\mathbf{A}_0 \times \mathbf{B}_0 \cdot \mathbf{A}_2) \\ &= \alpha_0(\mathbf{0}) - \alpha_1\mathbf{A}_2 \times \mathbf{B}_0 + \alpha_2\mathbf{A}_1 \cdot \mathbf{B}_0 \\ &= c_{10}\alpha_2 - c_{20}\alpha_1 \end{aligned}$$

Pseudocode follows. The code is organized to compute quantities only when needed. The code also detects when two face normals \mathbf{A}_i and \mathbf{B}_j are nearly parallel. Theoretically, if a parallel pair exists, it is sufficient to test only the face normals of the two OBBs for separation. Numerically, though, two nearly parallel faces can lead to all face normal tests reporting no separation along those directions. The cross-product directions are tested next, but $\mathbf{A}_i \times \mathbf{B}_j$ is nearly the zero vector and can cause the system to report that the OBBs are not intersecting when in fact they are.

```
bool TestIntersection (OBB box0, OBB box1)
{
    // OBB: center C; axes U[0], U[1], U[2];
    //           extents e[0], e[1], e[2]
```

Table 6.2 Potential Separating Directions for OBBs and Values for r_0 , r_1 , and r

D	r_0	r_1	r
\mathbf{A}_0	a_0	$b_0 c_{00} + b_1 c_{01} + b_2 c_{02} $	$ \alpha_0 $
\mathbf{A}_1	a_1	$b_0 c_{10} + b_1 c_{11} + b_2 c_{12} $	$ \alpha_1 $
\mathbf{A}_2	a_2	$b_0 c_{20} + b_1 c_{21} + b_2 c_{22} $	$ \alpha_2 $
\mathbf{B}_0	$a_0 c_{00} + a_1 c_{10} + a_2 c_{20} $	b_0	$ \beta_0 $
\mathbf{B}_1	$a_0 c_{01} + a_1 c_{11} + a_2 c_{21} $	b_1	$ \beta_1 $
\mathbf{B}_2	$a_0 c_{02} + a_1 c_{12} + a_2 c_{22} $	b_2	$ \beta_2 $
$\mathbf{A}_0 \times \mathbf{B}_0$	$a_1 c_{20} + a_2 c_{10} $	$b_1 c_{02} + b_2 c_{01} $	$ c_{10}\alpha_2 - c_{20}\alpha_1 $
$\mathbf{A}_0 \times \mathbf{B}_1$	$a_1 c_{21} + a_2 c_{11} $	$b_0 c_{02} + b_2 c_{00} $	$ c_{11}\alpha_2 - c_{21}\alpha_1 $
$\mathbf{A}_0 \times \mathbf{B}_2$	$a_1 c_{22} + a_2 c_{12} $	$b_0 c_{01} + b_1 c_{00} $	$ c_{12}\alpha_2 - c_{22}\alpha_1 $
$\mathbf{A}_1 \times \mathbf{B}_0$	$a_0 c_{20} + a_2 c_{00} $	$b_1 c_{12} + b_2 c_{11} $	$ c_{20}\alpha_0 - c_{00}\alpha_2 $
$\mathbf{A}_1 \times \mathbf{B}_1$	$a_0 c_{21} + a_2 c_{01} $	$b_0 c_{12} + b_2 c_{10} $	$ c_{21}\alpha_0 - c_{01}\alpha_2 $
$\mathbf{A}_1 \times \mathbf{B}_2$	$a_0 c_{22} + a_2 c_{02} $	$b_0 c_{11} + b_1 c_{10} $	$ c_{22}\alpha_0 - c_{02}\alpha_2 $
$\mathbf{A}_2 \times \mathbf{B}_0$	$a_0 c_{10} + a_1 c_{00} $	$b_1 c_{22} + b_2 c_{21} $	$ c_{00}\alpha_1 - c_{10}\alpha_0 $
$\mathbf{A}_2 \times \mathbf{B}_1$	$a_0 c_{11} + a_1 c_{01} $	$b_0 c_{22} + b_2 c_{20} $	$ c_{01}\alpha_1 - c_{11}\alpha_0 $
$\mathbf{A}_2 \times \mathbf{B}_2$	$a_0 c_{12} + a_1 c_{02} $	$b_0 c_{21} + b_1 c_{20} $	$ c_{02}\alpha_1 - c_{12}\alpha_0 $

```

// values that are computed only when needed
double c[3][3];      // c[i][j] = Dot(box0.U[i],box1.U[j])
double absC[3][3];   // |c[i][j]|
double d[3];          // Dot(box1.C-box0.C,box0.U[i])

// interval radii and distance between centers
double r0, r1, r;
int i;

// cutoff for cosine of angles between box axes
const double cutoff = 0.999999;
bool existsParallelPair = false;

// compute difference of box centers
Vector diff = box1.C - box0.C;

// axis C0 + t * A0
for (i = 0; i < 3; ++i)
{
    c[0][i] = Dot(box0.U[0],box1.U[i]);
    absC[0][i] = |c[0][i]|;
    if (absC[0][i] > cutoff)
    {

```

```

        existsParallelPair = true;
    }
}
d[0] = Dot(diff,box0.U[0]);
r = |d[0]|;
r0 = box0.e[0];
r1 = box1.e[0] * absC[0][0] + box1.e[1] * absC[0][1]
    + box1.e[2] * absC[0][2];
if (r > r0 + r1)
{
    return false;
}

// axis C0 + t * A1
for (i = 0; i < 3; ++i)
{
    c[1][i] = Dot(box0.U[1],box1.U[i]);
    absC[1][i] = |c[1][i]|;
    if (absC[1][i] > cutoff)
    {
        existsParallelPair = true;
    }
}
d[1] = Dot(diff,box0.U[1]);
r = |d[1]|;
r0 = box0.e[1];
r1 = box1.e[0] * absC[1][0] + box1.e[1] * absC[1][1]
    + box1.e[2] * absC[1][2];
if (r > r0 + r1)
{
    return false;
}

// axis C0 + t * A2
for (i = 0; i < 3; ++i)
{
    c[2][i] = Dot(box0.U[2],box1.U[i]);
    absC[2][i] = |c[2][i]|;
    if (absC[2][i] > cutoff)
    {
        existsParallelPair = true;
    }
}
d[2] = Dot(diff,box0.U[2]);
r = |d[2]|;
r0 = box0.e[2];
r1 = box1.e[0] * absC[2][0] + box1.e[1] * absC[2][1]

```

```

        + box1.e[2] * absC[2][2];
if (r > r0 + r1)
{
    return false;
}

// axis C0 + t * B0
r = |Dot(diff,box1.U[0])|;
r0 = box0.e[0] * absC[0][0] + box0.e[1] * absC[1][0]
    + box0.e[2] * absC[2][0];
r1 = box1.e[0];
if (r > r0 + r1)
{
    return false;
}

// axis C0 + t * B1
r = |Dot(diff,box1.U[1])|;
r0 = box0.e[0] * absC[0][1] + box0.e[1] * absC[1][1]
    + box0.e[2] * absC[2][1];
r1 = box1.e[1];
if (r > r0 + r1)
{
    return false;
}

// axis C0 + t * B2
r = |Dot(diff,box1.U[2])|;
r0 = box0.e[0] * absC[0][2] + box0.e[1] * absC[1][2]
    + box0.e[2] * absC[2][2];
r1 = box1.e[2];
if (r > r0 + r1)
{
    return false;
}

if (existsParallelPair)
{
    // A pair of box axes was (effectively) parallel,
    // boxes must intersect.
    return true;
}

// axis C0 + t * A0 x B0
r = |d[2] * c[1][0] - d[1] * c[2][0]|;
r0 = box0.e[1] * absC[2][0] + box0.e[2] * absC[1][0];
r1 = box1.e[1] * absC[0][2] + box1.e[2] * absC[0][1];

```

```
    if (r > r0 + r1)
    {
        return false;
    }

    // axis C0 + t * A0 x B1
    r = |d[2] * c[1][1] - d[1] * c[2][1]|;
    r0 = box0.e[1] * absC[2][1] + box0.e[2] * absC[1][1];
    r1 = box1.e[0] * absC[0][2] + box1.e[2] * absC[0][0];
    if (r > r0 + r1)
    {
        return false;
    }

    // axis C0 + t * A0 x B2
    r = |d[2] * c[1][2] - d[1] * c[2][2]|;
    r0 = box0.e[1] * absC[2][2] + box0.e[2] * absC[1][2];
    r1 = box1.e[0] * absC[0][1] + box1.e[1] * absC[0][0];
    if (r > r0 + r1)
    {
        return false;
    }

    // axis C0 + t * A1 x B0
    r = |d[0] * c[2][0] - d[2] * c[0][0]|;
    r0 = box0.e[0] * absC[2][0] + box0.e[2] * absC[0][0];
    r1 = box1.e[1] * absC[1][2] + box1.e[2] * absC[1][1];
    if (r > r0 + r1)
    {
        return false;
    }

    // axis C0 + t * A1 x B1
    r = |d[0] * c[2][1] - d[2] * c[0][1]|;
    r0 = box0.e[0] * absC[2][1] + box0.e[2] * absC[0][1];
    r1 = box1.e[0] * absC[1][2] + box1.e[2] * absC[1][0];
    if (r > r0 + r1)
    {
        return false;
    }

    // axis C0 + t * A1 x B2
    r = |d[0] * c[2][2] - d[2] * c[0][2]|;
    r0 = box0.e[0] * absC[2][2] + box0.e[2] * absC[0][2];
    r1 = box1.e[0] * absC[1][1] + box1.e[1] * absC[1][0];
    if (r > r0 + r1)
    {
```

```

        return false;
    }

    // axis C0 + t * A2 x B0
    r = |d[1] * c[0][0] - d[0] * c[1][0]|;
    r0 = box0.e[0] * absC[1][0] + box0.e[1] * absC[0][0];
    r1 = box1.e[1] * absC[2][2] + box1.e[2] * absC[2][1];
    if (r > r0 + r1)
    {
        return false;
    }

    // axis C0 + t * A2 x B1
    r = |d[1] * c[0][1] - d[0] * c[1][1]|;
    r0 = box0.e[0] * absC[1][1] + box0.e[1] * absC[0][1];
    r1 = box1.e[0] * absC[2][2] + box1.e[2] * absC[2][0];
    if (r > r0 + r1)
    {
        return false;
    }

    // axis C0 + t * A2 x B2
    r = |d[1] * c[0][2] - d[0] * c[1][2]|;
    r0 = box0.e[0] * absC[1][2] + box0.e[1] * absC[0][2];
    r1 = box1.e[0] * absC[2][1] + box1.e[1] * absC[2][0];
    if (r > r0 + r1)
    {
        return false;
    }

    return true;
}

```

6.4.5 BOXES MOVING WITH CONSTANT LINEAR AND ANGULAR VELOCITY

OBBs may certainly be used as objects in and of themselves in an application. A classic application in the industry is having a moving vehicle run through a wall of bricks. A large number of bricks will demand a lot of performance from the physics engine. After the vehicle crashes through the wall, the collision detection system has a lot to handle. The bricks will have both nonzero linear and angular velocities, the actual values dependent on the interactions with other bricks. To avoid performance issues with the bisection approach to collision, we would like to predict collisions at later times and reduce the desired time step accordingly. But is that not what the differential equation solving is about, predicting future behavior from current state? Taking the time step with the solver just to predict that we should take half the time step puts us

right back in the bisection algorithm. The question: Can we predict collisions without actually running the solver?

Well, the answer is “almost.” For a physical simulation running at real-time rates, the time step will be a fraction of a second. During the time interval $[0, \Delta t]$, where $\Delta t > 0$ is small, the linear and angular velocities should not change very much. If you assume that the linear and angular velocities are constant over the time step, you can estimate the location of the center of mass and the orientation of the body at the end of that time. The general equations of motion for these quantities are $\dot{\mathbf{x}}(t) = \mathbf{v}(t)$ and $\dot{\mathbf{R}}(t) = \text{Skew}(\mathbf{w}(t))\mathbf{R}(t)$, where $\mathbf{v}(t)$ is linear velocity and $\mathbf{w}(t)$ is angular velocity. In mathematical terms the assumption of constancy over the time interval produces the approximate equations $\dot{\mathbf{x}}(t) = \mathbf{v}_0$ and $\dot{\mathbf{R}}(t) = \text{Skew}(\mathbf{w}_0)\mathbf{R}(t)$, where $\mathbf{v}_0 = \mathbf{v}(0)$ and $\mathbf{w}_0 = \mathbf{w}(0)$. These have exact solutions,

$$\mathbf{x}(t) = \mathbf{x}_0 + t\mathbf{v}_0, \quad \mathbf{R}(t) = \text{Rot}(t|\mathbf{w}_0|, \mathbf{w}_0/|\mathbf{w}_0|)R_0$$

where $\mathbf{x}_0 = \mathbf{x}(0)$, $R_0 = R(0)$, and $\text{Rot}(\theta, \mathbf{u})$ is the rotation matrix by an angle θ about an axis whose direction is the unit-length vector \mathbf{u} . We can run our collision detection system using $\mathbf{x}(t)$ and $R(t)$ produced by these equations to predict if any collisions will occur on the time interval $[0, \Delta t]$. If not, we can solve the differential equations using the desired step Δt . If collisions are predicted, the system should report the largest time $T \in [0, \Delta t]$ for which no collisions occur on the interval $[0, T]$. The time step for the differential equation solver is chosen to be T instead of Δt . Our estimates $\mathbf{x}(t)$ and $R(t)$ are essentially a numerical method of the Euler type for solving differential equations, but in our case we are using these estimates in conjunction with the collision system to provide an adaptive time step for the actual differential equation solver (such as Runge–Kutta) that our physical simulator is using.

A collision detection system built on the method of separating axes can handle constant linear and angular velocities with a minimum of computational effort when the objects are oriented bounding boxes.

Constant Linear Velocity

Consider two OBBs whose centers are moving with constant linear velocity, $\mathcal{C}_i + t\mathbf{V}_i$ for $i = 0, 1$ and $t \geq 0$. The OBB axes are assumed not to rotate over time; that is, there is no angular velocity. The general analysis that led to `TestIntersection` for convex polyhedra moving with constant linear velocities applies here. The difference is that the general case required `ComputeInterval` for computing the projection intervals of the polyhedra. The intervals are simpler to compute for OBBs. Partial pseudocode for the test-intersection query is listed below. The organization is similar to the pseudocode for testing stationary OBBs. Blocks of the form,

```
if (r > r0 + r1)
{
    return false;
}
```

are replaced by

```
speed = Dot(D,V);
if (NoIntersect(tmax,speed,min0,max0,min1,max1,tfirst,tlast))
{
    return false;
}
```

where `speed` is of type `double`, `D` is the relevant potential separating axis, and `V` is the velocity of the second box relative to the first. The input to `NoIntersect` consisted of two projection intervals $[min_0, max_0]$ and $[min_1, max_1]$ on a line $\mathcal{O} + tD$, where \mathcal{O} is the origin. Now we are projecting onto a line with the same direction but containing the center of the first box. A brief look at the code for `NoIntersect` will convince you that only the relative position of the projection intervals matters, not the absolute location of their centers. In the pseudocode that follows, the interval values are computed relative to the projected center of the first box.

```
bool TestIntersection (OBB box0, Vector V0, OBB box1, Vector V1,
                      double tmax, double& tfirst, double& tlast)
{
    // OBB: center C; axes U[0], U[1], U[2];
    //      extents e[0], e[1], e[2]

    // values that are computed only when needed
    double c[3][3];      // c[i][j] = Dot(box0.U[i],box1.U[j])
    double absC[3][3];   // |c[i][j]|
    double udc[3];        // Dot(box0.U[i],box1.C-box0.C)
    double udv[3];        // Dot(box0.U[i],V1-V0)

    double center, speed, r0, r1, min0, max0, min1, max1;
    int i;

    // cutoff for cosine of angles between box axes
    const double cutoff = 0.999999;
    bool existsParallelPair = false;

    // compute difference of box centers and velocities
    Vector CDiff = box1.C - box0.C;
    Vector VDiff = V1 - V0;

    tfirst = 0;
    tlast = INFINITY;

    // axis C0 + t * A0
    for (i = 0; i < 3; ++i)
    {
        c[0][i] = Dot(box0.U[0],box1.U[i]);
        absC[0][i] = |c[0][i]|;
        if (absC[0][i] > cutoff)
```

```

        {
            existsParallelPair = true;
        }
    }
    udc[0] = Dot(box0.U[0],CDiff);
    udv[0] = Dot(box0.U[0],VDiff);
    center = udc[0];
    speed = udv[0];
    r0 = box0.e[0];
    r1 = box1.e[0] * absC[0][0] + box1.e[1] * absC[0][1]
        + box1.e[2] * absC[0][2];
    min0 = -r0;
    max0 = +r0;
    min1 = center - r1;
    max1 = center + r1;
    if (NoIntersect(tmax,speed,min0,max0,min1,max1,tfirst,tlast))
    {
        return false;
    }

    //*** other face normal cases go here ***

    if (existsParallelPair)
    {
        // A pair of box axes was (effectively) parallel,
        // boxes must intersect.
        return true;
    }

    // axis C0 + t * A0 x B0
    center = udc[2] * c[1][0] - udc[1] * c[2][0];
    speed = udv[2] * c[1][0] - udv[1] * c[2][0];
    r0 = box0.e[1] * absC[2][0] + box0.e[2] * absC[1][0];
    r1 = box1.e[1] * absC[0][2] + box1.e[2] * absC[0][1];
    min0 = -r0;
    max0 = +r0;
    min1 = center - r1;
    max1 = center + r1;
    if (NoIntersect(tmax,speed,min0,max0,min1,max1,tfirst,tlast))
    {
        return false;
    }

    //*** other edge-edge cases go here ***

    return true;
}

```

The pseudocode for NoIntersect is the same used for convex polyhedra generally.

Constant Angular Velocity

The analysis for constant linear velocity is based on two things, the separating test in equation (6.59) and the time-varying difference between centers $\Delta(t) = \mathbf{D} \cdot (\mathcal{C}_t - \mathcal{C}_0) + t\mathbf{D} \cdot (\mathbf{V}_1 - \mathbf{V}_0) = c + t\sigma$. If you consider the first projection interval $[-r_0, r_0]$ to be stationary, the second projection interval is $[c + t\sigma - r_1, c + t\sigma + r_1]$. At time 0 its center is c and it moves with speed σ . Figure 6.35 shows the four cases of interest.

The first two rows of the figure show the moving interval on the right of the stationary one. In the first row $\sigma \geq 0$ and the intervals will never intersect. In the second row $\sigma < 0$ and the intervals will intersect at time $t = (r_0 + r_1 - c)/\sigma$. The last two rows of the figure show the moving interval on the left of the stationary one. In the third row $\sigma > 0$ and the intervals will intersect at time $t = -(r_0 + r_1 + c)/\sigma$. In the fourth row $\sigma \leq 0$ and the intervals will never intersect. The constant linear velocities of the bodies leads to a linear equation in t for computing the first time of contact.

We are not so lucky to obtain a simple formulation for bodies moving with constant angular velocities \mathbf{w}_k , $k = 0, 1$, but we can obtain a formulation nonetheless. The constant angular speeds are $\omega_k = |\mathbf{w}_k|$ and the unit-length directions for the axes of rotation are $\mathbf{U}_k = \mathbf{w}_k/|\mathbf{w}_k|$. The rotation matrices corresponding to the angular

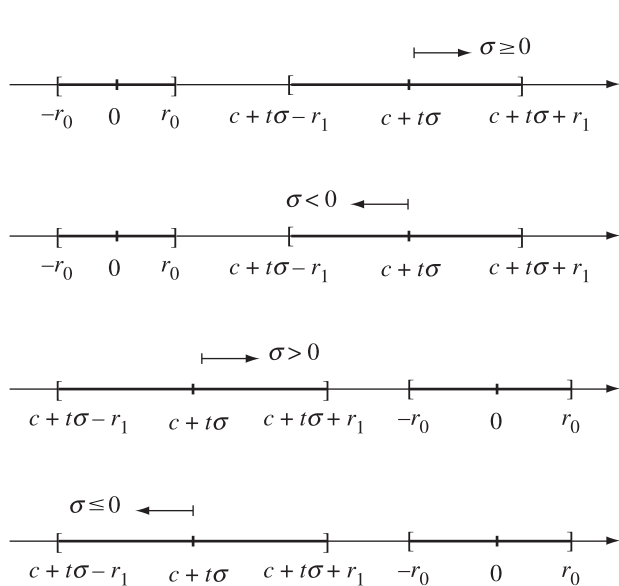


Figure 6.35 Two projected intervals, one stationary and one moving.

velocities are

$$R_k(t) = I + \sin(t\omega_k)S_k + (1 - \cos(t\omega_k))S_k^2$$

where $S_k = \text{Skew}(\mathbf{U}_k)$. Let \mathbf{A}_i and \mathbf{B}_j be the OBB axes at time zero. At a later time the axes are $R_0(t)\mathbf{A}_i$ and $R_1(t)\mathbf{B}_j$. The separation condition along an axis based on equation (6.59) is

$$|\mathbf{D}(t) \cdot \Delta| = r(t) > r_0(t) + r_1(t) = \sum_{i=0}^2 a_i |\mathbf{D}(t) \cdot R_0(t)\mathbf{A}_i| + \sum_{j=0}^2 b_j |\mathbf{D}(t) \cdot R_1(t)\mathbf{B}_j|$$

where $\Delta = \mathcal{C}_1 - \mathcal{C}_0$ does not vary with time (the box centers are stationary). The choices for potential separating direction $\mathbf{D}(t)$ are $R_0(t)\mathbf{A}_i$, $R_1(t)\mathbf{B}_j$, and $(R_0(t)\mathbf{A}_i) \times (R_1(t)\mathbf{B}_j)$.

To get an idea of the complexity of the separating equation, let us look at the case $\mathbf{D}(t) = R_0(t)\mathbf{A}_0$. The simplest distance quantity is $r_0(t) = a_0$. For $r(t)$ and $r_1(t)$, define $\sigma_i(t) = \sin(t\omega_i)$ and $\gamma_i(t) = \cos(t\omega_i)$. The quantity $r(t)$ is

$$\begin{aligned} r(t) &= |(\mathbf{A}_0 \cdot \Delta) + (S_0 \mathbf{A}_0 \cdot \Delta) \sigma_0(t) + (S_0^2 \mathbf{A}_0 \cdot \Delta) (1 - \gamma_0(t))| \\ &= |c_0 + c_1 \sin(\omega_0 t + \psi)| \end{aligned}$$

for some constants c_0 , c_1 , and ψ . The last equality follows from an application of trigonometric identities. The general term in the summation for $r_1(t)$ involves the absolute value of

$$\begin{aligned} R_0(t)\mathbf{A}_0 \cdot R_1(t)\mathbf{B}_j &= d_{00j} + d_{01j}\sigma_1(t) + d_{02j}(1 - \gamma_1(t)) \\ &\quad + d_{10j}\sigma_0(t) + d_{11j}\sigma_0(t)\sigma_1(t) + d_{12j}\sigma_0(t)(1 - \gamma_1(t)) \\ &\quad + d_{20j}(1 - \gamma_0(t)) + d_{21j}(1 - \gamma_0(t))\sigma_1(t) \\ &\quad + d_{22j}(1 - \gamma_0(t))(1 - \gamma_1(t)) \end{aligned}$$

where $d_{k\ell j} = S_0^k \mathbf{A}_0 \cdot S_1^\ell \mathbf{B}_j$. Trigonometric identities may be used to reduce this to

$$R_0(t)\mathbf{A}_0 \cdot R_1(t)\mathbf{B}_j = e_j + \sum_{i=0}^3 f_{ji} \sin(\lambda_i t + \phi_i)$$

where e_j , f_{ji} , and ϕ_i are constants. The frequencies are $\lambda_0 = \omega_0$, $\lambda_1 = \omega_1$, $\lambda_2 = \omega_0 + \omega_1$, and $\lambda_3 = \omega_0 - \omega_1$. The separating equation becomes

$$|c_0 + c_1 \sin(\lambda_0 t + \psi)| > a_0 + \sum_{j=0}^2 b_j \left| e_j + \sum_{i=0}^3 f_{ji} \sin(\lambda_i t + \phi_i) \right|$$

Computing the first time t for which you get equality in the above expression requires a numerical root finder. And keep in mind that the worst case is having to process all 15 separating axes, each yielding a complicated inequality of this form.

We could make yet another approximation and replace $\sin(\omega_k t) \doteq \omega_k t$ and $1 - \cos(\omega_k t) \doteq 0$. The separating equation for potential separating axis $R_0(t)\mathbf{A}_0$ with these approximations is of the form,

$$|g_0 + g_1 t| > a_0 + \sum_{j=0}^2 b_j |h_{j0} + h_{j1}t + h_{j2}t^2|$$

This looks less formidable, but still requires a bit of work to find when equality occurs.

6.4.6 GJK ALGORITHM

An alternative to the method of separating axes for determining when two convex polyhedra overlap is to compute the distance between the polyhedra. The distance is positive when the polyhedra are separated. The distance is zero when the polyhedra are just touching or overlapping.

An effective method for computing the distance was developed by E.G. Gilbert, D.W. Johnson, and S.S. Keerthi [GJK88] for convex polyhedra in 3D, but the ideas apply equally as well in 2D (and in any dimension for the generalization of convex polyhedra in that dimension). The algorithm has become known as the *GJK algorithm*, where the acronym is just the initial letters of the last names of the authors of the paper. The algorithm was later extended to handle convex objects in general [GF90]. An enhancement of the algorithm was also developed that computes penetration distances when the polyhedra are intersecting [Cam97].

A detailed description of the algorithm and its use in collision detection systems is in the book by Gino van den Bergen [vdB03]. The CD-ROM of the reference book has an implementation. Software is also available at [vdB01c]. Of great interest in this implementation is that special attention is paid to numerical issues that have plagued many other implementations of the GJK algorithm. Related materials are [vdB97, vdB99, vdB01b].

The ideas are illustrated here for convex polygons in 2D, but the concepts extend naturally to 3D.

Set Operations

The *Minkowski sum* of two sets A and B is defined as the set of all sums of vector pairs, one from each set. Formally, the set is $A + B = \{\mathbf{X} + \mathbf{Y} : \mathbf{X} \in A, \mathbf{Y} \in B\}$. The *negation* of a set B is $-B = \{-\mathbf{X} : \mathbf{X} \in B\}$. The *Minkowski difference* of the sets is $A - B = \{\mathbf{X} - \mathbf{Y} : \mathbf{X} \in A, \mathbf{Y} \in B\}$. Observe that $A - B = A + (-B)$. If the sets A and B are both convex, then the $A + B$, $-B$, and $A - B$ are all convex sets. If A is a convex polygon with n vertices and B is a convex polygon with m vertices, in worst case the sum $A + B$ has $n + m$ vertices. Figure 6.36 illustrates where A is

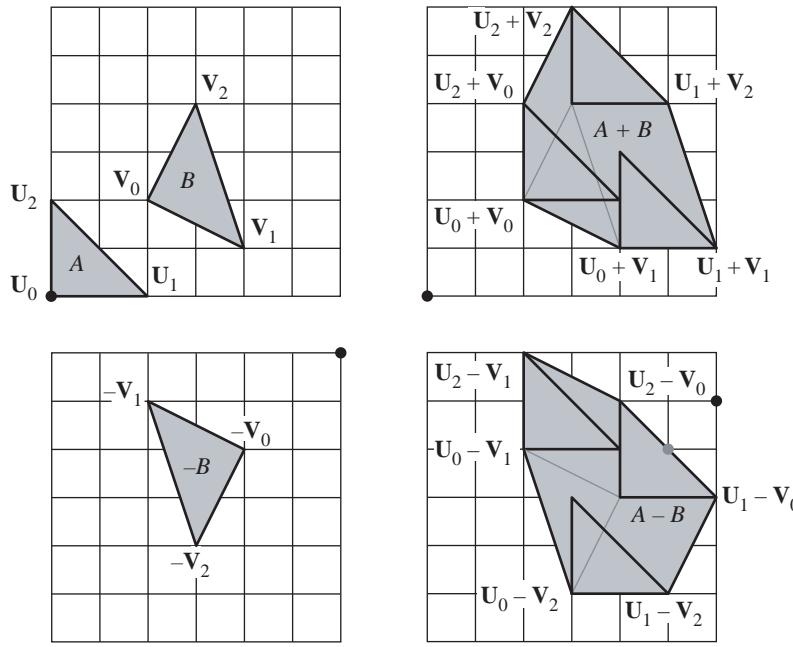


Figure 6.36 Triangles A and B and sets $A + B$, $-B$, and $A - B$. The black dots on the grid are the origin $(0,0)$. The gray point in the lower right grid is the closest point on $A - B$ to the origin.

the triangle $\langle \mathbf{U}_0, \mathbf{U}_1, \mathbf{U}_2 \rangle = \langle (0,0), (2,0), (0,2) \rangle$ and B is the triangle $\langle \mathbf{V}_0, \mathbf{V}_1, \mathbf{V}_2 \rangle = \langle (2,2), (4,1), (3,4) \rangle$. The origin $(0,0)$ is marked as a black dot.

The upper left of Figure 6.36 shows the original triangles. The lower left shows $-B$. The upper right of the figure shows $A + B$. To provide some geometric intuition on the sum, the figure shows three dark gray triangles corresponding to triangle A translated by each of the three vertices of triangle B . Triangle B itself is shown in lighter gray. Imagine painting the hexagon interior by the translated triangle A where you move $\mathbf{U}_0 + \mathbf{V}_0$ within triangle B . The same geometric intuition is illustrated in the drawing of $A - B$.

The distance between any two sets A and B is formally

$$\text{Distance}(A, B) = \min\{|\mathbf{X} - \mathbf{Y}| : \mathbf{X} \in A, \mathbf{Y} \in B\} = \min\{|\mathbf{Z}| : \mathbf{Z} \in A - B\}$$

The latter equation shows that the Minkowski difference can play an important role in distance calculations. The minimum distance is attained by a point in $A - B$ that is closest to the origin. Figure 6.36 illustrates this for two triangles. The closest point to the origin is the dark gray dot at the point $(-1, -1) \in A - B$. That point is generated

by $(1, 1) \in A$ and $(2, 2) \in B$, so the distance between A and B is $\sqrt{2}$ and is attained by the aforementioned points.

The heart of the distance calculation is how to efficiently search $A - B$ for the closest point to the origin. A straightforward algorithm is to compute $A - B$ directly, then iterate over the edges and computing the distance from each edge to the origin. The minimum such distance is the distance between A and B . However, this approach is not efficient in that it can take significant time to compute $A - B$ as the convex hull of the set of points $U - V$, where U is a vertex of A and V is a vertex of B . Moreover, an exhaustive search of the edges will process edges that are not even visible to the origin. The approach is $O(nm)$ where A has n vertices and B has m vertices since the convex hull can have nm vertices. The GJK algorithm is an iterative method designed to avoid the direct convex hull calculation and to localize the search to edges near the origin.

Overview of the Algorithm

The discussion here is for the general n -dimensional problem for convex objects A and B . Let $C = A - B$ where A and B are convex sets. As noted earlier, C itself is a convex set. If $\mathbf{0} \in C$, then the original sets intersect and the distance between them is zero. Otherwise, let $Z \in C$ be the closest point to the origin. It is geometrically clear that only one such point exists and must lie on the boundary of C . However, there can be many $X \in A$ and $Y \in B$ such that $X - Y = Z$. For example, this happens for two disjoint convex polygons in 2D whose closest features are a pair of parallel edges, one from each polygon.

The GJK algorithm is effectively a descent method that constructs a sequence of points on the boundary of C , each point having smaller distance to the origin than the previous point in the sequence. In fact, the algorithm generates a sequence of simplices with vertices in C (triangles in 2D, tetrahedra in 3D), each simplex having smaller distance to the origin than the previous simplex. Let S_k denote the simplex vertices at the k th step and let \bar{S}_k denote the simplex itself. The point $V_k \in \bar{S}_k$ is selected to be the closest point in \bar{S}_k to the origin. Initially, $S_0 = \emptyset$ (the empty set) and V_0 is an arbitrary point in C . The set C is projected onto the line through $\mathbf{0}$ with direction V_0 , the resulting projection being a closed and bounded interval on the line. The interval endpoint that is farthest left on the projection line is generated by a point $W_0 \in C$. The next set of simplex vertices is $S_1 = \{W_0\}$. Figure 6.37 illustrates this step.

Since S_1 is a singleton point set, $\bar{S}_1 = S_1$ and $V_1 = W_0$ is the closest point in \bar{S}_1 to the origin. The set C is now projected onto the line containing $\mathbf{0}$ with direction V_1 . The interval endpoint that is farthest left on the projection line is generated by a point $W_1 \in C$. The next set of simplex vertices is $S_2 = \{W_0, W_1\}$. Figure 6.38 illustrates this step.

The set \bar{S}_2 is the line segment $\langle W_0, W_1 \rangle$. The closest point in \bar{S}_2 to the origin is an edge-interior point V_2 . The set C is projected onto the line containing $\mathbf{0}$ with direction V_2 . The interval endpoint that is farthest left on the projection line is generated

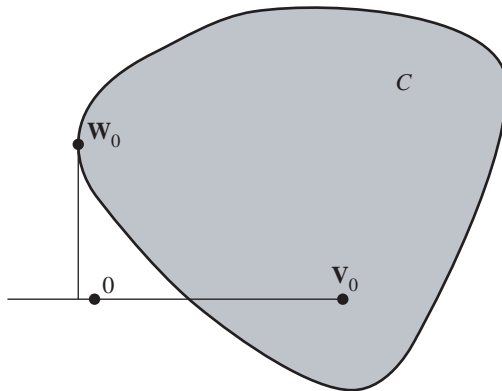


Figure 6.37 The first iteration in the GJK algorithm.

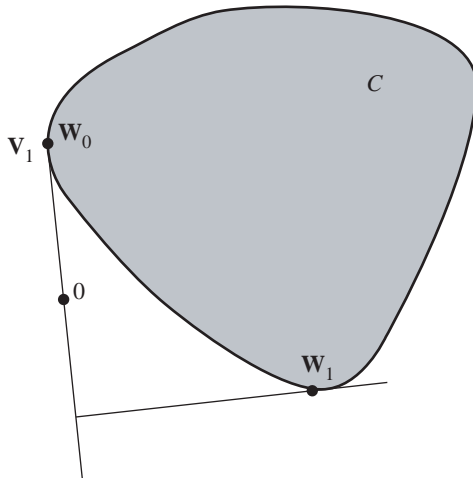


Figure 6.38 The second iteration in the GJK algorithm.

by a point $\mathbf{W}_2 \in C$. The next set of simplex vertices is $S_3 = \{\mathbf{W}_0, \mathbf{W}_1, \mathbf{W}_2\}$. Figure 6.39 illustrates this step.

The set \bar{S}_3 is the triangle $\langle \mathbf{W}_0, \mathbf{W}_1, \mathbf{W}_2 \rangle$. The closest point in \bar{S}_3 to the origin is a point \mathbf{V}_3 on the edge $\langle \mathbf{W}_0, \mathbf{W}_2 \rangle$. The next simplex vertex that is generated is \mathbf{W}_3 . The next set of simplex vertices is $S_4 = \langle \mathbf{W}_0, \mathbf{W}_2, \mathbf{W}_3 \rangle$. The old simplex vertex \mathbf{W}_1 is discarded. Figure 6.40 illustrates this step. The simplex \bar{S}_3 is shown in dark gray.

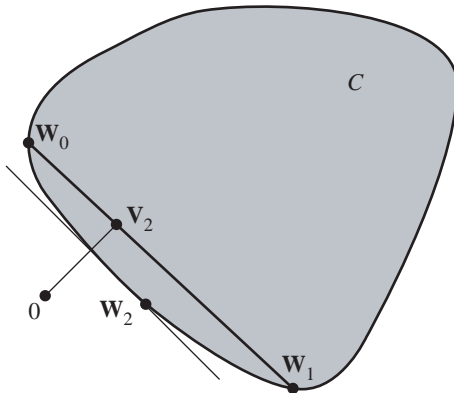


Figure 6.39 The third iteration in the GJK algorithm.

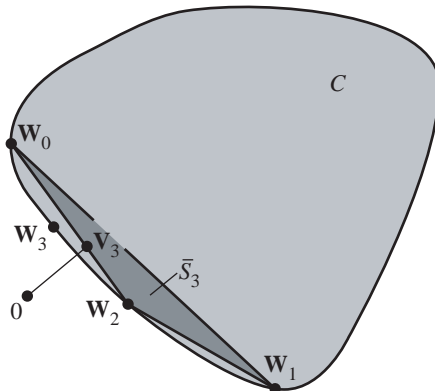


Figure 6.40 The fourth iteration in the GJK algorithm.

Generally, \mathbf{V}_{k+1} is chosen to be the closest point to the origin in the convex hull of $S_k \cup \{\mathbf{W}_k\}$. The next set of simplex vertices S_{k+1} is chosen to be set $M \subseteq S_k \cup \{\mathbf{W}_k\}$ with the fewest number of elements such that \mathbf{V}_{k+1} is in the convex hull of M . Such a set M must exist and is unique. The left half of Figure 6.41 shows the convex hull of $S_3 \cup \{\mathbf{W}_3\}$, a quadrilateral. The next iterate \mathbf{V}_4 is shown on that hull. The right half of Figure 6.41 shows the simplex \bar{S}_4 that was generated by $M = \{\mathbf{W}_0, \mathbf{W}_2, \mathbf{W}_3\}$.

Stated without proof, the sequence of iterates is monotonically decreasing in length, $|\mathbf{V}_{k+1}| \leq |\mathbf{V}_k|$. In fact, equality can occur only when $\mathbf{V}_k = \mathbf{Z}$, the closest point.

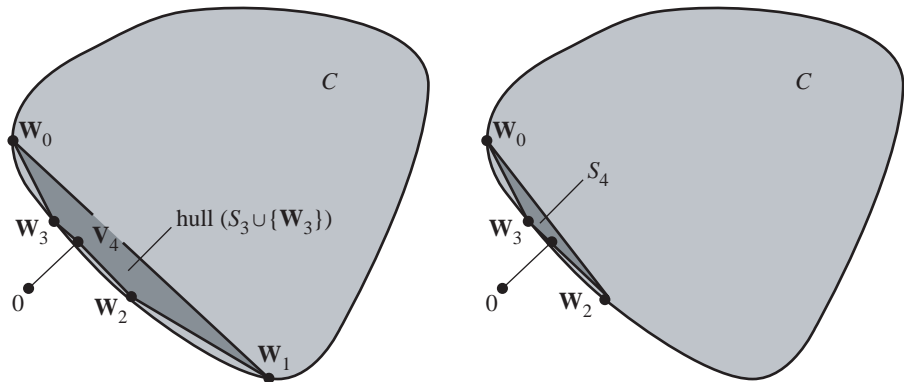


Figure 6.41 Left: Construction of V_{k+1} in the convex hull of $S_k \cup \{W_k\}$. Right: The new simplex \bar{S}_{k+1} generated from $M = \{W_0, W_2, W_3\}$.

For convex faceted objects, the closest point is reached in a finite number of steps. For general convex objects, the sequence can be infinite, but must converge to Z . If the GJK algorithm is implemented for such objects, some type of termination criterion must be used. Numerical issues arise when the algorithm is implemented in a floating point number system. One item to pay attention to is that the simplices eventually become flat in one or more dimensions.

Alternatives to GJK

The GJK algorithm is by no means the only algorithm for computing distance between convex polygons or convex polyhedra. The distance between two nonintersecting convex polygons can be computed using the method of rotating calipers [Pir]. This powerful method is useful for solving many other types of problems in computational geometry. Assuming both polyhedra have $O(n)$ vertices, an $O(n^2)$ algorithm, both in space and in time, for computing the distance is [CC86]. An asymptotically better algorithm is [DK90] and is $O(n)$ in space and $O(\log^2 n)$ in time. However, no implementation appears to be publicly available. The method is based on constructing a hierarchical representation of a polyhedron that is useful for solving other queries, for example in rapid determination of an extreme point of a polyhedron for a specified direction. In more recent times, the Lin-Canny algorithm [LC91] is $O(n)$ in space, empirically $O(n)$ in time, but maintains the closest pair of features to exploit frame coherence. After computing the distance in one frame, the polyhedra move slightly and the distance must be recalculated in the next frame. The incremental update is $O(1)$ in time. Implementations based on this method are I-Collide [CLMP95] and V-Clip [Mir98].

6.5 UNCONSTRAINED MOTION

For unconstrained motion, Newtonian dynamics may be used rather than Lagrangian dynamics to establish the equations of motion. The equations of motion for a single particle of mass m with world position \mathbf{x} , world velocity $\mathbf{v} = \dot{\mathbf{x}}$, and world acceleration $\mathbf{a} = \ddot{\mathbf{x}} = \ddot{\mathbf{x}}$ are in the form of Newton's second law:

$$m\ddot{\mathbf{x}} = m\dot{\mathbf{v}} = m\mathbf{a} = \mathbf{F}(t)$$

The right-hand side represents all forces applied to the particle. The dependence on time is indicated just to remind you that the force can change dynamically. This is a second-order differential equation in \mathbf{x} . Numerical differential equation solvers are typically set up to solve first-order systems. We can transform our single second-order equation into two first-order equations by allowing the velocity to be one of the variables: $\dot{\mathbf{x}} = \mathbf{v}$, $\dot{\mathbf{v}} = \mathbf{F}/m$. The vector $\mathbf{S}(t) = [\mathbf{x} \mathbf{v}]^T$ is referred to as the *state vector* for the system. The system of differential equations is

$$\frac{d\mathbf{S}}{dt} = \frac{d}{dt} \begin{bmatrix} \mathbf{x} \\ \mathbf{v} \end{bmatrix} = \begin{bmatrix} \dot{\mathbf{x}} \\ \dot{\mathbf{v}} \end{bmatrix} = \begin{bmatrix} \mathbf{v} \\ \frac{\mathbf{F}}{m} \end{bmatrix}$$

The physical simulation is a matter of updating the state vector over time using the differential equation solvers.

Newton's second law applies equally as well to a system of n particles. If the i th particle has mass m_i , position \mathbf{x}_i , velocity \mathbf{v}_i , and applied force \mathbf{F}_i , then the state vector is a list of all pairs of positions and velocities, $\mathbf{S} = [\mathbf{x}_1 \mathbf{v}_1 \cdots \mathbf{x}_n \mathbf{v}_n]^T$, and the system of differential equations is

$$\frac{d\mathbf{S}}{dt} = \frac{d}{dt} \begin{bmatrix} \mathbf{x}_1 \\ \mathbf{v}_1 \\ \vdots \\ \mathbf{x}_n \\ \mathbf{v}_n \end{bmatrix} = \begin{bmatrix} \dot{\mathbf{x}}_1 \\ \dot{\mathbf{v}}_1 \\ \vdots \\ \dot{\mathbf{x}}_n \\ \dot{\mathbf{v}}_n \end{bmatrix} = \begin{bmatrix} \mathbf{v}_1 \\ \frac{\mathbf{F}_1}{m_1} \\ \vdots \\ \mathbf{v}_n \\ \frac{\mathbf{F}_n}{m_n} \end{bmatrix}$$

This is conceptually the same as a system of one particle. The numerical differential equation solver just has to deal with more variables and equations.

A typical game application, though, has rigid bodies that are not single points. The physical concepts we introduced earlier come into play. Section 2.2.2 showed us the kinematics for a solid rigid body. In particular, we saw how to construct the position, velocity, and acceleration vectors for each point \mathcal{P} in the solid. We identified an object center point \mathcal{C} . As noted many times, the equations of motion greatly simplify when that point is chosen to be the center of mass of the object. The path of the center of mass was denoted by $\mathcal{X}(t; \mathcal{C})$. To work solely with vectors in this section, we will use the difference $\mathbf{x}(t) = \mathcal{X}(t; \mathcal{C}) - \mathcal{O}$, where \mathcal{O} is the origin of the world. The velocity

of the center of mass measured in world coordinates was denoted by $\mathbf{v}_{cen}(t)$. We will drop the subscript in this section and use just the notation $\mathbf{v}(t)$. The position and velocity are related by

$$\frac{d\mathbf{x}(t)}{dt} = \mathbf{v}(t) \quad (6.60)$$

A restatement of [equation \(2.56\)](#), the linear momentum of the rigid body is

$$\mathbf{p}(t) = m\mathbf{v}(t) \quad (6.61)$$

where m is the total mass of the body. Since the mass is a constant, we may keep track of either (linear) velocity or linear momentum in the state of the system. We choose the state to include \mathbf{x} and \mathbf{p} . The driving force behind the center of mass is $\mathbf{F}(t)$, the equations of motion provided by Newton's second law, [equation \(2.45\)](#),

$$\frac{d\mathbf{p}(t)}{dt} = \mathbf{F}(t) \quad (6.62)$$

The abstract operations to determine the location of the center of mass given an applied force $\mathbf{F}(t)$ are

1. Compute \mathbf{p} from \mathbf{F} by integrating [equation \(6.62\)](#).
2. Compute \mathbf{v} from \mathbf{p} by dividing by m in [equation \(6.61\)](#).
3. Compute \mathbf{x} from \mathbf{v} by integrating [equation \(6.60\)](#).

In practice these steps are handled simultaneously by a numerical differential equation solver.

An analogous set of equations tell us how the orientation matrix $R(t)$ is affected by an externally applied torque. The analogy to mass m is the inertia tensor (mass matrix) J defined in [equation \(2.85\)](#). Keep in mind that the inertia tensor is constructed relative to some coordinate system. In this section we are computing it relative to the center of mass of the object. The analogy to linear velocity \mathbf{v} is the angular velocity \mathbf{w} . The analogy to linear momentum is angular momentum \mathbf{L} . The relationship between angular velocity and the orientation matrix is [equation \(2.38\)](#),

$$\frac{dR(t)}{dt} = \text{Skew}(\mathbf{w}(t))R(t) \quad (6.63)$$

The relationship between angular momentum and angular velocity is [equation \(2.88\)](#),

$$\mathbf{L}(t) = J(t)\mathbf{w}(t) \quad (6.64)$$

The inertia tensor is measured in world coordinates. Since the object is moving and rotating, J does vary with time. The driving torque behind the orientation is $\boldsymbol{\tau}(t)$, the

equations of motion provided by [equation \(2.62\)](#),

$$\frac{d\mathbf{L}(t)}{dt} = \boldsymbol{\tau}(t) \quad (6.65)$$

The abstract operations to determine the orientation of the rigid body given an applied torque $\boldsymbol{\tau}(t)$ are analogous to those for determining the location:

1. Compute \mathbf{L} from $\boldsymbol{\tau}$ by integrating [equation \(6.65\)](#).
2. Compute \mathbf{w} from \mathbf{L} by dividing by J in [equation \(6.64\)](#). The division is in the matrix sense – you need to multiply by the inverse matrix J^{-1} .
3. Compute R from \mathbf{w} by integrating [equation \(6.63\)](#).

Recomputing the inertia tensor $J(t)$ and its inverse $J^{-1}(t)$ for each time step of the simulation can be expensive depending on how complex the shape of the rigid body. We can eliminate the direct computation by an observation. Recall that $\mathbf{r}(t; \mathcal{P}) = R(t)\mathbf{b}(\mathcal{P})$, where $R(t)$ is the orientation matrix and $\mathbf{b}(\mathcal{P})$ is the location of point \mathcal{P} measured in body coordinates. If B denotes the region of space that the rigid body occupies, the inertia tensor is

$$\begin{aligned} J(t) &= \int_B (|\mathbf{r}|^2 I - \mathbf{r}\mathbf{r}^T) dm, && \text{Definition of inertia tensor} \\ &= \int_B (|R\mathbf{b}|^2 I - (R\mathbf{b})(R\mathbf{b})^T) dm, && \text{Definition of } \mathbf{r} \\ &= \int_B (|\mathbf{b}|^2 I - R\mathbf{b}\mathbf{b}^T R^T) dm, && \text{Rotation preserves length} \\ &= \int_B (|\mathbf{b}|^2 RR^T - R\mathbf{b}\mathbf{b}^T R^T) dm, && \text{Rotations satisfy } I = RR^T \\ &= R \left(\int_B (|\mathbf{b}|^2 I - \mathbf{b}\mathbf{b}^T) dm \right) R^T, && R \text{ is constant with respect to the integration} \\ &= R(t)J_{\text{body}}R(t)^T \end{aligned} \quad (6.66)$$

where J_{body} is the inertia tensor measured in the body coordinate frame and is independent of time since the body is rigid. The inverse matrix is easy to compute,

$$J(t)^{-1} = R(t)J_{\text{body}}^{-1}R(t)^T \quad (6.67)$$

Another observation that leads to a robust implementation is that we can use quaternions to represent the orientation matrix. [Chapter 10](#) provides a large amount of background material on quaternions and how they relate to rotations. The main problem when numerically integrating [equation \(6.63\)](#) over many time steps is that

numerical error builds up, and the computed matrix $R(t)$ is no longer precisely a rotation matrix. We may easily correct for this situation. If $\hat{R}(t) = [\hat{\mathbf{u}}_0 \hat{\mathbf{u}}_1 \hat{\mathbf{u}}_2]$ is the output of the differential equation solver, Gram–Schmidt orthonormalization may be applied to its columns to generate a set of orthonormal vectors that become the columns of the orientation matrix, $R(t) = [\mathbf{u}_0 \mathbf{u}_1 \mathbf{u}_2]$. Specifically,

$$\mathbf{u}_0 = \frac{\hat{\mathbf{u}}_0}{|\hat{\mathbf{u}}_0|}, \quad \mathbf{u}_1 = \frac{\hat{\mathbf{u}}_1 - (\hat{\mathbf{u}}_1 \cdot \mathbf{u}_0)\mathbf{u}_0}{|\hat{\mathbf{u}}_1 - (\hat{\mathbf{u}}_1 \cdot \mathbf{u}_0)\mathbf{u}_0|}, \quad \mathbf{u}_2 = \mathbf{u}_0 \times \mathbf{u}_1$$

The orthonormalization does not have to be applied at every step, but often enough to avoid numerical problems. If $q(t)$ is a quaternion that represents $R(t)$, and if $\omega(t)$ is the (not necessarily unit length) quaternion that corresponds to the angular velocity $\mathbf{w}(t)$, then the differential equation for $q(t)$ equivalent to [equation \(6.63\)](#) is

$$\frac{dq(t)}{dt} = \frac{1}{2}\omega(t)q(t) \quad (6.68)$$

See [Chapter 10](#) for the derivation of this equation. A numerical integration still occurs and produces an output $\hat{q}(t)$ that can be normalized to unit length $q(t)$ to account for the numerical round-off errors, but the frequency of normalization can be chosen smaller than for rotation matrices. Treating $q(t)$ as a vector in four dimensions, the normalization is

$$q = \frac{\hat{q}}{|\hat{q}|}$$

where $|\hat{q}|$ is the length of the input 4-tuple. This normalization is less expensive to compute than Gram–Schmidt orthonormalization for rotation matrices.

Now to put all this together. For a single rigid body, the state vector is expanded to

$$\mathbf{S}(t) = \begin{bmatrix} \mathbf{x}(t) \\ q(t) \\ \mathbf{p}(t) \\ \mathbf{L}(t) \end{bmatrix} \quad (6.69)$$

The applied force is $\mathbf{F}(t)$ and the applied torque is $\boldsymbol{\tau}(t)$. The equations of motion are

$$\frac{d\mathbf{S}}{dt} = \frac{d}{dt} \begin{bmatrix} \mathbf{x} \\ q \\ \mathbf{p} \\ \mathbf{L} \end{bmatrix} = \begin{bmatrix} \dot{\mathbf{x}} \\ \dot{q} \\ \dot{\mathbf{p}} \\ \dot{\mathbf{L}} \end{bmatrix} = \begin{bmatrix} m^{-1}\mathbf{p} \\ \omega q/2 \\ \mathbf{F} \\ \boldsymbol{\tau} \end{bmatrix} \quad (6.70)$$

The force $\mathbf{F}(t)$ and torque $\boldsymbol{\tau}(t)$ are always computable at time t . The state values for $\mathbf{p}(t)$, $q(t)$, and $\mathbf{L}(t)$ at time t are maintained by the physics simulator. The orientation matrix $R(t)$ is computed from $q(t)$. The angular velocity is determined by [equations \(6.64\)](#) and [\(6.67\)](#), namely

$$\mathbf{w}(t) = J^{-1}(t)\mathbf{L}(t) = R(t)J_{\text{body}}^{-1}R(t)^T\mathbf{L}(t)$$

The corresponding quaternion ω is computed from $\mathbf{w}(t)$. After these calculations we know all the quantities on the right-hand side of [equation \(6.70\)](#) and can apply the numerical differential equation solver to compute the values at the next time $t + \Delta t$ for a suitably chosen step size $\Delta t > 0$.

For n rigid bodies, the state vector contains n blocks of values, each block the position, orientation, linear momentum, and angular momentum of a single rigid body. The state vector of the entire system is

$$\mathbf{S}(t) = \begin{bmatrix} \mathbf{x}_1(t) \\ q_1(t) \\ \mathbf{p}_1(t) \\ \mathbf{L}_1(t) \\ \vdots \\ \mathbf{x}_n(t) \\ q_n(t) \\ \mathbf{p}_n(t) \\ \mathbf{L}_n(t) \end{bmatrix} \quad (6.71)$$

For the i th rigid body, the applied force is $\mathbf{F}_i(t)$ and the applied torque is $\boldsymbol{\tau}_i(t)$. The equations of motion are

$$\frac{d\mathbf{S}}{dt} = \frac{d}{dt} \begin{bmatrix} \mathbf{x}_1(t) \\ q_1(t) \\ \mathbf{p}_1(t) \\ \mathbf{L}_1(t) \\ \vdots \\ \mathbf{x}_n(t) \\ q_n(t) \\ \mathbf{p}_n(t) \\ \mathbf{L}_n(t) \end{bmatrix} = \begin{bmatrix} \dot{\mathbf{x}}_1(t) \\ \dot{q}_1(t) \\ \dot{\mathbf{p}}_1(t) \\ \dot{\mathbf{L}}_1(t) \\ \vdots \\ \dot{\mathbf{x}}_n(t) \\ \dot{q}_n(t) \\ \dot{\mathbf{p}}_n(t) \\ \dot{\mathbf{L}}_n(t) \end{bmatrix} = \begin{bmatrix} m_1^{-1} \mathbf{p}_1 \\ \omega_1 q_1 / 2 \\ \mathbf{F}_1 \\ \boldsymbol{\tau}_1 \\ \vdots \\ m_n^{-1} \mathbf{p}_n \\ \omega_n q_n / 2 \\ \mathbf{F}_n \\ \boldsymbol{\tau}_n \end{bmatrix} = \mathbf{G}(t, \mathbf{S}) \quad (6.72)$$

The nonlinear system of differential equations $\dot{\mathbf{S}} = \mathbf{G}(t, \mathbf{S})$ is solved numerically to compute the state at any time during the physical simulation.

The main design goal of a rigid body class is to encapsulate the state handling to support a simulation of the form shown next. This is essentially part of the work implied by “update physics state” and “move objects” in [Section 6.1](#). At the moment

we are assuming unconstrained motion, so there is no pseudocode that corresponds to “resolve constraints” in the physics tick.

```
// initialization
RigidBody body[n];
double t = <your choice of initial time>;
double dt = <your choice of time step>;
for (int i = 0; i < n; ++i)
{
    // Set the initial state of the rigid bodies. X is position,
    // Q is a quaternion that represents the orientation, P is
    // linear momentum, and L is angular momentum.
    body[i].SetState(X[i], Q[i], P[i], L[i]);
}

// Part of the physics tick.
for (i = 0; i < n; ++i)
{
    body[i].Update(t, dt);
}
t += dt;
```

The class definition is shown next. The position is X , the orientation as a quaternion is Q , the linear momentum is P , the angular momentum is L , the orientation as a matrix is R , the linear velocity is V , and the angular velocity is W . The mass is $mass$ and the inertia tensor in body coordinates is $inertia$. The interface is written in a simplified manner for illustrative purposes. The actual interface in the source code is more extensive.

```
class RigidBody
{
public:
    RigidBody (double m, matrix inertia);
    virtual ~RigidBody () ;

    void SetState (point X, quaternion Q, vector P, vector L);
    void GetState (point& X, quaternion& Q, vector& P, vector& L);

    // force/torque function format
    typedef vector (*Function)
    (
        double,      // time of application
        point,       // position
        quaternion, // orientation
        vector,      // linear momentum
        vector,      // angular momentum
        matrix,      // orientation
        vector,      // linear velocity
    );
}
```

```

        vector      // angular velocity
    );

// for computing external forces and torques
void SetForceFunction (Function force);
void SetTorqueFunction (Function torque);

// Runge-Kutta fourth order differential equation solver
void Update (double t, double dt);

protected:
    // convert (Q,P,L) to (R,V,W)
    void Convert (quaternion Q, vector P, vector L,
                  matrix& R, vector& V, vector& W) const;

    // constant quantities
    double m_mass, m_invMass;
    matrix m_inertia, m_invInertia;

    // state variables
    vector m_X;          // position
    quaternion m_Q;       // orientation
    vector m_P;           // linear momentum
    vector m_L;           // angular momentum

    // derived state variables
    matrix m_R;           // orientation matrix
    vector m_V;           // linear velocity
    vector m_W;           // angular velocity

    // force and torque functions
    Function m_force;
    Function m_torque;
};

}

```

The constructor and the SetState member function make up the initialization portion of the physical simulation. The conversion from the primary state (quaternion orientation, linear momentum, and angular momentum) to the secondary state (matrix orientation, linear velocity, and angular velocity) is handled via the member function Convert. The conversions require access to the rigid body mass and inertia tensor, thus this function is nonstatic.

```

void RigidBody::Convert (quaternion Q, vector P, vector L,
                        matrix& R, vector& V, vector& W) const
{
    Q.ToRotationMatrix(R);
    V = m_invMass*P;
    W = R*m_invInertia*Transpose(R)*L;
}

```

Rather than having force and torque data members to store the current force and torque, we use function pointers. The force and torque vectors are required only during the differential equation update step, so there is no need to store the vectors with the rigid body. The force and torque functions take as input the current time and a list of state information. As noted earlier, one of the reasons the illustrative example code copies data from the state array to the rigid bodies during the multifunction evaluation differential equation solver is to make sure that the force and torque are computed with the current state values. These state values persist only for the lifetime of the update call of the solver since they are only needed temporarily by the multifunction evaluation algorithm. They may as well be stack variables, the main consequence being that the global state arrays are no longer necessary; each rigid body is now responsible for updating itself. The member function `Update` implements a Runge–Kutta fourth order solver.

```

void RigidBody::Update (double t, double dt)
{
    double halfdt = 0.5 * dt, sixthdt = dt / 6.0;
    double tphalfdt = t + halfdt, tpdt = t + dt;

    vector XN, PN, LN, VN, WN;
    quaternion QN;
    matrix RN;

    // A1 = G(t,S0), B1 = S0 + (dt / 2) * A1
    vector A1DXDT = m_V;
    quaternion A1DQDT = 0.5 * m_W * m_Q;
    vector A1DPDT = m_force(t,m_X,m_Q,m_P,m_L,m_R,m_V,m_W);
    vector A1DLDT = m_torque(t,m_X,m_Q,m_P,m_L,m_R,m_V,m_W);
    XN = m_X + halfdt * A1DXDT;
    QN = m_Q + halfdt * A1DQDT;
    PN = m_P + halfdt * A1DPDT;
    LN = m_L + halfdt * A1DLDT;
    Convert(QN,PN,LN,RN,VN,WN);

    // A2 = G(t + dt / 2,B1), B2 = S0 + (dt / 2) * A2
    vector A2DXDT = VN;
    quaternion A2DQDT = 0.5 * WN * QN;
    vector A2DPDT = m_force(tphalfdt,XN,QN,PN,LN,RN,VN,WN);
    vector A2DLDT = m_torque(tphalfdt,XN,QN,PN,LN,RN,VN,WN);
    XN = m_X + halfdt * A2DXDT;
    QN = m_Q + halfdt * A2DQDT;
    PN = m_P + halfdt * A2DPDT;
    LN = m_L + halfdt * A2DLDT;
    Convert(QN,PN,LN,RN,VN,WN);

    // A3 = G(t + dt / 2,B2), B3 = S0 + dt * A3
    vector A3DXDT = VN;
    quaternion A3DQDT = 0.5 * WN * QN;

```

```

vector A3DPDT = m_force(tphalfdt,XN,QN,PN,LN,RN,VN,WN);
vector A3DLDT = m_torque(tphalfdt,XN,QN,PN,LN,RN,VN,WN);
XN = m_X + dt * A3DXDT;
QN = m_Q + dt * A3DQDT;
PN = m_P + dt * A3DPDT;
LN = m_L + dt * A3DLDT;
Convert(QN,PN,LN,RN,VN,WN);

// A4 = G(t + dt,B3),
//      S1 = S0 + (dt / 6) * (A1 + 2 * A2 + 2 * A3 + A4)
vector A4DXDT = VN;
quaternion A4DQDT = 0.5 * WN * QN;
vector A4DPDT = m_force(tpdt,XN,QN,PN,LN,RN,VN,WN);
vector A4DLDT = m_torque(tpdt,XN,QN,PN,LN,RN,VN,WN);
m_X = m_X + sixthdt*(A1DXDT + 2.0*(A2DXDT + A3DXDT) + A4DXDT);
m_Q = m_Q + sixthdt*(A1DQDT + 2.0*(A2DQDT + A3DQDT) + A4DQDT);
m_P = m_P + sixthdt*(A1DPDT + 2.0*(A2DPDT + A3DPDT) + A4DPDT);
m_L = m_L + sixthdt*(A1DLDT + 2.0*(A2DLDT + A3DLDT) + A4DLDT);
Convert(m_Q,m_P,m_L,m_R,m_V,m_W);
}

```

After each call to `Update`, all rigid body state variables have correct and consistent information due to the last call to `Convert`.

6.6 ACCELERATION-BASED CONSTRAINED MOTION

The previous section was about the unconstrained motion of rigid bodies that are assumed not to interact with each other. We used the equations of motion that follow from Newtonian dynamics, a natural choice in the absence of constraints on the bodies. In realistic applications we, in fact, have to deal with interaction among many objects. A physics engine must decide what to do when two objects collide. The approach in [Bar01] is to force *nonpenetration constraints*. When one object collides with another, the two are not allowed to penetrate into each other. Despite the constraints imposed by collisions between objects, the Newtonian approach is still used to drive the physical simulation. The collision response for objects in contact falls into two categories based on how the objects collide at a point, either a *colliding contact* or a *resting contact*. When all contact points are known, the differential equation solver is interrupted during the simulation and the various physical parameters are adjusted based on the type of contact. The solver is then restarted using the new parameters. Adjustment of the physical parameters at points of colliding contact requires the introduction of *impulsive forces*. Adjustment of the physical parameters at points of resting contact requires computing *contact forces*. Sections 6.6.1 and 6.6.2 cover these topics in detail. The Baraff approach is quite popular with people interested in adding physical simulations to their games, but this approach is not the only

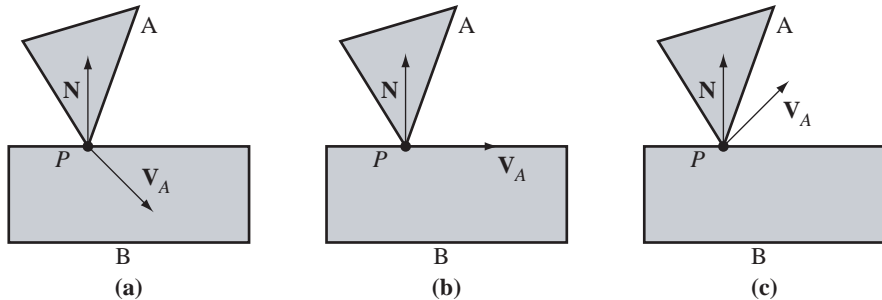


Figure 6.42 (a) Colliding contact. Body A attempts to penetrate into body B. (b) Resting contact. Body A rests on body B and attempts neither to penetrate into B nor to separate from B. Body A is allowed to slide along B. (c) Separation. Body A has a velocity that separates it from body B.

way to go about handling the physics. For example, Section 6.6.5 presents an alternative that is based on Lagrangian dynamics, a natural choice for dealing with motion in the presence of constraints.

6.6.1 COLLISION POINTS

Let us now define what is meant by colliding contact and resting contact. At a point of contact of two objects we need to decide how the objects will continue moving, the collision response so to speak. For example, if a rigid ball strikes a flat surface at an angle, you most likely want the ball to bounce away from the surface. In particular, your natural instinct is to reflect the velocity vector through the normal of the surface so that the angle of incidence is equal to the angle of reflection. This type of contact between moving rigid bodies is called *colliding contact* because the velocities of the bodies cause them to want to penetrate into each other. Figure 6.42(a) shows a point of colliding contact.

The velocity of body A, shown in Figure 6.42(a) as \mathbf{V}_A , has direction into the body B at the point of contact P . If A has zero velocity at P or has velocity perpendicular to the surface of body B at P , the point of contact is said to be a *resting contact*. This situation is shown in part (b). The last possibility is that bodies A and B are separating, as shown in part (c). The figure also shows a normal vector \mathbf{N} to the surface of body B at the contact point P . The algebraic quantity that distinguishes between the three cases is the magnitude of the velocity \mathbf{V}_A in the direction of the normal \mathbf{N} :

$$\begin{aligned} \mathbf{N} \cdot \mathbf{V}_A < 0 & \text{ Colliding contact} \\ \mathbf{N} \cdot \mathbf{V}_A = 0 & \text{ Resting contact} \\ \mathbf{N} \cdot \mathbf{V}_A > 0 & \text{ Separation} \end{aligned} \quad (6.73)$$

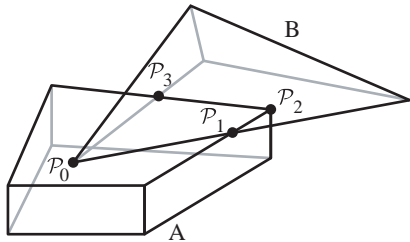


Figure 6.43 The reduced contact set for two convex polyhedra A and B.

The dot product $\mathbf{N} \cdot \mathbf{V}_A$ is the speed of body A in the normal direction.

Recall that we are restricting our attention to rigid bodies in the shape of convex polyhedra. The contact set between two convex polyhedra is potentially more complicated than just a single point that arises because of a vertex–face intersection. The set is infinite in the case of edge–face or face–face intersections. To simplify matters we will work with a *reduced contact set* that consists only of vertex–face or edge–edge intersections, the latter case only when the edges are not parallel. If the collision system detects an edge–face intersection, we will record only an edge endpoint (a vertex) if it is contained in the face and an edge–edge intersection point if the edge overlaps an edge of the face. If a face–face intersection is detected, the only recorded points are vertices of one face contained in the other face or edge–edge intersections, one edge from each face. Figure 6.43 illustrates this.

The point P_0 is generated by a vertex of B and a face of A; the point P_2 is generated by a vertex of A and a face of B; and points P_1 and P_3 are generated by edges of A and B.

The reduction to a finite point set helps to minimize the time spent in the physical simulation. However, this is only an approximation to the actual physics. If our target goal is N frames per second, the computational time available for one frame is $1/N$ seconds. If the physics simulation does not use all of this time, ideally we would calculate the line segment of intersection in an edge–face intersection or the polygon of intersection in a face–face intersection, then proceed with the collision response accordingly. We also process the reduced contact set a point at a time. The collision response becomes dependent on the order and is not quite physically correct. This can be a problem, especially when a rigid body makes simultaneous contact with two (or more) other rigid bodies.

6.6.2 COLLISION RESPONSE FOR COLLIDING CONTACT

Let us now formulate how our physics simulation will respond at a point of colliding contact. Let t_0 denote the first time of contact between a pair of rigid bodies A and B.

Let \mathcal{P}_0 be the contact point. If the point is a vertex–face intersection, we choose the convention that the vertex is from the first body and the face is from the second body. Let \mathbf{N}_0 be the unit-length, outer pointing normal for the face. If the point is an edge–edge intersection, let \mathbf{N}_0 be the unit-length cross product of the edge directions. The vector is chosen to point outside the second body of the pair. For a brief time interval before the collision, the path of the point on the first body contributing to the intersection is $\mathcal{P}_A(t)$ for $t \leq t_0$, and $\mathcal{P}_A(t_0) = \mathcal{P}_0$. During that same time interval the second body is (potentially) moving; the path of the point on it that contributes to the intersection is $\mathcal{P}_B(t)$ for $t \leq t_0$, and $\mathcal{P}_B(t_0) = \mathcal{P}_0$. Backing up in time, the normal vector at the point on the second body contributing to the intersection is $\mathbf{N}(t)$, and $\mathbf{N}(t_0) = \mathbf{N}_0$. The signed distance between the body points contributing to the intersection, as measured in the normal direction, is

$$d(t) = \mathbf{N}(t) \cdot (\mathcal{P}_A(t) - \mathcal{P}_B(t)) \quad (6.74)$$

The velocity component in the normal direction has magnitude,

$$\dot{d}(t) = \mathbf{N}(t) \cdot (\dot{\mathcal{P}}_A(t) - \dot{\mathcal{P}}_B(t)) + \dot{\mathbf{N}}(t) \cdot (\mathcal{P}_A(t) - \mathcal{P}_B(t)) \quad (6.75)$$

At the instant of contact, $d(t_0) = 0$ and $\dot{d}(t_0) = \mathbf{N}_0 \cdot (\dot{\mathcal{P}}_A(t_0) - \dot{\mathcal{P}}_B(t_0))$. The quantity $\dot{d}(t_0)$ is exactly what was mentioned in [equation \(6.73\)](#) for determining the type of contact point that \mathcal{P}_0 is.

In [Section 2.2](#) on kinematics, we derived the velocity equation for a particle, namely [equation \(2.43\)](#). We have two particles in motion, hence two velocity equations:

$$\dot{\mathcal{P}}_A = \mathbf{v}_A + \mathbf{w}_A \times \mathbf{r}_A, \quad \dot{\mathcal{P}}_B = \mathbf{v}_B + \mathbf{w}_B \times \mathbf{r}_B \quad (6.76)$$

where \mathbf{v}_C is the velocity of the center of mass \mathcal{X}_C of body C (C is either A or B), \mathbf{w}_C is the angular velocity of the body about its center of mass, and $\mathbf{r}_C = \mathcal{P}_C - \mathcal{X}_C$ is the location of the point relative to the center of mass. [Equation \(2.43\)](#) also had a term $D\mathbf{r}_C/Dt$, but for rigid bodies it is the zero vector. At the contact time, the speed of \mathcal{P}_0 in the normal direction \mathbf{N}_0 is

$$\dot{d}(t_0) = \mathbf{N}_0 \cdot ((\mathbf{v}_A(t_0) + \mathbf{w}_A(t_0) \times \mathbf{r}_A(t_0)) - (\mathbf{v}_B(t_0) + \mathbf{w}_B(t_0) \times \mathbf{r}_B(t_0))) \quad (6.77)$$

All the quantities on the right-hand side of this equation are known during the physics simulation at the contact time and are stored as part of the state information of the rigid body, just as in the case of unconstrained motion. Thus, after the collision detection system reports all contact points, we may iterate over them and determine which of them are colliding contacts, resting contacts, or separating points.

Impulses

To prevent interpenetration at \mathcal{P}_0 when $\dot{d}(t_0) < 0$, the relative velocity $\dot{\mathcal{P}}_A(t) - \dot{\mathcal{P}}_B(t)$ must be changed in a discontinuous manner. Of course, this is not physically possible since any forces acting on the bodies take some time to change the velocity smoothly.

EXAMPLE 6.2

To illustrate, consider a one-dimensional problem where a particle located at $x(t)$ on a line travels with constant velocity $\dot{x}(t) = v_0 > 0$. The implication, of course, is that no forces are acting on the particle. The path of motion is $x(t) = x_0 + v_0 t$, where x_0 is the initial position of the particle. If the particle strikes an object located at $x_1 > x_0$ at time $t_0 > 0$, so that $x_1 = x_0 + v_0 t_0$, you would expect the object to give way so that over some time interval $[t_0, t_0 + \varepsilon]$, for a small positive ε . During this interval the particle and object remain in contact at the common position $x(t) = x_1 + p(t)$ for some function $p(t)$ such that $p(t_0) = 0$, $\dot{p}(t_0) = v_0$, $p(t_0 + \varepsilon) = 0$, and $p(t) > 0$ for $t \in (t_0, t_0 + \varepsilon)$. For illustrative purposes, let $p(t) = v_0(t - t_0)(t_0 + \varepsilon - t)/\varepsilon$ whose graph is a parabola. During the interval of contact the velocity of the particle is $\dot{x}(t) = \dot{p}(t) = v_0(\varepsilon - 2(t - t_0))/\varepsilon$. At the first contact, $v_0 = \dot{x}(t_0) = \dot{p}(t_0)$. At time $t_0 + \varepsilon/2$ the particle and object come to rest, $\dot{x}(t_0 + \varepsilon/2) = 0$. The particle then reverses direction. At time $t_0 + \varepsilon$ the particle's velocity is $\dot{x}(t_0 + \varepsilon) = -v_0$.

The particle had velocity v_0 at time t_0 and now has the opposite velocity $-v_0$ at time $t_0 + \varepsilon$. The change in velocity occurred over a time period of duration $\varepsilon > 0$. This is true no matter how small the duration is, so consider taking a limit and let ε go to zero. Intuitively, by letting $\varepsilon = 0$, we have changed the velocity in a discontinuous manner:

$$\dot{x}(t) = \begin{cases} v_0, & t \leq t_0 \\ -v_0, & t > t_0 \end{cases}$$

Mathematically, however, the limit is not defined. Consider what has to happen to $p(t)$ as ε approaches zero. Figure 6.44 shows the graph of $p(t)$ for various values of ε . The interval on which $p(t) > 0$ gets smaller while the maximum value of p , namely v_0/ε , gets larger. The limiting function appears to be W

$$\delta(t - t_0) = \begin{cases} 0, & t \neq t_0 \\ \infty, & t = t_0 \end{cases}$$

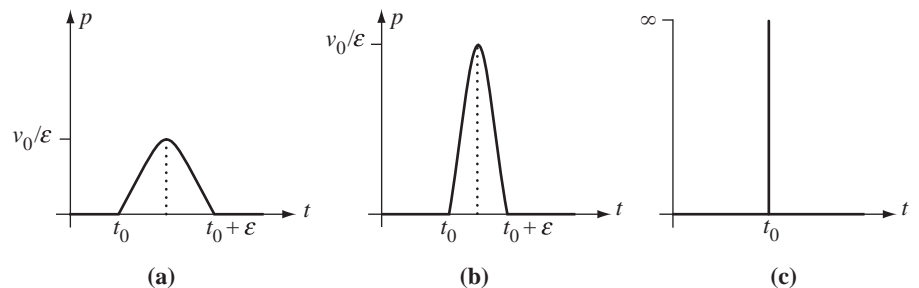


Figure 6.44 The effects on $p(t)$ as ε approaches zero: (a) Small ε ; (b) Smaller ε ; and (c) Really small ε (like zero).

(Example 6.2
continued)

The physicists refer to $\delta(t - t_0)$ as the *Dirac delta function*. It is not a function in the mathematical sense, but the mathematicians refer to such an entity as a *generalized function*. Its properties are defined in terms of integrals rather than using the informal definition. For example, one important property is

$$\int_0^t g(\tau) \delta(\tau - t_0) d\tau = \begin{cases} g(t_0) & \text{If } 0 \leq t_0 \leq t \\ 0 & \text{Otherwise} \end{cases} \quad (6.78)$$

In the special case when $g(t) \equiv 1$ we have $\int_0^t \delta(\tau - t_0) d\tau = u(t - t_0)$, where $u(s) = 1$ for $s \geq 0$ and $u(s) = 0$ for $s < 0$. The velocity of our particle is consequently $\dot{x}(t) = v_0(1 - 2u(t - t_0))$ and the acceleration is $\ddot{x}(t) = -2v_0\delta(t - t_0)$. The quantity $f(t) = -2mv_0\delta(t - t_0)$ is referred to as an *impulsive force*. ■

For a discussion of delta functions in the context of differential equations, see [Bra84]. A key idea discussed in that book is that an integration of Newton's second law of motion produces

$$mv(t) - mv(0) = \int_0^t \mathbf{F}(\tau) d\tau$$

The integral on the right-hand side of this equation is called the *impulse imparted by the force*. If we allow the force $\mathbf{F}(t)$ to include impulsive forces as motivated by Example 6.2, then we can cause a discontinuity in the linear momentum of the system. This is exactly what we do in our physical simulation at a point of colliding contact.

Computing the Change of Velocity

Rather than constructing an impulsive function that leads to a discontinuous change in velocity at a point of colliding contact, we will select the desired velocity to be used at that point *after* the impulse is applied. I mentioned earlier that the intuitive choice you want to make for the new velocity is a reflection of the old velocity through the normal vector. That is, if \mathbf{v}^- is the (relative) velocity before the impulse and \mathbf{N} is the unit-length outer pointing normal, you can write

$$\mathbf{v}^- = \mathbf{N}^\perp + (\mathbf{N} \cdot \mathbf{v}^-)\mathbf{N}$$

where \mathbf{N}^\perp is that portion of \mathbf{v}^- after projecting out the component in the \mathbf{N} direction. The velocity after the impulse is selected to be

$$\mathbf{v}^+ = \mathbf{N}^\perp - (\mathbf{N} \cdot \mathbf{v}^-)\mathbf{N}$$

Figure 6.45(a) illustrates the reflection.

The perfect reflection represents no loss of kinetic energy during the collision event. We may, however, want to incorporate loss of energy to make the collision response a bit more realistic. We can do this by introducing a *coefficient of restitution*,

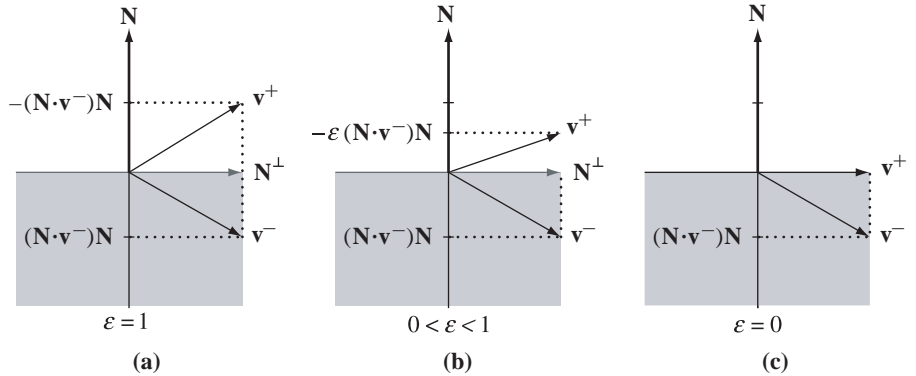


Figure 6.45 (a) Reflection of the preimpulse velocity \mathbf{v}^- through the contact normal to obtain the postimpulse velocity \mathbf{v}^+ . (b) An imperfect reflection that represents a loss of kinetic energy. (c) An imperfect reflection that represents a maximum loss of kinetic energy.

$\epsilon \in [0, 1]$, and generate a postimpulse velocity of

$$\mathbf{v}^+ = \mathbf{N}^\perp - \epsilon(\mathbf{N} \cdot \mathbf{v}^-)\mathbf{N}$$

Figure 6.45(c) shows such a vector. No kinetic energy is lost when $\epsilon = 1$ and the reflection is perfect. The maximum amount of kinetic energy is lost when $\epsilon = 0$ and the bodies remain in contact at the contact point, a change from colliding contact to resting contact.

In the following discussion, the contact time t_0 is omitted from function arguments for clarity. Let $\dot{\mathcal{P}}_A^-$ and $\dot{\mathcal{P}}_A^+$ denote preimpulse and postimpulse velocities for \mathcal{P}_0 as measured from body A. Let $\dot{\mathcal{P}}_B^-$ and $\dot{\mathcal{P}}_B^+$ denote the similar quantities for body B. From equation (6.76) we have

$$\dot{\mathcal{P}}_A^\pm = \mathbf{v}_A^\pm + \mathbf{w}_A^\pm \times \mathbf{r}_A, \quad \dot{\mathcal{P}}_B^\pm = \mathbf{v}_B^\pm + \mathbf{w}_B^\pm \times \mathbf{r}_B \quad (6.79)$$

where the use of the plus and minus superscripts on the velocity terms is clear from context. The impulsive force changes velocities at the contact time but not the positions of \mathcal{P}_0 relative to the centers of mass, so the \mathbf{r} terms do not require plus/minus superscripts.

Let us begin by postulating an impulsive force $\mathbf{F} = f\mathbf{N}_0$ that affects body A at the colliding contact point. The scalar f is the magnitude of the impulse that we need to compute to obtain the desired postimpulse velocity vector. The impulsive force has a contribution that changes the velocity of the center of mass, $f\mathbf{N}_0/m_A$, where m_A is the mass of body A. The preimpulse and postimpulse linear velocities are related by

$$\mathbf{v}_A^+ = \mathbf{v}_A^- + \frac{f\mathbf{N}_0}{m_A} \quad (6.80)$$

The corresponding change in linear momentum is $\mathbf{p}_A^+ = \mathbf{p}_A^- + f\mathbf{N}_0$. The impulsive force also has a contribution that changes the angular velocity of the body via an impulsive torque, $J_A^{-1}(\mathbf{r}_A \times f\mathbf{N}_0)$, where J_A is the inertia tensor at the contact time and is measured in world coordinates. The preimpulse and postimpulse angular velocities are related by

$$\mathbf{w}_A^+ = \mathbf{w}_A^- + J_A^{-1}(\mathbf{r}_A \times f\mathbf{N}_0) \quad (6.81)$$

The corresponding change in angular momentum is $\mathbf{L}_A^+ = \mathbf{L}_A^- + \mathbf{r}_A \times f\mathbf{N}_0$. Substituting equations (6.80) and (6.81) into the velocity equation (6.79) and applying a few algebraic steps produces

$$\dot{\mathcal{P}}_A^+ = \dot{\mathcal{P}}_A^- + f \left(\frac{\mathbf{N}_0}{m_A} + J_A^{-1}(\mathbf{r}_A \times \mathbf{N}_0) \times \mathbf{r}_A \right) \quad (6.82)$$

The opposite direction impulsive force $-F$ is applied to body B. A construction similar to the previous one produces $\mathbf{v}_B^+ = \mathbf{v}_B^- - f\mathbf{N}_0/m_B$, $\mathbf{p}_B^+ = \mathbf{p}_B^- - f\mathbf{N}_0$, $\mathbf{w}_B^+ = \mathbf{w}_B^- - J_B^{-1}(\mathbf{r}_B \times f\mathbf{N}_0)$, $\mathbf{L}_B^+ = \mathbf{L}_B^- - \mathbf{r}_B \times f\mathbf{N}_0$, and

$$\dot{\mathcal{P}}_B^+ = \dot{\mathcal{P}}_B^- - f \left(\frac{\mathbf{N}_0}{m_B} + J_B^{-1}(\mathbf{r}_B \times \mathbf{N}_0) \times \mathbf{r}_B \right) \quad (6.83)$$

Equations (6.82) and (6.83) are combined to form the relative velocity

$$\begin{aligned} \dot{\mathcal{P}}_A^+ - \dot{\mathcal{P}}_B^+ &= (\dot{\mathcal{P}}_A^- - \dot{\mathcal{P}}_B^-) + f \left(\frac{\mathbf{N}_0}{m_A} + \frac{\mathbf{N}_0}{m_B} + (J_A^{-1}(\mathbf{r}_A \times \mathbf{N}_0)) \times \mathbf{r}_A \right. \\ &\quad \left. + (J_B^{-1}(\mathbf{r}_B \times \mathbf{N}_0)) \times \mathbf{r}_B \right) \end{aligned} \quad (6.84)$$

The final step in computing the magnitude f involves our choice of how the postimpulse relative velocity relates to the preimpulse one. In particular, we choose a coefficient of restitution $\varepsilon \in [0, 1]$ and require that

$$\mathbf{N}_0 \cdot (\dot{\mathcal{P}}_A^+ - \dot{\mathcal{P}}_B^+) = -\varepsilon \mathbf{N}_0 \cdot (\dot{\mathcal{P}}_A^- - \dot{\mathcal{P}}_B^-) \quad (6.85)$$

Dot equation (6.84) with \mathbf{N}_0 , substitute equation (6.85) into the left-hand side, use equation (6.79), and solve to obtain

$$f = \frac{-(1 + \varepsilon)(\mathbf{N}_0 \cdot (\mathbf{v}_A^- - \mathbf{v}_B^-) + (\mathbf{w}_A^- \cdot (\mathbf{r}_A \times \mathbf{N}_0) - \mathbf{w}_B^- \cdot (\mathbf{r}_B \times \mathbf{N}_0)))}{m_A^{-1} + m_B^{-1} + (\mathbf{r}_A \times \mathbf{N}_0)^T J_A^{-1}(\mathbf{r}_A \times \mathbf{N}_0) + (\mathbf{r}_B \times \mathbf{N}_0)^T J_B^{-1}(\mathbf{r}_B \times \mathbf{N}_0)} \quad (6.86)$$

where $\mathbf{r}_A = \mathcal{P}_0 - \mathcal{X}_A$ and $\mathbf{r}_B = \mathcal{P}_0 - \mathcal{X}_B$. Some algebraic steps were performed to factor out the common expressions $\mathbf{r}_A \times \mathbf{N}_0$ and $\mathbf{r}_B \times \mathbf{N}_0$. The right-hand side of equation (6.86) depends only on constants $(\varepsilon, m_A^{-1}, J_A^{-1}, m_B^{-1}, J_B^{-1})$, preimpulse rigid body state $(\mathcal{X}_A, \mathbf{v}_A^-, \mathbf{w}_A^-, \mathcal{X}_B, \mathbf{v}_B^-, \mathbf{w}_B^-)$, and the contact information $(\mathcal{P}_0, \mathbf{N}_0)$. The

inverse inertia tensors J_A^{-1} and J_B^{-1} are positive definite, implying $\xi^T J_A^{-1} \xi > 0$ and $\xi^T J_B^{-1} \xi > 0$ for any $\xi \neq \mathbf{0}$. Consequently, the denominator of f must be positive, so the division is not of numerical concern in an implementation.

Pseudocode for processing a point of colliding contact follows and uses the RigidBody structure discussed in the illustrative implementation for unconstrained motion.

```

void ProcessCollidingContact (RigidBody A, RigidBody B, point P,
    vector N)
{
    // compute impulse force
    const double e = <coefficient of restitution>;
    vector rA = P - A.x;
    vector rB = P - B.x;
    vector kA = Cross(rA,N);
    vector kB = Cross(rB,N);
    vector uA = A.jinv * kA;
    vector uB = B.jinv * kB;
    double numer = -(1 + e) * (Dot(N,A.v - B.v) + Dot(A.w,kA)
        - Dot(B.w,kB));
    double denom = A.massinv + B.massinv + Dot(kA,uA)
        + Dot(kB,uB);
    double f = numer / denom;
    vector impulse = f * N;

    // apply impulse to bodies to change linear/angular momentum
    A.p += impulse;
    B.p -= impulse;
    A.L += f * kA;
    B.L -= f * kB;

    // compute derived quantities, linear/angular velocity
    A.v = A.p * A.massinv;
    B.v = B.p * B.massinv;
    A.w += f * uA;
    B.w += f * uB;
}

```

Notice that this function does not modify the centers of mass or orientations of the rigid bodies. Only the differential equation solver may change these quantities and only because of a positive increment in time. The colliding contact processing represents the application of an impulse at the current instant of time.

Before we look at a couple of simple examples, let us make an observation. In virtual environments you will want some immovable objects, the ground clearly an ideal candidate. We can simulate an immovable object by specifying that it has infinite mass and infinite principal moments, the former preventing translation of the center of mass, the latter preventing rotation about the center of mass. Since our

simulations are using only the inverse mass and inverse inertia tensor, we can instead set the inverse mass to zero and the inverse inertia tensor to the zero matrix. The velocities and momenta of an immovable object should also be set to zero. The values for the center of mass and orientation are irrelevant in the simulation.

EXAMPLE
6.3

Consider a constant density square traveling with constant linear velocity towards a sloped plane of 45 degrees from the horizontal. The square is assumed to have zero angular velocity (not rotating about its center). The sloped plane is immovable. The coefficient of restitution is assumed to be $\varepsilon = 1$ for a completely elastic collision. Gravity is not assumed here. Figure 6.46 illustrates.

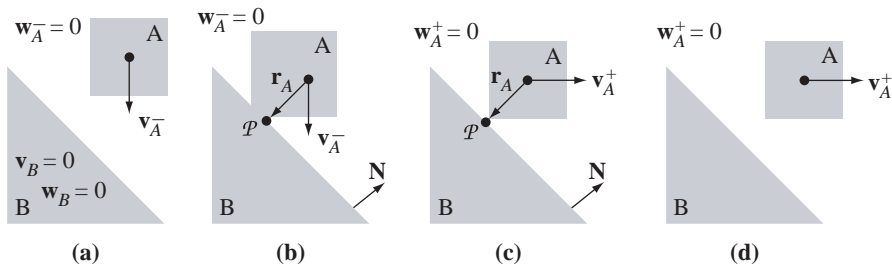


Figure 6.46

(a) The square traveling towards a sloped plane. (b) The preimpulse configuration at the instant of contact. (c) The postimpulse configuration at the instant of contact. (d) The square moving away from the plane.

The square is labeled as body A and the slope as body B. Since the slope is immovable, $v_B = w_B = \mathbf{0}$ always, and $m_B^{-1} = 0$ and $J_B^{-1} = 0$.

The point of contact is P and the unit-length outer pointing normal to the slope is N . The position of the contact point relative to body A is $\mathbf{r}_A = P - \mathcal{X}_A$ where \mathcal{X}_A is the center of mass of A. In this special situation of a square and 45 degree slope, the normal is $N = -\mathbf{r}_A/|\mathbf{r}_A|$, in which case $\mathbf{r}_A \times N = \mathbf{0}$. The impulse magnitude is $f = -2m_A N \cdot v_A^-$. The postimpulse linear velocity is $v_A^+ = v_A^- - 2(N \cdot v_A^-)N$ and the postimpulse angular velocity is $w_A^+ = w_A^- + f J_A^{-1}(\mathbf{r}_A \times N) = \mathbf{0}$. Therefore, the square travels downward and bounces to the right with no change in linear speed or angular velocity. ■

EXERCISE
6.4

Did you expect the result of Example 6.3 to be that the square obtains a nonzero angular velocity and starts to rotate after the impulse is applied? Speculate why the square maintains a zero angular velocity.

Suppose body A is rectangular in shape, but not a square, and axis-aligned as the square was. At the point of contact the normal N and the relative position \mathbf{r}_A are not

parallel, so $\mathbf{u} = \mathbf{r}_A \times \mathbf{N} \neq 0$. Show that the postimpulse velocities are

$$\mathbf{v}_A^+ = \mathbf{v}_A^- - \frac{2\mathbf{N} \cdot \mathbf{v}_A^-}{1 + \mathbf{u}^T m_A J_A^{-1} \mathbf{u}} \mathbf{N}, \quad \mathbf{w}_A^+ = -\frac{2\mathbf{N} \cdot \mathbf{v}_A^-}{1 + \mathbf{u}^T m_A J_A^{-1} \mathbf{u}} m_A J_A^{-1} \mathbf{u}$$

Make an intuitive argument that if the rectangle is wider than tall, the angular velocity corresponds to a clockwise rotation around the vector pointing out of the plane of the figure towards you. Similarly, argue that if the rectangle is taller than wide, the angular velocity corresponds to a counterclockwise rotation about that same vector. Now analyze the term $J_A^{-1} \mathbf{u}$ and show how its values relate to the direction of rotation. ■

Multiple Contact Points

[Example 6.3](#) and [Exercise 6.4](#) are useful as a simple verification of the ideas regarding impulses. Both involve a two-dimensional setting. What happens in a three-dimensional setting? Specifically, let us add thickness to the rectangle of [Exercise 6.4](#) and consider an axis-aligned box that is traveling vertically towards the sloped plane in such a way that the contact occurs along an entire edge of the box. [Figure 6.47](#) illustrates.

According to the convention mentioned earlier, the collision detection system will report only the endpoints of the edge as collision points. I previously made an innocuous statement about processing the collision points sequentially. The consequences of doing so must be weighed against the extra time needed to implement a system that can handle points simultaneously.

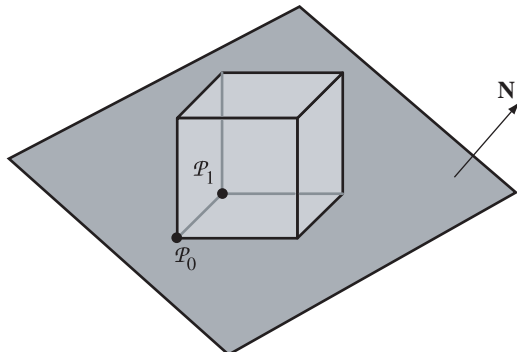


Figure 6.47 An axis-aligned box colliding with a sloped plane along an entire edge of the box, $(1 - s)\mathcal{P}_0 + s\mathcal{P}_1$ for $s \in [0, 1]$.

Let us process the contact points sequentially starting with \mathcal{P}_0 . The relative position in body A is $\mathbf{r}_0 = \mathcal{P}_0 - \mathcal{X}_A$. Define $\mathbf{u}_0 = \mathbf{r}_0 \times \mathbf{N}$. The magnitude of the impulsive force and the postimpulse velocities are

$$f_0 = -\frac{2m_A \mathbf{N} \cdot \mathbf{v}_A^-}{1 + \mathbf{u}_0^T m_A J_A^{-1} \mathbf{u}_0}, \quad \mathbf{v}_A^+ = \mathbf{v}_A^- + (f_0 \mathbf{N}) / m_A, \quad \mathbf{w}_A^+ = f_0 J_A^{-1} \mathbf{u}_0$$

In our full three-dimensional setting, $J_A^{-1} \mathbf{u}_0$ is not the zero vector! This means that the box's postimpulse angular velocity is not zero and the box will begin rotating. Now for the conundrum. Do we process the impulsive force at \mathcal{P}_1 next? Or should we run one time step of the differential equation solver first? Either way we have issues to consider. The impulsive force at \mathcal{P}_0 was used to change the state of the rigid body A. Point \mathcal{P}_1 was a collision point determined based on the previous state. If you were to run the differential equation solver first, it is quite possible that \mathcal{P}_1 would no longer be a collision point. In our example the angular velocity due to the impulse at \mathcal{P}_0 could rotate the corner at \mathcal{P}_1 up off the sloped plane, in which case we do not have to even consider that point. On the other hand, the angular velocity could cause that corner of the box to rotate through the plane, violating the nonpenetration constraint. To avoid this dilemma, perhaps we should process the impulse at \mathcal{P}_1 first. The dilemma here is that we just finished computing postimpulse velocities due to \mathcal{P}_0 . In order to retain a dependence on that point, you would most likely use the postimpulse velocities from \mathcal{P}_0 as preimpulse velocities for \mathcal{P}_1 . The relative position in body A is $\mathbf{r}_1 = \mathcal{P}_1 - \mathcal{X}_A$. Define $\mathbf{u}_1 = \mathbf{r}_1 \times \mathbf{N}$. The magnitude of the impulsive force and the postimpulse (post-postimpulse?) velocities are

$$f_1 = -\frac{2m_A \mathbf{N} \cdot \mathbf{v}_A^+}{1 + \mathbf{u}_1^T m_A J_A^{-1} \mathbf{u}_1}, \quad \mathbf{v}_A^{++} = \mathbf{v}_A^+ + (f_1 \mathbf{N}) / m_A, \quad \mathbf{w}_A^{++} = \mathbf{w}_A^+ + f_1 J_A^{-1} \mathbf{u}_1$$

It is not clear that this produces a reasonably correct physical response.

The simplest thing to do from an implementation perspective is to process a collision point and change the state of the rigid bodies sharing that point, the changes based on the impulsive force introduced at the point, then run the differential equation solver for one time step. Next, the collision detection system is enabled. If an interpenetration has occurred, rerun the differential equation solver using a smaller time step. Repeat until no interpenetrations occur or until a maximum number of iterations has occurred.

The latter constraint is necessary because it is quite possible that interpenetration occurs for any increase in time. In this case great care must be taken about how to proceed. You will need a system that can decide if motion is possible and, if so, what that motion is. This is where even commercial packages can run into problems. Getting a generic system to work in all cases is more of an art than a science. Invariably, you will need to use knowledge of the types of objects you have and the environment in which they are interacting in order to adapt the generic system for your application. A more complicated solution is to process the points simultaneously. In our example of a box colliding with a plane, let us make the problem even more general and determine how

to introduce an impulsive force that applies to the entire edge of intersection rather than just to endpoints of the edge.

Our approach requires a better understanding of delta functions, introduced in [Example 6.2](#). The delta function of that example was motivated as the limit of a function as a parameter ε was decreased to zero. [Equation \(6.78\)](#) shows the *selection property* of a delta function; integrating a function $g(t)$ against a delta function selects the function value $g(t_0)$, where t_0 is the discontinuity of the delta function. As shown in that example, the selection is for the time variable. Delta functions can be defined to select spatial variables as well.

EXAMPLE
6.4

Define the function $u(x, y, \eta, \varepsilon) = 1/(4\eta\varepsilon)$ for $|x| \leq \eta$ and $|y| \leq \varepsilon$, but zero otherwise, for $\eta > 0$ and $\varepsilon > 0$. The volume of the region bounded by the graph of $u(x, y, \eta, \varepsilon)$ and the xy -plane is 1 regardless of the choice of ε . For any continuous function $g(x, y)$, define the functions $\phi(x, y)$ and $\psi(y)$ so that $\partial\phi/\partial x = g(x, y)$ and $d\psi/dy = g(0, y)$. Consider the integral

$$I(\eta, \varepsilon) = \int_{\mathbb{R}^2} g(x, y) u(x, y, \eta, \varepsilon) dx dy = \int_{-\varepsilon}^{\varepsilon} \int_{-\eta}^{\eta} \frac{g(x, y)}{4\eta\varepsilon} dx dy$$

We may compute the limits of $I(\eta, \varepsilon)$ as η and ε approach zero. This is done informally here (with apologies to mathematicians who cringe at swapping the order of limit and integration without justification):

$$\begin{aligned} \lim_{\varepsilon \rightarrow 0} \lim_{\eta \rightarrow 0} I(\eta, \varepsilon) &= \lim_{\varepsilon \rightarrow 0} \lim_{\eta \rightarrow 0} \int_{-\varepsilon}^{\varepsilon} \int_{-\eta}^{\eta} \frac{g(x, y)}{4\eta\varepsilon} dx dy \\ &= \lim_{\varepsilon \rightarrow 0} \lim_{\eta \rightarrow 0} \int_{-\varepsilon}^{\varepsilon} \frac{\phi(\eta, y) - \phi(-\eta, y)}{4\eta\varepsilon} dy \quad \text{Definition of } \phi \\ &= \lim_{\varepsilon \rightarrow 0} \int_{-\varepsilon}^{\varepsilon} \lim_{\eta \rightarrow 0} \frac{\phi(\eta, y) - \phi(-\eta, y)}{4\eta\varepsilon} dy \quad \text{Swap limit, integration} \\ &= \lim_{\varepsilon \rightarrow 0} \int_{-\varepsilon}^{\varepsilon} \lim_{\eta \rightarrow 0} \frac{g(\eta, y) + g(-\eta, y)}{4\varepsilon} dy \quad \text{l'Hôpital's rule} \\ &= \lim_{\varepsilon \rightarrow 0} \int_{-\varepsilon}^{\varepsilon} \frac{g(0, y)}{2\varepsilon} dy \\ &= \lim_{\varepsilon \rightarrow 0} \frac{\psi(\varepsilon) - \psi(-\varepsilon)}{2\varepsilon} \quad \text{Definition of } \psi \\ &= \lim_{\varepsilon \rightarrow 0} \frac{g(0, \varepsilon) + g(0, -\varepsilon)}{2} \quad \text{l'Hôpital's rule} \\ &= g(0, 0) \end{aligned}$$

(Example 6.4
continued)

If we informally think of $\delta(x, y)$ as the limit of $u(x, y, \eta, \varepsilon)$ when η and ε goes to zero, we have the selection property

$$\begin{aligned} & \int_{y_1}^{y_2} \int_{x_1}^{x_2} g(x, y) \delta(x - x_0, y - y_0) dx dy \\ &= \begin{cases} g(x_0, y_0), & x_1 \leq x_0 \leq x_2, y_1 \leq y_0 \leq y_2 \\ 0 & \text{Otherwise} \end{cases} \end{aligned} \quad (6.87)$$

This is a two-dimensional analog of [equation \(6.78\)](#). ■

We can use the last example to formulate the impulse function at a single point of contact. The example showed the selection for a scalar function of two spatial variables, but the idea clearly extends to vector-valued functions of three spatial variables. The impulse occurs at a spatial point \mathcal{P}_0 and at a time t_0 , so the function may be defined using the selection property of the delta function, both in time and space. The function to which the selection is applied is $\mathbf{G}(\mathcal{X}, t) = f\mathbf{N}_0$, a constant in space and time. The formulation below is a bit loose with the mathematical notation so as not to cloud the issue with facts:

$$\begin{aligned} \mathbf{F} &= \iint_{\mathcal{X} \times t} \mathbf{G}(\mathcal{X}, t) \delta(t - t_0) \delta(\mathcal{X} - \mathcal{P}_0) d\mathcal{X} dt \\ &= \int_{\mathcal{X}} \mathbf{G}(\mathcal{X}, t_0) \delta(\mathcal{X} - \mathcal{P}_0) d\mathcal{X} \\ &= \mathbf{G}(\mathcal{P}_0, t_0) \\ &= f\mathbf{N}_0 \end{aligned}$$

Yet one more variation of the delta function is needed to handle the case of colliding contact of a box edge with the sloped plane.

EXAMPLE
6.5

Define $u(x, y, \varepsilon) = 1/(4\varepsilon)$ for $|x| \leq 1$ and $|y| \leq \varepsilon$, but zero otherwise, for $\varepsilon > 0$. The volume of the region bounded by the graph of $u(x, y, \varepsilon)$ and the xy -plane is 1 regardless of the choice of ε . For any continuous function $g(x, y)$, define the function $\phi(x, y)$ so that $\partial\phi/\partial y = g(x, y)$. Consider the integral,

$$I(\varepsilon) = \iint_{\mathbb{R}^2} g(x, y) u(x, y, \varepsilon) dy dx = \int_{-1}^1 \int_{-\varepsilon}^{\varepsilon} \frac{g(x, y)}{4\varepsilon} dy dx$$

We may compute the limit of $I(\varepsilon)$ as ε approaches zero. This is again done informally:

$$\begin{aligned}
 \lim_{\varepsilon \rightarrow 0} I(\varepsilon) &= \lim_{\varepsilon \rightarrow 0} \int_{-1-\varepsilon}^1 \int_{-\varepsilon}^{\varepsilon} \frac{g(x, y)}{4\varepsilon} dy dx \\
 &= \lim_{\varepsilon \rightarrow 0} \int_{-1}^1 \frac{\phi(x, \varepsilon) - \phi(x, -\varepsilon)}{4\varepsilon} dx \quad \text{Definition of } \phi \\
 &= \int_{-1}^1 \lim_{\varepsilon \rightarrow 0} \frac{\phi(x, \varepsilon) - \phi(x, -\varepsilon)}{4\varepsilon} dx \quad \text{Swap limit, integration} \\
 &= \int_{-1}^1 \lim_{\varepsilon \rightarrow 0} \frac{g(x, \varepsilon) + g(x, -\varepsilon)}{4} dx \quad \text{l'Hôpital's rule} \\
 &= (1/2) \int_{-1}^1 g(x, 0) dx
 \end{aligned}$$

You might have noticed that the right-hand side is the average value (in the integral sense of calculus) of $g(x, 0)$ over the line segment $(x, 0)$ for $|x| \leq 1$. Informally, $\int_{-1}^1 g(x, 0) dx$ “adds” up all the g values along the segment. The “total number of values” that are added is the length of the interval, in our case 2. The average is just the ratio of the these two numbers.

Informally, the delta function that is obtained by letting ε approach zero in $u(x, y, \varepsilon)$ has the *averaging property* rather than a selection property. The integral of $g(x, y)$ against the delta function produces the average value of g on the line segment connecting $(-1, 0)$ and $(1, 0)$. ■

Using some more informal notation, let S denote a line segment in space. Let $\mathbf{G}(\mathcal{X})$ be a vector-valued function of the spatial variable \mathcal{X} . Let $\delta(\mathcal{X}, S)$ denote the type of delta function we constructed in the last example. This delta function has the *averaging property*,

$$\int_{\mathcal{X}} \mathbf{G}(\mathcal{X}) \delta(\mathcal{X}, S) d\mathcal{X} = \frac{\int_{\mathcal{X} \in S} \mathbf{G}(\mathcal{X}) dS}{\int_{\mathcal{X} \in S} dS} = \frac{\int_{\mathcal{X} \in S} \mathbf{G}(\mathcal{X}) dS}{\text{Length}(S)} \quad (6.88)$$

Now we can address the problem of computing an impulsive force when the contact set is a line segment (the box edge in our example). Let f be a to-be-determined scalar constant, and let \mathbf{N} be the outward unit-length normal to the sloped plane. Let the edge have endpoints \mathcal{P}_0 and \mathcal{P}_1 . The edge is denoted by S and has an arc-length parameterization $(1 - s/\ell)\mathcal{P}_0 + (s/\ell)\mathcal{P}_1$ for $s \in [0, \ell]$, where $\ell = |\mathcal{P}_1 - \mathcal{P}_0|$.

The update of the linear velocity for body A is

$$\begin{aligned}
 \mathbf{v}_A^+ &= \mathbf{v}_A^- + m_A^{-1} \iint_{\mathcal{X} t} f \mathbf{N} \delta(t - t_0) \delta(\mathcal{X}, S) dt d\mathcal{X} \\
 &= \mathbf{v}_A^- + m_A^{-1} \int_{\mathcal{X}} f \mathbf{N} \delta(\mathcal{X}, S) d\mathcal{X} \\
 &= \mathbf{v}_A^- + m_A^{-1} \ell^{-1} \int_{\mathcal{X} \in S} f \mathbf{N} dS \\
 &= \mathbf{v}_A^- + m_A^{-1} \ell^{-1} (\ell f \mathbf{N}) \\
 &= \mathbf{v}_A^- + m_A^{-1} f \mathbf{N}
 \end{aligned} \tag{6.89}$$

The update of the linear velocity for body B is

$$\mathbf{v}_B^+ = \mathbf{v}_B^- - m_B^{-1} f \mathbf{N} \tag{6.90}$$

The update of the angular velocity for body A is

$$\begin{aligned}
 \mathbf{w}_A^+ &= \mathbf{w}_A^- + J_A^{-1} \iint_{\mathcal{X} t} \mathbf{r}_A(\mathcal{X}, t) \times f \mathbf{N} \delta(t - t_0) \delta(\mathcal{X}, S) dt d\mathcal{X} \\
 &= \mathbf{w}_A^- + J_A^{-1} \int_{\mathcal{X}} \mathbf{r}_A(\mathcal{X}, t_0) \times f \mathbf{N} \delta(\mathcal{X}, S) d\mathcal{X} \\
 &= \mathbf{w}_A^- + J_A^{-1} \ell^{-1} \int_{\mathcal{X} \in S} \mathbf{r}_A(\mathcal{X}, t_0) \times f \mathbf{N} dS \\
 &= \mathbf{w}_A^- + J_A^{-1} \ell^{-1} \left(\int_{\mathcal{X} \in S} \mathbf{r}_A(\mathcal{X}, t_0) dS \right) \times f \mathbf{N} \\
 &= \mathbf{w}_A^- + J_A^{-1} \ell^{-1} \left(\int_0^\ell (1 - s/\ell) \mathcal{P}_0 + (s/\ell) \mathcal{P}_1 - \mathcal{X}_A ds \right) \times f \mathbf{N} \\
 &= \mathbf{w}_A^- + J_A^{-1} ((\mathcal{P}_0 + \mathcal{P}_1)/2 - \mathcal{X}_A) \times f \mathbf{N} \\
 &= \mathbf{w}_A^- + J_A^{-1} \mathbf{r}_A(\mathcal{M}, t_0) \times f \mathbf{N}
 \end{aligned} \tag{6.91}$$

where $\mathcal{M} = (\mathcal{P}_0 + \mathcal{P}_1)/2$. The update of the angular velocity for body B is

$$\mathbf{w}_B^+ = \mathbf{w}_B^- - J_A^{-1} \mathbf{r}_A(\mathcal{M}, t_0) \times f \mathbf{N} \tag{6.92}$$

The update formulas for the angular velocities have a physically intuitive appeal. The torque applied to the line segment shows up as a torque applied to the center of mass of the line segment. The construction of [equation \(6.86\)](#) from [equations \(6.79\)](#) through

(6.85) is still valid for the line segment of contact, but applied to the midpoint. The magnitude of the impulse is therefore,

$$f = \frac{-(1+\varepsilon)(\mathbf{N} \cdot (\mathbf{v}_A^- - \mathbf{v}_B^-) + (\mathbf{w}_A^- \cdot (\mathbf{r}_A \times \mathbf{N}) - \mathbf{w}_B^- \cdot (\mathbf{r}_B \times \mathbf{N})))}{m_A^{-1} + m_B^{-1} + (\mathbf{r}_A \times \mathbf{N})^T J_A^{-1}(\mathbf{r}_A \times \mathbf{N}) + (\mathbf{r}_B \times \mathbf{N})^T J_B^{-1}(\mathbf{r}_B \times \mathbf{N})} \quad (6.93)$$

where $\mathbf{r}_A = \mathcal{M} - \mathcal{X}_A$ and $\mathbf{r}_B = \mathcal{M} - \mathcal{X}_B$.

EXERCISE
6.5

The collision system suggested in [Bar01] computes only a finite set of contact points (the reduced contact set; see Figure 6.43). If an edge of body A intersects a face of body B, only the endpoints of the edge, P_0 and P_1 , are stored by the system. Derive equations for the velocity updates and the impulse magnitude, analogous to equations (6.89) through (6.93), that correspond to applying an impulsive force simultaneously to the endpoints. (*Hint:* The delta function for a point and the delta function for a segment are limits of functions whose volumes are always 1.)

EXERCISE
6.6

Suppose your collision system computes the full set of intersection points for two colliding (but not interpenetrating) convex polyhedra. The set consists of either a single point, a line segment, or a convex polygon. We have seen how to compute an impulse force for a single point or for a line segment. If the intersection is a convex polygon, derive equations for the velocity updates and the impulse magnitude, analogous to equations (6.89) through (6.93).

Now suppose the collision system stores only the vertices of a convex polygon of intersection. Derive equations for the velocity updates and the impulse magnitude, analogous to equations (6.89) through (6.93), that correspond to applying an impulsive force simultaneously to the vertices. (*Hint:* Same as for Exercise 6.5.)

We finish the colliding contact discussion with an example that illustrates another problem with which a collision system must deal.

EXAMPLE
6.6

Consider a rectangle traveling downward and that intersects two other objects simultaneously. Figure 6.48 illustrates.

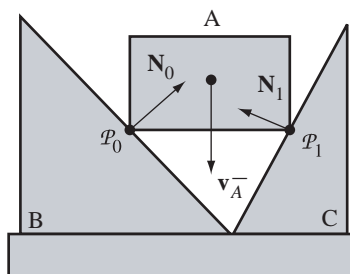


Figure 6.48

A rectangle travels downwards and intersects two objects simultaneously.

(Example 6.6
continued)

As shown in [Figure 6.48](#), body A intersects body B at \mathcal{P}_0 and body C at \mathcal{P}_1 . The outward unit-length normals at the contact points are \mathbf{N}_0 and \mathbf{N}_1 . The velocity of body A is $\mathbf{v}_A^- = (0, -\lambda)$ for $\lambda > 0$. The slope of the diagonal line of B is -1 and the slope of the diagonal line of C is 2 . As we saw in [Example 6.3](#), an impulsive force applied to \mathcal{P}_0 (with coefficient of restitution $\varepsilon = 1$) causes a postimpulse velocity

$$\begin{aligned}\mathbf{v}_A^+ &= \mathbf{v}_A^- + \frac{f_0 \mathbf{N}_0}{m_A} \\ &= \mathbf{v}_A^- - 2(\mathbf{N}_0 \cdot \mathbf{v}_A^-) \mathbf{N}_0 \\ &= (0, -\lambda) + (\lambda, \lambda) \\ &= (\lambda, 0)\end{aligned}$$

If we were to apply that impulse without considering the other contact point, body A tends to move to the right. It cannot because body C impedes the motion of body A in that direction. Similarly, if we apply the impulse at \mathcal{P}_1 , the postimpulse velocity is

$$\begin{aligned}\mathbf{v}_A^+ &= \mathbf{v}_A^- + \frac{f_1 \mathbf{N}_1}{m_A} \\ &= \mathbf{v}_A^- - 2(\mathbf{N}_1 \cdot \mathbf{v}_A^-) \mathbf{N}_1 \\ &= (0, -\lambda) + (-4\lambda/5, \lambda/5) \\ &= (-4\lambda/5, -3\lambda/5)\end{aligned}$$

Body B impedes the motion of body A in this direction. Applying simultaneous impulses (see [Exercise 6.5](#)), the postimpulse velocity is

$$\begin{aligned}\mathbf{v}_A^+ &= \mathbf{v}_A^- + \frac{f_0 \mathbf{N}_0 + f_1 \mathbf{N}_1}{2m_A} \\ &= (\lambda/10, -4\lambda/5)\end{aligned}$$

The implied motion is to the right and downward, in which case both bodies B and C impede the motion of A. So how do you handle this situation in a physically meaningful manner? Two choices are (1) require body A to stop, or (2) require body A to bounce upward.

If body A is very heavy compared to bodies B and C, the first choice is reasonable. The choice is also reasonable when you have a body that you want to collide with an immovable surface, and you want the body not to bounce at the instant of collision but to slide down the surface. The initial contact is colliding contact, but you want the component of velocity in the surface-normal direction set to zero rather than reflected as in the impulse approach. This is an instantaneous change from being a colliding contact to a resting contact. The body still has a nonzero velocity, but it is now orthogonal to the surface normal, so the body can slide along the surface.

If instead you want the body to bounce upward, you will need an algorithm to determine the new velocity of the center of mass of A. This might be as simple as

reversing the direction and choosing $\mathbf{v}_A^+ = -\mathbf{v}_A^-$. Of course, you also need to compute a new angular velocity \mathbf{w}_A^+ . If the slope of the diagonal edge for C were chosen to be 1, the symmetry of the contact would imply $\mathbf{w}_A^+ = \mathbf{0}$. With a slope of 2 as shown in Figure 6.48, your physical intuition says that body A should “slip downhill” a little bit more at \mathcal{P}_1 than at \mathcal{P}_0 . The normals at the contact points can be used to generate the angular velocity. For our current example, you might arbitrarily choose $\mathbf{w}_A^+ = \xi \mathbf{N}_0 \times \mathbf{N}_1$, where ξ is the x -component of $\mathbf{N}_0 + \mathbf{N}_1$. ■

Simultaneous Processing of Contact Points

Either choice in Example 6.6 appears to require feedback from the user or application about how to update the rigid body parameters when there are multiple colliding contact points for that body. In hopes that we can build a collision detection and response system that is completely automated, let us reconsider how impulse forces were chosen.

By definition, at a point of colliding contact the magnitude of the velocity in the normal direction at the point of contact is negative. Equation (6.75) provides us with a formula for the relative velocity. At the instant of contact, $\dot{d}(t_0) = \mathbf{N}_0 \cdot (\dot{\mathcal{P}}_A(t_0) - \dot{\mathcal{P}}_B(t_0))$, where \mathbf{N}_0 is the normal at the contact point \mathcal{P}_0 . The paths on bodies A and B for the points that meet at time t_0 are $\mathcal{P}_A(t)$ and $\mathcal{P}_B(t)$, with $\mathcal{P}_A(t_0) = \mathcal{P}_0 = \mathcal{P}_B(t_0)$. The relative velocity between the points on the path is $\dot{\mathcal{P}}_A(t) - \dot{\mathcal{P}}_B(t)$. The construction of impulse functions was based on two assumptions:

1. The points of colliding contact will be processed one at a time.
2. The relative velocity must be reflected through the contact normal using equation (6.85).

In light of Example 6.6, both of these assumptions create problems.

What we want physically is to avoid interpenetration of body A into body B when $\dot{d}(t_0) < 0$ is negative. To avoid the interpenetration, body B must exert a *contact force* C on body A at the point of contact. Such a force must satisfy four conditions:

1. C acts only at the instant of contact, not before and not later.
2. C must be a repulsive force. It cannot act like glue between the bodies.
3. C must prevent the interpenetration of the bodies.
4. The system cannot gain kinetic energy from the introduction of this contact force.

We postulate an impulsive force of the form $\mathbf{C} = f \mathbf{N}_0$ for some scalar $f \geq 0$ at the point of contact \mathcal{P}_0 . The use of an impulsive force satisfies condition 1. To satisfy condition 2, we need $f \geq 0$ so that the force repels the first body away from the second one.

Let us consider what condition 3 means at a single contact point such as the configuration of Example 6.3 (using a square or a rectangle). The pre- and postimpulse

velocities are related by [equation \(6.84\)](#), but with $m_B^{-1} = 0$, $J_B^{-1} = 0$, and $\dot{\mathcal{P}}_B = \mathcal{O}$:

$$\dot{\mathcal{P}}_A^+ - \mathcal{O} = (\dot{\mathcal{P}}_A^- - \mathcal{O}) + f \left(\frac{\mathbf{N}_0}{m_A} + (\mathbf{J}_A^{-1}(\mathbf{r}_A \times \mathbf{N}_0)) \times \mathbf{r}_A \right)$$

The normal component of the preimpulse world velocity is $\dot{d}^- = \mathbf{N}_0 \cdot (\dot{\mathcal{P}}_A^- - \mathcal{O})$ and the normal component of the postimpulse world velocity is $\dot{d}^+ = \mathbf{N}_0 \cdot (\dot{\mathcal{P}}_A^+ - \mathcal{O})$. Thus,

$$\dot{d}^+ = \dot{d}^- + f \left(m_A^{-1} + (\mathbf{r}_A \times \mathbf{N}_0)^T \mathbf{J}_A^{-1} (\mathbf{r}_A \times \mathbf{N}_0) \right) \quad (6.94)$$

If $\dot{d}^- \geq 0$, the bodies are separating so we may select $f = 0$ (no impulse), in which case $\dot{d}^+ = \dot{d}^-$ (no change in world velocity). If $\dot{d}^- < 0$, body A is trying to penetrate into body B. We must prevent this by choosing $f > 0$ large enough so that $\dot{d}^+ \geq 0$. If $f_0 > 0$ is chosen so that $\dot{d}^+ = 0$, we have met our constraint of nonpenetration. But any choice of $f > f_0$ leads to $\dot{d}^+ > 0$ and we still satisfy the constraint. The larger we choose f , the larger the impulse, and consequently the larger the magnitude of the normal component of the postimpulse velocity. An unwanted degree of freedom exists in the simplest of configurations.

This is where condition 4 comes into play. By choosing a sufficiently large value for f , we obtain a postimpulse value for \dot{d}^+ that exceeds $|\dot{d}^-|$, causing an increase in the kinetic energy of the system. We need to bound the postimpulse value so that the kinetic energy remains the same or even decreases; that is, the constraint $\dot{d}^+ \leq |\dot{d}^-|$ is required. We are still analyzing the case for $\dot{d}^- < 0$, so the constraint is $\dot{d}^+ \leq -\dot{d}^-$. Combining this with [equation \(6.94\)](#) we obtain

$$f \leq \frac{-2\dot{d}^-}{m_A^{-1} + (\mathbf{r}_A \times \mathbf{N}_0)^T \mathbf{J}_A^{-1} (\mathbf{r}_A \times \mathbf{N}_0)} = f_{\max} \quad (6.95)$$

where the last equality defines f_{\max} . This equation tells us that we need an impulsive force to generate a nonnegative postimpulse velocity $\dot{d}^+ \geq 0$, but the impulsive force cannot be too large. This limits our choice of f to a bounded interval $[0, f_{\max}]$, but we still have a degree of freedom to eliminate. We can do so by setting a goal for the postimpulse velocity to be as close as possible to the reflected preimpulse velocity while satisfying all the constraints of the system. In our special configuration of one contact point, we can choose $f = f_{\max}$ and the postimpulse velocity is the reflection of the preimpulse velocity, just as we saw in [Example 6.3](#).

Now for a slightly more complicated example, the multiple contact configuration of [Example 6.6](#). The impulse equation for linear velocity is

$$\mathbf{v}_A^+ = \mathbf{v}_A^- + \frac{f_0 \mathbf{N}_0 + f_1 \mathbf{N}_1}{m_A}$$

and the impulse equation for angular velocity is

$$\mathbf{w}_A^+ = \mathbf{w}_A^- + \mathbf{J}_A^{-1} (f_0 \mathbf{r}_0 \times \mathbf{N}_0 + f_1 \mathbf{r}_1 \times \mathbf{N}_1)$$

Define $\mathbf{r}_i = \mathcal{X}_A - \mathcal{P}_i$, where \mathcal{X}_A is the center of mass of body A and \mathcal{P}_i are the collision points, $i = 0, 1$. The outer normals at the collision points are \mathbf{N}_i . Bodies B and C are not moving. The preimpulse and postimpulse world velocities of body A are related by

$$\dot{\mathcal{P}}_A^+ - \mathcal{O} = (\dot{\mathcal{P}}_A^- - \mathcal{O}) + \sum_{i=0}^1 f_i \left(\frac{\mathbf{N}_i}{m_A} + (J_A^{-1}(\mathbf{r}_i \times \mathbf{N}_i)) \times \mathbf{r}_i \right)$$

The normal component of the preimpulse world velocity at the i th contact point is $\dot{d}_i^- = \mathbf{N}_i \cdot (\dot{\mathcal{P}}_i^- - \mathcal{O})$ and the normal component of the postimpulse world velocity is $\dot{d}_i^+ = \mathbf{N}_i \cdot (\dot{\mathcal{P}}_i^+ - \mathcal{O})$. Thus,

$$\begin{aligned}\dot{d}_0^+ &= \dot{d}_0^- + a_{00}f_0 + a_{01}f_1 \\ \dot{d}_1^+ &= \dot{d}_1^- + a_{10}f_0 + a_{11}f_1\end{aligned}$$

for appropriate constants a_{ij} . Our constraints to satisfy conditions 1, 2, and 3 are $f_i \geq 0$ and $\dot{d}_i^+ \geq 0$. Condition 4 may be satisfied by requiring $\dot{d}_i^+ \leq |\dot{d}_i^-|$.

As in the example of a single point of contact, we must analyze cases based on the signs of \dot{d}_i^- . Taking a hint from that example, let us set goals for what we want \dot{d}_i^+ to be. If $\dot{d}_0^- \geq 0$, our goal is $\dot{d}_0^+ = \dot{d}_0^-$. In the single-point example, we would choose $f_0 = 0$ to support the goal. This two-point example causes us to think twice about doing so. The choice for $f_0 = 0$ does not directly force the goal. Instead, we get $\dot{d}_0^+ = \dot{d}_0^- + a_{01}f_1$. Well, we can always then choose $f_1 = 0$ so that $\dot{d}_0^+ = \dot{d}_0^-$ as desired. Unfortunately the other postimpulse velocity equation becomes $\dot{d}_1^+ = \dot{d}_1^-$, which is a problem when $\dot{d}_1^- < 0$, the implication being that body A will penetrate body C. The two postimpulse velocity equations are coupled, causing us to obtain our goal not as “equality”; but “get as close as you can.”

More formally, if $\dot{d}_i^- \geq 0$, our goal for \dot{d}_i^+ is to make it as close to \dot{d}_i^- as possible while maintaining its nonnegativity. If $\dot{d}_i^- < 0$, our goal for \dot{d}_i^+ is to make it as close to $-\dot{d}_i^-$ as possible while maintaining its nonnegativity. We can achieve these goals in the sense of least squares, whereby we minimize the length of a vector rather than requiring the vector to be zero. Define:

$$b_i = \begin{cases} 0, & \dot{d}_i^- \geq 0 \\ 2\dot{d}_i^-, & \dot{d}_i^- < 0 \end{cases}$$

We want to choose (f_0, f_1) to make the length of the vector $(a_{00}f_0 + a_{01}f_1 + b_0, a_{10}f_0 + a_{11}f_1 + b_1)$ as small as possible. The minimization is constrained by $f_i \geq 0$ and $a_{i0}f_0 + a_{i1}f_1 + \dot{d}_i^- \geq 0$ for $i = 0, 1$. You should recognize this as a convex quadratic programming problem which we will discuss in Chapter 14.

Let us look at an even more complicated example and set up the general formulation for choosing the impulsive functions at all the contact points simultaneously.

EXAMPLE
6.7

Four rigid bodies with six points of contact are shown in Figure 6.49.

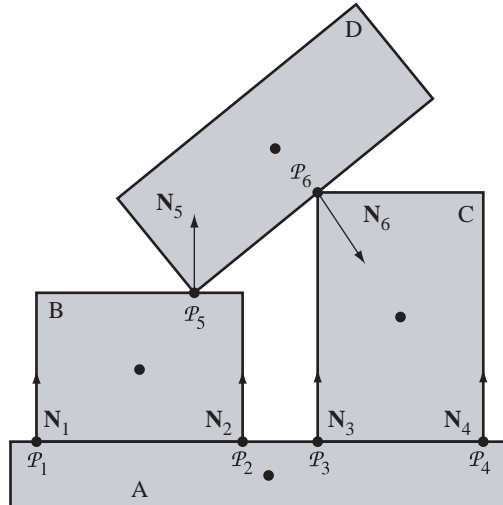


Figure 6.49

Four rigid bodies with six points of contact. The centers of mass of the four bodies are also shown.

It is irrelevant to us whether the contact points are colliding or resting. We require impulsive contact forces $\mathbf{C}_i = f_i \mathbf{N}_i$ for $1 \leq i \leq 6$. Using the same superscript notation as before for indicating preimpulse and postimpulse quantities, the simultaneous updates of the linear momenta of the centers of mass using the impulsive forces are

$$\begin{aligned} m_A \mathbf{v}_A^+ &= m_A \mathbf{v}_A^- - f_1 \mathbf{N}_1 - f_2 \mathbf{N}_2 - f_3 \mathbf{N}_3 - f_4 \mathbf{N}_4 \\ m_B \mathbf{v}_B^+ &= m_B \mathbf{v}_B^- + f_1 \mathbf{N}_1 + f_2 \mathbf{N}_2 - f_5 \mathbf{N}_5 \\ m_C \mathbf{v}_C^+ &= m_C \mathbf{v}_C^- + f_3 \mathbf{N}_3 + f_4 \mathbf{N}_4 + f_6 \mathbf{N}_6 \\ m_D \mathbf{v}_D^+ &= m_D \mathbf{v}_D^- + f_5 \mathbf{N}_5 - f_6 \mathbf{N}_6 \end{aligned}$$

The simultaneous updates of the angular momenta using the impulsive torques are

$$\begin{aligned} J_A \mathbf{w}_A^+ &= J_A \mathbf{w}_A^- - f_1 \mathbf{r}_A^1 \times \mathbf{N}_1 - f_2 \mathbf{r}_A^2 \times \mathbf{N}_2 - f_3 \mathbf{r}_A^1 \times \mathbf{N}_3 - f_4 \mathbf{r}_A^1 \times \mathbf{N}_4 \\ J_B \mathbf{w}_B^+ &= J_B \mathbf{w}_B^- + f_1 \mathbf{r}_B^1 \times \mathbf{N}_1 + f_2 \mathbf{r}_B^2 \times \mathbf{N}_2 - f_5 \mathbf{r}_B^5 \times \mathbf{N}_5 \\ J_C \mathbf{w}_C^+ &= J_C \mathbf{w}_C^- + f_3 \mathbf{r}_C^3 \times \mathbf{N}_3 + f_4 \mathbf{r}_C^4 \times \mathbf{N}_4 + f_6 \mathbf{r}_C^6 \times \mathbf{N}_6 \\ J_D \mathbf{w}_D^+ &= J_D \mathbf{w}_D^- + f_5 \mathbf{r}_D^5 \times \mathbf{N}_5 - f_6 \mathbf{r}_D^6 \times \mathbf{N}_6 \end{aligned}$$

where $\mathbf{r}_\gamma^i = \mathcal{P}_i - \mathcal{X}_\gamma$ for body γ and contact point i .

Each contact point leads to a relative velocity equation which we will index by i . For example, consider the contact point \mathcal{P}_1 involving bodies A and B. By our convention, the pair of bodies is ordered as (B, A) since a vertex of B intersects a face of A.

$$\begin{aligned}
\dot{d}_1^+ &= \mathbf{N}_1 \cdot ((\mathbf{v}_B^+ + \mathbf{w}_B^+ \times \mathbf{r}_B^1) - (\mathbf{v}_A^+ + \mathbf{w}_A^+ \times \mathbf{r}_A^1)) \\
&= \mathbf{N}_1 \cdot \left[m_B^{-1} (f_1 \mathbf{N}_1 + f_2 \mathbf{N}_2 - f_5 \mathbf{N}_5) \right. \\
&\quad + \left(J_B^{-1} (f_1 \mathbf{r}_B^1 \times \mathbf{N}_1 + f_2 \mathbf{r}_B^2 \times \mathbf{N}_2 - f_5 \mathbf{r}_B^5) \right) \times \mathbf{r}_B^1 \\
&\quad - m_A^{-1} (-f_1 \mathbf{N}_1 - f_2 \mathbf{N}_2 - f_3 \mathbf{N}_3 - f_4 \mathbf{N}_4) \\
&\quad \left. - \left(J_A^{-1} (-f_1 \mathbf{r}_A^1 \times \mathbf{N}_1 - f_2 \mathbf{r}_A^2 \times \mathbf{N}_2 - f_3 \mathbf{r}_A^3 \times \mathbf{N}_3 - f_4 \mathbf{r}_A^4 \times \mathbf{N}_4) \right) \times \mathbf{r}_A^1 \right] + \dot{d}_1^- \\
&= a_{11} f_1 + a_{12} f_2 + a_{13} f_3 + a_{14} f_4 + a_{15} f_5 + a_{16} f_6 + \dot{d}_1^-
\end{aligned}$$

where

$$\begin{aligned}
a_{11} &= \mathbf{N}_1 \cdot \left[\left(m_B^{-1} \mathbf{N}_1 + \left(J_B^{-1} (\mathbf{r}_B^1 \times \mathbf{N}_1) \right) \times \mathbf{r}_B^1 \right) - \left(-m_A^{-1} \mathbf{N}_1 - \left(J_A^{-1} (\mathbf{r}_A^1 \times \mathbf{N}_1) \right) \times \mathbf{r}_A^1 \right) \right] \\
a_{12} &= \mathbf{N}_1 \cdot \left[\left(m_B^{-1} \mathbf{N}_2 + \left(J_B^{-1} (\mathbf{r}_B^2 \times \mathbf{N}_2) \right) \times \mathbf{r}_B^1 \right) - \left(-m_A^{-1} \mathbf{N}_2 - \left(J_A^{-1} (\mathbf{r}_A^2 \times \mathbf{N}_2) \right) \times \mathbf{r}_A^1 \right) \right] \\
a_{13} &= \mathbf{N}_1 \cdot \left[(\mathbf{0}) - \left(-m_A^{-1} \mathbf{N}_3 - \left(J_A^{-1} (\mathbf{r}_A^3 \times \mathbf{N}_3) \right) \times \mathbf{r}_A^1 \right) \right] \\
a_{14} &= \mathbf{N}_1 \cdot \left[(\mathbf{0}) - \left(-m_A^{-1} \mathbf{N}_4 - \left(J_A^{-1} (\mathbf{r}_A^4 \times \mathbf{N}_4) \right) \times \mathbf{r}_A^1 \right) \right] \\
a_{15} &= \mathbf{N}_1 \cdot \left[\left(-m_B^{-1} \mathbf{N}_5 - \left(J_B^{-1} (\mathbf{r}_B^5 \times \mathbf{N}_5) \right) \times \mathbf{r}_B^1 \right) - (\mathbf{0}) \right] \\
a_{16} &= \mathbf{N}_1 \cdot [(\mathbf{0}) - (\mathbf{0})] \\
\dot{d}_1^- &= \mathbf{N}_1 \cdot [(\mathbf{v}_B^- + \mathbf{w}_B^- \times \mathbf{r}_B^1) - (\mathbf{v}_A^- + \mathbf{w}_A^- \times \mathbf{r}_A^1)]
\end{aligned}$$

These expressions were not simplified to be suggestive of the general formula and an algorithm to compute it. The simplest term to explain is $a_{16} = 0$. The two bodies sharing the contact point \mathcal{P}_1 are B and A. Point \mathcal{P}_6 is not part of either of these bodies, so the contact force $f_6 \mathbf{N}_6$ does not contribute to resolution at \mathcal{P}_1 . The term a_{12} has a couple of similar expressions, one involving values for body B, the other involving values for body A. The different subscripts B and A are one difference. The other difference is that the second expression has minus signs. This has to do with the fact that if the contact force on the first body is $\pm f \mathbf{N}$, then the contact force on the second body is $\mp f \mathbf{N}$ (reversed direction). Both expressions occur in a_{12} because \mathcal{P}_2 is also shared by bodies B and A. The second expression in the term a_{13} occurs because \mathcal{P}_3 is part of body A, thus indirectly affecting body B. However, the first expression is $\mathbf{0}$ because \mathcal{P}_3 is not a point of body B. Finally, a_{11} contains both expressions since \mathcal{P}_1 is shared by both bodies.

Similar expressions can be constructed for the other contact points to obtain $\dot{d}_i^+ = \sum_{j=1}^6 a_{ij} f_j + \dot{d}_i^-$ for $1 \leq i \leq 6$. ■

In the general case we have a collection of rigid bodies and n contact points \mathcal{P}_i for $1 \leq i \leq n$. The velocity at \mathcal{P}_i in the normal direction \mathbf{N}_i has magnitude

$$\dot{d}_i^+ = \sum_{i=1}^n a_{ij} f_j + \dot{d}_i^- \quad (6.96)$$

where the contact force at \mathcal{P}_i is $\pm f_i \mathbf{N}_i$, the sign chosen based on the body that is sharing the contact point. The general formula for the a_{ij} is listed next; the pair of bodies is (α, β) :

$$a_{ij} = \sigma_\alpha^{ij} \left(m_\alpha^{-1} \mathbf{N}_i \cdot \mathbf{N}_j + (\mathbf{r}_\alpha^i \times \mathbf{N}_i)^T J_\alpha^{-1} (\mathbf{r}_\alpha^j \times \mathbf{N}_j) \right) - \sigma_\beta^{ij} \left(m_\beta^{-1} \mathbf{N}_i \cdot \mathbf{N}_j + (\mathbf{r}_\beta^i \times \mathbf{N}_i)^T J_\beta^{-1} (\mathbf{r}_\beta^j \times \mathbf{N}_j) \right) \quad (6.97)$$

where σ_γ^{ij} is $+1$ when \mathcal{P}_j is in the body γ and the force direction is $+\mathbf{N}_j$, is -1 when \mathcal{P}_j is in the body γ and the force direction is $-\mathbf{N}_j$, or is 0 when \mathcal{P}_j is not in the body γ . Convince yourself from the physical situation that $a_{ji} = a_{ij}$; that is, the matrix $A = [a_{ij}]$ is symmetric. You can also verify this by direct manipulation of the general formula for the a_{ij} values. The preimpulse velocities are

$$\dot{d}_i^- = \mathbf{N}_i \cdot \left[(\mathbf{v}_\alpha^- + \mathbf{w}_\alpha^- \times \mathbf{r}_\alpha^i) - (\mathbf{v}_\beta^- + \mathbf{w}_\beta^- \times \mathbf{r}_\beta^i) \right] \quad (6.98)$$

Let us reformulate our conditions using vector and matrix notation. Let \mathbf{f} be the $n \times 1$ vector that stores the magnitudes of the impulsive forces. The magnitudes are nonnegative, a condition we may write succinctly as $\mathbf{f} \geq \mathbf{0}$. Let $\dot{\mathbf{d}}^-$ be the $n \times 1$ vector that stores the preimpulse velocities and let $\dot{\mathbf{d}}^+$ be the $n \times 1$ vector that stores the postimpulse velocities. To avoid interpenetrations we need $\dot{\mathbf{d}}^+ \geq \mathbf{0}$. Equation (6.96) is written as $\dot{\mathbf{d}}^+ = A\mathbf{f} + \dot{\mathbf{d}}^-$ where $A = [a_{ij}]$ is an $n \times n$ matrix. Define the $n \times 1$ vector \mathbf{b} to have i th component $b_i = 0$ if $\dot{d}_i^- \geq 0$ and $b_i = 2\dot{d}_i^-$ if $\dot{d}_i^- < 0$. Define the $n \times 1$ vector \mathbf{c} to have i th component $c_i = |\dot{d}_i^-|$.

The problem is abstracted to the following. We want to choose \mathbf{f} to minimize the convex quadratic function $|A\mathbf{f} + \mathbf{b}|^2$ subject to the constraints $\mathbf{f} \geq \mathbf{0}$ (forces are repulsive), $A\mathbf{f} + \mathbf{b} \geq \mathbf{0}$ (bodies cannot interpenetrate), and $A\mathbf{f} + \mathbf{b} \leq \mathbf{c}$ (kinetic energy cannot be gained via impulses). This is a convex quadratic programming problem that can be formulated as a linear complementarity problem (LCP) and solved using the Lemke algorithm of Chapter 14.

An illustrative implementation will be provided later in this chapter. For now it is sufficient to mention the general order of operations:

1. The collision detection system calculates all contact points for the current state of the rigid bodies.
2. The contact points and rigid body states are used to compute the matrix A and vector $\dot{\mathbf{d}}^-$.

3. The LCP solver computes \mathbf{f} and $\dot{\mathbf{d}}^+$. We are guaranteed of no interpenetration since $\dot{\mathbf{d}}^+ \geq \mathbf{0}$ is a postcondition of the LCP solver.
4. The postimpulse velocities are computed from \mathbf{f} and the normal vectors at the collision points. These velocities replace the preimpulse values in the rigid bodies.
5. The differential equation solver computes the new positions and orientations of the rigid bodies.
6. Repeat step 1.

This process will be modified when we take into account that some of the contact points are resting contact, as described in [Section 6.6.3](#).

EXERCISE 6.7

The postcondition of any system that instantaneously updates the linear and angular velocities for a collection of rigid bodies is that no instantaneous interpenetration can occur at any contact point. The original design of processing the colliding points sequentially does not satisfy this postcondition (see [Example 6.6](#)). The LCP-based method of this subsection does satisfy the postcondition. The sequential processing is conceptually simpler to implement. The LCP-based method requires a high-powered piece of software that is difficult to implement (robustly). Is there a middle ground?

Explore the following two concepts (mentally or programmatically, whatever):

1. In sequential processing, postimpulse velocities at a contact point shared by two bodies is computed, call them \mathbf{v}_A^+ and \mathbf{v}_B^+ . Before actually updating the rigid body states, determine if the new velocity is consistent with the postcondition. That is, if body A has contact points \mathcal{P}_i and contact normals \mathbf{N}_i for $1 \leq i \leq n$, and if body B has contact points \mathcal{Q}_j and contact normals \mathbf{M}_j for $1 \leq j \leq m$, compute the values $\alpha_i = \mathbf{N}_i \cdot \mathbf{v}_A^+$ and $\beta_j = \mathbf{M}_j \cdot \mathbf{v}_B^+$. If $\alpha_i \geq 0$ for all i and $\beta_j \geq 0$ for all j , then the postcondition is satisfied. If satisfied, update the rigid body states for these two bodies, call the differential equation solver, and proceed as usual. If not satisfied, repeat the process on the next contact point. If the set of current contact points becomes empty because the postcondition was never satisfied, set the new velocities to be zero.
2. In simultaneous processing, iterate over the rigid bodies. For a body A, let \mathcal{P}_i be the contact points contained by that body and let \mathbf{N}_i be the contact normals, $1 \leq i \leq n$. Assume that any body B that shares a contact point with A is at rest. Construct vectors \mathbf{v}^+ and \mathbf{w}^+ using impulsive forces so that if body A is updated with these velocities, no interpenetration can occur with any neighboring body B. If at least one of these velocities is nonzero, update the state of body A, call the differential equation solver, and proceed as usual. If both velocities are forced to be zero, repeat the process on the next rigid body.

Both concepts require that your collision detection system support a query whose input is a rigid body and whose output is the set of current contact points and normals for that body.

6.6.3 COLLISION RESPONSE FOR RESTING CONTACT

If two rigid bodies A and B are in contact at time t_0 at a point \mathcal{P}_0 , and if \mathbf{N}_0 is an outward, unit-length normal for body B, we distinguish between colliding contact, resting contact, or separation based on the normal component of the velocity of body A relative to body B. [Equation \(6.74\)](#) provides us with the function $d(t)$, a measure of signed distance between the two body points $\mathcal{P}_A(t)$ and $\mathcal{P}_B(t)$ that meet at \mathcal{P}_0 at time t_0 . By the definition, $d(t_0) = 0$. The relative velocity has a normal component given by [equation \(6.75\)](#). That component is $\dot{d}(t)$. A contact point is a colliding contact when $\dot{d}(t_0) < 0$ (body A moves into body B), a separation contact when $\dot{d}(t_0) > 0$ (body A moves away from body B), or a resting contact when $\dot{d}(t_0) = 0$. The latter case is the one we now analyze.

At a resting contact \mathcal{P}_0 the distance and relative velocity are zero. If body A has an acceleration $a\mathbf{N}_0$ relative to body B at \mathcal{P}_0 with $a < 0$, body A is attempting to accelerate into body B at the instant of contact. Clearly, we need to measure the relative acceleration to determine if this situation occurs. The relative acceleration is provided by the time derivative $\ddot{d}(t)$, which we can compute by differentiating [equation \(6.75\)](#):

$$\ddot{d}(t) = \mathbf{N}(t) \cdot (\ddot{\mathcal{P}}_A(t) - \ddot{\mathcal{P}}_B(t)) + 2\dot{\mathbf{N}}(t) \cdot (\dot{\mathcal{P}}_A(t) - \dot{\mathcal{P}}_B(t)) + \ddot{\mathbf{N}} \cdot (\mathcal{P}_A(t) - \mathcal{P}_B(t)) \quad (6.99)$$

At the time of contact, $\ddot{d}(t_0) = \mathbf{N}_0 \cdot (\ddot{\mathcal{P}}_A(t_0) - \ddot{\mathcal{P}}_B(t_0)) + 2\dot{\mathbf{N}}(t_0) \cdot (\dot{\mathcal{P}}_A(t_0) - \dot{\mathcal{P}}_B(t_0))$, where the last term of [equation \(6.99\)](#) is zero since $\mathcal{P}_A(t_0) = \mathcal{P}_0 = \mathcal{P}_B(t_0)$. In order to compute the relative acceleration, we need a formula for the normal $\mathbf{N}(t)$ so that we can compute the first derivative and evaluate $\dot{\mathbf{N}}(t_0)$. We have two cases to consider. The first case is for a vertex–face intersection, where $\mathbf{N}(t_0)$ is the face normal of body B. [Equation \(2.42\)](#) tells us how a vector quantity changes in the world coordinate system of a body. The normal vector derivative for this case is

$$\dot{\mathbf{N}}(t) = \mathbf{w}_B(t) \times \mathbf{N}(t) \quad (6.100)$$

where $D\mathbf{N}/Dt = \mathbf{0}$ since the body is rigid. The angular velocity of body B is used since the normal rotates with B. The second case is for an edge–edge intersection, where the normal is formed by taking the cross product of an edge of A and an edge of B, then normalized. Since each edge rotates due to the angular velocity of its respective body, the normal derivative is more complicated to compute. As a function of time the normal is $\mathbf{N}(t) = \mathbf{E}_A(t) \times \mathbf{E}_B(t)/L(t)$ with $L(t) = |\mathbf{E}_A(t) \times \mathbf{E}_B(t)|$. Using the product and quotient rules from vector calculus, the derivative is

$$\dot{\mathbf{N}} = \frac{L(\mathbf{E}_A \times \dot{\mathbf{E}}_B + \dot{\mathbf{E}}_A \times \mathbf{E}_B) - \dot{L}(\mathbf{E}_A \times \mathbf{E}_B)}{L^2} = \frac{\mathbf{E}_A \times \dot{\mathbf{E}}_B + \dot{\mathbf{E}}_A \times \mathbf{E}_B - \dot{L}\mathbf{N}}{L}$$

Now since $L^2 = (\mathbf{E}_A \times \mathbf{E}_B) \cdot (\mathbf{E}_A \times \mathbf{E}_B)$, its derivative is $2L\dot{L} = 2(\mathbf{E}_A \times \mathbf{E}_B) \cdot (\dot{\mathbf{E}}_A \times \mathbf{E}_B + \mathbf{E}_A \times \dot{\mathbf{E}}_B)$, in which case

$$\dot{L} = (\mathbf{E}_A \times \dot{\mathbf{E}}_B + \dot{\mathbf{E}}_A \times \mathbf{E}_B) \cdot \mathbf{N}$$

Using equation (2.42), the edge derivatives are $\dot{\mathbf{E}}_A = \mathbf{w}_A \times \mathbf{E}_A$ and $\dot{\mathbf{E}}_B = \mathbf{w}_B \times \mathbf{E}_B$. Combining all these steps produces

$$\mathbf{U} = \mathbf{E}_A \times (\mathbf{w}_B \times \mathbf{E}_B) + (\mathbf{w}_A \times \mathbf{E}_A) \times \mathbf{E}_B, \quad \dot{\mathbf{N}} = \frac{\mathbf{U} - (\mathbf{U} \cdot \mathbf{N})\mathbf{N}}{L} \quad (6.101)$$

An implementation for computing the normal derivative acts on whether the contact point is a vertex–face or an edge–edge intersection and uses either equation (6.100) or equation (6.101), accordingly.

We also need to compute $\dot{\mathcal{P}}_A(t) - \dot{\mathcal{P}}_B(t)$ and $\ddot{\mathcal{P}}_A(t) - \ddot{\mathcal{P}}_B(t)$. These follow from an application of equations (2.43) and (2.44), the latter equation containing linear acceleration terms with $\dot{\mathbf{v}} = \mathbf{a}$ and angular acceleration terms that can be evaluated using equation (2.90), $\dot{\mathbf{w}} = J^{-1}(\boldsymbol{\tau} - \mathbf{w} \times J\mathbf{w})$. The final formula for the relative acceleration at the point and time of contact is

$$\begin{aligned} \ddot{d}(t_0) &= \mathbf{N}_0 \cdot ((\dot{\mathbf{v}}_A + \dot{\mathbf{w}}_A \times \mathbf{r}_A + \mathbf{w}_A \times (\mathbf{w}_A \times \mathbf{r}_A)) \\ &\quad - (\dot{\mathbf{v}}_B + \dot{\mathbf{w}}_B \times \mathbf{r}_B + \mathbf{w}_B \times (\mathbf{w}_B \times \mathbf{r}_B))) \\ &\quad + 2(\mathbf{w}_B \times \mathbf{N}_0) \cdot ((\mathbf{v}_A + \mathbf{w}_A \times \mathbf{r}_A) - (\mathbf{v}_B + \mathbf{w}_B \times \mathbf{r}_B)) \\ &= \mathbf{N}_0 \cdot \left(\left(\mathbf{a}_A + \left(J_A^{-1} \boldsymbol{\tau}_A \right) \times \mathbf{r}_A \right) - \left(\mathbf{a}_B + \left(J_B^{-1} \boldsymbol{\tau}_B \right) \times \mathbf{r}_B \right) \right) + e \end{aligned} \quad (6.102)$$

where the second equality groups the acceleration and torque terms together for our later convenience. The term e contains all the remaining terms from the first equality, including those portions from the torque equation of the form $J^{-1}(\mathbf{w} \times J\mathbf{w})$.

To avoid the interpenetration of body A into body B when $\ddot{d}(t_0) < 0$, body B must exert a *contact force* \mathbf{C} on body A. Such a force must satisfy three conditions:

1. \mathbf{C} must prevent the interpenetration of the bodies.
2. \mathbf{C} must be a repulsive force. It cannot act like glue between the bodies.
3. \mathbf{C} must become zero when the bodies separate.

We postulate that $\mathbf{C} = g\mathbf{N}_0$ for some scalar $g \geq 0$ at the point of contact \mathcal{P}_0 . The value of g is chosen to satisfy condition 1. The nonnegativity of the magnitude g satisfies condition 2. To satisfy condition 3 we specify that $g\ddot{d}(t_0) = 0$. If the bodies separate an instant after the contact, we have $\ddot{d}(t_0 + \varepsilon) > 0$ and $g = 0$ is required. If $\ddot{d}(t_0) = 0$, the bodies are not separating, so the choice of g is irrelevant.

Just as for colliding contact, the contact force at a resting contact of a rigid body A has a contribution to changing the velocity of the center of mass, $gm_A^{-1}\mathbf{N}_0$, and a contribution to changing the angular velocity of the body about its center, $g(J_A^{-1}(\mathbf{r}_A \times \mathbf{N}_0)) \times \mathbf{r}_A$. The computation of contact forces must be done simultaneously for all points of contact, each point contributing terms of this type. We use Example 6.7 to illustrate, the same one that was used to illustrate computing impulse forces for the simultaneous handling of contact points.

EXAMPLE 6.8 Let \mathbf{F}_γ denote the external forces applied to body γ and let \mathbf{T}_γ denote the external torques applied to body γ . The external forces contribute to the linear acceleration of the centers of mass, and the external torques contribute to the angular acceleration of the bodies about their centers of mass. The postulated contact forces $g_i \mathbf{N}_i$ at the points of contact \mathcal{P}_i contribute as well. A quick glance at Figure 6.49 will convince you that the resolution of forces at the centers of mass produces

$$\begin{aligned} m_A \mathbf{a}_A &= -g_1 \mathbf{N}_1 - g_2 \mathbf{N}_2 - g_3 \mathbf{N}_3 - g_4 \mathbf{N}_4 + \mathbf{F}_A \\ m_B \mathbf{a}_B &= g_1 \mathbf{N}_1 + g_2 \mathbf{N}_2 - g_5 \mathbf{N}_5 + \mathbf{F}_B \\ m_C \mathbf{a}_C &= g_3 \mathbf{N}_3 + g_4 \mathbf{N}_4 + g_6 \mathbf{N}_6 + \mathbf{F}_C \\ m_D \mathbf{a}_D &= g_5 \mathbf{N}_5 - g_6 \mathbf{N}_6 + \mathbf{F}_D \end{aligned}$$

The torque resolution is

$$\begin{aligned} \boldsymbol{\tau}_A &= -g_1 \mathbf{r}_A^1 \times \mathbf{N}_1 - g_2 \mathbf{r}_A^2 \times \mathbf{N}_2 - g_3 \mathbf{r}_A^1 \times \mathbf{N}_3 - g_4 \mathbf{r}_A^4 \times \mathbf{N}_4 + \mathbf{T}_A \\ \boldsymbol{\tau}_B &= g_1 \mathbf{r}_B^1 \times \mathbf{N}_1 + g_2 \mathbf{r}_B^2 \times \mathbf{N}_2 - g_5 \mathbf{r}_B^5 \times \mathbf{N}_5 + \mathbf{T}_B \\ \boldsymbol{\tau}_C &= g_3 \mathbf{r}_C^3 \times \mathbf{N}_3 + g_4 \mathbf{r}_C^4 \times \mathbf{N}_4 + g_6 \mathbf{r}_C^6 \times \mathbf{N}_6 + \mathbf{T}_C \\ \boldsymbol{\tau}_D &= g_5 \mathbf{r}_D^5 \times \mathbf{N}_5 - g_6 \mathbf{r}_D^6 \times \mathbf{N}_6 + \mathbf{T}_D \end{aligned}$$

where $\mathbf{r}_\gamma^i = \mathcal{P}_i - \mathcal{X}_\gamma$ for body γ and contact point i .

Each contact point leads to a relative acceleration equation of the form in equation (6.102), so we will index those equations with i . In each equation the acceleration terms we grouped together can have their accelerations and torques replaced by the expressions we obtained in the resolution of forces. For example, consider the contact point \mathcal{P}_1 involving bodies A and B. By our convention, the pair of bodies is ordered as (B, A) , because a vertex of B intersects a face of A:

$$\begin{aligned} \ddot{\mathbf{d}}_1 &= \mathbf{N}_1 \cdot \left(\left(\mathbf{a}_B + \left(J_B^{-1} \boldsymbol{\tau}_B \right) \times \mathbf{r}_B^1 \right) - \left(\mathbf{a}_A + \left(J_A^{-1} \boldsymbol{\tau}_A \right) \times \mathbf{r}_A^1 \right) \right) + e_1 \\ &= \mathbf{N}_1 \cdot \left[m_B^{-1} (g_1 \mathbf{N}_1 + g_2 \mathbf{N}_2 - g_5 \mathbf{N}_5 + \mathbf{F}_B) \right. \\ &\quad \left. + \left(J_B^{-1} (g_1 \mathbf{r}_B^1 \times \mathbf{N}_1 + g_2 \mathbf{r}_B^2 \times \mathbf{N}_2 - g_5 \mathbf{r}_B^5 + \mathbf{T}_B) \right) \times \mathbf{r}_B^1 \right. \\ &\quad \left. - m_A^{-1} (-g_1 \mathbf{N}_1 - g_2 \mathbf{N}_2 - g_3 \mathbf{N}_3 - g_4 \mathbf{N}_4 + \mathbf{F}_A) \right. \\ &\quad \left. - \left(J_A^{-1} (-g_1 \mathbf{r}_A^1 \times \mathbf{N}_1 - g_2 \mathbf{r}_A^2 \times \mathbf{N}_2 - g_3 \mathbf{r}_A^3 \times \mathbf{N}_3 \right. \right. \\ &\quad \left. \left. - g_4 \mathbf{r}_A^4 \times \mathbf{N}_4 + \mathbf{T}_A) \right) \times \mathbf{r}_A^1 \right] + e_1 \\ &= a_{11} g_1 + a_{12} g_2 + a_{13} g_3 + a_{14} g_4 + a_{15} g_5 + a_{16} g_6 + b_1 \end{aligned}$$

where the a_{ij} are exactly the same as those computed in Example 6.7! The term b_1 is

$$b_1 = e_1 + \mathbf{N}_1 \cdot \left[\left(m_B^{-1} \mathbf{F}_B + \left(J_B^{-1} \mathbf{T}_B \right) \times \mathbf{r}_B^1 \right) - \left(m_A^{-1} \mathbf{F}_A + \left(J_A^{-1} \mathbf{T}_A \right) \times \mathbf{r}_A^1 \right) \right]$$

Similar expressions can be constructed for the other contact points to obtain $\ddot{d}_i = \sum_{j=1}^6 a_{ij}g_j + b_i$ for $1 \leq i \leq 6$. ■

In the general case we have a collection of rigid bodies and n contact points \mathcal{P}_i for $1 \leq i \leq n$. The acceleration at \mathcal{P}_i in the normal direction \mathbf{N}_i has magnitude

$$\ddot{d}_i = \sum_{j=1}^n a_{ij}g_j + b_i \quad (6.103)$$

where the a_{ij} are provided by [equation \(6.97\)](#). The general formula for the b_i is listed below:

$$b_i = e_i + \mathbf{N}_i \cdot \left[\left(m_\alpha^{-1} \mathbf{F}_\alpha + (J_\alpha^{-1} \mathbf{T}_\alpha) \times \mathbf{r}_\alpha^i \right) - \left(m_\beta^{-1} \mathbf{F}_\beta + (J_\beta^{-1} \mathbf{T}_\beta) \times \mathbf{r}_\beta^i \right) \right] \quad (6.104)$$

where

$$\begin{aligned} e_i &= \mathbf{N}_i \cdot \left[\left((J_\alpha^{-1} (\mathbf{L}_\alpha \times \mathbf{w}_\alpha)) \times \mathbf{r}_\alpha^i + \mathbf{w}_\alpha \times (\mathbf{w}_\alpha \times \mathbf{r}_\alpha^i) \right) \right. \\ &\quad \left. - \left((J_\beta^{-1} (\mathbf{L}_\beta \times \mathbf{w}_\beta)) \times \mathbf{r}_\beta^i + \mathbf{w}_\beta \times (\mathbf{w}_\beta \times \mathbf{r}_\beta^i) \right) \right] \\ &\quad + 2\dot{\mathbf{N}}_i \cdot \left[(\mathbf{v}_\alpha + \mathbf{w}_\alpha \times \mathbf{r}_\alpha^i) - (\mathbf{v}_\beta + \mathbf{w}_\beta \times \mathbf{r}_\beta^i) \right] \end{aligned} \quad (6.105)$$

and where \mathbf{F}_γ is the external force and \mathbf{T}_γ is the external torque on body γ . The quantity $\mathbf{L}_\gamma = J_\gamma \mathbf{w}_\gamma$ is the angular momentum of body γ .

We now know how to compute the accelerations \ddot{d}_i , given the contact forces. However, the original problem was to choose the contact forces to prevent interpenetration. Let us reformulate our conditions using vector and matrix notation. Let \mathbf{g} be the $n \times 1$ vector that stores the magnitudes of the contact forces. The magnitudes are all non-negative. We may write this succinctly as $\mathbf{g} \geq \mathbf{0}$, a shortcut for stating $g_i \geq 0$ for all i . Let $\ddot{\mathbf{d}}$ be the $n \times 1$ vector that stores the accelerations. To avoid interpenetrations we need $\ddot{\mathbf{d}} \geq \mathbf{0}$. If the bodies separate at resting contact point i an instant after the contact has occurred, we require that the contact force become zero. The mathematical formulation is $\ddot{d}_i g_i = 0$. In vector notation this is $\ddot{\mathbf{d}} \circ \mathbf{g} = \mathbf{0}$. Finally, [equation \(6.103\)](#) is written as $\ddot{\mathbf{d}} = A\mathbf{g} + \mathbf{b}$, where $A = [a_{ij}]$ is an $n \times n$ matrix and $\mathbf{b} = [b_i]$ is an $n \times 1$ vector.

In summary, given A and \mathbf{b} , we need to compute $\ddot{\mathbf{d}}$ and \mathbf{g} that satisfy $\ddot{\mathbf{d}} = A\mathbf{g} + \mathbf{b}$ subject to the constraints $\ddot{\mathbf{d}} \geq \mathbf{0}$ and $\mathbf{g} \geq \mathbf{0}$ and subject to the complementarity condition $\ddot{\mathbf{d}} \circ \mathbf{g} = \mathbf{0}$. This is a linear complementarity problem (LCP) which we discuss briefly in [Section 5.2.2](#) and cover in [Chapter 14](#) in more detail. In particular, it is of the form of [equation \(14.5\)](#) where M is our A , \mathbf{q} is our \mathbf{b} , \mathbf{w} is our $\ddot{\mathbf{d}}$, and \mathbf{z} is our \mathbf{g} .

The order of operations listed for handling colliding contact is modified to the following:

1. The collision detection system calculates all contact points for the current state of the rigid bodies.
2. The contact points and rigid body states are used to compute the matrix A , vector $\dot{\mathbf{d}}^-$, and vector \mathbf{b} .
3. The LCP solver computes \mathbf{f} and $\dot{\mathbf{d}}^+$ from the inputs A and $\dot{\mathbf{d}}^-$. The LCP solver computes \mathbf{g} and $\ddot{\mathbf{d}}$ from the inputs A and \mathbf{b} . We are guaranteed of no interpenetration since $\dot{\mathbf{d}}^+ \geq \mathbf{0}$ and $\ddot{\mathbf{d}} \geq \mathbf{0}$ are postconditions of the LCP solver.
4. The postimpulse velocities are computed from \mathbf{f} and the normal vectors at the collision points. These velocities replace the preimpulse values in the rigid bodies.
5. The resting contact forces involving the \mathbf{g} are included when computing the total forces and torques on the rigid bodies.
6. The differential equation solver computes the new positions and orientations of the rigid bodies.
7. Repeat step 1.

The next section expands on this.

6.6.4 AN ILLUSTRATIVE IMPLEMENTATION

The rigid bodies are convex polyhedral solids. We will assume the existence of a collision detection system that handles convex polyhedra. Section 6.4 provides details of such a system. The structure `RigidBodies` used earlier will also be used here. We need another structure for representing contact points:

```
struct Contact
{
    RigidBody A;           // body containing vertex
    RigidBody B;           // body containing face
    point P;               // contact point
    vector N;              // outward unit-length normal of face
    vector EA;              // edge from A
    vector EB;              // edge from B
    bool isVFCContact; // true if vertex-face, false if edge-edge
}
```

If the contact point is a vertex–face intersection, then \mathbf{N} is valid but the edges \mathbf{EA} and \mathbf{EB} are not. If the contact point is an edge–edge intersection, then all fields are valid. All point and vector quantities are assumed to be in world coordinates.

The highest level view of the physical simulation is listed below. It is assumed that the initialization of the rigid bodies results in no interpenetrations.

```

void DoSimulation ()
{
    // For the arrays, size() indicates the number of array
    // elements.

    array<RigidBody> body;
    for (i = 0; i < body.size(); ++i)
    {
        body[i].Initialize(<parameters>);
    }

    array<Contact> contact;

    double t = <your choice of initial time>;
    double dt = <your choice of time step>;

    while (application_running)
    {
        DoCollisionDetection(t,dt,body,contact);
        if (contact.size() > 0)
        {
            DoCollisionResponse(t,dt,body,contact);
        }

        t += dt;
    }
}

```

The function `DoCollisionDetection` removes all old contact points from the array `contact` before inserting new ones.

The collision response function is

```

void DoCollisionResponse (double t, double dt,
    array<RigidBody> body, array<Contact> contact)
{
    matrix A;
    vector preRelVel, postRelVel, impulseMag;
    vector restingB, relAcc, restingMag;

    ComputeLCPMatrix(contact,A);

    // guarantee no interpenetration by postRelVel >= 0
    ComputePreImpulseVelocity(contact,preRelVel);
    Minimize(A,preRelVel,postRelVel,impulseMag);
    DoImpulse(contact,impulseMag);

    // guarantee no interpenetration by relAcc >= 0
    ComputeRestingContactVector(contact,restingB);
}

```

```

    LCPSolver(A,restingB,relAcc,restingMag);
    DoMotion(t,dt,contact,restingMag,body);
}

// Minimize |A * f + b|^2 subject to f >= 0, c - b >= A * f >= -b.
// The i-th component of b is b[i] = 0 if dneg[i] >= 0 and
// b[i] = 2 * dneg[i] if dneg[i] < 0. The i-th component of
// c is c[i] = |dneg[i]|. The inputs are A and dneg. The
// outputs are dpos and f.
//
void Minimize (matrix A, vector dneg, vector& dpos, vector& f);

// The parameter names match those in the chapter discussing
// LCP. The input is the matrix M and vector q. The output
// is the vector w and the vector z.
//
void LCPSolver (matrix M, vector q, vector& w, vector& z);

```

The function `ComputeLCPMatrix` computes the matrix $A = [a_{ij}]$ whose entries are defined by [equation \(6.97\)](#).

```

void ComputeLCPMatrix (array<Contact> contact, matrix& A)
{
    for (i = 0; i < contact.size(); ++i)
    {
        Contact ci = contact[i];
        vector rANi = Cross(ci.P - ci.A.x,ci.N);
        vector rBNi = Cross(ci.P - ci.B.x,ci.N);

        for (j = 0; j < contact.size(); ++j)
        {
            Contact cj = contact[j];
            vector rANj = Cross(cj.P - cj.A.x,cj.N);
            vector rBNj = Cross(cj.P - cj.B.x,cj.N);

            A[i][j] = 0;

            if (ci.A == cj.A)
            {
                A[i][j] += ci.A.massinv * Dot(ci.N,cj.N);
                A[i][j] += Dot(rANi,ci.A.jinv * rANj);
            }
            else if (ci.A == cj.B)
            {
                A[i][j] -= ci.A.massinv * Dot(ci.N,cj.N);
                A[i][j] -= Dot(rANi,ci.A.jinv * rANj);
            }
        }
    }
}

```

```

    if (ci.B == cj.A)
    {
        A[i][j] -= ci.B.massinv * Dot(ci.N,cj.N);
        A[i][j] -= Dot(rBNi,ci.B.jinv * rBNj);
    }
    else if (ci.B == cj.B)
    {
        A[i][j] += ci.B.massinv * Dot(ci.N,cj.N);
        A[i][j] += Dot(rBNi,ci.B.jinv * rBNj);
    }
}
}

```

The function `ComputePreImpulseVelocity` computes the preimpulse velocities \dot{d}_i^- defined by equation (6.98).

```

void ComputePreImpulseVelocity (array<Contact> contact,
    vector& ddot)
{
    for (i = 0; i < contact.size(); ++i)
    {
        contact ci = contact[i];
        RigidBody A = ci.A;
        RigidBody B = ci.B;

        vector rAi = ci.P - A.x;
        vector rBi = ci.P - B.x;
        vector vela = A.v + Cross(A.w,rAi);
        vector velB = B.v + Cross(B.w,rBi);
        ddot[i] = Dot(ci.N,velA - velB);
    }
}

```

The function `ComputeRestingContactVector` computes the vector $\mathbf{b} = [b_i]$ defined by equation (6.104). The derivative of the normal vector is computed using equations (6.100) and (6.101).

```

void ComputeRestingContactVector (array<Contact> contact, vector& b)
{
    for (i = 0; i < contact.size(); ++i)
    {
        contact ci = contact[i];
        RigidBody A = ci.A, B = ci.B;

        // body A terms
        vector rAi = ci.P - ci.A.x;
        vector wAxrAi = Cross(A.w,rAi);
    }
}

```

```

vector At1 = A.massinv * A.force;
vector At2 = Cross(A.jinv * (A.torque + Cross(A.L,A.w)),rAi);
vector At3 = Cross(A.w,wAxrAi);
vector At4 = A.v + wAxrAi;

// body B terms
vector rBi = ci.P - ci.B.x;
vector wBxrBi = Cross(B.w,rBi);
vector Bt1 = B.massinv * B.force;
vector Bt2 = Cross(B.jinv * (B.torque + Cross(B.L,B.w)),rBi);
vector Bt3 = Cross(B.w,wBxrBi);
vector Bt4 = B.v + wBxrBi;

// compute the derivative of the contact normal
vector Ndot;
if (ci.isVFCContact)
{
    Ndot = Cross(B.w,ci.N);
}
else
{
    vector EAdot = Cross(A.w,ci.EA);
    vector EBdot = Cross(B.w,ci.EB);
    vector U = Cross(ci.EA,EBdot) + Cross(EAdot,ci.EB);
    Ndot = (U - Dot(U,ci.N) * ci.N) / Length(ci.N);
}

b[i] = Dot(ci.N,At1 + At2 + At3 - Bt1 - Bt2 - Bt3) +
       2*Dot(Ndot,At4 - Bt4);
}
}

```

The function `DoImpulse` has the responsibility of replacing the preimpulse linear and angular velocities by the postimpulse vectors. The motivation was given in [Example 6.7](#). That example shows that it suffices to iterate over the contacts and impulse magnitudes and incrementally update the velocities.

```

void DoImpulse (array<Contact> contact, vector f)
{
    for (i = 0; i < contact.size(); ++i)
    {
        contact ci = contact[i];

        // update linear/angular momentum
        vector impulse = f[i] * ci.N;
        ci.A.p += impulse;
    }
}

```

```

        ci.B.p -= impulse;
        ci.A.L += Cross(ci.P - ci.A.x, impulse);
        ci.B.L -= Cross(ci.P - ci.B.x, impulse);

        // compute linear/angular velocity
        ci.A.v = ci.A.massinv * ci.A.p;
        ci.B.v = ci.B.massinv * ci.B.p;
        ci.A.w = ci.A.jinv * ci.A.L;
        ci.B.w = ci.B.jinv * ci.B.L;
    }
}

```

Finally, the function `DoMotion` implements the differential equation solver. It also must incorporate the resting contact forces into the solver in addition to any externally applied forces. We used a Runge–Kutta method for solving the differential equations for unconstrained motion. This method uses multiple function evaluations and requires some careful programming to handle the forces and torques. The structure `RigidBody` in the illustrative implementation for unconstrained motion has two members, force and torque, that are intended to store the current externally applied force and torque at the current time of the simulation. To support solvers that use multiple function evaluations and to avoid the copying in the illustrative implementation, we designed a C++ class `RigidBody` that had function members for computing the external force and torque. Let us modify this class by adding two data members to store the current external force and torque in addition to having the force and torque function members. Moreover, we will add two data members to store the resting contact forces. Only the modified interface is shown:

```

class RigidBody
{
public:
    void AppendInternalForce (vector intForce)
    {
        m_internalForce += intForce;
    }

    void AppendInternalTorque (vector intTorque)
    {
        m_internalTorque += intTorque;
    }

protected:
    // external force/torque at current time of simulation
    vector m_externalForce, m_externalTorque;

    // Resting contact force/torque. Initially zero, changed by
    // simulator before call to ODE solver, ODE solver uses for

```

```

// motion of bodies, then reset to zero for next pass.
vector m_internalForce, m_internalTorque;

// force/torque functions (same as before)
Function m_force, m_torque;
};

```

The initialization of the rigid body objects must now include calling the force and torque member functions `m_force` and `m_torque` to initialize the data members `m_externalForce` and `m_externalTorque`. The member function `RigidBody::Update` must also be modified to support these changes. The old function had the following lines of code for the first step of the Runge–Kutta solver:

```

// A1 = G(t,S0), B1 = S0 + (dt / 2) * A1
:
vector A1DPDT = m_force(t,m_X,m_Q,m_P,m_L,m_R,m_V,m_W);
vector A1DLDT = m_torque(t,m_X,m_Q,m_P,m_L,m_R,m_V,m_W);
:

```

The force and torque evaluation are at the current time, but we are now storing those values in the rigid body itself. The new function replaces these lines by

```

// A1 = G(t,S0), B1 = S0 + (dt / 2) * A1
:
vector A1DPDT = m_externalForce + m_internalForce;
vector A1DLDT = m_externalTorque + m_internalTorque;
:
m_internalForce = 0;
m_internalTorque = 0;

// A2 = G(t + dt / 2,B1), B2 = S0 + (dt / 2) * A2
:
:

// A3 = G(t + dt / 2,B2), B3 = S0 + dt * A3
:
:

// A4 = G(t + dt,B3),
//      S1 = S0 + (dt / 6) * (A1 + 2 * A2 + 2 * A3 + A4)
:

```

The inclusion of the internal quantities takes into account that, just before the update function is called, the collision response system needs to set the internal quantities to support resting contact. After using the internal values for the first step, I have set them to zero. They are not used in steps two, three, or four because the time in those steps is later than the current time; separation potentially has occurred and the resting contact forces must become zero as specified in our analysis. However, it is possible that after the half-step in time, resting contact still exists, so you might want to use the internal force and torque terms in the later steps.

The dilemma is that we are now in the middle of running the differential equation solver. If we want more accurate information about contact after the first step, we would have to exit after the first step and rerun the other parts of the collision system to once again find out which intersections are resting contacts. By doing so, our solver is nothing more than an Euler's method and we suffer from its lack of robustness and stability. I chose to zero out the internal values for simplicity. You might very well experiment and rewrite the solver to use the internal values for all the steps. One last change must be made to the solver to maintain the invariant that the external force and torque members are those of the current simulation time. Two lines of code must be added to the end of `RigidBody::Update` after the fourth step is complete:

```
// A4 = G(t + dt,B3),
//     S1 = S0 + (dt / 6) * (A1 + 2 * A2 + 2 * A3 + A4)
//
Convert(m_Q,m_P,m_L,m_R,m_V,m_W);

// new lines to make force and torque correspond to new time t+dt
m_externalForce = m_force(tpdt,m_X,m_Q,m_P,m_L,m_R,m_V,m_W);
m_externalTorque = m_torque(tpdt,m_X,m_Q,m_P,m_L,m_R,m_V,m_W);

void DoMotion (double t, double dt, array<Contact> contact,
               vector g, array<RigidBody> body)
{
    // update internal force/torque
    for (i = 0; i < contact.size(); i++)
    {
        contact ci = contact[i];
        vector resting = g[i] * ci.N;
        ci.A.AppendInternalForce(resting);
        ci.A.AppendInternalTorque(Cross(ci.p - ci.A.x,resting));
        ci.B.AppendInternalForce(-resting);
        ci.B.AppendInternalTorque(-Cross(ci.p - ci.B.x,resting));
    }

    // update rigid bodies
    for (i = 0; i < body.size(); i++)
    {
        body[i].Update(t,dt);
    }
}
```

6.6.5 LAGRANGIAN DYNAMICS

The extensive system for constrained motion that we have studied so far is designed to be general. Other than requiring the rigid bodies to be modeled as convex polyhedra, no assumptions are made about how the environment might constrain the objects.

In fact, the main role of the collision detection system is to determine the constraints dynamically, then let the collision response system know what it has to work with. Such a general dynamics system is useful for many game applications but is not necessary for all situations arising in a game. Just as game designers will take into account the strengths and limitations of a graphics engine when deciding on the complexity of art content, they will also consider the strengths and limitations of a physics engine.

For example, automatic and efficient occlusion culling in a graphics engine is a difficult task to implement. Portal systems are particularly useful for limiting the depth complexity of an indoor scene while allowing the player to move in unconstrained ways. However, if a level is built in such a way that the player looks through a door (portal) of a room and can see through another door across the room, followed by a long path of visible doors of yet more adjacent rooms, the portal system performance can decrease quite rapidly. Yes, a general portal system is quite powerful, but it has its limitations. A level designer will arrange for such a configuration not to happen, knowing that the portal system is good for a couple of doors along the line of sight. Thus, the designer establishes the constraints during development time to keep the performance reasonable at runtime.

Careful consideration of how to build an environment to allow the physics engine to perform well is also called for. For example, suppose that a game requires a character to navigate through a room filled with boxes in order to reach an exit on the other side of the room. The environment is designed to make it challenging – no open path is available when the character enters the room. In order to reach the exit, boxes must be moved around, some of them easy to move, others too heavy to move. Moreover, the player must discover that some boxes need to be moved but that can happen only when they are pushed by other boxes; the other boxes block the path to ones that need to be moved. A general collision system can be used for this environment. Since the boxes are in resting contact with the floor, the system must compute the appropriate contact forces to keep the boxes from sinking through the floor. The collision detection system also spends a lot of time reporting that the boxes are intersecting the floor! No doubt we will want the floor to have friction. As commercial physics engine developers will remind you regularly, getting the general collision system to work correctly in the presence of static and dynamic friction is quite a difficult chore.

But we know that the boxes are on the floor and will remain so – that is our design. Let us take advantage of the fact that we know a constraint of the system at development time. What better way to take advantage of known constraints than by using Lagrangian dynamics? We covered this topic in extensive detail in [Section 3.2](#). At the end of that section we even derived the equations of motion for a box moving over a rough plane. And if you did your homework ([Exercise 3.31](#)), you are ready to test out the environment you just built! Well, not quite. We still have the dynamic situation of boxes being pushed by the character and colliding with other boxes. A collision detection system is still required, but even this system can be specialized for our environment.

Two of our boxes can collide only with edge–face or face–face contact. Although the general collision detection system can handle this as contact between 3D objects,

we can do better. If you view the boxes from above, they all appear as rectangles. The specialized collision detection system needs to work only in 2D. An edge–face intersection in 3D is detected as a vertex–edge intersection in 2D. A face–face intersection in 3D is detected as an edge–edge intersection in 2D. The Lagrangian equations of motion for this collection of boxes will involve only floor variables (x, y) but not the height variable z . The outline of how the system works is analogous to what the general system did, except that now we are working in only two dimensions.

There is a drawback to what I just described. The collision system is specifically written for this room (and similar rooms if you like). In the object-oriented approach, the general differential equation solver was built into the `RigidBody` class. In our Lagrangian setting, the equations of motion depend on the constraints. Moreover, our intent is that the constraints are known at development time. A general collision system is a reusable component, a good thing as any software engineer will tell you. The Lagrangian approach might very well lead to building a lot of components that are not reusable, thus increasing your development costs. Hopefully, the Lagrangian components you build, such as for a room of objects sitting on a floor, will be useful across levels and across games.

Can we find middle ground? That is, can we use Lagrangian dynamics even if our constraints change dynamically? I think so, but I believe such an engine will require a lot of thought be put into its design. To illustrate what I have in mind, consider a book on a table as shown in Figure 6.50.

The book can be pushed around the table, all the while using the Lagrangian equations of motion with the constraint that the center of mass of the book is a constant height above the table. If the book is pushed to the edge of the table and a small part of it extends past the edge, the book remains on the table, our constraint still applies, and the Lagrangian equations of motion remain as they are. However, if the book is pushed far enough past the table's edge, gravity will exert enough force to make the book start to fall off the table. The collision detection system is constantly reporting to us the polygon of intersection between the book and the table. This information is what we use to decide if the book rests on the table or if the area of intersection is small enough that torque causes the book to lift off the table and start to fall to the floor.

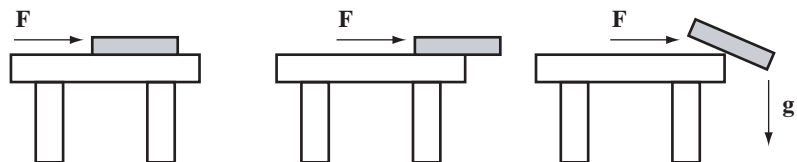


Figure 6.50 A book resting on a table. Forces applied to the book include only gravitational (force vertically downward) and those used to push the book around the table (force has only a horizontal component).

At the instant the book starts to fall, our constraint of constant height center of mass is invalid and we need a new set of equations of motion. The book will slide along the edge of the table while rotating about a line through its center of mass (the line perpendicular to the plane of the figure), constraints that might be difficult to dynamically convert to equations of motion. A physics engine that is a hybrid between the general collision system and a Lagrangian-based one appears to be called for. In our book-table example, once the book starts to fall, we enable the general system. Once the book strikes the floor and attains a resting position, we switch back to the Lagrangian-based engine.

I will leave the ideas at that. The development of an engine of this type is a challenge I pose to those of you who have the energy and desire to follow such a path!

6.7 VELOCITY-BASED CONSTRAINED MOTION

In this section I will describe velocity-based methods for the dynamics of particle systems and rigid body systems. The approach uses constraints for pairs of objects. The constraints are functions of position and orientation but not of linear and angular momentum. This makes the approach different from that of [Section 6.6](#).

The primary reference for this approach is [\[Cat05\]](#). One of the problems with the algorithm in [Section 6.6](#) is that the LCP solver is formulated to handle all the constraints simultaneously. The more rigid bodies in the system and the more contact points between them in a single physics tick, the more expensive it is to use a global LCP solver such as the Lemke algorithm. Effectively, the approach is NP-hard. [\[Cat05\]](#) discusses an iterative algorithm that handles each pair of colliding bodies one at a time has better performance. Catto points out the advantages of the algorithm, which include a more robust algorithm based on handling penetrations (the non penetration requirements for the impulse-based algorithm are difficult to make robust) and the ease of modeling and the uniformity of handling both joint and contact constraints.

The aforementioned paper talks about constraint forces, and the algorithm must explicitly compute them, both for equality and inequality constraints. I will first motivate the idea of computing constraint forces and the *principle of virtual work*, as discussed in [\[Wit97\]](#), and show how to extend these from a single particle to particle systems and rigid body systems.

6.7.1 CONSTRAINT ON A PARTICLE

This first part of this section analyzes the dynamics of a particle constrained to a surface. The second part analyzes the dynamics when the particle is constrained to a curve.

Particle Constrained to a Surface

Consider a single particle constrained to a surface defined implicitly by $C(\mathbf{x}) = 0$. The particle position is $\mathbf{x}(t)$, indicating that it varies with time. Thus,

$$C(\mathbf{x}(t)) = 0 \quad (6.106)$$

for all time t .

First Derivative of Constraint

The time derivative must also be equal to zero for all t , as shown next

$$0 = \dot{C}(\mathbf{x}(t)) = \nabla C \cdot \dot{\mathbf{x}} \quad (6.107)$$

where the dot over C denotes the first-order time derivative. The first-order spatial derivatives of C are stored in the 3×1 vector ∇C . The right-most equality is an application of the chain rule for differentiation. The dot over \mathbf{x} also denotes the time derivative, in which case $\dot{\mathbf{x}}$ is the velocity of the particle.

Second Derivative of Constraint

The second-order time derivative must as well be zero for all t ,

$$0 = \ddot{C}(\mathbf{x}(t)) = \nabla C \cdot \ddot{\mathbf{x}} + \dot{\mathbf{x}}^T \nabla \otimes \nabla C \dot{\mathbf{x}} \quad (6.108)$$

where the double dots over C denote the second-order time derivative. The double dots over \mathbf{x} also denote the second-order time derivative, in which case $\ddot{\mathbf{x}}$ is the acceleration of the particle. The term $\nabla \otimes \nabla C$ is the matrix of second-order spatial derivatives of C .

Equations of Motion

The external force applied to the particle is \mathbf{F} . This force most likely tries to move the particle off the surface, so a constraint force $\hat{\mathbf{F}}$ must prevent this. Newton's second law requires

$$m\ddot{\mathbf{x}} = \mathbf{F} + \hat{\mathbf{F}}$$

Substituting this into the equation (6.108) leads to

$$0 = \nabla C \cdot \left(\frac{\mathbf{F} + \hat{\mathbf{F}}}{m} \right) + \dot{\mathbf{x}}^T \nabla \otimes \nabla C \dot{\mathbf{x}} \quad (6.109)$$

which is one equation in the three unknown components of the constraint force.

Computing the Constraint Force

We have to provide information to eliminate the remaining two degrees of freedom in the constraint force. This is accomplished by appealing to the principle of virtual work: The constraint force cannot do work within the surface. This means the constraint force at a point on the surface has no component in any of the tangential directions at that point, which implies that the constraint force is normal to the surface. In fact, the velocity of the particle is a tangent vector, so the constraint force must be orthogonal to the velocity. The principle of virtual work makes sense in the following way. In the absence of external forces, if the constraint force were allowed to have a nonzero tangential component at a point, the constraint force would move a particle at the point along the surface, which is not an appealing physical consequence.

For implicitly defined surfaces, the gradient of the defining function is known to be normal to the surface. Thus, the constraining force is of the form

$$\hat{\mathbf{F}} = \lambda \nabla C \quad (6.110)$$

The scalar λ is a single degree of freedom. Substituting equation (6.110) into equation (6.109) leads to

$$\lambda = -\frac{\nabla C \cdot \mathbf{F} + m \dot{\mathbf{x}}^T \nabla \otimes \nabla C \dot{\mathbf{x}}}{|\nabla C|^2} \quad (6.111)$$

in which case the magnitude of the constraint force is $\lambda |\nabla C|$.

Particle Constrained to a Curve

The same ideas may be applied even when a particle is constrained to lie on a spatial curve. Assume that the curve is the intersection of two implicitly defined surfaces; that is, we have two constraints $C_0(\mathbf{x}) = 0$ and $C_1(\mathbf{x}) = 0$. Applying a construction similar to that for a surface,

$$\begin{aligned} 0 &= \nabla C_0 \cdot (\mathbf{F} + \hat{\mathbf{F}}) + m \dot{\mathbf{x}}^T \nabla \otimes \nabla C_0 \dot{\mathbf{x}} \\ 0 &= \nabla C_1 \cdot (\mathbf{F} + \hat{\mathbf{F}}) + m \dot{\mathbf{x}}^T \nabla \otimes \nabla C_1 \dot{\mathbf{x}} \end{aligned} \quad (6.112)$$

These are two equations in the three unknowns of $\hat{\mathbf{F}}$. We need one additional restriction. Appealing to the principle of virtual work, the constraint force must have no component in the tangential direction to the curve,

$$0 = \mathbf{T} \cdot \hat{\mathbf{F}} = \frac{\dot{\mathbf{x}}}{|\dot{\mathbf{x}}|} \cdot \hat{\mathbf{F}} \quad (6.113)$$

where \mathbf{T} is a unit-length tangent vector. If \mathbf{N} is a unit-length normal and \mathbf{B} is a unit-length binormal, the constraint force may be written in terms of the Frenet–Serret

frame,

$$\hat{\mathbf{F}} = \lambda_0 \mathbf{T} + \lambda_1 \mathbf{N} + \lambda_2 \mathbf{B} \quad (6.114)$$

Equation (6.113) trivially implies

$$\lambda_0 = 0 \quad (6.115)$$

Substituting equation (6.114) into equation (6.112) leads to

$$\begin{bmatrix} \lambda_1 \\ \lambda_2 \end{bmatrix} = \frac{1}{\Delta} \begin{bmatrix} \nabla C_1 \cdot \mathbf{B} - \nabla C_0 \cdot \mathbf{B} \\ -\nabla C_1 \cdot \mathbf{N} \quad \nabla C_0 \cdot \mathbf{N} \end{bmatrix} \begin{bmatrix} \nabla C_0 \cdot \mathbf{F} + m\dot{\mathbf{x}}^T \nabla \otimes \nabla C_0 \dot{\mathbf{x}} \\ \nabla C_1 \cdot \mathbf{F} + m\dot{\mathbf{x}}^T \nabla \otimes \nabla C_1 \dot{\mathbf{x}} \end{bmatrix} \quad (6.116)$$

where $\Delta = (\nabla C_0 \cdot \mathbf{B})(\nabla C_1 \cdot \mathbf{N}) - (\nabla C_0 \cdot \mathbf{N})(\nabla C_1 \cdot \mathbf{B})$. Once again we have determined explicitly the constraint force.

6.7.2 CONSTRAINTS ON A PARTICLE SYSTEM

The ideas of Section 6.7.1 apply to a system of n particles. The goal of this section is to motivate the extension of the ideas to a system of rigid bodies, so the assumptions made here for the particles are similar to the assumptions for rigid bodies.

Particle Constraints

Let particle i have constant mass m_i and time-varying position \mathbf{x}_i . We allow constraints between pairs of particles. The k th constraint is of the form

$$C_k(\mathbf{x}_{i_k}, \mathbf{x}_{j_k}) = 0$$

and represents the restrictions between the particles of index i_k and j_k . Let \mathbf{x} store consecutively the positions \mathbf{x}_i ; that is, \mathbf{x} can be thought of as a $3n \times 1$ vector. The constraint function can be written as $C_k(\mathbf{x})$, but it is understood that only two of the 3-tuple components of \mathbf{x} are allowed to take part in the constraint. Assuming m constraints, an $m \times 1$ vector $\mathbf{C}(\mathbf{x})$ may be used to store them. The vector-valued constraint equation is then

$$\mathbf{C}(\mathbf{x}) = \mathbf{0} \quad (6.117)$$

This is the extension of equation (6.106) for one particle to a system of particles.

First Derivative of Constraints

The time derivative of the constraint vector must be equal to zero for all t . Using block tensor index notation, the constraint vector equation is written as $\dot{C}_k(\mathbf{x}) = 0$, where k is a free index. The time derivative is computed using the chain rule,

$$\dot{C}_k = C_{k,i} \dot{\mathbf{x}}_i$$

where $C_{k,i}$ is the 3×1 vector of first-order partial derivatives of C_k with respect to the components of \mathbf{x}_i . In the subscript of C , any index before the comma denotes a “component” and any index after the comma denotes “differentiate with respect to the component.” The repeated index i indicates you must sum over that index. The index k is still a free index. I will use the suggestive vector notation $\partial C_k / \partial \mathbf{x}_i$ to represent the quantity $C_{k,i}$.

For example, consider a system of four particles subject to the two constraints

$$\mathbf{C}(\mathbf{x}_1, \mathbf{x}_2, \mathbf{x}_3, \mathbf{x}_4) = \begin{bmatrix} C_1(\mathbf{x}_1, \mathbf{x}_2) \\ C_2(\mathbf{x}_2, \mathbf{x}_4) \end{bmatrix} = \begin{bmatrix} 0 \\ 0 \end{bmatrix} = \mathbf{0}$$

The time derivative is

$$\begin{aligned} \dot{\mathbf{C}} &= \begin{bmatrix} \dot{C}_1(\mathbf{x}_1, \mathbf{x}_2) \\ \dot{C}_2(\mathbf{x}_2, \mathbf{x}_4) \end{bmatrix} = \begin{bmatrix} \frac{\partial C_1}{\partial \mathbf{x}_1} \dot{\mathbf{x}}_1 + \frac{\partial C_1}{\partial \mathbf{x}_2} \dot{\mathbf{x}}_2 + \frac{\partial C_1}{\partial \mathbf{x}_3} \dot{\mathbf{x}}_3 + \frac{\partial C_1}{\partial \mathbf{x}_4} \dot{\mathbf{x}}_4 \\ \frac{\partial C_2}{\partial \mathbf{x}_1} \dot{\mathbf{x}}_1 + \frac{\partial C_2}{\partial \mathbf{x}_2} \dot{\mathbf{x}}_2 + \frac{\partial C_2}{\partial \mathbf{x}_3} \dot{\mathbf{x}}_3 + \frac{\partial C_2}{\partial \mathbf{x}_4} \dot{\mathbf{x}}_4 \end{bmatrix} \\ &= \begin{bmatrix} \frac{\partial C_1}{\partial \mathbf{x}_1} & \frac{\partial C_1}{\partial \mathbf{x}_2} & \frac{\partial C_1}{\partial \mathbf{x}_3} & \frac{\partial C_1}{\partial \mathbf{x}_4} \\ \frac{\partial C_2}{\partial \mathbf{x}_1} & \frac{\partial C_2}{\partial \mathbf{x}_2} & \frac{\partial C_2}{\partial \mathbf{x}_3} & \frac{\partial C_2}{\partial \mathbf{x}_4} \end{bmatrix} \begin{bmatrix} \dot{\mathbf{x}}_1 \\ \dot{\mathbf{x}}_2 \\ \dot{\mathbf{x}}_3 \\ \dot{\mathbf{x}}_4 \end{bmatrix} \\ &= DC \dot{\mathbf{x}} \end{aligned}$$

where DC is the matrix of first-order partial derivatives of C with respect to its independent variables. The matrix is sometimes referred to as the *Jacobian matrix*. In this particular example, observe that

$$DC = \begin{bmatrix} \frac{\partial C_1}{\partial \mathbf{x}_1} & \frac{\partial C_1}{\partial \mathbf{x}_2} & \mathbf{0} & \mathbf{0} \\ \mathbf{0} & \frac{\partial C_2}{\partial \mathbf{x}_2} & \mathbf{0} & \frac{\partial C_2}{\partial \mathbf{x}_4} \end{bmatrix}$$

The matrix DC is *sparse*, meaning the majority of its entries are zero. This is true because each component constraint may involve the interaction of only two particles.

In general, the first-order time derivative of the constraint vector is

$$\mathbf{0} = \dot{\mathbf{C}}(\mathbf{x}) = DC \dot{\mathbf{x}} \quad (6.118)$$

where DC is the Jacobian matrix of C . This is the extension of equation (6.107) for one particle to a system of particles.

Second Derivative of Constraints

The second-order time derivative must also be zero for all t . Using block tensor index notation, we had $\dot{C}_k = C_{k,i}\dot{\mathbf{x}}_i$. Applying another time derivative using the product rule and then the chain rule,

$$\ddot{C}_k = C_{k,i}\ddot{\mathbf{x}}_i + \dot{C}_{k,i}\dot{\mathbf{x}}_i = C_{k,i}\ddot{\mathbf{x}}_i + C_{k,ij}\dot{\mathbf{x}}_i\dot{\mathbf{x}}_j$$

where $C_{k,ij}$ is the 3×3 matrix of second-order partial derivatives of C_k with respect to the components of \mathbf{x}_i and \mathbf{x}_j . Indices before a comma are components and indices after a comma are variables that you differentiate with respect to. Repeated indices are summed, the remaining ones free. I will use the suggestive notation $\partial^2 C_k / \partial \mathbf{x}_i \partial \mathbf{x}_j$ to represent the quantity $C_{k,ij}$.

Using the previous example of four particles with two constraints, the second-order time derivative of the k th component is

$$\begin{aligned} \ddot{C}_k &= \left[\frac{\partial C_k}{\partial \mathbf{x}_1} \frac{\partial C_k}{\partial \mathbf{x}_2} \frac{\partial C_k}{\partial \mathbf{x}_3} \frac{\partial C_k}{\partial \mathbf{x}_4} \right] \begin{bmatrix} \dot{\mathbf{x}}_1 \\ \dot{\mathbf{x}}_2 \\ \dot{\mathbf{x}}_3 \\ \dot{\mathbf{x}}_4 \end{bmatrix} \\ &\quad + \left[\dot{\mathbf{x}}_1^T \dot{\mathbf{x}}_2^T \dot{\mathbf{x}}_3^T \dot{\mathbf{x}}_4^T \right] \begin{bmatrix} \frac{\partial^2 C_k}{\partial \mathbf{x}_1^2} & \frac{\partial^2 C_k}{\partial \mathbf{x}_1 \partial \mathbf{x}_2} & \frac{\partial^2 C_k}{\partial \mathbf{x}_1 \partial \mathbf{x}_3} & \frac{\partial^2 C_k}{\partial \mathbf{x}_1 \partial \mathbf{x}_4} \\ \frac{\partial^2 C_k}{\partial \mathbf{x}_2 \partial \mathbf{x}_1} & \frac{\partial^2 C_k}{\partial \mathbf{x}_2^2} & \frac{\partial^2 C_k}{\partial \mathbf{x}_2 \partial \mathbf{x}_3} & \frac{\partial^2 C_k}{\partial \mathbf{x}_2 \partial \mathbf{x}_4} \\ \frac{\partial^2 C_k}{\partial \mathbf{x}_3 \partial \mathbf{x}_1} & \frac{\partial^2 C_k}{\partial \mathbf{x}_3 \partial \mathbf{x}_2} & \frac{\partial^2 C_k}{\partial \mathbf{x}_3^2} & \frac{\partial^2 C_k}{\partial \mathbf{x}_3 \partial \mathbf{x}_4} \\ \frac{\partial^2 C_k}{\partial \mathbf{x}_4 \partial \mathbf{x}_1} & \frac{\partial^2 C_k}{\partial \mathbf{x}_4 \partial \mathbf{x}_2} & \frac{\partial^2 C_k}{\partial \mathbf{x}_4 \partial \mathbf{x}_3} & \frac{\partial^2 C_k}{\partial \mathbf{x}_4^2} \end{bmatrix} \begin{bmatrix} \dot{\mathbf{x}}_1 \\ \dot{\mathbf{x}}_2 \\ \dot{\mathbf{x}}_3 \\ \dot{\mathbf{x}}_4 \end{bmatrix} \end{aligned}$$

There are two such equations for our example.

Observe that $C_{k,ij}$ is a triply indexed quantity. Unlike vectors (1 index) and matrices (2 indices), we have no convention for writing coordinate-free expressions. For example, given an $r \times c$ matrix $M = [M_{ij}]$ and a $c \times 1$ vector $\mathbf{V} = [V_j]$, the product of M and \mathbf{V} is written as $M\mathbf{V}$ with a corresponding tensor expression of $M_{ij}V_j$ (i is free, j is summed). Regardless, let us write a coordinate-free expression for $\ddot{\mathbf{C}}$ generally, with the understanding that the term involving the triply indexed tensor is computed correctly according to the tensor expression we derived for \dot{C}_k ,

$$\mathbf{0} = \ddot{\mathbf{C}} = DC\ddot{\mathbf{x}} + \dot{\mathbf{x}}^T D \otimes DC\dot{\mathbf{x}} \quad (6.119)$$

where $D \otimes DC$ is the coordinate-free expression representing the triply index tensor $C_{k,ij}$. Notice that the expression involves two “derivative operators” D that is applied

to all the components of \mathbf{C} . The coordinate-free expression $\dot{\mathbf{x}}^T D \otimes DC\dot{\mathbf{x}}$ represents the tensor expression $C_{k,ij}\dot{\mathbf{x}}_i\dot{\mathbf{x}}_j$. [Equation \(6.119\)](#) is the extension of [equation \(6.108\)](#) for one particle to a system of particles. The matrix $C_{k,ij}$ is sometimes referred to as the *Hessian matrix* for C_k . The collection of these matrices (as k varies) may be called the *Hessian tensor* for \mathbf{C} .

Equations of Motion

The external force applied to particle i is \mathbf{F}_i . To ensure that the constraints are satisfied, a constraint force per particle is required, call it $\hat{\mathbf{F}}_i$. Newton's second law requires

$$m_i\ddot{\mathbf{x}}_i = \mathbf{F}_i + \hat{\mathbf{F}}_i$$

for all i . Define the $n \times n$ diagonal matrix $M = \text{Diag}(m_1, \dots, m_n)$. Let \mathbf{F} represent the $n \times 1$ vector of external force vectors and let $\hat{\mathbf{F}}$ represent the 3×1 vector of constraint force vectors. Newton's second law for the particle system is

$$M\ddot{\mathbf{x}} = \mathbf{F} + \hat{\mathbf{F}}$$

Substituting this into [equation \(6.119\)](#) leads to

$$\mathbf{0} = DCM^{-1}(\mathbf{F} + \hat{\mathbf{F}}) + \dot{\mathbf{x}}^T D \otimes DC\dot{\mathbf{x}} \quad (6.120)$$

This a set of m equations (number of constraints) in the n unknown vector components (number of constraint force components) of $\hat{\mathbf{F}}$. As in the case of a single particle, we want to formulate an expression for $\hat{\mathbf{F}}$ and then substitute this expression into [equation \(6.120\)](#) to help solve for the constraint force.

Computing the Constraint Force

We make an appeal to the principle of virtual work once again. The constraint force $\hat{\mathbf{F}}$ cannot do work in the velocity direction $\dot{\mathbf{x}}$. This means $\hat{\mathbf{F}}$ must be orthogonal to $\dot{\mathbf{x}}$. [Equation \(6.118\)](#) states that $DC\dot{\mathbf{x}} = \mathbf{0}$, where DC is the Jacobian matrix. By definition, $\dot{\mathbf{x}}$ is in $\text{kernel}(DC)$. By the fundamental theorem of linear algebra (see [Section 7.4.7](#)), $\text{range}((DC)^T)$ is the orthogonal complement of $\text{kernel}(DC)$, so $\hat{\mathbf{F}}$ must be in the range of $(DC)^T$,

$$\hat{\mathbf{F}} = (DC)^T \boldsymbol{\lambda} \quad (6.121)$$

for some unknown $m \times 1$ vector $\boldsymbol{\lambda}$.

Substitute [equation \(6.121\)](#) into [equation \(6.120\)](#) and rearrange terms to obtain

$$GM^{-1}G^T \boldsymbol{\lambda} = - (GM^{-1}\mathbf{F} + \dot{\mathbf{x}}^T H\dot{\mathbf{x}}) \quad (6.122)$$

where $G = D\mathbf{C}$ is the Jacobian matrix and $H = D \otimes DC$ is the Hessian tensor. If $GM^{-1}G^T$ is invertible, then we can solve directly

$$\lambda = -(GM^{-1}G^T)^{-1}(GM^{-1}\mathbf{F} + \dot{\mathbf{x}}^T H \dot{\mathbf{x}})$$

which is the analog of equation (6.111) for a single particle.

The invertibility happens, however, only when G is of full rank. Generally, G might not be full rank, in which case there are infinitely many solutions λ to equation (6.122). We may compute one of them using a least-squares or minimum-norm approach (use the generalized inverse, called the *Moore–Penrose inverse*). Alternatively, one of the solutions may be computed by an iterative method for solving linear systems. For example, Gauss–Seidel iteration may be used (see Section 7.2.6).

6.7.3 CONSTRAINT ON A RIGID BODY

Consider a rigid body whose position \mathbf{x} and orientation q are constrained. The position is a vector but the orientation is a quaternion. Although we can work with mixed units, the discussion in this section converts everything to real-valued vector calculations. In particular, we will represent the quaternion with a 4-tuple vector \mathbf{q} and impose a single constraint on the rigid body that involves the position vector and the orientation vector,

$$C(\mathbf{x}(t), \mathbf{q}(t)) = 0 \quad (6.123)$$

which is true for all time t .

Recall from Section 2.2.2 that the world position of a time-varying point in a rigid body is of the form

$$\mathbf{p}(t) = \mathbf{x}(t) + R(t)\mathbf{b} = \mathbf{x}(t) + \mathbf{r}(t)$$

where $\mathbf{x}(t)$ is the time-varying center of mass, $R(t)$ is the time-varying orientation of the point about the center of mass, and \mathbf{b} is the body coordinates of the point. The offset of the point from the center of mass is $\mathbf{r}(t) = R(t)\mathbf{b}$.

In practice, a constraint on the rigid body involves center of mass \mathbf{x} and orientation R . However, the equations of motion are $\dot{\mathbf{x}} = \mathbf{v}$ and $\dot{q} = \omega q/2$, where \mathbf{v} is the linear velocity, $q = q_0 + q_1 i + q_2 j + q_3 k$ is the unit quaternion that represents R , and $\omega = w_1 i + w_2 j + w_3 k$ is the not-necessarily-unit quaternion that represents the angular velocity. Although the orientation differential equation introduces i , j , and k , the constraint itself may be thought of as $C(\mathbf{x}, R) = 0$ and does not contain i , j , or k terms.

Let us eliminate the quaternion notation, choosing instead to represent q by $\mathbf{q} = (q_0, q_1, q_2, q_3)$ and ω by $\mathbf{w} = (w_1, w_2, w_3)$. Some algebra will show that in vector form,

the orientation differential equation is

$$\dot{\mathbf{q}} = \begin{bmatrix} \dot{q}_0 \\ \dot{q}_1 \\ \dot{q}_2 \\ \dot{q}_3 \end{bmatrix} = \frac{1}{2} \begin{bmatrix} -q_1 & -q_2 & -q_3 \\ q_0 & q_3 & -q_2 \\ -q_3 & q_0 & q_1 \\ q_2 & -q_1 & q_0 \end{bmatrix} \begin{bmatrix} w_1 \\ w_2 \\ w_3 \end{bmatrix} = \frac{1}{2} Q \mathbf{w} \quad (6.124)$$

where the last equality defines the 4×3 matrix Q . Observe that $Q^T Q = I$, the 3×3 identity.

Also recall that the relationship between a rotation matrix R and the quaternion q representing it is

$$R = \begin{bmatrix} 1 - 2q_2^2 - 2q_3^2 & 2(q_1 q_2 - q_0 q_3) & 2(q_1 q_3 + q_0 q_2) \\ 2(q_1 q_2 + q_0 q_3) & 1 - 2q_1^2 - 2q_3^2 & 2(q_2 q_3 - q_0 q_1) \\ 2(q_1 q_3 - q_0 q_2) & 2(q_2 q_3 + q_0 q_1) & 1 - 2q_1^2 - 2q_2^2 \end{bmatrix} \quad (6.125)$$

Any constraint involving R can replace it with this matrix that contains entries from \mathbf{q} , in which case we need only consider constraints of the form in [equation \(6.123\)](#).

First Derivative of Constraint

The time derivative of $C(\mathbf{x}, \mathbf{q}) = 0$ must also be equal to zero for all t ,

$$0 = \dot{C} = \frac{\partial C}{\partial \mathbf{x}} \dot{\mathbf{x}} + \frac{\partial C}{\partial \mathbf{q}} \dot{\mathbf{q}} = \left[\frac{\partial C}{\partial \mathbf{x}} \frac{\partial C}{\partial \mathbf{q}} \right] \left[\begin{bmatrix} \dot{\mathbf{x}} \\ \dot{\mathbf{q}} \end{bmatrix} \right]$$

where $\partial C / \partial \mathbf{x}$ denotes the 1×3 vector of the first-order partial derivatives of C with respect to the components of \mathbf{x} . The symbol $\partial C / \partial \mathbf{q}$ denotes the 1×4 vector of the first-order partial derivatives of C with respect to the components of \mathbf{q} . The right-most equality is a factorization into a matrix times a vector. The matrix stores the first-order partial derivatives of C . You should recall that this is the Jacobian matrix for C .

The vector in the factorization stores the linear velocity in its first component. However, the second component is the rate of change of orientation. Velocity-based methods insist that the linear velocity and *angular velocity* be stored explicitly. We must make use of [equation \(6.124\)](#) and factor once more,

$$0 = \dot{C} = \left[\frac{\partial C}{\partial \mathbf{x}} \frac{1}{2} \frac{\partial C}{\partial \mathbf{q}} Q \right] \left[\begin{bmatrix} \mathbf{v} \\ \mathbf{w} \end{bmatrix} \right] = G \mathbf{V} \quad (6.126)$$

where we define

$$G = \left[\frac{\partial C}{\partial \mathbf{x}} \frac{1}{2} \frac{\partial C}{\partial \mathbf{q}} Q \right], \quad \mathbf{V} = \left[\begin{bmatrix} \mathbf{v} \\ \mathbf{w} \end{bmatrix} \right]$$

Please observe that G is *not the Jacobian matrix of C* . [Equation \(6.126\)](#) is the extension of [equation \(6.107\)](#) from a particle to a rigid body.

Second Derivative of Constraint

The second-order time derivative of C must be zero for all t ,

$$\begin{aligned}\ddot{C} &= \frac{\partial C}{\partial \mathbf{x}} \ddot{\mathbf{x}} + \frac{\partial \dot{C}}{\partial \mathbf{x}} \dot{\mathbf{x}} + \frac{\partial C}{\partial \mathbf{q}} \ddot{\mathbf{q}} + \frac{\partial \dot{C}}{\partial \mathbf{q}} \dot{\mathbf{q}} \\ &= \frac{\partial C}{\partial \mathbf{x}} \ddot{\mathbf{x}} + \dot{\mathbf{x}}^T \left(\frac{\partial^2 C}{\partial \mathbf{x}^2} \dot{\mathbf{x}} + \frac{\partial^2 C}{\partial \mathbf{x} \partial \mathbf{q}} \dot{\mathbf{q}} \right) + \frac{\partial C}{\partial \mathbf{q}} \ddot{\mathbf{q}} + \dot{\mathbf{q}}^T \left(\frac{\partial^2 C}{\partial \mathbf{q} \partial \mathbf{x}} \dot{\mathbf{x}} + \frac{\partial^2 C}{\partial \mathbf{q}^2} \dot{\mathbf{q}} \right) \\ &= \frac{\partial C}{\partial \mathbf{x}} \ddot{\mathbf{x}} + \frac{\partial C}{\partial \mathbf{q}} \ddot{\mathbf{q}} + \dot{\mathbf{x}}^T \frac{\partial^2 C}{\partial \mathbf{x}^2} \dot{\mathbf{x}} + 2\dot{\mathbf{x}}^T \frac{\partial^2 C}{\partial \mathbf{x} \partial \mathbf{q}} \dot{\mathbf{q}} + \dot{\mathbf{q}}^T \frac{\partial^2 C}{\partial \mathbf{q}^2} \dot{\mathbf{q}}\end{aligned}$$

where $\partial^2 C / \partial \mathbf{x}^2$ is the 3×3 matrix of second-order partial derivatives of C with respect to the components of \mathbf{x} , $\partial^2 C / \partial \mathbf{q}^2$ is the 4×4 matrix of second-order partial derivatives of C with respect to the components of \mathbf{q} , $\partial^2 C / \partial \mathbf{x} \mathbf{q}$ is the 3×4 matrix of second-order mixed partial derivatives of C , and $(\partial^2 C / \partial \mathbf{q} \partial \mathbf{x})^T = \partial^2 C / \partial \mathbf{x} \partial \mathbf{q}$.

We know that $\dot{\mathbf{x}} = \mathbf{v}$, so it is trivial to obtain the equation $\dot{\mathbf{v}} = \ddot{\mathbf{x}}$. We also know that $\dot{\mathbf{q}} = Q\mathbf{w}/2$ and want to derive a formula for $\ddot{\mathbf{q}}$ that includes the term $\dot{\mathbf{w}}$. Let us use tensor index notation to do so. The quaternion equation of motion is

$$\dot{q}_i = \frac{1}{2} Q_{ij} w_j$$

where q_i are the entries of \mathbf{q} , Q_{ij} are the entries of the matrix Q , and w_j are the entries of \mathbf{w} . The repeated index j indicates that you sum over it. The index i is a free index.

Observe that the entries of Q are individual components of \mathbf{q} with positive or negative signs. We can use a triply indexed tensor to write Q as

$$Q_{ij} = \sigma_{ijk} q_k$$

where the repeated index k indicates that you sum over it. The indices i and j are free indices. The tensor S_{ijk} has 48 entries: i has 4 values, j has 3 values, and k has 4 values, for a total of $4 * 3 * 4$ entries. Of these entries, 36 are zero, 6 are $+1$, and 6 are -1 . Using zero-based indexing, the $+1$ entries are $\sigma_{100}, \sigma_{113}, \sigma_{210}, \sigma_{221}, \sigma_{302}$, and σ_{320} . The -1 entries are $\sigma_{001}, \sigma_{012}, \sigma_{023}, \sigma_{122}, \sigma_{203}$, and σ_{311} . Thus,

$$\dot{q}_i = \frac{1}{2} \sigma_{ijk} w_j q_k$$

Computing the time derivative,

$$\ddot{q}_i = \frac{1}{2} \sigma_{ijk} (\dot{w}_j q_k + w_j \dot{q}_k) = \frac{1}{2} \sigma_{ijk} q_k \dot{w}_j + \frac{1}{4} \sigma_{ijk} w_j Q_{k\ell} w_\ell = \frac{1}{2} Q_{ij} \dot{w}_j + \frac{1}{4} \sigma_{ijk} w_j Q_{k\ell} w_\ell$$

If we define $C_{q,i}$ to be the i th component of $\partial C / \partial \mathbf{q}$ and matrix A to have components $A_{j\ell} = C_{q,i} \sigma_{ijk} Q_{k\ell}$, then

$$\frac{\partial C}{\partial \mathbf{q}} \ddot{\mathbf{q}} = \frac{1}{2} \frac{\partial C}{\partial \mathbf{q}} Q \dot{\mathbf{w}} + \frac{1}{4} \mathbf{w}^T A \mathbf{w}$$

Some tedious calculations will show the following. Define d_i to be the i th component of $\partial C / \partial \mathbf{q}$; then

$$A = \begin{bmatrix} -d_0 q_0 - d_1 q_1 - d_2 q_2 - d_3 q_3 & -d_0 q_3 - d_1 q_2 + d_2 q_1 + d_3 q_0 & d_0 q_2 - d_1 q_3 - d_2 q_0 + d_3 q_1 \\ d_0 q_3 + d_1 q_2 - d_2 q_1 + d_3 q_0 & -d_0 q_0 - d_1 q_1 - d_2 q_2 - d_3 q_3 & -d_0 q_1 + d_1 q_0 - d_2 q_3 + d_3 q_2 \\ -d_0 q_2 + d_1 q_3 + d_2 q_0 - d_3 q_1 & d_0 q_1 - d_1 q_0 + d_2 q_3 - d_3 q_2 & -d_0 q_0 - d_1 q_1 - d_2 q_2 - d_3 q_3 \end{bmatrix}$$

$$= \frac{\partial C}{\partial \mathbf{q}} \mathbf{q} I + S$$

where S is a skew-symmetric matrix. Consequently,

$$\mathbf{w}^T A \mathbf{w} = -\frac{\partial C}{\partial \mathbf{q}} \mathbf{q} \mathbf{w}^T \mathbf{w}$$

Substituting the formulas for $\dot{\mathbf{q}}$ and $\ddot{\mathbf{q}}$ into the equation for \ddot{C} leads to

$$\begin{aligned} \ddot{C} &= \left[\frac{\partial C}{\partial \mathbf{x}} \frac{1}{2} \frac{\partial C}{\partial \mathbf{q}} Q \right] \begin{bmatrix} \dot{\mathbf{v}} \\ \dot{\mathbf{w}} \end{bmatrix} \\ &\quad + [\mathbf{v}^T \mathbf{w}^T] \begin{bmatrix} \frac{\partial^2 C}{\partial \mathbf{x}^2} & \frac{1}{2} \frac{\partial^2 C}{\partial \mathbf{x} \partial \mathbf{q}} Q \\ \frac{1}{2} Q^T \left(\frac{\partial^2 C}{\partial \mathbf{x} \partial \mathbf{q}} \right)^T & \frac{1}{4} Q^T \left(\frac{\partial^2 C}{\partial \mathbf{q}^2} - \frac{\partial C}{\partial \mathbf{q}} q I \right) Q \end{bmatrix} \begin{bmatrix} \mathbf{v} \\ \mathbf{w} \end{bmatrix} \quad (6.127) \\ &= G \dot{\mathbf{V}} + \mathbf{V}^T H \mathbf{V} \end{aligned}$$

This is the extension of [equation \(6.108\)](#) for a single particle to a rigid body. The matrix G is not the Jacobian matrix of C and the matrix H is not the Hessian matrix of C .

6.7.4 CONSTRAINTS ON A RIGID BODY SYSTEM

The ideas of [Section 6.7.3](#) apply to a system of n rigid bodies.

Rigid Body Constraints

Let rigid body i have mass m_i , inertia tensor J_i in world coordinates, time-varying center of mass \mathbf{x}_i , and orientation vector \mathbf{q}_i . We allow constraints between pairs of rigid bodies. The k th constraint is of the form

$$C_k(\mathbf{x}_{i_k}, \mathbf{q}_{i_k}, \mathbf{x}_{j_k}, \mathbf{q}_{j_k}) = 0$$

and represents the restrictions between the rigid bodies of index i_k and j_k . Let \mathbf{x} store consecutively the positions \mathbf{x}_i and \mathbf{q} store consecutively the orientations \mathbf{q}_i . The constraint function can be written as $C_k(\mathbf{x}, \mathbf{q})$, but it is understood that only two of the rigid bodies are allowed to take part in the constraint. Assuming m constraints, an $m \times 1$ vector $\mathbf{C}(\mathbf{x}, \mathbf{q})$ may be used to store them. The vector-valued constraint equation is

$$\mathbf{C}(\mathbf{x}, \mathbf{q}) = \mathbf{0} \quad (6.128)$$

This is the extension of equation (6.123) for one rigid body to a system of rigid bodies.

The first-order time derivative must be equal to zero for all time t and is of the form

$$\mathbf{0} = \dot{\mathbf{C}} = G\mathbf{V} \quad (6.129)$$

where

$$\mathbf{V} = \begin{bmatrix} \mathbf{v}_1 \\ \mathbf{w}_1 \\ \vdots \\ \mathbf{v}_n \\ \mathbf{w}_n \end{bmatrix}$$

The matrix G is *not* the Jacobian matrix of \mathbf{C} . We already saw this for a single rigid body (see Section 6.7.3). This is the extension of equation (6.123) for one rigid body to a system of rigid bodies.

The second-order time derivative must be equal to zero for all time t and is of the form

$$\mathbf{0} = \ddot{\mathbf{C}} = G\dot{\mathbf{V}} + \mathbf{V}^T H \mathbf{V} \quad (6.130)$$

where H is a triply indexed tensor that is *not* the Hessian tensor of \mathbf{C} (see Section 6.7.3).

Equations of Motion

The rigid body with index i has mass m_i and inertia tensor J_i in world coordinates. Equation (6.66) shows how the inertia tensor in body coordinates relates to the inertia tensor in world coordinates. Specifically, if B_i is the inertia tensor in body coordinates, then $J_i = R(t)B_iR(t)^T$. The tensor B_i is a matrix of constants for a rigid body.

An external force on the body is \mathbf{F}_i and an external torque on the body is $\boldsymbol{\tau}_i$. These may be summarized as a single $6n \times 1$ vector,

$$\mathbf{F} = \begin{bmatrix} \mathbf{F}_1 \\ \boldsymbol{\tau}_1 \\ \vdots \\ \mathbf{F}_n \\ \boldsymbol{\tau}_n \end{bmatrix} \quad (6.131)$$

Body i also has an internal reaction force $\hat{\mathbf{F}}_i$ and an internal reaction torque $\hat{\boldsymbol{\tau}}_i$. These may be summarized as a single vector,

$$\hat{\mathbf{F}} = \begin{bmatrix} \hat{\mathbf{F}}_1 \\ \hat{\boldsymbol{\tau}}_1 \\ \vdots \\ \hat{\mathbf{F}}_n \\ \hat{\boldsymbol{\tau}}_n \end{bmatrix} \quad (6.132)$$

For the body i , Newton's equations of motion are

$$\frac{d(m_i \mathbf{v}_i)}{dt} = \mathbf{F}_i + \hat{\mathbf{F}}_i, \quad \frac{d(J_i \mathbf{w}_i)}{dt} = \boldsymbol{\tau}_i + \hat{\boldsymbol{\tau}}_i$$

These are mentioned in [equations \(6.62\)](#) and [\(6.65\)](#). The left-hand side of the second of these equations expands to

$$\frac{d(J_i \mathbf{w}_i)}{dt} = J_i \dot{\mathbf{w}}_i + \dot{J}_i \mathbf{w}$$

with

$$\begin{aligned} \dot{J}_i &= \frac{d}{dt} (RB_i R^T) \\ &= RB_i \dot{R}^T + \dot{R}B_i R^T \\ &= RB_i (\text{Skew}(\mathbf{w}_i)R)^T + (\text{Skew}(\mathbf{w}_i)R)B_i R^T \\ &= RB_i R^T \text{Skew}(\mathbf{w}_i)^T + \text{Skew}(\mathbf{w}_i) (RB_i R^T) \\ &= J_i \text{Skew}(\mathbf{w}_i)^T + \text{Skew}(\mathbf{w}_i)J_i \end{aligned}$$

and

$$\begin{aligned} \dot{J}_i \mathbf{w}_i &= J_i \text{Skew}(\mathbf{w}_i)^T \mathbf{w}_i + \text{Skew}(\mathbf{w}_i)J_i \mathbf{w}_i \\ &= -J_i \mathbf{w}_i \times \mathbf{w}_i + \mathbf{w}_i \times J_i \mathbf{w}_i \\ &= \mathbf{w}_i \times J_i \mathbf{w}_i \end{aligned}$$

The right-hand side of the previous equality is referred to as the *inertial torque*. It is assumed to be negligible in this application. Thus, the equations of motion become

$$m_i \dot{\mathbf{v}}_i = \mathbf{F}_i + \hat{\mathbf{F}}_i, \quad J_i \dot{\mathbf{w}}_i = \boldsymbol{\tau}_i + \hat{\boldsymbol{\tau}}_i$$

The masses and inertia tensors may be stored in a diagonal matrix,

$$\mathbf{M} = \text{Diag}(m_1 I, J_1, \dots, m_n I, J_n)$$

where I is the 3×3 identity matrix. The equations of motion for all the rigid bodies are summarized by

$$\begin{aligned} \mathbf{M} \dot{\mathbf{V}} &= \mathbf{F} + \hat{\mathbf{F}} \\ \mathbf{G} \mathbf{V} &= \mathbf{0} \end{aligned} \tag{6.133}$$

Equation (6.133) may be substituted into equation (6.130) to obtain

$$\mathbf{0} = GM^{-1}(\mathbf{F} + \hat{\mathbf{F}}) + \mathbf{V}^T H \mathbf{V} \tag{6.134}$$

As in the case for a system of particles, we want to formulate an expression for $\hat{\mathbf{F}}$ and then substitute this into equation (6.134) to help solve for the constraint force.

Computing the Constraint Force

The principle of virtual work applies, so the constraint force does no work in the velocity direction, which means that this force has components orthogonal to the velocity components. Equation (6.129) implies that \mathbf{V} is in $\text{kernel}(G)$. $\hat{\mathbf{F}}$ must be orthogonal to \mathbf{V} , so by the fundamental theorem of linear algebra (see Section 7.4.7), $\hat{\mathbf{F}}$ must be in $\text{range}(G^T)$, which implies

$$\hat{\mathbf{F}} = G^T \boldsymbol{\lambda} \tag{6.135}$$

for some unknown $m \times 1$ vector $\boldsymbol{\lambda}$.

Substitute equation (6.135) into equation (6.134) and rearrange terms to obtain

$$GM^{-1}G^T \boldsymbol{\lambda} = - (GM^{-1}\mathbf{F} + \mathbf{V}^T H \mathbf{V}) \tag{6.136}$$

As in the case of particle systems, the matrix $GM^{-1}G^T$ is usually not invertible, and there are in fact infinitely many solutions $\boldsymbol{\lambda}$. We may use an iterative method such as Gauss–Seidel iteration to compute a solution (see Section 7.2.6).

6.7.5 COMMENTS AND VARIATIONS ON THE ALGORITHM

The ideas of the previous sections are briefly summarized in [Cat05]. However, the paper does not consider computing the Hessian tensor H as we have done previously. I will discuss briefly the comments and variations on the algorithm presented in the

paper. The terminology changes slightly. First, the paper uses J instead of G and calls J the Jacobian matrix of \mathbf{C} (which it is not) – I will continue to use G . Second, the paper mentions the orientation differential equation $\dot{q} = q\omega/2$. To be consistent with the representation of rigid body world positions $\mathbf{p} = \mathbf{x} + R\mathbf{b}$, it is necessary to use $\dot{q} = \omega q/2$. The comments and variations include

- The constraints are simple enough that the matrix G may be computed by differentiating directly rather than applying a chain rule.
- A data structure is presented to show how to take advantage of the sparseness of G , which helps reduce memory usage and increases performance.
- Inequality constraints are allowed so that joint angles and contact points can be handled. The inequalities, however, are specified for the components of λ .
- A *constraint bias* is allowed, which means allowing $GV = \zeta \neq \mathbf{0}$. A consequence is that the constraint force can do work.
- The contact model allows interpenetration of bodies and deals with this appropriately.
- The friction model encapsulates both static and dynamic friction.
- A time-stepping algorithm is used to solve for λ . This turns out to be an approximation to [equation \(6.136\)](#), so the algorithm described in previous sections here is slightly different from that of the paper.
- A contact caching scheme is presented to help with robustness and increase performance of the algorithm.

Computing G Directly

An example in [\[Cat05\]](#) illustrates the direct calculation of G where the world positions of two body points, one per rigid body in the pair generating the constraint, are required to be separated by L units of distance. The constraint is

$$C = \frac{1}{2}(|\mathbf{p}_2 - \mathbf{p}_1|^2 - L^2) = 0$$

where $\mathbf{p}_1 = \mathbf{x}_1 + R_1\mathbf{b}_1$ and $\mathbf{p}_2 = \mathbf{x}_2 + R_2\mathbf{b}_2$. The time derivative of the constraint function is

$$\begin{aligned}\dot{C} &= (\mathbf{p}_2 - \mathbf{p}_1) \cdot (\dot{\mathbf{p}}_2 - \dot{\mathbf{p}}_1) \\ &= (\mathbf{p}_2 - \mathbf{p}_1) \cdot (\mathbf{v}_2 + \mathbf{w}_2 \times \mathbf{r}_2 - \mathbf{v}_1 - \mathbf{w}_1 \times \mathbf{r}_1) \\ &= [-\Delta^T - (\mathbf{r}_1 \times \Delta)^T \quad \Delta^T \quad (\mathbf{r}_2 \times \Delta)^T] \begin{bmatrix} \mathbf{v}_1 \\ \mathbf{w}_1 \\ \mathbf{v}_2 \\ \mathbf{w}_2 \end{bmatrix}\end{aligned}$$

where $\Delta = \mathbf{p}_2 - \mathbf{p}_1$. The matrix G is

$$G = [-\Delta^T - (\mathbf{r}_1 \times \Delta)^T \Delta^T (\mathbf{r}_2 \times \Delta)^T] \quad (6.137)$$

and depends implicitly on \mathbf{x}_1 , \mathbf{q}_1 , \mathbf{x}_2 , and \mathbf{q}_2 .

Data Structure for a Sparse Matrix

Recall that the first-order time derivative of the k th constraint function is the following, written in tensor index notation,

$$\dot{C}_k = C_{k,i}^{(x)} \dot{\mathbf{x}}_i + C_{k,i}^{(q)} \dot{\mathbf{q}}_i$$

where $C_{k,i}^{(x)}$ is the tensor representing $\partial C_k / \partial \mathbf{x}$ and $C_{k,i}^{(q)}$ is the tensor representing $\partial C_k / \partial \mathbf{q}$. The index i is repeated, so it is summed over. Only rigid bodies i_k and j_k take part in the constraint, so the summations have only four terms,

$$\dot{C}_k = C_{k,i_k}^{(x)} \dot{\mathbf{x}}_{i_k} + C_{k,i_k}^{(q)} \dot{\mathbf{q}}_{i_k} + C_{k,j_k}^{(x)} \dot{\mathbf{x}}_{j_k} + C_{k,j_k}^{(q)} \dot{\mathbf{q}}_{j_k}$$

Therefore, the k th row of G has only four nonzero entries. The k th row of G is

$$\left[0 \cdots 0 \frac{\partial C_k}{\partial \mathbf{x}_{i_k}} \frac{1}{2} \frac{\partial C_k}{\partial \mathbf{q}_{i_k}} Q_{i_k} 0 \cdots 0 \frac{\partial C_k}{\partial \mathbf{x}_{j_k}} \frac{1}{2} \frac{\partial C_k}{\partial \mathbf{q}_{j_k}} Q_{j_k} 0 \cdots 0 \right]$$

The matrix G is therefore sparse. To use the minimum amount of memory to store G , we need some mapping data structures. The *body map* is the $m \times 2$ matrix that stores the i_k and j_k indices for each of the m constraints,

$$B_{\text{map}} = \begin{bmatrix} i_1 & j_1 \\ \vdots & \vdots \\ i_m & j_m \end{bmatrix}$$

Each row G_k contains 12 nonzero entries. The vector $\partial C_k / \partial \mathbf{x}_{i_k}$ is 1×3 , representing 3 of the nonzero entries. The vector $\partial C_k / \partial \mathbf{q}_{i_k}$ is 1×4 and Q_{i_k} is 4×3 , so the product is 1×3 , representing 3 more nonzero entries. The 2 terms corresponding to j_k bring the total entries to 12. We can store all the nonzero entries in an $m \times 4$ block matrix whose entries are 1×3 vectors,

$$G_{\text{map}} = \begin{bmatrix} \frac{\partial C_1}{\partial \mathbf{x}_{i_1}} & \frac{1}{2} \frac{\partial C_1}{\partial \mathbf{q}_{i_1}} Q_{i_0} & \frac{\partial C_1}{\partial \mathbf{x}_{j_1}} & \frac{1}{2} \frac{\partial C_1}{\partial \mathbf{q}_{j_1}} Q_{j_0} \\ \vdots & \vdots & \vdots & \vdots \\ \frac{\partial C_m}{\partial \mathbf{x}_{i_m}} & \frac{1}{2} \frac{\partial C_m}{\partial \mathbf{q}_{i_m}} Q_{i_m} & \frac{\partial C_m}{\partial \mathbf{x}_{j_m}} & \frac{1}{2} \frac{\partial C_m}{\partial \mathbf{q}_{j_m}} Q_{j_m} \end{bmatrix}$$

Pseudocode for computing $\dot{\mathbf{C}} = \mathbf{G}\mathbf{V}$ is

```
float Cdot[m];
for (int k = 1; k <= m; ++k)
{
    int i_k = Bmap[k][1];
    int j_k = Bmap[k][2];
    Cdot[k] =
        Gmap[k][1]*linvel[i_k] + Gmap[k][2]*angvel[i_k] +
        Gmap[k][3]*linvel[j_k] + Gmap[k][4]*angvel[j_k];
}
```

The multiplications are between 1×3 vectors and 3×1 vectors, so they are really dot products. The computational work done inside the loop takes constant time, so the pseudocode is $O(m)$, which is linear in the number of constraints. Of course, $m = O(n^2)$, which says the number of constraints is in worst case quadratic in the number of rigid bodies. In practice, worstcase behavior is not expected (otherwise, redesign your game to reduce the number of interacting objects).

Computing the constraint force $\hat{\mathbf{F}} = \mathbf{G}^T\boldsymbol{\lambda}$ is an $O(m + n)$ process. Pseudocode is

```
Vector3 Fhat[2*n]; // force and torque per rigid body
for (int i = 1; i <= n; ++i)
{
    Fhat[2*i - 1] = Vector3::ZERO;
    Fhat[2*i      ] = Vector3::ZERO;
}
for (int k = 1; k <= m; ++k)
{
    int i_k = Bmap[k][1];
    int j_k = Bmap[k][2];
    Fhat[2*i_k - 1] += lambda[k]*Gmap[k][1]; // force
    Fhat[2*i_k      ] += lambda[k]*Gmap[k][2]; // torque
    Fhat[2*j_k - 1] += lambda[k]*Gmap[k][3]; // force
    Fhat[2*j_k      ] += lambda[k]*Gmap[k][4]; // torque
}
```

Inequality Constraints

The discussion in this section has been all about equality constraints. Inequality constraints must also be allowed to handle things like contact points during collision and joint angle limits. [Cat05] introduces this by allowing inequalities on the components of $\boldsymbol{\lambda}$; that is, a bounding interval $[\lambda_i^-, \lambda_i^+]$ may be specified for each component: $\lambda_i^- \leq \lambda_i \leq \lambda_i^+$. An equality constraint uses the entire real line, $\lambda_i \in (-\infty, +\infty)$. Inequality constraints have intervals that are not the entire real line, although it is not specified in the paper how you convert joint angle limits (conditions on constraint C_i) to an interval $(\lambda_i^-, \lambda_i^+)$.

When inequalities are introduced for the λ_i , the Gauss–Seidel iterations applied to equation (6.136) are not guaranteed to produce a solution that meets those

constraints. Instead, you must use *projected Gauss–Seidel iterations*, which amounts to clamping the current λ -values to the specified intervals after each iteration.

Constraint Bias

The principle of virtual work is discarded here, and the first-order time derivative $\dot{\mathbf{C}} = \mathbf{GV} = \mathbf{0}$ is relaxed to allow

$$\mathbf{GV} = \boldsymbol{\zeta} \neq \mathbf{0}$$

This has the consequence that the constraint force does work on the rigid bodies. To verify this, the work is the dot product of constraint force with velocity,

$$\mathbf{V}^T \hat{\mathbf{F}} = \mathbf{V}^T G^T \boldsymbol{\lambda} = (\mathbf{GV})^T \boldsymbol{\lambda} = \boldsymbol{\zeta}^T \boldsymbol{\lambda} \neq 0$$

The vector $\boldsymbol{\zeta}$ is called the *constraint bias* and may be a function of position and time. This is useful in the context of collision detection where penetration occurs and must be resolved.

Contact Model

The contact model is similar to that discussed in the acceleration-based dynamics, but penetration is allowed and must be resolved. Figure 6.51 shows two rigid bodies in contact at a single point.

The constraint function is the object separation measured as a signed distance along the normal direction \mathbf{N}_1 ,

$$C = (\mathbf{x}_2 + \mathbf{r}_2 - \mathbf{x}_1 - \mathbf{r}_1) \cdot \mathbf{N}_1$$

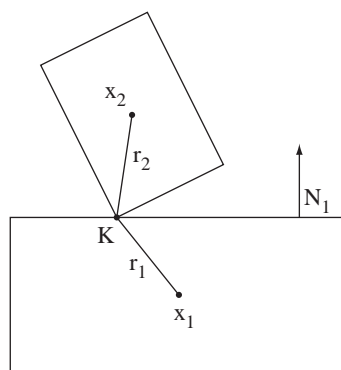


Figure 6.51 Two rigid bodies in contact at point \mathbf{K} . The centers of mass are \mathbf{x}_i and the offsets to the contact point are \mathbf{r}_i . The normal \mathbf{N}_1 is for rigid body 1.

Observe that $C > 0$ when the objects are separated, $C = 0$ when the objects are just touching, and $C < 0$ when the objects are overlapping (so there is penetration). The inequality constraint we want satisfied is $C \geq 0$.

The first-order time derivative of the constraint function is computed using the product rule

$$\dot{C} = (\mathbf{v}_2 + \mathbf{w}_2 \times \mathbf{r}_2 - \mathbf{v}_1 - \mathbf{w}_1 \times \mathbf{r}_1) \cdot \mathbf{N}_1 + (\mathbf{x}_2 + \mathbf{r}_2 - \mathbf{x}_1 - \mathbf{r}_1) \cdot \mathbf{w} \times \mathbf{N}_1$$

We used $\dot{\mathbf{N}}_1 = \mathbf{w} \times \mathbf{N}_1$, which follows from $\mathbf{N}_1 = R(t)\mathbf{b}_1$ for some body vector \mathbf{b}_1 . The derivative is

$$\dot{\mathbf{N}}_1 = \dot{R}\mathbf{b}_1 = \text{Skew}(\mathbf{w})R\mathbf{b}_1 = \text{Skew}(\mathbf{w})\mathbf{N}_1 = \mathbf{w} \times \mathbf{N}_1$$

In a simulation, the overlap is small, so the term

$$(\mathbf{x}_2 + \mathbf{r}_2 - \mathbf{x}_1 - \mathbf{r}_1) \cdot \mathbf{w} \times \mathbf{N}_1$$

itself is small and considered negligible – so it is discarded from the \dot{C} equation. The matrix G is determined by factoring the \dot{C} equation,

$$GV = \begin{bmatrix} -\mathbf{N}_1^T - (\mathbf{r}_1 \times \mathbf{N}_1)^T & \mathbf{N}_1^T & (\mathbf{r}_2 \times \mathbf{N}_1)^T \end{bmatrix} \begin{bmatrix} \mathbf{v}_1 \\ \mathbf{w}_1 \\ \mathbf{v}_2 \\ \mathbf{w}_2 \end{bmatrix}$$

The inequality for the λ component corresponding to the constraint force of the constraint is based on the following: The constraint force, which is parallel to \mathbf{N}_1 , must push the overlapping bodies apart but not pull them together. This implies $0 \leq \lambda < \infty$.

To undo any penetration, a Baumgarte scheme [Bau72] is used to push the bodies apart. A constraint bias is used,

$$\dot{C} = GV = -\beta C$$

where β is a constant that needs to be tuned for the method to work and where C is the constraint function. The equation $\dot{C} + \beta C = 0$ is a first-order linear differential equation whose solution is $C(t) = C(0) \exp(-\beta t)$. Since $C < 0$ when penetration occurs, we want C to vary towards zero over time, which forces $\beta > 0$. The constraint is part of the numerical differential equation solver, so we will solve $\dot{C} + \beta C = 0$ numerically. Using Euler's method, a simple analysis shows the numerical solver is stable as long as $0 < \beta < 2/\Delta t$ for time step $\Delta t > 0$ (see, for example, [BF01]). In practice, β should be chosen small enough for numerical stability but large enough to guarantee the penetration is undone over a reasonable amount of time.

Friction Model

A simplified friction model is used that treats static and dynamic friction in the same way. If \mathbf{N} is the contact normal at a contact point, two unit-length vectors \mathbf{U}_1 and \mathbf{U}_2 are chosen so that $\{\mathbf{U}_1, \mathbf{U}_2, \mathbf{N}\}$ is a right-handed orthonormal set. The friction force needs to prevent motion in the two tangential directions. Similar to how we formulated the constraint for the contact model, the time derivatives of the constraint functions are

$$\begin{aligned}\dot{C}_1 &= (\mathbf{v}_2 + \mathbf{w}_2 \times \mathbf{r}_2 - \mathbf{v}_1 - \mathbf{w}_1 \times \mathbf{r}_1) \cdot \mathbf{U}_1 \\ \dot{C}_2 &= (\mathbf{v}_2 + \mathbf{w}_2 \times \mathbf{r}_2 - \mathbf{v}_1 - \mathbf{w}_1 \times \mathbf{r}_1) \cdot \mathbf{U}_2\end{aligned}$$

By factoring, we have

$$G\mathbf{V} = \begin{bmatrix} -\mathbf{U}_1^T - (\mathbf{r}_1 \times \mathbf{U}_1)^T & \mathbf{U}_1^T (\mathbf{r}_2 \times \mathbf{U}_1)^T \\ -\mathbf{U}_2^T - (\mathbf{r}_1 \times \mathbf{U}_2)^T & \mathbf{U}_2^T (\mathbf{r}_2 \times \mathbf{U}_2)^T \end{bmatrix} \begin{bmatrix} \mathbf{v}_1 \\ \mathbf{w}_1 \\ \mathbf{v}_2 \\ \mathbf{w}_2 \end{bmatrix}$$

In practice it appears that there is no need for a constraint bias.

Coulomb's friction law requires the static and dynamic frictions to have magnitudes bounded by the normal force magnitude, thereby coupling the constraint force λ terms. To avoid this complication, a simplified model is used,

$$-\mu m_c g \leq \lambda_1 \leq \mu m_c g, \quad -\mu m_c g \leq \lambda_2 \leq \mu m_c g$$

where μ is the friction coefficient used both for static and dynamic friction (this is not the case for standard friction models). Each contact point is assigned some mass m_c . The typical choice is to distribute the mass uniformly among the contact points between the two interacting bodies.

Time Stepping

The equations of motion for the rigid body system are

$$M\ddot{\mathbf{V}} = \mathbf{F} + \hat{\mathbf{F}}$$

subject to the constraints $G\mathbf{V} = \boldsymbol{\zeta}$, where the constraint bias is included. In the section on computing the constraint force for a system of rigid bodies, I solved for $\dot{\mathbf{V}}$ in the equations of motion and substituted into the second-order time derivative of the constraints to obtain

$$GM^{-1}G^T \boldsymbol{\lambda} = - (GM^{-1}\mathbf{F} + \mathbf{V}^T H \mathbf{V})$$

where H is the Hessian tensor for the constraints. This system of equations may be solved using projected Gauss–Seidel iterations (so inequality constraints are allowed).

[Cat05] has an alternate approach. A first-order finite difference approximation is used for $\dot{\mathbf{V}}$, namely,

$$\dot{\mathbf{V}} \doteq \frac{\mathbf{V}^{(2)} - \mathbf{V}^{(1)}}{\Delta t}$$

where Δt is the time step, $\mathbf{V}^{(1)}$ is the velocity at the current time, and $\mathbf{V}^{(2)}$ is the new velocity that we need to compute. With the approximation, the equations of motion become

$$\mathbf{V}^{(2)} = \mathbf{V}^{(1)} + \Delta t M^{-1} (\mathbf{F} + G^T \boldsymbol{\lambda})$$

To satisfy the constraints (with bias), use $G\mathbf{V}^{(2)} = \boldsymbol{\zeta}$; then

$$\boldsymbol{\zeta} = G\mathbf{V}^{(1)} + \Delta t G M^{-1} (\mathbf{F} + G^T \boldsymbol{\lambda})$$

The equation may be rearranged to

$$G M^{-1} G^T \boldsymbol{\lambda} = \frac{\boldsymbol{\zeta} - G\mathbf{V}^{(1)}}{\Delta t} - G M^{-1} \mathbf{F}$$

and a solution is computed using projected Gauss–Seidel iterations.

The solution $\boldsymbol{\lambda}$ is substituted into the equation for $\mathbf{V}^{(2)} = (\mathbf{v}^{(2)}, \mathbf{w}^{(2)})$. The position and orientation are updated using standard first-order approximations to the differential equations of motion, namely,

$$\mathbf{x}^{(2)} = \mathbf{x}^{(1)} + \Delta t \mathbf{v}^{(2)}, \quad \mathbf{q}^{(2)} = \mathbf{q}^{(1)} + \frac{\Delta t}{2} Q^{(1)} \mathbf{w}^{(2)}$$

The integration scheme is semi-implicit Euler (*symplectic Euler*), because the new velocity is used to update the position. This integration scheme has good stability and conservation properties. That said, it would be of interest to compare this to the method that does not approximate $\dot{\mathbf{V}}$ and uses instead the quadratic term $\mathbf{V}^T H \mathbf{V}$ in the linear system for $\boldsymbol{\lambda}$.

Contact Caching

The projected Gauss–Seidel iterations may be slow to converge. The algorithms as stated here do not take advantage of space-time coherency for specifying the initial iterate $\boldsymbol{\lambda}_0$ in the linear system solving. [Cat05] describes a sophisticated scheme that caches contact points from the last frame. If possible, these are used to choose the initial values for $\boldsymbol{\lambda}_0$; otherwise, the initial values are set to zero. I leave it as an exercise for you to read the paper for the details of caching.

Mixed Linear Complementarity Problem

The algorithms in this section are considered to be *mixed linear complementarity problems* (MLCP). They are of the form

$$\begin{aligned}\mathbf{v} &= GM^{-1} G^T \boldsymbol{\lambda} - \boldsymbol{\eta} \\ \boldsymbol{\lambda}^- &\leq \boldsymbol{\lambda} \leq \boldsymbol{\lambda}^+ \\ v_i &= 0 \text{ if and only if } \lambda_i^- \leq \lambda_i \leq \lambda_i^+ \\ \lambda_i &= \lambda_i^- \text{ if and only if } v_i \geq 0 \\ \lambda_i &= \lambda_i^+ \text{ if and only if } v_i \leq 0\end{aligned}$$

where \mathbf{v} is referred to as the *constraint velocity*. The first two lines are part of the algorithms, regardless of whether you use the Hessian tensor term or the approximation of [Cat05]. The last three lines are complementarity conditions. The third line says the constraint can be satisfied as long as the λ component is within its interval bound. The last two lines state that the λ component will reach its bound only if the constraint is violated. For more details on MLCPs, see [CPS92].

6.8 VARIATIONS

Some of Chapter 6 has been about how to architect a general rigid body simulation using Newton's second law of motion, $\mathbf{F} = m\mathbf{a}$, and its implications for how position, orientation, linear velocity/momentum, and angular velocity/momentum change over time. In particular, a simulation based on impulsive forces to adjust linear and angular velocities and to prevent interpenetration and based on resting contact forces to prevent interpenetration was covered in detail. The simulation relies on a collision detection system to provide information about the constraints of motion. One requirement for a relatively simple system is that the rigid bodies be convex polyhedra. The intersection testing that we discussed uses the method of separating axes, both for stationary and for moving objects. The goal is for you to assemble a simulation of this type and see how it performs and what its strengths and weaknesses are. Academic and industrial researchers alike have tried various alternatives in building rigid body simulations. I briefly discuss a few of them here. References are provided to papers so that you can explore them once you are comfortable with the architecture of a simulation system as described in this book.

An alternative to impulsive forces is to use penalty-based methods in order to satisfy nonpenetration constraints. The idea is to track the distance between each pair of polytopes by maintaining the closest features for each pair [LC91, Lin93, CLMP95, Mir98]. This is done using Voronoi regions and allows an $O(1)$ update of the features (temporal and spatial coherence). An algorithm for tracking closest features using

BSP trees in the style of what was discussed earlier for extremal queries is [GV91] on multidimensional space partitioning. A recent paper on computing a directional lookup table for finding extremal points uses $O(n)$ preprocessing time for an $O(1)$ lookup [EL00]. Instead of using impulsive forces, the system internally modifies the simulation by adding springs between a pair of closest features that will lead to a colliding contact; the forces due to the springs are part of the force/torque calculations in the differential equation solver. As the distance between the closest features becomes small, the springs exert repulsive forces between the polytopes owning those features. A drawback of this approach is that the springs have large constants in the Hooke's law model, leading to stiff equations that cause numerical stability problems in the differential equation solver (see Chapter 13 on Numerical Methods and, in particular, Sections 13.9 and 13.10 on stability and stiff equations, respectively). Maintaining nonpenetration is also difficult with this approach.

People have also tried relaxing the constraint of nonpenetration. The differential equation solver computes the updates for position and orientation and the rigid bodies are moved. The objects may interpenetrate after the motion. The penetration distances can be computed for the polytopes and the objects are moved to undo the penetration. In this approach you need to compute distances between the polyhedra. The Gilbert-Johnson-Keerthi (GJK) distance algorithm [GJK88, vdB99, vdB01b] or the enhanced GJK distance algorithm [Cam97] is suitable for this system. The closest features [LC91] can be tracked to allow fast updating of the distance, another application of spatial and temporal coherence. The book [vdB03] covers these concepts in detail.

Variations have been tried regarding the linear complementarity problem (LCP) approach. The idea of contact force calculation is revisited in [Bar94], addressing both the issues of speed and of robustness when frictional forces are present. Nonlinear complementarity problems (NCP) have also been used to improve the robustness of calculation of contact forces. Resting contact has problems due to numerical round-off errors. The paper [BS99] deals with this by formulating the problem as an NCP. The brief paper [HKL⁺99] quickly summarizes the mathematics that goes into setting up an NCP problem for contact force calculation and provides pseudocode for an implementation. The NCP solver itself uses an LCP solver as a subtask. An energy-based approach for contact force computation is [Fau96]. An iterative scheme is used, the first pass handling force and torque computations and a global energy calculation. Subsequent passes redistribute energy about the system of objects. The method also handles static and sliding friction. A change of paradigm occurs in [RKC02b] and uses what is called *Gauss' principle of least constraints*. The LCP-based method is referred to as a *contact space formulation*. The number of degrees of freedom in this formulation is not explicit. The Gauss principle is formulated in what is called *motion space* and makes use of the explicit degrees of freedom to avoid unnecessary calculations. The abstract idea is that a *kinetic norm* is computed involving the constrained acceleration. In the current contact configuration, the norm is minimized to produce the constrained acceleration that is the closest acceleration to the unconstrained acceleration.

A variation on the impulsive force method allows you to simulate friction, as proposed by Gino van den Bergen [vdB01a] in the Usenet news group, `comp.games.development.programming.algorithms` excerpted as follows:

Contacts are resolved using impulses. At the time of collision, I have the contact points (I use only points, no higher-dimension simplices), a contact normal and a relative velocity for the contact points. The relative velocity is decomposed into a normal component and a tangential (along the surface) component. I compute the impulse in the direction of the normal that will result in the normal component of the relative velocity being set to zero. (In order to avoid, the objects drifting into each other, you'll have to do a correction using translations of the objects, such that the objects stay in contact, i.e., do not interpenetrate too much.)

I do the same for the tangential component. I compute the impulse that will set the relative velocity along the surface to zero. However, by applying this impulse, your objects will stick to the surface. They cannot slip since the friction is infinite. According to Coulomb's friction law, there is a maximum to the magnitude of the friction impulse that is proportional to the magnitude of the normal impulse. The ratio between the magnitude of the normal impulse and the magnitude of the maximum friction impulse is the friction coefficient. So, given the normal impulse, the magnitude of the maximum friction impulse is computed, and if the magnitude of the tangential impulse is greater than the maximum, the tangential impulse's magnitude is set to the maximum. In this way, it is possible to have slipping objects.

If the need for realism is really high, you should use different friction coefficients for slipping objects and “sticking” objects (the kinetic friction coefficient is usually smaller than the static coefficient for the same material), but I reckon that you can get by with only one coefficient. This is a games newsgroup after all. (Although, I guess that realistic racing games will use two coefficients for the maximum friction of the tyres.)

Finally, a lot of research has been done on collision detection systems themselves to develop fast, accurate, and robust systems. Some of the earliest work was simply based on algorithms for computing intersections of polyhedra. Nonconvex polyhedra naturally make the problem complicated, but hierarchical bounding volumes provide a relatively simple intersection system for two polyhedra represented as triangle meshes. The general idea is to localize where the intersections can occur by rapid culling of regions where they cannot be. Sphere trees were made popular by [Hub96] whereas oriented bounding box trees (OBB trees) and the method of separating axes were made popular by [GLM96]. A paper on hierarchical trees using axis-aligned bounding boxes is [vdB97]. The Wild Magic source code has an implementation for hierarchical bounding volumes. A templated class in the system is `BoundTree<Mesh, Bound>` and has an interface to support constructing bounding volume trees and supports the intersection queries. The template types `Mesh` and `Bound` must be classes that contained various member functions needed by `BoundTree`; the requirements are listed in the comments of the source files. The `CollisionGroup` and `CollisionRecord` classes

support the intersection query using the bounding volume trees of two objects. The *IntersectingCylinder* application shows how this collision system is used.

More sophisticated collision detection systems have been developed by one of the foremost groups in this area, the University of North Carolina GAMMA Research Group [GAM03]. GAMMA is the acronym for Geometric Algorithms for Modeling, Motion, and Animation). One of their original systems was RAPID (Robust and Accurate Polygon Interference Detection), which implements the OBB tree hierarchy of [GLM96] and is the basis for the Wild Magic code. RAPID did not use any coherence for intersection testing. Each test- or find-intersection query started anew the comparison between two OBB trees. If the tree is sufficiently deep, say 5 or 6 levels deep, the system can spend a lot of time comparing bounding volumes, especially when the two original triangle meshes are in close proximity to each other. Various systems have been built by UNC GAMMA over the years to improve on the disadvantages of the previous systems. Brief descriptions of some of these are provided here.

I-COLLIDE is an interactive and exact collision detection system that handles large environments of convex polyhedra [CLMP95]. Nonconvex polyhedra must be decomposed into convex polyhedra for this system to apply. The system uses temporal coherence via Voronoi regions as mentioned earlier in this section [LC91, Lin93]. *V-COLLIDE* [HLC⁺97] is a collision detection system that attempts to be more general than *I-COLLIDE* and is designed for environments with a large number of polygonal objects. The input models are allowed to be arbitrary (*polygon soups*). The system uses OBB trees as defined in RAPID but uses temporal coherence to speed up the location of possibly intersecting triangles in the system. The intersection candidate triangles are then tested for exact intersection. Similarities and differences among RAPID, *I-COLLIDE*, and *V-COLLIDE* are mentioned at [GAM03].

Another alternative intended to be more powerful than *I-COLLIDE* is *SWIFT*, Speedy Walking via Improved Feature Testing [EL00]. This is a package for collision detection, distance computation, and contact determination for polygonal objects undergoing rigid motions. The distance calculations can be approximate when the user specifies an error bound for the distance between objects or it can be exact. The contact determination uses bounding volume hierarchies and fast updating of closest features, just as earlier packages at UNC do. An evolution of the package is *SWIFT++* [EL01] and it supports nonconvex polyhedra. It also supports a proximity query that detects whether two objects are closer than a specified tolerance.

Other research at UNC includes *DEEP* (Dual-space Expansion for Estimating Penetration depth between convex polytopes) [KLM02]; *PIVOT* (Proximity Information from VOronoi Techniques) [IZLM01, IZLM02], systems that use graphics hardware acceleration to support the queries; *PQP* (Proximity Query Package) [LGML99], a system that uses sphere-swept volumes and supports overlap testing, distance computation, and tolerance verification; and *IMMPACT*, a system for partitioning and handling massive models for interactive collision detection [WLML99], where overlap graphs are used for localizing regions of interest. No surprise that *IMMPACT* also uses bounding volume hierarchies and spatial and temporal coherence.

Recent research regarding speedups, robustness, and accuracy of collision detection are provided by the following papers.

A non-UNC paper on a variation of I-COLLIDE and V-COLLIDE is called *Q-COLLIDE* [CW96], and it uses separating axes to determine intersections rather than tracking closest features, but still uses spatial and temporal coherence to speed up the calculations.

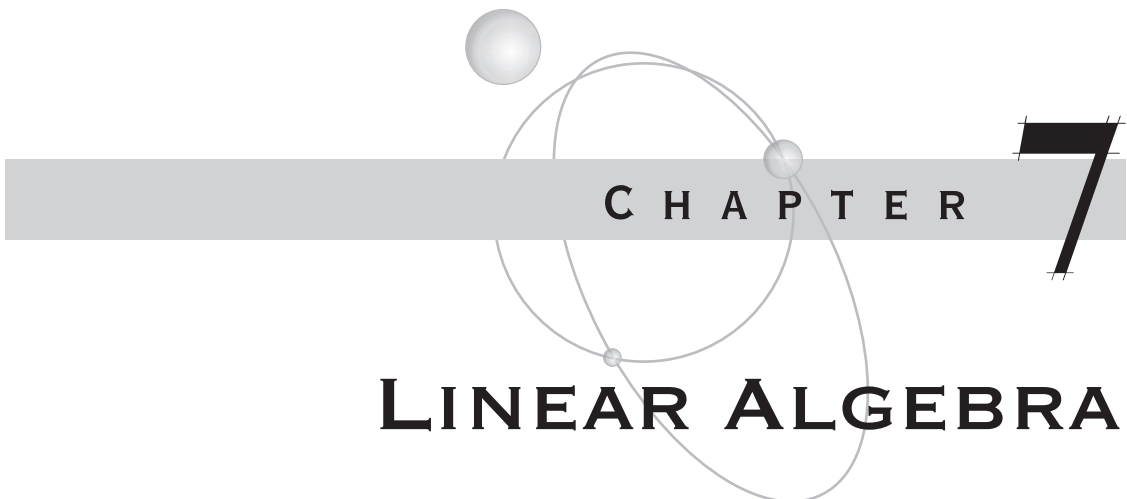
An efficient algorithm for collision detection for moving polyhedra is presented in [ST99]. Generally, it has been accepted that two polyhedra, each of $O(n)$ features (vertices, edges, or faces), requires $O(n^2)$ time to compute collisions. This paper shows that in the case of translational movements you can compute intersections in $O(n^{8/5} + \varepsilon)$ time, and in the case of rotational movements you can compute intersections in $O(n^{5/3} + \varepsilon)$ time; both are asymptotically subquadratic.

The paper [SSW99] describes the following setting. A polyhedron is moved through an environment that contains fixed polyhedral obstacles. Given a sequence of prescribed translations and rotations of the single polyhedron, the question is whether it can follow those transformations without colliding with the obstacles. Integer arithmetic is used for this algorithm. The maximum number of bits needed for intermediate calculations is shown to be $14L + 22$ where L is the maximal bit size for any input value. By knowing the maximum number of bits needed for the intermediate calculations, you can implement an exact arithmetic library with a fixed number of bytes for the integer type. The time performance of such a library is better than one supporting arbitrary precision arithmetic, the latter relying on dynamic memory management to allocate the integer objects. In a game application that uses floating point values to represent the data, an interface would be needed to hide the details of converting the floating point values to integer values needed as input in the exact arithmetic collision system.

A paper about reducing the time it takes to compute the collision time of two objects is [RKC00]. Under some restrictions on the object motion, it is shown that the collision time can be determined by solving polynomial equations of at most degree 3. A similar reduction to small degree polynomials can be made regarding the collision of two rotating OBBs. I showed earlier that the collision time of the intervals of projection of the OBBs onto a potential separating axis is a root to an equation $f(t) = 0$, where $f(t)$ involves sinusoids of different frequencies. By replacing sine and cosine by polynomials with a bounded error of approximation, the collision time is then computed as the root of a polynomial. Polynomial approximations to sine and cosine can be found on the CD-ROM in the source directory called Numerics.

In the discussion of OBBs moving with linear and/or angular velocity, I made the observation that during the time step of a differential equation solver, you can assume that an OBB is moving with constant linear velocity and constant angular velocity as an approximation to the theoretical motion (which you do not know; that is why the numerical solver is being used). Along these lines the papers [RKC01, RKC02a] propose arbitrary in-between motions to accurately predict the first time of contact.

These variations are by no means exhaustive. I apologize in advance for not including references to topics that readers believe should have been included here. An online search of some common terms in game physics (rigid body simulation, collision detection, etc.) will net you a *lot* of links. With a solid understanding of the material in this book, you should be able to quickly identify those links that are relevant to your pursuit of further knowledge in the field of game physics.



LINEAR ALGEBRA

7.1 A REVIEW OF NUMBER SYSTEMS

7.1.1 THE INTEGERS

We are all familiar with various number systems whose properties we take for granted. The simplest set of numbers is the *integers*. The basic operations on this set are addition and multiplication. Each operation takes a pair of integers and produces another integer. If n and m are integers, then $n + m$ and $n \cdot m$ are integers. The result of the operation does not depend on the order of the operands: $n + m = m + n$ and $n \cdot m = m \cdot n$. The operations are said to be *commutative*. When adding or multiplying three integers n , m , and p , the grouping of the operands is unimportant: $n + (m + p) = (n + m) + p$ and $n \cdot (m \cdot p) = (n \cdot m) \cdot p$. The operations are said to be *associative*. Because the grouping is unimportant, we may unambiguously write the sum as $n + m + p$ and the product as $n \cdot m \cdot p$. Multiplication is distributive across a sum: $n \cdot (m + p) = n \cdot m + n \cdot p$. The number zero is the *additive identity* in that $n + 0 = n$. Each integer n has an *additive inverse* $-n$ where $n + (-n) = 0$. This concept supports the definition of *subtraction* of two numbers n and m , namely $n - m = n + (-m)$. Finally, the number one is the *multiplicative identity* in that $n \cdot 1 = n$.

7.1.2 THE RATIONAL NUMBERS

The set of integers is deficient in a sense. Other than the numbers 1 and -1 , no integer has a *multiplicative inverse* that is itself an integer. If n is an integer such that $|n| \neq 1$,

there is no integer m for which $n \cdot m = 1$. The remedy for this is to define a superset of numbers that do have multiplicative inverses within that set. You are also familiar with this set, the *rational numbers*, that consists of all ratios n/m where n and m are integers and $m \neq 0$. A single rational number has many representations, for example $2/5$ and $4/10$ represent the same number. The standard representative is one for which the greatest common divisor of the numerator and denominator is 1. In the example, the greatest common divisor of 2 and 5 is 1, so this is the standard representative. The greatest common divisor of 4 and 10 is 2, so this number is not the standard, but can be reduced by dividing both numerator and denominator by 2. An integer n represented as a rational number is $n/1$, but for notational convenience, we still use n to represent the number.

Addition of rational numbers is based on addition of integers. If n_1/m_1 and n_2/m_2 are rational numbers, then the sum and product are defined by

$$\frac{n_1}{m_1} + \frac{n_2}{m_2} = \frac{n_1 \cdot m_2 + n_2 \cdot m_1}{m_1 \cdot m_2} \quad \text{and} \quad \frac{n_1}{m_1} \cdot \frac{n_2}{m_2} = \frac{n_1 \cdot n_2}{m_1 \cdot m_2}$$

The addition and multiplication operators on the left-hand sides of the definitions are those for the rational numbers. The addition and multiplication operators on the right-hand sides of the definitions are those for the integers. The rational operations have all the properties that the integer operations do: commutative, associative, and distributive. The rational number $0/1$ (or 0 for short) is the additive identity. The additive inverse of n/m is $(-n)/m$ (or $-n/m$ for short). The rational number $1/1$ (or 1 for short) is the multiplicative identity. The multiplicative inverse of n/m with $n \neq 0$ is m/n .

7.1.3 THE REAL NUMBERS

The rational numbers may also be thought of as deficient in the sense that certain algebraic equations with rational coefficients may not have rational roots. For example, the equation $16x^2 = 9$ has two rational roots, $x = \pm 3/4$. The equation $x^2 = 2$ does not have rational roots. Looking ahead, we need the concept of *irrational numbers*. The remedy is, once again, to define a superset of numbers, in this case the *real numbers*. The formal construction is nontrivial, normally taught in a course on real analysis, and is not presented here. The construction includes defining the addition and multiplication operations for real numbers in terms of the operations for rational numbers. The operations are commutative and associative and multiplication distributes across addition. The additive identity is the real number 0 and each number r has an additive inverse denoted $-r$. The multiplicative identity is the real number 1 and each nonzero number r has a multiplicative inverse denoted $1/r$. In this book, the set of real numbers is denoted by \mathbb{R} .

7.1.4 THE COMPLEX NUMBERS

And yet one more time we have another deficiency. Algebraic equations with real coefficients may not have real roots. We can now solve $x^2 = 2$ to obtain two real solutions $x = \pm\sqrt{2}$, but $x^2 = -1$ does not have real solutions since the square of a nonzero real number must be positive. The remedy is to define a subset of numbers, in this case the *complex numbers*. The symbol i is defined to be a complex number for which $i^2 = -1$. Complex numbers are written in the form $x + iy$, where x and y are real numbers. Addition is defined by

$$(x_1 + iy_1) + (x_2 + iy_2) = (x_1 + x_2) + i(y_1 + y_2)$$

and multiplication is defined by

$$(x_1 + iy_1) \cdot (x_2 + iy_2) = (x_1x_2 - y_1y_2) + i(x_1y_2 + x_2y_1)$$

The additive identity is $0 + i0$ (or 0 for short). The additive inverse of $x + iy$ is $(-x) + i(-y)$ (or $-x - iy$ for short). The multiplicative identity is $1 + i0$ (or 1 for short). The multiplicative inverse of $x + iy$, assuming not both x and y are zero, is

$$\frac{1}{x + iy} = \frac{x}{x^2 + y^2} - i\frac{y}{x^2 + y^2}$$

The addition and multiplication operators are commutative and associative and multiplication distributes across addition. The set of complex numbers is finally *complete* in the sense that the roots of any polynomial equation with complex-valued coefficients are always representable as complex numbers. This result is the fundamental theorem of algebra.

7.1.5 FIELDS

The arithmetic properties of the rational numbers, the real numbers, and the complex numbers may be abstracted. The general concept is a *field* that consists of a set F of numbers, an addition operator ($+$), and a multiplication operator (\cdot) that satisfy the following axioms. In the axioms, x , y , and z are elements of F .

1. $x + y$ is in F (set is closed under addition).
2. $x + y = y + x$ (addition is commutative).
3. $(x + y) + z = x + (y + z)$ (addition is associative).
4. There is an element 0 in F such that $x + 0 = x$ for all x in F (additive identity).
5. For each x in F , there is an element $-x$ in F such that $x + (-x) = 0$ (additive inverses).
6. $x \cdot y$ is in F (set is closed under multiplication).

7. $x \cdot y = y \cdot x$ (multiplication is commutative).
8. $(x \cdot y) \cdot z = x \cdot (y \cdot z)$ (multiplication is associative).
9. $x \cdot (y + z) = x \cdot y + x \cdot z$ (multiplication distributes across addition).
10. There is an element 1 in F such that $x \cdot 1 = c$ for all x in F (multiplicative identity).
11. For each $x \neq 0$ in F , there is an element x^{-1} such that $x \cdot x^{-1} = 1$ (multiplicative inverses).

This topic and related ones are usually presented in an undergraduate course in abstract algebra.

7.2 SYSTEMS OF LINEAR EQUATIONS

Suppose that a_1 through a_m and b are known constants and that x_1 through x_m are variables. The equation

$$a_1x_1 + \cdots + a_mx_m = b$$

is called a *linear equation*. A common problem in applications is to have to solve a system of n linear equations in m unknown variables. In most cases $n = m$, but the method of solution applies even if this is not the case. As we shall see, the system has no solutions, one solution, or infinitely many solutions. The method of solution involves elimination of one variable at a time from the equations. This phase is referred to as *forward elimination*. At the end of the phase, the first equation has m variables, the second equation has $m - 1$ variables, and so on, the last equation having 1 variable. The equations are then processed in reversed order to eliminate variables and obtain the final solution (if any). This phase is referred to as *back substitution*.

EXAMPLE
7.1

Here is a simple example for mixing two acid solutions to obtain a desired ratio of acid to water. Determine how many liters of a 10% and a 15% solution of acid must be used to produce 3 liters of a 12% solution of acid. Let x and y represent the number of liters of 10% and 15% solutions, respectively. Intuitively, $x > y$ since 12 is closer to 10 than 15. Two conservation rules apply. Conservation of volume implies

$$\begin{array}{ccc} x & + & y \\ \text{Liters of 10\% solution} & & \text{Liters of 15\% solution} & = & \text{Liters of 12\% solution} & = & 3 \end{array}$$

Conservation of acid implies

$$\begin{array}{ccc} 0.10x & + & 0.15y \\ \text{Acid in 10\% solution} & & \text{Acid in 15\% solution} & = & \text{Acid in 12\% solution} & = & 0.12(3) \end{array}$$

Thus, we have two equations in two unknowns, $x + y = 3$ and $0.10x + 0.15y = 0.36$. Forward elimination is used to remove x from the second equation. The first equation

implies $x = 3 - y$. Substitute in the second equation to eliminate x and obtain $0.36 = 0.10(3 - y) + 0.15y = 0.05y + 0.30$. The last equation is solved for $y = 6/5$. Back substitution is used to replace the occurrence of y in the first equation, $x = 3 - 6/5 = 9/5$. The final answer is that $9/5$ liters of the 10% solution and $6/5$ liters of the 15% solution combine to produce 3 liters of the 12% solution. ■

**EXAMPLE
7.2**

Here is an example of a system of three linear equations in three unknowns: (1) $x + y + z = 6$, (2) $x + 2y + 2z = 11$, and (3) $2x + 3y - 4z = 3$. The forward elimination process is applied first. Use the first equation to eliminate x in the other equations. Multiply [equation 1](#) by -1 and add to [equation 2](#):

$$\begin{array}{r} -x - y - z = -6 \\ x + 2y + 2z = 11 \\ \hline y + z = 5 \end{array}$$

Multiply [equation 1](#) by -2 and add to [equation 3](#):

$$\begin{array}{r} -2x - 2y - 2z = -12 \\ 2x + 3y - 4z = 3 \\ \hline y - 6z = -9 \end{array}$$

We now have two equations in two unknowns: $y + z = 5$ and $y - 6z = -9$. Multiply [equation 1](#) by -1 and add to [equation 2](#):

$$\begin{array}{r} -y - z = -5 \\ y - 6z = -9 \\ \hline -7z = -14 \end{array}$$

We now have one equation in one unknown: $-7z = 14$. In summary, forward elimination has produced the equations $x + y + z = 6$, $y + z = 5$, and $-7z = 14$. Back substitution is the next process. Solve [equation 3](#) for $z = 2$. Substitute this z value in [equation 2](#), $5 = y + z = y + 2$, and solve for $y = 3$. Substitute the z and y values in [equation 1](#), $6 = x + y + z = x + 3 + 2$, and solve for $x = 1$. The system has a single solution $x = 1$, $y = 3$, and $z = 2$. ■

There are a couple of snags that can be encountered in forward elimination. The next two examples illustrate these and how to get around them.

**EXAMPLE
7.3**

In this example, the right-hand side values are unimportant in the illustration. We simply put asterisks in these places. Consider

$$\begin{array}{r} x + y + z = * \\ 2x + 2y + 5z = * \\ 4x + 6y + 8z = * \end{array}$$

(Example 7.3
continued)

Use [equation 1](#) to eliminate x from [equations 2](#) and [3](#). Multiply [equation 1](#) by -1 and add to [equation 2](#). Multiply [equation 1](#) by -4 and add to [equation 3](#) to obtain the system

$$\begin{aligned}x + y + z &= * \\+ 3z &= * \\2y + 4z &= *\end{aligned}$$

There is no y -term in [equation 2](#), so you cannot use it to eliminate the y -term in [equation 3](#). In order to continue the formal elimination process, you must swap the last two equations. The swap has no effect on the algebraic process of solving the equations, but it is convenient in establishing an algorithm that a computer could use in solving systems. After swapping we have

$$\begin{aligned}x + y + z &= * \\2y + 4z &= * \\3z &= *\end{aligned}$$

Forward elimination is now complete and back substitution may be applied to obtain a solution. ■

EXAMPLE
7.4

In the following system, the constants on the right-hand sides of the equation are denoted a , b , and c , but are still considered to be known values:

$$\begin{aligned}x + y + z &= a \\2x + 2y + 5z &= b \\4x + 4y + 8z &= c\end{aligned}$$

Use [equation 1](#) to eliminate x from [equations 2](#) and [3](#). Multiply [equation 1](#) by -2 and add to [equation 2](#). Multiply [equation 1](#) by -4 and add to [equation 3](#). The resulting system is

$$\begin{aligned}x + y + z &= a \\3z &= b - 2a \\4z &= c - 4a\end{aligned}$$

There is no y -term in either [equation 2](#) or [3](#). Instead we proceed to the next variable, z , in the second equation and use it to eliminate z in the third equation. Multiply [equation 2](#) by $-4/3$ and add to [equation 3](#).

$$\begin{aligned}x + y + z &= a \\3z &= b - 2a \\0 &= (c - 4a) - 4(b - 2a)/3\end{aligned}$$

The last equation contains none of the original variables, but nonetheless must still be a true statement. That is, the constants a , b , and c , whatever they might be, must satisfy

$(c - 4a) - 4(b - 2a)/3 = 0$. If they do not, the system of equations has no solutions; no choice of x , y , and z can force the last equation to be true. For example, if $a = 1$, $b = -1$, and $c = 1$, $(c - 4a) - 4(b - 2a)/3 = 1 \neq 0$, and the system has no solutions. If the constants do satisfy the last equation, the first two equations can be manipulated further. The second equation is solved for $z = (b - 2a)/3$. Replacing this in the first equation and moving the constant terms to the right-hand side, we have

$$x + y = a - (b - 2a)/3 = (5a - b)/3$$

One of the variables may be freely chosen, the other variable depending on the choice. If y is freely chosen, then $x = (5a - b)/3 - y$. There are infinitely many choices for y (any real number), so the system of equations has infinitely many solutions. For example, if $a = 1$, $b = -1$, and $c = 0$, $(c - 4a) - 4(b - 2a)/3 = 0$ and the solutions are tabulated as

$$(x, y, z) = (-y + 2, y, -1) = y(-1, 1, 0) + (2, 0, -1)$$

which emphasizes the dependence on the free parameter y . ■

7.2.1 A CLOSER LOOK AT TWO EQUATIONS IN TWO UNKNOWNS

Let us take a closer look at the forward elimination for a system of two equations,

$$\begin{aligned} a_{11}x_1 + a_{12}x_2 &= b_1 \\ a_{21}x_1 + a_{22}x_2 &= b_2 \end{aligned}$$

The coefficients a_{ij} and the right-hand sides b_j are known constants. The x_j are the unknowns. For the sake of argument, assume $a_{11} \neq 0$ so that no row swapping is needed. To eliminate x_1 from [equation 2](#), multiply [equation 1](#) by a_{21}/a_{11} and subtract from [equation 2](#). The resulting system is

$$\begin{aligned} a_{11}x_1 + (a_{12})x_2 &= b_1 \\ \left(a_{22} - a_{12} * \frac{a_{21}}{a_{11}}\right)x_2 &= b_2 - b_1 * \frac{a_{21}}{a_{11}} \end{aligned}$$

Observe that you do not need to compute $a_{21} - a_{11} * a_{21}/a_{11}$ since the multiplier was chosen so that this term is zero. To solve using back substitution, solve the second equation for x_2 :

$$x_2 = \frac{b_2 - b_1 * \frac{a_{21}}{a_{11}}}{a_{22} - a_{12} * \frac{a_{21}}{a_{11}}}$$

Substitute this in the first equation and solve for x_1 :

$$x_1 = \frac{b_1 - a_{12} * x_2}{a_{11}}$$

The method of solution needs to be implemented for a computer. A practical concern is the amount of time required to compute a solution. The number of cycles for floating point addition/subtraction, multiplication, and division can vary on different processors. Historically, additions and subtractions were the fastest to compute, multiplication somewhat slower, and division the slowest. A speedy implementation had to be concerned about the cycle counts for the operations, sometimes replacing the slower operations with fast ones. For example, if addition requires α cycles and multiplication requires μ cycles, then the floating point expression $2*x$ requires μ cycles to compute. The expression written instead as $x+x$ requires α cycles. If $\alpha < \mu$, then the application most likely would choose to use the latter expression. A variation on this is to compute $3*x$ using μ cycles or $x+x+x$ using 2α cycles. Again, if the cost for an addition is less than half that for a multiplication, then the latter expression is a better choice for speed.

A more interesting example is in the product of two complex numbers, $(a + bi) * (c + di) = (a * c - b * d) + (a * d + b * c)i$. The expression on the right-hand side requires four multiplications and two additions for a cost of $4\mu + 2\alpha$ cycles. An alternate form of the right-hand side is $(d * (a - b) + a * (c - d)) + (d * (a - b) + b * (c + d))i$. The expression $d * (a - b)$ is common to the real and imaginary parts, so only needs to be computed once. The alternate form requires 3 multiplications and 5 additions for a cost of $3\mu + 5\alpha$. As long as an addition is less than one third the cost of a multiplication, the alternate form is cheaper to compute.

On some current-generation processors, additions and multiplications require the same number of cycles. Tricks of the form discussed previously are no longer of use in this setting. In fact, as hardware has evolved to eliminate the disparity between cycle counts for basic arithmetic operations, other issues have become important. Inexpensive comparisons were once used to steer the flow of computation along a path that minimizes the cycle count for arithmetic operations. Now comparisons can be more expensive to compute than additions or multiplications, so the steering might lead to a larger cycle count than by just using a direct path. Cache misses, floating point stalls, branch penalties, parallel integer and floating point units, and a collection of other issues must be dealt with when implementing algorithms. They will certainly make your programming life interesting!

Well, that was a long digression. How does it relate to linear systems? In the example of a system of two equations, the expressions that are computed, in order, are listed below:

1. Compute $c_1 = a_{21}/a_{11}$.
2. Compute $d_1 = a_{22} - a_{12} * c_1$.
3. Compute $e_1 = b_2 - b_1 * c_1$.
4. Solve for $x_2 = e_1/d_1$.
5. Compute $f_1 = b_1 - a_{12} * x_2$.
6. Solve for $x_1 = f_1/a_{11}$.

The algorithm requires three additions, three multiplications, and three divisions. Division is still typically more expensive to compute than additions and multiplications, so you might try to eliminate them (if possible). Convince yourself that the following sequence also leads to a solution:

1. Compute $c_2 = a_{11} * a_{22} - a_{21} * a_{12}$.
2. Compute $d_2 = a_{11} * b_2 - a_{21} * b_1$.
3. Solve for $x_2 = c_2/d_2$.
4. Compute $e_2 = b_1 - a_{12} * x_2$.
5. Solve for $x_1 = e_2/a_{11}$.

This algorithm requires three additions, five multiplications, and two divisions. The trade-off is that one division has been replaced by two multiplications. Whether that is a reduction in cycles depends on your processor. On most current processors, it is.

Other time-saving options depend on how you plan on using the solution (x_1, x_2) . For example, if your application needs only to compare the solution to see if it lies in a rectangle, the divisions are not required at all. Suppose the comparisons to be tested are $x_1 \in [u_1, v_1]$ and $x_2 \in [u_2, v_2]$. The pseudocode using x_1 and x_2 directly is

```
bool Contains (float x1, float x2, float u1, float v1, float u2,
               float v2)
{
    return u1 <= x1 && x1 <= v1 && u2 <= x2 && x2 <= v2;
```

The divisions can be avoided:

```
bool Contains (float e2, float a11, float c2, float d2, float u1,
               float v1, float u2, float v2)
{
    if (a11 > 0)
    {
        if (d2 > 0)
        {
            return a11 * u1 <= e2 && e2 <= a11 * v1
                && d2 * u2 <= c2 && c2 <= d2 * v2;
        }
        else
        {
            return a11 * u1 >= e2 && e2 >= a11 * v1
                && d2 * u2 >= c2 && c2 >= d2 * v2;
        }
    }
    else
    {
        if (d2 > 0)
```

```

    {
        return a11 * u1 >= e2 && e2 >= a11 * v1
        && d2 * u2 >= c2 && c2 >= d2 * v2;
    }
    else
    {
        return a11 * u1 <= e2 && e2 <= a11 * v1
        && d2 * u2 <= c2 && c2 <= d2 * v2;
    }
}
}

```

The two divisions have been replaced by four multiplications and two comparisons, in worst case. It is possible that not all multiplications are performed since an early return can occur if one of the Boolean subexpressions is false. On most current processors, the alternate method will reduce the cycle count.

7.2.2 GAUSSIAN ELIMINATION AND ELEMENTARY ROW OPERATIONS

I believe we now have a sufficient grasp on the methods of forward elimination and back substitution to look at the general setting. The total process is called *Gaussian elimination* and starts with n linear equations in m unknowns:

$$\begin{aligned} a_{11}x_1 + a_{12}x_2 + \cdots + a_{1m}x_m &= b_1 \\ a_{21}x_1 + a_{22}x_2 + \cdots + a_{2m}x_m &= b_2 \\ &\vdots \\ a_{n1}x_1 + a_{n2}x_2 + \cdots + a_{nm}x_m &= b_n \end{aligned}$$

where the coefficients a_{ij} and inputs b_i are known and where the x_j are unknown ($1 \leq i \leq n$, $1 \leq j \leq m$). The system can be written more concisely as

$$\sum_{j=1}^m a_{ij}x_j = b_i, \quad 1 \leq i \leq n$$

The coefficients a_{ij} can be written in tabular form, called a *matrix*, $A = [a_{ij}]$. The table has n rows indexed by i and m columns indexed by j . The numbers b_i can be written in tabular form, called a *column matrix*, $\mathbf{b} = [b_i]$. This table also has n rows indexed by i but only a single column. The variables x_j can be written as a column matrix, $\mathbf{x} = [x_j]$, that has m rows indexed by j . Using the tabular forms, the system may be suggestively written as $A\mathbf{x} = \mathbf{b}$, where the implied product $A\mathbf{x}$ denotes the operations necessary to reconstruct the left-hand sides of the equations in the system. In a later section I will define the general operation for multiplying matrices. The elimination process algebraically manipulates the entries of the A and \mathbf{b} matrices. The bookkeeping is concisely represented in terms of operations on A , \mathbf{b} , and the *augmented matrix* $[A|\mathbf{b}]$, the matrix with n rows and $m+1$ columns that is obtained by appending \mathbf{b} on the right of A .

Forward elimination is equivalent to applying what are called *elementary row operations* to the augmented matrix. These operations are

1. Interchange row i with row j . Notation: $R_i \leftrightarrow R_j$.
2. Multiply row i by a scalar $c \neq 0$. Notation: $cR_i \rightarrow R_i$.
3. Multiply row i by a scalar c_i , multiply row j by a scalar c_j , then add the results and replace row j . Notation: $c_i R_i + c_j R_j \rightarrow R_j$.

The sequential application of the operations is performed until the following rules are satisfied:

1. If row r has its first nonzero entry in column c , then every entry in column c below row r is zero.
2. If row r_1 has its first nonzero entry in column c_1 , row r_2 has its first nonzero entry in column c_2 , and $r_1 < r_2$, then $c_1 < c_2$ is required.
3. Each row having all zero entries must lie below any other row having at least one nonzero entry.

**EXAMPLE
7.5**

Solve $x_1 + x_2 + x_3 = 6$, $x_1 + 2x_2 + 2x_3 = 11$, $2x_1 + 3x_2 - 4x_3 = 3$. The augmented matrix is

$$[A|\mathbf{b}] = \left[\begin{array}{ccc|c} 1 & 1 & 1 & 6 \\ 1 & 2 & 2 & 11 \\ 2 & 3 & -4 & 3 \end{array} \right]$$

Apply elementary row operations to $[A|\mathbf{b}]$ so that the above rules are satisfied. For each row of the matrix, try to satisfy rule 1. The entry in the row which is used to eliminate the column entries below it is called a *pivot* and is nonzero. The pivots are indicated below by boxes. The process of getting from one matrix to another is denoted by the operator symbol \sim . The elementary row operations applied in that step are written below that symbol.

$$\left[\begin{array}{ccc|c} \boxed{1} & 1 & 1 & 6 \\ 1 & 2 & 2 & 11 \\ 2 & 3 & -4 & 3 \end{array} \right] \sim \left[\begin{array}{ccc|c} 1 & 1 & 1 & 6 \\ 0 & \boxed{1} & 1 & 5 \\ 0 & 1 & -6 & -9 \end{array} \right]$$

$$\sim \left[\begin{array}{ccc|c} 1 & 1 & 1 & 6 \\ 0 & 1 & 1 & 5 \\ 0 & 0 & -7 & -14 \end{array} \right]$$

$$\sim \left[\begin{array}{ccc|c} 1 & 1 & 1 & 6 \\ 0 & 1 & 1 & 5 \\ 0 & 0 & -7 & -14 \end{array} \right]$$

The system of equations corresponding to this reduced matrix is $x_1 + x_2 + x_3 = 6$, $x_2 + x_3 = 5$, and $-7x_3 = -14$. ■

Back substitution involves solving for x_n, x_{n-1}, \dots, x_1 , one at a time using the system obtained by forward elimination. In the last example we can solve the third equation for $x_3 = 2$. Substituting x_3 in the second equation: $x_2 = 5 - x_3 = 5 - 2 = 3$. Substituting x_2 and x_3 in the first equation: $x_1 = 6 - x_2 - x_3 = 6 - 3 - 2 = 1$.

We will now count operations, just like we did for the case of two equations in two unknowns. To simplify matters, let us assume that $m = n$ and that no rows need to be swapped. The first step of forward elimination is to zero out all entries below a_{11} in the first column.

$$\begin{aligned}
 [A|\mathbf{b}] &= \left[\begin{array}{cccc|c} a_{11} & a_{12} & \cdots & a_{1n} & b_1 \\ a_{21} & a_{22} & \cdots & a_{2n} & b_2 \\ \vdots & \vdots & & \vdots & \vdots \\ a_{n1} & a_{n2} & \cdots & a_{nn} & b_n \end{array} \right] \\
 &\sim \left[\begin{array}{ccccc|c} a_{11} & a_{12} & \cdots & a_{1n} & b_1 \\ 0 & a_{11}a_{22} - a_{21}a_{12} & \cdots & a_{11}a_{2n} - a_{21}a_{1n} & a_{11}b_2 - a_{21}b_1 \\ \vdots & \vdots & & \vdots & \vdots \\ 0 & a_{11}a_{n2} - a_{n1}a_{12} & \cdots & a_{11}a_{nn} - a_{n1}a_{1n} & a_{11}b_n - a_{n1}a_{11}b_1 \end{array} \right] \\
 &= \left[\begin{array}{cccc|c} a_{11} & a_{12} & \cdots & a_{1n} & b_1 \\ 0 & a'_{11} & \cdots & a'_{1,n-1} & b'_1 \\ \vdots & \vdots & & \vdots & \vdots \\ 0 & a'_{n-1,1} & \cdots & a'_{n-1,n-1} & b'_{n-1} \end{array} \right]
 \end{aligned}$$

Note that the $(n - 1) \times n$ submatrix consisting of the a'_{ij} and b'_i is set up for the next forward elimination step, thus leading to a recursive process.

Define C_n to be the cost of the arithmetic operations for solving the system of equations using Gaussian elimination. Let F_n be the cost of forward elimination and let B_n be the cost of back substitution; then $C_n = F_n + B_n$. The forward elimination phase takes an augmented matrix of size $n \times (n + 1)$ and reduces the problem to one involving an augmented matrix of size $(n - 1) \times n$. The cost for forward elimination on the reduced augmented matrix is F_{n-1} . The elimination requires $n - 1$ elementary row operations. Each row operation modifies n column entries; we do not count the replacement of the first column entry by zero. Each modified column entry requires 2 multiplications and 1 addition. If α represents the cost of an addition and μ represents the cost of a multiplication, the zeroing of the first column entries has a cost $(2\mu + \alpha)n(n - 1)$. The forward elimination cost must satisfy

$$F_n = (2\mu + \alpha)n(n - 1) + F_{n-1}, \quad n \geq 2$$

For a single equation in a single unknown ($n = 1$), no forward elimination is necessary, so $F_1 = 0$. This is an example of a *linear difference equation*. This equation,

though, is easy to solve. Note that

$$\begin{aligned} F_i - F_{i-1} &= (2\mu + \alpha)i(i-1) \\ \sum_{i=2}^n (F_i - F_{i-1}) &= \sum_{i=2}^n (2\mu + \alpha)i(i-1) \\ F_n - F_1 &= (2\mu + \alpha) \sum_{i=2}^n i(i-1) \\ F_n &= (2\mu + \alpha) \frac{n(n^2 - 1)}{3} \end{aligned}$$

The summation on the left-hand side is called a *telescoping sum*. The quantity $-F_j$ appears in one term of the summation, then appears as F_j in the next term and is cancelled. The cancellation occurs for all but F_1 and F_n . The right-hand summation is evaluated using standard formulas for summation, $\sum_{i=1}^n i = n(n+1)/2$ and $\sum_{i=1}^n i^2 = n(n+1)(2n+1)/6$. The number of operations for forward elimination is therefore on the order of n^3 .

Now let us compute the cost of back substitution. After forward elimination, the augmented matrix is of the form

$$\left[\begin{array}{cccc|c} \alpha_{11} & \alpha_{12} & \cdots & \alpha_{1n} & \beta_1 \\ 0 & \alpha_{22} & \cdots & \alpha_{2n} & \beta_2 \\ \vdots & \ddots & \ddots & \vdots & \vdots \\ 0 & 0 & \cdots & \alpha_{nn} & \beta_n \end{array} \right]$$

where $\alpha_{ij} = 0$ for $i > j$. The back substitution is

$$\begin{aligned} x_n &= \frac{\beta_n}{\alpha_{nn}} && \text{1 division} \\ x_{n-1} &= \frac{\beta_{n-1} - \alpha_{n-1,n} * x_n}{\alpha_{n-1,n-1}} && \text{1 multiply, 1 add, 1 division} \\ &\vdots \\ x_1 &= \frac{\beta_1 - \alpha_{12} * x_2 - \cdots - \alpha_{1n} * x_n}{\alpha_{11}} && \text{n-1 multiplies, n-1 adds, 1 division} \end{aligned}$$

If δ is the cost of a division and α and μ are as before,

$$\begin{aligned} B_n &= (\delta) + (\mu + \alpha + \delta) + \cdots + ((n-1)\mu + (n-1)\alpha + \delta) \\ &= \delta n + \sum_{i=0}^{n-1} (\mu + \alpha)i \\ &= \delta n + (\mu + \alpha) \frac{n(n-1)}{2} \end{aligned}$$

The number of operations is on the order of n^2 , so clearly forward elimination is the dominant cost in solving the system. The total cost for Gaussian elimination is

$$C_n = F_n + B_n = (2\mu + \alpha) \frac{n(n^2 - 1)}{3} + (\mu + \alpha) \frac{n(n - 1)}{2} + \delta n$$

A long story, but this is the classical method for solving linear systems and counting how many operations it takes to estimate the cost of solving systems. The cost is not particularly important for small n , but for very large n it becomes an issue.

EXERCISE

7.1

The forward elimination is designed to satisfy the constraint mentioned earlier: *If row r has its first nonzero entry in column c , then every entry in column c below row r is zero.* Change this constraint to: *If row r has its first nonzero entry in column c , then every other entry in column c is zero.* The entries above as well as below entry (r, c) must be zeroed out using elementary row operations. Determine the total cost C_n for this new elimination method. Compare it to the cost for Gaussian elimination. ■

7.2.3 NONSQUARE SYSTEMS OF EQUATIONS

Although I illustrated Gaussian elimination for systems of equations with the same number of unknowns as equations, the same process applies to systems with any number of equations and unknowns.

In general after application of the relevant elementary row operations, if row r has its first nonzero entry in column c , then the variable x_c is referred to as a *basic variable*. All other variables are referred to as *free variables*. The quantity of basic variables is called the *rank* of the matrix, denoted $\text{rank}(A)$, where A is the matrix of coefficients. Gaussian elimination allows us to solve for the basic variables in terms of the free variables.

If $Ax = b$ is the linear system, where A is an $n \times m$ matrix, then the following holds. If $\text{rank}(A) < \text{rank}([A|b])$, the system has no solutions. Otherwise, $\text{rank}(A) = \text{rank}([A|b])$. In this case, if $\text{rank}(A) = m$, then the system has a unique solution. Otherwise, $\text{rank}(A) < m$ and the system has infinitely many solutions; the number of free variables is $m - \text{rank}(A)$.

7.2.4 THE GEOMETRY OF LINEAR SYSTEMS

The previous sections were about the algebraic manipulations needed to solve a system of linear equations. The linear equations have geometric counterparts that, perhaps, provide greater insight about what the solution set of a system really is. Let us look at the simplest example, a system of two equations in two unknowns.

Consider $a_{11}x_1 + a_{12}x_2 = b_1$ and $a_{21}x_1 + a_{22}x_2 = b_2$. I assume that one of a_{11} and a_{12} is nonzero and one of a_{21} and a_{22} is nonzero. Each of these equations represents a line in the plane. The geometric possibilities are listed below.

1. The lines are not parallel. They intersect in a single point.
2. The lines are parallel and disjoint. They do not intersect.
3. The lines are the same. The set of points common to both is infinite.

Figure 7.1 shows these configurations.

The vector (a_{11}, a_{12}) is normal to the first line and the vector (a_{21}, a_{22}) is normal to the second line. If the two lines are parallel or the same line, then their normals are parallel. Consequently, one vector is a multiple of the other, say $(a_{11}, a_{12}) = t(a_{21}, a_{22})$ for some nonzero scalar t . Define $d = a_{11}a_{22} - a_{12}a_{21}$; then

$$d = a_{11}a_{22} - a_{12}a_{21} = ta_{21}a_{22} - ta_{22}a_{21} = 0$$

Conversely, the two lines are not parallel when $d \neq 0$, an algebraic condition that guarantees that the two lines intersect in a single point and the linear system has a unique solution. If $d = 0$, the lines are parallel and either disjoint or coincident. The second equation of the system can be multiplied by t to obtain

$$tb_2 = ta_{21}x_1 + ta_{22}x_2 = a_{11}x_1 + a_{12}x_2 = b_1$$

These equalities are valid only when $b_1 = tb_2$, in which case the two lines are coincident. Notice that $(a_{11}, a_{12}, b_1) = t(a_{21}, a_{22}, b_2)$ in this case. The value d is computed without explicitly computing the multiplier t . We may obtain a similar expression without t that indicates that the lines are coincident. Specifically, $(a_{11}, b_1) = t(a_{21}, b_2)$ implies $a_{11}b_2 - a_{21}b_1 = 0$. Equivalently, $(a_{12}, b_1) = t(a_{22}, b_2)$ implies $a_{12}b_1 - a_{22}b_2 = 0$. If $b_1 \neq tb_2$, the lines are parallel and disjoint. The algebraic equivalents to the three geometric possibilities mentioned earlier are summarized below.

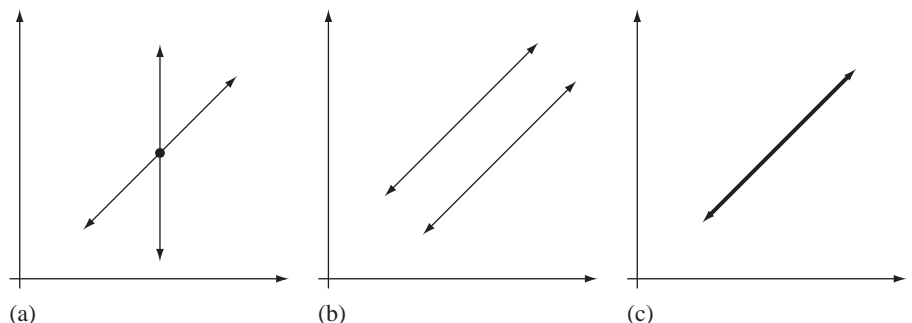


Figure 7.1 (a) Two nonparallel lines. (b) Two parallel and disjoint lines. (c) Two coincident lines (shown in bold black).

1. $a_{11}a_{22} - a_{12}a_{21} \neq 0$: The lines are not parallel. The linear system has a unique solution.
2. $a_{11}a_{22} - a_{12}a_{21} = 0$ and $a_{11}b_2 - a_{21}b_1 \neq 0$: The lines are parallel and disjoint. The linear system has no solution.
3. $a_{11}a_{22} - a_{12}a_{21} = 0$ and $a_{11}b_2 - a_{21}b_1 = 0$: The two lines are the same. The linear system has infinitely many solutions.

A similar algebra–geometry relationship exists for equations involving three variables. Consider three equations in three unknowns, $\sum_{j=1}^3 a_{ij}x_j = b_i$ for $1 \leq i \leq 3$. A single equation represents a plane in three dimensions. If this is the only equation of the system, the set of solutions is infinite and is represented by all the points on the plane. The possibilities for two equations in three unknowns are listed below.

1. The planes are not parallel. They intersect in a line.
2. The planes are parallel and disjoint. They do not intersect.
3. The planes are parallel and coincident.

Figure 7.2 shows these configurations.

Three equations in three unknowns lead to yet more possibilities.

1. No two planes are parallel.
 - (a) The planes intersect in a single point.
 - (b) The planes intersect in a line.
 - (c) The three planes have no common point.

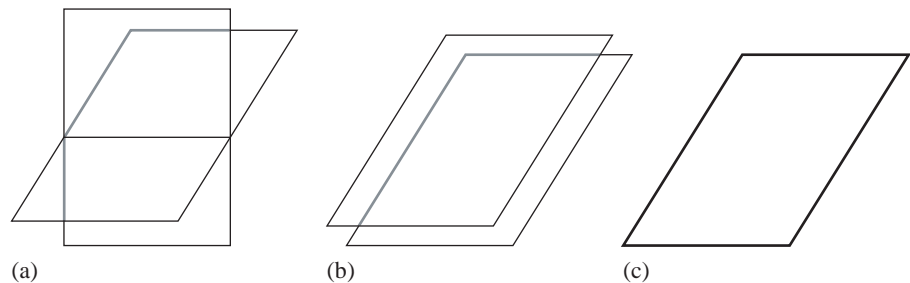


Figure 7.2 (a) Two nonparallel planes. (b) Two parallel and disjoint planes. (c) Two coincident planes (shown in bold black).

2. Two planes are parallel; the third is not parallel to them.
 - (a) The two parallel planes are disjoint. The three planes have no common point.
 - (b) The two parallel planes are coincident. The three planes intersect in a line.
3. All three planes are parallel.
 - (a) At least two planes are not coincident. The three planes have no common point.
 - (b) All planes are coincident. The intersection set is the common plane.

Figure 7.3 shows these configurations. The intersection set is either empty, a single point, a line, or a plane. Further geometric interpretations of linear equations and their solutions are discussed later in Section 7.2.4.

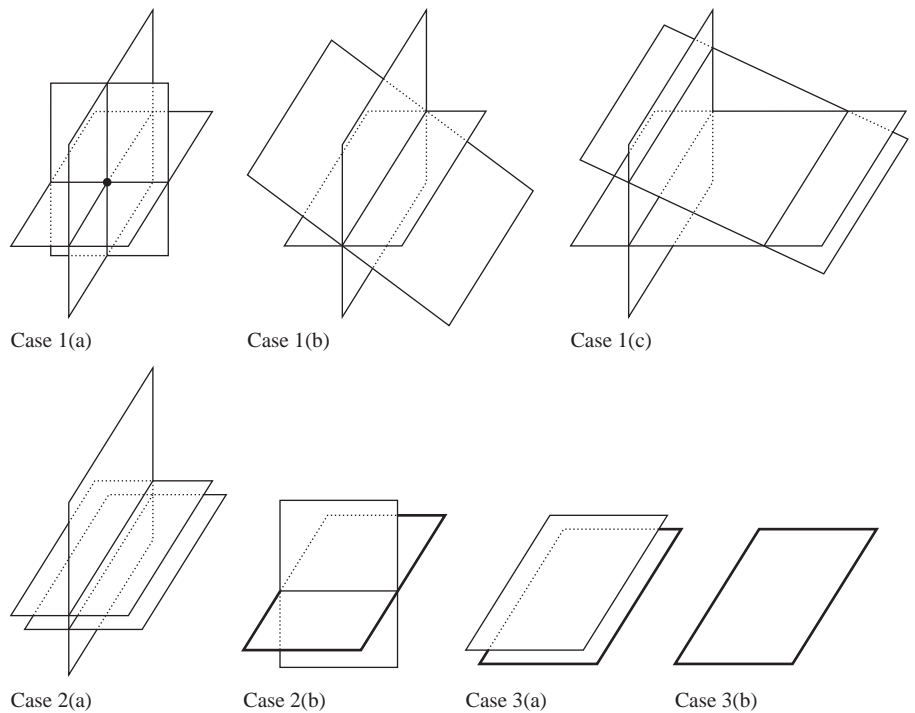


Figure 7.3 The coincident planes are shown in bold (black for visible portions, gray for hidden portions).

7.2.5 NUMERICAL ISSUES

The method of Gaussian elimination was discussed previously in mathematical terms without regard to numerical issues that can arise when implemented on a computer. The main issue is using the first nonzero entry in a row, the pivot, to zero out the column entries below it. The reciprocal of the pivot is required in the process. If the pivot is nearly zero, the division can be a source of numerical errors.

Consider a system whose augmented matrix is

$$\left[\begin{array}{cc|c} \varepsilon & 1 & 1 \\ 1 & 2 & -1 \end{array} \right] \quad (7.1)$$

where ε is a number that is nearly zero. If that entry is used as the pivot, then formally we can row-reduce the augmented matrix to

$$\left[\begin{array}{cc|c} 1 & 1/\varepsilon & 1/\varepsilon \\ 0 & 2 - 1/\varepsilon & -1 - 1/\varepsilon \end{array} \right]$$

This matrix now has very large entries due to $1/\varepsilon$. The numerical representations of some of the numbers are now suspect. For example, the floating point calculation for $2 - 1/\varepsilon$ could effectively ignore the 2 if $1/\varepsilon$ is so large that in matching the exponents of the two numbers to allow the floating point sum of the mantissas, the intermediate representation of 2 is the floating point number zero.

A better algorithm involves searching the entries in the first column of the augmented matrix and looking for the pivot that is largest in absolute magnitude. In the example we should have swapped the two equations:

$$\left[\begin{array}{cc|c} 1 & 2 & -1 \\ \varepsilon & 1 & 1 \end{array} \right] \quad (7.2)$$

The forward elimination produces

$$\left[\begin{array}{cc|c} 1 & 2 & -1 \\ 0 & 1 - 2\varepsilon & 1 + \varepsilon \end{array} \right]$$

The last equation is solved for $x_2 = (1 + \varepsilon)/(1 - 2\varepsilon)$. For ε nearly zero, the denominator is nearly 1 and the division is numerically well behaved. The other variable is $x_1 = -3/(1 - 2\varepsilon)$.

EXERCISE 7.2

Write a computer program to solve the system in [equation \(7.1\)](#) using Gaussian elimination so that the first pivot is ε . Allow this parameter to be supplied by the caller of the function for solving the system. The program should also have a function for solving the system in the form of [equation \(7.2\)](#), where ε is a parameter to the function. The test program should implement a loop that starts with $\varepsilon = 0.1$ and solves the system. On each successive iteration, replace ε by $\varepsilon/2$. The system should be solved using each of the two functions. Compare the results as ε becomes very small. ■

The search for a pivot entry of largest absolute magnitude is a good approach in solving systems. However, the next example shows that even this can be a problem. The system is

$$\begin{aligned}\varepsilon_1 x_1 + x_2 &= 1 \\ \varepsilon_2 x_1 + 2x_2 &= -1\end{aligned}$$

where ε_1 and ε_2 are both nearly zero. Regardless of which of these entries is largest in absolute magnitude, forward elimination will require a division by a number that is nearly zero. A close inspection of the system will show that we were unfortunate to name the variables as shown! Had we made x_2 the “first” variable and x_1 the “second” variable, the division problem disappears. That is, name $y_1 = x_2$ and $y_2 = x_1$ and obtain the system

$$\begin{aligned}y_1 + \varepsilon_1 y_2 &= 1 \\ 2y_1 + \varepsilon_2 y_2 &= -1\end{aligned}$$

The augmented matrix and the forward elimination are shown:

$$\left[\begin{array}{cc|c} 1 & \varepsilon_1 & 1 \\ 2 & \varepsilon_2 & -1 \end{array} \right] \sim \left[\begin{array}{cc|c} 1 & \varepsilon_1 & 1 \\ 0 & \varepsilon_2 - 2\varepsilon_1 & -3 \end{array} \right]$$

The forward elimination step is well behaved numerically, but now we need to solve for $x_2 = -3/(\varepsilon_2 - 2\varepsilon_1)$ where the denominator is nearly zero. This is unavoidable; the system is ill conditioned in the sense that if ε_1 and ε_2 really were zero, the equations would be $y_1 = 1$ and $2y_1 = -1$ implying that $y_1 = 1$ and $y_1 = -1/2$, an impossibility. Even so, the divisions in the back substitution can be deferred (by using back elimination instead) to make sure any numerical round-off errors from one division are not propagated (and magnified) through the remaining divisions. In our example, the operation is $R_1 \leftarrow (\varepsilon_2 - 2\varepsilon_1)R_1 - \varepsilon_1 R_2$:

$$\left[\begin{array}{cc|c} \varepsilon_2 - 2\varepsilon_1 & 0 & \varepsilon_1 + \varepsilon_2 \\ 0 & \varepsilon_2 - 2\varepsilon_1 & -3 \end{array} \right]$$

If the application decides inversion of $\varepsilon_2 - 2\varepsilon_1$ is justified, the division $\lambda = 1/(\varepsilon_2 - 2\varepsilon_1)$ is calculated once. The system solution is $y_1 = (\varepsilon_1 + \varepsilon_2)\lambda$ and $y_2 = -3\lambda$.

The renaming of x_1 and x_2 to y_2 and y_1 amounts to swapping *columns* of the augmented matrix. This is not an elementary row operation, so additional bookkeeping must be done to reconstruct the solution components in the order in which they were specified. You can do this by maintaining a permutation vector of indices. In the example the original variable indices are stored as $(1, 2)$. When the column swap is deemed appropriate, and memory swapping is actually performed in a computer implementation, the permutation vector indices are swapped to $(2, 1)$. If the final values obtained on the right-hand sides of the equations after Gaussian elimination are (c_1, c_2) and the permutation vector is (i_1, i_2) , one of $(1, 2)$ or $(2, 1)$, then the system solution is $x_{i_1} = c_1$ and $x_{i_2} = c_2$.

Generally, for a system of n equations in n unknowns, you can search the entire matrix of coefficients looking for the entry of largest absolute magnitude to be used as the pivot. This process is known as *full pivoting*. If that entry occurs in row r and column c , then rows r and 1 are swapped followed by a swap of column c and column 1. The original permutation vector is $(1, 2, \dots, c, \dots, n)$; the new vector is $(c, 2, \dots, 1, \dots, n)$. After both swaps, the entry in row 1 and column 1 is the largest absolute magnitude entry in the matrix. If nearly zero, the linear system is ill conditioned and you may choose to stop solving and notify the user of this situation. If you choose to continue, the division can be performed to make the pivot 1 and forward elimination commences. The process is repeated for the submatrix of $n - 1$ rows and $n - 1$ columns. Many column swaps can occur during the process. Let the final values obtained on the right-hand sides of the equation be listed as (c_1, \dots, c_n) . Let the permutation vector be (i_1, \dots, i_n) , a permutation of $(1, \dots, n)$. The system solution is $x_{ij} = c_j$ for $1 \leq j \leq n$.

7.2.6 ITERATIVE METHODS FOR SOLVING LINEAR SYSTEMS

As it turns out, Gaussian elimination is not the final word in solving systems. Iterative methods can be used. After all, why look for the exact mathematical solution when a good numerical approximation will do! Such algorithms are typically used in *sparse linear systems*. These systems have a large number of equations, but each equation involves only a small subset of the variables. The matrix A for the system is large, but has only a small number of nonzero entries. These algorithms are also used when the entries of A vary over time, in which case the solution at time t may be used as the initial guess for the iteration that estimates the solution at time $t + h$ for a small time step h . Assuming the entries of A vary continuously with time, the initial guess for time $t + h$ should be close enough to the true solution that only a few iterations are needed to obtain a good estimate. The iteration effectively makes use of time coherence to compute rapidly a solution. I will not go into great detail as this topic is quite extensive, but here are a few possibilities to ponder.

The first type of method we look at is known as a *splitting method*. I will illustrate for a system of two equations in two unknowns:

$$\begin{aligned} a_{11}x_1 + a_{12}x_2 &= b_1 \\ a_{21}x_1 + a_{22}x_2 &= b_2 \end{aligned}$$

For simplicity of the presentation, suppose that $a_{11} \neq 0$ and $a_{22} \neq 0$. The system can be rewritten as

$$x_1 = \frac{b_1 - a_{12}x_2}{a_{11}}$$

$$x_2 = \frac{b_2 - a_{21}x_1}{a_{22}}$$

The term *splitting* refers to splitting up the equations into the terms corresponding to the diagonal entries and the terms corresponding to the nondiagonal entries. Why bother with this form when it clearly does not give us a solution? The concept is to generate a sequence of iterates $x^{(1)}, x^{(2)}, \dots, x^{(n)}$ where n is large enough that $x^{(n)}$ is an acceptable approximation to the actual solution to the equation. At the same time we want n small enough to minimize the computational time in producing the approximation. Each iterate is of the form $x^{(i)} = (x_1^{(i)}, x_2^{(i)})$. The key idea is to relate the iterates by modifying the split equations to

$$x_1^{(i+1)} = \frac{b_1 - a_{12}x_2^{(i)}}{a_{11}}$$

$$x_2^{(i+1)} = \frac{b_2 - a_{21}x_1^{(i)}}{a_{22}}$$

The left-hand side is the next iterate and is obtained by substituting the current iterate into the right-hand side. Whether or not the sequence of iterates converges to the exact solution depends on your particular system. Another issue is that if any of the a_{ii} are nearly zero, the division by that small number can cause numerical problems. The splitting used here to illustrate the concept is not the only one. In fact, each equation on the right-hand side of the split system might very well contain all of the original variables. Such is the case when one of the a_{ii} is zero or nearly zero. Ideally, you want to split your terms so that you get rapid convergence and avoid numerical problems.

Standard splitting methods take advantage of the decomposition $A = L + D + U$, where L is the lower-triangular portion of A , D is the matrix of diagonal entries of A , and U is the upper-triangular portion of A . That is,

$$L = \begin{bmatrix} 0 & 0 & \cdots & 0 & 0 \\ a_{21} & 0 & \cdots & 0 & 0 \\ a_{31} & a_{32} & \ddots & 0 & 0 \\ \vdots & \vdots & \ddots & \vdots & \vdots \\ a_{n1} & a_{n2} & \cdots & a_{n,n-1} & 0 \end{bmatrix}, \quad D = \text{Diag}(a_{11}, a_{22}, \dots, a_{nn}),$$

$$U = \begin{bmatrix} 0 & a_{12} & a_{13} & \cdots & a_{1n} \\ 0 & 0 & a_{23} & \cdots & a_{2n} \\ \vdots & \vdots & \ddots & \ddots & \vdots \\ 0 & 0 & 0 & \cdots & a_{n-1,n} \\ 0 & 0 & 0 & \cdots & 0 \end{bmatrix}$$

The usual assumption is that none of the diagonal entries is zero.

The method I illustrated earlier for 2 equations is called the *Jacobi method*. The linear system is written as $D\mathbf{x} = \mathbf{b} - (L + U)\mathbf{x}$. The iterative formulation is

$$\mathbf{x}^{(k+1)} = D^{-1}(\mathbf{b} - (L + U)\mathbf{x}^{(k)}), \quad k \geq 0 \quad (7.3)$$

where $\mathbf{x}^{(0)}$ is the initial guess. The component-wise calculations for the iterates are

$$\mathbf{x}_i^{(k+1)} = \frac{1}{a_{ii}} \left(b_i - \sum_{j \neq i} a_{ij} x_j^{(k)} \right), \quad 1 \leq i \leq n \quad (7.4)$$

In practice, we must be concerned about convergence for an iterative method. That is, the limit of the iterates must be a solution to the linear system:

$$\mathbf{y} = \lim_{k \rightarrow \infty} \mathbf{x}^{(k)}$$

and $A\mathbf{y} = \mathbf{b}$. The analysis of convergence is an advanced topic in matrix analysis; for example, see [HJ85]. The Jacobi method is known to converge when A is *strictly diagonally dominant*. This means that

$$|a_{ii}| > \sum_{i \neq j} |a_{ij}| \quad (7.5)$$

for all i . In words, the diagonal entry in a row must have magnitude larger than the sum of the magnitudes of the other row entries – the diagonal entries are dominant. The term *strict* refers to the strict inequality in equation (7.5). The method is also known to converge when A is *irreducibly diagonally dominant*. Such a matrix must be diagonally dominant,

$$|a_{ii}| \geq \sum_{i \neq j} |a_{ij}| \quad (7.6)$$

and it must be *irreducible*. Matrix A is *reducible* when there exists a permutation matrix P for which $A' = P^T AP$ is an upper-triangular block matrix; that is, the lower-left $(n-r) \times r$ block of A' is zero for some r for which $1 \leq r < n$. Finally, a recent result shows a specific implementation of the Jacobi method that converges when A is *positive definite*; see [JBD09]. Such a matrix is symmetric and has the property that $\mathbf{x}^T A \mathbf{x} > 0$ for all nonzero \mathbf{x} . We will see in Section 7.5.3 that a positive definite matrix has all positive eigenvalues.

A different splitting is the *Gauss–Seidel method*. The linear system is written as $(L + D)\mathbf{x} = \mathbf{b} - U\mathbf{x}$. The iterative formulation is

$$\mathbf{x}^{(k+1)} = (L + D)^{-1}(\mathbf{b} - U\mathbf{x}^{(k)}), \quad k \geq 0 \quad (7.7)$$

where $\mathbf{x}^{(0)}$ is the initial guess. The component-wise calculations for the iterates are listed next. The inverse of $L + D$ is not computed explicitly; rather, it is computed by

forward elimination:

$$\mathbf{x}_i^{(k+1)} = \frac{1}{a_{ii}} \left(b_i - \sum_{j>i} a_{ij}x_j^{(k)} - \sum_{j*n*$$

As with the Jacobi method, this method converges for matrices that are strictly diagonally dominant, irreducibly diagonally dominant, or positive definite.

A variation of the Gauss–Seidel method is *successive over-relaxation*, which is an algorithm that can be used for any iterative method of the form $\mathbf{x}^{(k+1)} = \mathbf{F}(\mathbf{x}^{(k)})$. The next iterate is chosen to be a weighted sum of the previous iterate and the result of the iteration function

$$\mathbf{x}^{(k+1)} = (1 - w)\mathbf{x}^{(k)} + w\mathbf{F}(\mathbf{x}^{(k)}) \quad (7.9)$$

where w is a scalar. The idea is to accelerate the convergence of the method – fewer iterates should lead to a good numerical estimate of the solution. In general, it is difficult to know what to select for w . When applied to the Gauss–Seidel method of equation (7.7), where the right-hand side of that equation is $\mathbf{F}(\mathbf{x}^{(k)})$, the algorithm converges for $0 < w < 2$ when A is positive definite.

Another iterative method involves formulating the linear system $\mathbf{Ax} = \mathbf{b}$ as a minimization problem. The function to minimize is the squared length $f(\mathbf{x}) = |\mathbf{Ax} - \mathbf{b}|^2$, a quadratic function of \mathbf{x} which you see in least-squares error algorithms.

The illustration here is for a system of two equations in two unknowns. The two equations may be written as $a_{11}x_1 + a_{12}x_2 - b_1 = 0$ and $a_{21}x_1 + a_{22}x_2 - b_2 = 0$. The sum of squares of the left-hand sides must be zero:

$$f(x_1, x_2) = (a_{11}x_1 + a_{12}x_2 - b_1)^2 + (a_{21}x_1 + a_{22}x_2 - b_2)^2 = 0$$

Observe that $f(x_1, x_2) \geq 0$ no matter the choice of input. Assuming the system has a unique solution, the graph of this function is a paraboloid whose vertex lies in the $x_1 x_2$ -plane and is the solution to the system of equations. An iterative minimization algorithm takes the current iterate $\mathbf{x}^{(i)}$, where $f(\mathbf{x}^{(i)}) < 0$, and produces the next iterate $\mathbf{x}^{(i+1)}$ so that (hopefully) $f(\mathbf{x}^{(i+1)}) < f(\mathbf{x}^{(i)})$. You can visualize the iterates on the graph of f as a sequence of points $(x_1^{(i)}, x_2^{(i)}, f(x_1^{(i)}, x_2^{(i)}))$ for $i \geq 1$ that descend toward the vertex of the paraboloid. A good choice for generating the iterates is the *conjugate gradient method*, but other methods may be applied as well. See [PFTV88] for a discussion of numerical methods for function minimization.

7.3 MATRICES

Gaussian elimination applied to a system of linear equations is accomplished by setting up a table of numbers called an *augmented matrix*. The algebraic operations are applied only to the equation coefficients. The variable names themselves are unimportant in the manipulations. The concept of matrices is more powerful if we allow

additional structure to be placed on them. Part of that structure is introduced here in the context of solving linear systems of equations. More structure is introduced later where matrices are shown to be naturally related to the concept of a linear transformation.

The matrix of coefficients for the system of n equations in m unknowns is denoted $A = [a_{ij}]$ and has n rows and m columns. The column matrix for the right-hand side values is denoted $\mathbf{b} = [b_i]$ and has n rows and, of course, one column. Similarly, we define the column matrix $\mathbf{x} = [x_j]$ that has m rows and one column. The concise representation for a linear system using summation notation is

$$\sum_{j=1}^m a_{ij}x_j = b_i, \quad 1 \leq i \leq n$$

A suggestive shorthand notation is $A\mathbf{x} = \mathbf{b}$ and makes the linear system appear symbolically to be a single linear equation with known values A and \mathbf{b} and unknown value \mathbf{x} . For this to really make sense, we need to formalize what it means to multiply the matrices A and \mathbf{x} and obtain the product $A\mathbf{x}$. Consider a system with two equations and three unknowns: $a_{11}x_1 + a_{12}x_2 + a_{13}x_3 = b_1$, $a_{21}x_1 + a_{22}x_2 + a_{23}x_3 = b_2$. The symbolic form $A\mathbf{x} = \mathbf{b}$ with juxtaposed matrices is

$$\begin{bmatrix} a_{11} & a_{12} & a_{13} \\ a_{21} & a_{22} & a_{23} \end{bmatrix} \begin{bmatrix} x_1 \\ x_2 \\ x_3 \end{bmatrix} = \begin{bmatrix} b_1 \\ b_2 \end{bmatrix}$$

In order to recreate the linear equations, it appears that we need to multiply each row of A with the column \mathbf{x} , then equate the resulting product with the corresponding row of the column \mathbf{b} . For this to work, clearly the number of columns of A must equal the number of rows of \mathbf{x} . We will use this as motivation for defining the product of two matrices A and B . Let A have n rows and m columns. For the product $C = AB$ to make sense, the number of rows of B must be m . Let B have p columns. The product C itself is a matrix of numbers. Your intuition from the example of a linear system should convince you that C has n rows and p columns. Symbolically $AB = C$ is shown next.

$$\begin{bmatrix} a_{11} & a_{12} & \cdots & a_{1m} \\ a_{21} & a_{22} & \cdots & a_{2m} \\ \vdots & \vdots & \ddots & \vdots \\ a_{n1} & a_{n2} & \cdots & a_{nm} \end{bmatrix} \begin{bmatrix} b_{11} & b_{12} & \cdots & b_{1p} \\ b_{21} & b_{22} & \cdots & b_{2p} \\ \vdots & \vdots & \ddots & \vdots \\ b_{m1} & b_{m2} & \cdots & b_{mp} \end{bmatrix}$$

$$= \begin{bmatrix} (a_{11}b_{11} + a_{12}b_{21} + \cdots + a_{1m}b_{m1}) & (a_{11}b_{12} + a_{12}b_{22} + \cdots + a_{1m}b_{m2}) & \cdots & (a_{11}b_{1p} + a_{12}b_{2p} + \cdots + a_{1m}b_{mp}) \\ (a_{21}b_{11} + a_{22}b_{21} + \cdots + a_{2m}b_{m1}) & (a_{21}b_{12} + a_{22}b_{22} + \cdots + a_{2m}b_{m2}) & \cdots & (a_{21}b_{1p} + a_{22}b_{2p} + \cdots + a_{2m}b_{mp}) \\ \vdots & \vdots & \ddots & \vdots \\ (a_{n1}b_{11} + a_{n2}b_{21} + \cdots + a_{nm}b_{m1}) & (a_{n1}b_{12} + a_{n2}b_{22} + \cdots + a_{nm}b_{m2}) & \cdots & (a_{n1}b_{1p} + a_{n2}b_{2p} + \cdots + a_{nm}b_{mp}) \end{bmatrix}$$

$$= \begin{bmatrix} c_{11} & c_{12} & \cdots & c_{1p} \\ c_{21} & c_{22} & \cdots & c_{2p} \\ \vdots & \vdots & \ddots & \vdots \\ c_{n1} & c_{n2} & \cdots & c_{np} \end{bmatrix}$$

In summation notation, the general entry of the product is

$$c_{ij} = \sum_{k=1}^m a_{ik} b_{kj}$$

for $1 \leq i \leq n$ and $1 \leq j \leq p$.

EXAMPLE
7.6

Consider the matrices,

$$A = \begin{bmatrix} 1 & 0 & -1 \\ -1 & 2 & 0 \end{bmatrix} \quad \text{and} \quad B = \begin{bmatrix} -1 & 1 & 2 \\ 0 & 1 & -3 \\ -2 & 3 & 0 \end{bmatrix}$$

The product AB is

$$AB = \begin{bmatrix} 1 & 0 & -1 \\ -1 & 2 & 0 \end{bmatrix} \begin{bmatrix} -1 & 1 & 2 \\ 0 & 1 & -3 \\ -2 & 3 & 0 \end{bmatrix} = \begin{bmatrix} c_{11} & c_{12} & c_{13} \\ c_{21} & c_{22} & c_{23} \end{bmatrix}$$

To compute c_{ij} , use the summation formula shown earlier,

$$c_{ij} = a_{i1}b_{1j} + a_{i2}b_{2j} + a_{i3}b_{3j} = [a_{i1} \quad a_{i2} \quad a_{i3}] \begin{bmatrix} b_{1j} \\ b_{2j} \\ b_{3j} \end{bmatrix}$$

In the example, the product is

$$AB = \begin{bmatrix} 1 & -2 & 2 \\ 1 & 1 & -8 \end{bmatrix}$$

A matrix that has n rows and m columns is referred to as an $n \times m$ matrix. In defining the product $C = AB$, A is an $n \times m$ matrix, B is an $m \times p$ matrix, and C is an $n \times p$ matrix. It is important to note that the order of the matrices in a product is relevant. For example, if A is 2×3 and B is 3×4 , the product AB is defined and is 2×4 . On the other hand, BA is not defined since the number of columns of B is different from the number of rows of A . Now, it is possible that both products are defined. This is the case when A is $n \times m$ and B is $m \times n$. The product AB is $n \times n$ and the product BA is $m \times m$. If $n \neq m$, then AB and BA cannot be the same matrix since

their sizes are different. Even if $n = m$, the products still might differ. For example,

$$AB = \begin{bmatrix} 1 & 0 \\ 0 & 0 \end{bmatrix} \begin{bmatrix} 0 & 1 \\ 0 & 0 \end{bmatrix} = \begin{bmatrix} 0 & 1 \\ 0 & 0 \end{bmatrix} \neq \begin{bmatrix} 0 & 0 \\ 0 & 0 \end{bmatrix} = \begin{bmatrix} 0 & 1 \\ 0 & 0 \end{bmatrix} \begin{bmatrix} 1 & 0 \\ 0 & 0 \end{bmatrix} = BA$$

Matrix multiplication is therefore considered *not commutative*. It is the case that matrix multiplication is *associative*. That is, $A(BC) = (AB)C$ for matrices A , B , and C where the relevant pairwise products are defined.

7.3.1 SOME SPECIAL MATRICES

A few special types of matrices arise frequently in practice. Here are some that are of interest, some of general size $n \times m$ and some that are called *square matrices* where $n = m$ (number of rows and number of columns are the same).

The *diagonal entries* of an $n \times m$ matrix $A = [a_{ij}]$ are those entries a_{ii} . A square matrix $A = [a_{ij}]$ is a *diagonal matrix* if $a_{ij} = 0$ whenever $i \neq j$. That is, the nondiagonal terms are all zero. The diagonal terms can be anything, including zero. For example, consider

$$A = \begin{bmatrix} 1 & 2 & 3 \\ 4 & 5 & 6 \end{bmatrix} \quad \text{and} \quad B = \begin{bmatrix} 0 & 0 \\ 0 & 1 \end{bmatrix}$$

The diagonal entries of A are 1 and 5. The matrix B is diagonal. A shorthand notation for the diagonal matrix is to list only its diagonal entries, $B = \text{Diag}(0, 1)$.

A special diagonal matrix is the *identity matrix* I . All the diagonal entries are 1. The identity matrices for $n = 2$ and $n = 3$ are shown:

$$I = \begin{bmatrix} 1 & 0 \\ 0 & 1 \end{bmatrix} \quad \text{and} \quad I = \begin{bmatrix} 1 & 0 & 0 \\ 0 & 1 & 0 \\ 0 & 0 & 1 \end{bmatrix}$$

The identity matrix has the property that $IA = A$. That is, the product of the $n \times n$ identity matrix with the $n \times m$ matrix A does not change A .

If $A = [a_{ij}]$ is an $n \times m$ matrix, the *transpose* of A is the $m \times n$ matrix $A^T = [a_{ji}]$. That is, the entry a_{ij} in the i th row and j th column of A becomes the entry in the j th row and i th column of A^T . For example,

$$A = \begin{bmatrix} 1 & 2 & 3 \\ 4 & 5 & 6 \end{bmatrix} \quad \text{and} \quad A^T = \begin{bmatrix} 1 & 4 \\ 2 & 5 \\ 3 & 6 \end{bmatrix}$$

EXERCISE 7.3

Verify that the transpose satisfies the property $(AB)^T = B^T A^T$. ■

A square matrix A is *symmetric* if $A = A^T$. It is *skew-symmetric* if $A = -A^T$. For example, consider

$$A = \begin{bmatrix} 1 & 2 & 3 \\ 2 & 4 & 5 \\ 3 & 5 & 6 \end{bmatrix} \quad \text{and} \quad B = \begin{bmatrix} 0 & 1 & 2 \\ -1 & 0 & 3 \\ -2 & -3 & 0 \end{bmatrix}$$

The matrix A is symmetric and the matrix B is skew-symmetric. The diagonal entries of a skew-symmetric matrix are necessarily zero.

An $n \times m$ matrix $U = [u_{ij}]$ is said to be *upper echelon* if $u_{ij} = 0$ for $i > j$. In addition, if $n = m$, then U is said to be *upper triangular*. Similarly, an $n \times m$ matrix $L = [\ell_{ij}]$ is said to be *lower echelon* if $\ell_{ij} = 0$ for $i < j$. If $n = m$, then L is said to be *lower triangular*. For example, consider

$$U = \begin{bmatrix} 1 & 2 & 3 \\ 0 & 4 & 5 \end{bmatrix} \quad \text{and} \quad L = \begin{bmatrix} 1 & 0 \\ 2 & 3 \end{bmatrix}$$

The matrix U is upper echelon and the matrix L is lower triangular.

7.3.2 ELEMENTARY ROW MATRICES

Now that we have a concise symbolic representation of a system of equations, $Ax = \mathbf{b}$, let us review the forward elimination algorithm that reduces the augmented matrix $[A|\mathbf{b}]$. In our earlier discussion, the elimination was accomplished by applying elementary row operations to the augmented matrix in order to zero out various column entries below pivot elements. A reminder of the operations:

1. Interchange row i with row j . Notation: $R_i \leftrightarrow R_j$.
2. Multiply row i by a scalar $c \neq 0$. Notation: $cR_i \rightarrow R_i$.
3. Multiply row i by a scalar c_i , multiply row j by a scalar c_j , then add the results and replace row j . Notation: $c_i R_i + c_j R_j \rightarrow R_j$.

Each elementary row operation can be represented by a square matrix that multiplies the augmented matrix on its left.

Consider a general matrix A that is $n \times m$ (not necessarily an augmented matrix for a linear system). Let \mathcal{O} be an elementary row operation applied to A to obtain a matrix B of the same size as A . The notation introduced in Example 7.5 was $A \sim_{\mathcal{O}} B$. There is an $n \times n$ matrix E such that $B = EA$. The elementary row matrix E corresponding to the elementary row operation \mathcal{O} is obtained by applying \mathcal{O} to the $n \times n$ identity matrix: $I \sim_{\mathcal{O}} E$.

EXAMPLE
7.7

Consider the 3×4 matrix

$$A = \begin{bmatrix} 1 & -1 & 0 & 2 \\ 0 & 4 & -1 & -2 \\ 2 & 0 & 1 & 0 \end{bmatrix}$$

(Example 7.7
continued)

A type 1 operation is

$$A = \underset{R_1 \leftrightarrow R_2}{\sim} \begin{bmatrix} 0 & 4 & -1 & -2 \\ 1 & -1 & 0 & 2 \\ 2 & 0 & 1 & 0 \end{bmatrix} = \begin{bmatrix} 0 & 1 & 0 \\ 1 & 0 & 0 \\ 0 & 0 & 1 \end{bmatrix} A$$

A type 2 operation is

$$A = \underset{-2R_1 \rightarrow R_1}{\sim} \begin{bmatrix} -2 & 2 & 0 & -4 \\ 0 & 4 & -1 & -2 \\ 2 & 0 & 1 & 0 \end{bmatrix} = \begin{bmatrix} -2 & 0 & 0 \\ 0 & 1 & 0 \\ 0 & 0 & 1 \end{bmatrix} A$$

A type 3 operation is

$$A = \underset{-2R_1 + R_3 \rightarrow R_3}{\sim} \begin{bmatrix} 1 & -1 & 0 & 2 \\ 0 & 4 & -1 & -2 \\ 0 & 2 & 1 & -4 \end{bmatrix} = \begin{bmatrix} 1 & 0 & 0 \\ 0 & 1 & 0 \\ -2 & 0 & 1 \end{bmatrix} A$$

Observe that in all cases, the 3×3 elementary row matrices shown on the right-hand sides of the equations are obtained by applying the row operations to the 3×3 identity matrix. ■

The final result of forward elimination can be stated in terms of elementary row matrices applied to the augmented matrix $[A|\mathbf{b}]$. Namely, if E_1 through E_k are the elementary row matrices corresponding to the applied elementary row operations, then the final augmented matrix is the product

$$[U|\mathbf{v}] = E_k \cdots E_1 [A|\mathbf{b}]$$

The matrix $U = [u_{ij}]$ is upper echelon; that is, $u_{ij} = 0$ whenever $i > j$. The only possible nonzero entries are on or above the diagonal, the diagonal defined by entries where $i = j$. Back substitution is achieved by another sequence of elementary row operations, E_{k+1} through E_ℓ . The end result, assuming the diagonal entries of U are all nonzero is

$$[I|\mathbf{w}] = (E_\ell \cdots E_{k+1}) [U|\mathbf{v}] = (E_\ell \cdots E_1) [A|\mathbf{b}]$$

The solution to the linear system is $\mathbf{x} = \mathbf{w}$.

EXAMPLE
7.8

This example was shown earlier, but is revisited in terms of elementary row matrices. Solve $x_1 + x_2 + x_3 = 6$, $x_1 + 3x_2 + 2x_3 = 11$, $2x_1 + 3x_2 - 4x_3 = 3$. The forward elimination is

$$[A|b] = \left[\begin{array}{ccc|c} 1 & 1 & 1 & 6 \\ 1 & 2 & 2 & 11 \\ 2 & 3 & -4 & 3 \end{array} \right] \underset{-R_1 + R_2 \rightarrow R_2}{\sim} \left[\begin{array}{ccc|c} 1 & 1 & 1 & 6 \\ 0 & 1 & 1 & 5 \\ 2 & 3 & -4 & 3 \end{array} \right]$$

$$\begin{array}{c} \sim \\ -2R_1 + R_3 \rightarrow R_3 \end{array} \left[\begin{array}{ccc|c} 1 & 1 & 1 & 6 \\ 0 & 1 & 1 & 5 \\ 0 & 1 & -6 & -9 \end{array} \right]$$

$$\begin{array}{c} \sim \\ -R_2 + R_3 \rightarrow R_3 \end{array} \left[\begin{array}{ccc|c} 1 & 1 & 1 & 6 \\ 0 & 1 & 1 & 5 \\ 0 & 0 & -7 & -14 \end{array} \right] = [U|v]$$

The backward substitution is

$$\begin{array}{c} [U|v] = \left[\begin{array}{ccc|c} 1 & 1 & 1 & 6 \\ 0 & 1 & 1 & 5 \\ 0 & 0 & -7 & -14 \end{array} \right] \sim \\ -(1/7)R_3 \rightarrow R_3 \end{array} \left[\begin{array}{ccc|c} 1 & 1 & 1 & 6 \\ 0 & 1 & 1 & 5 \\ 0 & 0 & 1 & 2 \end{array} \right]$$

$$\begin{array}{c} \sim \\ -R_3 + R_2 \rightarrow R_2 \end{array} \left[\begin{array}{ccc|c} 1 & 1 & 1 & 6 \\ 0 & 1 & 0 & 3 \\ 0 & 0 & 1 & 2 \end{array} \right]$$

$$\begin{array}{c} \sim \\ -R_3 + R_1 \rightarrow R_1 \end{array} \left[\begin{array}{ccc|c} 1 & 1 & 0 & 4 \\ 0 & 1 & 0 & 3 \\ 0 & 0 & 1 & 2 \end{array} \right]$$

$$\begin{array}{c} \sim \\ -R_2 + R_1 \rightarrow R_1 \end{array} \left[\begin{array}{ccc|c} 1 & 0 & 0 & 1 \\ 0 & 1 & 0 & 3 \\ 0 & 0 & 1 & 2 \end{array} \right] = [I|w]$$

The solution is $x_1 = 1$, $x_2 = 3$, and $x_3 = 2$. The elementary row matrices listed in the order of operations shown previously are

$$E_1 = \begin{bmatrix} 1 & 0 & 0 \\ -1 & 1 & 0 \\ 0 & 0 & 1 \end{bmatrix}, \quad E_2 = \begin{bmatrix} 1 & 0 & 0 \\ 0 & 1 & 0 \\ -2 & 0 & 1 \end{bmatrix}, \quad E_3 = \begin{bmatrix} 1 & 0 & 0 \\ 0 & 1 & 0 \\ 0 & -1 & 1 \end{bmatrix},$$

$$E_4 = \begin{bmatrix} 1 & 0 & 0 \\ 0 & 1 & 0 \\ 0 & 0 & -1/7 \end{bmatrix}, \quad E_5 = \begin{bmatrix} 1 & 0 & 0 \\ 0 & 1 & -1 \\ 0 & 0 & 1 \end{bmatrix}, \quad E_6 = \begin{bmatrix} 1 & 0 & -1 \\ 0 & 1 & 0 \\ 0 & 0 & 1 \end{bmatrix},$$

$$E_7 = \begin{bmatrix} 1 & -1 & 0 \\ 0 & 1 & 0 \\ 0 & 0 & 1 \end{bmatrix}$$

7.3.3 INVERSE MATRICES

The linear system is symbolically written as $Ax = \mathbf{b}$. The product of the elementary row operations used in solving the system is $P = E_\ell \cdots E_1$. The application of

all the elementary row matrices at one time is $\mathbf{x} = PA\mathbf{x} = P\mathbf{b} = \mathbf{w}$. An implication of the construction is that $PA = I$, where I is the identity matrix. We use this as motivation for the *inverse* of a square matrix. That is, if A is an $n \times n$ matrix and if P is another $n \times n$ matrix for which $PA = I$, then P is the inverse of A and is denoted A^{-1} .

**EXAMPLE
7.9**

In the last example, the product of the elementary row matrices is

$$P = E_7 \cdots E_1 = \begin{bmatrix} 2 & -1 & 0 \\ -\frac{8}{7} & \frac{6}{7} & \frac{1}{7} \\ 1 & 1 & -1 \end{bmatrix}$$

It is easily verified that

$$PA = \begin{bmatrix} 2 & -1 & 0 \\ -\frac{8}{7} & \frac{6}{7} & \frac{1}{7} \\ 1 & 1 & -1 \end{bmatrix} \begin{bmatrix} 1 & 1 & 1 \\ 1 & 2 & 2 \\ 2 & 3 & -4 \end{bmatrix} = \begin{bmatrix} 1 & 0 & 0 \\ 0 & 1 & 0 \\ 0 & 0 & 1 \end{bmatrix} = I$$

As an exercise, also verify that $AP = I$. ■

**EXAMPLE
7.10**

Not all square matrices are invertible. The 2×2 zero matrix is clearly not invertible:

$$Z = \begin{bmatrix} 0 & 0 \\ 0 & 0 \end{bmatrix}$$

since $PZ = Z$ no matter which 2×2 matrix P you choose. A more interesting example of a noninvertible matrix is

$$A = \begin{bmatrix} 1 & -1 \\ -1 & 1 \end{bmatrix}$$

You may attempt to construct one, say,

$$P = \begin{bmatrix} a & b \\ c & d \end{bmatrix}$$

For this matrix to be the inverse, we need

$$\begin{bmatrix} 1 & 0 \\ 0 & 1 \end{bmatrix} = I = PA = \begin{bmatrix} a-b & b-a \\ c-d & d-c \end{bmatrix}$$

Equating the first row entries yields $a - b = 1$ and $b - a = 0$. The second of these forces $b = a$. Replacing in the first leads to $0 = 1$, a false statement. Thus, A is not invertible. ■

The elementary row matrices have inverses. The list of the elementary row operations and their inverse operations is provided:

Row Operation	Inverse Operation
$R_i \leftrightarrow R_j$	$R_i \leftrightarrow R_j$
$cR_i \rightarrow R_i$	$\frac{1}{c}R_i \rightarrow R_i$
$cR_i + R_j \rightarrow R_j$	$-cR_i + R_j \rightarrow R_j$

If E represents an elementary row operation, then E^{-1} denotes the matrix that represents the inverse operation.

EXAMPLE
7.11

The 3×3 elementary row matrix corresponding to the row operation $-2R_1 + R_3 \rightarrow R_3$ is

$$E = \begin{bmatrix} 1 & 0 & 0 \\ 0 & 1 & 0 \\ -2 & 0 & 1 \end{bmatrix}$$

The inverse row operation is $2R_1 + R_3 \rightarrow R_3$ and

$$E^{-1} = \begin{bmatrix} 1 & 0 & 0 \\ 0 & 1 & 0 \\ 2 & 0 & 1 \end{bmatrix}$$

It is easily shown that $E^{-1}E = I$, where I is the 3×3 identity matrix. ■

7.3.4 PROPERTIES OF INVERSES

Here are some important properties of inverses. The first one is quite subtle. The definition of inverse was that P is an inverse of A when $PA = I$. More precisely, P is a *left inverse*. I already pointed out that matrix multiplication is generally not commutative, so $PA = I$ does not immediately imply $AP = I$.

1. If $A^{-1}A = I$, then $AA^{-1} = I$. This is the same as saying that the inverse of A^{-1} is $A = (A^{-1})^{-1}$.
2. Inverses are unique.
3. If A and B are invertible, then so is AB . Its inverse is $(AB)^{-1} = B^{-1}A^{-1}$.

To prove the first item, I use the method of solution for linear systems as motivation. The system is $Ax = b$ and, assuming A is invertible, has solution $x = A^{-1}b$. Symbolically, this is obtained as

$$x = Ix = (A^{-1}A)x = A^{-1}(Ax) = A^{-1}b$$

Now replace this in the original equation to obtain

$$(AA^{-1})\mathbf{b} = A(A^{-1}\mathbf{b}) = A\mathbf{x} = \mathbf{b}$$

The column matrix \mathbf{b} can be anything you like. Regardless of the choice it is the case that $(AA^{-1})\mathbf{b} = \mathbf{b}$. Some clever choices will help us out. Define \mathbf{e}_i to be the $n \times 1$ row matrix with a 1 in row i and 0 in all other rows. For any $n \times n$ matrix M , the product $M\mathbf{e}_i$ is the $n \times 1$ matrix that stores the entries of M from the i th column. In particular, $(AA^{-1})\mathbf{e}_i = \mathbf{e}_i$, so the i th column of AA^{-1} is the vector \mathbf{e}_i . Consequently, AA^{-1} consists of columns \mathbf{e}_1 through \mathbf{e}_n , in that order, which is exactly the identity matrix I . It is always the case for an invertible matrix A that $A^{-1}A = I = AA^{-1}$.

The second item is proved as follows. Suppose that A has two inverses, B and C ; then $AB = I = BA$ and $AC = I = CA$. Also,

$$\begin{aligned} AB &= I && B \text{ is an inverse for } A \\ C(AB) &= C(I) && \text{Multiply by } C \\ (CA)B &= C && \text{Matrix multiplication is associative; } I \text{ is the identity} \\ (I)B &= C && C \text{ is an inverse for } A \\ B &= C && I \text{ is the identity} \end{aligned}$$

and so there is only one inverse.

The third item is proved by a simple set of calculations:

$$\begin{aligned} (B^{-1}A^{-1})(AB) &= B^{-1}(A^{-1}A)B && \text{Matrix multiplication is associative} \\ &= B^{-1}IB && A^{-1} \text{ is the inverse of } A \\ &= B^{-1}B && I \text{ is the identity} \\ &= I && B^{-1} \text{ is the inverse of } B \end{aligned}$$

By direct verification, $B^{-1}A^{-1}$ is the inverse of AB .

7.3.5 CONSTRUCTION OF INVERSES

This is illustrated with 3×3 matrices, but the ideas clearly carry over to the $n \times n$ case. Let

$$\mathbf{e}_1 = \begin{bmatrix} 1 \\ 0 \\ 0 \end{bmatrix}, \quad \mathbf{e}_2 = \begin{bmatrix} 0 \\ 1 \\ 0 \end{bmatrix}, \quad \mathbf{e}_3 = \begin{bmatrix} 0 \\ 0 \\ 1 \end{bmatrix}$$

Any 3×3 matrix $M = [m_{ij}]$ can be thought of as a *block matrix* consisting of three column vectors:

$$M = \left[\begin{array}{c|c|c} m_{11} & m_{12} & m_{13} \\ m_{21} & m_{22} & m_{23} \\ m_{31} & m_{32} & m_{33} \end{array} \right] = [M\mathbf{e}_1 \mid M\mathbf{e}_2 \mid M\mathbf{e}_3]$$

In particular, if A is invertible, then A^{-1} exists and

$$A^{-1} = [A^{-1}\mathbf{e}_1 \mid A^{-1}\mathbf{e}_2 \mid A^{-1}\mathbf{e}_3] = [\mathbf{v}_1 \mid \mathbf{v}_2 \mid \mathbf{v}_3]$$

where the column vectors \mathbf{v}_k ($k = 1, 2, 3$) are unknowns to be determined. Matching the similar entries in the block matrices yields

$$A^{-1}\mathbf{e}_k = \mathbf{v}_k \text{ or } A\mathbf{v}_k = \mathbf{e}_k, \quad k = 1, 2, 3$$

Each of these systems of equations can be solved separately by row-reducing $[A|\mathbf{e}_k]$ to $[I|\mathbf{v}_k]$. However, we can solve these systems simultaneously by row-reducing $[A|\mathbf{e}_1|\mathbf{e}_2|\mathbf{e}_3] = [A|I]$ to $[I|\mathbf{v}_1|\mathbf{v}_2|\mathbf{x}_3] = [I|A^{-1}]$.

EXAMPLE
7.12

Compute the inverse of

$$A = \begin{bmatrix} -2 & 1 & 1 \\ 0 & 1 & 1 \\ -3 & 0 & 6 \end{bmatrix}$$

Row-reduce:

$$[A|I] = \left[\begin{array}{ccc|ccc} -2 & 1 & 1 & 1 & 0 & 0 \\ 0 & 1 & 1 & 0 & 1 & 0 \\ -3 & 0 & 6 & 0 & 0 & 1 \end{array} \right] \sim -\frac{1}{2}R_1 \rightarrow R_1 \left[\begin{array}{ccc|ccc} 1 & -\frac{1}{2} & -\frac{1}{2} & -\frac{1}{2} & 0 & 0 \\ 0 & 1 & 1 & 0 & 1 & 0 \\ -3 & 0 & 6 & 0 & 0 & 1 \end{array} \right]$$

$$\sim 3R_1 + R_3 \rightarrow R_3 \left[\begin{array}{ccc|ccc} 1 & -\frac{1}{2} & -\frac{1}{2} & -\frac{1}{2} & 0 & 0 \\ 0 & 1 & 1 & 0 & 1 & 0 \\ 0 & -\frac{3}{2} & \frac{9}{2} & -\frac{3}{2} & 0 & 1 \end{array} \right]$$

$$\begin{aligned} \sim & \frac{1}{2}R_2 + R_1 \rightarrow R_1 \left[\begin{array}{ccc|ccc} 1 & 0 & 0 & -\frac{1}{2} & \frac{1}{2} & 0 \\ 0 & 1 & 1 & 0 & 1 & 0 \\ 0 & 0 & 6 & -\frac{3}{2} & \frac{3}{2} & 1 \end{array} \right] \\ \frac{3}{2}R_2 + R_3 \rightarrow R_3 & \left[\begin{array}{ccc|ccc} 1 & 0 & 0 & -\frac{1}{2} & \frac{1}{2} & 0 \\ 0 & 1 & 1 & 0 & 1 & 0 \\ 0 & 0 & 6 & -\frac{3}{2} & \frac{3}{2} & 1 \end{array} \right] \end{aligned}$$

$$\sim \frac{1}{6}R_3 \rightarrow R_3 \left[\begin{array}{ccc|ccc} 1 & 0 & 0 & -\frac{1}{2} & \frac{1}{2} & 0 \\ 0 & 1 & 1 & 0 & 1 & 0 \\ 0 & 0 & 1 & -\frac{1}{4} & \frac{1}{4} & \frac{1}{6} \end{array} \right]$$

(Example 7.12
continued)

$$\sim \begin{array}{l} \\ -R_3 + R_2 \rightarrow R_2 \end{array} \left[\begin{array}{ccc|ccc} 1 & 0 & 0 & -\frac{1}{2} & \frac{1}{2} & 0 \\ 0 & 1 & 0 & \frac{1}{4} & \frac{3}{4} & -\frac{1}{6} \\ 0 & 0 & 1 & -\frac{1}{4} & \frac{1}{4} & \frac{1}{6} \end{array} \right] = [I|A^{-1}]$$

■

EXAMPLE

7.13

The matrix

$$A = \begin{bmatrix} 1 & -1 \\ -2 & 2 \end{bmatrix}$$

has no inverse. Row-reduce:

$$[A|I] = \left[\begin{array}{cc|cc} 1 & -1 & 1 & 0 \\ -2 & 2 & 0 & 1 \end{array} \right] \sim 2R_1 + R_2 \rightarrow R_2 \quad \left[\begin{array}{cc|cc} 1 & -1 & 1 & 0 \\ 0 & 0 & 2 & 1 \end{array} \right]$$

This last matrix can never be row-reduced to the form $[I|B]$, so A has no inverse. ■**7.3.6 LU DECOMPOSITION**

The forward elimination of a matrix A produces an upper echelon matrix U . Suppose this happens with only row operations of the form $cR_i + R_j \rightarrow R_j$, $i < j$. Let E_1, \dots, E_k be the corresponding elementary row matrices; $U = E_k \cdots E_1 A$. The matrices E_i are all lower triangular, the product $E_k \cdots E_1$ is lower triangular, and $L = (E_k \cdots E_1)^{-1} = E_1^{-1} \cdots E_k^{-1}$ is lower triangular. Thus, $A = LU$ where L is lower triangular and U is upper echelon. This is called the *LU decomposition* of the matrix A .

EXAMPLE
7.14

$$A = \left[\begin{array}{ccccc} 1 & 0 & -4 & 0 & 6 \\ 5 & 1 & -3 & -3 & 9 \\ 6 & 3 & 7 & -3 & 1 \end{array} \right] \sim \begin{array}{l} \\ -5R_1 + R_2 \rightarrow R_2 \\ -6R_1 + R_3 \rightarrow R_3 \end{array} \left[\begin{array}{ccccc} 1 & 0 & -4 & 0 & 6 \\ 0 & 1 & 17 & -3 & -21 \\ 0 & 3 & 31 & -3 & -35 \end{array} \right]$$

$$\sim \begin{array}{l} \\ -3R_2 + R_3 \rightarrow R_3 \end{array} \left[\begin{array}{ccccc} 1 & 0 & -4 & 0 & 6 \\ 0 & 1 & 17 & -3 & -21 \\ 0 & 0 & -20 & 6 & 28 \end{array} \right] = U$$

The elementary row matrices corresponding to these operations are

$$E_1 = \begin{bmatrix} 1 & 0 & 0 \\ -5 & 1 & 0 \\ 0 & 0 & 1 \end{bmatrix}, E_2 = \begin{bmatrix} 1 & 0 & 0 \\ 0 & 1 & 0 \\ -6 & 0 & 1 \end{bmatrix}, E_3 = \begin{bmatrix} 1 & 0 & 0 \\ 0 & 1 & 0 \\ 0 & -3 & 1 \end{bmatrix}$$

We have

$$U = E_3 E_2 E_1 A = \begin{bmatrix} 1 & 0 & 0 \\ -5 & 1 & 0 \\ -6 & -3 & 1 \end{bmatrix} A$$

and

$$A = E_1^{-1} E_2^{-1} E_3^{-1} U = \begin{bmatrix} 1 & 0 & 0 \\ 5 & 1 & 0 \\ 6 & 3 & 1 \end{bmatrix} U = LU$$

The matrix U can be factored further by applying row operations of the type $cR_i \rightarrow R_i$ to obtain pivot values of 1. With a renaming of U to DU , we have the *LDU decomposition* of the matrix, $A = LDU$, where L is lower triangular, D is a diagonal matrix, and U is upper echelon with diagonal entries either 1 or 0.

EXAMPLE
7.15

This is the continuation of the last example.

$$U = E_3 E_2 E_1 A = \begin{bmatrix} 1 & 0 & -4 & 0 & 6 \\ 0 & 1 & 17 & -3 & -21 \\ 0 & 0 & -20 & 6 & 28 \end{bmatrix} \sim \begin{bmatrix} 1 & 0 & -4 & 0 & 6 \\ 0 & 1 & 17 & -3 & -21 \\ 0 & 0 & 1 & -\frac{3}{10} & -\frac{7}{5} \end{bmatrix}$$

$$-\frac{1}{20}R_3 \rightarrow R_3$$

The elementary row matrix representing this last row operation is

$$E_4 = \begin{bmatrix} 1 & 0 & 0 \\ 0 & 1 & 0 \\ 0 & 0 & -\frac{1}{20} \end{bmatrix}$$

Let $D = E_4^{-1} = \text{Diag}(1, 1, -20)$, a diagonal matrix. With a renaming of U to be the upper echelon matrix whose diagonal elements are 1,

$$A = LDU = \begin{bmatrix} 1 & 0 & 0 \\ 5 & 1 & 0 \\ 6 & 3 & 1 \end{bmatrix} \begin{bmatrix} 1 & 0 & 0 \\ 0 & 1 & 0 \\ 0 & 0 & -20 \end{bmatrix} \begin{bmatrix} 1 & 0 & -4 & 0 & 6 \\ 0 & 1 & 17 & -3 & -21 \\ 0 & 0 & 1 & -\frac{3}{10} & -\frac{7}{5} \end{bmatrix}$$

If row swappings are needed in the forward elimination, then the *LDU decomposition* method must be slightly modified, because matrices representing row swappings are not lower triangular. A matrix which represents swapping rows is called a *permutation matrix*.

EXAMPLE
7.16

$$A = \begin{bmatrix} 1 & 1 & 0 \\ 2 & 2 & 1 \\ -1 & 0 & 1 \end{bmatrix} \xrightarrow{\begin{array}{l} -2R_1 + R_2 \rightarrow R_2 \\ R_1 + R_3 \rightarrow R_3 \end{array}} \sim \begin{bmatrix} 1 & 1 & 0 \\ 0 & 0 & 1 \\ 0 & 1 & 1 \end{bmatrix} \xrightarrow{R_2 \leftrightarrow R_3} \sim \begin{bmatrix} 1 & 1 & 0 \\ 0 & 1 & 1 \\ 0 & 0 & 1 \end{bmatrix} = U$$

If E_k ($k = 1, 2, 3$) represent the row operations, then $U = E_3 E_2 E_1 A$. Consequently,

$$A = E_1^{-1} E_2^{-1} E_3^{-1} U = \begin{bmatrix} 1 & 0 & 0 \\ 2 & 0 & 1 \\ -1 & 1 & 0 \end{bmatrix} \begin{bmatrix} 1 & 1 & 0 \\ 0 & 1 & 1 \\ 0 & 0 & 1 \end{bmatrix}$$

The first matrix in the decomposition is not lower triangular. However, apply the operation $R_2 \leftrightarrow R_3$ to A first. Let $P = E_3$, a permutation matrix. Then

$$PA = \begin{bmatrix} 1 & 1 & 0 \\ -1 & 0 & 1 \\ 2 & 2 & 1 \end{bmatrix} = \begin{bmatrix} 1 & 0 & 0 \\ -1 & 1 & 0 \\ 2 & 0 & 1 \end{bmatrix} \begin{bmatrix} 1 & 1 & 0 \\ 0 & 1 & 1 \\ 0 & 0 & 1 \end{bmatrix} = LU$$

In general, the factorization can be written as $PA = LDU$, where

1. P represents row operations of type $R_i \leftrightarrow R_j$;
2. L is lower triangular, represents row operations of type $c_i R_i + R_j \rightarrow R_j$, and has diagonal entries 1;
3. D is diagonal and represents row operations of type $cR_i \rightarrow R_i$; and
4. U is upper echelon with diagonal entries 1.

In practice, we cannot expect to know which row swappings must be performed first in order to obtain $PA = LDU$. The following procedure allows us to postprocess the elementary row operations so that the row swappings are applied first. Apply row operations in the usual manner: Do $cR_i + R_j \rightarrow R_j$ and $R_i \leftrightarrow R_j$ first, $cR_i \rightarrow R_i$ last.

EXAMPLE
7.17

$$A = \begin{bmatrix} 1 & 3 & 0 \\ 2 & 6 & 1 \\ -1 & 0 & 2 \end{bmatrix} \xrightarrow{\begin{array}{l} -2R_1 + R_2 \rightarrow R_2 \\ R_1 + R_3 \rightarrow R_3 \end{array}} \sim \begin{bmatrix} 1 & 3 & 0 \\ 0 & 0 & 1 \\ 0 & 3 & 2 \end{bmatrix}$$

$$\xrightarrow{R_2 \leftrightarrow R_3} \sim \begin{bmatrix} 1 & 3 & 0 \\ 0 & 3 & 2 \\ 0 & 0 & 1 \end{bmatrix} \xrightarrow{\frac{1}{3}R_2 \rightarrow R_2} \begin{bmatrix} 1 & 3 & 0 \\ 0 & 1 & \frac{2}{3} \\ 0 & 0 & 1 \end{bmatrix}$$

Instead of switching rows 2 and 3 of A first and re-reducing, do the following. Write down the operations in the order applied:

$$-2R_1 + R_2 \rightarrow R_2, \quad R_1 + R_3 \rightarrow R_3, \quad R_2 \leftrightarrow R_3, \quad \frac{1}{3}R_2 \rightarrow R_2$$

The row swapping operations should appear *first*. Interchange the row swapping operation with the one directly to its left. In doing so, swap any row indices on that operation matching those of the row interchange. In the example,

$$-2R_1 + R_2 \rightarrow R_2, \quad R_2 \leftrightarrow R_3, \quad R_1 + R_2 \rightarrow R_2, \quad \frac{1}{3}R_2 \rightarrow R_2$$

and

$$R_2 \leftrightarrow R_3, \quad -2R_1 + R_3 \rightarrow R_3, \quad R_1 + R_2 \rightarrow R_2, \quad \frac{1}{3}R_2 \rightarrow R_2$$

give the correct ordering of the operations, with row swappings first. Therefore,

$$P = \begin{bmatrix} 1 & 0 & 0 \\ 0 & 0 & 1 \\ 0 & 1 & 0 \end{bmatrix}, \quad L = \begin{bmatrix} 1 & 0 & 0 \\ 1 & 1 & 0 \\ -2 & 0 & 1 \end{bmatrix}, \quad D = \begin{bmatrix} 1 & 0 & 0 \\ 0 & 3 & 0 \\ 0 & 0 & 1 \end{bmatrix}, \quad U = \begin{bmatrix} 1 & 3 & 0 \\ 0 & 1 & 2 \\ 0 & 0 & 1 \end{bmatrix}$$

The examples so far have been relatively simple. Here is a physics application that is a bit more in-depth. If you are not yet ready for the calculus portion of the problem (the exact solution), skip to the part after the point where an approximation is made to the second derivative function.

EXAMPLE 7.18

Given a homogeneous, thin rod of constant cross section and length 1, which is insulated except at its ends, a simple model of steady-state heat distribution in the rod is

$$\begin{aligned} -u''(x) &= f(x), \quad 0 < x < 1 \\ u(0) &= u(1) = 0 \end{aligned}$$

where $u(x)$ is the quantity of heat at position x , $f(x) \geq 0$ is a given heat source, and $u(0) = u(1) = 0$ represents fixed temperature 0 at the ends.

EXACT SOLUTION Integrate the differential equation $u''(x) = -f(x)$ from 0 to x to obtain

$$u'(x) = u'(0) - \int_0^x f(t) dt$$

where $u'(0)$ needs to be determined. Integrate again from 0 to x to obtain

$$u(x) = u(0) + u'(0)x - \int_0^x \int_0^s f(t) dt ds$$

(Example 7.18
continued)Using the conditions $u(0) = u(1) = 0$ yields

$$u'(0) = \int_0^1 \int_0^s f(t) dt ds$$

so that

$$u(x) = x \int_0^1 \int_0^s f(t) dt ds - \int_0^x \int_0^s f(t) dt ds$$

The double integral can be manipulated so that

$$u(x) = \int_0^1 G(x, t) f(t) dt$$

where

$$G(x, t) = \begin{cases} (1-t)x, & x \leq t \\ (1-x)t, & x \geq t \end{cases}$$

In most cases for $f(t)$, the integral for $u(x)$ cannot be evaluated symbolically to obtain a closed-form solution in terms of elementary functions. However, you can resort to numerical integration methods to obtain approximate values for $u(x)$.**APPROXIMATE SOLUTION** Find approximations to the values $u(jh)$ for $1 \leq j \leq n$, where $h = 1/(n+1)$ for some large positive integer n . From calculus,

$$u''(x) = \lim_{h \rightarrow 0} \frac{u(x+h) - 2u(x) + u(x-h)}{h^2}$$

The approximation below is reasonable for small values of h ,

$$u''(x) \doteq \frac{u(x+h) - 2u(x) + u(x-h)}{h^2}$$

Replace h by $1/(n+1)$ and $x = jh$, $j = 0, 1, \dots, n+1$. Define $u_j = u(jh)$ (so that $u_0 = u_{n+1} = 0$) and $f_j = f(jh)$. The differential equation is approximated by the second-order linear difference equation

$$\begin{aligned} -u_{j+1} + 2u_j - u_{j-1} &= h^2 f_j, \quad 1 \leq j \leq n \\ u_0 &= u_{n+1} = 0 \end{aligned}$$

We can rewrite this as a system of n equations in n unknowns as

$$A\mathbf{u} = \begin{bmatrix} 2 & -1 & 0 & 0 & \cdots & 0 \\ -1 & 2 & -1 & 0 & \cdots & 0 \\ 0 & -1 & 2 & -1 & \cdots & 0 \\ \vdots & \vdots & \vdots & \vdots & & \vdots \\ 0 & 0 & 0 & 0 & & 2 \end{bmatrix} \begin{bmatrix} u_1 \\ u_2 \\ u_3 \\ \vdots \\ u_n \end{bmatrix} = h^2 \begin{bmatrix} f_1 \\ f_2 \\ f_3 \\ \vdots \\ f_n \end{bmatrix} = h^2 \mathbf{f}$$

The matrix $n \times n$ matrix $A = [a_{ij}]$ can be written concisely as

$$a_{ij} = \begin{cases} 2, & i=j \\ -1, & i=j \pm 1 \\ 0, & \text{otherwise} \end{cases}.$$

Such a matrix is said to be *tridiagonal*.

Consider the case $n = 4$; then

$$A = \begin{bmatrix} 2 & -1 & 0 & 0 \\ -1 & 2 & -1 & 0 \\ 0 & -1 & 2 & -1 \\ 0 & 0 & -1 & 2 \end{bmatrix} \xrightarrow{\frac{1}{2}R_1 + R_2 \rightarrow R_2} \sim \begin{bmatrix} 2 & -1 & 0 & 0 \\ 0 & \frac{3}{2} & -1 & 0 \\ 0 & -1 & 2 & -1 \\ 0 & 0 & -1 & 2 \end{bmatrix}$$

$$\xrightarrow{\frac{2}{3}R_2 + R_3 \rightarrow R_3} \sim \begin{bmatrix} 2 & -1 & 0 & 0 \\ 0 & \frac{3}{2} & -1 & 0 \\ 0 & 0 & \frac{4}{3} & -1 \\ 0 & 0 & -1 & 2 \end{bmatrix} \xrightarrow{\frac{3}{4}R_3 + R_4 \rightarrow R_4} \sim \begin{bmatrix} 2 & -1 & 0 & 0 \\ 0 & \frac{3}{2} & -1 & 0 \\ 0 & 0 & \frac{4}{3} & -1 \\ 0 & 0 & 0 & \frac{5}{4} \end{bmatrix}$$

$$\begin{array}{l} \xrightarrow{\frac{1}{2}R_1 \rightarrow R_1} \begin{bmatrix} 1 & -\frac{1}{2} & 0 & 0 \\ 0 & 1 & -\frac{2}{3} & 0 \\ 0 & 0 & 1 & -\frac{3}{4} \\ 0 & 0 & 0 & 1 \end{bmatrix} \\ \xrightarrow{\frac{2}{3}R_2 \rightarrow R_2} \\ \xrightarrow{\frac{3}{4}R_3 \rightarrow R_3} \\ \xrightarrow{\frac{4}{5}R_4 \rightarrow R_4} \end{array}$$

(Example 7.18
continued)

Therefore,

$$A = \begin{bmatrix} 1 & 0 & 0 & 0 \\ -\frac{1}{2} & 1 & 0 & 0 \\ 0 & -\frac{2}{3} & 1 & 0 \\ 0 & 0 & -\frac{3}{4} & 1 \end{bmatrix} \begin{bmatrix} 2 & 0 & 0 & 0 \\ 0 & \frac{3}{2} & 0 & 0 \\ 0 & 0 & \frac{4}{3} & 0 \\ 0 & 0 & 0 & \frac{5}{4} \end{bmatrix} \begin{bmatrix} 1 & -\frac{1}{2} & 0 & 0 \\ 0 & 1 & -\frac{2}{3} & 0 \\ 0 & 0 & 1 & -\frac{3}{4} \\ 0 & 0 & 0 & 1 \end{bmatrix} = LDU$$

Note that $L^T = U$ and the diagonal entries of D are positive. Also note that A can be factored into

$$A = LDU = L\sqrt{D}\sqrt{D}U = (L\sqrt{D})(L\sqrt{D})^T = MM^T$$

where $\sqrt{\text{Diag}(d_1, \dots, d_n)} = \text{Diag}(\sqrt{d_1}, \dots, \sqrt{d_n})$. ■

A couple of observations are in order. First, if A is invertible, then its LDU decomposition is unique. The proof is by contradiction. Assume that we have two decompositions, $A = L_1 D_1 U_1 = L_2 D_2 U_2$. Then $(L_2^{-1} L_1) D_1 = D_2 (U_2 U_1^{-1})$. The left-hand side is lower triangular and the right-hand side is upper triangular. The only way this can happen is if both are diagonal. Since D_1 is invertible, $L_2^{-1} L_1$ must be diagonal. Since the diagonal entries of L_1 and L_2^{-1} are all 1, the diagonal of their product must all be 1. Therefore, $L_2^{-1} L_1 = I$ and $L_1 = L_2$. Similarly, $U_1 = U_2$. Finally, cancelling the L and U matrices yields $D_1 = D_2$. The conclusion is there can be only one decomposition.

Second, if A is symmetric, then U in the LDU decomposition must be $U = L^T$. That is, $A = LDL^T$. If in addition, the diagonal entries of D are nonnegative, then $A = (L\sqrt{D})(L\sqrt{D})^T$. To prove this, let $A = LDU$. Then $A = A^T = U^T D L^T$. This is another LDU decomposition for, so by the uniqueness we proved in the last paragraph, $U = L^T$. The additional factorization when D has nonnegative entries follows trivially.

7.4 VECTOR SPACES

The central theme of linear algebra is the study of vectors and the sets in which they live, called *vector spaces*. Our intuition about vectors comes from their manipulation in the xy -plane. The classical introduction in a physics setting introduces vectors to represent velocities, accelerations, or forces. In this setting, a vector is normally introduced as a quantity with *direction* and *magnitude*. As such, it does not matter where you place that vector in the plane – it is still the same vector. Figure 7.4 shows a vector \mathbf{v} occurring at two locations in the plane. The standard convention is used to draw the vector as an arrow to indicate its direction, the length of the arrow corresponding to its magnitude.

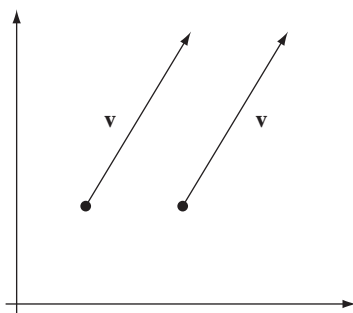


Figure 7.4 A vector v at two locations in the plane.

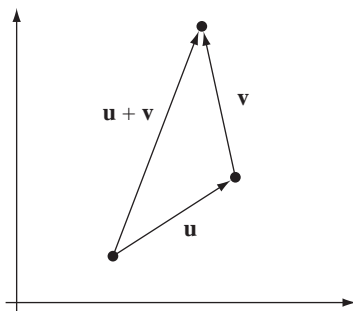


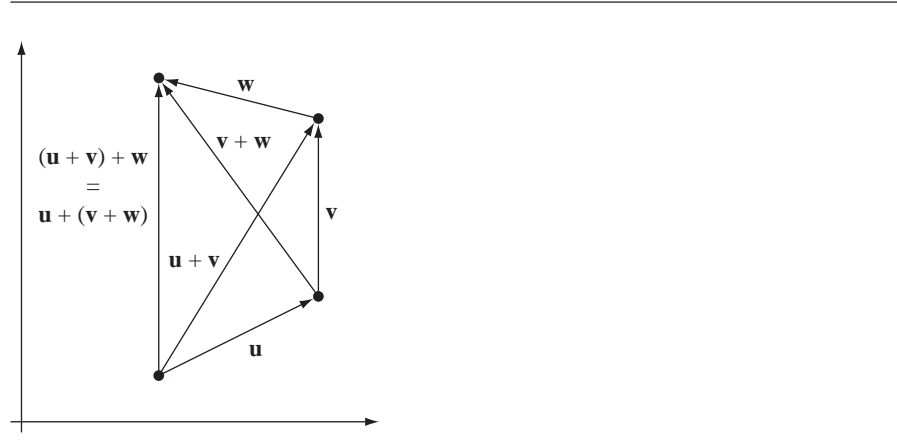
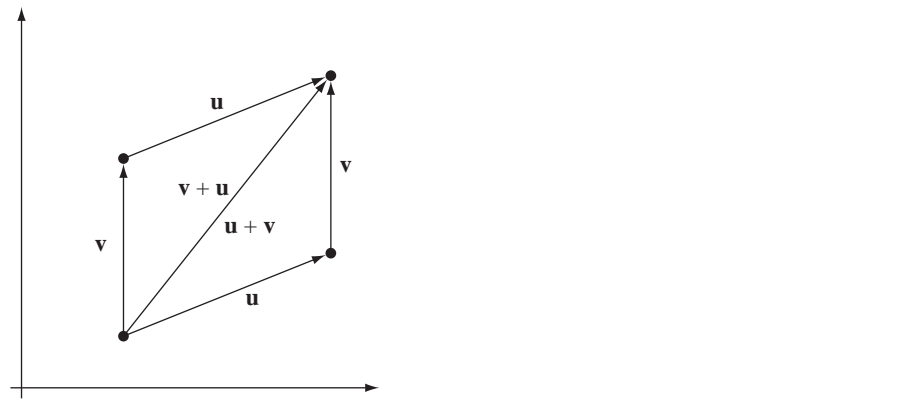
Figure 7.5 Addition of u and v .

Regardless of location, the two arrows have the same direction and same magnitude, so they represent the same vector.

The visual approach of drawing arrows is also used to motivate various operations on vectors. [Figure 7.5](#) illustrates the addition of two vectors u and v , the result denoted $u + v$.

You think of this as starting at the initial point of the arrow u , walking to the end of the arrow to get to the initial point of the arrow v , then walking to the end of that arrow to arrive at your final destination. That destination may be achieved by starting at the initial point of the arrow $u + v$ (placed conveniently at the initial point of u) and walking to the end of the arrow for the sum. The concept of aligning the vectors from initial point to final point and walking along the path may be used for motivation in the remaining rules mentioned next.

[Figure 7.6](#) illustrates that vector addition is associative: $u + (v + w) = (u + v) + w$. Not only is the grouping irrelevant, but also the ordering. [Figure 7.7](#) illustrates that vector addition is commutative: $u + v = v + u$.

Figure 7.6 Addition of \mathbf{u} , \mathbf{v} , and \mathbf{w} . Which pair of vectors is added first is irrelevant.Figure 7.7 Addition of \mathbf{u} and \mathbf{v} . The order of the vectors is irrelevant.

If you start at the initial point of an arrow \mathbf{v} , walk to its final point, then walk back to the initial point, the net effect is as if you never moved in the first place. The $\mathbf{0}$ is used to represent the zero vector that has length zero, but undefined direction, and corresponds to the net effect of no motion. As such, the following rule is suggested: $\mathbf{v} + \mathbf{0} = \mathbf{v}$. The arrow representing moving from the final point of \mathbf{v} to its initial point is denoted $-\mathbf{v}$ and is called the *additive identity* of \mathbf{v} . Figure 7.8 illustrates this vector.

Using our intuition about walking along the vectors, it is always true that $\mathbf{v} + (-\mathbf{v}) = \mathbf{0}$. The concept of an additive identity allows us to naturally define *subtraction*

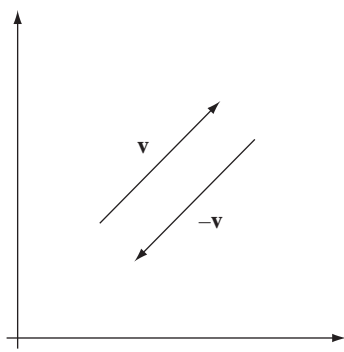


Figure 7.8 A vector v and its additive identity $-v$.

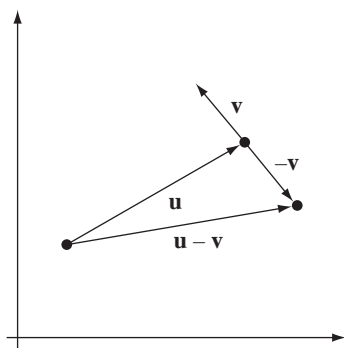


Figure 7.9 The vectors u and v and the difference $u - v$.

of a vector v from a vector u as $u - v = u + (-v)$. The quantity on the left of the equality is also referred to as the *difference* of u and v . Figure 7.9 shows two vectors and their difference.

Typically, though, the sum and difference vectors are visualized as the diagonals of a parallelogram formed by u and v . Figure 7.10 illustrates this.

The direction of a vector v can be preserved, but its length changed by a multiplicative factor $c > 0$. The resulting vector is denoted by cv . Figure 7.11 shows a vector whose length is scaled by 2. The vector $2v$ has the same direction as v but twice the length. The figure also shows the vector $(-2/3)v$, which may be thought of as having the direction of $-v$ but two-thirds of the length. We may as well allow c to be negative in the definition.

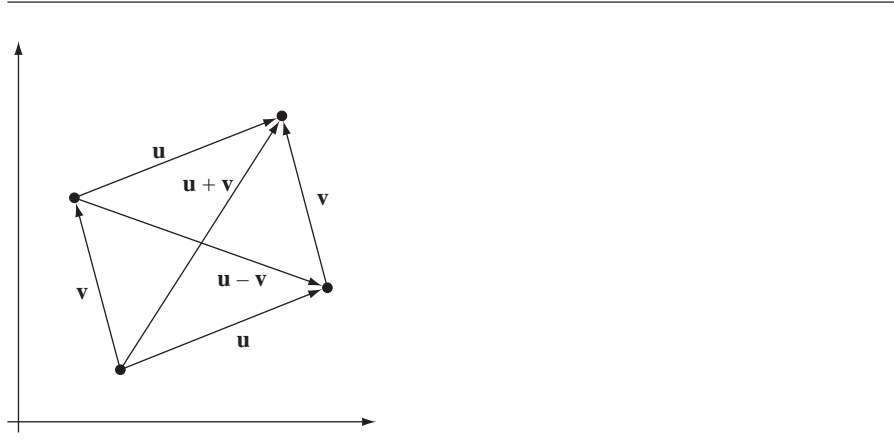


Figure 7.10 The vectors \mathbf{u} and \mathbf{v} , the parallelogram formed by them, and the sum $\mathbf{u} + \mathbf{v}$ and difference $\mathbf{u} - \mathbf{v}$ shown as diagonals of the parallelogram.

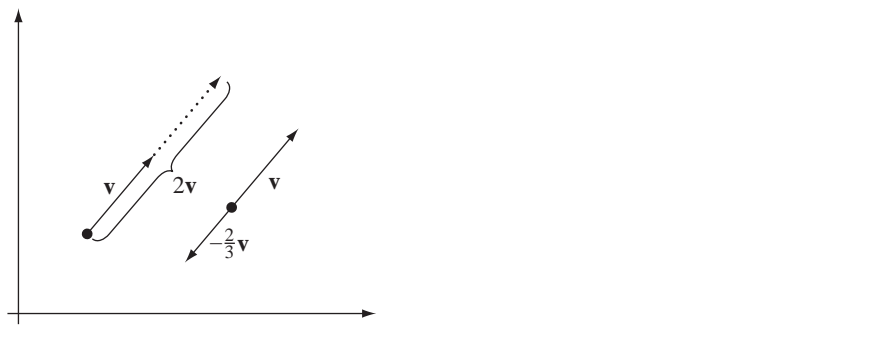


Figure 7.11 The vector \mathbf{v} and two scalar multiples of it, one positive and one negative.

A simple yet relevant observation: If you multiply a vector by the scalar 1, the length is unchanged. This suggests the rule $1 \cdot \mathbf{v} = \mathbf{v}$. The dot is included to emphasize that the left-hand side is a scalar multiple of the vector. It should also be intuitive that you can scale a vector by a , scale that vector by b , and obtain the same vector if you just scaled by ab . The formal rule is: $a(b\mathbf{v}) = (ab)\mathbf{v}$.

Figure 7.12 shows two distributive laws that apply to scalar multiplication of vectors. The left of the figure illustrates the rule for distributing across a scalar sum $(a + b)\mathbf{v} = a\mathbf{v} + b\mathbf{v}$. The right of the figure illustrates the rule for distributing across a vector sum $a(\mathbf{u} + \mathbf{v}) = a\mathbf{u} + a\mathbf{v}$.

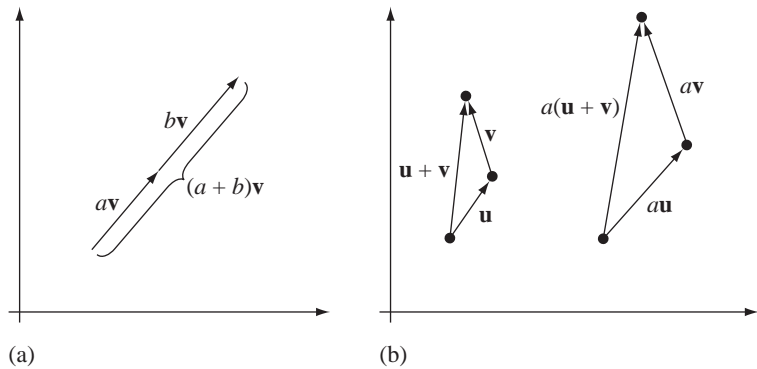


Figure 7.12 (a) Distributing across a scalar sum. (b) Distributing across a vector sum.

The various rules that apply to vectors in the plane also apply to vectors in space. More generally, a lot of systems in practice follow the same rules. The abstraction of the objects we call vectors and of the rules that apply to them leads us to the heart of linear algebra—vector spaces, as defined next.

7.4.1 DEFINITION OF A VECTOR SPACE

Let V be a set whose elements are called *vectors*. Assume that *equality* of vectors is well defined. Suppose that there are two operations, *vector addition* ($+$) and *scalar multiplication* (\cdot), such that the following properties hold. To help distinguish vectors from scalars, vectors are typeset in boldface. In the properties, $\mathbf{u}, \mathbf{v}, \mathbf{w} \in V$ and $a, b \in \mathbb{R}$. We can now state the following 10 axioms:

1. (Closure under $+$): $\mathbf{u} + \mathbf{v} \in V$
2. ($+$ is associative): $\mathbf{u} + (\mathbf{v} + \mathbf{w}) = (\mathbf{u} + \mathbf{v}) + \mathbf{w}$
3. ($+$ is commutative): $\mathbf{u} + \mathbf{v} = \mathbf{v} + \mathbf{u}$
4. (Additive identity): There is a vector $\mathbf{0} \in V$ such that $\mathbf{v} + \mathbf{0} = \mathbf{v}$ for any $\mathbf{v} \in V$
5. (Additive inverses): For each $\mathbf{v} \in V$ there is a vector $-\mathbf{v} \in V$ such that $\mathbf{v} + (-\mathbf{v}) = \mathbf{0}$
6. (Closure under \cdot): $c \cdot \mathbf{v} \in V$, written simply as $c\mathbf{v}$
7. (\cdot is distributive over real addition): $(a + b)\mathbf{v} = a\mathbf{v} + b\mathbf{v}$
8. (\cdot is distributive over vector addition): $a(\mathbf{u} + \mathbf{v}) = a\mathbf{u} + a\mathbf{v}$

9. (\cdot is associative): $a(b\mathbf{u}) = (ab)\mathbf{v}$
10. (Multiplicative identity): The number $1 \in \mathbb{R}$ has the property $1 \cdot \mathbf{v} = \mathbf{v}$

The triple $(V, +, \cdot)$ is called a *vector space* over the real numbers. As it turns out, any field of numbers is allowable, not just the field of real numbers. For example, the complex numbers or even the rational numbers could be used. There are also fields which have a finite number of elements; such fields could be used. In the applications in this book, the field of real numbers invariably is the appropriate choice.

A few comments are in order about the axioms for a vector space. First, the notation for the additive inverse of $\mathbf{v} \in V$, namely, $-\mathbf{v} \in V$, is not to be confused with the scalar multiple $-1 \cdot \mathbf{v}$. However, we will prove that in fact, $-\mathbf{v} = -1 \cdot \mathbf{v}$. Second, the zero vector is indicated as $\mathbf{0}$, but as we will see in a later example, there are vector spaces where the numerical value of $\mathbf{0}$ has nothing to do with “zero.” Third, the numerical value of the multiplicative identity 1 for a field may not be related to the number “one.” (For example, $S = \{0, 2, 4, 6, 8\}$ with addition and multiplication modulo 10 is an example of something called a *finite field*. It has additive identity 0 and multiplicative identity 6.)

EXAMPLE
7.19

This is the classic example of a vector space, n -tuples of numbers whose components are real numbers. Let $V = \mathbb{R}^n = \{(x_1, \dots, x_n) : x_k \in \mathbb{R}, k = 1, \dots, n\}$ be the set of ordered n -tuples of real numbers. Let $\mathbf{x}, \mathbf{y} \in V$, where $\mathbf{x} = (x_1, \dots, x_n)$ and $\mathbf{y} = (y_1, \dots, y_n)$, and let $c \in \mathbb{R}$.

Define *vector equality* by $\mathbf{x} = \mathbf{y}$ if and only if $x_k = y_k$ for every $k = 1, \dots, n$. That is, the vectors must be the same component-wise. Define *vector addition* by

$$\mathbf{x} + \mathbf{y} = (x_1, \dots, x_n) + (y_1, \dots, y_n) = (x_1 + y_1, \dots, x_n + y_n)$$

and define *scalar multiplication* by

$$c \cdot \mathbf{x} = c\mathbf{x} = c(x_1, \dots, x_n) = (cx_1, \dots, cx_n)$$

The triple $(\mathbb{R}^n, +, \cdot)$ is a vector space over the real numbers. The additive identity is $\mathbf{0} = (0, \dots, 0)$. For $\mathbf{x} = (x_1, \dots, x_n)$, the additive inverse is $-\mathbf{x} = (-x_1, \dots, -x_n)$. Each of the 10 axioms for a vector space must be verified. For example, the proof that axiom 3 is satisfied is given as:

$$\begin{aligned}
 \mathbf{x} + \mathbf{y} &= (x_1, \dots, x_n) + (y_1, \dots, y_n) && \text{Definition of } \mathbf{x} \text{ and } \mathbf{y} \\
 &= (x_1 + y_1, \dots, x_n + y_n) && \text{Definition of vector addition} \\
 &= (y_1 + x_1, \dots, y_n + x_n) && \text{Since real addition is commutative} \\
 &= (y_1, \dots, y_n) + (x_1, \dots, x_n) && \text{Definition of vector addition} \\
 &= \mathbf{y} + \mathbf{x} && \text{Definition of } \mathbf{x} \text{ and } \mathbf{y}
 \end{aligned}$$

The verification of the other axioms is left as an exercise. ■

EXAMPLE
7.20

Consider the set of all polynomials with real-valued coefficients,

$$V = \mathbb{R}[x] = \left\{ \sum_{k=0}^n a_k x^k : a_k \in \mathbb{R}, n \in \mathbb{W} \right\}$$

where $\mathbb{W} = \{0, 1, 2, \dots\}$ is the set of whole numbers. Let $\mathbf{p}, \mathbf{q} \in V$ where

$$\mathbf{p} = \sum_{i=0}^n p_i x^i \quad \text{and} \quad \mathbf{q} = \sum_{i=0}^m q_i x^i$$

In the following verifications, we can assume for the sake of argument that $n \geq m$.

Define *vector equality* by $\mathbf{p} = \mathbf{q}$ when $n = m$ and $p_k = q_k$ for all $k = 0, \dots, n$. Define *vector addition*, $\mathbf{p} + \mathbf{q}$, by

$$\mathbf{p} + \mathbf{q} = \sum_{i=0}^m (p_i + q_i) x^i + \sum_{i=m+1}^n p_i x^i$$

By convention, if in the summation $S = \sum_{i=L}^U t_i$, the lower index L is larger than the upper index U , then $S = 0$. Thus, in the above definition if $n = m$, in which case $m+1 > n$, the second summation is zero. Finally, define *scalar multiplication*, $c\mathbf{p}$ for $c \in \mathbb{R}$, by

$$c\mathbf{p} = \sum_{i=0}^n c p_i x^i$$

For example, if $\mathbf{p} = p_0 + p_1 x + p_2 x^2$ and $\mathbf{q} = q_0 + q_1 x$, then

$$\mathbf{p} + \mathbf{q} = (p_0 + q_0) + (p_1 + q_1)x + p_2 x^2 \quad \text{and} \quad c\mathbf{p} = (cp_0) + (cp_1)x + (cp_2)x^2.$$

The triple $(\mathbb{R}[x], +, \cdot)$ is a vector space. The additive identity is the zero polynomial, which can be represented as $\mathbf{0} = 0$, where the right-hand side denotes a constant polynomial (degree zero) whose only coefficient is the scalar zero. The additive inverse for $\mathbf{p} = \sum_{k=0}^n p_k x^k$ is

$$-\mathbf{p} = \sum_{k=0}^n (-p_k) x^k$$

Of course you need to verify the 10 axioms for a vector space. ■

EXAMPLE
7.21

Define $V = F(\mathbb{R}, \mathbb{R})$ to be the set of all real-valued functions of a real-valued variable. Two functions $f(x)$ and $g(x)$ are represented as the vectors $\mathbf{f}, \mathbf{g} \in V$. The vectors are *equal*, denoted $\mathbf{f} = \mathbf{g}$, whenever

$$f(x) = g(x), \quad \text{for all } x \in \mathbb{R}$$

(Example 7.21
continued)Define *vector addition*, $\mathbf{f} + \mathbf{g}$, to be the usual addition of functions:

$$(\mathbf{f} + \mathbf{g})(x) = f(x) + g(x), \quad \text{for all } x \in I$$

That is, the vector $\mathbf{f} + \mathbf{g}$ represents the function $f + g$. Note that the addition on the left represents vector addition, whereas the addition on the right is real addition. Let $c \in \mathbb{R}$ and $\mathbf{f} \in V$. Define *scalar multiplication*, $c \cdot \mathbf{f}$, to be the usual scalar multiplication for functions:

$$(c\mathbf{f})(x) = c \cdot f(x), \quad \text{for all } x \in I$$

The scalar multiplication on the left is that for V , but the scalar multiplication on the right is multiplication of real numbers. The triple $(F(\mathbb{R}, \mathbb{R}), +, \cdot)$ is a vector space. ■

EXAMPLE
7.22

The final example is a strange one, but illustrates how abstract the concept of vector space really is. Let $V = (0, \infty)$ denote the set of positive real numbers. Each positive number $x \in V$ is a vector. Define *vector equality* by $x = y$ when x and y are equal as real numbers. Define *vector addition*, denoted \oplus because of its lack of resemblance to real-valued addition, by $x \oplus y = xy$. That is, the vector addition of two positive numbers is defined to be their product! Define *scalar multiplication*, denoted \odot because of its lack of resemblance to real-valued multiplication, by $c \odot x = x^c$, where c is a scalar and x is a vector. That is, scalar multiplication of a positive number by a real number is defined to be the positive number raised to a power! Note that the additive identity is the positive number 1, *not the real number 0*. The multiplicative identity is the scalar $1 \in \mathbb{R}$. The additive inverse of x is the reciprocal $1/x$. The triple (V, \oplus, \odot) is a vector space, albeit a strange one. ■

Some consequences of the axioms for a vector space are listed here.

1. The additive identity $\mathbf{0}$ is unique.
2. The additive inverse of \mathbf{x} is unique.
3. For any \mathbf{x} , $0\mathbf{x} = \mathbf{0}$.
4. For any $c \in \mathbb{R}$, $c\mathbf{0} = \mathbf{0}$.
5. If $-\mathbf{x}$ is the additive inverse of \mathbf{x} , then $-\mathbf{x} = (-1) \cdot \mathbf{x}$.
6. If $c\mathbf{x} = \mathbf{0}$, then either $c = 0$ or $\mathbf{x} = \mathbf{0}$.

PROOF OF ITEM 1 Suppose there are two additive identities, call them $\mathbf{0}_1$ and $\mathbf{0}_2$. Then

$$\begin{aligned} \mathbf{0}_1 &= \mathbf{0}_1 + \mathbf{0}_2 && \text{Since } \mathbf{0}_2 \text{ is an additive identity} \\ &= \mathbf{0}_2 && \text{Since } \mathbf{0}_1 \text{ is an additive identity} \end{aligned}$$

so there can only be one additive identity.

PROOF OF ITEM 2 Suppose \mathbf{x} has two additive inverses, call them \mathbf{y} and \mathbf{z} . Then

$$\begin{aligned}
 \mathbf{z} &= \mathbf{z} + \mathbf{0} && \text{Since } \mathbf{0} \text{ is the additive identity} \\
 &= \mathbf{z} + (\mathbf{x} + \mathbf{y}) && \text{Since } \mathbf{y} \text{ is an additive inverse for } \mathbf{x} \\
 &= (\mathbf{z} + \mathbf{x}) + \mathbf{y} && \text{Since vector addition is associative} \\
 &= (\mathbf{x} + \mathbf{z}) + \mathbf{y} && \text{Since vector addition is commutative} \\
 &= \mathbf{0} + \mathbf{y} && \text{Since } \mathbf{z} \text{ is an additive inverse for } \mathbf{x} \\
 &= \mathbf{y} + \mathbf{0} && \text{Since vector addition is commutative} \\
 &= \mathbf{y} && \text{Since } \mathbf{0} \text{ is the additive identity}
 \end{aligned}$$

Therefore, \mathbf{x} has only one additive inverse.

PROOF OF ITEM 3 Let \mathbf{y} be the additive inverse for $0\mathbf{x}$. Then

$$\begin{aligned}
 0\mathbf{x} &= (0 + 0)\mathbf{x} && \text{Since } 0 = 0 + 0 \\
 &= 0\mathbf{x} + 0\mathbf{x} && \text{By axiom 7} \\
 0\mathbf{x} + \mathbf{y} &= (0\mathbf{x} + 0\mathbf{x}) + \mathbf{y} \\
 &= 0\mathbf{x} + (0\mathbf{x} + \mathbf{y}) && \text{By axiom 2} \\
 0 &= 0\mathbf{x} + \mathbf{0} && \text{Since } \mathbf{y} \text{ is the additive inverse for } 0\mathbf{x} \\
 &= 0\mathbf{x} && \text{Since } \mathbf{0} \text{ is the additive identity.}
 \end{aligned}$$

PROOF OF ITEM 4 Let $c \in \mathbb{R}$ and let \mathbf{y} be the additive inverse for $c\mathbf{0}$. Then

$$\begin{aligned}
 c\mathbf{0} &= c(\mathbf{0} + \mathbf{0}) && \text{Since } \mathbf{0} \text{ is the additive identity} \\
 &= c\mathbf{0} + c\mathbf{0} && \text{By axiom 8} \\
 c\mathbf{0} + \mathbf{y} &= (c\mathbf{0} + c\mathbf{0}) + \mathbf{y} \\
 &= c\mathbf{0} + (c\mathbf{0} + \mathbf{y}) && \text{By axiom 2} \\
 0 &= c\mathbf{0} + \mathbf{0} && \text{Since } \mathbf{y} \text{ is the additive inverse for } c\mathbf{0} \\
 &= c\mathbf{0} && \text{Since } \mathbf{0} \text{ is the additive identity}
 \end{aligned}$$

PROOF OF ITEM 5

$$\begin{aligned}
 \mathbf{x} + (-1)\mathbf{x} &= 1\mathbf{x} + (-1)\mathbf{x} && \text{By axiom 10} \\
 &= [1 + (-1)]\mathbf{x} && \text{By axiom 7} \\
 &= 0\mathbf{x} && \text{Since } 1 + (-1) = 0 \\
 &= \mathbf{0} && \text{By Item 3 proved earlier}
 \end{aligned}$$

The vector $(-1)\mathbf{x}$ is the additive inverse of \mathbf{x} . By item 2 shown previously, additive inverses are unique; therefore, $-\mathbf{x} = (-1)\mathbf{x}$.

PROOF OF ITEM 6 If $c = 0$, then the conclusion is clearly true. If $c \neq 0$, then

$$\begin{aligned} \mathbf{0} &= c\mathbf{x} && \text{By hypothesis} \\ \frac{1}{c}\mathbf{0} &= \frac{1}{c}(c\mathbf{x}) \\ \mathbf{0} &= \frac{1}{c}(c\mathbf{x}) && \text{By Item 4 proved earlier} \\ &= \left(\frac{1}{c}c\right)\mathbf{x} && \text{By axiom 9} \\ &= 1\mathbf{x} \\ &= \mathbf{x} && \text{By axiom 10} \end{aligned}$$

so $\mathbf{x} = \mathbf{0}$.

7.4.2 LINEAR COMBINATIONS, SPANS, AND SUBSPACES

Let $\mathbf{x}_k \in V$, a vector space, and let $c_k \in \mathbb{R}$ for $k = 1, \dots, n$. The expression

$$c_1\mathbf{x}_1 + \cdots + c_n\mathbf{x}_n = \sum_{k=1}^n c_k\mathbf{x}_k$$

is called a *linear combination* of the vectors.

EXAMPLE
7.23

All vectors in \mathbb{R}^2 can be written as a linear combination of the vectors $(1, 1)$ and $(1, -1)$. To prove this, we verify that each vector $(x, y) = c_1(1, 1) + c_2(1, -1)$ for some choice of c_1, c_2 .

$$\begin{aligned} (x, y) &= c_1(1, 1) + c_2(1, -1) \\ &= (c_1, c_1) + (c_2, -c_2) && \text{By definition of scalar multiplication} \\ &= (c_1 + c_2, c_1 - c_2) && \text{By definition of vector addition} \end{aligned}$$

Using the definition for vector equality, $x = c_1 + c_2$ and $y = c_1 - c_2$. We have two equations in the two unknowns c_1, c_2 . Solve these to obtain $c_1 = \frac{x+y}{2}$ and $c_2 = \frac{x-y}{2}$. Thus,

$$(x, y) = \frac{x+y}{2}(1, 1) + \frac{x-y}{2}(1, -1)$$

a unique representation of (x, y) as a linear combination of $(1, 1)$ and $(1, -1)$. ■

Let V be a vector space and let $A \subset V$. The *span* of A is the set

$$\text{Span}[A] = \left\{ \sum_{k=1}^n c_k\mathbf{x}_k : n > 0, c_k \in \mathbb{R}, \mathbf{x}_k \in A \right\}$$

That is, the span is the set of all finite linear combinations of vectors in A . The subset A need not be finite, and the number of terms in the sums can be arbitrarily large. For example, in the last example all vectors $(x, y) \in \mathbb{R}^2$ can be written as linear combinations of $(1, 1)$ and $(1, -1)$, which implies $\mathbb{R}^2 = \text{Span}[(1, 1), (1, -1)]$.

A general result may be stated now. Let $(V, +, \cdot)$ be a vector space. Let A be a nonempty subset of V . The triple $(\text{Span}[A], +, \cdot)$ is also a vector space. To prove this, we must verify the 10 axioms for a vector space.

1. Let $\mathbf{x}, \mathbf{y} \in \text{Span}[A]$. Then $\mathbf{x} = \sum_{i=1}^n a_i \mathbf{x}_i$ and $\mathbf{y} = \sum_{j=1}^m b_j \mathbf{y}_j$ for some $a_i, b_j \in \mathbb{R}$ and for some $\mathbf{x}_i, \mathbf{y}_j \in V$. Thus, $\mathbf{x} + \mathbf{y} = \sum_{i=1}^n a_i \mathbf{x}_i + \sum_{j=1}^m b_j \mathbf{y}_j = \sum_{k=1}^{n+m} c_k \mathbf{z}_k \in \text{Span}[A]$ where

$$c_k = \begin{cases} a_k, & 1 \leq k \leq n \\ b_{k-n}, & n+1 \leq k \leq n+m \end{cases}, \quad \mathbf{z}_k = \begin{cases} \mathbf{x}_k, & 1 \leq k \leq n \\ \mathbf{y}_{k-n}, & n+1 \leq k \leq n+m \end{cases}$$

2. Since $+$ is associative in V , it is associative in any subset of V . The set $\text{Span}[A]$ of linear combinations of elements in $A \subset V$ must itself be a subset of V . Thus, $+$ is associative in $\text{Span}[A]$.
3. Since $+$ is commutative in V , it is commutative in any subset of V . Thus, $+$ is commutative in $\text{Span}[A]$.
4. If $\mathbf{0}$ is the additive identity in V , then we show also that $\mathbf{0} \in \text{Span}[A]$. The set $A \neq \emptyset$ implies $\text{Span}[A] \neq \emptyset$. Let $\mathbf{x} \in \text{Span}[A]$. Then $\mathbf{x} = \sum_{i=1}^n a_i \mathbf{x}_i$ for some $a_i \in \mathbb{R}$ and for some $\mathbf{x}_i \in A$. Moreover, $\mathbf{x} + (-1)\mathbf{x} = \sum_{i=1}^n [a_i + (-1)a_i] \mathbf{x}_i \in \text{Span}[A]$. But $\mathbf{0} = \mathbf{x} + (-1)\mathbf{x}$ by an earlier result, so $\mathbf{0} \in \text{Span}[A]$.
5. Let $\mathbf{x} \in \text{Span}[A] \subset V$. We need to show that $-\mathbf{x} \in \text{Span}[A]$. Since \mathbf{x} is in the span, $\mathbf{x} = \sum_{i=1}^n a_i \mathbf{x}_i$ for some $a_i \in \mathbb{R}$ and for some $\mathbf{x}_i \in A$. Then $-\mathbf{x} = (-1)\mathbf{x} = \sum_{i=1}^n -a_i \mathbf{x}_i$ is a linear combination of elements of A , so $-\mathbf{x} \in \text{Span}[A]$.
6. Let $c \in \mathbb{R}$ and $\mathbf{x} \in \text{Span}[A]$. Then $\mathbf{x} = \sum_{i=1}^n a_i \mathbf{x}_i$ for some $a_i \in \mathbb{R}$ and for some $\mathbf{x}_i \in A$. But

$$\begin{aligned} c\mathbf{x} &= c \sum_{i=1}^n a_i \mathbf{x}_i \\ &= \sum_{i=1}^n c(a_i \mathbf{x}_i) \quad \text{by axiom 8 for } V \\ &= \sum_{i=1}^n (ca_i) \mathbf{x}_i \quad \text{by axiom 9 for } V \\ &\in \text{Span}[A] \end{aligned}$$

7. Since scalar multiplication is distributive over real addition in V , it is distributive in any subset of V . Thus, scalar multiplication is distributive over real addition in $\text{Span}[A]$.

8. Since scalar multiplication is distributive over vector addition in V , it is distributive in any subset of V . Thus, scalar multiplication is distributive over vector addition in $\text{Span}[A]$.
9. Since scalar multiplication is associative in V , it is associative in any subset of V . Thus, scalar multiplication is associative in $\text{Span}[A]$.
10. Since $1 \cdot \mathbf{x} = \mathbf{x}$ for all vectors in V , the same property is true in any subset. Thus, $1 \cdot \mathbf{x} = \mathbf{x}$ for $\mathbf{x} \in \text{Span}[A]$.

If a nonempty subset S of a vector space V is itself a vector space, S is said to be a *subspace* of V . For any given subset S , the 10 axioms for a vector space can be checked to see if S is a subspace. However, an analysis of the proof that the span of a set is a subspace shows that many of the vector space axioms are automatically satisfied just because of the fact that you are working with a subset of V . As it turns out, to show that $S \subset V$ is a subspace, we need only verify closure under scalar multiplication and vector addition. That is, $S \subset V$ is a subspace if and only if $a\mathbf{x} + b\mathbf{y} \in S$ for any $a, b \in \mathbb{R}$ and $\mathbf{x}, \mathbf{y} \in S$.

**EXAMPLE
7.24**

Let $V = \mathbb{R}^3$ and $S = \{(x_1, x_2, x_3) : x_1 = x_2\}$. The subset S is a subspace. To verify, let $a, b \in \mathbb{R}$ and $\mathbf{x}, \mathbf{y} \in S$; then

$$\begin{aligned} a\mathbf{x} + b\mathbf{y} &= a(x_1, x_2, x_3) + b(y_1, y_2, y_3) && \text{Notation} \\ &= a(x_1, x_1, x_3) + b(y_1, y_1, y_3) && \text{Since } \mathbf{x}, \mathbf{y} \in S \\ &= (ax_1, ax_1, ax_3) + (by_1, by_1, by_3) && \text{Definition of scalar multiplication} \\ &= (ax_1 + by_1, ax_1 + by_1, ax_3 + by_3) && \text{Definition of vector addition} \end{aligned}$$

Since the first two components of the last vector in the displayed equation are equal, that vector is in S . That is, $a\mathbf{x} + b\mathbf{y} \in S$ and S must be a subspace of V . ■

**EXAMPLE
7.25**

Let $V = \mathbb{R}^2$ and $S = \{(x_1, x_2) : x_2 = x_1 + 1\}$. The subset S is not a subspace for many reasons, one of which is that $(0, 0) \notin S$. ■

7.4.3 LINEAR INDEPENDENCE AND BASES

Let V be a vector space. If possible, we would like to find sets $A \subset V$ such that $\text{Span}[A] = V$. For example, let $V = \mathbb{R}^2$. If $A = \{(x, y) : x \geq 0\}$, then it is easily shown that $\text{Span}[A] = \mathbb{R}^2$. If $B = \{(1, 1), (1, -1)\}$, then also $\text{Span}[B] = \mathbb{R}^2$. In some sense, B is a “smaller” set than A . Given a suitable definition for “smallness,” we want to find the “smallest” sets $A \subset V$ for which $\text{Span}[A] = V$. The following concept gives us a handle on this. Let $(V, +, \cdot)$ be a vector space. The vectors $\mathbf{x}_1, \dots, \mathbf{x}_n \in V$. The vectors are *linearly dependent* if

$$\sum_{k=1}^n c_k \mathbf{x}_k = c_1 \mathbf{x}_1 + \cdots + c_n \mathbf{x}_n = \mathbf{0}$$

for some set of scalars c_1, \dots, c_n which are *not all zero*. If there is no such set of scalars, then the vectors are *linearly independent*. A set of vectors is said to be a *linearly independent set* (*linearly dependent set*) if the vectors in that set are linearly independent (linearly dependent).

EXAMPLE
7.26

For $V = \mathbb{R}^3$, the vectors $\mathbf{x}_1 = (1, 0, -1)$, $\mathbf{x}_2 = (2, 1, 0)$, $\mathbf{x}_3 = (0, 0, 1)$, $\mathbf{x} = (-1, 1, 2)$ are linearly dependent. Set:

$$\begin{aligned}(0, 0, 0) &= c_1(1, 0, -1) + c_2(2, 1, 0) + c_3(0, 0, 1) + c_4(-1, 1, 2) \\ &= (c_1 + 2c_2 - c_4, c_2 + c_4, -c_1 + c_3 + 2c_4)\end{aligned}$$

This equation can be formulated as a linear system of equations,

$$\begin{bmatrix} 1 & 2 & 0 & -1 \\ 0 & 1 & 0 & 1 \\ -1 & 0 & 1 & 2 \end{bmatrix} \begin{bmatrix} c_1 \\ c_2 \\ c_3 \\ c_4 \end{bmatrix} = \begin{bmatrix} 0 \\ 0 \\ 0 \end{bmatrix}$$

This system of three equations in four unknowns has infinitely many solutions. In particular, it must have a nonzero solution. We could also solve the system:

$$\begin{array}{lll} A & = & \begin{bmatrix} 1 & 2 & 0 & -1 \\ 0 & 1 & 0 & 1 \\ -1 & 0 & 1 & 2 \end{bmatrix} \\ & \sim & \begin{bmatrix} 1 & 2 & 0 & -1 \\ 0 & 1 & 0 & 1 \\ 0 & 2 & 1 & 1 \end{bmatrix} \\ R_1 + R_3 \rightarrow R_3 & & \\ & \sim & \begin{bmatrix} 1 & 0 & 0 & -3 \\ 0 & 1 & 0 & 1 \\ 0 & 0 & 1 & -1 \end{bmatrix} \\ -2R_2 + R_1 \rightarrow R_1 & & \\ -2R_2 + R_3 \rightarrow R_3 & & \\ & = & A_r \end{array}$$

The general solution is

$$\begin{bmatrix} c_1 \\ c_2 \\ c_3 \\ c_4 \end{bmatrix} = c_4 \begin{bmatrix} 3 \\ -1 \\ 1 \\ 1 \end{bmatrix}$$

Choose $c_4 = 1$; then $c_1 = 3$, $c_2 = -1$, and $c_3 = 1$. We can write

$$3(1, 0, -1) - 1(2, 1, 0) + 1(0, 0, 1) + 1(-1, 1, 2) = (0, 0, 0)$$

and the vectors are linearly dependent. ■

EXAMPLE 7.27 In $V = \mathbb{R}^2$, the vectors $(1, 1)$ and $(1, -1)$ are linearly independent. Let $c_1(1, 1) + c_2(1, -1) = (0, 0)$. Then $(c_1 + c_2, c_1 - c_2) = (0, 0)$ and so $c_1 + c_2 = 0$, $c_1 - c_2 = 0$. The *only* solution to this system is $c_1 = c_2 = 0$, so the vectors are linearly independent. ■

EXAMPLE 7.28 Let $V = F(\mathbb{R}, \mathbb{R})$ be the vector space of all real-valued functions whose domain is the set of real numbers. The vectors \mathbf{f} and \mathbf{g} that represent the functions $f(x) = \sin x$ and $g(x) = \cos x$, respectively, are linearly independent. The vector $\mathbf{h} = c_1\mathbf{f} + c_2\mathbf{g}$ represents the function $h(x) = c_1 f(x) + c_2 g(x)$. Setting $\mathbf{h} = \mathbf{0}$ is equivalent to requiring $h(x) \equiv 0$; that is, $h(x) = 0$ is true for *all* values of x . In particular, $0 = h(0) = c_1 \sin(0) + c_2 \cos(0) = c_2$ and $0 = h(\pi/2) = c_1 \sin(\pi/2) + c_2 \cos(\pi/2) = c_1$. Since both $c_1 = 0$ and $c_2 = 0$, the vectors \mathbf{f} and \mathbf{g} are linearly independent. ■

The following result is an important one. Let V be a vector space and let $A = \{\mathbf{x}_i \in V : i = 1, \dots, n\}$ be a linearly independent set of vectors. Each vector $\mathbf{x} \in \text{Span}[A]$ has a *unique representation* $\mathbf{x} = \sum_{i=1}^n a_i \mathbf{x}_i$. The proof of this result is by contradiction. Suppose that there are two distinct representations $\mathbf{x} = \sum_{i=1}^n a_i \mathbf{x}_i$ and $\mathbf{x} = \sum_{i=1}^n b_i \mathbf{x}_i$, where not all $a_i = b_i$. Subtract \mathbf{x} from itself:

$$\mathbf{0} = \mathbf{x} - \mathbf{x} = \sum_{i=1}^n a_i \mathbf{x}_i - \sum_{i=1}^n b_i \mathbf{x}_i = \sum_{i=1}^n (a_i - b_i) \mathbf{x}_i = \sum_{i=1}^n c_i \mathbf{x}_i$$

where $c_i = a_i - b_i$. Because the vectors in A are linearly independent, all $c_i = 0$, so $a_i = b_i$ for all $i = 1, \dots, n$, a contradiction to the assumption that not all $a_i = b_i$. Thus, there can be only one representation of \mathbf{x} . The value a_i in the unique representation are called the *coefficients of \mathbf{x} with respect to A* .

EXAMPLE 7.29 In an earlier example we had shown that $\mathbb{R}^2 = \text{Span}[\{(1, 1), (1, -1)\}]$, where

$$\mathbf{x} = (x_1, x_2) = \frac{x_1 + x_2}{2}(1, 1) + \frac{x_1 - x_2}{2}(1, -1)$$

The coefficients of \mathbf{x} with respect to $A = \{(1, 1), (1, -1)\}$ are $\frac{x_1+x_2}{2}$ and $\frac{x_1-x_2}{2}$ where the order is important. ■

A couple of useful algorithms are provided for manipulating sets based on linear independence or dependence.

Removing vectors from a linearly dependent set to obtain a linearly independent set. Let $\mathbf{x}_1, \dots, \mathbf{x}_n$ ($n \geq 2$) be linearly dependent vectors; then $\sum_{k=1}^n c_k \mathbf{x}_k = \mathbf{0}$ for coefficients c_k that are not all zero. Suppose that $c_m \neq 0$ for some index m . We can solve for \mathbf{x}_m to obtain

$$\mathbf{x}_m = - \sum_{\substack{k=1 \\ k \neq m}}^n \frac{c_k}{c_m} \mathbf{x}_k$$

Moreover,

$$\text{Span}[\{\mathbf{x}_1, \dots, \mathbf{x}_n\} \setminus \{\mathbf{x}_m\}] = \text{Span}[\{\mathbf{x}_1, \dots, \mathbf{x}_n\}]$$

because for any vector \mathbf{y} which is a linear combination of the \mathbf{x}_k , just replace the \mathbf{x}_m term by the relationship given above for \mathbf{x}_m as a linear combination of the other \mathbf{x}_k .

Inserting vectors into a linearly independent set to retain a linearly independent set. Let $A = \{\mathbf{x}_1, \dots, \mathbf{x}_n\}$ be a linearly independent set. Let $\mathbf{y} \notin \text{Span}[A]$; then $A \cup \{\mathbf{y}\}$, the union of A and the singleton set containing \mathbf{y} , is also a linearly independent set. Consider the linear combination

$$c_0\mathbf{y} + c_1\mathbf{x}_1 + \cdots + c_n\mathbf{x}_n = \mathbf{0}$$

If $c_0 \neq 0$, then we can solve the equation for \mathbf{y} ,

$$\mathbf{y} = -\frac{c_1}{c_0}\mathbf{x}_1 - \cdots - \frac{c_n}{c_0}\mathbf{x}_n \in \text{Span}[A]$$

a contradiction to the assumption that $\mathbf{y} \notin \text{Span}[A]$. It must be that $c_0 = 0$. Consequently, $c_1\mathbf{x}_1 + \cdots + c_n\mathbf{x}_n = \mathbf{0}$. But the \mathbf{x}_k are linearly independent, so $c_k = 0$ for $k = 1, \dots, n$. We have shown that $c_k = 0$ for $k = 0, \dots, n$, and so $A \cup \{\mathbf{y}\}$ is a linearly independent set.

This leads us to an important concept in linear algebra. Let V be a vector space with subset $A \subset V$. The set A is said to be a *basis* for V if A is linearly independent and $\text{Span}[A] = V$. The plural of the term *basis* is *bases*.

EXAMPLE
7.30

Let $V = \mathbb{R}^2$ with the usual vector addition and scalar multiplication. Accordingly,

1. $\{(1, 0), (0, 1)\}$ is a basis for V . It is easy to show that the two vectors are linearly independent. To show that they span V , note that

$$(x, y) = (x, 0) + (0, y) = x(1, 0) + y(0, 1)$$

2. $\{(1, 1), (1, -1), (0, 1)\}$ is not a basis for V because the vectors are linearly dependent:

$$1(1, 1) - 1(1, -1) - 2(0, 1) = (0, 0)$$

However, they do span V because

$$(x, y) = \frac{x+y-2}{2}(1, 1) + \frac{x-y+2}{2}(1, -1) + 2(0, 1)$$

3. $\{(0, 1)\}$ is not a basis for V . The set is linearly independent. However, $V \neq \text{Span}[\{(0, 1)\}]$ because $(1, 0) \in V$ but $(1, 0) \notin \text{Span}[\{(0, 1)\}]$. ■

The last example is designed to illustrate that, in fact, a basis for V is the smallest set of vectors whose span is V . The term smallest in this sense is the number of vectors in the set. Now it is the case that V can have many bases. For example, $\{(1, 0), (0, 1)\}$ and $\{(1, 1), (1, -1)\}$ are bases for \mathbb{R}^2 . Note that the two bases have the same number of elements. The number of elements of a set A , called the *cardinality* of the set, is denoted by $|A|$. The properties in the following list are valid for a vector space V that

has a basis B of cardinality $|B| = n$. The set A in the first three items is any subset of V .

1. If $|A| > n$, then A is linearly dependent. The contrapositive of this statement is, if A is linearly independent, then $|A| \leq n$.
2. If $\text{Span}[A] = V$, then $|A| \geq n$.
3. Every basis of V has cardinality n . The vector space is said to have dimension $\dim(V) = n$ and is referred to as a *finite dimensional vector space*.

PROOF OF ITEM 1 Let the known basis be $B = \{\mathbf{y}_1, \dots, \mathbf{y}_n\}$. Choose $A = \{\mathbf{x}_1, \dots, \mathbf{x}_{n+1}\}$ to be a linearly independent set of $n+1$ vectors, so $|A| = n+1$. Since B is a basis, each vector \mathbf{x}_i has a unique representation with respect to that basis,

$$\mathbf{x}_i = \sum_{j=1}^n c_{ij} \mathbf{y}_j$$

for $1 \leq i \leq n+1$. To show that the \mathbf{x}_i are linearly dependent, show that there are values d_i , not all zero, such that $\sum_{i=1}^{n+1} d_i \mathbf{x}_i = 0$:

$$\begin{aligned} 0 &= \sum_{i=1}^{n+1} d_i \mathbf{x}_i \\ &= \sum_{i=1}^{n+1} d_i \left(\sum_{j=1}^n c_{ij} \mathbf{y}_j \right) \\ &= \sum_{i=1}^{n+1} \sum_{j=1}^n d_i c_{ij} \mathbf{y}_j \\ &= \sum_{j=1}^n \left(\sum_{i=1}^{n+1} d_i c_{ij} \right) \mathbf{y}_j \end{aligned}$$

Since the \mathbf{y}_j are linearly independent, $\sum_{i=1}^{n+1} c_{ij} d_i = 0$ for $1 \leq j \leq n$. But this is a system of n equations in $n+1$ unknowns, so there must be a nonzero solution. That is, there must be a solution for which not all d_i are zero. Indeed, the \mathbf{x}_i must be linearly dependent and A is a linearly dependent set.

PROOF OF ITEM 2 The proof is by contradiction. Suppose that $A \subset V$ and $V = \text{Span}[A]$. Assume that $|A| = m < n$, say $A = \{\mathbf{x}_1, \dots, \mathbf{x}_m\}$. Remove linearly dependent vectors until we have a set $A' = \{\mathbf{y}_1, \dots, \mathbf{y}_\ell\}$ which is linearly independent and for which $V = \text{Span}[A']$. Because we have potentially removed vectors from the set, $\ell \leq m < n$. The fact that A' is a linearly independent set and the fact that the span of A' is V means that A' is a basis for V with cardinality ℓ . The basis B is a set whose cardinality $|B| = n > \ell$, to which (by item 1), B must be a linearly dependent set, a contradiction to B being a basis. The assumption $|A| < n$ cannot be valid, so in fact $|A| \geq n$.

PROOF OF ITEM 3 The basis B for V has cardinality n , the number mentioned in the first two items. Let C be a basis for V . Since C is a linearly independent set, item 1 says that $|C| \leq n$. Since $V = \text{Span}[C]$, item 2 says that $|C| \geq n$. The two conditions require that $|C| = n$.

EXAMPLE
7.31

Observe that $\dim(\mathbb{R}^n) = n$ since a basis is given by $\{\mathbf{e}_1, \dots, \mathbf{e}_n\}$, where \mathbf{e}_j is the n -tuple whose j th component is 1, and all other components are 0. It is easy to verify that these vectors are linearly independent. To see that they span \mathbb{R}^n :

$$\begin{aligned}(x_1, \dots, x_n) &= (x_1, 0, \dots, 0) + (0, x_2, 0, \dots, 0) + \cdots + (0, \dots, 0, x_n) \\&= x_1(1, 0, \dots, 0) + x_2(0, 1, 0, \dots, 0) + \cdots + x_n(0, \dots, 0, 1) \\&= x_1\mathbf{e}_1 + x_2\mathbf{e}_2 + \cdots + x_n\mathbf{e}_n \\&= \sum_{i=1}^n x_i\mathbf{e}_i\end{aligned}$$

The basis of vectors $\{\mathbf{e}_1, \dots, \mathbf{e}_n\}$ is called the *standard Euclidean basis* for \mathbb{R}^n .

The vector space \mathbb{R}^n is an example of a finite dimensional vector space; that is, $\dim(\mathbb{R}^n)$ is a finite number. Not all vector spaces are finite dimensional. For example, $F(\mathbb{R}, \mathbb{R})$, the set of all real-valued functions whose domain is the real numbers, is infinite dimensional. ■

The remaining material in this section is restricted to the vector spaces \mathbb{R}^n . The concepts generalize to other vector spaces, but for the purposes of this book are not necessary to investigate in detail.

7.4.4 INNER PRODUCTS, LENGTH, ORTHOGONALITY, AND PROJECTION

Let $\mathbf{x} = (x_1, \dots, x_n), \mathbf{y} = (y_1, \dots, y_n) \in \mathbb{R}^n$. When they are represented as $n \times 1$ column vectors, the *standard inner product* of \mathbf{x} and \mathbf{y} is the real number,

$$\langle \mathbf{x}, \mathbf{y} \rangle = \mathbf{x}^T \mathbf{y} = \sum_{i=1}^n x_i y_i \quad (7.10)$$

The inner product satisfies the conditions $\langle c\mathbf{x} + \mathbf{y}, \mathbf{z} \rangle = c\langle \mathbf{x}, \mathbf{z} \rangle + \langle \mathbf{y}, \mathbf{z} \rangle$ and $\langle \mathbf{x}, c\mathbf{y} + \mathbf{z} \rangle = c\langle \mathbf{x}, \mathbf{y} \rangle + \langle \mathbf{x}, \mathbf{z} \rangle$. It is possible to define other inner products that satisfy the same constraints, hence the use of the adjective *standard* in this definition. Treating \mathbf{x} and \mathbf{y} as n -tuples, a common notation for the standard inner product is $\mathbf{x} \cdot \mathbf{y}$, called the *dot product*. The *length* of \mathbf{x} is defined by

$$|\mathbf{x}| = \sqrt{\mathbf{x} \cdot \mathbf{x}} = \sqrt{\sum_{i=1}^n x_i^2} \quad (7.11)$$

The dot product is related to *orthogonality* of vectors. Two vectors \mathbf{x} and \mathbf{y} are *orthogonal* (perpendicular) if and only if $\mathbf{x} \cdot \mathbf{y} = 0$. To see that this is true, Figure 7.13 shows two orthogonal vectors drawn in the plane that they span.

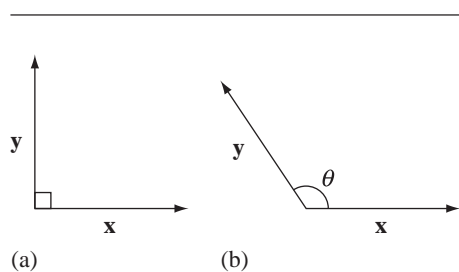


Figure 7.13 (a) Two orthogonal vectors drawn in the plane spanned by them. (b) Two nonorthogonal vectors and the angle between them.

Applying the Pythagorean theorem,

$$\begin{aligned}
 |\mathbf{x}|^2 + |\mathbf{y}|^2 &= |\mathbf{x} - \mathbf{y}|^2 \\
 &= (\mathbf{x} - \mathbf{y}) \cdot (\mathbf{x} - \mathbf{y}) \\
 &= (\mathbf{x} \cdot \mathbf{x}) - (\mathbf{x} \cdot \mathbf{y}) - (\mathbf{y} \cdot \mathbf{x}) + (\mathbf{y} \cdot \mathbf{y}) \\
 &= |\mathbf{x}|^2 + |\mathbf{y}|^2 - 2\mathbf{x} \cdot \mathbf{y}
 \end{aligned}$$

Subtracting $|x|^2 + |y|^2$ from both sides and dividing by -2 yields $x \cdot y = 0$. The argument is reversible; the converse of the Pythagorean theorem is, if $|x|^2 + |y|^2 = |x - y|^2$, then the triangle must be a right triangle. Thus, $x \cdot y = 0$ implies x and y are orthogonal.

An alternative formulation for the standard inner product is in terms of the angle θ between vectors \mathbf{x} and \mathbf{y} ,

$$\mathbf{x} \cdot \mathbf{y} = |\mathbf{x}| |\mathbf{y}| \cos \theta \quad (7.12)$$

Figure 7.13 shows a pair of vectors and the angle between them. The construction of equation (7.12) uses the same geometry argument for a triangle having sides \mathbf{x} , \mathbf{y} , and $\mathbf{x} - \mathbf{y}$, but now the *law of cosines* for a general triangle applies. In the special case of a right triangle, $\theta = \pi/2$ and $\cos(\pi/2) = 0$, in which case $\mathbf{x}^\top \mathbf{y} = 0$ and the vectors are orthogonal. Equation (7.10) defines the dot product in terms of coordinates, but equation (7.12) is referred to as a *coordinate-free* description since the individual coordinates of the vectors are not part of the equation.

The dot product is similarly related to *projection* of vectors. If \mathbf{u} is a unit length vector and \mathbf{v} is any vector, the projection of \mathbf{v} onto \mathbf{u} is illustrated in Figure 7.14.

The left part of the figure motivates the algebraic construction. If θ is the angle between \mathbf{v} and \mathbf{u} , then basic trigonometry tells us $\cos\theta = L/|\mathbf{v}|$. Solving for L and using $|\mathbf{u}| = 1$, we have $L = |\mathbf{v}|\cos\theta = |\mathbf{v}||\mathbf{u}|\cos\theta = \mathbf{v} \cdot \mathbf{u}$. The projection of \mathbf{v} onto \mathbf{u} is

$$\text{proj}(\mathbf{v}, \mathbf{u}) \equiv (\mathbf{v} \cdot \mathbf{u})\mathbf{u} \quad (7.13)$$

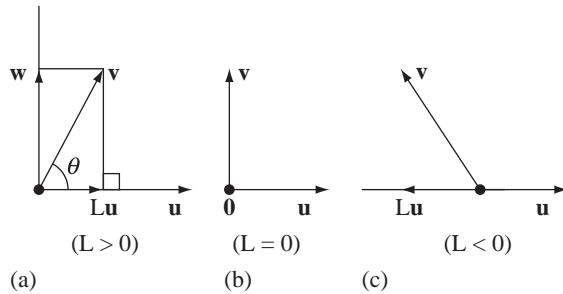


Figure 7.14 The projection of vectors onto a unit length vector \mathbf{u} . (a) \mathbf{v} projects to $L\mathbf{u}$ with $L > 0$. The angle θ between \mathbf{u} and \mathbf{v} is shown. The vector \mathbf{w} is obtained as $\mathbf{w} = \mathbf{v} - L\mathbf{u}$ and is itself a projection. (b) \mathbf{v} is perpendicular to \mathbf{u} , so the projection onto \mathbf{u} is the zero vector $\mathbf{0}$. (c) The projection is $L\mathbf{u}$ with $L < 0$.

As illustrated in two dimensions in Figure 7.14, the vector obtained by subtracting the projection of \mathbf{v} from itself is

$$\mathbf{w} = \mathbf{v} - (\mathbf{v} \cdot \mathbf{u})\mathbf{u} \quad (7.14)$$

and is necessarily orthogonal to \mathbf{u} . The calculation is simple:

$$\mathbf{u} \cdot \mathbf{w} = \mathbf{u} \cdot \mathbf{v} - (\mathbf{v} \cdot \mathbf{u})\mathbf{u} \cdot \mathbf{u} = \mathbf{u} \cdot \mathbf{v} - \mathbf{u} \cdot \mathbf{v} = 0$$

One last observation: The vector \mathbf{u} was deemed to be unit length. Projection is still well defined if the vector is not unit length. Let \mathbf{d} be a non-unit-length vector in the direction of \mathbf{u} ; then $\mathbf{u} = \mathbf{d}/|\mathbf{d}|$. Replacing this in equation (7.13), but changing the left-hand side argument from \mathbf{u} to \mathbf{d} to indicate the target of the projection is \mathbf{d} ,

$$\text{proj}(\mathbf{v}, \mathbf{d}) = \left(\mathbf{v} \cdot \frac{\mathbf{d}}{|\mathbf{d}|} \right) \frac{\mathbf{d}}{|\mathbf{d}|} = \left(\frac{\mathbf{v} \cdot \mathbf{d}}{\mathbf{d} \cdot \mathbf{d}} \right) \mathbf{d} \quad (7.15)$$

A set of nonzero vectors $\{\mathbf{x}_1, \dots, \mathbf{x}_m\}$ consisting of *mutually orthogonal* vectors (each pair is orthogonal) must be a linearly independent set. To see this:

$$\begin{aligned} \mathbf{0} &= \sum_{i=1}^m c_i \mathbf{x}_i \\ \mathbf{x}_j^T \mathbf{0} &= \mathbf{x}_j^T \sum_{i=1}^m c_i \mathbf{x}_i \\ 0 &= \sum_{i=1}^m c_i \mathbf{x}_j \cdot \mathbf{x}_i \quad \text{Since inner product is distributive} \\ &= c_j \mathbf{x}_j^T \mathbf{x}_j \quad \text{Since } \mathbf{x}_i^T \mathbf{x}_j = 0 \text{ for } i \neq j \end{aligned}$$

Since $\mathbf{x}_j \neq \mathbf{0}$, $\mathbf{x}_j \cdot \mathbf{x}_j$ is not zero and it must be that $c_j = 0$. The argument is valid for every $j = 1, \dots, m$, so all c_j are zero and the vectors are linearly independent. A set of mutually orthogonal vectors is said to be an *orthogonal set of vectors*. Additionally, if all the vectors in the set are unit length, the set is said to be an *orthonormal set of vectors*.

It is always possible to construct an orthonormal set of vectors $\{\mathbf{u}_1, \dots, \mathbf{u}_m\}$ from any linearly independent set of vectors, $\{\mathbf{v}_1, \dots, \mathbf{v}_m\}$. The process is referred to as *Gram–Schmidt orthonormalization*.

EXAMPLE
7.32

Consider $\mathbf{v}_1 = (1, 2)$ and $\mathbf{v}_2 = (-3, 0)$ in \mathbb{R}^2 . Figure 7.15 illustrates the process, one based on projection of the input vectors. Choose

$$\mathbf{u}_1 = \frac{\mathbf{v}_1}{|\mathbf{v}_1|} = \frac{(1, 2)}{\sqrt{5}}$$

so that \mathbf{u}_1 is a unit vector in the direction of \mathbf{v}_1 . The component of \mathbf{v}_2 in the direction of \mathbf{u}_1 can be removed, the remainder vector necessarily orthogonal to \mathbf{u}_1 ,

$$\mathbf{w}_2 = \mathbf{v}_2 - (\mathbf{u}_1 \cdot \mathbf{v}_2) \mathbf{u}_1 = \frac{6}{5}(-2, 1)$$

It is easily verified that $\mathbf{u}_1 \cdot \mathbf{w}_2 = 0$. The remainder is not necessarily unit length, but we can normalize it to obtain

$$\mathbf{u}_2 = \frac{\mathbf{w}_2}{|\mathbf{w}_2|} = \frac{(-2, 1)}{\sqrt{5}}$$

The set $\{\mathbf{u}_1, \mathbf{u}_2\}$ is orthonormal.

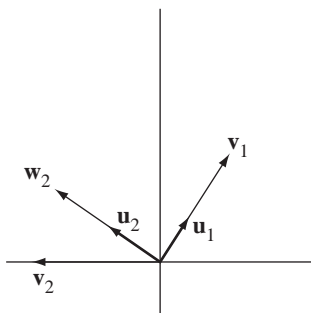


Figure 7.15

Gram–Schmidt orthonormalization applied to two vectors in the plane. ■

EXAMPLE
7.33

Let $\{\mathbf{v}_1, \mathbf{v}_2, \mathbf{v}_3\}$ be a linearly independent set in \mathbb{R}^3 . Figure 7.16 illustrates a typical case.

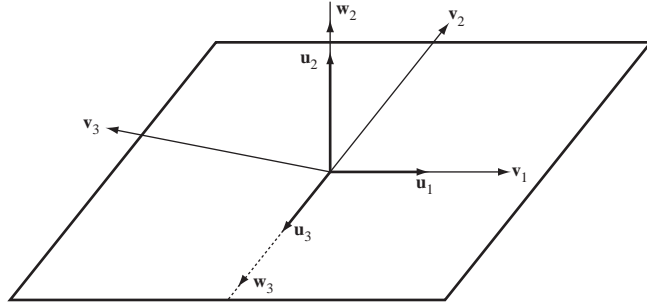


Figure 7.16

Gram-Schmidt orthonormalization applied to three vectors in space.

Let \mathbf{u}_1 , \mathbf{w}_2 , and \mathbf{u}_2 be constructed as in the last example,

$$\mathbf{u}_1 = \frac{\mathbf{v}_1}{|\mathbf{v}_1|}, \quad \mathbf{w}_2 = \mathbf{v}_2 - (\mathbf{u}_1 \cdot \mathbf{v}_2) \mathbf{u}_1, \quad \text{and} \quad \mathbf{u}_2 = \frac{\mathbf{w}_2}{|\mathbf{w}_2|}$$

The components of \mathbf{v}_3 in the directions of \mathbf{u}_1 and \mathbf{u}_2 can be removed, the remainder vector necessarily orthogonal to both \mathbf{u}_1 and \mathbf{u}_2 ,

$$\mathbf{w}_3 = \mathbf{v}_3 - (\mathbf{v}_3 \cdot \mathbf{u}_1) \mathbf{u}_1 - (\mathbf{v}_3 \cdot \mathbf{u}_2) \mathbf{u}_2$$

It is easily verified that $\mathbf{u}_1 \cdot \mathbf{w}_3 = 0$ and $\mathbf{u}_2 \cdot \mathbf{w}_3 = 0$. The remainder is normalized to obtain

$$\mathbf{u}_3 = \frac{\mathbf{w}_3}{|\mathbf{w}_3|}$$

The set $\{\mathbf{u}_1, \mathbf{u}_2, \mathbf{u}_3\}$ is orthonormal. ■

The process for n vectors is iterative,

$$\mathbf{u}_1 = \frac{\mathbf{v}_1}{|\mathbf{v}_1|} \quad \text{and} \quad \mathbf{u}_j = \frac{\mathbf{v}_j - \sum_{i=1}^{j-1} (\mathbf{v}_j \cdot \mathbf{u}_i) \mathbf{u}_i}{\left| \mathbf{v}_j - \sum_{i=1}^{j-1} (\mathbf{v}_j \cdot \mathbf{u}_i) \mathbf{u}_i \right|}, \quad 2 \leq j \leq n \quad (7.16)$$

The key idea, as shown in the examples, is that each new input vector from the original linearly independent set has components removed in the direction of the already constructed vectors in the orthonormal set. The remainder is then normalized to produce the next vector in the orthonormal set.

7.4.5 DOT PRODUCT, CROSS PRODUCT, AND TRIPLE PRODUCTS

In the last section we defined the dot product of two vectors \mathbf{u} and \mathbf{v} and named it $\mathbf{u} \cdot \mathbf{v}$. We saw its relationship to projection of one vector onto another and found it to be a useful concept for constructing an orthonormal set of vectors from a linearly independent set of vectors.

Cross Product

In three dimensions we have another type of product between vectors \mathbf{u} and \mathbf{v} that fits in naturally with the topics of the last section, namely, the *cross product*, a vector we will denote by $\mathbf{u} \times \mathbf{v}$. This vector is required to be perpendicular to each of its two arguments, and its length is required to be the area of the parallelogram formed by its arguments. Figure 7.17 illustrates the cross product.

Your intuition should tell you that there are infinitely many vectors that are perpendicular to both \mathbf{u} and \mathbf{v} , all such vectors lying on a normal line to the plane spanned by \mathbf{u} and \mathbf{v} . Of these, only two have the required length. We need to make a selection between the two. The standard convention uses what is called the *right-hand rule*. If you place your right hand so the fingers point in the direction of \mathbf{u} (the first argument) as shown Figure 7.17(a), then rotate your fingers towards \mathbf{v} (the second argument) so that you make a closed fist, the cross product is selected to be that vector in which direction your thumb points.

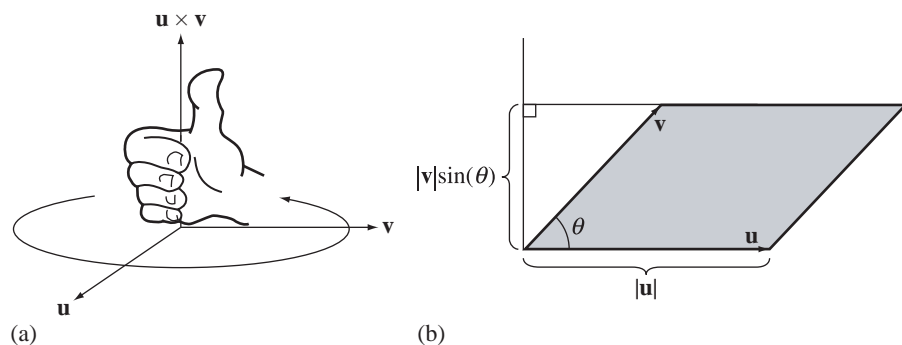


Figure 7.17 (a) The cross product of \mathbf{u} and \mathbf{v} according to the right-hand rule. (b) The parallelogram formed by \mathbf{u} and \mathbf{v} with angle θ and parallelogram base length and height marked.

The area of the parallelogram is $\alpha = bh$ where b is the length of the base (the length of \mathbf{u}) and h is the height (the length of the projection of \mathbf{v} onto a vector perpendicular to \mathbf{u}):

$$\alpha = bh = |\mathbf{u}||\mathbf{v}| \sin(\theta) \quad (7.17)$$

Let \mathbf{w} be a unit-length vector perpendicular to both \mathbf{u} and \mathbf{v} and in the direction consistent with the right-hand rule. The coordinate-free definition of the cross product is therefore,

$$\mathbf{u} \times \mathbf{v} = (|\mathbf{u}||\mathbf{v}| \sin(\theta)) \mathbf{w} \quad (7.18)$$

A coordinate-dependent definition can be constructed by solving a system of two linear equations in three unknowns plus the length and direction constraints. Let $\mathbf{u} \times \mathbf{v} = (x_1, x_2, x_3)$. The orthogonality conditions are

$$\begin{aligned} 0 &= \mathbf{u} \cdot (\mathbf{u} \times \mathbf{v}) = (u_1, u_2, u_3) \cdot (x_1, x_2, x_3) = u_1 x_1 + u_2 x_2 + u_3 x_3 \\ 0 &= \mathbf{v} \cdot (\mathbf{u} \times \mathbf{v}) = (v_1, v_2, v_3) \cdot (x_1, x_2, x_3) = v_1 x_1 + v_2 x_2 + v_3 x_3 \end{aligned}$$

We solve this system symbolically by choosing x_3 to be the free parameter and solve for x_1 and x_2 as basic parameters:

$$\begin{aligned} u_1 x_1 + u_2 x_2 &= -u_3 x_3 \\ v_1 x_1 + v_2 x_2 &= -v_3 x_3 \end{aligned}$$

Multiplying the first equation by v_2 , the second equation by u_2 , and subtracting second from first yields

$$(u_1 v_2 - u_2 v_1)x_1 = (u_2 v_3 - u_3 v_2)x_3$$

Multiplying the first equation by v_1 , the second equation by u_1 , and subtracting the first from the second yields

$$(u_1 v_2 - u_2 v_1)x_2 = (u_3 v_1 - u_1 v_3)x_3$$

The term $u_1 v_2 - u_2 v_1$ appears on the left-hand side of both equations, so a convenient replacement for the free parameter is $x_3 = t(u_1 v_2 - u_2 v_1)$, where t now is the free variable. In terms of t , the two basic parameters are $x_1 = t(u_2 v_3 - u_3 v_2)$ and $x_2 = t(u_3 v_1 - u_1 v_3)$. Thus,

$$(x_1, x_2, x_3) = t(u_2 v_3 - u_3 v_2, u_3 v_1 - u_1 v_3, u_1 v_2 - u_2 v_1)$$

The value of t is determined by the length and direction constraints. In the enforcement of the length constraint, we use [equations \(7.18\)](#) and [\(7.12\)](#):

$$\begin{aligned}
 |\mathbf{u} \times \mathbf{v}|^2 &= |\mathbf{u}|^2 |\mathbf{v}|^2 \sin^2 \theta \\
 &= |\mathbf{u}|^2 |\mathbf{v}|^2 (1 - \cos^2 \theta) \\
 &= |\mathbf{u}|^2 |\mathbf{v}|^2 \left(1 - \frac{(\mathbf{u} \cdot \mathbf{v})^2}{|\mathbf{u}|^2 |\mathbf{v}|^2}\right) \\
 &= |\mathbf{u}|^2 |\mathbf{v}|^2 - (\mathbf{u} \cdot \mathbf{v})^2 \\
 &= (u_1^2 + u_2^2 + u_3^2)(v_1^2 + v_2^2 + v_3^2) - (u_1 v_1 + u_2 v_2 + u_3 v_3)^2 \\
 &= (u_2 v_3 - u_3 v_2)^2 + (u_3 v_1 - u_1 v_3)^2 + (u_1 v_2 - u_2 v_1)^2
 \end{aligned} \tag{7.19}$$

The last equality is obtained by quite a few algebraic manipulations, albeit simple ones. From earlier,

$$|\mathbf{u} \times \mathbf{v}|^2 = |(x_1, x_2, x_3)|^2 = t^2 ((u_2 v_3 - u_3 v_2)^2 + (u_3 v_1 - u_1 v_3)^2 + (u_1 v_2 - u_2 v_1)^2)$$

For the last two displayed equations to be equal we need $t^2 = 1$. The direction constraint narrows our final choice to $t = 1$. That is, the coordinate-dependent definition for the cross product of two vectors is

$$\mathbf{u} \times \mathbf{v} = (u_2 v_3 - u_3 v_2, u_3 v_1 - u_1 v_3, u_1 v_2 - u_2 v_1) \tag{7.20}$$

The coordinate-dependent and coordinate-free descriptions of the dot product are [equations \(7.10\)](#) and [\(7.12\)](#), respectively. The coordinate-dependent and coordinate-free descriptions of the cross product are [equations \(7.20\)](#) and [\(7.18\)](#), respectively.

There are a couple of important properties of the cross product of which to be aware. First, the cross product is not commutative; in general $\mathbf{u} \times \mathbf{v}$ and $\mathbf{v} \times \mathbf{u}$ are not the same vector. The two vectors, however, point in opposite directions. The cross product is said to be *anticommutative*,

$$\mathbf{v} \times \mathbf{u} = -\mathbf{u} \times \mathbf{v} \tag{7.21}$$

The geometric intuition for this identity is given in [Figure 7.17](#). If you apply the right-hand rule to \mathbf{v} and \mathbf{u} , in that order, you should get a vector that is opposite in direction to $\mathbf{u} \times \mathbf{v}$. [Equation \(7.21\)](#) is simple to verify algebraically by use of [equation \(7.20\)](#). The other important property is that the cross product is a linear transformation in each component (called a *bilinear transformation*). That is,

$$\begin{aligned}
 (\mathbf{c}\mathbf{u} + \mathbf{w}) \times \mathbf{v} &= \mathbf{c}(\mathbf{u} \times \mathbf{v}) + (\mathbf{w} \times \mathbf{v}) \quad \text{Linear in first component} \\
 \mathbf{u} \times (\mathbf{c}\mathbf{v} + \mathbf{w}) &= \mathbf{c}(\mathbf{u} \times \mathbf{v}) + (\mathbf{u} \times \mathbf{w}) \quad \text{Linear in second component}
 \end{aligned} \tag{7.22}$$

EXERCISE
7.4

Prove that the identities in [equations \(7.21\)](#) and [\(7.22\)](#) are true. ■

EXERCISE
7.5

If $\mathbf{u} + \mathbf{v} + \mathbf{w} = \mathbf{0}$, then $\mathbf{u} \times \mathbf{v} = \mathbf{v} \times \mathbf{w} = \mathbf{w} \times \mathbf{u}$. What is the geometric interpretation of this statement? ■

Triple Scalar Product

The cross product of two vectors \mathbf{v} and \mathbf{w} is a vector that can be dotted with a third vector \mathbf{u} to obtain a scalar, $v = \mathbf{u} \cdot \mathbf{v} \times \mathbf{w}$. No parentheses are needed about the cross product portion. If you were to compute the dot product of \mathbf{u} and \mathbf{v} , the resulting scalar cannot be crossed with \mathbf{w} since we have defined no such operation between scalars and vectors. The quantity $\mathbf{u} \cdot \mathbf{v} \times \mathbf{w}$ is referred to as the *triple scalar product* of the three vectors. This quantity has an important geometric interpretation as a *signed volume* of a parallelepiped. Figure 7.18 illustrates this where \mathbf{u} forms an acute angle with $\mathbf{v} \times \mathbf{w}$.

The volume v of the parallelepiped is the product area of the base $\alpha = |\mathbf{v}| |\mathbf{w}| \sin \theta$ as determined by equation (7.17) and the height $h = |\mathbf{u}| \cos \phi$ as determined by the dot product between \mathbf{u} and $\mathbf{v} \times \mathbf{w}$,

$$\begin{aligned} v &= \mathbf{u} \cdot \mathbf{v} \times \mathbf{w} = |\mathbf{v} \times \mathbf{w}| |\mathbf{u}| \cos \phi \\ &= (|\mathbf{v}| |\mathbf{w}| \sin \theta) (|\mathbf{u}| \cos \phi) = \alpha h = |\mathbf{u}| |\mathbf{v}| |\mathbf{w}| \sin \theta \cos \phi \end{aligned} \quad (7.23)$$

In the configuration of vectors in Figure 7.18, the volume is $v > 0$. If \mathbf{u} were to form an obtuse angle with $\mathbf{v} \times \mathbf{w}$, $\phi \in (\pi/2, \pi)$, then $v < 0$ and $|v|$ is the volume. If $\phi = \pi/2$, then $v = 0$ and the parallelepiped is degenerate (all three vectors are coplanar) and has volume zero. Thus, v is referred to as a signed volume. Observe that equation (7.23) is a coordinate-free description of the triple scalar product. The coordinate-dependent formulas for dot product and cross product allow us to construct

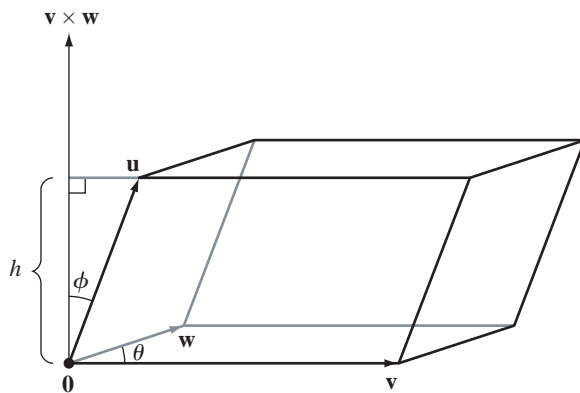


Figure 7.18 A parallelepiped formed by vectors \mathbf{u} , \mathbf{v} , and \mathbf{w} where \mathbf{u} forms an acute angle with $\mathbf{v} \times \mathbf{w}$. The angle between \mathbf{v} and \mathbf{w} is θ and the angle between \mathbf{u} and $\mathbf{v} \times \mathbf{w}$ is ϕ .

a coordinate-dependent description of the triple scalar product,

$$\begin{aligned}\mathbf{u} \cdot \mathbf{v} \times \mathbf{w} &= (u_1, u_2, u_3) \cdot (v_1, v_2, v_3) \times (w_1, w_2, w_3) \\ &= u_1(v_2 w_3 - v_3 w_2) + u_2(v_3 w_1 - v_1 w_3) + u_3(v_1 w_2 - v_2 w_1)\end{aligned}\quad (7.24)$$

EXERCISE
7.6

Prove the following:

1. The identity in equation (7.24)
2. $\mathbf{u} \times \mathbf{v} \cdot \mathbf{w} = \mathbf{u} \cdot \mathbf{v} \times \mathbf{w}$
3. $\mathbf{u} \cdot \mathbf{w} \times \mathbf{v} = -\mathbf{u} \cdot \mathbf{v} \times \mathbf{w}$
4. If $\{\mathbf{u}, \mathbf{v}, \mathbf{w}\}$ is an orthonormal set of vectors, then $|\mathbf{u} \cdot \mathbf{v} \times \mathbf{w}| = 1$

■

EXERCISE
7.7

Let \mathbf{u} , \mathbf{v} , and \mathbf{w} be linearly independent vectors.

1. Prove that any vector \mathbf{p} has the representation,

$$\mathbf{p} = \frac{(\mathbf{p} \cdot \mathbf{v} \times \mathbf{w})\mathbf{u} + (\mathbf{u} \cdot \mathbf{p} \times \mathbf{w})\mathbf{v} + (\mathbf{u} \cdot \mathbf{v} \times \mathbf{p})\mathbf{w}}{\mathbf{u} \cdot \mathbf{v} \times \mathbf{w}}$$

2. Prove that any vector \mathbf{p} has the representation,

$$\mathbf{p} = \frac{(\mathbf{w} \cdot \mathbf{p})\mathbf{u} \times \mathbf{v} + (\mathbf{u} \cdot \mathbf{p})\mathbf{v} \times \mathbf{w} + (\mathbf{v} \cdot \mathbf{p})\mathbf{w} \times \mathbf{u}}{\mathbf{u} \cdot \mathbf{v} \times \mathbf{w}}$$

■

Triple Vector Product

Another type of product of three vectors \mathbf{u} , \mathbf{v} , and \mathbf{w} is the *triple vector product* $\mathbf{p} = \mathbf{u} \times (\mathbf{v} \times \mathbf{w})$, itself a vector. For the sake of argument, let us assume that $\mathbf{v} \times \mathbf{w}$ is not the zero vector (the two vectors are linearly independent). The cross product of two vectors is perpendicular to each of those vectors. In our case, \mathbf{p} must be perpendicular to $\mathbf{v} \times \mathbf{w}$. But $\mathbf{v} \times \mathbf{w}$ is perpendicular to the plane spanned by \mathbf{v} and \mathbf{w} , so \mathbf{p} must lie in that plane. Figure 7.19 illustrates this.

Consequently, there must be scalars s and t such that $\mathbf{u} \times (\mathbf{v} \times \mathbf{w}) = s\mathbf{v} + t\mathbf{w}$. The scalars can be computed in a coordinate-dependent manner, but the algebraic details will be quite tedious. The following construction is coordinate-free.

Consider the special case

$$\mathbf{v} \times (\mathbf{v} \times \mathbf{w}) = s\mathbf{v} + t\mathbf{w} \quad (7.25)$$

Dotting equation (7.25) with \mathbf{v} and using the fact that \mathbf{v} is perpendicular to the cross product $\mathbf{v} \times \mathbf{w}$, we have

$$0 = \mathbf{v} \cdot \mathbf{v} \times (\mathbf{v} \times \mathbf{w}) = (\mathbf{v} \cdot \mathbf{v})s + (\mathbf{v} \cdot \mathbf{w})t \quad (7.26)$$

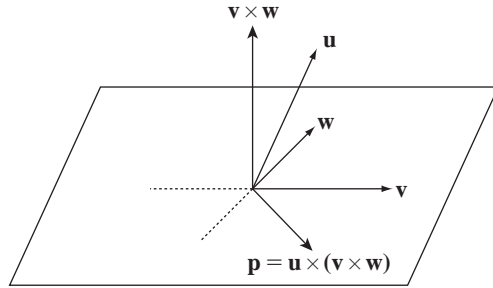


Figure 7.19 The triple vector product $\mathbf{p} = \mathbf{u} \times (\mathbf{v} \times \mathbf{w})$. Note that \mathbf{p} must lie in the plane spanned by \mathbf{v} and \mathbf{w} .

Now dot [equation \(7.25\)](#) with \mathbf{w} . The left-hand side is

$$\begin{aligned}\mathbf{w} \cdot \mathbf{v} \times (\mathbf{v} \times \mathbf{w}) &= (\mathbf{w} \times \mathbf{v}) \cdot (\mathbf{v} \times \mathbf{w}) \\ &= -(\mathbf{v} \times \mathbf{w}) \cdot (\mathbf{v} \times \mathbf{w}) \quad \text{By } \text{equation (7.21)} \\ &= -|\mathbf{v} \times \mathbf{w}|^2\end{aligned}$$

The second equation in s and t is

$$-|\mathbf{v} \times \mathbf{w}|^2 = (\mathbf{v} \cdot \mathbf{w})s + (\mathbf{w} \cdot \mathbf{w})t \quad (7.27)$$

The [equations \(7.26\)](#) and [\(7.27\)](#) are a system of two linear equations in two unknowns that can be written in matrix form as

$$\begin{bmatrix} \mathbf{v} \cdot \mathbf{v} & \mathbf{v} \cdot \mathbf{w} \\ \mathbf{v} \cdot \mathbf{w} & \mathbf{w} \cdot \mathbf{w} \end{bmatrix} \begin{bmatrix} s \\ t \end{bmatrix} = \begin{bmatrix} 0 \\ -|\mathbf{v} \times \mathbf{w}|^2 \end{bmatrix}$$

The matrix of coefficients on the right-hand side is inverted to produce the solution

$$\begin{bmatrix} s \\ t \end{bmatrix} = \frac{1}{(\mathbf{v} \cdot \mathbf{v})(\mathbf{w} \cdot \mathbf{w}) - (\mathbf{v} \cdot \mathbf{w})^2} \begin{bmatrix} \mathbf{w} \cdot \mathbf{w} & -\mathbf{v} \cdot \mathbf{w} \\ -\mathbf{v} \cdot \mathbf{w} & \mathbf{v} \cdot \mathbf{v} \end{bmatrix} \begin{bmatrix} 0 \\ -|\mathbf{v} \times \mathbf{w}|^2 \end{bmatrix} = \begin{bmatrix} \mathbf{v} \cdot \mathbf{w} \\ -\mathbf{v} \cdot \mathbf{v} \end{bmatrix}$$

where we have used the fact that $|\mathbf{v} \times \mathbf{w}|^2 = (\mathbf{v} \cdot \mathbf{v})(\mathbf{w} \cdot \mathbf{w}) - (\mathbf{v} \cdot \mathbf{w})^2$ from the derivation in [equation \(7.19\)](#). Therefore, we have the identity,

$$\mathbf{v} \times (\mathbf{v} \times \mathbf{w}) = (\mathbf{v} \cdot \mathbf{w})\mathbf{v} - (\mathbf{v} \cdot \mathbf{v})\mathbf{w} \quad (7.28)$$

This identity may be used to construct a formula for the general case. We need to determine scalars s and t such that

$$\mathbf{u} \times (\mathbf{v} \times \mathbf{w}) = s\mathbf{v} + t\mathbf{w} \quad (7.29)$$

Dotting equation (7.29) with \mathbf{u} produces

$$(\mathbf{u} \cdot \mathbf{v})s + (\mathbf{u} \cdot \mathbf{w})t = \mathbf{u} \cdot \mathbf{u} \times (\mathbf{v} \times \mathbf{w}) = 0 \quad (7.30)$$

Dotting equation (7.29) with \mathbf{v} produces

$$\begin{aligned} (\mathbf{v} \cdot \mathbf{v})s + (\mathbf{v} \cdot \mathbf{w})t &= \mathbf{u} \times (\mathbf{v} \times \mathbf{w}) \cdot \mathbf{v} \\ &= \mathbf{u} \cdot (\mathbf{v} \times \mathbf{w}) \times \mathbf{v} && \text{By Exercise 7.6, item 2} \\ &= -\mathbf{u} \cdot \mathbf{v} \times (\mathbf{v} \times \mathbf{w}) && \text{By equation (7.21)} \\ &= -\mathbf{u} \cdot ((\mathbf{v} \cdot \mathbf{w})\mathbf{v} - (\mathbf{v} \cdot \mathbf{v})\mathbf{w}) && \text{By equation (7.28)} \\ &= (\mathbf{v} \cdot \mathbf{v})(\mathbf{u} \cdot \mathbf{w}) - (\mathbf{v} \cdot \mathbf{w})(\mathbf{u} \cdot \mathbf{v}) \end{aligned} \quad (7.31)$$

The equations (7.30) and (7.31) are a system of two linear equations in two unknowns that can be written in matrix form as

$$\begin{bmatrix} \mathbf{u} \cdot \mathbf{v} & \mathbf{u} \cdot \mathbf{w} \\ \mathbf{v} \cdot \mathbf{v} & \mathbf{v} \cdot \mathbf{w} \end{bmatrix} \begin{bmatrix} s \\ t \end{bmatrix} = \begin{bmatrix} 0 \\ (\mathbf{v} \cdot \mathbf{v})(\mathbf{u} \cdot \mathbf{w}) - (\mathbf{v} \cdot \mathbf{w})(\mathbf{u} \cdot \mathbf{v}) \end{bmatrix}$$

The matrix of coefficients on the right-hand side is inverted to produce the solution

$$\begin{aligned} \begin{bmatrix} s \\ t \end{bmatrix} &= \frac{1}{(\mathbf{u} \cdot \mathbf{v})(\mathbf{v} \cdot \mathbf{w}) - (\mathbf{u} \cdot \mathbf{w})(\mathbf{v} \cdot \mathbf{v})} \begin{bmatrix} \mathbf{v} \cdot \mathbf{w} & -\mathbf{u} \cdot \mathbf{w} \\ -\mathbf{v} \cdot \mathbf{v} & \mathbf{u} \cdot \mathbf{v} \end{bmatrix} \begin{bmatrix} 0 \\ (\mathbf{v} \cdot \mathbf{v})(\mathbf{u} \cdot \mathbf{w}) - (\mathbf{v} \cdot \mathbf{w})(\mathbf{u} \cdot \mathbf{v}) \end{bmatrix} \\ &= \begin{bmatrix} \mathbf{u} \cdot \mathbf{w} \\ -\mathbf{u} \cdot \mathbf{v} \end{bmatrix} \end{aligned}$$

Therefore, we have the identity,

$$\mathbf{u} \times (\mathbf{v} \times \mathbf{w}) = (\mathbf{u} \cdot \mathbf{w})\mathbf{v} - (\mathbf{u} \cdot \mathbf{v})\mathbf{w} \quad (7.32)$$

A similar formula is

$$(\mathbf{u} \times \mathbf{v}) \times \mathbf{w} = (\mathbf{u} \cdot \mathbf{w})\mathbf{v} - (\mathbf{v} \cdot \mathbf{w})\mathbf{u} \quad (7.33)$$

Equations (7.32) and (7.33) show that, in general, $\mathbf{u} \times (\mathbf{v} \times \mathbf{w}) \neq (\mathbf{u} \times \mathbf{v}) \times \mathbf{w}$. That is, the *cross product operation is not associative*.

EXERCISE 7.8

Prove the following:

1. The identity in equation (7.33)
2. $(\mathbf{u} \times \mathbf{v}) \cdot (\mathbf{w} \times \mathbf{p}) = (\mathbf{u} \cdot \mathbf{w})(\mathbf{v} \cdot \mathbf{p}) - (\mathbf{u} \cdot \mathbf{p})(\mathbf{v} \cdot \mathbf{w})$
3. $(\mathbf{u} \times \mathbf{v}) \times (\mathbf{w} \times \mathbf{p}) = (\mathbf{u} \times \mathbf{v} \cdot \mathbf{p})\mathbf{w} - (\mathbf{u} \times \mathbf{v} \cdot \mathbf{w})\mathbf{p}$



7.4.6 ORTHOGONAL SUBSPACES

Let U and V be subspaces of \mathbb{R}^n . The subspaces are said to be *orthogonal subspaces* if $\mathbf{x} \cdot \mathbf{y} = 0$ for every $\mathbf{x} \in U$ and for every $\mathbf{y} \in V$.

EXAMPLE
7.34

Let $U = \text{Span}[(1, 1)]$ and $V = \text{Span}[(1, -1)]$ in \mathbb{R}^2 . Geometrically, these sets are perpendicular lines in \mathbb{R}^2 passing through the origin. A vector $\mathbf{x} \in U$ is of the form $\mathbf{x} = a(1, 1)$ and a vector $\mathbf{y} \in V$ is of the form $\mathbf{y} = b(1, -1)$. The inner product is $(a, a) \cdot (b, -b) = ab - ab = 0$, so U and V are orthogonal subspaces. ■

EXAMPLE
7.35

Let $U = \text{Span}[(1, 0, 0, 0), (1, 1, 0, 0)]$ and $V = \text{Span}[(0, 0, 4, 5)]$. Let $\mathbf{x} \in U$ and $\mathbf{y} \in V$; then

$$\mathbf{x} = a \begin{bmatrix} 1 \\ 0 \\ 0 \\ 0 \end{bmatrix} + b \begin{bmatrix} 1 \\ 1 \\ 0 \\ 0 \end{bmatrix} = \begin{bmatrix} a+b \\ b \\ 0 \\ 0 \end{bmatrix}, \quad \mathbf{y} = c \begin{bmatrix} 0 \\ 0 \\ 4 \\ 5 \end{bmatrix} = \begin{bmatrix} 0 \\ 0 \\ 4c \\ 5c \end{bmatrix}$$

and so

$$\mathbf{x} \cdot \mathbf{y} = [a+b \quad b \quad 0 \quad 0] \begin{bmatrix} 0 \\ 0 \\ 4c \\ 5c \end{bmatrix} = (a+b)(0) + (b)(0) + (0)(4c) + (0)(5c) = 0$$

The subspaces are therefore orthogonal. ■

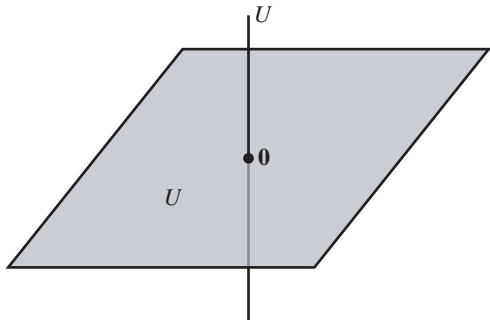
Given two subspaces U and V , some analysis of the subspaces is applied to verify that they are (or are not) orthogonal subspaces. For example, $U = \text{Span}[(1, 1, 0)]$ and $V = \text{Span}[(1, -1, 0)]$ are orthogonal subspaces since a general vector in U is $(a, a, 0)$, a general vector in V is $(b, -b, 0)$, and $(a, a, 0) \cdot (b, -b, 0) = 0$, regardless of choice for a and b . Geometrically, the two subspaces are perpendicular lines containing the origin. Vectors on the line representing V are perpendicular to any vector in U , but there are other vectors perpendicular to those in U that are *not* in V . Specifically, the plane containing the origin and having the normal vector $(1, 1, 0)$ is a subspace W that is orthogonal to U , and V is a strict subset of W . The general problem, then, is to find the largest dimension subspace V of \mathbb{R}^n that is orthogonal to a specified subspace U . That subspace is called the *orthogonal complement* of U and is denoted by U^\perp . The formal set definition is

$$U^\perp = \{\mathbf{x} \in \mathbb{R}^n : \mathbf{x} \cdot \mathbf{y} = 0 \text{ for all } \mathbf{y} \in U\} \quad (7.34)$$

Figure 7.20 illustrates this concept for \mathbb{R}^3 .

Figure 7.20 suggests that the orthogonal complement of U^\perp is U itself; that is, $(U^\perp)^\perp = U$. This is true for finite dimensional vector spaces, but there are examples of infinite dimensional vector spaces for which it is not true. The most you can say in those spaces is that $U \subseteq (U^\perp)^\perp$, something that is easily verified just by the definition of U^\perp . For finite dimensional vector spaces, the proof that $(U^\perp)^\perp = U$ is presented next.

Let us consider the trivial case first. If $U = \{\mathbf{0}\}$, the subspace consisting of only the zero vector, the orthogonal complement is $U^\perp = \mathbb{R}^n$ since every vector is trivially

Figure 7.20 A subspace U of \mathbb{R}^3 and its orthogonal complement U^\perp .

perpendicular to the zero vector. Conversely, the only vector perpendicular to all vectors in \mathbb{R}^n is the zero vector, so $(U^\perp)^\perp = (\mathbb{R}^n)^\perp = \{\mathbf{0}\} = U$.

The nontrivial cases require a bit more work. Let U be a nontrivial subspace of \mathbb{R}^n . It has a basis $A = \{\mathbf{u}_1, \dots, \mathbf{u}_m\}$, $1 < m < n$, that is an orthonormal set of vectors. Given any basis of U , it is always possible to construct an orthonormal one from it using Gram–Schmidt orthonormalization. Let B be a basis for \mathbb{R}^n . The set A can be extended to a basis for \mathbb{R}^n by attempting to insert, one at a time, the vectors from B into A . The insertion of a vector is allowed only if the resulting set of vectors is linearly independent. See the subsection on linear independence and bases to understand why this algorithm works. Let the resulting basis for \mathbb{R}^n be $\{\mathbf{u}_1, \dots, \mathbf{u}_m, \mathbf{v}_1, \dots, \mathbf{v}_{n-m}\}$. Now define:

$$\mathbf{w}_i = \mathbf{v}_i - \sum_{j=1}^m (\mathbf{v}_i \cdot \mathbf{u}_j) \mathbf{u}_j, \quad 1 \leq i \leq n-m$$

The set $C = \{\mathbf{w}_1, \dots, \mathbf{w}_{n-m}\}$ is linearly independent. To see this, set

$$\begin{aligned} \mathbf{0} &= \sum_{i=1}^{n-m} c_i \mathbf{w}_i \\ &= \sum_{i=1}^{n-m} c_i \mathbf{v}_i - \sum_{j=1}^m \left(\sum_{i=1}^{n-m} c_i \sum_{j=1}^m (\mathbf{v}_i \cdot \mathbf{u}_j) \right) \mathbf{u}_j \\ &= \sum_{i=1}^{n-m} c_i \mathbf{v}_i + \sum_{j=1}^m d_j \mathbf{u}_j \end{aligned}$$

where the last equality defines the coefficients d_j . The right-hand side is a linear combination of basis vectors for \mathbb{R}^n , so all the c_i and d_j must be zero. Since all the c_i are zero, the set of \mathbf{w}_i vectors are in fact linearly independent. Moreover, observe that

$$\begin{aligned}\mathbf{u}_k \cdot \mathbf{w}_i &= \mathbf{u}_k \cdot \mathbf{v}_i - \sum_{j=1}^m (\mathbf{v}_i \cdot \mathbf{u}_j) \mathbf{u}_k \cdot \mathbf{u}_j \\ &= \mathbf{u}_k \cdot \mathbf{v}_i - \sum_{j=1}^m (\mathbf{v}_i \cdot \mathbf{u}_j) \begin{cases} 1, & j = k \\ 0, & j \neq k \end{cases} \\ &= \mathbf{u}_k \cdot \mathbf{v}_i - \mathbf{u}_k \cdot \mathbf{v}_i \\ &= 0\end{aligned}$$

The $n - m$ vectors in C are all orthogonal to the m vectors in A . The set C is therefore a basis for U^\perp . The construction applies equally to U^\perp to obtain a basis D of m vectors for $(U^\perp)^\perp$. At this point we know that $U \subseteq (U^\perp)^\perp$ and that $\dim(U) = m = \dim((U^\perp)^\perp)$, the last condition disallowing proper containment; that is, $U = (U^\perp)^\perp$.

7.4.7 THE FUNDAMENTAL THEOREM OF LINEAR ALGEBRA

Let us revisit linear systems of equations. Given an $n \times m$ matrix A , there are four subspaces associated with it: $\text{kernel}(A)$, $\text{range}(A)$, $\text{kernel}(A^T)$, and $\text{range}(A^T)$. Each of these subspaces is discussed in this section.

Kernel of A

Define the *kernel* or *nullspace* of A to be the set

$$\text{kernel}(A) = \{\mathbf{x} \in \mathbb{R}^m : A\mathbf{x} = \mathbf{0}\}$$

This subset of \mathbb{R}^m is a subspace. As discussed earlier we only need to verify that $a\mathbf{x} + b\mathbf{y} \in \text{kernel}(A)$ for any $a, b \in \mathbb{R}$ and any $\mathbf{x}, \mathbf{y} \in \text{kernel}(A)$. This is the case since

$$A(a\mathbf{x} + b\mathbf{y}) = aA\mathbf{x} + bA\mathbf{y} = a\mathbf{0} + b\mathbf{0} = \mathbf{0}$$

If $U = EA$, where E is a product of elementary row matrices and U is upper echelon, then $A\mathbf{x} = \mathbf{0}$ and $U\mathbf{x} = \mathbf{0}$ have the same set of solutions. Therefore, $\text{kernel}(A) = \text{kernel}(U)$. A basis for $\text{kernel}(A)$ is constructed by solving the system $A\mathbf{x} = \mathbf{0}$. If $r = \text{rank}(A)$, then $\dim(\text{kernel}(A)) = m - r$.

EXAMPLE Consider $A\mathbf{x} = \mathbf{0}$ where

7.36

$$A = \begin{bmatrix} 1 & 3 & 2 \\ 2 & 6 & 9 \\ 3 & 9 & 8 \end{bmatrix} \xrightarrow{-2R_1 + R_2 \rightarrow R_2} \begin{bmatrix} 1 & 3 & 2 \\ 0 & 0 & 5 \\ 0 & 0 & 2 \end{bmatrix} \xrightarrow{\frac{1}{5}R_2 \rightarrow R_2} \begin{bmatrix} 1 & 3 & 2 \\ 0 & 0 & 1 \\ 0 & 0 & 2 \end{bmatrix}$$

$$\xrightarrow{-2R_2 + R_1 \rightarrow R_1} \begin{bmatrix} 1 & 3 & 0 \\ 0 & 0 & 1 \\ 0 & 0 & 0 \end{bmatrix} = U$$

$$\xrightarrow{-2R_2 + R_3 \rightarrow R_3} \begin{bmatrix} 1 & 3 & 0 \\ 0 & 0 & 1 \\ 0 & 0 & 0 \end{bmatrix}$$

The basic variables are x_1 and x_3 , and the only free variable is x_2 . The general solution is

$$\mathbf{x} = \begin{bmatrix} x_1 \\ x_2 \\ x_3 \end{bmatrix} = \begin{bmatrix} -3x_2 \\ x_2 \\ 0 \end{bmatrix} = x_2 \begin{bmatrix} -3 \\ 1 \\ 0 \end{bmatrix}$$

so that $\text{kernel}(A) = \text{Span}([-3, 1, 0])$ and $\dim(\text{kernel}(A)) = 1$. ■

EXAMPLE

7.37

Suppose A is a matrix such that its complete row-reduced form is

$$U = \begin{bmatrix} 1 & 2 & -1 & 0 & 3 & -1 \\ 0 & 0 & 0 & 1 & 2 & -1 \\ 0 & 0 & 0 & 0 & 0 & 0 \\ 0 & 0 & 0 & 0 & 0 & 0 \end{bmatrix}$$

The basic variables are x_1 and x_4 , and the free variables are x_2 , x_3 , x_5 , and x_6 . The general solution is

$$\mathbf{x} = \begin{bmatrix} x_1 \\ x_2 \\ x_3 \\ x_4 \\ x_5 \\ x_6 \end{bmatrix} = \begin{bmatrix} -2x_2 + x_3 - 3x_5 + x_6 \\ x_2 \\ x_3 \\ -2x_5 + x_6 \\ x_5 \\ x_6 \end{bmatrix} = x_2 \begin{bmatrix} -2 \\ 1 \\ 0 \\ 0 \\ 0 \\ 0 \end{bmatrix} + x_3 \begin{bmatrix} 1 \\ 0 \\ 1 \\ 0 \\ 0 \\ 0 \end{bmatrix} + x_5 \begin{bmatrix} -3 \\ 0 \\ 0 \\ -2 \\ 1 \\ 0 \end{bmatrix} + x_6 \begin{bmatrix} 1 \\ 0 \\ 0 \\ 1 \\ 0 \\ 1 \end{bmatrix}$$

The kernel is

$$\text{kernel}(A) = \text{Span}([-2, 1, 0, 0, 0, 0), (1, 0, 1, 0, 0, 0), (-3, 0, 0, -2, 1, 0), (1, 0, 0, 1, 0, 1)]$$

with $\dim(\text{kernel}(A)) = 4$. ■

Range of A

Let A be written as a block matrix of $n \times 1$ column vectors,

$$A = [\boldsymbol{\alpha}_1 | \cdots | \boldsymbol{\alpha}_m]$$

where $\alpha_k = [a_{ik}]$ for $1 \leq k \leq m$. The expression Ax can be written as a linear combination of these columns:

$$Ax = \sum_{k=1}^m a_{ik}x_k = x_1\alpha_1 + \cdots + x_m\alpha_m$$

Treating A as a function $A : \mathbb{R}^m \rightarrow \mathbb{R}^n$, the *range* of the function is

$$\text{range}(A) = \{y \in \mathbb{R}^n : y = Ax \text{ for some } x \in \mathbb{R}^m\} = \text{Span}[\alpha_1, \dots, \alpha_m]$$

This subset of \mathbb{R}^n is a subspace since the span of any subset is itself a subspace. The columns of A are not required to be linearly independent, in which case they do not form a basis for the range.

Suppose that $U = EA$ where E is a product of elementary row matrices and U is upper echelon. It is usually the case that $\text{range}(A) \neq \text{range}(U)$. However, if the pivot elements of U are in columns k_1, \dots, k_r where $r = \text{rank}(A)$, then the corresponding columns of A form a basis for the $\text{range}(A)$. That is,

$$\text{range}(A) = \text{Span}[\alpha_{k_1}, \dots, \alpha_{k_r}]$$

with $\dim(\text{range}(A)) = r$. We prove this assertion. Write U in terms of its column vectors, $U = [\mathbf{u}_1 | \cdots | \mathbf{u}_m]$. Construct the block matrices $\tilde{U} = [\mathbf{u}_{k_1} | \cdots | \mathbf{u}_{k_r}]$ and $\tilde{A} = [\alpha_{k_1} | \cdots | \alpha_{k_r}]$. Note that

$$\tilde{U} = \begin{bmatrix} I_{r \times r} \\ 0_{(n-r) \times r} \end{bmatrix}$$

where $I_{r \times r}$ is an identity matrix, $r = \text{rank}(A)$, and $0_{(n-r) \times r}$ is a block matrix with all zero entries. Also note that $U = EA$ implies $\tilde{U} = E\tilde{A}$.

Set $\sum_{j=1}^r c_j \alpha_{k_j} = 0$. To show linear independence, we need to show that the only possibility is $c_j = 0$ for all $j = 1, \dots, r$. But this equation is simply $\tilde{A}\mathbf{c} = \mathbf{0}$ where $\mathbf{c} = [c_j]$ is an $r \times 1$ column vector, so

$$\mathbf{0} = \tilde{A}\mathbf{c} = E^{-1}\tilde{U}\mathbf{c} = E^{-1}\begin{bmatrix} I_{r \times r} \\ 0_{(n-r) \times r} \end{bmatrix}\mathbf{c}$$

which implies

$$\begin{bmatrix} I_{r \times r} \\ 0_{(n-r) \times r} \end{bmatrix}\mathbf{c} = E\mathbf{0} = \mathbf{0}$$

The only solution is $\mathbf{c} = \mathbf{0}$, and so the vectors $\alpha_{k_1}, \dots, \alpha_{k_r}$ are linearly independent.

Moreover, $\text{range}(A) = \text{Span}[\alpha_{k_1}, \dots, \alpha_{k_r}]$. The proof is as follows. Suppose $\{\alpha_{k_1}, \dots, \alpha_{k_r}, \alpha_\ell\}$ is a linearly independent set for some $\ell \notin \{k_1, \dots, k_r\}$; then $[\tilde{A} | \alpha_\ell]\mathbf{c} = \mathbf{0}$, where \mathbf{c} is $(r+1) \times 1$, has the unique solution $\mathbf{c} = \mathbf{0}$. Consequently,

$$\mathbf{0} = E[\tilde{A} | \alpha_\ell]\mathbf{c} = [E\tilde{A} | E\alpha_\ell]\mathbf{c} = [\tilde{U} | \mathbf{b}]\mathbf{c}$$

This row-reduced system has more unknowns than equations, so it has infinitely many solutions \mathbf{c} , a contradiction to the uniqueness $\mathbf{c} = \mathbf{0}$. Therefore, $\{\alpha_{k_1}, \dots, \alpha_{k_r}\}$ is the maximal linearly independent set of columns of A and must form a basis for the range of A .

EXAMPLE
7.38

Consider the same matrix A as in the last example:

$$A = \begin{bmatrix} 1 & 3 & 2 \\ 2 & 6 & 9 \\ 3 & 9 & 8 \end{bmatrix} \sim \begin{bmatrix} 1 & 3 & 0 \\ 0 & 0 & 1 \\ 0 & 0 & 0 \end{bmatrix} = U$$

Then

$$\tilde{U} = \begin{bmatrix} 1 & 0 \\ 0 & 1 \\ 0 & 0 \end{bmatrix}, \tilde{A} = \begin{bmatrix} 1 & 2 \\ 2 & 9 \\ 3 & 8 \end{bmatrix}$$

and

$$\text{range}(A) = \text{Span}[(1, 2, 3), (2, 9, 8)], \text{range}(U) = \text{Span}[(1, 0, 0), (0, 1, 0)]$$

Note that $\text{range}(A) \neq \text{range}(U)$. ■

Kernel of A^T

As a function, $A^T : \mathbb{R}^n \rightarrow \mathbb{R}^m$ since A^T is an $m \times n$ matrix when A is an $n \times m$ matrix. The kernel of A^T is

$$\text{kernel}(A^T) = \{\mathbf{y} \in \mathbb{R}^m : A^T \mathbf{y} = \mathbf{0}\}$$

and is a subspace of \mathbb{R}^n . Construction of a basis is similar to that of $\text{kernel}(A)$. Since $\text{rank } A^T = \text{rank}(A) = r$, $\dim(\text{kernel}(A^T)) = n - r$.

Range of A^T

Write A^T as a block matrix of column vectors: $A^T = [\beta_1 | \cdots | \beta_n]$ where β_i is an $m \times 1$ column vector for each $i = 1, \dots, n$. The range of the transpose is

$$\text{range}(A^T) = \text{Span}[\beta_1, \dots, \beta_n]$$

and is a subspace of \mathbb{R}^m with dimension $\dim(\text{range}(A^T)) = r$.

These four subspaces are related by the following theorem.

The Fundamental Theorem of Linear Algebra ■ If A is an $n \times m$ matrix with subspaces $\text{kernel}(A)$ and $\text{range}(A)$, and if A^T is the $m \times n$ transpose of A with subspaces $\text{kernel}(A^T)$ and $\text{range}(A^T)$, then $\text{kernel}(A) = \text{range}(A^T)^\perp$, $\text{kernel}(A)^\perp = \text{range}(A^T)$, $\text{kernel}(A^T) = \text{range}(A)^\perp$, and $\text{kernel}(A^T)^\perp = \text{range}(A)$.

Proof ■ Let us prove that $\text{kernel}(A) = \text{range}(A^T)^\perp$. To prove that $\text{kernel}(A) \subseteq \text{range}(A^T)^\perp$, let $\mathbf{x} \in \text{kernel}(A)$ so that $A\mathbf{x} = \mathbf{0}$. For each $\mathbf{y} \in \text{range}(A^T)$, $\mathbf{y} = A^T\mathbf{z}$ for some $\mathbf{z} \in \mathbb{R}^n$. Consequently,

$$\mathbf{x}^T \mathbf{y} = \mathbf{x}^T (A^T \mathbf{z}) = (\mathbf{x}^T A^T) \mathbf{z} = (A\mathbf{x})^T \mathbf{z} = \mathbf{0}^T \mathbf{z} = 0$$

and so \mathbf{x} is orthogonal to all vectors in $\text{range}(A^T)$. That is, $\mathbf{x} \in \text{range}(A^T)^\perp$. ■

To prove that $\text{range}(A^T)^\perp \subseteq \text{kernel}(A)$, let $\mathbf{x} \in \text{range}(A^T)^\perp$; then $\mathbf{x}^T \mathbf{y} = 0$ for all $\mathbf{y} \in \text{range}(A^T)$. As \mathbf{z} varies over all vectors in \mathbb{R}^n , $\mathbf{y} = A^T\mathbf{z}$ varies over all vectors in $\text{range}(A^T)$. Thus, $\mathbf{0} = \mathbf{x}^T (A^T \mathbf{z}) = (A\mathbf{x})^T \mathbf{z}$ for all $\mathbf{z} \in \mathbb{R}^n$. In particular, the equation is true for the Euclidean basis vectors $\mathbf{e}_1, \dots, \mathbf{e}_n$: $(A\mathbf{x})^T \mathbf{e}_i = 0$. In block matrix form,

$$(A\mathbf{x})^T = [(A\mathbf{x})^T \mathbf{e}_1 | \cdots | (A\mathbf{x})^T \mathbf{e}_n] = [0 | \cdots | 0] = \mathbf{0}^T$$

so $A\mathbf{x} = \mathbf{0}$ and $\mathbf{x} \in \text{kernel}(A)$. The containment has been shown in both directions, so $\text{kernel}(A) = \text{range}(A^T)^\perp$.

We proved earlier that $(U^\perp)^\perp = U$. This result and the one of the previous paragraph implies that $\text{range}(A^T) = (\text{range}(A^T)^\perp)^\perp = \text{kernel}(A)$. The other two subspace equalities are valid by replacing A with A^T in the previous constructions. Figure 7.21 illustrates the relationship between the four subspaces. They are drawn to indicate the orthogonality to each other. Note that $\mathbf{x} = \mathbf{x}_k + \mathbf{x}_r$ since $\text{kernel}(A)$ and $\text{range}(A^T)$ are orthogonal subspaces.

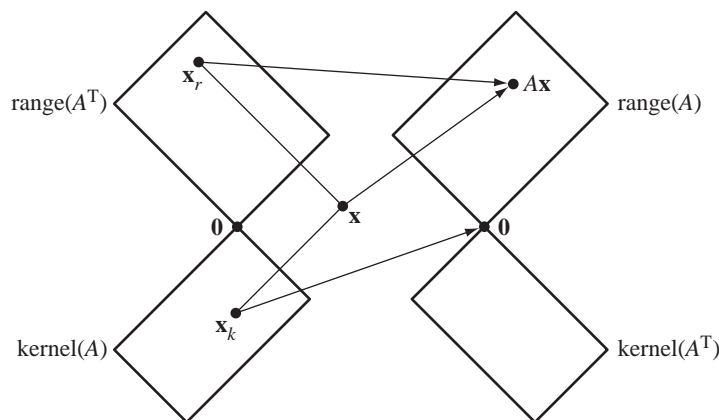


Figure 7.21 The four fundamental subspaces.

7.4.8 PROJECTION AND LEAST SQUARES

The projection \mathbf{p} of a vector $\mathbf{b} \in \mathbb{R}^n$ onto a line through the origin with direction \mathbf{a} (not necessarily unit length) is provided by [equation \(7.15\)](#). I will write this in a different form by grouping together the terms involving \mathbf{a} . This form appears strange at first but is suggestive of what is to follow:

$$\mathbf{p} = \mathbf{a} (\mathbf{a}^T \mathbf{a})^{-1} \mathbf{a}^T \mathbf{b} \quad (7.35)$$

The line is a one-dimensional subspace of \mathbb{R}^n . The projection of \mathbf{b} onto a higher dimensional subspace S may be similarly constructed. In this context, projection of a vector \mathbf{b} onto a subspace S will amount to finding the point in S that is closest to \mathbf{b} . [Figure 7.22](#) illustrates this for a two-dimensional subspace in \mathbb{R}^3 .

The quantity $\mathbf{a}^T \mathbf{a}$ appears in [equation \(7.35\)](#). For higher dimensional subspaces, the analogous quantity is $\mathbf{A}^T \mathbf{A}$, where \mathbf{A} is a matrix.

The construction of a projection onto a subspace is motivated by attempting to solve the system of linear equations $A\mathbf{x} = \mathbf{b}$, where A is an $n \times m$ matrix, \mathbf{x} is an $m \times 1$ column matrix, and \mathbf{b} is an $n \times 1$ column matrix. A solution exists if and only if $\mathbf{b} \in \text{range}(A)$. If \mathbf{b} is not in the range of A , an application might be satisfied with a vector \mathbf{x} that is “close enough”; that is, find an \mathbf{x} so that $A\mathbf{x} - \mathbf{b}$ is as close to the zero vector as possible. Rather than attempting to solve the linear system, we can instead try to find \mathbf{x} that minimizes the length $|A\mathbf{x} - \mathbf{b}|^2$. This is called the *least squares problem*. “Least” refers to minimum, and “squares” refers to the distance-squared quantity to be minimized. If the squared distance has a minimum of zero, any such \mathbf{x} that attains that minimum must be a solution to the linear system. If the minimum distance is positive, the linear system has no solution, but the minimization problem always does.

Geometrically, the minimizing process amounts to finding the point $\mathbf{p} \in \text{range}(A)$ that is closest to \mathbf{b} . Such a point \mathbf{p} always exists and is obtained by a *projection onto* $\text{range}(A)$. As shown in [Figure 7.22](#), there is also always a point $\mathbf{q} \in \text{range}(A)^\perp = \text{kernel}(A^T)$ such that the distance from \mathbf{b} to $\text{kernel}(A^T)$ is a minimum. The figure

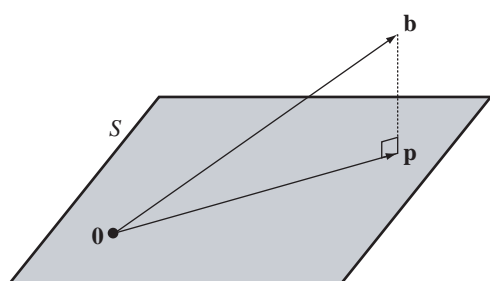


[Figure 7.22](#) The projection $\mathbf{p} \in S$ of $\mathbf{b} \in \mathbb{R}^3$, where S is a two-dimensional subspace of \mathbb{R}^3 (a plane through the origin).

should also make it clear that the quantity $|Ax - \mathbf{b}|^2$ is minimized if and only if $Ax - \mathbf{b} \in \text{kernel}(A^T)$. Since $\mathbf{p} \in \text{range}(A)$, there must be a vector $\mathbf{x} \in \mathbb{R}^m$ such that $\mathbf{p} = Ax$, and $Ax - \mathbf{b} \in \text{kernel}(A^T)$. Therefore, $|Ax - \mathbf{b}|^2$ is a minimum and $A^T(Ax - \mathbf{b}) = 0$. The equations $A^T Ax = A^T \mathbf{b}$ are called the *normal equations* corresponding to the linear system $Ax = \mathbf{b}$.

Solving the normal equations requires the following information. If A is an $n \times m$ matrix, then $A^T A$ is symmetric and $\text{rank}(A^T A) = \text{rank}(A)$. The symmetry of $A^T A$ follows from $(A^T A)^T = A^T (A^T)^T = A^T A$. The equality of the ranks is proved by showing that $\text{kernel}(A) = \text{kernel}(A^T A)$. Let $\mathbf{x} \in \text{kernel}(A)$; then $Ax = \mathbf{0}$. Multiply by A^T to obtain

$$\mathbf{0} = A^T \mathbf{0} = A^T Ax$$

which implies $\mathbf{x} \in \text{kernel}(A^T A)$. Thus, $\text{kernel}(A) \subseteq \text{kernel}(A^T A)$. To show the subset inclusion in the other direction, let $\mathbf{x} \in \text{kernel}(A^T A)$; then $A^T Ax = \mathbf{0}$. Multiply by \mathbf{x}^T to obtain

$$\mathbf{0} = \mathbf{x}^T \mathbf{0} = \mathbf{x}^T A^T Ax = |Ax|^2$$

The length of Ax is zero, so $Ax = \mathbf{0}$ is the only possibility. This implies $\mathbf{x} \in \text{kernel}(A)$, so we have shown $\text{kernel}(A^T A) \subseteq \text{kernel}(A)$. The subset inclusion is true in both directions, so $\text{kernel}(A) = \text{kernel}(A^T A)$. The equality of the ranks follows by a direct application of the fundamental theorem of linear algebra. As we saw earlier, $\dim(\text{kernel}(A)) + \text{rank}(A) = m$. Similarly, $\dim(\text{kernel}(A^T A)) + \text{rank}(A^T A) = m$. Since $\dim(\text{kernel}(A)) = \dim(\text{kernel}(A^T A))$, a subtraction of the two equations leads to $\text{rank}(A) = \text{rank}(A^T A)$.

A consequence of this result is that if the columns of A are linearly independent, then $A^T A$ is an invertible matrix. The linear independence of the columns means that $m = \text{rank}(A) = \text{rank}(A^T A)$. The matrix $A^T A$ is an $m \times m$ matrix of full rank m , so it must be invertible. In this case the normal equations have the unique solution $\mathbf{x} = (A^T A)^{-1} A^T \mathbf{b}$. Finally, the projection of \mathbf{b} onto $\text{range}(A)$ is

$$\mathbf{p} = Ax = A(A^T A)^{-1} A^T \mathbf{b} \quad (7.36)$$

Observe the similarity in form between this and equation (7.35). Also observe that the matrix $M = (A^T A)^{-1} A^T$ has the property $MA = I$. It is called the *left inverse* of A , but note that A is *not* a square matrix! The product $P = AM = A(A^T A)^{-1} A^T$ is not generally the identity matrix. Geometrically, this is clear since $\mathbf{p} = P\mathbf{b}$. And P cannot be the identity when $\mathbf{b} \notin \text{range}(A)$.

Let us take a closer look at the *projection matrix* $P = A(A^T A)^{-1} A^T$. As shown previously, the projection of \mathbf{b} onto $\text{range}(A)$ is $\mathbf{p} = P\mathbf{b}$. If we attempt to project \mathbf{p} itself onto $\text{range}(A)$, nothing should happen since \mathbf{p} is already in the range. That is,

$$P\mathbf{b} = \mathbf{p} = P\mathbf{p} = P^2\mathbf{b}$$

This equation suggests that $P^2 = P$, intuitively saying that projecting a second time does not produce anything different from projecting once. We can verify the identity using the definition of P :

$$\begin{aligned} P^2 &= (A(A^T A)^{-1} A^T)(A(A^T A)^{-1} A^T) \\ &= A(A^T A)^{-1} (A^T A)(A^T A)^{-1} A^T = A(A^T A)^{-1} A^T = P \end{aligned}$$

Also notice that

$$\begin{aligned} P^T &= (A(A^T A)^{-1} A^T)^T \\ &= (A^T)^T ((A^T A)^{-1})^T A^T = A((A^T A)^T)^{-1} A^T = A(A^T A)^{-1} A^T = P \end{aligned}$$

so P is a symmetric matrix. Finally, Figure 7.22 suggests the following. Let Q be the projection matrix onto $\text{kernel}(A^T)$. The subspaces $\text{range}(A)$ and $\text{kernel}(A^T)$ are orthogonal complements of each other. The sum of the projections onto those subspaces should be the original vector. That is, $\mathbf{b} = P\mathbf{b} + Q\mathbf{b} = (P + Q)\mathbf{b}$. This equation is true for all vectors \mathbf{b} , so it must be that $P + Q = I$, or $Q = I - P$. A projection onto one subspace followed by a projection onto the orthogonal complement should always produce the zero vector. Algebraically, we can see this is true: $PQ = P(I - P) = P - P^2 = 0$, which is the zero matrix.

So far all is well as long as the $m \times m$ matrix $A^T A$ is invertible, which is the case if and only if $\text{rank}(A) = m$. What if $r = \text{rank}(A) < m$? The range of A is spanned by the columns of A . Let the columns of A be denoted \mathbf{c}_i for $1 \leq i \leq m$. Reorder the columns as \mathbf{c}_{i_j} for $1 \leq i_j \leq m$, where the first r vectors are linearly independent ($1 \leq j \leq r$) and the last $m - r$ vectors are dependent on them ($r < j \leq m$). The left-hand side of the equation $Ax = \mathbf{b}$ is expanded into a linear combination of the columns of A , then reordered:

$$\mathbf{b} = Ax = \sum_{i=1}^m x_i \mathbf{c}_i = \sum_{j=1}^r x_{i_j} \mathbf{c}_{i_j} + \sum_{j=r+1}^m x_{i_j} \mathbf{c}_{i_j}$$

The dependent \mathbf{c}_{i_j} terms are written as linear combinations of the independent ones. The linear combination of the dependent vectors becomes a linear combination of the independent vectors and is folded into the already existing combination of independent vectors:

$$\mathbf{b} = \sum_{j=1}^r y_{i_j} \mathbf{c}_{i_j} = C\mathbf{y}$$

where y_{i_j} is a linear combination of x_{i_j} and the x_{i_k} where $r < k \leq m$. We now have a linear system where the $n \times r$ matrix C has linearly independent columns. Moreover, by the construction $\text{range}(C) = \text{range}(A)$, and the projection \mathbf{p} of \mathbf{b} onto the range of A is exactly the projection onto the range of C . Thus, the projection matrix is

$$P = C(C^T C)^{-1} C^T \mathbf{b}$$

Since all we need is C , and not a vector \mathbf{y} from the previous construction, it is enough to identify the columns of A that form a basis for $\text{range}(A)$ and use them to construct C , then P .

7.4.9 LINEAR TRANSFORMATIONS

The discussion of systems of linear equations naturally leads to the concept of a matrix, whether it be the $n \times m$ coefficient matrix A of the system, the $m \times 1$ column matrix \mathbf{x} of the unknown variables, or the $n \times 1$ column matrix of outputs \mathbf{b} . The definition for the product of matrices was motivated by solving linear systems using elementary row operations that are represented by matrices. In this section we will discover an approach to defining matrices and operations on them, one that is more natural in the framework of vector spaces.

Let V and W be vector spaces. A function $L : V \rightarrow W$ is said to be a *linear transformation* whenever

1. $L(\mathbf{x} + \mathbf{y}) = L(\mathbf{x}) + L(\mathbf{y})$ for all $\mathbf{x}, \mathbf{y} \in V$, and
2. $L(c\mathbf{x}) = cL(\mathbf{x})$ for all $c \in \mathbb{R}$ and for all $\mathbf{x} \in V$.

In words, the linear transformation of a sum of vectors is the sum of linear transformations of those vectors, and the linear transformation of a scalar multiple of a vector is the scalar multiple of the linear transformation of that vector. The two conditions can be summarized as a single condition, $L(c\mathbf{x} + \mathbf{y}) = cL(\mathbf{x}) + L(\mathbf{y})$ for all $c \in \mathbb{R}$ and for all $\mathbf{x}, \mathbf{y} \in V$. We will refer to V as the *domain* of L and W as the *codomain* of L . The last term is used to avoid confusion in nomenclature. Sometimes W is said to be the *range of the function*, but in our development we use the term *range* to refer to the set of vectors in W that are obtained by applying the function to the domain vectors. In many cases the range is a proper subset of W .

A couple of simple consequences of the definition: $L(\mathbf{0}) = \mathbf{0}$ and $L(-\mathbf{x}) = -L(\mathbf{x})$. The first identity follows from

$$L(\mathbf{0}) = L(0\mathbf{0}) = (0)L(\mathbf{0}) = \mathbf{0}$$

The first and third equalities are a consequence of the fact that the scalar zero multiplied by any vector is the zero vector. The second equality is valid since L is a linear transformation (item 2 in the definition). The second identity is proved similarly:

$$L(-\mathbf{x}) = L(-1\mathbf{x}) = (-1)L(\mathbf{x}) = -L(\mathbf{x})$$

In a finite dimensional vector space, if a vector is written as an n -tuple $\mathbf{x} = (x_1, \dots, x_n)$, you would write $L(\mathbf{x}) = L((x_1, \dots, x_n))$. In these specific cases the extra parentheses are dropped for readability: $L(x_1, \dots, x_n)$.

EXAMPLE 7.39 Define $L : \mathbb{R}^3 \rightarrow \mathbb{R}^2$ by $L(x_1, x_2, x_3) = (x_1 + x_2, x_1 - 3x_3)$. Let $c \in \mathbb{R}$, $\mathbf{x} = (x_1, x_2, x_3)$, and $\mathbf{y} = (y_1, y_2, y_3)$; then

$$\begin{aligned} L(c\mathbf{x} + \mathbf{y}) &= L(c(x_1, x_2, x_3) + (y_1, y_2, y_3)) \\ &= L(ax_1 + by_1, ax_2 + by_2, ax_3 + by_3) \\ &= ((cx_1 + y_1) + (cx_2 + y_2), (cx_1 + y_1) - 3(cx_3 + y_3)) \\ &= (c(x_1 + x_2) + (y_1 + y_2), c(x_1 - 3x_3) + (y_1 - 3y_3)) \\ &= c(x_1 + x_2, x_1 - 3x_3) + (y_1 + y_2, y_1 - 3y_3) \\ &= cL(\mathbf{x}) + L(\mathbf{y}) \end{aligned}$$

so L is a linear transformation.

If $\{\mathbf{e}_1, \mathbf{e}_2, \mathbf{e}_3\}$ is the standard Euclidean basis, then $\mathbf{x} = (x_1, x_2, x_3) = x_1\mathbf{e}_1 + x_2\mathbf{e}_2 + x_3\mathbf{e}_3$ and

$$L(\mathbf{x}) = L(x_1\mathbf{e}_1 + x_2\mathbf{e}_2 + x_3\mathbf{e}_3) = x_1L(\mathbf{e}_1) + x_2L(\mathbf{e}_2) + x_3L(\mathbf{e}_3)$$

since L is linear. Thus, L is determined completely by the values of $L(\mathbf{e}_i)$ for $1 \leq i \leq 3$. As we will see, in general L is determined by its values for any specified basis.

In column vector form,

$$L(\mathbf{x}) = L\left(\begin{bmatrix} x_1 \\ x_2 \\ x_3 \end{bmatrix}\right) = \begin{bmatrix} x_1 + x_2 \\ x_1 - 3x_3 \end{bmatrix} = \begin{bmatrix} 1 & 1 & 0 \\ 1 & 0 & -3 \end{bmatrix} \begin{bmatrix} x_1 \\ x_2 \\ x_3 \end{bmatrix} = A\mathbf{x}$$

The transformation $L(\mathbf{x})$ is represented by a matrix multiplication $A\mathbf{x}$. Since the k th column of A is $A\mathbf{e}_k$, $L(\mathbf{e}_k)$ is the k th column of A :

$$L\left(\begin{bmatrix} 1 \\ 0 \\ 0 \end{bmatrix}\right) = \begin{bmatrix} 1 \\ 1 \end{bmatrix}, \quad L\left(\begin{bmatrix} 0 \\ 1 \\ 0 \end{bmatrix}\right) = \begin{bmatrix} 1 \\ 0 \end{bmatrix}, \quad L\left(\begin{bmatrix} 0 \\ 0 \\ 1 \end{bmatrix}\right) = \begin{bmatrix} 0 \\ -3 \end{bmatrix}$$

This relationship naturally ties together linear transformations and matrices. ■

EXAMPLE 7.40 Let P be the vector space of all polynomials with real coefficients. Define $L : P \rightarrow P$ by $L(p(x)) = p'(x)$. That is,

$$L\left(\sum_{i=0}^n p_i x^i\right) = \sum_{i=1}^n i p_i x^i = \sum_{j=0}^{n-1} (j+1) p_{j+1} x^j$$

You should recognize L as differentiation of the polynomial $p(x)$. Let $p(x) = \sum_{i=0}^n p_i x^i$ and $q(x) = \sum_{i=0}^m q_i x^i$, where $n \leq m$. If we define $p_i = 0$ for $i > n$, then

$p(x) = \sum_{i=0}^m p_i x^i$ so that the upper limits of summation on $p(x)$ and $q(x)$ are the same. Let $c \in \mathbb{R}$; then

$$\begin{aligned}
 L(cp(x) + q(x)) &= L\left(c \sum_{i=0}^m p_i x^i + \sum_{i=0}^m q_i x^i\right) \\
 &= L\left(\sum_{i=0}^m (cp_i + q_i)x^i\right) && \text{Using vector space operations} \\
 &= \sum_{j=0}^{m-1} (j+1)(cp_{j+1} + q_{j+1})x^j && \text{Definition of } L \\
 &= c \sum_{j=0}^{m-1} (j+1)p_j x^j + \sum_{j=0}^{m-1} (j+1)q_j x^j && \text{Using vector space} \\
 &&& \text{operations} \\
 &= cL(p(x)) + L(q(x)) && \text{Definition of } L
 \end{aligned}$$

This proves that L is a linear transformation. ■

The next result establishes for certain the relationship between linear transformations and matrices: $L : \mathbb{R}^m \rightarrow \mathbb{R}^n$ is a linear transformation if and only if $L(\mathbf{x}) = A\mathbf{x}$ for some $n \times m$ matrix $A = [a_{ij}]$. The proof follows.

Define the function $L(\mathbf{x}) = A\mathbf{x}$, where \mathbf{x} is treated as an $m \times 1$ column vector and where $L(\mathbf{x})$ is treated as an $n \times 1$ column vector. For $c \in \mathbb{R}$ and $\mathbf{x}, \mathbf{y} \in \mathbb{R}^m$,

$$\begin{aligned}
 L(c\mathbf{x} + \mathbf{y}) &= A(c\mathbf{x} + \mathbf{y}) && \text{Definition of } L \\
 &= A(c\mathbf{x}) + A\mathbf{y} && \text{Matrix multiplication is distributive} \\
 &= c(A\mathbf{x}) + A\mathbf{y} && \text{Property of matrix arithmetic} \\
 &= cL(\mathbf{x}) + L(\mathbf{y}) && \text{Definition of } L
 \end{aligned}$$

This proves that L is a linear transformation.

Conversely, let $L : \mathbb{R}^m \rightarrow \mathbb{R}^n$ be a linear transformation, where \mathbf{x} and $L(\mathbf{x})$ are treated as column vectors. Let $\{\mathbf{e}_1, \dots, \mathbf{e}_n\}$ be the standard Euclidean basis for \mathbb{R}^n ; then $L(\mathbf{e}_k) \in \mathbb{R}^m$ for all k . As such, these vectors can be represented as

$$L(\mathbf{e}_k) = \begin{bmatrix} a_{1k} \\ \vdots \\ a_{mk} \end{bmatrix}_{m \times 1}, \quad k = 1, \dots, n$$

If $\mathbf{x} = \sum_{k=1}^n x_k \mathbf{e}_k$, then

$$\begin{aligned}
L(\mathbf{x}) &= L\left(\sum_{k=1}^n x_k \mathbf{e}_k\right) \\
&= \sum_{k=1}^n x_k L(\mathbf{e}_k) \quad \text{Since } L \text{ is linear} \\
&= \sum_{k=1}^n x_k \begin{bmatrix} a_{1k} \\ \vdots \\ a_{mk} \end{bmatrix} \\
&= \sum_{k=1}^n \begin{bmatrix} a_{1k}x_k \\ \vdots \\ a_{mk}x_k \end{bmatrix} \\
&= \begin{bmatrix} \sum_{k=1}^n a_{1k}x_k \\ \vdots \\ \sum_{k=1}^n a_{mk}x_k \end{bmatrix} \\
&= A\mathbf{x}
\end{aligned}$$

The argument actually provides the construction of the $n \times m$ matrix A given L .

EXAMPLE
7.41

Define $L : \mathbb{R}^2 \rightarrow \mathbb{R}^2$ by $L(x_1, x_2) = (3x_1 + 6x_2, -2x_1 + x_2)$. In column vector form,

$$L\left(\begin{bmatrix} 1 \\ 0 \end{bmatrix}\right) = \begin{bmatrix} 3 \\ -2 \end{bmatrix}, \quad L\left(\begin{bmatrix} 0 \\ 1 \end{bmatrix}\right) = \begin{bmatrix} 6 \\ 1 \end{bmatrix}$$

and

$$L\left(\begin{bmatrix} x_1 \\ x_2 \end{bmatrix}\right) = \begin{bmatrix} 3 & 6 \\ -2 & 1 \end{bmatrix} \begin{bmatrix} x_1 \\ x_2 \end{bmatrix} = \begin{bmatrix} 3x_1 + 6x_2 \\ -2x_1 + x_2 \end{bmatrix}$$

The transformation has been written as $L(\mathbf{x}) = A\mathbf{x}$, where

$$A = [L(e_1) \ L(e_2)]_{2 \times 2} = \begin{bmatrix} 3 & 6 \\ -2 & 1 \end{bmatrix}$$

This representation depends on our choice of the Euclidean basis for \mathbb{R}^2 . That is,

$$\begin{bmatrix} x_1 \\ x_2 \end{bmatrix} = x_1 \begin{bmatrix} 1 \\ 0 \end{bmatrix} + x_2 \begin{bmatrix} 0 \\ 1 \end{bmatrix} \text{ and}$$

$$L\left(\begin{bmatrix} x_1 \\ x_2 \end{bmatrix}\right) = (3x_1 + 6x_2) \begin{bmatrix} 1 \\ 0 \end{bmatrix} + (-2x_1 + x_2) \begin{bmatrix} 0 \\ 1 \end{bmatrix}$$

What happens if you use different bases? Let $L : V \rightarrow W$ be a linear transformation where V has basis $F = \{\mathbf{f}_1, \dots, \mathbf{f}_m\}$ and W has basis $G = \{\mathbf{g}_1, \dots, \mathbf{g}_n\}$. Treating the elements of V and W as column vectors, we can represent L by $L(\mathbf{x}) = A\mathbf{x}$, where A depends on the definition for L , the basis F for V , and the basis G for W . A vector $\mathbf{x} \in V$ is represented in the F basis as $\mathbf{x} = \sum_{j=1}^m x_j \mathbf{f}_j$. Each vector $L(\mathbf{f}_j) \in W$ is represented in the G basis as $L(\mathbf{f}_j) = \sum_{i=1}^n a_{ij} \mathbf{g}_i$. The linear transformation is expanded as

$$\begin{aligned} L(\mathbf{x}) &= L\left(\sum_{j=1}^m x_j \mathbf{f}_j\right) \\ &= \sum_{j=1}^m x_j L(\mathbf{f}_j) \\ &= \sum_{j=1}^m x_j \left(\sum_{i=1}^n a_{ij} \mathbf{g}_i \right) \\ &= \sum_{i=1}^n \left(\sum_{j=1}^m a_{ij} x_j \right) \mathbf{g}_i \\ &= \sum_{i=1}^n y_i \mathbf{g}_i \end{aligned}$$

where the last equality defines the $y_i = \sum_{j=1}^m a_{ij} x_j$. The coefficient vector \mathbf{x} , which is $m \times 1$, and the coefficient vector \mathbf{y} , which is $n \times 1$, are related by the matrix equation $\mathbf{y} = A\mathbf{x}$, where $A = [a_{ij}]$ is an $n \times m$ matrix. This matrix represents the linear transformation *with respect to the chosen bases F and G*. Different choices for bases will lead to different matrices for A .

EXAMPLE 7.42

Let $L : \mathbb{R}^2 \rightarrow \mathbb{R}^2$ be given by $L(x_1, x_2) = (3x_1 + 6x_2, -2x_1 + x_2) = (y_1, y_2)$. The standard Euclidean basis is $E = \{(1, 0), (0, 1)\}$. The matrix representation of L where E is the basis used for both the domain and codomain is

$$\mathbf{y}_E = \begin{bmatrix} 3 & 6 \\ -2 & 1 \end{bmatrix} \mathbf{x}_E$$

(Example 7.42
continued)

The notations \mathbf{x}_E and \mathbf{y}_E indicate that the vectors are to be represented in the basis E . The input 2-tuple (x_1, x_2) and output 2-tuple (y_1, y_2) have the obvious representations in E as

$$\mathbf{x}_E = \begin{bmatrix} x_1 \\ x_2 \end{bmatrix} \text{ and } \mathbf{y}_E = \begin{bmatrix} y_1 \\ y_2 \end{bmatrix}$$

Choose different bases, $F = \{\mathbf{f}_1, \mathbf{f}_2\} = \{(1, 1), (1, -1)\}$ for the domain and $G = \{\mathbf{g}_1, \mathbf{g}_2\} = \{(0, 1), (1, 0)\}$ for the codomain. The representation of (x_1, x_2) in the F basis is

$$\mathbf{x}_F = \frac{x_1 + x_2}{2}(1, 1) + \frac{x_1 - x_2}{2}(1, -1) = \frac{x_1 + x_2}{2}\mathbf{f}_1 + \frac{x_1 - x_2}{2}\mathbf{f}_2$$

The representation of (y_1, y_2) in the G basis is

$$\mathbf{y}_G = y_2(0, 1) + y_1(1, 0) = y_2\mathbf{g}_1 + y_1\mathbf{g}_2$$

The linear transformation applied to the F basis vectors has results written in the G basis,

$$\begin{aligned} L(\mathbf{f}_1) &= L(1, 1) = (9, -1) = -1(0, 1) + 9(1, 0) = -\mathbf{g}_1 + 9\mathbf{g}_2 \\ L(\mathbf{f}_2) &= L(1, -1) = (-3, -3) = -3(0, 1) - 3(1, 0) = -3\mathbf{g}_1 - 3\mathbf{g}_2 \end{aligned}$$

so the matrix, which represents L with respect to the bases F and G , is

$$A = \begin{bmatrix} -1 & -3 \\ 9 & -3 \end{bmatrix}$$

A quick verification shows

$$\begin{bmatrix} y_2 \\ y_1 \end{bmatrix} = \mathbf{y}_G = A\mathbf{x}_F = \begin{bmatrix} -1 & -3 \\ 9 & -3 \end{bmatrix} \begin{bmatrix} \frac{x_1 + x_2}{2} \\ \frac{x_1 - x_2}{2} \end{bmatrix} = \begin{bmatrix} -2x_1 + x_2 \\ 3x_1 + 6x_2 \end{bmatrix}$$

and reproduces exactly the linear transformation $(y_1, y_2) = (3x_1 + 6x_2, -2x_1 + x_2)$. ■

EXAMPLE
7.43

Let P_n be the set of polynomials with real-valued coefficients and of degree at most n . That is,

$$P_n = \left\{ \sum_{i=0}^n a_i x^i : a_i \in \mathbb{R} \right\}$$

Define $L : P_1 \rightarrow P_2$ by

$$L(p(x)) = \int_0^x p(t) dt$$

You should recognize this as the definite integral of the polynomial over the interval $[0, x]$ where the upper limit x is variable. Polynomials in P_1 are of the form $p(x) = a_0 + a_1x$ and polynomials in P_2 are of the form $p(x) = b_0 + b_1x + b_2x^2$. The linear transformation can be restated as $L(a_0 + a_1x) = a_0x + (a_1/2)x^2$. A basis for P_1 is $F = \{\mathbf{f}_1, \mathbf{f}_2\} = \{1, x\}$ and a basis for P_2 is $G = \{\mathbf{g}_1, \mathbf{g}_2, \mathbf{g}_3\} = \{1, x, x^2\}$. Applying the linear transformation to the F basis vectors produces

$$L(\mathbf{f}_1) = L(1) = x = 0 \cdot 1 + 1 \cdot x + 0 \cdot x^2 = \mathbf{g}_2$$

$$L(\mathbf{f}_2) = L(x) = \frac{1}{2}x^2 = 0 \cdot 1 + 0 \cdot x + \frac{1}{2} \cdot x^2 = (1/2)\mathbf{g}_3$$

The matrix A that represents the linear transformation with respect to the bases F and G is

$$A = \begin{bmatrix} 0 & 0 \\ 1 & 0 \\ 0 & \frac{1}{2} \end{bmatrix}$$

In terms of the polynomial coefficients, the application of the matrix is

$$A \begin{bmatrix} a_0 \\ a_1 \end{bmatrix} = \begin{bmatrix} 0 \\ a_0 \\ \frac{a_1}{2} \end{bmatrix}$$

Let $L : V \rightarrow V$ be a linear transformation where V is both the domain and codomain and has dimension n . A matrix representation of L is an $n \times n$ matrix. We have seen that the matrix representation depends on the bases selected for the domain and codomain. If a basis $F = \{\mathbf{f}_1, \dots, \mathbf{f}_n\}$ is chosen for domain and codomain with corresponding matrix representation A , and a basis $G = \{\mathbf{g}_1, \dots, \mathbf{g}_n\}$ is chosen for domain and codomain with corresponding matrix representation B , the question is how are A and B related? The key idea is *change of basis*, the process of representing basis vectors in F in terms of the basis G . Each vector \mathbf{f}_j is represented in G as

$$\mathbf{f}_j = \sum_{i=1}^n c_{ij}\mathbf{g}_i, \quad 1 \leq j \leq n$$

The matrix $C = [c_{ij}]$ is called the *change of basis matrix* and itself represents a linear transformation from V to V . Figure 7.23 is a diagram that indicates how all the matrices map V to itself. The bases are explicitly paired with V for clarity.

To get from (V, F) to (V, F) you can directly apply matrix A . Or you can go from (V, F) to (V, G) by applying matrix C , then from (V, G) to (V, G) by applying matrix B , then from (V, G) to (V, F) by applying the inverse matrix C^{-1} . The two alternatives

$$\begin{array}{ccc} (V, F) & \xrightarrow{A} & (V, F) \\ C \downarrow & & \downarrow C \\ (V, G) & \xrightarrow{B} & (V, G) \end{array}$$

Figure 7.23 A linear transformation from V to V with respect to two different bases (horizontal arrows). The change of basis for V (vertical arrows).

suggest that $A = C^{-1}BC$. This is in fact the case as the following algebraic construction shows. The inverse matrix C^{-1} has entries name d_{ij} . The basis vectors in G are related to the basis vectors in F by

$$\mathbf{g}_i = \sum_{\ell=1}^n d_{\ell i} \mathbf{f}_{\ell}$$

The linear transformation is expanded as

$$\begin{aligned} L(\mathbf{f}_j) &= L\left(\sum_{k=1}^n c_{kj} \mathbf{g}_k\right) && \text{Using the change of basis matrix } C \\ &= \sum_{k=1}^n c_{kj} L(\mathbf{g}_k) && \text{Since } L \text{ is linear} \\ &= \sum_{k=1}^n c_{kj} \left(\sum_{i=1}^n b_{ik} \mathbf{g}_i \right) && \text{Using the matrix } B \text{ that represents } L \\ &= \sum_{i=1}^n \sum_{k=1}^n b_{ik} c_{kj} \mathbf{g}_i \\ &= \sum_{i=1}^n \sum_{k=1}^n b_{ik} c_{kj} \left(\sum_{\ell=1}^n d_{\ell i} \mathbf{f}_{\ell} \right) && \text{Using the change of basis matrix } C^{-1} \\ &= \sum_{\ell=1}^n \left(\sum_{i=1}^n \sum_{k=1}^n d_{\ell i} b_{ik} c_{kj} \right) \mathbf{f}_{\ell} \\ &= \sum_{\ell=1}^n a_{\ell j} \mathbf{f}_{\ell} && \text{Using the matrix } A \text{ that represents } L \end{aligned}$$

so $a_{\ell j} = \sum_{i=1}^n \sum_{k=1}^n d_{\ell i} b_{ik} c_{kj}$. Using the definition of matrix multiplication, we have $A = C^{-1}BC$.

The relationship between A and B is called a *similarity relationship*. In general if A and B are square matrices for which there exists an invertible matrix C with

$A = C^{-1}BC$, then A and B are said to be *similar*. The importance of similarity of matrices will become more apparent in Sections 7.5.2 and 7.5.3 on eigenvalues and eigenvectors.

EXAMPLE
7.44

Consider the linear transformation $L : \mathbb{R}^2 \rightarrow \mathbb{R}^2$ defined by $L(x_1, x_2) = (x_1 - 3x_2, x_1 + x_2)$. Two bases for \mathbb{R}^2 are $F = \{(2, 1), (1, -1)\}$, and $G = \{(0, 1), (1, 0)\}$.

Compute the matrix A representing $L : (\mathbb{R}^2, F) \rightarrow (\mathbb{R}^2, F)$. Solve

$$L(\mathbf{f}_1) = L(2, 1) = (-1, 3) = a_{11}(2, 1) + a_{21}(1, -1) = a_{11}\mathbf{f}_1 + a_{21}\mathbf{f}_2$$

$$L(\mathbf{f}_2) = L(1, -1) = (4, 0) = a_{12}(2, 1) + a_{22}(1, -1) = a_{12}\mathbf{f}_1 + a_{22}\mathbf{f}_2$$

The coefficients a_{ij} are solutions to

$$\begin{bmatrix} 2 & 1 \\ 1 & -1 \end{bmatrix} \begin{bmatrix} a_{11} & a_{12} \\ a_{21} & a_{22} \end{bmatrix} = \begin{bmatrix} -1 & 4 \\ 3 & 0 \end{bmatrix}$$

therefore,

$$A = \begin{bmatrix} a_{11} & a_{12} \\ a_{21} & a_{22} \end{bmatrix} = \begin{bmatrix} 2 & 1 \\ 1 & -1 \end{bmatrix}^{-1} \begin{bmatrix} -1 & 4 \\ 3 & 0 \end{bmatrix} = \begin{bmatrix} \frac{2}{3} & \frac{4}{3} \\ \frac{3}{3} & \frac{3}{3} \\ -\frac{7}{3} & \frac{4}{3} \end{bmatrix}$$

and

$$L(\mathbf{f}_1) = \frac{2}{3}\mathbf{f}_1 - \frac{7}{3}\mathbf{f}_2, \quad L(\mathbf{f}_2) = \frac{4}{3}\mathbf{f}_1 + \frac{4}{3}\mathbf{f}_2$$

Compute the matrix B representing $L : (\mathbb{R}^2, G) \rightarrow (\mathbb{R}^2, G)$. Solve

$$L(\mathbf{g}_1) = L(0, 1) = (-3, 1) = b_{11}(0, 1) + b_{21}(1, 0) = b_{11}\mathbf{g}_1 + b_{21}\mathbf{g}_2$$

$$L(\mathbf{g}_2) = L(1, 0) = (1, 1) = b_{12}(0, 1) + b_{22}(1, 0) = b_{12}\mathbf{g}_1 + b_{22}\mathbf{g}_2$$

The coefficients b_{ij} are solutions to

$$\begin{bmatrix} 0 & 1 \\ 1 & 0 \end{bmatrix} \begin{bmatrix} b_{11} & b_{12} \\ b_{21} & b_{22} \end{bmatrix} = \begin{bmatrix} -3 & 1 \\ 1 & 1 \end{bmatrix}$$

therefore,

$$B = \begin{bmatrix} b_{11} & b_{12} \\ b_{21} & b_{22} \end{bmatrix} = \begin{bmatrix} 0 & 1 \\ 1 & 0 \end{bmatrix}^{-1} \begin{bmatrix} -3 & 1 \\ 1 & 1 \end{bmatrix} = \begin{bmatrix} 1 & 1 \\ -3 & 1 \end{bmatrix}$$

and

$$L(\mathbf{g}_1) = \mathbf{g}_1 - 3\mathbf{g}_2, \quad L(\mathbf{g}_2) = \mathbf{g}_1 + \mathbf{g}_2$$

Finally, compute the change of basis matrix C from

$$\mathbf{f}_1 = (2, 1) = c_{11}(0, 1) + c_{21}(1, 0) = c_{11}\mathbf{g}_1 + c_{21}\mathbf{g}_2$$

$$\mathbf{f}_2 = (1, -1) = c_{12}(0, 1) + c_{22}(1, 0) = c_{12}\mathbf{g}_1 + c_{22}\mathbf{g}_2$$

(Example 7.44
continued)

the solution being

$$C = \begin{bmatrix} 1 & -1 \\ 2 & 1 \end{bmatrix}, \quad C^{-1} = \frac{1}{3} \begin{bmatrix} 1 & 1 \\ -2 & 1 \end{bmatrix}$$

The similarity relationship between A and B is

$$C^{-1}BC = \frac{1}{3} \begin{bmatrix} 1 & 1 \\ -2 & 1 \end{bmatrix} \begin{bmatrix} 1 & 1 \\ -3 & 1 \end{bmatrix} \begin{bmatrix} 1 & -1 \\ 2 & 1 \end{bmatrix} = \frac{1}{3} \begin{bmatrix} 2 & 4 \\ -7 & 4 \end{bmatrix} = A$$

There is one last topic on vector spaces to consider, finally. Composition of linear transformations is the foundation for the definition of matrix multiplication. Let $R : \mathbb{R}^n \rightarrow \mathbb{R}^p$ and $S : \mathbb{R}^m \rightarrow \mathbb{R}^n$ be linear transformations, say $\mathbf{y} = S(\mathbf{x})$ and $\mathbf{z} = R(\mathbf{y})$. The composition is $T = R \circ S(\mathbf{x}) = R(S(\mathbf{x}))$ and is a linear function $T : \mathbb{R}^m \rightarrow \mathbb{R}^p$. The circle symbol denotes composition of functions. To see that T is linear, let $c \in \mathbb{R}$ and $\mathbf{x}_1, \mathbf{x}_2 \in \mathbb{R}^m$:

$$\begin{aligned} T(c\mathbf{x}_1 + \mathbf{x}_2) &= R(S(c\mathbf{x}_1 + \mathbf{x}_2)) && \text{Definition of } T \\ &= R(cS(\mathbf{x}_1) + S(\mathbf{x}_2)) && S \text{ is linear} \\ &= cR(S(\mathbf{x}_1)) + R(S(\mathbf{x}_2)) && R \text{ is linear} \\ &= cT(\mathbf{x}_1) + T(\mathbf{x}_2) && \text{Definition of } T \end{aligned}$$

If A is a matrix representation of R and B is a matrix representation of S , with respect to specified bases, of course, then what is the matrix representation of T with respect to those same bases? The answer is simply put: $R(\mathbf{y})$ is represented by $\mathbf{z} = A\mathbf{y}$, and $S(\mathbf{x})$ is represented by $\mathbf{y} = B\mathbf{x}$. The composition is $\mathbf{z} = A\mathbf{y} = A(B\mathbf{x}) = (AB)\mathbf{x} = C\mathbf{x}$. The matrix representing T is C and is a product of A and B . Observe that A is $p \times n$, B is $n \times m$, and C is $p \times m$.

7.5 ADVANCED TOPICS

7.5.1 DETERMINANTS

A *determinant* is a scalar quantity associated with a square matrix and is encountered frequently in applications. You are most likely familiar with the determinant formulas for 2×2 and 3×3 matrices. I will take a closer look at these definitions and provide a geometric interpretation for them.

Determinant of a 2×2 Matrix

The determinant for a 2×2 matrix A is defined by

$$\det(A) = \det \begin{bmatrix} a_{11} & a_{12} \\ a_{21} & a_{22} \end{bmatrix} = a_{11}a_{22} - a_{12}a_{21} \quad (7.37)$$

which is a simple enough formula to commit to memory. As it turns out, $\det(A)$ is nonzero if and only if A is an invertible matrix. Formally, the inverse of A is the matrix,

$$A^{-1} = \frac{1}{a_{11}a_{22} - a_{12}a_{21}} \begin{bmatrix} a_{22} & -a_{12} \\ -a_{21} & a_{11} \end{bmatrix}$$

Verify for yourself that $AA^{-1} = A^{-1}A = I$, where I is the identity matrix. Observe that the scalar before the matrix is the reciprocal of the determinant, $1/\det(A)$, so clearly the determinant must not be zero in order that A^{-1} exist. This algebraic requirement is perhaps unsatisfying to someone wanting a geometric understanding of the problem. Let us go ahead and take a closer look.

Let $\mathbf{i} = [1 \ 0]^T$ and $\mathbf{j} = [0 \ 1]^T$ be the standard basis vectors for \mathbb{R}^2 . These vectors are transformed to $A\mathbf{i} = [a_{11} \ a_{21}]^T$ and $A\mathbf{j} = [a_{12} \ a_{22}]^T$, the columns of the matrix A . Figure 7.24 shows the unit-area square whose sides are determined by the basis vectors and shows various possibilities for the transformed square.

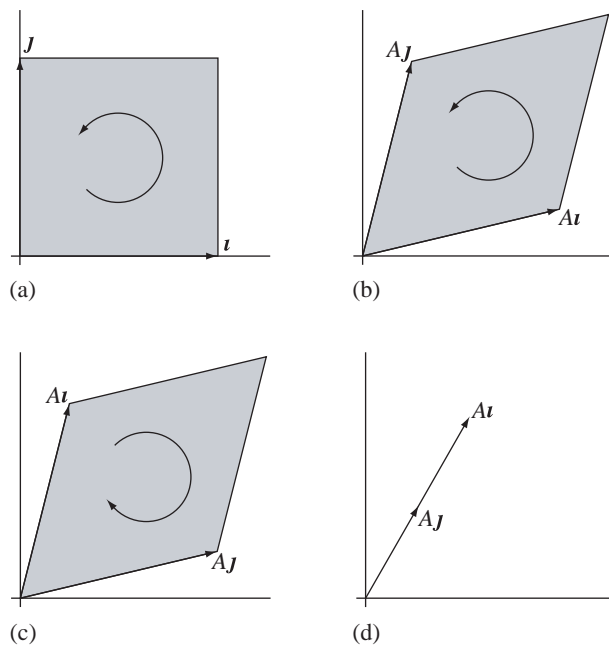


Figure 7.24 (a) A unit-area square. (b) The parallelogram obtained by transforming the square when the transformed basis vectors have the same order as the basis vectors. (c) The parallelogram obtained by transforming the square when the transformed basis vectors have the opposite order as the basis vectors. (d) The basis vectors mapped to parallel vectors, in which case A is not invertible.

Although Figure 7.24(d) shows $A\mathbf{i}$ and $A\mathbf{j}$ as nonzero vectors, either or both can be the zero vector; that is, one or both columns of A can be the zero vector. It is also possible that the transformed basis vectors are nonzero but point in opposite directions.

Set $\mathbf{u} = A\mathbf{i}$ and $\mathbf{v} = A\mathbf{j}$. The area of the parallelogram formed by \mathbf{u} and \mathbf{v} is $\alpha = bh$, where b is the base (the length of \mathbf{u}) and where h is the height (the length of the projection of \mathbf{v} onto a vector perpendicular to \mathbf{u}). We will do the calculations in squared form, that is, $\alpha^2 = b^2 h^2$. The squared base is just

$$b^2 = |\mathbf{u}|^2$$

The squared height is calculated from the aforementioned projection that is calculated using equation (7.15):

$$\mathbf{p} = \mathbf{v} - \frac{\mathbf{u} \cdot \mathbf{v}}{|\mathbf{u}|^2} \mathbf{u}$$

The squared height is

$$h^2 = |\mathbf{p}|^2 = \left| \mathbf{v} - \frac{\mathbf{u} \cdot \mathbf{v}}{|\mathbf{u}|^2} \mathbf{u} \right|^2 = |\mathbf{v}|^2 - \frac{2(\mathbf{u} \cdot \mathbf{v})^2}{|\mathbf{u}|^2} + \frac{(\mathbf{u} \cdot \mathbf{v})^2}{|\mathbf{u}|^2} = |\mathbf{v}|^2 - \frac{(\mathbf{u} \cdot \mathbf{v})^2}{|\mathbf{u}|^2}$$

The squared area is

$$\begin{aligned} \alpha^2 &= b^2 h^2 \\ &= |\mathbf{u}|^2 |\mathbf{p}|^2 \\ &= |\mathbf{u}|^2 |\mathbf{v}|^2 - (\mathbf{u} \cdot \mathbf{v})^2 \\ &= (a_{11}^2 + a_{21}^2)(a_{12}^2 + a_{22}^2) - (a_{11}a_{12} + a_{21}a_{22})^2 \\ &= a_{11}^2 a_{22}^2 + a_{21}^2 a_{12}^2 - 2a_{11}a_{12}a_{21}a_{22} \\ &= (a_{11}a_{22} - a_{12}a_{21})^2 \\ &= (\det(A))^2 \end{aligned}$$

The area of the parallelogram is $\alpha = |\det(A)|$, the absolute value of the determinant of the matrix. To distinguish between the two cases corresponding to Figure 7.24(b), (c) we will use a *signed area*. Part (b) occurs when the order of the basis vectors is preserved; we will assign a positive area to that parallelogram. Part (c) occurs when the order is switched; we will assign a negative area to that parallelogram. The signed area formula (using the same variable name) is $\alpha = \det(A)$. This equation captures all the geometry in parts (a)–(c) of the figure, part (d) representing the case when the determinant is zero. In this case, the parallelogram is degenerate and may be considered to bound a region of zero area.

Determinant of a 3×3 Matrix

The determinant for a 3×3 matrix is defined by

$$\begin{aligned}\det(A) &= \det \begin{bmatrix} a_{11} & a_{12} & a_{13} \\ a_{21} & a_{22} & a_{23} \\ a_{31} & a_{32} & a_{33} \end{bmatrix} \\ &= a_{11}(a_{22}a_{33} - a_{23}a_{32}) + a_{12}(a_{23}a_{31} - a_{21}a_{33}) + a_{13}(a_{21}a_{32} - a_{22}a_{31}) \\ &= a_{11}a_{22}a_{33} + a_{12}a_{23}a_{31} + a_{13}a_{21}a_{32} - a_{13}a_{22}a_{31} - a_{12}a_{21}a_{33} - a_{11}a_{23}a_{32}\end{aligned}\tag{7.38}$$

This equation is more difficult to commit to memory than its 2×2 counterpart. One method that is taught to help remember the formula is the *butterfly rule* as shown in Figure 7.25.

The matrix is written down and its first two columns are repeated after it. The three terms along each directed arrow are multiplied together. The diagonals from upper left to lower right are given a plus sign (use the product as is). The diagonals from lower left to upper right are given a minus sign (negate the product before using it). (Important note: The butterfly rule does not apply to larger matrices.)

The inverse of a 3×3 matrix A is formally

$$A^{-1} = \frac{1}{\det(A)} \begin{bmatrix} a_{22}a_{33} - a_{23}a_{32} & a_{13}a_{32} - a_{12}a_{33} & a_{12}a_{23} - a_{13}a_{22} \\ a_{23}a_{31} - a_{21}a_{33} & a_{11}a_{33} - a_{13}a_{31} & a_{13}a_{21} - a_{11}a_{23} \\ a_{21}a_{32} - a_{22}a_{31} & a_{12}a_{31} - a_{11}a_{32} & a_{11}a_{22} - a_{12}a_{21} \end{bmatrix}$$

and may be verified by symbolically calculating $AA^{-1} = A^{-1}A = I$, where I is the identity matrix. As in the 2×2 case, the scalar before the matrix is the reciprocal of the determinant, $1/\det(A)$, so the determinant must be nonzero for the inverse to exist.

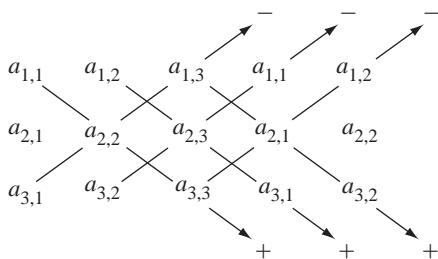


Figure 7.25 An illustration of the butterfly rule for the determinant of a 3×3 matrix.

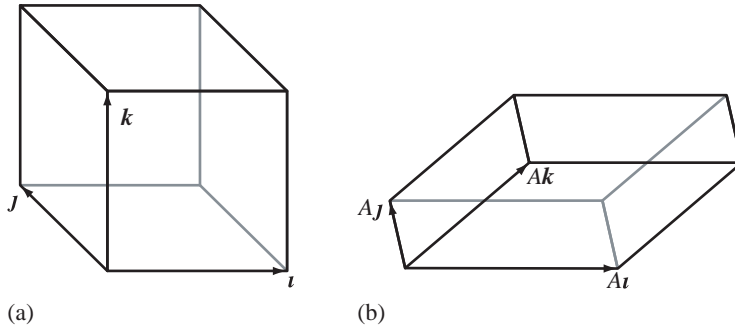


Figure 7.26 (a) A unit-volume cube. (b) The parallelepiped obtained by transforming the cube when the transformed basis vectors have the same order as the basis vectors.

The geometric interpretation of the determinant for a 3×3 matrix is analogous to that of the 2×2 matrix. Let $\mathbf{i} = [1 \ 0 \ 0]^T$, $\mathbf{j} = [0 \ 1 \ 0]^T$, and $\mathbf{k} = [0 \ 0 \ 1]^T$ be the standard basis vectors for \mathbb{R}^3 . These vectors are transformed to $A\mathbf{i} = [a_{11} \ a_{21} \ a_{31}]^T$, $A\mathbf{j} = [a_{12} \ a_{22} \ a_{32}]^T$, and $A\mathbf{k} = [a_{13} \ a_{23} \ a_{33}]^T$, the columns of the matrix A . Figure 7.26 shows a typical situation when the transformed vectors are linearly independent and have the same ordering as the basis vectors.

The degenerate cases that have zero volume occur when all three transformed vectors are coplanar or collinear. The signed volume v of a parallelepiped formed by $A\mathbf{i}$, $A\mathbf{j}$, and $A\mathbf{k}$ is computed in a coordinate-dependent manner using equation (7.24):

$$\begin{aligned} v &= A\mathbf{i} \cdot (A\mathbf{j} \times A\mathbf{k}) \\ &= (a_{11}, a_{21}, a_{31}) \cdot (a_{12}, a_{22}, a_{32}) \times (a_{13}, a_{23}, a_{33}) \\ &= a_{11}(a_{22}a_{33} - a_{23}a_{32}) + a_{12}(a_{23}a_{31} - a_{21}a_{33}) + a_{13}(a_{21}a_{32} - a_{22}a_{31}) \\ &= \det(A) \end{aligned}$$

This is exactly the determinant as defined by equation (7.38).

Formal Construction of Determinant Functions

A general and formal construction of the determinant function is given next. First, though, we need to define a few concepts. Let V and W be vector spaces. Recall that a function $L : V \rightarrow W$ is a linear transformation if $L(cx + \mathbf{y}) = cL(\mathbf{x}) + L(\mathbf{y})$ for all $c \in \mathbb{R}$ and for all $\mathbf{x}, \mathbf{y} \in V$. Define $V^n = \{(\mathbf{x}_1, \dots, \mathbf{x}_n) : \mathbf{x}_j \in V \text{ for all } j\}$, the set of n -tuples of vectors from V . A function $L : V^n \rightarrow W$ is a *multilinear transformation* if

it is linear with respect to each argument. That is, $L(\mathbf{x}_1, \dots, \mathbf{x}_n)$ satisfies the conditions:

$$\begin{aligned} L(c\mathbf{x}_1 + \mathbf{y}_1, \mathbf{x}_2, \dots, \mathbf{x}_n) &= cL(\mathbf{x}_1, \mathbf{x}_2, \dots, \mathbf{x}_n) + L(\mathbf{y}_1, \mathbf{x}_2, \dots, \mathbf{x}_n) \\ L(\mathbf{x}_1, c\mathbf{x}_2 + \mathbf{y}_2, \dots, \mathbf{x}_n) &= cL(\mathbf{x}_1, \mathbf{x}_2, \dots, \mathbf{x}_n) + L(\mathbf{x}_1, \mathbf{y}_2, \dots, \mathbf{x}_n) \\ &\vdots \\ L(\mathbf{x}_1, \mathbf{x}_2, \dots, c\mathbf{x}_n + \mathbf{y}_n) &= cL(\mathbf{x}_1, \mathbf{x}_2, \dots, \mathbf{x}_n) + L(\mathbf{x}_1, \mathbf{x}_2, \dots, \mathbf{y}_n) \end{aligned}$$

You have already seen an example of a multilinear function, the dot product $L(\mathbf{x}, \mathbf{y}) = \mathbf{x} \cdot \mathbf{y}$.

Let $S = \{1, \dots, n\}$. A *permutation on S* is any one-to-one, onto function $\sigma : S \rightarrow S$. For example, if $S = \{1, 2, 3\}$, then $\sigma(1) = 2$, $\sigma(2) = 1$, and $\sigma(3) = 3$ defines a permutation. Typically, we indicate the permutation by listing the elements of S and $\sigma(S)$ as n -tuples. In the last example, $S = (1 \ 2 \ 3)$ and $\sigma(S) = (2 \ 1 \ 3)$. A *transposition* is a permutation that swaps two elements in S . The permutation σ in the last example is a transposition since 1 and 2 were swapped. The permutation $\sigma(1 \ 2 \ 3) = (3 \ 1 \ 2)$ is not a transposition. However, a permutation can always be factored into a composition of transpositions.

EXAMPLE
7.45

Let $S = (1 \ 2 \ 3 \ 4 \ 5)$ and define σ by $\sigma(1 \ 2 \ 3 \ 4 \ 5) = (4 \ 3 \ 5 \ 2 \ 1)$. Begin swapping pairs of numbers. The circle symbol denotes composition of functions.

$$\begin{aligned} (1 \ 2 \ 3 \ 4 \ 5) & S \\ (4 \ 2 \ 3 \ 1 \ 5) & \text{Transpose } 1, 4, \tau_1(S) \\ (4 \ 3 \ 2 \ 1 \ 5) & \text{Transpose } 2, 3, \tau_2(\tau_1(S)) = \tau_2 \circ \tau_1(S) \\ (4 \ 3 \ 2 \ 5 \ 1) & \text{Transpose } 1, 5, \tau_3(\tau_2 \circ \tau_1(S)) = \tau_3 \circ \tau_2 \circ \tau_1(S) \\ (4 \ 3 \ 5 \ 2 \ 1) & \text{Transpose } 2, 5, \tau_4(\tau_3 \circ \tau_2 \circ \tau_1(S)) = \tau_4 \circ \tau_3 \circ \tau_2 \circ \tau_1(S) = \sigma(S) \end{aligned}$$

Note that $\tau_1(S) = (4 \ 2 \ 3 \ 1 \ 5)$, $\tau_2(S) = (1 \ 3 \ 2 \ 4 \ 5)$, $\tau_3(S) = (5 \ 2 \ 3 \ 4 \ 1)$, and $\tau_4(S) = (1 \ 5 \ 3 \ 4 \ 2)$. ■

The factorization of a permutation into transpositions is not unique. However, the parity of the number of transpositions in the factorizations is. That is, if a permutation can be factored into an even number of transpositions, then any other factorization contains an even number of transpositions. We call such a permutation an *even permutation*. A similar statement can be made for a permutation with an odd number of transpositions in the factorization. We call such a permutation an *odd permutation*.

Let V be a vector space with $\dim(V) = n$. A *determinant function* is any function $\Delta : V^n \rightarrow \mathbb{R}$ such that:

1. Δ is a multilinear transformation; and
2. Δ is skew-symmetric with respect to all arguments. That is, given a permutation σ on $\{1, \dots, n\}$, $\Delta(\mathbf{x}_{\sigma(1)}, \dots, \mathbf{x}_{\sigma(n)}) = \epsilon_{\sigma}(\mathbf{x}_1, \dots, \mathbf{x}_n)$, where $\epsilon_{\sigma} = 1$ if σ is even, and $\epsilon_{\sigma} = -1$ if σ is odd.

We will work with $V = \mathbb{R}^n$, so V^n is the set of n -tuples of vectors in \mathbb{R}^n . If we represent the vectors as $n \times 1$ row vectors, the n -tuple of rows may be represented as an $n \times n$ matrix. In this framework the domain of a determinant function is the set of all $n \times n$ matrices. When the argument is explicitly a matrix A , we will use $\det(A)$ to denote a determinant. If we specify an additional constraint,

$$3. \Delta(\mathbf{e}_1, \dots, \mathbf{e}_n) = 1$$

where the \mathbf{e}_j are the standard Euclidean basis vectors, then the three conditions uniquely determine Δ .

Assuming the three conditions, let us proceed to construct the determinant function. If $\{\mathbf{x}_1, \dots, \mathbf{x}_n\}$ is a set of linearly dependent vectors, then $\Delta(\mathbf{x}_1, \dots, \mathbf{x}_n) = 0$. For simplicity, let \mathbf{x}_n be dependent on the other vectors in the set. That is, $\mathbf{x}_n = \sum_{i=1}^{n-1} c_i \mathbf{x}_i$ for some coefficients c_i that are not all zero; then

$$\Delta(\mathbf{x}_1, \dots, \mathbf{x}_n) = \Delta(\mathbf{x}_1, \dots, \sum_{i=1}^{n-1} c_i \mathbf{x}_i) = \sum_{i=1}^{n-1} c_i \Delta(\mathbf{x}_1, \dots, \mathbf{x}_{n-1}, \mathbf{x}_i)$$

where the last equality is a consequence of Δ being a multilinear transformation. Define $(y_1, \dots, y_i, \dots, y_n) = (\mathbf{x}_1, \dots, \mathbf{x}_i, \dots, \mathbf{x}_i)$. If σ is a transposition of i and n , then σ is odd, and by condition 2 in the definition of a determinant function:

$$\begin{aligned} \Delta(x_1, \dots, x_i, \dots, x_i) &= \Delta(y_1, \dots, y_i, \dots, y_n) \\ &= -\Delta(y_{\sigma(1)}, \dots, y_{\sigma(i)}, \dots, y_{\sigma(n)}) \\ &= -\Delta(y_1, \dots, y_n, \dots, y_i) \\ &= -\Delta(x_1, \dots, x_i, \dots, x_i) \end{aligned}$$

The only way a number can equal its negative is if that number is zero, $\Delta(x_1, \dots, x_i, \dots, x_i) = 0$. Replacing this in the summation expansion for $\Delta(x_1, \dots, x_n)$ produces $\Delta(x_1, \dots, x_n) = 0$.

Let $c \in \mathbb{R}$ and $i \neq j$. Replace the j th argument \mathbf{x}_j in the determinant function by $c\mathbf{x}_i + \mathbf{x}_j$; then

$$\Delta(x_1, \dots, x_i, \dots, cx_i + x_j, \dots, x_n) = \Delta(x_1, \dots, x_n)$$

That is, the determinant function does not change value. To see that this is true, use the linearity in component i :

$$\begin{aligned} \Delta(x_1, \dots, x_i, \dots, cx_i + x_j, \dots, x_n) &= c\Delta(x_1, \dots, x_i, \dots, x_i, \dots, x_n) \\ &\quad + \Delta(x_1, \dots, x_i, \dots, x_j, \dots, x_n) \\ &= c(0) + \Delta(x_1, \dots, x_i, \dots, x_j, \dots, x_n) \end{aligned}$$

where the zero term is obtained by the argument of the previous paragraph.

We are now ready to construct the determinant function. Let $\mathbf{e}_1, \dots, \mathbf{e}_n$ be the standard Euclidean basis vectors. Let $\mathbf{x}_i = \sum_{j=1}^n a_{ji} \mathbf{e}_j$ for $1 \leq i \leq n$. Using linearity of Δ a component at a time:

$$\begin{aligned}\Delta(x_1, \dots, x_n) &= \Delta\left(\sum_{j_1=1}^n a_{j_1 1} e_{j_1}, \sum_{j_2=1}^n a_{j_2 2} e_{j_2}, \dots, \sum_{j_n=1}^n a_{j_n 1} e_{j_n}\right) \\ &= \sum_{j_1=1}^n a_{j_1 1} \Delta\left(e_{j_1}, \sum_{j_2=1}^n a_{j_2 2} e_{j_2}, \dots, \sum_{j_n=1}^n a_{j_n 1} e_{j_n}\right) \\ &= \sum_{j_1=1}^n \sum_{j_2=1}^n a_{j_1 1} a_{j_2 2} \Delta\left(e_{j_1}, e_{j_2}, \dots, \sum_{j_n=1}^n a_{j_n 1} e_{j_n}\right) \\ &\quad \vdots \\ &= \sum_{j_1=1}^n \sum_{j_2=1}^n \cdots \sum_{j_n=1}^n a_{j_1 1} a_{j_2 2} \cdots a_{j_n n} \Delta(e_{j_1}, e_{j_2}, \dots, e_{j_n})\end{aligned}$$

If $j_u = j_v$ for some $u \neq v$, then $\Delta(\mathbf{e}_{j_1}, \dots, \mathbf{e}_{j_u}, \dots, \mathbf{e}_{j_v}, \dots, \mathbf{e}_{j_n}) = 0$ using the skew-symmetry of Δ . Therefore, in the above summations, the only nonzero terms occur when all components of the multi-index (j_1, j_2, \dots, j_n) are distinct. Each such multi-index is just a permutation of the numbers 1 through n . That is, $(j_1, j_2, \dots, j_n) = \sigma(1, \dots, n)$ for some permutation σ . Consequently,

$$\begin{aligned}\Delta(x_1, \dots, x_n) &= \sum_{\sigma} a_{\sigma(1) 1} a_{\sigma(2) 2} \cdots a_{\sigma(n) n} \Delta(e_{\sigma(1)}, e_{\sigma(2)}, \dots, e_{\sigma(n)}) \\ &= \sum_{\sigma} \epsilon_{\sigma} a_{\sigma(1) 1} a_{\sigma(2) 2} \cdots a_{\sigma(n) n}\end{aligned}$$

where the summation is over all permutations σ (there are $n!$ of them) and where we have used condition 3 in the definition of the determinant function.

EXAMPLE
7.46

Let $n = 2$. Let A be the block matrix whose first row is vector \mathbf{x}_1 and whose second row is vector \mathbf{x}_2 . There are only two permutations on $\{1, 2\}$, namely $\sigma_1(1, 2) = (1, 2)$ and $\sigma_2(1, 2) = (2, 1)$ with $\epsilon_{\sigma_1} = +1$ and $\epsilon_{\sigma_2} = -1$. The determinant of A is

$$\begin{aligned}\det(A) &= \Delta(\mathbf{x}_1, \mathbf{x}_2) \\ &= \sum_{\sigma} \epsilon_{\sigma} a_{\sigma(1) 1} a_{\sigma(2) 2} \\ &= (+1)a_{\sigma_1(1) 1} a_{\sigma_1(2) 2} + (-1)a_{\sigma_2(1) 1} a_{\sigma_2(2) 2} \\ &= a_{11}a_{22} - a_{21}a_{12}\end{aligned}$$

EXAMPLE 7.47 For $n = 3$, let A be a matrix whose rows are \mathbf{x}_1 , \mathbf{x}_2 , and \mathbf{x}_3 . There are six permutations on $\{1, 2, 3\}$, so

$$\begin{aligned}\det(A) &= \Delta(\mathbf{x}_1, \mathbf{x}_2, \mathbf{x}_3) \\ &= \sum_{\sigma} \epsilon_{\sigma} a_{\sigma(1)1} a_{\sigma(2)2} a_{\sigma(3)3} \\ &= a_{11}a_{22}a_{33} + a_{12}a_{23}a_{31} + a_{13}a_{21}a_{32} - a_{31}a_{22}a_{13} - a_{21}a_{12}a_{33} - a_{11}a_{32}a_{23}\end{aligned}$$

■

EXERCISE 7.9 Compute the formal expression for the determinant when $n = 4$.

■

We now take a closer look at the determinant function in terms of its application to matrices. Let $A = [a_{ij}]$ be an $n \times n$ matrix. Let m_{ij} be the determinant of the $(n-1) \times (n-1)$ matrix obtained from A by deleting row i and column j . The value m_{ij} is called the *minor* of a_{ij} . The *cofactor* of a_{ij} is defined by $c_{ij} = (-1)^{i+j} m_{ij}$.

EXAMPLE 7.48 Let

$$A = \begin{bmatrix} -2 & 1 & 1 \\ 0 & 1 & 1 \\ -3 & 0 & 6 \end{bmatrix}$$

The minors are

$$m_{11} = \det \begin{bmatrix} 1 & 1 \\ 0 & 6 \end{bmatrix} = 6, \quad m_{12} = \det \begin{bmatrix} 0 & 1 \\ -3 & 6 \end{bmatrix} = 3, \quad m_{13} = \det \begin{bmatrix} 0 & 1 \\ -3 & 0 \end{bmatrix} = 3$$

$$m_{21} = \det \begin{bmatrix} 1 & 1 \\ 0 & 6 \end{bmatrix} = 6, \quad m_{22} = \det \begin{bmatrix} -2 & 1 \\ -3 & 6 \end{bmatrix} = -9, \quad m_{23} = \det \begin{bmatrix} -2 & 1 \\ -3 & 0 \end{bmatrix} = 3$$

$$m_{31} = \det \begin{bmatrix} 1 & 1 \\ 1 & 1 \end{bmatrix} = 0, \quad m_{32} = \det \begin{bmatrix} -2 & 1 \\ 0 & 1 \end{bmatrix} = -2, \quad m_{33} = \det \begin{bmatrix} -2 & 1 \\ 0 & 1 \end{bmatrix} = -2$$

The matrix of minors is

$$M = [m_{ij}] = \begin{bmatrix} 6 & 3 & 3 \\ 6 & -9 & 3 \\ 0 & -2 & -2 \end{bmatrix}$$

To obtain the matrix of cofactors, the minors are multiplied by either 1 or -1 depending on whether $i + j$ is even or odd. The matrix of cofactors is

$$C = [c_{ij}] = \begin{bmatrix} +(6) & -(3) & +(3) \\ -(6) & +(-9) & -(3) \\ +(0) & -(-2) & +(-2) \end{bmatrix} = \begin{bmatrix} 6 & -3 & 3 \\ -6 & -9 & -3 \\ 0 & 2 & -2 \end{bmatrix}$$

■

The *cofactor expansion of A by row k* is $\sum_{j=1}^n a_{kj}c_{kj}$. The *cofactor expansion of A by column k* is $\sum_{i=1}^n a_{ik}c_{ik}$. For an $n \times n$ matrix, there are $2n$ such summations to compute; all summations have the same value $\det(A)$.

**EXAMPLE
7.49**

Consider the matrix,

$$A = \begin{bmatrix} -2 & 1 & 1 \\ 0 & 1 & 1 \\ -3 & 0 & 6 \end{bmatrix}$$

from the last example. Expanding by row 1:

$$\det A = a_{11}c_{11} + a_{12}c_{12} + a_{13}c_{13} = (-2)(6) + (1)(-3) + (1)(3) = -12$$

Expanding by column 2:

$$\det A = a_{12}c_{12} + a_{22}c_{22} + a_{32}c_{32} = (1)(-3) + (1)(-9) + (0)(2) = -12 \quad \blacksquare$$

**EXAMPLE
7.50**

Let us compute the determinant of the matrix:

$$A = \begin{bmatrix} -5 & 0 & 1 & 6 \\ 2 & -1 & 3 & 7 \\ 4 & 4 & -5 & -8 \\ 1 & -1 & 6 & 2 \end{bmatrix}$$

Because any cofactor expansion will produce the determinant, you should choose to expand by that row or column that contains the maximum number of zeros. In any term $a_{ij}c_{ij}$ where $a_{ij} = 0$, you do not need to compute c_{ij} . Expand by row 1:

$$\begin{aligned} \det A &= +(-5) \det \begin{bmatrix} -1 & 3 & 7 \\ 4 & -5 & -8 \\ -1 & 6 & 2 \end{bmatrix} + (1) \det \begin{bmatrix} 2 & -1 & 7 \\ 4 & 4 & -8 \\ 1 & -1 & 2 \end{bmatrix} - (6) \det \begin{bmatrix} 2 & -1 & 3 \\ 4 & 4 & -5 \\ 1 & -1 & 6 \end{bmatrix} \\ &= +(-5)(95) + (1)(-40) - (6)(43) = -773 \end{aligned} \quad \blacksquare$$

We will now compute the number of arithmetic operations it takes to evaluate the determinant of an $n \times n$ matrix by a row or column expansion. Let θ_n be the number of such operations.

- Case $n = 1$. For $A = [a]$, there are no operations required. Therefore, $\theta_1 = 0$.
- Case $n = 2$. For $A = [a_{ij}]$, expanding by row 1 produces the quantity $\det A = a_{11} \det[a_{22}] - a_{12} \det[a_{21}]$. This requires 2 multiplications and 1 addition (subtraction). Therefore, $\theta_2 = 2\theta_1 + 2 + 1 = 3$.
- Case $n = 3$. Expanding A by row 1 produces

$$\det A = a_{11} \det \begin{bmatrix} a_{22} & a_{23} \\ a_{32} & a_{33} \end{bmatrix} - a_{12} \det \begin{bmatrix} a_{21} & a_{23} \\ a_{31} & a_{33} \end{bmatrix} + a_{13} \det \begin{bmatrix} a_{21} & a_{22} \\ a_{31} & a_{32} \end{bmatrix}.$$

Each 2×2 matrix requires θ_2 operations. Additionally, there are 3 multiplications and 2 additions. Therefore, $\theta_3 = 3\theta_2 + 3 + 2 = 14$.

Inductively, the determinant of A reduces to a combination of n determinants of $(n-1) \times (n-1)$ matrices. Each of these requires θ_{n-1} operations. Additionally, there are n multiplications and $n-1$ additions. Therefore, $\theta_n = n\theta_{n-1} + 2n - 1$ operations are required. This is a first-order linear difference equation with initial data $\theta_1 = 0$ whose solution is (for $n \geq 2$):

$$\theta_n = \sum_{i=1}^{n-1} \frac{n!}{(i+1)!} (2i+1) > n!$$

This is a lot of operations, even for values of n on the order of 10.

EXERCISE
7.10

An earlier exercise had you compute the formal expression for the determinant when $n = 4$. Verify that $\theta_4 = 63$. Derive an alternate formula for $n = 4$ that uses 47 operations. ■

The determinant can be evaluated in a more reasonable amount of time by row-reducing the matrix, as we will see later. Row reductions require on the order of n^3 operations. For large n , this is much smaller than $n!$. A computer program written to evaluate determinants should avoid cofactor expansion for large n . For small n the overhead costs of Gaussian elimination may outweigh the costs of using a cofactor expansion. The best advice is to profile the function to determine when to switch between the two methods. On current hardware, cofactor expansion for $n \leq 4$ appears to be a reasonable choice.

Some properties of the determinant for a matrix A follow immediately from the definition and constructions given previously. If any row of A has all zero entries, then $\det(A) = 0$. This is a consequence of the linearity in *any* component of the determinant function. A linear transformation has the property $L(\mathbf{0}) = \mathbf{0}$. The same is true for a multilinear transformation that has a zero in any component. The proof is exactly the same used for a linear transformation.

The determinants of elementary row operations are easy to construct. A swap of two rows of A is equivalent to transposing two arguments in the determinant function. Condition 2 of the definition for a determinant function is that the function is skew-symmetric with respect to its arguments; a transposition of two arguments changes the sign of the determinant. If E is an elementary row matrix for swapping two rows, then $\det(E) = -1$. Multiplication of a row of A by a nonzero scalar c is equivalent to replacing an argument of the determinant function with a scalar times the original argument. By multilinearity, that scalar can be factored outside the function: $\Delta(\dots, c\mathbf{x}_j, \dots) = c\Delta(\dots, \mathbf{x}_j, \dots)$. If E is an elementary row matrix that represents multiplying a row by a nonzero scalar, then $\det(E) = c$. Finally, if E is the elementary row matrix to add to row j a nonzero scalar multiple of row i , then $\det(E) = 1$. We proved this earlier when we showed that replacing argument \mathbf{x}_j by $c\mathbf{x}_i + \mathbf{x}_j$ in the determinant function Δ did not change the function's value. An application of

two elementary row operations is equivalent to a composition of two linear functions of the argument of the determinant function. The last section on transformations showed us that composition of linear functions is represented by multiplication of matrices of the functions involved in the composition. Therefore, if E_1 and E_2 are two elementary row matrices, then

$$\det(E_1 E_2) = \det(E_1) \det(E_2)$$

That is, the determinant of a product is the product of the determinants.

Forward plus backward elimination of the $n \times n$ matrix A reduces that matrix to an upper echelon matrix U that either is the identity I or is a matrix with at least one row of zeros. The determinant of the identity is 1, just a restatement of condition 3 in the definition for the determinant function. If U has a row of zeros, then $\det(U) = 0$, as proved earlier. Therefore, $\det(U)$ is 0 or 1. If E_1 through E_m are the elementary row matrices used in the elimination, then

$$E_m \cdots E_1 A = U$$

The determinant of a product was shown to be the product of the determinants, so

$$\det(E_m) \cdots \det(E_1) \det(A) = \det(U)$$

Because elementary row matrices all have nonzero determinants,

$$\det(A) = \frac{\det(U)}{\det(E_m) \cdots \det(E_1)} \quad (7.39)$$

The full elimination can be done with the order of n^3 operations, clearly asymptotically better than cofactor expansion that uses the order of $n!$ operations. Actually, we need only apply forward elimination. The backward elimination is not necessary. For an invertible matrix A , after forward elimination, the matrix U is upper triangular. The determinant of such a matrix is just the product of its diagonal entries.

EXERCISE

7.11

Prove that the determinant of an upper triangular matrix is the product of its diagonal entries. ■

EXERCISE

7.12

For an invertible matrix A , prove that $\det(A^{-1}) = 1/\det(A)$. ■

7.5.2 EIGENVALUES AND EIGENVECTORS

Eigenvalues and eigenvectors represent a topic vital to the study of difference and differential equations and to the analysis of the stability of mathematical models that describe physical phenomena. It is also a topic that many shy away from, but please do not since you need it later!

Although we have been working with vector spaces \mathbb{R}^n , the initial discussion here will involve the vector space of n -tuples of complex numbers, \mathbb{C}^n , whose scalar field is

itself the set of complex numbers. Let A be an $n \times n$ matrix of complex-valued entries. The scalar $\lambda \in \mathbb{C}$ is said to be an *eigenvalue* of A if there is a nonzero vector \mathbf{x} such that $A\mathbf{x} = \lambda\mathbf{x}$. In this case, \mathbf{x} is said to be an *eigenvector corresponding to λ* . Geometrically, an eigenvector is a vector that when transformed does not change direction. If $\lambda \neq 1$, the length changes, but if $\lambda = 1$, the eigenvector changes neither direction nor length.

EXAMPLE
7.51

The number -1 is an eigenvalue for

$$A = \begin{bmatrix} -1 & 0 & 0 \\ 1 & 1 & 0 \\ 0 & 1 & 1 \end{bmatrix}$$

with a corresponding eigenvector $\mathbf{x} = (-4, 2, -1)$ (written as a 3-tuple). To verify this,

$$A\mathbf{x} = \begin{bmatrix} -1 & 0 & 0 \\ 1 & 1 & 0 \\ 0 & 1 & 1 \end{bmatrix} \begin{bmatrix} -4 \\ 2 \\ -1 \end{bmatrix} = \begin{bmatrix} 4 \\ -2 \\ 1 \end{bmatrix} = (-1) \begin{bmatrix} -4 \\ 2 \\ -1 \end{bmatrix}$$

■

Let λ be an eigenvalue of the $n \times n$ matrix A . The *eigenspace of λ* is the set

$$S_\lambda = \{\mathbf{x} \in \mathbb{C}^n : A\mathbf{x} = \lambda\mathbf{x}\}$$

This set is a subspace of \mathbb{C}^n . The proof is simple. Let $c \in \mathbb{C}$ and let $\mathbf{x}, \mathbf{y} \in S_\lambda$. By definition of S_λ , $A\mathbf{x} = \lambda\mathbf{x}$ and $A\mathbf{y} = \lambda\mathbf{y}$. Applying A to the linear combination,

$$A(c\mathbf{x} + \mathbf{y}) = cA\mathbf{x} + A\mathbf{y} = c\lambda\mathbf{x} + \lambda\mathbf{y} = \lambda(c\mathbf{x} + \mathbf{y})$$

This shows that $c\mathbf{x} + \mathbf{y} \in S_\lambda$, so S_λ is a subspace. An alternate proof is to note that $S_\lambda = \text{kernel}(A - \lambda I)$. We had proved earlier that the kernel of a matrix is a subspace.

The method of construction of eigenvalues λ and eigenvectors \mathbf{x} is as follows. Observe that

$$A\mathbf{x} = \lambda\mathbf{x} \Leftrightarrow A\mathbf{x} = \lambda I\mathbf{x} \Leftrightarrow A\mathbf{x} - \lambda I\mathbf{x} = 0 \Leftrightarrow (A - \lambda I)\mathbf{x} = \mathbf{0}$$

We want *nonzero* solutions \mathbf{x} to this homogeneous system of equations. The only way this can happen is if $(A - \lambda I)$ is *not* invertible. For if it were invertible, then $\mathbf{x} = (A - \lambda I)^{-1}\mathbf{0} = \mathbf{0}$ is the only possible solution. An equivalent condition for $(A - \lambda I)$ not to be invertible is that $p(\lambda) = \det(A - \lambda I) = 0$. This determinant is a polynomial in λ of degree n since A is $n \times n$. The eigenvalues are therefore roots of the polynomial equation $p(\lambda) = 0$. The equation $\det(A - \lambda I) = 0$ is called the *characteristic equation* for the matrix A .

The fundamental theorem of algebra states that every polynomial of degree n with complex coefficients can be factored as

$$p(\lambda) = \prod_{i=1}^k (\lambda - \lambda_i)^{m_i}$$

where λ_i , $1 \leq i \leq k$, are the distinct roots of the equation $p(\lambda) = 0$ and where $\sum_{i=1}^k m_i = n$. For each root λ_i , solve the system $(A - \lambda_i I)\mathbf{x} = \mathbf{0}$ to find the corresponding eigenvectors.

EXAMPLE
7.52

Find the eigenvalues and corresponding eigenspaces for

$$A = \begin{bmatrix} -2 & 0 \\ 1 & 4 \end{bmatrix}.$$

Solve $\det(A - \lambda I) = 0$:

$$0 = \det(A - \lambda I) = \det \begin{bmatrix} -2 - \lambda & 0 \\ 1 & 4 - \lambda \end{bmatrix} = (-2 - \lambda)(4 - \lambda).$$

The eigenvalues are the roots $\lambda = -2, 4$. For each eigenvalue solve the system $(A - \lambda I)\mathbf{x} = \mathbf{0}$. Start with $\lambda = -2$ and solve $(A + 2I)\mathbf{x} = \mathbf{0}$:

$$A + 2I = \begin{bmatrix} 0 & 0 \\ 1 & 6 \end{bmatrix} \sim \begin{bmatrix} 1 & 6 \\ 0 & 0 \end{bmatrix}$$

If $\mathbf{x} = (x_1, x_2)$, then x_1 is basic and x_2 is free with $x_1 + 6x_2 = 0$. Therefore, $\mathbf{x} = x_2(-6, 1)$ and $S_{-2} = \text{Span}[(-6, 1)]$. Now select $\lambda = 4$ and solve $(A - 4I)\mathbf{x} = \mathbf{0}$:

$$A - 4I = \begin{bmatrix} -6 & 0 \\ 1 & 0 \end{bmatrix} \sim \begin{bmatrix} 1 & 0 \\ 0 & 0 \end{bmatrix}$$

If $\mathbf{x} = (x_1, x_2)$, then x_1 is basic and x_2 is free with $x_1 = 0$. Therefore, $\mathbf{x} = x_2(0, 1)$ and $S_4 = \text{Span}[(0, 1)]$. ■

EXAMPLE
7.53

Find the eigenvalues and corresponding eigenspaces for

$$A = \begin{bmatrix} 1 & -1 & 4 \\ 3 & 2 & -1 \\ 2 & 1 & -1 \end{bmatrix}$$

Solve $\det(A - \lambda I) = 0$:

$$\begin{aligned} 0 &= \det(A - \lambda I) = \begin{bmatrix} 1 - \lambda & -1 & 4 \\ 3 & 2 - \lambda & -1 \\ 2 & 1 & -1 - \lambda \end{bmatrix} \\ &= +(1 - \lambda) \det \begin{bmatrix} 2 - \lambda & -1 \\ 1 & -1 - \lambda \end{bmatrix} - (-1) \det \begin{bmatrix} 3 & -1 \\ 2 & -1 - \lambda \end{bmatrix} + (4) \det \begin{bmatrix} 3 & 2 - \lambda \\ 2 & 1 \end{bmatrix} \\ &= (1 - \lambda)[(2 - \lambda)(-1 - \lambda) + 1] + [3(-1 - \lambda) + 2] + 4[3 - 2(2 - \lambda)] \\ &= -\lambda^3 + 2\lambda^2 + 5\lambda - 6 \\ &= -(\lambda + 2)(\lambda - 1)(\lambda - 3) \end{aligned}$$

(Example 7.53
continued)

The eigenvalues are the roots $\lambda = -2, 1, 3$. For each eigenvalue, solve the system $(A - \lambda I)\mathbf{x} = \mathbf{0}$. For $\lambda = -2$, solve $(A + 2I)\mathbf{x} = \mathbf{0}$:

$$A + 2I = \begin{bmatrix} 3 & -1 & 4 \\ 3 & 4 & -1 \\ 2 & 1 & 1 \end{bmatrix} \sim \begin{bmatrix} 1 & 0 & 1 \\ 0 & 1 & -1 \\ 0 & 0 & 0 \end{bmatrix}$$

where the row operations are $-R_3 + R_1 \rightarrow R_1$, $-3R_1 + R_2 \rightarrow R_2$, $-2R_1 + R_3 \rightarrow R_3$, $\frac{1}{10}R_2 \rightarrow R_2$, $-5R_2 + R_3 \rightarrow R_3$, and $2R_2 + R_1 \rightarrow R_1$. If $\mathbf{x} = (x_1, x_2, x_3)$, then the only free variable is x_3 , so $S_{-2} = \text{Span}((-1, 1, 1))$.

For $\lambda = 1$, solve $(A - I)\mathbf{x} = \mathbf{0}$:

$$A - I = \begin{bmatrix} 0 & -1 & 4 \\ 3 & 1 & -1 \\ 2 & 1 & -2 \end{bmatrix} \sim \begin{bmatrix} 1 & 0 & 1 \\ 0 & 1 & -4 \\ 0 & 0 & 0 \end{bmatrix}$$

where the row operations are $-R_3 + R_2 \rightarrow R_2$, $R_1 \leftrightarrow R_2$, $-2R_1 + R_3 \rightarrow R_3$, $R_2 + R_3 \rightarrow R_3$, and $-R_2 \rightarrow R_2$. If $\mathbf{x} = (x_1, x_2, x_3)$, then the only free variable is x_3 , so $S_1 = \text{Span}((-1, 4, 1))$.

For $\lambda = 3$ solve $(A - 3I)\mathbf{x} = \mathbf{0}$:

$$A - 3I = \begin{bmatrix} -2 & -1 & 4 \\ 3 & -1 & -1 \\ 2 & 1 & -4 \end{bmatrix} \sim \begin{bmatrix} 1 & 0 & -1 \\ 0 & 1 & -2 \\ 0 & 0 & 0 \end{bmatrix}$$

where the row operations are $R_1 + R_2 \rightarrow R_2$, $R_1 + R_3 \rightarrow R_3$, $R_1 \leftrightarrow R_2$, $2R_1 + R_2 \rightarrow R_2$, $-\frac{1}{5}R_2 \rightarrow R_2$, and $2R_2 + R_1 \rightarrow R_1$. If $\mathbf{x} = (x_1, x_2, x_3)$, then the only free variable is x_3 , so $S_3 = \text{Span}((1, 2, 1))$. ■

EXAMPLE 7.54

This next example shows that the dimension of the eigenspace can be larger than one. Let

$$A = \begin{bmatrix} 1 & -1 & 2 \\ 0 & 1 & 0 \\ 0 & 0 & 1 \end{bmatrix}$$

Solve $\det(A - \lambda I) = 0$:

$$\det(A - \lambda I) = \det \begin{bmatrix} 1 - \lambda & -1 & 2 \\ 0 & 1 - \lambda & 0 \\ 0 & 0 & 1 - \lambda \end{bmatrix} = (1 - \lambda)^3$$

so $\lambda = 1$ is the only eigenvalue. Solve $(A - I)\mathbf{x} = \mathbf{0}$:

$$A - I = \begin{bmatrix} 0 & -1 & 2 \\ 0 & 0 & 0 \\ 0 & 0 & 0 \end{bmatrix} \sim \begin{bmatrix} 0 & 1 & -2 \\ 0 & 0 & 0 \\ 0 & 0 & 0 \end{bmatrix}$$

If $\mathbf{x} = (x_1, x_2, x_3)$, then x_1 and x_3 are free variables with $x_2 - 2x_3 = 0$. Thus, $\mathbf{x} = x_1(1, 0, 0) + x_3(0, 2, 1)$ and $S_1 = \text{Span}((1, 0, 0), (0, 2, 1))$. ■

Suppose that A is an $n \times n$ matrix with real-valued entries. If λ is an eigenvalue of A that has a nonzero imaginary part and has corresponding eigenvector \mathbf{x} , then $\bar{\lambda}$, the complex conjugate of λ , is also an eigenvalue of A and has corresponding eigenvector $\bar{\mathbf{x}}$, the componentwise complex conjugate of vector \mathbf{x} . Define the complex conjugate of a matrix $A = [a_{ij}]$ by $\bar{A} = [\bar{a}_{ij}]$; then the following sequence of steps is valid:

$$A\mathbf{x} = \lambda\mathbf{x}, \overline{A\mathbf{x}} = \overline{\lambda}\bar{\mathbf{x}}, \bar{A}\bar{\mathbf{x}} = \bar{\lambda}\bar{\mathbf{x}}, A\bar{\mathbf{x}} = \bar{\lambda}\bar{\mathbf{x}}$$

where we have used $\bar{A} = A$ since A has only real-valued entries. The last statement indicates that $\bar{\lambda}$ is an eigenvalue of A with a corresponding eigenvector $\bar{\mathbf{x}}$.

EXAMPLE
7.55

Let

$$A = \begin{bmatrix} \cos \theta & -\sin \theta \\ \sin \theta & \cos \theta \end{bmatrix}$$

where θ is not an integer multiple of π . This matrix represents rotation of vectors in the plane by θ radians (counterclockwise rotation when $\theta > 0$). An intuitive argument is that there should be no real-valued eigenvalues since any vector must have its direction changed by the rotation. The algebraic construction is to solve $\det(A - \lambda I) = 0$:

$$\det(A - \lambda I) = \begin{bmatrix} \cos \theta - \lambda & -\sin \theta \\ \sin \theta & \cos \theta - \lambda \end{bmatrix} = (\cos \theta - \lambda)^2 + \sin^2 \theta = 0$$

so the eigenvalues are $\lambda = \cos \theta \pm i \sin \theta$. For $\lambda = \cos \theta + i \sin \theta$, solve $(A - \lambda I)\mathbf{x} = \mathbf{0}$:

$$A - \lambda I = \sin \theta \begin{bmatrix} -i & -1 \\ 1 & -i \end{bmatrix} \sim \sin \theta \begin{bmatrix} 1 & -i \\ 0 & 0 \end{bmatrix}$$

If $\mathbf{x} = (x_1, x_2)$, then x_2 is the free parameter with $x_1 - ix_2 = 0$. Therefore, $\mathbf{x} = x_2(i, 1)$ and $S_\lambda = \text{Span}[(i, 1)] \subset \mathbb{C}^2$. The other eigenvalue is the complex conjugate $\bar{\lambda} = \cos \theta - i \sin \theta$. The eigenvectors are $\bar{\mathbf{x}} = x_2(-i, 1)$ and the eigenspace is $S_{\bar{\lambda}} = \text{Span}[(-i, 1)]$. ■

Let A be an $n \times n$ matrix with n linearly independent eigenvectors $\mathbf{x}_1, \dots, \mathbf{x}_n$. If $\lambda_1, \dots, \lambda_n$ are the corresponding eigenvalues, not necessarily distinct, and if $S = [\mathbf{x}_1 \cdots \mathbf{x}_n]$, then $P^{-1}AP = \text{Diag}(\lambda_1, \dots, \lambda_n) =: D$. The proof is as follows:

$$\begin{aligned} AP &= A[x_1 | \cdots | x_n] && \text{Definition of } S \\ &= [Ax_1 | \cdots | Ax_n] && \text{Distributive property of block multiplication} \\ &= [\lambda_1 x_1 | \cdots | \lambda_n x_n] && \text{Since } \lambda_i \text{ are eigenvalues} \\ &= [x_1 | \cdots | x_n] \text{Diag}(\lambda_1, \dots, \lambda_n) \\ &= PD \end{aligned}$$

Since the columns of P are the linearly independent eigenvectors of A , P must be invertible; thus, $AP = PD$ implies $P^{-1}AP = D$. For example, we had

$$A = \begin{bmatrix} -2 & 0 \\ 1 & 4 \end{bmatrix}, \lambda_1 = -2, S_{-2} = \text{Span}[(-6, 1)], \lambda_2 = 4, S_4 = \text{Span}[(0, 1)]$$

Therefore,

$$P = \begin{bmatrix} -6 & 0 \\ 1 & 1 \end{bmatrix} \text{ and } P^{-1}AP = \text{Diag}(-2, 4)$$

Recall from the section on linear transformations that the condition $P^{-1}AP = D$ means that A and D are similar matrices. Not all $n \times n$ matrices have n linearly independent eigenvectors. However, it might still be possible to find a similarity transformation $P^{-1}AP = D$ where D is diagonal. If so, A is said to be *diagonalizable*.

A specific instance where A is diagonalizable is when it has n distinct eigenvalues λ_1 through λ_n . Let \mathbf{x}_1 through \mathbf{x}_n be corresponding eigenvectors. This set of eigenvectors is linearly independent. The proof of this fact is by mathematical induction. The first case is $n = 2$. Let $c_1\mathbf{x}_1 + c_2\mathbf{x}_2 = \mathbf{0}$. Multiply by A to obtain

$$\mathbf{0} = A(c_1\mathbf{x}_1 + c_2\mathbf{x}_2) = c_1A\mathbf{x}_1 + c_2A\mathbf{x}_2 = c_1\lambda_1\mathbf{x}_1 + c_2\lambda_2\mathbf{x}_2$$

Replace $c_2\mathbf{x}_2 = -c_1\mathbf{x}_1$ in this equation and group terms to obtain

$$c_1(\lambda_1 - \lambda_2)\mathbf{x}_1 = \mathbf{0}$$

where $\mathbf{x}_1 \neq \mathbf{0}$ since it is an eigenvector and $\lambda_1 \neq \lambda_2$ by assumption, so $c_1 = 0$. Replacing in the original equation yields $c_2\mathbf{x}_2 = \mathbf{0}$. Again, $\mathbf{x}_2 \neq \mathbf{0}$ because it is an eigenvector, so it must be that $c_2 = 0$. Therefore, \mathbf{x}_1 and \mathbf{x}_2 are linearly independent.

The inductive hypothesis is that \mathbf{x}_1 through \mathbf{x}_k are linearly independent. We need to use this to show that \mathbf{x}_1 through \mathbf{x}_{k+1} are linearly independent. Let $c_1\mathbf{x}_1 + \cdots + c_{k+1}\mathbf{x}_{k+1} = \mathbf{0}$. Multiply by A to obtain

$$\begin{aligned} 0 &= A(c_1\mathbf{x}_1 + \cdots + c_{k+1}\mathbf{x}_{k+1}) = c_1A\mathbf{x}_1 + \cdots + c_{k+1}A\mathbf{x}_{k+1} \\ &= c_1\lambda_1\mathbf{x}_1 + \cdots + c_{k+1}\lambda_{k+1}\mathbf{x}_{k+1} \end{aligned}$$

Replace $c_{k+1}\mathbf{x}_{k+1} = -c_1\mathbf{x}_1 - \cdots - c_k\mathbf{x}_k$ in this equation and group terms to obtain

$$c_1(\lambda_1 - \lambda_{k+1})\mathbf{x}_1 + \cdots + c_k(\lambda_k - \lambda_{k+1})\mathbf{x}_k = \mathbf{0}$$

By the inductive hypothesis, the k vectors in the linear combination are linearly independent, so all the coefficients must be zero: $c_i(\lambda_i - \lambda_{k+1}) = 0$. The eigenvalues are distinct, so $\lambda_i \neq \lambda_{k+1}$ for $1 \leq i \leq k$, thus forcing $c_i = 0$ for $1 \leq i \leq k$. Replacing in the original equation yields $c_{k+1}\mathbf{x}_{k+1} = \mathbf{0}$. And, again, $\mathbf{x}_{k+1} \neq \mathbf{0}$ since it is an eigenvector, so it must be that $c_{k+1} = 0$. Therefore, the vectors \mathbf{x}_1 through \mathbf{x}_{k+1} are

linearly independent. The result is true for all $n \geq 2$ by the principle of mathematical induction.

Generally, two similar matrices A and B have the same characteristic polynomial, so their eigenvalues are identical. Because the matrices are similar, $B = P^{-1}AP$ for some invertible matrix P . The characteristic polynomial of B , $\det(B - \lambda I) = 0$ can be manipulated as

$$\begin{aligned} 0 &= \det(B - \lambda I) \\ &= \det(P^{-1}AP - \lambda P^{-1}IP) \\ &= \det(P^{-1}(A - \lambda I)P) \\ &= \det(P^{-1}) \det(A - \lambda I) \det(P) \\ &= \det(A - \lambda I) \end{aligned}$$

because $\det(P^{-1}) \det(P) = \det(P^{-1}P) = \det(I) = 1$. Although the eigenvalues are the same for A and B , the corresponding eigenvectors are not necessarily the same, but are related. Define $\mathbf{y} = P^{-1}\mathbf{x}$ where $A\mathbf{x} = \lambda\mathbf{x}$. Multiplying the eigensystem by P^{-1} and replacing $\mathbf{x} = P\mathbf{y}$ leads to

$$B\mathbf{y} = P^{-1}AP\mathbf{y} = \lambda P^{-1}P\mathbf{y} = \lambda\mathbf{y}$$

The vector $\mathbf{y} = P^{-1}\mathbf{x}$ is an eigenvector for B corresponding to λ whenever \mathbf{x} is an eigenvector for A with respect to the same eigenvalue.

7.5.3 EIGENDECOMPOSITION FOR SYMMETRIC MATRICES

A special class of matrices that arises most frequently in applications, especially physics applications, is the class of $n \times n$ *symmetric matrices* with real-valued entries. A symmetric matrix A satisfies the condition that $A^T = A$. Within the class of symmetric matrices are subclasses of importance.

- If $\mathbf{x}^T A \mathbf{x} > 0$ for all $\mathbf{x} \neq \mathbf{0}$, then A is said to be *positive definite*.
- If $\mathbf{x}^T A \mathbf{x} \geq 0$ for all $\mathbf{x} \neq \mathbf{0}$, then A is said to be *positive semidefinite* or *nonnegative definite*.
- If $\mathbf{x}^T A \mathbf{x} < 0$ for all $\mathbf{x} \neq \mathbf{0}$, then A is said to be *negative definite*.
- If $\mathbf{x}^T A \mathbf{x} \leq 0$ for all $\mathbf{x} \neq \mathbf{0}$, then A is said to be *negative semidefinite* or *nonpositive definite*.

The eigenvalues of a real-valued symmetric matrix must themselves be real-valued, and the corresponding eigenvectors are naturally real-valued. If A were to

have a possibly complex-valued eigenvector \mathbf{x} , then $\bar{\mathbf{x}}^T A \mathbf{x}$ must be real-valued. To see this:

$$\begin{aligned}
\bar{\mathbf{x}}^T A \mathbf{x} &= \sum_{i,j} \bar{x}_i a_{ij} x_j \\
&= \sum_{i=j} \bar{x}_i a_{ij} x_j + \sum_{i < j} \bar{x}_i a_{ij} x_j + \sum_{i > j} \bar{x}_i a_{ij} x_j \\
&= \sum_i a_{ii} |x_i|^2 + \sum_{i < j} \bar{x}_i a_{ij} x_j + \sum_{j > i} \bar{x}_j a_{ji} x_i && \text{Interchange names on } i \text{ and } j \\
&= \sum_i a_{ii} |x_i|^2 + \sum_{i < j} \bar{x}_i a_{ij} x_j + \sum_{i < j} x_i a_{ij} \bar{x}_j && \text{Since } A \text{ is symmetric} \\
&= \sum_i a_{ii} |x_i|^2 + \sum_{i < j} (\bar{x}_i a_{ij} x_j + x_i a_{ij} \bar{x}_j) \\
&= \sum_i a_{ii} |x_i|^2 + \sum_{i < j} 2\operatorname{Re}(\bar{x}_i a_{ij} x_j) && \operatorname{Re}(z) \text{ denotes the real part of } z
\end{aligned}$$

The right-hand side of the last equality is a real number, so $\bar{\mathbf{x}}^T A \mathbf{x}$ is real-valued. Also, $\bar{\mathbf{x}}^T \mathbf{x} = |\mathbf{x}|^2$, another real number. Since \mathbf{x} is an eigenvector, $A \mathbf{x} = \lambda \mathbf{x}$, where λ is the corresponding eigenvalue. Thus, $\bar{\mathbf{x}}^T A \mathbf{x} = \lambda \bar{\mathbf{x}}^T \mathbf{x}$ and

$$\lambda = \frac{\bar{\mathbf{x}}^T A \mathbf{x}}{\bar{\mathbf{x}}^T \mathbf{x}}$$

The right-hand side is the ratio of real numbers, so it must be real-valued itself. That is, the eigenvalue λ must be real. Moreover, since the eigenvalues are real, the nonzero solutions to $(A - \lambda I)\mathbf{x} = \mathbf{0}$ must be real-valued.

Another interesting result for a real-valued symmetric matrix: If λ_1 and λ_2 are distinct eigenvalues for A , then corresponding eigenvectors \mathbf{x}_1 and \mathbf{x}_2 are orthogonal. The proof is straightforward:

$$\begin{aligned}
\lambda_1 \mathbf{x}_1^T \mathbf{x}_2 &= (\lambda_1 \mathbf{x}_1)^T \mathbf{x}_2 \\
&= (A \mathbf{x}_1)^T \mathbf{x}_2 && \mathbf{x}_1 \text{ is an eigenvector for } \lambda_1 \\
&= \mathbf{x}_1^T A^T \mathbf{x}_2 \\
&= \mathbf{x}_1^T A \mathbf{x}_2 && A \text{ is symmetric} \\
&= \mathbf{x}_1^T (\lambda_2 \mathbf{x}_2) && \text{Since } \mathbf{x}_2 \text{ is an eigenvector for } \lambda_2 \\
&= \lambda_2 \mathbf{x}_1^T \mathbf{x}_2
\end{aligned}$$

But then $(\lambda_1 - \lambda_2) \mathbf{x}_1^T \mathbf{x}_2 = 0$ and $\lambda_1 \neq \lambda_2$ imply that $\mathbf{x}_1^T \mathbf{x}_2 = 0$. That is, \mathbf{x}_1 and \mathbf{x}_2 are orthogonal.

We are now in a position to characterize the eigenvectors for a real-valued symmetric matrix A . The construction makes use of a more general result that applies to square matrices. If A is a square matrix, there always exists an orthogonal matrix Q such that $Q^T A Q = U$, where U is an upper triangular matrix. The diagonal entries of

U are necessarily the eigenvalues of A . The proof is as follows. Let λ_1 be an eigenvalue for A . There is at least one linearly independent eigenvector \mathbf{y}_1 corresponding to it. Let $\mathbf{x}_1 = \mathbf{y}_1 / |\mathbf{y}_1|$ such that \mathbf{x}_1 is a unit-length eigenvector. Define the matrix,

$$Q_1 = [\mathbf{x}_1 | \mathbf{z}_2 | \cdots | \mathbf{z}_n]$$

where $\{\mathbf{z}_2, \dots, \mathbf{z}_n\}$ is an orthonormal basis for the orthogonal complement of $\text{Span}[\mathbf{x}_1]$. The matrix Q_1 is orthogonal by construction and

$$Q_1^T A Q_1 = \left[\begin{array}{c|cccc} \lambda_1 & * & \cdots & * \\ \hline 0 & * & \cdots & * \\ \vdots & \vdots & & \vdots \\ 0 & * & \cdots & * \end{array} \right]$$

The process is recursively applied to the lower right-hand corner submatrix to obtain an orthogonal matrix P_2 such that

$$Q_2 = \left[\begin{array}{c|c} 1 & 0 \\ \hline 0 & P_2 \end{array} \right] \text{ and } Q_2^T (Q_1^T A Q_1) Q_2 = \left[\begin{array}{cc|cccc} \lambda_1 & * & * & \cdots & * \\ 0 & \lambda_2 & * & \cdots & * \\ 0 & 0 & * & \cdots & * \\ \vdots & \vdots & \vdots & & \vdots \\ 0 & 0 & * & \cdots & * \end{array} \right]$$

At the last step of the reduction, we have $Q = \prod_{i=1}^n Q_i$ and $Q^T A Q = U$, where U is upper triangular and its diagonal entries are the eigenvalues of A .

The primary consequence of this result is that if A is symmetric and $Q^T A Q = U$, where Q is orthogonal and U is upper triangular, then in fact U must be a diagonal matrix. This follows from $U^T = (Q^T A Q)^T = Q^T A^T (Q^T)^T = Q^T A Q = U$, which forces U to be symmetric. The only upper triangular symmetric matrices are the diagonal matrices. The diagonal entries of U are the eigenvalues of A and the columns of Q are the corresponding eigenvectors. This means that an $n \times n$ real-valued symmetric matrix always has n linearly independent eigenvectors.

Finally, an important classification for the “definite” matrices: The symmetric matrix A is (positive, nonnegative, negative, nonpositive) definite if and only if its eigenvalues are (positive, nonnegative, negative, nonpositive). Let us prove this for the case of positive definite matrices. The other cases are similar.

- (\Rightarrow): Let A be positive definite. Let λ be an eigenvalue for A with corresponding eigenvector \mathbf{x} ; then $A\mathbf{x} = \lambda\mathbf{x}$, $\mathbf{x}^T A \mathbf{x} = \mathbf{x}^T (\lambda\mathbf{x}) = \lambda \mathbf{x}^T \mathbf{x}$, and so $\lambda = (\mathbf{x}^T A \mathbf{x}) / (\mathbf{x}^T \mathbf{x})$. But A is positive definite, so $\mathbf{x}^T A \mathbf{x} > 0$. Moreover, $\mathbf{x}^T \mathbf{x}$ is the squared length of \mathbf{x} , so it is positive. Thus, $\lambda = (\mathbf{x}^T A \mathbf{x}) / (\mathbf{x}^T \mathbf{x}) > 0$. The argument works for every eigenvalue of A .
- (\Leftarrow): Let λ be an eigenvalue for A and assume that $\lambda > 0$. Then as in the first part, $0 < \lambda = (\mathbf{x}^T A \mathbf{x}) / (\mathbf{x}^T \mathbf{x})$, where \mathbf{x} is a corresponding eigenvector. Therefore, $\mathbf{x}^T A \mathbf{x} > 0$ for every eigenvector of A . Since A is symmetric, it must have a set

of linearly independent eigenvectors $\mathbf{x}_1, \dots, \mathbf{x}_n$ given by the columns of Q in the decomposition. Let $\mathbf{x} = a_1\mathbf{x}_1 + \cdots + a_n\mathbf{x}_n \neq \mathbf{0}$; then

$$\begin{aligned}\mathbf{x}^T A \mathbf{x} &= \left(\sum_{i=1}^n a_i \mathbf{x}_i \right)^T A \left(\sum_{j=1}^n a_j \mathbf{x}_j \right) \\ &= \left(\sum_{i=1}^n a_i \mathbf{x}_i^T \right) \left(\sum_{j=1}^n a_j \mathbf{x}_j \right) \\ &= \left(\sum_{i=1}^n a_i \mathbf{x}_i^T \right) \left(\sum_{j=1}^n \lambda_j a_j \mathbf{x}_i \right) \\ &= \sum_{i,j} \lambda_j a_i a_j \mathbf{x}_i^T \mathbf{x}_j \\ &= \sum_i \lambda_i a_i^2 \quad \mathbf{x}_i \text{ are orthonormal} \\ &> 0 \quad \text{since } \lambda_i > 0 \text{ and } \mathbf{x} \neq \mathbf{0}\end{aligned}$$

Similar arguments apply to negative, nonpositive, or nonnegative definite matrices.

The eigenvalues of a symmetric matrix can be calculated directly by solving the characteristic equation $\det(A - \lambda I) = 0$; however, for large n , root finding in this manner is typically ill conditioned. A better approach reduces A to a tridiagonal matrix T via a finite sequence of similarity transformations by orthogonal matrices (i.e., Householder reduction) followed by an iterative reduction to a diagonal matrix using the QR algorithm. In the second phase, the reductions involve more similarity transformations by orthogonal matrices. In the end, $A = RDR^{-1}$, where D is a diagonal matrix whose diagonal entries are the eigenvalues of A , and R is an orthogonal matrix whose columns are the corresponding linearly independent eigenvectors, ordered according to the eigenvalue ordering on the diagonal of D .

7.5.4 S + N DECOMPOSITION

Given a square matrix A , we are going to show that it may be decomposed into a sum $A = S + N$, where S is diagonalizable (the S comes from *semisimple*, a term that is synonymous with diagonalizable) and N is *nilpotent*, a matrix for which $N^p = 0$ for some $p > 0$, but $N^i \neq 0$ for $0 < i < p$, and $SN = NS$. The decomposition allows us to efficiently compute powers A^k that arise in solving linear difference equations and to compute the exponential e^A (a formal power series $e^A = \sum_{k=0}^{\infty} A^k / k!$) that arise in solving linear differential equations. Both types of equations occur in physics applications.

Let V be an n -dimensional vector space. Let V_1, \dots, V_r be subspaces of V . V is said to be the *direct sum* of the V_i if every $\mathbf{x} \in V$ can be written uniquely as $\mathbf{x} = \sum_{i=1}^r \mathbf{x}_i$, where $\mathbf{x}_i \in V_i$. The notation for indicating that V is the direct sum of the subspaces is

$$V = V_1 \oplus \cdots \oplus V_r = \bigoplus_{i=1}^r V_i$$

We have already seen this concept in the section introducing orthogonal subspaces. If U is an m -dimensional subspace of \mathbb{R}^n and U^\perp is its $(n-m)$ -dimensional orthogonal complement, we proved that $\mathbb{R}^n = U \oplus U^\perp$ by constructing a basis of vectors, the first m in U and the last $n-m$ in U^\perp . A special case comes from the fundamental theorem of linear algebra. If A is an $n \times m$ matrix, then $\mathbb{R}^m = \text{kernel}(A) \oplus \text{range}(A^T)$ and $\mathbb{R}^m = \text{kernel}(A^T) \oplus \text{range}(A)$. Let's look at a last example. Let $\{\mathbf{f}_1, \dots, \mathbf{f}_n\}$ be a basis for \mathbb{R}^n ; then $\mathbb{R}^n = \bigoplus_{i=1}^n \text{Span}[\mathbf{f}_i]$ since every vector in \mathbb{R}^n can be written uniquely as a linear combination of basis vectors.

Linear transformations can be decomposed in a manner similar to the vector space. Let $L : V \rightarrow V$ be a linear transformation. Let $L_i : V_i \rightarrow V_i$ for $1 \leq i \leq r$ be linear transformations. Define $L(V_i) = \{L(\mathbf{x}) : \mathbf{x} \in V_i\}$. L is said to be the *direct sum* of the L_i if

1. $V = \bigoplus_{i=1}^r V_i$ (V is the direct sum of the V_i);
2. $L(V_i) \subseteq V_i$ for all i (V_i is *invariant* under L); and
3. $L(\mathbf{x}) = L_i(\mathbf{x})$ for $\mathbf{x} \in V_i$ (L restricted to the set V_i is just the transformation L_i).

The notation for indicating L is a direct sum of the transformations is

$$L = L_1 \oplus \cdots \oplus L_r = \bigoplus_{i=1}^r L_i$$

A direct sum of transformations is applied as follows:

$$L(\mathbf{x}) = \left(\bigoplus_{i=1}^r L_i \right) \left(\sum_{i=1}^r \mathbf{x}_i \right) = \sum_{i=1}^r L_i(\mathbf{x}_i)$$

If L_i is represented by the matrix A_i with respect to the basis β_i for V_i , then the union of the bases $\beta = \bigcup_{i=1}^r \beta_i$ is a basis for V and the diagonal block matrix $A = \text{Diag}(A_1, \dots, A_r)$ represents L with respect to β .

EXAMPLE
7.56

Let $V = \mathbb{R}^2$ and $L(x_1, x_2) = (-2x_1, x_1 + 4x_2)$. The matrix that represents L with respect to basis $B_1 = \{(1, 0), (0, 1)\}$ is

$$M = \begin{bmatrix} -2 & 0 \\ 1 & 4 \end{bmatrix}$$

(Example 7.56
continued)

Another basis for V is $B_2 = \{\mathbf{v}_1, \mathbf{v}_2\}$, where $\mathbf{v}_1 = (-6, 1)$ and $\mathbf{v}_2 = (0, 1)$. Note that \mathbf{v}_1 is an eigenvector of M corresponding to the eigenvalue $\lambda_1 = -2$ and \mathbf{v}_2 is an eigenvector of A corresponding to the eigenvalue $\lambda_2 = 4$. Let $V_i = \text{Span}[\mathbf{v}_i]$ for each i , so $\mathbb{R}^2 = \text{Span}[\mathbf{v}_1] \oplus \text{Span}[\mathbf{v}_2]$, a direct sum of the eigenspaces of M .

Define $L_1 : V_1 \rightarrow V_1$ by $L_1(\alpha \mathbf{v}_1) = -2\alpha \mathbf{v}_1$. Since V_1 is 1-dimensional, we can think of L_1 as $L_1(\alpha) = -2\alpha$. Its matrix of representation is $A_1 = [-2]$. Similarly, define $L_2 : V_2 \rightarrow V_2$ by $L_2(\beta \mathbf{v}_2) = 4\beta \mathbf{v}_2$. As a one-dimensional transformation, $L_2(\beta) = 4\beta$ and the matrix representation is $A_2 = [4]$. Observe that

$$\begin{aligned} L(\alpha(-6, 1)) &= \alpha L(-6, 1) = \alpha(12, -2) = -2\alpha(-6, 1) = L_1(\alpha(-6, 1)) \\ L(\beta(0, 1)) &= \beta L(0, 1) = \beta(0, 4) = 4\beta(0, 1) = L_2(\beta(0, 1)) \end{aligned}$$

Consequently, L is the direct sum $L = L_1 \oplus L_2$. The matrix representing L with respect to the basis B_2 is

$$A = \text{Diag}(A_1, A_2) = \begin{bmatrix} -2 & 0 \\ 0 & 4 \end{bmatrix}$$

The intent of the example is to show that the behavior of L is determined by its behavior on certain special subspaces. In this particular case, the subspaces are 1-dimensional eigenspaces and L acts like the classic linear function $f(x) = ax$ on each eigenspace. In some cases it is possible to have eigenspaces of dimension larger than 1, but the vector space V is a direct sum of eigenspaces. The representation of L as a direct sum of transformations on the eigenspaces is constructed in a manner similar to the example. In other cases, though, V is not a direct sum of eigenspaces, but it is a direct sum of *generalized eigenspaces*.

Since a change of basis is a similarity transformation between two matrix representations of a linear transformation $L : V \rightarrow V$, the characteristic polynomials of the matrix representations are the same (we proved this earlier), call it

$$p(\lambda) = \prod_{k=1}^r (\lambda - \lambda_k)^{n_k}$$

where $\dim(V) = \sum_{k=1}^r n_k$ and where the λ_k are the distinct roots of the polynomial. This allows us to refer to eigenvalues λ_k of L rather than having to explicitly associate the eigenvalues with a specific matrix A that represents L . Similarly, we will refer to the eigenspace of λ_k as the set $\text{kernel}(L - \lambda_k I)$ without reference to a specific matrix A since $L - \lambda_k I$ is itself a linear transformation with a kernel and a range. The *generalized eigenspace of L corresponding to λ_k* is the set

$$E_k = \text{kernel}(L - \lambda_k I)^{n_k}$$

The sets E_k are invariant subspaces of L ; that is, $L(E_k) \subseteq E_k$. To see this, select $\mathbf{y} \in L(E_k)$; then $\mathbf{y} = L(\mathbf{x})$ for some $\mathbf{x} \in E_k$. Also,

$$\begin{aligned}
 (L - \lambda_k I)^{n_k}(\mathbf{y}) &= (L - \lambda_k I)^{n_k}(L(\mathbf{x})) \\
 &= ((L - \lambda_k I)^{n_k} \circ L)(\mathbf{x}) && \text{Definition of composition} \\
 &= (L \circ (L - \lambda_k I)^{n_k})(\mathbf{x}) && L \text{ Commutes with itself} \\
 &= L(L - \lambda_k I)^{n_k}(\mathbf{x})) && \text{Definition of composition} \\
 &= L(\mathbf{0}) && \text{Since } \mathbf{x} \in E_k \\
 &= \mathbf{0} && L \text{ is a linear transformation}
 \end{aligned}$$

Thus, $\mathbf{y} \in E_k$ and so $L(E_k) \subseteq E_k$.

The main result is now stated, without proof. Let $L : V \rightarrow V$ be a linear transformation. The vector space is a direct sum of the generalized eigenspaces, $V = \bigoplus_{k=1}^r E_k$, where E_k is the generalized eigenspace of L with respect to eigenvalue λ_k . The proof involves showing that (1) E_k has a basis of n_k vectors and (2) eigenvectors corresponding to distinct eigenvalues are linearly independent. If L_k is the restriction of L to E_k , a consequence of the direct sum decomposition and the result $L(E_k) \subseteq E_k$ (proved in the last paragraph) is that L can be decomposed as $L = \bigoplus_{k=1}^r L_k$.

The most important consequence of the direct sum decomposition is that there are transformations S and N such that $L = S + N$ (a sum of transformations), any matrix representation of S is a diagonalizable matrix, any matrix representation of N is a nilpotent matrix, and the order of composition of S and N is irrelevant: $SN = NS$. To prove this, let us look at the special case when there is a single eigenvalue λ_1 . The characteristic polynomial is $p(\lambda) = (\lambda - \lambda_1)^n$. The generalized eigenspace is $E = \text{kernel}(L - \lambda_1 I)^n$. Define $S = \lambda_1 I$ and $N = L - \lambda_1 I$. Clearly $S \circ N = N \circ S$ since the identity transformation commutes with any transformation. $E = \text{kernel}(N^n)$ implies $N^n = 0$ since the only transformation which maps everything to 0 is the zero transformation.

Let L_k be the restriction of L to E_k . Each L_k has characteristic polynomial $(\lambda - \lambda_k)_k^n$ (just the special case mentioned in the previous paragraph) so $L_k = S_k + N_k$, where $S_k = \lambda_k I$ and $N_k = L_k - \lambda_k I$ are defined on E_k with $S_k N_k = N_k S_k$. Define $S = \bigoplus_{k=1}^r S_k$ and $N = \bigoplus_{k=1}^r N_k$. First,

$$\begin{aligned}
 L &= \bigoplus_{k=1}^r L_k \\
 &= \bigoplus_{k=1}^r (S_k + N_k) \\
 &= \bigoplus_{k=1}^r S_k + \bigoplus_{k=1}^r N_k \\
 &= S + N
 \end{aligned}$$

so $L = S + N$ as claimed. Second,

$$\begin{aligned} SN &= \left(\bigoplus_{k=1}^r S_k \right) \left(\bigoplus_{k=1}^r N_k \right) \\ &= \bigoplus_{k=1}^r S_k N_k \\ &= \bigoplus_{k=1}^r N_k S_k \\ &= \left(\bigoplus_{k=1}^r N_k \right) \left(\bigoplus_{k=1}^r S_k \right) \\ &= NS \end{aligned}$$

so $SN = NS$ as claimed.

EXAMPLE
7.57

Let $L : \mathbb{R}^3 \rightarrow \mathbb{R}^3$ be defined by $L(x_1, x_2, x_3) = (x_1 - x_2 + 2x_3, x_2, x_3)$. The matrix representing L with respect to the Euclidean basis is

$$A = \begin{bmatrix} 1 & -1 & 2 \\ 0 & 1 & 0 \\ 0 & 0 & 1 \end{bmatrix}$$

The characteristic polynomial is $p(\lambda) = -(\lambda - 1)^3$, so

$$S = \lambda I = I, \quad N = A - I = \begin{bmatrix} 0 & -1 & 2 \\ 0 & 0 & 0 \\ 0 & 0 & 0 \end{bmatrix}$$

Note that $N^2 = 0$, so N is nilpotent. Clearly S is diagonalizable since it is already diagonal. \blacksquare

EXAMPLE
7.58

Let $L : \mathbb{R}^3 \rightarrow \mathbb{R}^3$ be defined by $L(x_1, x_2, x_3) = (-x_1 + x_2 - 2x_3, -x_2 + 4x_3, x_3)$. The matrix representing L with respect to the Euclidean basis is

$$A = \begin{bmatrix} -1 & 1 & -2 \\ 0 & -1 & 4 \\ 0 & 0 & 1 \end{bmatrix}$$

The characteristic polynomial is $p(\lambda) = -(\lambda + 1)^2(\lambda - 1)$. The generalized eigenspaces are $E_1 = \ker(A + I)^2$ and $E_2 = \ker(A - I)$. To construct these, row-reduce:

$$(A + I)^2 = \begin{bmatrix} 0 & 0 & 0 \\ 0 & 0 & 8 \\ 0 & 0 & 4 \end{bmatrix} \sim \begin{bmatrix} 0 & 0 & 1 \\ 0 & 0 & 0 \\ 0 & 0 & 0 \end{bmatrix}$$

so that $E_1 = \text{Span}[(1, 0, 0), (0, 1, 0)]$. Also,

$$A - I = \begin{bmatrix} -2 & 1 & -2 \\ 0 & -2 & 4 \\ 0 & 0 & 0 \end{bmatrix} \sim \begin{bmatrix} 1 & 0 & 0 \\ 0 & 1 & -2 \\ 0 & 0 & 0 \end{bmatrix}$$

so that $E_2 = \text{Span}[(0, 2, 1)]$.

Restrict L to E_1 :

$$\begin{aligned} L(\alpha(1, 0, 0) + \beta(0, 1, 0)) &= \alpha L(1, 0, 0) + \beta L(0, 1, 0) \\ &= \alpha(-1, 0, 0) + \beta(1, -1, 0) \\ &= (\beta - \alpha)(1, 0, 0) + (-\beta)(0, 1, 0) \end{aligned}$$

Therefore, $L_1(\alpha, \beta) = (\beta - \alpha, -\beta)$. Similarly, restrict L to E_2 :

$$\begin{aligned} L(\gamma(0, 2, 1)) &= \gamma L(0, 2, 1) \\ &= \gamma(0, 2, 1) \end{aligned}$$

so $L_2(\gamma) = \gamma$.

The matrix representing L_1 with respect to the basis $\{(1, 0, 0), (0, 1, 0)\}$ is

$$A_1 = [L_1(1, 0) \mid L_1(0, 1)] = \begin{bmatrix} -1 & 1 \\ 0 & -1 \end{bmatrix}$$

and the matrix representing L_2 with respect to the basis $\{(0, 2, 1)\}$ is

$$A_2 = [L_2(1)] = [1]$$

We can write $A_1 = S_1 + N_1$, where

$$S_1 = \begin{bmatrix} -1 & 0 \\ 0 & -1 \end{bmatrix}, \quad N_1 = \begin{bmatrix} 0 & 1 \\ 0 & 0 \end{bmatrix}$$

and $A_2 = S_2 + N_2$, where

$$S_2 = [1], \quad N_2 = [0]$$

Therefore, $L = L_1 \oplus L_2$ is represented by

$$B = \text{Diag}(A_1, A_2) = \left[\begin{array}{cc|c} -1 & 1 & 0 \\ 0 & -1 & 0 \\ \hline 0 & 0 & 1 \end{array} \right] = \left[\begin{array}{cc|c} -1 & 0 & 0 \\ 0 & -1 & 0 \\ \hline 0 & 0 & 1 \end{array} \right] + \left[\begin{array}{cc|c} 0 & 1 & 0 \\ 0 & 0 & 0 \\ \hline 0 & 0 & 0 \end{array} \right] = S + N$$

The original matrix A and this matrix B are similar, $B = P^{-1}AP$. The columns of the matrix P consist of the generalized eigenvectors

$$P = \begin{bmatrix} 1 & 0 & 0 \\ 0 & 1 & 2 \\ 0 & 0 & 1 \end{bmatrix}, \quad P^{-1} = \begin{bmatrix} 1 & 0 & 0 \\ 0 & 1 & -2 \\ 0 & 0 & 1 \end{bmatrix}$$

(Example 7.58
continued)

The decomposition is not necessarily unique. For example, we could choose $E_1 = \text{Span}[(1, 1, 0), (1, -1, 0)]$; then

$$\begin{aligned} L(\alpha(1, 1, 0) + \beta(1, -1, 0)) &= \alpha(0, -1, 0) + \beta(-2, 1, 0) \\ &= -\left(\frac{\alpha + \beta}{2}\right)(1, 1, 0) + \frac{\alpha - 3\beta}{2}(1, -1, 0) \end{aligned}$$

and

$$L_1(\alpha, \beta) = \left(-\frac{\alpha + \beta}{2}, \frac{\alpha - 3\beta}{2}\right)$$

The matrix representing L_1 with respect to this new basis is

$$A_1 = \begin{bmatrix} -\frac{1}{2} & -\frac{1}{2} \\ \frac{1}{2} & -\frac{3}{2} \end{bmatrix} = \begin{bmatrix} -1 & 0 \\ 0 & -1 \end{bmatrix} + \begin{bmatrix} \frac{1}{2} & -\frac{1}{2} \\ \frac{1}{2} & \frac{1}{2} \end{bmatrix} = S_1 + N_1$$

Finally,

$$B = \text{Diag}(A_1, A_2) = S + N = \left[\begin{array}{cc|c} -1 & 0 & 0 \\ 0 & -1 & 0 \\ \hline 0 & 0 & 1 \end{array} \right] + \left[\begin{array}{cc|c} \frac{1}{2} & -\frac{1}{2} & 0 \\ \frac{1}{2} & -\frac{1}{2} & 0 \\ \hline 0 & 0 & 0 \end{array} \right]$$

■

7.5.5 APPLICATIONS

Three applications of interest regarding eigendecomposition are computing the powers of a matrix, computing the exponential of a matrix, and constructing the local extrema of multivariate functions. We discuss each application in this section.

Powers of a Matrix

The decomposition of a matrix $A = S + N$ where S is diagonalizable, N is nilpotent with $N^p = 0$ and $N^i \neq 0$ for $i < p$, and $SN = NS$ allows us to efficiently evaluate powers A^j for $j \geq 2$. Because $SN = NS$, the binomial expansion formula applies to $(S + N)^j$. That is,

$$A^j = (S + N)^j = \sum_{k=0}^j \binom{j}{k} S^{j-k} N^k = \sum_{k=0}^{\min(j,p-1)} \binom{j}{k} S^{j-k} N^k \quad (7.40)$$

The last equality follows because $N^k = 0$ for $k \geq p$. Since S is diagonalizable, $S = PDP^{-1}$ for some diagonal matrix D . The powers on S are efficiently computed as $S^{j-k} = (PDP^{-1})^{j-k} = PD^{j-k}P^{-1}$.

Let us do an operation count to see why the right-hand side of equation (7.40) is a more efficient way of computing A^j than the obvious iterative product. We will do this in general for an $n \times n$ matrix. Let Θ_j denote the number of operations needed to compute A^j in the usual manner. The product A^2 requires n multiplications and $n - 1$ additions per entry. The matrix has n^2 entries, so the total operations is given by $\Theta_2 = n^2(2n - 1)$. For $j > 2$, $A^j = A \cdot A^{j-1}$, so each additional multiplication requires $n^2(2n - 1)$ operations. The total count is $\Theta_j = (j - 1)n^2(2n - 1)$ for $j \geq 2$.

Define Φ_j to be the number of operations needed to compute A^j using the $S + N$ decomposition. The simplest case is when A is already diagonalizable, $A = PDP^{-1}$, so that $N = 0$. The powers are $A^j = PD^jP^{-1}$. The product DP^{-1} requires n^2 multiplications. Once computed and cached, the next product is $D^2P^{-1} = D(DP^{-1})$, which takes an additional n^2 multiplications. Once D^jP^{-1} is computed in this manner, the last multiplication on the left by P requires $n^2(2n - 1)$ operations. The total count is $\Phi_j = jn^2 + n^2(2n - 1)$. It is the case that $\Phi_j \geq \Theta_j$ when $j \geq 1 + (2n - 1)/(2n - 2)$.

When $N \neq 0$, the operation count increases as the power of nilpotency, p , becomes large. Consider the case when $N \neq 0$, but $N^2 = 0$; then

$$A^j = S^j + jS^{j-1}N = PD^jP^{-1} + jPD^{j-1}P^{-1}N = PD^{j-1}(DP^{-1} + jP^{-1}N)$$

PD^{j-1} requires $(j - 1)n^2$ multiplications; DP^{-1} requires n^2 multiplications; $P^{-1}N$ requires $n^2(2n - 1)$ operations; the product $j(P^{-1}N)$ requires an additional n^2 multiplications; the sum $(DP^{-1}) + (jP^{-1}N)$ requires n^2 additions; and finally $(PD^{j-1})(DP^{-1} + jP^{-1}N)$ uses $n^2(2n - 1)$ operations. The total count is $\Phi_j = (j - 1)n^2 + 2n^2(2n + 1)$. It is the case that $\Phi_j \geq \Theta_j$ when $j \geq 1 + (2n + 1)/(2n - 2)$. The break-even point for j occurs when $N^2 = 0$ is larger than in the case $N = 0$.

As it turns out, the power of nilpotency p is bounded by the matrix size, $p < n$. Even though A^j might be more cheaply computed for small j using the obvious multiplication, as j becomes large the $S + N$ decomposition will be cheaper.

Exponential of a Matrix

A system of ordinary differential equations with constant coefficients is of the form

$$\frac{d\mathbf{x}}{dt} = A\mathbf{x}, \quad t \geq 0, \quad \mathbf{x}(0) = \mathbf{x}_0$$

where A is an $n \times n$ matrix of constants and \mathbf{x}_0 is a specified initial condition. As we will see, the solution is

$$\mathbf{x}(t) = e^{tA}\mathbf{x}_0, \quad t \geq 0$$

where e^{tA} is the power series for the function $f(x) = e^x$ formally evaluated with the matrix argument tA . Recall that

$$e^x = \sum_{k=0}^{\infty} \frac{x^k}{k!}$$

is a power series that converges for any real-valued x . Although not proved here, the formal series

$$e^{tA} = \sum_{k=0}^{\infty} \frac{t^k}{k!} A^k$$

also converges for any real-valued matrix A . We could use the $A = S + N$ decomposition to calculate A^k for each k , but we can actually do better. The exponential of a matrix happens to satisfy the condition $e^{A+B} = e^A e^B$ whenever $AB = BA$. However, do not make the mistake of using this formula when $AB \neq BA$; the formula is not true in these cases. Using $A = S + N$, the fact that $SN = NS$, and the exponential identity,

$$e^{tA} = e^{t(S+N)} = e^{tS+tN} = e^{tS} e^{tN}$$

The right-hand side requires evaluating the power series for e^x twice. The power series for e^{tS} is simplified by using the fact that S is diagonalizable, $S = PDP^{-1}$. The series is

$$\begin{aligned} e^{tS} &= \sum_{k=0}^{\infty} \frac{t^k}{k!} S^k \\ &= \sum_{k=0}^{\infty} \frac{t^k}{k!} (PDP^{-1})^k \\ &= \sum_{k=0}^{\infty} \frac{t^k}{k!} PD^k P^{-1} \\ &= P \left(\sum_{k=0}^{\infty} \frac{t^k}{k!} D^k \right) P^{-1} \\ &= Pe^{tD} P^{-1} \end{aligned}$$

The diagonal matrix is $D = \text{Diag}(d_1, \dots, d_n)$ and the exponential of tD is

$$e^{tD} = e^{\text{Diag}(td_1, \dots, td_n)} = \text{Diag}(e^{td_1}, \dots, e^{td_n})$$

The power series for e^{tN} is actually a finite sum since $N^p = 0$ for some positive power p . That is,

$$e^{tN} = \sum_{k=0}^{\infty} \frac{t^k}{k!} N^k = \sum_{k=0}^{p-1} \frac{t^k}{k!} N^k$$

In summary, the exponential of A is

$$e^{tA} = P \text{Diag}(e^{td_1}, \dots, e^{td_n}) P^{-1} \sum_{k=0}^{p-1} \frac{t^k}{k!} N^k \quad (7.41)$$

Local Extrema of Multivariate Functions

Let $y = f(x)$ for $x \in \mathbb{R}$, where f is twice differentiable for all x . The *critical points* for f are those points x_0 such that $f'(x_0) = 0$. At such a point, three possibilities occur for the function as illustrated in Figure 7.27.

In studying calculus you discussed the concept of *Taylor polynomials*. If f is twice differentiable at x_0 , then for x near x_0 ,

$$f(x) = f(x_0) + \frac{f'(x_0)}{1!}(x - x_0) + \frac{f''(x_0)}{2!}(x - x_0)^2 + R(x, x_0)$$

where R is a remainder term such that

$$\lim_{x \rightarrow x_0} \frac{R(x, x_0)}{(x - x_0)^2}$$

Suppose that $f'(x_0) = 0$; then

$$f(x) = f(x_0) + \frac{1}{2}(x - x_0)^2 \left[f''(x_0) + 2\frac{R(x, x_0)}{(x - x_0)^2} \right]$$

where

$$\lim_{x \rightarrow x_0} \left[f''(x_0) + 2\frac{R(x, x_0)}{(x - x_0)^2} \right] = f''(x_0)$$

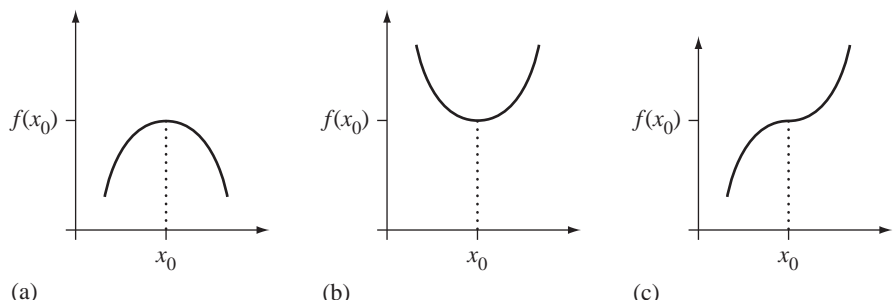


Figure 7.27 Three graphs showing critical points. (a) $f(x_0)$ is a local maximum. (b) $f(x_0)$ is a local minimum. (c) $(x_0, f(x_0))$ is a point of inflection for the graph of f .

Consequently,

$$\operatorname{sign} \left[f''(x_0) + 2 \frac{R(x, x_0)}{(x - x_0)^2} \right] = \operatorname{sign} f''(x_0)$$

for x sufficiently close to x_0 , where

$$\operatorname{sign}(x) = \begin{cases} 1, & x > 0 \\ 0, & x = 0 \\ -1, & x < 0 \end{cases}$$

From the above we can develop the *second derivative test*: If $f'(x_0) = 0$, then

1. $f(x_0)$ is a local maximum if $f''(x_0) < 0$
2. $f(x_0)$ is a local minimum if $f''(x_0) > 0$
3. No conclusion can be made if $f''(x_0) = 0$. A more detailed analysis is required to understand the behavior of the graph of f at $(x_0, f(x_0))$.

The idea is that for x near x_0 , $f''(x_0) > 0$ implies that $f''(x_0) + 2R(x, x_0)/(x - x_0)^2 > 0$, so $f(x) \geq f(x_0)$ for x near x_0 . A similar argument holds if $f''(x_0) < 0$ [$f(x) \leq f(x_0)$ for x near x_0].

The concept of Taylor polynomials can be generalized to functions $w = f(\mathbf{x})$, where $\mathbf{x} \in \mathbb{R}^n$. We will look at the case $n = 2$. A function $f(x_1, x_2)$ is *differentiable at* (x_1, x_2) if the partial first derivatives,

$$f_{x_1}(x_1, x_2) = \frac{\partial f(x_1, x_2)}{\partial x_1} \text{ and } f_{x_2}(x_1, x_2) = \frac{\partial f(x_1, x_2)}{\partial x_2}$$

exist. Similarly, $f(x_1, x_2)$ is *twice differentiable at* (x_1, x_2) if the partial second derivatives,

$$f_{x_1 x_1} = \frac{\partial^2 f}{\partial x_1^2}, \quad f_{x_1 x_2} = \frac{\partial^2 f}{\partial x_2 \partial x_1}, \quad f_{x_2 x_1} = \frac{\partial^2 f}{\partial x_1 \partial x_2}, \quad \text{and} \quad f_{x_2 x_2} = \frac{\partial^2 f}{\partial x_2^2}$$

exist.

Let $\mathbf{x} = (x_1, x_2)$ and $\mathbf{x}_0 = (a, b)$. If $f(\mathbf{x})$ is twice differentiable at \mathbf{x}_0 , then

$$f(\mathbf{x}) = f(\mathbf{x}_0) + Df(\mathbf{x}_0)(\mathbf{x} - \mathbf{x}_0) + \frac{D^2 f(\mathbf{x}_0)}{2!} (\mathbf{x} - \mathbf{x}_0)^2 + R(\mathbf{x}, \mathbf{x}_0)$$

where the implied operations are defined by

1. $Df(\mathbf{x}) = \nabla f(\mathbf{x}) = (f_{x_1}(x_1, x_2), f_{x_2}(x_1, x_2))$ (the gradient of f)
2. $Df(\mathbf{x})\mathbf{y} = \mathbf{y}^T \nabla f(\mathbf{x}) = \sum_{i=1}^2 f_{x_i} y_i$
3. $D^2 f(\mathbf{x}) = [f_{x_i x_j}] = \begin{bmatrix} f_{x_1 x_1} & f_{x_1 x_2} \\ f_{x_2 x_1} & f_{x_2 x_2} \end{bmatrix}$
4. $D^2 f(\mathbf{x})\mathbf{y}\mathbf{z} = \mathbf{y}^T D^2 f(\mathbf{x})\mathbf{z} = \sum_{i=1}^2 \sum_{j=1}^2 f_{x_i x_j} y_i z_j$

Generally,

$$D^n f(\mathbf{x}) \mathbf{y}^n = \sum_{i_1=1}^2 \cdots \sum_{i_n=1}^2 f_{x_{i_1} \cdots x_{i_n}} y_{i_1} \cdots y_{i_n}$$

The quantity $R(\mathbf{x}, \mathbf{x}_0)$ in the above Taylor polynomial expansion has the property

$$\lim_{\mathbf{x} \rightarrow \mathbf{x}_0} \frac{R(\mathbf{x}, \mathbf{x}_0)}{|\mathbf{x} - \mathbf{x}_0|^2} = 0$$

The second derivative test is the following. If $Df(\mathbf{x}_0) = \mathbf{0}$, then

1. $f(\mathbf{x}_0)$ is a local maximum if $D^2 f(\mathbf{x}_0)(\mathbf{x} - \mathbf{x}_0)^2 < 0$ for all \mathbf{x} near \mathbf{x}_0
2. $f(\mathbf{x}_0)$ is a local minimum if $D^2 f(\mathbf{x}_0)(\mathbf{x} - \mathbf{x}_0)^2 > 0$ for all \mathbf{x} near \mathbf{x}_0
3. No conclusion can be made otherwise without more information.

Using our results about the characterization of definite matrices, the second derivative test may be rephrased as follows. If $Df(\mathbf{x}_0) = \mathbf{0}$, then

1. $f(\mathbf{x}_0)$ is a local maximum if $D^2 f(\mathbf{x}_0)$ is negative definite;
2. $f(\mathbf{x}_0)$ is a local minimum if $D^2 f(\mathbf{x}_0)$ is positive definite;
3. No conclusion can be made if $D^2 f(\mathbf{x}_0)$ is neither positive definite nor negative definite. A more detailed analysis is required to understand the behavior of the graph of f at $(\mathbf{x}_0, f(\mathbf{x}_0))$.

Figure 7.28 shows a graph of f for various possibilities.

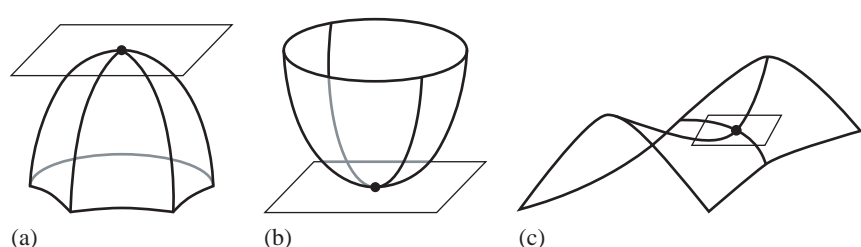


Figure 7.28 Three graphs showing critical points. (a) $f(\mathbf{x}_0)$ is a local maximum. (b) $f(\mathbf{x}_0)$ is a local minimum. (c) $(\mathbf{x}_0, f(\mathbf{x}_0))$ is a saddle point on the graph of f . The tangent planes at the graph points are shown in all three figures.

EXAMPLE
7.59

Consider $f(x_1, x_2) = x_1^4 + 4x_1^2x_2 + x_1^2 + 5x_2^2 - 2x_1x_2$; then

$$Df(x_1, x_2) = (4x_1^3 + 8x_1x_2 + 2x_1 - 2x_2, 4x_1^2 + 10x_2 - 2x_1)$$

and

$$D^2f(x_1, x_2) = \begin{bmatrix} 12x_1^2 + 8x_2 + 2 & 8x_1 - 2 \\ 8x_1 - 2 & 10 \end{bmatrix}$$

Solve $Df = (0, 0)$:

$$4x_1^3 + 8x_1x_2 + 2x_1 - 2x_2 = 0$$

$$4x_1^2 + 10x_2 - 2x_1 = 0$$

The second equation implies $x_2 = \frac{x_1 - 2x_1^2}{5}$. Replacing in the first equation yields $0 = \frac{4}{5}x_1(x_1 + 1)(x_1 + 2)$. The critical points are $(0, 0)$, $(-1, -3/5)$, and $(-2, -2)$.

- Case 1: $(0, 0)$

$$D^2f(0, 0) = \begin{bmatrix} 2 & -2 \\ -2 & 10 \end{bmatrix}$$

$$\det(D^2f(0, 0) - \lambda I) = \lambda^2 - 12\lambda + 16 = 0$$

so the eigenvalues are $\lambda \doteq 1.53, 0.76$. Thus, $D^2f(0, 0)$ is positive definite and $f(0, 0) = 0$ is a local minimum.

- Case 2: $(-1, -3/5)$

$$D^2f(-1, -3/5) = \begin{bmatrix} \frac{46}{5} & -10 \\ -10 & 10 \end{bmatrix}$$

$$\det(D^2f(-1, -3/5) - \lambda I) = \lambda^2 - \frac{96}{5}\lambda - 8 = 0$$

so the eigenvalues are $\lambda \doteq 19.61, -0.41$. The second derivative test gives no conclusions. Actually, the function has a *saddle point* at $(-1, -3/5)$.

- Case 3: $(-2, -2)$

$$D^2f(-2, -2) = \begin{bmatrix} 34 & -18 \\ -18 & 10 \end{bmatrix}$$

$$\det(D^2f(-2, -2) - \lambda I) = \lambda^2 - 44\lambda + 16 = 0$$

so the eigenvalues are $\lambda \doteq 43.63, 0.37$. Thus, $D^2f(-2, -2)$ is positive definite and $f(-2, -2) = 0$ is a local minimum.

Note that $f(x_1, x_2) = (x_1 - x_2)^2 + (x_1^2 + 2x_2)^2$, so 0 is the absolute minimum for the function. ■

AFFINE ALGEBRA

8.1 INTRODUCTION

As we saw earlier, linear algebra is the study of vectors and vector spaces. In two dimensions, a vector was treated as a quantity with direction and magnitude. It does not matter where you place the vector in the plane; it represents the same vector (see Figure 7.4) since the directions and magnitudes are the same. In physics applications, among others, the location of the vector, that is, where its initial point is, may very well be significant. For example, if a particle has a certain velocity at a given instant, the velocity vector necessarily applies to the *position* of the particle at that instant. Similarly, the same force applied to two different positions on a rod have different effects on the rod. The *point* of application of the force is relevant.

Clearly, there needs to be a distinction between *points* and *vectors*. This is the essence of *affine algebra*. Let V be a vector space of dimension n . Let A be a set of elements that are called *points*. A is referred to as an n -dimensional *affine space* whenever the following conditions are met:

1. For each ordered pair of points $\mathcal{P}, \mathcal{Q} \in A$, there is a unique vector in V called the *difference vector* and denoted by $\Delta(\mathcal{P}, \mathcal{Q})$.
2. For each point $\mathcal{P} \in A$ and $\mathbf{v} \in V$, there is a unique point $\mathcal{Q} \in A$ such that $\mathbf{v} = \Delta(\mathcal{P}, \mathcal{Q})$.
3. For any three points $\mathcal{P}, \mathcal{Q}, \mathcal{R} \in A$, it must be that $\Delta(\mathcal{P}, \mathcal{Q}) + \Delta(\mathcal{Q}, \mathcal{R}) = \Delta(\mathcal{P}, \mathcal{R})$.

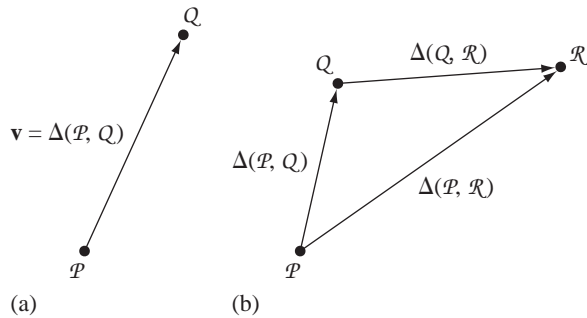


Figure 8.1 (a) A vector v connecting two points P and Q . (b) The sum of vectors, each vector determined by two points.

Figure 8.1 illustrates these three items.

If P and Q are specified, v is uniquely determined (item 1). If P and v are specified, Q is uniquely determined (item 2). [Figure 8.1\(b\)](#) illustrates item 3.

The formal definition for an affine space introduced the difference vector $\Delta(P, Q)$. [Figure 8.1](#) gives you the geometric intuition about the difference, specifically that it appears to be a subtraction operation for two points. However, certain consequences of the definition may be proved directly without having a concrete formulation for an actual subtraction of points.

A few consequences of the definition for an affine algebra follow.

1. $\Delta(P, P) = \mathbf{0}$
2. $\Delta(Q, P) = -\Delta(P, Q)$
3. If $\Delta(P_1, Q_1) = \Delta(P_2, Q_2)$, then $\Delta(P_1, P_2) = \Delta(Q_1, Q_2)$

The first consequence follows immediately from item 3 in the definition where Q is replaced by P , $\Delta(P, P) + \Delta(P, P) = \Delta(P, P)$. The vector $\Delta(P, P)$ is subtracted from both sides to obtain $\Delta(P, P) = \mathbf{0}$.

The second consequence also follows from item 3 in the definition where R is replaced by P , $\Delta(P, Q) + \Delta(Q, P) = \Delta(P, P) = \mathbf{0}$. The last equality is what we just proved in the previous paragraph. The first vector is subtracted from both sides to obtain $\Delta(Q, P) = -\Delta(P, Q)$.

The third consequence is called the *parallelogram law*. [Figure 8.2](#) illustrates. Item 3 in the definition can be applied in two ways:

$$\Delta(P_1, P_2) + \Delta(P_2, Q_2) = \Delta(P_1, Q_2) \text{ and } \Delta(P_1, Q_1) + \Delta(Q_1, Q_2) = \Delta(P_1, Q_2)$$

Subtracting these leads to

$$\mathbf{0} = \Delta(P_1, P_2) + \Delta(P_2, Q_2) - \Delta(P_1, Q_1) - \Delta(Q_1, Q_2) = \Delta(P_1, P_2) - \Delta(Q_1, Q_2)$$

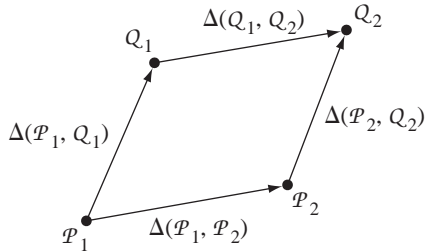


Figure 8.2 The parallelogram law for affine algebra.

where the last equality is valid since we assumed $\Delta(\mathcal{P}_1, \mathcal{Q}_1) = \Delta(\mathcal{P}_2, \mathcal{Q}_2)$. Therefore, $\Delta(\mathcal{P}_1, \mathcal{P}_2) = \Delta(\mathcal{Q}_1, \mathcal{Q}_2)$.

In the formal sense of affine algebra, points and vectors are distinct entities. We have already used two different fonts to help distinguish between them: \mathcal{P} is a point, \mathbf{v} is a vector. Even so, the following example shows how powerful the formal setting is. Given a vector space V , the points may be defined as the elements of V themselves, namely $A = V$. If \mathcal{P} and \mathcal{Q} are points, the corresponding vectors are labeled \mathbf{p} and \mathbf{q} . Think of the vectors geometrically as $\mathcal{P} - \mathcal{O}$ and $\mathcal{Q} - \mathcal{O}$, respectively, where \mathcal{O} is the origin. The difference vector of the points is $\Delta(\mathcal{P}, \mathcal{Q}) = \mathbf{q} - \mathbf{p}$, a subtraction of the two vectors. The three items in the definition for affine space can be easily verified. The example also shows that you must be steadfast in maintaining that points and vectors are different abstract quantities, even if you happen to represent them in a computer program in the same way, say as n -tuples of numbers.

Any further discussion of affine spaces in the abstract will continue to use the notation $\Delta(\mathcal{P}, \mathcal{Q})$ for the vector difference of two points. However, in situations that have a computational flavor, we will instead use the more intuitive notation $\mathcal{Q} - \mathcal{P}$ with the warning that the subtraction operator is a convenient notation that is not necessarily indicative of the actual mechanism used to compute the vector difference of two points in a particular application. We also use the suggestive notation $\mathcal{Q} = \mathcal{P} + \mathbf{v}$ when $\mathbf{v} = \Delta(\mathcal{P}, \mathcal{Q})$.

To avoid inadvertent confusion between points and vectors in a computer implementation, separate data structures for points and vectors are recommended. For example, in C++ you can define the vector class by

```
template class <T real, int n> Vector
{
public:
    // construction
    Vector ();
    Vector (const real tuple[n]);
    Vector (const Vector& v);
```

```

// tuple access as an array
operator const real* () const;
operator real* ();
real operator[] (int i) const;
real& operator[] (int i);

// assignment and comparison
Vector& operator= (const Vector& v);
bool operator== (const Vector& v) const;
bool operator!= (const Vector& v) const;

// arithmetic operations
Vector operator+ (const Vector& v) const;
Vector operator- (const Vector& v) const;
Vector operator* (real scalar) const;
Vector operator/ (real scalar) const;
Vector operator- () const;
friend Vector operator* (real scalar, const Vector& v);

private:
    real m_tuple[n];
};

```

where `real` allows you to support both `float` and `double` and where `n` is the dimension of the underlying vector space. The point class is defined by

```

template class <T real, int n> Point
{
public:
    // construction
    Point ();
    Point (const real tuple[n]);
    Point (const Point& p);

    // tuple access as an array
    operator const real* () const;
    operator real* ();
    real operator[] (int i) const;
    real& operator[] (int i);

    // assignment and comparison
    Point& operator= (const Point& p);
    bool operator== (const Point& p) const;
    bool operator!= (const Point& p) const;

    // arithmetic operations
    Point operator+ (const Vector& v) const;

```

```

Vector operator- (const Point& p) const;

private:
    real m_tuple[n];
};

```

Of course, these are just the basic operations, but other members can be added as needed for your applications.

8.2 COORDINATE SYSTEMS

Let A be an n -dimensional affine space. Let a fixed point $\mathcal{O} \in A$ be labeled as the *origin* and let $\{\mathbf{v}_1, \dots, \mathbf{v}_n\}$ be a basis for V . The set $\{\mathcal{O}; \mathbf{v}_1, \dots, \mathbf{v}_n\}$ is called an *affine coordinate system*. Each point $P \in A$ can be uniquely represented in the coordinate system as follows. The difference $\mathcal{P} - \mathcal{O}$ is a vector and can be represented uniquely with respect to the basis for V ,

$$\mathcal{P} - \mathcal{O} = \sum_{i=1}^n a_i \mathbf{v}_i$$

or using our suggestive notation for sum of a point and a vector,

$$\mathcal{P} = \mathcal{O} + \sum_{i=1}^n a_i \mathbf{v}_i$$

The numbers (a_1, \dots, a_n) are called the *affine coordinates* of \mathcal{P} relative to the specified coordinate system. The origin \mathcal{O} has coordinates $(0, \dots, 0)$. [Figure 8.3](#) shows three coordinate systems in the plane.

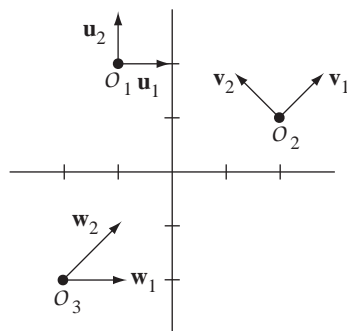


[Figure 8.3](#) Three coordinate systems in the plane. Observe that the vectors in the coordinate system are not required to be unit length or perpendicular in pairs.

A natural question is how to change coordinates from one system to another. Let $\{\mathcal{O}_1; \mathbf{u}_1, \dots, \mathbf{u}_n\}$ and $\{\mathcal{O}_2; \mathbf{v}_1, \dots, \mathbf{v}_n\}$ be two affine coordinate systems for A . A point $P \in A$ has affine coordinates (a_1, \dots, a_n) and (b_1, \dots, b_n) , respectively. The origin \mathcal{O}_2 has affine coordinates (c_1, \dots, c_n) in the first coordinate system. The relationship

$$\mathcal{P} = \mathcal{O}_1 + \sum_{i=1}^n a_i \mathbf{u}_i = \mathcal{O}_2 + \sum_{i=1}^n b_i \mathbf{v}_i = \mathcal{O}_1 + \sum_{i=1}^n c_i \mathbf{u}_i + \sum_{i=1}^n b_i \mathbf{v}_i$$

implies

$$\sum_{i=1}^n b_i \mathbf{v}_i = \sum_{i=1}^n (a_i - c_i) \mathbf{u}_i$$

The two bases are related by a change of basis transformation, $\mathbf{u}_i = \sum_{j=1}^n m_{ji} \mathbf{v}_j$ for $1 \leq i \leq n$, so

$$\sum_{i=1}^n b_i \mathbf{v}_i = \sum_{i=1}^n (a_i - c_i) \sum_{j=1}^n m_{ji} \mathbf{v}_j$$

Renaming the index i to j on the left-hand side and rearranging terms on the right-hand side,

$$\sum_{j=1}^n b_j \mathbf{v}_j = \sum_{j=1}^n \left(\sum_{i=1}^n m_{ji} (a_i - c_i) \right) \mathbf{v}_j$$

The uniqueness of the representation for a vector requires

$$b_j = \sum_{i=1}^n m_{ji} (a_i - c_i), \quad 1 \leq j \leq n$$

which is the desired relationship between the coordinate systems.

EXAMPLE
8.1

Here are two coordinate systems in the plane, the ones shown in Figure 8.3. The origin of the first is $\mathcal{O}_1 = (-1, 2)$ and the basis vectors (coordinate axis directions) are $\mathbf{u}_1 = (1, 0)$ and $\mathbf{u}_2 = (0, 1)$. The origin of the second is $\mathcal{O}_2 = (2, 1)$ and the basis vectors are $\mathbf{v}_1 = (1, 1)/\sqrt{2}$ and $\mathbf{v}_2 = (-1, 1)/\sqrt{2}$. Let us represent the origin of the second system in terms of the first:

$$(3, -1) = (2, 1) - (-1, 2) = \mathcal{O}_2 - \mathcal{O}_1 = c_1 \mathbf{u}_1 + c_2 \mathbf{u}_2 = c_1 (1, 0) + c_2 (0, 1) = (c_1, c_2)$$

The change of basis matrix is determined by $\mathbf{u}_1 = m_{11} \mathbf{v}_1 + m_{21} \mathbf{v}_2$ and $\mathbf{u}_2 = m_{12} \mathbf{v}_1 + m_{22} \mathbf{v}_2$. In block matrix form where the basis vectors are written as columns,

$$\begin{bmatrix} 1 & 0 \\ 0 & 1 \end{bmatrix} = [\mathbf{u}_1 \mathbf{u}_2] = [\mathbf{v}_1 \mathbf{v}_2] \begin{bmatrix} m_{11} & m_{12} \\ m_{21} & m_{22} \end{bmatrix} = \frac{1}{\sqrt{2}} \begin{bmatrix} 1 & -1 \\ 1 & 1 \end{bmatrix} \begin{bmatrix} m_{11} & m_{12} \\ m_{21} & m_{22} \end{bmatrix}$$

The solution is

$$\begin{bmatrix} m_{11} & m_{12} \\ m_{21} & m_{22} \end{bmatrix} = \frac{1}{\sqrt{2}} \begin{bmatrix} 1 & 1 \\ -1 & 1 \end{bmatrix}$$

If $\mathcal{P} = \mathcal{O}_1 + a_1\mathbf{u}_1 + a_2\mathbf{u}_2 = \mathcal{O}_2 + b_1\mathbf{v}_1 + b_2\mathbf{v}_2$, then

$$\begin{bmatrix} b_1 \\ b_2 \end{bmatrix} = \begin{bmatrix} m_{11} & m_{12} \\ m_{21} & m_{22} \end{bmatrix} \begin{bmatrix} a_1 - c_1 \\ a_2 - c_2 \end{bmatrix} = \frac{1}{\sqrt{2}} \begin{bmatrix} a_1 + a_2 - 2 \\ -a_1 + a_2 + 4 \end{bmatrix}$$

The point $(0, 0)$ is represented as $\mathcal{O}_1 + (1)\mathbf{u}_1 + (-2)\mathbf{u}_2$ in the first coordinate system. Using the change of coordinate relationship above, verify that the representation in the second coordinate system is $\mathcal{O}_2 + (-3/\sqrt{2})\mathbf{v}_1 + (1/\sqrt{2})\mathbf{v}_2$. Carefully sketch a picture to convince yourself that the coordinates are accurate. ■

EXERCISE
8.1

How does the analysis of [Example 8.1](#) change when you have the common origin $\mathcal{O}_1 = \mathcal{O}_2 = (0, 0)$? In the first coordinate system, let R be the matrix that represents a counterclockwise rotation about the origin by an angle $\pi/4$. What is the matrix R ? How is it related to the change of basis matrix? ■

EXERCISE
8.2

Repeat the construction in [Example 8.1](#), but use the coordinate system $\{\mathcal{O}_3; \mathbf{w}_1, \mathbf{w}_2\}$ instead of $\{\mathcal{O}_2; \mathbf{v}_1, \mathbf{v}_2\}$, where $\mathcal{O}_3 = (-2, -2)$, $\mathbf{w}_1 = (1, 0)$, and $\mathbf{w}_2 = (1, 1)$. ■

8.3 SUBSPACES

Let A be an affine space. An *affine subspace* of A is a set $A_1 \subseteq A$ such that $V_1 = \{\Delta(\mathcal{P}, \mathcal{Q}) \in V : \mathcal{P}, \mathcal{Q} \in S\}$ is a subspace of V . The geometric motivation for this definition is quite simple. If $V = \mathbb{R}^3$, the one-dimensional subspaces are lines through the origin and the two-dimensional subspaces are planes through the origin. If A is the set of points in space, the one-dimensional subspaces are lines (not necessarily through the origin) and the two-dimensional subspaces are planes (not necessarily through the origin). That is, the affine subspaces are just translations of the vector subspaces.

Let A_1 and A_2 be affine subspaces of A with corresponding vector subspaces V_1 and V_2 of V , respectively. The subspaces are said to be *parallel* if $V_1 \subseteq V_2$ or if $V_2 \subseteq V_1$. If it is the case that $V_1 \subseteq V_2$, then as sets either A_1 and A_2 are disjoint ($A_1 \cap A_2 = \emptyset$) or A_1 is contained in A_2 ($A_1 \subseteq A_2$).

EXAMPLE
8.2

Let A be the set of points in space and $V = \mathbb{R}^3$. Let $\mathcal{P} = (0, 0, 1)$, $\mathbf{u}_1 = (1, 0, 0)$, and $\mathbf{u}_2 = (0, 1, 0)$. Let $\mathcal{Q} = (0, 0, 2)$ and $\mathbf{v}_1 = (1, 1, 0)$. The sets $A_1 = \{\mathcal{P} + s_1\mathbf{u}_1 + s_2\mathbf{u}_2 : s_1, s_2 \in \mathbb{R}\}$ and $A_2 = \{\mathcal{Q} + t_1\mathbf{v}_1 : t_1 \in \mathbb{R}\}$ are parallel, affine subspaces. In this case, A_1 and A_2 are disjoint. If instead $A_2 = \{\mathcal{P} + t_1\mathbf{v}_1 : t_1 \in \mathbb{R}\}$, A_1 and A_2 are still parallel subspaces, but A_2 is a proper subset of A_1 . ■

EXERCISE
8.3

Let A be the set of points in space and $V = \mathbb{R}^3$. Let $\mathcal{P} = (0, 0, 0)$, $\mathbf{u} = (1, 0, 0)$, $\mathcal{Q} = (0, 0, 1)$, and $\mathbf{v} = (0, 1, 0)$. Are the sets $A_1 = \{\mathcal{P} + s\mathbf{u} : s \in \mathbb{R}\}$ and $A_2 = \{\mathcal{Q} + t\mathbf{v} : t \in \mathbb{R}\}$ parallel subspaces? ■

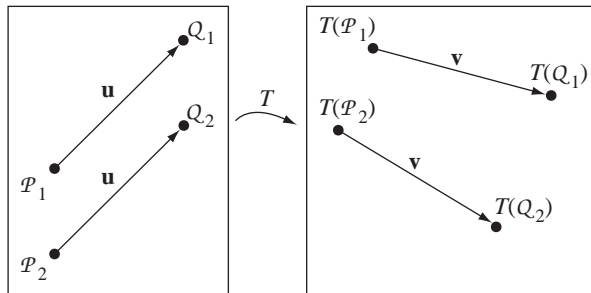


Figure 8.4 An illustration of condition 1 of the definition for affine transformation.

8.4 TRANSFORMATIONS

Just as we defined linear transformations for vector spaces, we can define *affine transformations* for affine spaces. Let A be an affine space with vector space V and vector difference operator Δ_A . Let B be an affine space with vector space W and vector difference operator Δ_B . An affine transformation is a function $T : A \rightarrow B$ such that the following are true:

1. $\Delta_A(\mathcal{P}_1, \mathcal{Q}_1) = \Delta_A(\mathcal{P}_2, \mathcal{Q}_2)$ implies that $\Delta_B(T(\mathcal{P}_1), T(\mathcal{Q}_1)) = \Delta_B(T(\mathcal{P}_2), T(\mathcal{Q}_2))$.
2. The function $L : V \rightarrow W$ defined by $L(\Delta_A(\mathcal{P}, \mathcal{Q})) = \Delta_B(T(\mathcal{P}), T(\mathcal{Q}))$ is a linear transformation.

Figure 8.4 illustrates condition 1 in the definition. Setting $\mathbf{u} = \Delta_A(\mathcal{P}_1, \mathcal{Q}_1)$ and $\mathbf{v} = \Delta_B(T(\mathcal{P}_1), T(\mathcal{Q}_1))$, in geometric terms the condition states that no matter what point \mathcal{P} is used as the initial point for \mathbf{u} , the initial point for \mathbf{v} must be $T(\mathcal{P})$. Condition 2 just states that the vectors themselves must be transformed linearly.

If \mathcal{O}_A is selected as the origin for A and if $\mathcal{O}_B = T(\mathcal{O}_A)$ is selected as the origin for B , then the affine transformation is of the form

$$T(\mathcal{O}_A + \mathbf{x}) = T(\mathcal{O}_A) + L(\mathbf{x}) = \mathcal{O}_B + L(\mathbf{x})$$

Consider the special case when the two affine spaces are the same $B = A$, $W = V$, and $\Delta_B = \Delta_A$. Define $\mathcal{O}_B - \mathcal{O}_A = \mathbf{b}$. The affine transformation is now of the form

$$T(\mathcal{O}_A + \mathbf{x}) = \mathcal{O}_A + \mathbf{b} + L(\mathbf{x})$$

Thus, for a fixed origin \mathcal{O}_A and for a specific matrix representation M of the linear transformation L , the induced action of the affine transformation on the vector space

elements is

$$\mathbf{y} = M\mathbf{x} + \mathbf{b} \quad (8.1)$$

Hopefully this form should look familiar! If M is the identity matrix, then the affine transformation is a *translation* by \mathbf{b} . If M is an orthogonal matrix with determinant 1 and \mathbf{b} is the zero vector, the affine transformation is a pure *rotation* about the origin. If M is an orthogonal matrix of determinant 1 and \mathbf{b} is any vector, the affine transformation is called a *rigid motion*, quite an important concept for physics applications.

8.5 BARYCENTRIC COORDINATES

The definition of an affine space allows for computing the difference of two points and for computing the sum of a point and a vector. The latter operation is the natural way you “move” from one point to another. The sum of two points is just not defined. However, there is an operation on two points that does make intuitive sense, that of a weighted average of two points. If \mathcal{P} and \mathcal{Q} are two points and $\mathbf{v} = \mathcal{Q} - \mathcal{P}$, then $\mathcal{Q} = \mathcal{P} + \mathbf{v}$. For each $t \in \mathbb{R}$, the quantity $t\mathbf{v}$ is, of course, a vector, so $\mathcal{P} + t\mathbf{v}$ is a point itself. Using our suggestive notation for subtraction of points, we have

$$\mathcal{P} + t\mathbf{v} = \mathcal{P} + t(\mathcal{Q} - \mathcal{P})$$

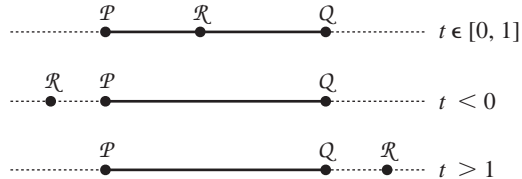
It is an error to distribute the multiplication by t across the difference of points, because the definition of affine algebra does not allow the operation of a scalar times a point. That is, $t(\mathcal{Q} - \mathcal{P})$ is well defined since t is a scalar and $\mathcal{Q} - \mathcal{P}$ is a vector, but $t\mathcal{Q} - t\mathcal{P}$ is ill-defined. But let’s go ahead and distribute anyway, then combine the \mathcal{P} terms to obtain

$$\mathcal{R} = (1 - t)\mathcal{P} + t\mathcal{Q} \quad (8.2)$$

\mathcal{R} is said to be a *barycentric combination* of \mathcal{P} and \mathcal{Q} with *barycentric coordinates* $1 - t$ and t , respectively. Observe that the sum of the coordinates is 1, a necessity for a pair of numbers to be barycentric coordinates. For $t \in [0, 1]$, \mathcal{R} is a point on the line segment connecting \mathcal{P} and \mathcal{Q} . For $t < 0$, \mathcal{R} is on the line through \mathcal{P} and \mathcal{Q} with \mathcal{P} between \mathcal{R} and \mathcal{Q} . Similarly, for $t > 1$, \mathcal{R} is on the line with \mathcal{Q} between \mathcal{R} and \mathcal{P} . Figure 8.5 illustrates these cases.

To support barycentric combinations, the C++ template code for points has one additional member function. The other two arithmetic operations are shown just for comparison.

```
template class <T real, int n> Point
{
public:
    // return_point = this + v
```

Figure 8.5 Various barycentric combinations of two points \mathcal{P} and \mathcal{Q} .

```

Point operator+ (const Vector& v) const;

// return_vector = this - p
Vector operator- (const Point& p) const;

// return_point = (1 - t) * this + t * p,
// a barycentric combination
Point operator+ (real t, const Point& p) const;
}

```

8.5.1 TRIANGLES

The concept of barycentric coordinates extends to three noncolinear points \mathcal{P} , \mathcal{Q} , and \mathcal{R} . The points, of course, form a triangle. Two vectors located at \mathcal{P} are $\mathbf{u} = \mathcal{Q} - \mathcal{P}$ and $\mathbf{v} = \mathcal{R} - \mathcal{P}$. For any scalars s and t , $s\mathbf{u}$ and $t\mathbf{v}$ are vectors and may be added to any point to obtain another point. In particular,

$$\mathcal{P} + s\mathbf{u} + t\mathbf{v} = \mathcal{P} + s(\mathcal{Q} - \mathcal{P}) + t(\mathcal{R} - \mathcal{P})$$

is a point. Just as equation (8.2) was motivated by distributing the scalar product across the differences and collected terms, we do the same here to obtain

$$\mathcal{B} = (1 - s - t)\mathcal{P} + s\mathcal{Q} + t\mathcal{R} \quad (8.3)$$

\mathcal{B} is said to be a *barycentric combination* of \mathcal{P} , \mathcal{Q} , and \mathcal{R} with *barycentric coordinates* $c_1 = 1 - s - t$, $c_2 = s$, and $c_3 = t$, respectively. As with a barycentric combination of two points, the barycentric coordinates must sum to one: $c_1 + c_2 + c_3 = 1$. The location of \mathcal{B} relative to the triangle formed by the three points is illustrated in Figure 8.6.

The signs of c_1 , c_2 , and c_3 are listed as ordered triples. On a boundary between two regions, not including the vertices, one of the c_i is 0. At a vertex, two of the c_i are 0, the other coordinate necessarily 1. The coordinates cannot be simultaneously negative since the sum of three negative numbers cannot be 1.

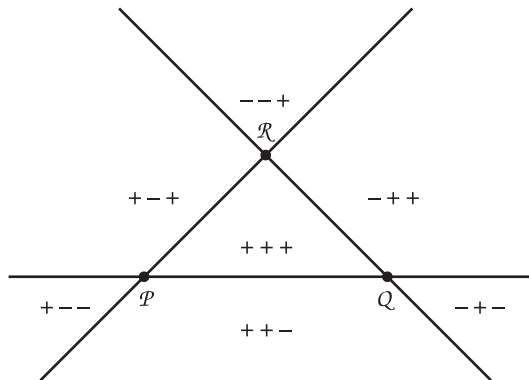


Figure 8.6 The triangle partitions the plane into seven regions. The signs of c_1 , c_2 , and c_3 are listed as ordered triples.

EXERCISE
8.4

Linear interpolation over a triangle. A real-valued function $f(x, y)$, unknown to you, has been sampled at three noncolinear points (x_i, y_i) with function values f_i , $0 \leq i \leq 2$. If you are given the information that $f : \mathbb{R}^2 \rightarrow \mathbb{R}$ is an affine transformation, construct an explicit formula for f . ■

8.5.2 TETRAHEDRA

The concept of barycentric coordinates also extends to four noncoplanar points \mathcal{P}_i , $0 \leq i \leq 3$. The points form a tetrahedron. Using a construction similar to that for a segment and a triangle, a *barycentric combination* of the points is

$$\mathcal{B} = (1 - c_1 - c_2 - c_3)\mathcal{P}_0 + c_1\mathcal{P}_1 + c_2\mathcal{P}_2 + c_3\mathcal{P}_3 \quad (8.4)$$

The values $c_0 = 1 - c_1 - c_2 - c_3$, c_1 , c_2 , and c_3 are the *barycentric coordinates* of \mathcal{B} and they sum to 1. The tetrahedron partitions space into 15 regions, each region labeled with an ordered quadruple of signs for the four coefficients. The only invalid combination of signs is all negative since the sum of four negative numbers cannot equal 1.

EXERCISE
8.5

Linear interpolation over a tetrahedron. A real-valued function $f(x, y, z)$, unknown to you, has been sampled at four noncoplanar points (x_i, y_i, z_i) with function values f_i , $0 \leq i \leq 3$. If you are given the information that $f : \mathbb{R}^3 \rightarrow \mathbb{R}$ is a linear transformation, construct an explicit formula for f . ■

8.5.3 SIMPLICES

We have seen barycentric coordinates relative to a segment, a triangle, and a tetrahedron. The concept extends to affine spaces of n -tuples for any $n \geq 2$. The name of the object that generalizes triangle and tetrahedron is *simplex* (plural *simplices*). A simplex is formed by $n + 1$ points \mathcal{P}_i , $0 \leq i \leq n$, such that the set of vectors $\{\mathcal{P}_i - \mathcal{P}_0\}_{i=1}^n$ are linearly independent. A *barycentric combination of the points* is

$$\mathcal{B} = \sum_{i=0}^n c_i \mathcal{P}_i \quad (8.5)$$

and the c_i are the *barycentric coordinates* of \mathcal{B} with respect to the given points. As before, the coefficients sum to 1, $\sum_{i=0}^n c_i = 1$.

Although we tend to work in 2D or 3D, let us be abstract for a moment and ask the same question we did for segments, triangles, and tetrahedra. A segment, a simplex in \mathbb{R} , partitioned \mathbb{R} into three regions. A triangle, a simplex in \mathbb{R}^2 , partitioned \mathbb{R}^2 into seven regions. A tetrahedron, a simplex in \mathbb{R}^3 , partitioned \mathbb{R}^3 into 15 regions. How many regions in \mathbb{R}^n are obtained by a partitioning of a simplex? The sequence with increasing dimension is 3, 7, 15, so you might guess that the answer is $2^{n+1} - 1$. This is correct. An intuitive reason is supported by looking at the signs of the $n + 1$ coefficients. Each region is labeled with an ordered $(n + 1)$ -tuple of signs, each sign positive or negative. There are two choices of sign for each of the $n + 1$ components, leading to 2^{n+1} possibilities. As in the cases we've already looked at, all negative signs are not allowed since the sum would be negative and you cannot obtain a sum of 1. This means only $(2^{n+1} - 1)$ tuples of signs are possible.

A more geometric approach to counting the regions is based on an analysis of the components of the simplices. A segment has two vertices. The interior of the segment is formed by both vertices, so you can think of that region as occurring as the only possibility when choosing two vertices from a set of two vertices. That is, the number of interior regions is $C(2, 2) = 1$, where

$$C(n, k) = \frac{n!}{k!(n-k)!}$$

is the number of combinations of n items choosing k at a time. The segment has two exterior regions, each formed by a single vertex. The number of such regions is $C(2, 1) = 2$, because you have two vertices, but choose only one at a time. The total number of regions in the partition of the line is $C(2, 1) + C(2, 2) = 2 + 1 = 3$.

A triangle has three vertices. The interior is formed by choosing all three vertices. The number of interior regions is $C(3, 3) = 1$. Figure 8.6 shows that each edge has a corresponding exterior region. An edge is formed by two vertices and you have three vertices to choose from. The total number of edges is $C(3, 2) = 3$. The figure also shows that each vertex has a corresponding exterior region. The total number of vertices is $C(3, 1) = 3$. The total number of regions in the partition of the plane is $C(3, 1) + C(3, 2) + C(3, 3) = 3 + 3 + 1 = 7$.

The same argument applies to a tetrahedron with four vertices. The interior is formed by all four vertices; the number of interior regions is $C(4, 4) = 1$. A face is formed by three vertices; there are $C(4, 3) = 4$ such possibilities. An edge is formed by two vertices; there are $C(4, 2) = 6$ such possibilities. Finally, there are $C(4, 1) = 4$ vertices. An exterior region is associated with each vertex, each edge, and each face. The total number of regions is $C(4, 1) + C(4, 2) + C(4, 3) + C(4, 4) = 4 + 6 + 4 + 1$.

Consider now the general case, a simplex formed by $n + 1$ points. The components, so to speak, of the simplex are classified by how many vertices form them. If a component uses k vertices, let's call that a k -vertex component. The interior of the simplex is the only $(n + 1)$ -vertex component. Each k -vertex component where $1 \leq k < n + 1$ has a single exterior region associated with it. The total number of regions is therefore

$$C(n+1, n+1) + C(n+1, n) + \cdots + C(n+1, 1) = \sum_{k=1}^{n+1} C(n+1, k) = 2^{n+1} - 1$$

The term $C(n, k)$ indicates the number of k -vertex components, the number of combinations of n vertices choosing k at a time. Where did that last equality come from? Recall the binomial expansion for a power of a sum of two values:

$$\begin{aligned} (x+y)^m &= C(m, 0)x^m + C(m, 1)x^{m-1}y + \cdots + C(m, m-1)xy^{m-1} + C(m, m)y^m \\ &= \sum_{k=0}^m C(m, k)x^{m-k}y^k \end{aligned}$$

Setting $x = 1$, $y = 1$, and $m = n + 1$, we arrive at

$$2^{n+1} = (1+1)^{n+1} = \sum_{k=0}^{n+1} C(n+1, k) = 1 + \sum_{k=1}^{n+1} C(n+1, k)$$

8.5.4 LENGTH, AREA, VOLUME, AND HYPERVOLUME

The constructions in this section are designed to show that the area of a triangle (simplex in 2D) can be computed as a sum (in an integration sense) of lengths of line segments (simplices in 1D). I also show that the volume of a tetrahedron (simplex in 3D) can be computed as a sum of areas of triangles (simplices in 2D). These two facts indicate the process is recursive in dimension. Intuitively, a simplex in 4D has a “volume,” so to speak, that can be computed as a sum of volumes of tetrahedra (simplices in 3D). Sometimes this is called a *hypervolume*, but that leads us to wanting names for the similar concept in yet higher dimensions. I will use the term *hypervolume* for any dimension and note that hypervolume in 1D is length, hypervolume in 2D is area, and hypervolume in 3D is volume. Given a simplex formed by points \mathcal{P}_i for $0 \leq i \leq n$, the hypervolume is denoted $H(\mathcal{P}_0, \dots, \mathcal{P}_n)$.

Length of a Segment

A line segment with endpoints \mathcal{P}_0 and \mathcal{P}_1 is a simplex with two vertices. The length of the simplex is $|\mathcal{P}_1 - \mathcal{P}_0|$. Using our notation for hypervolume,

$$H(\mathcal{P}_0, \mathcal{P}_1) = |\mathcal{P}_1 - \mathcal{P}_0| \quad (8.6)$$

Area of a Triangle

Recall that the area of a triangle with base length b and height h is $A = bh/2$. Figure 8.7(a) shows the standard drawing one normally uses to show b and h . Figure 8.7(b) shows a triangle viewed as the union of line segments of varying lengths. The drawing shows the bottom edge aligned with the x -axis, but the ensuing arguments do not depend on this. The area of the triangle may be thought of as the sum of the lengths of all the line segments in the union. This is an informal and mathematically nonrigorous view of the situation, but intuitively it works quite well. The number of line segments is infinite, one segment per y -value in the interval $[0, h]$. The sum cannot be computed in the usual sense. In this setting it becomes an integration of the lengths as a function of y .

Select a value of $y \in [0, h]$. The line segment has two endpoints, one on the triangle edge from \mathcal{P}_0 to \mathcal{P}_2 and one on the triangle edge from \mathcal{P}_1 to \mathcal{P}_2 . The fraction of the distance along each edge on which the endpoints lie is $y/h \in [0, 1]$. That is, the endpoints are the barycentric combinations $(1 - y/h)\mathcal{P}_0 + (y/h)\mathcal{P}_2$

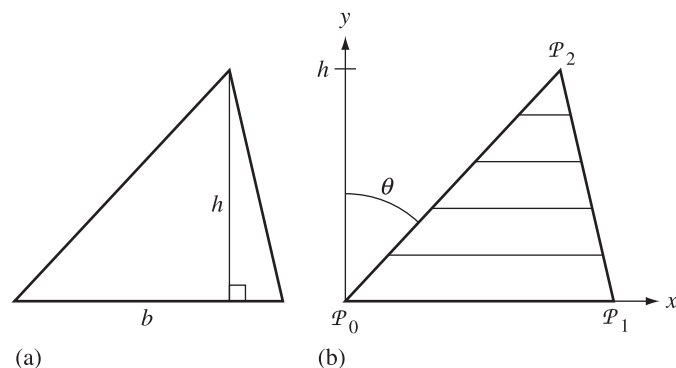


Figure 8.7 (a) A triangle with base length b and height h marked. The area of the triangle is $bh/2$. (b) A triangle viewed as a union of an infinite number of line segments of varying lengths (only a few are shown). The area of the triangle is the sum of the lengths of those line segments.

and $(1 - y/h)\mathcal{P}_1 + (y/h)\mathcal{P}_2$. The length of the segment is the length of the vector connecting the endpoints,

$$\mathbf{v} = ((1 - y/h)\mathcal{P}_1 + (y/h)\mathcal{P}_2) - (1 - y/h)\mathcal{P}_0 + (y/h)\mathcal{P}_2 = (1 - y/h)(\mathcal{P}_1 - \mathcal{P}_0)$$

The length of the segment as a function of y is

$$L(y) = |\mathbf{v}| = (1 - y/h)|\mathcal{P}_1 - \mathcal{P}_0| = (1 - y/h)b$$

where b is the length of the base of the triangle. To “add” all the values $L(y)$ for $y \in [0, h]$ in order to obtain the area A , we need to integrate

$$A = \int_0^h L(y) dy = \int_0^h (1 - y/h)b dy = b \left[\frac{-h(1 - y/h)^2}{2} \right]_0^h = \frac{bh}{2}$$

In terms of our hypervolume notation,

$$H(\mathcal{P}_0, \mathcal{P}_1, \mathcal{P}_2) = \frac{h}{2} H(\mathcal{P}_0, \mathcal{P}_1) \quad (8.7)$$

where $h = |\mathcal{P}_2 - \mathcal{P}_0| \cos \theta$ with θ the angle as shown in [Figure 8.7](#).

The height h also may be computed as the length of the projection of $\mathcal{P}_2 - \mathcal{P}_0$ onto the vertical axis. A convenient vector to use, whose direction is that of the vertical axis, is the following. Let $\mathcal{P}_1 - \mathcal{P}_0 = \mathbf{v} = (v_1, v_2)$. A perpendicular vector in the direction of the positive vertical axis as shown in [Figure 8.7](#) is $-\text{Perp}(\mathcal{P}_0, \mathcal{P}_1)$ where

$$\text{Perp}(\mathcal{P}_0, \mathcal{P}_1) = (v_2, -v_1) \quad (8.8)$$

is called the *perp* vector. You will notice that the perp vector itself is in the direction of the *negative* vertical axis as shown in [Figure 8.7](#). Using the coordinate-free definition of dot product, [equation \(7.12\)](#),

$$(\mathcal{P}_2 - \mathcal{P}_0) \cdot (-\text{Perp}(\mathcal{P}_0, \mathcal{P}_1)) = |\mathcal{P}_2 - \mathcal{P}_0| |\text{Perp}(\mathcal{P}_0, \mathcal{P}_1)| \cos \theta = h |\text{Perp}(\mathcal{P}_0, \mathcal{P}_1)|$$

The perp vector has the same length as $\mathcal{P}_1 - \mathcal{P}_0$, so the dot product in the previous equation is twice the area of the triangle, bh . This gives us the nonrecursive formula for the area of a triangle,

$$H(\mathcal{P}_0, \mathcal{P}_1, \mathcal{P}_2) = -\frac{1}{2} (\mathcal{P}_2 - \mathcal{P}_0) \cdot \text{Perp}(\mathcal{P}_0, \mathcal{P}_1) \quad (8.9)$$

Volume of a Tetrahedron

The volume of a tetrahedron may be computed in the same intuitive way that was used for the area of a triangle. Let \mathcal{P}_i , $0 \leq i \leq 3$, denote the vertices of the tetrahedron. The base of the tetrahedron will be selected as the triangle formed by \mathcal{P}_i , $0 \leq i \leq 2$. The tetrahedron may be informally thought of as an infinite union of triangles that are parallel to its base. [Figure 8.8](#) shows a tetrahedron and one of its triangle slices.

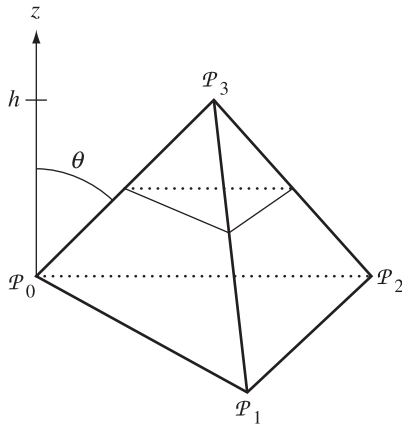


Figure 8.8 A tetrahedron with base formed by \mathcal{P}_0 , \mathcal{P}_1 , and \mathcal{P}_2 . A triangle slice parallel to the base is shown. The direction perpendicular to the base is marked as the positive z -axis.

Select a value of $z \in [0, h]$. The corresponding triangle has three vertices, one on each tetrahedron edge with endpoints \mathcal{P}_i and \mathcal{P}_3 for $0 \leq i \leq 2$. The fraction of the distance along each edge on which the endpoints lie is $z/h \in [0, 1]$. The endpoints are the barycentric combinations $\mathcal{Q}_i = (1 - z/h)\mathcal{P}_i + (z/h)\mathcal{P}_3$ for $0 \leq i \leq 2$. If $A(z)$ denotes the area of this triangle, the volume of the tetrahedron is

$$V = \int_0^h A(z) dz$$

We would like to use [equation \(8.9\)](#) to compute $A(z)$, but there is a problem. Even though that equation is written in a coordinate-free manner, it is implicitly tied to 2D points via the definition of the perp vector in [equation \(8.8\)](#) that requires points in two dimensions. For the time being, let's instead use the area formula from [equation \(7.17\)](#). We will later return to the issue of the perp vector and provide a definition that is valid in any dimension.

Set $\mathbf{v}_i = \mathcal{Q}_i - \mathcal{Q}_0 = (1 - z/h)(\mathcal{P}_i - \mathcal{P}_0)$ for $1 \leq i \leq 2$. The triangle slice is half of a parallelogram formed by \mathbf{v}_1 and \mathbf{v}_2 , so using [equation \(7.17\)](#) the area of the triangle is

$$A(z) = \frac{1}{2} |\mathbf{v}_1 \times \mathbf{v}_2| = \frac{(1 - z/h)^2}{2} |(\mathcal{P}_1 - \mathcal{P}_0) \times (\mathcal{P}_2 - \mathcal{P}_0)| = (1 - z/h)^2 b$$

where b is the area of the base of the tetrahedron. The volume of the tetrahedron is

$$V = \int_0^h A(z) dz = \int_0^h (1 - z/h)^2 b dz = b \left[\frac{-h(1 - z/h)^3}{3} \right]_0^h = \frac{bh}{3}$$

In our hypervolume notation, the volume is

$$H(\mathcal{P}_0, \mathcal{P}_1, \mathcal{P}_2, \mathcal{P}_3) = \frac{h}{3} H(\mathcal{P}_0, \mathcal{P}_1, \mathcal{P}_2) \quad (8.10)$$

where $h = |\mathcal{P}_3 - \mathcal{P}_0| \cos \theta$ with θ the angle shown in [Figure 8.8](#).

The height may also be computed as the length of the projection of $\mathcal{P}_3 - \mathcal{P}_0$ onto the vertical axis. We already know a vector with that direction, the cross product $(\mathcal{P}_1 - \mathcal{P}_0) \times (\mathcal{P}_2 - \mathcal{P}_0)$. Using [equation \(8.8\)](#) as motivation, define

$$\text{Perp}(\mathcal{P}_0, \mathcal{P}_1, \mathcal{P}_2) = (\mathcal{P}_1 - \mathcal{P}_0) \times (\mathcal{P}_2 - \mathcal{P}_0) \quad (8.11)$$

Using the coordinate-free definition of dot product, [equation \(7.12\)](#),

$$\begin{aligned} (\mathcal{P}_3 - \mathcal{P}_0) \cdot \text{Perp}(\mathcal{P}_0, \mathcal{P}_1, \mathcal{P}_2) &= |\mathcal{P}_3 - \mathcal{P}_0| |\text{Perp}(\mathcal{P}_0, \mathcal{P}_1, \mathcal{P}_2)| \cos \theta \\ &= h |\text{Perp}(\mathcal{P}_0, \mathcal{P}_1, \mathcal{P}_2)| = 2hb \end{aligned}$$

where b is the area of the triangle base of the tetrahedron. Dividing by 6 we have a nonrecursive formula for the volume,

$$H(\mathcal{P}_0, \mathcal{P}_1, \mathcal{P}_2, \mathcal{P}_3) = \frac{1}{6} (\mathcal{P}_3 - \mathcal{P}_0) \cdot \text{Perp}(\mathcal{P}_0, \mathcal{P}_1, \mathcal{P}_2) \quad (8.12)$$

Hypervolume of a Simplex

Notice the strong similarities between [equations \(8.7\)](#) and [\(8.10\)](#) and between [equations \(8.9\)](#) and [\(8.12\)](#). The first pair of equations suggests that for a simplex formed from $n + 1$ points \mathcal{P}_i , $0 \leq i \leq n$, the recursive formula for the hypervolume is

$$H(\mathcal{P}_0, \dots, \mathcal{P}_n) = \frac{h}{n} H(\mathcal{P}_0, \dots, \mathcal{P}_{n-1}) \quad (8.13)$$

where $h = |\mathcal{P}_n - \mathcal{P}_0| \cos \theta$ with θ the angle between $\mathcal{P}_n - \mathcal{P}_0$ and a vector that is perpendicular to the base of the simplex. The base is itself a simplex but formed by n points \mathcal{P}_i for $0 \leq i \leq n - 1$. As we saw in the cases $n = 2$ and $n = 3$, we want the perpendicular vector chosen so that θ is an acute angle. In 2D we used $-\text{Perp}(\mathcal{P}_0, \mathcal{P}_1)$ and in 3D we used $\text{Perp}(\mathcal{P}_0, \mathcal{P}_1, \mathcal{P}_2)$. This suggests that in general dimension n , we will use a vector $(-1)^{n+1} \text{Perp}(\mathcal{P}_0, \dots, \mathcal{P}_{n-1})$, where the perp vector $\text{Perp}(\mathcal{P}_0, \dots, \mathcal{P}_{n-1})$ is appropriately defined. The second pair of equations suggests the nonrecursive formula

$$H(\mathcal{P}_0, \dots, \mathcal{P}_n) = \frac{(-1)^{n+1}}{n!} (\mathcal{P}_n - \mathcal{P}_1) \cdot \text{Perp}(\mathcal{P}_0, \dots, \mathcal{P}_{n-1}) \quad (8.14)$$

This leaves us with the task of finding a formula for $\text{Perp}(\mathcal{P}_0, \dots, \mathcal{P}_{n-1})$, hopefully in a way that applies to any dimensional input points. We accomplish this last goal by introducing an indexed quantity that stores information about permutations. In

tensor calculus, this is called the *Levi–Civita permutation tensor*, but the name and tensor calculus are not really important in our context.

Let's look at the 2D problem first. The doubly-indexed quantity e_{ij} for $1 \leq i \leq 2$ and $1 \leq j \leq 2$ represents four numbers, each number in the set $\{-1, 0, 1\}$. The value is 0 if the two indices are the same: $e_{11} = 0$ and $e_{22} = 0$. The other values are $e_{12} = 1$ and $e_{21} = -1$. The choice of 1 or -1 is based on whether the ordered index pair (i, j) is an even or odd permutation of $(1, 2)$. In the current case, $(1, 2)$ is an even permutation of $(1, 2)$ (zero transpositions, zero is an even number) so $e_{12} = 1$. The pair $(2, 1)$ is an odd permutation of $(1, 2)$ (one transposition, one is an odd number) so $e_{21} = -1$. You should notice that $e_{ji} = -e_{ij}$. Treating e_{ij} as the elements of a 2×2 matrix E , that matrix is skew-symmetric: $E^T = -E$.

The arguments of the area function and perp operation are points. Since the area and perp vector are invariant under translations, we may as well replace the arguments by vectors $\mathbf{v}^{(i)} = \mathcal{P}_i - \mathcal{P}_0$ for $i \geq 1$. In 2D, $\mathbf{v}^{(i)} = (v_1^{(i)}, v_2^{(i)})$. Thus,

$$(u_1, u_2) = \mathbf{u} = \text{Perp}(\mathbf{v}^{(1)}) = (v_2^{(1)}, -v_1^{(1)}) = (e_{12}v_2^{(1)}, e_{21}v_1^{(1)})$$

In summation notation the components of \mathbf{u} are

$$u_j = \sum_{i=1}^2 e_{ji} v_i^{(1)} \quad (8.15)$$

The area of the triangle is

$$\begin{aligned} H(\mathbf{v}^{(1)}, \mathbf{v}^{(2)}) &= -\frac{1}{2} \mathbf{v}^{(2)} \cdot \text{Perp}(\mathbf{v}^{(1)}) \quad \text{Using equation (8.9)} \\ &= -\frac{1}{2} \sum_{i=1}^2 \sum_{j=1}^2 e_{ji} v_j^{(2)} v_i^{(1)} \quad \text{Using equation (8.15)} \\ &= \frac{1}{2} \sum_{i=1}^2 \sum_{j=1}^2 e_{ij} v_i^{(1)} v_j^{(2)} \quad e_{ij} = -e_{ji} \text{ and swapping terms} \end{aligned} \quad (8.16)$$

In 3D the triply-indexed permutation tensor is e_{ijk} for $1 \leq i \leq 3$, $1 \leq j \leq 3$, and $1 \leq k \leq 3$. Each value is in the set $\{-1, 0, 1\}$. If any pair of indices is the same, the value is zero; for example, $e_{111} = 0$, $e_{112} = 0$, and $e_{233} = 0$ (there are 21 zero elements). Otherwise, $e_{ijk} = 1$ if (i, j, k) is an even permutation of $(1, 2, 3)$ or $e_{ijk} = -1$ if (i, j, k) is an odd permutation of $(1, 2, 3)$. Under these conditions only six elements are nonzero: $e_{123} = e_{231} = e_{312} = 1$ and $e_{132} = e_{321} = e_{213} = -1$. As in the 2D case, if a pair of indices is swapped, the sign is changed: $e_{jik} = e_{ikj} = e_{kji} = -e_{ijk}$. Define $\mathbf{v}^{(i)} = \mathcal{P}_i - \mathcal{P}_0 = (v_1^{(i)}, v_2^{(i)}, v_3^{(i)})$, $1 \leq i \leq 3$; then

$$\begin{aligned} (u_1, u_2, u_3) &= \mathbf{u} \\ &= \text{Perp}(\mathbf{v}^{(1)}, \mathbf{v}^{(2)}) \end{aligned}$$

$$\begin{aligned}
&= \mathbf{v}^{(1)} \times \mathbf{v}^{(2)} \\
&= \left(v_2^{(1)} v_3^{(2)} - v_3^{(1)} v_2^{(2)}, v_3^{(1)} v_1^{(2)} - v_1^{(1)} v_3^{(2)}, v_1^{(1)} v_2^{(2)} - v_2^{(1)} v_1^{(2)} \right) \\
&= \left(e_{123} v_2^{(1)} v_3^{(2)} + e_{132} v_3^{(1)} v_2^{(2)}, e_{231} v_3^{(1)} v_1^{(2)} + e_{213} v_1^{(1)} v_3^{(2)}, \right. \\
&\quad \left. e_{312} v_1^{(1)} v_2^{(2)} + e_{321} v_2^{(1)} v_1^{(2)} \right)
\end{aligned}$$

In summation notation the components of \mathbf{u} are

$$u_k = \sum_{i=1}^3 \sum_{j=1}^3 e_{kij} v_i^{(1)} v_j^{(2)} \quad (8.17)$$

The volume of the tetrahedron is

$$\begin{aligned}
&H(\mathbf{v}^{(1)}, \mathbf{v}^{(2)}, \mathbf{v}^{(3)}) \\
&= \frac{1}{6} \mathbf{v}^{(3)} \cdot \text{Perp}(\mathbf{v}^{(1)}, \mathbf{v}^{(2)}) \quad \text{Using equation (8.12)} \\
&= \frac{1}{6} \sum_{i=1}^3 \sum_{j=1}^3 \sum_{k=1}^3 e_{kij} v_k^{(3)} v_i^{(1)} v_j^{(2)} \quad \text{Using equation (8.17)} \\
&= \frac{1}{6} \sum_{i=1}^3 \sum_{j=1}^3 \sum_{k=1}^3 -e_{ikj} v_i^{(1)} v_j^{(2)} v_k^{(3)} \quad e_{kij} = -e_{ikj} \text{ and swapping terms} \\
&= \frac{1}{6} \sum_{i=1}^3 \sum_{j=1}^3 \sum_{k=1}^3 e_{ijk} v_i^{(1)} v_j^{(2)} v_k^{(3)} \quad e_{ijk} = -e_{ijk}
\end{aligned} \quad (8.18)$$

The last couple of steps are just to swap the k into the last position. In 2D one swap was required. In 3D two swaps were required.

The pattern holds for general dimension n . The permutation tensor is an n -indexed quantity $e_{i_1 \dots i_n}$ that is zero if any pair of indices is repeated, is 1 if (i_1, \dots, i_n) is an even permutation of $(1, \dots, n)$, or is -1 if (i_1, \dots, i_n) is an odd permutation of $(1, \dots, n)$. Only $n!$ values are nonzero where $n!$ is the number of permutations of n numbers. The vectors of interest are $\mathbf{v}^{(i)} = \mathcal{P}_i - \mathcal{P}_0$ for $1 \leq i \leq n$. The vector $(u_1, \dots, u_n) = \mathbf{u} = \text{Perp}(\mathbf{v}^{(1)}, \dots, \mathbf{v}^{(n)})$ has components

$$u_j = \sum_{i_1=1}^n \dots \sum_{i_{n-1}=1}^n e_{i_n i_1 \dots i_{n-1}} v_{i_1}^{(1)} \dots v_{i_{n-1}}^{(n-1)} \quad (8.19)$$

The hypervolume of the simplex is

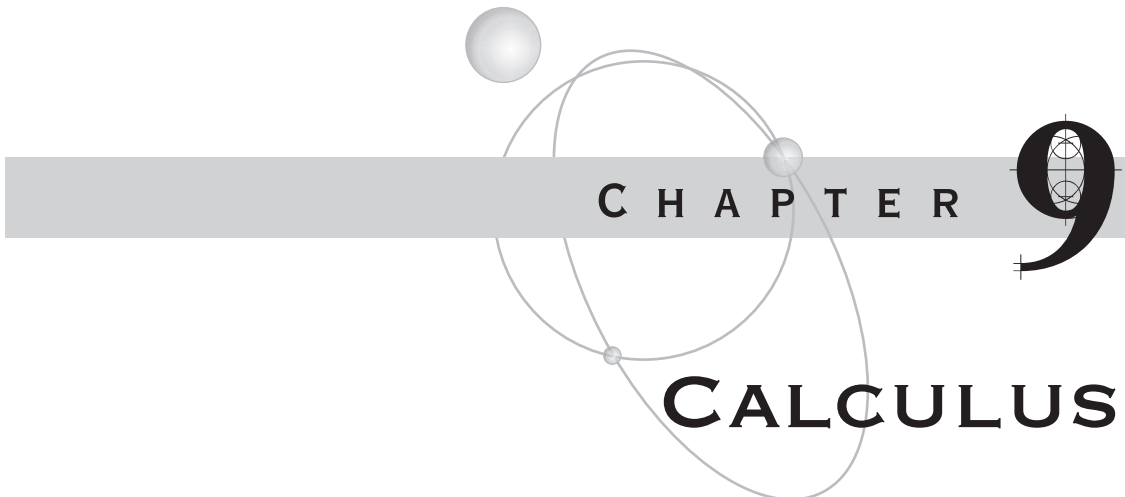
$$\begin{aligned}
 H(\mathbf{v}^{(1)}, \dots, \mathbf{v}^{(n)}) &= \frac{(-1)^{n+1}}{n!} \mathbf{v}^{(n)} \cdot \text{Perp}(\mathbf{v}^{(1)}, \dots, \mathbf{v}^{(n-1)}) && \text{Using equation (8.14)} \\
 &= \frac{(-1)^{n+1}}{n!} \sum_{i_1=1}^n \cdots \sum_{i_n=1}^n e_{i_n i_1 \cdots i_{n-1}} v_{i_n}^{(n)} v_{i_1}^{(1)} \cdots v_{i_{n-1}}^{(n-1)} && \text{Using equation (8.19)} \\
 &= \frac{1}{n!} \sum_{i_1=1}^n \cdots \sum_{i_n=1}^n e_{i_n i_1 \cdots i_{n-1}} v_{i_1}^{(1)} \cdots v_{i_{n-1}}^{(n-1)} v_{i_n}^{(n)}
 \end{aligned} \tag{8.20}$$

The last equation is the result of swapping i_n with each of the $n - 1$ other indices. Each swap introduces a factor of -1 , so the total swaps introduces the factor $(-1)^{n-1}$. Combining with the other sign factor $(-1)^{n+1}$ results in a factor of $(-1)^{n-1}(-1^{n+1}) = (-1)^{2n} = 1$.

The final interesting observation is that the summations in the hypervolume [equation \(8.20\)](#) are just the determinant of a matrix. The n -indexed quantity $e_{i_1 \dots i_n}$ is the same quantity as e_σ introduced in the section on determinants. If the vectors $\mathbf{v}^{(i)}$ are written as the columns of an $n \times n$, say $[\mathbf{v}^{(1)} | \dots | \mathbf{v}^{(n)}]$, then the hypervolume of the simplex is

$$H(\mathbf{v}^{(1)}, \dots, \mathbf{v}^{(n)}) = \frac{1}{n!} \det [\mathbf{v}^{(1)} | \dots | \mathbf{v}^{(n)}] \tag{8.21}$$

The formula was developed with a certain ordering in mind for the input vectors. For general ordering, [equation \(8.21\)](#) can produce negative numbers, in which case the formula generates the *signed hypervolume*. To be sure you have the nonnegative hypervolume, just take the absolute value of the right-hand side of the equation.



CHAPTER 9

CALCULUS

This appendix provides a brief summary of topics in calculus that you should be familiar with in order to fully understand how to model a physical system and implement the physical simulation on a computer. Calculus occurs in two flavors, *differential calculus* and *integral calculus*. Both disciplines are founded on the concepts of *infinitesimal quantities* and a *limit*, the measurement of what happens to a quantity as one or more parameters are varied.

Calculus involves processing functions, the topic further subdivided based on the number of independent and dependent variables. *Univariate calculus* studies functions $y = f(x)$, where x is an independent variable and y is the dependent variable. Formally, the function is written as $f : \mathcal{D} \rightarrow \mathcal{R}$, where $\mathcal{D} \subset \mathbb{R}$ is the *domain* of the function and $\mathcal{R} \subset \mathbb{R}$ is the *range* of the function. To be somewhat loose with the notation, an emphasis will be placed on the sets containing the domain and range by writing $f : \mathbb{R} \rightarrow \mathbb{R}$. The domain and range are most likely proper subsets of \mathbb{R} , but those will be known within the context of the problem at hand.

Multivariate calculus studies functions $y = f(x_1, \dots, x_n)$, where x_1 through x_n are n independent variables and y is a single dependent variable. The function may be written as $f : \mathbb{R}^n \rightarrow \mathbb{R}$, where \mathbb{R}^n denotes the set of n -tuples of real numbers. As indicated in the last paragraph, the domain of f may be a proper subset of \mathbb{R}^n and the range of f may be a proper subset of \mathbb{R} .

The next natural extension is to study a collection of functions $y_i = f_i(x_1, \dots, x_n)$ for $1 \leq i \leq m$. We now have n independent variables and m dependent variables. Using vector notation, let $\mathbf{Y} = (y_1, \dots, y_m)$, $\mathbf{X} = (x_1, \dots, x_n)$, and $\mathbf{F} = (f_1, \dots, f_m)$. The function may be written as $\mathbf{Y} = \mathbf{F}(\mathbf{X})$, or $\mathbf{F} : \mathbb{R}^n \rightarrow \mathbb{R}^m$. This coordinate-free representation looks just like the univariate case where $n = m = 1$. For physical applications

attention is focused on the case of $n = 1$ and $m = 2$ or $m = 3$. That is, $y_i = f_i(t)$ for all i with a single independent variable t (time). Extensive discussion of this case is already a large portion of [Chapter 2](#)!

[Section 9.1](#) is a summary of the key ideas for univariate calculus, whereas [Section 9.2](#) is a summary for multivariate calculus. [Section 9.3](#) provides a few applications that are related to physical simulations. Optimization involves computing maxima and minima of functions. Constrained optimization also involves computing maxima and minima, but with additional constraints related to the problem at hand. This appendix will cover only *equality constraints* that can be solved using the method of Lagrange multipliers. *Inequality constraints* are a bit more challenging, but we actually talk about these in this book! See [Chapter 14](#) for the details. The final topic in [Section 9.3](#) on applications section covers approximation of derivatives by finite differences. This topic is relevant to constructing numerical methods for solving differential equations.

9.1 UNIVARIATE CALCULUS

Differential calculus generalizes the idea of the rate of change of a quantity over a fixed time interval to the limit of rate of change over time intervals of decreasing duration. The prototypical example is a measurement of speed of an object traveling along a straight line path. If the position of an object at an initial time t_{initial} is x_{initial} and the position at a final time t_{final} is x_{final} , the average speed of the object on the time interval is

$$s_{\text{average}} = \frac{x_{\text{final}} - x_{\text{initial}}}{t_{\text{final}} - t_{\text{initial}}}$$

The measurement is the difference of final and initial positions divided by the difference of final and initial times. As an average, the measurement does not give you any information about the position or speed of the object at intermediate times. It is simply a statistic that summarizes the behavior of the object on the given time interval.

If we think of the position as a function of time, say $x(t)$, the initial position of the object at time t is $x_{\text{initial}} = x(t)$, the final position at time $t + \Delta t$ for some $\Delta t > 0$ is $x_{\text{final}} = x(t + \Delta t)$, and the average speed is

$$s_{\text{average}}([t, t + \Delta t]) = \frac{x(t + \Delta t) - x(t)}{\Delta t}$$

I have included the time interval on the left-hand side to stress over which time interval the average is computed. Now suppose we are able to compute the position of the object at any time. Consider how the average speed changes as we look at smaller

and smaller time intervals; that is, we will choose smaller values of Δt to make the measurements. [Example 9.1](#) illustrates.

EXAMPLE
9.1

Suppose the position is measured as $x(t) = t(1 - t)$ for $t \in [0, 1]$. The initial position is $x(0) = 0$ and the final position is $x(1) = 0$; that is, the object starts and ends at the same position. The average speed for the time interval $[0, 1]$ is $s_{\text{average}} = 0$. Although you know the object is moving, it does begin and end at the same position. If you looked at the object at the initial time, closed your eyes for one second, and then opened them, you would see the object in the same position. In this sense an average speed of zero is meaningful!

Now suppose that you opened your eyes after a half a second. The position of the object is $x(1/2) = 1/4$ and the average speed on the time interval $[0, 1/2]$ is $s_{\text{average}} = (1/4 - 0)/(1/2 - 0) = 1/2$. In fact, you now know that the object has moved because you kept your eyes closed for a shorter period of time. It has moved away from you, so a nonzero average speed makes sense.

[Table 9.1](#) displays average speed calculations on intervals $[0, \Delta t]$ of decreasing duration.

Table 9.1

Average Speed Calculations on Intervals $[0, \Delta t]$ with Decreasing Δt

Δt	$x(\Delta t)$	s_{average}
1	0	0
0.5	0.25	0.5
0.25	0.1875	0.75
0.125	0.109375	0.875
0.01	0.0099	0.99
0.001	0.000999	0.999
0.0001	0.00009999	0.9999

The pattern in our example is evident. As we make Δt smaller, the average speed is apparently getting closer to 1. ■

In [Example 9.1](#), we say that in the limit as Δt approaches zero, the average speed approaches 1. At time zero, the value 1 is said to be the *instantaneous speed* of the object. This measurement is only valid for time zero. At any other time we may go through the same process to reach an instantaneous measurement as a limit of average measurements. The instantaneous speed is referred to as the *derivative* of position and is denoted by dx/dt or $x'(t)$. The former notation uses *infinitesimals* dx and dt . Think of dx/dt intuitively as specifying a really small (infinitesimal) change in position per really small (infinitesimal) change in time. Before we introduce the formal construction of the derivative, let us take a closer look at what it means to be a limit.

9.1.1 LIMITS

Given a univariate function $f(x)$ that may be computed for values of x near a specified value c , we can repeat the experiment of [Example 9.1](#) by looking at how the function values change for values of x closer and closer to c . If those function values appear to be getting close to some number L , we may formally state this using *limit notation*:

$$\lim_{x \rightarrow c} f(x) = L$$

The notation $x \rightarrow c$ means that you think of choosing x closer and closer to c , or phrased mathematically: The limit as x approaches c of $f(x)$ is L . The intuition for what a limit is should come from our earlier example. A more formal presentation uses the limit notation. The mathematicians say: For each $\varepsilon > 0$ you can find a $\delta > 0$ such that $|f(x) - L| < \varepsilon$ whenever $|x - c| < \delta$. In less formal terms, think of ε as an error tolerance that you select to be small. Your goal is to make the function values $f(x)$ to be within this tolerance of the number L ; that is, $|f(x) - L| < \varepsilon$ is just a requirement on how large the absolute error can be between the function values and L . The allowable error is most likely not met by any value of x you so choose. Rather, the error will cause you to constrain your attention to values of x close to c . That is, as long as $|x - c|$ is small enough (i.e., the absolute difference is smaller than δ), then you will achieve your goal of bounding the function error.

Visually you can think of this process as “boxing the point $(f(x), L)$ ” in the xy -plane. An example will illustrate this.

EXAMPLE 9.2

Let $f(x) = x^2 + x$ and let $c = 1$. [Table 9.2](#) shows various function values for x near c .

Table 9.2

Function Values for x Near c

x	$f(x)$
0.9	1.71
0.99	1.9701
0.999	1.997001
1.001	2.003001
1.01	2.0301
1.1	2.31

The pattern shows that as x approaches 1, $f(x)$ approaches 2. In our limit notation,

$$\lim_{x \rightarrow 1} (x^2 + x) = 2$$

The graph of $f(x)$ near $x = 1$ is shown in [Figure 9.1](#)

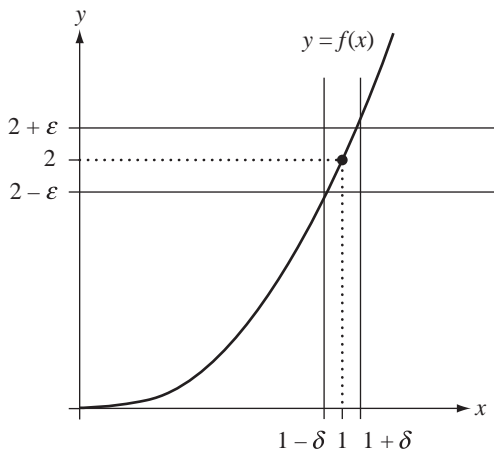


Figure 9.1

The graph of $f(x) = x^2 + x$ for x near 1.

The point $(c, L) = (1, 2)$ is “boxed” in by two pairs of parallel lines. You get to choose $\varepsilon > 0$ and require the function values to be within that tolerance of $L = 2$. The horizontal parallel lines provide two edges of the box. In order for you to be on the graph of $f(x)$ and within the horizontal strip, vertical bars must be drawn sufficiently close to 1. If you find a pair of such bars, any pair closer to 1 will also work, but one pair is all you need. This boxing process must succeed for any choice of ε , no matter how small. Of course, the smaller you choose ε , the smaller you expect to have to choose δ . ■

This process of boxing in (c, L) is made formal mathematically by actually constructing δ as a function of ε . We will not go into such a construction. The intuition is what is important.

In [Example 9.2](#) you might ask yourself why we bothered with the formalism in the first place. Clearly, if you evaluate the function at $x = 1$, you get $f(1) = 1^2 + 1 = 2$. As it turns out, it is not always possible to evaluate $f(x)$ to see what its limit is. For example,

$$f(x) = \frac{\sin(x)}{x}$$

is defined for all $x \neq 0$. You cannot evaluate $f(0)$ because the denominator is zero. However, the limit as x approaches 0 does exist:

$$\lim_{x \rightarrow 0} \frac{\sin(x)}{x} = 1$$

Construct a table of numbers x and $f(x)$ for x closer and closer to zero to see why this is the case. The formal proof of the limit is provided in standard calculus textbooks and requires some trigonometry, algebra, and a bit of patience to complete.

9.1.2 LIMITS OF A SEQUENCE

The concept of a limit was discussed in terms of a *continuous variable* x ; that is, x is a real-valued number that is allowed to approach some other real-valued number. A similar concept exists for a limit of a sequence of numbers f_n for $n \geq 1$. The formal notation for a sequence is $\{f_n\}_{n=1}^{\infty}$ to indicate that the index n is a positive integer and is allowed to become increasingly large. For example, $f_n = 1/n$ denotes a sequence of real numbers 1, 1/2, 1/3, and so on. You should notice that the numbers in this sequence are decreasing in size as n increases. In fact, your intuition should tell you that the numbers have a limiting value of zero.

Just as we had a formal notation for a limit of a function, we have one for a limit of a sequence. The definitions are quite similar. We say that the limit of the sequence $\{f_n\}_{n=1}^{\infty}$ as n increases without bound is L , denoted as

$$\lim_{n \rightarrow \infty} f_n = L$$

when the following is true: For each $\varepsilon > 0$ you can find an integer $N > 0$ such that $|f_n - L| < \varepsilon$ whenever $n \geq N$. The intuition is similar to that of a function. Your goal is to make the sequence values f_n be within the error tolerance ε of the number L ; that is, $|f_n - L| < \varepsilon$ is just a requirement on how large the absolute error can be between the sequence values and L . In order for this to happen, you most likely have to choose n significantly large, the condition indicated by $n \geq N$. Generally, as you choose ε smaller, the index N becomes larger. In our example of $f_n = 1/n$, we believe that the limit is $L = 0$. If you choose a small $\varepsilon > 0$, $|f_n - L| = |1/n| < \varepsilon$ happens whenever $n > 1/\varepsilon$. You may choose N to be the smallest integer that is larger than $1/\varepsilon$. Clearly, the smaller you choose ε , the larger N is.

Limits of sequences are more commonly encountered when working with iterative methods in computer science. Although we have not reached the point in the appendix where we discuss derivatives, you no doubt are familiar with derivatives since computational physics requires that you be so. An iterative method that you most likely encountered is Newton's method for estimating the root of a function $F(x) = 0$. An initial guess x_0 is made for the root. The guess is refined by a sequence

$$x_{n+1} = x_n - \frac{F(x_n)}{F'(x_n)}, \quad n \geq 0$$

where $F'(x)$ is the derivative of $F(x)$. What you hope is that the limit

$$\lim_{n \rightarrow \infty} x_n = L$$

really is a root to F , namely $F(L) = 0$. In order to have a good estimate, you get to choose how close to the root L you would like to be by selecting the error tolerance ε . The corresponding index N tells you how many times to apply the iteration method before you can be confident that x_N is an estimate that meets your tolerance criterion.

9.1.3 CONTINUITY

[Example 9.2](#) illustrated the limit $L = 2$ of a function $f(x) = x^2 + x$ as x approaches $c = 1$. As noted earlier, the function value $f(1)$ and limit 2 are the same number. This happens for most functions you tend to encounter in your applications. The property has a special name. If

$$\lim_{x \rightarrow c} f(x) = f(c)$$

then f is said to be *continuous* at $x = c$. The idea is shown in [Figure 9.1](#). The graph of $f(x)$ at $x = 1$ is a solid curve; that is, the graph to the left of $(1, f(1))$ and the graph to the right of $(1, f(1))$ both meet at the common point $(1, f(1))$.

The function $f(x) = \sin(x)/x$ is not continuous at $x = 0$ because the function is not even defined there. However, if we extend the function as follows:

$$g(x) = \begin{cases} \frac{\sin(x)}{x}, & x \neq 0 \\ 1, & x = 0 \end{cases}$$

The function $g(x)$ is continuous at $x = 0$, because $\lim_{x \rightarrow 0} g(x) = 1 = g(0)$.

If $\lim_{x \rightarrow c} f(x) = L$ exists and $f(c)$ is defined, but $f(c) \neq L$, the function f is said to be *discontinuous* at c . For example, consider

$$f(x) = \begin{cases} 1, & x > 0 \\ 0, & x = 0 \\ -1, & x < 0 \end{cases}$$

The graph of this function is shown in [Figure 9.2](#).

The function is discontinuous at $x = 0$. In fact, no matter how we define $f(0)$, we cannot make this function continuous at zero because there is no way to make a “solid” connection between the graph to the left of zero and the graph to the right of zero.

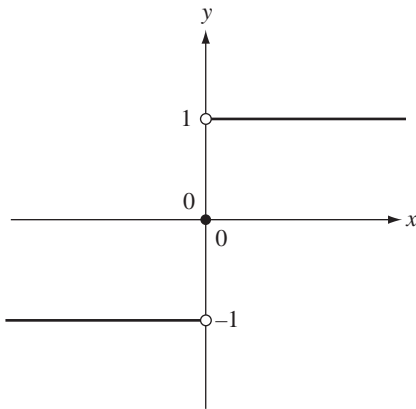


Figure 9.2 The graph of a function that is discontinuous at $x = 0$.

9.1.4 DIFFERENTIATION

As motivation for the concept of derivative and differentiation, let us return to our initial example of computing the instantaneous speed of an object whose position at time t is $x(t)$. By an intuitive limiting process, we computed this speed to be a limit of average speeds of the form $(x(t + \Delta t) - x(t)) / \Delta t$. In formal terms the limit is

$$x'(t) = \lim_{\Delta t \rightarrow 0} \frac{x(t + \Delta t) - x(t)}{\Delta t}$$

The function $x'(t)$ is referred to as the *derivative* of $x(t)$. The derivative exists only when the limit on the right-hand side of the definition exists.

The derivative has a geometric implication that is quite important. Consider the position function in our ongoing example, $x(t) = t(1 - t)$ for $t \in [0, 1]$. Figure 9.3 shows the graph of the function.

The line containing $(0, x(0))$ and $(t_2, x(t_2))$ is called a *secant line* of the graph. The average speed $(x(t_2) - x(0)) / (t_2 - 0)$ is the slope of the secant line. The line through $(0, x(0))$ and $(t_1, x(t_1))$ is yet another secant line and has slope given by the average speed $(x(t_1) - x(0)) / (t_1 - 0)$. As t_1 is chosen to be closer and closer to zero, the limit of the secant lines is the dark gray line shown in the figure. This is called the *tangent line* of the graph at the point $(0, x(0))$. The derivative $x'(t)$ may therefore be viewed as the slope of the tangent line to the graph at $(t, x(t))$.

In the example $x(t) = t(1 - t)$, we had a good guess at the instantaneous speed at $t = 0$ by looking at the average speeds for values of t close to zero. This would be quite a time-consuming process at other values of t . Instead, we can construct a

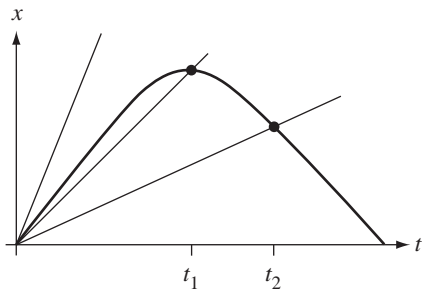


Figure 9.3 The graph of $x(t) = t(1-t)$ with two points marked at times t_1 and t_2 . The light gray lines connecting the origin $(0,0)$ to $(t_1, x(t_1))$ and $(t_2, x(t_2))$ are secant lines to the graph. The dark gray line is the tangent line to the graph at $(0, x(0)) = (0,0)$.

general formula for the derivative by directly applying the limit definition.

$$\begin{aligned}x'(t) &= \lim_{\Delta t \rightarrow 0} \frac{x(t + \Delta t) - x(t)}{\Delta t} \\&= \lim_{\Delta t \rightarrow 0} \frac{(t + \Delta t)(1 - t - \Delta t) - t(1 - t)}{\Delta t} \\&= \lim_{\Delta t \rightarrow 0} \frac{(\Delta t)(1 - 2t - \Delta t) - (\Delta t)^2}{\Delta t} \\&= \lim_{\Delta t \rightarrow 0} (1 - 2t - \Delta t) \\&= 1 - 2t\end{aligned}$$

The last equality is valid since $1 - 2t - \Delta t$ is a continuous function of Δt ; that is, we can just evaluate the argument of the limit with $\Delta t = 0$. Notice that $x'(0) = 1$, but we can evaluate $x'(t)$ at any other t of our choosing.

A function f with domain $[a, b]$ is said to be *differentiable at $x \in (a, b)$* with derivative,

$$f'(x) = \lim_{h \rightarrow 0} \frac{f(x + h) - f(x)}{h}$$

as long as the limit on the right-hand side exists. For most functions we work with, the derivative exists for all points in the domain, but sometimes we meet functions for which this is not the case. The typical example is the function $f(x) = |x|$. The graph consists of two rays, $y = x$ for $x \geq 0$ and $y = -x$ for $x < 0$. The derivative for $x > 0$ is $f'(x) = 1$ (the slope of the ray for $x > 0$). The derivative for $x < 0$ is $f'(x) = -1$.

Table 9.3 Derivatives of Some Common Functions

$f(x)$	$f'(x)$	$f(x)$	$f'(x)$
x^p	px^{p-1}	$\cot(x)$	$\csc^2(x)$
$\sin(x)$	$\cos(x)$	$\exp(x)$	$\exp(x)$
$\cos(x)$	$-\sin(x)$	$\ln(x)$	$\frac{1}{x}$
$\tan(x)$	$\sec^2(x)$		

(the slope of the ray for $x < 0$). However, $f'(0)$ is not defined, so f is not differentiable at $x = 0$. The graph of f has a *cusp*, or *kink*, at the origin.

In a standard calculus course you will spend a lot of time constructing derivatives for many functions that you will encounter in your applications. Table 9.3 provides some common derivatives without going through the formal constructions here.

The function $\exp(x)$ is the natural exponential function and $\ln(x)$ is the natural logarithm function. Derivatives of other functions can be found in calculus or other reference books.

Also of use are some standard identities for working with derivatives. The *product rule* is

$$\frac{d}{dx} (f(x)g(x)) = f(x)g'(x) + f'(x)g(x) \quad (9.1)$$

The notation on the left-hand side indicates the derivative of the product of two functions $f(x)$ and $g(x)$. The right-hand side is that derivative. For example, if $f(x) = x^2$ and $g(x) = \sin(x)$, then

$$\frac{d}{dx} (x^2 \sin(x)) = x^2 \cos(x) + 2x \sin(x)$$

The *quotient rule* is

$$\frac{d}{dx} \left(\frac{f(x)}{g(x)} \right) = \frac{f'(x)g(x) - f(x)g'(x)}{(g(x))^2} \quad (9.2)$$

Using the same f and g as in the last example,

$$\frac{d}{dx} \left(\frac{x^2}{\sin(x)} \right) = \frac{2x \sin(x) - x^2 \cos(x)}{\sin^2(x)}$$

The *chain rule* tells you how to compute the derivative of a composition of two functions, $f(g(x))$,

$$\frac{d}{dx} (f(g(x))) = f'(g(x))g'(x) \quad (9.3)$$

You compute the derivative of $f(y)$ with respect to its argument y , evaluate it at $y = g(x)$, then multiply by the derivative of $g(x)$. Once again using the same f and g as before, the composition is $f(g(x)) = (\sin(x))^2$. The derivative is

$$\frac{d}{dx}(\sin(x))^2 = 2(\sin(x))\cos(x)$$

9.1.5 L'HÔPITAL'S RULE

In some instances, a limit of a quotient of functions needs to be evaluated where both numerator and denominator become zero at the target independent variable value. A rule for evaluating such limits is *L'Hôpital's rule*, named after Guillaume François Antoine Marquis de L'Hôpital (in the 1600s) who wrote the first introductory differential calculus text book in which the rule appeared.

Specifically, if $f(x)$ and $g(x)$ are continuous functions at $x = c$ and $f(c) = g(c) = 0$, an attempt to evaluate

$$\lim_{x \rightarrow c} \frac{f(x)}{g(x)}$$

by direct substitution of $x = c$ fails because the fraction $0/0$ is an *indeterminate form*. If the functions are differentiable at $x = c$ and if $g'(c) \neq 0$, then the limit is, in fact,

$$\lim_{x \rightarrow c} \frac{f(x)}{g(x)} = \lim_{x \rightarrow c} \frac{f'(x)}{g'(x)} = \frac{f'(c)}{g'(c)}$$

For example,

$$\lim_{x \rightarrow 0} \frac{\sin(x)}{x} = \lim_{x \rightarrow 0} \frac{\cos(x)}{1} = \cos(0) = 1$$

which is a result I stated earlier without proof.

9.1.6 INTEGRATION

The other flavor of calculus is *integral calculus*. The concept is motivated by the desire to compute the area of an irregular-shaped region. We are familiar with area formulas for standard geometric objects. The area of a square of width W and height H is $A = WH$. The area of a circle of radius R is $A = \pi R^2$. However, consider as an example the following the region in the first quadrant of the xy -plane bounded by the x -axis and the graph of $y = x(1 - x)$. The graph is a parabola. The natural approach to solving this problem is to attempt to decompose it into regions for which we do know how to compute the area. What is more natural than trying rectangles? Figure 9.4 shows an attempt to fill the region with a few rectangles, all of whose bases are on the x -axis.

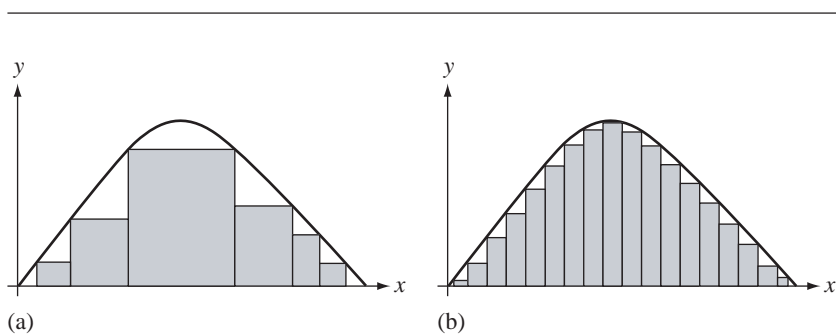


Figure 9.4 An attempt to compute the area bounded by a parabola and the x -axis by filling it with rectangles.

The problem, of course, is that no matter how many rectangles we select, we cannot fill the region. However, the more rectangles we choose and the smaller their widths, the more we can fill the bounded region. The sum of the areas of the rectangles in Figure 9.4(b) provides a better approximation to the true area than does the sum of the areas of the rectangles in Figure 9.4(a).

Have we failed in the attempt? No, as long as we rely on our old friend the limit to help us out. Intuitively, if we let the maximum width of the rectangles approach zero, all the time requiring more rectangles, in a limiting sense we can fill the region with rectangles. The classical argument from a physicist's or engineer's perspective is to think of choosing a rectangle whose width is *infinitesimal*, call this width dx . The rectangle is positioned at x on the axis. The height of the rectangle is just the function value $f(x)$. The rectangle has an *infinitesimal area*, $dA = f(x)dx$, which is just the product of the (infinitesimal) width and height. Sum up all such rectangles as x varies over the relevant domain to obtain the area of the region. The *summation* is not finite, so to speak, so rather than using the standard capital sigma (Σ) to denote the summation, historically a large S-shaped symbol was used (S for sum). In our example the area is indicated by the notation,

$$A = \int_0^1 x(1-x) dx$$

The right-hand side is referred to as the *definite integral* of $f(x) = x(1-x)$ on the domain $[0, 1]$. For a function $f(x)$ on a domain $[a, b]$, the definite integral is

$$\int_a^b f(x) dx \quad (9.4)$$

The function $f(x)$ is referred to as the *integrand* of the definite integral.

The process of computing the definite integrals is called *integration*. Our intuitive approach leads us to believe that the sum of the infinitesimal areas should be the area of the bounded region, but to obtain the actual area we would need to provide more formal details on computing a general formula for the area. Once again these are details you discuss in a standard calculus course. For our purposes, we just need to know the end result, the mechanical means by which you *integrate* the function $f(x)$. One of the most important results from calculus relates differentiation and integration:

Fundamental Theorem of Calculus. If $F(x) = \int_a^x f(\xi) d\xi$ is the definite integral of $f(\xi)$ on the interval $[a, x]$, then $F'(x) = f(x)$. That is, the derivative of $F(x)$ is just the integrand $f(x)$. The function $F(x)$ is said to be an *antiderivative* of $f(x)$. The relationship is sometimes written concisely as

$$\frac{d}{dx} \int_a^x f(\xi) d\xi = f(x)$$

which says that the derivative is the inverse operation of integration.

The result is general knowledge for us, but historically differential calculus and integral calculus were developed independently. Pierre de Fermat and René Descartes worked on the aspects of computing tangent lines to graphs (differential calculus) whereas Bonaventura Francesco Cavalieri and Christiaan Huygens worked on the aspects of calculating areas (integral calculus), all of this in the 1600s. Also in the 1600s, Isaac Newton and Gottfried Wilhelm von Leibniz independently discovered that, in fact, differentiation and integration were directly related, the result being the fundamental theorem of calculus.

With the fundamental theorem at hand, let us revisit the problem of computing the area bounded by a parabola and the x -axis. We had stated this as a definite integral, $A = \int_0^1 x(1-x) dx$. An antiderivative $F(x)$ for $f(x) = x(1-x) = x - x^2$ is a function for which $F'(x) = f(x)$. Using our knowledge about derivatives of polynomial terms, we can integrate a polynomial term in the reverse manner. That is, an antiderivative of x^p is $x^{p+1}/(p+1)$ as long as $p \neq -1$. An antiderivative of $x - x^2$ is therefore $F(x) = x^2/2 - x^3/3$. The antiderivative mentioned in the fundamental theorem has the property that $F(a) = 0$, but in general an antiderivative can be any function for which $F'(x) = f(x)$. That is, the antiderivative is not unique. When we choose one, we integrate by

$$\int_a^b f(x) dx = F(x)|_a^b = F(b) - F(a)$$

where the vertical bar in the middle expression is a notation that says to evaluate F at the top number and subtract from it F evaluated at the bottom number.

The area of the bounded region is, therefore,

$$A = \int_0^1 x(1-x) dx = \left. \frac{x^2}{2} - \frac{x^3}{3} \right|_0^1 = \left(\frac{1}{2} - \frac{1}{3} \right) - \left(\frac{0}{2} - \frac{0}{3} \right) = \frac{1}{6}$$

9.2 MULTIVARIATE CALCULUS

Multivariate calculus involves studying functions $y = f(x_1, \dots, x_n)$ with n independent variables x_1 through x_n and one dependent variable y . The heart of the topic is once again *limits*, but the introduction of multiple independent variables makes it somewhat more challenging and interesting. For the sake of making the constructions look like the ones for univariate functions, define $\mathbf{x} = (x_1, \dots, x_n)$ and $y = f(\mathbf{x})$.

9.2.1 LIMITS AND CONTINUITY

If we choose values of \mathbf{x} close to a specified point \mathbf{c} and if the corresponding function values $f(\mathbf{x})$ are close to a number L , we say that L is the limit of $f(\mathbf{x})$ as \mathbf{x} approaches \mathbf{c} . The formal notation is

$$\lim_{\mathbf{x} \rightarrow \mathbf{c}} f(\mathbf{x}) = L$$

The mathematical definition is just like the one for univariate functions. The limit exists and is the value L if for each $\varepsilon > 0$, there is a $\delta > 0$ such that $|f(\mathbf{x}) - L| < \varepsilon$ whenever $|\mathbf{x} - \mathbf{c}| < \delta$. The value ε may once again be viewed as an error tolerance. In order to make $f(\mathbf{x})$ differ from L by no more than the tolerance, we need to choose \mathbf{x} suitably close to \mathbf{c} . The value δ tells you how close. Observe that $|\mathbf{y}|$ denotes the length of the vector \mathbf{y} . This definition applies for any number $n \geq 1$ of independent variables, so the univariate case $n = 1$ is automatically covered by the definition.

The function $f(\mathbf{x})$ is said to be *continuous at \mathbf{c}* whenever f is defined at \mathbf{c} , the limit of f as \mathbf{x} approaches \mathbf{c} exists, and the limit is

$$\lim_{\mathbf{x} \rightarrow \mathbf{c}} f(\mathbf{x}) = f(\mathbf{c})$$

Many functions you will encounter in physical applications are continuous. For example, polynomial functions are continuous at all points and the process of computing the limit is simply one of evaluating the function.

9.2.2 DIFFERENTIATION

A univariate function $y = f(x)$ that is differentiable has derivative $dy/dx = f'(x)$, a measure of instantaneous rate of change of f at the value x . We can make similar measurements of instantaneous rates of change for a multivariate function

$y = f(x_1, \dots, x_n)$ with respect to each independent variable. If x_i is the independent variable of interest, the rate of change is called the *partial derivative of f with respect to x_i* . Its definition is similar to the one for univariate functions,

$$\frac{\partial f}{\partial x_i} = \lim_{h \rightarrow 0} \frac{f(x_1, \dots, x_i + h, \dots, x_n) - f(x_1, \dots, x_i, \dots, x_n)}{h}$$

The term *partial* is used to indicate that the rate of change is with respect to only one of the variables. The univariate differential operator was named d/dx and uses a regular Roman letter d . The partial derivative operator is $\partial/\partial x_i$; the symbol ∂ is used to indicate that the setting involves multiple independent variables.

EXAMPLE
9.3

When working with two independent variables, rather than indexing them, we sometimes use $z = f(x, y)$. The partial derivatives are $\partial f / \partial x$ and $\partial f / \partial y$. Consider $z = f(x, y) = x^2 y^3$. The partial derivatives are

$$\frac{\partial f}{\partial x} = 2xy^3, \quad \frac{\partial f}{\partial y} = 3x^2y^2$$

Notice that in computing $\partial f / \partial x$, the variable y was treated as a constant as far as x is concerned. As a function of x alone, think of $F(x) = cx^2$ (the constant c is y^3) whose derivative is $F'(x) = 2cx^2$. ■

All the derivative formulas that you know for univariate functions apply to multivariate functions. You simply treat the function as one that depends only on the independent variable x_i of interest, with all other $x_j (j \neq i)$ treated as constants. The product rule and quotient rule both apply to multivariate differentiation.

The Chain Rule

The chain rule, that differentiation rule that applies to composition of functions, is more complicated when multiple independent variables are present. The issue is that each independent variable may be a function of other variables; composition can occur in multiple components. For example, consider the function $g(y_1, y_2) = f(x_1(y_1, y_2), x_2(y_1, y_2), x_3(y_1, y_2))$, where f is a function of three independent variables x_1 , x_2 , and x_3 , but each of these variables is a function of two other variables y_1 and y_2 . The resulting composition is named $g(y_1, y_2)$, a function of two independent variables. We would like to see how g varies with respect to each of the independent variables. As y_1 varies, notice that each of the three components of f varies since those components are compositions involving y_1 . You should expect that the rate of change of g with respect to y_1 involves the rates of change of f with respect to all of its independent variables. In fact, the partial derivative of g with respect to y_1 is

$$\frac{\partial g}{\partial y_1} = \frac{\partial f}{\partial x_1} \frac{\partial x_1}{\partial y_1} + \frac{\partial f}{\partial x_2} \frac{\partial x_2}{\partial y_1} + \frac{\partial f}{\partial x_3} \frac{\partial x_3}{\partial y_1}$$

Each term in the summation on the right-hand side looks like the term you see in the univariate version of the chain rule. Similarly, the partial derivative of g with respect to y_2 is

$$\frac{\partial g}{\partial y_2} = \frac{\partial f}{\partial x_1} \frac{\partial x_1}{\partial y_2} + \frac{\partial f}{\partial x_2} \frac{\partial x_2}{\partial y_2} + \frac{\partial f}{\partial x_3} \frac{\partial x_3}{\partial y_2}$$

Generally, if f depends on n independent variables x_1 through x_n and each of the x_i depends on m independent variables y_1 through y_m , then the partial derivative of f when viewed as a function of the y_j is

$$\frac{\partial}{\partial y_j} f(x_1, \dots, x_n) = \sum_{i=1}^n \frac{\partial f}{\partial x_i} \frac{\partial x_i}{\partial y_j}$$

In the event that the x_i depend only on another single variable t – say $x_i(t)$ are the components as functions of t – then the notation changes slightly (but not the idea):

$$\frac{d}{dt} f(x_1, \dots, x_n) = \sum_{i=1}^n \frac{\partial f}{\partial x_i} \frac{dx_i}{dt}$$

The change is due to the fact that f viewed as a function of t alone is univariate, so the d notation is used rather than ∂ .

We used the chain rule many times in our coverage of Lagrangian dynamics to compute the partial derivatives of the kinetic energy function.

Directional Derivatives

Consider a multivariate function $f(\mathbf{x})$ where $\mathbf{x} \in \mathbb{R}^n$. The partial derivatives measure rates of change with respect to each independent variable of the function. Effectively, the rate of change is measured with respect to the direction vector associated with the independent variable. For example, the function $f(x_1, x_2)$ has partial derivatives,

$$\frac{\partial f}{\partial x_1} = \lim_{h \rightarrow 0} \frac{f(x_1 + h, x_2) - f(x_1, x_2)}{h}$$

The measurements are made in the $x_1 x_2$ -plane in the direction $(1, 0)$ associated with x_1 . That is, the limit formula can be thought of as

$$\frac{\partial f}{\partial x_1} = \lim_{h \rightarrow 0} \frac{f((x_1, x_2) + h(1, 0)) - f((x_1, x_2))}{h}$$

Similarly,

$$\frac{\partial f}{\partial x_2} = \lim_{h \rightarrow 0} \frac{f(x_1, x_2 + h) - f(x_1, x_2)}{h} = \lim_{h \rightarrow 0} \frac{f((x_1, x_2) + h(0, 1)) - f((x_1, x_2))}{h}$$

and the rate of change is measured in the direction $(0, 1)$ associated with x_2 .

It is natural to ask how f changes in another unit-length direction (u_1, u_2) . Using the pattern you see in the partial derivatives, that rate of change should be as shown:

$$\lim_{h \rightarrow 0} \frac{f((x_1, x_2) + h(u_1, u_2)) - f((x_1, x_2))}{h}$$

As it turns out, this quantity can be shown to be equal to

$$u_1 \frac{\partial f}{\partial x_1} + u_2 \frac{\partial f}{\partial x_2}$$

which is a weighted sum of the partial derivatives of f . The sum is called the *directional derivative of f* in the specified direction. We can write this in a coordinate-free manner by defining $\mathbf{x} = (x_1, x_2)$ and $\mathbf{u} = (u_1, u_2)$, and by defining the *gradient of f* to be the vector of partial derivatives of f , namely

$$\nabla f = \left(\frac{\partial f}{\partial x_1}, \frac{\partial f}{\partial x_2} \right)$$

The directional derivative at \mathbf{x} in the direction \mathbf{u} is $\mathbf{u} \cdot \nabla f(\mathbf{x})$. This form of the directional derivative applies to any number of independent variables,

$$\mathbf{u} \cdot \nabla f(\mathbf{x}) = \sum_{i=1}^n u_i \frac{\partial f}{\partial x_i}$$

EXAMPLE
9.4

Let $f(x, y) = x^2y^3$. The directional derivative at $(1, 2)$ in the direction $(3/5, 4/5)$ is

$$(3/5, 4/5) \cdot (2xy^3, 3x^2y^2)|_{(1,2)} = (3/5, 4/5) \cdot (16, 12) = 19.2$$

The vertical bar notation means that you evaluate the variable terms on the right using the specific point that occurs as a subscript on the bar. ■

The partial derivatives $\partial f / \partial x$ and $\partial f / \partial y$ of $f(x, y)$ have a geometric interpretation, just as the ordinary derivative $f'(x)$ of $f(x)$ did. In the univariate case, $f'(x)$ is the slope of the tangent line to the graph of $f(x)$ at x . That is, the tangent line at $(x, f(x))$ has direction $(1, f'(x))$. In the multivariate case, and assuming the function is differentiable, the graph at $(x, y, f(x, y))$ has a *tangent plane*. If you walk in a specific direction in the xy -plane, there is a corresponding *tangent line* in the tangent plane. If the planar direction is $(1, 0)$, the corresponding tangent line has direction $(1, 0, \partial f / \partial x)$. If the direction is $(0, 1)$, the tangent line has direction $(0, 1, \partial f / \partial y)$. Generally, the direction (u_1, u_2) in the xy -plane generates a tangent line whose direction is

$$\left(u_1, u_2, u_1 \frac{\partial f}{\partial x} + u_2 \frac{\partial f}{\partial y} \right)$$

In coordinate-free form, this vector is $(\mathbf{u}, \mathbf{u} \cdot \nabla f)$. Given two linearly independent tangent line directions, the tangent plane normal \mathbf{N} must be the normalized cross

product of those directions. In particular, as long as $\nabla f \neq \mathbf{0}$, the tangent line directions corresponding to $(1, 0)$ and $(0, 1)$ are linearly independent and the tangent plane normal is

$$\mathbf{N} = \frac{(1, 0, \partial f / \partial x) \times (0, 1, \partial f / \partial y)}{|(1, 0, \partial f / \partial x) \times (0, 1, \partial f / \partial y)|} = \frac{(-\partial f / \partial x, -\partial f / \partial y, 1)}{\sqrt{1 + (\partial f / \partial x)^2 + (\partial f / \partial y)^2}}$$

9.2.3 INTEGRATION

The motivation for the definite integral of a univariate function was based on computing the area bounded by the graph of a function $f(x)$ and the x -axis. A similar motivation applies for multivariate functions. In particular, let us consider bivariate functions $f(x, y)$ that are nonnegative. Let $\mathcal{D} \subset \mathbb{R}^2$ be the domain of the function whose boundary is a simple closed curve. The region \mathcal{R} bounded by the graph of $z = f(x, y)$, the xy -plane, and the boundary of \mathcal{D} extruded vertically, has a finite volume. We can attempt to “fill” \mathcal{R} with vertical rectangular solids whose bases are axis-aligned in the xy -plane. Figure 9.5 shows the bases of some rectangular solids as an attempt to fill the region.

Naturally, just as in the univariate case, we cannot fill \mathcal{R} with a finite number of rectangular solids because the graph of the function has variable slope. Moreover, we cannot even fill \mathcal{D} with rectangular bases because its shape is also not a union of a finite number of rectangles. In a limiting sense, though, we can obtain better and better approximations by using rectangles with smaller area bases and lots more of them. From the infinitesimal perspective, if an axis-aligned rectangular base is chosen to be very small, say of dimensions dx by dy , and placed at $(x, y) \in \mathcal{D}$, the height of the rectangle is $f(x, y)$. The infinitesimal volume covered by the rectangular solid is the product of the infinitesimal area of the base, $dx dy$, with the height $f(x, y)$, namely

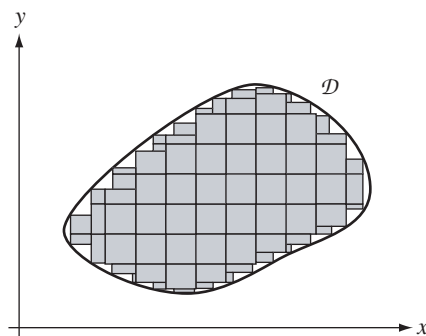


Figure 9.5 Bases of some rectangular solids as an attempt to fill the domain \mathcal{D} .

$dV = f(x, y)dx dy$. If we “add” these up for all $(x, y) \in \mathcal{D}$, we obtain the volume

$$V = \int_{\mathcal{D}} f(x, y)dx dy$$

a multidimensional integral. The question is how do we make sense of this and evaluate it. The answer is to use *iterated integration* by decomposing the domain so that we can fix y , integrate with respect to x , then integrate with respect to y . When we use iterated integrals, the integral sign in the last displayed equation is replaced by two integral signs.

**EXAMPLE
9.5**

Let us compute the volume of the solid bounded by the graph of $f(x, y) = 4 - x^2 - y^2$ on the closed disk \mathcal{D} , $x^2 + y^2 \leq 1$. The volume is

$$V = \iint_{\mathcal{D}} 4 - x^2 - y^2 dx dy$$

A fixed value of y in the domain corresponds to a horizontal line segment that touches the left and right hemispheres of the disk. The x values on that segment vary from $-\sqrt{1-y^2}$ to $\sqrt{1-y^2}$. The y values themselves vary from -1 to 1 . The iterated integral is

$$V = \int_{-1}^1 \int_{-\sqrt{1-y^2}}^{\sqrt{1-y^2}} 4 - x^2 - y^2 dx dy$$

Treating y as a constant, the “innermost integral” is evaluated.

$$\begin{aligned} V &= \int_{-1}^1 \left(\int_{-\sqrt{1-y^2}}^{\sqrt{1-y^2}} 4 - x^2 - y^2 dx \right) dy \\ &= \int_{-1}^1 (4 - y^2)x - \frac{1}{3}x^3 \Big|_{-\sqrt{1-y^2}}^{\sqrt{1-y^2}} dy \\ &= 2 \int_{-1}^1 (4 - y^2)\sqrt{1 - y^2} - \frac{1}{3}(1 - y^2)^{3/2} dy \end{aligned}$$

The last integral is univariate. Although one is apparently taught in calculus courses that closed-form antiderivatives are the goal, in practice that is typically not the case. An integral of the type we now have can be approximated using numerical integration algorithms. ■

The same iterated integration method applies in more dimensions. The technical challenge in higher dimensions is invariably the decomposition of the domain of the function in order to construct the limits of integration. However, numerical methods do exist for numerical integration without having to formally decompose the domain. These methods are discussed in standard numerical analysis textbooks such as [BF01].

Other examples of multivariate integrals are found in [Section 2.5](#). Computing centers of mass and inertia tensors are the main application of multivariate integration in a physics simulation.

9.3 APPLICATIONS

This section contains a few applications that are relevant to physical simulation. The first section is on optimization of a function, the process of constructing minima and/or maxima of the function. An illustrative example of optimization for a univariate function is provided: determining whether or not an oriented bounding box intersects a plane where the box is both translating and rotating in space. The specified time interval is $[0, T]$. The distance between the box and plane is time-varying, say $D(t)$. The box will intersect the plane if the minimum value of $D(t)$ on $[0, T]$ is zero. An example for multivariate function is provided and arises in the problem of computing the closest point on a triangle to a specified point.

Constrained optimization involves computing minima and/or maxima of a function, but with additional constraints on the variables. Only equality constraints are considered here. The method of solution uses Lagrange multipliers. An illustrative example of constrained optimization is provided: computing the distance between two objects whose boundary surfaces are level surfaces, ellipsoids being the prototypical case.

Finally, in constructing numerical methods for solving differential equations, we need to approximate derivatives by finite differences. The numerical methods of [Chapter 13](#) all require such approximations. The last application discussed here is about obtaining approximations of a specified order of error.

9.3.1 OPTIMIZATION

The ideas for optimization are first summarized for univariate functions. The extension of the ideas to multivariate functions is then provided.

Univariate Functions

Let $f(x)$ be a differentiable function with domain $[a, b]$. We wish to locate the value x_{\min} for which $f(x_{\min})$ is a minimum. That is, $f(x_{\min}) \leq f(x)$ for all $x \in [a, b]$. Similarly, we want to locate the value x_{\max} for which $f(x)$ is a maximum: $f(x) \leq f(x_{\max})$ for all $x \in [a, b]$. A typical function with these values is shown in [Figure 9.6](#).

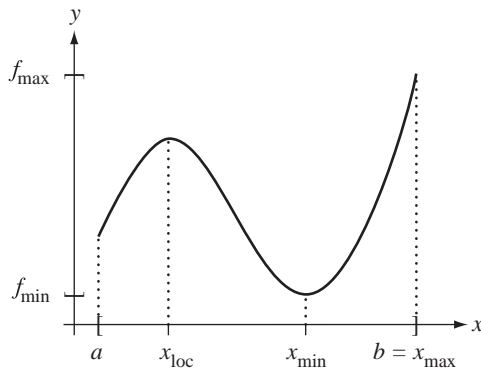


Figure 9.6 The graph of a function $f(x)$ on its domain $[a, b]$.

The function has a *local maximum* at x_{loc} . Such a point has the property that $f(x) \leq f(x_{\text{loc}})$ for all x *nearby* x_{loc} . That is, the maximum value for the function is only relevant in the locale near x_{loc} . The function has a *local minimum* at x_{min} . Such a point has the property that $f(x) \geq f(x_{\text{min}})$ for all x *nearby* x_{min} . That is, the minimum value for the function is only relevant in the locale near x_{min} . In this particular example the local minimum happens to be the *global minimum* for the function. The *global maximum* for the function occurs at $x_{\text{max}} = b$, an endpoint of the domain interval.

Generally, a *global extremum* (minimum or maximum) occurs at a point where the derivative of the function exists and is zero, or where the derivative does not exist, or at an endpoint of the interval. The process of function optimization involves locating all such candidate points, evaluating the function at these points, and choosing the optimum value. In Figure 9.6 we would find x_{loc} and x_{min} as solutions to $f'(x) = 0$ and we would look at $x = a$ and $x = b$ since they are the endpoints of the domain interval. An analysis of $f(a), f(b), f(x_{\text{loc}})$, and $f(x_{\text{min}})$ shows that $f_{\text{min}} = f(x_{\text{min}})$ and $f_{\text{max}} = f(b)$.

The technical challenge in computing global extrema is, of course, solving the equation $f'(x) = 0$ and/or determining where $f'(x)$ is undefined. Even when $f(x)$ is a polynomial, implementing fast and robust numerical methods to solve for zeros of the derivative is sometimes difficult.

EXAMPLE
9.6

Compute the global extrema of $f(x) = x^3 - 2x^2 - 4x - 5$ on the interval $[-1, 3]$. The derivative of f is $f'(x) = 3x^2 - 4x - 4$. The roots to $f'(x) = 0$ are computed using the quadratic equation: $x = 2$ and $x = -2/3$. The function values that contain the extrema are $f(-1) = -4$, $f(3) = -8$, $f(2) = -13$, and $f(-2/3) = -95/27 \doteq -3.518$. The global minimum is $f_{\text{min}} = -13$ and the global maximum is $f_{\text{max}} = -95/27$. ■

EXAMPLE
9.7

An oriented bounding box (OBB) is translating and rotating through space. Its center at time t is $\mathbf{C}(t)$. The box axis directions are $\mathbf{U}_0(t)$, $\mathbf{U}_1(t)$, and $\mathbf{U}_2(t)$. The directions are unit-length and mutually perpendicular. The extents (half-widths) along each axis are e_0 , e_1 , and e_2 . Points in the OBB are

$$\mathbf{X}(t) = \mathbf{C}(t) + R(t)\mathbf{Y}$$

where $R(t) = [\mathbf{U}_0(t) | \mathbf{U}_1(t) | \mathbf{U}_2(t)]$ is a rotation matrix whose columns are the box axis directions and where $\mathbf{Y}(t) = (y_0, y_1, y_2)$ with $|y_i| \leq e_i$ for all i .

We are interested in when the OBB will first contact a stationary plane given by $\mathbf{N} \cdot \mathbf{X} = d$, where \mathbf{N} is a unit-length normal to the plane and \mathbf{X} is any point on the plane. At first time of contact, the distance between the OBB and the plane is a minimum.

At time zero, the OBB and plane are assumed not to be intersecting and the OBB is on the side of the plane to which the normal points. The distance from the OBB to the plane at time t is the distance between the plane and a corner of the OBB that is closest to the plane. This corner has the property that its projection onto the normal line $s\mathbf{N}$ is closer to the plane than are other corners (possibly two or more corners are equally close). The projection of any OBB point $\mathbf{X}(t)$ is $s(t)\mathbf{N}$, where

$$s(t) = \mathbf{N} \cdot \mathbf{X}(t) = \mathbf{N} \cdot (\mathbf{C}(t) + R(t)\mathbf{Y})$$

At first time of contact it is the case that $s = d$, the plane constant. The smallest $s(t)$ for all points occurs at one of the eight corners. These corners occur for one of the eight possibilities $\mathbf{Y} = (\pm e_0, \pm e_1, \pm e_2)$. The eight projection values are

$$\begin{aligned} s(t) &= \mathbf{N} \cdot \mathbf{X}(t) \\ &= \mathbf{N} \cdot (\mathbf{C}(t) \pm e_0 \mathbf{U}_0(t) \pm e_1 \mathbf{U}_1(t) \pm e_2 \mathbf{U}_2(t)) \\ &= \mathbf{N} \cdot \mathbf{C}(t) \pm e_0 \mathbf{N} \cdot \mathbf{U}_0(t) \pm e_1 \mathbf{N} \cdot \mathbf{U}_1(t) \pm e_2 \mathbf{N} \cdot \mathbf{U}_2(t) \end{aligned}$$

The closest corner occurs when $s(t)$ is as small as possible, so

$$s(t) = \mathbf{N} \cdot \mathbf{C}(t) - e_0 |\mathbf{N} \cdot \mathbf{U}_0(t)| - e_1 |\mathbf{N} \cdot \mathbf{U}_1(t)| - e_2 |\mathbf{N} \cdot \mathbf{U}_2(t)|$$

Because we required the OBB to be initially on the side of the plane to which \mathbf{N} points, it is the case that $s(0) > d$. If we define $f(t) = (s(t) - d)^2$ and limit our collision query to $t \in [0, T]$ for some user-specified maximum time $T > 0$, we have reduced the problem to calculating the minimum of $f(t)$ on the interval $[0, T]$ and testing if that minimum is zero. The roots to $f'(t) = 0$ occur when $s(t) = d$ or when $s'(t) = 0$. The ease or difficulty with which we can solve this problem depends on the simplicity or complexity of the translation $\mathbf{C}(t)$ and the orientation matrix $R(t)$. ■

Multivariate Functions

Locating the global extrema of multivariate functions has similarities to the univariate case but is geometrically more challenging. The abstract idea of the univariate case extends naturally. A global extremum must occur either at a point where the “derivative” is zero, a point where the “derivative” is undefined, or at a boundary

point of the domain. The “derivative” in the multivariate case is the gradient vector of the function $f(\mathbf{x})$, namely ∇f .

When we have n independent variables, the equation $\nabla f = \mathbf{0}$ represents n equations in n unknowns. The equations are generally nonlinear, so numerical methods must be applied to solve them. The standard method is a multidimensional Newton’s method. Once the solutions are found, they can be classified as maxima points, minima points, or saddle points by using second-order partial derivatives. The classification requires knowing about eigenvalues and eigenvectors and is covered in detail in [Section 7.5.2](#).

The analysis of the function f restricted to its boundary points can itself be complicated depending on the function, but in fact the analysis is one of *recursive descent in dimension*. Consider a bivariate function $f(x, y)$ with an irregular-shaped domain \mathcal{D} in the xy -plane. Suppose that the boundary of \mathcal{D} is a simple closed curve parameterized by $(x(t), y(t))$ for $t \in [a, b]$. The restriction of f to the boundary is $g(t) = f(x(t), y(t))$. The global extrema of $g(t)$ on $[a, b]$ may be found. This is a one-dimensional problem (one independent parameter t) whereas finding the points where $\nabla f = \mathbf{0}$ is a two-dimensional problem (two independent variables x and y). Thus, the analysis of the boundary is in fewer dimensions than that of the interior of \mathcal{D} .

The recursive descent for a function $f(x, y, z)$ is similar. Let \mathcal{D} be the domain of the function whose boundary is a simple closed surface. The candidate extrema in the interior of \mathcal{D} are obtained by solving $\nabla f = \mathbf{0}$, a system of three equations in three unknowns. The boundary surface can be parameterized by two variables, say s and t , that parameterization being $(x(s, t), y(s, t), z(s, t))$. The parameter domain is denoted \mathcal{P} ; that is, each parameter pair $(s, t) \in \mathcal{P}$. The function f restricted to the boundary is $g(s, t) = f(x(s, t), y(s, t), z(s, t))$. We now need to compute the global extrema of $g(s, t)$ for $(s, t) \in \mathcal{P}$. This is a two-dimensional problem whereas, the original was in three dimensions. The two-dimensional problem involves determining where $\nabla g = \mathbf{0}$, a system of two equations in two unknowns. The global extrema of g on the boundary of \mathcal{P} (a curve) is performed by parameterizing the boundary by a parameter r . The boundary curve is $(s(r), t(r))$ for $r \in [a, b]$ and the restriction of g to the boundary is $h(r) = g(s(r), t(r))$. The reduction in dimension has led us to a one-dimensional problem.

EXAMPLE 9.8

Compute the global minimum of $f(s, t) = a_{00}s^2 + 2a_{01}st + a_{11}t^2 + 2b_0s + 2b_1t + c$ for (s, t) in the triangular domain $s \geq 0$, $t \geq 0$, and $s + t \leq 1$. We will assume that $a_{00} > 0$ and $a_{00}a_{11} - a_{01}^2 > 0$ so that the graph of f is a paraboloid opening upwards, thus a global minimum exists.

The gradient of f is

$$\nabla f = 2(a_{00}s + a_{01}t + b_0, a_{01}s + a_{11}t + b_1)$$

The equation $\nabla f = \mathbf{0}$ leads to two linear equations in the two unknowns s and t . The solution is

$$\bar{s} = \frac{-a_{11}b_0 + a_{01}b_1}{a_{00}a_{11} - a_{01}^2}, \quad \bar{t} = \frac{+a_{01}b_0 - a_{00}b_1}{a_{00}a_{11} - a_{01}^2}$$

(Example 9.8
continued)

If (\bar{s}, \bar{t}) is inside the triangular domain, then $f(\bar{s}, \bar{t})$ must be the global minimum since the graph is a paraboloid opening upwards. If it is not in the triangular domain, then we need to search for the minimum of f restricted to the boundary.

On the boundary $s = 0$ with $t \in [0, 1]$, the function is $g(t) = f(0, t) = a_{11}t^2 + 2b_1t + c$. The minimum of g occurs when $g'(t) = 0$ or at $t = 0$ or $t = 1$. The equation $g'(t) = 0$ has solution

$$\hat{t} = -\frac{b_1}{a_{11}}$$

The candidate minima are $g(0) = c$, $g(1) = a_{11} + 2b_1 + c$, and $g(\hat{t})$.

On the boundary $t = 0$ with $s \in [0, 1]$, the function is $h(s) = f(s, 0) = a_{00}s^2 + 2b_0s + c$. The minimum of h occurs when $h'(s) = 0$ or at $s = 0$ or $s = 1$. The equation $h'(s) = 0$ has solution

$$\hat{s} = -\frac{b_0}{a_{00}}$$

The candidate minima are $h(0) = c$, $h(1) = a_{00} + 2b_0 + c$, and $h(\hat{s})$.

Finally, on the boundary $s + t = 1$ with $s \in [0, 1]$, the function is $p(s) = f(s, 1-s) = (a_{00} - 2a_{01} + a_{11})s^2 + 2(a_{01} - a_{11} + b_0 - b_1)s + (a_{11} + 2b_1 + c)$. The minimum of p occurs when $p'(s) = 0$ or at $s = 0$ or $s = 1$. The equation $p'(s) = 0$ has solution

$$\tilde{s} = \frac{-a_{01} + a_{11} - b_0 + b_1}{a_{00} - 2a_{01} + a_{11}}$$

The candidate minima are $p(0) = a_{11} + 2b_1 + c$, $p(1) = a_{00} + 2b_0 + c$, and $p(\tilde{s})$.

The global minimum is the smallest of $g(0)$, $g(1)$, $g(\hat{t})$, $h(1)$, $h(\hat{s})$, and $p(\tilde{s})$. Notice that $g(0)$ corresponds to $f(0, 0)$, $g(1)$ corresponds to $f(0, 1)$, and $h(1)$ corresponds to $f(1, 0)$, the function values at the vertices of the triangular domain. The values $g(\hat{t})$, $h(\hat{s})$, and $p(\tilde{s})$ correspond to local minima on the lines containing the edges of the triangular domain.

By the way, this exact problem arises when computing the distance from a point to a triangle in 2D or in 3D. The s and t values are the variables of the standard parameterization for a triangle. The point (s, t) at which the global minimum of f occurs corresponds to the closest point on the triangle to the specified point. ■

EXERCISE 9.1

Establish the connection just described in Example 9.8 between distance from point to triangle and minimization of $f(s, t)$.

9.3.2 CONSTRAINED OPTIMIZATION

We have already seen that local extrema of multivariate functions $f(\mathbf{x})$ occur when the gradient is zero, $\nabla f(\mathbf{x}) = \mathbf{0}$. Sometimes an additional equality constraint is placed on the independent variable, say $g(\mathbf{x}) = 0$ for some multivariate function g . The

constraint causes dependencies within the set of independent variables, thus reducing the number of independent ones.

Constrained optimization is the term used to refer to problems of this type. A classical method for handling these is called the *method of Lagrange multipliers*. The method involves introducing another parameter into the problem, call it λ , and analyzing

$$h(\mathbf{x}, \lambda) = f(\mathbf{x}) + \lambda g(\mathbf{x})$$

The constraint $g = 0$ generally causes a reduction from n independent variables to $n - 1$. The introduction of λ raises this back to n independent variables. The function h is optimized in the manner mentioned earlier, by determining those \mathbf{x} and λ for which the gradient of h is zero. Notice that the gradient of h has one more component than the gradient of f . To stress this difference, we use the notation

$$\nabla h = \left(\frac{\partial h}{\partial x}, \frac{\partial h}{\partial \lambda} \right) = (\nabla f + \lambda \nabla g, g)$$

Setting $\nabla h = \mathbf{0}$ leads to $\nabla f + \lambda \nabla g = \mathbf{0}$ and $g = 0$. The second equation is just the constraint with which we started. The first equation is solved by dotting with ∇g ,

$$\lambda = -\frac{\nabla f \cdot \nabla g}{|\nabla g|^2}$$

assuming of course that ∇g is not identically the zero vector. Resubstituting this in the first equation, we obtain

$$\nabla f - \frac{\nabla f \cdot \nabla g}{|\nabla g|^2} \nabla g = \mathbf{0}$$

This equation provides n equations in the n unknown variables x_1 through x_n and may be solved by numerical methods for multidimensional root finding.

If m multiple constraints are specified, say $g_j(\mathbf{x}) = 0$ for $1 \leq j \leq m$, the same introduction of parameters λ_j allows for a similar method of solution. The λ_j are called *Lagrange multipliers*. The new function to optimize is

$$h(\mathbf{x}, \lambda_1, \dots, \lambda_m) = f(\mathbf{x}) + \sum_{j=1}^m \lambda_j g_j(\mathbf{x})$$

The gradient of h is

$$\nabla h = \left(\frac{\partial h}{\partial x}, \frac{\partial h}{\partial \lambda_1}, \dots, \frac{\partial h}{\partial \lambda_m} \right) = \left(\nabla f + \sum_{j=1}^m \lambda_j \nabla g_j, g_1, \dots, g_m \right)$$

Setting the first component of the gradient vector to the zero vector yields

$$\nabla f + \sum_{j=1}^m \lambda_j \nabla g_j = \mathbf{0} \tag{9.5}$$

Setting the other components to zero reproduces the constraints $g_j = 0$ for all j . Dotting equation (9.5) with ∇g_i for $1 \leq i \leq m$ gives us a set of m equations in the m unknown Lagrange multipliers,

$$\sum_{j=1}^m \nabla g_i \cdot \nabla g_j \lambda_j = -\nabla f \cdot \nabla g_i$$

If $A = [a_{ij}]$ is an $m \times m$ matrix with $a_{ij} = \nabla g_i \cdot \nabla g_j$, if $\mathbf{B} = [b_i]$ is an $m \times 1$ vector with $b_i = -\nabla f \cdot \nabla g_i$, and if $\boldsymbol{\Lambda} = [\lambda_j]$, the system of equations is $A\boldsymbol{\Lambda} = \mathbf{B}$, a linear system that can be solved whenever A is invertible: $\boldsymbol{\Lambda} = A^{-1}\mathbf{B}$. The λ_j from the solution are resubstituted into equation (9.5), thereby giving us a single vector-valued equation of n equations in the n unknowns x_1 through x_n .

EXAMPLE 9.9

Two ellipsoids are defined implicitly by the quadratic equations $g_j(\mathbf{x}) = \mathbf{x}^T A_j \mathbf{x} + \mathbf{b}_j^T \mathbf{x} + c_j = 0$, $j = 1$ and $j = 2$. The 3×3 matrices A_j are positive definite (symmetric with positive eigenvalues). Let us assume that the ellipsoids are separated, so the distance between them is positive. How do we go about computing the distance?

Let \mathbf{x} be a point on the first ellipsoid, so $g_1(\mathbf{x}) = 0$. Let \mathbf{y} be a point on the second ellipsoid, so $g_2(\mathbf{y}) = 0$. The squared distance between these two points is

$$f(\mathbf{x}, \mathbf{y}) = |\mathbf{x} - \mathbf{y}|^2$$

We wish to select \mathbf{x} and \mathbf{y} that minimize $f(\mathbf{x}, \mathbf{y})$ subject to the constraints that $g_1(\mathbf{x}) = 0$ and $g_2(\mathbf{y}) = 0$. The number of independent variables is six, three for the first ellipsoid and three for the second ellipsoid. Each constraint reduces the number of independent variables by one, leaving us (implicitly) with four independent variables. This makes sense in that \mathbf{x} and \mathbf{y} each lie on an ellipsoid, a two-dimensional surface. We have two degrees of freedom for each point, a total of four degrees of freedom.

Using the method of Lagrange multipliers, define

$$\begin{aligned} h(\mathbf{x}, \mathbf{y}, \lambda_1, \lambda_2) &= f(\mathbf{x}, \mathbf{y}) + \lambda_1 g_1(\mathbf{x}) + \lambda_2 g_2(\mathbf{y}) \\ &= |\mathbf{x} - \mathbf{y}|^2 + \lambda_1 (\mathbf{x}^T A_1 \mathbf{x} + \mathbf{b}_1^T \mathbf{x} + c_1) + \lambda_2 (\mathbf{y}^T A_2 \mathbf{y} + \mathbf{b}_2^T \mathbf{y} + c_2) \end{aligned}$$

Setting the gradient of h to zero yields four vector-valued equations

$$\begin{aligned} \partial h / \partial \mathbf{x} &= 2(\mathbf{x} - \mathbf{y}) + \lambda_1 (2A_1 \mathbf{x} + \mathbf{b}_1) = \mathbf{0} \\ \partial h / \partial \mathbf{y} &= 2(\mathbf{y} - \mathbf{x}) + \lambda_2 (2A_2 \mathbf{y} + \mathbf{b}_2) = \mathbf{0} \\ \partial h / \partial \lambda_1 &= \mathbf{x}^T A_1 \mathbf{x} + \mathbf{b}_1^T \mathbf{x} + c_1 = 0 \\ \partial h / \partial \lambda_2 &= \mathbf{y}^T A_2 \mathbf{y} + \mathbf{b}_2^T \mathbf{y} + c_2 = 0 \end{aligned} \tag{9.6}$$

The last two equations of equation (9.6) are just the original constraints. The first two equations have a geometric interpretation. The minimum distance between the ellipsoids is attained by points \mathbf{x} on the first and \mathbf{y} on the second and is the closest pair of points, one point per ellipsoid. Sketch a picture to convince yourself that the vector connecting these two, $\mathbf{x} - \mathbf{y}$, is perpendicular to both ellipsoids at the closest

points. The gradient vectors of the implicitly defined surfaces are perpendicular to their respective surfaces. The gradient of the first ellipsoid is $\nabla g_1(\mathbf{x}) = 2A_1\mathbf{x} + \mathbf{b}_1$, the gradient of the second is $\nabla g_2(\mathbf{y}) = 2A_2\mathbf{y} + \mathbf{b}_2$. The vectors $\mathbf{x} - \mathbf{y}$ and $2A_1\mathbf{x} + \mathbf{b}_1$ are parallel so some linear combination of the two vectors must be the zero vector. This is exactly what the first equation in (9.6) says. The same argument applies to $\mathbf{x} - \mathbf{y}$ and $2A_2\mathbf{y} + \mathbf{b}_2$; the second equation of (9.6) says the two vectors are parallel.

The first two equations of (9.6) may be solved directly to obtain the Lagrange multipliers, then we resubstitute the multipliers into the equations to obtain the following system of two equations in two vector-valued unknowns:

$$\mathbf{x} - \mathbf{y} - \frac{(\mathbf{x} - \mathbf{y}) \cdot (2A_1\mathbf{x} + \mathbf{b}_1)}{|2A_1\mathbf{x} + \mathbf{b}_1|^2} (2A_1\mathbf{x} + \mathbf{b}_1) = \mathbf{0}$$

and

$$\mathbf{x} - \mathbf{y} - \frac{(\mathbf{x} - \mathbf{y}) \cdot (2A_2\mathbf{y} + \mathbf{b}_2)}{|2A_2\mathbf{y} + \mathbf{b}_2|^2} (2A_2\mathbf{y} + \mathbf{b}_2) = \mathbf{0}$$

A multidimensional numerical root finder may be used to compute the solutions. ■

9.3.3 DERIVATIVE APPROXIMATIONS BY FINITE DIFFERENCES

In numerical methods for solving ordinary differential equations of the type shown in Chapter 13, and in numerical methods for solving partial differential equations, we invariably need to use approximations to ordinary derivatives and to partial derivatives in order to establish the iterative method itself. The following material shows how to obtain such approximations.

Given a small value $h > 0$, the d th order derivative satisfies the following equation where the integer order of error $p > 0$ may be selected as desired,

$$\frac{h^d}{d!} F^{(d)}(x) + O(h^{d+p}) = \sum_{i=i_{\min}}^{i_{\max}} C_i F(x + ih) \quad (9.7)$$

for some choice of extreme indices i_{\min} and i_{\max} and for some choice of coefficients C_i . The equation becomes an approximation by throwing away the $O(h^{d+p})$ term. The vector $\vec{C} = (C_{i_{\min}}, \dots, C_{i_{\max}})$ is called the *template* for the approximation. Approximations for the derivatives of multivariate functions are constructed as tensor products of templates for univariate functions.

Derivatives of Univariate Functions

The following approximations are valid for the derivative of $F(x)$. A *forward difference approximation* is

$$F'(x) = \frac{F(x + h) - F(x)}{h} + O(h) \quad (9.8)$$

a *backward difference approximation* is

$$F'(x) = \frac{F(x) - F(x-h)}{h} + O(h) \quad (9.9)$$

and a *centered difference approximation* is

$$F'(x) = \frac{F(x+h) - F(x-h)}{2h} + O(h^2) \quad (9.10)$$

The approximations are obtained by throwing away the error terms indicated by the O notation. The order of the error for each of these approximations is easily seen from formal expansions as Taylor series about the value x ,

$$F(x+h) = F(x) + hF'(x) + \frac{h^2}{2!}F''(x) + \dots = \sum_{n=0}^{\infty} \frac{h^n}{n!} F^{(n)}(x)$$

and

$$F(x-h) = F(x) - hF'(x) + \frac{h^2}{2!}F''(x) + \dots = \sum_{n=0}^{\infty} (-1)^n \frac{h^n}{n!} F^{(n)}(x)$$

where $F^{(n)}(x)$ denotes the n th order derivative of F . The first equation leads to the forward difference $F'(x) = (F(x+h) - F(x))/h + O(h)$. The second equation leads to the backward difference $F'(x) = (F(x) - F(x-h))/h + O(h)$. Both approximations have error $O(h)$. The centered difference is obtained by subtracting the second equation from the first to obtain $(F(x+h) - F(x-h))/(2h) + O(h^2)$.

Higher-order approximations to the first derivative can be obtained by using more Taylor series, more terms in the Taylor series, and cleverly weighting the various expansions in a sum. For example,

$$F(x+2h) = \sum_{n=0}^{\infty} \frac{(2h)^n}{n!} F^{(n)}(x) \quad \text{and} \quad F(x-2h) = \sum_{n=0}^{\infty} (-1)^n \frac{(2h)^n}{n!} F^{(n)}(x)$$

lead to a forward difference approximation with second-order error,

$$F'(x) = \frac{-F(x+2h) + 4F(x+h) - 3F(x)}{2h} + O(h^2) \quad (9.11)$$

to a backward difference approximation with second-order error,

$$F'(x) = \frac{3F(x) - 4F(x-h) + F(x-2h)}{2h} + O(h^2) \quad (9.12)$$

and to a centered difference approximation with fourth-order error,

$$F'(x) = \frac{-F(x+2h) + 8F(x+h) - 8F(x-h) + F(x-2h)}{12h} + O(h^4) \quad (9.13)$$

Higher-order derivatives can be approximated in the same way. For example, a forward difference approximation to $F''(x)$ is

$$F''(x) = \frac{F(x+2h) - 2F(x+h) + F(x)}{h^2} + O(h) \quad (9.14)$$

and centered difference approximations are

$$F''(x) = \frac{F(x+h) - 2F(x) + F(x-h)}{h^2} + O(h^2) \quad (9.15)$$

and

$$F''(x) = \frac{-F(x+2h) + 16F(x) - 30F(x) + 16F(x-h) - F(x-2h)}{12h^2} + O(h^4) \quad (9.16)$$

Each of these formulas is easily verified by expanding the $F(x+ih)$ terms in a formal Taylor series and computing the weighted sums on the right-hand sides. However, of greater interest is to select the order of derivative d and the order of error p and determine the weights C_i for the sum in equation (9.7). A formal Taylor series for $F(x+ih)$ is

$$F(x+ih) = \sum_{n=0}^{\infty} i^n \frac{h^n}{n!} F^{(n)}(x)$$

Replacing this in equation (9.7) yields

$$\begin{aligned} \frac{h^d}{d!} F^{(d)}(x) + O(h^{d+p}) &= \sum_{i=i_{\min}}^{i_{\max}} C_i \sum_{n=0}^{\infty} i^n \frac{h^n}{n!} F^{(n)}(x) \\ &= \sum_{n=0}^{\infty} \left(\sum_{i=i_{\min}}^{i_{\max}} i^n C_i \right) \frac{h^n}{n!} F^{(n)}(x) \\ &= \sum_{n=0}^{d+p-1} \left(\sum_{i=i_{\min}}^{i_{\max}} i^n C_i \right) \frac{h^n}{n!} F^{(n)}(x) + O(h^{d+p}) \end{aligned}$$

Multiplying by $d!/h^d$, the desired approximation is

$$F^{(d)}(x) = \frac{d!}{h^d} \sum_{n=0}^{d+p-1} \left(\sum_{i=i_{\min}}^{i_{\max}} i^n C_i \right) \frac{h^n}{n!} F^{(n)}(x) + O(h^p) \quad (9.17)$$

In order for equation (9.17) to be satisfied, it is necessary that

$$\sum_{i=i_{\min}}^{i_{\max}} i^n C_i = \begin{cases} 0, & 0 \leq n \leq d+p-1 \text{ and } n \neq d \\ 1, & n = d \end{cases} \quad (9.18)$$

Table 9.4 Parameters for Various Finite Difference Approximations

Equation	d	p	Approximation	i_{\min}	i_{\max}
(9.8)	1	1	forward	0	1
(9.9)	1	1	backward	-1	0
(9.10)	1	2	centered	-1	1
(9.11)	1	2	forward	0	2
(9.12)	1	2	backward	-2	0
(9.13)	1	4	centered	-2	2
(9.14)	2	1	forward	0	2
(9.15)	2	2	centered	-1	1
(9.16)	2	4	centered	-2	2

This is a set of $d + p$ linear equations in $i_{\max} - i_{\min} + 1$ unknowns. If we constrain the number of unknowns to be $d + p$, the linear system has a unique solution. A *forward difference approximation* occurs if we set $i_{\min} = 0$ and $i_{\max} = d + p - 1$. A *backward difference approximation* occurs if we set $i_{\max} = 0$ and $i_{\min} = -(d + p - 1)$. A *centered difference approximation* occurs if we set $i_{\max} = -i_{\min} = (d + p - 1)/2$ where it appears that $d + p$ is necessarily an odd number. As it turns out, p can be chosen to be even regardless of the parity of d and $i_{\max} = \lfloor (d + p - 1)/2 \rfloor$.

Table 9.4 indicates the choices for d and p , the type of approximation (forward, backward, or centered), and the corresponding equation number.

EXAMPLE
9.10

Approximate $F^{(3)}(x)$ with a forward difference with error $O(h)$, $d = 3$, and $p = 1$. We need $i_{\min} = 0$ and $i_{\max} = 3$. The linear system from equation (9.18) is

$$\begin{bmatrix} 1 & 1 & 1 & 1 \\ 0 & 1 & 2 & 3 \\ 0 & 1 & 4 & 9 \\ 0 & 1 & 8 & 27 \end{bmatrix} \begin{bmatrix} C_0 \\ C_1 \\ C_2 \\ C_3 \end{bmatrix} = \begin{bmatrix} 0 \\ 0 \\ 0 \\ 1 \end{bmatrix}$$

and has solution $(C_0, C_1, C_2, C_3) = (-1, 3, -3, 1)/6$. Equation (9.17) becomes

$$F^{(3)}(x) = \frac{-F(x) + 3F(x + h) - 3F(x + 2h) + F(x + 3h)}{h^3} + O(h)$$

Approximate $F^{(3)}(x)$ with a centered difference with error $O(h^2)$, so $d = 3$ and $p = 2$. We need $i_{\max} = -i_{\min} = 2$. The linear system from equation (9.18) is

$$\begin{bmatrix} 1 & 1 & 1 & 1 & 1 \\ -2 & -1 & 0 & 1 & 2 \\ 4 & 1 & 0 & 1 & 4 \\ -8 & -1 & 0 & 1 & 8 \\ 16 & 1 & 0 & 1 & 16 \end{bmatrix} \begin{bmatrix} C_{-2} \\ C_{-1} \\ C_0 \\ C_1 \\ C_2 \end{bmatrix} = \begin{bmatrix} 0 \\ 0 \\ 0 \\ 1 \\ 0 \end{bmatrix}$$

and has solution $(C_{-2}, C_{-1}, C_0, C_1, C_2) = (-1, 2, 0, -2, 1)/12$. Equation (9.17) becomes

$$F^{(3)}(x) = \frac{-F(x-2h) + 2F(x-h) - 2F(x+h) + F(x+2h)}{2h^3} + O(h^2)$$

Finally, approximate with a centered difference with error $O(h^4)$, so $d = 3$ and $p = 4$. We need $i_{\max} = -i_{\min} = 3$. The linear system from equation (9.18) is

$$\begin{bmatrix} 1 & 1 & 1 & 1 & 1 & 1 \\ -3 & -2 & -1 & 0 & 1 & 2 & 3 \\ 9 & 4 & 1 & 0 & 1 & 4 & 9 \\ -27 & -8 & -1 & 0 & 1 & 8 & 27 \\ 81 & 16 & 1 & 0 & 1 & 16 & 81 \\ -243 & -32 & -1 & 0 & 1 & 32 & 243 \\ 729 & 64 & 1 & 0 & 1 & 64 & 729 \end{bmatrix} \begin{bmatrix} C_{-3} \\ C_{-2} \\ C_{-1} \\ C_0 \\ C_1 \\ C_2 \\ C_3 \end{bmatrix} = \begin{bmatrix} 0 \\ 0 \\ 0 \\ 1 \\ 0 \\ 0 \\ 0 \end{bmatrix}$$

and has solution $(C_{-3}, C_{-2}, C_{-1}, C_0, C_1, C_2, C_3) = (1, -8, 13, 0, -13, 8, -1)/48$. Equation (9.17) becomes

$$F^{(3)}(x) = \frac{F(x-3h) - 8F(x-2h) + 13F(x-h) - 13F(x+h) + 8F(x+2h) - F(x+3h)}{8h^3} + O(h^4)$$

■

EXAMPLE
9.11

Approximate $F^{(4)}(x)$ with a forward difference with error $O(h)$, so $d = 4$ and $p = 1$. We need $i_{\min} = 0$ and $i_{\max} = 4$. The linear system from equation (9.18) is

$$\begin{bmatrix} 1 & 1 & 1 & 1 & 1 \\ 0 & 1 & 2 & 3 & 4 \\ 0 & 1 & 4 & 9 & 16 \\ 0 & 1 & 8 & 27 & 64 \\ 0 & 1 & 16 & 81 & 256 \end{bmatrix} \begin{bmatrix} C_0 \\ C_1 \\ C_2 \\ C_3 \\ C_4 \end{bmatrix} = \begin{bmatrix} 0 \\ 0 \\ 0 \\ 0 \\ 1 \end{bmatrix}$$

and has solution $(C_0, C_1, C_2, C_3, C_4) = (1, -4, 6, -4, 1)/24$. Equation (9.17) becomes

$$F^{(4)}(x) = \frac{F(x) - 4F(x+h) + 6F(x+2h) - 4F(x+3h) + F(x+4h)}{h^4} + O(h).$$

Approximate $F^{(4)}(x)$ with a centered difference with error $O(h^2)$, $d = 4$, and $p = 2$. We need $i_{\max} = -i_{\min} = 2$. The linear system from equation (9.18) is

$$\begin{bmatrix} 1 & 1 & 1 & 1 & 1 \\ -2 & -1 & 0 & 1 & 2 \\ 4 & 1 & 0 & 1 & 4 \\ -8 & -1 & 0 & 1 & 8 \\ 16 & 1 & 0 & 1 & 16 \end{bmatrix} \begin{bmatrix} C_{-2} \\ C_{-1} \\ C_0 \\ C_1 \\ C_2 \end{bmatrix} = \begin{bmatrix} 0 \\ 0 \\ 0 \\ 0 \\ 1 \end{bmatrix}$$

(Example 9.11
continued) and has solution $(C_{-2}, C_{-1}, C_0, C_1, C_2) = (1, -4, 6, -4, 1)/24$. Equation (9.17) becomes

$$F^{(4)}(x) = \frac{F(x-2h) - 4F(x-h) + 6F(x) - 4F(x+h) + F(x+2h)}{h^4} + O(h^2)$$

Finally, approximate with a centered difference with error $O(h^4)$, $d = 4$, and $p = 4$. We need $i_{\max} = -i_{\min} = 3$. The linear system from equation (9.18) is

$$\begin{bmatrix} 1 & 1 & 1 & 1 & 1 & 1 \\ -3 & -2 & -1 & 0 & 1 & 2 & 3 \\ 9 & 4 & 1 & 0 & 1 & 4 & 9 \\ -27 & -8 & -1 & 0 & 1 & 8 & 27 \\ 81 & 16 & 1 & 0 & 1 & 16 & 81 \\ -243 & -32 & -1 & 0 & 1 & 32 & 243 \\ 729 & 64 & 1 & 0 & 1 & 64 & 729 \end{bmatrix} \begin{bmatrix} C_{-3} \\ C_{-2} \\ C_{-1} \\ C_0 \\ C_1 \\ C_2 \\ C_3 \end{bmatrix} = \begin{bmatrix} 0 \\ 0 \\ 0 \\ 0 \\ 1 \\ 0 \\ 0 \end{bmatrix}$$

and has solution $(C_{-3}, C_{-2}, C_{-1}, C_0, C_1, C_2, C_3) = (-1, 12, -39, 56, -39, 12, -1)/144$. Equation (9.17) becomes

$$\begin{aligned} F^{(4)}(x) \\ = \frac{-F(x-3h) + 12F(x-2h) - 39F(x-h) + 56F(x) - 39F(x+h) + 12F(x+2h) - F(x+3h)}{6h^4} \\ + O(h^4) \end{aligned}$$

Derivatives of Bivariate Functions

For functions with more variables, the partial derivatives can be approximated by grouping together all of the same variables and applying the univariate approximation for that group. For example, if $F(x, y)$ is our function, then some partial derivative approximations are

$$\begin{aligned} f_x(x, y) &\doteq \frac{F(x+h, y) - F(x-h, y)}{2h} \\ f_y(x, y) &\doteq \frac{F(x, y+k) - F(x, y-k)}{2k} \\ f_{xx}(x, y) &\doteq \frac{F(x+h, y) - 2f(x, y) + F(x-h, y)}{h^2} \\ f_{yy}(x, y) &\doteq \frac{F(x, y+k) - 2f(x, y) + F(x, y-k)}{k^2} \\ f_{xy}(x, y) &\doteq \frac{F(x+h, y+k) - F(x+h, y-k) - F(x-h, y+k) + F(x-h, y-k)}{4hk} \end{aligned}$$

Each of these can be verified in the limit: the x -derivatives by taking the limit as h approaches zero, the y -derivatives by taking the limit as y approaches zero, and the mixed second-order derivative by taking the limit as both h and k approach zero.

The derivatives F_x , F_y , F_{xx} , and F_{yy} just use the univariate approximation formulas. The mixed derivative requires slightly more work. The important observation is that the approximation for F_{xy} is obtained by applying the x -derivative approximation for F_x , then applying the y -derivative approximation to the previous approximation. That is,

$$\begin{aligned} f_{xy}(x, y) &\doteq \frac{F(x+h, y) - F(x-h, y)}{2h} \\ &\doteq \frac{\frac{F(x+h, y+k) - F(x-h, y+k)}{2h} - \frac{F(x+h, y-k) - F(x-h, y-k)}{2h}}{2k} \\ &= \frac{F(x+h, y+k) - F(x+h, y-k) - F(x-h, y+k) + F(x-h, y-k)}{4hk} \end{aligned}$$

The approximation implied by equation (9.7) may be written as

$$\frac{h^m}{m!} \frac{d^m}{dx^m} F(x) \doteq \sum_{i=i_{\min}}^{i_{\max}} C_i^{(m)} F(x + ih) \quad (9.19)$$

The inclusion of the superscript on the C coefficients is to emphasize that those coefficients are constructed for each order m . For bivariate functions, we can use the natural extension of equation (9.19) by applying the approximation in x first, then applying the approximation in y to that approximation, just as in our example of F_{xy} .

$$\begin{aligned} \frac{k^n}{n!} \frac{\partial^n}{\partial y^n} \frac{h^m}{m!} \frac{\partial^m}{\partial x^m} F(x, y) &\doteq \frac{k^n}{n!} \frac{\partial^n}{\partial y^n} \sum_{i=i_{\min}}^{i_{\max}} C_i^{(m)} F(x + ih, y) \\ &\doteq \sum_{i=i_{\min}}^{i_{\max}} \sum_{j=j_{\min}}^{j_{\max}} C_i^{(m)} C_j^{(n)} F(x + ih, y + jk) \\ &= \sum_{i=i_{\min}}^{i_{\max}} \sum_{j=j_{\min}}^{j_{\max}} C_{i,j}^{(m,n)} F(x + ih, y + jk) \end{aligned} \quad (9.20)$$

where the last equality defines

$$C_{i,j}^{(m,n)} = C_i^{(m)} C_j^{(n)}$$

The coefficients for the bivariate approximation are just the tensor product of the coefficients for each of the univariate approximations.

Derivatives of Multivariate Functions

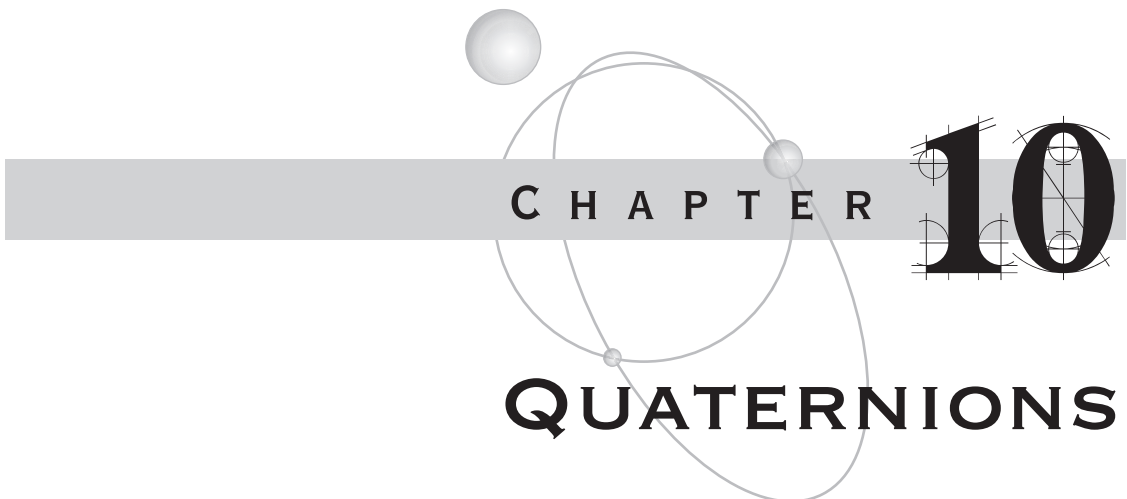
The approximation concept extends to any number of variables. Let (x_1, \dots, x_n) be those variables and let $F(x_1, \dots, x_n)$ be the function to approximate. The approximation is

$$\begin{aligned} & \left(\frac{h_1^{m_1}}{m_1!} \frac{\partial^{m_1}}{\partial x_1^{m_1}} \cdots \frac{h_n^{m_n}}{m_n!} \frac{\partial^{m_n}}{\partial x_n^{m_n}} \right) F(x_1, \dots, x_n) \\ & \doteq \sum_{i_1=i_1^{\min}}^{i_1^{\max}} \cdots \sum_{i_n=i_n^{\min}}^{i_n^{\max}} C_{(i_1, \dots, i_n)}^{(m_1, \dots, m_n)} F(x_1 + i_1 h_1, \dots, x_n + i_n h_n) \end{aligned} \quad (9.21)$$

where

$$C_{(i_1, \dots, i_n)}^{(m_1, \dots, m_n)} = C_{i_1}^{(m_1)} \cdots C_{i_n}^{(m_n)}$$

a tensor product of the coefficients of the n univariate approximations.



Qaternions are a powerful way to represent rotations within computer graphics and physics applications. Unfortunately, the mathematical complexity of quaternions seems to discourage some practitioners from any attempt at understanding them. As an aid to such understanding, a section is provided that constructs a matrix representing rotation about an arbitrary axis. The matrix is based on knowing how to rotate about the z -axis and uses the concept of change of basis from linear algebra. Afterwards, two sections are presented, each with a different view of what a quaternion is. [Section 10.2](#) is the classical approach that defines quaternions in terms of symbols i , j , and k and shows how they are related to rotation. [Section 10.3](#) motivates the idea of a quaternion based solely on concepts from linear algebra. In this setting a quaternion is a rotation matrix in 4D whose geometric actions are easy to understand.

[Section 10.4](#) discusses how to interpolate a sequence of quaternions. This is useful for smooth animation and for smooth motion of objects. [Section 10.5](#) discusses how to differentiate a quaternion function of time, which is used in the differential equations of motion.

10.1 ROTATION MATRICES

Let us review a concept that you are no doubt already familiar with, rotation in the xy -plane. The rotation of the vector (x, y) about the origin by an angle $\theta > 0$ is the vector (x', y') specified by

$$x' = \cos(\theta)x - \sin(\theta)y, \quad y' = \sin(\theta)x + \cos(\theta)y$$

The formula is derivable using a standard trigonometric construction. The direction of rotation is counterclockwise about the origin. In vector-matrix form the equation is

$$\begin{bmatrix} x' \\ y' \end{bmatrix} = \begin{bmatrix} \cos(\theta) & -\sin(\theta) \\ \sin(\theta) & \cos(\theta) \end{bmatrix} \begin{bmatrix} x \\ y \end{bmatrix}$$

If we now add a third dimension, the rotation of the vector (x, y, z) about the z -axis by an angle $\theta > 0$ is just a rotation of the (x, y) portion about the origin in the xy -plane. The rotated vector (x', y', z') is specified by

$$\begin{bmatrix} x' \\ y' \\ z' \end{bmatrix} = \begin{bmatrix} \cos(\theta) & -\sin(\theta) & 0 \\ \sin(\theta) & \cos(\theta) & 0 \\ 0 & 0 & 1 \end{bmatrix} \begin{bmatrix} x \\ y \\ z \end{bmatrix}$$

Setting $\mathbf{v} = [x \ y \ z]^T$, $\mathbf{v}' = [x' \ y' \ z']^T$, $s = \sin(\theta)$, and $c = \cos(\theta)$, the rotation is $\mathbf{v}' = R_0 \mathbf{v}$, where R_0 is the rotation matrix,

$$R_0 = \begin{bmatrix} c & -s & 0 \\ s & c & 0 \\ 0 & 0 & 1 \end{bmatrix} \quad (10.1)$$

The standard coordinate axis directions, represented as 3×1 vectors, are $\mathbf{i} = [1 \ 0 \ 0]^T$, $\mathbf{j} = [0 \ 1 \ 0]^T$, and $\mathbf{k} = [0 \ 0 \ 1]^T$. Observe that

$$R_0 \mathbf{i} = \begin{bmatrix} c \\ s \\ 0 \end{bmatrix} = c\mathbf{i} + s\mathbf{j}, \quad R_0 \mathbf{j} = \begin{bmatrix} -s \\ c \\ 0 \end{bmatrix} = -s\mathbf{i} + c\mathbf{j}, \quad R_0 \mathbf{k} = \begin{bmatrix} 0 \\ 0 \\ 1 \end{bmatrix} = \mathbf{k} \quad (10.2)$$

The vectors $R_0 \mathbf{i}$, $R_0 \mathbf{j}$, and $R_0 \mathbf{k}$ are the columns of the rotation matrix R_0 .

The equation for rotation of a vector $\mathbf{v} \in \mathbb{R}^3$ by an angle $\theta > 0$ about an axis with unit-length direction \mathbf{d} is derived next. Let \mathbf{a} and \mathbf{b} be vectors in the plane that contains the origin and has normal \mathbf{d} . Moreover, choose these vectors so that $\{\mathbf{a}, \mathbf{b}, \mathbf{d}\}$ is a right-handed orthonormal set: each vector is unit length; the vectors are mutually perpendicular; and $\mathbf{a} \times \mathbf{b} = \mathbf{d}$, $\mathbf{b} \times \mathbf{d} = \mathbf{a}$, and $\mathbf{d} \times \mathbf{a} = \mathbf{b}$. Figure 10.1 shows a typical choice.

The orthonormal set of vectors may be used as a basis for \mathbb{R}^3 , both as domain and range of the rotational transformation. The matrix R_0 in equation (10.1) represents the rotation in this basis. A matrix R_1 that represents the rotation in the standard basis will transform \mathbf{a} , \mathbf{b} , and \mathbf{d} as

$$R_1 \mathbf{a} = c\mathbf{a} + s\mathbf{b}, \quad R_1 \mathbf{b} = -s\mathbf{a} + c\mathbf{b}, \quad R_1 \mathbf{d} = \mathbf{d} \quad (10.3)$$

The similarity between equations (10.3) and equations (10.2) is no coincidence. The equations in (10.2) may be collected into a single equation using the convenient

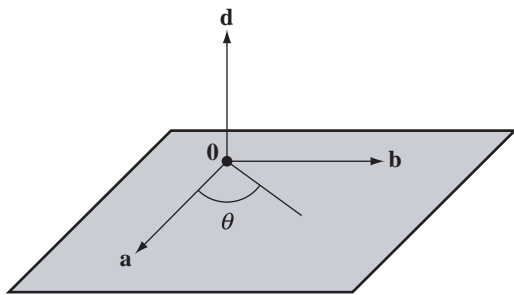


Figure 10.1 A right-handed orthonormal set of vectors. A rotation is desired about \mathbf{d} by the angle $\theta > 0$.

bookkeeping that block matrices provide,

$$R_1 [\mathbf{a} \mid \mathbf{b} \mid \mathbf{d}] = [c\mathbf{a} + s\mathbf{b} \mid -s\mathbf{a} + c\mathbf{b} \mid \mathbf{d}] = [\mathbf{a} \mid \mathbf{b} \mid \mathbf{d}] \begin{bmatrix} c & -s & 0 \\ s & c & 0 \\ 0 & 0 & 1 \end{bmatrix}$$

The matrix $P = [\mathbf{a} \mid \mathbf{b} \mid \mathbf{d}]$ is itself a rotation since $\{\mathbf{a}, \mathbf{b}, \mathbf{d}\}$ is a right-handed orthonormal set, so its inverse is just its transpose. The last displayed equation is $R_1 P = PR_0$. Solving for $R_1 = PR_0P^T$, we have

$$\begin{aligned} R_1 &= [\mathbf{a} \mid \mathbf{b} \mid \mathbf{d}] \begin{bmatrix} c & -s & 0 \\ s & c & 0 \\ 0 & 0 & 1 \end{bmatrix} [\mathbf{a} \mid \mathbf{b} \mid \mathbf{d}]^T \\ &= [\mathbf{a} \mid \mathbf{b} \mid \mathbf{d}] \begin{bmatrix} c & -s & 0 \\ s & c & 0 \\ 0 & 0 & 1 \end{bmatrix} \begin{bmatrix} \mathbf{a}^T \\ \mathbf{b}^T \\ \mathbf{d}^T \end{bmatrix} \\ &= [\mathbf{a} \mid \mathbf{b} \mid \mathbf{d}] \begin{bmatrix} c\mathbf{a}^T - s\mathbf{b}^T \\ s\mathbf{a}^T + c\mathbf{b}^T \\ \mathbf{d}^T \end{bmatrix} \\ &= \mathbf{a}(c\mathbf{a}^T - s\mathbf{b}^T) + \mathbf{b}(s\mathbf{a}^T + c\mathbf{b}^T) + \mathbf{d}\mathbf{d}^T \\ &= c(\mathbf{a}\mathbf{a}^T + \mathbf{b}\mathbf{b}^T) + s(\mathbf{b}\mathbf{a}^T - \mathbf{a}\mathbf{b}^T) + \mathbf{d}\mathbf{d}^T \end{aligned} \tag{10.4}$$

Keep in mind that $\mathbf{a}\mathbf{a}^T$ is the product of a 3×1 matrix and a 1×3 matrix, the result being a 3×3 matrix. This is not the same as $\mathbf{a}^T\mathbf{a}$, a product of a 1×3 matrix and a 3×1 matrix, the result being a 1×1 matrix (a scalar). Similarly, $\mathbf{b}\mathbf{b}^T$, $\mathbf{d}\mathbf{d}^T$, $\mathbf{b}\mathbf{a}^T$,

and \mathbf{ab}^T are 3×3 matrices. From a computational perspective, R_1 is easily computed from [equation \(10.4\)](#), but requires selecting \mathbf{a} and \mathbf{b} for the specified axis direction \mathbf{d} . Your intuition, though, should tell you that the rotation about the axis is independent of which pair of orthonormal vectors you choose in the plane. The following construction shows how to remove the dependence.

The representation of \mathbf{v} in the basis $\{\mathbf{a}, \mathbf{b}, \mathbf{d}\}$ is

$$\mathbf{v} = (\mathbf{a} \cdot \mathbf{v})\mathbf{a} + (\mathbf{b} \cdot \mathbf{v})\mathbf{b} + (\mathbf{d} \cdot \mathbf{v})\mathbf{d} = \alpha\mathbf{a} + \beta\mathbf{b} + \delta\mathbf{d} \quad (10.5)$$

where the last equality defines α , β , and δ as the dot products of the basis vectors with \mathbf{v} . This renaming is done for simplicity of notation in the ensuing constructions. A couple of vector quantities of interest are

$$\mathbf{d} \times \mathbf{v} = \mathbf{d} \times (\alpha\mathbf{a} + \beta\mathbf{b} + \delta\mathbf{d}) = \alpha\mathbf{d} \times \mathbf{a} + \beta\mathbf{d} \times \mathbf{b} + \delta\mathbf{d} \times \mathbf{d} = -\beta\mathbf{a} + \alpha\mathbf{b} \quad (10.6)$$

and

$$\mathbf{d} \times (\mathbf{d} \times \mathbf{v}) = \mathbf{d} \times (\alpha\mathbf{b} - \beta\mathbf{a}) = \alpha\mathbf{d} \times \mathbf{b} - \beta\mathbf{d} \times \mathbf{a} = -\alpha\mathbf{a} - \beta\mathbf{b} \quad (10.7)$$

The cross product $\mathbf{d} \times \mathbf{v}$ can be written as a matrix multiplied by a vector:

$$\begin{aligned} \mathbf{d} \times \mathbf{v} &= \begin{bmatrix} d_1 \\ d_2 \\ d_3 \end{bmatrix} \times \begin{bmatrix} v_1 \\ v_2 \\ v_3 \end{bmatrix} \\ &= \begin{bmatrix} d_2 v_3 - d_3 v_2 \\ d_3 v_1 - d_1 v_3 \\ d_1 v_2 - d_2 v_1 \end{bmatrix} \\ &= \begin{bmatrix} 0 & -d_3 & d_2 \\ d_3 & 0 & -d_1 \\ -d_2 & d_1 & 0 \end{bmatrix} \begin{bmatrix} v_1 \\ v_2 \\ v_3 \end{bmatrix} \\ &= D\mathbf{v} \end{aligned} \quad (10.8)$$

where the last equality defines the 3×3 matrix D . This matrix is skew-symmetric since $D^T = -D$. The cross product $\mathbf{d} \times (\mathbf{d} \times \mathbf{v})$ is written as a matrix multiplied by a vector by applying [equation \(10.8\)](#) twice:

$$\mathbf{d} \times (\mathbf{d} \times \mathbf{v}) = D(\mathbf{d} \times \mathbf{v}) = D(D\mathbf{v}) = D^2\mathbf{v} \quad (10.9)$$

We now take a closer look at the vectors $\mathbf{v} = I\mathbf{v}$, $\mathbf{d} \times \mathbf{v} = D\mathbf{v}$ and $\mathbf{d} \times (\mathbf{d} \times \mathbf{v}) = D^2\mathbf{v}$ to determine how \mathbf{a} , \mathbf{b} , and their various products are related to the matrices I , D , and D^2 .

First, observe that equation (10.5) may be manipulated as

$$\begin{aligned} I\mathbf{v} &= \mathbf{v} \\ &= (\mathbf{a} \cdot \mathbf{v})\mathbf{a} + (\mathbf{b} \cdot \mathbf{v})\mathbf{b} + (\mathbf{d} \cdot \mathbf{v})\mathbf{d} \\ &= \mathbf{a}(\mathbf{a}^T\mathbf{v}) + \mathbf{b}(\mathbf{b}^T\mathbf{v}) + \mathbf{d}(\mathbf{d}^T\mathbf{v}) \\ &= (\mathbf{a}\mathbf{a}^T + \mathbf{b}\mathbf{b}^T + \mathbf{d}\mathbf{d}^T)\mathbf{v} \end{aligned}$$

The equation is true for all vectors \mathbf{v} , so

$$I = \mathbf{a}\mathbf{a}^T + \mathbf{b}\mathbf{b}^T + \mathbf{d}\mathbf{d}^T \quad (10.10)$$

Second, equations (10.5), (10.6), and (10.8) imply the relationship

$$\begin{aligned} D\mathbf{v} &= \mathbf{d} \times \mathbf{v} \\ &= \alpha\mathbf{b} - \beta\mathbf{a} \\ &= (\mathbf{a} \cdot \mathbf{v})\mathbf{b} - (\mathbf{b} \cdot \mathbf{v})\mathbf{a} \\ &= \mathbf{b}(\mathbf{a}^T\mathbf{v}) - \mathbf{a}(\mathbf{b}^T\mathbf{v}) \\ &= (\mathbf{b}\mathbf{a}^T - \mathbf{a}\mathbf{b}^T)\mathbf{v} \end{aligned}$$

This equation is true for all vectors \mathbf{v} , so

$$D = \mathbf{b}\mathbf{a}^T - \mathbf{a}\mathbf{b}^T \quad (10.11)$$

Third, equations (10.5), (10.7), and (10.9) imply the relationship

$$\begin{aligned} D^2\mathbf{v} &= \mathbf{d} \times (D\mathbf{v}) \\ &= -\alpha\mathbf{a} - \beta\mathbf{b} \\ &= (\mathbf{d} \cdot \mathbf{v})\mathbf{d} - \mathbf{v} \\ &= \mathbf{d}(\mathbf{d}^T\mathbf{v}) - \mathbf{v} \\ &= (\mathbf{d}\mathbf{d}^T - I)\mathbf{v} \end{aligned}$$

This equation is true for all vectors \mathbf{v} , so

$$D^2 = \mathbf{d}\mathbf{d}^T - I \quad (10.12)$$

Combining these relationships with equation (10.4),

$$\begin{aligned} R_1 &= c(\mathbf{a}\mathbf{a}^T + \mathbf{b}\mathbf{b}^T) + s(\mathbf{b}\mathbf{a}^T - \mathbf{a}\mathbf{b}^T) + \mathbf{d}\mathbf{d}^T && \text{Restatement of equation (10.4)} \\ &= c(I - \mathbf{d}\mathbf{d}^T) + s(\mathbf{b}\mathbf{a}^T - \mathbf{a}\mathbf{b}^T) + \mathbf{d}\mathbf{d}^T && \text{By equation (10.10)} \\ &= c(I - \mathbf{d}\mathbf{d}^T) + sD + \mathbf{d}\mathbf{d}^T && \text{By equation (10.11)} \\ &= I + sD + (1 - c)(\mathbf{d}\mathbf{d}^T - I) \\ &= I + sD + (1 - c)D^2 && \text{By equation (10.12)} \end{aligned} \quad (10.13)$$

This equation provides the rotation matrix R_1 in terms of the unit-length axis direction \mathbf{d} stored as the matrix D and the angle θ occurring in $s = \sin(\theta)$ and $c = \cos(\theta)$. The application of the rotation matrix to a vector is

$$\begin{aligned} R_1 \mathbf{v} &= (I + sD + (1 - c)D^2)\mathbf{v} \\ &= I\mathbf{v} + sD\mathbf{v} + (1 - c)D^2\mathbf{v} \\ &= \mathbf{v} + s\mathbf{d} \times \mathbf{v} + (1 - c)\mathbf{d} \times (\mathbf{d} \times \mathbf{v}) \end{aligned} \quad (10.14)$$

Make sure you understand the constructions used to obtain equations (10.4) and (10.13). The same idea is used in Section 10.3 to motivate how a quaternion is related to a rotation matrix in four dimensions.

10.2 THE CLASSICAL APPROACH

A *quaternion* is specified by the abstract quantity $q = w + xi + yj + zk$, where w, x, y , and z are real numbers. This quantity can be thought of as a vector $(w, x, y, z) \in \mathbb{R}^4$. As it turns out, the quaternions that are related to rotations are unit-length quaternions, those quaternions for which the length of (w, x, y, z) is 1. As vectors in \mathbb{R}^4 , the unit-length quaternions are located on the hypersphere of radius 1, given algebraically as $w^2 + x^2 + y^2 + z^2 = 1$. Many practitioners use the term quaternion in place of unit-length quaternion. In this section I will use quaternion to mean any quantity of the form $w + xi + yj + zk$ and unit-length quaternion when I intend the vector (w, x, y, z) to have length 1.

10.2.1 ALGEBRAIC OPERATIONS

Addition of two quaternions is defined by

$$\begin{aligned} q_0 + q_1 &= (w_0 + x_0i + y_0j + z_0k) + (w_1 + x_1i + y_1j + z_1k) \\ &= (w_0 + w_1) + (x_0 + x_1)i + (y_0 + y_1)j + (z_0 + z_1)k \end{aligned} \quad (10.15)$$

Scalar multiplication of a quaternion by a real number c is defined by

$$cq = c(w + xi + yj + zk) = (cw) + (cx)i + (cy)j + (cz)k \quad (10.16)$$

The *subtraction* operation is defined as a consequence of these two definitions, $q_0 - q_1 = q_0 + (-1)q_1$.

Multiplications are allowed between quaternions. The symbols i , j , and k have multiplicative properties similar to pure imaginary numbers: $i^2 = -1$, $j^2 = -1$, and $k^2 = -1$. They also have multiplicative properties that are superficially similar to cross products of the 3D vectors \mathbf{i} , \mathbf{j} , and \mathbf{k} : $ij = -ji = k$, $jk = -kj = i$, and $ki = -ik = j$. Observe that $ij \neq ji$, so multiplication is not a commutative operation. The analogy to cross products is not fully valid, though. Multiplication is associative; for example,

$(ij)k = -1 = i(jk)$, but the cross product operation is not associative. Generally, the product of quaternions is defined by allowing the distributive law to apply and by using the various product formulas for the i , j , and k terms:

$$\begin{aligned} q_0 q_1 &= (w_0 + x_0 i + y_0 j + z_0 k)(w_1 + x_1 i + y_1 j + z_1 k) \\ &= (w_0 w_1 - x_0 x_1 - y_0 y_1 - z_0 z_1) \\ &\quad + (w_0 x_1 + w_1 x_0 + y_0 z_1 - z_0 y_1)i \\ &\quad + (w_0 y_1 + w_1 y_0 + z_0 x_1 - x_0 z_1)j \\ &\quad + (w_0 z_1 + w_1 z_0 + x_0 y_1 - y_0 x_1)k \end{aligned} \quad (10.17)$$

As noted multiplication is not generally commutative. The product in the other order obtained from equation (10.17) by interchanging the 0 and 1 subscripts is

$$\begin{aligned} q_1 q_0 &= (w_1 + x_1 i + y_1 j + z_1 k)(w_0 + x_0 i + y_0 j + z_0 k) \\ &= (w_0 w_1 - x_0 x_1 - y_0 y_1 - z_0 z_1) \\ &\quad + (w_0 x_1 + w_1 x_0 + y_1 z_0 - y_0 z_1)i \\ &\quad + (w_0 y_1 + w_1 y_0 + z_1 x_0 - z_0 x_1)j \\ &\quad + (w_0 z_1 + w_1 z_0 + x_1 y_0 - x_0 y_1)k \end{aligned} \quad (10.18)$$

The w -components of $q_0 q_1$ and $q_1 q_0$ are the same. On the other hand, the last two terms of each of the i -, j -, and k -components in the second equation of 10.18 are opposite in sign to their counterparts in the first equation. Those terms should remind you of the components of a cross product. Symbolically, equations (10.17) and (10.18) are different, but it is possible for *some* quaternions (but not all) that $q_0 q_1 = q_1 q_0$. For this to happen we need

$$\begin{aligned} (x_0, y_0, z_0) \times (x_1, y_1, z_1) &= (y_0 z_1 - y_1 z_0, z_0 x_1 - z_1 x_0, x_0 y_1 - y_0 x_1) \\ &= (y_1 z_0 - y_0 z_1, z_1 x_0 - z_0 x_1, x_1 y_0 - x_0 y_1) \\ &= (x_1, y_1, z_1) \times (x_0, y_0, z_0) \end{aligned}$$

The only way the two cross products can be the same for a pair of vectors is if they are parallel. In summary, $q_0 q_1 = q_1 q_0$ if and only if $(x_1, y_1, z_1) = t(x_0, y_0, z_0)$ for some real-valued scalar t .

The complex number $\zeta = w + xi$ has *real part* w and *imaginary part* x . I refer to xi as the *imaginary portion* of ζ . To allow a closer parallel between properties of quaternions and properties of complex numbers, a quaternion may be written as $q = w + \hat{v}$, where $\hat{v} = xi + yj + zk$. The separation of quaternions into two portions allows us to think of w as the *real part* of q and \hat{v} as the *imaginary portion* of q . The conjugate of ζ is defined as $\bar{\zeta} = w - xi$; that is, the sign of the imaginary portion is changed. A consequence is that $\zeta \bar{\zeta} = w^2 + x^2$. The right-hand side is called the norm of ζ and is denoted $N(\zeta) = \zeta \bar{\zeta}$. As long as $N(\zeta) \neq 0$, the multiplicative inverse of ζ exists and is $\zeta^{-1} = \bar{\zeta}/N(\zeta)$. If $N(\zeta) = 1$, the complex number is said to be unit length. Similar definitions apply to a quaternion $q = w + \hat{v}$. The *conjugate* is

$$q^* = w - \hat{v} \quad (10.19)$$

For historical reasons and reasons of mathematical nomenclature, a superscript asterisk is used to denote the conjugate rather than an overline bar as is done for complex numbers. The *norm* of q is $N(q) = qq^* = w^2 + x^2 + y^2 + z^2$ and the *length* of q is naturally defined as the square root of the norm, $L(q) = \sqrt{N(q)}$. If $L(q) = 1$, q is said to be *unit length*. As long as $N(q) \neq 0$, the *inverse* of q is $q^{-1} = q^*/N(q)$. If $L(q) = 1$, the inverse and conjugate are the same, $q^{-1} = q^*$. For purposes of rotations the norm, length, and inverse do not play a role, so I mention them here merely for completeness.

The polar form of a unit-length complex number is $\zeta = \cos \phi + i \sin \phi$. A unit-length quaternion has a similar representation,

$$q = \cos \phi + \hat{d} \sin \phi \quad (10.20)$$

where $\hat{d} = xi + yj + zk$ and $x^2 + y^2 + z^2 = 1$. Note the similarity in form to ζ . The imaginary number i has the property $i^2 = -1$. The imaginary portion \hat{d} has the similar property $\hat{d}^2 = -1$. The polar form is important in understanding how unit-length quaternions are related to rotations, the topic of the [Section 10.2.2](#).

The representation of any quaternion as $q = w + \hat{v}$ may be viewed in a sense as a coordinate-free description. We may identify $\hat{v} = xi + yj + zk$ with the vector $\mathbf{v} = (x, y, z)$. This allows us to define two operations on the imaginary portions based on how those operations apply to vectors. The *dot product* of \hat{v}_0 and \hat{v}_1 is denoted $\hat{v}_0 \cdot \hat{v}_1$ and defined to be the real-valued vector dot product $\mathbf{v}_0 \cdot \mathbf{v}_1$. The *cross product* of \hat{v}_0 and \hat{v}_1 is denoted $\hat{v}_0 \times \hat{v}_1$, another quaternion with zero w component. Its x , y , and z values are the components of the vector cross product $\mathbf{v}_0 \times \mathbf{v}_1$. In this formulation, the product of two quaternions is

$$(w_0 + \hat{v}_0)(w_1 + \hat{v}_1) = (w_0 w_1 - \hat{v}_0 \cdot \hat{v}_1) + w_0 \hat{v}_1 + w_1 \hat{v}_0 + \hat{v}_0 \times \hat{v}_1 \quad (10.21)$$

We will make use of this identity in the next section. Other identities are provided:

1. $(q^*)^* = q$
2. $(pq)^* = q^* p^*$
3. If $\hat{d} = xi + yj + zk$ with $x^2 + y^2 + z^2 = 1$, then $\hat{d}^2 = -1$
4. $(w_0 + \hat{v}_0)(w_1 + \hat{v}_1) = (w_1 + \hat{v}_1)(w_0 + \hat{v}_0)$ if and only if $\hat{v}_0 \times \hat{v}_1 = 0$

I leave the proofs of these as an exercise.

10.2.2 RELATIONSHIP OF QUATERNIONS TO ROTATIONS

A vector \mathbf{v} is to be rotated about an axis with unit-length direction \mathbf{d} by an angle θ . The sense of the rotation is counterclockwise: If you look at the origin of a plane perpendicular to \mathbf{d} , your view direction is $-\mathbf{d}$, and $\theta > 0$, then any vector in that plane is rotated counterclockwise about the origin. Let \mathbf{u} be the rotation of \mathbf{v} about axis \mathbf{d} by angle θ . [Figure 10.1](#) illustrates the rotation.

The quaternions \hat{d} , \hat{v} , and \hat{u} are those identified with the vectors \mathbf{d} , \mathbf{v} , and \mathbf{u} . Define the quaternion $q = \gamma + \sigma \hat{d}$, where $\gamma = \cos(\theta/2)$ and $\sigma = \sin(\theta/2)$. The quaternion $\hat{u} = q\hat{v}q^*$ has zero w -component; the left-hand side is written as if there is no w -component, but we do need to verify this. The vector \mathbf{u} turns out to be the rotation of \mathbf{v} . The formal calculations are shown:

$$\begin{aligned}
 q\hat{v}q^* &= (\gamma + \sigma \hat{d})(0 + \hat{v})(\gamma - \sigma \hat{d}) && \text{Definition of } q \text{ and } q^* \\
 &= (-\sigma \hat{d} \cdot \hat{v} + \gamma \hat{v} + \sigma \hat{d} \times \hat{v})(\gamma - \sigma \hat{d}) && \text{Using equation (10.21)} \\
 &= [(-\sigma \hat{d} \cdot \hat{v})(\gamma) - (\gamma \hat{v} + \sigma \hat{d} \times \hat{v})(-\sigma \hat{d})] \\
 &\quad + (\gamma)(\gamma \hat{v} + \sigma \hat{d} \times \hat{v}) + (-\sigma \hat{d} \cdot \hat{v})(-\sigma \hat{d}) && \text{Using equation (10.21)} \\
 &\quad + (\gamma \hat{v} + \sigma \hat{d} \times \hat{v}) \times (-\sigma \hat{d}) \\
 &= \gamma^2 \hat{v} + \sigma^2 (\hat{d} \cdot \hat{v}) \hat{d} + 2\sigma\gamma \hat{d} \times \hat{v} + \sigma^2 \hat{d} \times (\hat{d} \times \hat{v})
 \end{aligned}$$

The last equality uses the facts that $(\hat{d} \times \hat{v}) \cdot \hat{d} = 0$, $\hat{v} \times \hat{d} = -\hat{d} \times \hat{v}$ and $\hat{d} \times (\hat{d} \times \hat{v}) = -(\hat{d} \times \hat{v}) \times \hat{d}$, the same identities that the vector counterparts of \hat{d} and \hat{v} satisfy. Continuing with the calculations:

$$\begin{aligned}
 q\hat{v}q^* &= (1 - \sigma^2)\hat{v} + 2\sigma\gamma \hat{d} \times \hat{v} + \sigma^2 [(\hat{d} \cdot \hat{v})\hat{d} + \hat{d} \times (\hat{d} \times \hat{v})] \\
 &= \hat{v} + 2\sigma\gamma \hat{d} \times \hat{v} + \sigma^2 [(\hat{d} \cdot \hat{v})\hat{d} - \hat{v} + \hat{d} \times (\hat{d} \times \hat{v})]
 \end{aligned}$$

An identity from vector algebra is $\mathbf{d} \times (\mathbf{d} \times \mathbf{v}) = (\mathbf{d} \cdot \mathbf{v})\mathbf{d} - (\mathbf{d} \cdot \mathbf{d})\mathbf{v} = (\mathbf{d} \cdot \mathbf{v})\mathbf{d} - \mathbf{v}$, the last equality a consequence of \mathbf{d} being unit length. The quaternion counterpart satisfies the same identity, so

$$q\hat{v}q^* = \hat{v} + 2\sigma\gamma \hat{d} \times \hat{v} + 2\sigma^2 \hat{d} \times (\hat{d} \times \hat{v})$$

Recall also the trigonometric identities $\sin\theta = 2\sin(\theta/2)\cos(\theta/2) = 2\sigma\gamma$ and $1 - \cos\theta = 2\sin^2(\theta/2) = 2\sigma^2$, so we finally arrive at

$$q\hat{v}q^* = \hat{v} + (\sin\theta)\hat{d} \times \hat{v} + (1 - \cos\theta)\hat{d} \times (\hat{d} \times \hat{v}) \quad (10.22)$$

This is the quaternion counterpart of equation (10.14), the general rotation of \mathbf{v} about an axis \mathbf{d} by an angle θ . The vector \mathbf{u} corresponding to $\hat{u} = q\hat{v}q^*$ is therefore the rotation of \mathbf{v} .

The rotation matrix R corresponding to the quaternion q may be obtained by symbolically computing the right-hand side of $\hat{u} = q\hat{v}q^*$ and factoring the coefficients of the i -, j -, and k -terms to obtain $\mathbf{u} = R\mathbf{v}$, where

$$R = \begin{bmatrix} 1 - 2y^2 - 2z^2 & 2xy - 2wz & 2xz + 2wy \\ 2xy + 2wz & 1 - 2x^2 - 2z^2 & 2yz - 2wx \\ 2xz - 2wy & 2yz + 2wx & 1 - 2x^2 - 2y^2 \end{bmatrix} \quad (10.23)$$

Composition of rotations is easily stated in terms of quaternion algebra. If p and q are unit-length quaternions that represent rotations, and if \hat{v} is the quaternion identified with vector \mathbf{v} , then the rotation represented by q is accomplished by $\hat{u} = q\hat{v}q^*$

as shown earlier. The vector \mathbf{u} identified with \hat{u} is further modified by the rotation represented by p :

$$\begin{aligned} p\hat{u}p^* &= p(q\hat{v}q^*)p^* \\ &= (pq)\hat{v}(q^*p^*) \quad \text{Quaternion multiplication is associative} \\ &= (pq)\hat{v}(pq)^* \quad \text{Property of conjugation} \end{aligned}$$

This equation shows that the composite rotation is represented by the quaternion product pq .

10.3 A LINEAR ALGEBRAIC APPROACH

The classical approach of the last section is unappealing to those who are new to the topic because it neither appeals to the geometric nature of quaternions nor indicates what reasoning led to the definitions in the first place. This section provides a geometric understanding of quaternions, one that is based only on concepts of linear algebra. Instead of analyzing a rotation in three dimensions, we analyze it in a four-dimensional setting. A unit-length quaternion is shown to correspond to a rotation matrix in 4D and a transformation equation analogous to [equation \(10.22\)](#) is constructed. The construction is motivated by a change of basis, the same motivation used in the construction of [equations \(10.4\)](#) and [\(10.13\)](#).

Let us return to the standard basis $\{\mathbf{i}, \mathbf{j}, \mathbf{k}\}$ and the rotation matrix R_0 from [equation \(10.1\)](#) that represents rotation about the z -axis by angle θ . Instead of viewing the rotation as an operation on vectors $\mathbf{v} = (x, y, z) \in \mathbb{R}^3$, let us look at it as an operation on vectors $\tilde{\mathbf{v}} = (x, y, z, w) \in \mathbb{R}^4$. The inclusion of the fourth component gives us an additional degree of freedom that allows the creation of a more efficient representation of rotations than what is possible in three dimensions. By efficient, I mean in the sense of a computer implementation. The 4D representation requires less memory than its 3D counterpart. Composition of rotations in 3D involves multiplication of rotation matrices. Composition using the 4D representation can be computed faster than its 3D counterpart.

A natural choice for representing the rotation in 4D is

$$\mathcal{R}_0 = \left[\begin{array}{cccc} c & -s & 0 & 0 \\ s & c & 0 & 0 \\ 0 & 0 & 1 & 0 \\ 0 & 0 & 0 & 1 \end{array} \right] = \left[\begin{array}{c|c} R_0 & \mathbf{0} \\ \mathbf{0}^T & 1 \end{array} \right] = \left[\begin{array}{c|c} R_{xy} & \mathbf{0} \\ \mathbf{0}^T & I \end{array} \right] \quad (10.24)$$

where the first equality defines a 2×2 block matrix whose upper-left block is the 3×3 rotation matrix, whose upper-right block is the 3×1 zero vector, whose lower-left block is the 1×3 zero vector, and whose lower-right block is the scalar 1. The second equality defines a 2×2 block matrix where each block is itself a 2×2 matrix. The matrix R_{xy} is just the rotation within the xy -plane, the matrices $\mathbf{0}$ and $\mathbf{0}^T$ have all zeros, and I is the 2×2 identity matrix. The vector (x, y, z, w) is transformed to

$(cx - sy, sx + cy, z, w)$. The next step, a strange thing to do at first glance, is the key observation in the construction. The rotation by angle θ within the xy -plane can be thought of as a composition of two rotations, each by angle $\theta/2$:

$$R_{xy} = \begin{bmatrix} c & -s \\ s & c \end{bmatrix} = \begin{bmatrix} \gamma & -\sigma \\ \sigma & \gamma \end{bmatrix} \begin{bmatrix} \gamma & -\sigma \\ \sigma & \gamma \end{bmatrix} = H^2$$

where $\sigma = \sin(\theta/2)$, $\gamma = \cos(\theta/2)$, and H is the rotation matrix for the half-angle $\theta/2$ that controls the rotation in the xy -plane. The matrix in [equation \(10.24\)](#) may be factored into

$$\mathcal{R}_0 = \left[\begin{array}{c|c} H & 0 \\ \hline 0^T & I \end{array} \right] \left[\begin{array}{c|c} H & 0 \\ \hline 0^T & I \end{array} \right]$$

Although certainly the simplest factorization you might think of, the identity matrix I that keeps z and w fixed during the rotations can be replaced by H and H^T . That is, we actually can allow z and w to change during each half-angle rotation in the xy -plane *as long as we make sure z returns to its original value after both operations*. The corresponding factorization is

$$\mathcal{R}_0 = \left[\begin{array}{c|c} H & 0 \\ \hline 0^T & H \end{array} \right] \left[\begin{array}{c|c} H & 0 \\ \hline 0^T & H^T \end{array} \right] =: \bar{\mathcal{Q}}_0 \mathcal{Q}_0 \quad (10.25)$$

where the last equality defines the matrices \mathcal{Q}_0 and $\bar{\mathcal{Q}}_0$, themselves rotations in 4D. In summary, the half-angle rotation H is applied twice to (x, y) to obtain the full-angle rotation in the xy -plane. The inverse half-angle rotation H^T is applied to (z, w) , a rotation within the zw -plane, but that rotation is undone by H in the second operation, the end result being that (z, w) is unchanged by the composition. [Figure 10.2](#) illustrates this.

What does this really gain us? For the 3D rotation matrix R_0 we have a loss rather than a gain. The 3D matrix requires storing two precomputed numbers, s and c . The zeros and one are in known positions and do not need to be stored in general memory. The application of R to (x, y, z) is computed as $R_{xy}(x, y)$ since z is unchanged. This requires a product of a 2×2 matrix and a 2×1 vector that uses 6 operations (4 multiplications and 2 additions). The 4D matrix requires storing σ and γ – no change in memory requirements. However, the blind application of the right-hand-side matrices in [equation \(10.25\)](#) leads to computing terms $H(x, y)$, $H(H(x, y))$, $H^T(z, w)$, and $H(H^T(z, w))$ for a total of 24 operations. We could be clever and realize that (z, w) will not change, but that still leaves us with computing $H(x, y)$ and $H(H(x, y))$ for a total of 12 operations. Being even more clever, we realize that $H^2 = R_{xy}$ and just compute $R_{xy}(x, y)$. This just brings us full circle with no gain.

The real gain occurs by constructing a 4D rotation matrix \mathcal{R}_1 that corresponds to the general 3D rotation matrix R_1 constructed by [equations \(10.4\)](#) and [\(10.13\)](#). We need to “lift” all our basis vectors into \mathbb{R}^4 by appending a zero w -component. These vectors will be written as block matrices to preserve the notion of the first three

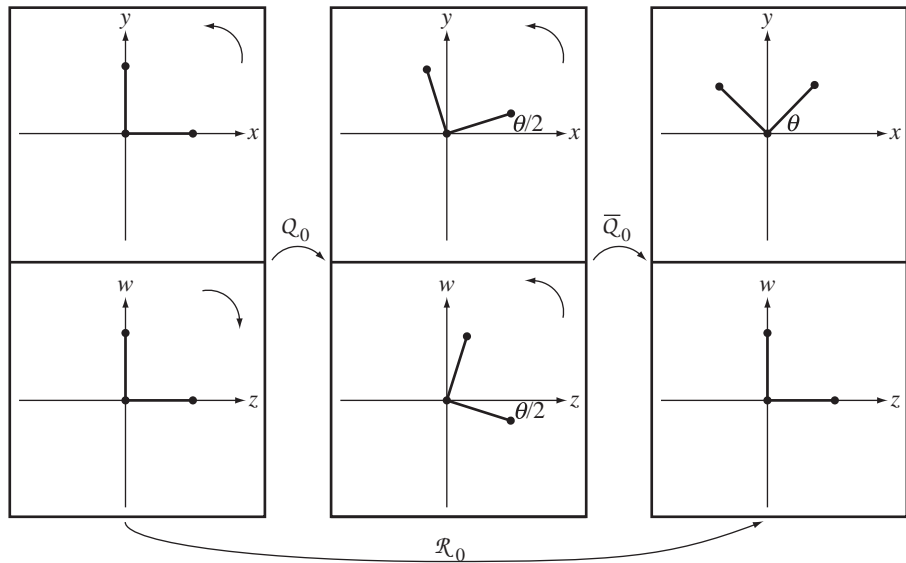


Figure 10.2 A 3D rotation about the z -axis that is represented as the product of two 4D rotations.

components living in \mathbb{R}^3 . Additional vectors are defined to allow us to have a standard basis and an alternate basis for \mathbb{R}^4 . The standard basis is $\{\tilde{\mathbf{i}}, \tilde{\mathbf{j}}, \tilde{\mathbf{k}}, \tilde{\mathbf{l}}\}$, where

$$\tilde{\mathbf{i}} = \begin{bmatrix} \mathbf{i} \\ 0 \end{bmatrix}, \quad \tilde{\mathbf{j}} = \begin{bmatrix} \mathbf{J} \\ 0 \end{bmatrix}, \quad \tilde{\mathbf{k}} = \begin{bmatrix} \mathbf{k} \\ 0 \end{bmatrix}, \quad \tilde{\mathbf{l}} = \begin{bmatrix} \mathbf{0} \\ 1 \end{bmatrix} \quad (10.26)$$

The alternate basis is $\{\tilde{\mathbf{a}}, \tilde{\mathbf{b}}, \tilde{\mathbf{d}}, \tilde{\mathbf{l}}\}$, where

$$\tilde{\mathbf{a}} = \begin{bmatrix} \mathbf{a} \\ 0 \end{bmatrix}, \quad \tilde{\mathbf{b}} = \begin{bmatrix} \mathbf{b} \\ 0 \end{bmatrix}, \quad \tilde{\mathbf{d}} = \begin{bmatrix} \mathbf{d} \\ 0 \end{bmatrix} \quad (10.27)$$

The construction in equation (10.4) is mimicked by choosing $\mathcal{P} = [\tilde{\mathbf{a}} | \tilde{\mathbf{b}} | \tilde{\mathbf{d}} | \tilde{\mathbf{l}}]$ and computing

$$\mathcal{R}_1 = \mathcal{P}\mathcal{R}_0\mathcal{P}^T = \mathcal{P}\bar{\mathcal{Q}}_0\mathcal{Q}_0\mathcal{P}^T = (\mathcal{P}\bar{\mathcal{Q}}_0\mathcal{P}^T)(\mathcal{P}\mathcal{Q}_0\mathcal{P}^T) =: \bar{\mathcal{Q}}_1\mathcal{Q}_1$$

where the last equality defines \mathcal{Q}_1 and $\bar{\mathcal{Q}}_1$. The matrix \mathcal{Q}_0 represents a general 4D rotation with respect to the alternate basis. The matrix \mathcal{Q}_1 represents the same rotation,

but with respect to the standard basis and is obtained by

$$\begin{aligned} \mathcal{Q}_1 &= \mathcal{P} \mathcal{Q}_0 \mathcal{P}^T \\ &= [\tilde{\mathbf{a}} | \tilde{\mathbf{b}} | \tilde{\mathbf{d}} | \tilde{\ell}] \left[\begin{array}{c|c|c|c} \gamma & -\sigma & 0 & 0 \\ \hline \sigma & \gamma & 0 & 0 \\ 0 & 0 & \gamma & \sigma \\ 0 & 0 & -\sigma & \gamma \end{array} \right] \left[\begin{array}{c} \tilde{\mathbf{a}}^T \\ \tilde{\mathbf{b}}^T \\ \tilde{\mathbf{d}}^T \\ \tilde{\ell}^T \end{array} \right] \\ &= \gamma (\tilde{\mathbf{a}}\tilde{\mathbf{a}}^T + \tilde{\mathbf{b}}\tilde{\mathbf{b}}^T + \tilde{\mathbf{d}}\tilde{\mathbf{d}}^T + \tilde{\ell}\tilde{\ell}^T) + \sigma (\tilde{\mathbf{b}}\tilde{\mathbf{a}}^T - \tilde{\mathbf{a}}\tilde{\mathbf{b}}^T + \tilde{\mathbf{d}}\tilde{\ell}^T - \tilde{\ell}\tilde{\mathbf{d}}^T) \end{aligned} \quad (10.28)$$

A construction analogous to the one that produced equation (10.10) may be used to obtain

$$\mathcal{I} = \tilde{\mathbf{a}}\tilde{\mathbf{a}}^T + \tilde{\mathbf{b}}\tilde{\mathbf{b}}^T + \tilde{\mathbf{d}}\tilde{\mathbf{d}}^T + \tilde{\ell}\tilde{\ell}^T \quad (10.29)$$

where \mathcal{I} is the 4×4 identity matrix. The equation (10.11) extends to four dimensions as

$$\tilde{\mathbf{b}}\tilde{\mathbf{a}}^T - \tilde{\mathbf{a}}\tilde{\mathbf{b}}^T = \left[\begin{array}{c} \mathbf{b} \\ 0 \end{array} \right] \left[\begin{array}{c|c} \mathbf{a}^T & 0 \end{array} \right] - \left[\begin{array}{c} \mathbf{a} \\ 0 \end{array} \right] \left[\begin{array}{c|c} \mathbf{b}^T & 0 \end{array} \right] = \left[\begin{array}{c|c} \mathbf{b}\mathbf{a}^T - \mathbf{a}\mathbf{b}^T & \mathbf{0} \\ \hline \mathbf{0}^T & 0 \end{array} \right] = \left[\begin{array}{c|c} D & \mathbf{0} \\ \hline \mathbf{0}^T & 0 \end{array} \right]$$

It is easy to verify that

$$\tilde{\mathbf{d}}\tilde{\ell}^T - \tilde{\ell}\tilde{\mathbf{d}}^T = \left[\begin{array}{c|c} 0 & \mathbf{d} \\ \hline -\mathbf{d}^T & 0 \end{array} \right]$$

The two matrices may be added to form a new matrix,

$$\mathcal{D} = \left[\begin{array}{c|c} D & \mathbf{d} \\ \hline -\mathbf{d}^T & 0 \end{array} \right] = \tilde{\mathbf{b}}\tilde{\mathbf{a}}^T - \tilde{\mathbf{a}}\tilde{\mathbf{b}}^T + \tilde{\mathbf{d}}\tilde{\ell}^T - \tilde{\ell}\tilde{\mathbf{d}}^T \quad (10.30)$$

Equations (10.29) and (10.30) are replaced in equation (10.28) leading to the representation:

$$\mathcal{Q}_1 = \gamma \mathcal{I} + \sigma \mathcal{D} = \left[\begin{array}{c|c} \gamma I + \sigma D & \sigma \mathbf{d} \\ \hline -\sigma \mathbf{d}^T & \gamma \end{array} \right] \quad (10.31)$$

where I is the 3×3 identity and D is the skew-symmetric matrix defined in the last section. A similar construction leads to

$$\overline{\mathcal{Q}}_1 = \left[\begin{array}{c|c} \gamma I + \sigma D & -\sigma \mathbf{d} \\ \hline \sigma \mathbf{d}^T & \gamma \end{array} \right] \quad (10.32)$$

A quick calculation that uses equation (10.13) will verify that

$$\mathcal{R}_1 = \overline{\mathcal{Q}}_1 \mathcal{Q}_1 = \left[\begin{array}{c|c} \gamma I + \sigma D & -\sigma \mathbf{d} \\ \hline \sigma \mathbf{d}^T & \gamma \end{array} \right] \left[\begin{array}{c|c} \gamma I + \sigma D & \sigma \mathbf{d} \\ \hline -\sigma \mathbf{d}^T & \gamma \end{array} \right] = \left[\begin{array}{c|c} R_1 & \mathbf{0} \\ \hline \mathbf{0}^T & 1 \end{array} \right]$$

The application to a vector $\mathbf{v} \in \mathbb{R}^3$ is to apply \mathcal{R}_1 as shown:

$$\begin{bmatrix} \mathbf{v}' \\ 0 \end{bmatrix} = \mathcal{R}_1 \begin{bmatrix} \mathbf{v} \\ 0 \end{bmatrix}$$

The 3D result is $\mathbf{v}' = R_1 \mathbf{v}$.

The matrix \mathcal{Q}_1 has a special form:

$$\mathcal{Q}_1 = \begin{bmatrix} \gamma & -\sigma d_3 & \sigma d_2 & \sigma d_1 \\ \sigma d_3 & \gamma & -\sigma d_1 & \sigma d_2 \\ -\sigma d_2 & \sigma d_1 & \gamma & \sigma d_3 \\ -\sigma d_1 & -\sigma d_2 & -\sigma d_3 & \gamma \end{bmatrix} = \begin{bmatrix} w & -z & y & x \\ z & w & -x & y \\ -y & x & w & z \\ -x & -y & -z & w \end{bmatrix} \quad (10.33)$$

where the last equality defines $x = \sigma d_1$, $y = \sigma d_2$, $z = \sigma d_3$, and $w = \gamma$. The names x , y , z , and w of these quantities are not to be confused with the names of the variable components for vectors in \mathbb{R}^4 . I use these names because that is the standard choice for the components of a quaternion to which \mathcal{Q}_1 happens to be related. Although \mathcal{Q}_1 has 16 entries, only four of them are unique – the last column values. Moreover, \mathcal{Q}_1 uses those same four values. The 4×4 matrix \mathcal{Q} requires less storage than the nine values for a 3×3 rotation matrix.

One issue that has not yet been addressed is composition of rotations. Let us do so now. Let $\mathcal{R} = \overline{\mathcal{Q}}\mathcal{Q}$ and $\mathcal{S} = \overline{\mathcal{P}}\mathcal{P}$ be two of our 4D rotations that correspond to 3D rotation matrices R and S , respectively. The composition in the 4D setting is

$$\mathcal{SR} = (\overline{\mathcal{P}}\mathcal{P})(\overline{\mathcal{Q}}\mathcal{Q}) = \overline{\mathcal{P}}(\mathcal{P}\overline{\mathcal{Q}})\mathcal{Q} = \overline{\mathcal{P}}(\overline{\mathcal{Q}}\mathcal{P})\mathcal{Q} = (\overline{\mathcal{P}}\mathcal{Q})(\mathcal{P}\mathcal{Q})$$

The astute reader will say, Wait a moment, and remind me that matrix multiplication is generally not commutative, so how can we switch the order in $\mathcal{P}\overline{\mathcal{Q}} = \overline{\mathcal{Q}}\mathcal{P}$? As it turns out, the matrices \mathcal{P} and $\overline{\mathcal{Q}}$ do commute. This can be verified with a moderate amount of symbolic manipulation. What this means is that we can store \mathcal{Q} to represent \mathcal{R} , store \mathcal{P} to represent \mathcal{S} , and compute the product $\mathcal{P}\mathcal{Q}$ and store to represent the composition \mathcal{SR} . If \mathcal{Q} is stored as the 4-tuple (x_0, y_0, z_0, w_0) and \mathcal{P} is stored as the 4-tuple (x_1, y_1, z_1, w_1) , we need compute only the unique values in $\mathcal{P}\mathcal{Q}$, call them (x_2, y_2, z_2, w_2) . We can do this by computing \mathcal{P} times the last column of \mathcal{Q} , the result being the last column of \mathcal{P} :

$$\begin{bmatrix} x_2 \\ y_2 \\ z_2 \\ w_2 \end{bmatrix} = \begin{bmatrix} w_1 & -z_1 & y_1 & x_1 \\ z_1 & w_1 & -x_1 & y_1 \\ -y_1 & x_1 & w_1 & z_1 \\ -x_1 & -y_1 & -z_1 & w_1 \end{bmatrix} \begin{bmatrix} x_0 \\ y_0 \\ z_0 \\ w_0 \end{bmatrix} = \begin{bmatrix} w_1 x_0 - z_1 y_0 + y_1 z_0 + x_1 w_0 \\ z_1 x_0 + w_1 y_0 - x_1 z_0 + y_1 w_0 \\ -y_1 x_0 + x_1 y_0 + w_1 z_0 + z_1 w_0 \\ -x_1 x_0 - y_1 y_0 - z_1 z_0 + w_1 w_0 \end{bmatrix}$$

The product $\mathcal{P}\mathcal{Q}$ effectively represents the composition of the 3D rotations. Notice that the right-hand side values in the equation are those of equation (10.18), the

definition for quaternion multiplication, when computing $q_1 q_0 = (w_1 + x_1 i + y_1 j + z_1 k)(w_0 + x_0 i + y_0 j + z_0 k)$. To rotate a vector using $\mathcal{R} = \overline{\mathcal{Q}}\mathcal{Q}$,

$$\tilde{\mathbf{u}} = \begin{bmatrix} \mathbf{u} \\ 0 \end{bmatrix} = \overline{\mathcal{Q}}\mathcal{Q} \begin{bmatrix} \mathbf{v} \\ 0 \end{bmatrix} = \overline{\mathcal{Q}}\mathcal{Q}\tilde{\mathbf{v}}.$$

This is the matrix equivalent of [equation \(10.22\)](#).

10.4 INTERPOLATION OF QUATERNIONS

An application that benefits from a quaternion representation of rotation is *keyframe animation*. The rotational keyframes must be interpolated to produce reasonable in-between rotations. The quaternions representing the rotations can themselves be interpolated in a natural manner, as described in this section.

10.4.1 SPHERICAL LINEAR INTERPOLATION

The 4-tuple (x, y, z, w) that represents the matrix \mathcal{Q} was already shown to be unit length when viewed as a vector in \mathbb{R}^4 . That means it is a point on the hypersphere of radius 1 that is centered at the origin of \mathbb{R}^4 . This is just a fancy way of stating the geometry associated with the algebraic equation $x^2 + y^2 + z^2 + w^2 = 1$.

A standard problem in computer graphics and animation is to interpolate two 3D rotation matrices R_0 and R_1 for various choices of $t \in [0, 1]$. The interpolant is denoted $R(t)$, a rotation matrix itself, and it is required that $R(0) = R_0$ and $R(1) = R_1$. The 4-tuple representations of the rotation matrices and the corresponding hypersphere geometry allow for a simple yet elegant interpolation called *spherical linear interpolation*, or *slerp* for short. If $\mathbf{q}_i = (x_i, y_i, z_i, w_i)$ are the 4-tuple representations for R_i ($i = 0, 1$) and if $\mathbf{q}(t)$ is the 4-tuple representing $R(t)$, then a reasonable geometric condition to impose is that $\mathbf{q}(t)$ lie on the hyperspherical arc connecting \mathbf{q}_0 and \mathbf{q}_1 . Moreover, the angle between $\mathbf{q}(t)$ and \mathbf{q}_0 should be proportional to the angle ϕ between \mathbf{q}_0 and \mathbf{q}_1 with constant of proportionality t . [Figure 10.3](#) illustrates this by showing the plane spanned by \mathbf{q}_0 and \mathbf{q}_1 and the circular arc connecting them within that plane.

The angle $\phi \in (0, \pi)$ between \mathbf{q}_0 and \mathbf{q}_1 is indirectly obtained by a dot product, $\cos(\phi) = \mathbf{q}_0 \cdot \mathbf{q}_1$. The interpolant is required to be of the form $\mathbf{q}(t) = c_0(t)\mathbf{q}_0 + c_1(t)\mathbf{q}_1$ for some to-be-determined coefficient functions $c_0(t)$ and $c_1(t)$. Construction of $\mathbf{q}(t)$ uses only trigonometry and solving two equations in two unknowns. As t uniformly varies between 0 and 1, the values $\mathbf{q}(t)$ are required to uniformly vary along the circular arc from \mathbf{q}_0 to \mathbf{q}_1 . That is, the angle between $\mathbf{q}(t)$ and \mathbf{q}_0 is $t\phi$ and the angle between $\mathbf{q}(t)$ and \mathbf{q}_1 is $(1 - t)\phi$. Dotting the equation for $\mathbf{q}(t)$ with \mathbf{q}_0 yields

$$\cos(t\phi) = c_0(t) + \cos(\phi)c_1(t)$$

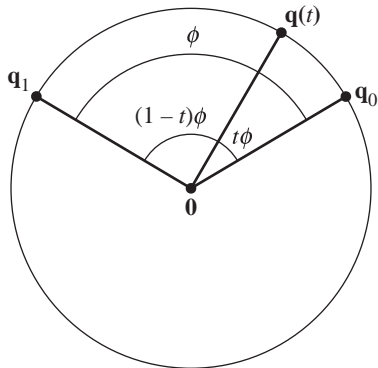


Figure 10.3 Illustration of the spherical linear interpolation, or slerp, of two vectors.

and dotting the equation with \mathbf{q}_1 yields

$$\cos((1-t)\phi) = \cos(\phi)c_0(t) + c_1(t)$$

These are two equations in the two unknowns c_0 and c_1 . The solution for c_0 is

$$c_0(t) = \frac{\cos(t\phi) - \cos(\phi)\cos((1-t)\phi)}{1 - \cos^2(\phi)} = \frac{\sin((1-t)\phi)}{\sin(\phi)}$$

The last equality is obtained by applying double-angle formulas for sine and cosine. By symmetry, $c_1(t) = c_0(1-t)$. Or solve the equations for

$$c_1(t) = \frac{\cos((1-t)\phi) - \cos(\phi)\cos(t\phi)}{1 - \cos^2(\phi)} = \frac{\sin(t\phi)}{\sin(\phi)}$$

The spherical linear interpolation is

$$\text{slerp}(t; \mathbf{q}_0, \mathbf{q}_1) = \frac{\sin((1-t)\phi)\mathbf{q}_0 + \sin(t\phi)\mathbf{q}_1}{\sin\phi} \quad (10.34)$$

for $0 \leq t \leq 1$. It is easy to verify that $\text{slerp}(0; \mathbf{q}_0, \mathbf{q}_1) = \mathbf{q}_0$ and $\text{slerp}(1; \mathbf{q}_0, \mathbf{q}_1) = \mathbf{q}_1$. Using trigonometry applied directly to equation (10.34), you can also verify that $|\text{slerp}(t; \mathbf{q}_0, \mathbf{q}_1)| = 1$ for all t .

The derivative of slerp with respect to time is

$$\text{slerp}'(t; \mathbf{q}_0, \mathbf{q}_1) = \frac{-\phi \cos((1-t)\phi)\mathbf{q}_0 + \phi \cos(t\phi)\mathbf{q}_1}{\sin\phi} \quad (10.35)$$

It is easy to verify that $\text{slerp}'(0; \mathbf{q}_0, \mathbf{q}_1) = \phi(-(\cos\phi)\mathbf{q}_0 + \mathbf{q}_1)/\sin\phi$, and $\text{slerp}'(1; \mathbf{q}_0, \mathbf{q}_1) = \phi(-\mathbf{q}_0 + (\cos\phi)\mathbf{q}_1)/\sin\phi$. Using trigonometry applied directly

to equation (10.35), you can also verify that $|\text{slerp}'(t; \mathbf{q}_0, \mathbf{q}_1)| = \phi$ for all t . The derivative vector has constant length, so a uniform sampling of t produces a uniform sampling of points on the circular arc.

If you were to specify a unit-length vector \mathbf{T} that is tangent to the unit hypersphere at a point \mathbf{q} on the hypersphere, and if you specify an angular speed ϕ , a circular arc starting at \mathbf{q} in the direction of \mathbf{T} is

$$\mathbf{p}(t) = \cos(t\phi)\mathbf{q} + \sin(t\phi)\mathbf{T} \quad (10.36)$$

for $t \geq 0$. In terms of the slerp function, \mathbf{q} is the starting point \mathbf{q}_0 , ϕ is the angle between \mathbf{q}_0 and the ending point \mathbf{q}_1 , and $\mathbf{T} = \text{slerp}'(0; \mathbf{q}_0, \mathbf{q}_1)/\phi$.

10.4.2 SPHERICAL QUADRATIC INTERPOLATION

In many applications there is a need for higher-order interpolation than what slerp provides. This section introduces *spherical quadratic interpolation* as an iteration of slerp operations to produce a higher-order result. The motivation for this comes from *quadratic interpolation* of four points in the plane that form a convex quadrilateral, call the points \mathbf{v}_i for $0 \leq i \leq 3$. Figure 10.4 shows a typical configuration.

Bilinear interpolation is used to generate points inside the quadrilateral. To represent the linear interpolation, or lerp, of the two input vectors, we use the notation

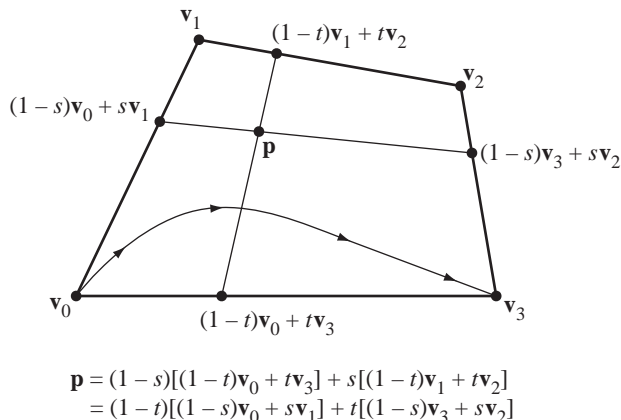


Figure 10.4 Four points forming a convex quadrilateral. Any interior point of the quadrilateral can be generated using bilinear interpolation with parameters s and t . The curve connecting \mathbf{v}_0 and \mathbf{v}_3 indicates that we want a particular function $s = f(t)$ with $f(0) = f(1) = 0$.

$\text{lerp}(r; \mathbf{a}, \mathbf{b}) = (1 - r)\mathbf{a} + r\mathbf{b}$ for $r \in [0, 1]$. The bottom and top edges are linearly interpolated using parameter $t \in [0, 1]$. The interpolated point for the bottom edge is

$$\mathbf{u}_0 = (1 - t)\mathbf{v}_0 + t\mathbf{v}_3 = \text{lerp}(t; \mathbf{v}_0, \mathbf{v}_3)$$

and the interpolated point for the top edge is

$$\mathbf{u}_1 = (1 - t)\mathbf{v}_1 + t\mathbf{v}_2 = \text{lerp}(t; \mathbf{v}_1, \mathbf{v}_2)$$

The line segment connecting \mathbf{u}_0 and \mathbf{u}_1 can be itself generated by linear interpolation of the endpoints using parameter $s \in [0, 1]$. Such points are of the form,

$$\begin{aligned}\mathbf{p} &= (1 - s)\mathbf{u}_0 + s\mathbf{u}_1 \\ &= (1 - s)[(1 - t)\mathbf{v}_0 + t\mathbf{v}_3] + s[(1 - t)\mathbf{v}_1 + t\mathbf{v}_2] \\ &= \text{lerp}(s; \text{lerp}(t; \mathbf{v}_0, \mathbf{v}_3), \text{lerp}(t; \mathbf{v}_1, \mathbf{v}_2))\end{aligned}$$

We want a curve that connects the initial point \mathbf{v}_0 and the final point \mathbf{v}_3 . This requires imposing a functional constraint $s = f(t)$ for some function f . It is necessary that $f(t) \in [0, 1]$ since $s \in [0, 1]$. For the curve to contain the initial point and final point, we need $f(0) = 0$ and $f(1) = 1$, respectively. The function $f(t)$ should also be symmetric about the t -interval midpoint $1/2$ so that the curve generated by the ordered input points and the curve generated by the reverse-ordered input points are the same. The constraint is therefore $f(1 - t) = f(t)$ for all $t \in [0, 1]$. The simplest function to use that satisfies the constraints is the quadratic $f(t) = ct(1 - t)$ for some $c \leq 4$; the bound on c guarantees $f(t) \leq 1$. Although there are many choices for c , a natural one is $c = 2$ so that at the midpoint $t = 1/2$, the interpolation produces the average of the four points. The curve is given parametrically as

$$\mathbf{p}(t) = \text{quad}(t; \mathbf{v}_0, \mathbf{v}_1, \mathbf{v}_2, \mathbf{v}_3) = \text{lerp}(2t(1 - t); \text{lerp}(t; \mathbf{v}_0, \mathbf{v}_3), \text{lerp}(t; \mathbf{v}_1, \mathbf{v}_2)) \quad (10.37)$$

A couple of observations are in order. First, as a function of s and t the interpolation scheme is bilinear. The coefficients of the input points are quadratic functions, hence the name *quadratic interpolation*. However, once the constraint $s = 2t(1 - t)$ is imposed, the coefficients are *cubic polynomials* in t , so the name “quadratic interpolation” is a misnomer. Second, equation (10.37) is *not* the cubic Bézier curve corresponding to four control points. The Bézier curve is

$$\begin{aligned}\mathbf{b}(t) &= (1 - t)^3\mathbf{v}_0 + 3(1 - t)^2t\mathbf{v}_1 + 3(1 - t)t^2\mathbf{v}_2 + t^3\mathbf{v}_3 \\ &= \text{lerp}(t; \text{lerp}(t; \text{lerp}(t; \mathbf{v}_0, \mathbf{v}_1), \text{lerp}(t; \mathbf{v}_1, \mathbf{v}_2)), \\ &\quad \text{lerp}(t; \text{lerp}(t; \mathbf{v}_1, \mathbf{v}_2), \text{lerp}(t; \mathbf{v}_2, \mathbf{v}_3)))\end{aligned}$$

The coefficient of \mathbf{v}_0 in equation (10.37) is $(1 - 2t(1 - t))(1 - t)$ and is not the same as the coefficient of \mathbf{v}_0 in $\mathbf{b}(t)$, namely $(1 - t)^3$. The Bézier curve has end tangents $\mathbf{b}'(0) = 3(\mathbf{v}_1 - \mathbf{v}_0)$ and $\mathbf{b}'(1) = 3(\mathbf{v}_3 - \mathbf{v}_2)$. The quadratic interpolation curve has end tangents $\mathbf{p}'(0) = (\mathbf{v}_3 - \mathbf{v}_0) + 2(\mathbf{v}_1 - \mathbf{v}_0)$ and $\mathbf{p}'(1) = (\mathbf{v}_3 - \mathbf{v}_0) - 2(\mathbf{v}_2 - \mathbf{v}_3)$.

Using the analogy of the iterated lerp function to define the quad function, we define the *squad* function of quaternions as

$$\text{squad}(t; \mathbf{q}_0, \mathbf{q}_1, \mathbf{q}_2, \mathbf{q}_3) = \text{slerp}(2t(1-t); \text{slerp}(t, \mathbf{q}_0, \mathbf{q}_3), \text{slerp}(t, \mathbf{q}_1, \mathbf{q}_2)) \quad (10.38)$$

You may verify that $\text{squad}(0; \mathbf{q}_0, \mathbf{q}_1, \mathbf{q}_2, \mathbf{q}_3) = \mathbf{q}_0$ and $\text{squad}(1; \mathbf{q}_0, \mathbf{q}_1, \mathbf{q}_2, \mathbf{q}_3) = \mathbf{q}_3$.

10.5 DERIVATIVES OF TIME-VARYING QUATERNIONS

In [equation \(6.68\)](#) of [Section 6.5](#) we stated that the derivative of a time-varying quaternion $q(t)$ is

$$\frac{dq(t)}{dt} = \frac{1}{2}\omega(t)q(t)$$

where $\omega(t)$ is the quaternion representation of the angular velocity vector $\mathbf{w}(t) = (w_1, w_2, w_3)$. As such, $\omega(t) = w_1\mathbf{i} + w_2\mathbf{j} + w_3\mathbf{k}$; that is, $\omega(t)$ has zero real part. It is not necessary that $\omega(t)$ be a unit-length quaternion since we know that the angular velocity $\mathbf{w}(t)$ is not necessarily a unit-length vector.

The derivative formula is proved according to the following construction that is a slightly more formal and detailed version of what occurs in the fine book [\[Kui99\]](#). Let $q(t) = \cos(\theta(t)/2) + u(t)\sin(\theta(t)/2)$, where $u = u_1\mathbf{i} + u_2\mathbf{j} + u_3\mathbf{k}$ with $u_1^2 + u_2^2 + u_3^2 = 1$. The rotation angle for $q(t)$ is θ and the rotation axis has unit-length direction $\mathbf{u} = (u_1, u_2, u_3)$. The quaternions $q(t+h)$ and $q(t)$ are both unit length, so the product $q(t+h)q^{-1}(t)$ is unit length; write it as

$$q(t+h)q^{-1}(t) = p(t, h) = \cos(\alpha(t, h)/2) + v(t, h)\sin(\alpha(t, h)/2) \quad (10.39)$$

where $v = v_1\mathbf{i} + v_2\mathbf{j} + v_3\mathbf{k}$ with $v_1^2 + v_2^2 + v_3^2 = 1$. The quaternion $p(t, h)$ has angle of rotation $\alpha(t, h)$ and rotation axis direction $\mathbf{v} = (v_1, v_2, v_3)$. When $h = 0$ the left-hand side is $q(t)q^{-1}(t) = 1$, so $\alpha(t, 0) = 0$. Multiplying [equation \(10.39\)](#) by $q(t)$, subtracting $q(t)$, and dividing by h leads to

$$\frac{q(t+h) - q(t)}{h} = \frac{\cos(\alpha(t, h)/2) - 1 + v(t, h)\sin(\alpha(t, h)/2)}{h}q(t)$$

Taking the limit as h goes to zero:

$$\begin{aligned} \frac{dq}{dt} &= \lim_{h \rightarrow 0} \frac{q(t+h) - q(t)}{h} \\ &= \lim_{h \rightarrow 0} \left(\frac{\cos(\alpha(t, h)/2) - 1 + v(t, h)\sin(\alpha(t, h)/2)}{h} q(t) \right) \\ &= \left(\lim_{h \rightarrow 0} \frac{\cos(\alpha(t, h)/2) - 1}{h} + v(t, 0) \lim_{h \rightarrow 0} \frac{\sin(\alpha(t, h)/2)}{h} \right) q(t) \end{aligned}$$

$$\begin{aligned}
&= \left(\lim_{h \rightarrow 0} \frac{-(\alpha_h(t, h)/2) \sin(\alpha(t, h)/2)}{1} + u(t) \lim_{h \rightarrow 0} \frac{(\alpha_h(t, h)/2) \cos(\alpha(t, h)/2)}{1} \right) q(t) \\
&= (\alpha_h(t, 0)/2) u(t) q(t)
\end{aligned}$$

where the next to last equality uses L'Hôpital's rule and $\alpha_h(t, h) = \partial \alpha(t, h) / \partial h$. So we have

$$\frac{dq}{dt} = \frac{1}{2} (\alpha_h(t, 0) u(t)) q(t) = \frac{1}{2} \omega q \quad (10.40)$$

Alternatively, we can use the approach taken in [DKL98]. Specify $q(t) = \gamma + \sigma u$, where $\gamma = \cos(\theta(t)/2)$, $\sigma = \sin(\theta(t)/2)$, and $u = u(t)$ has zero real part and its corresponding vector \mathbf{u} is unit length. Differentiating directly with respect to t :

$$\begin{aligned}
\frac{dq}{dt} &= -(\dot{\theta}/2)\sigma + \sigma \dot{u} + (\dot{\theta}/2)\gamma u \\
&= (\dot{\theta}/2)(\gamma u - \sigma) + \sigma \dot{u} \\
&= (\dot{\theta}/2)uq + \sigma \dot{u} \\
&= \frac{1}{2} (\dot{\theta}u + 2\sigma \dot{u}q^{-1})q
\end{aligned}$$

Since $\mathbf{u} \cdot \mathbf{u} = 1$, the derivative $\dot{\mathbf{u}}$ satisfies $\mathbf{u} \cdot \dot{\mathbf{u}} = 0$; that is, $\dot{\mathbf{u}}$ is perpendicular to \mathbf{u} . Consider:

$$\begin{aligned}
\dot{u}q^{-1} &= \dot{u}(\gamma - \sigma u) \\
&= \gamma \dot{u} - \sigma \dot{u}u \\
&= \gamma \dot{u} - \sigma(-\dot{u} \cdot u + \dot{u} \times u) \quad \text{By equation (10.21)} \\
&= \gamma \dot{u} - \sigma(\dot{u} \times u) \quad \text{Since } \dot{u} \text{ and } u \text{ are perpendicular as vectors} \\
&= 0 + (\gamma \dot{u} - \sigma(\dot{u} \times u))
\end{aligned}$$

The last equality stresses the fact that the real part is zero. This is true since \dot{u} and $\dot{u} \times u$ both have zero real parts. The derivative of $q(t)$ is therefore,

$$\begin{aligned}
\frac{dq}{dt} &= \frac{1}{2} (\dot{\theta}u + 2\sigma\gamma\dot{u} - 2\sigma^2\dot{u} \times u)q \\
&= \frac{1}{2} (\dot{\theta}u + \sin(\theta)\dot{u} + (\cos(\theta) - 1)\dot{u} \times u)q \\
&= \frac{1}{2} \omega q
\end{aligned} \quad (10.41)$$

Notice that u , \dot{u} , and $\dot{u} \times u$ in the term for angular velocity form an orthonormal set as vectors. Compare this to [equation \(2.40\)](#) to see, indeed, that the quaternion $\omega(t)$ does correspond to the angular velocity vector $\mathbf{w}(t)$.

Yet another approach is given in [KKS96] and uses logarithmic and exponential maps. However, this complicated approach is unnecessary as evidenced by the simplicity of the preceding proofs.

CHAPTER 11

DIFFERENTIAL EQUATIONS

This chapter is a brief summary of the basic concepts you need for working with *ordinary differential equations*. The modifier *ordinary* refers to equations that involve functions of a single independent variable. Rates of change of functions of multiple independent variables fall under the topic of *partial differential equations*, something we will not cover here. Thus, I will refer to ordinary differential equations in this chapter only by the term *differential equations*. A very good undergraduate textbook on the topic of ordinary differential equations is [Bra84] and it emphasizes an applied approach of the flavor of the problems in this book. A graduate textbook that is oriented towards physical applications and covers the advanced mathematical topics you need to fully understand the analysis of the physical models is [HS74].

Since our applications have time-varying quantities in physical simulations, the independent variable in the differential equations is always time t . The derivatives of dependent variables will use the dot notation. For example, if $x(t)$ is a function of t , the first derivative with respect to t is denoted $\dot{x}(t)$ and the second derivative is denoted $\ddot{x}(t)$.

11.1 FIRST-ORDER EQUATIONS

A *first-order differential equation* of a real-valued function $x(t)$ of the independent variable t is

$$\dot{x} = f(t, x) \quad (11.1)$$

The function $f(t, x)$ is a known quantity. The left-hand side of the equation is the formal expression for the first derivative of x with respect to t , which measures the rate of change of x over time. The right-hand side is what we wish the rate of change to be. For the sake of illustration, suppose that $x(t)$ measures the position of an object moving along a straight line. The velocity of the object is $\dot{x}(t)$ and the acceleration is $\ddot{x}(t)$. [Equation \(11.1\)](#) is what we want the velocity to be. Knowing the velocity $\dot{x}(t)$ at any time t , our goal is to determine what the position $x(t)$ is at any time. In a sense we want to integrate the velocity to obtain position.

An instinctive method for solving for position is the following. If we were to specify an initial position $x(0)$, [equation \(11.1\)](#) tells us immediately that the initial velocity is $\dot{x}(0) = f(0, x(0))$. We can differentiate equation (11.1) with respect to t and apply the chain rule from calculus to obtain

$$\ddot{x}(t) = f_t(t, x) + f_x(t, x) \dot{x}(t)$$

where $f_t = \partial f / \partial t$ and $f_x = \partial f / \partial x$. The initial acceleration is therefore $\ddot{x}(0) = f_t(0, x(0)) + f_x(0, x(0))\dot{x}(0)$. Assuming that $f(t, x)$ is differentiable of all orders, we could continue differentiating and evaluating to obtain the value of every derivative of $x(t)$. If $x^{(n)}(t)$ denotes the n th derivative of $x(t)$, then we can compute the initial values of all derivatives $x^{(n)}(0)$. If you recall from calculus, the formal Taylor series of $x(t)$ expanded about $t = 0$ is

$$x(t) = \sum_{n=0}^{\infty} \frac{x^{(n)}(0)}{n!} t^n$$

If we can compute all the derivatives of $x(t)$ at time 0, it appears that we have an expression for $x(t)$. I used the term *formal*. The right-hand side is an infinite sum. As you are aware, such a sum does not necessarily have a value. The general topic in calculus is *convergence* (or *divergence*) of the series. Moreover, not all functions have a Taylor series representation. Functions that do and for which the series converges for some interval of t are called *analytic functions*.

Unfortunately, the reality is that the Taylor series approach is not useful, especially for a computer application. We do not have the luxury of computing an infinite number of derivatives! At any rate, the process would require some general expression for partial derivatives of $f(t, x)$. Since f arises in our physical applications as applied forces, we might not even know a formula for it. In most cases $f(t, x)$ itself is not an analytic function which means, most likely, that $x(t)$ is not representable as a Taylor series. What we need to do instead is numerically solve the equation. That is the topic of [Chapter 13](#). We will look at a few relevant concepts for differential equations before pursuing numerical methods for solving them.

An *initial value problem* for a first-order differential equation is of the form,

$$\dot{x} = f(t, x), \quad t \geq t_0, \quad x(t_0) = x_0 \tag{11.2}$$

The differential equation is specified together with a selected initial time t_0 and initial function value $x_0 = x(t_0)$. These are the types of problems we will see in practice. Some initial value problems can be solved in closed form. For example, consider

$$\dot{x} = f(t), \quad t \geq t_0, \quad x(t_0) = x_0$$

where $f(t)$ depends only on time. Formally we can write the solution as an integral,

$$x(t) = x_0 + \int_{t_0}^t f(\tau) d\tau$$

If a closed-form exists for $\int f(t) dt$, we can immediately write down the solution for $x(t)$. For example, if $f(t) = t^p$, a polynomial term, then $\int f(t) dt = t^{p+1}/(p+1)$. The solution to the differential equation is then $x(t) = x_0 + (t^{p+1} - t_0^{p+1})/(p+1)$. In many cases, though, we do not have a closed-form for $\int f(t) dt$. The integral itself must be evaluated numerically using a standard numerical integrator.

Another type of problem that can be solved in closed form, so to speak, is a *first-order linear differential equation*. This is of the form,

$$\dot{x} = a(t)x + b(t), \quad t \geq t_0, \quad x(t_0) = x_0 \quad (11.3)$$

where $a(t)$ and $b(t)$ are known functions of time. If $b(t) = 0$ for all t , the equation $\dot{x} = a(t)x$ is said to be *homogeneous*. The formal solution is

$$x(t) = x_0 + \exp\left(\int_{t_0}^t a(\tau) d\tau\right) \left[x_0 + \int_{t_0}^t \exp\left(-\int_{t_0}^s a(\tau) d\tau\right) b(s) ds \right]$$

If we can integrate the various integrals in this equation in closed form, we can easily evaluate $x(t)$. If not, numerical integrators are required. The homogeneous equation (11.3) can be solved in closed form when the coefficient $a(t)$ is a constant for all time. That is, $\dot{x} = ax$ for some constant a with $x(t_0) = x_0$ has the solution,

$$x(t) = e^{a(t-t_0)} x_0 \quad (11.4)$$

as you can well verify.

Another special type of equation is a *separable equation*. These are of the form,

$$dx/dt = \dot{x} = f(t)/g(x), \quad t \geq t_0, \quad x(t_0) = x_0$$

The variables may be *separated* and placed on different sides of the equation, $g(x) dx = f(t) dt$, then integrated:

$$\int_{x_0}^x g(\xi) d\xi = \int_{t_0}^t f(\tau) d\tau$$

The same issue occurs regarding closed formulas for the integrals. If we do not have closed formulas, we must resort to numerical integration to estimate a solution. Even if we do have closed formulas, there is still a potential problem. If $G(x)$ is an antiderivative of $g(x)$, that is $dG/dx = g$, and if $F(t)$ is an antiderivative of $f(t)$, so that $dF/dt = f$, then the separated and integrated equation becomes $G(x) - G(x_0) = F(t) - F(t_0)$. To solve explicitly for x , we need to be able to invert the function $G(x)$; that is, $x = G^{-1}(F(t) - F(t_0) + G(x_0))$. The inversion might not be possible in closed form, and once again you must resort to numerical techniques. We already saw an application of separable equations to solving the simple pendulum problem, [Example 3.4](#). The separation was not for numerically solving the angle as a function of time; rather, it was to determine an estimate for the period of the pendulum.

The existence of closed formulas for the integrals or for inverse functions might be of pedagogic importance in a class on differential equations but not so in applications. The numerical differential equation solvers work directly with $f(t, x)$ in the equation and only require evaluations of that function.

11.2 EXISTENCE, UNIQUENESS, AND CONTINUOUS DEPENDENCE

Perhaps you might object to the title of this section – just like a mathematician to cloud the issue with facts! There is a good chance that the tutorials you find about physics simulations using differential equations of motion do not discuss the topic mentioned in the section title. Our interest is in numerically solving the initial value problem of [equation \(11.2\)](#). You can apply your favorite numerical solver to the differential equations of your application. A computer is quite happy to produce output without any thought, so to speak. The fundamental question on computer output: Can you trust it?

In the case of the initial value problem, in order for you to trust your output you really should be assured that the problem *has a solution*. This is the *existence question* about the initial value problem. Does there exist a solution to the problem? If there is a solution, your chances of finding it with a computer have just improved. If there is no solution, your output is useless. Better to do some type of analysis before implementing the problem or running a program to solve the problem. To make an analogy, consider solving a linear system of equations $A\mathbf{x} = \mathbf{b}$, where the $n \times n$ coefficient matrix A and the $n \times 1$ vector \mathbf{b} are inputs into the program. The output must be the solution \mathbf{x} , an $n \times 1$ vector. Well, it is quite possible that the linear system does not have a solution. Your linear system solver must be prepared to inform you that is the case. If you implemented Gaussian elimination to row-reduce the augmented matrix $[A | \mathbf{b}]$ to upper echelon form $H = [U | \mathbf{c}]$, where U is upper triangular, there is no solution to the system when $\text{rank}(U) < \text{rank}(H)$. The consequence of not trapping the rank condition is that you most likely will generate an exception due to division by zero.

Even if there is a solution, you still might not be able to trust the output of the program. What if there are multiple solutions to the same initial value problem? This is the *uniqueness question* about the initial value problem. Using our analogy of linear systems, it is possible that $\mathbf{Ax} = \mathbf{b}$ has multiple solutions. In fact, the theory says that if it has two solutions, it must have infinitely many solutions. This happens when $\text{rank}(U) = \text{rank}(H) < n$. An algorithm based on Gaussian elimination can trap this, report that there are multiple solutions, and terminate. However, your application might want to know more information. For example, the output might be a basis for the affine space of solutions. In the case of differential equations, if the initial value problem has multiple solutions, the physical modeling is more than likely in error. We expect that the modeling produces equations of motion for which there *exists a unique solution*.

Although I will not delve into the gory mathematical details, you can find in [Bra84], as well as in any other textbook on differential equations, the following theorem regarding existence and uniqueness of a solution to the initial value problem 11.2 of equation (11.2).

Theorem ■ Let $f(t, x)$ and $f_x(t, x)$ be continuous in the rectangle R defined by $t_0 \leq t \leq t_0 + a$ and $|x - x_0| \leq b$ for some positive constants a and b . Let $M = \max_{(t,x) \in R} |f(t, x)|$, a bound on the absolute value of $f(t, x)$ on the rectangle. Define $\alpha = \min(a, b/M)$. The initial value problem $\dot{x} = f(t, x)$ with $x(t_0) = x_0$ has a unique solution $x(t)$ defined for $t_0 \leq t \leq t_0 + \alpha$. ■

The bound M is guaranteed because a continuous function on a closed and bounded rectangle must have a minimum and a maximum, a standard result from calculus. The proof is not important to us, but the result is. As long as our function $f(t, x)$ has a continuous derivative in x in a small region about the initial point (t_0, x_0) , we have a unique solution. In fact, weaker conditions on f than having a continuous x -derivative still lead to existence-uniqueness results. But for all practical purposes the types of functions you expect to occur in the equations of motion will have continuous derivatives.

If your application “switches on and off” input forces and torques, you do not even have a continuous function. The theory of differential equations will provide you with yet more tools on showing existence and uniqueness, so feel free to investigate this topic in detail. A field of particular interest is *control theory*, by which you try to select $f(t, x)$ to force the solution $x(t)$ to behave in certain ways. For example, a pendulum with a metal end is swinging between two electric magnets. The magnets are either on or off; you get to choose their on/off status over time in order to get the pendulum to stop in the minimum amount of time.

The third portion of the section title is about *continuous dependence* of the solution on the input parameters. If there exists a unique solution for each choice of initial values (t_0, x_0) , we can write the solution to indicate its dependence on the values: $x(t; t_0, x_0)$. Our concern is that this function is continuous in t_0 and x_0 . Why should

we care? Think about it from the perspective of numerical round-off errors. If a small change in the input x_0 results in a very large change in the solution near initial time, we have an ill-conditioned problem whose numerical errors can propagate and lead to significantly incorrect outputs. In the applications we encounter with physical simulation, invariably we do have continuous dependence, so we will not concern ourselves at the moment with theoretical results.

11.3 SECOND-ORDER EQUATIONS

A *second-order differential equation* of a real-valued function $x(t)$ of the independent variable t is

$$\ddot{x} = f(t, x, \dot{x}) \quad (11.5)$$

The function $f(t, x, \dot{x})$ is a known quantity. The left-hand side of the equation is the formal expression for the second derivative of x with respect to t . For physical applications where $x(t)$ measures position, the second derivative measures acceleration, the rate of change of velocity $\dot{x}(t)$. The right-hand side is what we wish the rate of change to be. From this second-derivative information we wish to construct $x(t)$ itself. The *initial value problem* for the second-order equation is

$$\ddot{x} = f(t, x, \dot{x}), \quad t \geq t_0, \quad x(t_0) = x_0, \quad \dot{x}(t_0) = \dot{x}_0 \quad (11.6)$$

where t_0 , x_0 , and \dot{x}_0 are user-supplied inputs.

The initial value problem for a second-order linear differential equation is

$$\ddot{x} = a(t)\dot{x} + b(t)x + c(t), \quad t \geq t_0, \quad x(t_0) = x_0, \quad \dot{x}(t_0) = \dot{x}_0 \quad (11.7)$$

The homogeneous equation is the case $c(t) = 0$ for all t . Additionally, the equation with constant coefficients is

$$\ddot{x} = a\dot{x} + bx, \quad t \geq t_0, \quad x(t_0) = x_0, \quad \dot{x}(t_0) = \dot{x}_0$$

From the classical theory, at least one solution is of the form $x(t) = e^{rt}$ for a constant r that is possibly complex-valued. To determine r , compute the derivatives $\dot{x}(t) = re^{rt}$ and $\ddot{x}(t) = r^2e^{rt}$ and substitute into the equation to obtain

$$0 = \ddot{x} - a\dot{x} - bx = r^2e^{rt} - are^{rt} - be^{rt} = (r^2 - ar - b)e^{rt}$$

For this equation to be true for all t , we need $r^2 - ar - b = 0$, a quadratic equation in r . If the equation has two distinct real roots r_1 and r_2 , both $e^{r_1 t}$ and $e^{r_2 t}$ are solutions to the differential equation. The solution to the initial value problem is

$$x(t) = \frac{r_2 x_0 - \dot{x}_0}{r_2 - r_1} e^{r_1(t-t_0)} - \frac{r_1 x_0 - \dot{x}_0}{r_2 - r_1} e^{r_2(t-t_0)} \quad (11.8)$$

This equation is valid even if the roots are distinct, complex-valued numbers. However, the coefficients are then complex-valued and the exponential functions have powers that are complex-valued. If the roots are $\alpha \pm i\beta$, where $\beta \neq 0$, then Euler's identity $e^{i\theta} = \cos \theta + i \sin(\theta)$ yields

$$e^{(\alpha+i\beta)t} = e^{\alpha t}(\cos(\beta t) + i \sin(\beta t))$$

Some complex arithmetic applied to our solution in order to rearrange it into only real-valued expressions leads to

$$x(t) = \left(x_0 \cos(\beta(t - t_0)) + \frac{\dot{x}_0 - \alpha x_0}{\beta} \sin(\beta(t - t_0)) \right) e^{\alpha(t - t_0)} \quad (11.9)$$

Finally, the quadratic equation can have a repeated real root $r = a/2$ (when $b = -a^2/4$). The theory shows that two solutions to the differential equation are e^{rt} and te^{rt} . The solution to the initial value problem is

$$x(t) = (x_0 + (\dot{x}_0 - rx_0)(t - t_0)) e^{r(t-t_0)} \quad (11.10)$$

An understanding of this example is important for higher-order linear equations with constant coefficients. In particular, the relationship between the roots of the quadratic equation $r^2 - ar - b = 0$ and the types of solutions to the differential equation, namely e^{rt} , $e^{\alpha t} \cos(\beta t)$, $e^{\alpha t} \sin(\beta t)$, and te^{rt} , is important.

The theory of differential equations includes analysis of second-order equations in the form of [equation \(11.6\)](#). From our perspective we want only to solve the initial value problem numerically. We can do so by formulating the second-order equation as two first-order equations. If we define $v(t) = \dot{x}$, then $\dot{v} = \ddot{x} = f(t, x, \dot{x}) = f(t, x, v)$. The *first-order system of equations with initial conditions* corresponding to [equation \(11.6\)](#) is

$$\begin{bmatrix} \dot{x} \\ \dot{v} \end{bmatrix} = \begin{bmatrix} v \\ f(t, x, v) \end{bmatrix}, \quad t \geq t_0, \quad \begin{bmatrix} x(t_0) \\ v(t_0) \end{bmatrix} = \begin{bmatrix} x_0 \\ \dot{x}_0 \end{bmatrix} \quad (11.11)$$

To be suggestive of the form of [equation \(11.2\)](#), define $\mathbf{y} = [x \ v]^T$, $\mathbf{g}(t, \mathbf{y}) = [v \ f(t, x, v)]^T$, and $\mathbf{y}_0 = [x_0 \ \dot{x}_0]^T$. The initial value problem for the first-order system is

$$\dot{\mathbf{y}} = \mathbf{g}(t, \mathbf{y}), \quad t \geq t_0, \quad \mathbf{y}(t_0) = \mathbf{y}_0 \quad (11.12)$$

The importance of maintaining the form of the equation has to do with developing numerical methods for solving it. Methods that apply to [equation \(11.2\)](#) naturally extend to systems in the form of [equation \(11.12\)](#). The repackaging also applies to a system of n second-order equations to generate a first-order system of $2n$ equations. This latter case is exactly what we do in our physical simulations. For instance, see [Example 3.10](#).

11.4 GENERAL-ORDER DIFFERENTIAL EQUATIONS

The *n*th order differential equation of a real-valued function $x(t)$ of the independent variable t is

$$x^{(n)} = f(t, x, x^{(1)}, \dots, x^{(n-1)}) \quad (11.13)$$

where $x^{(k)}(t)$ denotes the k th order derivative of $x(t)$. The function $f(t, y_1, \dots, y_n)$ is a known quantity. The left-hand side of the equation is the formal expression for the n th order derivative of x with respect to t . The right-hand side is what we wish that derivative to be. We wish to construct $x(t)$ itself from the equation. The *initial value problem* for the n th order equation is

$$x^{(n)} = f(t, x, x^{(1)}, \dots, x^{(n-1)}), \quad t \geq t_0, \quad x^{(k)}(t_0) = x_0^{(k)}, \quad 0 \leq k \leq n-1 \quad (11.14)$$

where t_0 and $x_0^{(k)}$ for $0 \leq k \leq n-1$ are user-supplied inputs.

The initial value problem for an n th order linear differential equation is

$$x^{(n)} = \sum_{k=0}^{n-1} a_k(t) x^{(k)} + b(t), \quad t \geq t_0, \quad x^{(k)}(t_0) = x_0^{(k)}, \quad 0 \leq k \leq n-1 \quad (11.15)$$

The homogeneous equation is the case $b(t) = 0$ for all t . Additionally, the equation with constant coefficients is

$$x^{(n)} = \sum_{k=0}^{n-1} a_k x^{(k)}, \quad t \geq t_0, \quad x^{(k)}(t_0) = x_0^{(k)}, \quad 0 \leq k \leq n-1 \quad (11.16)$$

for some constants a_k for $0 \leq k \leq n-1$. Using the second-order linear equation with constant coefficients as the model, we expect a general solution of the form $x(t) = e^{rt}$. The derivatives are $x^{(k)}(t) = r^k e^{rt}$. Substituting into the differential equation leads to

$$0 = x^{(n)} - \sum_{k=0}^{n-1} a_k x^{(k)} = r^n e^{rt} - \sum_{k=0}^{n-1} a_k r^k e^{rt} = \left(r^n - \sum_{k=0}^{n-1} a_k r^k \right) e^{rt} = p(r) e^{rt}$$

where $p(r)$ is a polynomial of degree n and is called the *characteristic polynomial* for the differential equation. The only way to make $p(r)e^{rt} = 0$ for all t is if $p(r) = 0$. Thus, r must be a root of a polynomial. The fundamental theorem of algebra states that $p(r)$ is factorable into

$$p(r) = \prod_{j=1}^d (r - r_j)^{m_j}$$

where r_1 through r_d are the distinct roots, m_j is the multiplicity of root r_j , and $\sum_{j=1}^d m_j = n$. We know that the a_k are real-valued, so if a nonreal root occurs, say

$r = \alpha + i\beta$ for $\beta \neq 0$, then its conjugate $\bar{r} = \alpha - i\beta$ is also a root. The values r and \bar{r} are considered to be distinct roots, of course. Thus, nonreal roots occur in pairs. If r_j is a real-valued root, the contribution to the solution of the differential equation is the set of functions $t^\ell e^{r_j t}$ for $0 \leq \ell < m_j$. If $r_j = \alpha_j + i\beta_j$ is a nonreal root, the contribution of r_j and \bar{r}_j to the solution of the differential equation is the set of functions $t^\ell e^{\alpha_j t} \cos(\beta_j t)$ and $t^\ell e^{\alpha_j t} \sin(\beta_j t)$ for $0 \leq \ell < m_j$. If the real-valued roots are indexed by $1 \leq j \leq J_0$ and the complex-valued roots have indices $J_0 < j \leq d$, the general solution to the initial value problem is of the form,

$$x(t) = \sum_{j=1}^{J_0} \sum_{\ell=0}^{m_j-1} C_{\ell,j} t^\ell e^{r_j t} + \sum_{j=J_0+1}^d \sum_{\ell=0}^{m_j-1} [D_{\ell,j} \cos(\beta_j t) + E_{\ell,j} \sin(\beta_j t)] t^\ell e^{\alpha_j t} \quad (11.17)$$

where the n constants $C_{\ell,j}$, $D_{\ell,j}$, and $E_{\ell,j}$ are determined by the initial conditions of the problem.

Just as we converted the second-order equation to a first-order system, we may convert the n th order equation to a system. Define $y_k(t) = x^{(k-1)}(t)$ for $1 \leq k \leq n$. Differentiating the equation we obtain

$$\dot{y}_k(t) = \frac{dx^{(k-1)}(t)}{dt} = x^{(k)}(t) = y_{k+1}(t)$$

The last equation is

$$\dot{y}_n(t) = y_{n+1}(t) = x^{(n)}(t) = f(t, x, x^{(1)}, \dots, x^{(n-1)}) = f(t, y_1, \dots, y_n)$$

In vector form, define $\mathbf{y} = [y_1 \cdots y_n]^\top$, $\mathbf{g}(t, \mathbf{y}) = [y_2 \cdots y_n f(t, y_1, \dots, t_n)]^\top$, and $\mathbf{y}_0 = [x_0 \ x_0^{(1)} \ \cdots \ x_0^{(n-1)}]^\top$. The initial value problem for the first-order system is

$$\dot{\mathbf{y}} = \mathbf{g}(t, \mathbf{y}), \quad t \geq t_0, \quad \mathbf{y}(t_0) = \mathbf{y}_0 \quad (11.18)$$

which is identical to [equation \(11.12\)](#) except for the dimension of \mathbf{y} . Thus, numerical solvers for first-order systems are all that we need to solve n th order equations.

11.5 SYSTEMS OF LINEAR DIFFERENTIAL EQUATIONS

We have already observed that an n th order differential equation can be reformulated as a system of n first-order equations. This applies to linear differential equations, of course. A special case of interest, both generally and for physical applications, is the n th order linear equation with constant coefficients. These equations arise in the stability analysis of the differential equation, a topic discussed in [Section 11.6](#).

The n th order homogeneous linear equation with constant coefficients is [equation \(11.16\)](#) and has general solution given by [equation \(11.17\)](#). We can reformulate

the equation and its solution in vector-matrix form. Recall that we defined an $n \times 1$ vector \mathbf{y} whose components are $y_k(t) = x^{(k-1)}(t)$ for $1 \leq k \leq n$. The system of equations is

$$\dot{\mathbf{y}} = A\mathbf{y}, \quad t \geq t_0, \quad \mathbf{y}(t_0) = \mathbf{y}_0 \quad (11.19)$$

where A is an $n \times n$ matrix of constants and where \mathbf{y}_0 is the vector of initial conditions for the original equation. The matrix A is specifically

$$A = \begin{bmatrix} 0 & 1 & 0 & \cdots & 0 & 0 \\ 0 & 0 & 1 & \cdots & 0 & 0 \\ \vdots & \vdots & \vdots & \ddots & \vdots & \vdots \\ 0 & 0 & 0 & \cdots & 1 & 0 \\ 0 & 0 & 0 & \cdots & 0 & 1 \\ a_0 & a_1 & a_2 & \cdots & a_{n-2} & a_{n-1} \end{bmatrix}$$

The solution to the system of equations may be written as

$$\mathbf{y}(t) = e^{A(t-t_0)}\mathbf{y}_0 \quad (11.20)$$

where $e^{A(t-t_0)}$ is formally the exponential of a matrix power. Of course we need to define what this means. Notice the similarity of this solution to the one for a single first-order, linear, constant coefficient, homogeneous [equation \(11.4\)](#).

Recall that the Taylor series for the exponential function is

$$e^x = \sum_{k=0}^{\infty} \frac{x^k}{k!}$$

and that it converges for any real-valued input x . If we formally replace x by an $n \times n$ matrix of constants A , we have an expression for exponentiating a matrix:

$$e^A = \sum_{k=0}^{\infty} \frac{A^k}{k!}$$

An advanced course on matrix analysis covers the topic of convergence of such a series; for example, see [\[HJ85\]](#). The series does in fact converge for any matrix. The practical issue, though, is evaluating the series in order to compute the differential equation solution in [equation \(11.20\)](#). Since we already know the format of the general solution for the n th order equation with constant coefficients, [equation \(11.17\)](#), we expect that evaluation of the exponential $e^{A(t-t_0)}$ to depend somehow on the roots of the characteristic polynomial $p(r) = r^n - \sum_{k=0}^{n-1} a_k r^k$.

The characteristic polynomial does, in fact, show up in the problem. From linear algebra, the characteristic equation of a square matrix A is defined to be $\det(rI - A) = 0$. The determinant is indeed the characteristic polynomial $p(r) = \det(rI - A)$. A fact well known in linear algebra is the Cayley–Hamilton theorem that states

$p(A) = 0$, whereby you replace r formally by the matrix A in the characteristic polynomial. In our case we obtain the equation,

$$A^n = \sum_{k=0}^{n-1} a_k A^k$$

The n th power of A is decomposed into a linear combination of smaller powers of the matrix. The ramification for evaluating e^A is that the term A^n in the power series formula can be replaced by a linear combination of smaller powers. The next term is

$$\begin{aligned} A^{n+1} &= A \cdot A^n \\ &= A \sum_{k=0}^{n-1} a_k A^k \\ &= A(a_0 I + a_1 A + \cdots + a_{n-1} A^{n-1}) \\ &= a_0 I + a_1 A^2 + \cdots + a_{n-1} A^n \\ &= a_0 I + a_1 A^2 + \cdots + a_{n-1} \sum_{k=0}^{n-1} a_k A^k \\ &= \sum_{k=0}^{n-1} b_k A^k \end{aligned}$$

where the constants b_k are computed by grouping together like powers of A . We can repeat this procedure to obtain

$$A^{n+m} = \sum_{k=0}^{n-1} c_{m,k} A^k$$

for any $m \geq 0$. When $m = 0$ we have $c_{0,k} = a_k$ and when $m = 1$ we have $c_{1,k} = b_k$ from the formula we derived for A^{n+1} . Replacing in the power series:

$$\begin{aligned} \sum_{k=0}^{\infty} \frac{A^k}{k!} &= \sum_{k=0}^{n-1} \frac{A^k}{k!} + \sum_{k=n}^{\infty} \frac{A^k}{k!} \\ &= \sum_{k=0}^{n-1} \frac{A^k}{k!} + \sum_{m=0}^{\infty} \frac{A^{n+m}}{(n+m)!} \\ &= \sum_{k=0}^{n-1} \frac{A^k}{k!} + \sum_{m=0}^{\infty} \sum_{k=0}^{n-1} \frac{c_{m,k}}{(n+m)!} A^k \end{aligned}$$

$$\begin{aligned}
&= \sum_{k=0}^{n-1} \frac{A^k}{k!} + \sum_{k=0}^{n-1} \left(\sum_{m=0}^{\infty} \frac{c_{m,k}}{(n+m)!} \right) A^k \\
&= \sum_{k=0}^{n-1} \left(\frac{1}{k!} + \sum_{m=0}^{\infty} \frac{c_{m,k}}{(n+m)!} \right) A^k \\
&= \sum_{k=0}^{n-1} d_k A^k
\end{aligned}$$

where the last equation defines $d_k = \sum_{m=0}^{\infty} c_{m,k}/(n+m)!$. Thus, the infinite sum is replaced by a finite sum of the powers A^k with $k < n$. Unfortunately, this does not help us reach our final goal of computability because the d_k are still infinite sums.

Well, it takes quite a bit more of the power of linear algebra to get us to our goal. We need to be able to decompose A in such a way as to make the computation of e^A a reasonable endeavor. The motivation comes from *diagonalizable matrices*. The matrix A is diagonalizable if there exists a diagonal matrix D and an invertible matrix P such that $A = PDP^{-1}$. Powers of such matrices are easy to compute. For example,

$$A^2 = (PDP^{-1})(PDP^{-1}) = PD(P^{-1}P)DP^{-1} = PDIDP^{-1} = PD^2P^{-1}$$

The square of a diagonal matrix $D = \text{Diag}(d_1, \dots, d_n)$ is $D^2 = \text{Diag}(d_1^2, \dots, d_n^2)$. Repeating the process we see that

$$A^k = (PDP^{-1})^k = PD^kP^{-1}$$

where $D^k = \text{Diag}(d_1^k, \dots, d_n^k)$. The exponential matrix is

$$e^A = \sum_{k=0}^{\infty} \frac{A^k}{k!} = \sum_{k=0}^{\infty} \frac{PD^kP^{-1}}{k!} = P \left(\sum_{k=0}^{\infty} \frac{D^k}{k!} \right) P^{-1} = P \text{Diag}(e^{d_1}, \dots, e^{d_n}) P^{-1}$$

A special case where A is diagonalizable is when it is a symmetric matrix. The factorization is $A = RDR^T$, where the columns of R are eigenvectors of A and the diagonal entries of D are eigenvalues. Not all matrices are diagonalizable, so what to do? A handful of decomposition formulas can help you compute e^A , some good for mathematical reasons and others good for numerical reasons. Your best bet numerically is to use what is called the *S plus N decomposition*. The mathematical details of the decomposition are presented in [HS74]. A square matrix A with real-valued entries can always be decomposed as $A = S + N$, where S is a *semisimple matrix* and where N is a *nilpotent matrix*. A real-valued matrix N is said to be nilpotent if $N^p = 0$ for some power $p > 0$, but $N^k \neq 0$ for powers $1 \leq k < p$. A real-valued matrix S is said to be semisimple if, as an operator on n -tuples of complex number,

it is diagonalizable. If we were to attempt to use the diagonalizability of S directly, we would have $S = PDP^{-1}$ for a diagonal matrix D and an invertible matrix P . The problem is that D can have nonreal diagonal terms (complex conjugate roots of the characteristic equation) and P can have nonreal terms. To avoid the nonreal values we need to factor $S = PEP^{-1}$, where P is a real-valued invertible matrix and where E is of the form,

$$E = \begin{bmatrix} r_1 & & & & \\ & \ddots & & & \\ & & r_{J_0} & & \\ & & & \begin{bmatrix} \alpha_{J_0+1} & -\beta_{J_0+1} \\ \beta_{J_0+1} & \alpha_{J_0+1} \end{bmatrix} & & \\ & & & & \ddots & \\ & & & & & \begin{bmatrix} \alpha_d & -\beta_d \\ \beta_d & \alpha_d \end{bmatrix} \end{bmatrix} \quad (11.21)$$

where the distinct real-valued roots of the characteristic equation are r_j for $1 \leq j \leq J_0$ and the distinct nonreal roots are $r_j = \alpha_j \pm i\beta_j$ for $J_0 < j \leq d$. The factorization $S = PEP^{-1}$ is always possible for a semisimple matrix.

First, it is important to know that the properties of the exponential function of a matrix are not always the same as for real numbers. If a and b are real numbers, then $e^{a+b} = e^a e^b = e^b e^a = e^{b+a}$. If A and B are matrices, generally $e^{A+B} \neq e^A e^B$ and generally $e^A e^B \neq e^B e^A$. The failure for equality of $e^A e^B$ and $e^B e^A$ should be intuitive; you are already aware that matrix multiplication is not commutative. The failure for equality of e^{A+B} and $e^A e^B$ is not obvious. Now these terms are equal under very special conditions, in particular when the input matrices themselves commute, $AB = BA$.

The decomposition $A = S + N$ has the property that $SN = NS$, so in fact we can write $e^A = e^{S+N} = e^S e^N$. Since S is semisimple, it is factorable as $S = PEP^{-1}$ where P is invertible and E is a matrix of the form in [equation \(11.21\)](#). Since N is nilpotent, the infinite sum of e^N is really a finite one because $N^k = 0$ for $k \geq p$,

$$e^N = \sum_{k=0}^{\infty} \frac{N^k}{k!} = \sum_{k=0}^{p-1} \frac{N^k}{k!}$$

Combining these leads to a concise formula for e^A ,

$$e^A = e^S e^N = Pe^E P^{-1} \sum_{k=0}^{p-1} \frac{N^k}{k!}$$

when $D = \text{Diag}(d_1, \dots, d_n)$. The only remaining computation is e^E , a matrix which is shown to be

$$e^E = \begin{bmatrix} e^{r_1} & & & & \\ & \ddots & & & \\ & & e^{r_{j_0}} & & \\ & & & e^{\alpha_{j_0+1}} \begin{bmatrix} \cos(\beta_{j_0+1}) & -\sin(\beta_{j_0+1}) \\ \sin(\beta_{j_0+1}) & \cos(\beta_{j_0+1}) \end{bmatrix} & \\ & & & & \ddots \\ & & & & e^{\alpha_d} \begin{bmatrix} \cos(\beta_d) & -\sin(\beta_d) \\ \sin(\beta_d) & \cos(\beta_d) \end{bmatrix} \end{bmatrix} \quad (11.22)$$

The solution to the linear system of differential equations in equation (11.20) is, therefore,

$$\mathbf{y}(t) = e^{A(t-t_0)} \mathbf{y}_0 = \left(P e^{E(t-t_0)} P^{-1} \sum_{k=0}^{p-1} \frac{N^k (t-t_0)^k}{k!} \right) \mathbf{y}_0 \quad (11.23)$$

The bulk of the work in computing the solution is therefore in numerically computing the decomposition $A = S + N$ and factoring $S = PEP^{-1}$.

11.6 EQUILIBRIA AND STABILITY

An intuitive description of the concepts of *equilibria* and *stability* of solutions comes from the simple pendulum problem of Example 3.4. The differential equation that models the motion of the pendulum relative to the vertical, and measured in terms of the angle $\theta(t)$ formed with the vertical, is

$$\ddot{\theta} + \frac{g}{L} \sin \theta = 0, \quad t \geq 0, \quad \theta(0) = \theta_0, \quad \dot{\theta}(0) = \dot{\theta}_0$$

If we were to let the pendulum hang straight down and not give it an initial push, it would remain in the vertical position forever. The initial conditions for this configuration are $\theta_0 = 0$ and $\dot{\theta}_0 = 0$. The solution to the differential equation is $\theta(t) \equiv 0$, where the three-barred symbol denotes “equal for all t .” This solution is referred to as an *equilibrium solution*. Moreover, the solution is *stable* in the sense that if you were to just slightly push the pendulum, the motion is about the equilibrium solution and remains so for all time.

Now suppose you were to position the pendulum so that it was vertically upward and had no initial velocity. The initial conditions are $\theta_0 = \pi$ and $\dot{\theta}_0$. Observe that $\theta(t) \equiv \pi$ is a solution to the differential equation with the specified initial conditions. This solution is also an equilibrium solution, but it is *unstable* in the sense that if you were to just slightly push the pendulum, the motion would take the pendulum far away from $\theta_0 = \pi$.

We can write the simple pendulum model as a system of equations of the form of [equation \(11.18\)](#) by defining $y_1 = \theta(t)$, $y_2 = \dot{\theta}(t)$, $\mathbf{y}(t) = [y_1 \ y_2]^T$, $\mathbf{y}_0 = [\theta_0 \ \dot{\theta}_0]$, and $\mathbf{g}(t, \mathbf{y}) = [y_2 - (g/L) \sin y_1]^T$, namely

$$\dot{\mathbf{y}} = \mathbf{g}(t, \mathbf{y})$$

In this form the equilibrium solutions are $\mathbf{y} \equiv (0, 0)$ and $\mathbf{y} \equiv (\pi, 0)$.

In general, an *equilibrium solution* to [equation \(11.18\)](#) is $\mathbf{y}(t) \equiv \mathbf{y}_0$, where $\mathbf{g}(t, \mathbf{y}_0) \equiv 0$. Just as in the pendulum problem we want to know if we start the system near an equilibrium solution, will it remain nearby for all time (stable)? Or will it immediately move away from the equilibrium (unstable)? To answer this question we need a formal definition for stability. The definition is more general in that it may be applied to *any* solution of the differential equation, not just to an equilibrium solution. The intuitive concept is that a solution is stable when other solutions nearby at initial time tend to stay nearby for all time.

The classical stability results are developed for *autonomous systems of equations*. These are differential equations where the right-hand side does not explicitly depend on t ; that is, the differential equation is $\dot{\mathbf{y}} = \mathbf{g}(\mathbf{y})$.

Definition ■ Let $\mathbf{y} = \phi(t)$ be a solution to $\dot{\mathbf{y}} = \mathbf{g}(\mathbf{y})$. The solution is *stable* if every solution $\psi(t)$ of the differential equation that is close to $\phi(t)$ at initial time $t = 0$ remains close for all future time. In mathematical terms, this is reminiscent of the definition for a limit: For each choice of $\varepsilon > 0$ there is a $\delta > 0$ such that $|\psi(t) - \phi(t)| < \varepsilon$ whenever $|\psi(0) - \phi(0)| < \delta$.

If at least one solution $\psi(t)$ does not remain close, then $\phi(t)$ is said to be *unstable*. ■

For a stable solution the ε - δ definition says that you select the maximum amount of error ε you can tolerate between $\psi(t)$ and $\phi(t)$. The value δ , which depends on your choice of ε , tells you how close to $\phi(0)$ you have to start in order to stay within that error.

11.6.1 STABILITY FOR CONSTANT-COEFFICIENT LINEAR SYSTEMS

The stability of solutions for constant-coefficient linear systems $\dot{\mathbf{y}} = A\mathbf{y}$ is completely determinable. The motivation for the general results is provided by the following example.

Consider a second-order equation with characteristic polynomial $r^2 - ar - b = 0$. Suppose that the polynomial has two distinct real-valued roots r_1 and r_2 . The solution to the initial value problem is listed in [equation \(11.8\)](#). Generally,

$$x(t) = C_1 e^{r_1 t} + C_2 e^{r_2 t}$$

An equilibrium solution is $\phi(t) \equiv 0$. In order for $x(t)$ to remain close to $\phi(t)$ for all time, we need to understand what happens to $x(t)$ as t becomes large (as $t \rightarrow \infty$ in the mathematical vernacular). The behavior of $x(t)$ for large t is dependent, of course, on the behavior of its components $e^{r_1 t}$ and $e^{r_2 t}$. If $r_1 < 0$ and $r_2 < 0$, both exponentials decay to zero, in which case $\lim_{t \rightarrow \infty} x(t) = 0$. In fact, $x(t)$ remains “close” to zero. However, if $r_1 > 0$, the exponential term $e^{r_1 t}$ becomes unbounded regardless of the value of r_2 and $x(t)$ does not stay close to zero. The same instability occurs if $r_2 > 0$ regardless of the value of r_1 . That brings us to the case of $r_1 = 0$ and $r_2 < 0$ (or similarly, $r_1 < 0$ and $r_2 = 0$). The solution is $x(t) = C_1 + C_2 e^{r_2 t}$ and the limiting behavior is $\lim_{t \rightarrow \infty} x(t) = C_1$. The solution remains close to zero but does not approach zero when $C_1 \neq 0$. Being stable does not require the limit to be zero, only that you stay close for all time. Thus, the equilibrium solution is stable when $r_1 \leq 0$ and $r_2 \leq 0$ but unstable when either $r_1 > 0$ or $r_2 > 0$.

If the roots of the characteristic equation are $\alpha \pm i\beta$, where $\beta \neq 0$, the initial value problem has a solution provided by [equation \(11.9\)](#). Generally,

$$x(t) = (C_1 \cos(\beta t) + C_2 \sin(\beta t)) e^{\alpha t}$$

The graph of this function has sinusoidal oscillations, but the amplitude is exponential. If $\alpha < 0$, then the amplitude decays to zero over time. That is, $\lim_{t \rightarrow \infty} x(t) = 0$. The equilibrium solution $\phi(t) \equiv 0$ is stable in this case. If $\alpha > 0$, the oscillations are unbounded and the equilibrium solution is unstable. If $\alpha = 0$, the function $x(t)$ remains bounded for all time, which means it remains close to the zero solution (“close” in the sense that it does not move unboundedly away from the zero solution). The equilibrium solution is stable when $\alpha \leq 0$, but unstable when $\alpha > 0$.

Another case occurs when the characteristic polynomial has a repeated real root $r = a/2$. [Equation \(11.10\)](#) provides the solution to the initial value problem. Generally,

$$x(t) = (C_1 + C_2 t) e^{rt}$$

If $r < 0$, the solution decays to zero; the equilibrium solution is stable. If $r > 0$, the solution becomes unbounded; the equilibrium solution is unstable. If $r = 0$, $x(t)$ still becomes unbounded (generally for any nonzero C_2) and the equilibrium solution is unstable. This behavior is slightly different than the previous cases when a root was zero or the real part of a root was zero: The equilibrium solution is stable when $r < 0$ but unstable when $r \geq 0$. The general stability result is listed next without proof.

Theorem ■ Consider the constant-coefficient linear equation $\dot{\mathbf{y}} = A\mathbf{y}$.

1. Every solution is stable if all the eigenvalues of A have negative real parts.
2. Every solution is unstable if at least one eigenvalue of A has positive real part.
3. Suppose that the eigenvalues of A all have real parts that are zero or negative. List those eigenvalues with zero real part as $r_j = i\beta_j$ for $1 \leq j \leq \ell$ and let the multiplicity of r_j relative to the characteristic equation be m_j . Every solution is stable if A has m_j linearly independent eigenvectors for each r_j . Otherwise, every solution is unstable. ■

The first two conditions of the theorem are clearly illustrated by our example for a second-order equation, when the characteristic roots are distinct. The third condition was illustrated regardless of whether the characteristic roots are repeated or distinct. In the case of two distinct real roots, when $r_1 = 0$ and $r_2 < 0$ we had stability. The matrix A has an eigenvalue $r = 0$ of multiplicity 1 and one linearly independent eigenvector to go with it. In the case of two distinct nonreal roots, when $\alpha = 0$ we had stability. Each nonreal root is an eigenvalue of A with multiplicity 1, each eigenvalue having one linearly independent eigenvector to go with it. In the case of a repeated real root, the matrix A has an eigenvalue $r = a/2$ of multiplicity 2, but only one linearly independent eigenvector $(1, a/2)$, so the equilibrium solution is unstable.

Notice that when all the eigenvalues of A have negative real parts, the limit of any solution $x(t)$ as t approaches infinity is 0. Thus, the equilibrium solution $\phi(t) \equiv 0$ is stable. The limit being zero is quite a strong condition. In this case we say that the zero solution is *asymptotically stable*. The concept applies to any solution:

Definition ■ Let $\mathbf{y} = \phi(t)$ be a solution to $\dot{\mathbf{y}} = \mathbf{g}(\mathbf{y})$. The solution is *asymptotically stable* if it is stable and if every solution $\psi(t)$ that is close to $\phi(t)$ at initial time $t = 0$ approaches $\phi(t)$ as t approaches infinity. ■

11.6.2 STABILITY FOR GENERAL AUTONOMOUS SYSTEMS

This last section shows the stability properties for constant-coefficient, linear systems of equations. Other than the mass–spring systems, our physics applications were invariably nonlinear. We would still like to know the stability of the physical systems at equilibrium points. Consider the general autonomous system,

$$\dot{\mathbf{y}} = A\mathbf{y} + \mathbf{g}(\mathbf{y})$$

where A is an $n \times n$ matrix of constants and where $\mathbf{g}(\mathbf{y})$ is an $n \times 1$ vector for which $\mathbf{g}(\mathbf{y})/\|\mathbf{y}\|$ is continuous and which is zero when \mathbf{y} is zero. The norm of the vector is the *max norm*, $\|\mathbf{y}\| = \max\{|y_1|, \dots, |y_n|\}$, and is not the length of the vector. The stability analysis is summarized by the following.

Theorem ■ Consider the equilibrium solution $\mathbf{y}(t) \equiv \mathbf{0}$ of $\dot{\mathbf{y}} = A\mathbf{y} + \mathbf{g}(\mathbf{y})$, where $\mathbf{g}(\mathbf{y})/\|\mathbf{y}\|$ is continuous and $\lim_{\mathbf{y} \rightarrow \mathbf{0}} \mathbf{g}(\mathbf{y})/\|\mathbf{y}\| = \mathbf{0}$.

1. The equilibrium solution is asymptotically stable if all the eigenvalues of A have negative real parts.
2. The equilibrium solution is unstable if at least one eigenvalue of A has positive real part.
3. The stability of the equilibrium solution cannot be determined from the stability of the equilibrium solution for the linear system $\dot{\mathbf{y}} = A\mathbf{y}$ when all the eigenvalues of A have real parts zero or negative with at least one eigenvalue having real part zero. ■

The classical way this result is applied to a general autonomous system $\dot{\mathbf{y}} = \mathbf{f}(\mathbf{y})$, where $\mathbf{f}(\mathbf{0}) = \mathbf{0}$, is to use Taylor's theorem with remainder from calculus to write

$$\mathbf{f}(\mathbf{y}) = \mathbf{f}(\mathbf{0}) + A\mathbf{y} + \mathbf{g}(\mathbf{y}) = A\mathbf{y} + \mathbf{g}(\mathbf{y})$$

where A is the matrix of first-order partial derivatives of $\mathbf{f}(\mathbf{y})$ evaluated at zero and $\mathbf{g}(\mathbf{y})$ is the remainder term of second- and higher-order expressions.

The three conditions of the theorem mimic those shown in the theorem for stability of linear systems with constant matrix A . The last condition is problematic. In the case of linear systems, having some eigenvalues with negative real parts and the rest with zero real parts puts you on the border of stability versus instability. This is a particular problem in the numerical solution of differential equations. If you have a physical model for which theoretically there is a zero eigenvalue of the linearized system, numerical error can make it appear as if the model actually has a small positive eigenvalue, causing the numerical solution to behave erratically.

As an example consider the damped, simple pendulum problem. The equation of motion is $\ddot{\theta} + (g/L)\sin\theta = -c\dot{\theta}$, $c > 0$, where the right-hand side represents viscous friction at the pendulum joint. Setting $y_1 = \theta$, $y_2 = \dot{\theta}$, $\mathbf{y} = [y_1 \ y_2]^T$, and

$$\mathbf{f}(\mathbf{y}) = \begin{bmatrix} f_1(y_1, y_2) \\ f_2(y_1, y_2) \end{bmatrix} = \begin{bmatrix} y_2 \\ -\frac{g}{L} \sin y_1 - cy_2 \end{bmatrix}$$

the system that models the pendulum is $\dot{\mathbf{y}} = \mathbf{f}(\mathbf{y})$, where $\mathbf{f}(\mathbf{0}) = \mathbf{0}$. The linearized system is $\dot{\mathbf{y}} = A\mathbf{y}$, where

$$A = \left[\begin{array}{cc} \frac{\partial f_1(y_1, y_2)}{\partial y_1} & \frac{\partial f_1(y_1, y_2)}{\partial y_2} \\ \frac{\partial f_2(y_1, y_2)}{\partial y_1} & \frac{\partial f_2(y_1, y_2)}{\partial y_2} \end{array} \right] \Big|_{(y_1, y_2)=(0,0)} = \begin{bmatrix} 0 & 1 \\ -\frac{g}{L} & -c \end{bmatrix}$$

The eigenvalues are $r = (-c \pm \sqrt{c^2 - 4g/L})/2$. If $c > 0$ and $c^2 \geq 4g/L$, the eigenvalues are negative real numbers and we have asymptotic stability of $\mathbf{y} \equiv \mathbf{0}$. What

this means physically is that if you start the pendulum nearly vertical and give it a small velocity, it will move to the vertical position and stop without oscillating about the vertical position (strong damping). If $c > 0$ and $c^2 < 4g/L$, the eigenvalues are complex-valued with nonzero imaginary parts and negative real parts. If you start the pendulum nearly vertical and give it a small velocity, it will oscillate about the vertical position and eventually stop in the vertical position (weak damping). If you remove the damping so that $c = 0$, the eigenvalues are $\pm i\beta$ for a value $\beta \neq 0$. The theorem does not provide us any information on the stability in this case. A more detailed analysis will show that the zero solution is stable, but not asymptotically stable. That is, if you start the pendulum in a nearly vertical position and give it a small velocity, it will oscillate about the vertical forever (never stopping).

If you have shied away from eigenvalues and eigenvectors, change your ways! The eigendecomposition of a matrix is related to solving linear systems of differential equations that in turn occur as part of a physical simulation. And you want to program physics in a game environment, do you not? We did not avoid eigenvalues and eigenvectors in the regular chapters of this book, but one topic I intentionally avoided was choosing a differential equation solver for the equations of motion of a physical model. Part of the decision process involves choosing a step size for the numerical solver. This choice depends on the physical stability of equilibria of the system, an analysis that requires eigendecomposition. The choice also depends on the numerical stability of the solver. The relationship between physical stability and numerical stability is discussed in the next chapter.



ORDINARY DIFFERENCE EQUATIONS

12.1 DEFINITIONS

Let $\{y_k\}_{k=0}^{\infty}$ be a sequence of numbers whose terms are dependent based on the equation,

$$y_{k+n} = f(k, y_k, y_{k+1}, \dots, y_{k+n-1}) \quad (12.1)$$

for some function f , for some $n > 0$, and for all $k \geq 0$. The equation is called an *explicit nth-order difference equation*. The first n sequence terms y_0 through y_{n-1} are called the *initial values* for the difference equation. Once selected, the next term is determined from the previous terms by $y_n = f(0, y_0, \dots, y_{n-1})$. The terms y_1 through y_n may in turn be used to construct y_{n+1} . The process is repeated as often as an application requires. The adjective *explicit* refers to the explicit occurrence of the next term y_{k+n} on the left-hand side of the equation. An *implicit nth-order difference equation* is

$$F(k, y_k, \dots, y_{k+n}) = 0 \quad (12.2)$$

For all practical purposes, the function is assumed to be differentiable in its last component with $\partial F / \partial y_{k+n} \neq 0$ for any generated sequence. If it is possible to solve the implicit equation in closed form for y_{k+n} , then the solution is an explicit equation.

In many cases it is not possible to solve in closed form, so y_{k+n} must be calculated by some numerical method.

If the function in the definition for an explicit difference equation does not have a k -component, that is $y_{k+n} = f(y_k, \dots, y_{k+n-1})$, then the equation is said to be *autonomous*. The autonomous implicit difference equation is $F(y_k, \dots, y_{k+n}) = 0$.

In some applications, the behavior of y_k in the limit as k becomes infinite is important to know. The possibilities are that the limit is a finite number, is infinite ($+\infty$ or $-\infty$), or does not exist.

EXAMPLE
12.1

The equation $y_{k+1} = y_k^2$, $y_0 \geq 0$, is an explicit, autonomous, first-order difference equation. It is of the form $y_{k+1} = f(y_k)$, where $f(u) = u^2$. In this example we can construct a general formula. The first few terms of the sequence are

$$y_1 = y_0^2, \quad y_2 = y_1^2 = (y_0^2)^2 = y_0^4, \quad y_3 = y_2^2 = (y_0^4)^2 = y_0^8, \dots, \quad y_k = y_0^{2^k}$$

A check to make sure we observed the correct pattern:

$$y_{k+1} = y_0^{2^{k+1}} = \left(y_0^{2^k}\right)^2 = y_k^2,$$

and in fact we do have a solution. If $y_0 = 0$, all terms in the sequence are zero. If $y_0 = 1$, all terms in the sequence are 1. For $0 < y_0 < 1$, the sequence terms decrease in size and $\lim_{k \rightarrow \infty} y_k = 0$. For $y_0 > 1$, the sequence terms increase in size and $\lim_{k \rightarrow \infty} y_k = +\infty$. ■

EXAMPLE
12.2

The equation $y_{k+1}^3 + (k+1)y_k^2 - 1 = 0$ is an implicit, nonautonomous, first-order difference equation. It is of the form $F(k, y_k, y_{k+1}) = 0$, where $F(k, u, v) = v^3 + (k+1)u^2 - 1$. This equation may be solved explicitly as

$$y_{k+1} = (1 - (k+1)y_k^2)^{1/3}$$

A few iterations are shown:

$$\begin{aligned} y_1 &= (1 - y_0^2)^{1/3} \\ y_2 &= (1 - 2y_1^2)^{1/3} = \left(1 - 2(1 - y_0^2)^{2/3}\right)^{1/3} \\ y_3 &= (1 - 3y_2^2)^{1/3} = \left(1 - 3\left(1 - 2(1 - y_0^2)^{2/3}\right)^{2/3}\right)^{1/3} \end{aligned}$$

A general solution for this example is intractable, but it can be shown that the limiting behavior is $\lim_{k \rightarrow \infty} y_k = -\infty$. ■

EXAMPLE
12.3

The equation $y_{k+2} + \exp(-y_{k+2}) - y_{k+1} - y_k = 0$ is an autonomous, implicit, second-order difference equation. The initial values are y_0 and y_1 . It is not possible to explicitly solve for y_{k+2} . Define $g(x) = x + \exp(-x) - c$, where $c = y_{k+1} + y_k$.

The value y_{k+2} is a root to $g(x) = 0$. First, $g(x) = 0$ might not have roots. The first and second derivatives are $g'(x) = 1 - \exp(-x)$ and $g''(x) = \exp(-x)$. The first derivative is zero when $x = 0$. The second derivative is always positive. These conditions imply that $g(x)$ has a global minimum at $x = 0$, so $g(x) \geq g(0) = 1 - c$. If $c < 1$, then $g(x) > 0$ for all x , which means g has no roots. In order to have a next (real-valued) term y_{k+2} in the sequence, it is necessary that $y_{k+1} + y_k \geq 1$. If this constraint is met, then $g(0) < 0$. Because $g(0)$ is a global minimum and $g''(x) > 0$, there are exactly two roots to $g(x) = 0$. We will always choose the positive one.

Let's look at constructing y_2 when the initial values satisfy the constraint $c = y_1 + y_0 \geq 1$. We must solve $g(x) = 0$ for its positive root. Newton's method can be applied to approximate the root. For $x \geq 0$, define $h(x) = x - c$. A quick sketch of the graph shows that the $h(x) < g(x)$, so the positive root must be in $(0, c)$ since $h(c) = 0$. We may as well choose the initial guess for Newton's method to be $x_0 = c$. The other iterates are

$$x_{j+1} = x_j - \frac{g(x_j)}{g'(x_j)}, \quad j \geq 0$$

This is yet another ordinary difference equation, an autonomous and first-order one. A few iterates x_j are generated until some stopping condition is met, usually a combination of making sure $g(x_j)$ is close to zero and $|x_{j+1} - x_j|$ is close to zero. The last iterate is the number used for y_2 . The iterate y_3 can now be computed in a similar manner as long as $c = y_2 + y_1 \geq 1$. Assuming $y_{k+1} + y_k \geq 1$ at each step of the process, the limit as k becomes infinite exists, call it L , and it must be a solution to $0 = L + \exp(-L) - 2L$ (replace the y_k , y_{k+1} , and y_{k+2} terms in the difference equation by L). This simplifies to $\exp(-L) = L$. The equation cannot be solved in closed form. A numerical construction leads to the approximation $L \doteq 0.567143$. Observe that when the y_k terms are close to L , $y_{k+1} + y_k$ will in fact be larger than 1 (the sum is approximately 1.134286). ■

EXAMPLE 12.4

Compute an approximation to $1/\sqrt{x}$ for $x > 0$. Let $y = 1/\sqrt{x}$. Equivalently, $x = 1/y^2$. We may formulate the problem in terms of root finding. For a specified x , define $g(y) = 1/y^2 - x$. The root to $g(y) = 0$ is the number $1/\sqrt{x}$. Applying Newton's method, let y_0 be some initial guess to the root. The other iterates are determined by

$$y_{k+1} = y_k - \frac{g(y_k)}{g'(y_k)} = y_k - \frac{\frac{1}{y_k^2} - x}{-\frac{2}{y_k^3}} = \frac{y_k(3 - xy_k^2)}{2}$$

Once again we have an autonomous, first-order, explicit difference equation. The number of iterations to produce a reasonable approximation to $1/\sqrt{x}$ depends on how good an initial guess you choose. Suppose that x is written as $x = (1+m)2^e$, where $0 \leq m < 1$; then $1/\sqrt{x} = 1/\sqrt{1+m}2^{-e/2}$. This reduces the problem to computing $1/\sqrt{z}$ for $0 \leq z < 2$, where $z = 1+m$. Now we need to select a good initial

(Example 12.4
continued)

guess. One way to do this is to approximate the function $R(m) = 1/\sqrt{1+m}$ for $m \in [0, 1]$ by a straight line $L(m)$ and use $L(m)$ as the approximation to $R(m)$. One such line is $L(m) = 0.966215 - 0.25m$.

To illustrate, let $m = 0.5$. Using a hand calculator, $1/\sqrt{1+m} = 1/\sqrt{1.5} \doteq 0.81649658$. The initial guess is $y_0 = L(0.5) = 0.841215$. A couple of iterations of Newton's method are shown next:

$$y_1 = \frac{y_0(3 - (1 + m)y_0^2)}{2} = 0.81536277, \quad y_2 = \frac{y_1(3 - (1 + m)y_1^2)}{2} = 0.81649422$$

One iteration is a reasonable approximation. Two iterations is a really good approximation. ■

12.2 LINEAR EQUATIONS

A restricted class of explicit difference equations is the set of *n th-order linear difference equations*,

$$a_k^{(n)} y_{k+n} + a_k^{(n-1)} y_{k+n-1} + \cdots + a_k^{(1)} y_{k+1} + a_k^{(0)} y_k = b_k, \quad k \geq 0 \quad (12.3)$$

where the $a_k^{(m)}$ and b_k coefficients are known sequences. The initial values for the equation are y_0 through y_n . The order of the equation is degenerate if $a_k^{(n)} = 0$ for some k . In many applications we have $a_k^{(n)} \neq 0$ for all k . In this case the [equation \(12.3\)](#) is of the form

$$y_{k+n} + a_k^{(n-1)} y_{k+n-1} + \cdots + a_k^{(1)} y_{k+1} + a_k^{(0)} y_k = b_k, \quad k \geq 0 \quad (12.4)$$

which will be used in the remainder of this section. The linear difference equation is *homogeneous* if $b_k = 0$ for all k ; otherwise, it is *nonhomogeneous*. The theory of linear difference equations is analogous to the theory of ordinary differential equations as the following sections will show.

12.2.1 FIRST-ORDER LINEAR EQUATIONS

The first-order linear equation is

$$y_{k+1} + a_k y_k = b_k, \quad k \geq 0 \quad (12.5)$$

The initial value y_0 and the coefficient sequences a_k and b_k are known quantities.

The homogeneous equation sets $b_k = 0$ for all k . The *homogeneous solution* is presented here with h_k denoting the sequence. The equation is rewritten as $h_{k+1} = -a_k h_k$ for $k \geq 0$ with $h_0 = y_0$. The first few iterations are

$$h_1 = -a_0 h_0 = -a_0 y_0, \quad h_2 = -a_1 h_1 = a_1 a_0 y_0, \quad h_3 = -a_2 h_2 = -a_2 a_1 a_0 y_0$$

The observed pattern of terms leads to

$$h_k = \left(\prod_{i=0}^{k-1} (-a_i) \right) y_0, \quad k \geq 0 \quad (12.6)$$

where the “capital pi” symbol (Π) denotes a product of terms, analogous to “capital sigma” (Σ) denoting a sum of terms. The convention for products is $\prod_{i=\ell}^u T_i = 1$ whenever $u < \ell$. A similar convention for sums is $\sum_{i=\ell}^u T_i = 0$ whenever $u < \ell$.

A *particular solution* is a sequence p_k such that $p_{k+1} + a_k p_k = b_k$ for $k \geq 0$, but with initial value $p_0 = 0$. This equation can also be solved by iterating and observing the pattern:

$$\begin{aligned} p_1 &= b_0 - a_0 p_0 = b_0, \quad p_2 = b_1 - a_1 p_1 = b_1 - a_1 b_0, \\ p_3 &= b_2 - a_2 p_2 = b_2 - a_2 b_1 + a_2 a_1 b_0 \end{aligned}$$

The observed pattern of terms leads to

$$p_k = \sum_{i=1}^k \left(\prod_{j=i}^{k-1} (-a_j) \right) b_i, \quad k \geq 0 \quad (12.7)$$

The *general solution* to equation (12.5) is the sum of the homogeneous solution (12.6) and particular solution (12.7):

$$y_k = h_k + p_k, \quad k \geq 0 \quad (12.8)$$

12.2.2 SECOND-ORDER LINEAR EQUATIONS

The second-order linear equation is

$$y_{k+2} + a_k y_{k+1} + b_k y_k = c_k, \quad k \geq 0 \quad (12.9)$$

where y_0 and y_1 are known initial values. The coefficient sequences a_k , b_k , and c_k are known quantities. Establishing a pattern for the solution by writing down the first few iterates is difficult at best, although it can be done as we will see in the section on systems of equations.

For now, let us take a look at the homogeneous equation where $c_k = 0$ for all k . The homogeneous solution h_k can be written as two other solutions u_k and v_k , where the second sequence is not a constant multiplied by the first. In this sense the sequences u_k and v_k are linearly independent. Any linear combination of the sequences is also a homogeneous solution, so $h_k = \alpha u_k + \beta v_k$, where α and β are chosen so that $y_0 = h_0 = \alpha u_0 + \beta v_0$ and $y_1 = h_1 = \alpha u_1 + \beta v_1$.

Define $\Delta_k = u_k v_{k+1} - u_{k+1} v_k$. This quantity is analogous to the *Wronskian* of two linearly independent solutions to a second-order linear differential equation. The initial value is $\Delta_0 = u_0 v_1 - u_1 v_0$. We know that $u_{k+2} + a_k u_{k+1} + b_k u_k = 0$ and

$v_{k+2} + a_k v_{k+1} + b_k v_k = 0$. Multiplying the first equation by v_{k+1} , the second equation by u_{k+1} , and subtracting produces

$$0 = (u_{k+2}v_{k+1} - u_{k+1}v_{k+2}) + b_k(u_k v_{k+1} - u_{k+1}v_k) = -\Delta_{k+1} + b_k \Delta_k$$

which is a first-order equation whose solution is

$$\Delta_k = \prod_{i=0}^{k-1} b_i, \quad k \geq 1, \quad \Delta_0 = u_0 v_1 - u_1 v_0$$

If we happen to know in advance the solution u_k , we can determine v_k from the first-order equation in the v -terms:

$$u_k v_{k+1} - u_{k+1} v_k = \prod_{i=0}^{k-1} b_i$$

Another method for obtaining one homogeneous solution from another is *reduction of order*. If u_k is a known homogeneous solution, we attempt a solution of the form $v_k = \lambda_k u_k$. Replacing this in the homogeneous equation yields

$$\begin{aligned} 0 &= v_{k+2} + a_k v_{k+1} + b_k v_k \\ &= \lambda_{k+2} u_{k+2} + a_k \lambda_{k+1} u_{k+1} + b_k \lambda_k u_k \\ &= \lambda_{k+2} u_{k+2} + \lambda_{k+1}(-u_{k+2} - b_k u_k) + b_k \lambda_k u_k \\ &= u_{k+2}(\lambda_{k+2} - \lambda_{k+1}) - b_k u_k(\lambda_{k+1} - \lambda_k) \\ &= u_{k+2} D_{k+1} - b_k u_k D_k \end{aligned}$$

where $D_k = \lambda_{k+1} - \lambda_k$. The term D_k satisfies a first-order linear equation which we know how to solve,

$$\lambda_{k+1} - \lambda_k = D_k = \prod_{i=0}^{k-1} \frac{b_i u_i}{u_{i+2}}$$

Summing over k and canceling all the common terms on the left,

$$\lambda_n - \lambda_0 = \sum_{k=0}^{n-1} \prod_{i=0}^{k-1} \frac{b_i u_i}{u_{i+2}}$$

The value λ_0 is chosen so that the solutions u_k and v_k are linearly independent.

Now let us try to construct a particular solution p_k whose initial values are $p_0 = p_1 = 0$. The method shown here is analogous to the *variation of parameters* that is used for second-order linear differential equations. Let u_k and v_k be linearly independent solutions to the homogeneous equation. Assume that a particular solution is

of the form $p_k = d_k u_k + e_k v_k$. The initial values for p_k require $d_0 = d_1 = e_0 = e_1 = 0$. Replacing this in equation (12.9) yields

$$\begin{aligned} c_k &= p_{k+2} + a_k p_{k+1} + b_k p_k \\ &= (d_{k+2} u_{k+2} + e_{k+2} v_{k+2}) + a_k (d_{k+1} u_{k+1} + e_{k+1} v_{k+1}) + b_k (d_k u_k + e_k v_k) \\ &= (d_{k+2} u_{k+2} + e_{k+2} v_{k+2}) - d_{k+1} (u_{k+2} + b_k u_k) - e_{k+1} (v_{k+2} + b_k v_k) \\ &\quad + b_k (d_k u_k + e_k v_k) \\ &= [u_{k+2}(d_{k+2} - d_{k+1}) + v_{k+2}(e_{k+2} - e_{k+1})] - b_k [u_k(d_{k+1} - d_k) + v_k(e_{k+1} - e_k)] \end{aligned}$$

As in the variation of parameters for ordinary differential equations, an arbitrary equation may be selected to relate the parameters d_k and e_k . The simplest is to require $u_k(d_{k+1} - d_k) + v_k(e_{k+1} - e_k) = 0$. The previously displayed equation reduces to $u_{k+2}(d_{k+2} - d_{k+1}) + v_{k+2}(e_{k+2} - e_{k+1}) = 0$. Incrementing the index k by 1 in the arbitrary equation and defining $D_k = d_{k+2} - d_{k+1}$ and $E_k = e_{k+2} - e_{k+1}$, the two equations are written as the system,

$$\begin{bmatrix} u_{k+1} & v_{k+1} \\ u_{k+2} & v_{k+2} \end{bmatrix} \begin{bmatrix} D_k \\ E_k \end{bmatrix} = \begin{bmatrix} 0 \\ c_k \end{bmatrix}, \quad k \geq 0$$

The solution follows where $\Delta_k = u_k v_{k+1} - u_{k+1} v_k$:

$$\begin{bmatrix} d_{k+2} - d_{k+1} \\ e_{k+2} - e_{k+1} \end{bmatrix} = \begin{bmatrix} D_k \\ E_k \end{bmatrix} = \frac{1}{\Delta_{k+1}} \begin{bmatrix} -c_k v_{k+1} \\ c_k u_{k+1} \end{bmatrix}$$

Summing over k , canceling all the common terms on the left, and using $d_1 = e_1 = 0$, we obtain

$$d_k = - \sum_{i=0}^{k-2} \frac{c_i v_{i+1}}{\Delta_{i+1}}, \quad e_k = \sum_{i=0}^{k-2} \frac{c_i u_{i+1}}{\Delta_{i+1}}$$

and

$$p_k = \sum_{i=0}^{k-2} \frac{c_i (u_i v_k - u_k v_i)}{u_i v_{i+1} - u_{i+1} v_i}, \quad k \geq 2, \quad p_0 = p_1 = 0 \quad (12.10)$$

12.3 CONSTANT COEFFICIENT EQUATIONS

For the general linear difference equation, obtaining closed-form homogeneous solutions can be difficult, if not impossible. A special class of linear equations includes those whose coefficient sequences are all constants:

$$y_{k+n} + a_{n-1} y_{k+n-1} + \cdots + a_1 y_{k+1} + a_0 y_k = 0 \quad (12.11)$$

where the a_j are constant and $a_0 \neq 0$. We attempt a solution of the form $y_k = r^k$, where $r \neq 0$ is a constant. Replacing this in equation (12.11) and dividing by r^k leads to

$$r^n + a_{n-1}r^{n-1} + \cdots + a_1r + a_0 = 0$$

This is a polynomial equation, say $p(r) = 0$, whose roots may be found in closed-form for $1 \leq n \leq 4$ or by numerical root finding for any n .

Let r_1 through r_ℓ be the distinct roots of $p(r)$. Let each root r_j have multiplicity m_j . That is, the polynomial is factored into

$$p(r) = \prod_{j=1}^{\ell} (r - r_j)^{m_j}$$

Necessarily, $n = \sum_{j=1}^{\ell} m_j$. If r is a real-valued root with multiplicity m , then by the construction, r^k is a solution to the difference equation. However, there are m linearly independent solutions to the difference equation corresponding to r :

$$r^k, kr^k, k^2r^k, \dots, k^{m-1}r^k$$

If r is a complex-valued root with nonzero imaginary part, say $r = \alpha + \beta i$ with $\beta \neq 0$, and if r has multiplicity m , then the conjugate \bar{r} is also a root with multiplicity m . There are $2m$ linearly independent solutions corresponding to r and \bar{r} . In complex-valued form, these are

$$r^k, kr^k, \dots, k^{m-1}r^k; \bar{r}^k, k\bar{r}^k, \dots, k^{m-1}\bar{r}^k$$

Using the polar representation $r = \rho(\cos \theta + i \sin \theta)$, the real-valued form for the solutions are generated from $k^t r^k$ and $k^t \bar{r}^k$ by taking combinations $k^t(r^k + \bar{r}^k)/2$ and $k^t(r^k - \bar{r}^k)/(2i)$. These are

$$k^t \rho^k \cos(k\theta), \quad k^t \rho^k \sin(k\theta), \quad 0 \leq t \leq m-1$$

When a root r has multiplicity $m > 1$, the question is how did we arrive at the solutions $k^t r^k$ for $t > 0$? The answer is variation of parameters, a method discussed earlier in this section. As an example, consider the fourth-order equation,

$$y_{k+4} - 3y_{k+3} - 6y_{k+2} + 28y_{k+1} - 24 = 0$$

The polynomial equation obtained by trying a solution $y_k = r^k$ is $p(r) = r^4 - 3r^3 - 6r^2 + 28r - 24 = 0$. The polynomial factors into $p(r) = (r-2)^3(r+3)$. The root $r = 2$ has multiplicity 3, and the root $r = -3$ has multiplicity 1. Two linearly independent solutions to the difference equation are $y_k = 2^k$ and $y_k = (-3)^k$. Since $r = 2$ has multiplicity larger than one, attempt a reduction by $y_k = a_k 2^k$ for some sequence a_k .

Replacing this in the difference equation yields

$$\begin{aligned} 0 &= y_{k+4} - 3y_{k+3} - 6y_{k+2} + 28y_{k+1} - 24 \\ &= a_{k+4}2^{k+4} - 3a_{k+3}2^{k+3} - 6a_{k+2}2^{k+2} + 28a_{k+1}2^{k+1} - 24a_k2^k \\ &= 8 \cdot 2^k(2a_{k+4} - 3a_{k+3} - 3a_{k+2} + 7a_{k+1} - 3a_k) \end{aligned}$$

Consequently, the a_k satisfy yet another fourth-order constant coefficient equation,

$$2a_{k+4} - 3a_{k+3} - 3a_{k+2} + 7a_{k+1} - 3a_k = 0$$

An important observation is that the sum of the coefficients is zero. This allows the following reduction:

$$\begin{aligned} 0 &= 2a_{k+4} - 3a_{k+3} - 3a_{k+2} + 7a_{k+1} - 3a_k \\ &= 2(a_{k+4} - a_{k+3}) - a_{k+3} - 3a_{k+2} + 7a_{k+1} - 3a_k \\ &= 2(a_{k+4} - a_{k+3}) - (a_{k+3} - a_{k+2}) - 4a_{k+2} + 7a_{k+1} - 3a_k \\ &= 2(a_{k+4} - a_{k+3}) - (a_{k+3} - a_{k+2}) - 4(a_{k+2} - a_{k+1}) + 3a_{k+1} - 3a_k \\ &= 2(a_{k+4} - a_{k+3}) - (a_{k+3} - a_{k+2}) - 4(a_{k+2} - a_{k+1}) + 3(a_{k+1} - a_k) \end{aligned}$$

Define $b_k = a_{k+1} - a_k$. The previous equation is restated as

$$2b_{k+3} - b_{k+2} - 4b_{k+1} + 3b_k = 0$$

This is a third-order equation, a reduction in order by one from the original equation. The sum of the coefficients in this equation is also zero, allowing yet another reduction:

$$\begin{aligned} 0 &= 2b_{k+3} - b_{k+2} - 4b_{k+1} + 3b_k \\ &= 2(b_{k+3} - b_{k+2}) + b_{k+2} - 4b_{k+1} + 3b_k \\ &= 2(b_{k+3} - b_{k+2}) + (b_{k+2} - b_{k+1}) - 3b_{k+1} + 3b_k \\ &= 2(b_{k+3} - b_{k+2}) + (b_{k+2} - b_{k+1}) - 3(b_{k+1} - b_k) \end{aligned}$$

Define $c_k = b_{k+1} - b_k$. The previous equation is restated as

$$2c_{k+2} + c_{k+1} - 3c_k = 0$$

The order has been reduced by one again. The sum of the coefficients in this equation is zero, allowing yet one more reduction:

$$\begin{aligned} 0 &= 2c_{k+2} + c_{k+1} - 3c_k \\ &= 2(c_{k+2} - c_{k+1}) + 3(c_{k+1} - c_k) \end{aligned}$$

Define $d_k = c_{k+1} - c_k$. The previous equation is restated as

$$2d_{k+1} + 3d_k = 0$$

The general solution is $d_k = d_0(-3/2)^k$, but as it turns out, we need consider only the instance when $d_0 = 0$, in which case $d_k = 0$ for all k . Backtracking, we now know that $c_{k+1} - c_k = d_k = 0$. The c_k must be constant, so choose $c_k = c_0 \neq 0$ for all k . Backtracking again, $b_{k+1} - b_k = c_k = c_0$. Summing over k and canceling terms lead to $b_k = b_0 + \sum_{i=0}^{k-1} c_0 = b_0 + c_0 k$. Backtracking for the last time, $a_{k+1} - a_k = b_k = b_0 + c_0 k$. Summing over k and canceling terms lead to

$$a_k = a_0 + \sum_{i=0}^{k-1} (b_0 + c_0 i) = a_0 + b_0 k + c_0(k-1)k/2 = \alpha + \beta k + \gamma k^2$$

for appropriately selected values α , β , and γ . The choice of $\alpha = 1$ and $\beta = \gamma = 0$ leads to $a_k = 1$ and the already known solution 2^k . The choice of $\beta = 1$ and $\alpha = \gamma = 0$ leads to $a_k = k$ and a new solution $k2^k$. The choice of $\gamma = 1$ and $\alpha = \beta = 0$ leads to $a_k = k^2$ and a new solution k^22^k .

12.4 SYSTEMS OF EQUATIONS

Equation (12.1) provides a relationship between the terms of a single sequence. Some applications might involve multiple sequences that are interrelated. For example, two sequences $\{x_k\}_{k=0}^{\infty}$ and $\{y_k\}_{k=0}^{\infty}$ might be interrelated by

$$\begin{aligned} x_{k+n} &= f_0(k, x_k, \dots, x_{k+n-1}, y_k, \dots, y_{k+n-1}) \\ y_{k+n} &= f_1(k, x_k, \dots, x_{k+n-1}, y_k, \dots, y_{k+n-1}) \end{aligned}$$

for some $n > 0$, for all $k \geq 0$, and for some specified functions f_0 and f_1 . The initial values are x_0 through x_{n-1} and y_0 through y_{n-1} . The pair of equations is evaluated to obtain the next terms x_n and y_n , which in turn can be used to generate subsequent terms. The pair of relationships is an example of a *system of difference equations*. The system in the example can be written in vector form. Define:

$$\mathbf{u}_k = \begin{bmatrix} x_k \\ y_k \end{bmatrix} \text{ and } \mathbf{f}(k, (s_0, t_0), \dots, (s_{n-1}, t_{n-1})) = \begin{bmatrix} f_0(k, s_0, \dots, s_{n-1}, t_0, \dots, t_{n-1}) \\ f_1(k, s_0, \dots, s_{n-1}, t_0, \dots, t_{n-1}) \end{bmatrix}$$

In terms of these quantities, the system is

$$\mathbf{u}_{k+n} = \mathbf{f}(k, \mathbf{u}_k, \dots, \mathbf{u}_{k+n-1}), \quad k \geq 0$$

with initial values \mathbf{u}_0 through \mathbf{u}_{n-1} . Systems may contain explicit equations (as in our example), implicit equations, or a mixture of both.

A convenient use for a system of equations is in solving the n th-order linear equation (12.4). Define the vector sequence:

$$\mathbf{u}_k = \begin{bmatrix} u_k^{(0)} \\ u_k^{(1)} \\ \vdots \\ u_k^{(n-1)} \end{bmatrix} = \begin{bmatrix} y_k \\ y_{k+1} \\ \vdots \\ y_{k+n-1} \end{bmatrix}$$

Increasing the index by 1,

$$\begin{aligned} \mathbf{u}_{k+1} &= \begin{bmatrix} y_{k+1} \\ y_{k+2} \\ \vdots \\ y_{k+n} \end{bmatrix} \\ &= \begin{bmatrix} y_{k+1} \\ y_{k+2} \\ \vdots \\ b_k - a_k^{(n-1)} y_{k+n-1} - \cdots - a_k^{(0)} y_k \end{bmatrix} \\ &= \begin{bmatrix} u_k^{(1)} \\ u_k^{(2)} \\ \vdots \\ b_k - a_k^{(n-1)} u_k^{(n-1)} - \cdots - a_k^{(0)} u_k^{(0)} \end{bmatrix} \end{aligned}$$

In matrix form, the system is

$$\mathbf{u}_{k+1} + A_k \mathbf{u}_k = \mathbf{B}_k, \quad k \geq 0 \quad (12.12)$$

where \mathbf{u}_0 is a known quantity and where A_k is an $n \times n$ matrix and \mathbf{B}_k is an $n \times 1$ vector given by

$$A_k = \begin{bmatrix} 0 & 1 & 0 & \cdots & 0 \\ 0 & 0 & 1 & \cdots & 0 \\ \vdots & \vdots & \vdots & \ddots & \vdots \\ 0 & 0 & 0 & \cdots & 1 \\ a_k^{(0)} & a_k^{(1)} & a_k^{(2)} & \cdots & a_k^{(n-1)} \end{bmatrix} \text{ and } \mathbf{B}_k = \begin{bmatrix} 0 \\ 0 \\ \vdots \\ b_k \end{bmatrix}$$

Equation (12.12) has exactly the form of equation (12.5) and can be solved symbolically in the same way. The homogeneous solution is

$$\mathbf{h}_k = \left(\prod_{i=0}^{k-1} (-A_i) \right) \mathbf{u}_0, \quad k \geq 0 \quad (12.13)$$

The particular solution is

$$\mathbf{p}_k = \sum_{i=1}^k \left(\prod_{j=i}^{k-1} (-A_j) \right) \mathbf{B}_i, \quad k \geq 0 \quad (12.14)$$

The general solution to equation (12.12) is the sum of the homogeneous solution (12.13) and particular solution (12.14),

$$\mathbf{u}_k = \mathbf{h}_k + \mathbf{p}_k, \quad k \geq 0 \quad (12.15)$$

CHAPTER 13

NUMERICAL METHODS

This chapter is the most fitting one for a computer implementation of a physical simulation. The focus of the book has been on understanding the basic concepts of physics, modeling a physical system, and deriving the equations of motion for that system. The physical simulation itself requires us to implement methods that numerically solve the differential equations that we derive. Many choices exist for numerical solvers. Each choice has its trade-offs to consider, the usual one being an exchange of speed for accuracy and/or stability. We want the solver to be fast, accurate, and robust. In most cases it is not possible to obtain all three simultaneously. A variety of algorithms for numerically solving differential equations are provided here, some to give you a flavor of the ideas even if they are not the best choices for a real application. The issue of stability is revisited, as promised in the chapter on differential equations.

To keep the discussion simple, let us look at a single first-order differential equation with initial conditions,

$$\dot{x} = f(t, x), \quad t \geq t_0, \quad x(t_0) = x_0 \quad (13.1)$$

The methods presented here extend easily to vector-valued functions that we encounter in the physics applications. Much of the analysis depends on looking at the derivatives of $x(t)$. In particular, recall the following result from calculus:

Taylor's Theorem ■ If $x(t)$ and its derivatives $x^{(k)}(t)$ for $1 \leq k \leq n$ are continuous on the closed interval $[t_0, t_1]$ and $x^{(n)}(t)$ is differentiable on the open interval (t_0, t_1) ,

then there exists $\bar{t} \in [t_0, t_1]$ such that

$$x(t_1) = \sum_{k=0}^n \frac{x^{(k)}(t_0)}{k!} (t_1 - t_0)^k + \frac{x^{(n+1)}(\bar{t})}{(n+1)!} (t_1 - t_0)^{n+1}$$

By convention $x^{(0)}(t) = x(t)$. The polynomial $P_n(t) = \sum_{k=0}^n x^{(k)}(t_0)(t - t_0)^k / k!$ is called the *Taylor polynomial of degree n* and may be used to approximate $x(t)$. The *remainder term* is $R_n(t) = x^{(n+1)}(\bar{t})(t - t_0)^{n+1} / (n+1)!$. In practice we estimate a bound M for which $|x^{(n+1)}(t)| \leq M$ for all $t \in [t_0, t_1]$, thus leading to a bound on the total error $|R_n(t)| \leq M(t_1 - t_0)^{n+1} / (n+1)!$ for $t \in [t_0, t_1]$. ■

13.1 EULER'S METHOD

No discussion of numerical methods is complete without mentioning Euler's method, a very simple and popular method for solving differential equations. Its attraction is its simplicity. Its downfall is its large amount of truncation error compared to other methods and its lack of stability and accuracy for many practical examples.

Euler's method is a matter of using Taylor's theorem with $n = 2$ on the interval $[t_i, t_{i+1}]$, where $h = t_{i+1} - t_i > 0$. Using dot notation, since we only have a couple of derivatives to look at,

$$x(t_{i+1}) = x(t_i) + \dot{x}(t_i)h + \ddot{x}(\bar{t})\frac{h^2}{2} = x(t_i) + hf(t_i, x(t_i)) + \ddot{x}(\bar{t})\frac{h^2}{2}$$

for some $\bar{t} \in [t_i, t_{i+1}]$. Observe that we replaced $\dot{x}(t_i)$ by $f(t_i, x(t_i))$ since we know that $x(t)$ is a solution to the differential equation (13.1). Define $x_i = x(t_i)$ for all i ; keep in mind that x_i refers to the exact value of the solution to the differential equation at time t_i . Discarding the remainder term and using y_i to denote the *approximation* to x_i , we obtain Euler's method,

$$y_{i+1} = y_i + hf(t_i, y_i), \quad i \geq 0, \quad y_0 = x_0 \tag{13.2}$$

Certainly this is an easy method to implement. The important question, though, is how well y_i approximates x_i for large i . In particular we would like to know a bound on the error term $|x_i - y_i|$.

In Chapter 11, “Differential Equations,” we mentioned an existence and uniqueness theorem whose hypotheses included the continuity of the partial derivative $f_x(t, x)$ on a rectangle containing the initial point (t_0, x_0) . This condition implies

$$|f(t, x) - f(t, \bar{x})| \leq L|x - \bar{x}|$$

for some constant $L > 0$ and for any (t, x) and (t, \bar{x}) in the rectangle. Let us assume that there is a value $M > 0$ for which $|\ddot{x}(t)| \leq M$ for all t of interest in our differential

equation solving. We can use these facts to obtain an upper bound on the error term $|x_i - y_i|$. Specifically,

$$\begin{aligned} |x_{i+1} - y_{i+1}| &= \left| x_i + hf(t_i, x_i) + \ddot{x}(\bar{t}) \frac{h^2}{2} - y_i - hf(t_i, y_i) \right| \\ &\leq |x_i - y_i| + h|f(t_i, x_i) - f(t_i, y_i)| + Mh^2/2 \\ &\leq |x_i - y_i| + L|x_i - y_i| + Mh^2/2 \\ &= (1 + Lh)|x_i - y_i| + Mh^2/2 \end{aligned}$$

Define $e_i = |x_i - y_i|$. The preceding inequality is of the form $e_{i+1} \leq (1 + Lh)e_i + c$ for $c > 0$. We know that $e_0 = 0$. The inequality for $i = 1$ is

$$e_1 \leq (1 + Lh)e_0 + c = c$$

The inequality for $i = 2$ is

$$e_2 \leq (1 + Lh)e_1 + c \leq (1 + Lh)c + c = ((1 + Lh) + 1)c$$

For $i = 3$ the inequality is

$$e_3 \leq (1 + Lh)e_2 + c \leq (1 + Lh)((1 + Lh) + 1)c = ((1 + Lh)^2 + (1 + Lh) + 1)c$$

You should recognize the pattern and deduce that in general,

$$\begin{aligned} e_i &\leq c \sum_{j=0}^{i-1} (1 + Lh)^j \\ &= \frac{Mh^2}{2} \frac{(1 + Lh)^i - 1}{Lh} \\ &\leq \frac{Mh^2}{2} \frac{e^{iLh} - 1}{Lh} \\ &= \frac{M(e^{L(t_i - t_0)} - 1)}{2L} h \\ &\leq Kh \end{aligned} \tag{13.3}$$

for $i \geq 1$. We have used the fact that $(1 + x)^p \leq e^{px}$ for $x \geq 0$ and $p > 0$. We also used $t_i = t_0 + ih$. The final bound K is a constant that absorbs M and L , and uses the fact that $\exp(L(t_i - t_0))$ is bounded when we are solving the differential equation on an already specified interval $[t_0, T]$, namely $\exp(L(t_i - t_0)) \leq \exp(L(T - t_0))$. The bound K is independent of h ; the smaller h is, the more iterations it takes to get to time T , but K is independent of this process.

What we have shown is that the amount of error e_i between the true value of the iterate x_i and the approximate value y_i is bounded by $e_i \leq Kh$ for some constant K . If you were to halve the step size, you would expect only half the error and a better

approximation. However, it takes you twice as many steps to reach the maximum time T . This is one of the promised trade-offs you have to decide on: smaller errors in exchange for more computing time.

The analysis that led to the inequality of equation (13.3) is based on truncation error in the mathematical formulation. That is, we discarded the remainder term from Taylor's theorem and argued how much error occurs in the iterates. As you are well aware, a full numerical analysis of the problem must also deal with errors introduced by a floating point number system. In particular, when you compute $y_i + hf(t_i, y_i)$ using floating point arithmetic, a small round-off error will occur. If δ_{i+1} is the round-off error that occurs when computing y_{i+1} , we can formulate yet another equation for determining the actual floating point values obtained from Euler's method:

$$z_{i+1} = z_i + hf(t_i, z_i) + \delta_{i+1}$$

The iterate z_i is the floating point number that occurs when trying to compute the theoretical value y_i . An argument similar to the one used in the truncation error can be applied to estimate the error $|x_i - z_i|$. Specifically,

$$\begin{aligned} |x_{i+1} - z_{i+1}| &= \left| x_i + hf(t_i, x_i) + \ddot{x}(\bar{t}) \frac{h^2}{2} - z_i - hf(t_i, z_i) - \delta_{i+1} \right| \\ &\leq (1 + Lh)|x_i - z_i| + \frac{Mh^2}{2} + \delta \end{aligned}$$

where δ is an upper bound on all the $|\delta_i|$ values. Define $\varepsilon = |x_i - z_i|$. In this case ε_0 is not necessarily zero since the floating point representation z_0 for x_0 might not be an exact representation. The inequality for $i = 1$ is

$$\varepsilon_1 \leq (1 + Lh)\varepsilon_0 + (Mh^2/2 + \delta)$$

The inequality for $i = 2$ is

$$\varepsilon_2 \leq (1 + Lh)\varepsilon_1 + \delta \leq (1 + Lh)^2\varepsilon_0 + ((1 + Lh) + 1)(Mh^2/2 + \delta)$$

For $i = 3$ the inequality is

$$\varepsilon_3 \leq (1 + Lh)\varepsilon_2 + \delta \leq (1 + Lh)^3\varepsilon_0 + ((1 + Lh)^2 + (1 + Lh) + 1)(Mh^2/2 + \delta)$$

The pattern leads to the closed form,

$$\begin{aligned} \varepsilon_i &\leq (1 + Lh)^i\varepsilon_0 + \left(\frac{Mh^2}{2} + \delta \right) \sum_{j=0}^{i-1} (1 + Lh)^j \\ &\leq \varepsilon_0 e^{L(T-t_0)} + \frac{e^{L(T-t_0)} - 1}{L} \left(\frac{Mh}{2} + \frac{\delta}{h} \right) \\ &= K_0 + K_1 h + K_2 \frac{1}{h} \end{aligned} \tag{13.4}$$

for $i \geq 1$ and for some constants K_0 , K_1 , and K_2 .

The inequality of [equation \(13.4\)](#) differs from that of [equation \(13.3\)](#) in that a term $1/h$ occurs in [equation \(13.4\)](#). The general folklore of numerical differential equation solvers is that to get a better approximation you choose a smaller step size. This analysis shows that in fact this is not always true. Inequality [\(13.4\)](#) shows that as you let h approach zero, the error can become unbounded. Please keep in mind that the bound we produced using the inequality is exactly that – a bound. The actual error can be less; but then again, it might reach the upper bound. Also notice that $(Mh/2 + \delta/h)$ has a global minimum at $h = \sqrt{2\delta/M}$. This choice of h produces the smallest error bound. For an actual floating point number system, the chances are that $\sqrt{2\delta/M}$ is sufficiently small that you would never decrease h to such a small number in your numerical solver.

The analysis of this section was quite lengthy, but I include it to let you know that this is what numerical analysis of an algorithm is all about. You have errors due to mathematical approximations in the algorithms and errors due to representation in a floating point number system. In order to have some assurance of the accuracy of the output of the computer, you might consider doing analyses of this type yourself.

13.2 HIGHER-ORDER TAYLOR METHODS

Euler's method is the algorithm obtained by using the first-degree Taylor polynomial of $x(t)$ to approximate $x(t+h)$. Higher-order approximations may be used, the class of such algorithms called *higher-order Taylor methods*. For example, Taylor's theorem when using a second-degree polynomial is

$$x(t_{i+1}) = x(t_i) + h\dot{x}(t_i) + \frac{h^2}{2}\ddot{x}(t_i) + \frac{h^3}{6}x^{(3)}(\bar{t})$$

where $h = t_{i+1} - t_i$ and for some $\bar{t} \in [t_i, t_{i+1}]$. We know that $\dot{x}(t) = f(t, x(t))$ since $x(t)$ is a solution to the differential equation. An expression for $\ddot{x}(t)$ is obtained by differentiating the differential equation and using the chain rule from calculus,

$$\ddot{x}(t) = \frac{d}{dt}f(t, x(t)) = f_t(t, x(t)) + f_x(t, x(t))\dot{x}(t) = f_t(t, x(t)) + f_x(t, x(t))f(t, x(t))$$

where $f_t = \partial f / \partial t$ and $f_x = \partial f / \partial x$. The numerical method for degree $n = 2$ is

$$y_{i+1} = y_i + hf(t_i, y_i) + \frac{h^2}{2}(f_t(t_i, y_i) + f_x(t_i, y_i)f(t_i, y_i)), \quad i \geq 0, \quad y_0 = x_0 \quad (13.5)$$

Euler's method is a Taylor method of degree 1 and has approximation error bound Kh for some constant K . The degree n Taylor method can be shown to have an error bound Kh^n for some constant K , so generally you expect more accuracy than Euler's method for a given step size h .

The technical problem with Taylor methods is that you need to formally compute the partial derivatives of $f(t, x)$. In many applications such as our physics examples where f represents external forces and torques, we do not have the luxury of computing derivatives since we do not know ahead of time a closed form for f itself.

13.3 METHODS VIA AN INTEGRAL FORMULATION

The initial value problem of equation (13.1) may be formally integrated to obtain

$$x(t_{i+1}) = x(t_i) + \int_{t_i}^{t_{i+1}} f(t, x(t)) dt \quad (13.6)$$

Define $\phi(t) = f(t, x(t))$; for the sake of illustration, suppose that $\phi(t) > 0$. The integral of equation (13.6) represents the area bounded by the graph of $\phi(t)$, the t -axis, and the vertical lines $t = t_i$ and $t = t_{i+1}$. Figure 13.1(a) illustrates.

Figure 13.1(b) shows an approximation of the area by a rectangle,

$$\int_{t_i}^{t_{i+1}} f(t, x(t)) dt = \int_{t_i}^{t_{i+1}} \phi(t) dt \doteq (t_{i+1} - t_i)\phi(t_i) = (t_{i+1} - t_i)f(t_i, x_i)$$

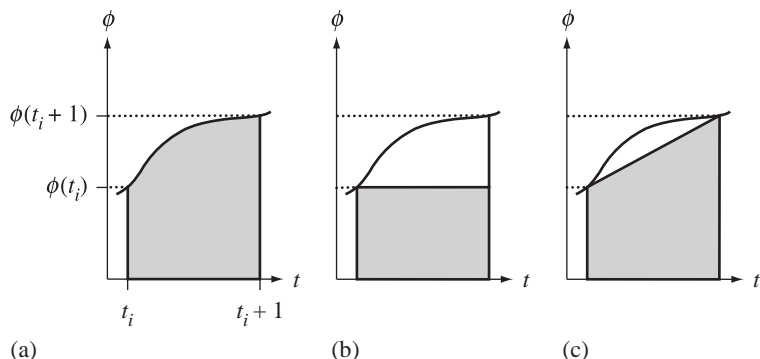


Figure 13.1 (a) Area under a curve. (b) Approximation of the area by a rectangle (leads to Euler's method). (c) Approximation of the area by a trapezoid (leads to the modified Euler method).

If $x_i = x(t_i)$, y_i is an approximation to x_i , and $h = t_{i+1} - t_i$, then substituting the integral approximation into equation (13.6) produces Euler's method: $y_{i+1} = y_i + hf(t_i, y_i)$.

Figure 13.1(c) shows an approximation of the area by a trapezoid,

$$\int_{t_i}^{t_{i+1}} f(t, x(t)) dt \doteq (t_{i+1} - t_i) \frac{f(t_i, x_i) + f(t_{i+1}, x_{i+1})}{2}$$

This leads to a numerical algorithm for approximations y_i to x_i ,

$$y_{i+1} = y_i + \frac{h}{2}(f(t_i, y_i) + f(t_{i+1}, y_{i+1})), \quad i \geq 0, \quad y_0 = x_0 \quad (13.7)$$

Unfortunately, we cannot immediately use this equation since the quantity we wish to determine, y_{i+1} , occurs on both the left and right sides of the equality. One modification to remedy this is to use an Euler step for the term on the right, $y_{i+1} = y_i + hf(t_i, y_i)$:

$$y_{i+1} = y_i + \frac{h}{2}(f(t_i, y_i) + f(t_i + h, y_i + hf(t_i, y_i))) \quad (13.8)$$

This is referred to as the *modified Euler's method* and is an *explicit method*, because y_{i+1} is defined explicitly in terms of the quantities t_i and y_i computed at the previous time.

The method in equation (13.9) is referred to as an *implicit method* since y_{i+1} is defined implicitly by the equation. Implicit equations can use Newton's method for root finding to determine the unknown quantity. In our example, if we define

$$g(z) = \left(x_i + \frac{h}{2}f(t_i, x_i) \right) + \frac{h}{2}f(t_i + h, z) - z$$

then y_{i+1} is a root of $g(z) = 0$; that is, $g(y_{i+1}) = 0$. A reasonable starting guess for z is $z_0 = y_i$. The Newton iterates are

$$z_{j+1} = z_j - \frac{g(z_j)}{g'(z_j)}, \quad j \geq 0$$

You may well compute iterates until you are assured of convergence to a root that is used for y_{i+1} . An alternative that uses a bounded amount of time is just to iterate once and use that as your choice for y_{i+1} , in which case

$$y_{i+1} = y_i - \frac{(h/2)(f(t_i + h, y_i) + f(t_i, y_i))}{(h/2)f_x(t_i + h, y_i) - 1} \quad (13.9)$$

This does require knowing the partial derivative $f_x(t, x)$ so that you may evaluate it.

An implicit method that occurs in a simpler manner is to think of Euler's method as an algorithm that uses a forward difference to approximate the first derivative of $x(t)$. That is,

$$\dot{x}(t_i) = \lim_{h \rightarrow 0} \frac{x(t_i + h) - x(t_i)}{h} \doteq \frac{x(t_i + h) - x(t_i)}{h} = \frac{x_{i+1} - x_i}{h}$$

Choosing y_i as the approximation to x_i and substituting into the differential equation leads to the approximation $(y_{i+1} - y_i)/h = f(t_i, y_i)$ or $y_{i+1} = y_i + hf(t_i, y_i)$, which is Euler's method. If we were to use a backward difference to approximate the first derivative:

$$\dot{x}(t_{i+1}) = \lim_{h \rightarrow 0} \frac{x(t_{i+1}) - x(t_{i+1} - h)}{h} \doteq \frac{x(t_{i+1}) - x(t_{i+1} - h)}{h} = \frac{x_{i+1} - x_i}{h}$$

then substituting into the differential equation and multiplying by h leads to an *implicit Euler's method*,

$$y_{i+1} = y_i + hf(t_{i+1}, y_{i+1}) \quad (13.10)$$

The equation is implicit since x_{i+1} occurs on both sides of the equality. Just as we tried earlier, define $g(z) = y_i + hf(t_i + h, z) - z$ and compute y_{i+1} as a root of $g(z) = 0$. Using Newton's method with an initial iterate $z_0 = x_i$ and iterating only once, we have

$$y_{i+1} = y_i - \frac{hf(t_i + h, y_i)}{hf_x(t_i + h, y_i) - 1} \quad (13.11)$$

This also requires knowing the partial derivative $f_x(t, x)$ in order that you may evaluate it.

13.4 RUNGE-KUTTA METHODS

The Taylor methods of Section 13.2 have high-order truncation errors, a good thing for an algorithm, but the methods require that you compute partial derivatives of $f(t, x)$. Runge–Kutta methods are designed to have the same high-order truncation error, yet use only evaluations of the function $f(t, x)$. The derivations require the extension of Taylor's theorem to bivariate functions.

Taylor's Theorem ■ Let $f(t, x)$ and its partial derivatives of orders 1 through $n + 1$ be continuous on a rectangular domain D . Let $(t_0, x_0) \in D$. For every $(t, x) \in D$, there is a $\bar{t} \in [t_0, t]$ and a $\bar{x} \in [x_0, x]$ such that $f(t, x) = P_n(t, x) + R_n(t, x)$, where

$$P_n(t, x) = \sum_{j=0}^n \frac{1}{j!} \sum_{i=0}^j \binom{j}{i} \frac{\partial^i f(t_0, x_0)}{\partial t^{j-i} \partial x^i} (t - t_0)^{j-i} (x - x_0)^i$$

is the *Taylor polynomial of degree n* and where

$$R_n(t, x) = \sum_{i=0}^{n+1} \binom{n+1}{i} \frac{\partial^{n+1} f(\bar{t}, \bar{x})}{\partial t^{n+1-i} \partial x^i} (t - t_0)^{n+1-i} (x - x_0)^i$$

is the remainder term. ■

The Taylor polynomial you see quite often in practice is the one that includes the first- and second-order partial derivatives:

$$\begin{aligned} P_2(t, x) &= f(t_0, x_0) + f_t(t_0, x_0)(t - t_0) + f_x(t_0, x_0)(x - x_0) \\ &\quad + \frac{1}{2} f_{tt}(t_0, x_0)(t - t_0)^2 + f_{tx}(t_0, x_0)(t - t_0)(x - x_0) + \frac{1}{2} f_{xx}(t_0, x_0)(x - x_0)^2 \\ &= f(t_0, x_0) + Df(t_0, x_0)^T \begin{bmatrix} t - t_0 \\ x - x_0 \end{bmatrix} \\ &\quad + \frac{1}{2} \begin{bmatrix} t - t_0 & x - x_0 \end{bmatrix} D^2 f(t_0, x_0) \begin{bmatrix} t - t_0 \\ x - x_0 \end{bmatrix} \end{aligned}$$

where $Df(t, x)$ is called the *gradient* of $f(t, x)$ (a list of the first-order partial derivatives) and $D^2 f(t, x)$ is called the *Hessian matrix* of $f(t, x)$ (a list of the second-order partial derivatives).

13.4.1 SECOND-ORDER METHODS

The application of Taylor's theorem to the solution $x(t)$ produces the equation $x(t+h) = x(t) + h\dot{x}(t) + \frac{h^2}{2}\ddot{x}(t) + R(t)$ for a remainder $R(t)$ that is of order $O(h^3)$. Using $\dot{x} = f(t, x)$ and $\ddot{x} = f_t + f_{xx}$ as we did in deriving Taylor's method in [equation \(13.5\)](#), we have

$$x(t+h) = x(t) + hf(t, x) + \frac{h^2}{2} (f_t(t, x) + f(t, x)f_x(t, x)) + R(t) \quad (13.12)$$

As indicated, the equation requires evaluating the first-order partial derivatives of f . What we would like to do instead is replace the derivative evaluations by function evaluations. This is possible through an approximation that will change the remainder term R . Specifically, we want to obtain a formal expression,

$$x(t+h) = x(t) + haf(t+b, x(t)+c) + \bar{R}(t)$$

for some choice of a , b , and c and a remainder $\bar{R}(t)$ that is of order $O(h^3)$. Using Taylor's theorem for bivariate functions, we have

$$af(t+b, x+c) = af(t, x) + abf_t(t, x) + acf_x(t, x)c + S(t)$$

where $S(t)$ is $O(h^2)$. The right-hand side appears to be of the form shown in [equation \(13.12\)](#). Matching terms we obtain $a = 1$, $ab = h/2$, and $ac = (h/2)f$. The error terms match up as $R(t) = hS(t) + \bar{R}(t)$. Consequently, $a = 1$, $b = h/2$, and $c = hf/2$, so that

$$x(t+h) = x(t) + hf \left(t + \frac{h}{2}, x(t) + \frac{h}{2}f(t, x(t)) \right) + R(t)$$

This suggests a numerical method for solving the differential equation,

$$y_{i+1} = y_i + hf \left(t_i + \frac{h}{2}, y_i + \frac{h}{2}f(t_i, y_i) \right) \quad (13.13)$$

and is called the *midpoint method*.

The midpoint method occurred as a result of using a Taylor polynomial of degree 1 to approximate $x(t)$. The numerical method has error of order $O(h^2)$. The hope is that an approximation using a Taylor polynomial of degree 2 will lead to a method whose error is of order $O(h^3)$. As it turns out, we can use the same method of construction but only obtain $O(h^2)$ methods. From Taylor's theorem,

$$\begin{aligned} x(t+h) &= x(t) + hf(t, x) + \frac{h^2}{2} \frac{d}{dt} f(t, x) + \frac{h^3}{6} \frac{d^2}{dt^2} f(t, x) + R(t) \\ &= x(t) + hf + \frac{h^2}{2} (f_t + ff_x) + \frac{h^3}{6} (f_{tt} + 2ff_{tx} + f^2 f_{xx}) \\ &\quad + f_x(f_t + ff_x) + R(t) \end{aligned} \quad (13.14)$$

where $R(t)$ is of order $O(h^4)$. To replace the derivative evaluations by function evaluations, we postulate a formal expression,

$$x(t+h) = x(t) + h(a_1 f(t, x(t)) + a_2 f(t+b, x(t)+c)) + \bar{R}(t)$$

for some choice of a_1 , a_2 , b , and c and a remainder $\bar{R}(t)$ that is of order $O(h^4)$. Using Taylor's theorem to expand the expression involving the functions,

$$\begin{aligned} a_1 f(t, x) + a_2 f(t+b, x+c) &= a_1 f + a_2 (bf_t + cf_x + (b^2/2)f_{tt} + bcf_{tx} \\ &\quad + (c^2/2)f_{xx}) + S(t) \end{aligned}$$

where $S(t)$ is of order $O(h^3)$. The right-hand side is *almost* of the form in [equation \(13.14\)](#), except there is no subexpression involving $f_x(f_t + ff_x)$. Regardless, let us try to match as many terms as possible. We can match the f , f_t , and f_x terms: $a_1 + a_2 = 1$, $a_2 b = h/2$, and $a_2 c = hf/2$. The remaining matches overconstrain the problem. This, and the inability to match the term $f_x(f_t + ff_x)$, means that those terms must become part of the remainder $S(t)$, forcing it to be of order $O(h^2)$ instead.

Our matched terms involve four parameters but only three equations. This gives us some flexibility in choosing them. One choice is $a_1 = a_2 = 1/2$, $b = h$, and $c = hf$,

leading to the numerical method,

$$y_{i+1} = y_i + \frac{h}{2}(f(t_i, y_i) + f(t_i + h, y_i + hf(t_i, y_i))) \quad (13.15)$$

You will notice that this is the *modified Euler method* (13.8) derived by other means. Another choice of parameters is $a_1 = 1/4$, $a_2 = 3/4$, $b = 2h/3$, and $c = 2hf/3$, leading to the numerical method,

$$y_{i+1} = y_i + \frac{h}{4} \left(f(t_i, y_i) + 3f \left(t_i + \frac{2}{3}h, y_i + \frac{2}{3}hf(t_i, y_i) \right) \right) \quad (13.16)$$

This is referred to as *Heun's method*.

13.4.2 THIRD-ORDER METHODS

The inability to match some of the higher-order terms had to do with choosing an expression with a singly nested evaluation of f . That is, we have attempted to replace derivative evaluations by function evaluations using a term of the form $f(t + \alpha, x + \beta f(t, x))$. We can actually match the higher-order terms if we include a doubly nested term,

$$f(t + \alpha_1, x + \beta_1 f(t + \alpha_2, x + \beta_2 f(t, x)))$$

The method of construction is to expand this using Taylor's theorem. The algebraic details are tedious because you have to first expand $f(t + \alpha_2, x + \beta_2 f)$, substitute it in the second component of the outermost f , and expand that. A symbolic mathematics package is quite useful here, not that Runge and Kutta could have benefited, because their development of the ideas was in about 1900!

A couple of numerical methods of third-order that are obtainable from this construction are

$k_1 = hf(t_i, y_i)$	No nesting
$k_2 = hf \left(t_i + \frac{h}{2}, y_i + \frac{k_1}{2} \right)$	Singly nested
$k_3 = hf(t_i + h, y_i - k_1 + 2k_2)$	Doubly nested
$y_{i+1} = y_i + \frac{1}{6}(k_1 + 2k_2 + k_3)$	

(13.17)

which for lack of a proper name we will call the *RK3a method*, and

$$\begin{aligned} k_1 &= hf(t_i, y_i) \\ k_2 &= hf\left(t_i + \frac{h}{3}, y_i + \frac{k_1}{3}\right) \\ k_3 &= hf\left(t_i + \frac{2h}{3}, y_i + \frac{2k_2}{3}\right) \\ y_{i+1} &= y_i + \frac{1}{4}(k_1 + 3k_3) \end{aligned} \tag{13.18}$$

which we will call the *RK3b method*.

13.4.3 FOURTH-ORDER METHOD

To obtain a fourth-order method, the Taylor polynomial used to approximate $x(t)$ is

$$x(t+h) \doteq x(t) + hf + \frac{h^2}{2} \frac{df}{dt} + \frac{h^3}{6} \frac{d^2f}{dt^2} + \frac{h^4}{24} \frac{d^3f}{dt^3}$$

The symbolic expansion of d^3f/dt^3 is quite complicated. The replacement of derivative evaluations by function evaluations uses a matching scheme by postulating a combination of function terms, one term with no nesting, one singly nested term, one doubly nested term, and one triply nested term. The details of matching are not shown here as they are quite complicated. The resulting numerical method is

$$\begin{aligned} k_1 &= hf(t_i, y_i) && \text{No nesting} \\ k_2 &= hf\left(t_i + \frac{h}{2}, y_i + \frac{k_1}{2}\right) && \text{Singly nested} \\ k_3 &= hf\left(t_i + \frac{h}{2}, y_i + \frac{k_2}{2}\right) && \text{Doubly nested} \\ k_4 &= hf(t_i + h, y_i + k_3) && \text{Triply nested} \\ y_{i+1} &= y_i + \frac{1}{6}(k_1 + 2k_2 + 2k_3 + k_4) \end{aligned} \tag{13.19}$$

and is known as *a Runge–Kutta fourth-order method* (or the *RK4a method*). I specifically used the article *a*, not *the*. Other fourth-order methods are possible, just like the midpoint, modified Euler, and Heun methods were different second-order methods. A concise summary of many of these methods may be found in [AS65, Section 25.5].

Two of these are

$$\begin{aligned}
 k_1 &= hf(t_i, y_i) \\
 k_2 &= hf\left(t_i + \frac{h}{3}, y_i + \frac{k_1}{3}\right) \\
 k_3 &= hf\left(t_i + \frac{2h}{3}, y_i - \frac{k_1}{3} + k_2\right) \\
 k_4 &= hf(t_i + h, y_i + k_1 - k_2 + k_3) \\
 y_{i+1} &= y_i + \frac{1}{8}(k_1 + 3k_2 + 3k_3 + k_4)
 \end{aligned} \tag{13.20}$$

which I will refer to as the *RK4b method*. The other is

$$\begin{aligned}
 k_1 &= hf(t_i, y_i) \\
 k_2 &= hf\left(t_i + \frac{h}{2}, y_i + \frac{k_1}{2}\right) \\
 k_3 &= hf\left(t_i + \frac{h}{2}, y_i + \left(-\frac{1}{2} + \sqrt{\frac{1}{2}}\right)k_1 + \left(1 - \sqrt{\frac{1}{2}}\right)k_2\right) \\
 k_4 &= hf\left(t_i + h, y_i - \sqrt{\frac{1}{2}}k_2 + \left(1 + \sqrt{\frac{1}{2}}\right)k_3\right) \\
 y_{i+1} &= y_i + \frac{1}{6}\left(k_1 + 2\left(1 - \sqrt{\frac{1}{2}}\right)k_2 + 2\left(1 + \sqrt{\frac{1}{2}}\right)k_3 + k_4\right)
 \end{aligned} \tag{13.21}$$

which is known as *Gill's method*.

13.5 MULTISTEP METHODS

The methods previously discussed in this chapter are referred to as 1-step methods. Each numerical method computes y_{i+1} using information only about y_i . Euler's method is an explicit 1-step method, $y_{i+1} = y_i + hf(t_i, y_i)$. We also mentioned the implicit Euler's method – a 1-step method, $y_{i+1} = y_i + hf(t_{i+1}, y_{i+1})$ – that requires root finding to solve for y_{i+1} . *Multistep methods* are a generalization of these two equations. An m -step method generates the iterate y_{i+1} from the previous iterates y_i through $y_{i-(m-1)}$. The general method is summarized by

$$y_{i+1} = \sum_{j=0}^{m-1} a_j y_{i-j} + h \sum_{j=0}^m b_j f(t_{i+1-j}, y_{i+1-j}), \quad i \geq m-1 \tag{13.22}$$

where the method is *implicit* if $b_0 \neq 0$ (y_{i+1} occurs on the right-hand side) or *explicit* if $b_0 = 0$ (y_{i+1} does not occur on the right-hand side). Initial conditions are required to start the iteration and must include known values for y_0 through y_{m-1} . In practice you typically know only y_0 at time t_0 . The other iterates can be generated by using a one-step method, a bootstrapping process of sorts.

The differential equation in its integral form is mentioned in [equation \(13.6\)](#). For $f > 0$ the motivation for numerical methods was to approximate the area under the curve $\phi(t) = f(t, x(t))$ for $t_i \leq t \leq t_{i+1}$. Multistep methods are derivable in a similar manner. The approximation by the area of a rectangle is equivalent to approximating $\phi(t)$ by a constant function $P(t) = \phi(t_i)$ and integrating. The approximation by the area of a trapezoid is equivalent to approximating $\phi(t)$ by a linear function $P(t) = \phi(t_i) + (\phi(t_{i+1}) - \phi(t_i))(t - t_i)/(t_{i+1} - t_i)$ but led to an implicit method because of the occurrence of the future value $\phi(t_{i+1})$. We may approximate $\phi(t)$ by a polynomial $P(t)$ of higher degree and obtain either explicit or implicit methods.

The explicit m -step method using the higher-degree approximation is to choose $P(t)$ as the interpolating polynomial of degree $m - 1$ of the iterates (t_j, y_j) for $i - m + 1 \leq j \leq i$. If we set $t = t_i + sh$, where s is a continuous variable and $f_i = f(t_i, y_i)$, the polynomial is

$$P(t) = f_i + s\nabla f_i + \frac{s(s+1)}{2}\nabla^2 f_i + \cdots + \frac{s(s+1)\cdots(s+m-2)}{(m-1)!}\nabla^{m-1} f_i$$

where $\nabla^j f_i$ terms are backward differences defined by $\nabla f_i = f_i - f_{i-1}$, and $\nabla^{k+1} f_i = \nabla(\nabla^k f_i)$ for $k \geq 1$. The numerical method obtained by integrating $P(t)$ and using it as an approximation to the integral is referred to as the *Adams-Basforth m -step method*. The local truncation error is $O(h^m)$. Some special cases are shown:

$$\begin{aligned} y_{i+1} &= y_i + h f_i, && \text{Euler's method} \\ y_{i+1} &= y_i + \frac{h(3f_i - f_{i-1})}{2} && \text{2-step method} \\ y_{i+1} &= y_i + \frac{h(23f_i - 16f_{i-1} + 5f_{i-2})}{12} && \text{3-step method} \\ y_{i+1} &= y_i + \frac{h(55f_i - 59f_{i-1} + 37f_{i-2} - 9f_{i-3})}{24} && \text{4-step method} \\ y_{i+1} &= y_i + \frac{h(1901f_i - 2774f_{i-1} + 2616f_{i-2} - 1274f_{i-3} + 251f_{i-4})}{720} && \text{5-step method} \end{aligned} \tag{13.23}$$

The derivation of the two-step method uses $P(t) = f_i + s(f_i - f_{i-1})$ and

$$\int_{t_i}^{t_{i+1}} P(t) dt = h \int_0^1 f_i + s(f_i - f_{i-1}) ds = h(f_i + (f_i - f_{i-1})/2) = (h/2)(3f_i - f_{i-1})$$

A small observation: The coefficients of the f -terms add up to the denominator of the h -term.

In the Adams–Bashforth explicit solver the polynomial $P(t)$ interpolates the iterates occurring at times $t \leq t_i$. The values of $P(t)$ for $t \in [t_i, t_{i+1}]$ are *extrapolated*. In a sense the solver *predicts* the value y_{i+1} by this extrapolation. An implicit solver is obtained by interpolating the iterates at times $t \leq t_{i+1}$. For example, if a 2-step implicit method interpolates (t_{i-1}, f_{i-1}) , (t_i, f_i) , and (t_{i+1}, f_{i+1}) by a quadratic polynomial,

$$P(t) = f_i + \left(\frac{f_{i+1} - f_{i-1}}{2h} \right) (t - t_i) + \left(\frac{f_{i+1} - 2f_i + f_{i-1}}{2h^2} \right) (t - t_i)^2$$

The integral is

$$\int_{t_i}^{t_{i+1}} P(t) dt = \frac{h}{12} (5f_{i+1} + 8f_i - f_{i-1})$$

The implicit solver is $y_{i+1} = y_i + (h/12)(5f_{i+1} + 8f_i - f_{i-1})$. The m -step implicit method obtained in this manner is referred to as the *Adams–Moulton m -step method*. In general the local truncation error of an m -step implicit method is $O(h^{m+1})$, one degree larger than for an m -step explicit method. As a rule of thumb you get better accuracy with the implicit method, but the cost is that you have to solve the implicit equation for y_{i+1} . Some special cases are shown:

$$\begin{aligned} y_{i+1} &= y_i + h(f_{i+1} + f_i) && \text{Trapezoid method} \\ y_{i+1} &= y_i + \frac{h(5f_{i+1} + 8f_i - f_{i-1})}{12} && \text{2-step method} \\ y_{i+1} &= y_i + \frac{h(9f_{i+1} + 19f_i - 5f_{i-1} + f_{i-2})}{24} && \text{3-step method} \\ y_{i+1} &= y_i + \frac{h(251f_{i+1} + 646f_i - 264f_{i-1} + 106f_{i-2} - 19f_{i-3})}{720} && \text{4-step method} \end{aligned} \tag{13.24}$$

13.6 PREDICTOR–CORRECTOR METHODS

The Adams–Bashforth m -step solver is an explicit method that interpolates the iterates through time t_i with a polynomial and integrates the polynomial on $[t_i, t_{i+1}]$. As such we are using the polynomial to extrapolate the behavior for times $t \geq t_i$. The resulting approximation is used to generate the iterate y_{i+1} . The Adams–Moulton m -step solver is an implicit method that interpolates the iterates through time t_{i+1}

with a polynomial and integrates the polynomial on $[t_i, t_{i+1}]$. We are using the polynomial to interpolate the behavior for times $t \geq t_i$, but since we do not know y_{i+1} we obtain the implicit behavior. Rather than solve the implicit equation via a root finder or fixed point iteration, something not guaranteed to be stable or robust, we use the two methods together. The pair forms what is called a *predictor-corrector method*. The explicit method is used to *predict* the value of y_{i+1} . This value is used on the right-hand side of the implicit equation to *correct* the value. The left-hand side of the implicit equation is the corrected value. Of course, you may iterate the corrector portion of the system by taking the left-hand side value and feeding it back to the right-hand side, effectively implementing a fixed-point iteration that hopefully converges.

13.7 EXTRAPOLATION METHODS

In this section we look at the prospect of applying extrapolation methods to increase the accuracy of our approximations to the solutions of differential equations. The basic approach will be to compute three approximations to $x(t)$ using different step sizes whose ratios in pairs are integers; each approximation will require a different number of iterations. The approximations are all $O(h^2)$ but can be combined to produce an approximation that is $O(h^6)$.

13.7.1 RICHARDSON EXTRAPOLATION

Accurate approximations may be obtained from low-order formulas using a method called *Richardson extrapolation* [RG27]. Let Q be an unknown quantity which is approximated by $A(h)$. Think of $A(h)$ as a black-box process that can approximate Q depending on some parameter h that you may choose as you like. For our purposes h is the step size in the differential equation solver. Suppose that the approximation is of the following form for some constant c_1 :

$$Q = A(h) + c_1 h^2 + O(h^4) = A(h) + O(h^2)$$

We can generate another approximation with the process by selecting $h/2$ instead, namely

$$Q = A(h/2) + c_1 h^2/4 + O(h^4) = A(h/2) + O(h^2)$$

In practice, of course, we would use $A(h)$ or $A(h/2)$ as the approximation since we do not know what c_1 is; after all, A represents a black-box process. The two approximations can be combined to eliminate the quadratic term in h , even though we do

not know c_1 . Specifically, another approximation for the quantity is

$$\begin{aligned} Q &= \frac{1}{3} (4(A(h/2) + c_1 h^2/4 + O(h^4)) - (A(h) + c_1 h^2 + O(h^4))) \\ &= \frac{4A(h/2) - A(h)}{3} + O(h^4) \end{aligned}$$

That is, the value $(4A(h/2) - A(h))/3$ is an approximation for Q , but the surprising conclusion is that the error is $O(h^4)$ rather than $O(h^2)$ of the two original approximations.

Define $A_1(h) = A(h)$ and $A_2(h) = (4A(h/2) - A(h))/3$. We have seen that $Q = A_2(h) + O(h^4)$. If additionally we know that

$$Q = A_2(h) + c_2 h^4 + O(h^6)$$

we can repeat the process. Using half the input parameter, we have another approximation,

$$Q = A_2(h/2) + c_2 h^4/16 + O(h^6)$$

The two approximations combine to produce

$$Q = \frac{16A_2(h/2) - A_2(h)}{15} + O(h^6)$$

with yet another increase in the order of the error. Define $A_3(h) = (16A_2(h/2) - A_2(h))/15$. Assuming more structure in the error terms so that powers $c_k h^{2k}$ appear for constants c_k , further repetitions lead to the approximation,

$$Q = A_k(h) + O(h^{2k}), \quad A_k(h) = \frac{4^{k-1} A_{k-1}(h/2) - A_{k-1}(h)}{4^{k-1} - 1}$$

13.7.2 APPLICATION TO DIFFERENTIAL EQUATIONS

Let us look at the application of a slight variation of the Richardson extrapolation to numerical methods for differential equations. The method is attributed to [Gra65]. The differential equation is $\dot{x} = f(t, x)$. Suppose we have a numerical method of the form,

$$y_{i+1} = y_i + h\phi(t_i, y_i, h)$$

Let $A(t, h)$ denote the process of solving the numerical method to approximate $y(t)$. As long as the approximation is of the form

$$x(t) = A(t, h) + \sum_{k=1}^n c_k(t) h^{2k} + O(h^{2n+2})$$

where the $c_k(t)$ are independent of h , we can use extrapolation to produce a high-order approximation from low-order ones. Choose a value $h > 0$ and choose three step sizes $h_j = h/q_j$, $0 \leq j \leq 2$, where the q_j are positive integers. We solve the numerical method for these step sizes. The approximation using h_j requires q_j steps. The actual solutions are

$$\begin{aligned} x(t) &= A(t, h_j) + c_1(t)h_j^2 + c_2(t)h_j^4 + O(h^6) \\ &= A(t, h_j) + \frac{c_1(t)}{q_j^2} h^2 + \frac{c_2(t)}{q_j^4} h^4 + O(h^6) \end{aligned}$$

for $0 \leq j \leq 2$.

Define $A_{j,0} = A(t, h_j)$ for $0 \leq j \leq 2$. We can combine the first two equations for $x(t)$ to eliminate the h^2 term:

$$x(t) = \frac{q_1^2 A_{1,0} - q_0^2 A_{0,0}}{q_1^2 - q_0^2} - \frac{c_2(t)}{q_0^2 q_1^2} h^4 + O(h^6) = A_{1,1} - \frac{c_2(t)}{q_0^2 q_1^2} h^4 + O(h^6)$$

where the last equality defines $A_{1,1}$. We can also combine the last two equations to eliminate the h^2 term:

$$x(t) = \frac{q_2^2 A_{2,0} - q_1^2 A_{1,0}}{q_2^2 - q_1^2} - \frac{c_2(t)}{q_1^2 q_2^2} h^4 + O(h^6) = A_{2,1} - \frac{c_2(t)}{q_1^2 q_2^2} h^4 + O(h^6)$$

where the last equality defines $A_{2,1}$. Both combined equations have error terms of $O(h^4)$, whereas the original ones had error terms of $O(h^2)$. Combining the combined equations to eliminate the h^4 term,

$$x(t) = \frac{q_2^2 A_{1,1} - q_0^2 A_{2,1}}{q_2^2 - q_0^2} + O(h^6) = A_{2,2} + O(h^6)$$

where the last equality defines $A_{2,2}$, a quantity that approximates $x(t)$ with error term $O(h^6)$ rather than the errors $O(h^2)$ that occurred in the initial approximations. You may view this construction as building a table of approximations,

$$\begin{array}{ccc} A_{0,0} & & \\ A_{1,0} & A_{1,1} & \\ A_{2,0} & A_{2,1} & A_{2,2} \end{array}$$

where an entry $A_{i,j}$ is obtained by combining $A_{i,j-1}$ and $A_{i-1,j-1}$ in the appropriate manner. The first column represents different $O(h^2)$ approximations to the solution, the second column represents $O(h^4)$ approximations, and the third column represents an $O(h^6)$ approximation.

Although the presentation here uses three approximations of $O(h^2)$ to construct an approximation of $O(h^6)$, it is clear that the ideas easily extend to using m approximations of $O(h^2)$ generated from step sizes $h_j = h/q_j$ for m distinct integers q_j in

order to obtain a final approximation of $O(h^{2m})$. The table of approximations is

$$\begin{matrix} A_{0,0} & & & \\ A_{1,0} & A_{1,1} & & \\ A_{2,0} & A_{2,1} & A_{2,2} & \\ \vdots & \vdots & \vdots & \ddots \\ A_{m-1,0} & A_{m-1,1} & A_{m-1,2} & \cdots & A_{m-1,m-1} \end{matrix} \quad (13.25)$$

where the entries in column j represent approximations of order $O(h^{2(j+1)})$.

13.7.3 POLYNOMIAL INTERPOLATION AND EXTRAPOLATION

Given points (t_i, y_i) for $0 \leq i \leq n$, the interpolating polynomial of degree n is Lagrange polynomial,

$$P(t) = \sum_{i=0}^n y_i \left(\prod_{\substack{j=1 \\ j \neq i}}^n (t - t_j) \right)$$

Direct evaluation of the right-hand side is not the recommended way to compute $P(t)$ on a computer. A more robust method uses a recursion formula for Lagrange polynomials, called *Neville's method*. For $i \geq j$ define $P_{i,j}(t)$ to be the interpolating polynomial of degree j of (t_k, y_k) , where $i - j \leq k \leq i$. The recursion is started by $P_{i,0} = y_i$ for $0 \leq i \leq n$ and the recursion itself is

$$P_{i,j}(t) = \frac{(t - t_{i-j})P_{i,j-1}(t) - (t - t_i)P_{i-1,j-1}(t)}{t_i - t_{i-j}} \quad (13.26)$$

for $1 \leq j \leq n$ and $j \leq i \leq n$. The resulting values can be stored in a table identical to the format shown in equation (13.25) with $P_{i,j}$ as the general term rather than $A_{i,j}$. This is no coincidence! The construction is in essence a Richardson extrapolation.

The diagonal term $P_{i,i}$ is determined by the inputs (t_j, y_j) for $0 \leq j \leq i$. An application might want to add new points to the system and continuing evaluation until the diagonal terms do not change significantly. That is, the application supplies an error tolerance $\varepsilon > 0$ and requires a stopping condition $|P_{i,i} - P_{i-1,i-1}| < \varepsilon$. If the condition is met, $P_{i,i}$ is the output of the method. If the condition is not met, the application provides another data point (t_{i+1}, y_{i+1}) and evaluates another row in the table.

13.7.4 RATIONAL POLYNOMIAL INTERPOLATION AND EXTRAPOLATION

A set of points (t_i, y_i) for $0 \leq i \leq n$ can be interpolated by rational polynomials rather than by polynomials. The idea is that some functions are not well interpolated by

polynomials but do have reasonable approximations by rational polynomials. The form of the interpolating rational polynomial is chosen to be

$$R(t) = \frac{\sum_{i=0}^{d_p} p_i t^i}{\sum_{i=0}^{d_q} q_i t^i}$$

where the degrees of the polynomials satisfy $d_p + d_q = n$. The coefficients allow us one arbitrary choice, so we set $q_0 = 1$. If we choose any other nonzero value for q_0 , we can always divide the coefficients in both numerator and denominator by q_0 so that in fact the constant term of the denominator becomes 1.

Bulirsch and Stoer developed an algorithm for interpolating and extrapolating rational polynomials that is similar to the algorithm for polynomial interpolation and extrapolation [BS64]. If n is even, the degrees of the numerator and denominator are equal, $d_p = d_q = n/2$. If n is odd, the denominator is one degree larger than the numerator, $d_p = \lfloor n/2 \rfloor$ and $d_q = d_p + 1$. The recursion is started with $R_{i,0} = y_i$ for $0 \leq i \leq n$ and the recursion itself is

$$R_{i,j}(t) = R_{i,j-1}(t) + \frac{R_{i,j-1}(t) - R_{i-1,j-1}(t)}{\left(\frac{t-t_{i-j}}{t-t_i}\right)\left(1 - \frac{R_{i,j-1}(t) - R_{i-1,j-1}(t)}{R_{i,j-1}(t) - R_{i-1,j-2}(t)}\right) - 1} \quad (13.27)$$

for $1 \leq j \leq n$ and $j \leq i \leq n$. In evaluating the recursion, it is understood that $R_{i,j} = 0$ whenever $i < j$.

Just as for polynomials, the diagonal term $R_{i,i}$ is determined by the inputs (t_i, y_i) for $0 \leq j \leq i$. The application supplies an error tolerance $\varepsilon > 0$ and requires a stopping condition $|R_{i,i} - R_{i-1,i-1}| < \varepsilon$. If the condition is met, $R_{i,i}$ is the output of the method. If the condition is not met, the application provides another data point (t_{i+1}, y_{i+1}) and evaluates another row in the table.

13.7.5 MODIFIED MIDPOINT METHOD

The *modified midpoint method* is a numerical method for solving a differential equation that takes a large step in time to produce an approximation. If y_i is an approximation to $x(t_i)$, we wish to approximate $x(t_i + H)$ using n substeps, each of size $h = H/n$. The approximation is denoted y_{i+n} to reflect the fact that we are approximating $x(t_i + nh) = x(t_{i+n})$.

The process is initialized with $z_0 = y_i$. The first iterate is generated by Euler's method,

$$z_1 = z_0 + hf(t_i, z_0)$$

Other iterates are generated by

$$z_{j+1} = z_j + 2hf(t + jh, z_j), \quad 1 \leq j \leq n - 1$$

The final approximation is

$$y_{i+n} = \frac{1}{2}(z_n + z_{n-1} + hf(t + nh, z_n))$$

This process is part of the Bulirsch–Stoer numerical method for solving a differential equation, as we will see in the next section.

13.7.6 BULIRSCH–STOER METHOD

The Bulirsch–Stoer method [BS64] is designed to obtain highly accurate solutions to a differential equation for which $f(t, x)$ is smooth and to do so with a minimal amount of computation. The idea is analogous to the method we discussed in an earlier section that uses polynomial extrapolation to improve the order of the error term. The final, highly accurate approximation was generated by combining the low accuracy approximations in the appropriate manner. The Bulirsch–Stoer method uses the modified midpoint method for solving the differential equation for a sequence of decreasing step sizes and uses rational polynomial extrapolation to improve the accuracy.

A step size $H > 0$ is chosen and the equation is solved three times using the modified midpoint method with substep counts of $q_0 = 2$, $q_1 = 4$, and $q_2 = 6$. These values are used to construct a table of rational polynomial approximations, the table of the form in [equation \(13.25\)](#) and consisting of three rows. The differential equation is solved again by the modified midpoint method using substep counts generated by $q_j = 2q_{j-2}$ for $j \geq 3$. For each numerical solution, the rational polynomial approximation table has a new row added and a comparison is made between the new diagonal term $R_{i,i}$ and the old one $R_{i-1,i-1}$, as mentioned in [Section 13.7.4](#) on rational polynomial interpolation and extrapolation. If the difference is suitably small, the value $R_{i,i}$ is used as the approximation to $x(t + H)$. If not, the next substep count is used and the process is repeated.

13.8 VERLET INTEGRATION

A numerical method that has its origins in molecular dynamics is due to Verlet [Ver67]. The method and its variations were made popular in the game programming industry through the work of Thomas Jakobsen [Jak01]. The scheme is based on Taylor's theorem using

$$\begin{aligned}\mathbf{x}(t + h) &= \mathbf{x}(t) + \dot{\mathbf{x}}(t)h + \frac{1}{2}\ddot{\mathbf{x}}(t)h^2 + \frac{1}{6}\mathbf{x}^{(3)}(t)h^3 + O(h^4) \\ \mathbf{x}(t - h) &= \mathbf{x}(t) - \dot{\mathbf{x}}(t)h + \frac{1}{2}\ddot{\mathbf{x}}(t)h^2 - \frac{1}{6}\mathbf{x}^{(3)}(t)h^3 + O(h^4)\end{aligned}$$

The first expansion is forward in time, the second backward in time. Summing these and keeping only the $\mathbf{x}(t + h)$ term on the left-hand side leads to

$$\mathbf{x}(t + h) = 2\mathbf{x}(t) - \mathbf{x}(t - h) + \ddot{\mathbf{x}}(t)h^2 + O(h^4)$$

The velocity terms cancel as well as the third-order terms, leaving an approximation error on the order of $O(h^4)$. Assuming the physical system is modeled by Newton's second law of motion, $\ddot{\mathbf{x}} = \mathbf{F}(t, \mathbf{x}, \dot{\mathbf{x}})/m$, the iteration scheme is

$$\mathbf{y}_{i+1} = 2\mathbf{y}_i - \mathbf{y}_{i-1} + \frac{h^2}{m}\mathbf{F}(t_i, \mathbf{y}_i, \dot{\mathbf{y}}_i), \quad i \geq 1 \quad (13.28)$$

The iterate \mathbf{y}_i is an approximation to the position $\mathbf{x}(t_i)$ and $\dot{\mathbf{y}}_i$ is an approximation to the velocity $\dot{\mathbf{x}}(t_i)$. In this most general form of the force function, the general iteration scheme requires estimates of the velocity.

One of the main advantages of the Verlet approach is that the difference method is *reversible in time*, something that a differential equation for a physical model satisfies when the force is conservative. The reversibility shows up in that we could just have easily solved for $\mathbf{y}_{i-1} = 2\mathbf{y}_i - \mathbf{y}_{i+1} + h^2\mathbf{F}(t_i, \mathbf{y}_i, \dot{\mathbf{y}}_i)/m$ and iterate to approximate position *backward in time*. The implication of reversibility in time is that the method maintains conservation of energy, at least when treating the quantities in the equation as true real numbers. On a computer, numerical round-off errors can cause an apparent change in energy. Another advantage is that only one evaluation of \mathbf{F} is required per time step, as compared to the multiple evaluations in methods such as the ones of Runge–Kutta type. The computational time is minimized to some extent. The disadvantage of the Verlet method is that it is not as accurate as other methods. Variations on the method were developed in attempts to maintain the advantages of reversibility in time and minimum computational time but improve accuracy. We will discuss a few of these variations later in this section.

13.8.1 FORCES WITHOUT A VELOCITY COMPONENT

In its original formulation, the force is assumed to depend only on time and position, $\mathbf{F}(t, \mathbf{x})$. This rules out frictional forces, of course, which depend on velocity. Moreover, in nearly all applications you see to molecular dynamics, the force is conservative, $\mathbf{F}(\mathbf{x}) = -\nabla V(\mathbf{x})$, where V is the potential energy function. The iteration scheme in this restricted case is a two-step method and requires two initial positional conditions. The initial value problem for the second-order differential equation has one positional condition \mathbf{y}_0 and one velocity condition $\dot{\mathbf{y}}_0$. The second positional condition can be generated with an Euler step:

$$\mathbf{y}_0, \dot{\mathbf{y}}_0 \text{ are specified}$$

$$\begin{aligned} \mathbf{y}_1 &= \mathbf{y}_0 + h\dot{\mathbf{y}}_0 \\ \mathbf{y}_{i+1} &= 2\mathbf{y}_i - \mathbf{y}_{i-1} + \frac{h^2}{m}\mathbf{F}(t_i, \mathbf{y}_i), \quad i \geq 1 \end{aligned} \quad (13.29)$$

This fits the mold of an explicit two-step method of the form in [equation \(13.22\)](#).

Notice that the method does not calculate velocity explicitly. The new position is computed from the previous two steps and the force on the particle. If an estimate of velocity is required by your application, you have a couple of possibilities. One is to use the previous two positions and select $\dot{\mathbf{y}}_{i+1} = (\mathbf{y}_i - \mathbf{y}_{i-1})/h$, an $O(h)$ approximation. The other possibility is to use a centered difference $\dot{\mathbf{y}}_i = (\mathbf{y}_{i+1} - \mathbf{y}_{i-1})/(2h)$, an $O(h^2)$ approximation at the same cost of calculation as the $O(h)$ one. The trade-off, though, is that you have to wait until the $(i + 1)$ -th time step to estimate the velocity at the i th time step.

13.8.2 FORCES WITH A VELOCITY COMPONENT

If frictional forces are part of the physical model and/or if you need to compute the velocity for the purposes of computing the energy of the system, then the velocity approximations must be generated. The force is of the form $\mathbf{F}(t, \mathbf{x}, \dot{\mathbf{x}})$. An application using forces of this type does need approximations to the velocity at each time step in order to evaluate the force function. A few variations are possible.

Using our suggestion for estimating velocity when the force does not have a velocity component, an explicit method is provided by

$$\begin{aligned} \mathbf{y}_0, \dot{\mathbf{y}}_0 &\text{ are specified} \\ \mathbf{y}_1 &= \mathbf{y}_0 + h\dot{\mathbf{y}}_0 \\ \dot{\mathbf{y}}_i &= \frac{1}{h}(\mathbf{y}_i - \mathbf{y}_{i-1}), \quad i \geq 1 \\ \mathbf{y}_{i+1} &= 2\mathbf{y}_i - \mathbf{y}_{i-1} + \frac{h^2}{m}\mathbf{F}(t_i, \mathbf{y}_i, \dot{\mathbf{y}}_i), \quad i \geq 1 \end{aligned} \tag{13.30}$$

The $\dot{\mathbf{y}}_i$ term must be evaluated first, then used in the evaluation of \mathbf{y}_{i+1} . Notice that $\dot{\mathbf{y}}_1 = \dot{\mathbf{y}}_0$, so effectively the explicit method assumes no change in velocity over the first time step.

The other suggestion for estimating velocity when the force does not have a velocity component leads to an implicit method:

$$\begin{aligned} \mathbf{y}_0, \dot{\mathbf{y}}_0 &\text{ are specified} \\ \mathbf{y}_1 &= \mathbf{y}_0 + h\dot{\mathbf{y}}_0 \\ \dot{\mathbf{y}}_i &= \frac{1}{2h}(\mathbf{y}_{i+1} - \mathbf{y}_{i-1}), \quad i \geq 1 \\ \mathbf{y}_{i+1} &= 2\mathbf{y}_i - \mathbf{y}_{i-1} + \frac{h^2}{m}\mathbf{F}(t_i, \mathbf{y}_i, \dot{\mathbf{y}}_i), \quad i \geq 1 \end{aligned} \tag{13.31}$$

As with any implicit method, you must decide how to solve for the implicit quantity \mathbf{y}_{i+1} . A fixed point iteration or Newton's method each requires a force-function evaluation per iteration, something that would negate the advantage of minimum

computational time in the Verlet method. A cheaper alternative is to use a predictor-corrector approach where you predict $\dot{\mathbf{y}}_i = (\mathbf{y}_i - \mathbf{y}_{i-1})/h$, use it to compute \mathbf{y}_{i+1} from the other difference equation, then correct the value with $\dot{\mathbf{y}}_i = (\mathbf{y}_{i+1} - \mathbf{y}_{i-1})/(2h)$.

13.8.3 SIMULATING DRAG IN THE SYSTEM

The iteration of the Verlet equation can be modified to simulate drag in the system. The difference equation is rewritten as

$$\mathbf{y}_{i+1} = \mathbf{y}_i + (\mathbf{y}_i - \mathbf{y}_{i-1}) + \frac{h^2}{m} \mathbf{F}(t, \mathbf{y}_i, \dot{\mathbf{y}}_i)$$

The term $\mathbf{y}_i - \mathbf{y}_{i-1}$ is related to an estimate of velocity. Drag is introduced by including a *drag coefficient* $\delta \in [0, 1]$,

$$\mathbf{y}_{i+1} = \mathbf{y}_i + (1 - \delta)(\mathbf{y}_i - \mathbf{y}_{i-1}) + \frac{h^2}{m} \mathbf{F}(t, \mathbf{y}_i, \dot{\mathbf{y}}_i)$$

A reasonable requirement is that you choose δ to be a small positive number, say on the order of 10^{-2} .

13.8.4 LEAPFROG METHOD

The velocity estimates in the standard Verlet approach might not be as accurate as an application requires. The estimate $\dot{\mathbf{y}}_i = (\mathbf{y}_i - \mathbf{y}_{i-1})/h$ is $O(h)$ and the estimate $\dot{\mathbf{y}}_i = (\mathbf{y}_{i+1} - \mathbf{y}_i)/(2h)$ is $O(h^2)$. The *leapfrog method* is designed to improve on the velocity estimates.

Let us take a different look at the velocity by using Taylor's theorem:

$$\begin{aligned}\dot{\mathbf{x}}(t+h) &= \dot{\mathbf{x}}(t) + h\ddot{\mathbf{x}}(t) + \frac{h^2}{2}\mathbf{x}^{(3)}(t) + \frac{h^3}{6}\mathbf{x}^{(4)}(t) + \frac{h^4}{24}\mathbf{x}^{(5)}(t) + O(h^5) \\ \dot{\mathbf{x}}(t-h) &= \dot{\mathbf{x}}(t) - h\ddot{\mathbf{x}}(t) + \frac{h^2}{2}\mathbf{x}^{(3)}(t) - \frac{h^3}{6}\mathbf{x}^{(4)}(t) + \frac{h^4}{24}\mathbf{x}^{(5)}(t) + O(h^5)\end{aligned}$$

Subtracting leads to

$$\dot{\mathbf{x}}(t+h) = \dot{\mathbf{x}}(t-h) + 2h\ddot{\mathbf{x}}(t) + \frac{h^3}{3}\mathbf{x}^{(4)}(t) + O(h^5) = \dot{\mathbf{x}}(t-h) + 2h\ddot{\mathbf{x}}(t) + O(h^3)$$

This represents a time step of h . If we were to use half the step $h/2$, the equation becomes

$$\dot{\mathbf{x}}(t+h/2) = \dot{\mathbf{x}}(t-h/2) + h\ddot{\mathbf{x}}(t) + \frac{h^3}{24}\mathbf{x}^{(4)}(t) + O(h^5) = \dot{\mathbf{x}}(t-h/2) + h\ddot{\mathbf{x}}(t) + O(h^3)$$

The order term is $O(h^3)$ in either case, and the third-order term includes $\mathbf{x}^{(4)}(t)$ in both cases. By using only a half step, the second equation produces a coefficient of

$h^3/24$, which is $1/8$ of the coefficient generated by the full step h . The intuitive appeal is that the error generated by the second equation is less than that of the first, so the velocity estimates should be better than with the straightforward Verlet method.

We need to estimate the position as well, but our goal is to approximate the positions using the full step h . The previous paragraph tells us how to estimate the velocities for half steps $h/2$. The leapfrog method interleaves the velocity and position iteration. The informal manner in which you normally see the leapfrog method stated is

$$\begin{aligned}\mathbf{v}(t + h/2) &= \mathbf{v}(t - h/2) + h\mathbf{a}(t) \\ \mathbf{x}(t + h) &= \mathbf{x}(t) + h\mathbf{v}(t + h/2)\end{aligned}$$

where $\mathbf{x}(t)$ is position, $\mathbf{v}(t)$ is velocity, and $\mathbf{a}(t)$ is acceleration given by \mathbf{F}/m . The velocity is updated on the time interval $[t - h/2, t + h/2]$ by using the acceleration computation at the midpoint t of the interval. The position is updated on the time interval $[t, t + h]$ by using the velocity estimate at the midpoint of the interval, $t + h/2$. As with any second-order differential equation, the initial conditions $\mathbf{x}(0)$ and $\mathbf{v}(0)$ must be specified. The leapfrog method requires $\mathbf{v}(h/2)$, not $\mathbf{v}(0)$, to approximate the first position $\mathbf{x}(h) = \mathbf{x}(0) = h\mathbf{v}(h/2)$. We may not use $\mathbf{v}(h/2) = \mathbf{v}(-h/2) + h\mathbf{a}(0)$ since we have no information about the velocity at negative times. Instead, we should estimate $\mathbf{v}(h/2) = \mathbf{v}(0) + (h/2)\mathbf{a}(0)$, an Euler iterate for the half-step $h/2$.

The implicit assumption in this formulation is that the force \mathbf{F} is a function of time t and position $\mathbf{x}(t)$ only. If the force were also to depend on velocity $\mathbf{v}(t)$, then the velocity approximations involve times $t - h/2$, t , and $t + h/2$, thereby requiring velocity estimates at all times $t + ih/2$ for $i \geq 0$. In this setting, the method is no longer the one intended by leapfrog, yet is still a valid numerical method.

When the force is of the form $\mathbf{F}(t, \mathbf{x})$, the formulation of the difference equations in the style to which we have become accustomed is shown next, where $t_i = ih/2$ and initial time is 0.

$\mathbf{y}_0, \dot{\mathbf{y}}_0$ are specified

$$\begin{aligned}\dot{\mathbf{y}}_1 &= \dot{\mathbf{y}}_0 + \frac{h}{m} \mathbf{F}(0, \mathbf{y}_0) \\ \dot{\mathbf{y}}_{i+1} &= \dot{\mathbf{y}}_{i-1} + \frac{h}{m} \mathbf{F}(t_i, \mathbf{y}_i), \quad i \geq 1 \\ \mathbf{y}_{i+2} &= \mathbf{y}_i + h\dot{\mathbf{y}}_{i+1}, \quad i \geq 0\end{aligned}\tag{13.32}$$

Notice the “leapfrog” behavior in that the velocity iterates are computed for the odd indices and the position iterates are computed for the even indices. When the force is of the form $\mathbf{F}(t, \mathbf{x}, \dot{\mathbf{x}})$, the formulation is in terms of an explicit two-step solver. The step size $H = h/2$, where h is the original step size and $t_i = iH$ where initial time is 0.

$\mathbf{y}_0, \dot{\mathbf{y}}_0$ are specified

$$\mathbf{y}_1 = \mathbf{y}_0 + H\dot{\mathbf{y}}_0$$

$$\begin{aligned}\dot{\mathbf{y}}_1 &= \dot{\mathbf{y}}_0 + \frac{H}{m} \mathbf{F}(0, \mathbf{y}_0, \dot{\mathbf{y}}_0) \\ \mathbf{y}_{i+2} &= \mathbf{y}_i + 2H\dot{\mathbf{y}}_{i+1}, \quad i \geq 0 \\ \dot{\mathbf{y}}_{i+2} &= \dot{\mathbf{y}}_i + \frac{2H}{m} \mathbf{F}(t_{i+1}, \mathbf{y}_{i+1}, \dot{\mathbf{y}}_{i+1}), \quad i \geq 0\end{aligned}\tag{13.33}$$

An Euler step is also needed to estimate \mathbf{y}_1 . The position and velocity iterates are computed for all indices, so no leap-frogging going on here.

The general rule of thumb on the advantages of the leapfrog over the standard Verlet method is that the position and velocity estimates are better but come at the cost of slightly more computation time.

13.8.5 VELOCITY VERLET METHOD

Another variation on the Verlet method is called the *velocity Verlet method*. The velocity estimate is produced using an integral formulation of the same type that led to equation (13.7), using $d\mathbf{v}/dt = \mathbf{a}(t)$ and an integration:

$$\mathbf{v}(t+h) = \mathbf{v}(t) + \int_t^{t+h} \mathbf{a}(\tau) d\tau \doteq \mathbf{v}(t) + \frac{h}{2}(\mathbf{a}(t) + \mathbf{a}(t+h))$$

This provides a slightly better estimate than what the leapfrog method used. Specifically, Taylor's theorem gives us

$$\mathbf{v}(t+h) - \mathbf{v}(t-h) - 2h\mathbf{a}(t) = \frac{h^3}{6}\ddot{\mathbf{a}}(t) + O(h^5)$$

Taylor expansions for velocity and acceleration are

$$\begin{aligned}\mathbf{v}(t+h) &= \mathbf{v}(t) + h\mathbf{a}(t) + \frac{h^2}{2}\dot{\mathbf{a}}(t) + \frac{h^3}{6}\ddot{\mathbf{a}}(t) + O(h^4) \\ \mathbf{a}(t+h) &= \mathbf{a}(t) + h\dot{\mathbf{a}}(t) + \frac{h^2}{2}\ddot{\mathbf{a}}(t) + O(h^4)\end{aligned}$$

so that

$$\mathbf{v}(t+h) - \mathbf{v}(t) - (h/2)(\mathbf{a}(t) + \mathbf{a}(t+h)) = -\frac{h^3}{12}\ddot{\mathbf{a}}(t) + O(h^4)$$

The velocity in the leapfrog method is

$$\mathbf{v}(t+h) = \mathbf{v}(t-h) + 2h\mathbf{a}(t) + \frac{h^3}{6}\ddot{\mathbf{a}}(t) + O(h^5)$$

and the velocity using the velocity Verlet method is

$$\mathbf{v}(t+h) = \mathbf{v}(t) + \frac{h}{2}(\mathbf{a}(t) + \mathbf{a}(t+h)) - \frac{h^3}{12}\ddot{\mathbf{a}}(t) + O(h^4)$$

All other things being equal, you expect the latter velocity estimate to have about half the error of the former since the coefficient of the h^3 term is half that in the other expression. The price for less error, though, is more computational time. The leapfrog method uses one evaluation of acceleration whereas the velocity Verlet method uses two evaluations. But the comparison is not quite fair. The leapfrog computes velocity on every other time step. The velocity Verlet method computes velocity on each time step. If you need the velocity information in the leapfrog method, such as in the implicit scheme of equation (13.33), then both methods use the same number of acceleration evaluations. The velocity Verlet produces a better estimate for the same cost.

The position in the velocity Verlet method is estimated from Taylor's theorem. The numerical method stated in the manner in which it normally is found in the literature is

$$\begin{aligned}\mathbf{x}(t+h) &= \mathbf{x}(t) + h\mathbf{v}(t) + \frac{h^2}{2}\mathbf{a}(t) \\ \mathbf{v}(t+h) &= \mathbf{v}(t) + \frac{h}{2}(\mathbf{a}(t) + \mathbf{a}(t+h))\end{aligned}$$

Once again the implicit assumption is that the force is of the form $\mathbf{F}(t, \mathbf{x})$ with no explicit dependence on velocity. The idea of the iteration is that $\mathbf{x}(t)$, $\mathbf{v}(t)$, and $\mathbf{a}(t) = \mathbf{F}(t, \mathbf{x}(t))/m$ are known. The next position $\mathbf{x}(t+h)$ is calculated from the first difference equation. This value is used to compute $\mathbf{a}(t+h) = \mathbf{F}(t+h, \mathbf{x}(t+h))/m$ and is substituted into the second difference equation to obtain the next velocity $\mathbf{v}(t+h)$. Many literature sources describe the process with one intermediate step. First, $\mathbf{x}(t+h)$ is computed. Second, the velocity for a half-step is computed, $\mathbf{v}(t+h/2) = \mathbf{v}(t) + (h/2)\mathbf{a}(t)$. Third, $\mathbf{a}(t+h) = \mathbf{F}(t+h, \mathbf{x}(t+h))/m$ is computed. Fourth, the velocity for the full-step is computed, $\mathbf{v}(t+h) = \mathbf{v}(t+h/2) + (h/2)\mathbf{a}(t+h)$. However, it is not necessary to do so in an implementation unless for some reason you need estimates of the velocities at the half-steps. In our standard formulation, the numerical method is

$\mathbf{y}_0, \dot{\mathbf{y}}_0$ are specified

$$\begin{aligned}\mathbf{y}_{i+1} &= \mathbf{y}_i + h\dot{\mathbf{y}}_i + \frac{h^2}{2m}\mathbf{F}(t_i, \mathbf{y}_i), \quad i \geq 0 \\ \dot{\mathbf{y}}_{i+1} &= \dot{\mathbf{y}}_i + \frac{h}{2m}(\mathbf{F}(t_i, \mathbf{y}_i) + \mathbf{F}(t_{i+1}, \mathbf{y}_{i+1})), \quad i \geq 0\end{aligned}\tag{13.34}$$

The \mathbf{y}_{i+1} term must be computed first since it is used in the equation to produce $\dot{\mathbf{y}}_{i+1}$.

When the force is of the form $\mathbf{F}(t, \mathbf{x}, \dot{\mathbf{x}})$, the numerical method becomes implicit:

$\mathbf{y}_0, \dot{\mathbf{y}}_0$ are specified

$$\mathbf{y}_{i+1} = \mathbf{y}_i + h\dot{\mathbf{y}}_i + \frac{h^2}{2m}\mathbf{F}(t_i, \mathbf{y}_i, \dot{\mathbf{y}}_i), \quad i \geq 0 \quad (13.35)$$

$$\dot{\mathbf{y}}_{i+1} = \dot{\mathbf{y}}_i + \frac{h}{2m} (\mathbf{F}(t_i, \mathbf{y}_i, \dot{\mathbf{y}}_i) + \mathbf{F}(t_{i+1}, \mathbf{y}_{i+1}, \dot{\mathbf{y}}_{i+1})), \quad i \geq 0$$

The implicitness is because $\dot{\mathbf{y}}_{i+1}$ occurs on both sides of the last difference equation. As always, a predictor-corrector method could be used. For example, you could predict $\dot{\mathbf{y}}_{i+1} = (\mathbf{y}_{i+1} - \mathbf{y}_i)/h$ and substitute in the right-hand side of the last difference equation to obtain the correction for $\dot{\mathbf{y}}_{i+1}$.

The velocity Verlet method gives you the best estimates of velocity of all the Verlet-style methods, but the cost is additional function evaluations. It is a one-step method, whereas the other explicit Verlet methods are two-step methods.

13.8.6 GEAR'S FIFTH-ORDER PREDICTOR-CORRECTOR METHOD

A method that is sometimes used as an alternative to the velocity Verlet method is called *Gear's fifth-order predictor-corrector method* [Gea71]. The prediction portion of the algorithm is based once again on Taylor's Theorem,

$$\begin{aligned} \mathbf{x}(t+h) &= \mathbf{x}(t) + h\mathbf{x}^{(1)}(t) + \frac{h^2}{2!}\mathbf{x}^{(2)}(t) + \frac{h^3}{3!}\mathbf{x}^{(3)}(t) + \frac{h^4}{4!}\mathbf{x}^{(4)}(t) + \frac{h^5}{5!}\mathbf{x}^{(5)}(t) + O(h^6) \\ \mathbf{x}^{(1)}(t+h) &= \mathbf{x}^{(1)}(t) + h\mathbf{x}^{(2)}(t) + \frac{h^2}{2!}\mathbf{x}^{(3)}(t) + \frac{h^3}{3!}\mathbf{x}^{(4)}(t) + \frac{h^4}{4!}\mathbf{x}^{(5)}(t) + O(h^5) \\ \mathbf{x}^{(2)}(t+h) &= \mathbf{x}^{(2)}(t) + h\mathbf{x}^{(3)}(t) + \frac{h^2}{2!}\mathbf{x}^{(4)}(t) + \frac{h^3}{3!}\mathbf{x}^{(5)}(t) + O(h^4) \\ \mathbf{x}^{(3)}(t+h) &= \mathbf{x}^{(3)}(t) + h\mathbf{x}^{(4)}(t) + \frac{h^2}{2!}\mathbf{x}^{(5)}(t) + O(h^3) \\ \mathbf{x}^{(4)}(t+h) &= \mathbf{x}^{(4)}(t) + h\mathbf{x}^{(5)}(t) + O(h^2) \\ \mathbf{x}^{(5)}(t+h) &= \mathbf{x}^{(5)}(t) + O(h) \end{aligned}$$

Subscripting the predicted values with p and the corrected values with c , the matrix form of the prediction step is

$$\begin{bmatrix} \mathbf{x}_p(t+h) \\ h\mathbf{x}_p^{(1)}(t+h) \\ \frac{h^2}{2!}\mathbf{x}_p^{(2)}(t+h) \\ \frac{h^3}{3!}\mathbf{x}_p^{(3)}(t+h) \\ \frac{h^4}{4!}\mathbf{x}_p^{(4)}(t+h) \\ \frac{h^5}{5!}\mathbf{x}_p^{(5)}(t+h) \end{bmatrix} = \begin{bmatrix} 1 & 1 & 1 & 1 & 1 & 1 \\ 0 & 1 & 2 & 3 & 4 & 5 \\ 0 & 0 & 1 & 3 & 6 & 10 \\ 0 & 0 & 0 & 1 & 4 & 10 \\ 0 & 0 & 0 & 0 & 1 & 5 \\ 0 & 0 & 0 & 0 & 0 & 1 \end{bmatrix} \begin{bmatrix} \mathbf{x}_c(t) \\ h\mathbf{x}_c^{(1)}(t) \\ \frac{h^2}{2!}\mathbf{x}_c^{(2)}(t) \\ \frac{h^3}{3!}\mathbf{x}_c^{(3)}(t) \\ \frac{h^4}{4!}\mathbf{x}_c^{(4)}(t) \\ \frac{h^5}{5!}\mathbf{x}_c^{(5)}(t) \end{bmatrix}$$

Notice that the nonzero entries of the columns of the 6×6 matrix are the rows of Pascal's triangle. The predicted values are used to evaluate the force function and obtain a corrected second-derivative,

$$\mathbf{x}_c^{(2)}(t+h) = \frac{1}{m} \mathbf{F}(t+h, \mathbf{x}_p(t+h), \dot{\mathbf{x}}_p(t+h))$$

Define:

$$\Delta = \frac{h^2}{2!} (\mathbf{x}_c^{(2)}(t+h) - \mathbf{x}_p^{(2)}(t+h))$$

The corrected values are

$$\begin{bmatrix} \mathbf{x}_c(t+h) \\ h\mathbf{x}_c^{(1)}(t+h) \\ \frac{h^2}{2!}\mathbf{x}_c^{(2)}(t+h) \\ \frac{h^3}{3!}\mathbf{x}_c^{(3)}(t+h) \\ \frac{h^4}{4!}\mathbf{x}_c^{(4)}(t+h) \\ \frac{h^5}{5!}\mathbf{x}_c^{(5)}(t+h) \end{bmatrix} = \begin{bmatrix} \mathbf{x}_p(t+h) \\ h\mathbf{x}_p^{(1)}(t+h) \\ \frac{h^2}{2!}\mathbf{x}_p^{(2)}(t+h) \\ \frac{h^3}{3!}\mathbf{x}_p^{(3)}(t+h) \\ \frac{h^4}{4!}\mathbf{x}_p^{(4)}(t+h) \\ \frac{h^5}{5!}\mathbf{x}_p^{(5)}(t+h) \end{bmatrix} + \Delta \begin{bmatrix} \lambda \\ 251/360 \\ 1 \\ 11/18 \\ 1/6 \\ 1/60 \end{bmatrix}$$

where $\lambda = 3/16$ if the force is of the form $\mathbf{F}(t, \mathbf{x})$ or $\lambda = 3/20$ if the force is of the form $\mathbf{F}(t, \mathbf{x}, \dot{\mathbf{x}})$. Starting the iteration does require that estimates be made for the second- and higher-order derivatives at initial time.

Compared to the velocity Verlet method, the Gear method will require more memory usage, potentially of importance if your physical system has a large number

of rigid bodies. The trade-off, though, is that the Gear method makes one function evaluation per time step, whereas the velocity Verlet method uses two function evaluations. Thus, we have the classic space versus time trade-off. Experience in the molecular dynamics field has shown that the velocity estimates from the velocity Verlet method tend to degenerate over time faster than those computed in the Gear method. The Gear method also has a higher degree of energy conservation with a larger time step compared to the velocity Verlet method. However, the Gear method is not reversible in time as are the Verlet methods.

Finally, if you should want to choose variable step sizes for the Verlet methods rather than fixed step sizes, see [HOS99].

13.9 NUMERICAL STABILITY AND ITS RELATIONSHIP TO PHYSICAL STABILITY

Stability of solutions to a system of differential equations was discussed in Section 11.6. The intuitive description is that a solution $\phi(t)$ is *stable* if each solution $\psi(t)$ that starts out close to $\phi(t)$ remains close to it for all time. In effect this is a statement about the *continuous dependence of a solution on its initial conditions*. If $\dot{\mathbf{x}} = \mathbf{f}(t, \mathbf{x})$ is the system of differential equations with initial data $\mathbf{x}(t_0) = \mathbf{x}_0$, the solution is denoted $\mathbf{x}(t; \mathbf{x}_0)$. If we compare solutions $\mathbf{x}(t; \mathbf{x}_0 + \delta)$ and $\mathbf{x}(t; \mathbf{x}_0)$, where δ is a nonzero vector of small length, we want to know about the differences $|\mathbf{x}(t; \mathbf{x}_0 + \delta) - \mathbf{x}(t; \mathbf{x}_0)|$ as time t increases. We do know that $|\mathbf{x}(t_0; \mathbf{x}_0 + \delta) - \mathbf{x}(t_0; \mathbf{x}_0)| = |(\mathbf{x}_0 + \delta) - \mathbf{x}_0| = |\delta|$, which is small. The question is whether or not the differences remain bounded or become unbounded with increasing time. I will refer to this measure of stability as *physical stability* since the differential equations are obtained as the equations of motion for a physical system.

Our earlier discussion involved understanding the stability of linear systems $\dot{\mathbf{x}} = A\mathbf{x}$ for which A has constant entries. As we saw, the stability is directly related to the signs on the real parts of the eigenvalues of A . If all eigenvalues have negative real parts, the system is stable. If at least one eigenvalue has positive real part, the system is unstable. If all eigenvalues have negative or zero real parts with at least one eigenvalue having zero real part, the stability depends on the dimension of the eigenspace of the eigenvalue.

We then used our knowledge of linear stability to determine the stability properties of equilibrium solutions to nonlinear autonomous systems $\dot{\mathbf{x}} = \mathbf{f}(\mathbf{x})$. For the sake of argument, let us assume that the equilibrium solution of interest is $\mathbf{x}(t) \equiv \mathbf{0}$. If this were not the case and $\mathbf{x}(t) \equiv \mathbf{x}_0 \neq \mathbf{0}$ were an equilibrium solution, we could always transform the system to one that does have a zero equilibrium solution by $\mathbf{y} = \mathbf{x} - \mathbf{x}_0$ and $\mathbf{F}(\mathbf{y}) = \mathbf{f}(\mathbf{y} + \mathbf{x}_0)$, so $\dot{\mathbf{y}} = \mathbf{F}(\mathbf{y})$ has the equilibrium solution $\mathbf{y}(t) \equiv \mathbf{0}$. Taylor's theorem allows us to write

$$\mathbf{f}(\mathbf{x}) = A\mathbf{x} + \mathbf{R}(\mathbf{x})$$

where A is the matrix of first-order derivatives of the components of \mathbf{f} that are evaluated at $\mathbf{0}$. The remainder \mathbf{R} consists of quadratic and higher-order terms. The *linearized system* is $\dot{\mathbf{x}} = A\mathbf{x}$. If the eigenvalues of A all have negative real parts, then the equilibrium solution of the physical system is stable. If at least one eigenvalue has positive real part, the equilibrium solution is unstable. No immediate conclusions can be drawn when the eigenvalues have negative or zero real parts with at least one having zero real part.

This result addresses the physical stability of the equilibrium solution. However, we will solve $\dot{\mathbf{x}} = \mathbf{f}(\mathbf{x})$ using a numerical method. It is important that the approximations generated by the method are themselves close to the true solution. The concept of closeness in this context is referred to as *numerical stability*. In general, to obtain numerical stability, you will need to carefully choose your step size h in the numerical solvers. The end result of our discussion will be that you can do this safely only by understanding the relationship between numerical stability and physical stability.

13.9.1 STABILITY FOR SINGLE-STEP METHODS

Three concepts are of interest: *consistency*, *convergence*, and *stability*. Recall that the *local truncation error* refers to the terms we discard when generating a numerical method from something such as a Taylor expansion. For example, Euler's method arose from Taylor's theorem in representing a solution to $\dot{x} = f(t, x)$ as

$$x(t_{i+1}) = x(t_i) + h\dot{x}(t_i) + \frac{h^2}{2}\ddot{x}(\bar{t}_i) = x(t_i) + hf(t_i, x(t_i)) + \frac{h^2}{2}\ddot{x}(\bar{t}_i)$$

where $\bar{t}_i \in [t_i, t_{i+1}]$, but whose value is generally unknown to us. We discarded the second-order term to obtain the numerical method,

$$y_{i+1} = y_i + hf(t_i, y_i)$$

where y_i is the approximation to $x(t_i)$. The discarded term is the local truncation error for Euler's method and is of order $O(h^2)$. As we make h small, the local truncation error for a single iteration is small. If we can make the local truncation errors become small for n iterations, that is a good thing for our numerical method. This leads us to the definition that follows.

Definition ■ Let τ_i denote the local truncation error at the i th step of the numerical method. The method is said to be *consistent* with the differential equation it approximates if

$$\lim_{h \rightarrow 0} \max_{1 \leq i \leq n} |\tau_i| = 0$$

Intuitively, this says that for very small step sizes, the local truncation error made at any time t is very small. ■

According to this definition, Euler's method is consistent.

In general having very small local truncation errors at any time is not enough to guarantee that y_i is a good approximation to $x(t_i)$. We need a definition about closeness.

Definition ■ A numerical method is said to be *convergent* with respect to the differential equation if

$$\lim_{h \rightarrow 0} \max_{1 \leq i \leq n} |x(t_i) - y_i| = 0$$

Intuitively, this says that for very small step sizes, the maximum error at any time t between the approximation and the true solution is very small. ■

Our derivation that led to the inequality of [equation \(13.3\)](#) shows that Euler's method is convergent.

Our last definition is about stability itself.

Definition ■ A numerical method is said to be *stable* if small changes in the initial data for the differential equation produce correspondingly small changes in the subsequent approximations. In formal terms, let x_0 and x_1 be two initial values for the differential equation. Let y_i be the approximation to $x(t_i; x_0)$ and let \bar{y}_i be the approximation to $x(t_i; x_1)$. For each $\varepsilon > 0$, there is a $\delta > 0$ sufficiently small so that $|y_i - \bar{y}_i| < \varepsilon$ whenever $|x_1 - x_0| < \delta$. ■

This definition is a statement about continuous dependence of solutions on the initial data. The relationship between consistency, convergence, and stability for a one-step numerical method is summarized by the following result.

Theorem ■ Consider the initial value problem $\dot{x} = f(t, x)$ for $t \in [t_0, t_0 + \alpha]$ with initial data $x(t_0) = x_0$. Let a numerical method for the equation be of the form $y_0 = x_0$ and $y_{i+1} = y_i + h\phi(t_i, y_i, h)$ for $i \geq 0$. If there is a value $h_0 > 0$ such that $\phi(t, y, h)$ is continuous on the domain,

$$D = \{(t, y, h) : t \in [t_0, t_0 + \alpha], y \in \mathbb{R}, h \in [0, h_0]\}$$

and if there exists a constant $L > 0$ such that

$$|\phi(t, y, h) - \phi(t, \bar{y}, h)| \leq L|y - \bar{y}|$$

for all $(t, y, h), (t, \bar{y}, h) \in D$, which is called a *Lipschitz condition*.

1. The numerical method is stable.
2. The method is convergent if and only if it is consistent; that is, if and only if $\phi(t, x, 0) = f(t, x, 0)$ for all $t \in [t_0, t_0 + \alpha]$.

3. If the local truncation errors are bounded by $|\tau_i| \leq T(h)$ for some function $B(h)$ independent of i and for $h \in [0, h_0]$, then $|x(t_i) - y_i| \leq B(h) \exp(L(t_i - t_0))/L$. ■

The condition in item 2 of the conclusion is easily verified for all the single-step numerical methods we have encountered. Notice that for Euler's method, $\phi(t, y, 0) = f(t, y)$. The same is true for the Runge–Kutta methods. Item 3 of the conclusion gives us an upper bound on the error of the approximation and looks similar to what we derived for Euler's method.

13.9.2 STABILITY FOR MULTISTEP METHODS

A stability result for multistep methods is only slightly more complicated than the one for single-step methods. The general multistep method can be formulated as

$$y_{i+1} = \sum_{j=0}^{m-1} a_j y_{i-j} + hF(t_i, h, y_{i+1}, y_i, \dots, y_{i+1-m}), \quad i \geq 0$$

with start-up conditions $y_i = b_i$ for selected constants b_i with $0 \leq i \leq m-1$. Since we started with a differential equation with initial condition $x(t_0) = x_0$, we choose $y_0 = x_0$. The other start-up values are generated by some single-step method. The prototypical explicit method is Adams–Bashforth and the prototypical implicit method is Adams–Moulton.

The concepts of convergence and stability are the same as for single-step methods, but consistency requires there be a slight bit more to it. The local truncation errors for a multistep method are of the form,

$$\tau_{i+1} = \frac{x(t_{i+1}) - \sum_{j=0}^{m-1} x(t_{i-j})}{h} - F(t_i, h, x(t_{i+1}), \dots, x(t_{i+1-m}))$$

The analysis of the algorithm for the m -step Adams–Bashforth method will show that the local truncation error is $\tau_{i+1} = O(h^m)$. The m -step Adams–Moulton method has local truncation error of $\tau_{i+1} = O(h^{m+1})$. The definition for consistency of a multistep method includes the same condition we used for single-step methods,

$$\lim_{h \rightarrow 0} \max_{1 \leq i \leq n} |\tau_i| = 0$$

so the local truncation errors go to zero as the step size becomes small but, in addition we need to make sure that the local truncation errors for the start-up conditions become small, also.

$$\lim_{h \rightarrow 0} \max_{1 \leq i \leq m-1} |x(t_i) - b_i| = 0$$

The result for multistep methods that is the analogy of the one for single-step methods follows.

Theorem ■ Consider the initial value problem $\dot{x} = f(t, x)$ for $t \in [t_0, t_0 + \alpha]$ with initial data $x(t_0) = x_0$. Consider a multistep method of the form $y_{i+1} = \sum_{j=0}^{m-1} a_j y_{i-j} + hF(t_i, h, y_{i+1}, y_i, \dots, y_{i+1-m})$ with start-up conditions $y_0 = x_0$ and $y_i = b_i$ for specified constants b_i with $1 \leq i \leq m - 1$. Suppose that $F \equiv 0$ whenever $f \equiv 0$. Suppose that F satisfies a Lipschitz condition,

$$|F(t_i, h, y_{i+1}, \dots, y_{i+1-m}) - F(t_i, h, \bar{y}_{i+1}, \dots, \bar{y}_{i+1-m})| \leq L \sum_{j=0}^m |y_{i+1-j} - \bar{y}_{i+1-j}|$$

for each i with $m - 1 \leq i \leq n$. Define the polynomial $p(\lambda) = \lambda^m - \sum_{j=0}^{m-1} a_j \lambda^{m-1-j}$.

1. The numerical method is stable if and only if all roots of $p(\lambda) = 0$ satisfy $|\lambda| \leq 1$ and any root such that $|\lambda| = 1$ must be a simple root (multiplicity is 1).
2. If the numerical method is consistent with the differential equation, the method is stable if and only if it is convergent. ■

The important aspect of this theorem for practical purposes is the analysis of the roots of $p(\lambda)$. Note that the roots can be nonreal. Also note that $p(1) = 0$ because of the way the a_j were defined for multistep methods. Thus, $\lambda = 1$ is always a root and has magnitude $|\lambda| = 1$. If $\lambda = 1$ is the only root of magnitude 1, all other roots satisfying $|\lambda| < 1$, then the numerical method is said to be *strongly stable*. If more than one root has magnitude one, the others satisfying $|\lambda| < 1$, the numerical method is said to be *weakly stable*. If any root has magnitude $|\lambda| > 1$, the numerical method is said to be *unstable*.

13.9.3 CHOOSING A STABLE STEP SIZE

In fact, we can go one step further. The analysis of the roots of $p(\lambda)$ when using the linearized equation instead of the original $\mathbf{f}(x)$ allows us to decide what step sizes h lead to stability, an important issue for solving the equations on a computer. More details can be found in Chapter 5 of [BF01], although they are listed in the section on stiff equations. A presentation of the material in the context of game development may also be found in [Rho01].

Assuming an equilibrium solution of $\mathbf{x}(t) \equiv \mathbf{0}$, the linearized equation is $\dot{\mathbf{x}} = A\mathbf{x}$, where A is an $n \times n$ matrix of constants occurring in the expansion $\mathbf{f}(x) = Ax + \mathbf{R}$. Let us assume that the eigenvalues of A all have negative real parts so that the equilibrium solution is physically stable. For each eigenvalue λ , consider what is called the *modal equation*, $\dot{\mathbf{x}} = \lambda \mathbf{x}$. An m -step method ($m \geq 1$) is applied to the modal equation. The resulting difference equation is linear and has a characteristic polynomial of the type

$p(z)$ whose coefficients involve the eigenvalue λ and the step size h . This polynomial includes the linear contribution from the function F in the multistep method. The conditions of $|z| \leq 1$ for all roots and unit-magnitude roots being simple are required for a stable method. These in turn impose conditions on how we can choose h .

The best way to illustrate this is with an example. We will once again revisit the simple pendulum problem of [Example 3.4](#).

EXAMPLE

13.1

The equation of motion for a simple pendulum with viscous friction at the joint is

$$\ddot{\theta} + b\dot{\theta} + c \sin(\theta) = 0, \quad t \geq 0, \quad \theta(0) = \theta_0, \quad \dot{\theta}(0) = \dot{\theta}_0$$

where $b \geq 0$ represents the coefficient of viscous friction ($b = 0$ for a frictionless joint) and $c = g/L > 0$, where g is the gravitational constant and L is the length of the pendulum rod. The angle $\theta(t)$ is measured from the vertical position. The initial angle is θ_0 and the initial angular speed is $\dot{\theta}_0$. We may write this equation as a first-order system $\dot{\mathbf{x}} = \mathbf{f}(t, \mathbf{x})$ by defining

$$\mathbf{x} = \begin{bmatrix} x_1 \\ x_2 \end{bmatrix} = \begin{bmatrix} \theta \\ \dot{\theta} \end{bmatrix}, \quad \mathbf{f}(t, \mathbf{x}) = \begin{bmatrix} f_1 \\ f_2 \end{bmatrix} = \begin{bmatrix} \dot{\theta} \\ -b\dot{\theta} - c \sin(\theta) \end{bmatrix} = \begin{bmatrix} x_2 \\ -bx_2 - c \sin(x_1) \end{bmatrix}$$

In fact the system is autonomous since \mathbf{f} does not depend explicitly on t , only on x_1 and x_2 . The first-derivative matrix is

$$D\mathbf{f}(\mathbf{x}) = \begin{bmatrix} \frac{\partial f_1}{\partial x_1} & \frac{\partial f_1}{\partial x_2} \\ \frac{\partial f_2}{\partial x_1} & \frac{\partial f_2}{\partial x_2} \end{bmatrix} = \begin{bmatrix} 0 & 1 \\ -c \cos(x_1) & -b \end{bmatrix}$$

The equilibrium solutions of the system are $\mathbf{x}_0(t) \equiv (0, 0)$ and $\mathbf{x}_1(t) \equiv (\pi, 0)$. The first equilibrium solution corresponds to the pendulum hanging vertically downward with no angular speed. Physically you expect this to be stable. If you move the pendulum slightly, you expect it to stay near the vertical. The second solution corresponds to the pendulum positioned vertically upward with no angular speed. Physically you expect this to be unstable because any slight movement of the pendulum will cause it to fall downward. Let us see what the mathematical model has to say about this.

The first-derivative matrix at the first equilibrium solution is

$$D\mathbf{f}(0, 0) = \begin{bmatrix} 0 & 1 \\ -c & -b \end{bmatrix}$$

and has the characteristic equation $\lambda^2 + b\lambda + c = 0$. For the case of viscous friction where $b > 0$, the roots are

$$\lambda = \frac{-b \pm \sqrt{b^2 - 4c}}{2}$$

(Example 13.1
continued)

Both roots are negative real numbers when $b^2 \geq 4c$ or are complex numbers with negative real parts when $b^2 < 4c$. In either case the real parts are both negative, so $(0,0)$ is a stable equilibrium solution. For the case of no friction where $b = 0$, the roots are

$$\lambda = 0 \pm ci$$

Both roots are complex-valued with zero real parts. Each root is an eigenvalue of $Df(0,0)$ with one linearly independent eigenvector. According to our theorem on stability of linear systems, the equilibrium solution is stable. Thus, the equilibrium solution $(0,0)$ is stable for any $b \geq 0$, so the mathematical model appears to be a reasonable match to what we expect physically.

The first-derivative matrix at the second equilibrium solution is

$$Df(\pi, 0) = \begin{bmatrix} 0 & 1 \\ c & -b \end{bmatrix}$$

and has the characteristic equation $\lambda^2 + b\lambda - c = 0$. The roots are

$$\lambda = \frac{-b \pm \sqrt{b^2 + 4c}}{2}$$

Regardless of $b = 0$ or $b > 0$, both roots are real-valued with one negative and one positive. The second equilibrium solution is therefore unstable, once again showing that the mathematical model exhibits properties that we expect in the physical system.

Before doing the analysis for numerical stability, let us try four different numerical methods for the simple pendulum problem where $b = 0$, $c = 1$, $\theta_0 = 0.1$, $\dot{\theta}_0 = 1.0$, and $h = 0.1$. The experiments generate $n = 256$ iterates. The test driver is

```
double c = 1.0f; // global constant used by numerical methods
void SolveSystem (double* (*NumericalMethod)(double,double,double,int))
{
    int n = 256;
    double theta0 = 0.1, dtheta0 = 1.0, h = 0.1;
    double theta* = NumericalMethod(theta0,dtheta0,h,n);
    // plot the output...
}
```

EXPLICIT EULER'S METHOD The numerical method is

$$\mathbf{y}_{i+1} = \mathbf{y}_i + h\mathbf{f}(t_i, \mathbf{y}_i)$$

with initial data $\mathbf{y}_0 = (\theta_0, \dot{\theta}_0)$. Pseudocode for generating the iterates is

```
double* ExplicitEuler (double theta0, double dtheta0, double h, int n)
{
    double* theta = new double[n];
    for (int i = 0; i < n; i++)
```

```

{
    double theta1 = theta0 + h * dtheta0;
    double dtheta1 = dtheta0 - h * c * sin(theta0);
    theta[i] = theta1;
    theta0 = theta1;
    dtheta0 = dtheta1;
}
return theta;
}

```

Figure 13.2 shows a plot of the output of the numerical method.

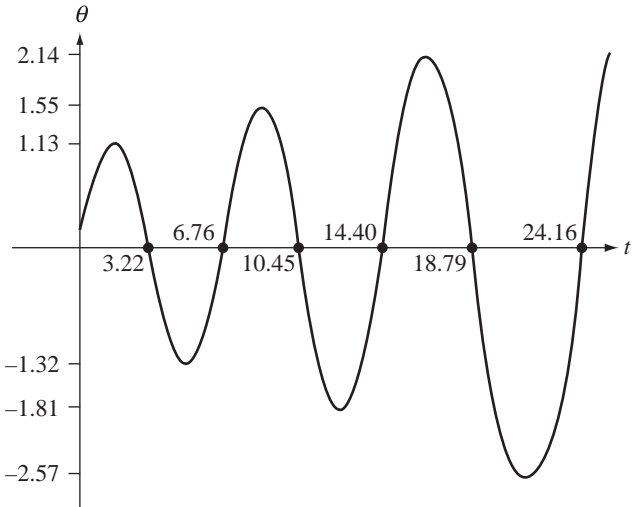


Figure 13.2

The explicit Euler's method applied to the simple pendulum problem. The image shows a plot of the pendulum angles over time.

Observe that the angles are becoming unbounded over time, contrary to how the physical solution should behave. The true solution should be periodic, implying that the maximum angles are all the same and the minimum angles are all the same. Also, the time between two consecutive zeros should be a constant. The results should make you question whether choosing Euler's method without analysis was a good thing to do.

IMPLICIT EULER'S METHOD The numerical method is

$$\mathbf{y}_{i+1} = \mathbf{y}_i + h\mathbf{f}(t_{i+1}, \mathbf{y}_{i+1})$$

(Example 13.1
continued)

with initial data $\mathbf{y}_0 = (\theta_0, \dot{\theta}_0)$. The iterate \mathbf{y}_{i+1} appears on both sides of the equation. For the simple pendulum, $\mathbf{y}_i = (\theta_i, \dot{\theta}_i)$ and the iteration scheme is

$$\theta_{i+1} = \theta_i + h\dot{\theta}_{i+1}, \quad \dot{\theta}_{i+1} = \dot{\theta}_i - hc \sin(\theta_{i+1})$$

My implementation combines these into a single equation,

$$\theta_{i+1} + h^2 c \sin(\theta_{i+1}) - \theta_i - h\dot{\theta}_i = 0$$

and applies Newton's method to $g(z) = z + h^2 c \sin(z) - \theta_i - h\dot{\theta}_i$ with initial guess $z_0 = \theta_i$ and

$$z_{m+1} = z_m - \frac{g(z_m)}{g'(z_m)}, \quad m \geq 0$$

where $g'(z) = 1 + h^2 c \cos(z)$. The final iterate z_M is chosen to be the value θ_{i+1} . Pseudocode for generating the differential equation iterates is

```
double* ImplicitEuler (double theta0, double dtheta0, double h,
int n)
{
    const int maxIterations = 32;
    double* theta = new double[n];
    for (int i = 0; i < n; i++)
    {
        double theta1 = theta0;
        for (int j = 0; j < maxIterations; j++)
        {
            double g = theta1 + h * h * c * sin(theta1) - theta0
                - h * dtheta0;
            double gder = 1.0 + h * h * c * cos(theta1);
            theta1 -= g / gder;
        }
        double dtheta1 = dtheta0 - h * c * sin(theta1);
        theta[i] = theta1;
        theta0 = theta1;
        dtheta0 = dtheta1;
    }
    return theta;
}
```

For simplicity, no convergence or stopping criterion is used in the inner loop that constructs the Newton's iterates; the loop just runs a fixed number of times. A more sophisticated loop with an eye towards minimizing inner loop cycles may certainly be tried. [Figure 13.3](#) shows a plot of the output of the numerical method.

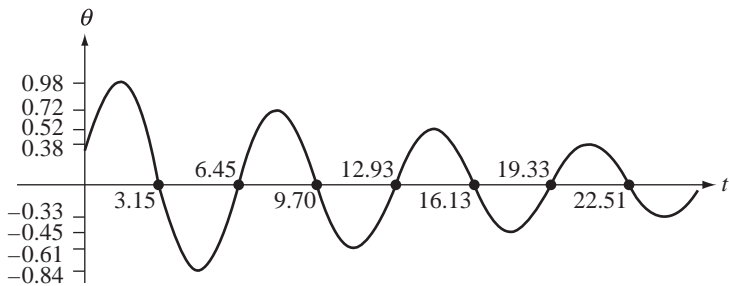


Figure 13.3

The implicit Euler method applied to the simple pendulum problem. The image shows a plot of the pendulum angles over time.

Now the angles are damped over time, contrary to how the physical solution should behave, although in this case someone observing the numerical pendulum behavior might think the physical system had friction at the joint causing the oscillations to dampen. The time between two consecutive zeros in Euler's method was significantly increasing over time. In the implicit Euler method, the time between zeros is only gradually decreasing.

RUNGE-KUTTA FOURTH-ORDER METHOD The numerical method is

$$\begin{aligned} \mathbf{k}_1 &= h\mathbf{f}(t_i, \mathbf{y}_i) \\ \mathbf{k}_2 &= h\mathbf{f}(t_i + h/2, \mathbf{y}_i + \mathbf{k}_1/2) \\ \mathbf{k}_3 &= h\mathbf{f}(t_i + h/2, \mathbf{y}_i + \mathbf{k}_2/2) \\ \mathbf{k}_4 &= h\mathbf{f}(t_i + h, \mathbf{y}_i + \mathbf{k}_3) \\ \mathbf{y}_{i+1} &= \mathbf{y}_i + (\mathbf{k}_1 + 2\mathbf{k}_2 + 2\mathbf{k}_3 + \mathbf{k}_4)/6 \end{aligned}$$

with initial data $\mathbf{y}_0 = (\theta_0, \dot{\theta}_0)$. Pseudocode for generating the iterates is

```
double* RungeKutta (double theta0, double dtheta0, double h, int n)
{
    double* theta = new double[n];
    for (int i = 0; i < n; i++)
    {
        double K1theta = h * dtheta0;
        double K1dtheta = -h * c * sin(theta0);
        double theta1 = theta0 + 0.5 * K1theta;
        double dtheta1 = dtheta0 + 0.5 * K1dtheta;
        double K2theta = h * dtheta1;
        double K2dtheta = -h * c * sin(theta1);
```

(Example 13.1
continued)

```

        thetal = theta0 + 0.5 * K2theta;
        dthetal = dtheta0 + 0.5 * K2dtheta;
        double K3theta = h * dthetal;
        double K3dtheta = -h * c * sin(theta1);
        thetal = theta0 + K3theta;
        dthetal = dtheta0 + K3dtheta;
        double K4theta = h * dthetal;
        double K4dtheta = -h * c * sin(theta1);
        thetal = theta0 + (K1theta + 2.0 * K2theta
            + 2.0 * K3theta + K4theta) / 6.0;
        dthetal = dtheta0 + (K1dtheta + 2.0 * K2dtheta
            + 2.0 * K3dtheta + K4dtheta) / 6.0;
        theta[i] = thetal;
        theta0 = thetal;
        dtheta0 = dthetal;
    }
    return theta;
}

```

Figure 13.4 shows a plot of the output of the numerical method.

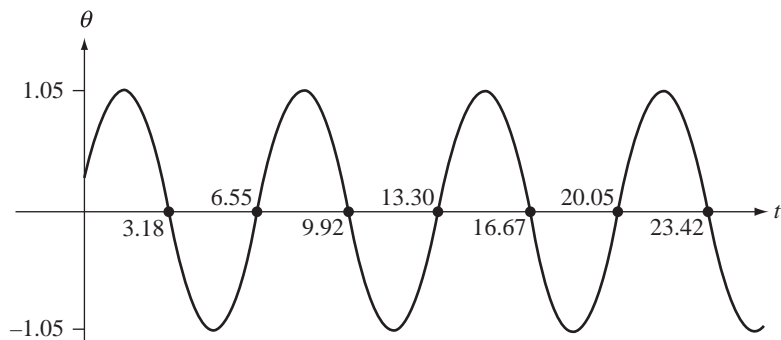


Figure 13.4

The Runge–Kutta fourth-order method applied to the simple pendulum problem. The image shows a plot of the pendulum angles over time.

The results appear to indicate that this method is stable. The zeros of $\theta(t)$ are evenly spaced, and the four maximum values, in order of increasing time, are 1.05289, 1.05117, 1.05285, and 1.05249. The four minimum values are -1.05232 , -1.05291 , -1.05221 , and -1.05293 .

LEAPFROG METHOD This is a two-step method,

$$y_{i+2} = y_i + 2hf(t_i, y_{i+1})$$

where the initial data is y_0 and the first iterate is generated by an Euler step, $y_1 = y_0 + hf(t_0, y_0)$. Pseudocode for generating the iterates is

```
double* Leapfrog (double theta0, double dtheta0, double h, int n)
{
    double* theta = new double[n];

    // generate first iterate with Euler's to start up the process
    double theta1 = theta0 + h * dtheta0;
    double dtheta1 = dtheta0 - h * c * sin(theta0);
    theta[0] = theta1;

    for (int i = 1; i < n; i++)
    {
        double theta2 = theta0 + 2.0 * h * dtheta1;
        double dtheta2 = dtheta0 - 2.0 * h * c * sin(theta1);
        theta[i] = theta2;
        theta0 = theta1;
        dtheta0 = dtheta1;
        theta1 = theta2;
        dtheta1 = dtheta2;
    }
    return theta;
}
```

Figure 13.5 shows a plot of the output of the numerical method.

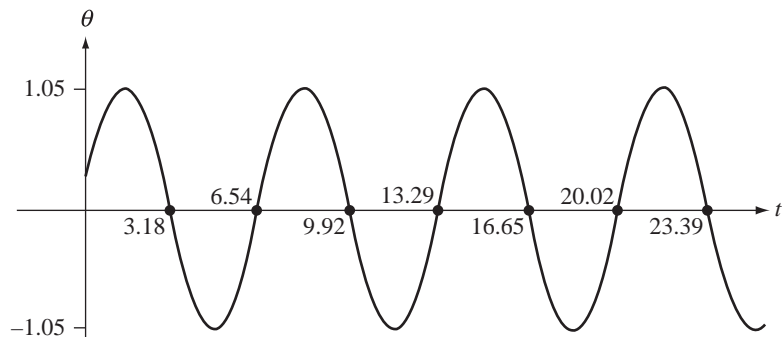


Figure 13.5

The leapfrog method applied to the simple pendulum problem. The image shows a plot of the pendulum angles over time.

The results appear to indicate that this method is stable. The zeros of $\theta(t)$ are evenly spaced, and the four maximum values, in order of increasing time, are 1.05816,

(Example 13.1
continued)

1.05079, 1.05582, and 1.05810. The four minimum values are -1.05750 , -1.05410 , -1.05730 , and -1.05820 .

We now analyze the numerical stability of the four methods for the physically stable equilibrium solution $(0, 0)$ when $b = 0$ and $c = 1$. The eigenvalues of $Df(0, 0)$ are $\lambda = \pm i$. The modal equation is $\dot{\mathbf{x}} = \lambda \mathbf{x}$. We apply the numerical methods using $\mathbf{f}(t, \mathbf{x}) = \lambda \mathbf{x}$.

EXPLICIT EULER'S METHOD The application to the modal equation is

$$\mathbf{y}_{i+1} = \mathbf{y}_i + h\lambda \mathbf{y}_i = (1 + h\lambda) \mathbf{y}_i$$

The characteristic polynomial equation $p(z) = 0$ of a linear difference equation is obtained by subtracting all terms to the left-hand side of the equation and formally replacing \mathbf{y}_{i+j} by z^j for $j \geq 0$. In this case the characteristic polynomial is

$$p(z) = z - (1 + h\lambda)$$

and has the single root $z = 1 + h\lambda$. For stability we need $|z| \leq 1$, so $|1 + h\lambda| \leq 1$. This is an inequality that defines a set of points in the complex plane. We can plot the set in terms of the complex variable $h\lambda$. Figure 13.6 shows the region for $|1 + h\lambda| \leq 1$.

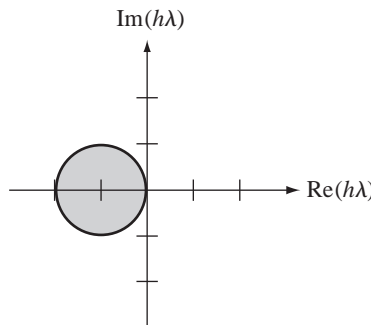


Figure 13.6

The region of stability for the explicit Euler method is shown in gray.

Regardless of choice of $h > 0$, $h\lambda = \pm hi$ is never inside the gray region. The explicit Euler's method is not stable for the simple pendulum problem for any choice of h and cannot be used to obtain good approximations.

IMPLICIT EULER'S METHOD The application to the modal equation is

$$\mathbf{y}_{i+1} = \mathbf{y}_i + h\lambda \mathbf{y}_{i+1}$$

The characteristic polynomial is

$$p(z) = (1 - h\lambda)z - 1$$

and has the single root $z = 1/(1 - h\lambda)$. For stability we need $|z| \leq 1$, so $|1 - h\lambda| \geq 1$. Figure 13.7 shows the region of stability.

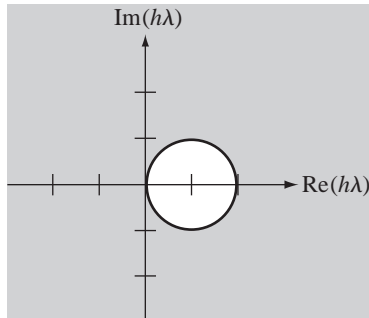


Figure 13.7

The region of stability for the implicit Euler method is shown in gray.

Regardless of choice of $h > 0$, $h\lambda = \pm hi$ is always inside the gray region. The implicit Euler method is always stable for the simple pendulum problem for any choice of h . However, the approximations are not accurate over time.

RUNGE-KUTTA FOURTH-ORDER METHOD The application to the modal equation is

$$\mathbf{k}_1 = h\lambda \mathbf{y}_i$$

$$\mathbf{k}_2 = h\lambda(1 + h\lambda/2)\mathbf{y}_i$$

$$\mathbf{k}_3 = h\lambda(1 + (h\lambda/2)(1 + h\lambda/2))\mathbf{y}_i$$

$$\mathbf{k}_4 = h\lambda(1 + h\lambda(1 + (h\lambda/2)(1 + h\lambda/2)))\mathbf{y}_i$$

These combine to form

$$\mathbf{y}_{i+1} = \left[1 + (h\lambda) + \frac{1}{2}(h\lambda)^2 + \frac{1}{6}(h\lambda)^3 + \frac{1}{24}(h\lambda)^4 \right] \mathbf{y}_i = q(h\lambda) \mathbf{y}_i$$

where the last equality defines the fourth-degree polynomial $q(h\lambda)$. The characteristic polynomial is

$$p(z) = z - q(h\lambda)$$

(Example 13.1
continued)

and has a single root $z = q(h\lambda)$. For stability we need $|q(h\lambda)| \leq 1$. Figure 13.8 shows the region of stability.

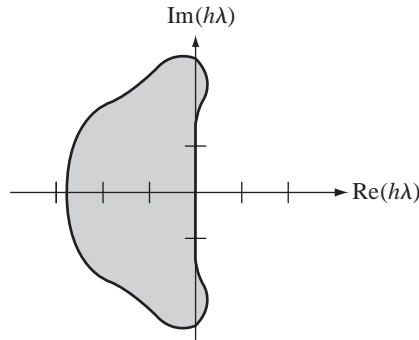


Figure 13.8

The region of stability for the Runge–Kutta fourth-order method is shown in gray.

Although Figure 13.8 does not show this, the right boundary of the gray region is slightly to the right of the imaginary axis, except at the origin, which is a point on the boundary. An evaluation at $h = 0.1$ for either eigenvalue $\pm i$ shows that $|q(\pm 0.1i)| \doteq 0.999999986 < 1$. Thus, the Runge–Kutta method is stable for the simple pendulum problem and it turns out to be accurate over time.

LEAPFROG METHOD The application to the modal equation is

$$\mathbf{y}_{i+2} = \mathbf{y}_i + 2h\lambda \mathbf{y}_{i+1}$$

The characteristic polynomial is

$$p(z) = z^2 - 2h\lambda z - 1$$

and has two roots $z = h\lambda \pm \sqrt{1 + (h\lambda)^2}$. For stability we need two conditions satisfied, $|h\lambda + \sqrt{1 + (h\lambda)^2}| \leq 1$ and $|h\lambda - \sqrt{1 + (h\lambda)^2}| \leq 1$. Figure 13.9 shows the region of stability. The region consists of the line segment $z = wi$, where $|w| \leq 1$. In our case $z = \pm 0.1i$, so the leapfrog method is stable for the simple pendulum problem with our chosen step size.

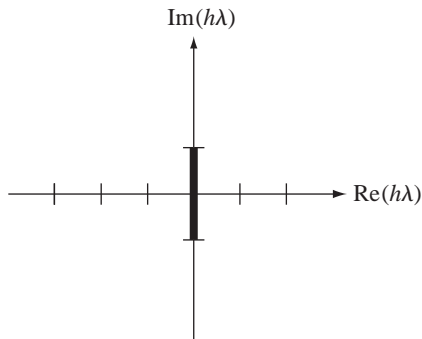


Figure 13.9

The region of stability for the leapfrog method is shown in black and consists of a line segment on the imaginary axis. ■

13.10 STIFF EQUATIONS

When dealing with a system of differential equations, numerical stability is clearly important in order that the output of the numerical method be meaningful. A somewhat related problem that can also occur is the problem of *stiffness*. These types of problems arise when the differential equation has two or more functional terms that have widely different scales. If the solution relevant to the application is the one that yields a steady state, a transient term that rapidly decays to zero can affect the calculations and generate significant error. The prototypical behavior is illustrated by a second-order linear equation or, equivalently, a system of two first-order linear equations.

EXAMPLE

13.2

Consider the second-order equation,

$$\ddot{x} = c^2 x, \quad t \geq 0, \quad x(0) = x_0, \quad \dot{x}(0) = \dot{x}_0$$

where $c > 0$ is a constant. The solution is

$$x(t) = \left(\frac{cx_0 + \dot{x}_0}{2c} \right) e^{ct} + \left(\frac{cx_0 - \dot{x}_0}{2c} \right) e^{-ct}$$

A physical application will no doubt be interested only in the steady state solution that has the decaying term e^{-ct} . We can make this happen by choosing the initial conditions so that $\dot{x}_0 = -cx_0$. The solution for such conditions is

$$x(t) = x_0 e^{-ct}$$

(Example 13.2
continued)

and has the property $\lim_{t \rightarrow \infty} x(t) = 0$. Choosing $c^2 = 2$, $x_0 = 1$, $\dot{x}_0 = -\sqrt{2}$, and $h = 0.01$, the Runge–Kutta fourth-order method produces iterates as shown in Figure 13.10.

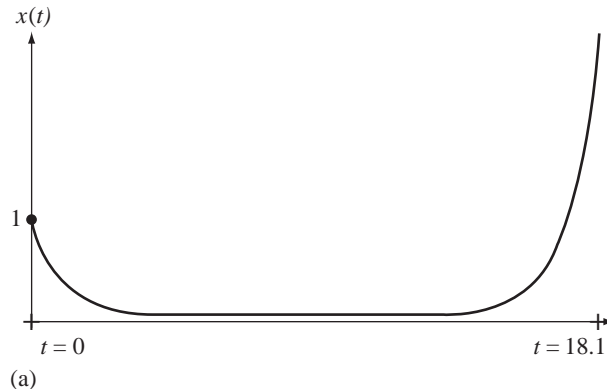


Figure 13.10

(a) An approximation to $x(t)$ using the Runge–Kutta fourth-order method. (b) The graph of the actual solution $x_0 e^{-ct}$.

As you can see, the approximation appears to be stable and accurate for quite some time, but then becomes unbounded. Two problems are occurring here. The first is that we cannot exactly represent $c = \sqrt{2}$ on the computer, so our theoretical requirement of $cx_0 + \dot{x}_0 = 0$ cannot be enforced. Numerical errors cause $cx_0 + \dot{x}_0 = \varepsilon$ for a very small value of $\varepsilon \neq 0$. This causes the functional term e^{ct} to influence the approximations and cause the unbounded behavior as shown in Figure 13.10. Even if we could represent the initial data exactly, the numerical method still introduces errors, both local truncation errors and round-off errors. This, too, causes e^{ct} to affect the solution eventually. Consequently, this problem is stiff. ■

You might be tempted to conclude that the problem occurs only because of the occurrence of a positive eigenvalue $c > 0$ and a negative one $-c < 0$. However,

even if the theoretical solution has two negative eigenvalues, stiffness can occur. The following example from [BF01] illustrates this.

EXAMPLE

13.3

Consider the first-order linear system,

$$\begin{aligned}\dot{x} &= 9x + 24y + 5\cos(t) - \frac{1}{3}\sin(t) \\ \dot{y} &= -24x - 51y - 9\cos(t) + \frac{1}{3}\sin(t)\end{aligned}$$

with initial data $x(0) = 4/3$ and $y(0) = 2/3$. The solution is

$$\begin{aligned}x(t) &= 2e^{-3t} - e^{-39t} + \frac{1}{3}\cos(t) \\ y(t) &= -e^{-3t} + 2e^{-39t} - \frac{1}{3}\cos(t)\end{aligned}$$

The homogeneous linear system is physically stable about the equilibrium solution $(0,0)$ since the eigenvalues of the first-derivative matrix are $\lambda = -3$ and $\lambda = -39$. The Runge–Kutta fourth-order method was used to numerically solve this problem with step sizes of $h = 0.1$ and $h = 0.05$. Table 13.1 shows the iterates for times between 0 and 1. It also shows the actual values.

Table 13.1 The Actual and Approximate Values for the Solution to the System of Equations

t	$x(t)$	$y(t)$	x_i	y_i	x_i	y_i
			$h = 0.05$		$h = 0.1$	
0.1	1.793063	-1.032002	1.712221	-0.870315	-2.645182	7.844543
0.2	1.423902	-0.874681	1.414072	-0.855015	-18.451691	38.876595
0.3	1.131577	-0.724999	1.130526	-0.722892	-87.473297	176.484833
0.4	0.909409	-0.608214	0.909278	-0.607948	-394.077576	789.365967
0.5	0.738788	-0.515658	0.738752	-0.515581	-1760.050049	3521.062256
0.6	0.605710	-0.440411	0.605684	-0.440356	-7848.706055	15698.184570
0.7	0.499860	-0.377404	0.499837	-0.377355	-34990.457031	69981.546875
0.8	0.413671	-0.322953	0.413650	-0.322908	-155983.609375	311967.750000
0.9	0.341614	-0.274409	0.341595	-0.274368	-695351.062500	1390702.750000
1.0	0.279675	-0.229888	0.279658	-0.229852	-3099763.500000	6199527.500000

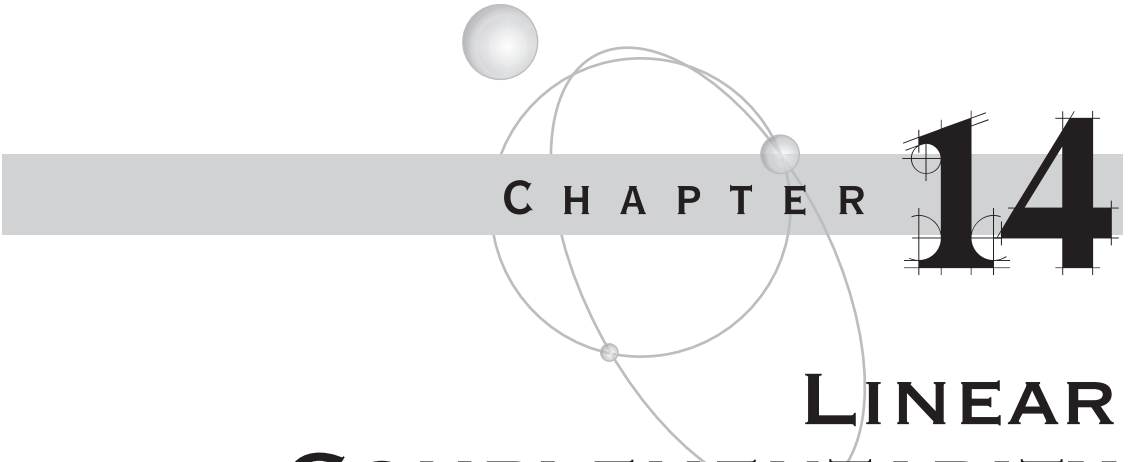
As you can see, the method appears to be stable when $h = 0.05$ but not when $h = 0.1$. The differences in behavior for the two step sizes is explained by something we already talked about: determining if the chosen step size puts us in the region of stability associated with the numerical method. The region of stability for the Runge–Kutta

(Example 13.3
continued)

fourth-order (RK4) method is shown in Figure 13.8. The eigenvalues for the current problem are $\lambda_1 = -3$ and $\lambda_2 = -39$. For step size $h = 0.1$, $h\lambda_1 = -0.3$ is in the region of stability, but $h\lambda_2 = -3.9$ is *outside* the region (to the left of it). However, when $h = 0.05$, both $h\lambda_1 = -0.15$ and $h\lambda_2 = -1.95$ are *inside* the region, so the RK4 method is stable. Our experiments agree with this analysis. ■

As the last example shows, the analysis of numerical stability for the linearized system is important for choosing a step size for which the method is stable and, hopefully, that avoids the problems of stiffness. Numerical methods that lead to as large a region of stability as possible are clearly desirable. Of course, since the physical stability requires eigenvalues with negative real parts and since the step sizes are positive, the only relevant portion of the region of stability is that part in the left half of the complex plane. For example, the region of stability for the implicit Euler's method includes the entire left half of the complex plane. In general, if the region of stability for a numerical method includes the entire left half of the complex plane, the method is called *A-stable*. Another example of an A-stable method is the trapezoid method listed in equation (13.7). This happens to be the only multistep method that is A-stable.

Although I have not discussed the topic here, the numerical methods of this chapter all use fixed-size steps. A class of numerical methods that might be important to you are those involving variable-size steps. It is not clear if variable step sizes gain you much in a real-time physics simulation, but if you do decide to use such a method, you need to balance the desire to choose large steps against the need to retain stability and avoid stiffness. Error monitoring is implemented in methods using variable step sizes in order to allow you to decide that the local truncation errors warrant choosing a larger step size. However, that larger step could take you outside the region of stability. Your implementation should additionally determine, if possible, whether the desired larger step size keeps you in the region of stability.



CHAPTER

14

LINEAR COMPLEMENTARITY AND MATHEMATICAL PROGRAMMING

The collision response system of a generic physics engine described in [Chapter 6](#) enforces nonpenetration constraints among all the rigid bodies participating in a physical simulation. When a set of rigid bodies collides simultaneously, the system must guarantee that the velocities and accelerations of the objects do not cause a pair of rigid bodies to start to interpenetrate at a contact point. The mathematical model that arises from the nonpenetration constraints requires us to solve a couple of problems in the form of what is called a *linear complementarity problem* (LCP), which we discussed briefly in [Chapter 6](#). As it turns out, calculation of distances between convex polygons or convex polyhedra can be formulated as an LCP. The applications to nonpenetration and to distance calculations are presented at the end of this chapter. The first part of the chapter is devoted to showing how you can solve an LCP.

The Lemke algorithm is a pivoting method for solving an LCP and is motivated by the classical linear programming problem. We discuss this problem first as well as how you go about solving it. Convex quadratic programming is also solvable by converting to an LCP. The typical convex quadratic functions you encounter are squared distance functions that arise when attempting to compute the separation distance between two convex objects. Linear and quadratic programming are special cases of what is



known as *mathematical programming*, a term not to be confused with programming mathematical algorithms.

Applications are provided at the end of the chapter for computing distance between a point and a convex polygon, distance between a point and a convex polyhedron, distance between two convex polygons, and distance between two convex polyhedra. The application to computing contact forces in order to enforce nonpenetration constraints in the collision response system is also summarized, although you will need to read [Chapter 6](#) to see exactly how the LCP formulation is derived. Source code is provided on the CD-ROM for solving the LCP problem and is based on the algorithm discussed in this chapter, using both direct numerical calculations in the pivoting scheme and using symbolic manipulations to handle degenerate behavior in the system.

14.1 LINEAR PROGRAMMING

The topic of *linear programming* has to do with maximizing a linear function subject to a set of linear inequality constraints. Let us first look at the problem in two dimensions to obtain some intuition about how to solve such problems in higher dimensions.

14.1.1 A TWO-DIMENSIONAL EXAMPLE

Consider the problem of maximizing the linear function $f(x_1, x_2) = x_1 + x_2$ subject to the linear inequality constraints $x_1 \geq 0$, $x_2 \geq 0$, $2x_1 + x_2 \leq 2$, and $x_1 + 2x_2 \leq 3$. [Figure 14.1](#) shows two ways of visualizing the problem.

The four inequality constraints define a convex quadrilateral in the plane. [Figure 14.1\(a\)](#) shows four level curves $f(x_1, x_2) = c$ in the quadrilateral: $c = 1/3$, $c = 2/3$, $c = 1$, and $c = 3/2$. The largest value of c for any level curve in the quadrilateral is $c = 5/3$ and occurs at the vertex $(1/3, 4/3)$. [Figure 14.1\(b\)](#) shows the graph of $x_3 = f(x_1, x_2)$, a plane in three dimensions. The point on the portion of the plane over the quadrilateral domain with largest x_3 value occurs at $(x_1, x_2, x_3) = (1/3, 4/3, 5/3)$.

The example shows that the maximization problem has two important aspects. The first aspect is determining the region defined by the linear inequality constraints. Each constraint defines a half plane. Points satisfying two constraints must be in the intersection of the half planes implied by the constraints. Generally, the intersection of the half planes of all the constraints is either the empty set, in which case the maximization problem has no solution, or a convex set that is possibly unbounded. In most applications the constraints are set up to generate a bounded convex set. Because the boundary of the convex sets is generated by the lines corresponding to equality in the linear inequality constraints, a bounded convex set must be a solid convex polygon. An unbounded convex set has a boundary consisting of linear components (lines, rays, or line segments). [Figure 14.2](#) illustrates various cases.

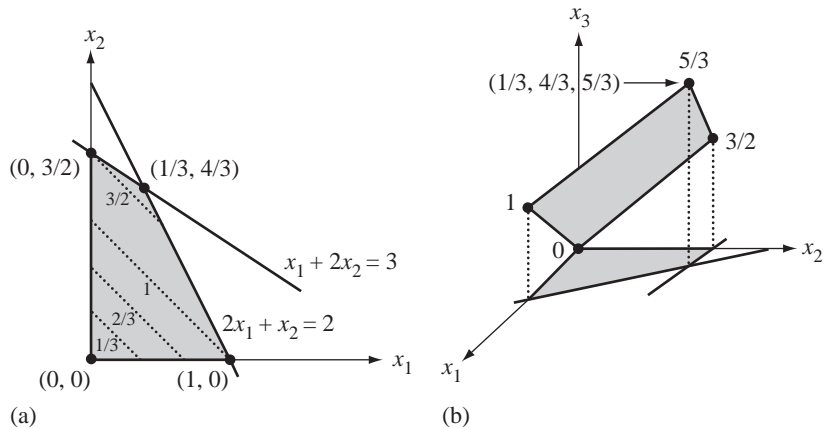


Figure 14.1 (a) Various level curves $f(x_1, x_2) = c$ (straight lines) superimposed on the quadrilateral region implied by the constraints. (b) The graph of $x_3 = f(x_1, x_2)$ (a plane) over the quadrilateral region. The x_3 values at four points on the plane are shown.

The second important aspect is locating the maximum of the linear function when restricted to the convex domain. Figure 14.1 suggests that the maximum of $f(\mathbf{x})$ occurs at a vertex \mathbf{x} on the convex polygon boundary. This is a correct observation. If f happened to be constant, the maximum is that constant and occurs at every point in the domain, and so at a vertex. If f is not identically a constant, at a point \mathbf{y} in the

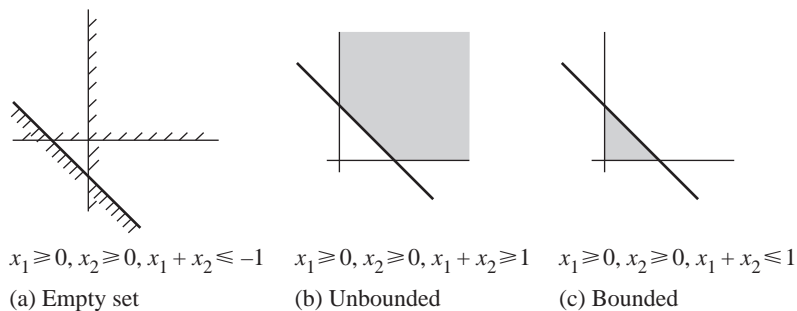


Figure 14.2 (a) Constraints with no solution. The hash marks indicate on which side of the lines the half planes occur. (b) Constraints defining an unbounded convex set. (c) Constraints defining a bounded convex set.

interior of the polygon the gradient $\mathbf{d} = \nabla f(\mathbf{y})$ is in the direction of largest increase of f . The function $g(t) = f(\mathbf{y} + t\mathbf{d})$ is strictly increasing in t , so the function value at \mathbf{y} is smaller than function values at points nearby on the ray $\mathbf{y} + \varepsilon\mathbf{d}$. This means $f(\mathbf{y})$ cannot be a maximum for f . The same argument applies on the convex polygon itself to show that the maximum must occur at a vertex. If f is identically a constant on an edge, the maximum along the edge is that constant and occurs at every point of the edge, and so at a vertex. If the function values along an edge are strictly monotone, the maximum must occur at one of the edge endpoints.

In order to simplify our discussions from here on, let us assume that the constraints force generates a nonempty bounded convex set. For most physics applications this is a reasonable assumption to make since the constraints are naturally formed based on physical information that indicates a solution is to be expected.

14.1.2 SOLUTION BY PAIRWISE INTERSECTIONS

We have already argued that $f(x_1, x_2)$ must attain its maximum at a vertex of the bounded convex polygonal domain. A natural approach to finding the maximum is to construct all the vertices, evaluate f at each, then select the maximum of these values. Each vertex occurs as the intersection of two lines determined by inequality constraints, so we proceed by solving all possible systems of two equations in two unknowns. In our ongoing example, we have four inequality constraints. If we choose two at a time, the total number of systems is six. The systems and solutions are listed in [Table 14.1](#).

You probably already noticed that the systems produce six points, yet the convex domain shown in [Figure 14.1](#) has only four vertices. Two of the points produced by the system are not in the convex domain. We need to eliminate those points by testing all inequality constraints. Any point not satisfying one of the constraints is discarded. In the presence of a floating point number system, you need to be careful about this step, perhaps by introducing an error tolerance when making the comparison of the constraint. In the example, the point $(0, 2)$ is discarded because it fails to satisfy $x_1 + 2x_2 \leq 3$. The point $(3, 0)$ is discarded because it fails to satisfy $2x_1 + x_2 \leq 2$.

Table 14.1 Solving All Possible Systems of Two Equations in Two Unknowns

System	Solution
$x_1 = 0, x_1 = 0$	$(0, 0)$
$x_1 = 0, 2x_1 + x_2 = 2$	$(0, 2)$
$x_1 = 0, x_1 + 2x_2 = 3$	$(0, 3/2)$
$x_2 = 0, 2x_1 + x_2 = 2$	$(1, 0)$
$x_2 = 0, x_1 + 2x_2 = 3$	$(3, 0)$
$2x_1 + x_2 = 2, x_1 + 2x_2 = 3$	$(1/3, 4/3)$

The function is evaluated at the remaining 4 points: $f(0,0) = 0$, $f(0,3/2) = 3/2$, $f(1,0) = 1$, and $f(1/3,4/3) = 5/3$. The maximum is $5/3$ and occurs at the vertex $(1/3,4/3)$.

If m constraints are specified, $(a_i, b_i) \cdot (x_1, x_2) \leq c_i$ for $1 \leq i \leq m$, the number of linear systems to solve is the number of ways of choosing two items from a set of m , namely $m! / (2!(m-2)!) = m(m-1)/2$. For a large number of constraints, the computational effort will be quite large. Each point (x_1, x_2) obtained as the solution of a system of equations is tested by $(a_i, b_i) \cdot (x_1, x_2) \leq c_i$. If this inequality is false, the point is discarded. The function $f(x_1, x_2)$ is evaluated at the remaining points and the maximum is selected. Figure 14.3 shows two possible scenarios for constraints.

Figure 14.3(a) has five inequality constraints. The line of each constraint is drawn and the light gray segment is attached to each point to the side corresponding to the half plane represented by the constraint. All 10 intersections of pairs of lines are shown as black dots of which five are vertices of the convex domain. Each constraint contributes an edge to the domain. The right of the figure has six inequality constraints. The 15 intersections of pairs of lines are shown as black dots of which only four are vertices of the convex domain. Only four constraints contribute to edges of the domain. The other two are *redundant constraints* in the sense that if you were to ignore those constraints, the convex domain is unaffected and the optimization of the objective function produces the same result. Notice that redundant constraints jointly generate nine of the 30 pairwise intersections. Had these constraints not occurred, we would have to solve only six linear systems.

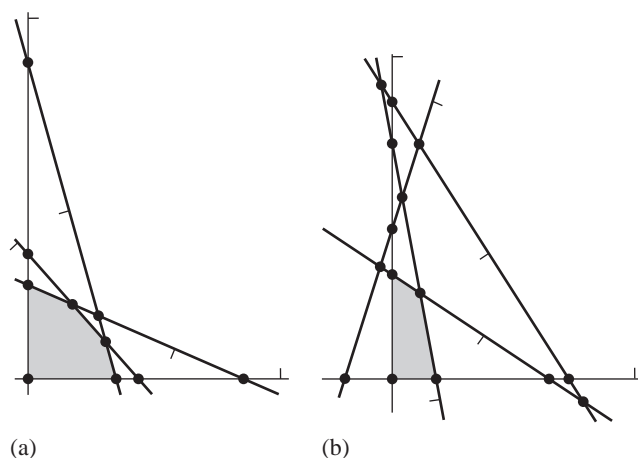


Figure 14.3 (a) All five constraints are relevant to forming the convex domain. (b) Two of the six constraints are redundant, because only four of the constraints form the convex domain.

Given m constraints, the pairwise intersection method of the last section requires solving on the order of m^2 linear systems. Effectively this is an exhaustive search for a vertex of the convex domain that produces the maximum function value. In the general dimensional case when you have n independent variables x_1 through x_n and $m > n$ constraints, the exhaustive search for a vertex of the convex domain requires solving all possible combinations of m equations choosing n at a time for a total of $m!/(n!(m-2)!)$. This can be quite an expensive endeavor. The exhaustive search turns out to be suboptimal. A better method that uses a smart search is the *simplex method* invented by Dantzig [Dan63]. We will take a look at this for the general dimensional case.

14.1.3 STATEMENT OF THE GENERAL PROBLEM

Stated in its most general terms for $\mathbf{x} \in \mathbb{R}^n$, the *linear programming* problem is about maximizing the linear function $f(\mathbf{x}) = \mathbf{c}^T \mathbf{x}$ subject to the n nonnegativity constraints $\mathbf{x} \geq \mathbf{0}$ and the m linear inequality constraints $A\mathbf{x} \leq \mathbf{b}$. The $m \times n$ matrix A , the $n \times 1$ column vector \mathbf{c} , and the $m \times 1$ column matrix \mathbf{b} are all application-specified values. The inequality notation for vectors is shorthand to denote that the inequality holds for each pair of components, that is, $(u_1, \dots, u_k) \geq (v_1, \dots, v_k)$ if and only if $u_i \geq v_i$ for $1 \leq i \leq k$. The function f is called the *objective function*. Any vector that satisfies the inequality constraints is called a *feasible vector*. A feasible vector that maximizes the objective function is called an *optimal feasible vector*; there may be more than one such vector. The constraints trim \mathbb{R}^n to a convex domain (possibly empty or nonempty and possibly unbounded). Each vertex of the domain is a solution to exactly n of the $n+m$ constraints and is called a *feasible basis vector*. Using our motivation in two dimensions, the feasible basis vectors are the only feasible vectors that need to be searched for optimality.

The method of solution requires two changes to the constraints $A\mathbf{x} \leq \mathbf{b}$. We are interested in constructing feasible basis vectors which, by definition, are the vertices of the convex domain. These vectors occur as solutions to constraints where the inequality has been replaced by equality. This suggests that we eliminate inequalities in the first place. The first change is therefore to introduce new nonnegative variables called *slack variables*; these take up the slack, so to speak, between the two sides of the inequalities. For a constraint $a_1x_1 + \dots + a_nx_n \leq b$, the slack is $s = b - a_1x_1 - \dots - a_nx_n \geq 0$. The single inequality constraint is replaced by a new equality constraint $a_1x_1 + \dots + a_nx_n + s = b$ and a new nonnegativity constraint $s \geq 0$. In total m slack variables are introduced, s_i for $1 \leq i \leq m$, and stored in the $m \times 1$ column vector \mathbf{s} . In matrix notation, the constraints $A\mathbf{x} \leq \mathbf{b}$ and $\mathbf{x} \geq \mathbf{0}$ are transformed to

$$A\mathbf{x} + \mathbf{s} = \mathbf{b}, \quad \mathbf{x} \geq \mathbf{0}, \quad \mathbf{s} \geq \mathbf{0} \tag{14.1}$$

where the zero vectors are of the appropriate size in their respective contexts. This form of the linear programming problem is called the *normal form*. The pair (\mathbf{x}, \mathbf{s}) has $n + m$ components, so is a vector in \mathbb{R}^{n+m} . Each equation in $A\mathbf{x} + \mathbf{s} = \mathbf{b}$ represents a hyperplane in \mathbb{R}^{n+m} . These bound a convex domain in \mathbb{R}^{n+m} whose vertices we must search. A vertex (\mathbf{x}, \mathbf{s}) of interest is one for which \mathbf{x} maximizes the objective function. The \mathbf{s} component of that solution is simply discarded.

A search of the vertices implied by the normal-form constraints, [equation \(14.1\)](#), will involve starting at one vertex, then visiting another vertex whose objective function value is larger than that of the current vertex. This requires finding an initial vertex to start the search. To support this, the second change is to introduce more new nonnegative variables called *artificial variables*. For an equality constraint $a_1x_1 + \cdots + a_nx_n + s = b$ where s is the appropriate slack variable, an artificial variable will be set to the difference of the two sides of the equation. We require that the right-hand side be nonnegative. If $b \geq 0$, the new variable w is set to $w = b - a_1x_1 - \cdots - a_nx_n - s \geq 0$. If $b < 0$, a multiplication by -1 must occur first, $w = -b + a_1x_1 + \cdots + a_nx_n + s \geq 0$. In total, m artificial variables are introduced, w_i for $1 \leq i \leq m$, and stored in the $m \times 1$ column vector \mathbf{w} . In matrix notation,

$$\mathbf{w} = D(\mathbf{b} - A\mathbf{x} - \mathbf{s}), \quad \mathbf{x} \geq \mathbf{0}, \quad \mathbf{s} \geq \mathbf{0}, \quad \mathbf{w} \geq \mathbf{0} \quad (14.2)$$

where $D = \text{Diag}(d_1, \dots, d_m)$ with $d_i = 1$ if $b_i \geq 0$ or $d_i = -1$ if $b_i < 0$. The linear programming problem in this form is called the *restricted normal form*. We associate an *auxiliary objective function* with the constraints of [equation \(14.2\)](#),

$$g(\mathbf{w}) = - \sum_{i=1}^m w_i = \sum_{i=1}^m d_i \left(\sum_{j=1}^n a_{ji}x_j - b_i + s_i \right)$$

Since $w_i \geq 0$ for all i , $g(\mathbf{w}) \leq 0$. The goal is to maximize $g(\mathbf{w})$. If the maximum occurs at $\mathbf{w} \neq \mathbf{0}$, then it is not possible to construct a pair (\mathbf{x}, \mathbf{s}) that solves the linear system in the constraints [\(14.1\)](#). In this case, the original linear programming problem has no solution because the inequality constraints are inconsistent. However, if the maximum does occur at $\mathbf{w} = \mathbf{0}$, we will have found a pair (\mathbf{x}, \mathbf{s}) that is the initial vertex to start a search in the normal-form problem to maximize the original objective function. The search for a maximum of g will always start with $\mathbf{x} = \mathbf{0}$ and $\mathbf{s} = \mathbf{0}$. In this case the initial artificial variables are $\mathbf{w} = D\mathbf{b} \geq \mathbf{0}$.

The normal form and restricted normal form can be solved with the same methods. The simplex method refers to the two-phase process of solving the restricted normal form in optimizing the auxiliary objective function to find an initial feasible basis vector, then solving the normal form in optimizing the objective function, the search starting at the feasible vector found in the first phase. The method is illustrated in [Example 14.1](#).

EXAMPLE
14.1

The objective function is $f(x_1, x_2) = x_1 + x_2$ and is to be maximized with respect to the constraints $x_1 \geq 0$, $x_2 \geq 0$, $-x_1 + x_2 \leq 2$, $2x_1 - x_2 \leq -1$, and $3x_1 + x_2 \leq 3$. Figure 14.4 shows the convex domain implied by the constraints.

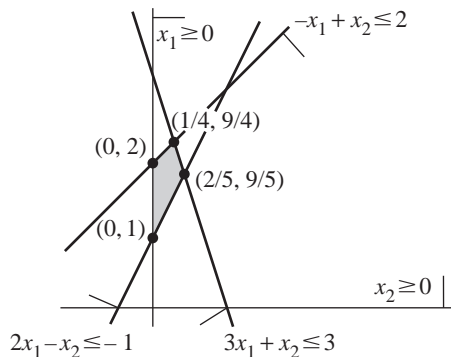


Figure 14.4

The convex domain implied by the two nonnegativity constraints and three linear inequality constraints of the example.

To convert to normal form requires three slack variables, s_1 , s_2 , and s_3 :

$$\begin{aligned} -x_1 + x_2 + s_1 &= 2 \\ 2x_1 - x_2 + s_2 &= -1 \\ 3x_1 + x_2 + s_3 &= 3 \end{aligned}$$

To convert to restricted normal form requires three artificial variables, w_1 , w_2 , and w_3 :

$$\begin{aligned} w_1 &= 2 + x_1 - x_2 - s_1 \\ w_2 &= 1 + 2x_1 - x_2 + s_2 \\ w_3 &= 3 - 3x_1 - x_2 - s_3 \end{aligned}$$

The auxiliary objective function is $g = -(w_1 + w_2 + w_3) = -6 + 3x_2 + s_1 - s_2 + s_3$. As mentioned earlier, the search for a maximum of g always starts with $(x_1, x_2) = (0, 0)$ and $(s_1, s_2, s_3) = (0, 0, 0)$, in which case $(w_1, w_2, w_3) = (2, 1, 3)$ are the initial artificial variables and $g = -6$. The goal is to modify the variables to increase g to zero.

The classic method of setup involves storing the various coefficients and constants in a *tableau*. Table 14.2 shows the tableau for this example.

Table 14.2

Tableau of Coefficients and Constants (Example 14.1)

	<i>Value</i>	x_1	x_2	s_1	s_2	s_3
g	-6	0	3	1	-1	1
w_1	2		1	-1	-1	0
w_2	1		2	-1	0	1
w_3	3		-3	-1	0	0

The value column initially contains the constant terms in the equations for g , w_1 , w_2 , and w_3 and represents the fact that we will always be thinking of the variables in the other columns as being zero. The entries in the other column are the coefficients of those variables in the auxiliary objective function g and in the equality constraints.

Let us analyze the coefficients in the g -row after the value column. The x_1 coefficient is zero since x_1 does not occur in that function. No matter how you modify x_1 , g will not change, so we may ignore x_1 at this step of the process. The x_2 coefficient is 3, a positive number. If we increase the value of x_2 from its current value of zero, g will also increase, thereby giving us a chance to force it to become zero. The column entry for x_2 in the w_1 -row tells us how w_1 depends on x_2 . The coefficient is -1, a negative number, so any increase in x_2 will result in a decrease in w_1 . Since we require $w_1 \geq 0$, we cannot increase x_2 by an arbitrary amount. In fact, the most we can increase is to $x_2 = 2$, in which case $w_1 = 0$.

Similarly in the w_2 -row and w_3 -row, the coefficients are negative, which means that an increase in x_2 will result in decreases in w_2 and w_3 . As we increase x_2 , all the w_i will decrease simultaneously. When the first w_i value reaches zero, we can no longer increase x_2 . Of course, if the coefficient of x_2 in a z -equation is positive, there is no limit on increasing x_2 , so we need consider only z -equations for which the x_2 coefficient is negative. The maximum value to which we can increase x_2 is the minimum of the negatives of the ratios of the constant terms and the coefficients. In our current case the ratios for the w_1 -row, w_2 -row, and w_3 -row are $2 = -(2/(-1))$, $1 = -(1/(-1))$, and $1 = -(3/(-3))$, respectively. The w_2 -row limits the increase of x_2 to 1.

Once the row corresponding to the limiting increase is identified, the next step is to make the row variable (basic variable) a column variable (nonbasic variable) and vice versa. In our example we solve for x_2 in the w_2 equation to obtain

$$x_2 = 1 - w_2 + 2x_1 + s_2$$

This equation is substituted into the x_2 terms in the g equation and the other equality constraints:

$$\begin{aligned} g &= -6 + 3x_2 + s_1 - s_2 + s_3 = -3 - 3w_2 + 6x_1 + s_1 + 2s_2 + s_3 \\ w_1 &= 2 + x_1 - x_2 - s_1 = 1 - x_1 + w_2 - s_1 - s_2 \\ w_3 &= 2 - 5x_1 + w_2 - s_2 - s_3 \end{aligned}$$

(Example 14.1
continued)

Table 14.3

The tableau is updated in Table 14.3 by swapping the row variable w_2 with the column variable x_2 ,

Updated Tableau: Exchanging w_2 with x_2

	Value	x_1	w_2	s_1	s_2	s_3
g	-3	6	-3	1	2	1
w_1	1	-1	1	-1	-1	0
x_2	1	2	-1	0	1	0
w_3	2	-5	1	0	-1	-1

The invariant in this process is that the resulting tableau represent a linear programming problem in restricted normal form.

We repeat the process. The column variables are thought of as having value zero. The x_1 coefficient in the g -row is positive, so an increase in x_1 results in an increase in g . The x_1 coefficients in the w_1 -row and w_3 -row are negative, so w_1 and w_3 will decrease when x_1 is increased. The limiting factor is the minimum of the ratios $1 = -(1/(-1))$ and $2/5 - (2/(-5))$; that is, w_3 will reach zero before w_1 does. We now need to exchange x_1 and w_3 by solving for

$$x_1 = \frac{1}{5}(2 + w_2 - w_3 - s_2 - s_3)$$

and substituting in the g equation and the other constraints:

$$\begin{aligned} g &= -3 + 6x_1 - 3w_2 + s_2 + s_3 = -\frac{3}{5} - \frac{6}{5}w_3 - \frac{9}{5}w_2 + s_1 + \frac{4}{5}s_2 - \frac{1}{5}s_3 \\ w_1 &= 1 - x_1 + w_2 - s_1 - s_2 = \frac{3}{5} + \frac{1}{5}w_3 + \frac{4}{5}w_2 - s_1 - \frac{4}{5}s_2 + \frac{1}{5}s_3 \\ x_2 &= 1 + 2x_1 - w_2 + s_2 = \frac{9}{5} - \frac{2}{5}w_3 - \frac{3}{5}w_2 + \frac{3}{5}s_2 - \frac{2}{5}s_3 \end{aligned}$$

Table 14.4 shows the updated tableau.

Table 14.4

Updated Tableau: Exchanging x_1 with w_3

	Value	w_3	w_2	s_1	s_2	s_3
g	$-\frac{3}{5}$	$-\frac{6}{5}$	$-\frac{9}{5}$	1	$\frac{4}{5}$	$-\frac{1}{5}$
w_1	$\frac{3}{5}$	$\frac{1}{5}$	$\frac{4}{5}$	-1	$-\frac{4}{5}$	$\frac{1}{5}$
x_2	$\frac{9}{5}$	$-\frac{2}{5}$	$-\frac{3}{5}$	0	$\frac{3}{5}$	$-\frac{2}{5}$
x_1	$\frac{2}{5}$	$-\frac{1}{5}$	$\frac{1}{5}$	0	$-\frac{1}{5}$	$-\frac{1}{5}$

And yet one more repetition of the process. The coefficient of s_1 in the g -row is positive, so an increase in s_1 results in an increase in g . Note that in this step we are increasing a slack variable, not one of the original variables, to increase the auxiliary objective function. The only negative coefficient in the s_1 column is in the w_1 row, so we may increase s_1 until w_1 is zero. We exchange w_1 and s_1 by solving for

$$s_1 = \frac{3}{5} + \frac{1}{5}w_3 + \frac{4}{5}w_2 - w_1 - \frac{4}{5}s_2 + \frac{1}{5}s_3$$

and substituting in the g equation and the other constraints:

$$\begin{aligned} g &= -\frac{3}{5} - \frac{6}{5}w_3 - \frac{9}{5}w_2 + s_1 + \frac{4}{5}s_2 - \frac{1}{5}s_3 = 0 - w_1 - w_2 - w_3 \\ x_2 &= \frac{9}{5} - \frac{2}{5}w_3 - \frac{3}{5}w_2 + \frac{3}{5}s_2 - \frac{2}{5}s_3 \\ x_1 &= \frac{2}{5} - \frac{1}{5}w_3 + \frac{1}{5}w_2 - \frac{1}{5}s_2 - \frac{1}{5}s_3 \end{aligned}$$

Table 14.5 shows the updated tableau.

Table 14.5

Updated Tableau: Exchanging w_1 with s_1

	<i>Value</i>	w_3	w_2	w_1	s_2	s_3
g	0	-1	-1	-1	0	0
s_1	$\frac{3}{5}$	$\frac{1}{5}$	$\frac{4}{5}$	-1	$-\frac{4}{5}$	$\frac{1}{5}$
x_2	$\frac{9}{5}$	$-\frac{2}{5}$	$-\frac{3}{5}$	0	$\frac{3}{5}$	$-\frac{2}{5}$
x_1	$\frac{2}{5}$	$-\frac{1}{5}$	$\frac{1}{5}$	0	$-\frac{1}{5}$	$-\frac{1}{5}$

The current value of g is zero and none of the coefficients in the g row is positive, so it is no longer possible to increase any of the nonbasic variables s_2 , s_3 , w_1 , w_2 , or w_3 and obtain an increase in g . That is, g does have a maximum of zero and is obtained when $s_2 = s_3 = w_1 = w_2 = w_3 = 0$. The basic variables are x_1 , x_2 , and s_1 and have values $x_1 = 2/5$, $x_2 = 9/5$, and $s_1 = 3/5$. The vector $(x_1, x_2, s_1, s_2, s_3) = (2/5, 9/5, 3/5, 0, 0)$ is a feasible basis vector for the normal form, [equation \(14.1\)](#), and is the starting point for the search to maximize $f(x_1, x_2) = x_1 + x_2$. Just to verify, replace the feasible vector in the constraints as in [equation \(14.2\)](#), written as $Ax + s - b$:

$$-x_1 + x_2 + s_1 - 2 = -2/5 + 9/5 + 3/5 - 2 = 0$$

$$2x_1 - x_2 + s_2 + 1 = 4/5 - 9/5 + 1 = 0$$

$$3x_1 + x_2 + s_3 - 3 = 6/5 + 9/5 - 3 = 0$$

(Example 14.1
continued)

The slack variable s_1 is positive, but the other two are zero. In terms of what is shown in [Figure 14.4](#), $(x_1, x_2) = (2/5, 9/5)$ is a vertex of the convex domain and is the intersection of $2x_1 - x_2 = -1$ and $3x_1 + x_2 = 3$ (slack variables $s_2 = s_3 = 0$). That vertex is not on the other line, but $-x_1 + x_2 < 2$ (slack variable $s_1 > 0$).

Now we are ready to maximize f . The artificial variables w_i are no longer needed, so the tableau no longer contains them. The tableau also contains a row representing f since the auxiliary function g is no longer needed. In terms of the nonbasic variables,

$$f = x_1 + x_2 = \left(\frac{2}{5} - \frac{1}{5}s_2 - \frac{1}{5}s_3 \right) + \left(\frac{9}{5} + \frac{3}{5}s_2 - \frac{2}{5}s_3 \right) = \frac{11}{5} + \frac{2}{5}s_2 - \frac{3}{5}s_3$$

and the initial tableau is shown in [Table 14.6](#).

Table 14.6

Maximizing f

	Value	s_2	s_3
f	$\frac{11}{5}$	$\frac{2}{5}$	$-\frac{3}{5}$
x_1	$\frac{2}{5}$	$-\frac{1}{5}$	$-\frac{1}{5}$
x_2	$\frac{9}{5}$	$\frac{3}{5}$	$\frac{2}{5}$
s_1	$\frac{3}{5}$	$\frac{4}{5}$	$\frac{1}{5}$

and s_2 and s_3 are nonbasic variables whose initial values are zero. The coefficient of s_2 in the f -row is positive, so an increase in s_2 leads to an increase in f . The negative coefficients in the s_2 column are in the x_1 -row and s_1 -row. The limiting increase is the minimum of $2 = -((2/5)/(-1/5))$ and $3/4 = -((3/5)/(-4/5))$, so the s_1 variable decreases to zero before x_1 does. Exchange s_1 and s_2 by solving for

$$s_2 = \frac{1}{4}(3 - 5s_1 + s_3)$$

and substituting in the f equation and the other constraints:

$$\begin{aligned} f &= \frac{11}{5} + \frac{2}{5}s_2 - \frac{3}{5} = \frac{5}{2} - \frac{1}{2}s_1 - \frac{1}{2}s_3 \\ x_1 &= \frac{2}{5} - \frac{1}{5}s_2 - \frac{1}{5}s_3 = \frac{1}{4} + \frac{1}{4}s_1 - \frac{1}{4}s_3 \\ x_2 &= \frac{9}{5} + \frac{3}{5}s_2 - \frac{2}{5}s_3 = \frac{9}{4} - \frac{3}{4}s_1 - \frac{1}{4}s_3 \end{aligned}$$

[Table 14.7](#) shows the updated tableau.

Table 14.7

Maximizing f : Exchanging s_1 with s_2

	Value	s_1	s_3
f	5 2	-1 2	-1 2
x_1	1 4	1 4	-1 4
x_2	9 4	3 4	-1 4
s_2	3 4	5 4	1 4

The coefficients of the nonbasic variables in the f -row are all negative, so no amount of increasing those variables will increase f . Thus, f has a maximum of $5/2$ and it occurs when $s_1 = s_3 = 0$. Consequently, the basic variables are $x_1 = 1/4$, $x_2 = 9/4$, and $s_2 = 3/4$. The pair $(x_1, x_2) = (1/4, 9/4)$ is another vertex of the convex domain shown in Figure 14.4. The slack variables s_1 and s_3 are both zero, therefore that vertex is generated as the intersection of the lines corresponding to $-x_1 + x_2 = 2$ and $3x_1 + x_2 = 3$. The slack variable $s_2 > 0$, so the vertex is not on the line of the other constraint; that is, $2x_1 - x_2 < -1$. ■

As is true in most algorithms, you have to deal with degenerate cases. The constant terms in the value column are constrained to be nonnegative, but in the previous example were always positive. If a zero constant term is encountered, the corresponding basic variable is zero whenever all the nonbasic variables are zero. The vector of basic and nonbasic variables in this case is referred to as a *degenerate feasible vector*. As suggested in [PFTV88], the zero constant term must be handled by exchanging the basic variable in that row with a nonbasic variable in a column, sometimes having to make several such exchanges. In fact, the description in [PFTV88] is incomplete because there are three types of degeneracies that can occur. We will discuss these in Section 14.2 showing that the linear programming problem is a special case of the linear complementarity problem (LCP). The method of solution of an LCP is well suited for dealing with the degeneracies.

14.1.4 THE DUAL PROBLEM

The linear programming problem has an associated problem called the *dual problem*. In this context the original problem is referred to as the *primal problem*. The motivation for the dual problem is provided by Example 14.1. We wanted to maximize $f(x_1, x_2) = x_1 + x_2$ subject to the nonnegativity constraints $x_1 \geq 0$ and $x_2 \geq 0$ and the linear inequality constraints $-x_1 + x_2 \leq 2$, $2x_1 - x_2 \leq -1$ and $3x_1 + x_2 \leq 3$. The simplex method was used to show that the maximum of f is $5/2$ and occurs at

$(x_1, x_2) = (1/4, 9/4)$. Before proceeding with the simplex method, we can in fact use the linear inequality constraints to obtain upper bounds on the maximum of f . For example,

$$f = x_1 + x_2 \leq 3x_1 + x_2 \leq 3$$

This guarantees that $\max(f) \leq 3$. We can also use combinations of constraints to obtain upper bounds:

$$f = x_1 + x_2 = 3(-x_1 + x_2) + 2(2x_1 - x_2) \leq 3(2) + 2(-1) = 4$$

This bound leads to $\max(f) \leq 4$, not as good a bound as the previous case but still a bound. Another possibility is

$$\begin{aligned} f &= x_1 + x_2 \leq 4x_1 + x_2 = 1(-x_1 + x_2) + 1(2x_1 - x_2) + 1(3x_1 + x_2) \\ &\leq 1(2) + 1(-1) + 1(3) = 4 \end{aligned}$$

again concluding that $\max(f) \leq 4$. Yet one more possibility is

$$f = x_1 + x_2 = \frac{1}{2}(-x_1 + x_2) + \frac{1}{2}(3x_1 + x_2) \leq \frac{1}{2}(2) + \frac{1}{2}(3) = \frac{5}{2}$$

We conclude that $\max(f) \leq 5/2$ but in fact got lucky in that the upper bound really happens to be the maximum value of f .

Perhaps we can choose just the right multipliers for the linear inequality constraints so that we will indeed obtain the maximum value for f . In the example let $y_1 \geq 0$, $y_2 \geq 0$, and $y_3 \geq 0$ be the multipliers for the constraints; that is,

$$y_1(-x_1 + x_2) \leq 2y_1, \quad y_2(2x_1 - x_2) \leq -y_2, \quad y_3(3x_1 + x_2) \leq 3y_3$$

The constraints are combined to form the following.

$$\begin{aligned} 2y_1 - y_2 + 3y_3 &\geq y_1(-x_1 + x_2) + y_2(2x_1 - x_2) + y_3(3x_1 + x_2) \\ &= (-y_1 + 2y_2 + 3y_3)x_1 + (y_1 - y_2 + y_3)x_2 \\ &\geq x_1 + x_2 = f \end{aligned}$$

The last inequality is what we want to be true, so we have to choose $y_1 \geq 0$, $y_2 \geq 0$, and $y_3 \geq 0$ to make that happen. Specifically, choose $-y_1 + 2y_2 + 3y_3 \geq 1$ and $y_1 - y_2 + y_3 \geq 1$. Our goal is to make the quantity $2y_1 - y_2 + 3y_3$ as small as possible. That is, we want to minimize $g(y_1, y_2, y_3) = 2y_1 - y_2 + 3y_3$ subject to the nonnegativity constraints $y_1 \geq 0$, $y_2 \geq 0$, and $y_3 \geq 0$ and the linear inequality constraints $-y_1 + 2y_2 + 3y_3 \geq 1$ and $y_1 - y_2 + y_3 \geq 1$. You will notice that this is nearly identical in structure to the original problem with the exceptions that we are now minimizing a function and have instead greater-or-equal constraints. This problem is referred to as the *dual problem* for the original problem.

In general, and using vector notation, the primal problem is

$$\text{Maximize } f(\mathbf{x}) = \mathbf{c}^T \mathbf{x} \text{ subject to } \mathbf{x} \geq \mathbf{0} \text{ and } \mathbf{Ax} \leq \mathbf{b} \quad (14.3)$$

The dual problem is

$$\text{Minimize } g(\mathbf{y}) = \mathbf{b}^T \mathbf{y} \text{ subject to } \mathbf{y} \geq \mathbf{0} \text{ and } A^T \mathbf{y} \geq \mathbf{c} \quad (14.4)$$

You should convince yourself from the previous example of why A^T , \mathbf{b} , and \mathbf{c} show up as they do in the general definition for the dual problem. The dual problem may be solved with the simplex method by introducing slack and artificial variables. Of course the process requires you to decrease the objective function values rather than increase as the primal problem requires.

A few relationships hold between the primal and dual problems. These are referred to as *weak duality*, *unboundedness property*, and *strong duality*.

Weak Duality Principle

If \mathbf{x} is a feasible vector for the primal problem and if \mathbf{y} is a feasible vector for the dual problem, then $f(\mathbf{x}) \leq g(\mathbf{y})$.

The proof is simple. Since \mathbf{x} is a feasible vector for the primal problem, we know that it satisfies the constraints $A\mathbf{x} \leq \mathbf{b}$. The components of the vectors $A\mathbf{x}$ and \mathbf{b} must be ordered by the inequality, so the transposition of the vectors satisfies the same ordering:

$$\mathbf{x}^T A^T = (A\mathbf{x})^T \leq \mathbf{b}^T$$

The \mathbf{y} components are nonnegative, so multiplying the previous equation by \mathbf{y} does not change the direction of inequality,

$$\mathbf{x}^T A^T \mathbf{y} \leq \mathbf{b}^T \mathbf{y}$$

Also, \mathbf{y} is a feasible vector for the dual problem so we know that it satisfies the constraints $\mathbf{c} \leq A^T \mathbf{y}$. Since \mathbf{x} has nonnegative components, multiplying by \mathbf{x} does not change the direction of the inequality,

$$\mathbf{x}^T \mathbf{c} \leq \mathbf{x}^T A^T \mathbf{y}$$

Combining this with the previous displayed equation yields

$$f(\mathbf{x}) = \mathbf{c}^T \mathbf{x} = \mathbf{x}^T \mathbf{c} \leq \mathbf{x}^T A^T \mathbf{y} \leq \mathbf{b}^T \mathbf{y} = g(\mathbf{y})$$

and the proof is complete.

Unboundedness Property

A linear programming problem is said to have an *unbounded solution* if you can make the objective function arbitrarily large. Figure 14.2(b) shows a domain for which the

objective function $f(\mathbf{x})$ can be made as large as you like by choosing values of \mathbf{x} far away from the origin. The unboundedness property is stated in three ways:

1. If the primal problem has an unbounded solution, then the dual problem has no solution and is said to be *infeasible*.
2. If the dual problem has an unbounded solution, then the primal problem is infeasible.
3. The primal problem has a finite optimal solution if and only if the dual problem has a finite optimal solution.

These results are direct consequences of the weak duality principle. For example, if the primal problem has an unbounded solution, then you can force $f(\mathbf{x})$ to be arbitrarily large by choosing appropriate feasible vectors. You can visualize this in 2D by sketching a convex domain for f . One of the boundary components will be a ray. Choose \mathbf{x} along that ray with increasing length to force the corresponding f values to become large. Given that you can do this, and given $f(\mathbf{x}) \leq g(\mathbf{y})$ for a feasible solution \mathbf{y} , you would also force g to become arbitrarily large. This cannot happen, so there is no such feasible vector \mathbf{y} and the dual problem cannot be solved.

Strong Duality Principle

If \mathbf{x} is a feasible vector for the primal problem and \mathbf{y} is a feasible vector for the dual problem, then these vectors optimize f and g if and only if $f(\mathbf{x}) = g(\mathbf{y})$.

Let us assume that \mathbf{x} is a feasible vector for the primal problem, \mathbf{y} is a feasible vector for the dual problem, and $f(\mathbf{x}) = g(\mathbf{y})$. From the weak duality principle we know that $f(\mathbf{u}) \leq g(\mathbf{v})$ for any feasible vectors \mathbf{u} and \mathbf{v} . Thus, $\max(f) \leq \min(g)$. The fact that equality occurs in $f(\mathbf{x}) = g(\mathbf{y})$ guarantees that $\max(f) = f(\mathbf{x})$ and $\min(g) = g(\mathbf{y})$.

The proof in the other direction is more complicated and is not proved here. The essence is that in constructing the optimal solution for the primal problem using the simplex method, the details of the construction also allow you to construct the optimal solution for the dual problem with the same function value as that of the primal solution.

14.2 THE LINEAR COMPLEMENTARITY PROBLEM

In the last section we saw a brief overview of the linear programming problem and introduced the concepts of primal problem and dual problem. The strong duality principle states that you can optimize the primal problem or optimize the dual problem to arrive at the same optimum value. An important consequence of this principle is called *complementary slackness*. The vector of slack variables for the primal problem is $\mathbf{s} = \mathbf{b} - A\mathbf{x} \geq 0$. The vector of slack variables for the dual problem is $\mathbf{u} = A^T\mathbf{y} - \mathbf{c}$. Complementary slackness presents the following challenge. If $\mathbf{x} = (x_1, \dots, x_n)$ is a

feasible vector for the primal problem and $\mathbf{y} = (y_1, \dots, y_m)$ is a feasible vector for the dual problem, then these vectors optimize f and g if and only if both of the following apply:

1. Either $x_j = 0$ or $u_j = 0$.
2. Either $y_i = 0$ or $s_i = 0$.

In vector notation we write these conditions as $\mathbf{x} \circ \mathbf{u} = \mathbf{0}$ and $\mathbf{y} \circ \mathbf{s} = \mathbf{0}$, where the circle operator defines a new vector whose components are the products of the components from the input vectors, $\mathbf{u} \circ \mathbf{v} = (u_1, \dots, u_k) \circ (v_1, \dots, v_k) = (u_1 v_1, \dots, u_k v_k)$.

The primal and dual problems combined fit the format for a more general problem (which we discussed briefly in [Chapter 6](#)) called the *linear complementarity problem* (LCP): Given a $k \times 1$ vector \mathbf{q} and a $k \times k$ matrix M , construct $k \times 1$ vectors \mathbf{w} and \mathbf{z} such that

$$\mathbf{w} = \mathbf{q} + M\mathbf{z}, \quad \mathbf{w} \circ \mathbf{z} = \mathbf{0}, \quad \mathbf{w} \geq \mathbf{0}, \quad \text{and} \quad \mathbf{z} \geq \mathbf{0} \quad (14.5)$$

The variables w_i and z_i are said to be *complementary*. The reduction of the primal and dual problems to this form is straightforward. The various quantities in the LCP are written in block matrix form as

$$\mathbf{q} = \begin{bmatrix} -\mathbf{c} \\ \mathbf{b} \end{bmatrix}, \quad M = \left[\begin{array}{c|c} 0 & A^T \\ -A & 0 \end{array} \right], \quad \mathbf{w} = \begin{bmatrix} \mathbf{u} \\ \mathbf{s} \end{bmatrix}, \quad \text{and} \quad \mathbf{z} = \begin{bmatrix} \mathbf{x} \\ \mathbf{y} \end{bmatrix} \quad (14.6)$$

Make sure you understand the difference in formulations for the linear programming problem and the linear complementarity problem. In the former problem your goal is to optimize a function based on various constraints. In the latter your goal is to satisfy the complementarity condition $\mathbf{w} \circ \mathbf{z} = \mathbf{0}$.

14.2.1 THE LEMKE ALGORITHM

The simplex method may be used to solve an LCP. Although the tableau method works fine, a modern approach uses slightly different terminology which we introduce here. The presentation here is based on Joel Friedman's nicely written online summary of LCP and MP [\[Fri98\]](#). The equation $\mathbf{w} = \mathbf{q} + M\mathbf{z}$ is considered to be a *dictionary* for the basic variables \mathbf{w} defined in terms of the nonbasic variables \mathbf{z} . The analogy to a dictionary makes sense since each w_i is a new "word" whose definition is provided in terms of already defined "words," z_j . If $\mathbf{q} \geq \mathbf{0}$, the dictionary is said to be *feasible*. In this case, the LCP has a trivial solution of $\mathbf{w} = \mathbf{q}$ and $\mathbf{z} = \mathbf{0}$.

If the dictionary is not feasible, then a two-phase algorithm called the *Lemke algorithm* [\[CPS92\]](#) is applied. The first phase of the algorithm adds an auxiliary variable $z_0 \geq 0$ by modifying the dictionary to

$$\mathbf{w} = \mathbf{q} + M\mathbf{z} + z_0 \mathbf{1}$$

where $\mathbf{1}$ is the appropriately sized vector whose components are all one. An exchange is made, much like that in the tableau method, between z_0 and some basic variable w_i . That is, z_0 enters the dictionary and w_i leaves the dictionary. Not just any exchange will do; we need an exchange that will make the modified dictionary feasible.

The second phase of the Lemke algorithm is designed to obtain a dictionary such that both of two conditions hold:

1. z_0 is nonbasic.
2. For each i either z_i or w_i is nonbasic.

Note that z_0 is nonbasic to start, enters the dictionary in the first phase, and eventually leaves the dictionary to once again become nonbasic. When z_0 leaves the dictionary, we know that as a nonbasic variable it is thought of as $z_0 = 0$ (just like in the tableau method) and the modified dictionary $\mathbf{w} = \mathbf{q} + M\mathbf{z} + z_0\mathbf{1}$ is restored to the original one $\mathbf{w} = \mathbf{q} + M\mathbf{z}$. The condition that z_i or w_i is nonbasic for each $i \geq 1$ means that either $z_i = 0$ or $w_i = 0$; that is, $\mathbf{w} \circ \mathbf{z} = \mathbf{0}$ and we have solved the LCP. A dictionary that satisfies conditions 1 and 2 is said to be a *terminal dictionary*. If the dictionary satisfies only condition 2, it is said to be a *balanced dictionary*. The first phase produces a balanced dictionary, but since z_0 is in the dictionary, the dictionary is nonterminal. The procedure to reach a terminal dictionary is iterative, each iteration designed so that a nonbasic variable enters the dictionary and a basic variable leaves the dictionary. The invariant of each iteration is that the dictionary remain feasible and balanced. To guarantee this happens and (hopefully) avoid returning to the same dictionary twice (a cycle so to speak), if a variable has just left the dictionary, then its complementary variable must enter the dictionary on the next iteration (a variable cannot leave on one iteration and enter on the next iteration and vice versa).

The Lemke algorithm is illustrated with a simple linear programming problem in Example 14.2.

EXAMPLE
14.2

Maximize $f(x_1, x_2) = 2x_1 + x_2$ with respect to the constraints $x_1 \geq 0$, $x_2 \geq 0$, and $x_1 + x_2 \leq 3$. The vectors and matrices implied by this are

$$A = \begin{bmatrix} 1 & 1 \end{bmatrix}, \quad \mathbf{b} = \begin{bmatrix} 3 \end{bmatrix}, \quad \text{and } \mathbf{c} = \begin{bmatrix} 2 \\ 1 \end{bmatrix}$$

Equation (14.6) makes the conversion to an LCP:

$$\mathbf{q} = \begin{bmatrix} -2 \\ -1 \\ 3 \end{bmatrix}, \quad M = \left[\begin{array}{cc|c} 0 & 0 & 1 \\ 0 & 0 & 1 \\ -1 & -1 & 0 \end{array} \right], \quad \mathbf{w} = \begin{bmatrix} u_1 \\ u_2 \\ s_1 \end{bmatrix} = \begin{bmatrix} w_1 \\ w_2 \\ w_3 \end{bmatrix} \quad \text{and}$$

$$\mathbf{z} = \begin{bmatrix} x_1 \\ x_2 \\ y_1 \end{bmatrix} = \begin{bmatrix} z_1 \\ z_2 \\ z_3 \end{bmatrix}$$

The initial dictionary with auxiliary variable z_0 is

$$\begin{aligned}w_1 &= -2 + z_0 + z_3 \\w_2 &= -1 + z_0 + z_3 \\w_3 &= 3 + z_0 - z_1 - z_2\end{aligned}$$

The first phase involves moving z_0 to the dictionary. To obtain a feasible dictionary, we need consider only solving for z_0 in an equation that has a negative constant term. Moreover, that constant term should be the largest in magnitude so that, when substituting the new z_0 equation into the other equations, all constant terms are guaranteed to be nonnegative. In this example the first equation is the one to use. We solve for z_0 (so w_1 leaves the dictionary) and substitute that expression into the other equations:

$$\begin{aligned}z_0 &= 2 + w_1 - z_3 \\w_2 &= 1 + w_1 \\w_3 &= 5 + w_1 - z_1 - z_2 - z_3\end{aligned}$$

The new constant vector is $(2, 1, 5) \geq (0, 0, 0)$, so we have a feasible dictionary. Since the z_i are nonbasic for all $i \geq 1$, we have a balanced dictionary. The dictionary is not terminal, because z_0 is still in it.

The second phase is now initiated. The variable w_1 just left the dictionary, so its complementary variable z_1 must now enter the dictionary. The only way this can happen is by solving the w_3 equation for z_1 . The other two equations have no z_1 terms in them, so no substitution by the newly formed z_1 equation is necessary:

$$\begin{aligned}z_0 &= 2 + w_1 - z_3 \\w_2 &= 1 + w_1 \\z_1 &= 5 + w_1 - w_3 - z_2 - z_3\end{aligned}$$

The variable w_3 left the dictionary, so its complementary variable z_3 must enter the dictionary. We have two equations involving z_3 . Just as in the tableau method, we should choose the one that limits an increase in z_3 so that the constant terms in the other equations remain nonnegative. The first equation is limiting since the ratio of constant term and negative z_3 coefficient is 2, whereas the ratio in the last equation is 5. Solving for z_3 and substituting in any other equations containing z_3 :

$$\begin{aligned}z_3 &= 2 + w_1 - z_0 \\w_2 &= 1 + w_1 \\z_1 &= 3 - w_3 + z_0 - z_2\end{aligned}$$

Because z_0 has left the dictionary to return as a nonbasic variable, the process is complete. The dictionary is terminal. The solution to the LCP is $z_0 = z_2 = w_1 = w_3 = 0$ (nonbasic variables are zero) and $z_3 = 2$, $w_2 = 1$, and $z_1 = 3$. In vector form $\mathbf{w} = (0, 1, 0)$ and $\mathbf{z} = (3, 0, 2)$. As required, $\mathbf{w} \circ \mathbf{z} = (0, 0, 0)$. ■

Now we look at a more complicated problem in the context of the LCP, [Example 14.1](#) solved earlier in this chapter.

EXAMPLE
14.3

We want to maximize $f(x_1, x_2) = x_1 + x_2$ with respect to the constraints $x_1 \geq 0$, $x_2 \geq 0$, $-x_1 + x_2 \leq 2$, $2x_1 - x_2 \leq -1$, and $3x_1 + x_2 \leq 3$. The vectors and matrices implied by this are

$$A = \begin{bmatrix} -1 & 1 \\ 2 & -1 \\ 3 & 1 \end{bmatrix}, \quad \mathbf{b} = \begin{bmatrix} 2 \\ -1 \\ 3 \end{bmatrix}, \quad \text{and } \mathbf{c} = \begin{bmatrix} 1 \\ 1 \end{bmatrix}$$

Equation (14.6) makes the conversion to an LCP:

$$\mathbf{q} = \begin{bmatrix} -1 \\ -1 \\ \hline 2 \\ -1 \\ 3 \end{bmatrix}, \quad M = \left[\begin{array}{cc|ccc} 0 & 0 & -1 & 2 & 3 \\ 0 & 0 & 1 & -1 & 1 \\ \hline 1 & -1 & 0 & 0 & 0 \\ -2 & 1 & 0 & 0 & 0 \\ -3 & -1 & 0 & 0 & 0 \end{array} \right], \quad \mathbf{w} = \begin{bmatrix} u_1 \\ u_2 \\ \hline s_1 \\ s_2 \\ s_3 \end{bmatrix} = \begin{bmatrix} w_1 \\ w_2 \\ \hline w_3 \\ w_4 \\ w_5 \end{bmatrix} \quad \text{and}$$

$$\mathbf{z} = \begin{bmatrix} x_1 \\ x_2 \\ \hline y_1 \\ y_2 \\ y_3 \end{bmatrix} = \begin{bmatrix} z_1 \\ z_2 \\ \hline z_3 \\ z_4 \\ z_5 \end{bmatrix}$$

The initial dictionary with auxiliary variable z_0 is

$$\begin{aligned} w_1 &= -1 + z_0 - z_3 + 2z_4 + 3z_5 \\ w_2 &= -1 + z_0 + z_3 - z_4 + z_5 \\ w_3 &= 2 + z_0 + z_1 - z_2 \\ w_4 &= -1 + z_0 - 2z_1 + z_2 \\ w_5 &= 3 + z_0 - 3z_1 - z_2 \end{aligned}$$

The first phase involves moving z_0 to the dictionary. We do so using the first equation, solve for z_0 (so w_1 leaves the dictionary), and substitute that expression into the other equations:

$$\begin{aligned} z_0 &= 1 + w_1 + z_3 - 2z_4 - 3z_5 \\ w_2 &= 0 + w_1 + 2z_3 - 3z_4 - 2z_5 \\ w_3 &= 3 + w_1 + z_1 - z_2 + z_3 - 2z_4 - 3z_5 \\ w_4 &= 0 + w_1 - 2z_1 + z_2 + z_3 - 2z_4 - 3z_5 \\ w_5 &= 4 + w_1 - 3z_1 - z_2 + z_3 - 2z_4 - 3z_5 \end{aligned}$$

The new constant vector is $(1, 0, 3, 0, 4) \geq (0, 0, 0, 0, 0)$, so we have a feasible dictionary. Since all z_i for $i \geq 1$ are nonbasic, we have a balanced dictionary. The dictionary is not terminal since z_0 is still in it. The tableau method requires extra care when any of the constant terms becomes zero. The Lemke algorithm is itself not exempt from the potential problems of zero constants as we will see.

The second phase is now initiated. The variable w_1 just left the dictionary, so its complementary variable z_1 must now enter the dictionary. We have three equations involving z_1 from which to choose one to solve for z_1 , but only two have negative coefficients for z_1 , the w_4 and w_5 equations. The limiting value for the ratio of the constant term and the negative of the z_1 coefficient comes from the w_4 equation, a ratio of 0 as compared to the ratio 4/3 for the w_5 equation. Solving the w_4 equation for z_1 and substituting into other equations:

$$\begin{aligned} z_0 &= 1 + w_1 + z_3 - 2z_4 - 3z_5 \\ w_2 &= 0 + w_1 + 2z_3 - 3z_4 - 2z_5 \\ w_3 &= 3 + \frac{3}{2}w_1 - \frac{1}{2}w_4 - \frac{1}{2}z_2 + \frac{3}{2}z_3 - 3z_4 - \frac{9}{2}z_5 \\ z_1 &= 0 + \frac{1}{2}w_1 - \frac{1}{2}w_4 + \frac{1}{2}z_2 + \frac{1}{2}z_3 - z_4 - \frac{3}{2}z_5 \\ w_5 &= 4 - \frac{1}{2}w_1 + \frac{3}{2}w_4 - \frac{5}{2}z_2 - \frac{1}{2}z_3 + z_4 + \frac{3}{2}z_5 \end{aligned}$$

The variable w_4 left the dictionary, so its complementary variable z_4 must enter the dictionary, all the while maintaining a feasible, balanced dictionary. Four equations contain z_4 with a negative coefficient. Two of the equations lead to a limiting ratio of zero. Choosing the w_2 equation, solving for z_4 , and substituting in other equations:

$$\begin{aligned} z_0 &= 1 + \frac{1}{3}w_1 + \frac{2}{3}w_2 - \frac{1}{3}z_3 - \frac{5}{3}z_5 \\ z_4 &= 0 + \frac{1}{3}w_1 - \frac{1}{3}w_2 + \frac{2}{3}z_3 - \frac{2}{3}z_5 \\ w_3 &= 3 + \frac{1}{2}w_1 + w_2 - \frac{1}{2}w_4 - \frac{1}{2}z_2 - \frac{1}{2}z_3 - \frac{5}{2}z_5 \\ z_1 &= 0 + \frac{1}{6}w_1 + \frac{1}{3}w_2 - \frac{1}{2}w_4 + \frac{1}{2}z_2 - \frac{1}{6}z_3 - \frac{5}{6}z_5 \\ w_5 &= 4 - \frac{1}{6}w_1 - \frac{1}{3}w_2 + \frac{3}{2}w_4 - \frac{5}{2}z_2 + \frac{1}{6}z_3 + \frac{5}{6}z_5 \end{aligned}$$

The variable w_2 left the dictionary, so z_2 must enter the dictionary. As before we need to maintain a feasible and balanced dictionary. Two equations contain z_2 with a negative coefficient, the w_5 equation providing a limiting ratio of 8/5 whereas the w_3 equation has a ratio of 6. Solving the w_5 equation for z_2 and substituting in other equations:

$$\begin{aligned} z_0 &= 1 + \frac{1}{3}w_1 + \frac{2}{3}w_2 - \frac{1}{3}z_3 - \frac{5}{3}z_5 \\ z_4 &= 0 + \frac{1}{3}w_1 - \frac{1}{3}w_2 + \frac{2}{3}z_3 - \frac{2}{3}z_5 \\ w_3 &= \frac{11}{5} + \frac{8}{15}w_1 + \frac{16}{15}w_2 - \frac{4}{5}w_4 + \frac{1}{5}w_5 - \frac{8}{15}z_3 - \frac{8}{3}z_5 \end{aligned}$$

(Example 14.3
continued)

$$z_1 = \frac{4}{5} + \frac{2}{15}w_1 + \frac{4}{15}w_2 - \frac{1}{5}w_4 - \frac{3}{15}w_5 - \frac{2}{15}z_3 - \frac{2}{3}z_5$$

$$z_2 = \frac{8}{5} - \frac{1}{15}w_1 - \frac{2}{15}w_2 + \frac{3}{5}w_4 - \frac{2}{5}w_5 + \frac{1}{15}z_3 + \frac{1}{3}z_5$$

The variable w_5 left the dictionary, so z_5 must enter the dictionary. Four equations contain z_5 with a negative coefficient. The limiting equation is the z_4 equation with a ratio of zero and must be solved for z_5 . In doing so, we are now in a predicament. The variable z_4 leaves the dictionary and on the next step w_4 must enter the dictionary. But an earlier step saw us removing w_4 from the dictionary and adding z_4 . Continuing along our present path, we will undo all the work we have done only to arrive back at the start. What we have is a *cycle* in the processing. This occurred due to the presence of a zero constant term. The problem occurred in the first phase; to move z_0 into the dictionary, we had multiple choices for the leaving variable, either choice forcing an equation to have a zero constant term. ■

With our last example in mind, now is a good time to mention two potential problems that might be encountered when using the Lemke algorithm:

1. Cycling due to degeneracies.
2. The variable complementary to the leaving variable cannot enter the dictionary.

The term *degeneracy* refers to a constant term becoming zero. As we saw in Example 14.3, a zero constant term arises when there are multiple choices for the leaving variable. *Cycling* refers to removing a variable from the dictionary that was inserted at an earlier step. In Example 14.3, the cycling occurs because of a degeneracy – a constant term became zero. As it turns out, if we can modify the algorithm to prevent degeneracies, no cycling can occur.

14.2.2 ZERO CONSTANT TERMS

The classical method for handling degeneracies is to apply a *perturbation* to the constant terms. The k th constant term is modified (perturbed) by a power ε^k for some small $\varepsilon \in (0, 1)$. The value of ε is made so that the choice of leaving variable is unambiguous, thus never forcing zero constant terms to occur. The perturbed problem is solved using the Lemke algorithm. The final solution will be a continuous function of ε , so we can evaluate the solution at $\varepsilon = 0$ (formally, take the limit as ε approaches zero) to obtain the solution to the original problem.

EXAMPLE
14.4

Maximize $f(x_1, x_2) = x_1 + x_2$ subject to the constraints $x_1 \geq 0$, $x_2 \geq 0$, and $x_1 + x_2 \leq 2$. The vectors and matrices implied by this are

$$A = \begin{bmatrix} 1 & 1 \end{bmatrix}, \quad \mathbf{b} = [2], \quad \text{and } \mathbf{c} = \begin{bmatrix} 1 \\ 1 \end{bmatrix}$$

Equation (14.6) makes the conversion to an LCP:

$$\mathbf{q} = \begin{bmatrix} -1 \\ -1 \\ 2 \end{bmatrix}, \quad M = \left[\begin{array}{cc|c} 0 & 0 & 1 \\ 0 & 0 & 1 \\ -1 & -1 & 0 \end{array} \right], \quad \mathbf{w} = \begin{bmatrix} u_1 \\ u_2 \\ s_1 \end{bmatrix} = \begin{bmatrix} w_1 \\ w_2 \\ w_3 \end{bmatrix}$$

$$\mathbf{z} = \begin{bmatrix} x_1 \\ x_2 \\ y_1 \end{bmatrix} = \begin{bmatrix} z_1 \\ z_2 \\ z_3 \end{bmatrix}$$

The initial dictionary with auxiliary variable z_0 is

$$\begin{aligned} w_1 &= -1 + z_0 + z_3 \\ w_2 &= -1 + z_0 + z_3 \\ w_3 &= 2 + z_0 - z_1 - z_2 \end{aligned}$$

The limiting equations for moving z_0 to the dictionary are the w_1 and w_2 equations, an ambiguous choice. Solving the first leads to $z_0 = 1 - z_3 + w_1$. Replacing it in the second produces $w_2 = 0 + w_1$, a degeneracy.

Instead, add powers of a small number $\varepsilon \in (0, 1)$ to the constant terms:

$$\begin{aligned} w_1 &= (-1 + \varepsilon) + z_0 + z_3 \\ w_2 &= (-1 + \varepsilon^2) + z_0 + z_3 \\ w_3 &= (2 + \varepsilon^3) + z_0 - z_1 - z_2 \end{aligned}$$

Because $\varepsilon^2 < \varepsilon$, we are forced to use the w_2 equation to solve for z_0 . Do so and substitute in the other equations:

$$\begin{aligned} w_1 &= (\varepsilon - \varepsilon^2) + w_2 \\ z_0 &= (1 - \varepsilon^2) + w_2 - z_3 \\ w_3 &= (3 + \varepsilon^3 - \varepsilon^2) + w_2 - z_1 - z_2 - z_3 \end{aligned}$$

Observe that the constant terms are all positive for small ε . The variable w_2 left the dictionary, so z_2 must now enter the dictionary. The only equation containing z_2 is the w_3 equation:

$$\begin{aligned} w_1 &= (\varepsilon - \varepsilon^2) + w_2 \\ z_0 &= (1 - \varepsilon^2) + w_2 - z_3 \\ z_2 &= (3 + \varepsilon^3 - \varepsilon^2) + w_2 - w_3 - z_1 - z_3 \end{aligned}$$

The variable w_3 left the dictionary, so z_3 must enter the dictionary. For small, positive ε , $1 - \varepsilon^2$ is smaller than $3 + \varepsilon^3 - \varepsilon^2$, so the limiting equation is the z_0 equation. Solve for z_3 and substitute in other equations,

$$\begin{aligned} w_1 &= (\varepsilon - \varepsilon^2) + w_2 \\ z_3 &= (1 - \varepsilon^2) + w_2 - z_0 \\ z_2 &= (2 + \varepsilon^3) - w_3 + z_0 - z_1 \end{aligned}$$

(Example 14.4
continued)

Because z_0 has left the dictionary, the process ends and the dictionary is terminal. The solution to the LCP is $\mathbf{w} = (w_1, w_2, w_3) = (\varepsilon - \varepsilon^2, 0, 0)$ and $\mathbf{z} = (z_1, z_2, z_3) = (0, 2 + \varepsilon^3, 1 - \varepsilon^2)$. Clearly, $\mathbf{w} \circ \mathbf{z} = (0, 0, 0)$. This argument applies for arbitrarily small ε , so we may take the limit as ε approaches zero to obtain $\mathbf{w} = (0, 0, 0)$ and $\mathbf{z} = (0, 2, 1)$. Because $x_1 = z_1 = 0$ and $x_2 = z_2 = 2$, the solution to the original linear programming problem is $\max(f) = f(0, 2) = 2$. ■

In order to evaluate the perturbed solution at $\varepsilon = 0$, a numerical implementation of the Lemke algorithm must allow for the inclusion of ε symbolically. This can be done by maintaining a data structure that implements a polynomial in ε (stored as an array of coefficients), one structure for each equation in the dictionary. The constant term of the polynomial is the constant term of the equation. The higher-order polynomial terms represent the perturbation of the constant term. The implementation also maintains a variable that represents the current value of ε so that the perturbed constant term in the equation can be computed by evaluating the corresponding polynomial at ε . When a terminal dictionary is found, the solution to the original problem is obtained by setting the nonbasic variables to zero and the basic variables to the constant terms of the polynomials.

If no degeneracies occur during the algorithm, there can be no cycling. The proof of this uses an analogy – referred to as the *museum principle* in [Fri98] – to visiting a finite collection of rooms that have the following properties:

1. Each room is labeled “stop” or “continue.”
2. All “continue” rooms have one or two doors.
3. If you reach a “stop” room, then your visiting stops.
4. If you reach a “continue” room with one door, then your visiting stops.
5. If you reach a “continue” room with two doors, then your visiting continues, but you must leave the room through the other door from which you entered.

The museum principle states that you will never enter a room twice; that is, your path of visitation does not have a cycle. This principle may be used to show that the second phase of the Lemke algorithm, in the absence of degeneracies, has no cycles and terminates in a finite number of steps.

The analogy is as follows. The feasible, balanced dictionaries are the rooms. Each door corresponds to the act of one variable entering the dictionary and another leaving. A room is labeled “stop” if it is a terminal dictionary. All other rooms are labeled “continue.” Each “continue” room corresponds to a feasible, balanced dictionary with z_0 as a basic variable. The dictionary has exactly one pair of complementary variables, both of which are nonbasic. The “continue” room has at most two doors; each of the complementary variables can enter the dictionary in at most one way. Finally, the first phase of the Lemke algorithm produces a “continue” room that has exactly one door, and this is the room in which you start the visitation. To see that there is only one door, consider that z_0 enters the dictionary and a basic variable w_i leaves

the dictionary, the choice of w_i made so that the constant terms of the equations are nonnegative. Because we have assumed that there are no degeneracies, there can be only one such w_i . The corresponding equation is solved for z_0 and the w_i term shows up as a nonbasic variable that has a positive coefficient (with value 1). Substituting the z_0 into all other equations, w_i shows up with a positive coefficient (with value 1) in every case. Because all the w_i coefficients are positive and the constant terms are nonnegative, w_i cannot reenter the dictionary. For if you were to solve for w_i , the constant term on the right-hand side would be a negative number, contradicting the fact the invariant of each step is that the dictionary is feasible. Thus, there is no door in which w_i can enter the room, in which case the room has one door (corresponding to z_i entering the dictionary). The rooms satisfy the conditions of the museum principle and the Lemke algorithm cannot cycle.

14.2.3 THE COMPLEMENTARY VARIABLE CANNOT LEAVE THE DICTIONARY

Degeneracies are one problem with the method of solving an LCP, but the perturbation method discussed earlier circumvents the problems. Another problem with the method is that at some point the variable complementary to the leaving variable cannot enter the dictionary, in which case you cannot proceed with the algorithm.

EXAMPLE
14.5

Maximize $f(x_1, x_2) = 2x_1 + x_2$ subject to the constraints $x_1 \geq 0$, $x_2 \geq 0$, and $-x_1 - x_2 \leq -1$. The initial dictionary with auxiliary variable z_0 is

$$\begin{aligned} w_1 &= -2 + z_0 - z_3 \\ w_2 &= -1 + z_0 - z_3 \\ w_3 &= -1 + z_0 + z_1 + z_2 \end{aligned}$$

The first phase is to move z_0 into the dictionary by solving the first equation, $z_0 = 2 + w_1 + z_3$, and substituting into the other equations,

$$\begin{aligned} z_0 &= 2 + w_1 + z_3 \\ w_2 &= 1 + w_1 \\ w_3 &= 1 + w_1 + z_1 + z_2 + z_3 \end{aligned}$$

The variable w_1 left the dictionary, so z_1 must enter it. The only equation containing z_1 is the last, but the coefficient of z_1 is positive. In solving for z_1 we would obtain a negative constant term, violating the feasibility of the dictionary. Therefore, z_1 cannot enter the dictionary. ■

A sketch of the convex domain defined by the constraints shows us what the problem is. The domain is unbounded, so in fact f is unbounded and has no maximum. The linear programming problem has no solution. Some general statements can be made about the matrix M in the LCP regarding the inability for the complementary variable to enter the dictionary.

First, some definitions. The matrix M is said to be *copositive* if $\mathbf{x}^T M \mathbf{x} \geq 0$ for all $\mathbf{x} \geq 0$. M is said to be *copositive-plus* if (1) it is copositive and (2) $\mathbf{x} \geq \mathbf{0}$, $M\mathbf{x} \geq \mathbf{0}$, and $\mathbf{x}^T M \mathbf{x} = 0$ imply $(M + M^T)\mathbf{x} = \mathbf{0}$. Recall from linear algebra that a matrix M is said to be positive-semidefinite if M is symmetric and $\mathbf{x}^T M \mathbf{x} \geq 0$ for all \mathbf{x} . In contrast, a copositive matrix is not required to be symmetric and the vectors for which we require $\mathbf{x}^T M \mathbf{x} \geq 0$ are only those whose components are all nonnegative.

A simple fact to verify is that the matrix M that comes from complementary slackness and is shown in equation (14.6) is copositive. For any skew-symmetric matrix M , it is the case that $\mathbf{z}^T M \mathbf{z} = 0$. Setting $M = [m_{ij}]$ and $\mathbf{z} = [z_i]$:

$$\begin{aligned}\mathbf{z}^T M \mathbf{z} &= \sum_{i=1}^n \sum_{j=1}^n z_i m_{ij} z_j \\ &= \sum_{i < j} z_i m_{ij} z_j + \sum_{i=j} z_i m_{ij} z_j + \sum_{i > j} z_i m_{ij} z_j \\ &= \sum_{i < j} z_i m_{ij} z_j + 0 - \sum_{i > j} z_i m_{ji} z_j && \text{skew-symmetry means } m_{ij} = -m_{ji} \\ &= \sum_{i < j} z_i m_{ij} z_j + 0 - \sum_{j > i} z_i m_{ij} z_j && \text{swapping names } i \text{ and } j \text{ in the last summation} \\ &= 0\end{aligned}$$

This is true for all \mathbf{z} , so is true for $\mathbf{z} \geq \mathbf{0}$. Thus, a skew-symmetric matrix is copositive. M in equation (14.6) is skew-symmetric, therefore copositive.

The main result of this section is the following:

Let M be copositive. If the Lemke algorithm reaches the stage where a complementary variable cannot leave the dictionary, then the linear complementarity problem has no solution.

The proof is somewhat tedious and not presented here. The consequence of the linear complementarity problem regarding a numerical implementation is that when you reach a stage where the complementary variable cannot leave the solution, the program terminates and reports to the caller that the LCP has no solution.

14.3 MATHEMATICAL PROGRAMMING

Now that we have a good understanding of linear programming, I will briefly discuss a generalization called *mathematical programming* (MP). The goal is to minimize $f(\mathbf{x})$ subject to the constraints $\mathbf{g}(\mathbf{x}) \leq \mathbf{0}$ where $f : \mathbb{R}^n \rightarrow \mathbb{R}$, the *objective function*, and $\mathbf{g} : \mathbb{R}^n \rightarrow \mathbb{R}^m$, the *constraining functions*, are arbitrary functions. The convention used in the mathematical programming is that the objective function is to be minimized. If an application requires maximizing f , you can minimize instead the function $-f$.

Here is some further terminology that will be used later. A point \mathbf{x} satisfying the constraints $\mathbf{g}(\mathbf{x}) \leq \mathbf{0}$ is said to be a *feasible point*. If $g_i(\mathbf{x}) = 0$ for some i , we say that g_i is *active* at \mathbf{x} .

EXAMPLE 14.6

The linear programming problem can be rephrased as a mathematical programming problem. The original problem is to maximize $\mathbf{c}^T \mathbf{x}$ subject to $\mathbf{x} \geq \mathbf{0}$ and $A\mathbf{x} \leq \mathbf{b}$. As a mathematical programming problem, the objective function is $f(\mathbf{x}) = -\mathbf{c}^T \mathbf{x}$, we want to minimize f , and the constraints are combined into $\mathbf{g}(\mathbf{x}) \leq \mathbf{0}$ as

$$\mathbf{g}(\mathbf{x}) = \begin{bmatrix} A\mathbf{x} - \mathbf{b} \\ -\mathbf{x} \end{bmatrix}$$

In this case f is a linear function and \mathbf{g} is an affine function. ■

EXAMPLE 14.7

You are given a set of points $\{(x_i, y_i)\}_{i=1}^n$ with at least three noncollinear points. Let (x_0, y_0) be the average of the points. Compute the minimum area, axis-aligned ellipse centered at the average that contains all the points.

The average is $(x_0, y_0) = (\sum_{i=1}^n (x_i, y_i))/n$. The axis-aligned ellipse centered at the average is of the form,

$$\left(\frac{x - x_0}{a}\right)^2 + \left(\frac{y - y_0}{b}\right)^2 = 1$$

where $a > 0$ and $b > 0$ are the half-lengths of the ellipse axes. The area of the ellipse is

$$\mathcal{A} = \pi ab.$$

We want to minimize the area and have all points contained in the ellipse. The containment leads to the constraints,

$$\left(\frac{x_i - x_0}{a}\right)^2 + \left(\frac{y_i - y_0}{b}\right)^2 \leq 1, \quad 1 \leq i \leq n$$

In terms of the notation of mathematical programming, the variables are a and b , the objective function is $f(a, b) = \pi ab$, and the constraint functions are $\mathbf{g}(a, b) = (g_1(a, b), \dots, g_n(a, b), g_{n+1}(a, b), g_{n+2}(a, b))$, where $g_i(a, b) = ((x_i - x_0)/a)^2 + ((y_i - y_0)/b)^2 - 1$, $g_{n+1}(a, b) = -a$, and $g_{n+2}(a, b) = -b$. Both f and \mathbf{g} are nonlinear functions.

The problem can be equivalently formulated in a manner that makes \mathbf{g} an affine function, potentially making the solution a bit easier to construct. Instead of variables a and b , let us choose $u = 1/a^2$ and $v = 1/b^2$. The constraint functions are $g_i(u, v) = (x_i - x_0)^2 u + (y_i - y_0)^2 v - 1$ for $1 \leq i \leq n$, $g_{n+1}(u, v) = -u$, and $g_{n+2}(u, v) = -v$, all affine functions of u and v . The objective function is $f(u, v) = \pi/\sqrt{uv}$. The uv -domain implied by $\mathbf{g}(u, v) \leq \mathbf{0}$ is a bounded region whose boundary is a convex polygon. The graph of f is shown in Figure 14.5. Even though f is nonlinear, the figure should convince you that the minimum must occur on the polygon boundary (not necessarily at a vertex). ■

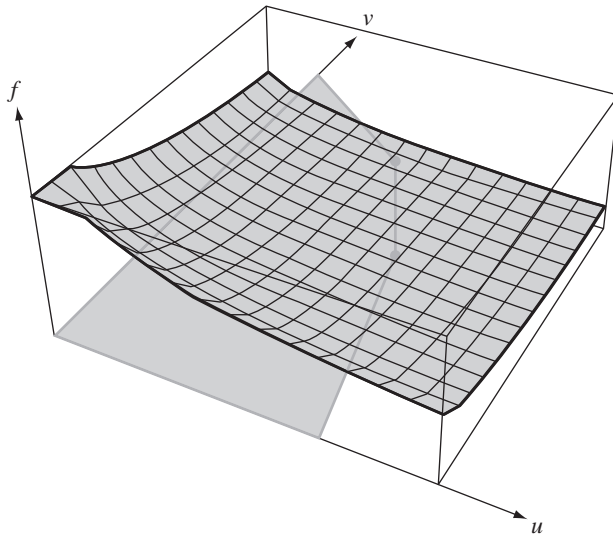


Figure 14.5 Graph of $f(u, v) = \pi / \sqrt{uv}$ in the first quadrant.

Two categories of mathematical programming problems are of interest to us. The first is called *quadratic programming*. The objective function has a quadratic term in addition to the linear term that appears in the linear programming problem. The constant term is omitted here since f can be minimized without it, then that constant is added back in to the result. The function is

$$f(\mathbf{x}) = \mathbf{x}^T S \mathbf{x} - \mathbf{c}^T \mathbf{x} \quad (14.7)$$

where S is a symmetric matrix. The constraint functions are still of the form used in linear programming, $\mathbf{g}(\mathbf{x}) = (\mathbf{A}\mathbf{x} - \mathbf{b}, -\mathbf{x}) \leq \mathbf{0}$.

The second category is *convex programming* and involves objective functions that are *convex functions*. A function $f(\mathbf{x})$ is said to be *convex* if its domain is a convex set and if

$$f((1-t)\mathbf{x} + t\mathbf{y}) \leq (1-t)f(\mathbf{x}) + tf(\mathbf{y}) \quad (14.8)$$

for all $t \in [0, 1]$ and for all \mathbf{x} and \mathbf{y} in the domain of the function. Since the domain of f is a convex set, $(1-t)\mathbf{x} + t\mathbf{y}$ is guaranteed to be in the domain for any $t \in [0, 1]$. Thus, the left-hand side of the inequality [equation \(14.8\)](#) is well defined since the input to f is in its domain. [Figure 14.6](#) illustrates the graphs of a convex function and a nonconvex function of one variable.

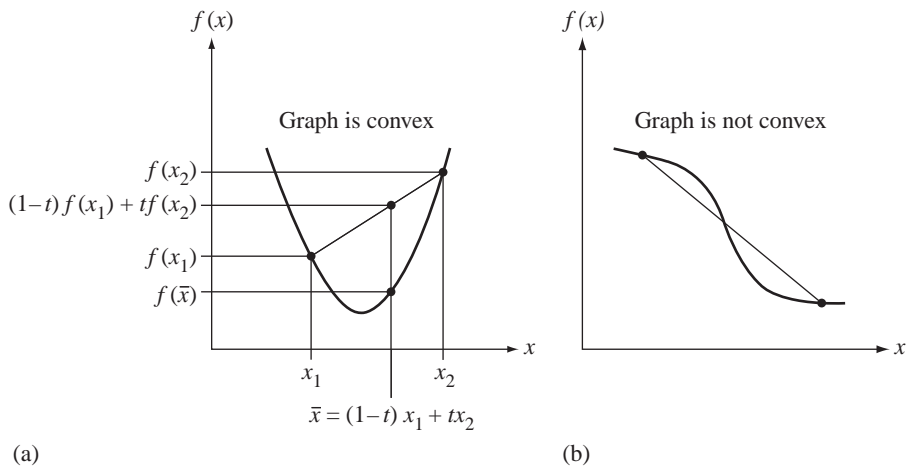


Figure 14.6 (a) The graph of a convex function. Any line segment connecting two graph points is always above the graph. (b) The graph of a nonconvex function. The line segment connecting two graph points is not always above the graph.

Visually, convexity means that any line segment connecting two points on the graph of the function must always lie above the graph. If $f(x)$ has a continuous second-order derivative, it is a convex function when $f''(x) \geq 0$. Figure 14.7 illustrates the graph of a convex function of two variables.

A line segment connecting any two points on the graph of the function must always lie above the graph. Generally, if $f(\mathbf{x})$ for $\mathbf{x} \in \mathbb{R}^n$ has continuous second-order partial derivatives, it is a convex function when the matrix of second-order partial derivatives is positive-semidefinite (the eigenvalues are all nonnegative).

In Example 14.7, the second formulation of the problem that has affine constraints in u and v is both a quadratic programming and a convex programming problem. That is, the objective function is a convex and quadratic function and the constraints are affine.

14.3.1 KARUSH–KUHN–TUCKER CONDITIONS

In calculus we have the concept of a local minimum of a function. If $f(\mathbf{x})$ is the function and \mathbf{x}_0 is a point for which $f(\mathbf{x}) \geq f(\mathbf{x}_0)$ for all \mathbf{x} sufficiently close to \mathbf{x}_0 , then \mathbf{x}_0 is referred to as a *local minimum for f*. In mathematical programming a similar concept can be defined. A point \mathbf{x}_0 is a *constrained local minimum* if $f(\mathbf{x}) \geq f(\mathbf{x}_0)$ for all **feasible** \mathbf{x} sufficiently close to \mathbf{x}_0 . That is, \mathbf{x} must be close to \mathbf{x}_0 and $\mathbf{g}(\mathbf{x}) \leq \mathbf{0}$. We will assume from here on that both f and \mathbf{g} are differentiable functions. The constraint

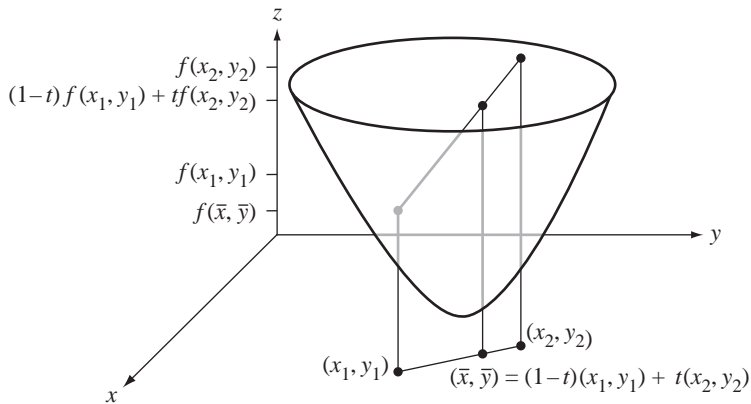


Figure 14.7 The graph of a convex function $f(x, y)$.

function is stored as an $m \times 1$ column vector. The gradient of $f(\mathbf{x})$, denoted $\nabla f(\mathbf{x})$, is stored as a $1 \times n$ row vector. The derivative matrix of $\mathbf{g}(\mathbf{x})$, denoted $D\mathbf{g}(\mathbf{x})$, is stored as an $m \times n$ matrix. The i th row corresponds to the gradient of the i th component, $\nabla g_i(\mathbf{x})$.

An important result for mathematical programming is stated here without proof: If \mathbf{x}_0 is a constrained local minimum for the MP problem, then there exists nonnegative u_i for $0 \leq i \leq m$, such that

$$u_0 \nabla f(\mathbf{x}_0) + \sum_{i=1}^m u_i \nabla g_i(\mathbf{x}_i) = \mathbf{0} \quad (14.9)$$

and such that $u_i = 0$ whenever $g_i(\mathbf{x}_i) < 0$. The left-hand side of equation (14.9) is effectively a summation over active constraints since the u_i are zero for inactive constraints. If the constraints of the MP problem are allowed to include equality constraints, equation (14.9) is still valid, except that the u_i for an equality constraint is allowed to be negative. By making this minor adjustment, the generalized result stated above includes the classical theory of Lagrange multipliers. One final observation: If $u_0 = 0$, equation (14.9) contains information only about the constraint functions and nothing about f . In most applications of interest, information about f allows us to choose $u_0 = 1$.

A feasible \mathbf{x} that satisfies equation (14.9) with $u_0 = 1$, the other u_i as specified in that equation, is said to be a *Karush–Kuhn–Tucker point*, or *KKT point* for short. The conditions for being a KKT point are summarized in vector notation:

$$\mathbf{g}(\mathbf{x}) \leq \mathbf{0}, \quad \nabla f(\mathbf{x}) + \mathbf{u}^T D\mathbf{g}(\mathbf{x}) = \mathbf{0} \quad \text{for a } \mathbf{u} \geq \mathbf{0}, \text{ and } \mathbf{u} \circ \mathbf{g}(\mathbf{x}) = \mathbf{0} \quad (14.10)$$

where \mathbf{u} is the $m \times 1$ vector whose components are u_1 through u_m mentioned in equation (14.9). Notice that the last expression of equation (14.10) is a complementarity condition.

Recall from calculus that the candidates for minimizing a differentiable function $f(x)$ on an interval $[a, b]$ are those points for which $f'(x) = 0$ and the endpoints $x = a$ and $x = b$. These points were named *critical points*. For a multivariate differentiable function $f(\mathbf{x})$ defined on a closed and bounded domain, the critical points are those for which $\nabla f(\mathbf{x}) = \mathbf{0}$ and boundary points of the domain. The KKT points are the analogy of critical points in the realm of mathematical programming. Specifically, a constrained local minimum of the MP problem must be a KKT point when the constraints are any of the following types:

1. The constraint function is affine, $\mathbf{g}(\mathbf{x}) = M\mathbf{x} + \mathbf{t}$ for a matrix M and vector \mathbf{t} .
2. The constraint components $g_i(\mathbf{x})$ are convex functions and there is at least one feasible \mathbf{x} at which all constraints are inactive.
3. For any feasible \mathbf{x} , the vectors $\nabla g_i(\mathbf{x})$ are linearly independent.

EXAMPLE 14.8

The linear programming problem is to minimize $f(\mathbf{x}) = -\mathbf{c}^T \mathbf{x}$ subject to $\mathbf{g}(\mathbf{x}) = (\mathbf{Ax} - \mathbf{b}, -\mathbf{x}) \leq \mathbf{0}$. The three KKT conditions for this problem are as follows.

The first condition is $\mathbf{g}(\mathbf{x}) \leq \mathbf{0}$, which simply states that \mathbf{x} is feasible.

The second condition is

$$\mathbf{0} = \nabla f(\mathbf{x}) + \mathbf{u}^T D\mathbf{g}(\mathbf{x}) = -\mathbf{c}^T + \mathbf{u}^T \begin{bmatrix} A \\ -I \end{bmatrix}$$

where I is the identity matrix of the appropriate size. Partitioning \mathbf{u} into two blocks of the appropriate sizes, $\mathbf{u} = (\mathbf{u}_d, \mathbf{u}_s)$, the last displayed equation is equivalent to

$$\mathbf{u}_s = -\mathbf{c} + A^T \mathbf{u}_d$$

That is, \mathbf{u}_s are the slack variables for the primal problem and \mathbf{u}_d are the regular variables for the dual problem. The condition $\mathbf{u} \geq \mathbf{0}$ is a statement of dual feasibility. Using the same block decomposition of \mathbf{u} as just described, the third condition is

$$\mathbf{0} = \mathbf{u} \circ \mathbf{g}(\mathbf{x}) = (\mathbf{u}_d, \mathbf{u}_s) \circ (\mathbf{Ax} - \mathbf{b}, -\mathbf{x})$$

or $\mathbf{u}_d \circ (\mathbf{Ax} - \mathbf{b}) = \mathbf{0}$ and $\mathbf{u}_s \circ \mathbf{x} = \mathbf{0}$, just statements of complementary slackness. ■

14.3.2 CONVEX QUADRATIC PROGRAMMING

The quadratic programming problem is to minimize $f(\mathbf{x}) = \mathbf{x}^T S \mathbf{x} - \mathbf{c}^T \mathbf{x} + K$ for a constant symmetric matrix S , a constant vector \mathbf{c} , and a constant scalar K , subject to $\mathbf{g}(\mathbf{x}) = (\mathbf{Ax} - \mathbf{b}, -\mathbf{x}) \leq \mathbf{0}$. We additionally want f to be a convex function; it is sufficient to require S to be positive-semidefinite.

The first KKT condition is a statement of feasibility: $\mathbf{Ax} \leq \mathbf{b}$ and $\mathbf{x} \geq 0$. The second KKT condition is

$$\mathbf{0} = \nabla f(\mathbf{x}) + \mathbf{u}^T Dg(\mathbf{x}) = 2\mathbf{x}^T S - \mathbf{c}^T + \mathbf{u}^T \begin{bmatrix} A \\ -I \end{bmatrix}$$

Using the decomposition of $\mathbf{u} = (\mathbf{u}_d, \mathbf{u}_2)$ as in the linear programming problem, the last equation implies

$$\mathbf{u}_s = -\mathbf{c} + 2S\mathbf{x} + A^T \mathbf{u}_d \quad (14.11)$$

and is called the *dual slack* equation. The third KKT condition is the same as in the linear programming problem,

$$\mathbf{u}_d \circ (\mathbf{Ax} - \mathbf{b}) = \mathbf{0} \text{ and } \mathbf{u}_s \circ \mathbf{x} = \mathbf{0} \quad (14.12)$$

and is called *complementary slackness*.

These conditions allow us to reformulate the quadratic programming problem as a linear complementarity problem,

$$\mathbf{w} = \mathbf{q} + M\mathbf{z}, \quad \mathbf{w} \circ \mathbf{z} = \mathbf{0}, \quad \mathbf{w} \geq \mathbf{0}, \quad \mathbf{z} \geq \mathbf{0}$$

where

$$\mathbf{x}_s = \mathbf{b} - \mathbf{Ax}, \quad \mathbf{q} = \begin{bmatrix} -\mathbf{c} \\ \mathbf{b} \end{bmatrix}, \quad M = \begin{bmatrix} 2S & A^T \\ -A & 0 \end{bmatrix}, \quad \mathbf{w} = \begin{bmatrix} \mathbf{u}_s \\ \mathbf{x}_s \end{bmatrix}, \quad \mathbf{z} = \begin{bmatrix} \mathbf{x} \\ \mathbf{u}_d \end{bmatrix}$$

The matrix M is copositive. To see this,

$$\mathbf{z}^T M \mathbf{z} = \mathbf{z}^T \begin{bmatrix} 2S & 0 \\ 0 & 0 \end{bmatrix} \mathbf{z} + \mathbf{z}^T \begin{bmatrix} 0 & A^T \\ -A & 0 \end{bmatrix} \mathbf{z} = \mathbf{z}^T \begin{bmatrix} 2S & 0 \\ 0 & 0 \end{bmatrix} \mathbf{z}$$

where the last equality is valid since the matrix involving just A and $-A$ is skew-symmetric, causing its quadratic form to be zero. The last matrix in the equations is positive-semidefinite since S is positive-semidefinite. The lower right-hand zero block only introduces zero eigenvalues in the larger matrix. As a result, M is also copositive-plus, which means that the Lemke algorithm may be applied, using a perturbation if necessary to eliminate degeneracies, and allowing for proper termination either because a solution is found or because a complementary variable could not leave the dictionary, in which case f has no minimum.

Because the linear complementarity problem is just a reformulated set of KKT conditions, any solution to it must be a KKT point. The additional assumption of convexity allows us to use the following result: If f and g_1 through g_m are convex functions, then any KKT point for the MP problem must be a global minimum.

In summary, the solution to a convex, quadratic programming problem may be constructed by solving the corresponding linear complementarity problem using the Lemke algorithm. That algorithm will properly terminate and produce either a

minimum for f or indicate that f has no minimum. Since f is convex and the affine constraints are convex, the minimum found by the algorithm must be the global minimum of f .

EXAMPLE
14.9

A solid triangle has vertices $(0, 0)$, $(1, 0)$, and $(0, 1)$. Compute the closest triangle point to $(1, 2)$. A sketch of the triangle and point will convince you that the closest point is on the edge connecting $(1, 0)$ and $(0, 1)$. Although you can use a simple geometric argument to construct the closest point, we will solve this as a convex quadratic programming problem.

We must minimize the squared distance $(x_1 - 1)^2 + (x_2 - 2)^2 = x_1^2 + x_2^2 - 2x_1 - 4x_2 + 5$, where (x_1, x_2) is any point in the solid triangle. We can ignore the constant term and equivalently minimize $f(x_1, x_2) = x_1^2 + x_2^2 - 2x_1 - 4x_2$. The interior of the triangle is the intersection of half planes: $x_1 \geq 0$, $x_2 \geq 0$ and $x_1 + x_2 \leq 1$. The quantities of interest in the quadratic programming problem are

$$S = \begin{bmatrix} 1 & 0 \\ 0 & 1 \end{bmatrix}, \quad \mathbf{c} = \begin{bmatrix} 2 \\ 4 \end{bmatrix}, \quad A = \begin{bmatrix} 1 & 1 \end{bmatrix}, \quad \text{and } \mathbf{b} = [1]$$

The quantities of interest in the linear complementarity problem are

$$M = \left[\begin{array}{cc|c} 2 & 0 & 1 \\ 0 & 2 & 1 \\ \hline -1 & -1 & 0 \end{array} \right] \quad \text{and} \quad \mathbf{q} = \begin{bmatrix} -2 \\ -4 \\ 1 \end{bmatrix}$$

The initial modified dictionary is

$$\begin{aligned} w_1 &= -2 + z_0 + 2z_1 + z_3 \\ w_2 &= -4 + z_0 + 2z_2 + z_3 \\ w_3 &= 1 + z_0 - z_1 - z_2 \end{aligned}$$

In the first phase, z_0 enters the dictionary and w_2 leaves the dictionary,

$$\begin{aligned} w_1 &= 2 + w_2 + 2z_1 - 2z_2 \\ z_0 &= 4 + w_2 - 2z_2 - z_3 \\ w_3 &= 5 + w_2 - z_1 - 3z_2 - z_3 \end{aligned}$$

Because w_2 left the dictionary, z_2 must enter it. The limiting equation is the w_1 equation, so solve that equation for z_2 and substitute in the others:

$$\begin{aligned} z_2 &= 1 - \frac{1}{2}w_1 + \frac{1}{2}w_2 + z_1 \\ z_0 &= 2 + w_1 - 2z_1 - z_3 \\ w_3 &= 2 + \frac{3}{2}w_1 - \frac{1}{2}w_2 - 4z_1 - z_3 \end{aligned}$$

(Example 14.9
continued)

Because w_1 left the dictionary, z_1 must enter it. The limiting equation is the w_3 equation, so solve that equation for z_1 and substitute in the others:

$$\begin{aligned} z_2 &= \frac{3}{2} - \frac{1}{8}w_1 + \frac{3}{8}w_2 - \frac{1}{4}w_3 - \frac{1}{4}z_3 \\ z_0 &= 1 + \frac{1}{4}w_1 + \frac{1}{4}w_2 + \frac{1}{2}w_3 - \frac{1}{2}z_3 \\ z_1 &= \frac{1}{2} + \frac{3}{8}w_1 - \frac{1}{8}w_2 - \frac{1}{4}w_3 - \frac{1}{4}z_3 \end{aligned}$$

Finally, w_3 left, so z_3 must enter. Two equations are limiting, the z_0 and z_1 equations. No need to apply a perturbation here. We know that cycling should not occur, so solve the z_0 equation for z_3 and substitute:

$$\begin{aligned} z_2 &= 1 - \frac{1}{4}w_1 + \frac{1}{4}w_2 - \frac{1}{2}w_3 + \frac{1}{2}z_0 \\ z_3 &= 2 + \frac{1}{2}w_1 + \frac{1}{2}w_2 + w_3 - 2z_0 \\ z_1 &= 0 + \frac{1}{4}w_1 - \frac{1}{4}w_2 - \frac{1}{2}w_3 + \frac{1}{2}z_0 \end{aligned}$$

The solution is $\mathbf{w} = (w_1, w_2, w_3) = (0, 0, 0)$ and $\mathbf{z} = (z_1, z_2, z_3) = (0, 1, 2)$. In terms of the original variables, $x_1 = z_1 = 0$ and $x_2 = z_2 = 1$. The closest point on the triangle to $(1, 2)$ is the vertex $(0, 1)$. ■

14.3.3 GENERAL DUALITY THEORY

The linear programming problem was referred to as the primal problem. We discovered an equivalent problem, called the dual problem. The mathematical programming problem has a similar concept of duality. The *primal MP problem* is

$$\text{Minimize } f(\mathbf{x}) \text{ subject to } \mathbf{g}(\mathbf{x}) \leq \mathbf{0}$$

Define $h(\mathbf{x}, \mathbf{u}) = f(\mathbf{x}) + \mathbf{u}^T \mathbf{g}(\mathbf{x})$. Notice that the (row) vector of derivatives of L with respect to \mathbf{x} , denoted $\partial h / \partial \mathbf{x}$, is $\partial h / \partial \mathbf{x} = \nabla f(\mathbf{x}) + \mathbf{u}^T D\mathbf{g}(\mathbf{x})$, exactly the expression that appears in the second KKT condition. Define the *Lagrangian function*,

$$L(\mathbf{u}) = \min_{\mathbf{x} \in \mathbb{R}^n} h(\mathbf{x}, \mathbf{u})$$

The *dual MP problem* is

$$\text{Maximize } L(\mathbf{u}) \text{ subject to } \mathbf{u} \geq \mathbf{0}$$

If $\min(f)$ is the minimum of the primal problem and $\max(L)$ is the maximum of the dual problem, then it is the case that $\max(L) \leq \min(f)$. The difference

$\min(f) - \max(L)$ is called the *duality gap*. For the linear programming problem we saw that the duality gap is zero.

We had used the terminology that \mathbf{x} is feasible if $\mathbf{g}(\mathbf{x}) \leq \mathbf{0}$. Similarly, we say that \mathbf{u} is *feasible* for the dual problem if $\mathbf{u} \geq \mathbf{0}$. Results similar to the Strong Duality principle for linear programming are the following:

1. If there are feasible vectors \mathbf{x} and \mathbf{u} such that $L(\mathbf{u}) = f(\mathbf{x})$, then \mathbf{x} is an optimal solution to the primal problem.
2. If there are feasible vectors \mathbf{x} and \mathbf{u} such that $f(\mathbf{x}) + \mathbf{u}^T \mathbf{g}(\mathbf{x}) = L(\mathbf{u})$ and $\mathbf{u} \circ \mathbf{g}(\mathbf{x}) = \mathbf{0}$, then \mathbf{x} is an optimal solution to the primal problem.

In either case, the duality gap is zero.

14.4 APPLICATIONS

A few applications of LCP methods are presented here. The first subsection includes distance calculations between a point and a convex polygon, a point and a convex polyhedron, two convex polygons, and two convex polyhedra. The second subsection is a brief summary of how one goes about computing impulsive forces and resting contact forces at points of contact between two rigid bodies represented as convex polyhedra.

14.4.1 DISTANCE CALCULATIONS

The origin of the coordinate system in any of these applications is always chosen to be $\mathbf{0}$. The distinction between point and vector is not necessary in this situation, so all quantities are typeset using vector notation.

Distance Between Point and Convex Polygon

Let \mathbf{V}_i for $0 \leq i \leq n - 1$ be the counterclockwise-ordered vertices for a convex polygon. The vertices may occur anywhere in the plane, but to support distance calculations using LCP methods, we require that all the vertices lie in the first quadrant. If the polygon is not in the first quadrant, it is always possible to place it there by a translation of all vertices. Let \mathbf{P} be a point that is outside the polygon. We wish to compute the distance between the point and the polygon.

In order to apply LCP methods to solve this problem, we need to formulate it in terms of convex quadratic programming as discussed in Section 14.3.2. The objective function must be of the form $f(\mathbf{x}) = \mathbf{x}^T \mathbf{S} \mathbf{x} - \mathbf{c}^T \mathbf{x} + K$, where \mathbf{S} is a positive-semidefinite matrix. The constraints are of the form $\mathbf{A}\mathbf{x} \leq \mathbf{b}$ and $\mathbf{x} \geq \mathbf{0}$. The objective function is simple enough to construct. The vector \mathbf{x} is a point that is inside the

polygon (includes points on the boundary). We want to choose \mathbf{x} to minimize the squared distance,

$$f(\mathbf{x}) = |\mathbf{x} - \mathbf{P}|^2 = \mathbf{x}^T I \mathbf{x} - 2\mathbf{P}^T \mathbf{x} + |\mathbf{P}|^2$$

where I is the 2×2 identity matrix. Clearly we should choose $S = I$, which is positive-definite, $\mathbf{c} = 2\mathbf{P}$, and $K = |\mathbf{P}|^2$. Since the polygon vertices are in the first quadrant, we know that $\mathbf{x} \geq \mathbf{0}$.

The remaining constraints occur because \mathbf{x} must be inside the polygon. If \mathbf{N}_i is an outer normal to the polygon edge with direction $\mathbf{V}_{i+1} - \mathbf{V}_i$, then \mathbf{x} is inside the polygon whenever $\mathbf{N}_i \cdot (\mathbf{x} - \mathbf{V}_i) \leq 0$ for all i . The matrix A in the constraints is created by selecting row i to be \mathbf{N}_i^T . The vector \mathbf{b} in the constraints is created by selecting row i to be $\mathbf{N}_i \cdot \mathbf{V}_i$.

The conversion to an LCP of the form $\mathbf{w} = \mathbf{q} + M\mathbf{z}$ with $\mathbf{w} \geq \mathbf{0}$, $\mathbf{z} \geq \mathbf{0}$, and $\mathbf{w} \circ \mathbf{z} = \mathbf{0}$ was discussed earlier. We choose inputs,

$$M = \left[\begin{array}{c|c} 2S & A^T \\ \hline -A & 0 \end{array} \right], \quad \mathbf{q} = \left[\begin{array}{c} -\mathbf{c} \\ \hline \mathbf{b} \end{array} \right]$$

The output \mathbf{w} is not important for this application, but the other output is $\mathbf{z} = [\mathbf{x} | \mathbf{u}_d]^T$. We need only the first block \mathbf{x} of the output, which corresponds to the closest point of the polygon to \mathbf{P} .

Pseudocode for computing the distance from \mathbf{P} to the polygon is listed below. The convex polygon object has an array of vertices denoted `vertex`.

```

double Distance (vector P, ConvexPolygon C)
{
    int n = C.vertex.size();

    // translate to first quadrant (if necessary)
    vector min = C.vertex[0];
    for (i = 1; i < n; i++)
    {
        if ( C.vertex[i].x < min.x )
            min.x = C.vertex[i].x;
        if ( C.vertex[i].y < min.y )
            min.y = C.vertex[i].y;
    }
    if ( min.x < 0 || min.y < 0 )
    {
        P -= min;
        for (i = 0; i < n; i++)
            C.vertex[i] -= min;
    }

    // compute coefficients of objective function
    matrix S[2][2] = identity_2; // the 2-by-2 identity matrix
    vector c = 2.0*P;

```

```

// double K = Dot(P,P); not needed in the code

// compute constraint matrix and vector
matrix A[n][2];
vector b[n];
for (i0 = n-1, i1 = 0; i1 < n; i0 = i1++)
{
    vector normal = Perp(C.vertex[i1]-C.vertex[i0]);
    A[i1][0] = normal.x;
    A[i1][1] = normal.y;
    b[i1] = Dot(normal,C.vertex[i0]);
}

// compute inputs for LCP solver
matrix M[n+2][n+2] = Block(2*S,Transpose(A),-A,zero_nxn);
vector q[n+2] = Block(-c,b);

// compute outputs
vector w[n+2], z[n+2];
LCPSolver(M,q,w,z);

// compute closest point and distance to P
vector closest(z[0],z[1]);
return sqrt(Dot(closest-P,closest-P));
}

// The parameter names match those in the section discussing LCP
// where w = q + Mz. The inputs are the matrix M and the vector
// q. The outputs are the vectors w and z.
void LCPSolver (Matrix M, Vector q, Vector& w, Vector& z);

```

The function `Perp` takes a vector (x, y) and returns $(y, -x)$. We also assume an implementation of an LCP solver of the form shown in the pseudocode. An actual implementation for an LCP solver is on the CD-ROM.

Distance Between Point and Convex Polyhedron

This problem is nearly identical in formulation to the one for computing the distance from a point to a convex polygon. The convex polyhedron must be translated to the first octant if it is not already located there. The polyhedron is made up of a collection of n faces. The only information we need from the polyhedron for the setup is for face i , a vertex \mathbf{V}_i , and an outer normal \mathbf{F}_i for that face. If the query point is \mathbf{P} , the objective function is still $f(\mathbf{x}) = |\mathbf{x} - \mathbf{P}|^2 = \mathbf{x}^T I \mathbf{x} - 2\mathbf{P}^T \mathbf{x} + |\mathbf{P}|^2$, where \mathbf{x} is a point inside the polyhedron. Because we have required the polyhedron to be in the first octant, we know that $\mathbf{x} \geq \mathbf{0}$. The constraint matrix A is $n \times 3$ with the transpose of the face normal \mathbf{N}_i^T as its i th row. The constraint vector \mathbf{b} is $n \times 1$ with i th row given by $\mathbf{N}_i \cdot \mathbf{V}_i$.

The conversion to an LCP of the form $\mathbf{w} = \mathbf{q} + M\mathbf{z}$ with $\mathbf{w} \geq \mathbf{0}$, $\mathbf{z} \geq \mathbf{0}$, and $\mathbf{w} \circ \mathbf{z} = \mathbf{0}$ was discussed earlier. We choose inputs,

$$M = \begin{bmatrix} 2S & A^T \\ -A & 0 \end{bmatrix}, \quad \mathbf{q} = \begin{bmatrix} -\mathbf{c} \\ \mathbf{b} \end{bmatrix}$$

The output \mathbf{w} is not important for this application, but the other output is $\mathbf{z} = [\mathbf{x} | \mathbf{u}_d]^T$. We need only the first block \mathbf{x} of the output, which corresponds to the closest point of the polygon to \mathbf{P} .

Pseudocode for computing the distance from \mathbf{P} to the polyhedron follows. The convex polyhedron object is assumed to have any data structures and methods that are necessary to support the calculations.

```

double Distance (vector P, ConvexPolyhedron C)
{
    int nv = C.vertex.size();

    // translate to first octant (if necessary)
    vector min = C.vertex[0];
    for (i = 1; i < nv; i++)
    {
        if ( C.vertex[i].x < min.x )
            min.x = C.vertex[i].x;
        if ( C.vertex[i].y < min.y )
            min.y = C.vertex[i].y;
        if ( C.vertex[i].z < min.z )
            min.y = C.vertex[i].y;
    }
    if ( min.x < 0 || min.y < 0 )
    {
        P -= min;
        for (i = 0; i < nv; i++)
            C.vertex[i] -= min;
    }

    // compute coefficients of objective function
    matrix S[3][3] = identity_3; // the 3-by-3 identity matrix
    vector c = 2.0*P;
    // double K = Dot(P,P); not needed in the code

    // compute constraint matrix and vector
    int n = C.face.size();
    matrix A[n][3];
    vector b[n];
    for (i = 0; i < n; i++)
    {
        A[i][0] = C.face[i].normal.x;
        A[i][1] = C.face[i].normal.y;
    }
}

```

```

        A[i][2] = C.face[i].normal.z;
        b[i] = Dot(C.face[i].normal,C.face[i].vertex);
    }

    // compute inputs for LCP solver
    matrix M[n+3][n+3] = Block(2*S,Transpose(A),-A,zero_nxn);
    vector q[n+3] = Block(-c,b);

    // compute outputs
    vector w[n+3], z[n+3];
    LCPSolver(M,q,w,z);

    // compute closest point and distance to P
    vector closest(z[0],z[1],z[2]);
    return sqrt(Dot(closest-P,closest-P));
}

```

As you can see, the structure of the code is nearly identical to that for convex polygons.

Distance Between Convex Polygons

Two convex polygons are specified, the first C_0 with vertices $\mathbf{V}_i^{(0)}$ for $0 \leq i < n_0$ and the second C_1 with vertices $\mathbf{V}_i^{(1)}$ for $0 \leq i < n_1$. Both sequences of vertices are counterclockwise ordered. As we had arranged in the point-object calculators discussed previously, a translation is applied (if necessary) to place both polygons in the first quadrant. Let \mathbf{P}_0 denote a point inside C_0 and let \mathbf{P}_1 denote a point inside C_1 . We want to choose one point in each polygon to minimize the squared distance $|\mathbf{P}_0 - \mathbf{P}_1|^2$. The setup to solve this using LCP methods is similar to that for computing distance between a point and a convex polygon, except that the unknown vector \mathbf{x} will be 4-dimensional. The unknown vector and the objective function are

$$\mathbf{x} = \begin{bmatrix} \mathbf{P}_0 \\ \mathbf{P}_1 \end{bmatrix}, f(\mathbf{x}) = |\mathbf{P}_0 - \mathbf{P}_1|^2 = [\mathbf{P}_0^T \mid \mathbf{P}_1^T] \begin{bmatrix} I & -I \\ -I & I \end{bmatrix} \begin{bmatrix} \mathbf{P}_0 \\ \mathbf{P}_1 \end{bmatrix} = \mathbf{x}^T S \mathbf{x}$$

where I is the 2×2 identity matrix. The matrix S is 4×4 , has diagonal blocks I and off-diagonal blocks $-I$. S is positive-semidefinite since it is symmetric and its eigenvalues are $\lambda = 0$ and $\lambda = 2$, both nonnegative numbers.

Since the polygons are in the first quadrant, both $\mathbf{P}_0 \geq \mathbf{0}$ and $\mathbf{P}_1 \geq \mathbf{0}$ and the non-negativity constraint $\mathbf{x} \geq \mathbf{0}$ are satisfied. The other constraints arise from requiring the points be in their convex polygons. Let $\mathbf{N}_i^{(j)}$ denote outer normals for polygon C_j for the edge of direction $\mathbf{V}_{i+1}^{(j)} - \mathbf{V}_i^{(j)}$. The point containment imposes the constraints,

$$\mathbf{N}_i^{(j)} \cdot (\mathbf{P}_j - \mathbf{V}_i^{(j)}) \leq 0$$

for $0 \leq i < n_j$. The constraint matrix A is $(n_0 + n_1) \times 4$ and is a block diagonal matrix $A = \text{Diag}(A_0, A_1)$, where A_j is $n_j \times 2$. The i th row of A_j is the transposed normal vector $N_i^{(j)}$. The constraint vector \mathbf{b} is $(n_0 + n_1) \times 1$ and consists of two blocks \mathbf{b}_j of size $n_j \times 1$. The i th row of \mathbf{b}_j is $N_i^{(j)} \cdot \mathbf{V}_i^{(j)}$. As before the inputs to the LCP solver are

$$M = \left[\begin{array}{c|c} 2S & A^T \\ \hline -A & 0 \end{array} \right], \quad \mathbf{q} = \begin{bmatrix} \mathbf{0} \\ \bar{\mathbf{b}} \end{bmatrix}$$

but in this case $\mathbf{c} = \mathbf{0}$. The output $\mathbf{z} = [\mathbf{x} | *]^T$ where the first block produces a pair of closest points on the polygons.

The pseudocode is similar yet again to what we had before.

```
double Distance (ConvexPolygon C0, ConvexPolygon C1)
{
    int n0 = C0.vertex.size(), n1 = C1.vertex.size();

    // translate to first quadrant (if necessary)
    vector min = C0.vertex[0];
    for (i = 1; i < n0; i++)
    {
        if ( C0.vertex[i].x < min.x )
            min.x = C0.vertex[i].x;
        if ( C0.vertex[i].y < min.y )
            min.y = C0.vertex[i].y;
    }
    for (i = 0; i < n1; i++)
    {
        if ( C1.vertex[i].x < min.x )
            min.x = C1.vertex[i].x;
        if ( C1.vertex[i].y < min.y )
            min.y = C1.vertex[i].y;
    }
    if ( min.x < 0 || min.y < 0 )
    {
        for (i = 0; i < n0; i++)
            C0.vertex[i] -= min;
        for (i = 0; i < n1; i++)
            C1.vertex[i] -= min;
    }

    // Compute coefficients of objective function, identity_2 is the
    // 2-by-2 identity matrix.
    matrix S[4][4] = Block(identity_2,-identity_2,
                           -identity_2,identity_2);
    vector c = zero_4; // the 4-by-1 zero vector
    // double K = 0; not needed in the code
```

```

// compute constraint matrix and vector
matrix A0[n0][2], A1[n1][2];
vector b0[n0], b1[n1];
for (i0 = n0-1, i1 = 0; i1 < n0; i0 = i1++)
{
    vector normal = Perp(C0.vertex[i1]-C0.vertex[i0]);
    A0[i1][0] = normal.x;
    A0[i1][1] = normal.y;
    b0[i1] = Dot(normal,C0.vertex[i0]);
}
for (i0 = n1-1, i1 = 0; i1 < n0; i0 = i1++)
{
    vector normal = Perp(C1.vertex[i1]-C1.vertex[i0]);
    A1[i1][0] = normal.x;
    A1[i1][1] = normal.y;
    b1[i1] = Dot(normal,C1.vertex[i0]);
}
matrix A[n0+n1][4] = BlockDiagonal(A0,A1);
vector b[n0+n1] = Block(b0,b1);

// compute inputs for LCP solver
int n = n0+n1;
matrix M[n+4][n+4] = Block(2*S,Transpose(A),-A,zero_nxn);
vector q[n+4] = Block(-c,b);

// compute outputs
vector w[n+4], z[n+4];
LCPSolver(M,q,w,z);

// compute closest points P0 in C0 and P1 in C1 and
// distance |P0-P1|
vector P0(z[0],z[1]), P1(z[2],z[3]);
return sqrt(Dot(P0-P1,P0-P1));
}

```

Distance Between Convex Polyhedra

The LCP formulation is similar to the previous ones. The convex polyhedra are C_0 and C_1 . A translation must be applied to make sure both polyhedra are in the first octant. Let the number of faces of C_j be denoted n_j . The outer-pointing normal for face i is $N_i^{(j)}$ and a vertex on the face for use in constraints is $V_i^{(j)}$. The goal is to find points $P_j \in C_j$ that minimize $|P_0 - P_1|$. The construction parallels that of distance between convex polygons. The unknown vector is $\mathbf{x}^T = [P_0^T | P_1^T]$ and is six-dimensional. The objective function is $f(\mathbf{x}) = \mathbf{x}^T S \mathbf{x}$, where S is a 6×6 matrix whose diagonal blocks are the 3×3 identity matrix I and whose off-diagonal blocks are $-I$.

The eigenvalues of S are 0 and 2, so S is positive-semidefinite. The constraint matrix A is $(n_0 + n_1) \times 6$ and the constraint vector \mathbf{b} is $(n_0 + n_1) \times 1$, both constructed similarly to what was done for convex polygons. Pseudocode is

```

double Distance (ConvexPolyhedron C0, ConvexPolyhedron C1)
{
    int nv0 = C0.vertex.size(), nv1 = C1.vertex.size();

    // translate to first octant (if necessary)
    vector min = C0.vertex[0];
    for (i = 1; i < nv0; i++)
    {
        if ( C0.vertex[i].x < min.x )
            min.x = C0.vertex[i].x;
        if ( C0.vertex[i].y < min.y )
            min.y = C0.vertex[i].y;
    }
    for (i = 0; i < nv1; i++)
    {
        if ( C1.vertex[i].x < min.x )
            min.x = C1.vertex[i].x;
        if ( C1.vertex[i].y < min.y )
            min.y = C1.vertex[i].y;
    }
    if ( min.x < 0 || min.y < 0 )
    {
        for (i = 0; i < nv0; i++)
            C0.vertex[i] -= min;
        for (i = 0; i < nv1; i++)
            C1.vertex[i] -= min;
    }

    // Compute coefficients of objective function, identity_3 is the
    // 3-by-3 identity matrix.
    matrix S[6][6] = Block(identity_3,-identity_3,
                           -identity_3,identity_3);
    vector c = zero_6; // the 6-by-1 zero vector
    // double K = 0; not needed in the code

    // compute constraint matrix and vector
    int n0 = C0.face.size(), n1 = C1.face.size();
    matrix A0[n0][2], A1[n1][2];
    vector b0[n0], b1[n1];
    for (i0 = n0-1, i1 = 0; i1 < n0; i0 = i1++)
    {
        vector normal = C0.face[i].normal;
        A0[i1][0] = normal.x;
        A0[i1][1] = normal.y;
        b0[i0] = C0.face[i].b;
        b1[i1] = C1.face[i].b;
    }
}

```

```

        A0[i1][2] = normal.z;
        b0[i1] = Dot(normal,C0.face[i].vertex);
    }
    for (i0 = n1-1, i1 = 0; i1 < n0; i0 = i1++)
    {
        vector normal = C1.face[i].normal;
        A1[i1][0] = normal.x;
        A1[i1][1] = normal.y;
        A1[i1][2] = normal.z;
        b1[i1] = Dot(normal,C1.face[i].vertex);
    }
    matrix A[n0+n1][6] = BlockDiagonal(A0,A1);
    vector b[n0+n1] = Block(b0,b1);

    // compute inputs for LCP solver
    int n = n0+n1;
    matrix M[n+6][n+6] = Block(2*S,Transpose(A),-A,zero_nxn);
    vector q[n+6] = Block(-c,b);

    // compute outputs
    vector w[n+6], z[n+6];
    LCPSolver(M,q,w,z);

    // compute closest points P0 in C0 and P1 in C1 and
    // distance |P0-P1|
    vector P0(z[0],z[1],z[2]), P1(z[3],z[4],z[5]);
    return sqrt(Dot(P0-P1,P0-P1));
}

```

Once again we have assumed that the data members and methods of the class for the convex polyhedron have enough structure to support the queries required in the distance calculator.

14.4.2 CONTACT FORCES

The derivation of contact forces for colliding rigid bodies is presented in detail in [Section 6.6](#). The impulsive force construction to modify the linear and angular velocities simultaneously for all contact points was formulated as the following abstract problem: Minimize $|Af + b|^2$ subject to the constraints $f \geq 0$, $Af + b \geq 0$, and $Af + b \leq c$, where A is a known $n \times n$ matrix and b and c are known $n \times 1$ vectors. The impulse magnitudes f are required by the collision response system. The postimpulse velocities $d^+ = Af + b$ are also required, but can be computed once f is known. The quadratic function expands to $f^T(A^T A)f + (2b^T A)f + |b|^2$. This is a classical problem of quadratic programming that can be formulated as a LCP.

To see this, [Section 14.3.2](#) lists a variable x , a quadratic function $x^T Sx - c^T x + K$, where S is a constant positive-definite symmetric matrix, c is a constant vector, and

K is a constant scalar. The section also mentions constraints $\mathbf{x} \geq \mathbf{0}$ and $A\mathbf{x} \leq \mathbf{b}$, where A is a constants matrix and \mathbf{b} is a constant vector. Please observe that the A , \mathbf{b} , and \mathbf{c} of the problems stated on page 496 are not the same as those of [Section 14.3.2](#). To make clear the differences, the variables of [Section 6.6.2](#) remain the same, namely, A , \mathbf{b} , and \mathbf{c} . Rename the variables of [Section 14.3.2](#) to A_0 , \mathbf{b}_0 , and \mathbf{c}_0 . The formulation of the problem of [Section 6.6.2](#) as an LCP is as follows. Define $S = A^T A$, $\mathbf{c}_0 = -2\mathbf{b}^T A$, and $K = |\mathbf{b}|^2$. The constraints of [Section 6.6.2](#) are restated as $-A\mathbf{x} \leq \mathbf{b}$ and $A\mathbf{x} \leq \mathbf{c} - \mathbf{b}$. The constraint matrix of [Section 14.3.2](#) is $A_0 = \{\{-A\}, \{A\}\}$, where the bracket notation means that A_0 is a 2×1 block matrix whose block of the first row is $-A$ and whose block of the second row is A . The constraint vector of [Section 14.3.2](#) is $\mathbf{b}_0 = \{\{\mathbf{b}\}, \{\mathbf{c} - \mathbf{b}\}\}$, also a 2×1 block matrix whose block of the first row is \mathbf{b} and whose block of the second row is $\mathbf{c} - \mathbf{b}$.

The resting contact force construction to prevent the rigid bodies from interpenetrating was formulated as [equation \(6.103\)](#), $\ddot{\mathbf{d}} = A\mathbf{g} + \dot{\mathbf{b}}$. The outer normals at the n contact points are as before. The resting contact forces are postulated as $g_i \mathbf{N}_i$, where $g_i \geq 0$ is required to satisfy the nonpenetration constraints. The force magnitudes are stored as a vector $\mathbf{g} \geq \mathbf{0}$. The acceleration of the first body in the direction \mathbf{N}_i has magnitude \ddot{d}_i . The magnitudes are stored as a vector $\ddot{\mathbf{d}}$. The nonpenetration constraint requires that $\ddot{\mathbf{d}} \geq \mathbf{0}$. The matrix A is the same one used for impulsive force calculations. The vector \mathbf{b} is defined by [equation \(6.104\)](#). We also had a complementarity condition $\ddot{\mathbf{d}} \circ \mathbf{g} = \mathbf{0}$. Once again an LCP solver can be applied, where $M = A$, $\mathbf{q} = \mathbf{b}$, $\mathbf{w} = \ddot{\mathbf{d}}$, and $\mathbf{z} = \mathbf{g}$. The outputs $\ddot{\mathbf{d}}$ and \mathbf{g} are what the collision response system needs to adjust the forces and torques that are used by the differential equation solver to update the rigid body states. Pseudocode for both of these problems is presented in [Section 6.6](#) immediately following their derivations.

BIBLIOGRAPHY

- [Ani97] M. Anitescu. *Modeling Rigid Multi Body Dynamics with Contact and Friction*. Doctoral dissertation, University of Iowa, Iowa City, Iowa, 1997.
- [AP97] M. Anitescu and F. A. Potra. Formulating dynamic multi-rigid-body contact problems with friction as solvable linear complementarity problems. *Nonlinear Dynamics*, 14:231–247, 1997.
- [Arv91] J. Arvo, editor. *Graphics Gems II*. Academic Press, San Diego, CA, 1991.
- [AS65] M. Abramowitz and I. A. Stegun. *Handbook of Mathematical Functions with Formulas, Graphs, and Mathematical Tables*. Dover Publications, Inc., New York, NY, 1965.
- [Bar84] A. Barr. Global and local deformations of solid primitives. *Proceedings of SIGGRAPH 1984*, pages 21–30, 1984.
- [Bar94] D. Baraff. Fast contact force computation for nonpenetrating rigid bodies. *Proceedings of SIGGRAPH 1994*, pages 23–34, 1994.
- [Bar01] D. Baraff. Physically based modeling: Rigid body simulation. <http://www.pixar.com/companyinfo/research/pbm2001/notesp.pdf>, 2001.
- [Bau72] J. Baumgarte. Stabilization of constraints and integrals of motion in dynamical systems. *Computer Methods in Applied Mechanics and Engineering*, 1:1–16, 1972.
- [BF01] R. L. Burden and J. D. Faires. *Numerical Analysis, 7th edition*. Brooks/Cole, Belmont, CA, 2001.
- [Bra84] M. Braun. *Differential Equations and Their Applications*, volume 15 of *Applied Mathematical Sciences*. Springer-Verlag, Heidelberg, Germany, 1984.
- [BS64] R. Bulirsch and J. Stoer. Fehlerabschätzungen und extrapolation mit rationalen Funktionen bei Verfahren von Richardson-typus. *Numerische Mathematik*, 6:413–427, 1964.
- [BS99] M. Buck and E. Schömer. Interactive rigid body manipulation with obstacle contacts. <http://www.mpi-sb.mpg.de/~schoemer/publications/JVCA98.pdf>, 1999.
- [Cam97] S. Cameron. Enhancing GJK: Computing minimum and penetration distances between convex polyhedra. *Proceedings of the IEEE Conference on Robotics and Automation*, pages 591–596, 1997.
- [Cat05] E. Catto. Iterative dynamics with temporal coherence. <http://www.continuousphysics.com/ftp/pub/test/physics/papers/iterativeDynamics.pdf>, 2005.

- [CBP05] S. Clavet, P. Beaudoin, and P. Poulin. Particle-based viscoelastic fluid simulation. In *Symposium on Computer Animation 2005*, pages 219–228, July 2005.
- [CC86] S. Cameron and R.K. Culley. Determining the minimum translational distance between convex polyhedra. In *Proc. IEEE Int. Conf. on Robotics and Automation*, pages 591–596, 1986.
- [CLMP95] J. Cohen, M. Lin, D. Manocha, and K. Ponamgi. I-COLLIDE: An interactive and exact collision detection system for large-scaled environments. *Proceedings of ACM International 3D Graphics Conference*, pages 189–196, 1995.
- [CLR90] T. H. Cormen, C. E. Leiserson, and R. L. Rivest. *Introduction to Algorithms*. MIT Press, Cambridge, MA, 1990.
- [Coq90] S. Coquillart. Extended free form deformation: A sculpturing tool for 3D geometric design. *Proceedings of SIGGRAPH 1990*, pages 187–193, 1990.
- [CPS92] R. W. Cottle, J. -S. Pang, and R. E. Stone. *The Linear Complementarity Problem*. Academic Press, San Diego, CA, 1992.
- [CRE01] E. Cohen, R. F. Riesenfeld, and G. Elber. *Geometric Modeling with Splines: An Introduction*. A. K. Peters, Natick, MA, 2001.
- [CW96] K. Chung and W. Wang. Quick collision detection of polytopes in virtual environments. *Proceedings of ACM Symposium on Virtual Reality Software and Technology*, pages 125–131, 1996.
- [Dan63] G. B. Dantzig. *Linear Programming and Extensions*. Princeton University Press, Princeton, NJ, 1963.
- [DK90] D. P. Dobkin and D. G. Kirkpatrick. Determining the separation of preprocessed polyhedra—a unified approach. In *Proceedings of the 17th International Colloquium on Automata, Languages, and Programming (ICALP), Lecture Notes in Computer Science*, volume 443, pages 400–413, Heidelberg, Germany, 1990. Springer-Verlag.
- [DKL98] E. B. Dam, M. Koch, and M. Lillholm. Quaternions, animation and interpolation. 103 pages, <http://citeseer.nj.nec.com/dam98quaternions.html>, 1998.
- [DZ91] M. J. Dehaemer and M. J. Zyda. Simplification of objects rendered by polygonal approximations. *Computer & Graphics*, 15(2):175–184, 1991.
- [Ebe07] D. H. Eberly. *3D Game Engine Design*. Morgan Kaufmann, San Francisco, CA, 2nd edition, 2007.
- [Ede87] H. Edelsbrunner. *Algorithms in Computational Geometry*. Springer-Verlag, Heidelberg, Germany, 1987.
- [EL00] S. Ehmann and M. C. Lin. Accelerated proximity queries between convex polyhedra using multi-level Voronoi marching. *Proceedings of IEEE/RSJ International Conference on Intelligent Robots and Systems 2000*, 2000.

- [EL01] S. Ehmann and M. C. Lin. Accurate and fast proximity queries between polyhedra using surface decomposition. In *Computer Graphics Forum (Proceedings of Eurographics 2001)*, page 11 pages, 2001.
- [EM85] H. Edelsbrunner and H. A. Maurer. Finding extreme points in three dimensions and solving the post-office problem in the plane. *Information Processing Letters*, 21:39–47, 1985.
- [EMF02] D. Enright, S. Marschner, and R. Fedkiw. Animation and rendering of complex water surfaces. In *Proceedings of SIGGRAPH 2002*, pages 243–255, 2002.
- [Eri03] C. Ericson. *Real Time Collision Detection*. Morgan Kaufmann, San Francisco, CA, 2003.
- [Far90] G. Farin. *Curves and Surfaces for Computer Aided Geometric Design: A Practical Guide*. Academic Press, San Diego, CA, 1990.
- [Far99] G. Farin. *NURBS: From Projective Geometry to Practical Use*. A. K. Peters, Natick, MA, 1999.
- [Fau96] F. Faure. An energy-based approach for contact force computation. In *Computer Graphics Forum (Proceedings of Eurographics 1996)*, volume 16, pages 357–366, 1996.
- [FF01] N. Foster and R. Fedkiw. Practical animation of liquids. In *Proceedings of SIGGRAPH 2001*, pages 23–30, 2001.
- [Fri98] J. Friedman. Linear complementarity and mathematical (non-linear) programming. <http://www.math.ubc.ca/~jf/courses/340/pap.pdf>, April 1998.
- [FSJ01] R. Fedkiw, J. Stam, and H.W. Jensen. Visualization of smoke. In *Proceedings of SIGGRAPH 2001*, pages 15–22, 2001.
- [GAM03] Geometric Algorithms for Modeling, Motion, and Animation). <http://www.cs.unc.edu/~geom>, 2003.
- [Gea71] C. W. Gear. *Numerical Initial-Value Problems in Ordinary Differential Equations*. Prentice-Hall, Englewood Cliffs, NJ, 1971.
- [GF90] E. G. Gilbert and C. -P. Foo. Computing the distance between general convex objects in three-dimensional space. *IEEE Transactions on Robotics and Automation*, 6(1):53–61, 1990.
- [GH97] M. Garland and P. Heckbert. Surface simplification using quadric error metrics. *Proceedings of SIGGRAPH 1997*, pages 209–216, 1997.
- [GJK88] E. G. Gilbert, D. W. Johnson, and S. S. Keerthi. A fast procedure for computing the distance between complex objects in three-dimensional space. *IEEE Journal of Robotics and Automation*, 4(2):193–203, 1988.
- [GLM96] S. Gottschalk, M. Lin, and D. Manocha. OBBTree: A hierarchical structure for rapid interference detection. *Proceedings of SIGGRAPH 1996*, pages 171–180, 1996.

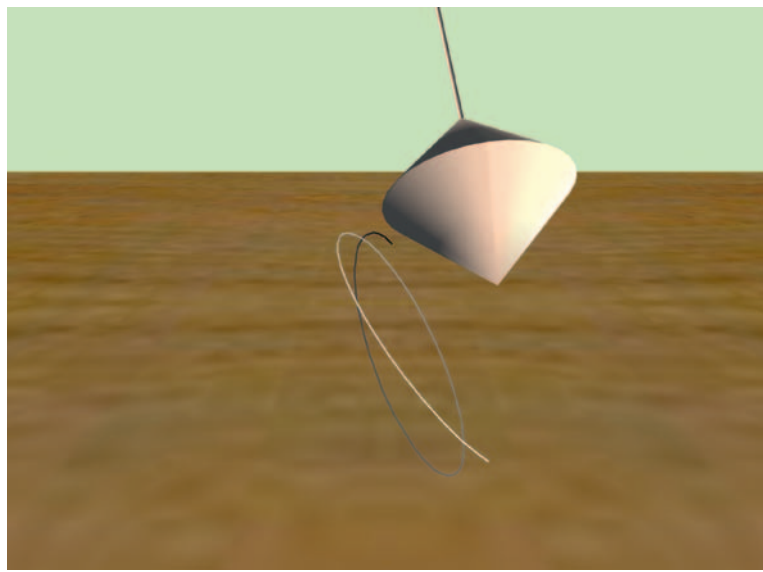
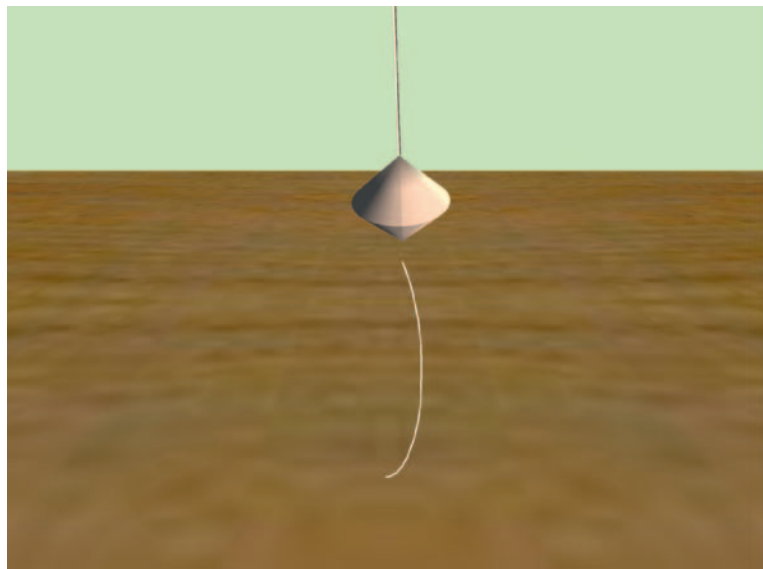
- [GP89] J. Griessmair and W. Purgathofer. Deformation of solids with trivariate B-splines. In *Proceedings of Eurographics 1989*, pages 134–148, 1989.
- [GPS02] H. Goldstein, C. Poole, and J. Safko. *Classical Mechanics, 3rd Edition*. Addison-Wesley, San Francisco, CA, 2002.
- [Gra65] W. B. Gragg. On extrapolation algorithms for ordinary initial-value problems. *SIAM Journal on Numerical Analysis*, 2:384–403, 1965.
- [GV91] G. Vanecik, Jr. Brep-index: A multi-dimensional space partitioning tree. In *ACM/SIGGRAPH Symposium on Solid Modeling Foundations and CAD Applications*, pages 35–44, 1991.
- [Har08] M. Harris. Cuda fluid simulation in nvidia physx. http://sa08.idav.ucdavis.edu/CUDA_physx_fluids.Harris.pdf, 2008.
- [HDD⁺93] H. Hoppe, T. DeRose, T. Duchamp, J. McDonald, and W. Stuetzle. Mesh optimization. *Proceedings of SIGGRAPH 1993*, pages 19–26, 1993.
- [Hec98] C. Hecker. Rigid body dynamics. <http://www.d6.com/users/checker/dynamics.htm>, 1998.
- [HJ85] R. A. Horn and C. R. Johnson. *Matrix Analysis*. Cambridge University Press, Cambridge, England, 1985.
- [HKK07] T. Harada, S. Koshizuka, and Y. Kawaguchi. Smoothed particle hydrodynamics on GPUs. In *Proc. of Computer Graphics International*, pages 63–70, 2007.
- [HKL⁺99] G. Hotz, A. Kerzmann, C. Lennerz, R. Schmid, E. Schmer, and T. Warken. Calculation of contact forces. In *Proceedings of the ACM Symposium on Virtual Reality Software and Technology 1999*, pages 180–181, 1999.
- [HLC⁺97] T. Hudson, M. Lin, J. Cohen, S. Gottschalk, and D. Manocha. V-COLLIDE: Accelerated collision detection for VRML. *Proceedings of VRML 1997*, page 7 pages, 1997.
- [HML99] G. Hirota, R. Maheshwari, and M. C. Lin. Fast volume-preserving free form deformation using multi-level optimization. *ACM Solid Modeling 1999*, pages 234–245, 1999.
- [HOS99] D. J. Hardy, D. I. Okunbor, and R. D. Skeel. Symplectic variable step-size integration for N-body problems. *Applied Numerical Mathematics*, 29:19–30, 1999.
- [HS74] M. W. Hirsch and S. Smale. *Differential Equations, Dynamical Systems, and Linear Algebra*. Academic Press, San Diego, CA, 1974.
- [Hub96] P. M. Hubbard. Approximating polyhedra with spheres for time-critical collision detection. *ACM Transactions on Graphics*, 15(3):179–210, 1996.
- [IZLM01] K. E. Hoff III, A. Zaferakis, M. Lin, and D. Manocha. Fast and simple 2D geometric proximity queries using graphics hardware. *Proceedings of ACM Symposium on Interactive 3D Graphics*, 2001.

- [IZLM02] K. E. Hoff III, A. Zaferakis, M. Lin, and D. Manocha. Fast 3D geometric proximity queries between rigid and deformable models using graphics hardware acceleration. Technical Report TR02-004, Department of Computer Science, University of North Carolina, 2002.
- [Jak01] T. Jakobsen. Advanced character physics. In *Game Developers Conference Proceedings 2001*, pages 383–401, San Francisco, CA, 2001. CMP Media, Inc.
- [JBD09] J. K. Johnson, D. Bickson, and D. Dolev. Fixing convergence of gaussian belief propagation. *CoRR*, abs/0901.4192, 2009.
- [Kir83] D. G. Kirkpatrick. Optimal search in planar subdivisions. *SIAM Journal on Computing*, 12:28–35, 1983.
- [KKS96] M.-J. Kim, M.-S. Kim, and S. Y. Shin. A compact differential formula for the first derivative of a unit quaternion curve. *The Journal of Visualization and Computer Animation*, 7(1):43–58, 1996.
- [KLM02] Y. J. Kim, M. C. Lin, and D. Manocha. DEEP: Dual-space expansion for estimating penetration depth between convex polytopes. *Proceedings of the IEEE International Conference on Robotics and Automation*, page 6 pages, 2002.
- [Kui99] J. B. Kuipers. *Quaternions and Rotation Sequences: A Primer with Applications to Orbits, Aerospace, and Virtual Reality*. Princeton University Press, Princeton, NJ, 1999.
- [LC87] W. E. Lorensen and H. Cline. Marching cubes: A high resolution 3D surface construction algorithm. *Proceedings of SIGGRAPH 1987*, pages 163–169, 1987.
- [LC91] M. C. Lin and J. F. Canny. A fast algorithm for incremental distance calculation. In *Proceedings of IEEE International Conference on Robotics and Automation*, pages 1008–1014, 1991.
- [Lev00] R. Levine. Collision of moving objects. On the game developer algorithms list at <http://www.sourceforge.net>, November 2000.
- [LGLM99] E. Larsen, S. Gottschalk, M. C. Lin, and D. Manocha. Fast proximity queries with swept sphere volumes. Technical Report TR99-018, Department of Computer Science, University of North Carolina, 1999.
- [Lin93] M. C. Lin. *Efficient Collision Detection for Animation and Robotics*. Doctoral dissertation, University of California at Berkeley, Berkeley, California, 1993.
- [MCG03] M. Müller, D. Charypar, and M. Gross. Particle-based fluid simulation for interactive applications. In *Proceedings of SIGGRAPH 2003*, pages 154–159, 2003.
- [MHHR06] M. Müller, B. Heidelberger, M. Hennex, and J. Ratcliff. Position based dynamics. In *Proceedings of Virtual Reality Interactions and Physical Simulations (VRIPhys)*, pages 71–80, 2006.
- [Mir96a] B. Mirtich. Fast and accurate computation of polyhedral mass properties. *Journal of Graphics Tools*, 1(2):31–50, 1996.

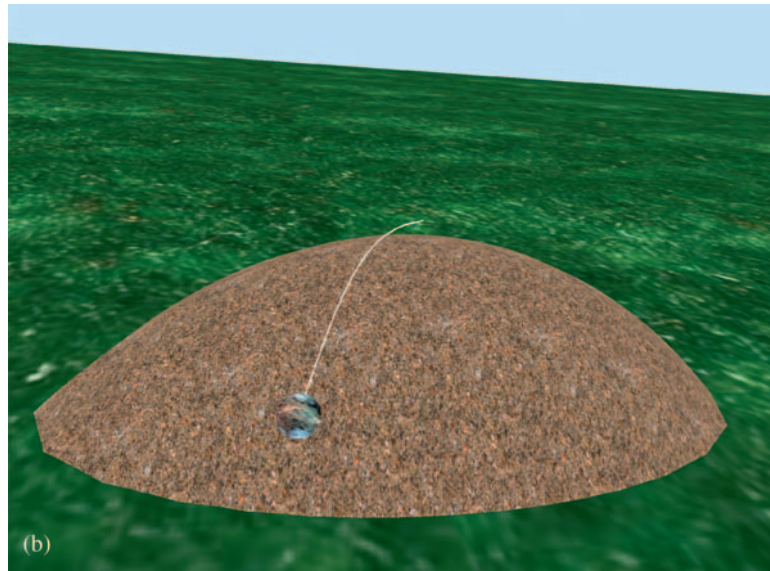
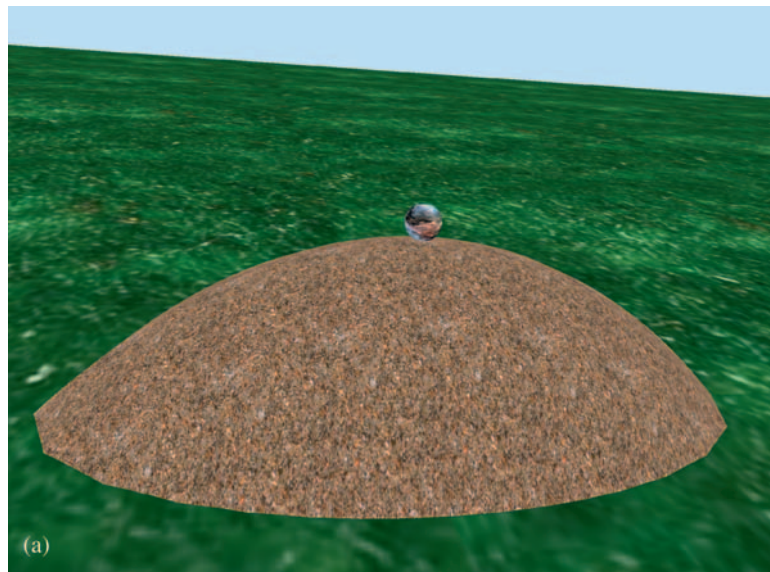
- [Mir96b] B. Mirtich. *Impulse-based dynamic simulation of rigid body systems*. Doctoral dissertation, University of California at Berkeley, Berkeley, California, 1996.
- [Mir98] B. Mirtich. V-Clip: Fast and robust polyhedral collision detection. *ACM Transactions on Graphics*, 17(3):177–208, 1998.
- [Mon92] J. J. Monaghan. Smoothed particle hydrodynamics. *Review of Astronomy and Astrophysics*, 30:543–574, 1992.
- [Mül08] M. Müller. Hierarchical position based dynamics. In *Proceedings of Virtual Reality Interactions and Physical Simulations (VRIPhys)*, 2008.
- [NFJ02] D. Q. Nguyen, R. Fedkiw, and H. W. Jensen. Physically based modeling and animation of fire. In *Proceedings of SIGGRAPH 2002*, pages 721–728, 2002.
- [OF03] S. Osher and R. Fedkiw. *Level Set Methods and Dynamic Implicit Surfaces*. Springer-Verlag, New York, NY, 2003.
- [O'R98] J. O'Rourke. *Computational Geometry in C*, 2nd ed. Cambridge University Press, Cambridge, England, 1998.
- [PFTV88] W. H. Press, B. P. Flannery, S. A. Teukolsky, and W. T. Vetterling. *Numerical Recipes in C: The Art of Scientific Computing*. Cambridge University Press, Cambridge, England, 1988.
- [Pir] H. Pirzadeh. Rotating calipers home page. <http://www.cs.mcgill.ca/orm/rotcal.html>.
- [PS85] F. P. Preparata and M. I. Shamos. *Computational Geometry: An Introduction*. Springer-Verlag, Heidelberg, Germany, 1985.
- [RG27] L. F. Richardson and J. A. Gaunt. The deferred approach to the limit. *Philosophical Transactions of the Royal Society of London*, 226A:299–361, 1927.
- [Rho01] G. S. Rhodes. Stable rigid-body physics. In *Game Developers Conference Proceedings 2001*, pages 651–669, San Francisco, CA, 2001. CMP Media, Inc.
- [RKC00] S. Redon, A. Kheddar, and S. Coquillart. An algebraic solution to the problem of collision detection for rigid polyhedral objects. In *Proceedings of IEEE International Conference on Robotics and Automation*, pages 3733–3738, 2000.
- [RKC01] S. Redon, A. Kheddar, and S. Coquillart. Contact: arbitrary in-between motions for continuous collision detection. In *Proceedings of the 10th IEEE International Workshop on Robot-Human Interactive Communication*, page 6 pages, 2001.
- [RKC02a] S. Redon, A. Kheddar, and S. Coquillart. Fast continuous collision detection between rigid bodies. In *Proceedings of Eurographics 2002*, page 9 pages, 2002.
- [RKC02b] S. Redon, A. Kheddar, and S. Coquillart. Gauss' least constraints principle and rigid body simulations. In *Proceedings of IEEE International Conference on Robotics and Automation*, page 6 pages, 2002.

- [Rog01] D. F. Rogers. *An Introduction to NURBS with Historical Perspective*. Morgan Kaufmann, San Francisco, CA, 2001.
- [SB08] H. Schechter and R. Bridson. Evolving sub-grid turbulence for smoke animation. In *Proceedings of the 2008 ACM/Eurographics Symposium on Computer Animation*, 2008.
- [SE02] P. J. Schneider and D. H. Eberly. *Geometric Tools for Computer Graphics*. Morgan Kaufmann, San Francisco, CA, 2002.
- [Set99] J. A. Sethian. *Level Set Methods and Fast Marching Methods*. Cambridge University Press, Cambridge, England, 1999.
- [SP86] T. Sederberg and S. Parry. Free-form deformation of solid geometric models. *Proceedings of SIGGRAPH 1986*, pages 151–160, 1986.
- [SP09] B. Solenthaler and R. Pajarola. Predictive-corrective incompressible SPH. In *Proceedings of SIGGRAPH 2009*, pages 1–6, 2009.
- [SRF05] A. Selle, N. Rasmussen, and R. Fedkiw. A vortex particle method for smoke, water and explosions. In *Proceedings of SIGGRAPH 2005*, pages 910–914, 2005.
- [SSW99] E. Schömer, J. Sellen, and M. Welsch. Exact geometric collision detection. <http://www.mpi-sb.mpg.de/~schoemer/publications/EGCD.pdf>, 1999.
- [ST99] E. Schömer and C. Tiel. Efficient collision detection for moving polyhedra. <http://www.mpi-sb.mpg.de/~schoemer/publications/ECDFMP.pdf>, 1999.
- [Sta03] J. Stam. Real-Time Fluid Dynamics for Games. In *Proceedings of the Game Developer Conference, March 2003*, March 2003.
- [Str88] G. Strang. *Linear Algebra and its Applications, 3rd edition*. International Thomson Publishing, 1988.
- [SZL92] W. J. Schroeder, J. A. Zarge, and W. E. Lorensen. Decimation of triangle meshes. *Proceedings of SIGGRAPH 1992*, pages 65–70, 1992.
- [Tur92] G. Turk. Re-tiling of polygonal surfaces. *Proceedings of SIGGRAPH 1992*, pages 55–64, 1992.
- [vdB97] G. van den Bergen. Efficient collision detection of complex deformable models using AABB trees. *Journal of Graphics Tools*, 2(4):1–13, 1997.
- [vdB99] G. van den Bergen. A fast and robust GJK implementation for collision detection of convex objects. *Journal of Graphics Tools*, 4(2):7–25, 1999.
- [vdB01a] G. van den Bergen. Physical behavior and resting contacts with friction. Post to the USENET news group *comp.games.development.programming.algorithms*, August 2001.
- [vdB01b] G. van den Bergen. Proximity queries and penetration depth computation on 3D game objects. In *Proceedings of the Game Developers Conference 2001*, pages 821–837, 2001.

- [vdB01c] G. van den Bergen. SOLID: Software library for interference detection. <http://www.win.tue.nl/gino/solid/>, 2001.
- [vdB03] G. van den Bergen. *Collision Detection in Interactive 3D Environments*. Morgan Kaufmann Publishers, San Francisco, CA, 2003.
- [Ver67] L. Verlet. Computer experiments on classical fluids. I. Thermodynamic properties of Lennard-Jones molecules. *Physical Review*, 159:98–103, 1967.
- [Ves04] M. Vesterlund. Simulation and rendering of a viscous fluid using smoothed particle hydrodynamics. <http://www.cs.umu.se/education/examina/Rapporter/MarcusVesterlund.pdf>, December 2004.
- [Wel67] D. A. Wells. *Lagrangian Dynamics*. Schaum’s Outline Series. McGraw-Hill, New York, 1967.
- [Wit97] A. Witkin. Physically based modeling: Principles and practice, constrained dynamics. In *SIGGRAPH 1997 Course Notes*, 1997.
- [WLML99] A. Wilson, E. Larsen, D. Manocha, and M. Lin. Partitioning and handling massive models for interactive collision detection. In *Computer Graphics Forum (Proceedings of Eurographics 1999)*, volume 18, pages 319–329, 1999.
- [YOH00] G. Yngve, J. O’Brien, and J. Hodgins. Animating explosions. In *Proceedings of SIGGRAPH 2000*, pages 29–36, 2000.
- [ZSP08] Y. Zhang, B. Solenthaler, and R. Pajarola. Adaptive sampling and rendering of fluids on the GPU. In *IEEE / EG Symposium on Point-Based Graphics*, 2008.



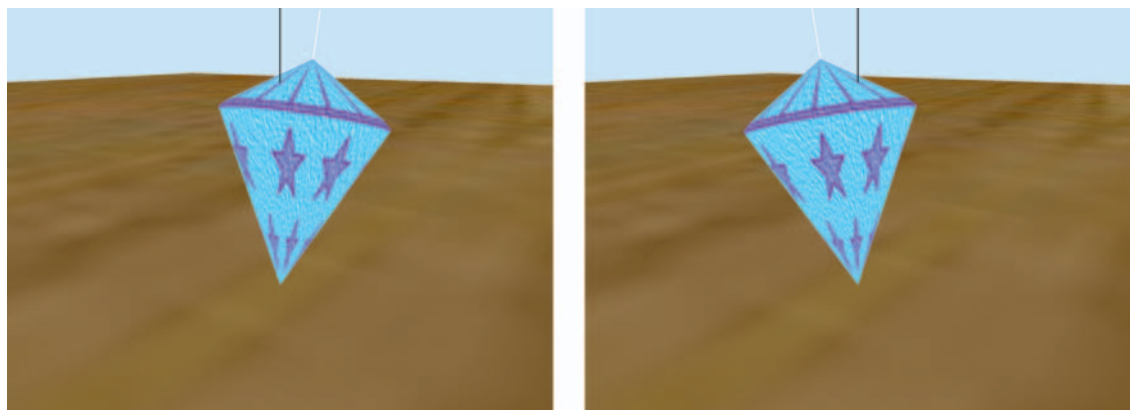
Color Plate 3.3 The Foucault pendulum. The figures show the path of the pendulum tip in the horizontal plane. New points on the path are colored white, but the intensity of the older points along the path gradually decreases.



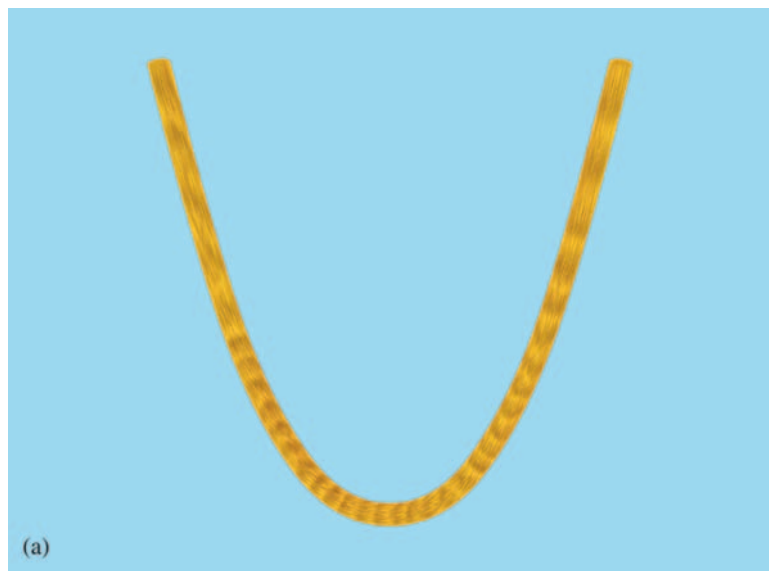
Color Plate 3.7 A ball rolling down a hill. Image (b) shows the path of the center of the ball as it rolls down the hill. The ball rotates at a speed commensurate with its downhill velocity.



Color Plate 3.14 A mass-pulley-spring system shown at two different times. The spring expands and compresses and the pulley disk rotates during the simulation. The system stops when a mass reaches the center line of the pulley or the ground.



Color Plate 3.25 Two snapshots of a freely spinning top. The black line is the vertical axis. The white line is the axis of the top.



Color Plate 4.2 A rope modeled as a linear chain of springs. Image (a) shows the rope at rest with only gravity acting on it. Image (b) shows the rope subject to a wind force whose direction changes by small random amounts.



(a)

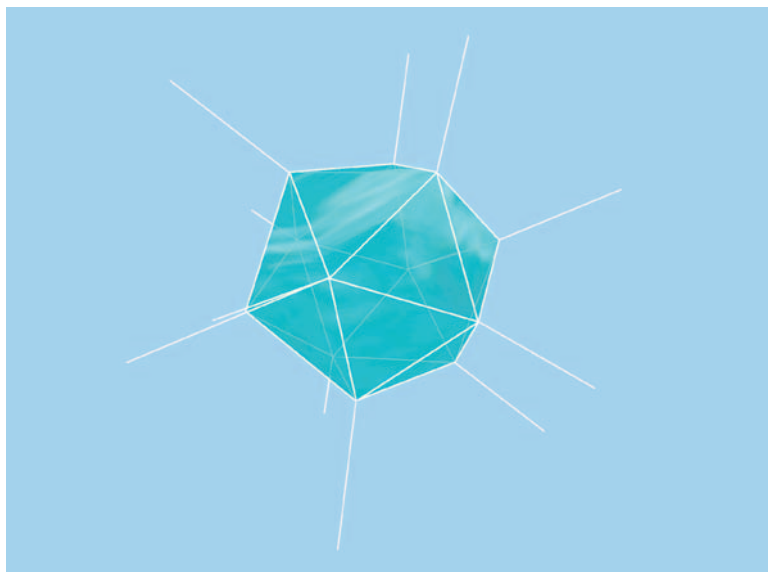
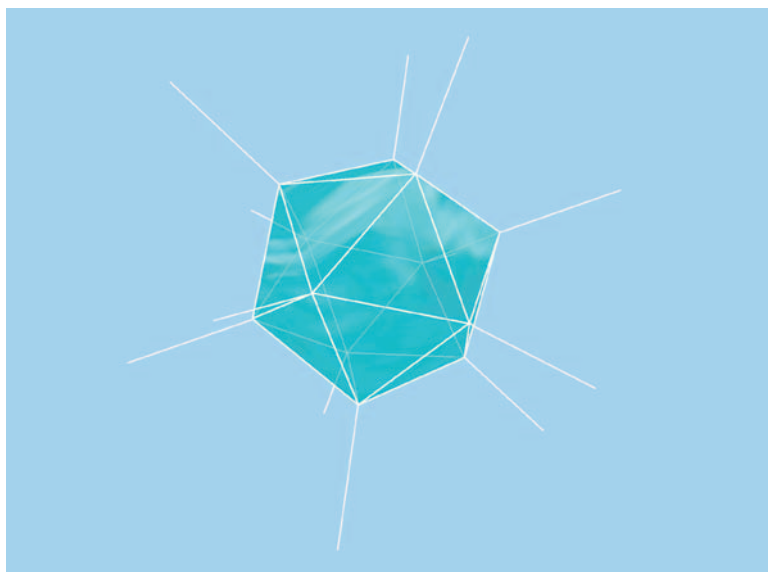


(b)

Color Plate 4.4 A cloth modeled as a rectangular array of springs. Wind forces make the cloth flap about. Notice that the cloth in image (b) is stretched in the vertical direction. The stretching occurs while the gravitational and spring forces balance out in the vertical direction during the initial portion of the simulation.



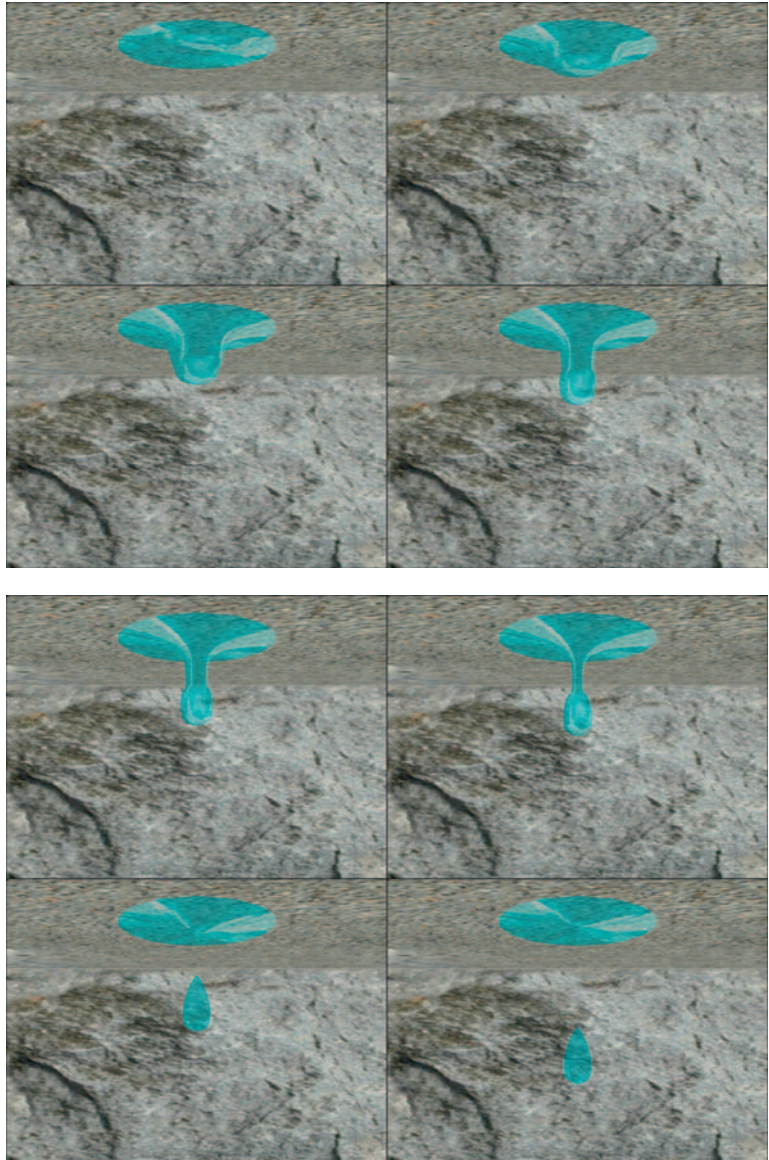
Color Plate 4.6 A gelatinous cube that is oscillating because of random forces. The cube is modeled by a three-dimensional array of mass connected by springs.



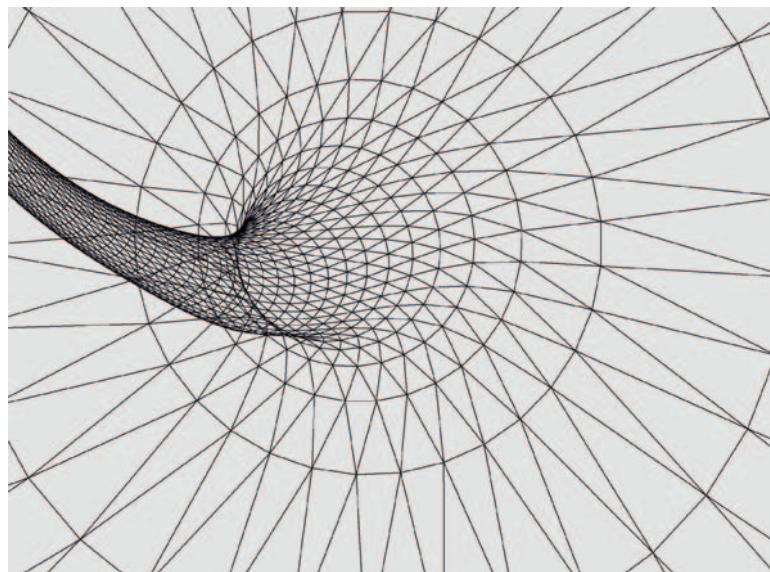
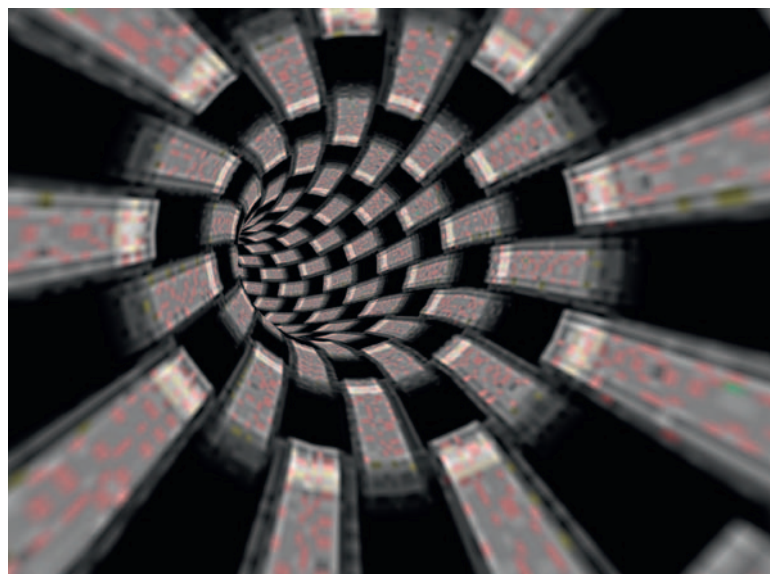
Color Plate 4.7 A gelatinous blob that is oscillating because of small, random forces. This blob has the masses located at the vertices of an icosahedron with additional masses of infinite weight to help stabilize the oscillations. The springs connecting the blob to the infinite masses are shown in white.



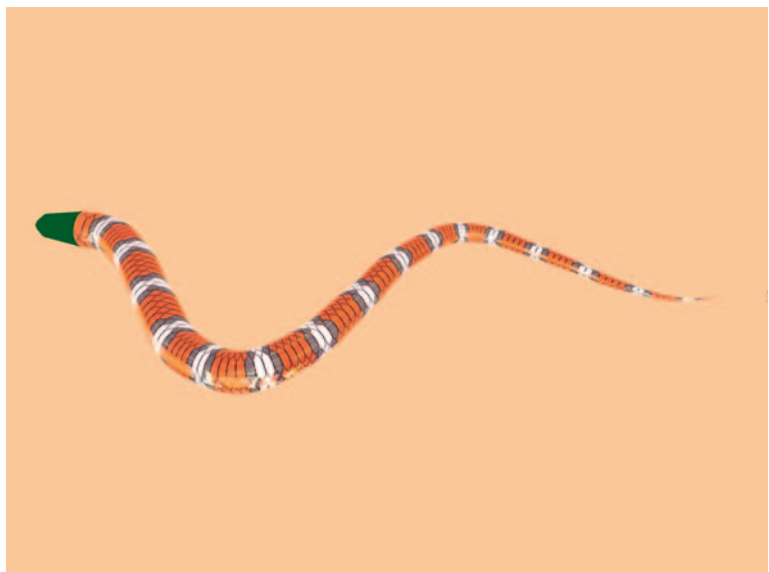
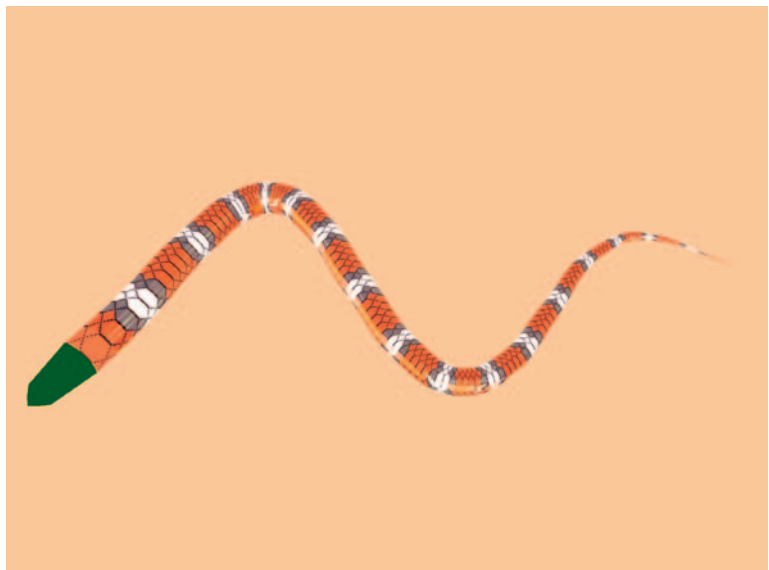
Color Plate 4.15 A skirt modeled by a generalized cylinder surface. Wind-like forces are acting on the skirt and are applied in the radial direction. Image (a) shows the skirt after wind is blowing it about. Image (b) shows a wireframe view of the skirt so that you can see it consists of two closed curve boundaries and is tessellated between.



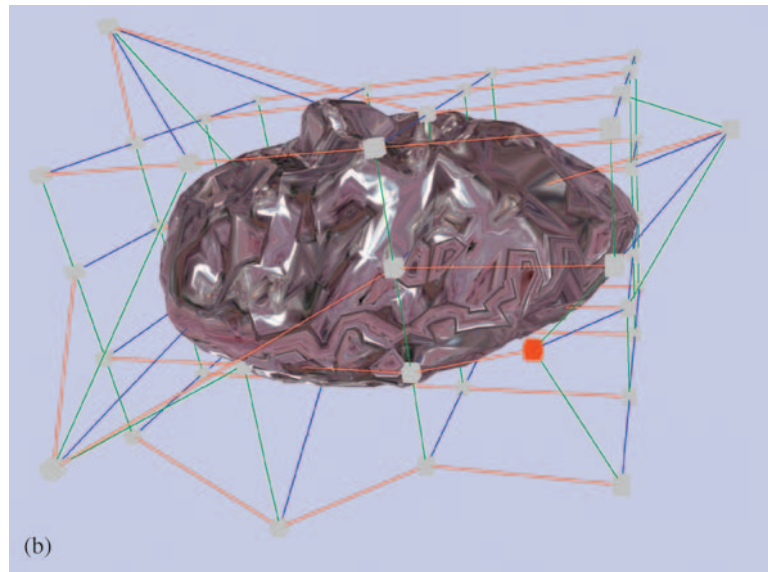
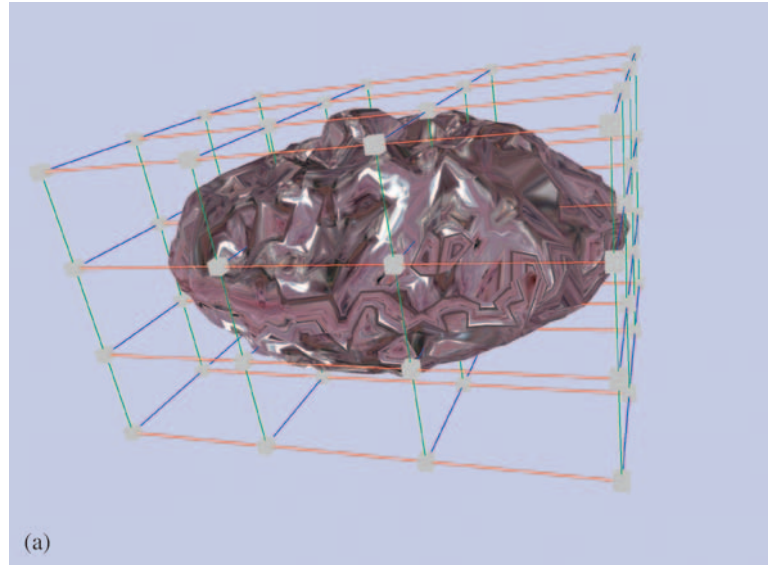
Color Plate 4.17 A water drop modeled as a control point surface of revolution. The surface dynamically changes to show the water drop forming, separating from the main body of water, then falling to the floor. The evolution is from left to right and top to bottom.



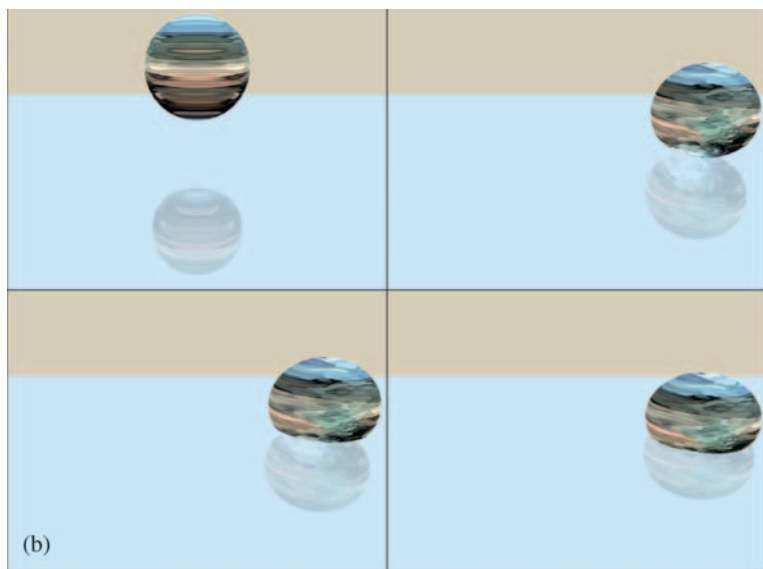
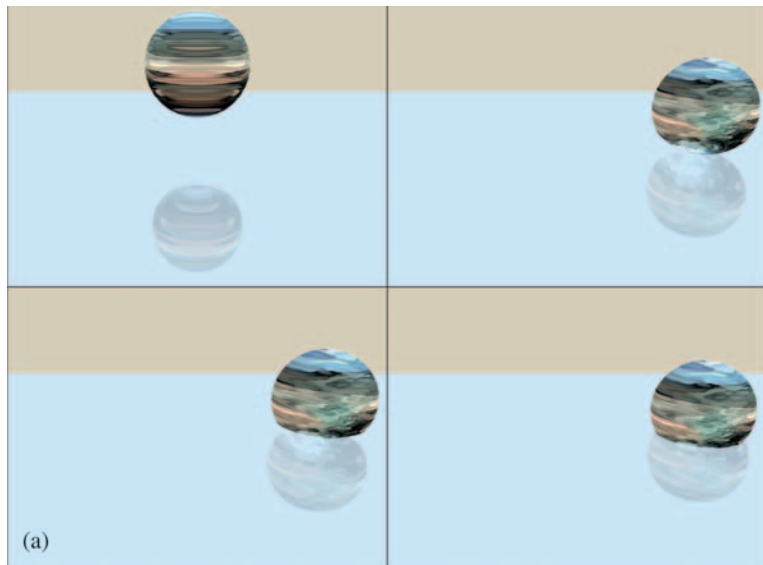
Color Plate 4.18 A closed tube surface whose central axis is a helix.



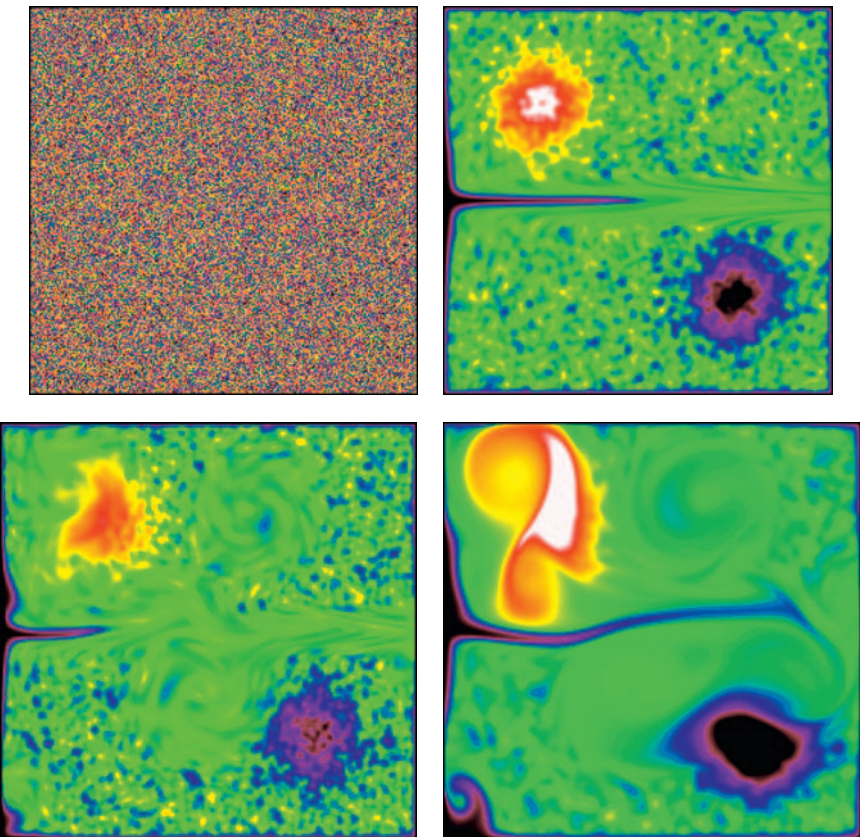
Color Plate 4.19 A wriggling snake modeled as a tube surface whose central curve is a control point curve.



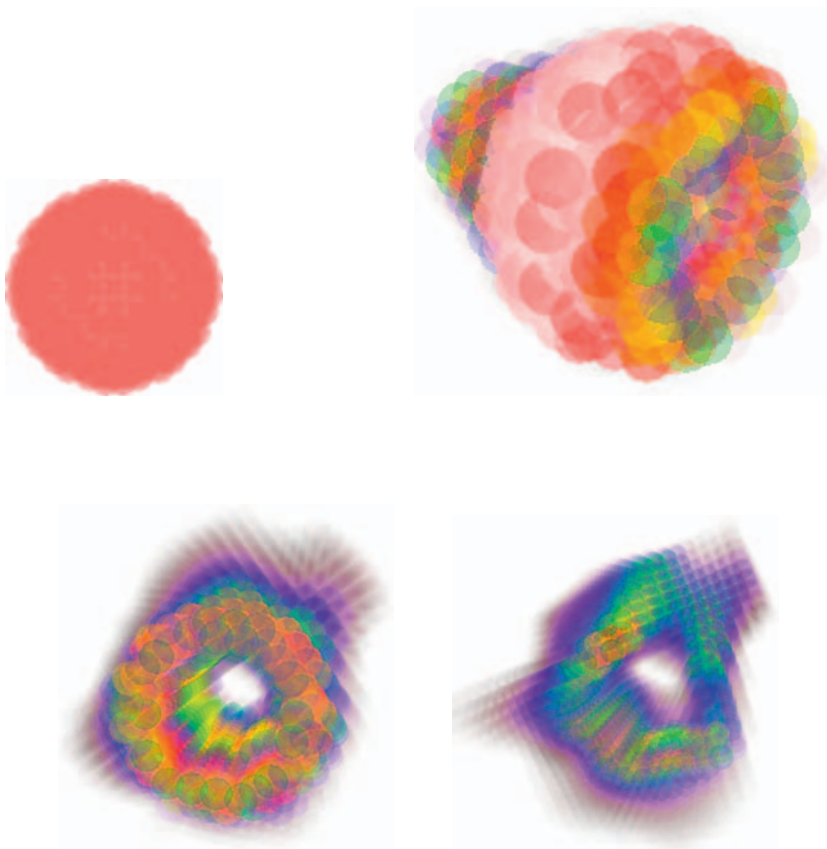
Color Plate 4.20 Free-form deformation. Image (a) shows the initial configuration where all control points are rectangularly aligned. Image (b) shows that some control points have been moved and the surface is deformed. The control point shown in red in (b) is the point at which the mouse was clicked on and moved.



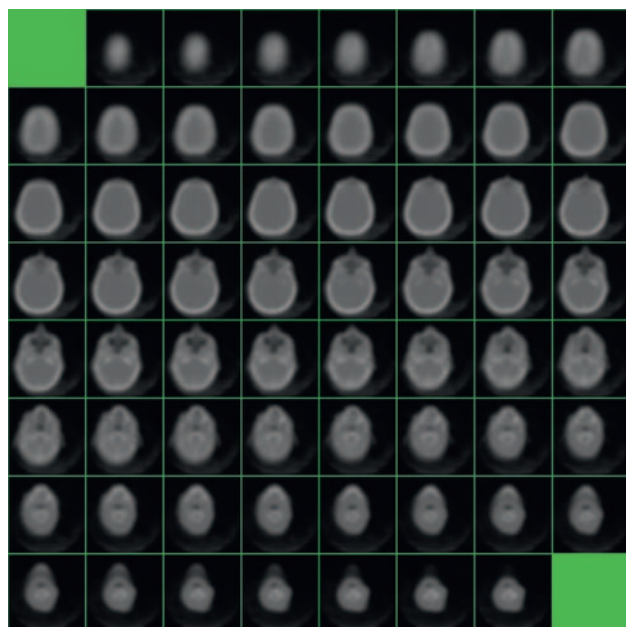
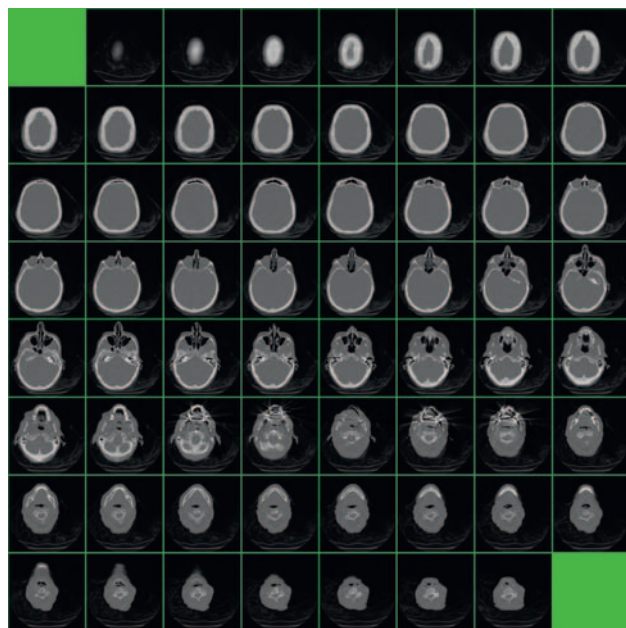
Color Plate 4.29 A bouncing ball with deformation based on implicit surfaces. Image (a) shows the bouncing ball with only the implicit surface deformation. Image (b) shows an additional deformation of nonuniform scaling by applying an affine transformation.



Color Plate 5.4 Image (a) [upper left]: The initial density is generated by a uniform random number generator. Image (b) [upper right]: The evolved density after a small period of time. The only force is due to a spike of wind moving from the left-center of the grid. The bright blob-like region is a density source. The dark blob-like region is a density sink. Image (c) [lower left]: Starting from the random initial density, eight vortices were added to the grid. They are shown in white in the equivalent gray-scale image of Figure 5.4; the direction of rotation is indicated by the arrows. You can see the swirl-like effects of the vortices. Image (d) [lower right]: The grid of image (c) is allowed to evolve further. The density source and sink are more pronounced, and the density is starting to become more homogeneous in regions centered at the vortices.



Color Plate 5.5 Image (a) [upper left]: The initial density is a spherical blob of constant density. Image (b) [upper right]: The evolved density after a small period of time. The only force is due to a spike of wind moving from the right-center of the grid; the scene has been rotated slightly so you can see the portion of the sphere on which the wind interacted first. There are no density sources or sinks. You can see the material being pushed out of the sphere by the wind. Image (c) [lower left]: Eight vortices were added to the grid, which causes the density to swirl around a bit. The scene was rotated so you can see the tunnel carved out by the wind. Image (d) [lower right]: The lower-left grid is allowed to evolve further.



Color Plate 5.6 Image (a) [top] shows the initial $128 \times 128 \times 64$ gray scale image (a CT image). The boundary voxels are drawn in light gray. The $z = 0$ slice is the upper left tile. The $z = 63$ slice is the lower right tile. Image (b) [bottom] shows the 3D image after a number of blurring operations.

INDEX

A

AABBs, *See* Axis-aligned bounding boxes
Absolute value signs, 379, 381
Acceleration, 16
 angular, 25
 centripetal, 17, 25
 drag, 30
 given contact force, 501
 normal, 17
 tangential, 17, 25
Acceleration-based constrained motion, 10, 473–512
 collision points, 474–475
 illustrative implementation, 502–509
 impulses, 476–478
 Lagrangian dynamics, 509–512
 multiple contact points, 483–491
 simultaneous processing of contact points, 491–497
 velocity, 476
Active intervals, 305, *See also* Intersecting intervals
Adams-Basforth explicit solver, 779
Adams-Basforth m -step method, 778, 797
Adams-Moulton m -step method, 779, 797
Addition, 546
 of quaternions, 718
 of vectors, 580f, 583, 585, 586
Additive identity, 539, 580, 585, 589
 of vector(s), 581f
Additive inverse, 539, 587
Adjacent indices, 165
AdjustVelocity, 270, 278
Advection
 density update by, 285
 velocity update by, 285
Advection team, 257–260
Affine algebra, 659–678
 barycentric coordinates, 667–678
 coordinate system, 663–665
 definition for, 660
 parallelogram law for, 661
 subspaces, 665
 transformations, 666–667
Affine coordinate systems, 663–665
Affine coordinates, 663
Affine function, 839
Affine transformation, 211
AGEIA Technologies, 5

Algebra

affine, 659–678
fundamental theorem of, 609–613, 638
linear, 539–658
vectors, 721
Algebraic operations, quaternion, 718–720
Algorithm
 bisection, 400
 broad-phase, 296
 conditionally stable, 254
Fluid2Da, 274
Fluid3Da, 274, 287
Fluid3Db, 287
GJK, 9, 299, 349, 459–464, 534
Lemke, 512, 813, 829–834, 836, 844
Lin-Canny, 464
Marching Cubes, 199–201, 206, 207
Marching Squares, 202
medium-phase, 297
Mirtich, 77
multifunction evaluation, 472
narrow-phase, 297
pseudocode for cylinders, 384
QR, 646
single-stage update, 289
sweep, 305
Taylor's theorem, 792
time-stepping, 526
transport, 258
Alternate basis, 724
Alternating-direction implicit method, 255
AMD Athlon XP 2800, 420
Analytic functions, 734
Angular acceleration, 25
Angular momentum, 41–42, 90
 angular velocity and, 466
 conservation of, 42, 237–238
 in unconstrained motion, 470
 simultaneous updates of, 494
 vector, 151
Angular speed, 25
Angular velocity, 25, 520
 angular momentum and, 466
 boxes moving with, 453–456
 determining, 468
 for body A, 488
 for body B, 488
 impulse equation for, 492
 in body coordinates, 149, 150
 in unconstrained motion, 470

- Angular velocity (*continued*)
 in world coordinates, 149
 OBBs moving with, 537
 of bodies about center of mass, 476
 of disks, 128
 of pipes, 128
 of rigid bodies, 148
 of tops, 150
 postimpulse, 480
 preimpulse, 480
 world coordinates of, 126–127
- Anticommutative cross product, 602
- Antisymmetry, 218
- Applied force, 78, 468, 469
- Approximation, 391
- Arbitrary configurations, mass-spring systems, 165
- Arbitrary equations, 759
- Arc(s)
 bisector, 419
 order of, 419
 sets of, 416
- Arc-arc intersection, 419
- Arc-length parameterization, 487–488
- Area(s)
 approximation of, by rectangles, 770f
 bounded by parabola, 690f
 infinitesimal, 87–88, 690
 of trapezoids, 778
 of triangles, 672–673
 signed, 628
 squared, 628
 under curves, 770f
 unit, of squares, 627f
- Array index, 75
- Array inputs, update function with, 319
- Artificial variables, 819, 820
- Associative, 539, 564, 589
- Associative property, 540
- A-stable method, 812
- Asymptotic sense, 400
- Asymptotic stability, 749
- Asynchronous sorting function, 333
- Augmented matrix, 548, 549, 557, 561
- Autonomous implicit difference equations, 754
- Autonomous ordinary difference equations, 755
- Autonomous systems of equations, 747
- Auxiliary objective function, 819, 820
- Auxiliary variables, 829
 in initial dictionary, 831, 832, 837
- Averaging property, of delta function, 487
- Axioms, 541
- Axis-aligned bounding boxes (AABBs), 298
 colliding with sloped plane, 483f
- culling, using a specialized processor, 335–349
- culling, using separate core of CPU, 330–335
- culling with, 304–349
- endpoints and, 321–323
- enumerations and, 321–323
- intersecting intervals, 304–312
- masks and, 321–323
- overlap test for, 319
- in single-threaded environment, 320–330
- Axis-aligned ellipse, 359–361, 360f, 361f, 371–372, 839
- Axis-aligned rectangles, 313f, 316
- `AxisAlignedBox`, 302

B

- Back substitution, 542, 544, 545, 550, 551
- Backward difference approximation, 706, 708
- Backward substitution, 567
- Bacon, Roger, 6
- Balanced dictionary, 830–832
- Balls, 104–106
 bouncing, 211
- Baraff approach, 473
- Baraff, David, 10, 295
- Barycentric combination, 667
 of simplices, 670–671
 of tetrahedra, 669
 of two points, 668f
- Barycentric coordinates
 affine algebra and, 667–678
 hypervolume, 671–678
 length, 671–678
 of simplices, 670–671
 tetrahedron, 669
 triangles, 668–669
 volume, 671–678
- Bases of tetrahedrons, 674f
- Basic variables, 552, 821
- Basis, 593
 alternate, 724
 change, 623
 different, 621
 Euclidean, 650
 of rectangular solids, 696f
 standard, 724
 standard Euclidean, 595
 vector spaces, 590–595
- Basis functions, 195
 B-spline, 168, 170
 data, 174
- Basis vectors, 624
 feasible, 818, 823
 in block matrix, 664–665

- BasisFunction class, 173, 183
- Bernstein polynomials, 183, 192
- Bézier curve, 730
 - Bézier rectangle patch, 192
 - Bézier volume patch, 192
- Bias, constraint, 526, 529
- Bilinear interpolation, 201, 258, 729
- Bilinear transformation, 602
- Binary space partitioning node (BSP node), 404, 418
- Binary space partitioning tree (BSP tree), 403, 404f, 413
 - external queries, 420t
 - for children of root, 416f
 - for spherical dual, 419
 - generating, 416
 - root of, 415f
- Binning, 302
- Binomial vectors, 21
- Bisection, 387, 390
 - algorithm, 400
 - approach, 421
 - method, 392, 401
- Bisectors
 - arcs, 419
 - choice of, 419
 - convex polygon with, 418f
- Bitmap pixels, 258
- Bivariate approximation, 711
- Bivariate functions, 701, 772
 - derivatives of, 710–711
 - Taylor’s theorem for, 773
- Black box, 425, 780
- Black vector, 425
- Blobs, gelatinous, 167
- Block decomposition, 843
- Block diagonal matrix, 852
- Block matrix, 570–571, 610, 633
 - 2×1 , 856
 - 2×2 , 722
 - basis vectors in, 664–665
 - constructing, 611
- Boards
 - generalized force of, 145
 - kinetic energy of, 144
 - on rough planes, 143–145
- Body axes, 27
- Body coordinates, 27
 - angular velocity in, 149, 150
 - body observer and, 28
 - for rigid bodies, 148
 - frame, 467
 - world observer and, 28
- Body map, 527
- Body observer, 27
 - body coordinate system as seen by, 28
- Body origin, 27
- Book, resting on table, 511f
- Bookkeeping, 548
- Boolean conditions, 293
- Boolean operations, 426
- Boolean return value, 325
 - BoxManager and, 328–329
- Boolean value, 377, 395
- Boolean variables, 331
- Booster rockets, 92
- Bouncing balls, 211
- BouncingBall, 210
- Boundaries, moving, 293
- Boundary cell, 293
- Boundary conditions, 267–268
 - Dirichlet, 221, 247, 250, 267, 272
 - insulated, 271
 - mixed, 272, 276
 - Neumann, 221, 248, 272, 276
- Boundary points, 700–701
- Boundary update function, 253, 269, 279
- Boundary value problems, 222, 269
- BoundaryFunctions, 250, 253, 262, 268
 - rhoBF, 265
 - uBF, 265
 - vBF, 266
- BoundaryType, 250
- Bounded convex sets, constraints defining, 815f
- Bounded regions, 839
- Bounding intervals, 173
- Bounding spheres, 299
 - culling with, 299–304
- Bounding volumes (BVs), 298
- Box(es), *See also* Axis-aligned bounding boxes;
 - Oriented bounding boxes
 - axes, 451
 - black, 425, 780
 - colliding contact, 485
 - collision, with edge-face contact, 510–511
 - collision, with face-face contact, 510–511
 - intersecting, 316–320
 - moving, 453–456
 - moving with angular velocity, 453–456
 - moving with constant linear velocity, 453–459
 - nonoverlapping, 320
 - on rough planes, 146–147
 - overlapping, 320
 - sloped plane and, 485
 - stationary, 425
 - BOX_DMA_TAG, 337, 347

- BoxManager, 317
 Boolean return value in, 328–329
 client of, 326
 CPU implementation, 345–349
 culling system, 323–330
 overlap test, 328
 overlapping, 342
 SPU implementation of, 335
 SPU manager, 338
- BoxManagerCPU, 345
- BoxState, 340, 345
- Branch penalties, 546
- Bridgman, P. W., 6
- Broad-phase algorithm, 296
- Broad-phase collision culling, 9
- Broderbund, 4
- BSP node, *See* Binary space partitioning node
- B-spline basis functions, 168
 recursive dependencies for, 170
- B-spline curves, 168–176
 closing, 175
 evaluation, 169–174
 open, nonuniform, closed, 176
 open, nonuniform, not closed, 176
 open, uniform, closed, 176
 open, uniform, not closed, 176
 periodic, closed, 176
 periodic, not closed, 176
- B-spline surfaces, 179–181
 evaluation, 181
- B-spline volume, 194
 function, 196
- BSplineSurface class, 173
- BSPNode, 406
- BSPTree node, 408
- Bulirsch-Stoer method, 785
- Bulk modulus, 157–158
- Bullet Physics Engine, 5
- Butterfly rule, 629
- BVs, *See* Bounding volumes
- C**
- C++, 507
- Cache misses, 546
- Calculus, 679–712
 applications, 698–712
 constrained optimization, 702–705
 differential, 679
 fundamental theorem of, 691
 integral, 679
 multivariate, 679, 692–698
 optimization, 698–702
 univariate, 679, 680–691
 vector, 214–230
- Candidate minima, 702
- Capsules, test-intersection query, 350–353
- Cardinality, 593–594
- Cartesian coordinates, 88
 planar motion in, 15–18
 spatial motion in, 19–22
- Cavalieri, Bonaventura Francesco, 691
- Cayley-Hamilton theorem, 742–743
- Center of mass, 42–54, 120–122, 147
 angular velocity of bodies about, 476
 velocity of, 126, 465–466
- Center points, OBB with, 446f
- Centered difference approximation, 706, 708
- Centers of mass, linear momentum of, 494
- Central axis, helix, 191
- Central processing units (CPUs), 4
 BoxManager and, 345–349
 memory, 336f
 relationships among, 336f
- Centripetal acceleration, 17, 25
- Chain rule, 102, 365, 366, 515, 526, 688, 769
 in multivariate calculus, 693–694
- Change of basis, 623
 matrix, 623
- Characteristic equation, 638
- Characteristic polynomials, 740, 743, 748
- Chutes, 108
- Circle
 ellipses moving towards, 367f
 transformed configuration of, 360f, 361f
 unit, 403f
- Classic linear function, 648
- Classical tube surface, 189
- Client code, of culling system, 334
- Closed curves
 control point deformation, 175
 line segment deformation in, 181
- Closed tube surface, 191
- Closest point, 362
- Cloth
 as rectangular array of springs, 163
 wind and, 163
- Codomain, 617, 621
- Coefficient(s)
 drag, 788
 matrix of, 562, 605–606
 negative, 821, 834
 of friction, 136
 of kinetic friction, 35
 of nonbasic variables, 825
 of restitution, 480
 of static friction, 35
 real-valued, 585, 622
 vector, 621
- velocity, 263

- Cofactors
 - expansion, 635, 636
 - matrix of, 634
- Coherence, 300
 - spatial, 300
 - temporal, 300–301
- Coincident lines, 553f
- Coincident planes, 555f
- Colliding contact, 473, 474
 - collision response for, 475–497
 - contact force and, 499–500
 - of box edge with sloped plane, 485
 - order of operations for handling, 502
 - points of, 491
 - pseudocode for processing, 481
- Collins, Steven, 5
- Collision culling. *See* Culling
- Collision detection, 296, 496–497, 502
 - constant linear velocity, 421–444
 - convex polyhedra separation, 435–436
 - edge-edge contact, 427
 - GJK algorithm, 459–464
 - implementation and timing, 420–421
 - method of separating axes, 394–395
 - separation of convex polygons, 422–426
 - stationary objects, 396–421
 - vertex-edge contact, 427
 - vertex-vertex contact, 427
 - with convex polyhedra, 390–464
- Collision points, 474–475, 493
 - processing, 484
- Collision response, 296, 855
 - for colliding contact, 475–497
 - for resting contact, 498–502
 - function, 503
- Collision system, 302, 489
 - intersection detection in, 391
- CollisionGroup**, 535
- Column matrix, 548, 562
 - $n \times 1$, 617
- Column variables, 821, 822
- Column vector, $m \times 1$, 819, 842
- Commutative operations, 539, 564, 589
- Commutative property, 540
- Complementary slackness, 828, 838, 843, 844
- Complementary variables, 829
 - in dictionary, 831, 833
 - leaving dictionary, 837–838
 - pairs of, 836
- Complete sets, 541
- Complex numbers, 541
 - imaginary part of, 719
 - product of, 546
 - real part of, 719
- Complex-valued roots, 760
- Compressible flow, 292
- Compressible fluids, 292
- Computation by direct parameterization of triangles, 72–74
- Compute function, 173
- ComputeClosestPoint, 368, 370, 374
- ComputeContact, 369, 374
- ComputeInterval, 409, 411, 423, 425, 428, 438, 454
- ComputeLPCMMatrix, 504
- ComputePreImpulseVelocity, 505
- ComputeRestingContactVector, 505
- Concurrent forces, 38
- Conditionally stable algorithms, 254
- Conjugate gradient method, 389, 561
- Conservation laws, 237–246
 - of mass, 238–242
 - of momentum, 242–246
- Conservation of energy, 292
- Conservation of volume, 542
- Conservative forces, 80–84
 - Lagrangian equations of motion and, 129–135
- Consistency
 - in numerical methods, 795
 - of Euler's method, 795
- Constant angular velocity, 457–459
- Constant coefficient equations, 759–762
- Constant density, 288f
- Constant linear velocity, 113f, 133, 350, 454–456
 - boxes moving with, 453–454
 - objects moving with, 421–444
- Constant scalar, 856
- Constant vectors, 87, 832, 856
- Constant-coefficient linear systems, stability for, 747–749
- Constants matrix, 856
- Constrained local minimum, 841
- Constrained motion, 297
- Constrained optimization, 702–705
- Constraining forces, 99, 159
 - determining, 109–111
- Constraining functions, 838
- Constrain(s)
 - matrix, 849, 852
 - vector, 849
- Constraint force, 514, 515, 816
 - computing, 518–519, 525
- Constraint(s)
 - bias, 526, 529
 - components, 843
 - defining bounded convex sets, 815f
 - defining unbounded convex set, 815f
 - equality, 680, 821

- Constraint(s) (*continued*)
 - first derivative of, 513, 515–516, 520
 - function, 839, 843
 - functions, 530, 839
 - in forming convex domain, 817f
 - inequality, 528–529, 680, 817
 - linear inequality, 820f, 826
 - matrix, 849, 852
 - nonnegativity, 820f, 825
 - nonpenetration, 473, 534
 - normal-form, 819
 - on particles, 512–515
 - on rigid bodies, 519–522
 - on rigid body system, 522–525
 - redundant, 817
 - second derivative of, 513, 517–518, 521–522
 - specified, 817
 - velocity, 533
- Construction of inverses, 570–572
- Contact caching scheme, 526, 532
- Contact force, 855–856
 - accelerations given, 501
 - choosing, 501
 - colliding contact and, 499–500
 - computation of, 499
 - resting, 856
- Contact forces, 473, 495
 - exerting, 499
- Contact manifold, 296
- Contact model, 529
- Contact points, 368, 496–497
 - edge-edge intersection, 499
 - finite set of, 489
 - multiple, 483–491
 - reporting, 393
 - rigid bodies, 529f
 - simultaneous processing of, 491–497
 - vertex-face intersection, 499, 502
- Contact set, 296
 - convex polygons for, 426–435
 - for convex polyhedra, 436–444
 - reduced, 475f
- Contact space formulation, 534
- Contact time, computing, 364–368
- Continuity
 - multivariate calculus, 692
 - univariate calculus, 685
- Continuous dependence
 - initial conditions and, 794
 - of differential equations, 736–738
- Continuous functions, 198, 239
- Continuous mass, 44–45
 - balancing, on a plane, 47
 - in three dimensions, 50–54
 - in two dimensions, 46–50
- Continuous material, 14
 - particle systems, 27–30
- Continuous variables, 206, 684
- Continuum of mass, 14
 - equations of motion for, 118–128
- Contradiction, 594
- Control point deformation, 168–192
 - B-spline curves, 168–176
 - closed curves, 175
 - evolution and, 179, 180
 - initial, 179
 - local control, 175
 - modifying, 176
 - NURBS curves and, 178
 - water drops and, 190
- Control theory, 737
- Control weights, 177, 183
- Convergence, 734, 795
 - in numerical methods, 796
- Convex domain, 816, 828
 - constraints, 817f
 - implied by nonnegativity constraints, 820
 - sketch of, 837
- Convex function, 363, 382, 384, 840
 - graphs of, 841f, 842f
- Convex objects
 - nonintersecting, 395f
 - projection methods, 377
- Convex polygons
 - as stationary objects, 396–408
 - boundary, 815
 - contact set for, 426–435
 - distance between, 851–853
 - distance between points and, 847–849
 - edge-edge contact in, 397f
 - intersecting, 397f, 432
 - nonintersecting, 397f
 - object, 848
 - planar, 408
 - pseudocode for intersecting, 422
 - separation of, 422–426
 - spherical, 417
 - vertex-edge contact in, 397f
 - vertex-vertex contact in, 397f
 - with bisectors, 418f
- Convex polyhedra, 300, 376, 377, 408–414
 - collision detection with, 390–464
 - contact set for, 436–444
 - distance between, 853–855
 - distance between points and, 849–851
 - edge-edge, 409
 - edge-edge contact, 436–437
 - edge-vertex, 409
 - edge-vertex contact, 436–437
 - external query for, 414–420

- face-edge, 409
- face-edge contact, 436–437
- face-face, 409
- face-face contact, 436–437
- face-vertex, 409
- face-vertex contact, 436–437
- nonpenetration of, 390
- point-in spherical-polygon test, 417f
- pseudocode for, 456
- separation of, 435–436
- spherical duals of, 414
- stationary, 421
- TestIntersection* for, 454
- vertex-vertex, 409
- vertex-vertex contact, 436–437
- Convex programming, 840
- Convex quadratic function, 496
- Convex quadratic programming, 843–846
- Convex quadratic programming problem, 493, 813
- Convex quadrilateral, 729f
 - points forming, 729f
- Convex set, 394f
- Convexity, 364
- ConvexPolygon, 399, 404
- ConvexPolyhedron, 410, 438
- Coordinate axis directions, 16, 664
- Coordinate axis stress vectors, 244
- Coordinate system, 16
 - affine algebra, 663–665
 - in planes, 663f
- Coordinate-dependent definition, 601, 602
- Coordinate-dependent formulas, 603
- Coordinate-free description, 596, 602, 603, 674, 675, 720
- Coordinate-free expression, 517
- Copositive matrix, 838, 844
- Copositive skew-symmetric matrix, 838
- CopyArray* function, 256
- Corners, 276
- Cosine, 449
 - law of, 596
- Coulumb's friction law, 531, 535
- Coupled system of second-order differential equations, 107
- Couples, 37
- CPUs, *See* Central processing units
- Crank-Nicholson scheme, 255
- Cray, Seymour, 3
- CreateEvent*, 332
- CreateThread*, 332
- Critical points, 655, 657f
 - KKT, 843
- Cross product, 720
 - anticommutative, 602
- operation, 606
- vector spaces, 600–606
- Cubes, *See also* Marching Cubes algorithm
 - gelatinous, 166
 - transforming, into parallelepiped, 630f
 - unit-volume, 630f
- Cubic polynomials, 730
- Culling, 298–349
 - AABB, 304–349
 - AABB, using specialized processor, 335–349
 - AABB, with separate core of CPU, 330–335
 - BoxManager, 323–330
 - client code and, 334
 - endpoints and, 321–323
 - enumerations and, 321–323
 - intersecting intervals, 304–312
 - masks and, 321–323
 - OBB, 445
 - occlusion, 510
 - sphere-based, 301, 303
 - with bounding spheres, 299–304
- Curl
 - free, 224
 - operator, 218
 - vector calculus, 217–218
 - vector fields and, 226–227
- Current *r*-interval, directions along, 390
- Current-generation processors, 546
- Curve(s), 7, *See also* Isocurve extraction
 - area under, 770f
 - B-spline, 168–176
 - Bézier, 730
 - binomials, 189
 - closed, 175, 181
 - geodesic, 3
 - level, 815f
 - linearly interpolating pairs of points on, 187
 - motion on, 100–102
 - NURBS, 177–179
 - particles constrained to, 514–515
 - pseudocode for, points, 172
 - surfaces built from, 184–192
 - torsion of, 21
- Curve mass, 14, 118
 - in three dimensions, 53–55
- Cusp, 688
- Cycling, 846
- Cylinders
 - axis directions, 380
 - axis perpendiculars, 380–382
 - nonintersection of convex objects by
 - projection methods, 377
 - parallel, 384
 - projection of, 378–379
 - pseudocode for algorithm, 384

- Cylinders (*continued*)

representation of, 376–377

separating axis for, 378–379

separation by projection onto a line, 377–378

separation tests involving cylinder axis directions, 380

separation tests involving cylinder axis perpendiculars, 380–382

separation tests involving other directions, 382–384

surfaces, 186

test-intersection query, 376–390

walls, 376
- Cylindrical coordinates, spatial motion in, 22–23
- D**
- $d \times v$ matrix, 716

D'Alembert's equation, 100, 102

DEC Gigi, 2

Decomposition of space, 301f

DEEP (Dual-space Expansion for Estimating Penetration depth between convex polytopes), 536

Definite integral, 623, 690

Definite matrices, 645

Deformable bodies, 8, 155–212

elasticity and, 156–158

mass-spring systems and, 158–167

strain and, 156–158

stress and, 156–158

Deformation tensor, 233

Degenerate feasible vectors, 825

Delta function, 485–486

averaging property of, 487

Density

constant, 288f

constant along flow lines, 242

diffusion, 284

dissipation, 291–292

equation, 247–249

evolved, 288f

initialization of, 280

sink, 275f

sources, 283

source-sink function, 292

total, update, 261–263

update, 266, 281, 283, 284

update by advection, 285

Dependent vectors, 616

Derivative(s), 131, 363

approximations, by finite differences, 705–710

directional, 214–215, 694–696

first, of constraint, 513

first-order, 383

first-order partial, 516, 750, 773

first-order time, 523

higher-order, 707

multivariate functions, 712

normal vector, 498

of bivariate functions, 710–711

of common functions, 688f

of univariate functions, 705–710

operators, 517

partial, 693, 695

positional, 110

relevant, 110, 113, 127, 133, 139

second test, 656, 657

second, matrix, 384

second, of constraint, 513

second-order, 383

second-order partial, 521, 773, 841

second-order time, 523

spatial, 249

 t , 356

time, 249, 521, 523

total, 111, 214–215

total time, 112

 X , 356

Derived state variables, 471

Descartes, Rene, 6, 691

DestroyEvent function, 332

Destructor, 346

Determinants, 626–637

functions, 630–637

of 2×2 matrix, 626–628

of 3×3 matrix, 629–630

Diagonal entries, 564

Diagonal matrix, 119, 360, 564, 573, 645, 654

block, 852

 $n \times m$ matrix, 564

Diagonalizable matrix, 649, 744

Dictionary, 829

balanced, 830, 831

complementary variables in, 831, 833

complementary variables leaving, 837–838

entering, 830

feasible, 831

initial, 831, 832

initial modified, 845

leaving, 830

terminal, 830, 832

Difference, 581

Minkowski, 459

vectors, 659

Difference approximation

backward, 706, 708

centered, 706, 708

- finite, 708t
- forward, 705–706, 708, 709
- Difference equations, 753–764
 - autonomous implicit, 754
 - constant coefficient, 759–762
 - explicit, 754
 - first-order linear, 756–757
 - homogeneous linear, 756
 - linear, 756–759
 - nonhomogeneous linear, 756
 - n*th order, 753
 - n*th order linear, 763
 - second-order, 754–755
 - second-order linear, 757–759
 - systems of, 762–764
- Differentiable, 687
- Differential calculus, 679
- Differential equations, 2, 10–11, 89, 152, 733–751, 767
 - constant-coefficient, 747–749
 - continuous dependence of, 736–738
 - equilibria, 746–751
 - existence of, 736–738
 - extrapolation methods and, 781–783
 - first-order, 733–738
 - first-order linear, 735
 - first-order nonlinear, 90
 - first-order systems of, 739
 - general-order, 740–741
 - hyperbolic, 257
 - integration of, 574
 - nonlinear, 90
 - nonlinear system of, 469
 - n*th order, 740
 - of motion, 713
 - ordinary, 733
 - orientation, 520
 - parabolic partial, 247
 - partial, 733
 - pseudocode for generating, 802
 - Runge-Kutta fourth order, 471
 - Runge-Kutta methods for, 507
 - second-order, 90, 107, 738–739
 - second-order linear, 124, 135
 - second-order linear systems of, 117
 - second-order system of ordinary, 91
 - solutions, 736
 - solver, 856
 - solvers, 465
 - solving, 97, 136
 - stability, 746–751
 - systems of, 108, 465
 - systems of linear, 741–746
 - unique solutions to, 737
 - uniqueness of, 736–738
- Differentiating equation, 498
- Differentiation, 102
 - univariate calculus, 686–689
 - vector field decomposition and, 225
- Diffusion, 216
 - density, 284
 - term, 249–257
 - times, 291
 - velocity, 284
- Dirac delta function, 222
- Direct memory access (DMA), 335
- Direct sums, 647
 - decomposition, 649
- Direct test, 364–365
- Directional derivative
 - multivariate calculus, 694–696
 - vector calculus, 214–215
- Dirichlet boundary conditions, 221, 247, 250, 267, 272
- Discontinuous functions, 685
 - graphs, 686f
- Discrete mass
 - balancing, 43
 - in one dimension, 43–44
 - in three dimensions, 50
 - in two dimensions, 45–46
- Disjoint lines, 553f
- Disjoint planes, 554
- Disk Operating System (DOS), 2
- Disks
 - angular velocity of, 128
 - on rough inclined plane, 128
- Disk-shaped body, deformations of, 198
- Displacement, infinitesimal, 100
- Dissipation
 - of density, 291–292
 - of velocity, 291–292
- Dissipative forces, 34–36
 - Lagrangian equations of motion and, 135–147
- Distance calculations, 847–855
 - between convex polygons, 851–853
 - between convex polyhedra, 853–855
 - between point and convex polyhedra, 849–851
- Distance functions
 - between point and convex polygon, 847–849
 - parallelogram-parallelogram, 351
 - segment-parallelogram, 351
- Distributions, 222
- Distributive property, 540
- Divergence, 734
- Divergence theorem, 67, 239
 - of stress, 245
 - vector calculus and, 215–217, 220–221
 - vector fields and, 226–227

- Diving boards, 129–130
 Divisions, avoiding, 547
 DMA, *See* Direct memory access
 Dobkin-Kirkpatrick hierarchy, 411, 413, 414, 418
DoCollisionResponse, 503
DoImpulse function, 506
 Domain, 617, 621, 679
 convex, 816, 817f, 828, 837
 triangular, 702
 unbounded, 837
 DOS, *See* Disk Operating System
 Dot equation, 605
 Dot notation, 766
 Dot product, 720
 vector spaces, 600–606
 Double integral, 118
 Double pendulum, 118, 131
 Drag
 acceleration, 30
 coefficient, 788
 simulation of, 788
 velocity, 29
 Dual problem, 825–828
 finite optimal solution to, 828
 infeasible, 828
 unboundedness property, 827–828
 weak duality principle, 827
 Dual slack equation, 844
 Duality
 gap, 847
 general, theory, 846–847
 strong, 828
 weak, 827, 828
 Dual-space Expansion for Estimating
 Penetration depth between convex
 polytopes, *See* DEEP
 Dynamic(s), 7, 86
 friction, 510
 Lagrangian, 8, 77, 85–86, 98–135, 474,
 509–512, 694
 Newtonian, 86–98
 viscosity, 245, 246
 Dynamically equivalent, 121
- E**
- Ear-clipping-based mesh construction, 208–212
 Earth
 motion of, 86–87
 orbit of, 88
 radius of, 91
 rockets leaving, 92
 world coordinate system and, 90–91
- Edge(s)
 moments of inertia for, 62
 products of inertia for, 62
 Edge mesh
 extracted, 208f
 triangle removal in, 209
 Edge-edge contact
 collision detection, 427
 convex polygons, 397f
 convex polyhedra, 436–437
 for moving triangles, 432f
 intersection calculator pseudocode, 433
 Edge-edge intersection, 475
 contact points, 499
 predicted, 426f
 Edge-face contact, box collision with, 510–511
 Edge-face intersection, 465, 475, 511
 Edge-interior point, 461
 Edge-interior voxels, 276
 Edge-vertex contact
 convex polyhedra, 436–437
 intersection calculator pseudocode, 433
 Eigendecomposition
 applications of, 652–658
 for symmetric matrices, 643–646
 of matrices, 751
 Eigenspaces, 638, 794
 generalized, 648
 one-dimensional, 648
 Eigensystems, 643
 Eigenvalues, 59, 625, 637–643, 749, 794
 positive, 810
 row operations, 640
 Eigenvectors, 625, 637–643, 649
 generalized, 651
 linearly independent, 641, 645, 646, 749
 Elasticity, deformable bodies and, 156–158
 Elementary row matrices, 565–567, 572
 3×3 , 566, 569
 inverses of, 569
 order of operations, 567
 Elementary row operations, 548–552
 interchanging rows, 549
 multiplying rows, 549
 Ellipses, 88–89
 axes, 839
 axis-aligned, 359–361, 360f, 361f, 371–372,
 839
 configuration at contact time, 359, 359f
 intersection of, 357f
 moving, 358–359
 points, 366
 stationary, 357–358
 sweeping regions bound by parallel lines,
 365f

- Ellipsoids
 - defined, 704
 - distance between, 704
 - moving, 371–376
 - stationary, 357–358
 - test-intersection query, 353–376
- Elliptical paraboloids, 105, 108
- Empty sets, 814
- Endpoints, 310
 - arrays, 325
 - class, 322
 - culling, 321–323
 - initializing, 341
 - ordering, 340
 - sorting of, 317
 - SPU, 339
- Energy, 77–84, 104
 - conservation of, 292
 - kinetic, 78–80, 102, 104, 106, 113, 116–117, 119, 123, 139, 144, 478f, 479, 491, 492, 694
 - potential, 80–84, 90, 130, 786
 - total potential, 130
 - work, 78–80
- Enumerations, culling, 321–323
- Equalities, 366
 - vector, 584–586
- Equality constraints, 680, 821
- Equations, *See also* Differential equations
 - arbitrary, 759
 - autonomous implicit difference, 754
 - autonomous ordinary difference, 755
 - autonomous systems of, 747
 - characteristic, 638
 - constant coefficient, 759–762
 - coupled system of second-order differential, 107
 - D'Alembert's, 100, 102
 - density, 247–249
 - difference, 753–764
 - differentiating, 498
 - dot, 606
 - dual slack, 844
 - Euler's, of motion, 8, 59, 147–154
 - explicit difference, 754
 - finite-difference, 268, 289
 - first, of motion, 93–94
 - first-order differential, 733–738
 - first-order linear difference, 756–757
 - first-order linear differential, 735
 - first-order ordinary difference, 755
 - first-order systems of differential, 739
 - fourth-order, 760
 - Frenet-Serret, 22
 - general-order differential, 740–741
 - hyperbolic differential, 257
 - impulse, 492
 - Lagrangian, of motion, 99, 100–147, 511
 - Laplace's, 213, 221–224
 - limiting, 845
 - linear, 542–561, 701–702, 756–759
 - linear difference, 756–759
 - linear systems of differential, 117
 - modal, 798, 806–808
 - Navier-Stokes, 9, 213, 244, 258, 263
 - Newton's, of motion, 524
 - nonhomogeneous linear difference, 756
 - nonlinear systems of differential, 469
 - nonsquare systems of, 552
 - normal, 615
 - n*th order differential, 740
 - n*th order difference, 753
 - n*th order linear difference, 763–764
 - of motion, 31, 750
 - ordinary difference, 755
 - ordinary differential, 91, 733
 - orientation differential, 520
 - parabolic partial differential, 247
 - partial differential, 733
 - Poisson's, 213, 221–224, 267, 269, 279, 294
 - polynomial, 356, 760, 806
 - quadratic, 201
 - Runge-Kutta fourth order differential, 471
 - second-order difference, 754–755
 - second-order differential, 90, 107, 738–739
 - second-order linear difference, 757–759
 - second-order linear differential, 124
 - second-order linear systems of differential, 117
 - second-order system of ordinary differential, 91
 - separating, 458
 - solving all possible systems of, 816t
 - stiff, 809–812, 811t
 - system of, 465
 - systems of difference, 762–764
 - systems of linear, 542–561
 - systems of linear differential, 741–746
 - third-order, 761
 - two, in two unknowns, 545–548
 - velocity, 263–270
 - w_4 , 833
 - Equilibrium, 38–40
 - differential equations, 746–751
 - solution, 746–749
 - stable solution, 750
 - unstable solution, 750
 - Erdos, Paul, 6
 - Ethernet, 6
 - Euclidean basis, 650

- Euclidean basis vectors, 613, 618, 632
 - standard, 633
- Euler step, 786, 790
- Euler's equations of motion, 8, 59, 147–154
- Euler's identity, 739
- Euler's method, 509, 530, 766–769
 - consistency of, 795
 - explicit, 800, 801f, 806–807
 - floating point values obtained from, 768
 - implicit, 772, 777, 806–807
 - modified, 770f, 771, 775
- Even permutation, 631
- EVENT_DMA_TAG, 337, 347
- Evolved density, 288f
- Existence, of differential equations, 736–738
- Explicit difference equation, 754
- Explicit Euler's method, 800, 806–807
 - region of stability for, 806f
 - simple pendulum and, 801f
- Explicit method, 255
- Explicit multistep method, 778
- Exponential function, 742
 - properties of, 745
- Exponential of matrices, 653–655
- Extended free form deformation, 196
- External force, 30, 500
 - on body, 524
 - sum of, 244
- External queries
 - BSP tree, 420t
 - for convex polyhedron, 414–420
- External torque, 501
- Externally applied force, 507
- Extrapolation, 779, 780–785
 - Bulirsch-Stoer method, 785
 - polynomial, 783
 - rational polynomial, 783–784
 - Richardson, 780–781
- Extrapolation methods, differential equation and, 781–783
- F**
- Face-edge contact, convex polyhedra, 436–437
- Face-face contact
 - box collision with, 510–511
 - convex polyhedra, 436–437
- Face-face intersection, 442, 465, 511
- Face-interior boundary values, 276
- Face-interior voxels, 276
- Faces
 - moments of inertia for, 63
 - products of inertia for, 63
- Face-vertex contact, convex polyhedra, 436–437
- Factorizations, 384
- Feasible, 829
- Feasible basis vector, 818, 823
- Feasible dictionary, 831
- Feasible points, 839
- Feasible vector, 818, 823, 828
 - optimal, 818
- Feasible vectors, degenerate, 825
- Fermat, Pierre de, 691
- Fields, 541–542
 - finite, 584
- FindContact, 370, 374
- Find-intersection query, 296, 377
 - geometric, 391
- FindIntersection, 432, 440
 - pseudocode, 431
- Finite differences, 705–710
 - derivative approximations by, 705–711
 - parameters for, 708t
- Finite dimensional vector space, 594, 607, 617
- Finite element methods, 247
- Finite field, 584
- Finite linear combinations, 589
- Finite optimal solution, to dual problem, 828
- Finite point set, 475
- Finite sets, of contact points, 489
- Finite-difference equations, 268, 289
- Finite-difference scheme, 255
- First derivative of constraint, 513, 515–516, 520
- First quadrant, 840f
- First-derivative matrix, 799–800
- First-order derivatives, 383
- First-order differential equation, 733–738
 - initial value problem, 734–735
 - linear, 735
- First-order finite difference approximation, 532
- First-order linear difference equations, 756–757
 - general solutions, 757
 - homogeneous solution to, 756–757
 - in v -terms, 758
 - particular solutions, 757
- First-order linear differential equations, 735
- First-order linear system, 811
- First-order ordinary difference equations, 755
- First-order partial derivatives, 516, 750, 773
- First-order systems of differential equations, with initial conditions, 739
- First-order time derivatives, 523
- Fixed axis, motion about, 24–25
- Fixed frame vectors, 92
- Floating point box values, 345
- Floating point numbers, 428
 - system, 769

- Floating point stalls, 546
- Floating point units, 546
- Floating point values, obtained from Euler's method, 768
- Flow line, 241
 - density along, 242
- Fluid(s), 213–294
 - compressible, 292
 - incompressible, 240
 - multiple, 293
 - obstacles in, region, 293
 - simulation, 293–294
- Fluid flow
 - advection term, 257–260
 - density equation, 247–249
 - diffusion term, 247–257
 - implementing models for, 247–274
 - simplified 3D model for, 274–290
 - simplified model for, 246–247
 - source-sink term, 260–261
 - total density update, 261–263
 - variations of simplified model, 290–294
- Fluid2Da algorithm, 274
- Fluid3Da algorithm, 287
- Fluid3Db algorithm, 287
- Force(s), 30–40, 472
 - applied, 78, 468, 469
 - concurrent, 38
 - conservative, 80–84, 129–135
 - constraining, 99, 109–111, 159
 - constraint, 514, 515, 816
 - contact, 473, 495, 499, 501, 855–856
 - dissipative, 34–36, 135–137
 - external, 30, 244, 500, 524
 - externally applied, 507
 - frictional, 135, 137, 142, 787
 - function, 787, 793
 - generalized, 101, 110, 113, 121, 124, 127, 139, 143, 145
 - gravitational, 32–33, 83, 87–88, 93, 105, 111, 116, 121, 130
 - impulsive, 469, 473, 478, 480, 484
 - inertial, 246
 - infinitesimal, 120
 - inverse-square, 216
 - moment of, 36
 - normal, 35
 - random, 166
 - reactive, 99
 - repulsive, 499
 - resolution of, 500
 - spring, 33–34
 - viscous, 36
 - wind as, 109, 161
- with velocity component, 787–788
- without velocity component, 786–787
- Force-function evaluation, 787
- Formal notation, 684
- Formal Taylor series, 707
- Formula, rotation, 148, 149
- Formulas
 - coordinate-dependent, 603
 - Mirtich's, 74–75
- Fortran, 1
- Forward difference approximation, 705–706, 708, 709
- Forward elimination, 556, 557
 - costs, 550
 - first step of, 550
 - in systems of linear equations, 542–544
- Forward transport method, 258, 259f
- Foucault pendulum, 92
- Fourth-order equation, 760
- Fourth-order error, 706
- Fourth-order Runge-Kutta method, 776–777
- Free index, 243
- Free variables, 552
- Free-form deformation, 8, 192–196
 - extended, 196
 - initial configuration, 197
 - of disk-shaped bodies, 198
 - time interval of, 210
- Freely spinning top, 150–154
- Frenet frame, 189
- Frenet-Serret equations, 22
- Friction, 34–35
 - coefficient of, 136
 - Coulomb's law, 531, 535
 - dynamic, 510
 - kinetic, 35, 136
 - model, 526, 531
 - static, 35, 510
 - viscous, 799
- Frictional force, 135, 137, 787
 - on rods, 142
- Friedman, Joel, 829
- Frustum, view, 299f
- Full pivoting, 558
- Function(s)
 - affine, 839
 - analytic, 734
 - asynchronous sorting, 333
 - auxiliary objective, 819, 820
 - B-spline basis, 168, 170
 - B-spline volume, 196
 - basis, 168, 170, 173, 195
 - bivariate, 701, 710–711, 772, 773
 - boundary update, 253, 269, 270
 - call, 393

- Function(s) (*continued*)
 classic linear, 648
 collision response, 503
 Compute, 173
 constraining, 838
 constraint, 530, 839, 843
 continuous, 198, 239
 convex, 363, 382, 384, 840, 841f, 842f
 convex quadratic, 496
 CopyArray, 256
 delta, 485–487
 derivatives of, 688t
 DestroyEvent, 332
 determinants, 630–637
 Dirac delta, 222
 discontinuous, 685, 686f
 distance, 351, 847–849
 DoImpulse, 506
 error, 682
 exponential, 742, 745
 force, 787, 793
 GetKey, 173
 global, 251, 276–277
 graphs, 699f
 harmonic, 221
 impulsive, 493–494
 initialization, 252
 initial-value, 248, 249
 Lagrangian, 129, 846
 linear, 778, 839
 main update, 341
 m_torque, 508
 Move, 325–326
 m_force, 508
 multivariate, 655–658, 712
 nonconvex, 841f
 nonstatic, 471
 objective, 818–820, 838, 851, 853
 optimizing, 703
 parallelogram-parallelogram distance, 351
 Perp, 405, 849
 position, 112
 potential energy, 786
 quadratic, 354
 range of, 617
 real-valued, 585
 scalar-valued, 218
 segment-parallelogram distance, 351
 segment-segment distance, 351
 SeparatedByOtherDirections, 389
 source-sink, 238
 squad, 731
 strictly convex, 381
 trigonometric, 117, 152
 univariate, 698–700, 705–710
 update, 252, 253, 259, 311, 315, 319, 326, 341, 342
 values, 682t
 volume, 194, 196
 Fundamental subspaces, 613f
 Fundamental theorem of algebra, 609–613, 638
 kernel of A , 609–610
 kernel of A^T , 612
 range of A , 610–612
 range of A^T , 612
 Fundamental theorem of calculus, 691
 Fundamental theorem of vector calculus, 224, 229–230
- G**
 Game logic tick, 297
 Game loop, 297
 GAMMA Research Group (Geometric Algorithms for Modeling, Motion, and Animation), 536
 Gases, 213–294
 Gates, William H., 3
 Gauss' principle of least constraints, 534
 Gauss-Seidel method, 255, 256, 258, 268, 519, 531, 560–561
 projected, 529
 Gaussian blurring, 263
 Gaussian elimination, 548–552, 550, 556, 636, 736
 total cost for, 552
 Gear's fifth-order predictor-corrector method, 792–794
 Gelatinous blobs, random forces and, 167
 Gelatinous cubes, random forces and, 166
 General autonomous systems, 749–751
 General duality theory, 846–847
 General solutions, first-order linear difference equations, 757
 General system, 82
 General-order differential equations, 740–741
 Generalized cylinder surfaces, 186–187
 obtaining, by linearly interpolating points on curves, 187
 skirts modeled by, 188
 Generalized eigenspaces, 648
 Generalized eigenvectors, 651
 Generalized force, 101, 110, 113, 121, 127, 139
 of boards, 145
 for pulleys, 124
 on rods, 143
 Geodesic curves, 3
 Geometric Algorithms for Modeling, Motion, and Animation, *See* GAMMA Research Group
 Geometry of linear systems, 552–555

- GetExtremeIndex, 408, 427
- GetIntersection, 393
- GetKey function, 174
- GetLargeIndependentSet, 412
- GetMaximumIndependentSet, 412
- GetMiddleIndex, 401
- GetNormal, 402, 410
- GetVertex, 396, 402
- Gilbert, E. G., 459
- Gill's method, 777
- GJK algorithm, 9, 299, 349, 534
 - alternatives to, 464
 - collision detection, 459–464
 - first iteration of, 462f
 - fourth iteration of, 463f
 - second iteration of, 462f
 - set operations, 459–461
 - third iteration of, 463f
- Global extremum, 699
- Global functions, 251, 276–277
- Global minimum, 699, 702
- Global values, 276
- Global variables, 251
- GPUs, *See* Graphics processing units
- Gradient, 214–215, 701, 773
 - defining, 695
 - vector, 361, 703
- Gram-Schmidt orthonormalization, 468, 598, 599f, 608
- Graphics processing units (GPUs), 4
- Graphs, 683f
 - convex function of, 841f, 842f
 - cusp in, 688
 - kink in, 688
 - left-most branch of, 363f
 - of critical points, 655f
 - of discontinuous functions, 686f
 - of functions, 699f
 - possibilities for, 367f
- Gravitational constant, 133
- Gravitational forces, 32–33, 83, 86–87, 93, 105, 111, 121, 136
 - on mass, 116
- Gravity, 482f
- Green's theorem, 67, 213
 - vector calculus, 221–224
- Greystone Technology, 4
- G-row, 823

- H**
- Half-steps, 791
- Handheld calculators, 1
- Hardy, G. H., 7
- Harmonic function, 221
- Havok.com, 5
- Helix, central axis as, 191
- Helmholtz decomposition, 213, 229, 267
- Hemicircles, 381
- Hemispheres, 382
 - root of, 415
- Hessian matrix, 518, 522, 773
- Hessian tensor, 518, 531
- Heun's method, 775
- Higher-order derivatives, 707
- Higher-order polynomials, 836
- Higher-order Taylor methods, 769–770
- Hollerith cards, 1
- Homogeneous linear difference equations, 756
- Homogeneous solutions, 735, 756–757
 - n th order linear difference equation, 763–764
 - reduction of order and, 758
- Hooke's Law, 34, 104, 156, 160, 162, 164
- Hygens, Christiaan, 691
- Hyperbolic differential equation, 257
- Hyperbolic isocurves, 204
- Hypervolume
 - barycentric coordinates, 671–678
 - of simplex, 675–678
 - signed, 678

- I**
- I-COLLIDE, 464, 536–537
- Identities, 102
 - additive, 539, 580, 581f, 585, 589
 - Euler's, 739
 - multiplicative, 539, 586
 - trigonometric, 131, 458, 721
 - vector algebra, 721
 - verifying, 616
- Identity matrix, 236, 378, 564, 843
 - 2×2 , 848, 851
 - 3×3 , 853
 - 4×4 , 725
- I-loop, 272
- Implicit equations, Newton's method for, 771
- Implicit Euler's method, 772, 777, 812
 - modal equation and, 806–807
 - region of stability for, 808f
 - simple pendulum and, 803f
- Implicit method, 255, 771, 787
 - alternating-direction, 255
- Implicit multistep methods, 778
- Implicit surface deformation, 196–212, 211
- Implicit test, 364
- Implied motion, 490
- Improper integrals, 97
- Impulse equation
 - for angular velocity, 492
 - for linear velocity, 492

- Impulses
 - acceleration-based constrained motion, 476–478
 - at spatial points, 486
- Impulsive forces, 473, 478, 480
 - causing postimpulse velocity, 490
 - processing, 484
- Impulsive functions, 493, 494
- Inclined plane, 35, 137
 - rough, 128
- Incompressible fluids, 240
- Indeterminate form, 689
- Indices
 - adjacent, 165
 - for overlapping intervals, 306–309
 - free, 243
 - modular, 402
 - permutation vector of, 557
 - positional, 234
 - tensor component, 234
 - vector, 415
 - vertex, 415
- Inductive hypothesis, 642
- Inequalities, 767, 768
 - constraints, 817
 - equations, 840
- Inequality constraints, 528–529, 680
 - linear, 820f
- Inertia, 30
 - moments of, 55–64
 - principal directions of, 59
 - products of, 55–64
 - tensor, 58
- Inertia tensor, 466
 - definition of, 467
 - in world coordinates, 466–467
 - measuring, 467
 - recomputing, 467
- Inertia tensor of solid polyhedron, 64–77
 - computation by direct parameterization of triangles, 72–74
 - computation by reduction to line integrals, 67–72
 - pseudocode for, 75–77
 - reduction of volume integrals, 65–66
- Inertial coordinates, 31, 99
- Inertial force, 246
- Inertial frame, 31
- Inertial torque, 525
- Infinite masses, 167, 481
- Infinite principal moments, 481
- Infinite sum, 744
- Infinitesimal areas, 87–88, 690
- Infinitesimal displacement, 100
- Infinitesimal forces, 120
- Infinitesimal mass, 238
- Infinitesimal strain tensor, 233
- Infinitesimal volume, 238, 696
- Infinitesimal width, 690
- Infinitesimals, 681
- Initial angular speed, 799
- Initial conditions, 247
 - continuous dependence and, 794
- Initial density, 275, 288f
- Initial dictionary, 831
 - auxiliary variables in, 831, 832, 837
- Initial modified dictionary, 845
- Initial points, 730
- Initial tableau, 824
- Initial value problem
 - first-order differential equation, 734–735
 - second-order differential equations, 738
- Initial-value function, 248
 - in lattice of points, 249
- Initialization function, 252
- Inner products, vector spaces, 595–599
- Innermost integrals, 697
- Input parameter, 781
- INSERT_EVENT, 322
- InsertFeature, 444
- Insertion sort, 310
 - nonoverlapping boxes in, 320
 - overlapping boxes in, 320
- InsertMoveQueue, 347
- Instantaneous speed, 681
- Insulated boundary conditions, 271
- Integers, 539
- Integrals
 - calculus, 679, 689
 - definite, 623, 690
 - double, 118
 - formation of, via numerical methods, 770–772
 - improper, 97
 - innermost, 697
 - line, 67–72, 219
 - projection, 71
 - single, 118
 - surface, 219–220
 - triple, 118
 - volume, 65–66, 220–221
- Integrand, 97
- Integration, iterated, 697
- Interior points, 159
- Internal reaction force, 524
- Internal values, 508
- Interpolation
 - polynomial, 783
 - rational polynomial, 783–784
- Intersecting boxes, 316–320

- Intersecting convex polygons, 397f
 Intersecting intervals, 304–312
 Intersecting rectangles, 312–316
 Intersection
 arc-arc, 419
 edge-edge, 426f, 475
 edge-face, 511
 face-face, 442, 511
 in collision system, 391
 not predicted, 426f
 OBB, pseudocode, 448–449
 pseudocode for, 422
 vertex-edge, 511
 vertex-face, 475, 502
 vertex-vertex, 426f
 Intersection calculator pseudocode, 441
 Interval radii, 449
 IntervalManager, 307
 Intervals
 x , 312, 313
 y , 312, 313
 active, 305
 bounding, 173
 intersecting, 304–312
 moving projected, 457f
 nonoverlapping, 309
 overlapping, 306–309
 parameter, 176
 projected, 457f
 projection, 447f, 457f
 stationary projected, 457f
 time, 210, 392
 values, 455
 Invariant, 647
 subspaces, 649
 Inverse
 additive, 539, 587
 construction of, 570–572
 elementary row matrix, 569
 left, 615
 matrix, 467, 567–569
 Moore-Penrose, 519
 multiplicative, 539
 of rotation matrix, 715
 of square matrices, 568
 properties of, 569–570
 Inverse-square force, 216
 Invertible matrix, 637
 Irrational numbers, 540
 Irreducibly diagonally dominant, 560
 Isocurve extraction
 hyperbolic, 204
 in 2D images, 201–206
 Isosceles triangles, 120
 Isosurface extraction, in 3D images, 206–212
 Isosurfaces, 199
 Iterated integration, 697
 Iteration scheme, 786
 Iterative method, 519
 for solving linear systems, 558–561

J
 Jacobi method, 560
 Jacobian matrix, 516, 520, 522, 526
 Jakobsen, Thomas, 785
 Jerk, 22
 Jittering, 5
 J-loop, 272
 Johnson, D. W., 459
 Juxtaposed matrices, 562

K
 Karush-Kuhn-Tucker conditions (KKT), 841–843
 critical points, 843
 reformulated set of, 844
 Keerthi, S. S., 459
 Kepler's laws, 32, 88–89, 132–133
 defined, 86–87
 first, 87–88
 third, 89–90
 Kepler, Johann, 86
 Kernel, 609–610
 Keyframe animation, 727
 Kilogram, 30
 Kinematics, 13, 476
 viscosity, 246
 Kinetic energy, 78–80, 102, 104, 106, 113, 694
 computing, 119
 for systems, 116–117
 gaining, 491
 in special cases, 119
 loss of, 479
 measurement of, 80
 of boards, 144
 of first mass, 123
 relevant derivatives of, 123, 139
 Kinetic friction, 136
 coefficient of, 35
 Kinetic norm, 534
 Kink, 688
 Knot vectors, 168
 and parameter intervals, 176
 periodic, 171
 types of, 169
 Knots, 168
 nonuniform, 169
 uniform, 169

L

- l'Hôpital's rule, 485, 732
 - in univariate calculus, 689
- Lagrange multipliers, 354, 358, 698
 - classical theory of, 842
 - method of, 703, 704
- Lagrangian dynamics, 7, 77, 85, 86, 98–135, 474, 694
 - acceleration-based constrained motion, 509–512
- Lagrangian equations of motion, 99, 100–147, 511
 - conservative forces in, 129–135
 - dissipative forces and, 135–147
 - for continuum of mass, 118–128
 - for particles, 100–111
 - for systems of particles, 115–118
 - interpretation of, 114–115
 - time-varying frames or constants, 114–115
- Lagrangian function, 129, 846
- Laminator, 14
- Laplace's equation, 213
 - vector calculus, 221–224
- Laplacian, vector calculus and, 215–217
- Lattice cells update function for, 259
- Lattice of points, 248f
 - initial-value function in, 249
- Law(s)
 - conservation, 237–246
 - Coulumb's friction, 531, 535
 - Hooke's, 34, 104, 156, 160, 162, 164
 - Kepler's, 32, 86–90, 132–133
 - of cosines, 596
 - parallelogram, 660, 661
- LCP, *See* Linear complementarity problem
- LDU decomposition, 573, 578
- Leaf node, 404, 408
- Leapfrog method, 788–790, 804–806
 - modal equation and, 808
 - region of stability for, 809f
- Leary, Timothy, 3
- Least squares, vector spaces, 614–617
- Left inverse, 615
- Leibniz, Gottfried Wilhelm von, 691
- Lemke algorithm, 512, 813, 830, 838
 - illustration of, 830
 - LCP and, 829–834, 844
 - museum principle and, 836
 - numerical implementation of, 836
 - zero constants and, 832
- Length
 - barycentric coordinates, 671–678
 - unit, 720
 - vector spaces, 595–599
- Level curves, 815f
- Level set extraction, 199–201
- Level surface, 200, 215
- Levi-Civita permutation tensor, 676
- Levine, Ron, 421
- Limiting equation, 845
- Limiting factor, 822
- Limiting ratios, 833
- Limits
 - in univariate calculus, 682–684
 - multivariate calculus, 692
 - of sequences, 684–685
- Lin-Canny algorithm, 464
- Line integrals, 219
 - computation by reduction to, 67–72
 - vector calculus, 219
- Line segments, 488–489
 - deformation of, into closed curve, 181
- Line(s)
 - coincident, 553f
 - disjoint, 553f
 - flow, 241, 242
 - integrals, 67–72, 219
 - nonparallel, 553f
 - parallel, 365f, 553f, 683
 - projection of cylinders onto, 378
 - secant, 686
 - separating, 377, 394
 - tangent, 686, 695
- Linear algebra, 539–658
 - quaternions and, 722–727
- Linear chains, 162
 - rope modeled as, 161
- Linear combinations
 - finite, 589
 - of smaller powers, 743
 - vector spaces, 588–590
- Linear complementarity problem (LCP), 11, 496–497, 501–502, 534, 813, 828–838
 - conversion to, 830, 832, 835, 848
 - inputs to, 852
 - Lemke algorithm, 829–834, 844
 - quantities of interest in, 845
 - solution to, 831
 - solver, 502, 512, 849
 - zero constant terms, 835–837
- Linear difference equations, 756–759
 - n*th order, 763
 - first-order, 756–757
 - homogeneous, 756
 - nonhomogeneous, 756
 - second-order, 757–759
- Linear differential equations
 - constant-coefficient, 747–749
 - second-order, 124, 135, 576
 - systems of, 741–746

- Linear equations, 701–702
 - difference, 756–759
 - first-order difference, 756–759
 - systems of, 542–559
 - Linear function, 778, 839
 - Linear independence
 - demonstrating, 611
 - vector spaces, 590–595
 - Linear inequality constraints, 820f, 826
 - Linear interpolation
 - over tetrahedron, 669f
 - over triangles, 669
 - Linear momentum, 31, 40–41
 - conservation of, 41
 - in unconstrained motion, 470
 - of centers of mass, 494
 - Linear programming (LP), 11, 814–828
 - dual problem, 825–828
 - general problem, 818–825
 - normal form, 819
 - pairwise intersections, 816–818
 - restricted normal form, 819
 - two-dimensional example, 814–816
 - Linear systems of differential equations, 117
 - Linear transformations, 617–626
 - matrices and, 618
 - properties of, 636
 - Linear translation, 232
 - Linear velocity
 - for body A, 488
 - for body B, 488
 - impulse equation for, 492
 - in unconstrained motion, 470
 - OBBs moving with, 537
 - preimpulse, 506
 - Linearized system, 795
 - Linearly dependent sets, *See also* Vector(s)
 - removing vectors from, 592
 - Linearly dependent vectors, 590
 - Linearly independent eigenvectors, 641, 645, 646, 749
 - Linearly independent sets, 591, 593, 604.
 - See also* Vector(s)
 - Linearly independent solutions
 - of second-order linear differential equations, 757
 - Wronskian of, 757
 - Linearly independent vectors, 593, 611
 - Linking steps, 411
 - Linux, 5
 - Lipschitz conditions, 798
 - Local control, 169
 - control point deformation, 175
 - Local coordinate frame, 121
 - Local maximum, 699
 - Local minimum, 699
 - constrained, 841
 - Local state arrays, 251
 - Local truncation error, 795
 - Lookup tables, 315, 318
 - initializing, 341
 - Move function and, 325–326
 - Lower echelon matrix, 565
 - Lower triangular matrix, 565, 574, 578
 - LP, *See* Linear programming
 - LU decomposition, 572–578
- M**
- $m \times 1$ column vector, 819, 842
 - $m \times 1$ vector, 704
 - $m \times m$ matrix, 563, 704
 - invertible, 616
 - $m \times p$ matrix, 563
 - `m_force`, 508
 - `M_torque` function, 508
 - Macintosh, 5
 - Main update function, 341
 - Marching Cubes algorithm, 199–201, 206
 - consequences of, 200
 - single triangle mesh, 207
 - table lookup of, 201
 - Marching Squares algorithm, 202
 - `MASK_INDEX0`, 322
 - `MASK_INDEX1`, 322
 - Masks, culling, 321–323
 - MASPAR, 3
 - Mass matrix, 58
 - Mass objects, represented as mass-spring systems, 159
 - Mass tensor of solid polyhedron, 64, 77
 - computation by direct parameterization of triangles, 72–74
 - computation by reduction to line integrals, 67–72
 - pseudocode for, 75–77
 - reduction of volume integrals, 65–66
 - Mass(es), 30
 - ball, 104–106
 - beads of, 102
 - center of, 120–122, 126, 147, 465–466, 494
 - conservation of, 238–242
 - continuum of, 14, 118–128
 - curve, 14, 118
 - discrete, 43–46, 50
 - distribution, 142
 - gravitational forces on, 116
 - infinite, 167, 481
 - infinitesimal, 238
 - kinetic energy of, 123
 - matrices, 58

- Mass(es) (*continued*)
 one-dimensional array of, 158–160
 planar, 122
 point, 122
 rigid body, 471
 surface, 14, 118, 219
 three-dimensional array of, 164–165
 two-dimensional array of, 160–164
 volume, 14, 50–52, 118, 164
- Mass-spring systems, 158–167
 arbitrary configurations, 165
 mass objects represented as, 159
 one-dimensional array of masses, 158–160
 surface mass represented as, 162
 three-dimensional array of masses, 164–165
 two-dimensional array of masses, 160–164
 volume mass represented as, 164
- Massless rods, 138
- Matching terms, 774
- Material derivative operator, 241
- Mathematica, 73, 75, 384
- Mathematical programming (MP), 11, 814, 838–856
 convex quadratic, 843–846
 general duality theory, 846
 KKT conditions, 841–843
- Matrices, 561–578
 1×1 , 715
 1×3 , 715
 2×1 block, 856
 2×2 identity, 848, 851
 2×2 zero, 568, 626–628
 3×1 , 715
 3×3 , 629–630
 3×3 elementary row, 566, 569
 3×3 identity, 853
 3×3 rotation, 726
 4×4 identity, 725
 6×6 , 793
 $d \times v$, 716
 $m \times 1$ column vector, 819, 842
 $m \times 1$, 704
 $m \times m$, matrix 563, 704
 invertible, 616
 $m \times p$, matrix 563
 $n \times 1$ column, 617
 $n \times m$, 563–564, 565, 612, 620, 647
 $n \times n$, 563, 568, 577, 634, 641, 645
 $n \times p$, 563
 3×3 identity, 525
 3D rotation, 723, 724
 4D rotation, 723, 724
 augmented, 548, 549, 557, 561
 block, 570–571, 610, 611, 633, 664–665, 722, 856
 block diagonal, 852
 change of basis, 623
 column, 548, 562, 617
 constants, 856
 constraint, 849, 852
 copositive, 838, 844
 copositive skew-symmetric, 838
 diagonal, 119, 360, 564, 573, 645, 654, 852
 diagonalizable, 649, 744
 eigendecomposition of, 751
 exponential of, 653–655
 first-derivative, 799–800
 Hessian, 518, 522, 773
 identity, 236, 378, 564, 725, 843, 848, 851, 853
 invertible, 637
 Jacobian, 516, 520, 523, 526
 lower echelon, 565
 lower triangular, 565, 574, 578
 LU decomposition, 572–578
 mass, 58
 nilpotent, 744
 noninvertible, 568
 of coefficients, 562, 605–606
 of cofactors, 634
 orientation, 466
 permutation, 573
 powers of, 652–653
 projection, 379
 properties of inverses, 569–570
 rank of, 552
 real-valued symmetric, 643–644
 rotation, 26, 360, 454, 468, 520, 713–718, 723, 724, 726
 rotation of, 91
 second derivative, 384
 semisimple, 744
 skew-symmetric, 231, 522, 565, 636, 725, 838
 special, 564–565
 symmetric, 616, 643–644
 upper echelon, 565, 573, 574, 637
 upper triangular, 565, 578, 637, 644
 zero, 568, 616
- Matrix multiplication, 564, 626, 726, 745
- Matrix notation, 496, 501
- Matrix representation, 626
- MAX_EVENTS, 326, 327, 334
- Maximum independent set, 411
- Measure theory, 223
- Medium-phase algorithm, 297
- Medium-phase collision culling, 9
- `mEndpoints`, 307
- Mesh construction, ear-clipping-based, 208–212

- Mesh vertex, 194, 195
 - positions, 195
- Metcalfe, Bob, 6
- Method of Langrange multipliers, 703
- Method of separating axes, 9, 299, 349, 393–394
- Middle index, 400
- Midpoint method, 774
 - modified, 784–785
- Midpoint Runge-Kutta method, 774
- Minkowski difference, 459
- Minkowski sum, 459
- Mirtich algorithm, implementing, 77
- Mirtich's formulas, 74–75
- Mirtich, Brian, 10, 295
- Mixed boundary conditions, 272, 276
- Mixed linear complementarity problem (MLCP), 533
 - MLCP*, *See* Mixed linear complementarity problem
- MLookup, 308
- MNumevents, 326
- MNumMoveQueue, 347, 348
- Modal equation, 798
 - implicit Euler's method and, 806–807
 - leapfrog method and, 808
 - Runge-Kutta fourth order method and, 807–808
- Modified Euler's method, 770f, 771, 775
- Modified midpoint method, 784, 785
- Modified signs, 205
- Modulus
 - bulk, 157–158
 - shear, 157
 - Young's, 157
- Moment of force, 36
- Moments of inertia, 55–64
 - for edges, 62
 - for faces, 63
 - in one dimension, 55
 - in three dimension, 56–64
 - in two dimension, 56
 - principal, 59
 - for vertices, 61
- Momentum, 40–54
 - angular, 41–42, 90, 151, 236–237, 466, 470, 494
 - conservation of, 242–246
 - linear, 31, 40–41, 470, 494
- Moore–Penrose inverse, 519
- Motion
 - acceleration-based constrained, 473–512
 - constrained, 297
 - differential equation of, 713
 - equations of, 31, 750
- Euler's equations of, 8, 59, 147–154
 - first equation of, 93–94
 - implied, 490
- Lagrangian equations of, 100–147, 511
- Newton's equations of, 524
- Newton's laws of, 7, 13, 30–31, 99, 115, 120, 465, 533, 786
 - of Earth, 86–87
 - of particles, 90–91
 - on curves, 100–102
 - on surfaces, 102–109
 - path of, 86, 108
 - planar, 15–19
 - plane of, 87–88
 - rigid, 667
 - rigid body, 85–154
 - second equation of, 94
 - space, 534
 - Sun and, 86–87
 - third equation of, 94
 - unconstrained, 465–473
 - velocity-based constrained, 10, 512–533
- Move function, lookup tables and, 325–326
- MoveBoxes, 324, 347, 348
 - Moving axis, motion about, 26–27
 - Moving boundaries, 293
 - Moving boxes, with constant linear and angular velocity, 453–459
- Moving ellipses
 - computing closest point, 362
 - computing negative root, 362–364
 - configuration at contact time, 359
 - contact time, 364–368
 - intersection of, 358–359
 - reduction to circle and axis-aligned ellipse, 359–361
 - source code, 368–371
- Moving ellipsoids, 371–376
 - source code, 372–376
- Moving frame, 16
- Moving objects, with constant linear velocity, 421–444
- Moving projected intervals, 457f
- MP, *See* Mathematical programming
- MSG_SHARED_BOX_HEAP_ADDRESS, 338
- MSG_SHARED_EVENT_HEAP_ADDRESS, 338
- MSG_TERMINATE, 338, 339, 348
- MSG_UPDATE_BEGIN, 348
- MTerminate, 331
- MType, 320
- Multi-index, 633
- Multifunction evaluation algorithm, 472
- Multilinear transformation, 630–631
- Multiple contact points, 483–491
- Multiple fluids, 293

- Multiplication, 546
 - matrix, 564, 626, 726, 745
 - scalar, 583, 584
- Multiplicative identity, 539, 586
- Multiplicative inverse, 539
- Multistep methods, 11
 - Adams-Basforth, 778, 797
 - Adams-Moulton, 779, 797
 - explicit, 778
 - implicit, 778
 - numerical methods, 777–779
 - stable for, 797–798
- Multivariate calculus, 679, 692–698
 - chain rule in, 693–694
 - continuity, 692
 - differentiation, 692–696
 - directional derivative, 694–696
 - integration, 696–698
 - limits, 692
- Multivariate functions, 655–658
 - derivatives, 712
 - optimization and, 700–702
- MUpdateAsynchronousEndEvent, 331
- MUpdateBegin, 332
- Museum principle, 836, 837
- Mutually orthogonal vectors, 597
- MXLookup, 317
- MYLookup, 317
- MZLookup, 317

- N**
- $n \times 1$ column matrix, 617
- $n \times m$ matrix, 563, 612, 647
 - construction of, 620
 - diagonal entries of, 564
 - diagonal matrix of, 564
 - lower echelon, 565
 - lower triangular, 565
 - upper echelon, 565
 - upper triangular, 565
- $n \times n$ matrix, 563, 568, 577, 634
 - symmetric, 645
 - with real-valued entries, 641
- $n \times p$ matrix, 563
- Narrow-phase algorithm, 297
- Navier-Stokes equation, 9, 213, 244, 258
 - simplified, 263
- NCP, *See* Nonlinear complementarity problems
- n -dimensional affine space, 659
- NEG_INFINITY, 337, 340, 346
- Negation of sets, 459
- Negative coefficients, 821, 834
- Negative constant term, 837
- Negative definite symmetric matrices, 643
- Negative root, computing, 362–364
- Negative semidefinite symmetric matrices, 643
- Negative vertical axis, 673
- Nested polytope, 411, 413
- NetImmerse, 4
- Neumann boundary conditions, 221, 247, 272, 276
 - in i -loop, 272
- Neumann boundary value problem, 223
- Neville's method, 783
- Newton Game Dynamics, 5
- Newton's equations of motion, 524
- Newton's iterates, 771, 802
- Newton's laws of motion, 7, 13, 30–31, 120
 - first, 31
 - second, 31, 99, 115, 465, 533, 786
 - third, 31
- Newton's method, 364, 367, 372, 755, 802
 - implicit equations and, 771
- Newton, Isaac, 691
- Newtonian dynamics, 86–98, 465
- Nilpotent, 650, 653
 - matrix, 744
- NoIntersect, 423, 428, 436, 438–439
 - input to, 455
 - pseudocode for, 456
- Non-unit-length vector, 597
- Nonbasic variables, 821, 824
 - coefficients of, 825
- Nonconvex function, graph of, 841f
- Nonconvex set, 394f
- Nonhomogeneous linear difference equations, 756
- Noninertial frame, 31, 99
- Nonintersecting convex objects, 395f
- Nonintersecting convex polygons, 397f
- Nonintersection, of convex objects, 377
- Noninvertible matrix, 568
- Nonlinear complementarity problems (NCP), 534
- Nonlinear differential equations, first-order, 90
- Nonlinear system of differential equations, 469
- Nonnegative definite symmetric matrices, 643
- Nonnegativity constraints, 825
 - convex domain implied by, 820f
- Nonoverlapping boxes, in insertion sort, 320
- Nonoverlapping intervals, 309
- Nonparallel lines, 553f
- Nonparallel planes, 554
- Nonpenetration constraints, 473, 534
- Nonpenetration of polyhedra, 390
- Nonpositive definite symmetric matrices, 643
- Nonrational uniform B-spline (NURBS), 8, 156, 168, 169

- curves, 177–179
- encapsulating, 183
- rectangle surface patch, 182
- surfaces, 182–184
 - with control points, 177
- Nonsquare systems of equations, 552
- Nonstatic functions, 471
- Nonuniform knots, 169
- Nonuniform scaling, 211
- Nonzero linear velocities, 453
- Nonzero scalars, 553, 636
- Nonzero solutions, 638
- Nonzero values, 172
- Nonzero velocity, 490
- Norm, 720
- Normal acceleration, 17
- Normal equations, 615
- Normal force, 35
- Normal form, 819
 - restricted, 819
- Normal stresses, 233
- Normal vector derivative, 498
- Normal-form constraints, 819
- Normalized projections, 381
- Normals, pseudocode generating, 185
- North Pole, 92
- Nth order difference equation, 753
 - implicit, 753
- Nth order differential equation, 740
- Nth order linear difference equation
 - homogeneous solution, 763–764
 - vector sequence in, 763
- Nullspace, 609
- NUM_ENDPOINTS, 340
- Numbers
 - complex, 541, 546, 719
 - irrational, 540
 - rational, 540
 - real, 540
 - systems, 539–542
- Numerical Design Ltd., 4
- Numerical issues, 556–558
- Numerical methods, 766–812
 - Bulirsch-Stoer method, 785
 - consistency in, 795
 - convergence in, 796
 - definition, 796
 - Euler's, 766–769
 - extrapolation, 780–785
 - higher-order Taylor, 769–770
 - in standard formulation, 791
 - modified midpoint, 784–785
 - multistep, 777–779
 - output of, 805f
 - polynomial extrapolation, 783
 - polynomial interpolation, 783
 - predictor-corrector, 779–780
 - rational polynomial extrapolation, 783–784
 - rational polynomial interpolation, 783–784
 - stability in, 796
 - stiff equations, 809–812
 - strongly stable, 798
 - unstable, 798
 - Verlet integration, 785–794
 - via integral formation, 770–772
 - weakly stable, 798
 - Numerical stability, 254
 - physical stability and, 794–809
 - Runge-Kutta fourth order method and, 803, 804
 - NURBS, *See* Nonrational uniform B-spline
 - NVIDIA Corporation, 5, 290
 - NVIDIA GeForce 9600 GT graphics card, 274

O

 - $O(h^2)$ approximations, 782
 - $O(h^6)$ approximations, 782
 - OBBs, *See* Oriented bounding boxes
 - Objective function, 818, 820, 838, 851, 853
 - auxiliary, 819, 820
 - Occlusion culling, 510
 - Odd permutation, 631
 - Olson, Ken, 1
 - One-dimensional array of masses, 158–160
 - One-dimensional eigenspaces, 648
 - One-dimensional subspaces, 665
 - Open Dynamics Engine, 5
 - Operators
 - curl, 218
 - derivative, 517
 - material derivative, 241
 - splitting method, 255
 - univariate differential, 693
 - Optimal feasible vector, 818
 - Optimization
 - calculus, 698–702
 - constrained, 702–705
 - multivariate functions in, 700–702
 - univariate functions, 698–700
 - Orbit, of Earth, 88
 - Ordinary difference equations, 755
 - autonomous, 755
 - first-order, 755
 - Ordinary differential equations, 733
 - second-order system of, 91
 - Ordinary differentiation, 111
 - Orientation differential equation, 520
 - Orientation matrix, 466, 700

- Oriented bounding boxes (OBBs), 349,
445–453, 535
culling in, 445
moving with angular velocity, 537
moving with linear velocity, 537
normal, 448
potential separating directions for, 449t
projection intervals of, 447f
pseudocode for intersection of, 448–449
rotating, 537
univariate functions and, 700
with center point, 446f
- Orthogonal camera, 421
- Orthogonal complement, 607
subspaces and, 608f
- Orthogonal sets, 598
- Orthogonal subspaces, 606–609, 647
- Orthogonality, vector spaces, 595–599
- Orthonormal basis, 384, 645
- Orthonormal sets, 189, 598
of vectors, 714f
right-handed, of vectors, 715f
- Orthonormalization, 468
Gram–Schmidt, 468, 598, 599f, 608
- Overlap processing, 342
- Overlap set update, 328
- Overlap test, 316
BoxManager, 328
for AABBs, 319
per-dimension, 328
- Overlapping boxes, in insertion sort, 320
- Overlapping intervals, indices for, 306–319
- P**
- Pairwise intersections, in linear programming,
816–818
- Parabola, 477
area bounded by, 690f
- Parabolic partial differential equations, 247
- Paraboloids, elliptical, 105, 108
- Parallel cylinders, 385
- Parallel integers, 546
- Parallel lines, 553f
boxing in by, 683
ellipses sweeping regions bounded by, 365f
- Parallel planes, 554, 555
- Parallel subspaces, 665
- Parallelepiped, 603f
transforming cubes into, 630f
- Parallelogram, 350
transforming square and, 627f
vectors and, 582f
- Parallelogram law, 660
for affine algebra, 661
- Parallelogram-parallelogram distance function, 351
- Parameter intervals, 176
- Parameter points, 389
- Partial derivatives, 693, 695
first-order, 516, 750, 773
second-order, 521, 773, 841
vector of, 695
- Partial differential equations, 733
- Particle systems, 14
and continuous materials, 27–30
constraints on, 515–519
equations of motions for, 115–118
- Particle(s)
constrained to curves, 514–515
constrained to surface, 513
constraint on, 512–515
Lagrangian equations of motion for,
100–111
multiple, on rough plane, 140–141
on rough planes, 137–138
single, 14–27
two, on rough planes, 138–140
velocity of, 477
vortex, 291
- Particular solutions, first-order linear
difference equations, 757
- Partitioning, 395
- Pascal's triangle, 793
- Pascals, 157
- Pendulum
angles, 805f
double, 118, 131
Foucault, 92–95
model, 747
plot of, 803f
simple, 96–99, 101, 110, 112, 750, 801f, 803f
triangle, 121
- Per-dimension overlap test, 328
- Per-dimension update, 326–327
- Periodic knot vector, 171
- Permutation, 631, 633
even, 631
odd, 631
tensor, 677
triply-indexed, tensor, 676
- Permutation matrix, 573
- Permutation tensor, 235
- Permutation vector, 557
- Perp function, 405, 849
- Perp vector, 673
- Perturbation method, 837, 846
- Physical realism, 5
- Physical stability, numerical stability and,
794–809

- Physics engines, 5, 295–538
- Physics tick, 297–298, 334
 - resolve constraints, 470
- PhysX, 5
- Picasso, Pablo, 2
- Pipes, 126
 - angular velocity of, 128
- PIVOT (Proximity Information from VOronoi Techniques), 536
- Pivots, 549
 - full, 558
- Pixels
 - ambiguous, 203
 - bitmap, 258
 - sign configurations of, 202
 - superimposition of, 204
 - vertex-edge table for, 205
- Planar bodies, 198
- Planar convex polygons, 408
- Planar lamina, 14
- Planar mass, 122
- Planar motion
 - in Cartesian coordinates, 15–18
 - in polar coordinates, 18–20
- Planar polygons, 201
- Plane(s)
 - coincident, 555f
 - coordinate systems in, 663f
 - disjoint, 554
 - half, 815f
 - inclined, 35, 128, 137
 - nonparallel, 554
 - parallel, 554, 555
 - rough, 137–147
 - sloped, 482f, 483f, 485
 - tangent, 695
- Playstation, 3, 5
- Point(s)
 - barycentric combination of, 668f
 - boundary, 700–701
 - center, 446f
 - closest, 362
 - collision, 474–475, 493
 - contact, 368, 393, 494f, 502, 529f
 - critical, 655, 657, 843
 - distance between convex polygons and, 847–849
 - distance between convex polyhedra, 849–851
 - edge-interior, 461
 - ellipse, 366
 - feasible, 839
 - forming convex quadrilateral, 729f
 - interior, 159
 - lattice of, 248f
 - linearly interpolating pairs of points on, 187
 - multiple contact, 483–491
 - of colliding contact, 491
 - parameter, 389
 - saddle, 658
 - singleton, 461
 - spatial, 486
 - vectors and, 659
- Point-in-spherical-polygon test, 417, 419
- Point-mass objects, 122
- Poisson's equation, 213, 267, 269, 294
 - solving, 279
 - vector calculus, 221–224
- Polar coordinates
 - coordinate form, 89
 - frame, 18
 - planar motion in, 18–19f
- Polar dual, of polygon, 403f
- Polar representation, 760
- Pollutants, 258n
- Polygon(s), *See also* Convex polygons;
 - Sub polygon
 - counterclockwise ordering of, 431
 - edge-normal direction of, 398f
 - edges, 418f
 - intersecting convex, 397f
 - nonintersecting, 397f
 - planar, 201
 - planar convex, 408
 - polar dual, 403f
 - separation of, 398f
 - soups, 536
- Polynomial(s), 650
 - Bernstein, 183, 192
 - characteristic, 740, 743, 748
 - cubic, 730
 - definite integral of, 623
 - extrapolation, 783
 - generation of, by vector fields, 66
 - higher-order, 836
 - interpolation, 783
 - quadratic, 356, 384
 - quartic, 182, 356
 - rational, 783–784
 - Taylor, 655–657, 773
 - vector space of, 618
- Polynomial equations, 356
 - characteristic, 806
 - obtaining, 760
- Polynomial function, 70
- Polytope, 390
 - moving, 392
 - nested, 411, 413
 - stationary, 391
 - velocities of, 393

- Portal systems, 510
- `POS_INFINITY`, 337, 340, 346
- Position function, 112
- Position-based constrained motion, 10
- Positional derivatives, 110
- Positional indices, 234
- Positive definite, 560, 855
- Positive definite symmetric matrices, 643
- Positive semidefinite, 844
- Positive semidefinite symmetric matrices, 643
- Positivity, 364, 366
- Postimpulse angular velocity, 480, 482
- Postimpulse configuration, 482f
- Postimpulse velocity, 479f, 483, 491–492
 - computing, 484
 - impulsive forces causing, 490
 - in sequential processing, 497
 - vector, 478
- Postimpulse world velocity, 492
- Potential energy, 80–84, 90
 - function, 786
 - total, 130
- Potential intersection, 349
- Potential normals, 20
- Potential separating directions, for OBBs, 449t
- Powell’s direction, 389
- Power series, 654
- Powers of matrices, 652–653
- Predictor-corrector method, Gear’s fifth-order, 792–794
- Predictor-corrector methods, 779–780
- Preimpulse angular velocity, 480
- Preimpulse configuration, 482f
- Preimpulse linear velocity, 506
- Preimpulse velocity, 478f, 491–492, 496
- Preimpulse world velocity, 492, 493
- Pressure, 157
 - on boundary, 243
 - separate, team, 291
- Primal MP problem, 847
- Primal problem, 825, 826
 - infeasible, 828
 - slack variables for, 843
- Primary state, 471
- Prince of Persia 3D*, 4
- Principal directions of inertia, 59
- Principal moments of inertia, 59
- `ProcessCollidingContact`, 481
- `ProcessEvent`s, 324, 347
- Producer-consumer model, 321
- Product(s)
 - cross, 600–606, 720
 - dot, 600–606, 720
 - inner, 595–599
 - rule, 239, 240, 498, 688
- triple, 600–606
- triple scalar, 603–604
- triple vector, 604–606, 605f
- Products of inertia, 55–64
 - for edges, 62
 - for faces, 63
 - for vertices, 61
- Project-All, timing for, 420t
- Projected Gauss–Seidel iterations, 529
- Projected intervals
 - moving, 457f
 - stationary, 457f
- Projection, 395
 - normalized, 381
 - of cylinders onto lines, 378
 - onto range, 614
 - vector spaces, 595–599, 614–617
- Projection integrals, 71
- Projection intervals, 427
 - of OBBs, 447f
 - separation of, 447
- Projection matrix, 379, 615
- Projection methods, nonintersection of convex objects by, 377
- `ProjInfo` objects, 428, 437–439
- Property
 - associative, 540
 - averaging, 487
 - commutative, 540
 - distributive, 540
 - selection, 485, 486
 - substitution, 222
 - unboundedness, 827–828
- Proximity Information from VOronoi Techniques, *See* PIVOT
- Pseudocode, 75–77, 171, 260, 396, 404, 425, 547
 - convex polyhedra for, 456
 - differential equation for, 802
 - edge–edge contact intersection calculator, 433
 - `FindIntersection`, 431
 - for algorithm, 384–390
 - for computing curve points, 172
 - for computing distance, 848, 850
 - for convex polygon intersection, 422
 - for generating iterates, 803, 805
 - for inertia tensor of solid polyhedron, 75–77
 - for insertion sort, 309
 - for mass tensor of solid polyhedron, 75–77
 - for OBB intersection, 448–449
 - for processing point of colliding contact, 481

- for test-intersection query, 454–455
- generating triangles, 185
- generating vertices, 185
- implementing, 77
- intersection calculator, 441
- interval values in, 455
- normals, 185
- overlapping, 349–350
- simulation portion of, 269–270, 277–278
- uniform texture coordinates, 185
- vertex–edge contact intersection calculator, 433
- vertex–vertex contact intersection calculator, 433
- Pulleys, 123
 - generalized forces for, 124
 - spring system, 125
 - systems of, 125
- Pure strain, 232

- Q**
- Q-COLLIDE, 537
- QR algorithm, 646
- Quadratic equation, 201
- Quadratic functions, 354, 855
- Quadratic interpolation, spherical, 729–731
- Quadratic polynomial, 356, 384
- Quadratic programming, 840
 - quantities of interest, 845
- Quadrilaterals, convex, 729f
- Quantities of interest
 - in linear complementarity problem, 845
 - in quadratic programming, 845
- Quartic polynomials, 182, 356
- Quaternions, 10, 467, 713–732
 - addition of, 718
 - algebraic operations and, 718–720
 - classical approach, 718–722
 - equation of motion, 521
 - interpolating, 713, 727–731
 - linear algebra and, 722–727
 - rotation matrix and, 713–718
 - rotations and, 720–722
 - scalar multiplication of, 718
 - spherical linear, 727–729
 - spherical linear interpolation of, 727–729
 - spherical quadratic interpolation of, 729–731
 - squad function of, 731
 - subtraction of, 718
- Quotient rule, 498, 688

- R**
- R-Plus, 4
- Radeon 9700, 5
- Random forces
 - gelatinous blobs and, 167
 - gelatinous cubes and, 166
- RAPID (Robust and Accurate Polygon Interface Detection), 536
- Rate of change, 88
- Rational numbers, 539–540
- Rational polynomial
 - extrapolation, 783–784
 - interpolation, 783–784
- Reactive force, 99
- Real numbers, 540
- Real-valued coefficients, 585, 622
- Real-valued entries
 - $n \times n$ matrix with, 641
- Real-valued functions, 585
- Real-valued matrices, 654
- Real-valued symmetric matrix, 643–644
- Receive port, relationships among, 336f
- ReceiveMessageFromSPU, 346
- Rectangle surface patch, 179–180
 - NURBS, 182
- RectangleManager, 313, 314
- Rectangles
 - approximation of area by, 770f
 - axis-aligned, 313f, 316
 - consisting of triangles, 184
 - intersecting, 312–316
 - traveling downwards, 489f
- Rectangular array, of springs, 163
- Rectangular solids, bases of, 696f
- Recursions, 168
- Recursive descent in dimension, 701
- Reduced contact set, 475f
- Reduction of order, 758
- Reduction of volume integrals, 65–66
- Redundant constraints, 817
- Reference system, 82
- Region of stability
 - explicit Euler's method, 806f
 - implicit Euler's method, 807f
 - leapfrog method, 809f
 - Runge-Kutta fourth order method, 808f
- Relative velocity, 480, 491
 - at resting contact, 498
- Relevant derivatives, 110, 113, 127, 133
 - of kinetic energy, 123, 139
- Remainder term, 766
- Repeated real root, 739
- Reported intersections, 306
- Repulsive forces, 499
- Resolution of forces, 500
- Resting contact, 474
 - collision response for, 498–502
 - relative velocity at, 498

- Restricted normal form, 819
 - `ResumeThread`, 332
 - Return value, 303
 - Reverse-ordered input, 730
 - Revolution surfaces, 187
 - water drops modeled as control points of, 190
 - Richardson extrapolation, 780–781
 - variation of, 781
 - Ridges, 3
 - Right-hand rule, 600
 - Right-handed orthonormal basis, 381
 - Rigid bodies, 13
 - angular velocity of, 148
 - body coordinates for, 148
 - classification, 14–15
 - collection of, 496
 - constraint on, 519–522
 - contact points, 529f
 - equations of motion, 523–525f
 - mass, 471
 - points of contact, 494f
 - simultaneous processing in, 497
 - solid, 465
 - states, 855–856
 - world coordinates for, 148
 - Rigid body kinematics, 15–30
 - single particle, 15–27
 - Rigid body motion, 85–154
 - Rigid body system, constraint on, 522–525
 - Rigid motion, 667
 - `RigidBody` class, 470, 481
 - RK3a method, 776
 - RK3b method, 776
 - RK4a method, 777, 812
 - RK4b method, 776, 777
 - Robust and Accurate Polygon Interface
 - Detection, *See* RAPID
 - Rods, 113, 128–129
 - frictional force on, 142
 - generalized force on, 143
 - massless, 138
 - on rough planes, 142–143
 - Rooms, properties of, 836
 - Root finding, 755
 - Ropes, as linear chains of springs, 161
 - Rotating calipers, 464
 - Rotation, 667
 - angle, 731
 - axis, 731
 - composition of, 721, 722
 - quaternions relationship to, 720–722
 - Rotation formula, 148, 149
 - Rotation matrix, 26, 91, 360, 454, 468, 520
 - 3×3 , 726
 - 3D, 723
 - 4D, 723, 724
 - inverse of, 715
 - quaternions and, 713–718
 - transpose of, 715
 - Rough planes, 137–138
 - boards on, 143–145
 - multiple particles on, 140–141
 - solid boxes on, 146–147
 - thin rods on, 142–143
 - two particles on, 138–140
 - Row operations, in eigenvalues, 640
 - Row-reducing, 571, 610
 - Runge–Kutta fourth order solver, 472
 - Runge–Kutta method, 11, 98, 454, 772–777, 786, 797
 - for differential equations, 507
 - Runge–Kutta solver, 508
 - fourth order, 472
 - Runge–Kutta fourth order, 471
 - Runge–Kutta fourth order differential equation, 471
 - Runge–Kutta fourth order method, 803, 810
 - approximation to, 810f
 - leapfrog method, 804–805
 - modal equation and, 807–808f
 - numerical stability and, 804
 - region of stability for, 808f
 - fourth-order, 776–777
 - mid point, 774
 - second-order, 773–775
 - Taylor’s theorem, 772–773
 - third-order, 775–776
- ## S
- $S + N$ decomposition, 646–652
 - Saddle points, 658
 - Scalar multiples, of vectors, 582f
 - Scalar multiplication, 583, 585, 586, 589
 - of quaternions, 718
 - of vectors, 584
 - Scalar potential, vector field decomposition, 224–226
 - Scalar-valued functions, 218
 - Schaum’s Outline Series, 86
 - Secant line, 686
 - Second derivative of constraint, 513, 517–518, 521–522
 - Second derivative test, 656, 657
 - Second-derivative matrix, 384
 - Second-order derivatives, 383
 - Second-order difference equation, 754–755

- Second-order differential equations, 90, 738–739
 - coupled systems of, 107
 - initial value problem, 738
- Second-order error, 706
- Second-order linear difference equations, 757–759
 - general solutions, 757–759
 - variation of parameters, 758
- Second-order linear differential equations, 124, 135, 576
 - Wronskian of linearly independent solutions, 757
- Second-order linear systems of differential equations, 117
- Second-order partial derivatives, 521, 773, 841
- Second-order Runge-Kutta methods, 773–775
- Second-order system of ordinary differential equations, 91
- Second-order time derivatives, 523
- Secondary state, 471
- Segment, length of, 672
- Segment-parallelogram distance function, 351
- Segment-segment distance function, 351
- Selection property, of delta function, 485–486
- Semi-implicit Euler, 532
- Semi-Langrangian method, 258
- Semisimple matrix, 744
- Send queue, relationships among, 336f
- Separate pressure team, 291
- Separated variables, 735
- SeparatedByCylinderPerpendiculars, 385, 386
- SeparatedByOtherDirections function, 389
- SeparatedCylinders, 385
- Separating axis, 377, 394, 398, 435
 - for two cylinders, 378–379
- Separating direction, 377, 395
- Separating equation, 458
- Separating line, 377, 394
- Separation tests, 385
 - involving cylinder axis directions, 380
 - involving cylinder axis perpendiculars, 380–382
 - involving other directions, 382–384
- Sequential processing, postimpulse velocities in, 497
- Set operations, GJK algorithm, 459–461
- Set(s)
 - bounded convex, 815f
 - cardinality of, 593–594
 - complete, 541
 - contact, 296, 426–444
 - convex, 394f
 - empty, 814
 - finite, 489
- finite point, 475
- linearly dependent, 592
- linearly independent, 591, 593, 604
- maximum independent, 411
- negation of, 459
- nonconvex, 394f
- of arcs, 416
- orthogonal, 598
- orthonormal, 189, 598, 714, 715f
- overlap, 328
- reduced contact, 475f
- triangles and, 460
- unbounded convex, 815f
- Set_bnd, 271
- SetRhoBoundary, 271
- SetState, member function, 471
- SetUBoundary, 271, 273
- SetVBoundary, 273
- Shear modulus, 157
- Shear stresses, 233
- Sign changes, 202
- Sign configurations, 202
- Signed area, 628
- Signed hypervolume, 678
- Signed volume, 603
- Similarity relationship, 624
- Simple pendulum, 96–99, 101, 110, 112
 - equation of motion, 750
 - explicit Euler's method and, 801f
 - implicit Euler's method and, 803f
 - model, 747
- Simplex method, 818
- Simplex vertices, 463, 464f
- Simplices
 - barycentric coordinates of, 670–671
 - hypervolume of, 675–678
- Simultaneous processing
 - of contact points, 491–497
 - rigid bodies in, 497
- Simultaneously diagonalizable, 236
- Singl integral, 118
- Single particles, 14
 - rigid body kinematics, 15–27
- Single-stage update algorithm, 289
- Single-step methods, 11
 - stability for, 795–797
- Single-threaded environment, AABBs in, 320–330
- Singleton point, 461
- Sinks, 238
- Sinusoidal oscillations, 748
- Sinusoidal terms, 136
- Skew-symmetric matrix, 231, 522, 636, 724
 - copositive, 838
- square, 565

- Skirts
 - modeling by generalized cylinder surface, 188
 - wind on, 188
 - Slack variables, 818, 820
 - for primal problem, 843
 - increasing, 823
 - positive, 824
 - Slerp, *See* Spherical linear interpolation
 - Slide rule, 1
 - Slipping objects, 535
 - Sloped plane
 - axis-aligned box colliding with, 483f
 - colliding contact of box edge with, 485
 - square traveling towards, 482f
 - Smoothed particle hydrodynamics (SPH), 294
 - Solid rigid bodies, 465
 - Solids, 14
 - Source code, 368–371
 - moving ellipsoids, 372–376
 - density, 292
 - Source-sink function, 238
 - Source-sink term, 260–261
 - SourceForge, 421
 - Sources, 238
 - Spans, vector spaces, 588–590
 - Sparse linear systems, 558
 - Sparse matrices, 516
 - data structure for, 527–528
 - spatial, motion, 19–24
 - Spatial coherence, 300
 - Spatial derivatives, 249
 - Spatial motion
 - in Cartesian coordinates, 19–22
 - in cylindrical coordinates, 22–23
 - in spherical coordinates, 23–24
 - Spatial points, 486
 - Specialized boundary handling, 270–274
 - Specialized processing unit (SPU)
 - AABB culling using, 335–349
 - BoxManager implementation, 335
 - endpoint class, 339
 - implementation, 335–343
 - memory, 336f
 - relationships among, 336f
 - Speed, 19
 - calculations, 681t
 - initial angular, 799
 - instantaneous, 681
 - Sphere class, 302
 - Sphere-based culling, 301, 303
 - Spheres, test-intersection query, 349
 - Spherical bodies, 210
 - Spherical coordinates, 23–24
 - Spherical duals
 - BSP tree for, 419
 - of convex polyhedra, 414
 - of tetrahedrons, 414f
 - with spherical convex polygons, 417
 - Spherical faces, 416
 - Spherical linear interpolation (slerp)
 - illustration of, 728f
 - of quaternions, 727–729
 - Spherical quadratic interpolation, of quaternions, 729–731
 - Splitting method, 558–559
 - Spring forces, 33–34
 - SPU, *See* Specialized processing unit
 - SpuConnect, 346
 - SpuSendMessage, 348
 - Squad function, 731
 - Square brackets, 73
 - Square matrices, 564
 - diagonal, 564
 - inverse of, 568
 - skew-symmetric, 565
 - symmetric, 565
 - Square root, 96
 - Squared area, 628
 - Squared base, 628
 - Squared height, 628
 - Squares
 - transforming parallelograms into, 627f
 - traveling towards sloped plane, 482f
 - unit-area, 627f
 - Stability
 - asymptotic, 749
 - conditional, 254
 - definition of, 747
 - differential equations, 746–751
 - for constant-coefficient linear systems, 747–749
 - for general autonomous systems, 749–751
 - for multistep methods, 797–798
 - for single-step methods, 795–797
 - in numerical methods, 796
 - numerical, 254, 794–809
 - of solutions, 747
 - physical, 794–809
 - region of, for explicit Euler method, 806f
 - region of, for implicit Euler method, 807f
 - region of, for leapfrog method, 809f
 - region of, for Runge-Kutta fourth order method, 808f
 - step size, 798–808
- Standard basis, 724
- Standard coordinate axis directions, 714
- Standard Euclidean basis, 595
- State variables, 471

- State vector, 465, 468, 469
 - blocks of values in, 469
- Static friction, 35, 510
 - coefficient of, 35
- Stationary
 - ellipsoids, 358
- Stationary box, 425
- Stationary ellipses, 353–356
 - test-intersection query for, 353–356
- Stationary objects
 - collision detection, 396–421
 - convex polygons and, 396–408
- Stationary polytope, 391
- Stationary projected intervals, 457f
- Sticking objects, 535
- Stiff equations, 809–812
 - systems of, 811t
- Stiffness, 11, 809
- Stoke’s theorem, 67, 213
 - vector calculus and, 219–220
- Strain
 - deformable bodies and, 156–158
 - fluids and, 230–237
 - gases and, 230–237
 - pure, 232
 - stress and, 236–237
 - tensor, 230–233
- Stress
 - deformable bodies and, 156–158
 - divergence of, 245
 - fluids and, 230–237
 - gases and, 230–237
 - normal, 233
 - shear, 233
 - simultaneously diagonalizable, 236
 - strain and, 236–237
 - tensor, 233–236, 245
- Strictly convex functions, 381
- Strictly diagonally dominant, 560
- Strong duality principle, 828
- Subpolygon, 418
- Subsectors, 404f
- Subspaces
 - affine algebra, 665
 - fundamental, 613f
 - invariant, 649
 - one-dimensional, 665
 - orthogonal, 606–609, 647
 - orthogonal complement and, 608
 - parallel, 665
 - two-dimensional, 614f, 665
 - vector spaces, 588–590
- Substitution property, 222
- Subtraction, 539
 - of quaternions, 718
 - of vectors, 580–581
- Successive over-relaxation, 561
- Suggestive notation, 661
- Sum(s)
 - direct, 647, 649
 - infinite, 744
 - Minkowski, 459
 - of external force, 244
 - of transformations, 649
 - telescoping, 551
- Summation, 690
- Summation notation, 563, 676–677
- Sun
 - Earth’s orbit and, 88
 - motion and, 86–87
- Surface integrals, vector calculus, 219–220
- Surface mass, 14, 118, 219
 - as mass-spring system, 162
 - in three dimensions, 52–53
- Surface(s)
 - B-spline, 179–181
 - built from curves, 184–192
 - classical tube, 189
 - closed tube, 191
 - control point, 190
 - cylinder, 186
 - generalized cylinder, 186–188
 - integrals, 219–220
 - level, 200, 215
 - NURBS, 182–184
 - particle constrained to, 513
 - revolution, 187, 190
 - tube, 189–193
- SwapBuffers, 277
- Sweep algorithm, 305
- SWIFT (Speedy Walking via Improved Feature Testing), 536
- Symmetric control points, 183
- Symmetric matrices, 744
 - $n \times n$, 645
 - eigendecomposition for, 643–646
 - negative definite, 643
 - negative semidefinite, 643
 - nonnegative definite, 643
 - nonpositive definite, 643
 - positive definite, 643
 - positive semidefinite, 643
 - real-valued, 643–644
- Symmetric matrix, 616
- Symmetric weights, 183
- Synergistic processing units, 349
- Systems of difference equations, 762–764

- Systems of linear differential equations, 741–746
 stability for constant-coefficient, 747–749
- Systems of linear equations
 forward elimination in, 542–559
 geometry of, 552–555
 iterative methods for solving, 558–561
 nonsquare, 552
 numerical issues, 556–558
 two equations in two unknowns, 545–548
- Systems of stiff equations, solutions of, 811t
- T**
- T -derivative, 356
 T -interval midpoint, 730
 Tableau, 820
 method, 832
 updated, 822–824
 Table-based mesh selection, 206–208
 Tangent line, 686, 695
 Tangent plane, 695
 Tangential acceleration, 17, 25
 Tangential component, 535
 Taylor expansions, 790
 Taylor methods, higher-order, 769–770
 Taylor polynomials, 655–657, 773, 774
 of degree n , 766
 Taylor series, 706, 734
 for exponential functions, 742
 formal, 707
 Taylor's theorem, 765, 768, 785, 788, 794
 algorithms based on, 792
 for bivariate functions, 72, 773
 Telekinesys, 5
 Telescoping sum, 551
 Temperature, 292
 Templates, 705
 Temporal coherence, 300–301, 309
 Tensor component indices, 234
 Tensor index notation, 527
 Tensors
 permutation, 235
 strain, 230–233
 stress, 233–236
 Terminal dictionary, 830, 832
 Test driver, 800
 Test-intersection query, 296, 297, 349–390
 capsules, 350–353
 cylinders, 376–377
 ellipsoids, 353–376
 geometric, 391
 moving ellipses, 358–371
 moving ellipsoids, 371–376
 pseudocode for, 454–455
 spheres, 349
 stationary ellipses, 353–356
 stationary ellipsoids, 357–358
 TestIntersection, 302, 398, 401, 408, 422, 427, 435, 437
 for convex polyhedra, 454
 formulation, 430
 rewriting, 439
 Tetrahedron, 234, 414f
 barycentric combination of, 669
 barycentric coordinates, 669
 base of, 674f
 linear interpolation over, 669
 spherical duals of, 414f
 vertex of, 671
 volume of, 673–675, 677
 Theorem
 Cayley–Hamilton, 742–743
 divergence, 67, 215–217, 220–221, 226–227, 239, 244
 fundamental, of algebra, 609–613
 fundamental, of calculus, 691
 fundamental, of vector calculus, 224, 229–230
 Green's, 67, 213, 221–224
 Stoke's, 67
 Stoke's theorem, 213, 219–220
 Taylor's, 765, 768, 773, 785, 788, 792, 794
 Third-order equations, 761
 Third-order Runge–Kutta methods, 775–776
 Three-dimensional array of masses, 164–165
 Time derivatives, 249, 516, 521
 first-order, 523
 second-order, 523
 Time intervals, 392
 of free-form deformation, 210
 Time step, 392
 Time stepping, velocity-based constrained motion, 531–532
 Time-stepping algorithm, 526
 Time-varying constraints, 111–114
 Time-varying deformations, 199
 Time-varying frames, 111–114
 Tmax, 75
 Tokamak Open Source Physics Engine, 5
 Tops
 angular velocity of, 150
 freely spinning, 150, 154
 Torque, 36–37, 151, 154, 472
 external, 501
 inertial, 525
 resolution, 500
 Torsion of curves, 21
 Total density update, 261–263

- Total derivative, 111, 214–215
 time, 112
 vector calculus, 214–215
- Total potential energy, 130
- Transfer of axes, 64
- Transformations, affine, 666–667
- Translation, 667
- Transport algorithm, 258
- Transpose, 564
 range of, 612
- Transposition, 631
- Trapezoids, area of, 778
- Triangle mesh, 192
 in Marching Cubes algorithm, 207
- Triangle(s)
 area of, 672–673
 barycentric coordinates, 668–669
 base length, 672
 computation by direct parameterization of, 72–74
 edge–edge contact for, 432f
 isosceles, 120
 linear interpolation over, 669f
 moving, 432f
 Pascal’s, 793
 pendulum, 121
 pseudocode generating, 185
 rectangles consisting of, 184
 removal, 209
 sets and, 460
 solid, 845
 uvw, 182
- Triangular domain, 702
- Triangulation, 411
- Tridiagonal, 577
- Trigonometric functions, 117, 152
- Trigonometric identities, 131, 458, 721
- Triple integral, 118
- Triple products, vector spaces, 600–606
- Triple scalar product, 603–604
- Triple vector product, 604–606f
- Triply indexed tensor, 521, 523
 permutation, 676
- Tube surfaces, 189–192
 closed, 191
 wriggling snake as, 193
- Turbo Pascal, 2
- Twice differentiable, 656
- Two-body problem, 132–134
- Two-dimensional array of masses, 160–163
- Two-dimensional linear programming, 814–816
- Two-dimensional subspaces, 614f, 665
- TYPE_MAXIMUM, 322, 337
- U**
- Umbrella parents, 413
- Unbounded convex set, constraints defining, 815f
- Unbounded domains, 837
- Unboundedness property, dual problem, 827–828
- Unconstrained motion, 465–473
- Uniform knots, 169
- Uniform random number generator, 275f
- Uniform texture coordinates, pseudocode generating, 185
- Unique representations, 592
- Uniqueness, of differential equations, 736–738
- Unit circle, 403f
- Unit disk, splitting, 404f
- Unit length, 720
- Unit-area square, 627f
- Unit-length direction, 695
- Unit-length tangent vector, 514–515
- Unit-length vector, 731
- Unit-length vector perpendicular, 601
- Unit-volume cube, 630f
- Univariate calculus, 679–691
 continuity, 685
 differentiation, 686–689
 integration, 689–692
 l’Hôpital’s rule, 689
 limits, 682–684
- Univariate differential operator, 693
- Univariate functions
 derivatives of, 705–710
 global extremum, 699
 global minimum, 699
 local maximum, 699
 local minimum, 699
 OBBs and, 700
 optimization, 698–700
- Universal gravitational constant, 32
- Unknown vector, 851
- Unknowns, two equations in two, 545–548
- Unstable solutions, 747
- Update function, 252, 311, 315, 326
 boundary, 253
 for lattice cells, 259
 main, 341
 per dimension, 342
 with array inputs, 319
- Update phase, 310
- UpdateAdvection, 270, 278
- UpdateAsynchronous, 331
- UpdateBoundary, 256
- Updated tableau, 822t–824
- UpdateDensityAdvection, 285
- UpdateDensityBoundary, 281

- UpdateDensityDiffusion, 284
 UpdateDensitySource, 283
 UpdateSource, 260
 UpdateVelocityAdvection, 286
 UpdateVelocityBoundary, 281
 UpdateVelocityDiffusion, 278
 UpdateVelocitySource, 278, 283
 Upper echelon matrix, 565, 573, 574, 637
 Upper triangular matrix, 565, 578, 637, 644
 Usenet groups, 10, 535
 User-specified maximum time, 702
 User-supplied inputs, 740
 uvw -triangle, 182
- V**
- V-Clip, 464
 V-COLLIDE, 536–537
 V-terms, first-order linear difference equations, 758
 Van den Bergen, Gino, 459, 535
 Variables, 822
 artificial, 819, 820
 auxiliary, 829, 831
 basic, 610, 821
 changes of, 360
 column, 821
 complementary, 829, 831, 833, 836–838
 continuous, 206, 684
 derived state, 471
 free, 552, 610
 nonbasic, 821, 824, 825
 real-valued, 585
 separated, 735
 slack, 818, 820, 823, 824, 843
 state, 471
 Variation of parameters, 758
 VAX 730, 2
 Vector calculus, 214–230
 curl and, 217–218
 directional derivative, 214–215
 divergence and, 215–217, 220–221
 fundamental theorem of, 224, 229–230
 gradient, 214–215
 Green's theorem, 221–224
 Laplace's equation, 221–224
 Laplacian and, 215–217
 line integrals, 219
 Poisson's equation, 221–224
 product rule of, 498
 quotient rule of, 498
 Stoke's theorem and, 219–220
 vector field decomposition and, 224–230
 vector fields and, 215–217
 volume integrals, 220–221
- Vector field decomposition
 curl and, 226–227
 differentiation and, 225
 divergence and, 226–227
 scalar potential, 224–226
 vector calculus and, 224–230
 vector potential and, 227–229
- Vector fields, 66
 curl and, 226–227
 divergence and, 226–227
 flow lines of, 241
 vector calculus and, 215–217
- Vector potential, vector field decomposition and, 227–229
- Vector(s), 579, *See also* Eigenvectors
 $1 \times n$ row, 842
 $m \times 1$ column, 819, 842
 addition of, 580, 583–586
 additive identity of, 581f
 algebra, 721
 angular momentum, 151
 basis, 624, 664
 binormal, 21
 black, 425
 class, 661
 coefficient, 621
 connecting points, 660f
 constant, 87, 832, 856
 constraint, 849
 coordinate axis stress, 244
 definition of, space, 583–588
 degenerate feasible, 825
 dependent, 616
 difference, 659
 direction of, 578
 equality, 584–586
 Euclidean basis, 613, 618, 632, 633
 feasible, 818, 823, 828
 feasible basis, 818, 823
 finite dimensional, space, 594, 617
 fixed frame, 92
 form, 245
 gradient, 361, 703
 indices, 415
 inserting, 593
 knot, 168
 linear combination of, 616
 linearly dependent, 590
 linearly independent, 593, 611
 magnitude of, 578
 mutually orthogonal, 597
 non-unit-length, 597
 notation, 496, 501, 826, 847
 of partial derivatives, 695
 optimal feasible, 818

- orthonormal set of, 714
- parallelograms and, 582f
- periodic knot, 171
- permutation, 557
- perp, 673
- perpendicular, 379
- points and, 659
- postimpulse velocity, 478
- removing, from linearly dependent sets, 592
- right-handed orthonormal set of, 715f
- scalar multiples of, 582f
- scalar multiplication of, 584
- spaces, 578–626
- state, 465, 468, 469
- subtraction of, 580–581
- unit-length, 731
- unknown, 851
- velocity, 111
- Velocity, 93, *See also* Angular velocity
 - acceleration-based constrained motion, 476
 - adjustment of, 278
 - center of mass, 126, 465–466
 - constant angular, 457–459
 - constant linear, 113, 133, 350, 421–444, 453–456
 - constraint, 533
 - diffusion, 284
 - dissipation, 291–292
 - divergence of, 278
 - drag, 29
 - equations, 263–270
 - fields, 267
 - for half-steps, 791
 - initialization of, 280
 - linear, 470, 488, 492, 506, 537
 - linear preimpulse, 506
 - nonzero, 490
 - nonzero linear, 453
 - of particles, 477
 - of polytopes, 393
 - postimpulse, 478f, 483, 484, 490, 491–492, 497
 - postimpulse angular, 480
 - postimpulse world, 492
 - preimpulse, 478f, 491–492, 496
 - preimpulse angular, 480
 - preimpulse world, 492, 493
 - relative, 480, 491, 498
 - sources, 283
 - update, 266, 283, 284
 - update by advection, 285
 - vector, 111
 - Verlet method, 790–792
 - world, 118–119, 492
- Velocity component
 - forces with, 787–788
 - forces without, 786–787
- Velocity equations, 263–270
- Velocity-based constrained motion, 10, 512–533
 - constraint bias, 529
 - contact caching scheme, 532
 - contact model, 529
 - friction model, 531
 - inequality constraints, 528–529
 - time stepping, 531–532
 - variations on, 525–533
- Verlet integration, 785–794
 - forces with velocity component, 787–788
 - forces without velocity component, 786–787
 - leapfrog method, 788–790
 - simulating drag in system, 788
- Verlet method, 791, 794
 - velocity, 790–792
- Vertex, 500
 - nm*, 461
 - indices, 415
 - of tetrahedrons, 671
 - simplex, 463, 464f
- Vertex–edge contact
 - collision detection, 427
- Vertex–edge intersection, 511
- Vertex–face intersection, 475, 476
 - contact points, 498, 502
- Vertex–vertex contact
 - collision detection, 427
 - convex polyhedra, 436–437
 - intersection calculator pseudocode, 433
- Vertex–vertex intersection, 426f
- Vertex–edge contact
 - convex polygons in, 397f
- Vertex–edge table, 165, 203
 - for pixels, 205
- Vertical asymptotes, 204
- Vertical axis, 105
- Vertical bar notation, 695
- Vertical edges, 172
- Vertices
 - moments of inertia, 61
 - products of inertia, 61
 - pseudocode generating, 185
- View frustum, 299f
- Virtual work, 514
- Viscosity, 34, 36
 - coefficient, 263
 - dynamic, 245, 246
 - kinematic, 246
- Viscous forces, 36
- Viscous friction, 799

- Volume
 barycentric coordinates, 671–678
 conservation of, 542
 evaluation, 194
 infinitesimal, 238, 696
 of tetrahedron, 673–675, 677
- Volume function, 194
 B-spline, 196
- Volume integrals
 reduction of, 65–66
 vector calculus, 220–221
- Volume mass, 14, 118
 as mass-spring systems, 164
 in three dimensions, 50–52
- Vortex particles, 291
- Vorticity confinement, 291
- Voxels, 207
 ambiguity for, 207
 corners, 276
 edge interior, 276
 extracted edge mesh, 208f
 face-interior, 276
 sharing faces, 207
- W**
 W_1 -row, 822
 W_2 -row, 821
 W_3 -row, 821, 822
 W_4 equation, 833
`WaitForObjectToSignal`, 333
`WaitForUpdateEnd`, 331, 333, 347
 Water drops, as control point surface of revolution, 190
 Watson, Thomas J., 2
 Weak damping, 751
 Weak duality principle, 827, 828
 Weight, 33
`WhichSide`, 399
 Wild Magic code, 368, 535
 Wild Magic Files, 350
 Wind, 109, 161
 cloth and, 163
 on skirts, 188
 Wire, 14
 Work energy, 78–80
 World coordinates, 27
 angular velocity in, 149
 for rigid bodies, 148
 inertia tensor in, 466–467
 of angular velocity, 126–127
 system, 90–91
- World observer, 27
 body coordinates as seen by, 28
- World velocity, 118–120
 postimpulse, 492
 preimpulse, 492, 493
- Wriggling snake, 192, 193
 tube surface as, 193
- Wronskian, of linearly independent solutions, 757
- X**
 Xbox 360, 335
- X-derivative, 356
- X-dimension, 315
- X-intervals, 312, 313f
- XS-G, 4
- Y**
 Y-dimension, 315
- Y-intervals, 312, 313f
- Young's modulus, 157
- Z**
 Z-offset texture, 289
 Zero constants
 Lemke algorithm and, 832
 terms, 835–837
 Zero matrix, 616
 2×2 , 568
 Zero vector yields, 703
 Zero-indexed entries, 427
- 1×1 matrix, 715
 1×3 matrix, 715
 $1 \times n$ row vector, 842
 2×1 block matrix, 856
 2×2 block matrix, 722
 2×2 identity matrix, 848, 851
 2×2 zero matrix, 568
 determinants of, 626–628
 3×1 matrix, 715
 3×3 elementary row matrix, 566, 569
 3×3 identity matrix, 853
 3×3 matrix, determinants of, 629–630
 4×4 identity matrix, 725
 6×6 matrix, 793
 2D images, isocurve extraction in, 201–206
 3×3 identity matrix, 525
 3×3 rotation matrix, 726
 3Com Corporation, 6
 3D images, isosurface extraction in, 206–212
 3D rotation matrix, 723, 724
 4D rotation matrix, 723, 724